Averages of *b*-hadron, *c*-hadron, and *τ*-lepton properties as of summer 2016

Y. Amhis et al. (HFLAV Group)

2017

This article was originally published at:
https://doi.org/10.1140/epjc/s10052-017-5058-4

Eur. Phys. J. C (2017) 77:895
https://doi.org/10.1140/epjc/s10052-017-5058-4

THE EUROPEAN PHYSICAL JOURNAL C

Regular Article - Experimental Physics

Averages of b-hadron, c-hadron, and τ-lepton properties as of summer 2016

Heavy Flavor Averaging Group (HFLAV): Y. Amhis[1,a], Sw. Banerjee[2,b], E. Ben-Haim[3,c], F. Bernlochner[4,d], A. Bozek[5,e], C. Bozzi[6,f], M. Chrząszcz[5,7,g], J. Dingfelder[4,h], S. Duell[4], M. Gersabeck[8,i], T. Gershon[9,j], D. Gerstel[10], P. Goldenzweig[11,k], R. Harr[12], K. Hayasaka[13,l], H. Hayashii[14,m], M. Kenzie[15,n], T. Kuhr[16,o], O. Leroy[10,p], A. Lusiani[17,18,q], X. R. Lyu[19,r], K. Miyabayashi[13,s], P. Naik[20,t], T. Nanut[21,u], A. Oyanguren Campos[22,v], M. Patel[23], D. Pedrini[24,w], M. Petrič[25], M. Rama[18,x], M. Roney[26], M. Rotondo[27,y], O. Schneider[28,z], C. Schwanda[29,aa], A. J. Schwartz[30,ab], J. Serrano[10], B. Shwartz[31,32,ac], R. Tesarek[33,ad], D. Tonelli[18,ae], K. Trabelsi[34,35,af], P. Urquijo[36], R. Van Kooten[37,ag], J. Yelton[38,ah], A. Zupanc[21,39,ai]

[1] LAL, Université Paris-Sud, CNRS/IN2P3, Orsay, France
[2] University of Louisville, Louisville, KY, USA
[3] LPNHE, Université Pierre et Marie Curie, Université Paris Diderot, CNRS/IN2P3, Paris, France
[4] University of Bonn, Bonn, Germany
[5] H. Niewodniczanski Institute of Nuclear Physics, Kraków, Poland
[6] INFN, sezione di Ferrara, Ferrara, Italy
[7] Physik-Institut, Universität Zürich, Zurich, Switzerland
[8] School of Physics and Astronomy, University of Manchester, Manchester, UK
[9] Department of Physics, University of Warwick, Coventry, UK
[10] Aix Marseille Univ, CNRS/IN2P3, CPPM, Marseille, France
[11] Institut für Experimentelle Kernphysik, Karlsruher Institut für Technologie, Karlsruhe, Germany
[12] Wayne State University, Detroit, MI, USA
[13] Niigata University, Niigata, Japan
[14] Nara Women's University, Nara, Japan
[15] Cavendish Laboratory, University of Cambridge, Cambridge, UK
[16] Ludwig-Maximilians-University, Munich, Germany
[17] Scuola Normale Superiore, Pisa, Italy
[18] INFN, sezione di Pisa, Pisa, Italy
[19] University of Chinese Academy of Sciences, Beijing, China
[20] H.H. Wills Physics Laboratory, University of Bristol, Bristol, UK
[21] J. Stefan Institute, Ljubljana, Slovenia
[22] Instituto de Fisica Corpuscular, Centro Mixto Universidad de Valencia-CSIC, Valencia, Spain
[23] Imperial College London, London, UK
[24] INFN, sezione di Milano-Bicocca, Milan, Italy
[25] European Organization for Nuclear Research (CERN), Geneva, Switzerland
[26] University of Victoria, Victoria, BC, Canada
[27] INFN, Laboratori Nazionali di Frascati, Frascati, Italy
[28] Institute of Physics, Ecole Polytechnique Fédérale de Lausanne (EPFL), Lausanne, Switzerland
[29] Institute of High Energy Physics, Vienna, Austria
[30] University of Cincinnati, Cincinnati, OH, USA
[31] Budker Institute of Nuclear Physics (SB RAS), Novosibirsk, Russia
[32] Novosibirsk State University, Novosibirsk, Russia
[33] Fermi National Accelerator Laboratory, Batavia, IL, USA
[34] High Energy Accelerator Research Organization (KEK), Tsukuba, Japan
[35] SOKENDAI (The Graduate University for Advanced Studies), Hayama, Japan
[36] School of Physics, University of Melbourne, Melbourne, VIC, Australia
[37] Indiana University, Bloomington, IN, USA
[38] University of Florida, Gainesville, FL, USA
[39] Faculty of Mathematics and Physics, University of Ljubljana, Ljubljana, Slovenia

Received: 14 June 2017 / Accepted: 10 July 2017 / Published online: 21 December 2017

Abstract This article reports world averages of measurements of b-hadron, c-hadron, and τ-lepton properties obtained by the Heavy Flavor Averaging Group using results available through summer 2016. For the averaging, common input parameters used in the various analyses are adjusted (rescaled) to common values, and known correlations are taken into account. The averages include branching fractions, lifetimes, neutral meson mixing parameters, CP violation parameters, parameters of semileptonic decays, and Cabbibo–Kobayashi–Maskawa matrix elements.

[a] e-mail: yasmine.sara.amhis@cern.ch
[b] e-mails: Swagato.Banerjee@cern.ch; swagato.banerjee@louisville.edu
[c] e-mail: benhaim@in2p3.fr
[d] e-mail: florian.bernlochner@cern.ch
[e] e-mail: bozek@belle2.ifj.edu.pl
[f] e-mail: bozzi@fe.infn.it
[g] e-mail: mchrzasz@cern.ch
[h] e-mails: jochen.christian.dingfelder@cern.ch; dingfelder@physik.uni-bonn.de
[i] e-mail: marco.gersabeck@manchester.ac.uk
[j] e-mail: T.J.Gershon@warwick.ac.uk
[k] e-mail: pablo.goldenzweig@kit.edu
[l] e-mail: hayasaka@hepl.phys.nagoya-u.ac.jp
[m] e-mail: hayashii@hepl.phys.nara-wu.ac.jp
[n] e-mail: matthew.william.kenzie@cern.ch
[o] e-mail: thomas.kuhr@lmu.de
[p] e-mail: olivier.leroy@in2p3.fr
[q] e-mails: alberto.lusiani@cern.ch; alberto.lusiani@pi.infn.it
[r] e-mail: xiaorui@ucas.ac.cn
[s] e-mail: miyabaya@cc.nara-wu.ac.jp
[t] e-mail: paras.naik@bristol.ac.uk
[u] e-mail: tara.nanut@ijs.si
[v] e-mail: Arantza.Oyanguren@ific.uv.es
[w] e-mail: daniele.pedrini@mib.infn.it
[x] e-mail: matteo.rama@pi.infn.it
[y] e-mail: marcello.rotondo@pd.infn.it
[z] e-mail: Olivier.Schneider@epfl.ch
[aa] e-mail: Christoph.Schwanda@oeaw.ac.at
[ab] e-mail: alan.j.schwartz@uc.edu
[ac] e-mail: shwartz@inp.nsk.su
[ad] e-mail: tesarek@fnal.gov
[ae] e-mail: diego.tonelli@ts.infn.it
[af] e-mails: karim.trabelsi@cern.ch; karim.trabelsi@kek.jp
[ag] e-mail: rvankoot@indiana.edu
[ah] e-mails: john.martin.yelton@cern.ch; yelton@phys.ufl.edu
[ai] e-mail: anze.zupanc@ijs.si

Contents

1 Introduction

Flavor dynamics plays an important role in elementary particle interactions. The accurate knowledge of properties of heavy flavor hadrons, especially b hadrons, plays an essential role for determining the elements of the Cabibbo–Kobayashi–Maskawa (CKM) quark-mixing matrix [1,2]. The operation of the Belle and BABAR e^+e^- B factory experiments led to a large increase in the size of available B-meson, D-hadron and τ-lepton samples, enabling dramatic improvement in the accuracies of related measurements. The CDF and D0 experiments at the Fermilab Tevatron have also

provided important results in heavy flavour physics, most notably in the B_s^0 sector. In the D-meson sector, the dedicated e^+e^- charm factory experiments CLEO-c and BESIII have made significant contributions. Run I of the CERN Large Hadron Collider delivered high luminosity, enabling the collection of even larger samples of b and c hadrons, and thus a further leap in precision in many areas, at the ATLAS, CMS, and (especially) LHCb experiments. With the LHC Run II ongoing, further improvements are keenly anticipated.

The Heavy Flavor Averaging Group (HFLAV)[1] was formed in 2002 to continue the activities of the LEP Heavy Flavor Steering Group [3]. This group was responsible for calculating averages of measurements of b-flavor related quantities. HFLAV has evolved since its inception and currently consists of seven subgroups:

- the "B Lifetime and Oscillations" subgroup provides averages for b-hadron lifetimes, b-hadron fractions in $\Upsilon(4S)$ decay and pp or $p\bar{p}$ collisions, and various parameters governing B^0–$\overline{B}^0$ and B_s^0–$\overline{B}_s^0$ mixing;
- the "Unitarity Triangle Parameters" subgroup provides averages for parameters associated with time-dependent CP asymmetries and $B \to DK$ decays, and resulting determinations of the angles of the CKM unitarity triangle;
- the "Semileptonic B Decays" subgroup provides averages for inclusive and exclusive B-decay branching fractions, and subsequent determinations of the CKM matrix element magnitudes $|V_{cb}|$ and $|V_{ub}|$;
- the "B to Charm Decays" subgroup provides averages of branching fractions for B decays to final states involving open charm or charmonium mesons;
- the "Rare Decays" subgroup provides averages of branching fractions and CP asymmetries for charmless, radiative, leptonic, and baryonic B-meson and b-baryon decays;
- the "Charm Physics" subgroup provides averages of numerous quantities in the charm sector, including branching fractions; properties of excited D^{**} and D_{sJ} mesons; properties of charm baryons; D^0–$\overline{D}^0$ mixing, CP, and T violation parameters; and D^+ and D_s^+ decay constants f_D and f_{D_s}.
- the "Tau Physics" subgroup provides averages for τ branching fractions using a global fit and elaborates the results to test lepton universality and to determine the CKM matrix element magnitude $|V_{us}|$; furthermore, it lists the τ lepton-flavor-violating upper limits and computes the combined upper limits.

[1] The group was originally known by the acronym "HFAG." Following feedback from the community, this was changed to HFLAV in 2017.

Subgroups consist of representatives from experiments producing relevant results in that area, i.e., representatives from BaBar, Belle, BESIII, CDF, CLEO(c), D0, and LHCb.

This article is an update of the last HFLAV preprint, which used results available by summer 2014 [5]. Here we report world averages using results available by summer 2016. In some cases, important new results made available in the latter part of 2016 have been included, or there have been minor revisions in the averages since summer 2016. All plots carry a timestamp indicating when they were produced. In general, we use all publicly available results that are supported by written documentation, including preliminary results presented at conferences or workshops. However, we do not use preliminary results that remain unpublished for an extended period of time, or for which no publication is planned. Close contacts have been established between representatives from the experiments and members of subgroups that perform averaging to ensure that the data are prepared in a form suitable for combinations.

Section 2 describes the methodology used for calculating averages. In the averaging procedure, common input parameters used in the various analyses are adjusted (rescaled) to common values, and, where possible, known correlations are taken into account. Sections 3–9 present world average values from each of the subgroups listed above. A brief summary of the averages presented is given in Sect. 10. A complete listing of the averages and plots, including updates since this document was prepared, are also available on the HFLAV web site: http://www.slac.stanford.edu/xorg/hflav.

2 Averaging methodology

The main task of HFLAV is to combine independent but possibly correlated measurements of a parameter to obtain the world's best estimate of that parameter's value and uncertainty. These measurements are typically made by different experiments, or by the same experiment using different data sets, or sometimes by the same experiment using the same data but using different analysis methods. In this section, the general approach adopted by HFLAV is outlined. For some cases, somewhat simplified or more complex algorithms are used; these are noted in the corresponding sections.

Our methodology focuses on the problem of combining measurements obtained with different assumptions about external (or "nuisance") parameters and with potentially correlated systematic uncertainties. It is important for any averaging procedure that the quantities measured by experiments be statistically well-behaved, which in this context means having a (one- or multi-dimensional) Gaussian likelihood function that is described by the central

value(s) $\boldsymbol{x}_i$ and covariance matrix $\boldsymbol{V}_i$. In what follows we assume $\boldsymbol{x}$ does not contain redundant information, i.e., if it contains n elements then n is the number of parameters being determined. A χ^2 statistic is constructed as

$$\chi^2(\boldsymbol{x}) = \sum_i^N (\boldsymbol{x}_i - \boldsymbol{x})^{\mathrm{T}} \boldsymbol{V}_i^{-1} (\boldsymbol{x}_i - \boldsymbol{x}), \tag{1}$$

where the sum is over the N independent determinations of the quantities $\boldsymbol{x}$. These are typically from different experiments; possible correlations of the systematic uncertainties are discussed below. The results of the average are the central values $\hat{\boldsymbol{x}}$, which are the values of $\boldsymbol{x}$ at the minimum of $\chi^2(\boldsymbol{x})$, and their covariance matrix

$$\hat{\boldsymbol{V}}^{-1} = \sum_i^N \boldsymbol{V}_i^{-1}. \tag{2}$$

We report the covariance matrices or the correlation matrices derived from the averages whenever possible. In some cases where the matrices are large, it is inconvenient to report them in this document; however, all results can be found on the HFLAV web pages.

The value of $\chi^2(\hat{\boldsymbol{x}})$ provides a measure of the consistency of the independent measurements of $\boldsymbol{x}$ after accounting for the number of degrees of freedom (dof), which is the difference between the number of measurements and the number of fitted parameters: $N \cdot n - n$. The values of $\chi^2(\hat{\boldsymbol{x}})$ and dof are typically converted to a confidence level (C.L.) and reported together with the averages. In cases where $\chi^2/\mathrm{dof} > 1$, we do not usually scale the resulting uncertainty, in contrast to what is done by the Particle Data Group [6]. Rather, we examine the systematic uncertainties of each measurement to better understand them. Unless we find systematic discrepancies among the measurements, we do not apply any additional correction to the calculated error. If special treatment is necessary to calculate an average, or if an approximation used in the calculation might not be sufficiently accurate (e.g., assuming Gaussian errors when the likelihood function exhibits non-Gaussian behavior), we include a warning message. Further modifications to the averaging procedures for non-Gaussian situations are discussed in Sect. 2.2.

For observables such as branching fractions, experiments typically report upper limits when the signal is not significant. Sometimes there is insufficient information available to combine upper limits on a parameter obtained by different experiments; in this case we usually report only the most restrictive upper limit. For branching fractions of lepton-flavor-violating decays of tau leptons, we calculate combined upper limits as discussed in Sect. 9.6.

2.1 Treatment of correlated systematic uncertainties

Consider two hypothetical measurements of a parameter x, which can be summarized as

$$x_1 \pm \delta x_1 \pm \Delta x_{1,1} \pm \Delta x_{1,2} \ldots$$
$$x_2 \pm \delta x_2 \pm \Delta x_{2,1} \pm \Delta x_{2,2} \ldots,$$

where the δx_k are statistical uncertainties and the $\Delta x_{k,i}$ are contributions to the systematic uncertainty. The simplest approach is to combine statistical and systematic uncertainties in quadrature:

$$x_1 \pm \left(\delta x_1 \oplus \Delta x_{1,1} \oplus \Delta x_{1,2} \oplus \cdots\right)$$
$$x_2 \pm \left(\delta x_2 \oplus \Delta x_{2,1} \oplus \Delta x_{2,2} \oplus \cdots\right),$$

and then perform a weighted average of x_1 and x_2 using their combined uncertainties, treating the measurements as independent. This approach suffers from two potential problems that we try to address. First, the values x_k may have been obtained using different assumptions for nuisance parameters; e.g., different values of the B^0 lifetime may have been used for different measurements of the oscillation frequency Δm_d. The second potential problem is that some systematic uncertainties may be correlated between measurements. For example, different measurements of Δm_d may depend on the same branching fraction used to model a common background.

The above two problems are related, as any quantity y_i upon which x_k depends gives a contribution $\Delta x_{k,i}$ to the systematic error that reflects the uncertainty Δy_i on y_i. We thus use the values of y_i and Δy_i assumed by each measurement in our averaging (we refer to these values as $y_{k,i}$ and $\Delta y_{k,i}$). To properly treat correlated systematic uncertainties among measurements requires decomposing the overall systematic uncertainties into correlated and uncorrelated components. As different measurements often quote different types of systematic uncertainties, achieving consistent definitions in order to properly treat correlations requires close coordination between HFLAV and the experiments. In some cases, a group of systematic uncertainties must be combined into a coarser description in order to obtain an average that is consistent among measurements. Systematic uncertainties that are uncorrelated with any other source of uncertainty are combined together with the statistical error, so that the only systematic uncertainties treated explicitly are those that are correlated with at least one other measurement via a consistently-defined external parameter y_i. When asymmetric statistical or systematic uncertainties are quoted by experiments, we symmetrize them since our combination method implicitly assumes Gaussian likelihoods (or parabolic log likelihoods) for each measurement.

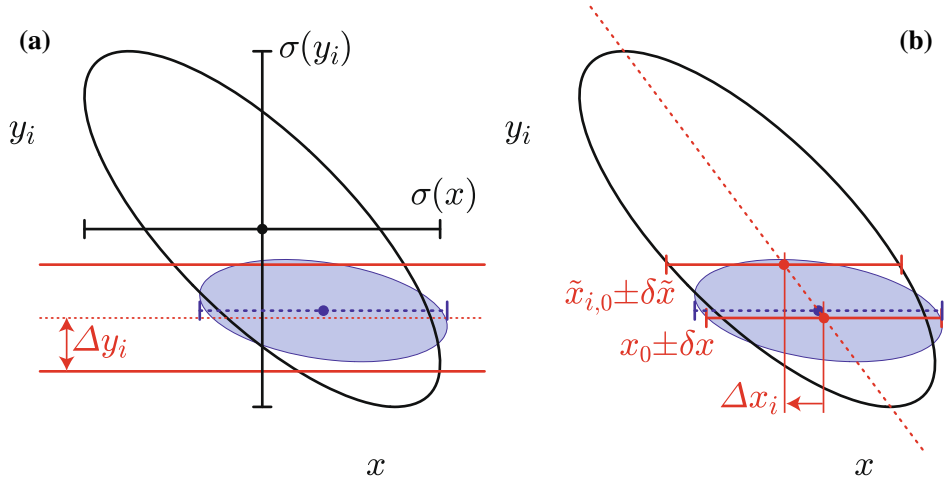

Fig. 1 Illustration of the possible dependence of a measured quantity x on a nuisance parameter y_i. The *left-hand plot* **a** compares the 68% confidence level contours of a hypothetical measurement's unconstrained (*large ellipse*) and constrained (*filled ellipse*) likelihoods, using the Gaussian constraint on y_i represented by the *horizontal band*. The *solid error bars* represent the statistical uncertainties $\sigma(x)$ and $\sigma(y_i)$ of the unconstrained likelihood. The *dashed error bar* shows the statistical error on x from a constrained simultaneous fit to x and y_i. The *right-hand plot* **b** illustrates the method described in the text of performing fits to x with y_i fixed at different values. The *dashed diagonal line* between these fit results has the slope $\rho(x, y_i)\sigma(y_i)/\sigma(x)$ in the limit of an unconstrained parabolic log likelihood. The result of the constrained simultaneous fit from **a** is shown as a *dashed error bar* on x

The fact that a measurement of x is sensitive to y_i indicates that, in principle, the data used to measure x could also be used for a simultaneous measurement of x and y_i. This is illustrated by the large contour in Fig. 1a. However, there often exists an external constraint Δy_i on y_i (represented by the horizontal band in Fig. 1a) that is more precise than the constraint $\sigma(y_i)$ from the x data alone. In this case one can perform a simultaneous fit to x and y_i, including the external constraint, and obtain the filled (x, y) contour and dashed one-dimensional estimate of x shown in Fig. 1a. For this procedure one usually takes the external constraint Δy_i to be Gaussian.

When the external constraints Δy_i are significantly more precise than the sensitivity $\sigma(y_i)$ of the data alone, the additional complexity of a constrained fit with extra free parameters may not be justified by the resulting increase in sensitivity. In this case the usual procedure is to perform a baseline fit with all y_i fixed to nominal values $y_{i,0}$, obtaining $x = x_0 \pm \delta x$. This baseline fit neglects the uncertainty due to Δy_i, but this error is subsequently recovered by repeating the fit separately for each external parameter y_i, with its value fixed to $y_i = y_{i,0} \pm \Delta y_i$. This gives the result $x = \tilde{x}_{0,i} \pm \delta\tilde{x}$ as illustrated in Fig. 1b. The shift in the central value $\Delta x_i = \tilde{x}_{0,i} - x_0$ is usually quoted as the systematic uncertainty due to the unknown value of y_i. If the unconstrained data can be represented by a Gaussian likelihood function, the shift will equal

$$\Delta x_i = \rho(x, y_i)\frac{\sigma(x)}{\sigma(y_i)}\,\Delta y_i, \tag{3}$$

where $\sigma(x)$ and $\rho(x, y_i)$ are the statistical uncertainty on x and the correlation between x and y_i in the unconstrained data, respectively. This procedure gives very similar results to that of the constrained fit with extra parameters: the central values x_0 agree to $\mathcal{O}(\Delta y_i/\sigma(y_i))^2$, and the uncertainties $\delta x \oplus \Delta x_i$ agree to $\mathcal{O}(\Delta y_i/\sigma(y_i))^4$.

To combine two or more measurements that share systematic uncertainty due to the same external parameter(s) y_i, we try to perform a constrained simultaneous fit of all measurements to obtain values of x and y_i. When this is not practical, e.g. if we do not have sufficient information to reconstruct the likelihoods corresponding to each measurement, we perform the two-step approximate procedure described below.

Consider two statistically-independent measurements, $x_1 \pm (\delta x_1 \oplus \Delta x_{1,i})$ and $x_2 \pm (\delta x_2 \oplus \Delta x_{2,i})$, of the quantity x as shown in Fig. 2a, b. For simplicity we consider only one correlated systematic uncertainty for each external parameter y_i. As our knowledge of the y_i improves, the measurements of x will shift to different central values and uncertainties. The first step of our procedure is to adjust the values of each measurement to reflect the current best knowledge of the external parameters y_i' and their ranges $\Delta y_i'$, as illustrated in Fig. 2c, d. We adjust the central values x_k and correlated systematic uncertainties $\Delta x_{k,i}$ linearly for each measurement (indexed by k) and each external parameter (indexed by i):

$$x_k' = x_k + \sum_i \frac{\Delta x_{k,i}}{\Delta y_{k,i}}\left(y_i' - y_{k,i}\right) \tag{4}$$

$$\Delta x_{k,i}' = \Delta x_{k,i}\frac{\Delta y_i'}{\Delta y_{k,i}}. \tag{5}$$

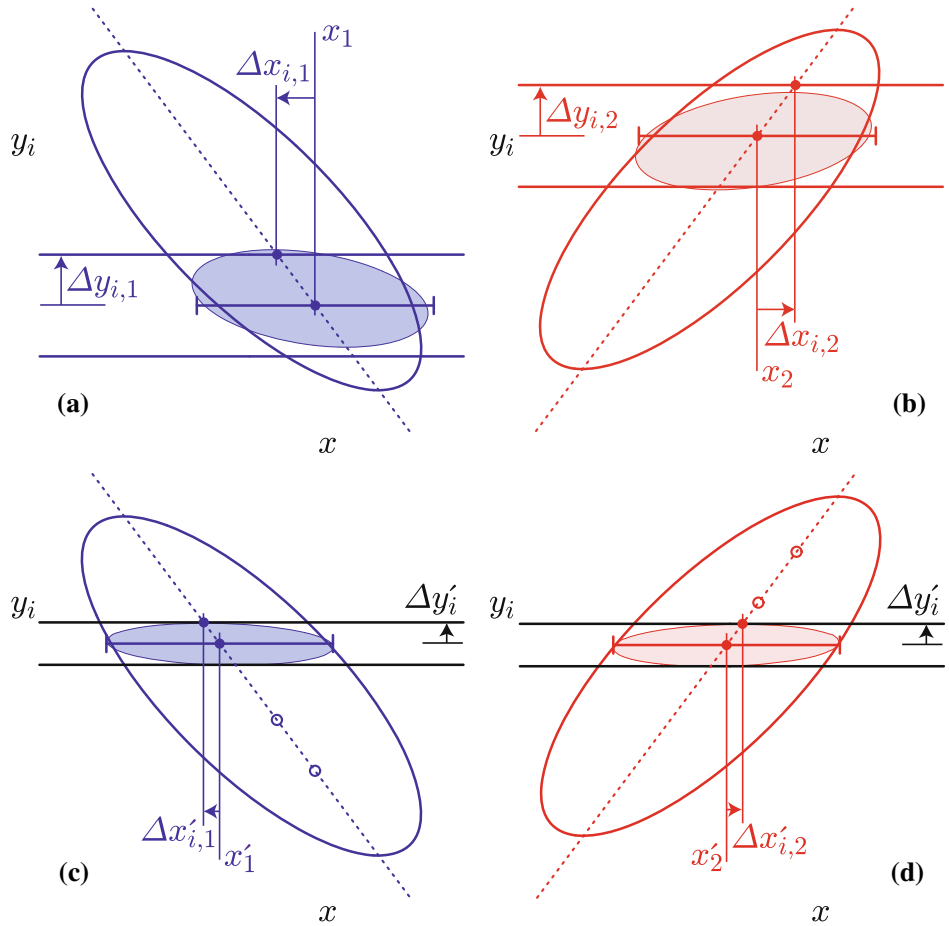

Fig. 2 Illustration of the HFLAV combination procedure for correlated systematic uncertainties. *Upper plots* **a**, **b** show examples of two individual measurements to be combined. The large (*filled*) *ellipses* represent their unconstrained (constrained) likelihoods, while *horizontal bands* indicate the different assumptions about the value and uncertainty of y_i used by each measurement. The *error bars* show the results of the method described in the text for obtaining x by performing fits with y_i fixed to different values. *Lower plots* **c**, **d** illustrate the adjustments to accommodate updated and consistent knowledge of y_i. O*pen circles mark* the central values of the unadjusted fits to x with y fixed; these determine the *dashed line* used to obtain the adjusted values

This procedure is exact in the limit that the unconstrained likelihood of each measurement is Gaussian.

The second step is to combine the adjusted measurements, $x_k' \pm (\delta x_k \oplus \Delta x_{k,1}' \oplus \Delta x_{k,2}' \oplus \cdots)$ by constructing the goodness-of-fit statistic

$$\chi^2_{\text{comb}}(x, y_1, y_2, \ldots) \equiv \sum_k \frac{1}{\delta x_k^2} \times \left[x_k' - \left(x + \sum_i (y_i - y_i') \frac{\Delta x_{k,i}'}{\Delta y_i'} \right) \right]^2 + \sum_i \left(\frac{y_i - y_i'}{\Delta y_i'} \right)^2. \quad (6)$$

We minimize this χ^2 to obtain the best values of x and y_i and their uncertainties, as shown in Fig. 3. Although this method determines new values for the y_i, we typically do not report them.

For comparison, the exact method we perform if the unconstrained likelihoods $\mathcal{L}_k(x, y_1, y_2, \ldots)$ are available is to minimize the simultaneous likelihood

$$\mathcal{L}_{\text{comb}}(x, y_1, y_2, \ldots) \equiv \prod_k \mathcal{L}_k(x, y_1, y_2, \ldots) \prod_i \mathcal{L}_i(y_i), \quad (7)$$

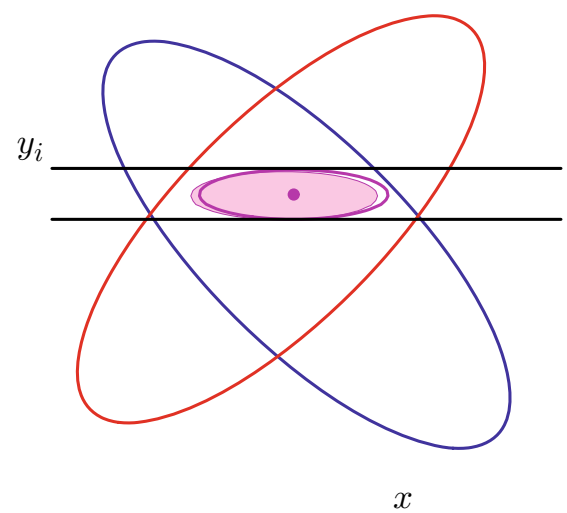

Fig. 3 Illustration of the combination of two hypothetical measurements of x using the method described in the text. The *ellipses* represent the unconstrained likelihoods of each measurement, and the *horizontal band* represents the latest knowledge about y_i that is used to adjust the individual measurements. The *filled small ellipse* shows the result of the exact method using $\mathcal{L}_{\text{comb}}$, and the *hollow small ellipse* and dot show the result of the approximate method using χ^2_{comb}

with an independent Gaussian constraint for each y_i:

$$\mathcal{L}_i(y_i) = \exp\left[-\frac{1}{2}\left(\frac{y_i - y_i'}{\Delta y_i'}\right)^2\right]. \tag{8}$$

The results of this exact method agree with those of the approximate method when the $\mathcal{L}_k$ are Gaussian and $\Delta y_i' \ll \sigma(y_i)$. If the likelihoods are non-Gaussian,, experiments need to provide $\mathcal{L}_k$ in order to perform a combination. If $\sigma(y_i) \approx \Delta y_i'$, experiments are encouraged to perform a simultaneous measurement of x and y_i so that their data will improve the world knowledge of y_i.

For averages where common sources of systematic uncertainty are important, central values and uncertainties are rescaled to a common set of input parameters following the prescription above. We use the most up-to-date values for common inputs, consistently across subgroups, taking values from within HFLAV or from the Particle Data Group when possible. The parameters and values used are listed in each subgroup section.

2.2 Treatment of non-Gaussian likelihood functions

For measurements with Gaussian errors, the usual estimator for the average of a set of measurements is obtained by minimizing

$$\chi^2(x) = \sum_k^N \frac{\left(x_k - x\right)^2}{\sigma_k^2}, \tag{9}$$

where x_k is the kth measured value of x and σ_k^2 is the variance of the distribution from which x_k was drawn. The value $\hat{x}$ at minimum χ^2 is the estimate for the parameter x. The true σ_k are unknown but typically the error as assigned by the experiment σ_k^{raw} is used as an estimator for it. However, caution is advised when σ_k^{raw} depends on the measured value x_k. Examples of this are multiplicative systematic uncertainties such as those due to acceptance, or the $\sqrt{N}$ dependence of Poisson statistics for which $x_k \propto N$ and $\sigma_k \propto \sqrt{N}$. Failing to account for this type of dependence when averaging leads to a biased average. Such biases can be avoided by minimizing

$$\chi^2(x) = \sum_k^N \frac{(x_k - x)^2}{\sigma_k^2(\hat{x})}, \tag{10}$$

where $\sigma_k(\hat{x})$ is the uncertainty on x_k that includes the dependence of the uncertainty on the value measured. As an example, consider the error due to acceptance for which $\sigma_k(\hat{x}) = (\hat{x}/x_k) \times \sigma_k^{\text{raw}}$. Inserting this into Eq. (10) leads to

$$\hat{x} = \frac{\sum_k^N x_k^3/(\sigma_k^{\text{raw}})^2}{\sum_k^N x_k^2/(\sigma_k^{\text{raw}})^2},$$

which is the correct behavior, i.e., weighting by the inverse square of the fractional uncertainty $\sigma_k^{\text{raw}}/x_k$. It is sometimes difficult to assess the dependence of σ_k^{raw} on $\hat{x}$ from the errors quoted by the experiments.

Another issue that needs careful treatment is that of correlations among measurements, e.g., due to using the same decay model for intermediate states to calculate acceptances. A common practice is to set the correlation coefficient to unity to indicate full correlation. However, this is not necessarily conservative and can result in underestimated uncertainty on the average. The most conservative choice of correlation coefficient between two measurements i and j is that which maximizes the uncertainty on $\hat{x}$ due to the pair of measurements,

$$\sigma_{\hat{x}(i,j)}^2 = \frac{\sigma_i^2\,\sigma_j^2\,(1-\rho_{ij}^2)}{\sigma_i^2 + \sigma_j^2 - 2\,\rho_{ij}\,\sigma_i\,\sigma_j}, \tag{11}$$

namely

$$\rho_{ij} = \min\left(\frac{\sigma_i}{\sigma_j}, \frac{\sigma_j}{\sigma_i}\right). \tag{12}$$

This corresponds to setting $\sigma_{\hat{x}(i,j)}^2 = \min(\sigma_i^2, \sigma_j^2)$. Setting $\rho_{ij} = 1$ when $\sigma_i \neq \sigma_j$ can lead to a significant underestimate of the uncertainty on $\hat{x}$, as can be seen from Eq. (11).

Finally, we carefully consider the various errors contributing to the overall uncertainty of an average. The covariance matrix describing the uncertainties of different measurements and their correlations is constructed, i.e., $\boldsymbol{V} = \boldsymbol{V}_{\text{stat}} + \boldsymbol{V}_{\text{sys}} + \boldsymbol{V}_{\text{theory}}$. If the measurements are from independent data samples, then $\boldsymbol{V}_{\text{stat}}$ is diagonal, but $\boldsymbol{V}_{\text{sys}}$ and $\boldsymbol{V}_{\text{theory}}$ may contain correlations. The variance on the average $\hat{x}$ can be written

$$\begin{aligned}\sigma_{\hat{x}}^2 &= \frac{\sum_{i,j}\left(\boldsymbol{V}^{-1}\left[\boldsymbol{V}_{\text{stat}} + \boldsymbol{V}_{\text{sys}} + \boldsymbol{V}_{\text{theory}}\right]\boldsymbol{V}^{-1}\right)_{ij}}{\left(\sum_{i,j}\boldsymbol{V}_{ij}^{-1}\right)^2} \\ &= \sigma_{\text{stat}}^2 + \sigma_{\text{sys}}^2 + \sigma_{\text{th}}^2.\end{aligned} \tag{13}$$

This breakdown of uncertainties is used in certain cases, but usually only a single, total uncertainty is quoted for an average.

3 Production fractions, lifetimes and mixing parameters of *b* hadrons

Quantities such as b-hadron production fractions, b-hadron lifetimes, and neutral B-meson oscillation frequencies have been studied in the nineties at LEP and SLC (e^+e^-colliders at $\sqrt{s} = m_Z$) as well as at the first version of the Tevatron ($p\bar{p}$ collider at $\sqrt{s} = 1.8$ TeV). This was followed by precise measurements of the B^0 and B^+ mesons performed at the

asymmetric B factories, KEKB and PEPII (e^+e^-colliders at $\sqrt{s} = m_{\Upsilon(4S)}$), as well as measurements related to the other b hadrons, in particular B_s^0, B_c^+ and Λ_b^0, performed at the upgraded Tevatron ($\sqrt{s} = 1.96$ TeV). Since a few years, the most precise measurements are coming from the LHC (pp collider at $\sqrt{s} = 7$ and 8 TeV), in particular the LHCb experiment.

In most cases, these basic quantities, although interesting by themselves, became necessary ingredients for the more refined measurements, such as those of decay-time dependent CP-violating asymmetries. It is therefore important that the best experimental values of these quantities continue to be kept up-to-date and improved.

In several cases, the averages presented in this section are needed and used as input for the results given in the subsequent sections. Within this section, some averages need the knowledge of other averages in a circular way. This coupling, which appears through the b-hadron fractions whenever inclusive or semi-exclusive measurements have to be considered, has been reduced drastically in the past several years with increasingly precise exclusive measurements becoming available and dominating practically all averages.

In addition to b-hadron fractions, lifetimes and oscillation frequencies, this section also deals with CP violation in the B^0 and B_s^0 mixing amplitudes, as well as the CP-violating phase $\phi_s^{c\bar{c}s} \simeq -2\beta_s$, which is the phase difference between the B_s^0 mixing amplitude and the $b \to c\bar{c}s$ decay amplitude. The angle β, which is the equivalent of β_s for the B^0 system, is discussed in Sect. 4.

Throughout this section published results that have been superseded by subsequent publications are ignored (i.e., excluded from the averages) and are only referred to if necessary.

3.1 b-hadron production fractions

We consider here the relative fractions of the different b-hadron species found in an unbiased sample of weakly decaying b hadrons produced under some specific conditions. The knowledge of these fractions is useful to characterize the signal composition in inclusive b-hadron analyses, to predict the background composition in exclusive analyses, or to convert (relative) observed rates into (relative) branching fraction measurements. We distinguish here the following three conditions: $\Upsilon(4S)$ decays, $\Upsilon(5S)$ decays, and high-energy collisions (including Z^0 decays).

3.1.1 b-hadron production fractions in $\Upsilon(4S)$ decays

Only pairs of the two lightest (charged and neutral) B mesons can be produced in $\Upsilon(4S)$ decays. Therefore only the following two branching fractions must be considered:

$$f^{+-} = \Gamma(\Upsilon(4S) \to B^+B^-)/\Gamma_{\text{tot}}(\Upsilon(4S)), \tag{14}$$

$$f^{00} = \Gamma(\Upsilon(4S) \to B^0\bar{B}^0)/\Gamma_{\text{tot}}(\Upsilon(4S)). \tag{15}$$

In practice, most analyses measure their ratio

$$\begin{aligned} R^{+-/00} &= f^{+-}/f^{00} \\ &= \Gamma(\Upsilon(4S) \to B^+B^-)/\Gamma(\Upsilon(4S) \to B^0\bar{B}^0), \end{aligned} \tag{16}$$

which is easier to access experimentally. Since an inclusive (but separate) reconstruction of B^+ and B^0 is difficult, exclusive decay modes to specific final states f, $B^+ \to f^+$ and $B^0 \to f^0$, are usually considered to perform a measurement of $R^{+-/00}$, whenever they can be related by isospin symmetry (for example $B^+ \to J/\psi K^+$ and $B^0 \to J/\psi K^0$). Under the assumption that $\Gamma(B^+ \to f^+) = \Gamma(B^0 \to f^0)$, i.e., that isospin invariance holds in these B decays, the ratio of the number of reconstructed $B^+ \to f^+$ and $B^0 \to f^0$ mesons, after correcting for efficiency, is proportional to

$$\begin{aligned} \frac{f^{+-}\,\mathcal{B}(B^+ \to f^+)}{f^{00}\,\mathcal{B}(B^0 \to f^0)} &= \frac{f^{+-}\,\Gamma(B^+ \to f^+)\,\tau(B^+)}{f^{00}\,\Gamma(B^0 \to f^0)\,\tau(B^0)} \\ &= \frac{f^{+-}}{f^{00}}\,\frac{\tau(B^+)}{\tau(B^0)}, \end{aligned} \tag{17}$$

where $\tau(B^+)$ and $\tau(B^0)$ are the B^+ and B^0 lifetimes respectively. Hence the primary quantity measured in these analyses is $R^{+-/00}\,\tau(B^+)/\tau(B^0)$, and the extraction of $R^{+-/00}$ with this method therefore requires the knowledge of the $\tau(B^+)/\tau(B^0)$ lifetime ratio.

The published measurements of $R^{+-/00}$ are listed in Table 1[2] together with the corresponding assumed values of $\tau(B^+)/\tau(B^0)$. All measurements are based on the above-mentioned method, except the one from Belle, which is a by-product of the B^0 mixing frequency analysis using dilepton events (but note that it also assumes isospin invariance, namely $\Gamma(B^+ \to \ell^+\text{X}) = \Gamma(B^0 \to \ell^+\text{X})$). The latter is therefore treated in a slightly different manner in the following procedure used to combine these measurements:

- each published value of $R^{+-/00}$ from CLEO and BaBar is first converted back to the original measurement of $R^{+-/00}\,\tau(B^+)/\tau(B^0)$, using the value of the lifetime ratio assumed in the corresponding analysis;
- a simple weighted average of these original measurements of $R^{+-/00}\,\tau(B^+)/\tau(B^0)$ from CLEO and BaBar is then computed, assuming no statistical or systematic correlations between them;
- the weighted average of $R^{+-/00}\,\tau(B^+)/\tau(B^0)$ is converted into a value of $R^{+-/00}$, using the latest average of

[2] An old and imprecise measurement from CLEO [11] is not included in Table 1 nor in the average.

Table 1 Published measurements of the B^+/B^0 production ratio in $\Upsilon(4S)$ decays, together with their average (see text). Systematic uncertainties due to the imperfect knowledge of $\tau(B^+)/\tau(B^0)$ are included

Experiment, year	References	Decay modes or method	Published value of $R^{+-/00} = f^{+-}/f^{00}$	Assumed value of $\tau(B^+)/\tau(B^0)$
CLEO, 2001	[7]	$J/\psi K^{(*)}$	$1.04 \pm 0.07 \pm 0.04$	1.066 ± 0.024
CLEO, 2002	[8]	$D^*\ell\nu$	$1.058 \pm 0.084 \pm 0.136$	1.074 ± 0.028
Belle, 2003	[9]	Dilepton events	$1.01 \pm 0.03 \pm 0.09$	1.083 ± 0.017
BaBar, 2005	[10]	$(c\bar{c})K^{(*)}$	$1.06 \pm 0.02 \pm 0.03$	1.086 ± 0.017
Average			1.059 ± 0.027 (tot)	1.076 ± 0.004

the lifetime ratios, $\tau(B^+)/\tau(B^0) = 1.076 \pm 0.004$ (see Sect. 3.2.3);

- the Belle measurement of $R^{+-/00}$ is adjusted to the current values of $\tau(B^0) = 1.520 \pm 0.004$ ps and $\tau(B^+)/\tau(B^0) = 1.076 \pm 0.004$ (see Sect. 3.2.3), using the quoted systematic uncertainties due to these parameters;
- the combined value of $R^{+-/00}$ from CLEO and BaBar is averaged with the adjusted value of $R^{+-/00}$ from Belle, assuming a 100% correlation of the systematic uncertainty due to the limited knowledge on $\tau(B^+)/\tau(B^0)$; no other correlation is considered.

The resulting global average,

$$R^{+-/00} = \frac{f^{+-}}{f^{00}} = 1.059 \pm 0.027, \tag{18}$$

is consistent with equal production rate of charged and neutral B mesons, although only at the $2.2\,\sigma$ level.

On the other hand, the BaBar collaboration has performed a direct measurement of the f^{00} fraction using an original method, which neither relies on isospin symmetry nor requires the knowledge of $\tau(B^+)/\tau(B^0)$. Its analysis, based on a comparison between the number of events where a single $B^0 \to D^{*-}\ell^+\nu$ decay could be reconstructed and the number of events where two such decays could be reconstructed, yields [12]

$$f^{00} = 0.487 \pm 0.010\,(\text{stat}) \pm 0.008\,(\text{syst}). \tag{19}$$

The two results of Eqs. (18) and (19) are of very different natures and completely independent of each other. Their product is equal to $f^{+-} = 0.516 \pm 0.019$, while another combination of them gives $f^{+-} + f^{00} = 1.003 \pm 0.029$, compatible with unity. Assuming[3] $f^{+-} + f^{00} = 1$, also consistent with CLEO's observation that the fraction of $\Upsilon(4S)$ decays to $B\overline{B}$ pairs is larger than 0.96 at 95% CL [16], the results of Eqs. (18) and (19) can be averaged (first converting Eq. (18) into a value of $f^{00} = 1/(R^{+-/00} + 1)$) to yield the following more precise estimates:

$$f^{00} = 0.486 \pm 0.006, \quad f^{+-} = 1 - f^{00} = 0.514 \pm 0.006, \quad \frac{f^{+-}}{f^{00}} = 1.058 \pm 0.024. \tag{20}$$

The latter ratio differs from one by $2.4\,\sigma$.

3.1.2 *b-hadron production fractions in $\Upsilon(5S)$ decays*

Hadronic events produced in e^+e^- collisions at the $\Upsilon(5S)$ (also known as $\Upsilon(10860)$) energy can be classified into three categories: light-quark (u, d, s, c) continuum events, $b\bar{b}$ continuum events, and $\Upsilon(5S)$ events. The latter two cannot be distinguished and will be called $b\bar{b}$ events in the following. These $b\bar{b}$ events, which also include $b\bar{b}\gamma$ events because of possible initial-state radiation, can hadronize in different final states. We define $f_{u,d}^{\Upsilon(5S)}$ as the fraction of $b\bar{b}$ events with a pair of non-strange bottom mesons ($B\bar{B}$, $B\bar{B}^*$, $B^*\bar{B}$, $B^*\bar{B}^*$, $B\bar{B}\pi$, $B\bar{B}^*\pi$, $B^*\bar{B}\pi$, $B^*\bar{B}^*\pi$, and $B\bar{B}\pi\pi$ final states, where B denotes a B^0 or B^+ meson and $\bar{B}$ denotes a $\bar{B}^0$ or B^- meson), $f_s^{\Upsilon(5S)}$ as the fraction of $b\bar{b}$ events with a pair of strange bottom mesons ($B_s^0\bar{B}_s^0$, $B_s^0\bar{B}_s^{*0}$, $B_s^{*0}\bar{B}_s^0$, and $B_s^{*0}\bar{B}_s^{*0}$ final states), and $f_{\not{B}}^{\Upsilon(5S)}$ as the fraction of $b\bar{b}$ events without any bottom meson in the final state. Note that the excited bottom-meson states decay via $B^* \to B\gamma$ and $B_s^{*0} \to B_s^0\gamma$. These fractions satisfy

$$f_{u,d}^{\Upsilon(5S)} + f_s^{\Upsilon(5S)} + f_{\not{B}}^{\Upsilon(5S)} = 1. \tag{21}$$

The CLEO and Belle collaborations have published measurements of several inclusive $\Upsilon(5S)$ branching fractions, $\mathcal{B}(\Upsilon(5S) \to D_sX)$, $\mathcal{B}(\Upsilon(5S) \to \phi X)$ and $\mathcal{B}(\Upsilon(5S) \to D^0X)$, from which they extracted the model-dependent estimates of $f_s^{\Upsilon(5S)}$ reported in Table 2. This extraction was performed under the implicit assumption $f_{\not{B}}^{\Upsilon(5S)} = 0$, using the relation

[3] A few non-$B\bar{B}$ decay modes of the $\Upsilon(4S)$ ($\Upsilon(1S)\pi^+\pi^-$, $\Upsilon(2S)\pi^+\pi^-$, $\Upsilon(1S)\eta$) have been observed with branching fractions of the order of 10^{-4} [13–15], corresponding to a partial width several times larger than that in the e^+e^-channel. However, this can still be neglected and the assumption $f^{+-} + f^{00} = 1$ remains valid in the present context of the determination of f^{+-} and f^{00}.

Table 2 Published measurements of $f_s^{\Upsilon(5S)}$, obtained assuming $f_{\not{B}}^{\Upsilon(5S)} = 0$ and quoted as in the original publications, except for the 2010 Belle measurement, which is quoted as $1 - f_{u,d}^{\Upsilon(5S)}$ with $f_{u,d}^{\Upsilon(5S)}$ from Ref. [17]. Our average of $f_s^{\Upsilon(5S)}$ assuming $f_{\not{B}}^{\Upsilon(5S)} = 0$, given on the penultimate line, does not include the most recent Belle result quoted on the last line (see footnote 4)

Experiment, year, dataset	Decay mode or method	Value of $f_s^{\Upsilon(5S)}$
CLEO, 2006, 0.42 fb^{-1} [18]	$\Upsilon(5S) \to D_s X$	$0.168 \pm 0.026^{+0.067}_{-0.034}$
	$\Upsilon(5S) \to \phi X$	$0.246 \pm 0.029^{+0.110}_{-0.053}$
	$\Upsilon(5S) \to B\bar{B}X$	$0.411 \pm 0.100 \pm 0.092$
	CLEO average of above 3	$0.21^{+0.06}_{-0.03}$
Belle, 2006, 1.86 fb^{-1} [19]	$\Upsilon(5S) \to D_s X$	$0.179 \pm 0.014 \pm 0.041$
	$\Upsilon(5S) \to D^0 X$	$0.181 \pm 0.036 \pm 0.075$
	Belle average of above 2	$0.180 \pm 0.013 \pm 0.032$
Belle, 2010, 23.6 fb^{-1} [17]	$\Upsilon(5S) \to B\bar{B}X$	$0.263 \pm 0.032 \pm 0.051$[a]
Average of all above after adjustments to inputs of Table 3		0.215 ± 0.031
Belle, 2012, 121.4 fb^{-1} [20]	$\Upsilon(5S) \to D_s X, D^0 X$	0.172 ± 0.030

Table 3 External inputs on which the $f_s^{\Upsilon(5S)}$ averages are based

Branching fraction	Value	Explanation and reference
$\mathcal{B}(B \to D_s X) \times \mathcal{B}(D_s \to \phi\pi)$	0.00374 ± 0.00014	Derived from [6]
$\mathcal{B}(B_s^0 \to D_s X)$	0.92 ± 0.11	Model-dependent estimate [21]
$\mathcal{B}(D_s \to \phi\pi)$	0.045 ± 0.004	[6]
$\mathcal{B}(B \to D^0 X) \times \mathcal{B}(D^0 \to K\pi)$	0.0243 ± 0.0011	Derived from [6]
$\mathcal{B}(B_s^0 \to D^0 X)$	0.08 ± 0.07	Model-dependent estimate [19,21]
$\mathcal{B}(D^0 \to K\pi)$	0.0393 ± 0.0004	[6]
$\mathcal{B}(B \to \phi X)$	0.0343 ± 0.0012	[6]
$\mathcal{B}(B_s^0 \to \phi X)$	0.161 ± 0.024	Model-dependent estimate [18]

$$\frac{1}{2}\mathcal{B}(\Upsilon(5S) \to D_s X) = f_s^{\Upsilon(5S)} \times \mathcal{B}(B_s^0 \to D_s X) + \left(1 - f_s^{\Upsilon(5S)} - f_{\not{B}}^{\Upsilon(5S)}\right) \times \mathcal{B}(B \to D_s X), \tag{22}$$

and similar relations for $\mathcal{B}(\Upsilon(5S) \to D^0 X)$ and $\mathcal{B}(\Upsilon(5S) \to \phi X)$. In Table 2 we list also the values of $f_s^{\Upsilon(5S)}$ derived from measurements of $f_{u,d}^{\Upsilon(5S)} = \mathcal{B}(\Upsilon(5S) \to B\bar{B}X)$ [17,18], as well as our average value of $f_s^{\Upsilon(5S)}$, all obtained under the assumption $f_{\not{B}}^{\Upsilon(5S)} = 0$.

However, the assumption $f_{\not{B}}^{\Upsilon(5S)} = 0$ is known to be invalid since the observation of the following final states in e^+e^- collisions at the $\Upsilon(5S)$ energy: $\Upsilon(1S)\pi^+\pi^-$, $\Upsilon(2S)\pi^+\pi^-$, $\Upsilon(3S)\pi^+\pi^-$ and $\Upsilon(1S)K^+K^-$ [22,23], $h_b(1P)\pi^+\pi^-$ and $h_b(2P)\pi^+\pi^-$ [24], and more recently $\Upsilon(1S)\pi^0\pi^0$, $\Upsilon(2S)\pi^0\pi^0$ and $\Upsilon(3S)\pi^0\pi^0$ [25]. The sum of the measurements of the corresponding visible cross-sections, adding also the contributions of the unmeasured $\Upsilon(1S)K^0\bar{K}^0$, $h_b(1P)\pi^0\pi^0$ and $h_b(2P)\pi^0\pi^0$ final states assuming isospin conservation, amounts to

$$\sigma^{\text{vis}}(e^+e^- \to (b\bar{b})hh) = 13.2 \pm 1.4\ \text{pb},$$
$$\text{for } (b\bar{b}) = \Upsilon(1S, 2S, 3S), h_b(1P, 2P) \text{ and } hh = \pi\pi, KK.$$

We divide this by the $b\bar{b}$ production cross section, $\sigma(e^+e^- \to b\bar{b}X) = 337 \pm 15$ pb, obtained as the average of the CLEO [21] and Belle [20][4] measurements, to obtain

$$\mathcal{B}(\Upsilon(5S) \to (b\bar{b})hh) = 0.039 \pm 0.004,$$
$$\text{for } (b\bar{b}) = \Upsilon(1S, 2S, 3S), h_b(1P, 2P) \text{ and } hh = \pi\pi, KK,$$

which is to be considered as a lower bound for $f_{\not{B}}^{\Upsilon(5S)}$.

Following the method described in Ref. [26], we perform a χ^2 fit of the original measurements of the $\Upsilon(5S)$ branching fractions of Refs. [17–19],[4] using the inputs of Table 3, the relations of Eqs. (21) and (22) and the one-sided Gaussian constraint $f_{\not{B}}^{\Upsilon(5S)} \geq \mathcal{B}(\Upsilon(5S) \to (b\bar{b})hh)$, to simultaneously extract $f_{u,d}^{\Upsilon(5S)}$, $f_s^{\Upsilon(5S)}$ and $f_{\not{B}}^{\Upsilon(5S)}$. Taking all known correlations into account, the best fit values are

$$f_{u,d}^{\Upsilon(5S)} = 0.761^{+0.027}_{-0.042}, \tag{23}$$

[4] Belle updated the analysis of Ref. [19] with the full $\Upsilon(5S)$ dataset. The resulting measurements of $\sigma(e^+e^- \to b\bar{b}X)$ and $f_s^{\Upsilon(5S)}$, which supersede those of Ref. [19], are quoted and used in Ref. [20]. However, no details are given. Because of the lack of relevant information, this measurement of $f_s^{\Upsilon(5S)}$ cannot be included in the averages presented here.

$$f_s^{\Upsilon(5S)} = 0.200^{+0.030}_{-0.031}, \tag{24}$$

$$f_{\not{B}}^{\Upsilon(5S)} = 0.039^{+0.050}_{-0.004}, \tag{25}$$

where the strongly asymmetric uncertainty on $f_{\not{B}}^{\Upsilon(5S)}$ is due to the one-sided constraint from the observed $(b\bar{b})hh$ decays. These results, together with their correlation, imply

$$f_s^{\Upsilon(5S)}/f_{u,d}^{\Upsilon(5S)} = 0.263^{+0.052}_{-0.044}, \tag{26}$$

in fair agreement with the results of a BABAR analysis [27], performed as a function of centre-of-mass energy.[5]

The production of B_s^0 mesons at the $\Upsilon(5S)$ is observed to be dominated by the $B_s^{*0}\bar{B}_s^{*0}$ channel, with $\sigma(e^+e^- \to B_s^{*0}\bar{B}_s^{*0})/\sigma(e^+e^- \to B_s^{(*)0}\bar{B}_s^{(*)0}) = (87.0 \pm 1.7)\%$ [28, 29]. The proportions of the various production channels for non-strange B mesons have also been measured [17].

3.1.3 b-hadron production fractions at high energy

At high energy, all species of weakly decaying b hadrons may be produced, either directly or in strong and electromagnetic decays of excited b hadrons. It is often assumed that the fractions of these different species are the same in unbiased samples of high-p_T b jets originating from Z^0 decays, from $p\bar{p}$ collisions at the Tevatron, or from pp collisions at the LHC. This hypothesis is plausible under the condition that the square of the momentum transfer to the produced b quarks, Q^2, is large compared with the square of the hadronization energy scale, $Q^2 \gg \Lambda^2_{\mathrm{QCD}}$. On the other hand, there is no strong argument that the fractions at different machines should be strictly equal, so this assumption should be checked experimentally. The available data show that the fractions depend on the kinematics of the produced b hadron. A simple phenomenological model appears to agree with all data and indicates that the fractions are constant if the b hadron is produced with sufficiently high transverse momentum from any collider. Unless otherwise indicated, these fractions are assumed to be equal at all high-energy colliders until demonstrated otherwise by experiment. Both CDF and LHCb report a p_T dependence for Λ_b^0 production relative to B^+ and B^0; the number of Λ_b^0 baryons observed at low p_T is enhanced with respect to that seen at LEP's higher p_T. Therefore we present three sets of complete averages: one set including only measurements performed at LEP, a second set including only measurements performed at the Tevatron, a third set including measurements performed at LEP, Tevatron and LHC. The LHCb production fractions results by themselves are still incomplete, lacking measurements of the production of weakly-decaying baryons heavier than Λ_b^0.

Contrary to what happens in the charm sector where the fractions of D^+ and D^0 are different, the relative amount of B^+ and B^0 is not affected by the electromagnetic decays of excited B^{*+} and B^{*0} states and strong decays of excited B^{**+} and B^{**0} states. Decays of the type $B_s^{**0} \to B^{(*)}K$ also contribute to the B^+ and B^0 rates, but with the same magnitude if mass effects can be neglected. We therefore assume equal production of B^+ and B^0 mesons. We also neglect the production of weakly decaying states made of several heavy quarks (like B_c^+ and doubly heavy baryons) which is known to be very small. Hence, for the purpose of determining the b-hadron fractions, we use the constraints

$$f_u = f_d \quad \text{and} \quad f_u + f_d + f_s + f_{\text{baryon}} = 1, \tag{27}$$

where f_u, f_d, f_s and f_{baryon} are the unbiased fractions of B^+, B^0, B_s^0 and b baryons, respectively.

We note that there are many measurements of the production cross-sections of different species of b hadrons. In principle these could be included in a global fit to determine the production fractions. We do not perform such a fit at the current time, and instead average only the explicit measurements of the production fractions.

The LEP experiments have measured $f_s \times \mathcal{B}(B_s^0 \to D_s^-\ell^+\nu_\ell X)$ [30–32], $\mathcal{B}(b \to \Lambda_b^0) \times \mathcal{B}(\Lambda_b^0 \to \Lambda_c^+\ell^-\bar{\nu}_\ell X)$ [33,34] and $\mathcal{B}(b \to \Xi_b^-) \times \mathcal{B}(\Xi_b^- \to \Xi^-\ell^-\bar{\nu}_\ell X)$ [35,36] from partially reconstructed final states including a lepton, f_{baryon} from protons identified in b events [37], and the production rate of charged b hadrons [38]. Ratios of b-hadron fractions have been measured by CDF using lepton+charm final states [39–41][6] and double semileptonic decays with $K^*\mu\mu$ and $\phi\mu\mu$ final states [42]. Measurements of the production of other heavy flavour baryons at the Tevatron are included in the determination of f_{baryon} [43–45][7] using the constraint

$$\begin{aligned} f_{\text{baryon}} &= f_{\Lambda_b^0} + f_{\Xi_b^0} + f_{\Xi_b^-} + f_{\Omega_b^-} \\ &= f_{\Lambda_b^0}\left(1 + 2\frac{f_{\Xi_b^-}}{f_{\Lambda_b^0}} + \frac{f_{\Omega_b^-}}{f_{\Lambda_b^0}}\right), \end{aligned} \tag{28}$$

where isospin invariance is assumed in the production of Ξ_b^0 and Ξ_b^-. Other b baryons are expected to decay strongly or electromagnetically to those baryons listed. For the production measurements, both CDF and D0 reconstruct their b baryons exclusively to final states which include a J/ψ and a hyperon ($\Lambda_b^0 \to J/\psi\Lambda$, $\Xi_b^- \to J/\psi\Xi^-$ and $\Omega_b^- \to J/\psi\Omega^-$). We assume that the partial decay width of a b

[5] The results of Ref. [27] are not included in the average since no numerical value is given for $f_s^{\Upsilon(5S)}/f_{u,d}^{\Upsilon(5S)}$.

[6] CDF updated their measurement of $f_{\Lambda_b^0}/f_d$ [39] to account for a measured p_T dependence between exclusively reconstructed Λ_b^0 and B^0 [41].

[7] D0 reports $f_{\Omega_b^-}/f_{\Xi_b^-}$. We use the CDF+D0 average of $f_{\Xi_b^-}/f_{\Lambda_b^0}$ to obtain $f_{\Omega_b^-}/f_{\Lambda_b^0}$ and then combine it with the CDF result.

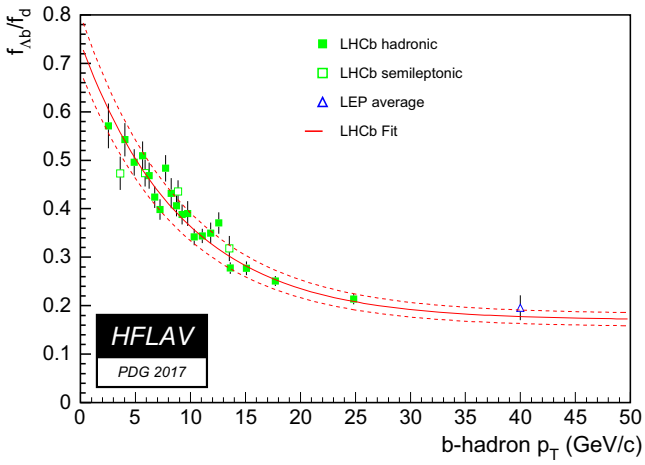

Fig. 4 Ratio of production fractions $f_{\Lambda_b^0}/f_d$ as a function of p_T of the b hadron from LHCb data for b hadrons decaying semileptonically [46] and fully reconstructed in hadronic decays [48]. The *curve* represents a fit to the LHCb hadronic data [48]. The computed LEP ratio is included at an approximate p_T in Z decays, but does not participate in any fit

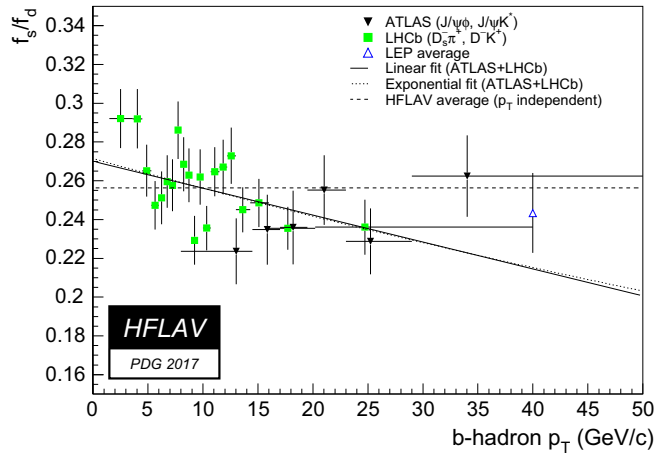

Fig. 5 Ratio of production fractions f_s/f_d as a function of p_T of the reconstructed b hadrons for the LHCb [47] and ATLAS [49] data. Note the suppressed zero for the vertical axis. The *curves* represent fits to the data: a linear fit (*solid*), and an exponential fit described in the text (*dotted*). The p_T independent value average of R_s (*dashed*) is shown for comparison. The computed LEP ratio is included at an approximate p_T in Z decays, but does not participate in any fit

baryon to a J/ψ and the corresponding hyperon is equal to the partial width of any other b baryon to a J/ψ and the corresponding hyperon. LHCb has also measured ratios of b-hadron fractions in charm+lepton final states [46] and in fully reconstructed hadronic two-body decays $B^0 \to D^-\pi^+$, $B_s^0 \to D_s^-\pi^+$ and $\Lambda_b^0 \to \Lambda_c^+\pi^-$ [47,48].

Both CDF and LHCb observe that the ratio $f_{\Lambda_b^0}/f_d$ depends on the p_T of the charm+lepton system [41,46].[8] CDF chose to correct an older result to account for the p_T dependence. In a second result, CDF binned their data in p_T of the charm+electron system [40]. The more recent LHCb measurement using hadronic decays [48] obtains the scale for $R_{\Lambda_b^0} = f_{\Lambda_b^0}/f_d$ from their previous charm + lepton data [46]. The LHCb measurement using hadronic data also bins the same data in pseudorapidity (η) and sees a linear dependence of $R_{\Lambda_b^0}$. Since η is not entirely independent of p_T it is impossible to tell at this time whether this dependence is just an artifact of the p_T dependence. Figure 4 shows the ratio $R_{\Lambda_b^0}$ as a function of p_T for the b hadron, as measured by LHCb. LHCb fits their scaled hadronic data to obtain

$$R_{\Lambda_b^0} = (0.151 \pm 0.030) + \exp\Big\{-(0.57 \pm 0.11) - (0.095 \pm 0.016)[\mathrm{GeV}/c]^{-1} \times p_T\Big\}. \quad (29)$$

A value of $R_{\Lambda_b^0}$ is also calculated for LEP and placed at the approximate p_T for the charm+lepton system, but this value does not participate in any fit.[9] Because the two LHCb results for $R_{\Lambda_b^0}$ are not independent, we use only their semileptonic data for the averages. Note that the p_T dependence of $R_{\Lambda_b^0}$ combined with the constraint from Eq. (27) implies a compensating p_T dependence in one or more of the production fractions, f_u, f_d, or f_s.

LHCb and ATLAS have investigated the p_T dependence of f_s/f_d using fully reconstructed B_s^0 and B^0 decays. LHCb reported 3σ evidence that the ratio $R_s = f_s/f_d$ decreases with p_T using fully reconstructed B_s^0 and B^0 decays and theoretical predictions for branching ratios [47]. Data from the ATLAS experiment [49] using decays of B_s^0 and B^0 to J/ψ final states and using theoretical predictions for branching ratios [50] indicates that R_s is consistent with no p_T dependence. Figure 5 shows the ratio R_s as a function of p_T measured by LHCb and ATLAS. Two fits are performed. The first fit, using a linear parameterization, yields $R_s = (0.2701 \pm 0.0058) - (0.00139 \pm 0.00044)[\mathrm{GeV}/c]^{-1} \times p_T$. A second fit, using a simple exponential, yields $R_s = \exp\big\{(-1.304 \pm 0.024) - (0.0058 \pm 0.0019)[\mathrm{GeV}/c]^{-1} \times p_T\big\}$. The two fits are nearly indistinguishable over the p_T range of the results, but the second gives a physical value for all p_T. R_s is also calculated for LEP and placed at the approximate p_T for the b hadron, though the LEP result doesn't participate in the fit. Our world average for R_s is also included in the figure for reference.

In order to combine or compare LHCb results with other experiments, the p_T-dependent $f_{\Lambda_b^0}/(f_u + f_d)$ is weighted by

[8] CDF compares the p_T distribution of fully reconstructed $\Lambda_b^0 \to \Lambda_c^+\pi^-$ with $\overline{B}^0 \to D^+\pi^-$, which gives $f_{\Lambda_b^0}/f_d$ up to a scale factor. LHCb compares the p_T in the charm+lepton system between Λ_b^0 and B^0 and B^+, giving $R_{\Lambda_b^0}/2 = f_{\Lambda_b^0}/(f_u + f_d) = f_{\Lambda_b^0}/2f_d$.

[9] The CDF semileptonic data would require significant corrections to obtain the p_T of the b hadron and be included on the same plot with the LHCb data. We do not have these corrections at this time.

Table 4 Comparison of average production fraction ratios from CDF [40,41] and LHCb [46]. The kinematic regime of the charm+lepton system reconstructed in each experiment is also shown

Quantity	CDF	LHCb
$f_s/(f_u+f_d)$	0.224 ± 0.057	0.134 ± 0.009
$f_{\Lambda_b^0}/(f_u+f_d)$	0.229 ± 0.062	0.240 ± 0.022
Average charm+lepton p_T	$\sim$13 GeV/c	$\sim$7 GeV/c
Pseudorapidity range	$-1 < \eta < 1$	$2 < \eta < 5$

the p_T spectrum.[10] Table 4 compares the p_T-weighted LHCb data with comparable averages from CDF. The average CDF and LHCb data are in agreement despite the b hadrons being produced in different kinematic regimes.

Ignoring p_T dependence, all these published results have been adjusted to the latest branching fraction averages [6] and combined following the procedure and assumptions described in Ref. [3], to yield $f_u = f_d = 0.404 \pm 0.006$, $f_s = 0.102 \pm 0.005$ and $f_{\text{baryon}} = 0.090 \pm 0.012$ under the constraints of Eq. (27). Repeating the combinations for LEP and the Tevatron, we obtain $f_u = f_d = 0.412 \pm 0.008$, $f_s = 0.088 \pm 0.013$ and $f_{\text{baryon}} = 0.089 \pm 0.012$ when using the LEP data only, and $f_u = f_d = 0.340 \pm 0.021$, $f_s = 0.101 \pm 0.015$ and $f_{\text{baryon}} = 0.218 \pm 0.047$ when using the Tevatron data only. As noted previously, the LHCb data are insufficient to determine a complete set of b-hadron production fractions. The world averages (LEP, Tevatron and LHC) for the various fractions are presented here for comparison with previous averages. Significant differences exist between the LEP and Tevatron fractions, therefore use of the world averages should be taken with some care. For these combinations other external inputs are used, e.g., the branching ratios of B mesons to final states with a D or D^* in semileptonic decays, which are needed to evaluate the fraction of semileptonic B_s^0 decays with a D_s^- in the final state.

Time-integrated mixing analyses performed with lepton pairs from $b\bar{b}$ events produced at high-energy colliders measure the quantity

$$\overline{\chi} = f'_d\,\chi_d + f'_s\,\chi_s, \tag{30}$$

where f'_d and f'_s are the fractions of B^0 and B_s^0 hadrons in a sample of semileptonic b-hadron decays, and where χ_d and χ_s are the B^0 and B_s^0 time-integrated mixing probabilities. Assuming that all b hadrons have the same semileptonic decay width implies $f'_i = f_i R_i$, where $R_i = \tau_i/\tau_b$ is the ratio of the lifetime τ_i of species i to the average b-hadron lifetime $\tau_b = \sum_i f_i \tau_i$. Hence measurements of the mixing probabilities $\overline{\chi}$, χ_d and χ_s can be used to improve our knowledge of f_u, f_d, f_s and f_{baryon}. In practice, the above relations yield another determination of f_s obtained from f_{baryon} and mixing information,

$$f_s = \frac{1}{R_s}\,\frac{(1+r)\overline{\chi} - (1 - f_{\text{baryon}} R_{\text{baryon}})\chi_d}{(1+r)\chi_s - \chi_d}, \tag{31}$$

where $r = R_u/R_d = \tau(B^+)/\tau(B^0)$.

The published measurements of $\overline{\chi}$ performed by the LEP experiments have been combined by the LEP Electroweak Working Group to yield $\overline{\chi} = 0.1259 \pm 0.0042$ [51].[11] This can be compared with the Tevatron average, $\overline{\chi} = 0.147 \pm 0.011$, obtained from D0 [52] and CDF [53]. The two averages deviate from each other by $1.8\,\sigma$; this could be an indication that the production fractions of b hadrons at the Z peak or at the Tevatron are not the same. We choose to combine these two results in a simple weighted average, assuming no correlations, and, following the PDG prescription, we multiply the combined uncertainty by 1.8to account for the discrepancy. Our world average is then $\overline{\chi} = 0.1284 \pm 0.0069$.

Introducing the $\overline{\chi}$ average in Eq. (31), together with our world average $\chi_d = 0.1860 \pm 0.0011$ [see Eq. (67) of Sect. 3.3.1], the assumption $\chi_s = 1/2$ [justified by Eq. (76) in Sect. 3.3.2], the best knowledge of the lifetimes (see Sect. 3.2) and the estimate of f_{baryon} given above, yields $f_s = 0.118 \pm 0.018$ (or $f_s = 0.111 \pm 0.011$ using only LEP data, or $f_s = 0.166 \pm 0.029$ using only Tevatron data), an estimate dominated by the mixing information. Taking into account all known correlations (including that introduced by f_{baryon}), this result is then combined with the set of fractions obtained from direct measurements (given above), to yield the improved estimates of Table 5, still under the constraints of Eq. (27). As can be seen, our knowledge on the mixing parameters reduces the uncertainty on f_s, quite substantially in the case of LEP data. It should be noted that the results are correlated, as indicated in Table 5.

3.2 b-hadron lifetimes

In the spectator model the decay of b hadrons H_b is governed entirely by the flavour changing $b \to Wq$ transition ($q = c, u$). For this very reason, lifetimes of all b hadrons are the same in the spectator approximation regardless of the (spectator) quark content of the H_b. In the early 1990's experiments became sophisticated enough to start seeing the differences of the lifetimes among various H_b

[10] In practice the LHCb data are given in 14 bins in p_T and η with a full covariance matrix [46]. The weighted average is calculated as $D^T C^{-1} M/\sigma$, where $\sigma = D^T C^{-1} D$, M is a vector of measurements, C^{-1} is the inverse covariance matrix and D^T is the transpose of the design matrix (vector of 1's).

[11] We use the $\bar{\chi}$ average of Eq. 5.39 in Ref. [51], obtained from a 10-parameter global fit of all electroweak data where the asymmetry measurements have been excluded.

Table 5 Time-integrated mixing probability $\overline{\chi}$ (defined in Eq. (30)), and fractions of the different b-hadron species in an unbiased sample of weakly decaying b hadrons, obtained from both direct and mixing measurements. The correlation coefficients between the fractions are also given. The last column includes measurements performed at LEP, Tevatron and LHC

Quantity		Z decays	Tevatron	LHCb [47]	All
Mixing probability	$\overline{\chi}$	0.1259 ± 0.0042	0.147 ± 0.011		0.1284 ± 0.0069
B^+ or B^0 fraction	$f_u = f_d$	0.407 ± 0.007	0.344 ± 0.021		0.404 ± 0.006
B_s^0 fraction	f_s	0.101 ± 0.008	0.115 ± 0.013		0.103 ± 0.005
b-baryon fraction	f_{baryon}	0.084 ± 0.011	0.196 ± 0.046		0.088 ± 0.012
B_s^0/B^0 ratio	f_s/f_d	0.249 ± 0.023	0.333 ± 0.041	0.256 ± 0.020[a]	0.256 ± 0.013
$\rho(f_s, f_u) = \rho(f_s, f_d)$		-0.629	$+0.153$		-0.143
$\rho(f_{\text{baryon}}, f_u) = \rho(f_{\text{baryon}}, f_d)$		-0.822	-0.959		-0.921
$\rho(f_{\text{baryon}}, f_s)$		$+0.074$	-0.426		-0.254

[a] This value has been updated with new inputs by LHCb to yield 0.259 ± 0.015 [54]

species. The first theoretical calculations of the spectator quark effects on H_b lifetime emerged only few years earlier [55].

Since then, such calculations are performed in the framework of the Heavy Quark Expansion (HQE) [55–57], using as most important assumption that of quark-hadron duality [58,59]. Since a few years, possible quark-hadron duality violating effects are severely constrained by experiments [60]. In these calculations, the total decay rate of an H_b is expressed as the sum of a series of expectation values of operators of increasing dimension, multiplied by the correspondingly higher powers of Λ_{QCD}/m_b:

$$\Gamma_{H_b} = |\text{CKM}|^2 \sum_n c_n \left(\frac{\Lambda_{\text{QCD}}}{m_b}\right)^n \langle H_b|O_n|H_b\rangle, \tag{32}$$

where $|\text{CKM}|^2$ is the relevant combination of CKM matrix elements. The coefficients c_n of this expansion, known as the Operator Product Expansion [61], can be calculated perturbatively. Hence, the HQE predicts Γ_{H_b} in the form of an expansion in both Λ_{QCD}/m_b and $\alpha_s(m_b)$. The precision of current experiments requires an expansion up to the next-to-leading order in QCD, i.e., the inclusion of corrections of the order of $\alpha_s(m_b)$ to the c_n terms. The non-perturbative parts of the calculation are grouped into the expectation values $\langle H_b|O_n|H_b\rangle$ of operators O_n. These can be calculated using lattice QCD or QCD sum rules, or can be related to other observables via the HQE. One may reasonably expect that powers of Λ_{QCD}/m_b provide enough suppression that only the first few terms of the sum in Eq. (32) matter.

Theoretical predictions are usually made for the ratios of the lifetimes (with $\tau(B^0)$ often chosen as the common denominator) rather than for the individual lifetimes, for this allows several uncertainties to cancel. The precision of the HQE calculations (see Refs. [62–67], and Refs. [68,69] for the latest updates) is in some instances already surpassed by the measurements, e.g., in the case of $\tau(B^+)/\tau(B^0)$. More accurate predictions are now a matter of progress in the evaluation of the non-perturbative hadronic matrix elements, in particular using lattice QCD where significant advances were made in the last decade. However, the following important conclusions can be drawn from the HQE, even in its present state, which are in agreement with experimental observations:

- The heavier the mass of the heavy quark, the smaller is the variation in the lifetimes among different hadrons containing this quark, which is to say that as $m_b \to \infty$ we retrieve the spectator picture in which the lifetimes of all H_b states are the same. This is well illustrated by the fact that lifetimes are rather similar in the b sector, while they differ by large factors in the charm sector ($m_c < m_b$).
- The non-perturbative corrections arise only at the order of $\Lambda_{\text{QCD}}^2/m_b^2$, which translates into differences among H_b lifetimes of only a few percent.
- It is only the difference between meson and baryon lifetimes that appears at the $\Lambda_{\text{QCD}}^2/m_b^2$ level. The splitting of the meson lifetimes occurs at the $\Lambda_{\text{QCD}}^3/m_b^3$ level, yet it is enhanced by a phase space factor $16\pi^2$ with respect to the leading free b decay.

To ensure that certain sources of systematic uncertainty cancel, lifetime analyses are sometimes designed to measure ratios of lifetimes. However, because of the differences in decay topologies, abundance (or lack thereof) of decays of a certain kind, *etc.*, measurements of the individual lifetimes are also common. In the following section we review the most common types of lifetime measurements. This discussion is followed by the presentation of the averaging of the various lifetime measurements, each with a brief description of its particularities.

3.2.1 Lifetime measurements, uncertainties and correlations

In most cases, the lifetime of an H_b state is estimated from a flight distance measurement and a $\beta\gamma$ factor which is used to convert the geometrical distance into the proper decay time. Methods of accessing lifetime information can roughly be divided in the following five categories:

1. *Inclusive (flavour-blind) measurements*. These early measurements were aimed at extracting the lifetime from a mixture of b-hadron decays, without distinguishing the decaying species. Often the knowledge of the mixture composition was limited, which made these measurements experiment-specific. Also, these measurements had to rely on Monte Carlo simulation for estimating the $\beta\gamma$ factor, because the decaying hadrons are not fully reconstructed. These were usually the largest statistics b-hadron lifetime measurements accessible to a given experiment, and could therefore serve as an important performance benchmark.
2. *Measurements in semileptonic decays of a specific H_b*. The W boson from $b \to Wc$ produces a $\ell\nu_l$ pair ($\ell = e, \mu$) in about 21% of the cases. The electron or muon from such decays provides a clean and efficient trigger signature. The c quark from the $b \to Wc$ transition and the other quark(s) making up the decaying H_b combine into a charm hadron, which is reconstructed in one or more exclusive decay channels. Knowing what this charmed hadron is allows one to separate, at least statistically, different H_b species. The advantage of these measurements is in the sample size, which is usually larger than in the case of exclusively reconstructed H_b decays. Some of the main disadvantages are related to the difficulty of estimating the lepton+charm sample composition and to the Monte Carlo reliance for the momentum (and hence $\beta\gamma$ factor) estimate.
3. *Measurements in exclusively reconstructed hadronic decays*. These have the advantage of complete reconstruction of the decaying H_b state, which allows one to infer the decaying species as well as to perform precise measurement of the $\beta\gamma$ factor. Both lead to generally smaller systematic uncertainties than in the above two categories. The downsides are smaller branching ratios and larger combinatorial backgrounds, especially in $H_b \to H_c\pi(\pi\pi)$ and multi-body H_c decays, or in a hadron collider environment with non-trivial underlying event. Decays of the type $H_b \to J/\psi H_s$ are relatively clean and easy to trigger, due to the $J/\psi \to \ell^+\ell^-$ signature, but their branching fraction is only about 1%.
4. *Measurements at asymmetric B factories*. In the $\Upsilon(4S) \to B\bar{B}$ decay, the B mesons (B^+ or B^0) are essentially at rest in the $\Upsilon(4S)$ frame. This makes direct lifetime measurements impossible in experiments at symmetric colliders producing $\Upsilon(4S)$ at rest. At asymmetric B factories the $\Upsilon(4S)$ meson is boosted resulting in B and $\bar{B}$ moving nearly parallel to each other with the same boost. The lifetime is inferred from the distance Δz separating the B and $\bar{B}$ decay vertices along the beam axis and from the $\Upsilon(4S)$ boost known from the beam energies. This boost is equal to $\beta\gamma \approx 0.55$ (0.43) in the BaBar (Belle) experiment, resulting in an average B decay length of approximately 250 (190) μm.
   In order to determine the charge of the B mesons in each event, one of them is fully reconstructed in a semileptonic or hadronic decay mode. The other B is typically not fully reconstructed, only the position of its decay vertex is determined from the remaining tracks in the event. These measurements benefit from large sample sizes, but suffer from poor proper time resolution, comparable to the B lifetime itself. This resolution is dominated by the uncertainty on the decay vertices, which is typically 50 (100) μm for a fully (partially) reconstructed B meson. With much larger samples in the future, the resolution and purity could be improved (and hence the systematics reduced) by fully reconstructing both B mesons in the event.
5. *Direct measurement of lifetime ratios*. This method, initially applied in the measurement of $\tau(B^+)/\tau(B^0)$, is now also used for other b-hadron species at the LHC. The ratio of the lifetimes is extracted from the proper time dependence of the ratio of the observed yields of two different b-hadron species, both reconstructed in decay modes with similar topologies. The advantage of this method is that subtle efficiency effects (partially) cancel in the ratio.

In some of the latest analyses, measurements of two (e.g., $\tau(B^+)$ and $\tau(B^+)/\tau(B^0)$) or three (e.g. $\tau(B^+)$, $\tau(B^+)/\tau(B^0)$, and Δm_d) quantities are combined. This introduces correlations among measurements. Another source of correlations among the measurements are the systematic effects, which could be common to an experiment or to an analysis technique across the experiments. When calculating the averages, such known correlations are taken into account.

3.2.2 Inclusive b-hadron lifetimes

The inclusive b-hadron lifetime is defined as $\tau_b = \sum_i f_i\tau_i$ where τ_i are the individual species lifetimes and f_i are the fractions of the various species present in an unbiased sample of weakly decaying b hadrons produced at a high-energy

Table 6 Measurements of average b-hadron lifetimes

Experiment	Method	Data set	τ_b (ps)	Refs.
ALEPH	Dipole	91	$1.511 \pm 0.022 \pm 0.078$	[70]
DELPHI	All track i.p. (2D)	91–92	$1.542 \pm 0.021 \pm 0.045$	[71][a]
DELPHI	Sec. vtx	91–93	$1.582 \pm 0.011 \pm 0.027$	[72][a]
DELPHI	Sec. vtx	94–95	$1.570 \pm 0.005 \pm 0.008$	[73]
L3	Sec. vtx + i.p.	91–94	$1.556 \pm 0.010 \pm 0.017$	[74][b]
OPAL	Sec. vtx	91–94	$1.611 \pm 0.010 \pm 0.027$	[75]
SLD	Sec. vtx	93	$1.564 \pm 0.030 \pm 0.036$	[76]
Average set 1 (b vertex)			1.572 ± 0.009	
ALEPH	Lepton i.p. (3D)	91–93	$1.533 \pm 0.013 \pm 0.022$	[77]
L3	Lepton i.p. (2D)	91–94	$1.544 \pm 0.016 \pm 0.021$	[74][b]
OPAL	Lepton i.p. (2D)	90–91	$1.523 \pm 0.034 \pm 0.038$	[78]
Average set 2 ($b \to \ell$)			1.537 ± 0.020	
CDF1	J/ψ vtx	92–95	$1.533 \pm 0.015^{+0.035}_{-0.031}$	[79]
Average set 3 ($b \to J/\psi$)			1.533 ± 0.036	

[a] The combined DELPHI result quoted in [72] is $1.575 \pm 0.010 \pm 0.026$ ps
[b] The combined L3 result quoted in [74] is $1.549 \pm 0.009 \pm 0.015$ ps

collider.[12] This quantity is certainly less fundamental than the lifetimes of the individual species, the latter being much more useful in comparisons of the measurements with the theoretical predictions. Nonetheless, we perform the averaging of the inclusive lifetime measurements for completeness and because they might be of interest as "technical numbers."

In practice, an unbiased measurement of the inclusive lifetime is difficult to achieve, because it would imply an efficiency which is guaranteed to be the same across species. So most of the measurements are biased. In an attempt to group analyses that are expected to select the same mixture of b hadrons, the available results (given in Table 6) are divided into the following three sets:

1. measurements at LEP and SLD that include any b-hadron decay, based on topological reconstruction (secondary vertex or track impact parameters);
2. measurements at LEP based on the identification of a lepton from a b decay; and
3. measurements at hadron colliders based on inclusive $H_b \to J/\psi X$ reconstruction, where the J/ψ is fully reconstructed.

The measurements of the first set are generally considered as estimates of τ_b, although the efficiency to reconstruct a secondary vertex most probably depends, in an analysis-specific way, on the number of tracks coming from the vertex, thereby depending on the type of the H_b. Even though these efficiency variations can in principle be accounted for using Monte Carlo simulations (which inevitably contain assumptions on branching fractions), the H_b mixture in that case can remain somewhat ill-defined and could be slightly different among analyses in this set.

On the contrary, the mixtures corresponding to the other two sets of measurements are better defined in the limit where the reconstruction and selection efficiency of a lepton or a J/ψ from an H_b does not depend on the decaying hadron type. These mixtures are given by the production fractions and the inclusive branching fractions for each H_b species to give a lepton or a J/ψ. In particular, under the assumption that all b hadrons have the same semileptonic decay width, the analyses of the second set should measure $\tau(b \to \ell) = (\sum_i f_i \tau_i^3)/(\sum_i f_i \tau_i^2)$ which is necessarily larger than τ_b if lifetime differences exist. Given the present knowledge on τ_i and f_i, $\tau(b \to \ell) - \tau_b$ is expected to be of the order of 0.003 ps. On the other hand, the third set measuring $\tau(b \to J/\psi)$ is expected to give an average smaller than τ_b because of the B_c^+ meson, which has a significantly larger probability to decay to a J/ψ than other b-hadron species.

Measurements by SLC and LEP experiments are subject to a number of common systematic uncertainties, such as those due to (lack of knowledge of) b and c fragmentation, b and c decay models, $\mathcal{B}(B \to \ell)$, $\mathcal{B}(B \to c \to \ell)$, $\mathcal{B}(c \to \ell)$, τ_c, and H_b decay multiplicity. In the averaging, these systematic uncertainties are assumed to be 100% correlated. The averages for the sets defined above (also given in Table 6) are

$$\tau(b \text{ vertex}) = 1.572 \pm 0.009 \text{ ps}, \tag{33}$$

$$\tau(b \to \ell) = 1.537 \pm 0.020 \text{ ps}, \tag{34}$$

[12] In principle such a quantity could be slightly different in Z decays, at the Tevatron or at the LHC, in case the fractions of b-hadron species are not exactly the same; see the discussion in Sect. 3.1.3.

Table 7 Measurements of the B^0 lifetime

Experiment	Method	Data set	$\tau(B^0)$ (ps)	Refs.
ALEPH	$D^{(*)}\ell$	91–95	$1.518 \pm 0.053 \pm 0.034$	[80]
ALEPH	Exclusive	91–94	$1.25^{+0.15}_{-0.13} \pm 0.05$	[81]
ALEPH	Partial rec. $\pi^+\pi^-$	91–94	$1.49^{+0.17+0.08}_{-0.15-0.06}$	[81]
DELPHI	$D^{(*)}\ell$	91–93	$1.61^{+0.14}_{-0.13} \pm 0.08$	[82]
DELPHI	Charge sec. vtx	91–93	$1.63 \pm 0.14 \pm 0.13$	[83]
DELPHI	Inclusive $D^*\ell$	91–93	$1.532 \pm 0.041 \pm 0.040$	[84]
DELPHI	Charge sec. vtx	94–95	$1.531 \pm 0.021 \pm 0.031$	[73]
L3	Charge sec. vtx	94–95	$1.52 \pm 0.06 \pm 0.04$	[85]
OPAL	$D^{(*)}\ell$	91–93	$1.53 \pm 0.12 \pm 0.08$	[86]
OPAL	Charge sec. vtx	93–95	$1.523 \pm 0.057 \pm 0.053$	[87]
OPAL	Inclusive $D^*\ell$	91–00	$1.541 \pm 0.028 \pm 0.023$	[88]
SLD	Charge sec. vtx ℓ	93–95	$1.56^{+0.14}_{-0.13} \pm 0.10$	[89][a]
SLD	Charge sec. vtx	93–95	$1.66 \pm 0.08 \pm 0.08$	[89][a]
CDF1	$D^{(*)}\ell$	92–95	$1.474 \pm 0.039^{+0.052}_{-0.051}$	[90]
CDF1	Excl. $J/\psi K^{*0}$	92–95	$1.497 \pm 0.073 \pm 0.032$	[91]
CDF2	Excl. $J/\psi K^0_S$, $J/\psi K^{*0}$	02–09	$1.507 \pm 0.010 \pm 0.008$	[92]
D0	Excl. $J/\psi K^{*0}$	03–07	$1.414 \pm 0.018 \pm 0.034$	[93]
D0	Excl. $J/\psi K^0_S$	02–11	$1.508 \pm 0.025 \pm 0.043$	[94]
D0	Inclusive $D^-\mu^+$	02–11	$1.534 \pm 0.019 \pm 0.021$	[95]
BaBar	Exclusive	99–00	$1.546 \pm 0.032 \pm 0.022$	[96]
BaBar	Inclusive $D^*\ell$	99–01	$1.529 \pm 0.012 \pm 0.029$	[97]
BaBar	Exclusive $D^*\ell$	99–02	$1.523^{+0.024}_{-0.023} \pm 0.022$	[98]
BaBar	Incl. $D^*\pi$, $D^*\rho$	99–01	$1.533 \pm 0.034 \pm 0.038$	[99]
BaBar	Inclusive $D^*\ell$	99–04	$1.504 \pm 0.013^{+0.018}_{-0.013}$	[100]
Belle	Exclusive	00–03	$1.534 \pm 0.008 \pm 0.010$	[101]
ATLAS	Excl. $J/\psi K^0_S$	2011	$1.509 \pm 0.012 \pm 0.018$	[102]
LHCb	Excl. $J/\psi K^{*0}$	2011	$1.524 \pm 0.006 \pm 0.004$	[103]
LHCb	Excl. $J/\psi K^0_S$	2011	$1.499 \pm 0.013 \pm 0.005$	[103]
LHCb	$K^+\pi^-$	2011	$1.524 \pm 0.011 \pm 0.004$	[104]
Average			1.520 ± 0.004	

[a] The combined SLD result quoted in [89] is $1.64 \pm 0.08 \pm 0.08$ ps

$$\tau(b \to J/\psi) = 1.533 \pm 0.036 \text{ ps}. \tag{35}$$

The differences between these averages are consistent both with zero and with expectations within less than 2σ.

3.2.3 B^0 and B^+ lifetimes and their ratio

After a number of years of dominating these averages the LEP experiments yielded the scene to the asymmetric B factories and the Tevatron experiments. The B factories have been very successful in utilizing their potential – in only a few years of running, BaBar and, to a greater extent, Belle, have struck a balance between the statistical and the systematic uncertainties, with both being close to (or even better than) an impressive 1% level. In the meanwhile, CDF and D0 have emerged as significant contributors to the field as the Tevatron Run II data flowed in. Recently, the LHCb experiment reached a further step in precision, improving by a factor ∼2 over the previous best measurements.

At the present time we are in an interesting position of having three sets of measurements (from LEP/SLC, B factories and Tevatron/LHC) that originate from different environments, are obtained using substantially different techniques and are precise enough for incisive comparison.

The averaging of $\tau(B^+)$, $\tau(B^0)$ and $\tau(B^+)/\tau(B^0)$ measurements is summarized in Tables 7, 8, and 9. For $\tau(B^+)/\tau(B^0)$ we average only the measurements of this quantity provided by experiments rather than using all available knowledge, which would have included, for example, $\tau(B^+)$

Table 8 Measurements of the B^+ lifetime

Experiment	Method	Data set	$\tau(B^+)$ (ps)	Refs.
ALEPH	$D^{(*)}\ell$	91–95	$1.648 \pm 0.049 \pm 0.035$	[80]
ALEPH	Exclusive	91–94	$1.58^{+0.21+0.04}_{-0.18-0.03}$	[81]
DELPHI	$D^{(*)}\ell$	91–93	$1.61 \pm 0.16 \pm 0.12$	[82][a]
DELPHI	Charge sec. vtx	91–93	$1.72 \pm 0.08 \pm 0.06$	[83][a]
DELPHI	Charge sec. vtx	94–95	$1.624 \pm 0.014 \pm 0.018$	[73]
L3	Charge sec. vtx	94–95	$1.66 \pm 0.06 \pm 0.03$	[85]
OPAL	$D^{(*)}\ell$	91–93	$1.52 \pm 0.14 \pm 0.09$	[86]
OPAL	Charge sec. vtx	93–95	$1.643 \pm 0.037 \pm 0.025$	[87]
SLD	Charge sec. vtx ℓ	93–95	$1.61^{+0.13}_{-0.12} \pm 0.07$	[89][b]
SLD	Charge sec. vtx	93–95	$1.67 \pm 0.07 \pm 0.06$	[89][b]
CDF1	$D^{(*)}\ell$	92–95	$1.637 \pm 0.058^{+0.045}_{-0.043}$	[90]
CDF1	Excl. $J/\psi K$	92–95	$1.636 \pm 0.058 \pm 0.025$	[91]
CDF2	Excl. $J/\psi K$	02–09	$1.639 \pm 0.009 \pm 0.009$	[92]
CDF2	Excl. $D^0\pi$	02–06	$1.663 \pm 0.023 \pm 0.015$	[105]
BaBar	Exclusive	99–00	$1.673 \pm 0.032 \pm 0.023$	[96]
Belle	Exclusive	00–03	$1.635 \pm 0.011 \pm 0.011$	[101]
LHCb	Excl. $J/\psi K$	2011	$1.637 \pm 0.004 \pm 0.003$	[103]
Average			1.638 ± 0.004	

[a] The combined DELPHI result quoted in [83] is 1.70 ± 0.09 ps
[b] The combined SLD result quoted in [89] is $1.66 \pm 0.06 \pm 0.05$ ps

Table 9 Measurements of the ratio $\tau(B^+)/\tau(B^0)$

Experiment	Method	Data set	Ratio $\tau(B^+)/\tau(B^0)$	Refs.
ALEPH	$D^{(*)}\ell$	91–95	$1.085 \pm 0.059 \pm 0.018$	[80]
ALEPH	Exclusive	91–94	$1.27^{+0.23+0.03}_{-0.19-0.02}$	[81]
DELPHI	$D^{(*)}\ell$	91–93	$1.00^{+0.17}_{-0.15} \pm 0.10$	[82]
DELPHI	Charge sec. vtx	91–93	$1.06^{+0.13}_{-0.11} \pm 0.10$	[83]
DELPHI	Charge sec. vtx	94–95	$1.060 \pm 0.021 \pm 0.024$	[73]
L3	Charge sec. vtx	94–95	$1.09 \pm 0.07 \pm 0.03$	[85]
OPAL	$D^{(*)}\ell$	91–93	$0.99 \pm 0.14^{+0.05}_{-0.04}$	[86]
OPAL	Charge sec. vtx	93–95	$1.079 \pm 0.064 \pm 0.041$	[87]
SLD	Charge sec. vtx ℓ	93–95	$1.03^{+0.16}_{-0.14} \pm 0.09$	[89][a]
SLD	Charge sec. vtx	93–95	$1.01^{+0.09}_{-0.08} \pm 0.05$	[89][a]
CDF1	$D^{(*)}\ell$	92–95	$1.110 \pm 0.056^{+0.033}_{-0.030}$	[90]
CDF1	Excl. $J/\psi K$	92–95	$1.093 \pm 0.066 \pm 0.028$	[91]
CDF2	Excl. $J/\psi K^{(*)}$	02–09	$1.088 \pm 0.009 \pm 0.004$	[92]
D0	$D^{*+}\mu$ $D^0\mu$ ratio	02–04	$1.080 \pm 0.016 \pm 0.014$	[106]
BaBar	Exclusive	99–00	$1.082 \pm 0.026 \pm 0.012$	[96]
Belle	Exclusive	00–03	$1.066 \pm 0.008 \pm 0.008$	[101]
LHCb	Excl. $J/\psi K^{(*)}$	2011	$1.074 \pm 0.005 \pm 0.003$	[103]
Average			1.076 ± 0.004	

[a] The combined SLD result quoted in [89] is $1.01 \pm 0.07 \pm 0.06$

and $\tau(B^0)$ measurements which did not contribute to any of the ratio measurements.

The following sources of correlated (within experiment/machine) systematic uncertainties have been considered:

- for SLC/LEP measurements – D^{**} branching ratio uncertainties [3], momentum estimation of b mesons from Z^0 decays (b-quark fragmentation parameter $\langle X_E \rangle = 0.702 \pm 0.008$ [3]), B_s^0 and b-baryon lifetimes (see Sects. 3.2.4, 3.2.6), and b-hadron fractions at high energy (see Table 5);
- for B-factory measurements – alignment, z scale, machine boost, sample composition (where applicable);
- for Tevatron/LHC measurements – alignment (separately within each experiment).

The resultant averages are:

$$\tau(B^0) = 1.520 \pm 0.004 \text{ ps}, \tag{36}$$

$$\tau(B^+) = 1.638 \pm 0.004 \text{ ps}, \tag{37}$$

$$\tau(B^+)/\tau(B^0) = 1.076 \pm 0.004. \tag{38}$$

3.2.4 B_s^0 lifetimes

Like neutral kaons, neutral B mesons contain short- and long-lived components, since the light (L) and heavy (H) eigenstates differ not only in their masses, but also in their total decay widths. Neglecting CP violation in $B_s^0 - \bar{B}_s^0$ mixing, which is expected to be very small [60,107–110] (see also Sect. 3.3.3), the mass eigenstates are also CP eigenstates, with the light state being CP-even and the heavy state being CP-odd. While the decay width difference $\Delta\Gamma_d$ can be neglected in the B^0 system, the B_s^0 system exhibits a significant value of $\Delta\Gamma_s = \Gamma_{s\mathrm{L}} - \Gamma_{s\mathrm{H}}$, where $\Gamma_{s\mathrm{L}}$ and $\Gamma_{s\mathrm{H}}$ are the total decay widths of the light eigenstate $B_{s\mathrm{L}}^0$ and the heavy eigenstate $B_{s\mathrm{H}}^0$, respectively. The sign of $\Delta\Gamma_s$ is known to be positive [111], i.e., $B_{s\mathrm{H}}^0$ lives longer than $B_{s\mathrm{L}}^0$. Specific measurements of $\Delta\Gamma_s$ and $\Gamma_s = (\Gamma_{s\mathrm{L}} + \Gamma_{s\mathrm{H}})/2$ are explained and averaged in Sect. 3.3.2, but the results for $1/\Gamma_{s\mathrm{L}} = 1/(\Gamma_s + \Delta\Gamma_s/2)$, $1/\Gamma_{s\mathrm{H}} = 1/(\Gamma_s - \Delta\Gamma_s/2)$ and the mean B_s^0 lifetime, defined as $\tau(B_s^0) = 1/\Gamma_s$, are also quoted at the end of this section.

Many B_s^0 lifetime analyses, in particular the early ones performed before the non-zero value of $\Delta\Gamma_s$ was firmly established, ignore $\Delta\Gamma_s$ and fit the proper time distribution of a sample of B_s^0 candidates reconstructed in a certain final state f with a model assuming a single exponential function for the signal. We denote such effective lifetime measurements [112] as $\tau_{\mathrm{single}}(B_s^0 \to f)$; their true values may lie *a priori* anywhere between $1/\Gamma_{s\mathrm{L}}$ and $1/\Gamma_{s,\mathrm{H}}$, depending on the proportion of $B_{s\mathrm{L}}^0$ and $B_{s\mathrm{H}}^0$ in the final state f. More recent determinations of effective lifetimes may be interpreted as measurements of the relative composition of $B_{s\mathrm{L}}^0$ and $B_{s\mathrm{H}}^0$ decaying to the final state f. Table 10 summarizes the effective lifetime measurements.

Averaging measurements of $\tau_{\mathrm{single}}(B_s^0 \to f)$ over several final states f will yield a result corresponding to an ill-defined observable when the proportions of $B_{s\mathrm{L}}^0$ and $B_{s\mathrm{H}}^0$ differ. Therefore, the effective B_s^0 lifetime measurements are broken down into several categories and averaged separately.

- $B_s^0 \to D_s^{\mp} X$ *decays* include mostly flavour-specific decays but also decays with an unknown mixture of light and heavy components. Measurements performed with such inclusive states are no longer used in averages.
- *Decays to flavour-specific final states*, i.e., decays to final states f with decay amplitudes satisfying $A(B_s^0 \to f) \neq 0$, $A(\bar{B}_s^0 \to \bar{f}) \neq 0$, $A(B_s^0 \to \bar{f}) = 0$ and $A(\bar{B}_s^0 \to f) = 0$, have equal fractions of $B_{s\mathrm{L}}^0$ and $B_{s\mathrm{H}}^0$ at time zero. Their total untagged time-dependent decay rates $\Gamma_s(t)$ have a mean value $\int_0^\infty t\Gamma_s(t)dt / \int_0^\infty \Gamma_s(t)dt$, called the *flavour-specific lifetime*, equal to [131]

$$\tau_{\mathrm{single}}(B_s^0 \to \text{flavour specific}) = \frac{1/\Gamma_{s\mathrm{L}}^2 + 1/\Gamma_{s\mathrm{H}}^2}{1/\Gamma_{s\mathrm{L}} + 1/\Gamma_{s\mathrm{H}}} = \frac{1}{\Gamma_s} \frac{1 + \left(\frac{\Delta\Gamma_s}{2\Gamma_s}\right)^2}{1 - \left(\frac{\Delta\Gamma_s}{2\Gamma_s}\right)^2}. \tag{39}$$

Because of the fast $B_s^0 - \bar{B}_s^0$ oscillations, possible biases of the flavour-specific lifetime due to a combination of $B_s^0/\bar{B}_s^0$ production asymmetry, CP violation in the decay amplitudes ($|A(B_s^0 \to f)| \neq |A(\bar{B}_s^0 \to \bar{f})|$), and CP violation in $B_s^0 - \bar{B}_s^0$ mixing ($|q_s/p_s| \neq 1$) are strongly suppressed, by a factor $\sim x_s^2$ (given in Eq. (75)). The $B_s^0/\bar{B}_s^0$ production asymmetry at LHCb and the CP asymmetry due to mixing have been measured to be compatible with zero with a precision below 3% [132] and 0.3% [see Eq. (83)], respectively. The corresponding effects on the flavour-specific lifetime, which therefore have a relative size of the order of 10^{-5} or smaller, can be neglected at the current level of experimental precision. Under the assumption of no production asymmetry and no CP violation in mixing, Eq. (39) is exact even for a flavour-specific decay with CP violation in the decay amplitudes. Hence any flavour-specific decay mode can be used to measure the flavour-specific lifetime.

The average of all flavour-specific B_s^0 lifetime measurements [95,104,116–122] is

$$\tau_{\mathrm{single}}(B_s^0 \to \text{flavour specific}) = 1.516 \pm 0.014 \text{ ps}. \tag{40}$$

Table 10 Measurements of the effective B_s^0 lifetimes obtained from single exponential fits

Experiment	Final state f		Data set		$\tau_{\text{single}}(B_s^0 \to f)$ (ps)	Refs.
ALEPH	$D_s h$	Ill-defined	91–95		$1.47 \pm 0.14 \pm 0.08$	[113]
DELPHI	$D_s h$	Ill-defined	91–95		$1.53^{+0.16}_{-0.15} \pm 0.07$	[114]
OPAL	D_s incl.	Ill-defined	90–95		$1.72^{+0.20+0.18}_{-0.19-0.17}$	[115]
ALEPH	$D_s^- \ell^+$	Flavour-specific	91–95		$1.54^{+0.14}_{-0.13} \pm 0.04$	[116]
CDF1	$D_s^- \ell^+$	Flavour-specific	92–96		$1.36 \pm 0.09^{+0.06}_{-0.05}$	[117]
DELPHI	$D_s^- \ell^+$	Flavour-specific	92–95		$1.42^{+0.14}_{-0.13} \pm 0.03$	[118]
OPAL	$D_s^- \ell^+$	Flavour-specific	90–95		$1.50^{+0.16}_{-0.15} \pm 0.04$	[119]
D0	$D_s^- \mu^+ X$	Flavour-specific	Run II	10.4 fb^{-1}	$1.479 \pm 0.010 \pm 0.021$	[95]
CDF2	$D_s^- \pi^+(X)$	Flavour-specific	02–06	1.3 fb^{-1}	$1.518 \pm 0.041 \pm 0.027$	[120]
LHCb	$D_s^- D^+$	Flavour-specific	11–12	3 fb^{-1}	$1.52 \pm 0.15 \pm 0.01$	[121]
LHCb	$D_s^- \pi^+$	Flavour-specific	11	1 fb^{-1}	$1.535 \pm 0.015 \pm 0.014$	[122]
LHCb	$\pi^+ K^-$	Flavour-specific	11	1.0 fb^{-1}	$1.60 \pm 0.06 \pm 0.01$	[104]
Average of above 9 Flavour-specific lifetime measurements					1.516 ± 0.014	
CDF1	$J/\psi\phi$	CP even+odd	92–95		$1.34^{+0.23}_{-0.19} \pm 0.05$	[79]
D0	$J/\psi\phi$	CP even+odd	02–04		$1.444^{+0.098}_{-0.090} \pm 0.02$	[123]
LHCb	$J/\psi\phi$	CP even+odd	11	1 fb^{-1}	$1.480 \pm 0.011 \pm 0.005$	[103]
Average of above 3 $J/\psi\phi$ lifetime measurements					1.479 ± 0.012	
ALEPH	$D_s^{(*)+} D_s^{(*)-}$	mostly CP even	91–95		$1.27 \pm 0.33 \pm 0.08$	[124]
LHCb	K^+K^-	CP-even	10	0.037 fb^{-1}	$1.440 \pm 0.096 \pm 0.009$	[125]
LHCb	K^+K^-	CP-even	11	1.0 fb^{-1}	$1.407 \pm 0.016 \pm 0.007$	[104]
Average of above 2 K^+K^- lifetime measurements					1.408 ± 0.017	
LHCb	$D_s^+ D_s^-$	CP-even	11–12	3 fb^{-1}	$1.379 \pm 0.026 \pm 0.017$	[121]
LHCb	$J/\psi\eta$	CP-even	11–12	3 fb^{-1}	$1.479 \pm 0.034 \pm 0.011$	[126]
Average of above 2 measurements of $1/\Gamma_{s\text{L}}$					1.422 ± 0.023	
LHCb	$J/\psi K_S^0$	CP-odd	11	1.0 fb^{-1}	$1.75 \pm 0.12 \pm 0.07$	[127]
CDF2	$J/\psi f_0(980)$	CP-odd	02–08	3.8 fb^{-1}	$1.70^{+0.12}_{-0.11} \pm 0.03$	[128]
D0	$J/\psi f_0(980)$	CP-odd	Run II	10.4 fb^{-1}	$1.70 \pm 0.14 \pm 0.05$	[129]
LHCb	$J/\psi\pi^+\pi^-$	CP-odd	11	1.0 fb^{-1}	$1.652 \pm 0.024 \pm 0.024$	[130]
Average of above 3 measurements of $1/\Gamma_{s\text{H}}$					1.658 ± 0.032	

- $B_s^0 \to J/\psi\phi$ decays contain a well-measured mixture of CP-even and CP-odd states. There are no known correlations between the existing $B_s^0 \to J/\psi\phi$ effective lifetime measurements; these are combined into the average $\tau_{\text{single}}(B_s^0 \to J/\psi\phi) = 1.479 \pm 0.012$ ps. A caveat is that different experimental acceptances may lead to different admixtures of the CP-even and CP-odd states, and simple fits to a single exponential may result in inherently different values of $\tau_{\text{single}}(B_s^0 \to J/\psi\phi)$. Analyses that separate the CP-even and CP-odd components in this decay through a full angular study, outlined in Sect. 3.3.2, provide directly precise measurements of $1/\Gamma_s$ and $\Delta\Gamma_s$ (see Table 21).
- Decays to CP eigenstates have also been measured, in the CP-even modes $B_s^0 \to D_s^{(*)+} D_s^{(*)-}$ by ALEPH [124], $B_s^0 \to K^+K^-$ by LHCb [104,125], $B_s^0 \to D_s^+ D_s^-$ by LHCb [121] and $B_s^0 \to J/\psi\eta$ by LHCb [126], as well as in the CP-odd modes $B_s^0 \to J/\psi f_0(980)$ by CDF [128] and D0 [129], $B_s^0 \to J/\psi\pi^+\pi^-$ by LHCb [130] and $B_s^0 \to J/\psi K_S^0$ by LHCb [127]. If these decays are dominated by a single weak phase and if CP violation can be neglected, then $\tau_{\text{single}}(B_s^0 \to CP\text{-even}) = 1/\Gamma_{s\text{L}}$ and $\tau_{\text{single}}(B_s^0 \to CP\text{-odd}) = 1/\Gamma_{s\text{H}}$ [see Eqs. (70) and (71) for approximate relations in presence of mixing-induced CP violation]. However, not all these modes can be considered as pure CP eigenstates: a small CP-odd component is most probably present in $B_s^0 \to D_s^{(*)+} D_s^{(*)-}$ decays. Furthermore the decays $B_s^0 \to K^+K^-$ and $B_s^0 \to J/\psi K_S^0$ may suffer from direct CP violation due to interfering tree and loop amplitudes. The averages for the effective lifetimes obtained for decays to pure CP-even ($D_s^+ D_s^-$, $J/\psi\eta$) and CP-odd ($J/\psi f_0(980)$,

Table 11 Measurements of the B_c^+ lifetime

Experiment	Method	Data set		$\tau(B_c^+)$ (ps)	Refs.
CDF1	$J/\psi\ell$	92–95	0.11 fb^{-1}	$0.46^{+0.18}_{-0.16} \pm 0.03$	[133]
CDF2	$J/\psi e$	02–04	0.36 fb^{-1}	$0.463^{+0.073}_{-0.065} \pm 0.036$	[134]
D0	$J/\psi\mu$	02–06	1.3 fb^{-1}	$0.448^{+0.038}_{-0.036} \pm 0.032$	[135]
CDF2	$J/\psi\pi$		6.7 fb^{-1}	$0.452 \pm 0.048 \pm 0.027$	[136]
LHCb	$J/\psi\mu$	12	2 fb^{-1}	$0.509 \pm 0.008 \pm 0.012$	[137]
LHCb	$J/\psi\pi$	11–12	3 fb^{-1}	$0.5134 \pm 0.0110 \pm 0.0057$	[138]
Average				0.507 ± 0.009	

$J/\psi\pi^+\pi^-$) final states, where CP conservation can be assumed, are

$$\tau_{\text{single}}(B_s^0 \to CP\text{-even}) = 1.422 \pm 0.023 \text{ ps}, \quad (41)$$

$$\tau_{\text{single}}(B_s^0 \to CP\text{-odd}) = 1.658 \pm 0.032 \text{ ps}. \quad (42)$$

As described in Sect. 3.3.2, the effective lifetime averages of Eqs. (40), (41) and (42) are used as ingredients to improve the determination of $1/\Gamma_s$ and $\Delta\Gamma_s$ obtained from the full angular analyses of $B_s^0 \to J/\psi\phi$ and $B_s^0 \to J/\psi K^+K^-$ decays. The resulting world averages for the B_s^0 lifetimes are

$$\tau(B_{s\text{L}}^0) = \frac{1}{\Gamma_{s\text{L}}} = \frac{1}{\Gamma_s + \Delta\Gamma_s/2} = 1.413 \pm 0.006 \text{ ps}, \quad (43)$$

$$\tau(B_{s\text{H}}^0) = \frac{1}{\Gamma_{s\text{H}}} = \frac{1}{\Gamma_s - \Delta\Gamma_s/2} = 1.609 \pm 0.010 \text{ ps}, \quad (44)$$

$$\tau(B_s^0) = \frac{1}{\Gamma_s} = \frac{2}{\Gamma_{s\text{L}} + \Gamma_{s\text{H}}} = 1.505 \pm 0.005 \text{ ps}. \quad (45)$$

3.2.5 B_c^+ lifetime

Early measurements of the B_c^+ meson lifetime, from CDF [133,134] and D0 [135], use the semileptonic decay mode $B_c^+ \to J/\psi\ell^+\nu$ and are based on a simultaneous fit to the mass and lifetime using the vertex formed with the leptons from the decay of the J/ψ and the third lepton. Correction factors to estimate the boost due to the missing neutrino are used. Correlated systematic errors include the impact of the uncertainty of the B_c^+ p_T spectrum on the correction factors, the level of feed-down from $\psi(2S)$ decays, Monte Carlo modeling of the decay model varying from phase space to the ISGW model, and mass variations. With more statistics, CDF2 was able to perform the first B_c^+ lifetime based on fully reconstructed $B_c^+ \to J/\psi\pi^+$ decays [136], which does not suffer from a missing neutrino. Recent measurements from LHCb, both with $B_c^+ \to J/\psi\mu^+\nu$ [137] and $B_c^+ \to J/\psi\pi^+$ [138] decays, achieve the highest level of precision.

All the measurements are summarized in Table 11 and the world average, dominated by the LHCb measurements, is determined to be

$$\tau(B_c^+) = 0.507 \pm 0.009 \text{ ps}. \quad (46)$$

3.2.6 Λ_b^0 and b-baryon lifetimes

The first measurements of b-baryon lifetimes, performed at LEP, originate from two classes of partially reconstructed decays. In the first class, decays with an exclusively reconstructed Λ_c^+ baryon and a lepton of opposite charge are used. These products are more likely to occur in the decay of Λ_b^0 baryons. In the second class, more inclusive final states with a baryon (p, $\bar{p}$, Λ, or $\bar{\Lambda}$) and a lepton have been used, and these final states can generally arise from any b baryon. With the large b-hadron samples available at the Tevatron and the LHC, the most precise measurements of b baryons now come from fully reconstructed exclusive decays.

The following sources of correlated systematic uncertainties have been considered: experimental time resolution within a given experiment, b-quark fragmentation distribution into weakly decaying b baryons, Λ_b^0 polarisation, decay model, and evaluation of the b-baryon purity in the selected event samples. In computing the averages the central values of the masses are scaled to $M(\Lambda_b^0) = 5619.51 \pm 0.23$ MeV/c^2 [6].

For measurements with partially reconstructed decays, the meaning of the decay model systematic uncertainties and the correlation of these uncertainties between measurements are not always clear. Uncertainties related to the decay model are dominated by assumptions on the fraction of n-body semileptonic decays. To be conservative, it is assumed that these are 100% correlated whenever given as an error. DELPHI varies the fraction of four-body decays from 0.0 to 0.3. In computing the average, the DELPHI result is corrected to a value of 0.2 ± 0.2 for this fraction. Furthermore the semileptonic decay results from LEP are corrected for a Λ_b^0 polar-

Table 12 Measurements of the b-baryon lifetimes

Experiment	Method	Data set	Lifetime (ps)	Refs.
ALEPH	$\Lambda\ell$	91–95	$1.20 \pm 0.08 \pm 0.06$	[34]
DELPHI	$\Lambda\ell\pi$ vtx	91–94	$1.16 \pm 0.20 \pm 0.08$	[139][b]
DELPHI	$\Lambda\mu$ i.p.	91–94	$1.10^{+0.19}_{-0.17} \pm 0.09$	[140][b]
DELPHI	$p\ell$	91–94	$1.19 \pm 0.14 \pm 0.07$	[139][b]
OPAL	$\Lambda\ell$ i.p.	90–94	$1.21^{+0.15}_{-0.13} \pm 0.10$	[141][c]
OPAL	$\Lambda\ell$ vtx	90–94	$1.15 \pm 0.12 \pm 0.06$	[141][c]
ALEPH	$\Lambda_c^+\ell$	91–95	$1.18^{+0.13}_{-0.12} \pm 0.03$	[34][a]
ALEPH	$\Lambda\ell^-\ell^+$	91–95	$1.30^{+0.26}_{-0.21} \pm 0.04$	[34][a]
DELPHI	$\Lambda_c^+\ell$	91–94	$1.11^{+0.19}_{-0.18} \pm 0.05$	[139][b]
OPAL	$\Lambda_c^+\ell$, $\Lambda\ell^-\ell^+$	90–95	$1.29^{+0.24}_{-0.22} \pm 0.06$	[119]
CDF1	$\Lambda_c^+\ell$	91–95	$1.32 \pm 0.15 \pm 0.07$	[142]
D0	$\Lambda_c^+\mu$	02–06	$1.290^{+0.119+0.087}_{-0.110-0.091}$	[143]
Average of above 6			$1.247^{+0.071-0.069}$	
CDF2	$\Lambda_c^+\pi$	02–06	$1.401 \pm 0.046 \pm 0.035$	[144]
CDF2	$J/\psi\Lambda$	02–11	$1.565 \pm 0.035 \pm 0.020$	[145]
D0	$J/\psi\Lambda$	02–11	$1.303 \pm 0.075 \pm 0.035$	[94]
ATLAS	$J/\psi\Lambda$	2011	$1.449 \pm 0.036 \pm 0.017$	[102]
CMS	$J/\psi\Lambda$	2011	$1.503 \pm 0.052 \pm 0.031$	[146]
LHCb	$J/\psi\Lambda$	2011	$1.415 \pm 0.027 \pm 0.006$	[103]
LHCb	$J/\psi pK$ (w.r.t. B^0)	11–12	$1.479 \pm 0.009 \pm 0.010$	[147]
Average of above 7			Λ_b^0 lifetime $= 1.470 \pm 0.010$	
ALEPH	$\Xi^-\ell^-X$	90–95	$1.35^{+0.37+0.15}_{-0.28-0.17}$	[35]
DELPHI	$\Xi^-\ell^-X$	91–93	$1.5^{+0.7}_{-0.4} \pm 0.3$	[148][d]
DELPHI	$\Xi^-\ell^-X$	92–95	$1.45^{+0.55}_{-0.43} \pm 0.13$	[36][d]
CDF2	$J/\psi\Xi^-$	02–11	$1.32 \pm 0.14 \pm 0.02$	[145]
LHCb	$J/\psi\Xi^-$	11–12	$1.55^{+0.10}_{-0.09} \pm 0.03$	[149]
LHCb	$\Xi_c^0\pi^-$ (w.r.t. Λ_b^0)	11–12	$1.599 \pm 0.041 \pm 0.022$	[150]
Average of above 3			Ξ_b^- lifetime $= 1.571 \pm 0.040$	
LHCb	$\Xi_c^+\pi^-$ (w.r.t. Λ_b^0)	11–12	$1.477 \pm 0.026 \pm 0.019$	[151]
Average of above 1			Ξ_b^0 lifetime $= 1.479 \pm 0.031$	
CDF2	$J/\psi\Omega^-$	02–11	$1.66^{+0.53}_{-0.40} \pm 0.02$	[145]
LHCb	$J/\psi\Omega^-$	11–12	$1.54^{+0.26}_{-0.21} \pm 0.05$	[149]
LHCb	$\Omega_c^0\pi^-$ (w.r.t. Ξ_b^-)	11–12	$1.78 \pm 0.26 \pm 0.05 \pm 0.06$	[152]
Average of above 3			Ω_b^- lifetime $= 1.64^{+0.18}_{-0.17}$	

[a] The combined ALEPH result quoted in [34] is 1.21 ± 0.11 ps
[b] The combined DELPHI result quoted in [139] is $1.14 \pm 0.08 \pm 0.04$ ps
[c] The combined OPAL result quoted in [141] is $1.16 \pm 0.11 \pm 0.06$ ps
[d] The combined DELPHI result quoted in [36] is $1.48^{+0.40}_{-0.31} \pm 0.12$ ps

isation of $-0.45^{+0.19}_{-0.17}$ [3] and a b fragmentation parameter $\langle x_E \rangle_b = 0.702 \pm 0.008$ [51].

The list of all measurements are given in Table 12. We do not attempt to average measurements performed with $p\ell$ or $\Lambda\ell$ correlations, which select unknown mixtures of b baryons. Measurements performed with $\Lambda_c^+\ell$ or $\Lambda\ell^+\ell^-$ correlations can be assumed to correspond to semileptonic Λ_b^0 decays. Their average ($1.247^{+0.071}_{0.069}$ ps)) is significantly different from the average using only measurements performed with exclusively reconstructed hadronic Λ_b^0 decays (1.470 ± 0.010 ps). The latter is much more precise and less prone to potential biases than the former. The discrepancy between the two averages is at the level of $3.1\,\sigma$ and assumed to be due to an experimental systematic effect in

the semileptonic measurements or to a rare statistical fluctuation. The best estimate of the Λ_b^0 lifetime is therefore taken as the average of the exclusive measurements only. The CDF $\Lambda_b^0 \to J/\psi\Lambda$ lifetime result [145] is larger than the average of all other exclusive measurements by $2.4\,\sigma$. It is nonetheless kept in the average without adjustment of input errors. The world average Λ_b^0 lifetime is then

$$\tau(\Lambda_b^0) = 1.470 \pm 0.010 \text{ ps}. \tag{47}$$

For the strange b baryons, we do not include the measurements based on inclusive $\Xi^{\mp}\ell^{\mp}$ [35,36,148] final states, which consist of a mixture of Ξ_b^- and Ξ_b^0 baryons. Instead we only average results obtained with fully reconstructed Ξ_b^-, Ξ_b^0 and Ω_b^- baryons, and obtain

$$\tau(\Xi_b^-) = 1.571 \pm 0.040 \text{ ps}, \tag{48}$$

$$\tau(\Xi_b^0) = 1.479 \pm 0.031 \text{ ps}, \tag{49}$$

$$\tau(\Omega_b^-) = 1.64^{+0.18}_{-0.17} \text{ ps}. \tag{50}$$

It should be noted that several b-baryon lifetime measurements from LHCb [147,150–152] were made with respect to the lifetime of another b hadron (i.e., the original measurement is that of a decay width difference). Before these measurements are included in the averages quoted above, we rescale them according to our latest lifetime average of that reference b hadron. This introduces correlations between our averages, in particular between the Ξ_b^- and Ξ_b^0 lifetimes. Taking this correlation into account leads to

$$\tau(\Xi_b^0)/\tau(\Xi_b^-) = 0.929 \pm 0.028. \tag{51}$$

3.2.7 *Summary and comparison with theoretical predictions*

Averages of lifetimes of specific b-hadron species are collected in Table 13. As described in the introduction to Sect. 3.2, the HQE can be employed to explain the hierarchy of $\tau(B_c^+) \ll \tau(\Lambda_b^0) < \tau(B_s^0) \approx \tau(B^0) < \tau(B^+)$, and used to predict the ratios between lifetimes. Recent predictions are compared to the measured lifetime ratios in Table 14.

The predictions of the ratio between the B^+ and B^0 lifetimes, 1.06 ± 0.02 [65,66] or $1.04^{+0.05}_{-0.01} \pm 0.02 \pm 0.01$ [68,69], are in good agreement with experiment.

The total widths of the B_s^0 and B^0 mesons are expected to be very close and differ by at most 1% [67–69,153,154]. This prediction is consistent with the experimental ratio $\tau(B_s^0)/\tau(B^0) = \Gamma_d/\Gamma_s$, which is smaller than 1 by $(1.0 \pm 0.4)\%$. The authors of Refs. [60,107] predict $\tau(B_s^0)/\tau(B^0) = 1.00050 \pm 0.00108 \pm 0.0225 \times \delta$, where δ quantifies a possible breaking of the quark-hadron duality. In this context, they interpret the 2.5σ difference between theory and experiment as being due to either new physics or a sizable duality violation. The key message is that improved experimental precision on this ratio is very welcome.

The ratio $\tau(\Lambda_b^0)/\tau(B^0)$ has particularly been the source of theoretical scrutiny since earlier calculations using the HQE [55–57,155] predicted a value larger than 0.90, almost $2\,\sigma$ above the world average at the time. Many predictions cluster around a most likely central value of 0.94 [159]. Calculations of this ratio that include higher-order effects predict a lower ratio between the Λ_b^0 and B^0 lifetimes [65–67] and reduce this difference. Since then the experimental average is now definitely settling at a value significantly larger than initially, in agreement with the latest theoretical predictions. A recent review [68,69] concludes that the long-standing Λ_b^0 lifetime puzzle is resolved, with a nice agreement between the precise experimental determination of $\tau(\Lambda_b^0)/\tau(B^0)$ and the less precise HQE prediction which needs new lattice calculations. There is also good agreement for the $\tau(\Xi_b^0)/\tau(\Xi_b^-)$ ratio.

The lifetimes of the most abundant b-hadron species are now all known to sub-percent precision. Neglecting the contributions of the rarer species (B_c^+ meson and b baryons other than the Λ_b^0), one can compute the average b-hadron lifetime from the individual lifetimes and production fractions as

Table 13 Summary of the lifetime averages for the different b-hadron species

b-Hadron species		Measured lifetime
B^+		1.638 ± 0.004 ps
B^0		1.520 ± 0.004 ps
B_s^0	$1/\Gamma_s =$	1.505 ± 0.005 ps
$B_{s\mathrm{L}}^0$	$1/\Gamma_{s\mathrm{L}} =$	1.413 ± 0.006 ps
$B_{s\mathrm{H}}^0$	$1/\Gamma_{s\mathrm{H}} =$	1.609 ± 0.010 ps
B_c^+		0.507 ± 0.009 ps
Λ_b^0		1.470 ± 0.010 ps
Ξ_b^-		1.571 ± 0.040 ps
Ξ_b^0		1.479 ± 0.031 ps
Ω_b^-		$1.64^{+0.18}_{-0.17}$

Table 14 Experimental averages of b-hadron lifetime ratios and Heavy-Quark Expansion (HQE) predictions [68,69]

Lifetime ratio	Experimental average	HQE prediction
$\tau(B^+)/\tau(B^0)$	1.076 ± 0.004	$1.04^{+0.05}_{-0.01} \pm 0.02 \pm 0.01$
$\tau(B_s^0)/\tau(B^0)$	0.990 ± 0.004	1.001 ± 0.002
$\tau(\Lambda_b^0)/\tau(B^0)$	0.967 ± 0.007	0.935 ± 0.054
$\tau(\Xi_b^0)/\tau(\Xi_b^-)$	0.929 ± 0.028	0.95 ± 0.06

$$\tau_b = \frac{f_d\tau(B^0)^2 + f_u\tau(B^+)^2 + 0.5 f_s\tau(B^0_{s\mathrm{H}})^2 + 0.5 f_s\tau(B^0_{s\mathrm{L}})^2 + f_{\mathrm{baryon}}\tau(\Lambda^0_b)^2}{f_d\tau(B^0) + f_u\tau(B^+) + 0.5 f_s\tau(B^0_{s\mathrm{H}}) + 0.5 f_s\tau(B^0_{s\mathrm{L}}) + f_{\mathrm{baryon}}\tau(\Lambda^0_b)}. \tag{52}$$

Using the lifetimes of Table 13 and the fractions in Z decays of Table 5, taking into account the correlations between the fractions (Table 5) as well as the correlation between $\tau(B_{s\mathrm{H}})$ and $\tau(B_{s\mathrm{L}})$ (-0.398), one obtains

$$\tau_b(Z) = 1.566 \pm 0.003 \text{ ps}. \tag{53}$$

This is in very good agreement with (and three times more precise than) the average of Eq. (33) for the inclusive measurements performed at LEP.

3.3 Neutral B-meson mixing

The $B^0 - \bar{B}^0$ and $B^0_s - \bar{B}^0_s$ systems both exhibit the phenomenon of particle-antiparticle mixing. For each of them, there are two mass eigenstates which are linear combinations of the two flavour states, B^0_q and $\bar{B}^0_q$,

$$|B^0_{q\mathrm{L}}\rangle = p_q|B^0_q\rangle + q_q|\bar{B}^0_q\rangle, \tag{54}$$

$$|B^0_{q\mathrm{H}}\rangle = p_q|B^0_q\rangle - q_q|\bar{B}^0_q\rangle, \tag{55}$$

where the subscript $q = d$ is used for the B^0_d $(= B^0)$ meson and $q = s$ for the B^0_s meson. The heaviest (lightest) of these mass states is denoted $B^0_{q\mathrm{H}}$ $(B^0_{q\mathrm{L}})$, with mass $m_{q\mathrm{H}}$ $(m_{q\mathrm{L}})$ and total decay width $\Gamma_{q\mathrm{H}}$ $(\Gamma_{q\mathrm{L}})$. We define

$$\Delta m_q = m_{q\mathrm{H}} - m_{q\mathrm{L}}, \quad x_q = \Delta m_q/\Gamma_q, \tag{56}$$

$$\Delta\Gamma_q = \Gamma_{q\mathrm{L}} - \Gamma_{q\mathrm{H}}, \quad y_q = \Delta\Gamma_q/(2\Gamma_q), \tag{57}$$

where $\Gamma_q = (\Gamma_{q\mathrm{H}} + \Gamma_{q\mathrm{L}})/2 = 1/\bar{\tau}(B^0_q)$ is the average decay width. Δm_q is positive by definition, and $\Delta\Gamma_q$ is expected to be positive within the Standard Model.[13]

There are four different time-dependent probabilities describing the case of a neutral B meson produced as a flavour state and decaying without CP violation to a flavour-specific final state. If CPT is conserved (which will be assumed throughout), they can be written as

$$\begin{cases} \mathcal{P}(B^0_q \to B^0_q) = \frac{1}{2}e^{-\Gamma_q t}\left[\cosh\left(\frac{1}{2}\Delta\Gamma_q t\right) + \cos\left(\Delta m_q t\right)\right] \\ \mathcal{P}(B^0_q \to \bar{B}^0_q) = \frac{1}{2}e^{-\Gamma_q t}\left[\cosh\left(\frac{1}{2}\Delta\Gamma_q t\right) - \cos\left(\Delta m_q t\right)\right]\left|q_q/p_q\right|^2 \\ \mathcal{P}(\bar{B}^0_q \to B^0_q) = \frac{1}{2}e^{-\Gamma_q t}\left[\cosh\left(\frac{1}{2}\Delta\Gamma_q t\right) - \cos\left(\Delta m_q t\right)\right]\left|p_q/q_q\right|^2 \\ \mathcal{P}(\bar{B}^0_q \to \bar{B}^0_q) = \frac{1}{2}e^{-\Gamma_q t}\left[\cosh\left(\frac{1}{2}\Delta\Gamma_q t\right) + \cos\left(\Delta m_q t\right)\right] \end{cases}, \tag{58}$$

where t is the proper time of the system (i.e., the time interval between the production and the decay in the rest frame of the B meson). At the B factories, only the proper-time difference Δt between the decays of the two neutral B mesons from the $\Upsilon(4S)$ can be determined, but, because the two B mesons evolve coherently (keeping opposite flavours as long as neither of them has decayed), the above formulae remain valid if t is replaced with Δt and the production flavour is replaced by the flavour at the time of the decay of the accompanying B meson in a flavour-specific state. As can be seen in the above expressions, the mixing probabilities depend on three mixing observables: Δm_q, $\Delta\Gamma_q$, and $|q_q/p_q|^2$, which signals CP violation in the mixing if $|q_q/p_q|^2 \neq 1$. Another (non independent) observable often used to characterize CP violation in the mixing is the so-called semileptonic asymmetry, defined as

$$\mathcal{A}^q_{\mathrm{SL}} = \frac{|p_q/q_q|^2 - |q_q/p_q|^2}{|p_q/q_q|^2 + |q_q/p_q|^2}. \tag{59}$$

All mixing observables depend on two complex numbers, M^q_{12} and Γ^q_{12}, which are the off-diagonal elements of the mass and decay 2×2 matrices describing the evolution of the $B^0_q - \bar{B}^0_q$ system. In the Standard Model the quantity $|\Gamma^q_{12}/M^q_{12}|$ is small, of the order of $(m_b/m_t)^2$ where m_b and m_t are the bottom and top quark masses. The following relations hold, to first order in $|\Gamma^q_{12}/M^q_{12}|$:

$$\Delta m_q = 2|M^q_{12}|\left[1 + \mathcal{O}\left(|\Gamma^q_{12}/M^q_{12}|^2\right)\right], \tag{60}$$

$$\Delta\Gamma_q = 2|\Gamma^q_{12}|\cos\phi^q_{12}\left[1 + \mathcal{O}\left(|\Gamma^q_{12}/M^q_{12}|^2\right)\right], \tag{61}$$

$$\begin{aligned}\mathcal{A}^q_{\mathrm{SL}} &= \mathrm{Im}\left(\Gamma^q_{12}/M^q_{12}\right) + \mathcal{O}\left(|\Gamma^q_{12}/M^q_{12}|^2\right) \\ &= \frac{\Delta\Gamma_q}{\Delta m_q}\tan\phi^q_{12} + \mathcal{O}\left(|\Gamma^q_{12}/M^q_{12}|^2\right),\end{aligned} \tag{62}$$

where

$$\phi^q_{12} = \arg\left(-M^q_{12}/\Gamma^q_{12}\right) \tag{63}$$

is the observable phase difference between $-M^q_{12}$ and Γ^q_{12} (often called the mixing phase). It should be noted that the theoretical predictions for Γ^q_{12} are based on the same HQE as the lifetime predictions.

In the next sections we review in turn the experimental knowledge on the B^0 decay-width and mass differences, the B^0_s decay-width and mass differences, CP violation in B^0 and B^0_s mixing, and mixing-induced CP violation in B^0_s decays.

[13] For reasons of symmetry in Eqs. (56) and (57), $\Delta\Gamma$ is sometimes defined with the opposite sign. The definition adopted in Eq. (57) is the one used by most experimentalists and many phenomenologists in B physics.

Table 15 Time-dependent measurements included in the Δm_d average. The results obtained from multi-dimensional fits involving also the B^0 (and B^+) lifetimes as free parameter(s) [98,100,101] have been converted into one-dimensional measurements of Δm_d. All the measurements have then been adjusted to a common set of physics parameters before being combined

Experiment and Refs.	Method		Δm_d in ps^{-1}	Δm_d in ps^{-1}
	Rec.	Tag	Before adjustment	After adjustment
ALEPH [163]	ℓ	Q_{jet}	$0.404 \pm 0.045 \pm 0.027$	
ALEPH [163]	ℓ	ℓ	$0.452 \pm 0.039 \pm 0.044$	
ALEPH [163]	Above two combined		$0.422 \pm 0.032 \pm 0.026$	$0.440 \pm 0.032 ^{+0.020}_{-0.019}$
ALEPH [163]	D^*	ℓ, Q_{jet}	$0.482 \pm 0.044 \pm 0.024$	$0.482 \pm 0.044 \pm 0.024$
DELPHI [164]	ℓ	Q_{jet}	$0.493 \pm 0.042 \pm 0.027$	$0.499 \pm 0.042 \pm 0.024$
DELPHI [164]	$\pi^*\ell$	Q_{jet}	$0.499 \pm 0.053 \pm 0.015$	$0.500 \pm 0.053 \pm 0.015$
DELPHI [164]	ℓ	ℓ	$0.480 \pm 0.040 \pm 0.051$	$0.495 \pm 0.040 ^{+0.042}_{-0.040}$
DELPHI [164]	D^*	Q_{jet}	$0.523 \pm 0.072 \pm 0.043$	$0.518 \pm 0.072 \pm 0.043$
DELPHI [165]	vtx	comb	$0.531 \pm 0.025 \pm 0.007$	$0.525 \pm 0.025 \pm 0.006$
L3 [166]	ℓ	ℓ	$0.458 \pm 0.046 \pm 0.032$	$0.466 \pm 0.046 \pm 0.028$
L3 [166]	ℓ	Q_{jet}	$0.427 \pm 0.044 \pm 0.044$	$0.439 \pm 0.044 \pm 0.042$
L3 [166]	ℓ	ℓ(IP)	$0.462 \pm 0.063 \pm 0.053$	$0.470 \pm 0.063 \pm 0.044$
OPAL [167]	ℓ	ℓ	$0.430 \pm 0.043 ^{+0.028}_{-0.030}$	$0.466 \pm 0.043 ^{+0.017}_{-0.016}$
OPAL [168]	ℓ	Q_{jet}	$0.444 \pm 0.029 ^{+0.020}_{-0.017}$	$0.481 \pm 0.029 \pm 0.013$
OPAL [169]	$D^*\ell$	Q_{jet}	$0.539 \pm 0.060 \pm 0.024$	$0.544 \pm 0.060 \pm 0.023$
OPAL [169]	D^*	ℓ	0.567 ± 0.089	$^{+0.029}_{-0.023} 0.572 \pm 0.089 ^{+0.028}_{-0.022}$
OPAL [88]	$\pi^*\ell$	Q_{jet}	$0.497 \pm 0.024 \pm 0.025$	$0.496 \pm 0.024 \pm 0.025$
CDF1 [170]	$D\ell$	SST	$0.471 ^{+0.078}_{-0.068} ^{+0.033}_{-0.034}$	$0.470 ^{+0.078}_{-0.068} ^{+0.033}_{-0.034}$
CDF1 [172]	μ	μ	$0.503 \pm 0.064 \pm 0.071$	$0.514 \pm 0.064 ^{+0.070}_{-0.069}$
CDF1 [173]	ℓ	ℓ, Q_{jet}	$0.500 \pm 0.052 \pm 0.043$	$0.546 \pm 0.052 \pm 0.036$
CDF1 [174]	$D^*\ell$	ℓ	$0.516 \pm 0.099 ^{+0.029}_{-0.035}$	$0.523 \pm 0.099 ^{+0.028}_{-0.035}$
D0 [175]	$D^{(*)}\mu$	OST	$0.506 \pm 0.020 \pm 0.016$	$0.506 \pm 0.020 \pm 0.016$
BaBar [176]	B^0	ℓ, K, NN	$0.516 \pm 0.016 \pm 0.010$	$0.521 \pm 0.016 \pm 0.008$
BaBar [178]	ℓ	ℓ	$0.493 \pm 0.012 \pm 0.009$	$0.487 \pm 0.012 \pm 0.006$
BaBar [98]	$D^*\ell\nu$	ℓ, K, NN	$0.492 \pm 0.018 \pm 0.014$	$0.493 \pm 0.018 \pm 0.013$
BaBar [100]	$D^*\ell\nu$(part)	ℓ	$0.511 \pm 0.007 \pm 0.007$	$0.513 \pm 0.007 \pm 0.007$
Belle [101]	B^0, $D^*\ell\nu$	comb	$0.511 \pm 0.005 \pm 0.006$	$0.513 \pm 0.005 \pm 0.006$
Belle [179]	$D^*\pi$(part)	ℓ	$0.509 \pm 0.017 \pm 0.020$	$0.513 \pm 0.017 \pm 0.019$
Belle [9]	ℓ	ℓ	$0.503 \pm 0.008 \pm 0.010$	$0.506 \pm 0.008 \pm 0.008$
LHCb [180]	B^0	OST	$0.499 \pm 0.032 \pm 0.003$	$0.499 \pm 0.032 \pm 0.003$
LHCb [181]	B^0	OST,SST	$0.5156 \pm 0.0051 \pm 0.0033$	$0.5156 \pm 0.0051 \pm 0.0033$
LHCb [182]	$D\mu$	OST,SST	$0.503 \pm 0.011 \pm 0.013$	$0.503 \pm 0.011 \pm 0.013$
LHCb [183]	$D^{(*)}\mu$	OST	$0.5050 \pm 0.0021 \pm 0.0010$	$0.5050 \pm 0.0021 \pm 0.0010$
World average (all above measurements included)				$0.5065 \pm 0.0016 \pm 0.0011$
– ALEPH, DELPHI, L3 and OPAL only				$0.493 \pm 0.011 \pm 0.009$
– CDF and D0 only				$0.509 \pm 0.017 \pm 0.013$
– BaBar and Belle only				$0.509 \pm 0.003 \pm 0.003$
– LHCb only				$0.5063 \pm 0.0019 \pm 0.0010$

3.3.1 B^0 mixing parameters $\Delta\Gamma_d$ and Δm_d

A large number of time-dependent B^0–$\bar{B}^0$ oscillation analyses have been performed in the past 20 years by the ALEPH, DELPHI, L3, OPAL, CDF, D0, BaBar, Belle and LHCb collaborations. The corresponding measurements of Δm_d are summarized in Table 15. Although a variety of different techniques have been used, the individual

Δm_d results obtained at different colliders have remarkably similar precision. The systematic uncertainties are comparable to the statistical uncertainties; they are often dominated by sample composition, mistag probability, or b-hadron lifetime contributions. Before being combined, the measurements are adjusted on the basis of a common set of input values, including the averages of the b-hadron fractions and lifetimes given in this report (see Sects. 3.1, 3.2). Some measurements are statistically correlated. Systematic correlations arise both from common physics sources (fractions, lifetimes, branching ratios of b hadrons), and from purely experimental or algorithmic effects (efficiency, resolution, flavour tagging, background description). Combining all published measurements listed in Table 15 and accounting for all identified correlations as described in Ref. [3] yields $\Delta m_d = 0.5065 \pm 0.0016 \pm 0.0011\ \text{ps}^{-1}$.

On the other hand, ARGUS and CLEO have published measurements of the time-integrated mixing probability χ_d [184,186,187], which average to $\chi_d = 0.182 \pm 0.015$. Following Ref. [187], the decay width difference $\Delta\Gamma_d$ could in principle be extracted from the measured value of $\Gamma_d = 1/\tau(B^0)$ and the above averages for Δm_d and χ_d (provided that $\Delta\Gamma_d$ has a negligible impact on the Δm_d and $\tau(B^0)$ analyses that have assumed $\Delta\Gamma_d = 0$), using the relation

$$\chi_d = \frac{x_d^2 + y_d^2}{2(x_d^2 + 1)}. \tag{64}$$

However, direct time-dependent studies provide much stronger constraints: $|\Delta\Gamma_d|/\Gamma_d < 18\%$ at 95% CL from DELPHI [165], $-6.8\% < \text{sign}(\text{Re}\lambda_{CP})\Delta\Gamma_d/\Gamma_d < 8.4\%$ at 90% CL from BaBar [188], and $\text{sign}(\text{Re}\lambda_{CP})\Delta\Gamma_d/\Gamma_d = (1.7 \pm 1.8 \pm 1.1)\%$ [190] from Belle, where $\lambda_{CP} = (q_d/p_d)(\bar{A}_{CP}/A_{CP})$ is defined for a CP-even final state (the sensitivity to the overall sign of $\text{sign}(\text{Re}\lambda_{CP})\Delta\Gamma_d/\Gamma_d$ comes from the use of B^0 decays to CP final states). In addition LHCb has obtained $\Delta\Gamma_d/\Gamma_d = (-4.4 \pm 2.5 \pm 1.1)\%$ [103] by comparing measurements of the $B^0 \to J/\psi K^{*0}$ and $B^0 \to J/\psi K^0_S$ decays, following the method of Ref. [191]. More recently ATLAS has measured $\Delta\Gamma_d/\Gamma_d = (-0.1 \pm 1.1 \pm 0.9)\%$ [192] using a similar method. Assuming $\text{Re}\lambda_{CP} > 0$, as expected from the global fits of the Unitarity Triangle within the Standard Model [193], a combination of these five results (after adjusting the DELPHI and BaBar results to $1/\Gamma_d = \tau(B^0) = 1.520 \pm 0.004$ ps) yields

$$\Delta\Gamma_d/\Gamma_d = -0.002 \pm 0.010, \tag{65}$$

an average consistent with zero and with the Standard Model prediction of $(3.97 \pm 0.90) \times 10^{-3}$ [107]. An independent result, $\Delta\Gamma_d/\Gamma_d = (0.50 \pm 1.38)\%$ [195], was obtained by the D0 collaboration from their measurements of the single muon and same-sign dimuon charge asymmetries, under the interpretation that the observed asymmetries are due to CP violation in neutral B-meson mixing and interference. This indirect determination was called into question [196] and is therefore not included in the above average, as explained in Sect. 3.3.3 (see Footnote 17).

Assuming $\Delta\Gamma_d = 0$ and using $1/\Gamma_d = \tau(B^0) = 1.520 \pm 0.004$ ps, the Δm_d and χ_d results are combined through Eq. (64) to yield the world average

$$\Delta m_d = 0.5064 \pm 0.0019\ \text{ps}^{-1}, \tag{66}$$

or, equivalently,

$$x_d = 0.770 \pm 0.004 \quad \text{and} \quad \chi_d = 0.1860 \pm 0.0011. \tag{67}$$

Figure 6 compares the Δm_d values obtained by the different experiments.

The B^0 mixing averages given in Eqs. (66) and (67) and the b-hadron fractions of Table 5 have been obtained in a fully consistent way, taking into account the fact that the fractions are computed using the χ_d value of Eq. (67) and that many individual measurements of Δm_d at high energy depend on the assumed values for the b-hadron fractions. Furthermore, this set of averages is consistent with the lifetime averages of Sect. 3.2.

3.3.2 B^0_s mixing parameters $\Delta\Gamma_s$ and Δm_s

The best sensitivity to $\Delta\Gamma_s$ is currently achieved by the recent time-dependent measurements of the $B^0_s \to J/\psi\phi$ (or more generally $B^0_s \to (c\bar{c})K^+K^-$) decay rates performed at CDF [197], D0 [198], ATLAS [199,200] CMS [201] and LHCb [202,203], where the CP-even and CP-odd amplitudes are statistically separated through a full angular analysis. These studies use both untagged and tagged B^0_s candidates and are optimized for the measurement of the CP-violating phase $\phi_s^{c\bar{c}s}$, defined later in Sect. 3.3.4. The LHCb collaboration analyzed the $B^0_s \to J/\psi K^+K^-$ decay, considering that the K^+K^- system can be in a P-wave or S-wave state, and measured the dependence of the strong phase difference between the P-wave and S-wave amplitudes as a function of the K^+K^- invariant mass [111]. This allowed, for the first time, the unambiguous determination of the sign of $\Delta\Gamma_s$, which was found to be positive at the $4.7\,\sigma$ level. The following averages present only the $\Delta\Gamma_s > 0$ solutions.

The published results [197–203] are shown in Table 16. They are combined taking into account, in each analysis, the correlation between $\Delta\Gamma_s$ and Γ_s. The results, displayed as the red contours labelled "$B^0_s \to (c\bar{c})KK$ measurements" in the plots of Fig. 7, are given in the first column of numbers of Table 17.

An alternative approach, which is directly sensitive to first order in $\Delta\Gamma_s/\Gamma_s$, is to determine the effective life-

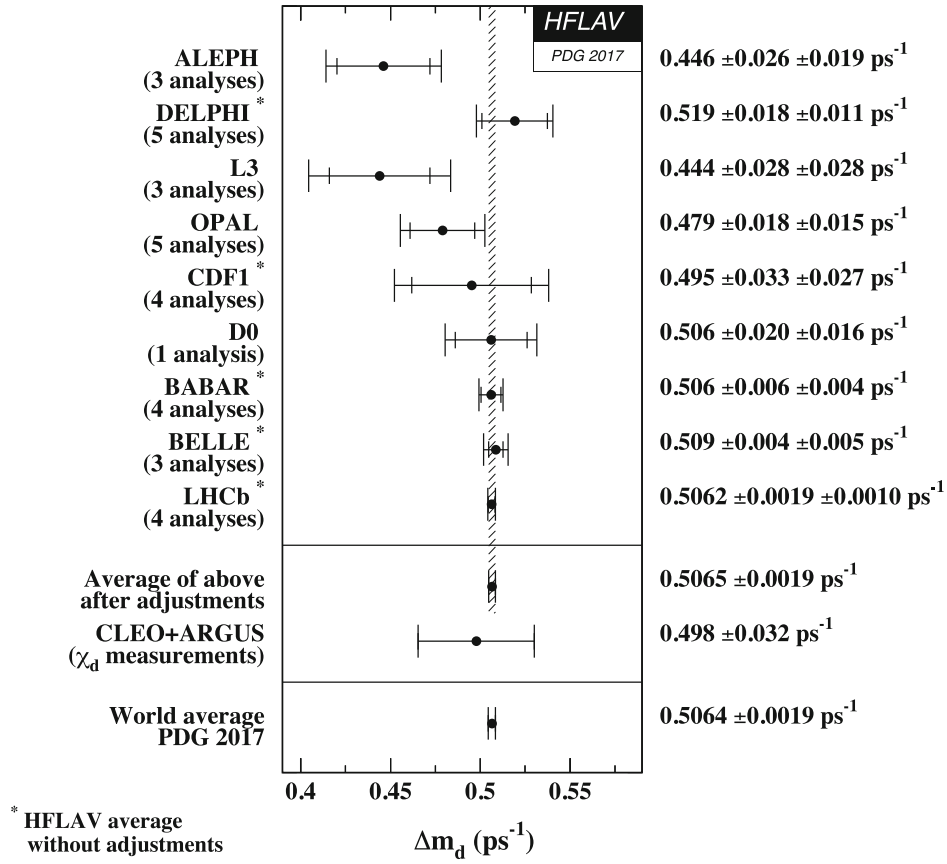

Fig. 6 The B^0–$\bar{B}^0$ oscillation frequency Δm_d as measured by the different experiments. The averages quoted for ALEPH, L3 and OPAL are taken from the original publications, while the ones for DELPHI, CDF, BABAR, Belle and LHCb are computed from the individual results listed in Table 15 without performing any adjustments. The time-integrated measurements of χ_d from the symmetric B factory experiments ARGUS and CLEO are converted to a Δm_d value using $\tau(B^0) = 1.520 \pm 0.004$ ps. The two global averages are obtained after adjustments of all the individual Δm_d results of Table 15 (see text)

Table 16 Measurements of $\Delta\Gamma_s$ and Γ_s using $B_s^0 \to J/\psi\phi$, $B_s^0 \to J/\psi K^+K^-$ and $B_s^0 \to \psi(2S)\phi$ decays. Only the solution with $\Delta\Gamma_s > 0$ is shown, since the two-fold ambiguity has been resolved in Ref. [111]. The first error is due to statistics, the second one to systematics. The last line gives our average

Exp.	Mode	Dataset	$\Delta\Gamma_s$ (ps^{-1})	Γ_s (ps^{-1})	Refs.
CDF	$J/\psi\phi$	9.6 fb^{-1}	$+0.068 \pm 0.026 \pm 0.009$	$0.654 \pm 0.008 \pm 0.004$	[197]
D0	$J/\psi\phi$	8.0 fb^{-1}	$+0.163^{+0.065}_{-0.064}$	$0.693^{+0.018}_{-0.017}$	[198]
ATLAS	$J/\psi\phi$	4.9 fb^{-1}	$+0.053 \pm 0.021 \pm 0.010$	$0.677 \pm 0.007 \pm 0.004$	[199]
ATLAS	$J/\psi\phi$	14.3 fb^{-1}	$+0.101 \pm 0.013 \pm 0.007$	$0.676 \pm 0.004 \pm 0.004$	[200]
ATLAS	Above 2 combined		$+0.085 \pm 0.011 \pm 0.007$	$0.675 \pm 0.003 \pm 0.003$	[200]
CMS	$J/\psi\phi$	19.7 fb^{-1}	$+0.095 \pm 0.013 \pm 0.007$	$0.6704 \pm 0.0043 \pm 0.0055$	[201]
LHCb	$J/\psi K^+K^-$	3.0 fb^{-1}	$+0.0805 \pm 0.0091 \pm 0.0032$	$0.6603 \pm 0.0027 \pm 0.0015$	[202]
LHCb	$\psi(2S)\phi$	3.0 fb^{-1}	$+0.066^{+0.041}_{-0.044} \pm 0.007$	$0.668 \pm 0.011 \pm 0.006$	[203]
All combined			$+0.084 \pm 0.007$	0.6654 ± 0.0022	

time of untagged B_s^0 candidates decaying to pure CP eigenstates; we use here measurements with $B_s^0 \to D_s^+ D_s^-$ [121], $B_s^0 \to J/\psi\eta$ [126], $B_s^0 \to J/\psi f_0(980)$ [128,129] and $B_s^0 \to J/\psi\pi^+\pi^-$ [130] decays. The precise extraction of $1/\Gamma_s$ and $\Delta\Gamma_s$ from such measurements, discussed in detail in Ref. [112], requires additional information in the form of theoretical assumptions or external inputs on weak phases and hadronic parameters. If f designates a final state in which both B_s^0 and $\bar{B}_s^0$ can decay, the ratio of the effective B_s^0 lifetime decaying to f relative to the mean B_s^0 lifetime is [112][14]

$$\frac{\tau_{\text{single}}(B_s^0 \to f)}{\tau(B_s^0)} = \frac{1}{1-y_s^2}\left[\frac{1 - 2A_f^{\Delta\Gamma} y_s + y_s^2}{1 - A_f^{\Delta\Gamma} y_s}\right], \tag{68}$$

[14] The definition of $A_f^{\Delta\Gamma}$ given in Eq. (69) has the sign opposite to that given in Ref. [112].

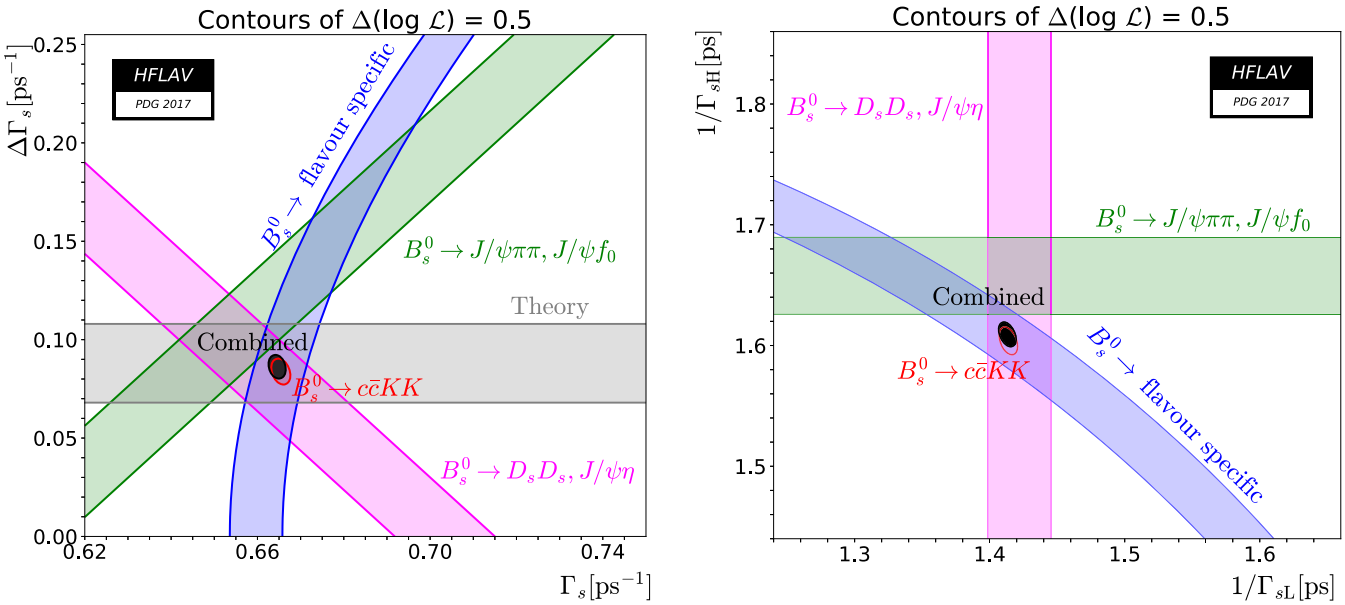

Fig. 7 Contours of $\Delta \ln L = 0.5$ (39% CL for the enclosed 2D regions, 68% CL for the bands) shown in the $(\Gamma_s, \Delta\Gamma_s)$ *plane on the left* and in the $(1/\Gamma_{s\mathrm{L}}, 1/\Gamma_{s\mathrm{H}})$ *plane on the right*. The average of all the $B_s^0 \to J/\psi\phi$, $B_s^0 \to J/\psi K^+K^-$ and $B_s^0 \to \psi(2S)\phi$ results is shown as the *red contour*, and the constraints given by the effective lifetime measurements of B_s^0 to flavour-specific, pure *CP*-odd and pure *CP*-even final states are shown as the *blue*, *green* and *purple bands*, respectively. The average taking all constraints into account is shown as the *grey-filled contour*. The *yellow band* is a theory prediction $\Delta\Gamma_s = 0.088 \pm 0.020\ \mathrm{ps}^{-1}$ [60,107] that assumes no new physics in B_s^0 mixing

Table 17 Averages of $\Delta\Gamma_s$, Γ_s and related quantities, obtained from $B_s^0 \to J/\psi\phi$, $B_s^0 \to J/\psi K^+K^-$ and $B_s^0 \to \psi(2S)\phi$ alone (first column), adding the constraints from the effective lifetimes measured in pure *CP* modes $B_s^0 \to D_s^+D_s^-$, $J/\psi\eta$ and $B_s^0 \to J/\psi f_0(980)$, $J/\psi\pi^+\pi^-$ (second column), and adding the constraint from the effective lifetime measured in flavour-specific modes $B_s^0 \to D_s^-\ell^+\nu X$, $D_s^-\pi^+$, $D_s^-D^+$ (third column, recommended world averages)

	$B_s^0 \to (c\bar{c})K^+K^-$ modes only (see Table 16)	$B_s^0 \to (c\bar{c})K^+K^-$ modes + pure *CP* modes	$B_s^0 \to (c\bar{c})K^+K^-$ modes + pure *CP* modes + flavour-specific modes
Γ_s	$0.6654 \pm 0.0022\ \mathrm{ps}^{-1}$	$0.6645 \pm 0.0021\ \mathrm{ps}^{-1}$	$0.6646 \pm 0.0020\ \mathrm{ps}^{-1}$
$1/\Gamma_s$	1.503 ± 0.005 ps	1.505 ± 0.005 ps	1.505 ± 0.005 ps
$1/\Gamma_{s\mathrm{L}}$	1.414 ± 0.007 ps	1.413 ± 0.006 ps	1.413 ± 0.006 ps
$1/\Gamma_{s\mathrm{H}}$	1.604 ± 0.011 ps	1.610 ± 0.011 ps	1.609 ± 0.010 ps
$\Delta\Gamma_s$	$+0.084 \pm 0.007\ \mathrm{ps}^{-1}$	$+0.086 \pm 0.006\ \mathrm{ps}^{-1}$	$+0.086 \pm 0.006\ \mathrm{ps}^{-1}$
$\Delta\Gamma_s/\Gamma_s$	$+0.126 \pm 0.010$	$+0.130 \pm 0.009$	$+0.130 \pm 0.009$
$\rho(\Gamma_s, \Delta\Gamma_s)$	–0.286	–0.267	–0.210

where

$$A_f^{\Delta\Gamma} = -\frac{2\mathrm{Re}(\lambda_f)}{1+|\lambda_f|^2}. \tag{69}$$

To include the measurements of the effective $B_s^0 \to D_s^+D_s^-$ (*CP*-even), $B_s^0 \to J/\psi f_0(980)$ (*CP*-odd) and $B_s^0 \to J/\psi\pi^+\pi^-$ (*CP*-odd) lifetimes as constraints in the $\Delta\Gamma_s$ fit,[15] we neglect sub-leading penguin contributions and possible direct *CP* violation. Explicitly, in Eq. (69), we set $A^{\Delta\Gamma}_{CP\text{-even}} = \cos\phi_s^{c\bar{c}s}$ and $A^{\Delta\Gamma}_{CP\text{-odd}} = -\cos\phi_s^{c\bar{c}s}$. Given the small value of $\phi_s^{c\bar{c}s}$, we have, to first order in y_s:

$$\tau_{\mathrm{single}}(B_s^0 \to CP\text{-even}) \approx \frac{1}{\Gamma_{s\mathrm{L}}}\left(1+\frac{(\phi_s^{c\bar{c}s})^2 y_s}{2}\right), \tag{70}$$

$$\tau_{\mathrm{single}}(B_s^0 \to CP\text{-odd}) \approx \frac{1}{\Gamma_{s\mathrm{H}}}\left(1-\frac{(\phi_s^{c\bar{c}s})^2 y_s}{2}\right). \tag{71}$$

The numerical inputs are taken from Eqs. (41) and (42) and the resulting averages, combined with the $B_s^0 \to J/\psi K^+K^-$ information, are indicated in the second column of numbers of Table 17. These averages assume $\phi_s^{c\bar{c}s} = 0$,

[15] The effective lifetimes measured in $B_s^0 \to K^+K^-$ (mostly *CP*-even) and $B_s^0 \to J/\psi K_S^0$ (mostly *CP*-odd) are not used because we can not quantify the penguin contributions in those modes.

Table 18 Measurements of Δm_s

Experiment	Method	Data set		Δm_s (ps^{-1})	Refs.
CDF2	$D_s^{(*)-}\ell^+\nu$, $D_s^{(*)-}\pi^+$, $D_s^-\rho^+$		1 fb^{-1}	$17.77 \pm 0.10 \pm 0.07$	[218]
LHCb	$D_s^-\pi^+$, $D_s^-\pi^+\pi^-\pi^+$	2010	0.034 fb^{-1}	$17.63 \pm 0.11 \pm 0.02$	[219]
LHCb	$D_s^-\mu^+X$	2011	1.0 fb^{-1}	$17.93 \pm 0.22 \pm 0.15$	[182]
LHCb	$D_s^-\pi^+$	2011	1.0 fb^{-1}	$17.768 \pm 0.023 \pm 0.006$	[220]
LHCb	$J/\psi K^+K^-$	2011–2012	3.0 fb^{-1}	$17.711^{+0.055}_{-0.057} \pm 0.011$	[202]
Average				$17.757 \pm 0.020 \pm 0.007$	

which is compatible with the $\phi_s^{c\bar{c}s}$ average presented in Sect. 3.3.4.

Information on $\Delta\Gamma_s$ can also be obtained from the study of the proper time distribution of untagged samples of flavour-specific B_s^0 decays [131], where the flavour (i.e., B_s^0 or $\bar{B}_s^0$) at the time of decay can be determined by the decay products. In such decays, e.g. semileptonic B_s^0 decays, there is an equal mix of the heavy and light mass eigenstates at time zero. The proper time distribution is then a superposition of two exponential functions with decay constants $\Gamma_{s\mathrm{L}}$ and $\Gamma_{s\mathrm{H}}$. This provides sensitivity to both $1/\Gamma_s$ and $(\Delta\Gamma_s/\Gamma_s)^2$. Ignoring $\Delta\Gamma_s$ and fitting for a single exponential leads to an estimate of Γ_s with a relative bias proportional to $(\Delta\Gamma_s/\Gamma_s)^2$, as shown in Eq. (39). Including the constraint from the world-average flavour-specific B_s^0 lifetime, given in Eq. (40), leads to the results shown in the last column of Table 17. These world averages are displayed as the grey contours labelled "Combined" in the plots of Fig. 7. They correspond to the lifetime averages $1/\Gamma_s = 1.505 \pm 0.005$ ps, $1/\Gamma_{s\mathrm{L}} = 1.413 \pm 0.006$ ps, $1/\Gamma_{s\mathrm{H}} = 1.609 \pm 0.010$ ps, and to the decay-width difference

$$\Delta\Gamma_s = +0.086 \pm 0.006\ \mathrm{ps}^{-1} \quad \text{and}$$
$$\Delta\Gamma_s/\Gamma_s = +0.130 \pm 0.009. \tag{72}$$

The good agreement with the Standard Model prediction $\Delta\Gamma_s = 0.088 \pm 0.020$ ps^{-1} [60,107] excludes significant quark-hadron duality violation in the HQE [204].

Estimates of $\Delta\Gamma_s/\Gamma_s$ obtained from measurements of the $B_s^0 \to D_s^{(*)+}D_s^{(*)-}$ branching fraction [124,205–207] have not been used, since they are based on the questionable [208,209] assumption that these decays account for all CP-even final states. The results of early lifetime analyses attempting to measure $\Delta\Gamma_s/\Gamma_s$ [79,85,114,118] have not been used either.

The strength of B_s^0 mixing has been known to be large for more than 20 years. Indeed the time-integrated measurements of $\overline{\chi}$ (see Sect. 3.1.3), when compared to our knowledge of χ_d and the b-hadron fractions, indicated that χ_s should be close to its maximal possible value of 1/2. Many searches of the time dependence of this mixing were performed by ALEPH [210], DELPHI [114,118,165,211], OPAL [212,213], SLD [214,215], CDF (Run I) [216] and D0 [217] but did not have enough statistical power and proper time resolution to resolve the small period of the B_s^0 oscillations.

B_s^0 oscillations have been observed for the first time in 2006 by the CDF collaboration [218], based on samples of flavour-tagged hadronic and semileptonic B_s^0 decays (in flavour-specific final states), partially or fully reconstructed in 1 fb^{-1} of data collected during Tevatron's Run II. More recently the LHCb collaboration obtained the most precise results using fully reconstructed $B_s^0 \to D_s^-\pi^+$ and $B_s^0 \to D_s^-\pi^+\pi^-\pi^+$ decays at the LHC [219,220]. LHCb has also observed B_s^0 oscillations with $B_s^0 \to J/\psi K^+K^-$ decays [202] and with semileptonic $B_s^0 \to D_s^-\mu^+X$ decays [182]. The measurements of Δm_s are summarized in Table 18.

A simple average of the CDF and LHCb results, taking into account the correlated systematic uncertainties between the three LHCb measurements, yields

$$\begin{aligned}\Delta m_s &= 17.757 \pm 0.020 \pm 0.007\ \mathrm{ps}^{-1}\\ &= 17.757 \pm 0.021\ \mathrm{ps}^{-1}\end{aligned} \tag{73}$$

and is illustrated in Fig. 8. The Standard Model prediction $\Delta m_s = 18.3 \pm 2.7$ ps^{-1} [60,107] is consistent with the experimental value, but has a much larger error dominated by the uncertainty on the hadronic matrix elements. The ratio $\Delta\Gamma_s/\Delta m_s$ can be predicted more accurately, 0.0048 ± 0.0008 [60,107], and is in good agreement with the experimental determination of

$$\Delta\Gamma_s/\Delta m_s = 0.00486 \pm 0.00034. \tag{74}$$

Multiplying the Δm_s result of Eq. (73) with the mean B_s^0 lifetime of Eq. (45), $1/\Gamma_s = 1.505 \pm 0.005$ ps, yields

$$x_s = 26.72 \pm 0.09. \tag{75}$$

With $2y_s = +0.130 \pm 0.009$ [see Eq. (72)] and under the assumption of no CP violation in B_s^0 mixing, this corresponds to

$$\chi_s = \frac{x_s^2 + y_s^2}{2(x_s^2+1)} = 0.499304 \pm 0.000005. \tag{76}$$

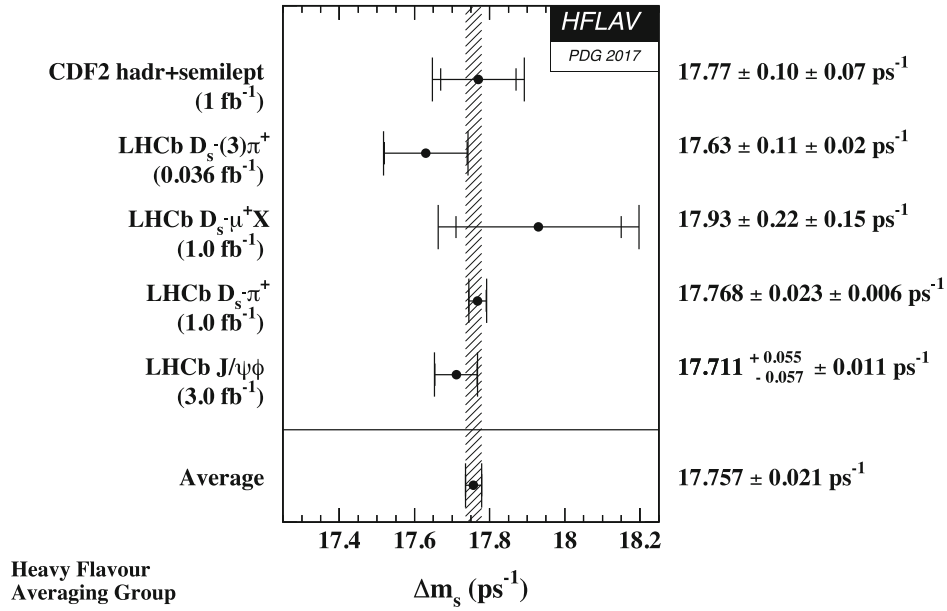

Fig. 8 Published measurements of Δm_s, together with their average

The ratio of the B^0 and B_s^0 oscillation frequencies, obtained from Eqs. (66) and (73),

$$\frac{\Delta m_d}{\Delta m_s} = 0.02852 \pm 0.00011, \tag{77}$$

can be used to extract the following magnitude of the ratio of CKM matrix elements,

$$\left|\frac{V_{td}}{V_{ts}}\right| = \xi \sqrt{\frac{\Delta m_d}{\Delta m_s}\frac{m(B_s^0)}{m(B^0)}} = 0.2053 \pm 0.0004 \pm 0.0032, \tag{78}$$

where the first quoted error is from experimental uncertainties (with the masses $m(B_s^0)$ and $m(B^0)$ taken from Ref. [6]), and where the second quoted error is from theoretical uncertainties in the estimation of the SU(3) flavour-symmetry breaking factor $\xi = 1.206 \pm 0.018 \pm 0.006$, obtained from recent three-flavour lattice QCD calculations [221,222]. Note that Eq. (78) assumes that Δm_s and Δm_d only receive Standard Model contributions.

3.3.3 *CP violation in B^0 and B_s^0 mixing*

Evidence for *CP* violation in B^0 mixing has been searched for, both with flavour-specific and inclusive B^0 decays, in samples where the initial flavour state is tagged. In the case of semileptonic (or other flavour-specific) decays, where the final state tag is also available, the asymmetry

$$\mathcal{A}_{\rm SL}^d = \frac{N(\bar{B}^0(t) \to \ell^+\nu_\ell X) - N(B^0(t) \to \ell^-\bar{\nu}_\ell X)}{N(\bar{B}^0(t) \to \ell^+\nu_\ell X) + N(B^0(t) \to \ell^-\bar{\nu}_\ell X)} \tag{79}$$

has been measured, either in decay-time-integrated analyses at CLEO [187,223], BaBar [224], CDF [225] and D0 [195], or in decay-time-dependent analyses at OPAL [168], ALEPH [226], BaBar [188,227,228] and Belle [229]. Note that the asymmetry of time-dependent decay rates in Eq. (79) is related to $|q_d/p_d|$ through Eq. (59) and is therefore time-independent. In the inclusive case, also investigated and published by ALEPH [226] and OPAL [87], no final state tag is used, and the asymmetry [230,231]

$$\frac{N(B^0(t) \to \text{all}) - N(\bar{B}^0(t) \to \text{all})}{N(B^0(t) \to \text{all}) + N(\bar{B}^0(t) \to \text{all})} \simeq \mathcal{A}_{\rm SL}^d \left[\frac{\Delta m_d}{2\Gamma_d}\sin(\Delta m_d\, t) - \sin^2\left(\frac{\Delta m_d\, t}{2}\right)\right] \tag{80}$$

must be measured as a function of the proper time to extract information on *CP* violation.

On the other hand, D0 [232] and LHCb [233] have studied the time-dependence of the charge asymmetry of $B^0 \to D^{(*)-}\mu^+\nu_\mu X$ decays without tagging the initial state, which would be equal to

$$\frac{N(D^{(*)-}\mu^+\nu_\mu X) - N(D^{(*)+}\mu^-\bar{\nu}_\mu X)}{N(D^{(*)-}\mu^+\nu_\mu X) + N(D^{(*)+}\mu^-\bar{\nu}_\mu X)} = \mathcal{A}_{\rm SL}^d \frac{1-\cos(\Delta m_d\, t)}{2} \tag{81}$$

in absence of detection and production asymmetries.

Table 19 summarizes the different measurements[16] of $\mathcal{A}_{\rm SL}^d$ and $|q_{\rm d}/p_{\rm d}|$: in all cases asymmetries compatible with zero have been found, with a precision limited by the available statistics.

A simple average of all measurements performed at the B factories [187,188,223,224,227,229] yields $\mathcal{A}_{\rm SL}^d =$

[16] A low-statistics result published by CDF using the Run I data [225] is not included in our averages, nor in Table 19.

Table 19 Measurements[16] of CP violation in B^0 mixing and their average in terms of both $\mathcal{A}^d_{\rm SL}$ and $|q_d/p_d|$. The individual results are listed as quoted in the original publications, or converted[18] to an $\mathcal{A}^d_{\rm SL}$ value. When two errors are quoted, the first one is statistical and the second one systematic. The ALEPH and OPAL results assume no CP violation in B^0_s mixing

Exp. and Refs.	Method	Measured $\mathcal{A}^d_{\rm SL}$	Measured $\lvert q_{\rm d}/p_{\rm d}\rvert$
CLEO [187]	Partial hadronic rec.	$+0.017\pm0.070\pm0.014$	
CLEO [223]	Dileptons	$+0.013\pm0.050\pm0.005$	
CLEO [223]	Average of above two	$+0.014\pm0.041\pm0.006$	
BaBar [188]	Full hadronic rec.	$1.029\pm0.013\pm0.011$	
BaBar [227]	Part. rec. $D^*X\ell\nu$	$+0.0006\pm0.0017^{+0.0038}_{-0.0032}$	$0.99971\pm0.00084\pm0.00175$
BaBar [224]	Dileptons	$-0.0039\pm0.0035\pm0.0019$	
Belle [229]	Dileptons	$-0.0011\pm0.0079\pm0.0085$	$1.0005\pm0.0040\pm0.0043$
Average of above 6 B-factory results		-0.0019 ± 0.0027 (tot)	1.0009 ± 0.0013 (tot)
D0 [232]	$B^0\to D^{(*)-}\mu^+\nu X$	$+0.0068\pm0.0045\pm0.0014$	
LHCb [233]	$B^0\to D^{(*)-}\mu^+\nu X$	$-0.0002\pm0.0019\pm0.0030$	
Average of above 8 pure B^0 results		$+0.0001\pm0.0020$ (tot)	1.0000 ± 0.0010 (tot)
D0 [195]	Muons and dimuons	-0.0062 ± 0.0043 (tot)	
Average of above 9 direct measurements		-0.0010 ± 0.0018 (tot)	1.0005 ± 0.0009 (tot)
OPAL [168]	Leptons	$+0.008\pm0.028\pm0.012$	
OPAL [87]	Inclusive (Eq. (80))	$+0.005\pm0.055\pm0.013$	
ALEPH [226]	Leptons	$-0.037\pm0.032\pm0.007$	
ALEPH [226]	Inclusive (Eq. (80))	$+0.016\pm0.034\pm0.009$	
ALEPH [226]	Average of above two	-0.013 ± 0.026 (tot)	
Average of above 13 results		-0.0010 ± 0.0018 (tot)	1.0005 ± 0.0009 (tot)
Best fit value from 2D combination of $\mathcal{A}^d_{\rm SL}$ and $\mathcal{A}^s_{\rm SL}$ results (see Eq. (82))		-0.0021 ± 0.0017 (tot)	1.0010 ± 0.0008 (tot)

-0.0019 ± 0.0027. Adding also the D0 [232] and LHCb [233] measurements obtained with reconstructed semileptonic B^0 decays yields $\mathcal{A}^d_{\rm SL}=+0.0001\pm0.0020$. As discussed in more detail later in this section, the D0 analysis with single muons and like-sign dimuons [195] separates the B^0 and B^0_s contributions by exploiting the dependence on the muon impact parameter cut; including the $\mathcal{A}^d_{\rm SL}$ result quoted by D0 in the average yields $\mathcal{A}^d_{\rm SL}=-0.0010\pm0.0018$. All the other B^0 analyses performed at high energy, either at LEP or at the Tevatron, did not separate the contributions from the B^0 and B^0_s mesons. Under the assumption of no CP violation in B^0_s mixing ($\mathcal{A}^s_{\rm SL}=0$), a number of these early analyses [52,87,168,226] quote a measurement of $\mathcal{A}^d_{\rm SL}$ or $|q_d/p_d|$ for the B^0 meson. However, these imprecise determinations no longer improve the world average of $\mathcal{A}^d_{\rm SL}$. The latter assumption makes sense within the Standard Model, since $\mathcal{A}^s_{\rm SL}$ is predicted to be much smaller than $\mathcal{A}^d_{\rm SL}$ [60,107], but may not be suitable in the presence of new physics.

The Tevatron experiments have measured linear combinations of $\mathcal{A}^d_{\rm SL}$ and $\mathcal{A}^s_{\rm SL}$ using inclusive semileptonic decays of b hadrons, $\mathcal{A}^b_{\rm SL}=+0.0015\pm0.0038(\text{stat})\pm0.0020(\text{syst})$ [225] and $\mathcal{A}^b_{\rm SL}=-0.00496\pm0.00153(\text{stat})\pm0.00072(\text{syst})$ [195], at CDF1 and D0 respectively. While the imprecise CDF1 result is compatible with no CP violation, the D0 result, obtained by measuring the single muon and like-sign dimuon charge asymmetries, differs by 2.8 standard deviations from the Standard Model expectation of $\mathcal{A}^{b,\rm SM}_{\rm SL}=(-2.3\pm0.4)\times10^{-4}$ [195,208]. With a more sophisticated analysis in bins of the muon impact parameters, D0 conclude that the overall deviation of their measurements from the SM is at the level of $3.6\,\sigma$. Interpreting the observed asymmetries in bins of the muon impact parameters in terms of CP violation in B-meson mixing and interference, and using the mixing parameters and the world b-hadron fractions of Ref. [234], the D0 collaboration extracts [195] values for $\mathcal{A}^d_{\rm SL}$ and $\mathcal{A}^s_{\rm SL}$ and their correlation coefficient,[17] as shown in Table 20. However, the various contributions to the total quoted errors from this analysis and from the external inputs are not given, so the adjustment of these results to different

[17] In each impact parameter bin i the measured same-sign dimuon asymmetry is interpreted as $A_i=K^s_i\mathcal{A}^s_{\rm SL}+K^d_i\mathcal{A}^d_{\rm SL}+\lambda K^{\rm int}_i\Delta\Gamma_d/\Gamma_d$, where the factors K^s_i, K^d_i and $K^{\rm int_i}$ are obtained by D0 from Monte Carlo simulation. The D0 publication [195] assumes $\lambda=1$, but it has been demonstrated subsequently that $\lambda\le0.49$ [196]. This particular point invalidates the $\Delta\Gamma_d/\Gamma_d$ result published by D0, but not the $\mathcal{A}^d_{\rm SL}$ and $\mathcal{A}^s_{\rm SL}$ results. As stated by D0, their $\mathcal{A}^d_{\rm SL}$ and $\mathcal{A}^s_{\rm SL}$ results assume the above expression for A_i, i.e. that the observed asymmetries are due to CP violation in B mixing. As long as this assumption is not shown to be wrong (or withdrawn by D0), we include the $\mathcal{A}^d_{\rm SL}$ and $\mathcal{A}^s_{\rm SL}$ results in our world average.

Table 20 Measurements of CP violation in B_s^0 and B^0 mixing, together with their correlations $\rho(\mathcal{A}_{\rm SL}^s, \mathcal{A}_{\rm SL}^d)$ and their two-dimensional average. Only total errors are quoted

Exp. and Refs.	Method	Measured $\mathcal{A}_{\rm SL}^s$	Measured $\mathcal{A}_{\rm SL}^d$	$\rho(\mathcal{A}_{\rm SL}^s, \mathcal{A}_{\rm SL}^d)$
B-factory average of Table 19			-0.0019 ± 0.0027	
D0 [232,235]	$B_{(s)}^0 \to D_{(s)}^{(*)-}\mu^+\nu X$	-0.0112 ± 0.0076	$+0.0068 \pm 0.0047$	+0.
LHCb [233,236]	$B_{(s)}^0 \to D_{(s)}^{(*)-}\mu^+\nu X$	$+0.0039 \pm 0.0033$	-0.0002 ± 0.0036	+0.13
Average of above		$+0.0016 \pm 0.0030$	$+0.0000 \pm 0.0019$	+0.066
D0 [195]	Muons and dimuons	-0.0082 ± 0.0099	-0.0062 ± 0.0043	−0.61
Average of all above		-0.0006 ± 0.0028	-0.0021 ± 0.0017	-0.054

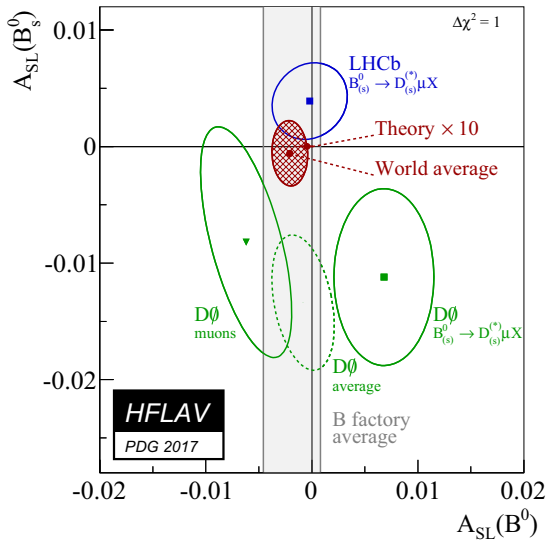

Fig. 9 Measurements of $\mathcal{A}_{\rm SL}^s$ and $\mathcal{A}_{\rm SL}^d$ listed in Table 20 (B-factory average as the *grey band*, D0 measurements as the *green ellipses*, LHCb measurements as the *blue ellipse*) together with their two-dimensional average (*red hatched ellipse*). The red point close to (0, 0) is the Standard Model prediction of Refs. [60,107] with error bars multiplied by 10. The prediction and the experimental world average deviate from each other by $0.5\,\sigma$

or more recent values of the external inputs cannot (easily) be done.

Finally, direct determinations of $\mathcal{A}_{\rm SL}^s$, also shown in Table 20, are obtained by D0 [235] and LHCb [236] from the time-integrated charge asymmetry of untagged $B_s^0 \to D_s^-\mu^+\nu X$ decays.

Using a two-dimensional fit, all measurements of $\mathcal{A}_{\rm SL}^s$ and $\mathcal{A}_{\rm SL}^d$ obtained by D0 and LHCb are combined with the B-factory average of Table 19. Correlations are taken into account as shown in Table 20. The results, displayed graphically in Fig. 9, are

$$\mathcal{A}_{\rm SL}^d = -0.0021 \pm 0.0017 \iff |q_d/p_d| = 1.0010 \pm 0.0008, \quad (82)$$

$$\mathcal{A}_{\rm SL}^s = -0.0006 \pm 0.0028 \iff |q_s/p_s| = 1.0003 \pm 0.0014, \quad (83)$$

$$\rho(\mathcal{A}_{\rm SL}^d, \mathcal{A}_{\rm SL}^s) = -0.054, \quad (84)$$

where the relation between $\mathcal{A}_{\rm SL}^q$ and $|q_q/p_q|$ is given in Eq. (59).[18] However, the fit χ^2 probability is only 4.5%. This is mostly due to an overall discrepancy between the D0 and LHCb averages at the level of $2.2\,\sigma$. Since the assumptions underlying the inclusion of the D0 muon results in the average[17] are somewhat controversial [237], we also provide in Table 20 an average excluding these results.

The above averages show no evidence of CP violation in B^0 or B_s^0 mixing. They deviate by $0.5\,\sigma$ from the very small predictions of the Standard Model (SM), $\mathcal{A}_{\rm SL}^{d,\rm SM} = -(4.7 \pm 0.6) \times 10^{-4}$ and $\mathcal{A}_{\rm SL}^{s,\rm SM} = +(2.22 \pm 0.27) \times 10^{-5}$ [60,107]. Given the current size of the experimental uncertainties, there is still significant room for a possible new physics contribution, in particular in the B_s^0 system. In this respect, the deviation of the D0 dimuon asymmetry [195] from expectation has generated a lot of excitement. However, the recent $\mathcal{A}_{\rm SL}^s$ and $\mathcal{A}_{\rm SL}^d$ results from LHCb are not precise enough yet to settle the issue. It was pointed out [238] that the D0 dimuon result can be reconciled with the SM expectations of $\mathcal{A}_{\rm SL}^s$ and $\mathcal{A}_{\rm SL}^d$ if there were non-SM sources of CP violation in the semileptonic decays of the b and c quarks. A recent Run 1 ATLAS study [239] of charge asymmetries in muon+jets $t\bar{t}$ events, in which a b-hadron decays semileptonically to a soft muon, yields results with limited statistical precision, compatible both with the D0 dimuon asymmetry and with the SM predictions. More experimental data, especially from Run 2 of LHC, is awaited eagerly.

At the more fundamental level, CP violation in B_s^0 mixing is caused by the weak phase difference ϕ_{12}^s defined in Eq. (63). The SM prediction for this phase is tiny [60,107],

$$\phi_{12}^{s,\rm SM} = 0.0046 \pm 0.0012; \quad (85)$$

[18] Early analyses and the PDG use the complex parameter $\epsilon_B = (p_q - q_q)/(p_q + q_q)$ for the B^0; if CP violation in the mixing is small, $\mathcal{A}_{\rm SL}^d \cong 4{\rm Re}(\epsilon_B)/(1 + |\epsilon_B|^2)$ and the average of Eq. (82) corresponds to ${\rm Re}(\epsilon_B)/(1 + |\epsilon_B|^2) = -0.0005 \pm 0.0004$.

however, new physics in B_s^0 mixing could change this observed phase to

$$\phi_{12}^s = \phi_{12}^{s,\mathrm{SM}} + \phi_{12}^{s,\mathrm{NP}}. \tag{86}$$

Using Eq. (62), the current knowledge of $\mathcal{A}_{\mathrm{SL}}^s$, $\Delta\Gamma_s$ and Δm_s, given in Eqs. (83), (72) and (73) respectively, yields an experimental determination of ϕ_{12}^s,

$$\tan\phi_{12}^s = \mathcal{A}_{\mathrm{SL}}^s \frac{\Delta m_s}{\Delta\Gamma_s} = -0.1 \pm 0.6, \tag{87}$$

which represents only a very weak constraint at present.

3.3.4 Mixing-induced CP violation in B_s^0 decays

CP violation induced by $B_s^0 - \bar{B}_s^0$ mixing has been a field of very active study and fast experimental progress in the past few years. The main observable is the *CP*-violating phase $\phi_s^{c\bar{c}s}$, defined as the weak phase difference between the $B_s^0 - \bar{B}_s^0$ mixing amplitude M_{12}^s and the $b \to c\bar{c}s$ decay amplitude.

The golden mode for such studies is $B_s^0 \to J/\psi\phi$, followed by $J/\psi \to \mu^+\mu^-$ and $\phi \to K^+K^-$, for which a full angular analysis of the decay products is performed to separate statistically the *CP*-even and *CP*-odd contributions in the final state. As already mentioned in Sect. 3.3.2, CDF [197], D0 [198], ATLAS [199,200], CMS [201] and LHCb [202,203] have used both untagged and tagged $B_s^0 \to J/\psi\phi$ (and more generally $B_s^0 \to (c\bar{c})K^+K^-$) events for the measurement of $\phi_s^{c\bar{c}s}$. LHCb [240] has used $B_s^0 \to J/\psi\pi^+\pi^-$ events, analyzed with a full amplitude model including several $\pi^+\pi^-$ resonances (e.g., $f_0(980)$), although the $J/\psi\pi^+\pi^-$ final state had already been shown to be almost *CP* pure with a *CP*-odd fraction larger than 0.977 at 95% CL [241]. In addition, LHCb has used the $B_s^0 \to D_s^+D_s^-$ channel [242] to measure $\phi_s^{c\bar{c}s}$.

All CDF, D0, ATLAS and CMS analyses provide two mirror solutions related by the transformation $(\Delta\Gamma_s, \phi_s^{c\bar{c}s}) \to (-\Delta\Gamma_s, \pi - \phi_s^{c\bar{c}s})$. However, the LHCb analysis of $B_s^0 \to J/\psi K^+K^-$ resolves this ambiguity and rules out the solution with negative $\Delta\Gamma_s$ [111], a result in agreement with the Standard Model expectation. Therefore, in what follows, we only consider the solution with $\Delta\Gamma_s > 0$.

We perform a combination of the CDF [197], D0 [198], ATLAS [199,200], CMS [201] and LHCb [202,203,240] results summarized in Table 21. This is done by adding the two-dimensional log profile-likelihood scans of $\Delta\Gamma_s$ and $\phi_s^{c\bar{c}s}$ from all $B_s^0 \to (c\bar{c})K^+K^-$ analyses and a one-dimensional log profile-likelihood of $\phi_s^{c\bar{c}s}$ from the $B_s^0 \to J/\psi\pi^+\pi^-$ and $B_s^0 \to D_s^+D_s^-$ analyses; the combined likelihood is then maximized with respect to $\Delta\Gamma_s$ and $\phi_s^{c\bar{c}s}$.

In the $B_s^0 \to J/\psi\phi$ and $B_s^0 \to J/\psi K^+K^-$ analyses, $\phi_s^{c\bar{c}s}$ and $\Delta\Gamma_s$ come from a simultaneous fit that determines also the B_s^0 lifetime, the polarisation amplitudes and strong phases. While the correlation between $\phi_s^{c\bar{c}s}$ and all other parameters is small, the correlations between $\Delta\Gamma_s$ and the polarisation amplitudes are sizable. However, since the various experiments use different conventions for the amplitudes and phases, a full combination including all correlations is not performed. Instead, our average only takes into account the correlation between $\phi_s^{c\bar{c}s}$ and $\Delta\Gamma_s$.

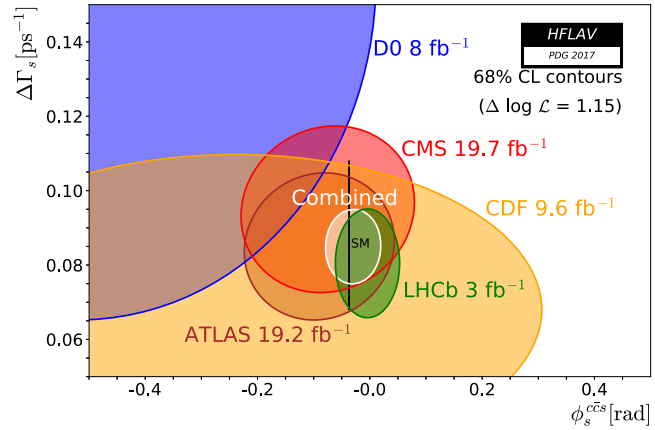

Fig. 10 68% CL regions in B_s^0 width difference $\Delta\Gamma_s$ and weak phase $\phi_s^{c\bar{c}s}$ obtained from individual and combined CDF [197], D0 [198], ATLAS [199,200], CMS [201] and LHCb [202,203,240,242] likelihoods of $B_s^0 \to J/\psi\phi$, $B_s^0 \to J/\psi K^+K^-$, $B_s^0 \to \psi(2S)\phi$, $B_s^0 \to J/\psi\pi^+\pi^-$ and $B_s^0 \to D_s^+D_s^-$ samples. The expectation within the Standard Model [60,107,193] is shown as the *black rectangle*

In the recent LHCb $B_s^0 \to J/\psi K^+K^-$ analysis [202], the $\phi_s^{c\bar{c}s}$ values are measured for the first time for each polarisation of the final state. Since those values are compatible within each other, we still use the unique value of $\phi_s^{c\bar{c}s}$ for our world average, corresponding to the one measured by the other-than-LHCb analyses. In the same analysis, the statistical correlation coefficient between $\phi_s^{c\bar{c}s}$ and $|\lambda|$ (which signals *CP* violation in the decay if different from unity) is measured to be very small (−0.02). We neglect this correlation in our average. Furthermore, the statistical correlation coefficient between $\phi_s^{c\bar{c}s}$ and $\Delta\Gamma_s$ is measured to be small (−0.08). When averaging LHCb results of $B_s^0 \to J/\psi K^+K^-$, $B_s^0 \to J/\psi\pi^+\pi^-$ and $B_s^0 \to D_s^+D_s^-$, we neglect this correlation coefficient (putting it to zero). Given the increasing experimental precision, we have also stopped using the two-dimensional $\Delta\Gamma_s - \phi_s^{c\bar{c}s}$ histograms provided by the CDF and D0 collaborations: we are now approximating those with two-dimensional Gaussian likelihoods.

We obtain the individual and combined contours shown in Fig. 10. Maximizing the likelihood, we find, as summarized in Table 21:

$$\Delta\Gamma_s = +0.085 \pm 0.007\ \mathrm{ps}^{-1}, \tag{88}$$

$$\phi_s^{c\bar{c}s} = -0.030 \pm 0.033. \tag{89}$$

The above $\Delta\Gamma_s$ average is consistent, but highly correlated with the average of Eq. (72). Our final recommended average

Table 21 Direct experimental measurements of $\phi_s^{c\bar{c}s}$, $\Delta\Gamma_s$ and Γ_s using $B_s^0 \to J/\psi\phi$, $J/\psi K^+K^-$, $\psi(2S)\phi$, $J/\psi\pi^+\pi^-$ and $D_s^+D_s^-$ decays. Only the solution with $\Delta\Gamma_s > 0$ is shown, since the two-fold ambiguity has been resolved in Ref. [111]. The first error is due to statistics, the second one to systematics. The last line gives our average

Exp.	Mode	Dataset	$\phi_s^{c\bar{c}s}$	$\Delta\Gamma_s$ (ps^{-1})	Refs.
CDF	$J/\psi\phi$	9.6 fb^{-1}	$[-0.60, +0.12]$, 68% CL	$+0.068 \pm 0.026 \pm 0.009$	[197]
D0	$J/\psi\phi$	8.0 fb^{-1}	$-0.55^{+0.38}_{-0.36}$	$+0.163^{+0.065}_{-0.064}$	[198]
ATLAS	$J/\psi\phi$	4.9 fb^{-1}	$+0.12 \pm 0.25 \pm 0.05$	$+0.053 \pm 0.021 \pm 0.010$	[199]
ATLAS	$J/\psi\phi$	14.3 fb^{-1}	$-0.110 \pm 0.082 \pm 0.042$	$+0.101 \pm 0.013 \pm 0.007$	[200]
ATLAS		Above 2 combined	$-0.090 \pm 0.078 \pm 0.041$	$+0.085 \pm 0.011 \pm 0.007$	[200]
CMS	$J/\psi\phi$	19.7 fb^{-1}	$-0.075 \pm 0.097 \pm 0.031$	$+0.095 \pm 0.013 \pm 0.007$	[201]
LHCb	$J/\psi K^+K^-$	3.0 fb^{-1}	$-0.058 \pm 0.049 \pm 0.006$	$+0.0805 \pm 0.0091 \pm 0.0032$	[202]
LHCb	$J/\psi\pi^+\pi^-$	3.0 fb^{-1}	$+0.070 \pm 0.068 \pm 0.008$	–	[240]
LHCb		Above 2 combined	-0.010 ± 0.039(tot)	–	[202]
LHCb	$\psi(2S)\phi$	3.0 fb^{-1}	$+0.23^{+0.29}_{-0.28} \pm 0.02$	$+0.066^{+0.41}_{-0.44} \pm 0.007$	[203]
LHCb	$D_s^+D_s^-$	3.0 fb^{-1}	$+0.02 \pm 0.17 \pm 0.02$	–	[242]
All combined			-0.030 ± 0.033	$+0.085 \pm 0.007$	

for $\Delta\Gamma_s$ is the one of Eq. (72), which includes all available information on $\Delta\Gamma_s$.

In the Standard Model and ignoring sub-leading penguin contributions, $\phi_s^{c\bar{c}s}$ is expected to be equal to $-2\beta_s$, where $\beta_s = \arg\left[-\left(V_{ts}V_{tb}^*\right)/\left(V_{cs}V_{cb}^*\right)\right]$ is a phase analogous to the angle β of the usual CKM unitarity triangle (aside from a sign change). An indirect determination via global fits to experimental data gives [193]

$$(\phi_s^{c\bar{c}s})^{\rm SM} = -2\beta_s = -0.0370 \pm 0.0006. \tag{90}$$

The average value of $\phi_s^{c\bar{c}s}$ from Eq. (89) is consistent with this Standard Model expectation.

From its measurements of time-dependent CP violation in $B_s^0 \to K^+K^-$ decays, the LHCb collaboration has determined the B_s^0 mixing phase to be $-2\beta_s = -0.12^{+0.14}_{-0.12}$ [243], assuming a U-spin relation (with up to 50% breaking effects) between the decay amplitudes of $B_s^0 \to K^+K^-$ and $B^0 \to \pi^+\pi^-$, and a value of the CKM angle γ of $(70.1 \pm 7.1)^\circ$. This determination is compatible with, and less precise than, the world average of $\phi_s^{c\bar{c}s}$ from Eq. (89).

New physics could contribute to $\phi_s^{c\bar{c}s}$. Assuming that new physics only enters in M_{12}^s (rather than in Γ_{12}^s), one can write [208,209]

$$\phi_s^{c\bar{c}s} = -2\beta_s + \phi_{12}^{s,\rm NP}, \tag{91}$$

where the new physics phase $\phi_{12}^{s,\rm NP}$ is the same as that appearing in Eq. (86). In this case

$$\phi_{12}^s = \phi_{12}^{s,\rm SM} + 2\beta_s + \phi_s^{c\bar{c}s} = 0.012 \pm 0.033, \tag{92}$$

where the numerical estimation was performed with the values of Eqs. (85), (89) and (90). Keeping in mind the approximation and assumption mentioned above, this can serve as a reference value to which the measurement of Eq. (87) can be compared.

4 Measurements related to unitarity triangle angles

The charge of the "$CP(t)$ and Unitarity Triangle angles" group is to provide averages of measurements obtained from analyses of decay-time-dependent asymmetries, and other quantities that are related to the angles of the Unitarity Triangle (UT). In cases where considerable theoretical input is required to extract the fundamental quantities, no attempt to do so is made. However, straightforward interpretations of the averages are given, where possible.

In Sect. 4.1 a brief introduction to the relevant phenomenology is given. In Sect. 4.2 an attempt is made to clarify the various different notations in use. In Sect. 4.3 the common inputs to which experimental results are rescaled in the averaging procedure are listed. We also briefly introduce the treatment of experimental errors. In the remainder of this section, the experimental results and their averages are given, divided into subsections based on the underlying quark-level decays. All the measurements reported are quantities determined from decay-time-dependent analyses, with the exception of several in Sect. 4.14, which are related to the UT angle γ and are obtained from decay-time-integrated analyses. In the compilations of measurements, indications of the sizes of the data samples used by each experiment are given. For the e^+e^- B factory experiments, this is quoted in terms of the number of $B\bar{B}$ pairs in the data sample, while the integrated luminosity is given for experiments at hadron colliders.

4.1 Introduction

The Standard Model Cabibbo–Kobayashi–Maskawa (CKM) quark mixing matrix V must be unitary. The CKM matrix has four free parameters and these are conventionally written by the product of three (complex) rotation matrices [244], where the rotations are characterised by the Euler mixing angles between the generations, θ_{12}, θ_{13} and θ_{23}, and one overall phase δ,

$$V = \begin{pmatrix} V_{ud} & V_{us} & V_{ub} \\ V_{cd} & V_{cs} & V_{cb} \\ V_{td} & V_{ts} & V_{tb} \end{pmatrix} = \begin{pmatrix} c_{12}c_{13} & s_{12}c_{13} & s_{13}e^{-i\delta} \\ -s_{12}c_{23} - c_{12}s_{23}s_{13}e^{i\delta} & c_{12}c_{23} - s_{12}s_{23}s_{13}e^{i\delta} & s_{23}c_{13} \\ s_{12}s_{23} - c_{12}c_{23}s_{13}e^{i\delta} & -c_{12}s_{23} - s_{12}c_{23}s_{13}e^{i\delta} & c_{23}c_{13} \end{pmatrix} \tag{93}$$

where $c_{ij} = \cos\theta_{ij}$, $s_{ij} = \sin\theta_{ij}$ for $i < j = 1, 2, 3$.

Following the observation of a hierarchy between the different matrix elements, the Wolfenstein parametrisation [245] is an expansion of V in terms of the four real parameters λ (the expansion parameter), A, ρ and η. Defining to all orders in λ [246]

$$\begin{aligned} s_{12} &\equiv \lambda, \\ s_{23} &\equiv A\lambda^2, \\ s_{13}e^{-i\delta} &\equiv A\lambda^3(\rho - i\eta), \end{aligned} \tag{94}$$

and inserting these into the representation of Eq. (93), unitarity of the CKM matrix is achieved to all orders. A Taylor expansion of V leads to the familiar approximation

$$V = \begin{pmatrix} 1 - \lambda^2/2 & \lambda & A\lambda^3(\rho - i\eta) \\ -\lambda & 1 - \lambda^2/2 & A\lambda^2 \\ A\lambda^3(1 - \rho - i\eta) & -A\lambda^2 & 1 \end{pmatrix} + \mathcal{O}\left(\lambda^4\right). \tag{95}$$

At order λ^5, the obtained CKM matrix in this extended Wolfenstein parametrisation is:

$$V = \begin{pmatrix} 1 - \frac{1}{2}\lambda^2 - \frac{1}{8}\lambda^4 & \lambda & A\lambda^3(\rho - i\eta) \\ -\lambda + \frac{1}{2}A^2\lambda^5\left[1 - 2(\rho + i\eta)\right] & 1 - \frac{1}{2}\lambda^2 - \frac{1}{8}\lambda^4(1 + 4A^2)A\lambda^2 & \\ A\lambda^3\left[1 - (1 - \frac{1}{2}\lambda^2)(\rho + i\eta)\right] & -A\lambda^2 + \frac{1}{2}A\lambda^4\left[1 - 2(\rho + i\eta)\right] & 1 - \frac{1}{2}A^2\lambda^4 \end{pmatrix} + \mathcal{O}\left(\lambda^6\right). \tag{96}$$

A non-zero value of η implies that the CKM matrix is not purely real in this, or any, parametrisation, and is the origin of

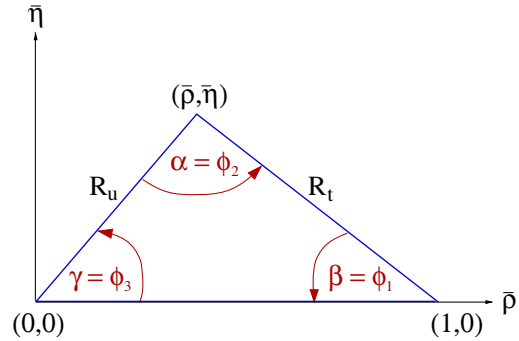

Fig. 11 The unitarity triangle

CP violation in the Standard Model. This is encapsulated in a parametrisation-invariant way through the Jarlskog parameter $J = \mathrm{Im}\left(V_{us}V_{cb}V_{ub}^*V_{cs}^*\right)$ [247].

The unitarity relation $V^\dagger V = \mathit{1}$ results in a total of nine expressions, that can be written as $\sum_{i=u,c,t} V_{ij}^* V_{ik} = \delta_{jk}$, where δ_{jk} is the Kronecker symbol. Of the off-diagonal expressions ($j \neq k$), three can be transformed into the other three (under $j \leftrightarrow k$, corresponding to complex conjugation). This leaves three relations in which three complex numbers sum to zero, which therefore can be expressed as triangles in the complex plane, together with three relations in which the squares of the elements in each column of the CKM matrix sum to unity. Similar relations are obtained for the rows of the matrix from $VV^\dagger = \mathit{1}$, so there are in total six triangle relations and six sums to unity. More details about unitarity triangles can be found in Refs. [248–251].

One of the triangle relations,

$$V_{ud}V_{ub}^* + V_{cd}V_{cb}^* + V_{td}V_{tb}^* = 0, \tag{97}$$

is of particular importance to the B system, being specifically related to flavour-changing neutral-current $b \to d$ transitions. The three terms in Eq. (97) are of the same order, $\mathcal{O}(\lambda^3)$, and this relation is commonly known as the Unitarity Triangle. For presentational purposes, it is convenient to rescale the triangle by $(V_{cd}V_{cb}^*)^{-1}$, as shown in Fig. 11.

Two popular naming conventions for the UT angles exist in the literature:

$$\alpha \equiv \phi_2 = \arg\left[-\frac{V_{td}V_{tb}^*}{V_{ud}V_{ub}^*}\right],$$
$$\beta \equiv \phi_1 = \arg\left[-\frac{V_{cd}V_{cb}^*}{V_{td}V_{tb}^*}\right],$$
$$\gamma \equiv \phi_3 = \arg\left[-\frac{V_{ud}V_{ub}^*}{V_{cd}V_{cb}^*}\right]. \quad (98)$$

In this document the (α, β, γ) set is used. The sides R_u and R_t of the Unitarity Triangle (the third side being normalised to unity) are given by

$$R_u = \left|\frac{V_{ud}V_{ub}^*}{V_{cd}V_{cb}^*}\right| = \sqrt{\overline{\rho}^2 + \overline{\eta}^2},$$
$$R_t = \left|\frac{V_{td}V_{tb}^*}{V_{cd}V_{cb}^*}\right| = \sqrt{(1-\overline{\rho})^2 + \overline{\eta}^2}. \quad (99)$$

where $\overline{\rho}$ and $\overline{\eta}$ define the apex of the Unitarity Triangle [246]

$$\overline{\rho} + i\overline{\eta} \equiv -\frac{V_{ud}V_{ub}^*}{V_{cd}V_{cb}^*} \equiv 1 + \frac{V_{td}V_{tb}^*}{V_{cd}V_{cb}^*}$$
$$= \frac{\sqrt{1-\lambda^2}\,(\rho + i\eta)}{\sqrt{1-A^2\lambda^4} + \sqrt{1-\lambda^2}A^2\lambda^4(\rho + i\eta)}. \quad (100)$$

The exact relation between (ρ, η) and $(\overline{\rho}, \overline{\eta})$ is

$$\rho + i\eta = \frac{\sqrt{1-A^2\lambda^4}(\overline{\rho} + i\overline{\eta})}{\sqrt{1-\lambda^2}\left[1 - A^2\lambda^4(\overline{\rho} + i\overline{\eta})\right]}. \quad (101)$$

By expanding in powers of λ, several useful approximate expressions can be obtained, including

$$\overline{\rho} = \rho\left(1 - \frac{1}{2}\lambda^2\right) + \mathcal{O}(\lambda^4),$$
$$\overline{\eta} = \eta\left(1 - \frac{1}{2}\lambda^2\right) + \mathcal{O}(\lambda^4),$$
$$V_{td} = A\lambda^3(1 - \overline{\rho} - i\overline{\eta}) + \mathcal{O}(\lambda^6). \quad (102)$$

Recent world average values for the Wolfenstein parameters, evaluated using many of the measurements reported in this document, are [252]

$$A = 0.8227^{+0.0066}_{-0.0136}, \quad \lambda = 0.22543^{+0.00042}_{-0.00031},$$
$$\overline{\rho} = 0.1504^{+0.0121}_{-0.0062}, \quad \overline{\eta} = 0.3540^{+0.0069}_{-0.0076}. \quad (103)$$

The relevant unitarity triangle for the $b \to s$ transition is obtained by replacing $d \leftrightarrow s$ in Eq. (97). Definitions of the set of angles $(\alpha_s, \beta_s, \gamma_s)$ can be obtained using equivalent relations to those of Eq. (98). However, this gives a value of β_s that is negative in the Standard Model, so that the sign is usually flipped in the literature; this convention, i.e. $\beta_s = \arg\left[-(V_{ts}V_{tb}^*)/(V_{cs}V_{cb}^*)\right]$, is also followed here and in Sect. 3. Since the sides of the $b \to s$ unitarity triangle are not all of the same order of λ, the triangle is squashed and $\beta_s \sim \lambda^2\eta$.

4.2 Notations

Several different notations for *CP* violation parameters are commonly used. This section reviews those found in the experimental literature, in the hope of reducing the potential for confusion, and to define the frame that is used for the averages.

In some cases, when B mesons decay into multibody final states via broad resonances (ρ, K^*, etc.), the experimental analyses ignore the effects of interference between the overlapping structures. This is referred to as the quasi-two-body (Q2B) approximation in the following.

4.2.1 CP asymmetries

The *CP* asymmetry is defined as the difference between the rate involving a b quark and that involving a $\bar{b}$ quark, divided by the sum. For example, the partial rate (or charge) asymmetry for a charged B decay would be given as

$$\mathcal{A}_f \equiv \frac{\Gamma(B^- \to f) - \Gamma(B^+ \to \bar{f})}{\Gamma(B^- \to f) + \Gamma(B^+ \to \bar{f})}. \quad (104)$$

4.2.2 Time-dependent CP asymmetries in decays to CP eigenstates

If the amplitudes for B^0 and $\overline{B}^0$ to decay to a final state f, which is a *CP* eigenstate with eigenvalue η_f, are given by A_f and $\overline{A}_f$, respectively, then the decay distributions for neutral B mesons, with known (i.e. "tagged") flavour at time $\Delta t = 0$, are given by

$$\Gamma_{\overline{B}^0 \to f}(\Delta t) = \frac{e^{-|\Delta t|/\tau(B^0)}}{4\tau(B^0)}\left[1 + \frac{2\,\mathrm{Im}(\lambda_f)}{1+|\lambda_f|^2}\sin(\Delta m \Delta t) - \frac{1-|\lambda_f|^2}{1+|\lambda_f|^2}\cos(\Delta m \Delta t)\right], \quad (105)$$

$$\Gamma_{B^0 \to f}(\Delta t) = \frac{e^{-|\Delta t|/\tau(B^0)}}{4\tau(B^0)}\left[1 - \frac{2\,\mathrm{Im}(\lambda_f)}{1+|\lambda_f|^2}\sin(\Delta m \Delta t) + \frac{1-|\lambda_f|^2}{1+|\lambda_f|^2}\cos(\Delta m \Delta t)\right]. \quad (106)$$

Here $\lambda_f = \frac{q}{p}\frac{\overline{A}_f}{A_f}$ contains terms related to B^0–$\overline{B}^0$ mixing and to the decay amplitude (the eigenstates of the $B^0\overline{B}^0$ system with physical masses and lifetimes are $|B_\pm\rangle = p|B^0\rangle \pm q|\overline{B}^0\rangle$). This formulation assumes *CPT* invariance, and neglects possible lifetime differences between the two physical states (see Sect. 3.3 where the mass difference Δm is also defined) in the neutral B meson system. The case

where non-zero lifetime differences are taken into account is discussed in Sect. 4.2.3.

The notation and normalisation used in Eqs. (105) and (106) are relevant for the e^+e^- B factory experiments. In this case, neutral B mesons are produced via the $e^+e^- \to \Upsilon(4S) \to B\overline{B}$ process, and the wavefunction of the produced $B\overline{B}$ pair evolves coherently until one meson decays. When one of the pair decays into a final state that tags its flavour, the flavour of the other at that instant is known. The evolution of the other neutral B meson is therefore described in terms of Δt, the difference between the decay times of the two mesons in the pair. At hadron collider experiments, t is usually used in place of Δt since the flavour tagging is done at production ($t = 0$); due to the nature of the production in hadron colliders (incoherent $b\bar{b}$ quark pair production with many additional associated particles), very different methods are used for tagging compared to those in e^+e^- experiments. Moreover, since negative values of t are not possible, the normalisation is such that $\int_0^{+\infty}(\Gamma_{\overline{B}^0\to f}(t) + \Gamma_{B^0\to f}(t))dt = 1$, rather than $\int_{-\infty}^{+\infty}(\Gamma_{\overline{B}^0\to f}(\Delta t) + \Gamma_{B^0\to f}(\Delta t))d(\Delta t) = 1$, as in Eqs. (105) and (106).

The time-dependent CP asymmetry, again defined as the difference between the rate involving a b quark and that involving a $\bar{b}$ quark, is then given by

$$\begin{aligned}\mathcal{A}_f(\Delta t) &\equiv \frac{\Gamma_{\overline{B}^0\to f}(\Delta t) - \Gamma_{B^0\to f}(\Delta t)}{\Gamma_{\overline{B}^0\to f}(\Delta t) + \Gamma_{B^0\to f}(\Delta t)} \\ &= \frac{2\,\mathrm{Im}(\lambda_f)}{1+|\lambda_f|^2}\sin(\Delta m\Delta t) \\ &\quad -\frac{1-|\lambda_f|^2}{1+|\lambda_f|^2}\cos(\Delta m\Delta t). \end{aligned} \tag{107}$$

While the coefficient of the $\sin(\Delta m\Delta t)$ term in Eq. (107) is customarily[19] denoted S_f:

$$S_f \equiv \frac{2\,\mathrm{Im}(\lambda_f)}{1+|\lambda_f|^2}, \tag{108}$$

different notations are in use for the coefficient of the $\cos(\Delta m\Delta t)$ term:

$$C_f \equiv -A_f \equiv \frac{1-|\lambda_f|^2}{1+|\lambda_f|^2}. \tag{109}$$

The C notation has been used by the BaBar collaboration (see e.g. Ref. [253]), and is also adopted in this document. The A notation has been used by the Belle collaboration (see e.g. Ref. [254]). When the final state is a CP eigenstate, the notation S_{CP} and C_{CP} is widely used, including in this document, instead of specifying the final state f. In addition, particularly when grouping together measurements with different final states mediated by the same quark-level transition, the S, C notation with a subscript indicating the transition is used.

Neglecting effects due to CP violation in mixing (by taking $|q/p| = 1$), if the decay amplitude contains terms with a single weak (i.e. CP violating) phase then $|\lambda_f| = 1$ and one finds $S_f = -\eta_f \sin(\phi_{\mathrm{mix}} + \phi_{\mathrm{dec}})$, $C_f = 0$, where $\phi_{\mathrm{mix}} = \arg(q/p)$ and $\phi_{\mathrm{dec}} = \arg(\overline{A}_f/A_f)$. Note that the B^0–$\overline{B}^0$ mixing phase ϕ_{mix} is approximately equal to 2β in the Standard Model (in the usual phase convention) [255,256].

If amplitudes with different weak phases contribute to the decay, no clean interpretation of S_f is possible without further input. In this document, only the theoretically cleanest channels are interpreted as measurements of the weak phase (e.g. $b \to c\bar{c}s$ transitions for $\sin(2\beta)$), though even in these cases some care is necessary. In channels in which the second amplitude is expected to be suppressed, the concept of an effective weak phase difference is sometimes used, e.g. $\sin(2\beta^{\mathrm{eff}})$ in $b \to q\bar{q}s$ transition.

If, in addition to having a weak phase difference, the decay amplitudes have different CP conserving strong phases, then $|\lambda_f| \neq 1$. Additional input is required for interpretation of the results. The coefficient of the cosine term becomes non-zero, indicating CP violation in decay.

Due to the fact that $\sin(\Delta m\Delta t)$ and $\cos(\Delta m\Delta t)$ are respectively odd and even functions of Δt, only small correlations (that can be induced by backgrounds, for example) between S_f and C_f are expected at an e^+e^- B factory experiment, where the range of Δt is $-\infty < \Delta t < +\infty$. The situation is different for measurements at hadron collider experiments, where the range of the time variable is $0 < t < +\infty$, so that more sizable correlations can be expected. We include the correlations in the averages where available.

Frequently, we are interested in combining measurements governed by similar or identical short-distance physics, but with different final states (e.g., $B^0 \to J/\psi K_S^0$ and $B^0 \to J/\psi K_L^0$). In this case, we remove the dependence on the CP eigenvalue of the final state by quoting $-\eta S_f$. In cases where the final state is not a CP eigenstate but has an effective CP content (see below), the reported $-\eta S$ is corrected by the effective CP.

4.2.3 *Time-dependent distributions with non-zero decay width difference*

A complete analysis of the time-dependent decay rates of neutral B mesons must also take into account the difference in lifetimes, denoted $\Delta\Gamma$, between the mass eigenstates. This is particularly important in the B_s^0 system, since a non-

[19] Occasionally one also finds Eq. (107) written as $\mathcal{A}_f(\Delta t) = \mathcal{A}_f^{\mathrm{mix}}\sin(\Delta m\Delta t) + \mathcal{A}_f^{\mathrm{dir}}\cos(\Delta m\Delta t)$, or similar.

negligible value of $\Delta\Gamma_s$ has been established (see Sect. 3.3 for the latest experimental constraints). The formalism given here is therefore appropriate for measurements of B_s^0 decays to a CP eigenstate f as studied at hadron colliders, but appropriate modifications for B^0 mesons or for the e^+e^- environment are straightforward to make.

Neglecting CP violation in mixing, the relevant replacements for Eqs. (105) and (106) are [257]

$$\Gamma_{\bar{B}_s^0\to f}(t) = \mathcal{N}\frac{e^{-t/\tau(B_s^0)}}{2\tau(B_s^0)}\Bigg[\cosh\left(\frac{\Delta\Gamma_s t}{2}\right) + S_f\sin(\Delta m_s t) - C_f\cos\left(\Delta m_s t\right) + A_f^{\Delta\Gamma}\sinh\left(\frac{\Delta\Gamma_s t}{2}\right)\Bigg], \tag{110}$$

and

$$\Gamma_{B_s^0\to f}(t) = \mathcal{N}\frac{e^{-t/\tau(B_s^0)}}{2\tau(B_s^0)}\Bigg[\cosh\left(\frac{\Delta\Gamma_s t}{2}\right) - S_f\sin\left(\Delta m_s t\right) + C_f\cos\left(\Delta m_s t\right) + A_f^{\Delta\Gamma}\sinh\left(\frac{\Delta\Gamma_s t}{2}\right)\Bigg], \tag{111}$$

where S_f and C_f are as defined in Eqs. (108) and (109), respectively, $\tau(B_s^0) = 1/\Gamma_s$ is defined in Sect. 3.2.4, and the coefficient of the sinh term is[20]

$$A_f^{\Delta\Gamma} = -\frac{2\,\mathrm{Re}(\lambda_f)}{1+|\lambda_f|^2}. \tag{112}$$

With the requirement $\int_0^{+\infty}[\Gamma_{\bar{B}_s^0\to f}(t) + \Gamma_{B_s^0\to f}(t)]dt = 1$, the normalisation factor is fixed to $\mathcal{N} = (1-(\frac{\Delta\Gamma_s}{2\Gamma_s})^2)/(1+\frac{A_f^{\Delta\Gamma}\Delta\Gamma_s}{2\Gamma_s})$.[21]

A time-dependent analysis of CP asymmetries in flavour-tagged B_s^0 decays to a CP eigenstate f can thus determine the parameters S_f, C_f and $A_f^{\Delta\Gamma}$. Note that, by definition,

$$(S_f)^2 + (C_f)^2 + (A_f^{\Delta\Gamma})^2 = 1, \tag{113}$$

and this constraint can be imposed or not in the fits. Since these parameters have sensitivity to both $\mathrm{Im}(\lambda_f)$ and $\mathrm{Re}(\lambda_f)$, alternative choices of parametrisation, including those directly involving CP violating phases (such as β_s), are possible. These can also be adopted for vector-vector final states.

The *untagged* time-dependent decay rate is given by

$$\Gamma_{\bar{B}_s^0\to f}(t) + \Gamma_{B_s^0\to f}(t) = \mathcal{N}\frac{e^{-t/\tau(B_s^0)}}{\tau(B_s^0)} \times\Bigg[\cosh\left(\frac{\Delta\Gamma_s t}{2}\right) + A_f^{\Delta\Gamma}\sinh\left(\frac{\Delta\Gamma_s t}{2}\right)\Bigg]. \tag{114}$$

Thus, an untagged time-dependent analysis can probe λ_f, through the dependence of $A_f^{\Delta\Gamma}$ on $\mathrm{Re}(\lambda_f)$, when $\Delta\Gamma_s \neq 0$. This is equivalent to determining the "*effective lifetime*" [112], as discussed in Sect. 3.2.4. The analysis of flavour-tagged B_s^0 mesons is, of course, more sensitive.

The discussion in this and the previous section is relevant for decays to CP eigenstates. In the following sections, various cases of time-dependent CP asymmetries in decays to non-CP eigenstates are considered. For brevity, these will be given assuming that the decay width difference $\Delta\Gamma$ is negligible. Modifications similar to those described here can be made to take into account a non-zero decay width difference.

4.2.4 *Time-dependent CP asymmetries in decays to vector-vector final states*

Consider B decays to states consisting of two spin-1 particles, such as $J/\psi K^{*0}(\to K_S^0\pi^0)$, $J/\psi\phi$, $D^{*+}D^{*-}$ and $\rho^+\rho^-$, which are eigenstates of charge conjugation but not of parity.[22] For such a system, there are three possible final states: in the helicity basis these can be written h_{-1}, h_0, h_{+1}. The h_0 state is an eigenstate of parity, and hence of CP, however CP transforms $h_{+1} \leftrightarrow h_{-1}$ (up to an unobservable phase). In the transversity basis, these states are transformed into $h_\parallel = (h_{+1}+h_{-1})/2$ and $h_\perp = (h_{+1}-h_{-1})/2$. In this basis all three states are CP eigenstates, and $h_\perp$ has the opposite CP to the others.

The amplitude for decays to the transversity basis states are usually given by $A_{0,\perp,\parallel}$, with normalisation such that $|A_0|^2 + |A_\perp|^2 + |A_\parallel|^2 = 1$. Given the relation between the CP eigenvalues of the states, the effective CP content of the vector-vector state is known if $|A_\perp|^2$ is measured. An alternative strategy is to measure just the longitudinally polarised component, $|A_0|^2$ (sometimes denoted by f_{long}), which allows a limit to be set on the effective CP since $|A_\perp|^2 \leq |A_\perp|^2 + |A_\parallel|^2 = 1 - |A_0|^2$. The value of the effective CP content can be used to treat the decay with the same formalism as for CP eigenstates. The most complete treatment for neutral B decays to vector-vector final states is, however, time-dependent angular analysis (also known as time-dependent transversity analysis). In such an analysis, interference between CP-even and CP-odd states pro-

[20] As ever, alternative and conflicting notations appear in the literature. One popular alternative notation for this parameter is $\mathcal{A}_{\Delta\Gamma}$. Particular care must be taken over the signs.

[21] The prefactor of $\mathcal{N}/2\tau(B_s^0)$ in Eqs. (108) and (109) has been chosen so that $\mathcal{N} = 1$ in the limit $\Delta\Gamma_s = 0$. In the e^+e^- environment, where the range is $-\infty < \Delta t < \infty$, the prefactor should be $\mathcal{N}/4\tau(B_s^0)$ and $\mathcal{N} = 1 - (\frac{\Delta\Gamma_s}{2\Gamma_s})^2$.

[22] This is not true for all vector-vector final states, e.g., $D^{*\pm}\rho^\mp$ is clearly not an eigenstate of charge conjugation.

vides additional sensitivity to the weak and strong phases involved.

In most analyses of time-dependent CP asymmetries in decays to vector-vector final states carried out to date, an assumption has been made that each helicity (or transversity) amplitude has the same weak phase. This is a good approximation for decays that are dominated by amplitudes with a single weak phase, such $B^0 \to J/\psi K^{*0}$, and is a reasonable approximation in any mode for which only very limited statistics are available. However, for modes that have contributions from amplitudes with different weak phases, the relative size of these contributions can be different for each helicity (or transversity) amplitude, and therefore the time-dependent CP asymmetry parameters can also differ. The most generic analysis, suitable for modes with sufficient statistics, allows for this effect; such an analysis has been carried out by LHCb for the $B^0 \to J/\psi \rho^0$ decay [258]. An intermediate analysis can allow different parameters for the CP-even and CP-odd components; such an analysis has been carried out by BaBar for the decay $B^0 \to D^{*+}D^{*-}$ [259]. The independent treatment of each helicity (or transversity) amplitude, as in the latest result on $B_s^0 \to J/\psi\phi$ [202] (discussed in Sect. 3), becomes increasingly important for high precision measurements.

4.2.5 *Time-dependent asymmetries: self-conjugate multiparticle final states*

Amplitudes for neutral B decays into self-conjugate multiparticle final states such as $\pi^+\pi^-\pi^0$, $K^+K^-K_S^0$, $\pi^+\pi^-K_S^0$, $J/\psi\pi^+\pi^-$ or $D\pi^0$ with $D \to K_S^0\pi^+\pi^-$ may be written in terms of CP-even and CP-odd amplitudes. As above, the interference between these terms provides additional sensitivity to the weak and strong phases involved in the decay, and the time-dependence depends on both the sine and cosine of the weak phase difference. In order to perform unbinned maximum likelihood fits, and thereby extract as much information as possible from the distributions, it is necessary to choose a model for the multiparticle decay, and therefore the results acquire some model dependence. In certain cases, model-independent methods are also possible, but the resulting need to bin the Dalitz plot leads to some loss of statistical precision. The number of observables depends on the final state (and on the model used); the key feature is that as long as there are regions where both CP-even and CP-odd amplitudes contribute, the interference terms will be sensitive to the cosine of the weak phase difference. Therefore, these measurements allow distinction between multiple solutions for, e.g., the two values of 2β from the measurement of $\sin(2\beta)$.

We now consider the various notations that have been used in experimental studies of time-dependent asymmetries in decays to self-conjugate multiparticle final states.

$B^0 \to D^{(*)}h^0$ with $D \to K_S^0\pi^+\pi^-$

The states $D\pi^0$, $D^*\pi^0$, $D\eta$, $D^*\eta$, $D\omega$ are collectively denoted $D^{(*)}h^0$. When the D decay model is fixed, fits to the time-dependent decay distributions can be performed to extract the weak phase difference. However, it is experimentally advantageous to use the sine and cosine of this phase as fit parameters, since these behave as essentially independent parameters, with low correlations and (potentially) rather different uncertainties. A parameter representing CP violation in the B decay can be simultaneously determined. For consistency with other analyses, this could be chosen to be C_f, but could equally well be $|\lambda_f|$, or other possibilities.

Belle performed an analysis of these channels with $\sin(2\phi_1)$ and $\cos(2\phi_1)$ as free parameters [260]. BaBar has performed an analysis in which $|\lambda_f|$ was also determined [261]. Belle has in addition performed a model-independent analysis [262] using as input information about the average strong phase difference between symmetric bins of the Dalitz plot determined by CLEO-c [263].[23] The results of this analysis are measurements of $\sin(2\phi_1)$ and $\cos(2\phi_1)$.

$B^0 \to D^{*+}D^{*-}K_S^0$

The hadronic structure of the $B^0 \to D^{*+}D^{*-}K_S^0$ decay is not sufficiently well understood to perform a full time-dependent Dalitz plot analysis. Instead, following Ref. [264], BaBar [265] and Belle [266] divide the Dalitz plane in two regions: $m(D^{*+}K_S^0)^2 > m(D^{*-}K_S^0)^2$ ($\eta_y = +1$) and $m(D^{*+}K_S^0)^2 < m(D^{*-}K_S^0)^2$ ($\eta_y = -1$); and then fit to a decay time distribution with asymmetry given by

$$\mathcal{A}_f(\Delta t) = \eta_y \frac{J_c}{J_0}\cos(\Delta m \Delta t) - \left[\frac{2J_{s1}}{J_0}\sin(2\beta) + \eta_y \frac{2J_{s2}}{J_0}\cos(2\beta)\right]\sin(\Delta m \Delta t)\,. \tag{115}$$

The fitted observables are $\frac{J_c}{J_0}$, $\frac{2J_{s1}}{J_0}\sin(2\beta)$ and $\frac{2J_{s2}}{J_0}\cos(2\beta)$, where the parameters J_0, J_c, J_{s1} and J_{s2} are the integrals over the half Dalitz plane $m(D^{*+}K_S^0)^2 < m(D^{*-}K_S^0)^2$ of the functions $|a|^2 + |\bar{a}|^2$, $|a|^2 - |\bar{a}|^2$, $\mathrm{Re}(\bar{a}a^*)$ and $\mathrm{Im}(\bar{a}a^*)$ respectively, where a and $\bar{a}$ are the decay amplitudes of $B^0 \to D^{*+}D^{*-}K_S^0$ and $\overline{B}^0 \to D^{*+}D^{*-}K_S^0$ respectively. The parameter J_{s2} (and hence J_{s2}/J_0) is predicted to be pos-

[23] The external input needed for this analysis is the same as in the model-independent analysis of $B^+ \to DK^+$ with $D \to K_S^0\pi^+\pi^-$, discussed in Sect. 4.14.5.

itive; assuming this prediction to be correct, it is possible to determine the sign of $\cos(2\beta)$.

$B^0 \to J/\psi\pi^+\pi^-$

Amplitude analyses of $B^0 \to J/\psi\pi^+\pi^-$ decays [258, 267] show large contributions from the $\rho(770)^0$ and $f_0(500)$ states, together with smaller contributions from higher resonances. Since modelling the $f_0(500)$ structure is challenging [268], it is difficult to determine reliably its associated CP violation parameters. Corresponding parameters for the $J/\psi\rho^0$ decay can, however, be determined. In the LHCb analysis [258], $2\beta^{\text{eff}}$ is determined from the fit; results are then converted into values for S_{CP} and C_{CP} to allow comparison with other modes. Here, the notation S_{CP} and C_{CP} denotes parameters obtained for the $J/\psi\rho^0$ final state accounting for the composition of CP-even and CP-odd amplitudes (while assuming that all amplitudes involve the same phases), so that no dilution occurs. Possible CP violation effects in the other amplitudes contributing to the Dalitz plot are treated as a source of systematic uncertainty.

Amplitude analyses have also been done for the $B_s^0 \to J/\psi\pi^+\pi^-$ decay, where the final state is dominated by scalar resonances including the $f_0(980)$ [240,241]. Time-dependent analyses of this B_s^0 decay allow a determination of $2\beta_s$, as discussed in Sect. 3.

$B^0 \to K^+K^-K^0$

Studies of $B^0 \to K^+K^-K^0$ [269–271] and of the related decay $B^+ \to K^+K^-K^+$ [271–273], show that the decay is dominated by a large nonresonant contribution with significant components from the intermediate K^+K^- resonances $\phi(1020)$, $f_0(980)$, and other higher resonances, as well as a contribution from χ_{c0}.

The full time-dependent Dalitz plot analysis allows the complex amplitudes of each contributing term to be determined from data, including CP violation effects (i.e. allowing the complex amplitude for the B^0 decay to be independent from that for $\overline{B}^0$ decay), although one amplitude must be fixed to serve as a reference. There are several choices for parametrisation of the complex amplitudes (e.g. real and imaginary part, or magnitude and phase). Similarly, there are various approaches to include CP violation effects. Note that positive definite parameters such as magnitudes are disfavoured in certain circumstances (they inevitably lead to biases for small values). In order to compare results between analyses, it is useful for each experiment to present results in terms of the parameters that can be measured in a Q2B analysis (such as $\mathcal{A}_f$, S_f, C_f, $\sin(2\beta^{\text{eff}})$, $\cos(2\beta^{\text{eff}})$, etc.)

In the BaBar analysis of the $B^0 \to K^+K^-K^0$ decay [271], the complex amplitude for each resonant contribution is written as

$$A_f = c_f(1+b_f)e^{i(\phi_f+\delta_f)},$$
$$\bar{A}_f = c_f(1-b_f)e^{i(\phi_f-\delta_f)}, \tag{116}$$

where b_f and δ_f introduce CP violation in the magnitude and phase respectively. Belle [270] use the same parametrisation but with a different notation for the parameters.[24] (The weak phase in B^0–$\bar{B}^0$ mixing (2β) also appears in the full formula for the time-dependent decay distribution.) The Q2B parameter of CP violation in decay is directly related to b_f,

$$\mathcal{A}_f = \frac{-2b_f}{1+b_f^2} \approx C_f, \tag{117}$$

and the mixing-induced CP violation parameter can be used to obtain $\sin(2\beta^{\text{eff}})$,

$$-\eta_f S_f \approx \frac{1-b_f^2}{1+b_f^2}\sin(2\beta_f^{\text{eff}}), \tag{118}$$

where the approximations are exact in the case that $|q/p| = 1$.

Both BaBar [271] and Belle [270] present results for c_f and ϕ_f, for each resonant contribution, and in addition present results for $\mathcal{A}_f$ and β_f^{eff} for $\phi(1020)K^0$, $f_0(980)K^0$ and for the remainder of the contributions to the $K^+K^-K^0$ Dalitz plot combined. BaBar also present results for the Q2B parameter S_f for these channels. The models used to describe the resonant structure of the Dalitz plot differ, however. Both analyses suffer from symmetries in the likelihood that lead to multiple solutions, from which we select only one for averaging.

$B^0 \to \pi^+\pi^-K_S^0$

Studies of $B^0 \to \pi^+\pi^-K_S^0$ [274,275] and of the related decay $B^+ \to \pi^+\pi^-K^+$ [272,276–278] show that the decay is dominated by components from intermediate resonances in the $K\pi$ ($K^*(892)$, $K_0^*(1430)$) and $\pi\pi$ ($\rho(770)$, $f_0(980)$, $f_2(1270)$) spectra, together with a poorly understood scalar structure that peaks near $m(\pi\pi) \sim 1300$ MeV/c^2 and is denoted f_X[25] and a large nonresonant component. There is also a contribution from the χ_{c0} state.

The full time-dependent Dalitz plot analysis allows the complex amplitudes of each contributing term to be determined from data, including CP violation effects. In

[24] $(c, b, \phi, \delta) \leftrightarrow (a, c, b, d)$. See Eq. (120).

[25] The f_X component may originate from either the $f_0(1370)$ or $f_0(1500)$ resonances, or from interference between those or other states and nonresonant amplitudes in this region.

the BABAR analysis [274], the magnitude and phase of each component (for both B^0 and $\overline{B}^0$ decays) are measured relative to $B^0 \to f_0(980)K_S^0$, using the following parametrisation

$$A_f = |A_f|e^{i\arg(A_f)} \quad \bar{A}_f = |\bar{A}_f|e^{i\arg(\bar{A}_f)}. \tag{119}$$

In the Belle analysis [275], the $B^0 \to K^{*+}\pi^-$ amplitude is chosen as the reference, and the amplitudes are parametrised as

$$A_f = a_f(1+c_f)e^{i(b_f+d_f)} \quad \bar{A}_f = a_f(1-c_f)e^{i(b_f-d_f)}. \tag{120}$$

In both cases, the results are translated into Q2B parameters such as $2\beta_f^{\rm eff}$, S_f, C_f for each CP eigenstate f, and parameters of CP violation in decay for each flavour-specific state. Relative phase differences between resonant terms are also extracted.

$B^0 \to \pi^+\pi^-\pi^0$

The $B^0 \to \pi^+\pi^-\pi^0$ decay is dominated by intermediate ρ resonances. Though it is possible, as above, to determine directly the complex amplitudes for each component, an alternative approach [279,280] has been used by both BABAR [281,282] and Belle [283,284]. The amplitudes for B^0 and $\overline{B}^0$ decays to $\pi^+\pi^-\pi^0$ are written as

$$\begin{aligned} A_{3\pi} &= f_+A_+ + f_-A_- + f_0A_0, \\ \bar{A}_{3\pi} &= f_+\bar{A}_+ + f_-\bar{A}_- + f_0\bar{A}_0, \end{aligned} \tag{121}$$

respectively. The symbols A_+, A_- and A_0 represent the complex decay amplitudes for $B^0 \to \rho^+\pi^-$, $B^0 \to \rho^-\pi^+$ and $B^0 \to \rho^0\pi^0$ while $\bar{A}_+$, $\bar{A}_-$ and $\bar{A}_0$ represent those for $\overline{B}^0 \to \rho^+\pi^-$, $\overline{B}^0 \to \rho^-\pi^+$ and $\overline{B}^0 \to \rho^0\pi^0$ respectively. The terms f_+, f_- and f_0 incorporate kinematic and dynamical factors and depend on the Dalitz plot coordinates. The full time-dependent decay distribution can then be written in terms of 27 free parameters, one for each coefficient of the form factor bilinears, as listed in Table 22. These parameters are sometimes referred to as "the Us and Is", and can be expressed in terms of A_+, A_-, A_0, $\bar{A}_+$, $\bar{A}_-$ and $\bar{A}_0$. If the full set of parameters is determined, together with their correlations, other parameters, such as weak and strong phases, parameters of CP violation in decay, etc., can be subsequently extracted. Note that one of the parameters (typically U_+^+) is often fixed to unity to provide a reference; this does not affect the analysis.

Table 22 Definitions of the U and I coefficients. Modified from Ref. [281]

Parameter	Description
U_+^+	Coefficient of $\lvert f_+\rvert^2$
U_0^+	Coefficient of $\lvert f_0\rvert^2$
U_-^+	Coefficient of $\lvert f_-\rvert^2$
U_0^-	Coefficient of $\lvert f_0\rvert^2\cos(\Delta m\Delta t)$
U_-^-	Coefficient of $\lvert f_-\rvert^2\cos(\Delta m\Delta t)$
U_+^-	Coefficient of $\lvert f_+\rvert^2\cos(\Delta m\Delta t)$
I_0	Coefficient of $\lvert f_0\rvert^2\sin(\Delta m\Delta t)$
I_-	Coefficient of $\lvert f_-\rvert^2\sin(\Delta m\Delta t)$
I_+	Coefficient of $\lvert f_+\rvert^2\sin(\Delta m\Delta t)$
$U_{+-}^{+,\rm Im}$	Coefficient of $\mathrm{Im}[f_+f_-^*]$
$U_{+-}^{+,\rm Re}$	Coefficient of $\mathrm{Re}[f_+f_-^*]$
$U_{+-}^{-,\rm Im}$	Coefficient of $\mathrm{Im}[f_+f_-^*]\cos(\Delta m\Delta t)$
$U_{+-}^{-,\rm Re}$	Coefficient of $\mathrm{Re}[f_+f_-^*]\cos(\Delta m\Delta t)$
$I_{+-}^{\rm Im}$	Coefficient of $\mathrm{Im}[f_+f_-^*]\sin(\Delta m\Delta t)$
$I_{+-}^{\rm Re}$	Coefficient of $\mathrm{Re}[f_+f_-^*]\sin(\Delta m\Delta t)$
$U_{+0}^{+,\rm Im}$	Coefficient of $\mathrm{Im}[f_+f_0^*]$
$U_{+0}^{+,\rm Re}$	Coefficient of $\mathrm{Re}[f_+f_0^*]$
$U_{+0}^{-,\rm Im}$	Coefficient of $\mathrm{Im}[f_+f_0^*]\cos(\Delta m\Delta t)$
$U_{+0}^{-,\rm Re}$	Coefficient of $\mathrm{Re}[f_+f_0^*]\cos(\Delta m\Delta t)$
$I_{+0}^{\rm Im}$	Coefficient of $\mathrm{Im}[f_+f_0^*]\sin(\Delta m\Delta t)$
$I_{+0}^{\rm Re}$	Coefficient of $\mathrm{Re}[f_+f_0^*]\sin(\Delta m\Delta t)$
$U_{-0}^{+,\rm Im}$	Coefficient of $\mathrm{Im}[f_-f_0^*]$
$U_{-0}^{+,\rm Re}$	Coefficient of $\mathrm{Re}[f_-f_0^*]$
$U_{-0}^{-,\rm Im}$	Coefficient of $\mathrm{Im}[f_-f_0^*]\cos(\Delta m\Delta t)$
$U_{-0}^{-,\rm Re}$	Coefficient of $\mathrm{Re}[f_-f_0^*]\cos(\Delta m\Delta t)$
$I_{-0}^{\rm Im}$	Coefficient of $\mathrm{Im}[f_-f_0^*]\sin(\Delta m\Delta t)$
$I_{-0}^{\rm Re}$	Coefficient of $\mathrm{Re}[f_-f_0^*]\sin(\Delta m\Delta t)$

4.2.6 *Time-dependent CP asymmetries in decays to non-CP eigenstates*

Consider a non-CP eigenstate f, and its conjugate $\bar{f}$. For neutral B decays to these final states, there are four amplitudes to consider: those for B^0 to decay to f and $\bar{f}$ (A_f and $A_{\bar{f}}$, respectively), and the equivalents for $\overline{B}^0$ ($\overline{A}_f$ and $\overline{A}_{\bar{f}}$). If CP is conserved in the decay, then $A_f = \overline{A}_{\bar{f}}$ and $A_{\bar{f}} = \overline{A}_f$.

The time-dependent decay distributions can be written in many different ways. Here, we follow Sect. 4.2.2 and define $\lambda_f = \frac{q}{p}\frac{\overline{A}_f}{A_f}$ and $\lambda_{\bar{f}} = \frac{q}{p}\frac{\overline{A}_{\bar{f}}}{A_{\bar{f}}}$. The time-dependent CP asymmetries that are sensitive to mixing-induced CP violation effects then follow Eq. (107):

$$\begin{aligned} \mathcal{A}_f(\Delta t) &\equiv \frac{\Gamma_{\overline{B}^0\to f}(\Delta t) - \Gamma_{B^0\to f}(\Delta t)}{\Gamma_{\overline{B}^0\to f}(\Delta t) + \Gamma_{B^0\to f}(\Delta t)} \\ &= S_f\sin(\Delta m\Delta t) - C_f\cos(\Delta m\Delta t), \end{aligned} \tag{122}$$

$$\begin{aligned} \mathcal{A}_{\bar{f}}(\Delta t) &\equiv \frac{\Gamma_{\overline{B}^0\to \bar{f}}(\Delta t) - \Gamma_{B^0\to \bar{f}}(\Delta t)}{\Gamma_{\overline{B}^0\to \bar{f}}(\Delta t) + \Gamma_{B^0\to \bar{f}}(\Delta t)} \\ &= S_{\bar{f}}\sin(\Delta m\Delta t) - C_{\bar{f}}\cos(\Delta m\Delta t), \end{aligned} \tag{123}$$

with the definitions of the parameters C_f, S_f, $C_{\bar{f}}$ and $S_{\bar{f}}$, following Eqs. (108) and (109).

The time-dependent decay rates are given by

$$\Gamma_{\overline{B}^0\to f}(\Delta t) = \frac{e^{-|\Delta t|/\tau(B^0)}}{8\tau(B^0)}(1+\langle\mathcal{A}_{f\bar{f}}\rangle) \times\Big[1+S_f\sin(\Delta m\Delta t)-C_f\cos(\Delta m\Delta t)\Big], \tag{124}$$

$$\Gamma_{B^0\to f}(\Delta t) = \frac{e^{-|\Delta t|/\tau(B^0)}}{8\tau(B^0)}(1+\langle\mathcal{A}_{f\bar{f}}\rangle) \times\Big[1-S_f\sin(\Delta m\Delta t)+C_f\cos(\Delta m\Delta t)\Big], \tag{125}$$

$$\Gamma_{\overline{B}^0\to \bar{f}}(\Delta t) = \frac{e^{-|\Delta t|/\tau(B^0)}}{8\tau(B^0)}(1-\langle\mathcal{A}_{f\bar{f}}\rangle) \times\Big[1+S_{\bar{f}}\sin(\Delta m\Delta t)-C_{\bar{f}}\cos(\Delta m\Delta t)\Big], \tag{126}$$

$$\Gamma_{B^0\to \bar{f}}(\Delta t) = \frac{e^{-|\Delta t|/\tau(B^0)}}{8\tau(B^0)}(1-\langle\mathcal{A}_{f\bar{f}}\rangle) \times\Big[1-S_{\bar{f}}\sin(\Delta m\Delta t)+C_{\bar{f}}\cos(\Delta m\Delta t)\Big], \tag{127}$$

where the time-independent parameter $\langle\mathcal{A}_{f\bar{f}}\rangle$ represents an overall asymmetry in the production of the f and $\bar{f}$ final states,[26]

$$\langle\mathcal{A}_{f\bar{f}}\rangle = \frac{\Big(|A_f|^2+|\overline{A}_f|^2\Big)-\Big(|A_{\bar{f}}|^2+|\overline{A}_{\bar{f}}|^2\Big)}{\Big(|A_f|^2+|\overline{A}_f|^2\Big)+\Big(|A_{\bar{f}}|^2+|\overline{A}_{\bar{f}}|^2\Big)}. \tag{128}$$

Assuming $|q/p|=1$, i.e. absence of CP violation in mixing, the parameters C_f and $C_{\bar{f}}$ can also be written in terms of the decay amplitudes as follows:

$$C_f = \frac{|A_f|^2-|\overline{A}_f|^2}{|A_f|^2+|\overline{A}_f|^2} \quad\text{and}\quad C_{\bar{f}} = \frac{|A_{\bar{f}}|^2-|\overline{A}_{\bar{f}}|^2}{|A_{\bar{f}}|^2+|\overline{A}_{\bar{f}}|^2}, \tag{129}$$

giving asymmetries in the decay amplitudes of B^0 and $\overline{B}^0$ to the final states f and $\bar{f}$ respectively. In this notation, the conditions for absence of CP violation in decay are $\langle\mathcal{A}_{f\bar{f}}\rangle = 0$ and $C_f = -C_{\bar{f}}$. Note that C_f and $C_{\bar{f}}$ are typically non-zero; e.g., for a flavour-specific final state, $\overline{A}_f = A_{\bar{f}} = 0$ ($A_f = \overline{A}_{\bar{f}} = 0$), they take the values $C_f = -C_{\bar{f}} = 1$ ($C_f = -C_{\bar{f}} = -1$).

The coefficients of the sine terms contain information about the weak phase. In the case that each decay amplitude contains only a single weak phase (i.e., no CP violation in decay as well as none in mixing), these terms can be written as

$$S_f = \frac{-2|A_f||\overline{A}_f|\sin(\phi_{\rm mix}+\phi_{\rm dec}-\delta_f)}{|A_f|^2+|\overline{A}_f|^2} \quad\text{and}$$
$$S_{\bar{f}} = \frac{-2|A_{\bar{f}}||\overline{A}_{\bar{f}}|\sin(\phi_{\rm mix}+\phi_{\rm dec}+\delta_f)}{|A_{\bar{f}}|^2+|\overline{A}_{\bar{f}}|^2}, \tag{130}$$

where δ_f is the strong phase difference between the decay amplitudes. If there is no CP violation, the condition $S_f = -S_{\bar{f}}$ holds. If decay amplitudes with different weak and strong phases contribute, no clean interpretation of S_f and $S_{\bar{f}}$ is possible.

The conditions for CP invariance $C_f = -C_{\bar{f}}$ and $S_f = -S_{\bar{f}}$ motivate a rotation of the parameters:

$$S_{f\bar{f}} = \frac{S_f+S_{\bar{f}}}{2}, \quad \Delta S_{f\bar{f}} = \frac{S_f-S_{\bar{f}}}{2}$$
$$C_{f\bar{f}} = \frac{C_f+C_{\bar{f}}}{2}, \quad \Delta C_{f\bar{f}} = \frac{C_f-C_{\bar{f}}}{2}. \tag{131}$$

With these parameters, the CP invariance conditions become $S_{f\bar{f}} = 0$ and $C_{f\bar{f}} = 0$. The parameter $\Delta C_{f\bar{f}}$ gives a measure of the "flavour-specificity" of the decay: $\Delta C_{f\bar{f}} = \pm 1$ corresponds to a completely flavour-specific decay, in which no interference between decays with and without mixing can occur, while $\Delta C_{f\bar{f}} = 0$ results in maximum sensitivity to mixing-induced CP violation. The parameter $\Delta S_{f\bar{f}}$ is related to the strong phase difference between the decay amplitudes of the B^0 meson to the f and to $\bar{f}$ final states. We note that the observables of Eq. (131) exhibit experimental correlations (typically of $\sim 20\%$, depending on the tagging purity, and other effects) between $S_{f\bar{f}}$ and $\Delta S_{f\bar{f}}$, and between $C_{f\bar{f}}$ and $\Delta C_{f\bar{f}}$. On the other hand, the final state specific observables of Eqs. (124)–(127) tend to have low correlations.

Alternatively, if we recall that the CP invariance conditions at the decay amplitude level are $A_f = \overline{A}_{\bar{f}}$ and $A_{\bar{f}} = \overline{A}_f$, we are led to consider the parameters [252]

$$\mathcal{A}_{f\bar{f}} = \frac{|\overline{A}_{\bar{f}}|^2-|A_f|^2}{|\overline{A}_{\bar{f}}|^2+|A_f|^2} \quad\text{and}\quad \mathcal{A}_{\bar{f}f} = \frac{|\overline{A}_f|^2-|A_{\bar{f}}|^2}{|\overline{A}_f|^2+|A_{\bar{f}}|^2}. \tag{132}$$

These are sometimes considered more physically intuitive parameters since they characterise CP violation in decay in decays with particular topologies. For example, in the case of $B^0\to\rho^\pm\pi^\mp$ (choosing $f=\rho^+\pi^-$ and $\bar{f}=\rho^-\pi^+$), $\mathcal{A}_{f\bar{f}}$ (also denoted $\mathcal{A}^{+-}_{\rho\pi}$) parametrises CP violation in decays in

[26] This parameter is often denoted $\mathcal{A}_f$ (or $\mathcal{A}_{CP}$), but here we avoid this notation to prevent confusion with the time-dependent CP asymmetry.

which the produced ρ meson does not contain the spectator quark, while $\mathcal{A}_{\bar{f}f}$ (also denoted $\mathcal{A}_{\rho\pi}^{-+}$) parametrises *CP* violation in decays in which it does. Note that we have again followed the sign convention that the asymmetry is the difference between the rate involving a b quark and that involving a $\bar{b}$ quark, cf. Eq. (104). Of course, these parameters are not independent of the other sets of parameters given above, and can be written

$$\mathcal{A}_{f\bar{f}} = -\frac{\langle\mathcal{A}_{f\bar{f}}\rangle + C_{f\bar{f}} + \langle\mathcal{A}_{f\bar{f}}\rangle\Delta C_{f\bar{f}}}{1 + \Delta C_{f\bar{f}} + \langle\mathcal{A}_{f\bar{f}}\rangle C_{f\bar{f}}} \quad \text{and}$$
$$\mathcal{A}_{\bar{f}f} = \frac{-\langle\mathcal{A}_{f\bar{f}}\rangle + C_{f\bar{f}} + \langle\mathcal{A}_{f\bar{f}}\rangle\Delta C_{f\bar{f}}}{-1 + \Delta C_{f\bar{f}} + \langle\mathcal{A}_{f\bar{f}}\rangle C_{f\bar{f}}}. \tag{133}$$

They usually exhibit strong correlations.

We now consider the various notations used in experimental studies of time-dependent *CP* asymmetries in decays to non-*CP* eigenstates.

$B^0 \to D^{*\pm} D^{\mp}$

The $(\langle\mathcal{A}_{f\bar{f}}\rangle, C_f, S_f, C_{\bar{f}}, S_{\bar{f}})$ set of parameters was used in early publications by both BaBar [285] and Belle [286] (albeit with slightly different notations) in the $D^{*\pm} D^{\mp}$ system ($f = D^{*+}D^-$, $\bar{f} = D^{*-}D^+$). In their most recent paper on this topic Belle [287] instead used the parametrisation $(A_{D^*D}, S_{D^*D}, \Delta S_{D^*D}, C_{D^*D}, \Delta C_{D^*D})$, while BaBar [259] give results in both sets of parameters. We therefore use the $(A_{D^*D}, S_{D^*D}, \Delta S_{D^*D}, C_{D^*D}, \Delta C_{D^*D})$ set.

$B^0 \to \rho^{\pm}\pi^{\mp}$

In the $\rho^{\pm}\pi^{\mp}$ system, the $(\langle\mathcal{A}_{f\bar{f}}\rangle, C_{f\bar{f}}, S_{f\bar{f}}, \Delta C_{f\bar{f}}, \Delta S_{f\bar{f}})$ set of parameters has been used originally by BaBar [288] and Belle [289], in the Q2B approximation; the exact names[27] used in this case are $(\mathcal{A}_{CP}^{\rho\pi}, C_{\rho\pi}, S_{\rho\pi}, \Delta C_{\rho\pi}, \Delta S_{\rho\pi})$, and these names are also used in this document.

Since $\rho^{\pm}\pi^{\mp}$ is reconstructed in the final state $\pi^+\pi^-\pi^0$, the interference between the ρ resonances can provide additional information about the phases (see Sect. 4.2.5). Both BaBar [281] and Belle [283,284] have performed time-dependent Dalitz plot analyses, from which the weak phase α is directly extracted. In such an analysis, the measured Q2B parameters are also naturally corrected for interference effects.

$B^0 \to D^{\mp}\pi^{\pm}, D^{*\mp}\pi^{\pm}, D^{\mp}\rho^{\pm}$

Time-dependent *CP* analyses have also been performed for the final states $D^{\mp}\pi^{\pm}$, $D^{*\mp}\pi^{\pm}$ and $D^{\mp}\rho^{\pm}$. In these theoretically clean cases, no penguin contributions are possible, so there is no *CP* violation in decay. Furthermore, due to the smallness of the ratio of the magnitudes of the suppressed ($b \to u$) and favoured ($b \to c$) amplitudes (denoted R_f), to a very good approximation, $C_f = -C_{\bar{f}} = 1$ (using $f = D^{(*)-}h^+$, $\bar{f} = D^{(*)+}h^-$ $h = \pi, \rho$), and the coefficients of the sine terms are given by

$$S_f = -2R_f \sin(\phi_{\text{mix}} + \phi_{\text{dec}} - \delta_f) \quad \text{and}$$
$$S_{\bar{f}} = -2R_f \sin(\phi_{\text{mix}} + \phi_{\text{dec}} + \delta_f). \tag{134}$$

Thus weak phase information can be cleanly obtained from measurements of S_f and $S_{\bar{f}}$, although external information on at least one of R_f or δ_f is necessary. (Note that $\phi_{\text{mix}} + \phi_{\text{dec}} = 2\beta + \gamma \equiv 2\phi_1 + \phi_3$ for all the decay modes in question, while R_f and δ_f depend on the decay mode.)

Again, different notations have been used in the literature. BaBar [290,291] defines the time-dependent probability function by

$$f^{\pm}(\eta, \Delta t) = \frac{e^{-|\Delta t|/\tau}}{4\tau} \times \left[1 \mp S_\zeta \sin(\Delta m \Delta t) \mp \eta C_\zeta \cos(\Delta m \Delta t)\right], \tag{135}$$

where the upper (lower) sign corresponds to the tagging meson being a B^0 ($\overline{B}^0$). The parameters η and ζ take the values $+1$ and $+$ (-1 and $-$) when the final state is, e.g., $D^-\pi^+$ ($D^+\pi^-$). However, in the fit, the substitutions $C_\zeta = 1$ and $S_\zeta = a \mp \eta b_i - \eta c_i$ are made, where the subscript i denotes tagging category. Neglecting b terms,

$$S_+ = a - c \quad \text{and} \quad S_- = a + c \;\Leftrightarrow$$
$$a = (S_+ + S_-)/2 \quad \text{and}$$
$$c = (S_- - S_+)/2, \tag{136}$$

in analogy to the parameters of Eq. (131). These are motivated by the possibility of *CP* violation on the tag side [292], which is absent for semileptonic B decays (mostly lepton tags). The parameter a is not affected by tag side *CP* violation. The parameter b only depends on tag side *CP* violation parameters and is not directly useful for determining UT angles. A clean interpretation of the c parameter is only possible for lepton-tagged events, so the BaBar measurements report c measured with those events only.

The parameters used by Belle in the analysis using partially reconstructed B decays [293], are similar to the S_ζ parameters defined above. However, in the Belle convention, a tagging B^0 corresponds to a $+$ sign in front of the sine coefficient; furthermore the correspondence between the super/subscript and the final state is opposite, so that $S_\pm$ (BaBar) $= -S^{\mp}$ (Belle). In this analysis, only lepton tags are used, so there is no effect from tag side *CP* violation. In the Belle analysis using fully reconstructed B decays [294],

[27] BaBar has used the notations $A_{CP}^{\rho\pi}$ [288] and $\mathcal{A}_{\rho\pi}$ [281] in place of $\mathcal{A}_{CP}^{\rho\pi}$.

Table 23 Conversion between the various notations used for CP violation parameters in the $D^{\pm}\pi^{\mp}$, $D^{*\pm}\pi^{\mp}$ and $D^{\pm}\rho^{\mp}$ systems. The b_i terms used by BaBar have been neglected. Recall that $(\alpha, \beta, \gamma) \equiv (\phi_2, \phi_1, \phi_3)$

	BaBar	Belle partial rec.	Belle full rec.
$S_{D^+\pi^-}$	$-S_- = -(a + c_i)$	–	$2R_{D\pi}\sin(2\phi_1 + \phi_3 + \delta_{D\pi})$
$S_{D^-\pi^+}$	$-S_+ = -(a - c_i)$	–	$2R_{D\pi}\sin(2\phi_1 + \phi_3 - \delta_{D\pi})$
$S_{D^{*+}\pi^-}$	$-S_- = -(a + c_i)$	S^+	$-2R_{D^*\pi}\sin(2\phi_1 + \phi_3 + \delta_{D^*\pi})$
$S_{D^{*-}\pi^+}$	$-S_+ = -(a - c_i)$	S^-	$-2R_{D^*\pi}\sin(2\phi_1 + \phi_3 - \delta_{D^*\pi})$
$S_{D^+\rho^-}$	$-S_- = -(a + c_i)$	–	–
$S_{D^-\rho^+}$	$-S_+ = -(a - c_i)$	–	–

Table 24 Translations used to convert the parameters measured by Belle to the parameters used for averaging in this document. The angular momentum factor L is -1 for $D^*\pi$ and $+1$ for $D\pi$. Recall that $(\alpha, \beta, \gamma) \equiv (\phi_2, \phi_1, \phi_3)$

	$D^*\pi$ partial rec.	$D^{(*)}\pi$ full rec.
a	$-(S^+ + S^-)$	$\frac{1}{2}(-1)^{L+1}\Big(2R_{D^{(*)}\pi}\sin(2\phi_1 + \phi_3 + \delta_{D^{(*)}\pi}) + 2R_{D^{(*)}\pi}\sin(2\phi_1 + \phi_3 - \delta_{D^{(*)}\pi})\Big)$
c	$-(S^+ - S^-)$	$\frac{1}{2}(-1)^{L+1}\Big(2R_{D^{(*)}\pi}\sin(2\phi_1 + \phi_3 + \delta_{D^{(*)}\pi}) - 2R_{D^{(*)}\pi}\sin(2\phi_1 + \phi_3 - \delta_{D^{(*)}\pi})\Big)$

this effect is measured and taken into account using $D^*\ell\nu$ decays; in neither Belle analysis are the a, b and c parameters used. In the latter case, the measured parameters are $2R_{D^{(*)}\pi}\sin(2\phi_1+\phi_3 \pm \delta_{D^{(*)}\pi})$; the definition is such that $S^{\pm}$ (Belle) $= -2R_{D^*\pi}\sin(2\phi_1 + \phi_3 \pm \delta_{D^*\pi})$. However, the definition includes an angular momentum factor $(-1)^L$ [295], and so for the results in the $D\pi$ system, there is an additional factor of -1 in the conversion.

Explicitly, the conversion then reads as given in Table 23, where we have neglected the b_i terms used by BaBar (which are zero in the absence of tag side CP violation). For the averages in this document, we use the a and c parameters, and give the explicit translations used in Table 24. It is to be fervently hoped that the experiments will converge on a common notation in future.

$B_s^0 \to D_s^{\mp}K^{\pm}$

The phenomenology of $B_s^0 \to D_s^{\mp}K^{\pm}$ decays is similar to that for $B^0 \to D^{\mp}\pi^{\pm}$, with some important caveats. The two amplitudes $b \to u$ and $b \to c$ amplitudes have the same level of Cabibbo-suppression (i.e. are of the same order in λ) though the former is suppressed by $\sqrt{\rho^2 + \eta^2}$. The large value of the ratio R of their magnitudes allows it to be determined from data, as the deviation of C_f and $C_{\bar{f}}$ from unity (in magnitude) can be observed. Moreover, the non-zero value of $\Delta\Gamma_s$ allows the determination of additional terms, $A_f^{\Delta\Gamma}$ and $A_{\bar{f}}^{\Delta\Gamma}$ (see Sect. 4.2.3), that break ambiguities in the solutions for $\phi_{\rm mix} + \phi_{\rm dec}$, which for $B_s^0 \to D_s^{\mp}K^{\pm}$ decays is equal to $\gamma - 2\beta_s$.

LHCb [296] has performed such an analysis with $B_s^0 \to D_s^{\mp}K^{\pm}$ decays. The absence of CP violation in decay is assumed, and the parameters that are determined from the fit are labelled C, $A^{\Delta\Gamma}$, $\bar{A}^{\Delta\Gamma}$, S, $\bar{S}$. These are trivially related to the definitions used in this section.

Time-dependent asymmetries in radiative B decays

As a special case of decays to non-CP eigenstates, let us consider radiative B decays. Here, the emitted photon has a distinct helicity, which is in principle observable, but in practice is not usually measured. Thus the measured time-dependent decay rates for B^0 decays are given by [297,298]

$$\begin{aligned}\Gamma_{\overline{B}^0\to X\gamma}(\Delta t) &= \Gamma_{\overline{B}^0\to X\gamma_L}(\Delta t) + \Gamma_{\overline{B}^0\to X\gamma_R}(\Delta t)\\ &= \frac{e^{-|\Delta t|/\tau(B^0)}}{4\tau(B^0)}\,[1 + (S_L + S_R)\times\sin(\Delta m\Delta t)\\ &\quad - (C_L + C_R)\cos(\Delta m\Delta t)]\,, \qquad (137)\\ \Gamma_{B^0\to X\gamma}(\Delta t) &= \Gamma_{B^0\to X\gamma_L}(\Delta t) + \Gamma_{B^0\to X\gamma_R}(\Delta t)\\ &= \frac{e^{-|\Delta t|/\tau(B^0)}}{4\tau(B^0)}\Big[1 - (S_L + S_R)\times\sin(\Delta m\Delta t)\\ &\quad + (C_L + C_R)\cos(\Delta m\Delta t)\Big], \qquad (138)\end{aligned}$$

where in place of the subscripts f and $\bar{f}$ we have used L and R to indicate the photon helicity. In order for interference between decays with and without B^0-$\overline{B}^0$ mixing to occur, the X system must not be flavour-specific, e.g., in case of $B^0 \to K^{*0}\gamma$, the final state must be $K_S^0\pi^0\gamma$. The sign of the sine term depends on the C eigenvalue of the X system. At leading order, the photons from $b \to q\gamma$ ($\bar{b} \to \bar{q}\gamma$) are predominantly left (right) polarised, with

corrections of order of m_q/m_b, thus interference effects are suppressed. Higher-order effects can lead to corrections of order $\Lambda_{\rm QCD}/m_b$ [299,300], though explicit calculations indicate that such corrections may be small for exclusive final states [301,302]. The predicted smallness of the S terms in the Standard Model results in sensitivity to new physics contributions.

The formalism discussed above is valid for any radiative decay to a final state where the hadronic system is an eigenstate of C. In addition to $K^0_S\pi^0\gamma$, experiments have presented results using B^0 decays to $K^0_S\eta\gamma$, $K^0_S\rho^0\gamma$ and $K^0_S\phi\gamma$. For the case of the $K^0_S\rho^0\gamma$ final state, particular care is needed, as due to the non-negligible width of the ρ^0 meson, decays selected as $B^0 \to K^0_S\rho^0\gamma$ can include a significant contribution from $K^{*\pm}\pi^\mp\gamma$ decays, which are flavour-specific and do not have the same oscillation phenomenology. It is therefore necessary to correct the fitted asymmetry parameter for a "dilution factor".

In the case of radiative B^0_s decays, the time-dependent decay rates of Eqs. (137) and (138) must be modified, in a similar way as discussed in Sect. 4.2.3, to account for the non-zero value of $\Delta\Gamma_s$. Thus, for decays such as $B^0_s \to \phi\gamma$, there is an additional observable, $A^{\Delta\Gamma}_{\phi\gamma}$, which can be determined from an untagged effective lifetime measurement [303].

4.2.7 Asymmetries in $B \to D^{(*)}K^{(*)}$ decays

CP asymmetries in $B \to D^{(*)}K^{(*)}$ decays are sensitive to γ. The neutral $D^{(*)}$ meson produced is an admixture of $D^{(*)0}$ (produced by a $b \to c$ transition) and $\overline{D}^{(*)0}$ (produced by a colour-suppressed $b \to u$ transition) states. If the final state is chosen so that both $D^{(*)0}$ and $\overline{D}^{(*)0}$ can contribute, the two amplitudes interfere, and the resulting observables are sensitive to γ, the relative weak phase between the two B decay amplitudes [304]. Various methods have been proposed to exploit this interference, including those where the neutral D meson is reconstructed as a CP eigenstate (GLW) [305,306], in a suppressed final state (ADS) [307,308], or in a self-conjugate three-body final state, such as $K^0_S\pi^+\pi^-$ (GGSZ or Dalitz) [309,310]. It should be emphasised that while each method differs in the choice of D decay, they are all sensitive to the same parameters of the B decay, and can be considered as variations of the same technique.

Consider the case of $B^\mp \to DK^\mp$, with D decaying to a final state f, which is accessible from both D^0 and $\overline{D}^0$. We can write the decay rates for B^- and B^+ ($\Gamma_\mp$), the charge averaged rate [$\Gamma = (\Gamma_- + \Gamma_+)/2$) and the charge asymmetry ($A = (\Gamma_- - \Gamma_+)/(\Gamma_- + \Gamma_+)$, see Eq. (104)] as

$$\Gamma_\mp \propto r_B^2 + r_D^2 + 2r_Br_D\cos(\delta_B + \delta_D \mp \gamma)\,, \tag{139}$$

$$\Gamma \propto r_B^2 + r_D^2 + 2r_Br_D\cos(\delta_B + \delta_D)\cos(\gamma)\,, \tag{140}$$

$$A = \frac{2r_Br_D\sin(\delta_B + \delta_D)\sin(\gamma)}{r_B^2 + r_D^2 + 2r_Br_D\cos(\delta_B + \delta_D)\cos(\gamma)}, \tag{141}$$

where the ratio of B decay amplitudes[28] is usually defined to be less than one,

$$r_B = \left|\frac{A(B^- \to \overline{D}^0K^-)}{A(B^- \to D^0K^-)}\right| = \left|\frac{A(B^+ \to D^0K^+)}{A(B^+ \to \overline{D}^0K^+)}\right|, \tag{142}$$

and the ratio of D decay amplitudes is correspondingly defined by

$$r_D = \left|\frac{A(D^0 \to f)}{A(\overline{D}^0 \to f)}\right|. \tag{143}$$

The relation between B^- and B^+ amplitudes given in Eq. (142) is a result of their being only one weak phase contributing to each amplitude in the Standard Model, which is the source of the theoretical cleanliness of this approach to measure γ [311]. The strong phase differences between the B and D decay amplitudes are given by δ_B and δ_D, respectively. The values of r_D and δ_D depend on the final state f: for the GLW analysis, $r_D = 1$ and δ_D is trivial (either zero or π); for other modes, values of r_D and δ_D are not trivial and for multibody final states they vary across the phase space. This can be quantified either by an explicit D decay amplitude model or by model-independent information. In the case that the multibody final state is treated inclusively, the formalism is modified by the inclusion of a coherence factor, usually denoted κ, while r_D and δ_D become effectively parameters corresponding to amplitude-weighted averages across the phase space.

Note that, for given values of r_B and r_D, the maximum size of A (at $\sin(\delta_B + \delta_D) = 1$) is $2r_Br_D\sin(\gamma)/(r_B^2 + r_D^2)$. Thus even for D decay modes with small r_D, large asymmetries, and hence sensitivity to γ, may occur for B decay modes with similar values of r_B. For this reason, the ADS analysis of the decay $B^\mp \to D\pi^\mp$ is also of interest.

The expressions of Eqs. (139)–(143) are for a specific point in phase space, and therefore are relevant where both B and D decays are to two-body final states. Additional coherence factors enter the expressions when the B decay is to a multibody final state (further discussion of multibody D decays can be found below). In particular, experiments have studied $B^+ \to DK^*(892)^+$, $B^0 \to DK^*(892)^0$ and $B^+ \to DK^+\pi^+\pi^-$ decays. Considering, for concreteness, the $B \to DK^*(892)$ case, the non-negligible width of the $K^*(892)$ resonance implies that contributions from other

[28] Note that here we use the notation r_B to denote the ratio of B decay amplitudes, whereas in Sect. 4.2.6 we used, e.g., $R_{D\pi}$, for a rather similar quantity. The reason is that here we need to be concerned also with D decay amplitudes, and so it is convenient to use the subscript to denote the decaying particle. Hopefully, using r in place of R will reduce the potential for confusion.

$B \to DK\pi$ decays can pass the selection requirements. Their effect on the Q2B analysis can be accounted for with a coherence factor [312], usually denoted κ, which tends to unity in the limit that the $K^*(892)$ resonance is the only signal amplitude contributing in the selected region of phase space. In this case, the hadronic parameters r_B and δ_B become effectively weighted averages across the selected phase space of the magnitude ratio and relative strong phase between the CKM-suppressed and -favoured amplitudes; these effective parameters are denoted $\bar{r}_B$ and $\bar{\delta}_B$ (the notations r_s, δ_s and r_S, δ_S are also found in the literature). An alternative, and in certain cases more advantageous, approach is Dalitz plot analysis of the full $B \to DK\pi$ phase space [313,314].

$B \to D^{(*)}K^{(*)}$ with $D \to CP$ eigenstate decays

In the GLW analysis, the measured quantities are the partial rate asymmetry and the charge averaged rate, which are measured both for CP-even and CP-odd D decays. The latter is defined as

$$R_{CP} = \frac{2\,\Gamma\left(B^+ \to D_{CP}K^+\right)}{\Gamma\left(B^+ \to \overline{D}^0 K^+\right)}. \tag{144}$$

It is experimentally convenient to measure R_{CP} using a double ratio,

$$R_{CP} = \frac{\Gamma\left(B^+ \to D_{CP}K^+\right)/\Gamma\left(B^+ \to \overline{D}^0 K^+\right)}{\Gamma\left(B^+ \to D_{CP}\pi^+\right)/\Gamma\left(B^+ \to \overline{D}^0 \pi^+\right)} \tag{145}$$

that is normalised both to the rate for the favoured $\overline{D}^0 \to K^+\pi^-$ decay, and to the equivalent quantities for $B^+ \to D\pi^+$ decays (charge conjugate processes are implicitly included in Eqs. (144) and (145)). In this way the constant of proportionality drops out of Eq. (140). Equation (145) is exact in the limit that the contribution of the $b \to u$ decay amplitude to $B^+ \to D\pi^+$ vanishes and when the flavour-specific rates $\Gamma(B^+ \to \overline{D}^0 h^+)$ ($h = \pi, K$) are determined using appropriately flavour-specific D decays. In reality, the decay $D \to K\pi$ is used, leading to a small source of systematic uncertainty. The CP asymmetry is defined as

$$A_{CP} = \frac{\Gamma(B^- \to D_{CP}K^-) - \Gamma(B^+ \to D_{CP}K^+)}{\Gamma(B^- \to D_{CP}K^-) + \Gamma(B^+ \to D_{CP}K^+)}. \tag{146}$$

$B \to D^{(*)}K^{(*)}$ with $D \to$ non-CP eigenstate two-body decays

For the ADS analysis, based on a suppressed $D \to f$ decay, the measured quantities are again the partial rate asymmetry, and the charge averaged rate. In this case it is sufficient to measure the rate in a single ratio (normalised to the favoured $D \to \bar{f}$ decay) since potential systematic uncertainties related to detection cancel naturally; the observed quantity is then

$$R_{\rm ADS} = \frac{\Gamma(B^- \to [f]_D K^-) + \Gamma(B^+ \to [\bar{f}]_D K^+)}{\Gamma(B^- \to [\bar{f}]_D K^-) + \Gamma(B^+ \to [f]_D K^+)}, \tag{147}$$

where the inclusion of charge-conjugate modes has been made explicit. The CP asymmetry is defined as

$$A_{\rm ADS} = \frac{\Gamma(B^- \to [f]_D K^-) - \Gamma(B^+ \to [f]_D K^+)}{\Gamma(B^- \to [f]_D K^-) + \Gamma(B^+ \to [f]_D K^+)}. \tag{148}$$

Since the uncertainty of $A_{\rm ADS}$ depends on the central value of $R_{\rm ADS}$, for some statistical treatments it is preferable to use an alternative pair of parameters [315]

$$R_- = \frac{\Gamma(B^- \to [f]_D K^-)}{\Gamma(B^- \to [\bar{f}]_D K^-)}$$
$$R_+ = \frac{\Gamma(B^+ \to [\bar{f}]_D K^+)}{\Gamma(B^+ \to [f]_D K^+)}, \tag{149}$$

where there is no implied inclusion of charge-conjugate processes. These parameters are statistically uncorrelated but may be affected by common sources of systematic uncertainty. We use the $(R_{\rm ADS}, A_{\rm ADS})$ set in our compilation where available.

In the ADS analysis, there are two additional unknowns (r_D and δ_D) compared to the GLW case. However, the value of r_D can be measured using decays of D mesons of known flavour, and δ_D can be measured from interference effects in decays of quantum-correlated $D\bar{D}$ pairs produced at the $\psi(3770)$ resonance. More generally, one needs access to two different linear admixtures of D^0 and $\bar{D}^0$ states in order to determine the relative phase: one such sample can be flavour tagged D mesons, which are available in abundant quantities in many experiments; the other can be CP-tagged D mesons from $\psi(3770)$ decays or could be mixed D mesons (or could be the combination of D^0 and $\bar{D}^0$ that is found in $B \to DK$ decays). In fact, the most precise information on both r_D and δ_D currently comes from global fits on charm mixing parameters, as discussed in Sect. 8.1.

The relation of $A_{\rm ADS}$ to the underlying parameters given in Eq. (141) and Table 25 is exact for a two-body D decay. For multibody decays, a similar formalism can be used with the introduction of a coherence factor [316]. This is most appropriate for doubly-Cabibbo-suppressed decays to non-self-conjugate final states, but can also be modified for use with singly-Cabibbo-suppressed decays [317]. For multibody self-conjugate final states, such as $K^0_S\pi^+\pi^-$, a Dalitz plot analysis (discussed below) is often more appropriate. However, in certain cases where the final state can be approximated as a CP eigenstate, a modified version of the GLW formalism can be used [318]. In such cases the observables

are denoted A_{qGLW} and R_{qGLW} to indicate that the final state is not a pure CP eigenstate.

$B \to D^{(*)}K^{(*)}$ with $D \to$ multibody final state decays

In the Dalitz plot (or GGSZ) analysis of D decays to multibody self-conjugate final states, once a model is assumed for the D decay, which gives the values of r_D and δ_D across the Dalitz plot, it is possible to perform a simultaneous fit to the B^+ and B^- samples and directly extract γ, r_B and δ_B. However, the uncertainties on the phases depend approximately inversely on r_B. Furthermore, r_B is positive definite and therefore tends to be overestimated (unless $\sigma(r_B) \ll r_B$), which leads to an underestimation of the uncertainty on γ that must be corrected statistically. An alternative approach is to extract from the data the "Cartesian" variables

$$\begin{aligned}(x_\pm, y_\pm) &= (\mathrm{Re}(r_B e^{i(\delta_B \pm \gamma)}), \mathrm{Im}(r_B e^{i(\delta_B \pm \gamma)})) \\ &= (r_B \cos(\delta_B \pm \gamma), r_B \sin(\delta_B \pm \gamma)). \end{aligned} \quad (150)$$

These variables tend to be statistically well-behaved, and are therefore appropriate for combination of results. The pairs of variables $(x_\pm, y_\pm)$ can be extracted from independent fits of the $B^\pm$ data samples.

The assumption of a model for the D decay leads to a non-negligible, and hard to quantify, source of uncertainty. To obviate this, it is possible to use instead a model-independent approach, in which the Dalitz plot (or, more generally, the phase space) is binned [309,319,320]. In this case, hadronic parameters describing the average strong phase difference in each bin between the suppressed and favoured decay amplitudes enter the equations. These parameters can be determined from interference effects in decays of quantum-correlated $D\bar{D}$ pairs produced at the $\psi(3770)$ resonance. Measurements of such parameters have been made for various different hadronic D decays by CLEO-c and BESIII.

If a multibody decay is dominated by one CP state, there will be additional sensitivity to γ in the numbers of events in the $B^\pm$ data samples. This can be taken into account in various ways. One possibility is to perform a GLW-like analysis, as mentioned above. An alternative approach proceeds by defining $z_\pm = x_\pm + iy_\pm$ and $x_0 = -\int \mathrm{Re}[f(s_1, s_2) f^*(s_2, s_1)] ds_1 ds_2$, where s_1, s_2 are the coordinates of invariant mass squared that define the Dalitz plot and f is the complex amplitude for D decay as a function of the Dalitz plot coordinates.[29] The fitted parameters $(\rho^\pm, \theta^\pm)$ are then defined by

$$\rho^\pm e^{i\theta^\pm} = z_\pm - x_0. \quad (151)$$

[29] The x_0 parameter gives a model-dependent measure of the net CP content of the final state [318,321]. It is closely related to the c_i parameters of the model dependent Dalitz plot analysis [309,319,320], and the coherence factor of inclusive ADS-type analyses [316], integrated over the entire Dalitz plot.

Table 25 Summary of relations between measured and physical parameters in GLW, ADS and Dalitz analyses of $B \to D^{(*)}K^{(*)}$ decays

GLW analysis	
$R_{CP\pm}$	$1 + r_B^2 \pm 2r_B \cos(\delta_B)\cos(\gamma)$
$A_{CP\pm}$	$\pm 2r_B \sin(\delta_B)\sin(\gamma)/R_{CP\pm}$
ADS analysis	
R_{ADS}	$r_B^2 + r_D^2 + 2r_B r_D \cos(\delta_B + \delta_D)\cos(\gamma)$
A_{ADS}	$2r_B r_D \sin(\delta_B + \delta_D)\sin(\gamma)/R_{\mathrm{ADS}}$
GGSZ Dalitz analysis ($D \to K_S^0\pi^+\pi^-$)	
$x_\pm$	$r_B \cos(\delta_B \pm \gamma)$
$y_\pm$	$r_B \sin(\delta_B \pm \gamma)$
Dalitz analysis ($D \to \pi^+\pi^-\pi^0$)	
$\rho^\pm$	$\lvert z_\pm - x_0\rvert$
$\theta^\pm$	$\tan^{-1}(\mathrm{Im}(z_\pm)/(\mathrm{Re}(z_\pm) - x_0))$

Table 26 Common inputs used in calculating the averages

$\tau(B^0)$ (ps)	1.520 ± 0.004
Δm_d (ps^{-1})	0.5064 ± 0.0019
$\Delta\Gamma_d/\Gamma_d$	-0.002 ± 0.010
$\lvert A_\perp\rvert^2(J/\psi K^*)$	0.209 ± 0.006

Note that the yields of $B^\pm$ decays are proportional to $1 + (\rho^\pm)^2 - (x_0)^2$. This choice of variables has been used by BaBar in the analysis of $B^+ \to DK^+$ with $D \to \pi^+\pi^-\pi^0$ [322]; for this D decay, and with the assumed amplitude model, a value of $x_0 = 0.850$ is obtained.

The relations between the measured quantities and the underlying parameters are summarised in Table 25. It must be emphasised that the hadronic factors r_B and δ_B are different, in general, for each B decay mode.

4.3 Common inputs and error treatment

The common inputs used for rescaling are listed in Table 26. The B^0 lifetime ($\tau(B^0)$), mixing parameter (Δm_d) and relative width difference ($\Delta\Gamma_d/\Gamma_d$) averages are provided by the HFLAV Lifetimes and Oscillations subgroup (Sect. 3). The fraction of the perpendicularly polarised component ($|A_\perp|^2$) in $B \to J/\psi K^*(892)$ decays, which determines the CP composition in these decays, is averaged from results by BaBar [323], Belle [324], CDF [325], D0 [93] and LHCb [326]. See also the HFLAV B to Charm Decay Parameters subgroup (Sect. 6).

At present, we only rescale to a common set of input parameters for modes with reasonably small statistical errors ($b \to c\bar{c}s$ transitions of B^0 mesons). Correlated systematic errors are taken into account in these modes as well. For all other modes, the effect of such a procedure is currently negligible.

Table 27 Results and averages for $S_{b\to c\bar{c}s}$ and $C_{b\to c\bar{c}s}$. The result marked (*) uses "hadronic and previously unused muonic decays of the J/ψ". We neglect a small possible correlation of this result with the main BABAR result [331] that could be caused by reprocessing of the data

Experiment	Sample size	$-\eta S_{b\to c\bar{c}s}$	$C_{b\to c\bar{c}s}$
BABAR [331]	$N(B\bar{B})$ = 465M	$0.687 \pm 0.028 \pm 0.012$	$0.024 \pm 0.020 \pm 0.016$
BABAR $\chi_{c0}K^0_S$ [274]	$N(B\bar{B})$ = 383M	$0.69 \pm 0.52 \pm 0.04 \pm 0.07$	$-0.29^{+0.53}_{-0.44} \pm 0.03 \pm 0.05$
BABAR $J/\psi K^0_S$ (*) [332]	$N(B\bar{B})$ = 88M	$1.56 \pm 0.42 \pm 0.21$	–
Belle [333]	$N(B\bar{B})$ = 772M	$0.667 \pm 0.023 \pm 0.012$	$-0.006 \pm 0.016 \pm 0.012$
B factory average		0.679 ± 0.020	0.005 ± 0.017
Confidence level		0.28 (1.2σ)	0.47 (0.5σ)
ALEPH [334]	$N(Z \to \text{hadrons})$ = 4M	$0.84^{+0.82}_{-1.04} \pm 0.16$	–
OPAL [335]	$N(Z \to \text{hadrons})$ = 4.4M	$3.2^{+1.8}_{-2.0} \pm 0.5$	–
CDF [336]	$\int \mathcal{L}\,dt = 110\ \text{pb}^{-1}$	$0.79^{+0.41}_{-0.44}$	–
LHCb [337]	$\int \mathcal{L}\,dt = 3\ \text{fb}^{-1}$	$0.731 \pm 0.035 \pm 0.020$	$-0.038 \pm 0.032 \pm 0.005$
Belle $\Upsilon(5S)$ [338]	$\int \mathcal{L}\,dt = 121\ \text{fb}^{-1}$	$0.57 \pm 0.58 \pm 0.06$	–
Average		0.691 ± 0.017	-0.004 ± 0.015

As explained in Sect. 1, we do not apply a rescaling factor on the error of an average that has $\chi^2/\text{dof} > 1$ (unlike the procedure currently used by the PDG [327]). We provide a confidence level of the fit so that one can know the consistency of the measurements included in the average, and attach comments in case some care needs to be taken in the interpretation. Note that, in general, results obtained from data samples with low statistics will exhibit some non-Gaussian behaviour. We average measurements with asymmetric errors using the PDG [327] prescription. In cases where several measurements are correlated (e.g. S_f and C_f in measurements of time-dependent CP violation in B decays to a particular CP eigenstate) we take these into account in the averaging procedure if the uncertainties are sufficiently Gaussian. For measurements where one error is given, it represents the total error, where statistical and systematic uncertainties have been added in quadrature. If two errors are given, the first is statistical and the second systematic. If more than two errors are given, the origin of the additional uncertainty will be explained in the text.

4.4 Time-dependent asymmetries in $b \to c\bar{c}s$ transitions

4.4.1 Time-dependent CP asymmetries in $b \to c\bar{c}s$ decays to CP eigenstates

In the Standard Model, the time-dependent parameters for B^0 decays governed by $b \to c\bar{c}s$ transitions are predicted to be $S_{b\to c\bar{c}s} = -\eta \sin(2\beta)$ and $C_{b\to c\bar{c}s} = 0$ to very good accuracy. Deviations from this relation are currently limited to the level of $\lesssim 1°$ on 2β [328–330]. The averages for $-\eta S_{b\to c\bar{c}s}$ and $C_{b\to c\bar{c}s}$ are provided in Table 27. The averages for $-\eta S_{b\to c\bar{c}s}$ are shown in Fig. 12.

Both BABAR and Belle have used the $\eta = -1$ modes $J/\psi K^0_S$, $\psi(2S)K^0_S$, $\chi_{c1}K^0_S$ and $\eta_c K^0_S$, as well as $J/\psi K^0_L$, which has $\eta = +1$ and $J/\psi K^{*0}(892)$, which is found to have η close to $+1$ based on the measurement of $|A_\perp|$ (see Sect. 4.3). The most recent Belle result does not use $\eta_c K^0_S$ or $J/\psi K^{*0}(892)$ decays.[30] ALEPH, OPAL, CDF and LHCb have used only the $J/\psi K^0_S$ final state. BABAR has also determined the CP violation parameters of the $B^0 \to \chi_{c0}K^0_S$ decay from the time-dependent Dalitz plot analysis of the $B^0 \to \pi^+\pi^- K^0_S$ mode (see Sect. 4.7.2). In addition, Belle has performed a measurement with data accumulated at the $\Upsilon(5S)$ resonance, using the $J/\psi K^0_S$ final state – this involves a different flavour tagging method compared to the measurements performed with data accumulated at the $\Upsilon(4S)$ resonance. A breakdown of results in each charmonium-kaon final state is given in Table 28.

It should be noted that, while the uncertainty in the average for $-\eta S_{b\to c\bar{c}s}$ is still limited by statistics, the precision for $C_{b\to c\bar{c}s}$ is close to being dominated by the systematic uncertainty, particularly for measurements from the e^+e^- B factory experiments. This occurs due to the possible effect of tag side interference [292] on the $C_{b\to c\bar{c}s}$ measurement, an effect which is correlated between different $e^+e^- \to \Upsilon(4S) \to B\bar{B}$ experiments. Understanding of this effect may continue to improve in future, allowing the uncertainty to reduce.

From the average for $-\eta S_{b\to c\bar{c}s}$ above, we obtain the following solutions for β (in $[0, \pi]$):

$$\beta = (21.9 \pm 0.7)° \quad \text{or} \quad \beta = (68.1 \pm 0.7)°. \tag{152}$$

[30] Previous analyses from Belle did include these channels [101], but it is not possible to obtain separate results for those modes from the published information.

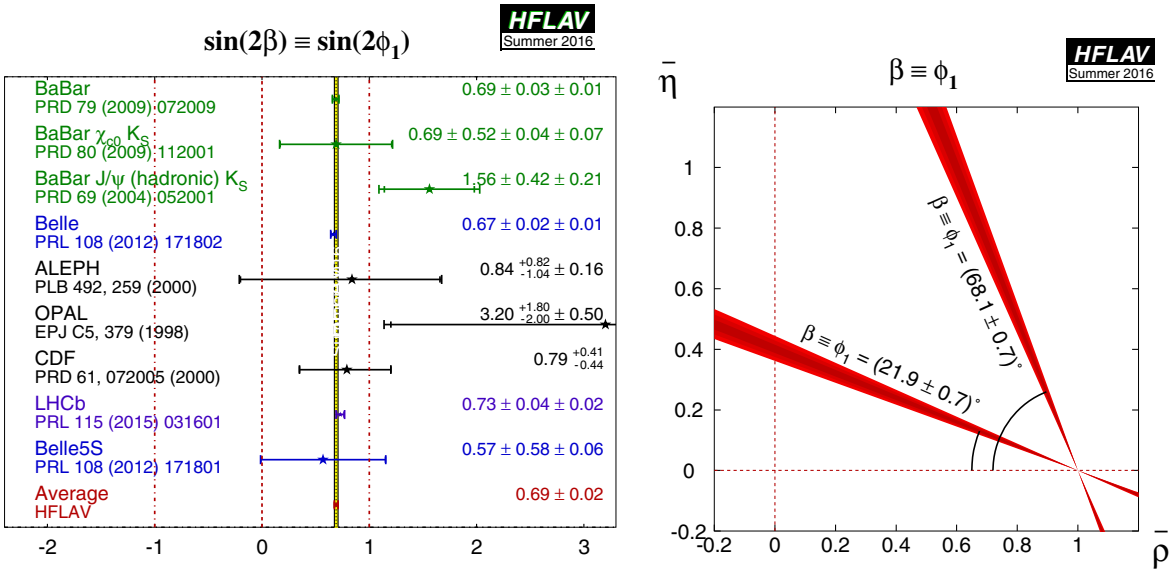

Fig. 12 (*Left*) Average of measurements of $S_{b\to c\bar{c}s}$, interpreted as $\sin(2\beta)$. (*Right*) Constraints on the $(\overline{\rho}, \overline{\eta})$ plane, obtained from the average of $-\eta S_{b\to c\bar{c}s}$ and Eq. (152). Note that the solution with the smaller (*larger*) value of β has $\cos(2\beta) > 0$ (<0)

Table 28 Breakdown of B factory results on $S_{b\to c\bar{c}s}$ and $C_{b\to c\bar{c}s}$

Mode	$N(B\bar{B})$	$-\eta S_{b\to c\bar{c}s}$	$C_{b\to c\bar{c}s}$
BaBar			
$J/\psi K^0_S$ [331]	465M	$0.657 \pm 0.036 \pm 0.012$	$0.026 \pm 0.025 \pm 0.016$
$J/\psi K^0_L$ [331]	465M	$0.694 \pm 0.061 \pm 0.031$	$-0.033 \pm 0.050 \pm 0.027$
$J/\psi K^0$ [331]	465M	$0.666 \pm 0.031 \pm 0.013$	$0.016 \pm 0.023 \pm 0.018$
$\psi(2S) K^0_S$ [331]	465M	$0.897 \pm 0.100 \pm 0.036$	$0.089 \pm 0.076 \pm 0.020$
$\chi_{c1} K^0_S$ [331]	465M	$0.614 \pm 0.160 \pm 0.040$	$0.129 \pm 0.109 \pm 0.025$
$\eta_c K^0_S$ [331]	465M	$0.925 \pm 0.160 \pm 0.057$	$0.080 \pm 0.124 \pm 0.029$
$J/\psi K^{*0}(892)$ [331]	465M	$0.601 \pm 0.239 \pm 0.087$	$0.025 \pm 0.083 \pm 0.054$
All [331]	465M	$0.687 \pm 0.028 \pm 0.012$	$0.024 \pm 0.020 \pm 0.016$
Belle			
$J/\psi K^0_S$ [333]	772M	$0.670 \pm 0.029 \pm 0.013$	$0.015 \pm 0.021^{+0.023}_{-0.045}$
$J/\psi K^0_L$ [333]	772M	$0.642 \pm 0.047 \pm 0.021$	$-0.019 \pm 0.026^{+0.041}_{-0.017}$
$\psi(2S) K^0_S$ [333]	772M	$0.738 \pm 0.079 \pm 0.036$	$-0.104 \pm 0.055^{+0.027}_{-0.047}$
$\chi_{c1} K^0_S$ [333]	772M	$0.640 \pm 0.117 \pm 0.040$	$0.017 \pm 0.083^{+0.026}_{-0.046}$
All [333]	772M	$0.667 \pm 0.023 \pm 0.012$	$-0.006 \pm 0.016 \pm 0.012$
Averages			
$J/\psi K^0_S$		0.665 ± 0.024	0.024 ± 0.026
$J/\psi K^0_L$		0.663 ± 0.041	-0.023 ± 0.030
$\psi(2S) K^0_S$		0.807 ± 0.067	-0.009 ± 0.055
$\chi_{c1} K^0_S$		0.632 ± 0.099	0.066 ± 0.074

In radians, these values are $\beta = (0.382 \pm 0.012)$, $\beta = (1.189 \pm 0.012)$.

This result gives a precise constraint on the $(\overline{\rho}, \overline{\eta})$ plane, as shown in Fig. 12. The measurement is in remarkable agreement with other constraints from CP conserving quantities, and with CP violation in the kaon system, in the form of the parameter ϵ_K. Such comparisons have been performed by various phenomenological groups, such as CKMfitter [252] and UTFit [339] (see also Refs. [340,341]).

Table 29 Averages from $B^0 \to J/\psi K^{*0}$ transversity analyses

Experiment	$N(B\bar{B})$	$\sin 2\beta$	$\cos 2\beta$	Correlation
BABAR [345]	88M	$-0.10 \pm 0.57 \pm 0.14$	$3.32^{+0.76}_{-0.96} \pm 0.27$	-0.37
Belle [324]	275M	$0.24 \pm 0.31 \pm 0.05$	$0.56 \pm 0.79 \pm 0.11$	0.22
Average		0.16 ± 0.28	1.64 ± 0.62	Uncorrelated averages
Confidence level		0.61 (0.5σ)	0.03 (2.2σ)	

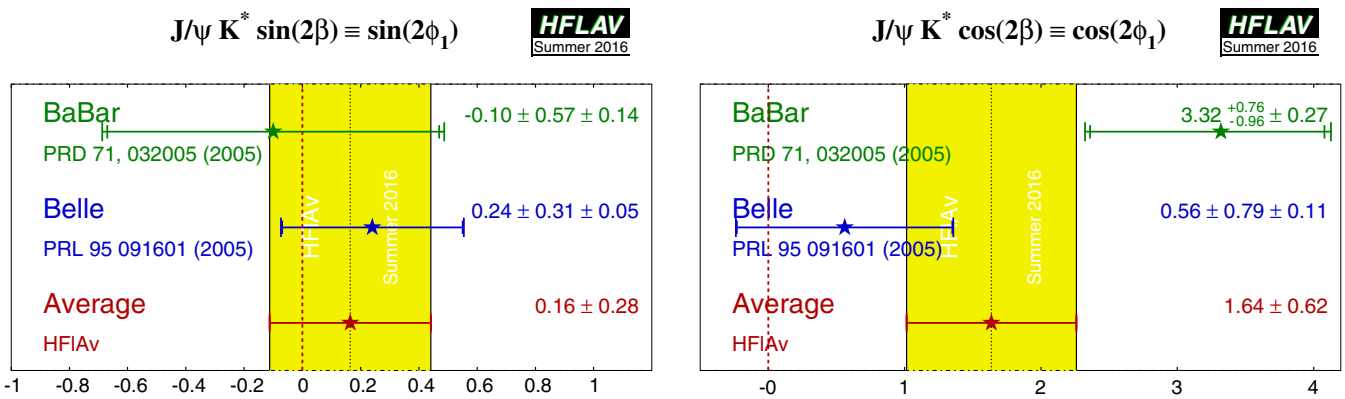

Fig. 13 Averages of (*left*) $\sin(2\beta) \equiv \sin(2\phi_1)$ and (*right*) $\cos(2\beta) \equiv \cos(2\phi_1)$ from time-dependent analyses of $B^0 \to J/\psi K^{*0}$ decays

4.4.2 *Time-dependent transversity analysis of $B^0 \to J/\psi K^{*0}$ decays*

B meson decays to the vector-vector final state $J/\psi K^{*0}$ are also mediated by the $b \to c\bar{c}s$ transition. When a final state that is not flavour-specific ($K^{*0} \to K^0_S \pi^0$) is used, a time-dependent transversity analysis can be performed allowing sensitivity to both $\sin(2\beta)$ and $\cos(2\beta)$ [342]. Such analyses have been performed by both B factory experiments. In principle, the strong phases between the transversity amplitudes are not uniquely determined by such an analysis, leading to a discrete ambiguity in the sign of $\cos(2\beta)$. The BABAR collaboration resolves this ambiguity using the known variation [343] of the P-wave phase (fast) relative to the S-wave phase (slow) with the invariant mass of the $K\pi$ system in the vicinity of the $K^*(892)$ resonance. The result is in agreement with the prediction from s quark helicity conservation, and corresponds to Solution II defined by Suzuki [344]. We include only the solutions consistent with this phase variation in Table 29 and Fig. 13.

At present the results are dominated by large and non-Gaussian statistical errors, and exhibit significant correlations. We perform uncorrelated averages, the interpretation of which has to be done with the greatest care. Nonetheless, it is clear that $\cos(2\beta) > 0$ is preferred by the experimental data in $J/\psi K^{*0}$ (for example, BABAR [345] find a confidence level for $\cos(2\beta) > 0$ of 89%).

4.4.3 *Time-dependent CP asymmetries in $B^0 \to D^{*+} D^{*-} K^0_S$ decays*

Both BABAR [265] and Belle [266] have performed time-dependent analyses of the $B^0 \to D^{*+} D^{*-} K^0_S$ decay, to obtain information on the sign of $\cos(2\beta)$. More information can be found in Sect. 4.2.5. The results are given in Table 30, and shown in Fig. 14.

From the above result and the assumption that $J_{s2} > 0$, BABAR infer that $\cos(2\beta) > 0$ at the 94% confidence level [265].

4.4.4 *Time-dependent analysis of B^0_s decays through the $b \to c\bar{c}s$ transition*

As described in Sect. 4.2.3, time-dependent analysis of decays such as $B^0_s \to J/\psi\phi$ probes the CP violating phase of B^0_s–$\bar{B}^0_s$ oscillations, ϕ_s.[31] The combination of results on $B^0_s \to J/\psi\phi$ decays, including also results from $B^0_s \to J/\psi\pi^+\pi^-$ and $B^0_s \to D^+_s D^-_s$ decays, is performed by the HFLAV Lifetimes and Oscillations subgroup, see Sect. 3.

[31] We use ϕ_s here to denote the same quantity labelled $\phi_s^{c\bar{c}s}$ in Sect. 3. It should not be confused with the parameter $\phi_{12} \equiv \arg[-M_{12}/\Gamma_{12}]$, which historically was also often referred to as ϕ_s.

Table 30 Results from time-dependent analysis of $B^0 \to D^{*+}D^{*-}K_S^0$

Experiment	$N(B\bar{B})$	$\frac{J_c}{J_0}$	$\frac{2J_{s1}}{J_0}\sin(2\beta)$	$\frac{2J_{s2}}{J_0}\cos(2\beta)$
BABAR [265]	230M	$0.76 \pm 0.18 \pm 0.07$	$0.10 \pm 0.24 \pm 0.06$	$0.38 \pm 0.24 \pm 0.05$
Belle [266]	449M	$0.60^{+0.25}_{-0.28} \pm 0.08$	$-0.17 \pm 0.42 \pm 0.09$	$-0.23^{+0.43}_{-0.41} \pm 0.13$
Average		0.71 ± 0.16	0.03 ± 0.21	0.24 ± 0.22
Confidence level		0.63 (0.5σ)	0.59 (0.5σ)	0.23 (1.2σ)

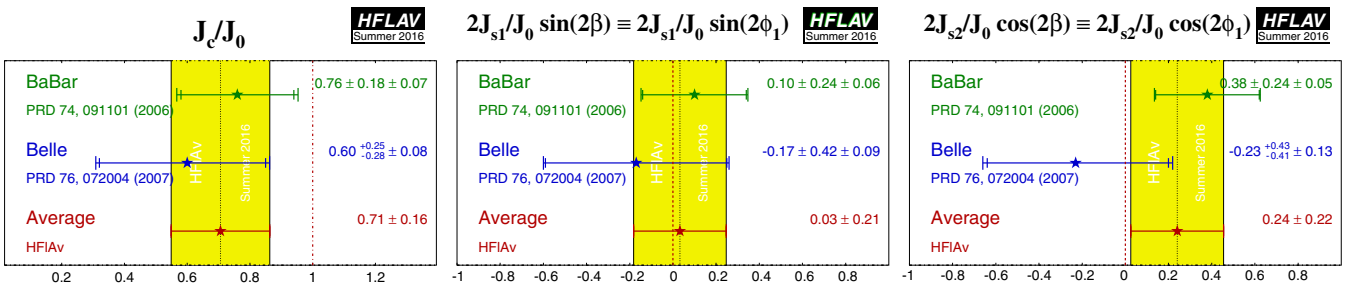

Fig. 14 Averages of (*left*) (J_c/J_0), (*middle*) $(2J_{s1}/J_0)\sin(2\beta)$ and (*right*) $(2J_{s2}/J_0)\cos(2\beta)$ from time-dependent analyses of $B^0 \to D^{*+}D^{*-}K_S^0$ decays

Table 31 Results from analyses of $B^0 \to D^{(*)}h^0$, $D \to CP$ eigenstates decays

Experiment	$N(B\bar{B})$	S_{CP}	C_{CP}	Correlation
BABAR and Belle [349]	1243M	$0.66 \pm 0.10 \pm 0.06$	$-0.02 \pm 0.07 \pm 0.03$	-0.05

4.5 Time-dependent *CP* asymmetries in colour-suppressed $b \to c\bar{u}d$ transitions

4.5.1 Time-dependent CP asymmetries: $b \to c\bar{u}d$ decays to CP eigenstates

Decays of B mesons to final states such as $D\pi^0$ are governed by $b \to c\bar{u}d$ transitions. If the final state is a *CP* eigenstate, e.g. $D_{CP}\pi^0$, the usual time-dependence formulae are recovered, with the sine coefficient sensitive to $\sin(2\beta)$. Since there is no penguin contribution to these decays, there is even less associated theoretical uncertainty than for $b \to c\bar{c}s$ decays such as $B \to J/\psi K_S^0$. Such measurements therefore allow to test the Standard Model prediction that the *CP* violation parameters in $b \to c\bar{u}d$ transitions are the same as those in $b \to c\bar{c}s$ [346]. Although there is an additional contribution from CKM suppressed $b \to u\bar{c}d$ amplitudes, which have a different weak phase compared to the leading $b \to c\bar{u}d$ transition, the effect is small and can be taken into account in the analysis [347,348].

Results are available from a joint analysis of BABAR and Belle data [349]. The following *CP*-even final states are included: $D\pi^0$ and $D\eta$ with $D \to K_S^0\pi^0$ and $D \to K_S^0\omega$; $D\omega$ with $D \to K_S^0\pi^0$; $D^*\pi^0$ and $D^*\eta$ with $D^* \to D\pi^0$ and $D \to K^+K^-$. The following *CP*-odd final states are included: $D\pi^0$, $D\eta$ and $D\omega$ with $D \to K^+K^-$, $D^*\pi^0$ and $D^*\eta$ with $D^* \to D\pi^0$ and $D \to K_S^0\pi^0$. All $B^0 \to D^{(*)}h^0$ decays are analysed together, taking into account the different *CP* factors (denoted $D_{CP}^{(*)}h^0$). The results are summarised in Table 31.

4.5.2 Time-dependent Dalitz plot analyses of $b \to c\bar{u}d$ decays

When multibody D decays, such as $D \to K_S^0\pi^+\pi^-$ are used, a time-dependent analysis of the Dalitz plot of the neutral D decay allows for a direct determination of the weak phase 2β. (Equivalently, both $\sin(2\beta)$ and $\cos(2\beta)$ can be measured.) This information can be used to resolve the ambiguity in the measurement of 2β from $\sin(2\beta)$ [350].

Results of such analyses are available from both Belle [260] and BABAR [261]. The decays $B \to D\pi^0$, $B \to D\eta$, $B \to D\omega$, $B \to D^*\pi^0$ and $B \to D^*\eta$ are used. (This collection of states is denoted by $D^{(*)}h^0$.) The daughter decays are $D^* \to D\pi^0$ and $D \to K_S^0\pi^+\pi^-$. The results are given in Table 32, and shown in Fig. 15. Note that BABAR quote uncertainties due to the D decay model separately from other

Table 32 Averages from $B^0 \to D^{(*)}h^0$, $D \to K_S^0\pi^+\pi^-$ analyses

Experiment	$N(B\bar{B})$	$\sin 2\beta$	$\cos 2\beta$	$\lvert\lambda\rvert$
		Model dependent		
BABAR [261]	383M	$0.29 \pm 0.34 \pm 0.03 \pm 0.05$	$0.42 \pm 0.49 \pm 0.09 \pm 0.13$	$1.01 \pm 0.08 \pm 0.02$
Belle [260]	386M	$0.78 \pm 0.44 \pm 0.22$	$1.87\,^{+0.40}_{-0.53}\,^{+0.22}_{-0.32}$	–
Average		0.45 ± 0.28	1.01 ± 0.40	1.01 ± 0.08
Confidence level		0.59 (0.5σ)	0.12 (1.6σ)	–
		Model independent		
Belle [262]	772M	$0.43 \pm 0.27 \pm 0.08$	$1.06 \pm 0.33\,^{+0.21}_{-0.15}$	–

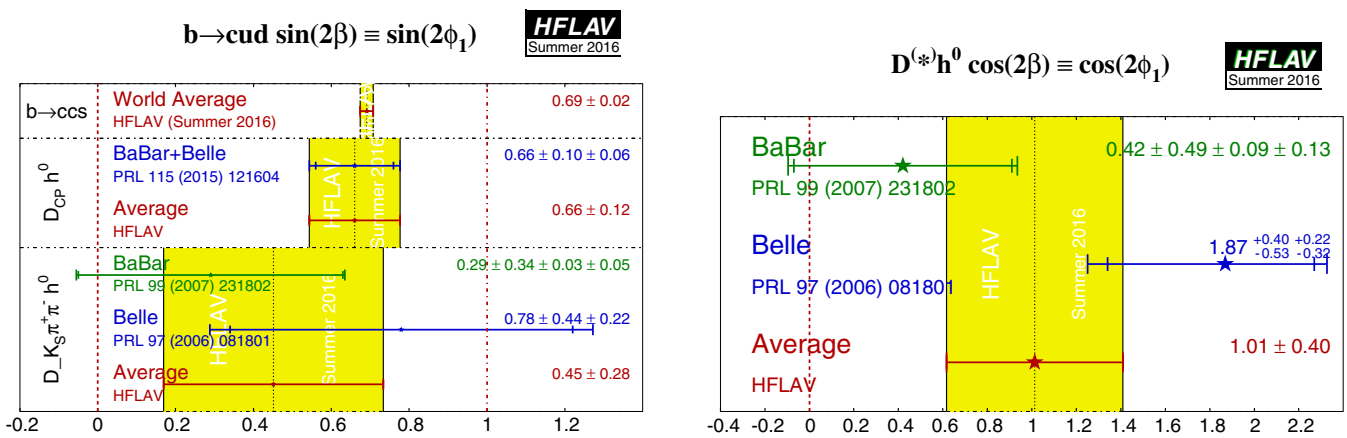

Fig. 15 Averages of (*left*) $\sin(2\beta)$ and (*right*) $\cos(2\beta)$ measured in colour-suppressed $b \to c\bar{u}d$ transitions

systematic errors as a third source of uncertainty, while Belle do not.

Again, it is clear that the data prefer $\cos(2\beta) > 0$. Indeed, Belle [260] determine the sign of $\cos(2\phi_1)$ to be positive at 98.3% confidence level, while BABAR [261] favour the solution of β with $\cos(2\beta) > 0$ at 87% confidence level. Note, however, that the Belle measurement has strongly non-Gaussian behaviour. Therefore, we perform uncorrelated averages, from which any interpretation has to be done with the greatest care.

A model-independent time-dependent analysis of $B^0 \to D^{(*)}h^0$ decays, with $D \to K_S^0\pi^+\pi^-$, has been performed by Belle [262]. The decays $B^0 \to D\pi^0$, $B^0 \to D\eta$, $B^0 \to D\eta'$, $B^0 \to D\omega$, $B^0 \to D^*\pi^0$ and $B^0 \to D^*\eta$ are used. The results are also included in Table 32. From these results, Belle disfavour the solution with the value of $\sin(2\phi_1)$ from $b \to c\bar{c}s$ transitions but a negative value for $\cos(2\phi_1)$, at $5.1\,\sigma$ significance. The solution with the $b \to c\bar{c}s$ value of $\sin(2\phi_1)$ and positive $\cos(2\phi_1)$ is consistent with the data at the level of $1.3\,\sigma$. Note that due to the strong statistical and systematic correlations, model-dependent results and model-independent results from the same experiment cannot be combined.

4.6 Time-dependent CP asymmetries in $b \to c\bar{c}d$ transitions

The transition $b \to c\bar{c}d$ can occur via either a $b \to c$ tree or a $b \to d$ penguin amplitude. The flavour changing neutral current $b \to d$ penguin can be mediated by any up-type quark in the loop, and hence the amplitude can be written as

$$\begin{aligned} A_{b\to d} &= F_u V_{ub} V_{ud}^* + F_c V_{cb} V_{cd}^* + F_t V_{tb} V_{td}^* \\ &= (F_u - F_c) V_{ub} V_{ud}^* + (F_t - F_c) V_{tb} V_{td}^*, \end{aligned} \tag{153}$$

where $F_{u,c,t}$ describe all factors except CKM suppression entering each quark loop diagram. In the last line, both terms are $\mathcal{O}(\lambda^3)$, so it can be seen that the $b \to d$ penguin amplitude contains terms with different weak phases at the same order of CKM suppression.

In the above, we have chosen to eliminate the F_c term using unitarity. However, we could equally well write

$$\begin{aligned} A_{b\to d} &= (F_u - F_t) V_{ub} V_{ud}^* + (F_c - F_t) V_{cb} V_{cd}^* \\ &= (F_c - F_u) V_{cb} V_{cd}^* + (F_t - F_u) V_{tb} V_{td}^*. \end{aligned} \tag{154}$$

Since the $b \to c\bar{c}d$ tree amplitude has the weak phase of $V_{cb}V_{cd}^*$, either of the above expressions allow the penguin amplitude to be decomposed into a part with weak phase the

Table 33 Averages for the $b \to c\bar{c}d$ modes, $B^0 \to J/\psi\pi^0$ and D^+D^-

Experiment	Sample size	S_{CP}	C_{CP}	Correlation
$J/\psi\pi^0$				
BABAR [353]	$N(B\bar{B}) = 466$M	$-1.23 \pm 0.21 \pm 0.04$	$-0.20 \pm 0.19 \pm 0.03$	0.20
Belle [354]	$N(B\bar{B}) = 535$M	$-0.65 \pm 0.21 \pm 0.05$	$-0.08 \pm 0.16 \pm 0.05$	-0.10
Average		-0.93 ± 0.15	-0.10 ± 0.13	0.04
Confidence level		0.15 (1.4σ)		
D^+D^-				
BABAR [259]	$N(B\bar{B}) = 467$M	$-0.65 \pm 0.36 \pm 0.05$	$-0.07 \pm 0.23 \pm 0.03$	-0.01
Belle [287]	$N(B\bar{B}) = 772$M	$-1.06^{+0.21}_{-0.14} \pm 0.08$	$-0.43 \pm 0.16 \pm 0.05$	-0.12
LHCb [355]	$\int \mathcal{L}\,dt = 3\,\text{fb}^{-1}$	$-0.54^{+0.17}_{-0.16} \pm 0.05$	$0.26^{+0.18}_{-0.17} \pm 0.02$	0.48
Average		-0.84 ± 0.12	-0.13 ± 0.10	0.18
Confidence level		0.027 (2.2σ)		

Table 34 Averages for the $b \to c\bar{c}d$ modes, $J/\psi\rho^0$, $D^{*+}D^{*-}$ and $D^{*\pm}D^{\mp}$

Experiment	$N(B\bar{B})$	S_{CP}	C_{CP}	$R_\perp$
$J/\psi\rho^0$				
LHCb [258]	3 fb^{-1}	$-0.66^{+0.13}_{-0.12}{}^{+0.09}_{-0.03}$	$-0.06 \pm 0.06^{+0.02}_{-0.01}$	0.198 ± 0.017
$D^{*+}D^{*-}$				
BABAR [259]	467M	$-0.70 \pm 0.16 \pm 0.03$	$0.05 \pm 0.09 \pm 0.02$	0.17 ± 0.03
BABAR part. rec. [356]	471M	$-0.49 \pm 0.18 \pm 0.07 \pm 0.04$	$0.15 \pm 0.09 \pm 0.04$	–
Belle [352]	772M	$-0.79 \pm 0.13 \pm 0.03$	$-0.15 \pm 0.08 \pm 0.02$	$0.14 \pm 0.02 \pm 0.01$
Average		-0.71 ± 0.09	-0.01 ± 0.05	0.15 ± 0.02
Confidence level			0.72 (0.4σ)	

Experiment	$N(B\bar{B})$	S_{CP+}	C_{CP+}	S_{CP-}	C_{CP-}	$R_\perp$
$D^{*+}D^{*-}$						
BABAR [259]	467M	$-0.76 \pm 0.16 \pm 0.04$	$0.02 \pm 0.12 \pm 0.02$	$-1.81 \pm 0.71 \pm 0.16$	$0.41 \pm 0.50 \pm 0.08$	0.15 ± 0.03

Experiment	$N(B\bar{B})$	S	C	ΔS	ΔC	$\mathcal{A}$
$D^{*\pm}D^{\mp}$						
BABAR [259]	467M	$-0.68 \pm 0.15 \pm 0.04$	$0.04 \pm 0.12 \pm 0.03$	$0.05 \pm 0.15 \pm 0.02$	$0.04 \pm 0.12 \pm 0.03$	$0.01 \pm 0.05 \pm 0.01$
Belle [287]	772M	$-0.78 \pm 0.15 \pm 0.05$	$-0.01 \pm 0.11 \pm 0.04$	$-0.13 \pm 0.15 \pm 0.04$	$0.12 \pm 0.11 \pm 0.03$	$0.06 \pm 0.05 \pm 0.02$
Average		-0.73 ± 0.11	0.01 ± 0.09	-0.04 ± 0.11	0.08 ± 0.08	0.03 ± 0.04
Confidence level		0.65 (0.5σ)	0.77 (0.3σ)	0.41 (0.8σ)	0.63 (0.5σ)	0.48 (0.7σ)

same as the tree amplitude and another part with a different weak phase, which can be chosen to be either β or γ. The choice of parametrisation cannot, of course, affect the physics [351]. In any case, if the tree amplitude dominates, there is little sensitivity to any phase other than that from B^0–$\overline{B}^0$ mixing.

The $b \to c\bar{c}d$ transitions can be investigated with studies of various different final states. Results are available from both BABAR and Belle using the final states $J/\psi\pi^0$, D^+D^-, $D^{*+}D^{*-}$ and $D^{*\pm}D^{\mp}$, and from LHCb using the final states $J/\psi\rho^0$ and D^+D^-; the averages of these results are given in Tables 33 and 34. The results using the CP eigenstate ($\eta = +1$) modes $J/\psi\pi^0$ and D^+D^- are shown in Fig. 16 and Fig. 17 respectively, with two-dimensional constraints shown in Fig. 18.

Results for the vector-vector mode $J/\psi\rho^0$ are obtained from a full time-dependent amplitude analysis of $B^0 \to J/\psi\pi^+\pi^-$ decays. LHCb [258] find a $J/\psi\rho^0$ fit fraction of $65.6 \pm 1.9\%$ and a longitudinal polarisation fraction of $56.7 \pm 1.8\%$ (uncertainties are statistical only; both results are consistent with those from a time-integrated amplitude analysis [267] where systematic uncertainties were also evaluated). Fits are performed to obtain $2\beta^{\text{eff}}$ in the cases that all transversity amplitudes are assumed to have

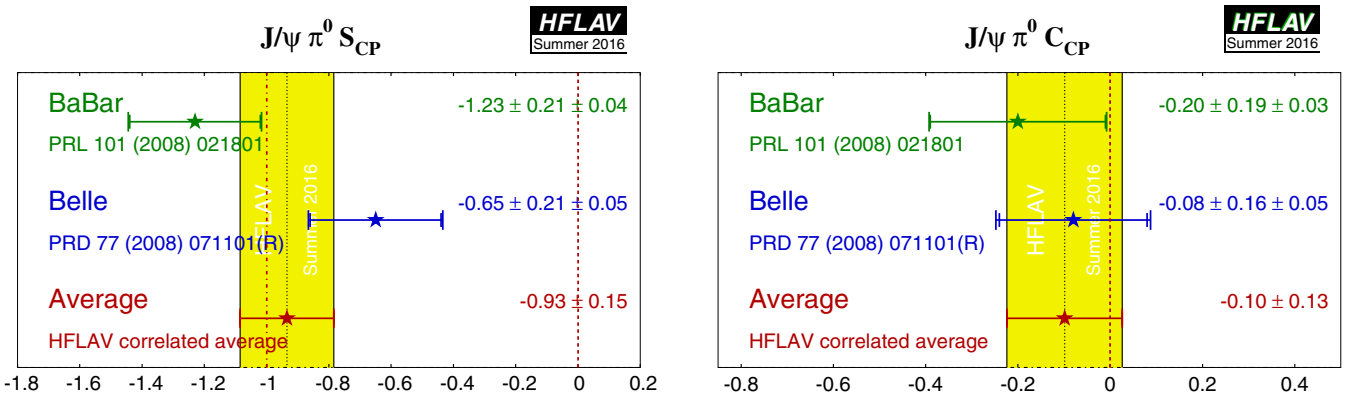

Fig. 16 Averages of (*left*) $S_{b\to c\bar{c}d}$ and (*right*) $C_{b\to c\bar{c}d}$ for the mode $B^0 \to J/\psi\pi^0$

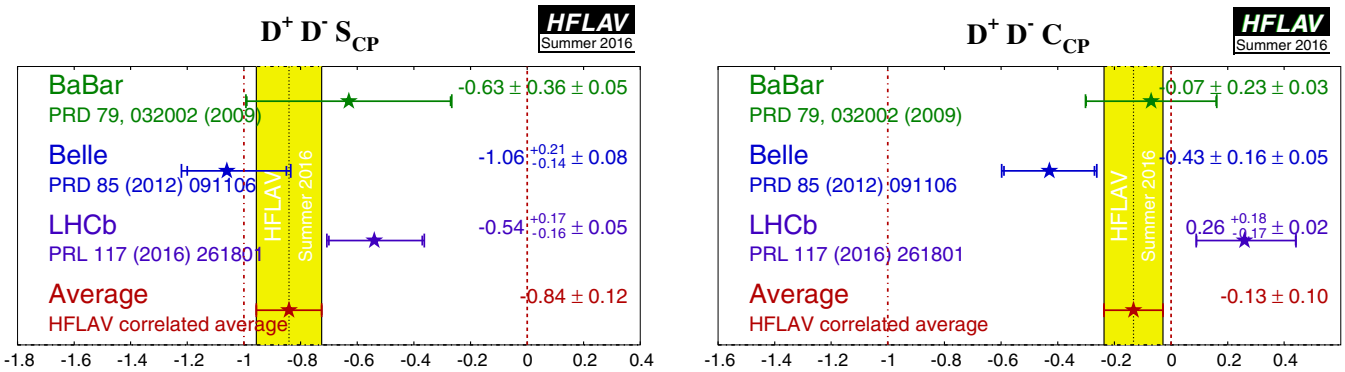

Fig. 17 Averages of (*left*) $S_{b\to c\bar{c}d}$ and (*right*) $C_{b\to c\bar{c}d}$ for the mode $B^0 \to D^+D^-$

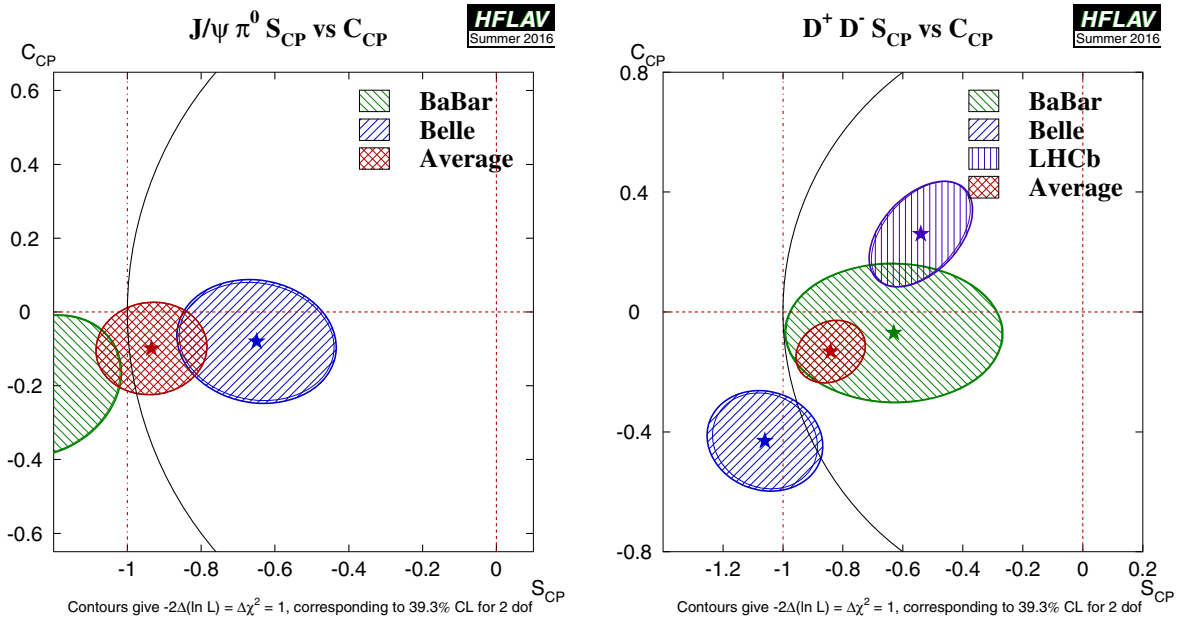

Fig. 18 Averages of two $b \to c\bar{c}d$ dominated channels, for which correlated averages are performed, in the S_{CP} *vs.* C_{CP} plane. (*Left*) $B^0 \to J/\psi\pi^0$ and (*right*) $B^0 \to D^+D^-$

the same *CP* violation parameter. A separate fit is performed allowing different parameters. The results in the former case are presented in terms of S_{CP} and C_{CP} in Table 34.

The vector-vector mode $D^{*+}D^{*-}$ is found to be dominated by the *CP*-even longitudinally polarised component; BABAR measures a *CP*-odd fraction of $0.158 \pm 0.028 \pm 0.006$ [259] while Belle measures a *CP*-odd fraction of

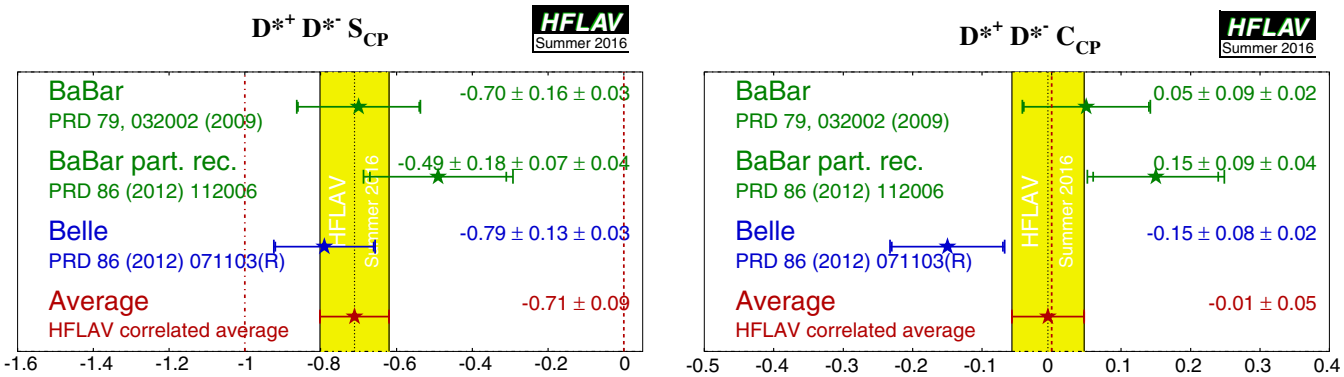

Fig. 19 Averages of (*left*) $S_{b\to c\bar{c}d}$ and (*right*) $C_{b\to c\bar{c}d}$ for the mode $B^0 \to D^{*+}D^{*-}$

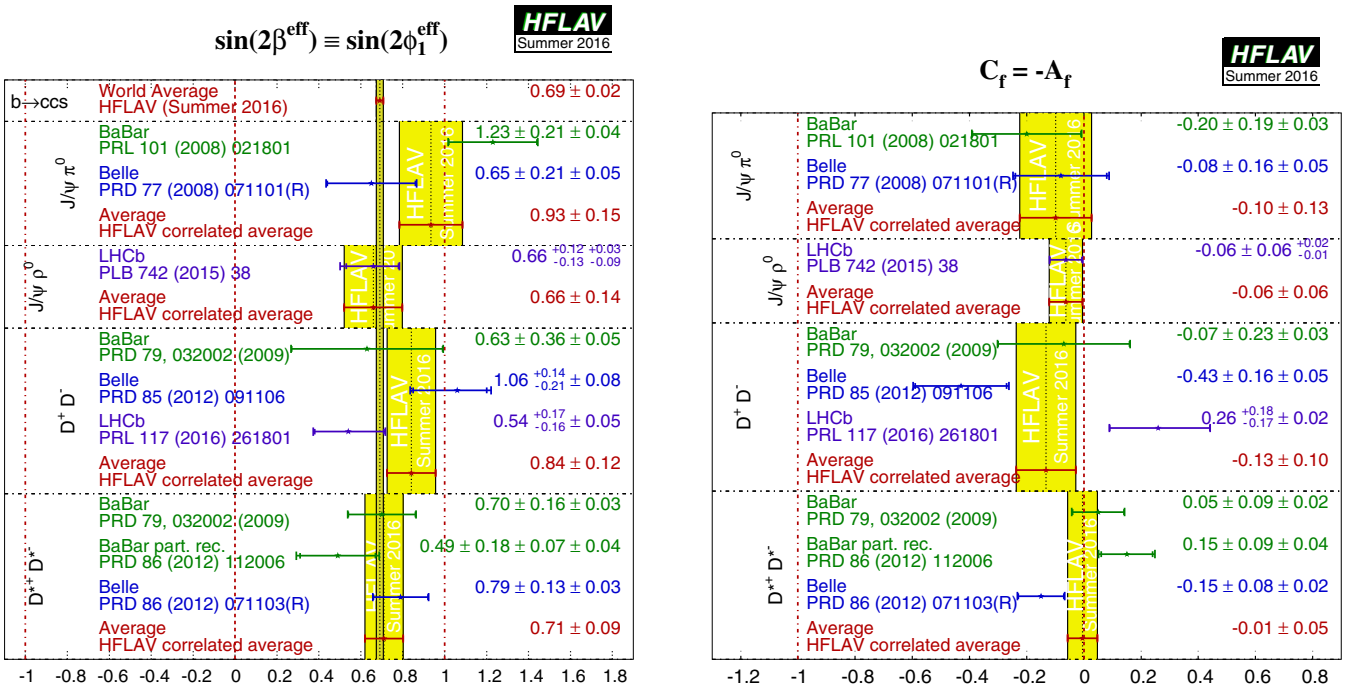

Fig. 20 Averages of (*left*) $-\eta S_{b\to c\bar{c}d}$ interpreted as $\sin(2\beta^{\text{eff}})$ and (*right*) $C_{b\to c\bar{c}d}$. The $-\eta S_{b\to c\bar{c}d}$ figure compares the results to the world average for $-\eta S_{b\to c\bar{c}s}$ (see Sect. 4.4.1)

$0.138 \pm 0.024 \pm 0.006$ [352]. These values, listed as $R_\perp$, are included in the averages, which ensures that the correlations are taken into account.[32] BABAR has also performed an additional fit in which the *CP*-even and *CP*-odd components are allowed to have different *CP* violation parameters S and C. These results are included in Table 34. Results using $D^{*+}D^{*-}$ are shown in Fig. 19.

As discussed in Sect. 4.2.6, the most recent papers on the non-*CP* eigenstate mode $D^{*\pm}D^{\mp}$ use the $(A, S, \Delta S, C, \Delta C)$ set of parameters, and we therefore perform the averages with this choice.

[32] Note that the BABAR value given in Table 34 differs from the value quoted here, since that in the table is not corrected for efficiency.

In the absence of the penguin contribution (tree dominance), the time-dependent parameters would be given by $S_{b\to c\bar{c}d} = -\eta\sin(2\beta)$, $C_{b\to c\bar{c}d} = 0$, $S_{+-} = \sin(2\beta+\delta)$, $S_{-+} = \sin(2\beta-\delta)$, $C_{+-} = -C_{-+}$ and $\mathcal{A} = 0$, where δ is the strong phase difference between the $D^{*+}D^-$ and $D^{*-}D^+$ decay amplitudes. In the presence of the penguin contribution, there is no clean interpretation in terms of CKM parameters; however, direct *CP* violation may be observed through any of $C_{b\to c\bar{c}d} \neq 0$, $C_{+-} \neq -C_{-+}$ or $A_{+-} \neq 0$.

The averages for the $b \to c\bar{c}d$ modes are shown in Figs. 20 and 21. Results are consistent with tree dominance, and with the Standard Model, though the Belle results in $B^0 \to D^+D^-$ [357] show an indication of *CP* violation in decay, and hence a non-zero penguin contribution. The average of $S_{b\to c\bar{c}d}$ in each of the $J/\psi\pi^0$, D^+D^- and $D^{*+}D^{*-}$

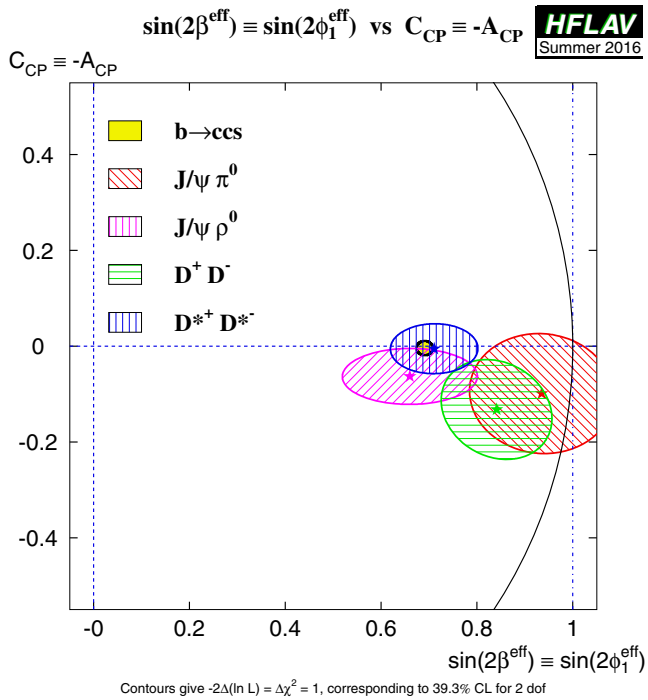

Fig. 21 Compilation of constraints in the $-\eta S_{b\to c\bar{c}d}$, interpreted as $\sin(2\beta^{\rm eff})$, *vs.* $C_{b\to c\bar{c}d}$ plane

final states is more than 5σ from zero, corresponding to observations of *CP* violation in these decay channels. Possible non-Gaussian effects due to some of the inputs measurements being outside the physical region ($S_{CP}^2 + C_{CP}^2 \leq 1$) should, however, be borne in mind.

4.6.1 Time-dependent CP asymmetries in B_s^0 decays mediated by $b \to c\bar{c}d$ transitions

Time-dependent *CP* asymmetries in B_s^0 decays mediated by $b \to c\bar{c}d$ transitions provide a determination of $2\beta_s^{\rm eff}$ where possible effects from penguin amplitudes may cause a shift from the value of $2\beta_s$ seen in $b \to c\bar{c}s$ transitions. Results in the $b \to c\bar{c}d$ case, with larger penguin effects, can be used together with flavour symmetries to derive limits on the possible size of penguin effects in the $b \to c\bar{c}s$ transitions [358,359].

The parameters have been measured in $B_s^0 \to J/\psi K_S^0$ decays by LHCb, as summarised in Table 35. The results supersede an earlier measurement of the effective lifetime, which is directly related to $A^{\Delta\Gamma}$, in the same mode [127], which is discussed in Sect. 3.

4.7 Time-dependent *CP* asymmetries in charmless $b \to q\bar{q}s$ transitions

Similarly to Eq. (153), the $b \to s$ penguin amplitude can be written as

$$\begin{aligned} A_{b\to s} &= F_u V_{ub} V_{us}^* + F_c V_{cb} V^*{}_{cs} + F_t V_{tb} V_{ts}^* \\ &= (F_u - F_c) V_{ub} V_{us}^* + (F_t - F_c) V_{tb} V_{ts}^*, \end{aligned} \tag{155}$$

using the unitarity of the CKM matrix to eliminate the F_c term. In this case, the first term in the last line is $\mathcal{O}(\lambda^4)$ while the second is $\mathcal{O}(\lambda^2)$. Therefore, in the Standard Model, this amplitude is dominated by $V_{tb}V_{ts}^*$, and to within a few degrees ($|\delta\beta^{\rm eff}| \equiv |\beta^{\rm eff} - \beta| \lesssim 2^\circ$ for $\beta \approx 20^\circ$) the time-dependent parameters can be written[33] $S_{b\to q\bar{q}s} \approx -\eta \sin(2\beta)$, $C_{b\to q\bar{q}s} \approx 0$, assuming $b \to s$ penguin contributions only ($q = u, d, s$).

Due to the suppression of the Standard Model amplitude, contributions of additional diagrams from physics beyond the Standard Model, with heavy virtual particles in the penguin loops, may have observable effects. In general, these contributions will affect the values of $S_{b\to q\bar{q}s}$ and $C_{b\to q\bar{q}s}$. A discrepancy between the values of $S_{b\to c\bar{c}s}$ and $S_{b\to q\bar{q}s}$ can therefore provide a clean indication of new physics [346,361–363].

However, there is an additional consideration to take into account. The above argument assumes that only the $b \to s$ penguin contributes to the $b \to q\bar{q}s$ transition. For $q = s$ this is a good assumption, which neglects only rescattering effects. However, for $q = u$ there is a colour-suppressed $b \to u$ tree diagram (of order $\mathcal{O}(\lambda^4)$), which has a different weak (and possibly strong) phase. In the case $q = d$, any light neutral meson that is formed from $d\bar{d}$ also has a $u\bar{u}$ component, and so again there is "tree pollution". The B^0 decays to $\pi^0 K_S^0$, $\rho^0 K_S^0$ and ωK_S^0 belong to this category. The mesons ϕ, f_0 and η' are expected to have predominant $s\bar{s}$ composition, which reduces the relative size of the possible tree pollution. If the inclusive decay $B^0 \to K^+K^-K^0$ (excluding ϕK^0) is dominated by a nonresonant three-body transition, an Okubo–Zweig–Iizuka-suppressed [364–366] tree-level diagram can occur through insertion of an $s\bar{s}$ pair. The corresponding penguin-type transition proceeds via insertion of a $u\bar{u}$ pair, which is expected to be favoured over the $s\bar{s}$ insertion by fragmentation models. Neglecting rescattering, the final state $K^0\overline{K}^0K^0$ (reconstructed as $K_S^0K_S^0K_S^0$) has no tree pollution [367]. Various estimates, using different theoretical approaches, of the values of $\Delta S = S_{b\to q\bar{q}s} - S_{b\to c\bar{c}s}$ exist in the literature [368–381]. In general, there is agreement that the modes ϕK^0, $\eta' K^0$ and $K^0\overline{K}^0K^0$ are the cleanest, with values of $|\Delta S|$ at or below the few percent level (ΔS is usually predicted to be positive). Nonetheless, the uncertainty is sufficient that interpretation is given in terms of $\sin(2\beta^{\rm eff})$.

[33] The presence of a small ($\mathcal{O}(\lambda^2)$) weak phase in the dominant amplitude of the s penguin decays introduces a phase shift given by $S_{b\to q\bar{q}s} = -\eta \sin(2\beta)(1 + \Delta)$. Using the CKMfitter results for the Wolfenstein parameters [252], one finds $\Delta \simeq 0.033$, which corresponds to a shift of 2β of $+2.1^\circ$. Nonperturbative contributions can alter this result.

Table 35 Measurements of CP violation parameters from $B_s^0 \to J/\psi K_S^0$

Experiment	$\int \mathcal{L}\,dt$	S_{CP}	C_{CP}	$A^{\Delta\Gamma}$
LHCb [360]	3 fb^{-1}	$0.49^{+0.77}_{-0.65} \pm 0.06$	$-0.28 \pm 0.41 \pm 0.08$	$-0.08 \pm 0.40 \pm 0.08$

4.7.1 *Time-dependent CP asymmetries: $b \to q\bar{q}s$ decays to CP eigenstates*

The averages for $-\eta S_{b\to q\bar{q}s}$ and $C_{b\to q\bar{q}s}$ can be found in Tables 36 and 37, and are shown in Figs. 22, 23 and 24. Results from both BaBar and Belle are averaged for the modes $\eta' K^0$ (K^0 indicates that both K_S^0 and K_L^0 are used) $K_S^0 K_S^0 K_S^0$, $\pi^0 K_S^0$ and ωK_S^0.[34] Results on ϕK_S^0 and $K^+K^-K_S^0$ (implicitly excluding ϕK_S^0 and $f_0 K_S^0$) are taken from time-dependent Dalitz plot analyses of $K^+K^-K_S^0$; results on $\rho^0 K_S^0$, $f_2 K_S^0$, $f_X K_S^0$ and $\pi^+\pi^-K_S^0$ nonresonant are taken from time-dependent Dalitz plot analyses of $\pi^+\pi^-K_S^0$ (see Sect. 4.7.2). The results on $f_0 K_S^0$ are from combinations of both Dalitz plot analyses. BaBar has also presented results with the final states $\pi^0\pi^0 K_S^0$ and $\phi K_S^0 \pi^0$.

Of these final states, ϕK_S^0, $\eta' K_S^0$, $\pi^0 K_S^0$, $\rho^0 K_S^0$, ωK_S^0 and $f_0 K_L^0$ have CP eigenvalue $\eta = -1$, while ϕK_L^0, $\eta' K_L^0$, $K_S^0 K_S^0 K_S^0$, $f_0 K_S^0$, $f_2 K_S^0$, $f_X K_S^0$, $\pi^0\pi^0 K_S^0$ and $\pi^+\pi^-K_S^0$ nonresonant have $\eta = +1$. The final state $K^+K^-K_S^0$ (with ϕK_S^0 and $f_0 K_S^0$ implicitly excluded) is not a CP eigenstate, but the CP-content can be absorbed in the amplitude analysis to allow the determination of a single effective S parameter. (In earlier analyses of the $K^+K^-K^0$ final state, its CP composition was determined using an isospin argument [383] and a moments analysis [384].) Throughout this section, $f_0 \equiv f_0(980)$ and $f_2 \equiv f_2(1270)$. Details of the assumed lineshapes of these states, and of the f_X (which is taken to have even spin), can be found in the relevant experimental papers [270,271,274,275].

The final state $\phi K_S^0 \pi^0$ is also not a CP eigenstate but its CP-composition can be determined from an angular analysis. Since the parameters are common to the $B^0 \to \phi K_S^0 \pi^0$ and $B^0 \to \phi K^+\pi^-$ decays (because only $K\pi$ resonances contribute), BaBar perform a simultaneous analysis of the two final states [391] (see Sect. 4.7.3).

It must be noted that Q2B parameters extracted from Dalitz plot analyses are constrained to lie within the physical boundary ($S_{CP}^2 + C_{CP}^2 < 1$) and consequently the obtained errors are highly non-Gaussian when the central value is close to the boundary. This is particularly evident in the BaBar results for $B^0 \to f_0 K^0$ with $f_0 \to \pi^+\pi^-$ [274]. These results must be treated with extreme caution.

[34] Belle [382] include the $\pi^0 K_L^0$ final state together with $\pi^0 K_S^0$ in order to improve the constraint on the parameter of CP violation in decay; these events cannot be used for time-dependent analysis.

As explained above, each of the modes listed in Tables 36 and 37 has potentially different subleading contributions within the Standard Model, and thus each may have a different value of $-\eta S_{b\to q\bar{q}s}$. Therefore, there is no strong motivation to make a combined average over the different modes. We refer to such an average as a "naïve s-penguin average". It is naïve not only because the theoretical uncertainties are neglected, but also since possible correlations of systematic effects between different modes are not included. In spite of these caveats there remains interest in the value of this quantity and therefore it is given here: $\langle -\eta S_{b\to q\bar{q}s}\rangle = 0.655 \pm 0.032$, with confidence level 0.77 (0.3σ). This value is in agreement with the average $-\eta S_{b\to c\bar{c}s}$ given in Sect. 4.4.1. (The average for $C_{b\to q\bar{q}s}$ is $\langle C_{b\to q\bar{q}s}\rangle = -0.006 \pm 0.026$ with confidence level 0.53 (0.6σ).)

From Table 36 it may be noted that the averages for $-\eta S_{b\to q\bar{q}s}$ in ϕK_S^0, $\eta' K^0$, $f_0 K_S^0$ and $K^+K^-K_S^0$ are all now more than 5σ away from zero, so that CP violation in these modes can be considered well established. There is no evidence (above 2σ) for CP violation in any $b \to q\bar{q}s$ decay.

4.7.2 *Time-dependent Dalitz plot analyses: $B^0 \to K^+K^-K^0$ and $B^0 \to \pi^+\pi^-K_S^0$*

As mentioned in Sect. 4.2.5 and above, both BaBar and Belle have performed time-dependent Dalitz plot analysis of $B^0 \to K^+K^-K^0$ and $B^0 \to \pi^+\pi^-K_S^0$ decays. The results are summarised in Tables 38 and 39. Averages for the $B^0 \to f_0 K_S^0$ decay, which contributes to both Dalitz plots, are shown in Fig. 25. Results are presented in terms of the effective weak phase (from mixing and decay) difference $\beta^{\rm eff}$ and the parameter of CP violation in decay $\mathcal{A}$ ($\mathcal{A} = -C$) for each of the resonant contributions. Note that Dalitz plot analyses, including all those included in these averages, often suffer from ambiguous solutions – we quote the results corresponding to those presented as solution 1 in all cases. Results on flavour specific amplitudes that may contribute to these Dalitz plots (such as $K^{*+}\pi^-$) are averaged by the HFLAV Rare Decays subgroup (Sect. 7).

For the $B^0 \to K^+K^-K^0$ decay, both BaBar and Belle measure the CP violation parameters for the ϕK^0, $f_0 K^0$ and "other $K^+K^-K^0$" amplitudes, where the latter includes all remaining resonant and nonresonant contributions to the charmless three-body decay. For the $B^0 \to \pi^+\pi^-K_S^0$ decay, BaBar reports CP violation parameters for all of the CP

Table 36 Averages of $-\eta S_{b\to q\bar{q}s}$ and $C_{b\to q\bar{q}s}$. Where a third source of uncertainty is given, it is due to model uncertainties arising in Dalitz plot analyses

Experiment	$N(B\bar{B})$	$-\eta S_{b\to q\bar{q}s}$	$C_{b\to q\bar{q}s}$	Correlation
ϕK^0				
BaBar [271]	470M	$0.66 \pm 0.17 \pm 0.07$	$0.05 \pm 0.18 \pm 0.05$	–
Belle [270]	657M	$0.90^{+0.09}_{-0.19}$	$-0.04 \pm 0.20 \pm 0.10 \pm 0.02$	–
Average		$0.74^{+0.11}_{-0.13}$	0.01 ± 0.14	Uncorrelated averages
$\eta' K^0$				
BaBar [385]	467M	$0.57 \pm 0.08 \pm 0.02$	$-0.08 \pm 0.06 \pm 0.02$	0.03
Belle [386]	772M	$0.68 \pm 0.07 \pm 0.03$	$-0.03 \pm 0.05 \pm 0.03$	0.03
Average		0.63 ± 0.06	-0.05 ± 0.04	0.02
Confidence level		0.53 (0.6σ)		
$K^0_S K^0_S K^0_S$				
BaBar [387]	468M	$0.94^{+0.21}_{-0.24} \pm 0.06$	$-0.17 \pm 0.18 \pm 0.04$	0.16
Belle [388]	535M	$0.30 \pm 0.32 \pm 0.08$	$-0.31 \pm 0.20 \pm 0.07$	–
Average		0.72 ± 0.19	-0.24 ± 0.14	0.09
Confidence level		0.26 (1.1σ)		
$\pi^0 K^0$				
BaBar [385]	467M	$0.55 \pm 0.20 \pm 0.03$	$0.13 \pm 0.13 \pm 0.03$	0.06
Belle [382]	657M	$0.67 \pm 0.31 \pm 0.08$	$-0.14 \pm 0.13 \pm 0.06$	-0.04
Average		0.57 ± 0.17	0.01 ± 0.10	0.02
Confidence level		0.37 (0.9σ)		
$\rho^0 K^0_S$				
BaBar [274]	383M	$0.35^{+0.26}_{-0.31} \pm 0.06 \pm 0.03$	$-0.05 \pm 0.26 \pm 0.10 \pm 0.03$	–
Belle [275]	657M	$0.64^{+0.19}_{-0.25} \pm 0.09 \pm 0.10$	$-0.03^{+0.24}_{-0.23} \pm 0.11 \pm 0.10$	–
Average		$0.54^{+0.18}_{-0.21}$	-0.06 ± 0.20	Uncorrelated averages
ωK^0_S				
BaBar [385]	467M	$0.55^{+0.26}_{-0.29} \pm 0.02$	$-0.52^{+0.22}_{-0.20} \pm 0.03$	0.03
Belle [389]	772M	$0.91 \pm 0.32 \pm 0.05$	$0.36 \pm 0.19 \pm 0.05$	-0.00
Average		0.71 ± 0.21	-0.04 ± 0.14	0.01
Confidence level		0.007 (2.7σ)		
$f_0 K^0$				
BaBar [271,274]	–	$0.74^{+0.12}_{-0.15}$	0.15 ± 0.16	–
Belle [270,275]	–	$0.63^{+0.16}_{-0.19}$	0.13 ± 0.17	–
Average		$0.69^{+0.10}_{-0.12}$	0.14 ± 0.12	Uncorrelated averages
$f_2 K^0_S$				
BaBar [274]	383M	$0.48 \pm 0.52 \pm 0.06 \pm 0.10$	$0.28^{+0.35}_{-0.40} \pm 0.08 \pm 0.07$	–
$f_X K^0_S$				
BaBar [274]	383M	$0.20 \pm 0.52 \pm 0.07 \pm 0.07$	$0.13^{+0.33}_{-0.35} \pm 0.04 \pm 0.09$	–

eigenstate components in the Dalitz plot model ($\rho^0 K^0_S$, $f_0 K^0_S$, $f_2 K^0_S$, $f_X K^0_S$ and nonresonant decays; see Sect. 4.2.5), while Belle reports the CP violation parameters for only the $\rho^0 K^0_S$ and $f_0 K^0_S$ amplitudes, although the used Dalitz plot model is rather similar.

4.7.3 *Time-dependent analyses of $B^0 \to \phi K^0_S \pi^0$*

The final state in the decay $B^0 \to \phi K^0_S \pi^0$ is a mixture of CP-even and CP-odd amplitudes. However, since only ϕK^{*0} resonant states contribute (in particular, $\phi K^{*0}(892)$, $\phi K^{*0}_0(1430)$ and $\phi K^{*0}_2(1430)$ are seen), the composition

Table 37 Averages of $-\eta S_{b\to q\bar{q}s}$ and $C_{b\to q\bar{q}s}$ (continued). Where a third source of uncertainty is given, it is due to model uncertainties arising in Dalitz plot analyses

Experiment	$N(B\bar{B})$	$-\eta S_{b\to q\bar{q}s}$	$C_{b\to q\bar{q}s}$	Correlation
$\pi^0\pi^0 K_S^0$				
BaBar [390]	227M	$-0.72 \pm 0.71 \pm 0.08$	$0.23 \pm 0.52 \pm 0.13$	-0.02
$\phi K_S^0\pi^0$				
BaBar [391]	465M	$0.97^{+0.03}_{-0.52}$	$-0.20 \pm 0.14 \pm 0.06$	–
$\pi^+\pi^- K_S^0$ nonresonant				
BaBar [274]	383M	$0.01 \pm 0.31 \pm 0.05 \pm 0.09$	$0.01 \pm 0.25 \pm 0.06 \pm 0.05$	–
$K^+K^-K^0$				
BaBar [271]	470M	$0.65 \pm 0.12 \pm 0.03$	$0.02 \pm 0.09 \pm 0.03$	–
Belle [270]	657M	$0.76^{+0.14}_{-0.18}$	$0.14 \pm 0.11 \pm 0.08 \pm 0.03$	–
Average		$0.68^{+0.09}_{-0.10}$	0.06 ± 0.08	Uncorrelated averages

can be determined from the analysis of $B \to \phi K^+\pi^-$ decays, assuming only that the ratio of branching fractions $\mathcal{B}(K^{*0} \to K_S^0\pi^0)/\mathcal{B}(K^{*0} \to K^+\pi^-)$ is the same for each excited kaon state.

BaBar [391] has performed a simultaneous analysis of $B^0 \to \phi K_S^0\pi^0$ and $B^0 \to \phi K^+\pi^-$ decays that is time-dependent for the former mode and time-integrated for the latter. Such an analysis allows, in principle, all parameters of the $B^0 \to \phi K^{*0}$ system to be determined, including mixing-induced CP violation effects. The latter is determined to be $\Delta\phi_{00} = 0.28 \pm 0.42 \pm 0.04$, where $\Delta\phi_{00}$ is half the weak phase difference between B^0 and $\overline{B}^0$ decays to the $\phi K_0^{*0}(1430)$ final state. As discussed above, this can also be presented in terms of the Q2B parameter $\sin(2\beta_{00}^{\rm eff}) = \sin(2\beta + 2\Delta\phi_{00}) = 0.97^{+0.03}_{-0.52}$. The highly asymmetric uncertainty arises due to the conversion from the phase to the sine of the phase, and the proximity of the physical boundary.

Similar $\sin(2\beta^{\rm eff})$ parameters can be defined for each of the helicity amplitudes for both $\phi K^{*0}(892)$ and $\phi K_2^{*0}(1430)$. However, the relative phases between these decays are constrained due to the nature of the simultaneous analysis of $B^0 \to \phi K_S^0\pi^0$ and $B^0 \to \phi K^+\pi^-$, decays and therefore these measurements are highly correlated. Instead of quoting all these results, BaBar provide an illustration of their measurements with the following differences:

$$\sin(2\beta - 2\Delta\delta_{01}) - \sin(2\beta) = -0.42^{+0.26}_{-0.34}, \quad (156)$$

$$\sin(2\beta - 2\Delta\phi_{\parallel 1}) - \sin(2\beta) = -0.32^{+0.22}_{-0.30}, \quad (157)$$

$$\sin(2\beta - 2\Delta\phi_{\perp 1}) - \sin(2\beta) = -0.30^{+0.23}_{-0.32}, \quad (158)$$

$$\sin(2\beta - 2\Delta\phi_{\perp 1}) - \sin(2\beta - 2\Delta\phi_{\parallel 1}) = 0.02 \pm 0.23, \quad (159)$$

$$\sin(2\beta - 2\Delta\delta_{02}) - \sin(2\beta) = -0.10^{+0.18}_{-0.29}, \quad (160)$$

where the first subscript indicates the helicity amplitude and the second indicates the spin of the kaon resonance. For the complete definitions of the $\Delta\delta$ and $\Delta\phi$ parameters, please refer to the BaBar paper [391].

Parameters of CP violation in decay for each of the contributing helicity amplitudes can also be measured. Again, these are determined from a simultaneous fit of $B^0 \to \phi K_S^0\pi^0$ and $B^0 \to \phi K^+\pi^-$ decays, with the precision being dominated by the statistics of the latter mode. Measurements of CP violation in decay, obtained from decay-time-integrated analyses, are tabulated by the HFLAV Rare Decays subgroup (Sect. 7).

4.7.4 Time-dependent CP asymmetries in $B_s^0 \to K^+K^-$

The decay $B_s^0 \to K^+K^-$ involves a $b \to u\bar{u}s$ transition, and hence has both penguin and tree contributions. Both mixing-induced and CP violation in decay effects may arise, and additional input is needed to disentangle the contributions and determine γ and $\beta_s^{\rm eff}$. For example, the observables in $B^0 \to \pi^+\pi^-$ can be related using U-spin, as proposed in Refs. [392,393].

The observables are $A_{\rm mix} = S_{CP}$, $A_{\rm dir} = -C_{CP}$, and $A_{\Delta\Gamma}$. They can all be treated as free parameters, but are physically constrained to satisfy $A_{\rm mix}^2 + A_{\rm dir}^2 + A_{\Delta\Gamma}^2 = 1$. Note that the untagged decay distribution, from which an "effective lifetime" can be measured, retains sensitivity to $A_{\Delta\Gamma}$; measurements of the $B_s^0 \to K^+K^-$ effective lifetime have been made by LHCb [104,125]. Compilations and averages of effective lifetimes are performed by the HFLAV Lifetimes and Oscillations subgroup, see Sect. 3.

The observables in $B_s^0 \to K^+K^-$ have been measured by LHCb [394], who do not impose the constraint mentioned above to eliminate $A_{\Delta\Gamma}$. The results are shown in Table 40, and correspond to evidence for CP violation both in the interference between mixing and decay, and in the $B_s^0 \to K^+K^-$ decay.

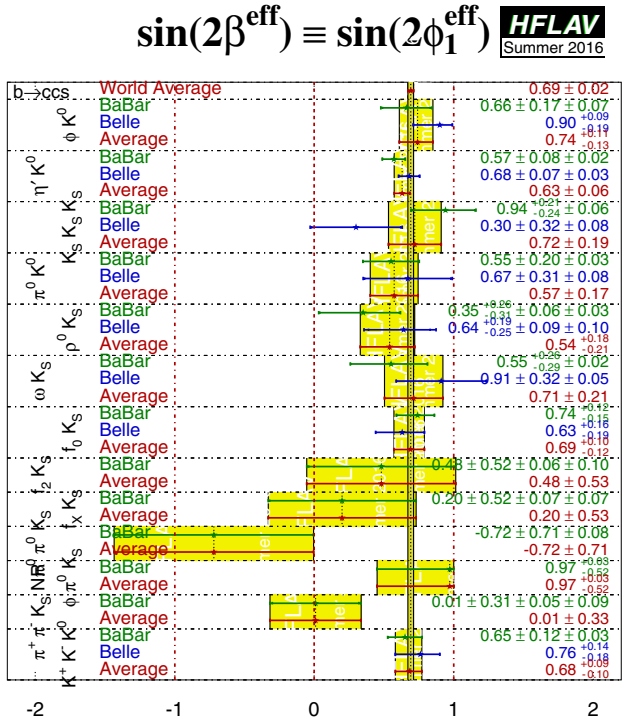

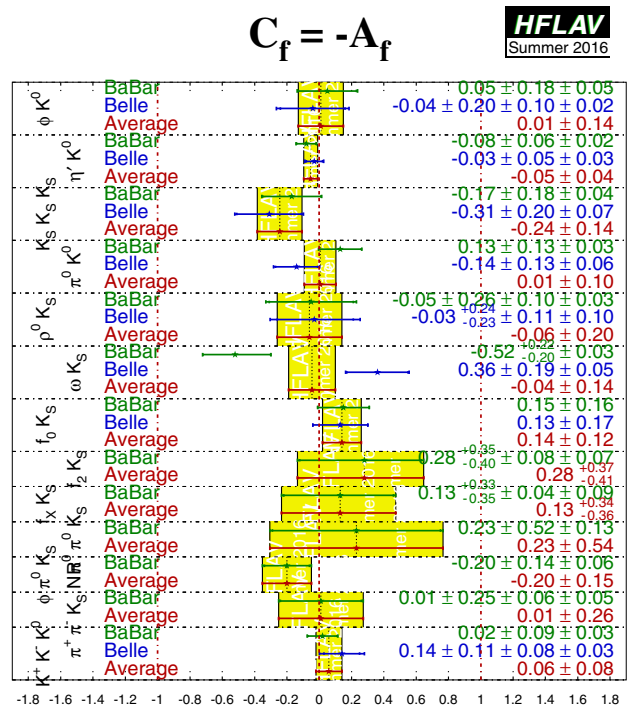

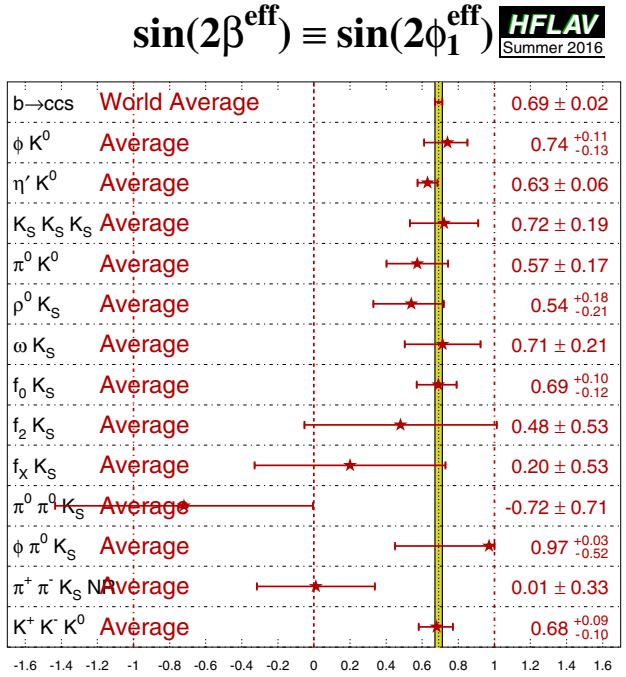

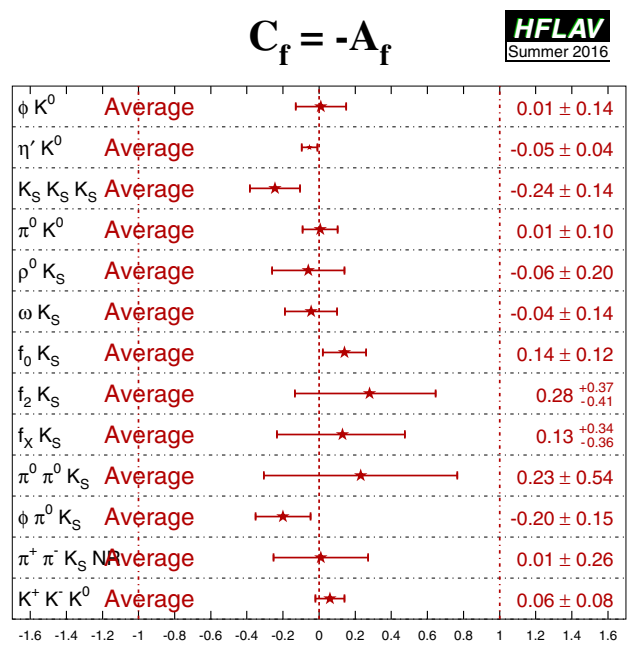

Fig. 22 (*Top*) Averages of (*left*) $-\eta S_{b\to q\bar{q}s}$, interpreted as $\sin(2\beta^{\rm eff}$ and (*right*) $C_{b\to q\bar{q}s}$. The $-\eta S_{b\to q\bar{q}s}$ figure compares the results to the world average for $-\eta S_{b\to c\bar{c}s}$ (see Sect. 4.4.1). (*Bottom*) Same, but only averages for each mode are shown. More figures are available from the HFLAV web pages

Interpretations of an earlier set of results [395], in terms of constraints on γ and $2\beta_s$, have been separately published by LHCb [243].

4.7.5 *Time-dependent CP asymmetries in $B_s^0 \to \phi\phi$*

The decay $B_s^0 \to \phi\phi$ involves a $b \to s\bar{s}s$ transition, and hence is a "pure penguin" mode (in the limit that the ϕ meson

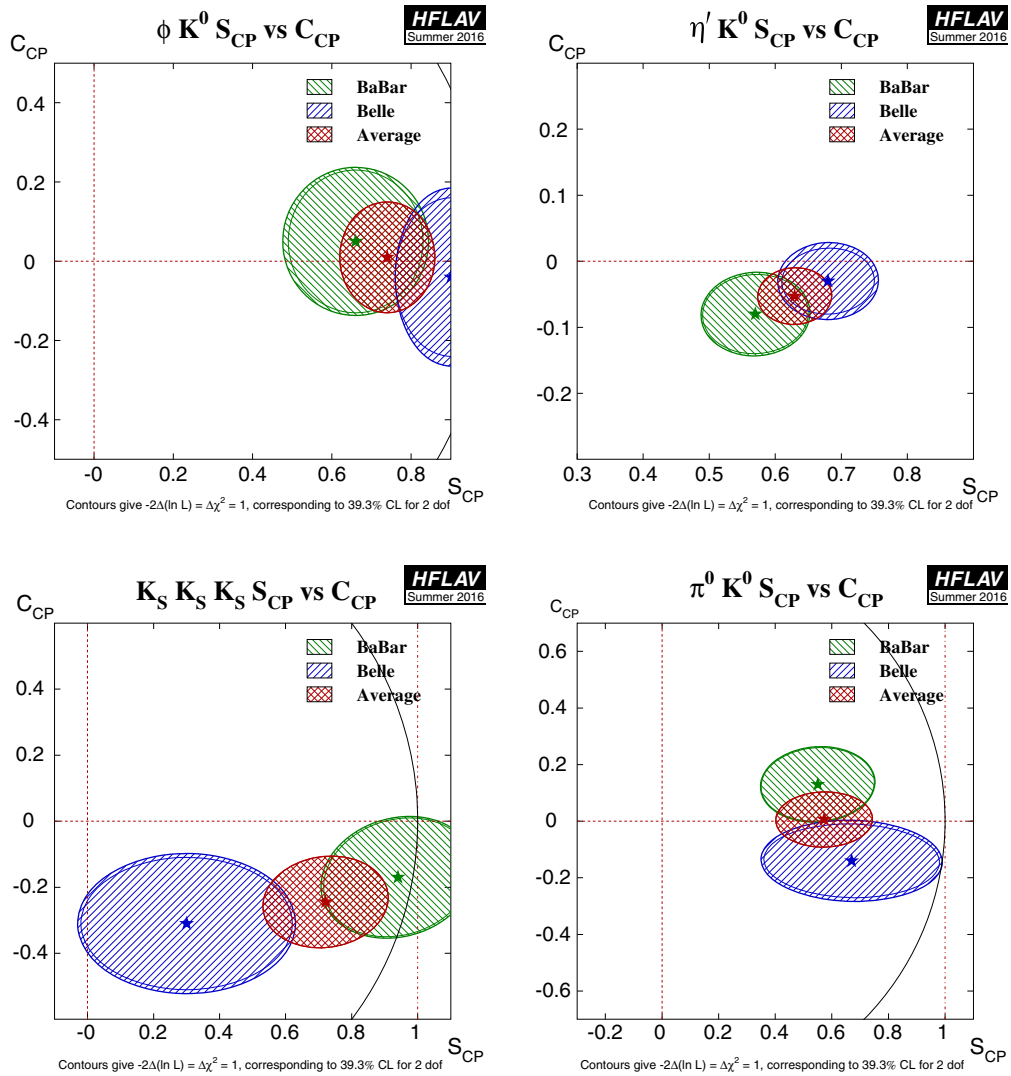

Fig. 23 Averages of four $b \to q\bar{q}s$ dominated channels, for which correlated averages are performed, in the S_{CP} *vs.* C_{CP} plane, where S_{CP} has been corrected by the *CP* eigenvalue to give $\sin(2\beta^{\text{eff}})$. (*Top left*) $B^0 \to \phi K^0$, (*top right*) $B^0 \to \eta' K^0$, (*bottom left*) $B^0 \to K_S^0 K_S^0 K_S^0$, (*bottom right*) $B^0 \to \pi^0 K_S^0$. More figures are available from the HFLAV web pages

is considered a pure $s\bar{s}$ state). Since the mixing phase and the decay phase are expected to cancel in the Standard Model, the prediction for the phase from the interference of mixing and decay is predicted to be $\phi_s(\phi\phi) = 0$ with low uncertainty [396]. Due to the vector-vector nature of the final state, angular analysis is needed to separate the *CP*-even and *CP*-odd contributions. Such an analysis also makes it possible to fit directly for $\phi_s(\phi\phi)$.

A constraint on $\phi_s(\phi\phi)$ has been obtained by LHCb using $3.0\,\text{fb}^{-1}$ of data [397]. The result is $\phi_s(\phi\phi) = -0.17 \pm 0.15 \pm 0.03$ rad where the first uncertainty is statistical and the second is systematic.

4.8 Time-dependent *CP* asymmetries in $b \to q\bar{q}d$ transitions

Decays such as $B^0 \to K_S^0 K_S^0$ are pure $b \to q\bar{q}d$ penguin transitions. As shown in Eq. (153), this diagram has different contributing weak phases, and therefore the observables are sensitive to their difference (which can be chosen to be either β or γ). Note that if the contribution with the top quark in the loop dominates, the weak phase from the decay amplitudes should cancel that from mixing, so that no *CP* violation (neither mixing-induced nor in decay) occurs. Non-zero contributions from loops with intermediate up and charm quarks can result in both types of effect (as usual, a strong phase difference is required for *CP* violation in decay to occur).

Both BaBar [398] and Belle [399] have performed time-dependent analyses of $B^0 \to K_S^0 K_S^0$ decays. The results are given in Table 41 and shown in Fig. 26.

4.9 Time-dependent asymmetries in $b \to s\gamma$ transitions

The radiative decays $b \to s\gamma$ produce photons which are highly polarised in the Standard Model. The decays $B^0 \to F\gamma$ and $\overline{B}^0 \to F\gamma$ produce photons with opposite helicities, and since the polarisation is, in principle, observable, these

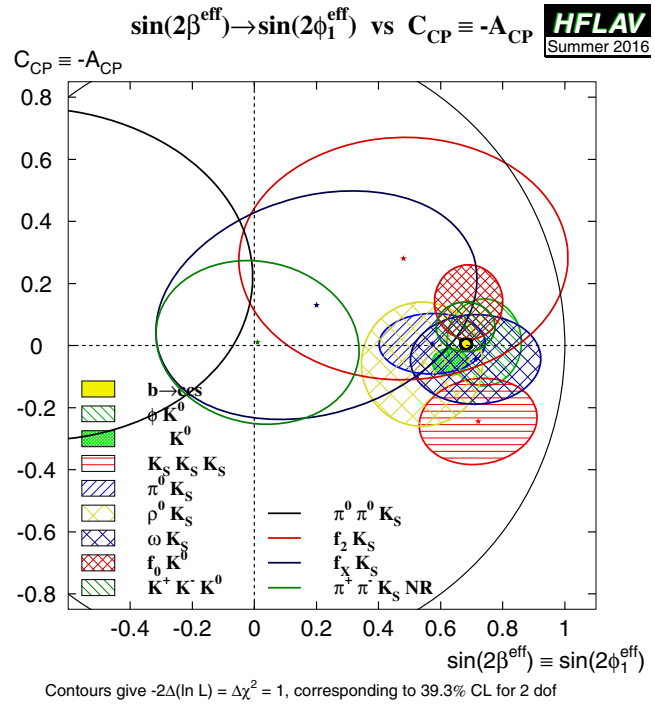

Fig. 24 Compilation of constraints in the $-\eta S_{b\to q\bar{q}s}$, interpreted as $\sin(2\beta^{\rm eff})$, *vs.* $C_{b\to q\bar{q}s}$ plane

final states cannot interfere. The finite mass of the s quark introduces small corrections to the limit of maximum polarisation, but any large mixing-induced CP violation would be a signal for new physics. Since a single weak phase dominates the $b \to s\gamma$ transition in the Standard Model, the cosine term is also expected to be small.

Atwood et al. [298] have shown that an inclusive analysis of $K^0_S\pi^0\gamma$ can be performed, since the properties of the decay amplitudes are independent of the angular momentum of the $K^0_S\pi^0$ system. However, if non-dipole operators contribute significantly to the amplitudes, then the Standard Model mixing-induced CP violation could be larger than the naïve expectation $S \simeq -2(m_s/m_b)\sin(2\beta)$ [299,300]. In this case, the CP parameters may vary over the $K^0_S\pi^0\gamma$ Dalitz plot, for example as a function of the $K^0_S\pi^0$ invariant mass.

With the above in mind, we quote two averages: one for $K^*(892)$ candidates only, and the other one for the inclusive $K^0_S\pi^0\gamma$ decay (including the $K^*(892)$). If the Standard Model dipole operator is dominant, both should give the same quantities (the latter naturally with smaller statistical error). If not, care needs to be taken in interpretation of the inclusive parameters, while the results on the $K^*(892)$ resonance remain relatively clean. Results from BaBar and Belle are used for both averages; both experiments use the invariant mass range $0.60 < M_{K^0_S\pi^0} < 1.80$ GeV/c^2 in the inclusive analysis.

Table 38 Results from time-dependent Dalitz plot analyses of the $B^0 \to K^+K^-K^0$ decay. Correlations (not shown) are taken into account in the average

Experiment	$N(B\bar{B})$	ϕK^0_S		$f_0 K^0_S$		$K^+K^-K^0_S$	
		$\beta^{\rm eff}$ (°)	$\mathcal{A}$	$\beta^{\rm eff}$ (°)	$\mathcal{A}$	$\beta^{\rm eff}$ (°)	$\mathcal{A}$
BaBar [271]	470M	$21 \pm 6 \pm 2$	$-0.05 \pm 0.18 \pm 0.05$	$18 \pm 6 \pm 4$	$-0.28 \pm 0.24 \pm 0.09$	$20.3 \pm 4.3 \pm 1.2$	$-0.02 \pm 0.09 \pm 0.03$
Belle [270]	657M	$32.2 \pm 9.0 \pm 2.6 \pm 1.4$	$0.04 \pm 0.20 \pm 0.10 \pm 0.02$	$31.3 \pm 9.0 \pm 3.4 \pm 4.0$	$-0.30 \pm 0.29 \pm 0.11 \pm 0.09$	$24.9 \pm 6.4 \pm 2.1 \pm 2.5$	$-0.14 \pm 0.11 \pm 0.08 \pm 0.03$
Average		24 ± 5	-0.01 ± 0.14	22 ± 6	-0.29 ± 0.20	21.6 ± 3.7	-0.06 ± 0.08
Confidence level					0.93 (0.1σ)		

Table 39 Results from time-dependent Dalitz plot analysis of the $B^0 \to \pi^+\pi^- K_S^0$ decay. Correlations (not shown) are taken into account in the average

Experiment	$N(B\bar{B})$	$\rho^0 K_S^0$		$f_0 K_S^0$	
		$\beta^{\rm eff}$	$\mathcal{A}$	$\beta^{\rm eff}$	$\mathcal{A}$
BABAR [274]	383M	$(10.2 \pm 8.9 \pm 3.0 \pm 1.9)^\circ$	$0.05 \pm 0.26 \pm 0.10 \pm 0.03$	$(36.0 \pm 9.8 \pm 2.1 \pm 2.1)^\circ$	$-0.08 \pm 0.19 \pm 0.03 \pm 0.04$
Belle [275]	657M	$(20.0^{+8.6}_{-8.5} \pm 3.2 \pm 3.5)^\circ$	$0.03^{+0.23}_{-0.24} \pm 0.11 \pm 0.10$	$(12.7^{+6.9}_{-6.5} \pm 2.8 \pm 3.3)^\circ$	$-0.06 \pm 0.17 \pm 0.07 \pm 0.09$
Average		16.4 ± 6.8	0.06 ± 0.20	20.6 ± 6.2	-0.07 ± 0.14
Confidence level			0.39 (0.9σ)		
Experiment	$N(B\bar{B})$	$f_2 K_S^0$		$f_X K_S^0$	
		$\beta^{\rm eff}$	$\mathcal{A}$	$\beta^{\rm eff}$	$\mathcal{A}$
BABAR [274]	383M	$(14.9 \pm 17.9 \pm 3.1 \pm 5.2)^\circ$	$-0.28^{+0.40}_{-0.35} \pm 0.08 \pm 0.07$	$(5.8 \pm 15.2 \pm 2.2 \pm 2.3)^\circ$	$-0.13^{+0.35}_{-0.33} \pm 0.04 \pm 0.09$
Experiment	$N(B\bar{B})$	$B^0 \to \pi^+\pi^- K_S^0$ nonresonant		$\chi_{c0} K_S^0$	
		$\beta^{\rm eff}$	$\mathcal{A}$	$\beta^{\rm eff}$	$\mathcal{A}$
BABAR [274]	383M	$(0.4 \pm 8.8 \pm 1.9 \pm 3.8)^\circ$	$-0.01 \pm 0.25 \pm 0.06 \pm 0.05$	$(23.2 \pm 22.4 \pm 2.3 \pm 4.2)^\circ$	$0.29^{+0.44}_{-0.53} \pm 0.03 \pm 0.05$

In addition to the $K_S^0\pi^0\gamma$ decay, both BABAR and Belle have presented results using the $K_S^0\rho\gamma$ mode, while BABAR (Belle) has in addition presented results using the $K_S^0\eta\gamma$ ($K_S^0\phi\gamma$) channel. For the $K_S^0\rho\gamma$ case, due to the non-negligible width of the ρ^0 meson, decays selected as $B^0 \to K_S^0\rho^0\gamma$ can include a significant contribution from $K^{*\pm}\pi^\mp\gamma$ decays, which are flavour-specific and do not have the same oscillation phenomenology. Both BABAR and Belle measure $S_{\rm eff}$ for all B decay candidates with the ρ^0 selection being $0.6 < m(\pi^+\pi^-) < 0.9$ GeV/c^2, obtaining $0.14 \pm 0.25^{+0.04}_{-0.03}$ (BABAR) and $0.09 \pm 0.27^{+0.04}_{-0.07}$ (Belle). These values are then corrected for a "dilution factor", that is evaluated with different methods in the two experiments: BABAR [400,401] obtains a dilution factor of $-0.78^{+0.19}_{-0.17}$ while Belle [402] obtains $+0.83^{+0.19}_{-0.03}$. Until the discrepancy between these values is understood, the average of the results should be treated with caution.

The results are given in Table 42, and shown in Figs. 27 and 28. No significant CP violation results are seen; the results are consistent with the Standard Model and with other measurements in the $b \to s\gamma$ system (see Sect. 7).

A similar analysis can be performed for radiative B_s^0 decays to, for example, the $\phi\gamma$ final state. As for other observables determined with self-conjugate final states produced in B_s^0 decays, the effective lifetime also provides sensitivity, and can be determined without tagging the initial flavour of the decaying meson. The LHCb collaboration has determined the associated parameter $A_{\Delta\Gamma}(\phi\gamma) = -0.98^{+0.46}_{-0.52}{}^{+0.23}_{-0.20}$ [407].

4.10 Time-dependent asymmetries in $b \to d\gamma$ transitions

The formalism for the radiative decays $b \to d\gamma$ is much the same as that for $b \to s\gamma$ discussed above. Assuming dominance of the top quark in the loop, the weak phase in decay should cancel with that from mixing, so that the mixing-induced CP violation parameter S_{CP} should be very small. Corrections due to the finite light quark mass are smaller compared to $b \to s\gamma$, since $m_d < m_s$, but QCD corrections of $\mathcal{O}\left(\Lambda_{\rm QCD}/m_b\right)$ may be sizable [299]. Large CP violation effects could be seen through a non-zero value of $C_{b\to d\gamma}$ since the top loop is not the only contribution.

Results using the mode $B^0 \to \rho^0\gamma$ are available from Belle and are given in Table 43.

4.11 Time-dependent CP asymmetries in $b \to u\bar{u}d$ transitions

The $b \to u\bar{u}d$ transition can be mediated by either a $b \to u$ tree amplitude or a $b \to d$ penguin amplitude. These transitions can be investigated using the time dependence of B^0 decays to final states containing light mesons. Results are

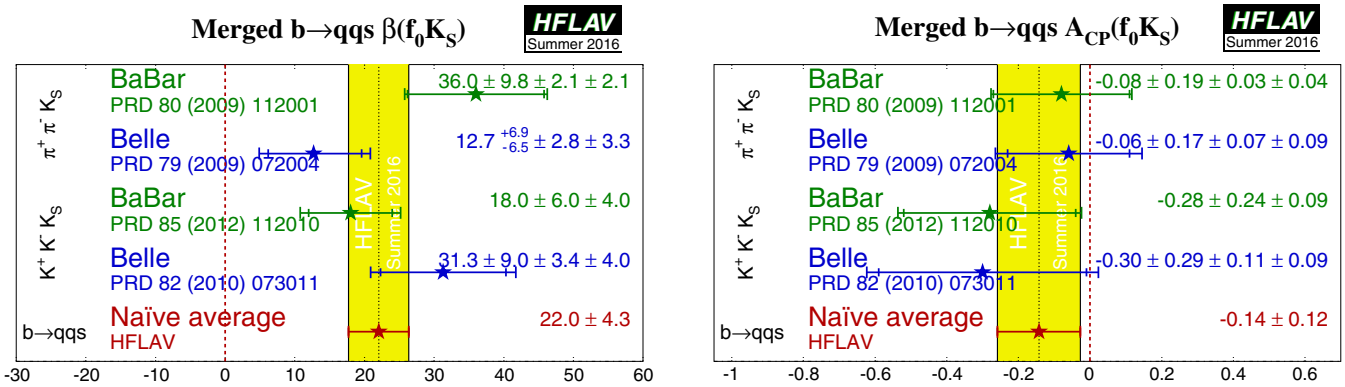

Fig. 25 Averages of (*left*) $\beta^{\rm eff} \equiv \phi_1^{\rm eff}$ and (*right*) A_{CP} for the $B^0 \to f_0 K_S^0$ decay including measurements from Dalitz plot analyses of both $B^0 \to K^+K^-K_S^0$ and $B^0 \to \pi^+\pi^-K_S^0$

Table 40 Results from time-dependent analysis of the $B_s^0 \to K^+K^-$ decay

Experiment	Sample size	S_{CP}	C_{CP}	$A^{\Delta\Gamma}$
LHCb [394]	$\int \mathcal{L}\,dt = 3.0\ \text{fb}^{-1}$	$0.22 \pm 0.06 \pm 0.02$	$0.24 \pm 0.06 \pm 0.02$	$-0.75 \pm 0.07 \pm 0.11$

Table 41 Results for $B^0 \to K_S^0 K_S^0$

Experiment	$N(B\bar{B})$	S_{CP}	C_{CP}	Correlation
BaBar [398]	350M	$-1.28\,^{+0.80}_{-0.73}\,^{+0.11}_{-0.16}$	$-0.40 \pm 0.41 \pm 0.06$	-0.32
Belle [399]	657M	$-0.38\,^{+0.69}_{-0.77} \pm 0.09$	$0.38 \pm 0.38 \pm 0.05$	0.48
Average		-1.08 ± 0.49	-0.06 ± 0.26	0.14
Confidence level		0.29 (1.1σ)		

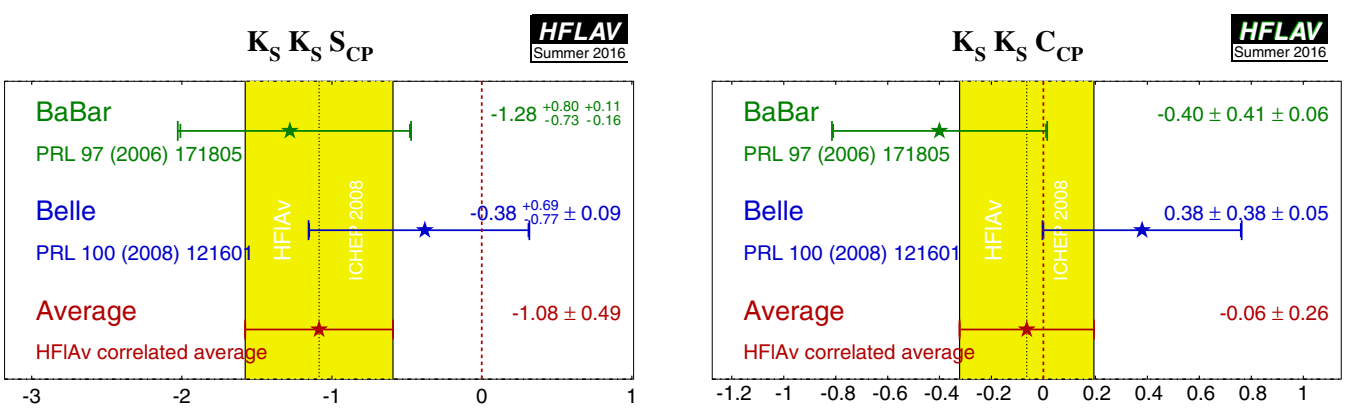

Fig. 26 Averages of (*left*) S_{CP} and (*right*) C_{CP} for the mode $B^0 \to K_S^0 K_S^0$

available from both BaBar and Belle for the *CP* eigenstate ($\eta = +1$) $\pi^+\pi^-$ final state and for the vector-vector final state $\rho^+\rho^-$, which is found to be dominated by the *CP*-even longitudinally polarised component (BaBar measures $f_{\rm long} = 0.992 \pm 0.024\,^{+0.026}_{-0.013}$ [409] while Belle measures $f_{\rm long} = 0.988 \pm 0.012 \pm 0.023$ [410]). BaBar has also performed a time-dependent analysis of the vector-vector final state $\rho^0\rho^0$ [411], in which they measure $f_{\rm long} = 0.70 \pm 0.14 \pm 0.05$; Belle measure a smaller branching fraction than BaBar for $B^0 \to \rho^0\rho^0$ [412] with corresponding signal yields too small to perform a time-dependent analysis; for the longitudinal polarisation they measure $f_{\rm long} = 0.21\,^{+0.18}_{-0.22} \pm 0.13$. LHCb has measured the branching fraction and longitudinal polarisation for $B^0 \to \rho^0\rho^0$, and for

Table 42 Averages for $b \to s\gamma$ modes

Experiment	$N(B\bar{B})$	$S_{CP}(b \to s\gamma)$	$C_{CP}(b \to s\gamma)$	Correlation
$K^*(892)\gamma$				
BABAR [403]	467M	$-0.03 \pm 0.29 \pm 0.03$	$-0.14 \pm 0.16 \pm 0.03$	0.05
Belle [404]	535M	$-0.32^{+0.36}_{-0.33} \pm 0.05$	$0.20 \pm 0.24 \pm 0.05$	0.08
Average		-0.16 ± 0.22	-0.04 ± 0.14	0.06
Confidence level		0.40 (0.9σ)		
$K^0_S\pi^0\gamma$ (including $K^*(892)\gamma$)				
BABAR [403]	467M	$-0.17 \pm 0.26 \pm 0.03$	$-0.19 \pm 0.14 \pm 0.03$	0.04
Belle [404]	535M	$-0.10 \pm 0.31 \pm 0.07$	$0.20 \pm 0.20 \pm 0.06$	0.08
Average		-0.15 ± 0.20	-0.07 ± 0.12	0.05
Confidence level		0.30 (1.0σ)		
$K^0_S\eta\gamma$				
BABAR [405]	465M	$-0.18^{+0.49}_{-0.46} \pm 0.12$	$-0.32^{+0.40}_{-0.39} \pm 0.07$	-0.17
$K^0_S\rho^0\gamma$				
BABAR [401]	471M	$-0.18 \pm 0.32^{+0.06}_{-0.05}$	$-0.39 \pm 0.20^{+0.03}_{-0.02}$	-0.09
Belle [402]	657M	$0.11 \pm 0.33^{+0.05}_{-0.09}$	$-0.05 \pm 0.18 \pm 0.06$	0.04
Average		-0.06 ± 0.23	-0.22 ± 0.14	-0.02
Confidence level		0.38 (0.9σ)		
$K^0_S\phi\gamma$				
Belle [406]	772M	$0.74^{+0.72}_{-1.05}{}^{+0.10}_{-0.24}$	$-0.35 \pm 0.58^{+0.10}_{-0.23}$	–

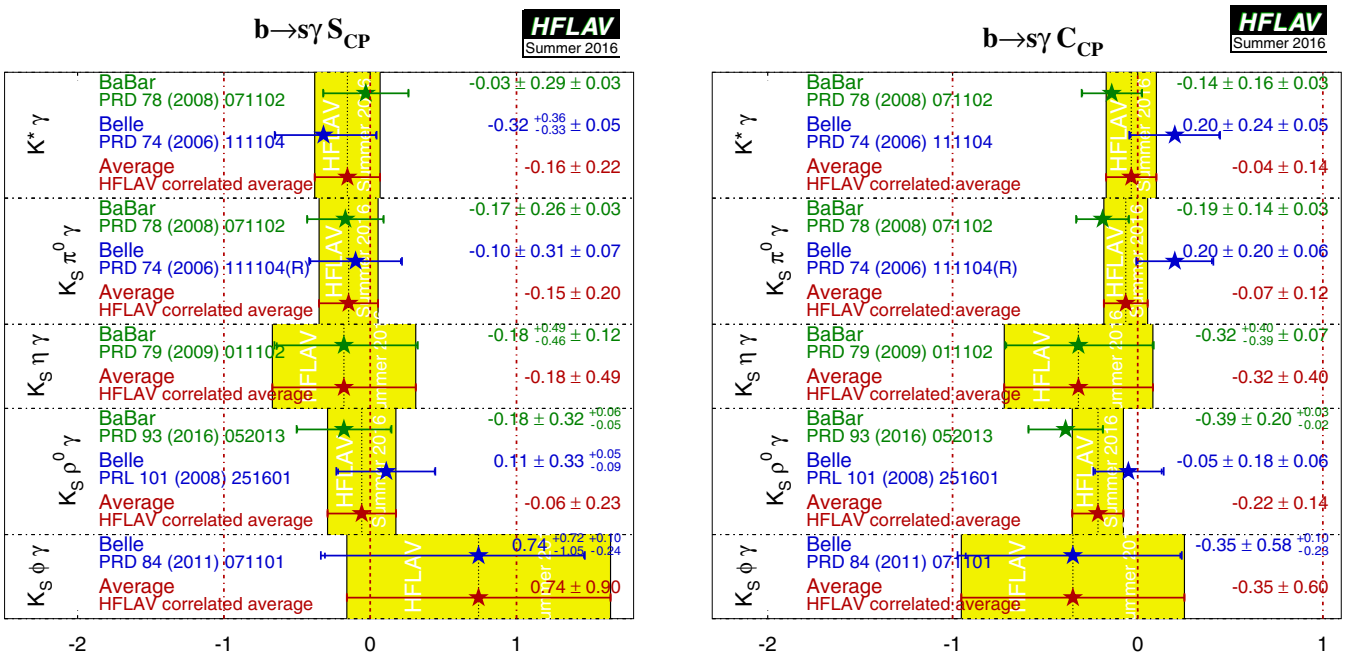

Fig. 27 Averages of (*left*) $S_{b\to s\gamma}$ and (*right*) $C_{b\to s\gamma}$. Recall that the data for $K^*\gamma$ is a subset of that for $K^0_S\pi^0\gamma$

the latter finds $f_{\rm long} = 0.745^{+0.048}_{-0.058} \pm 0.034$ [413], but has not yet performed a time-dependent analysis of this decay. The Belle measurement for $f_{\rm long}$ is thus in some tension with the other results. BABAR has furthermore performed a time-dependent analysis of the $B^0 \to a_1^{\pm}\pi^{\mp}$ decay [414]; further experimental input for the extraction of α from this channel is reported in a later publication [415].

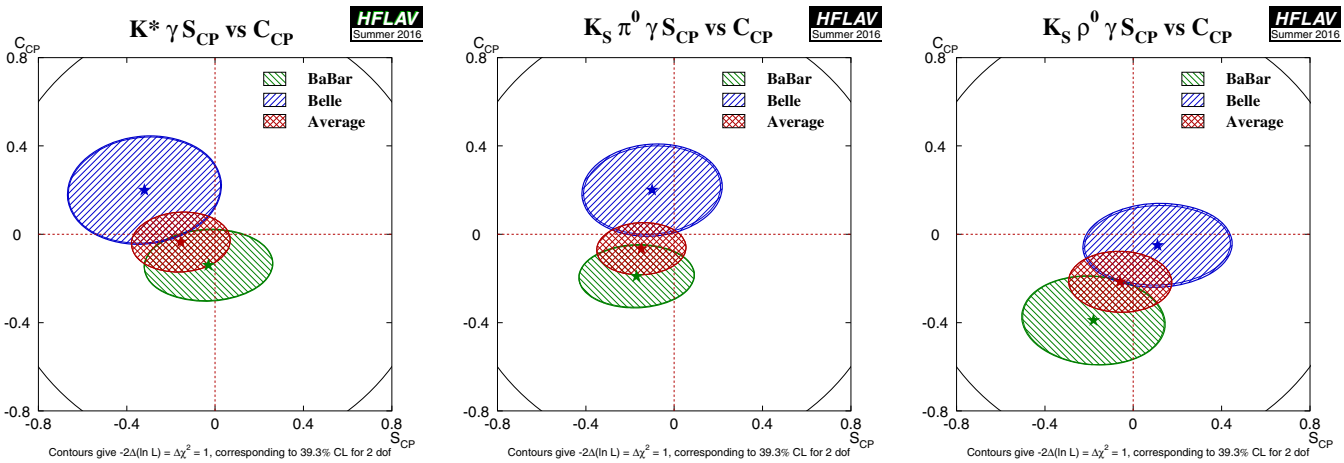

Fig. 28 Averages of three $b \to s\gamma$ dominated channels, for which correlated averages are performed, in the S_{CP} *vs.* C_{CP} plane. (*Left*) $B^0 \to K^*\gamma$, (*middle*) $B^0 \to K^0_S\pi^0\gamma$ (including $K^*\gamma$), (*right*) $B^0 \to K^0_S\rho\gamma$

Table 43 Averages for $B^0 \to \rho^0\gamma$

Experiment	$N(B\bar{B})$	S_{CP}	C_{CP}	Correlation
Belle [408]	657M	$-0.83 \pm 0.65 \pm 0.18$	$0.44 \pm 0.49 \pm 0.14$	-0.08

Results, and averages, of time-dependent *CP* violation parameters in $b \to u\bar{u}d$ transitions are listed in Table 44. The averages for $\pi^+\pi^-$ are shown in Fig. 29, and those for $\rho^+\rho^-$ are shown in Fig. 30, with the averages in the S_{CP} *vs.* C_{CP} plane shown in Fig. 31 and averages of *CP* violation parameters in $B^0 \to a_1^\pm\pi^\mp$ decay shown in Fig. 32.

If the penguin contribution is negligible, the time-dependent parameters for $B^0 \to \pi^+\pi^-$ and $B^0 \to \rho^+\rho^-$ are given by $S_{b\to u\bar{u}d} = \eta\sin(2\alpha)$ and $C_{b\to u\bar{u}d} = 0$. In the presence of the penguin contribution, *CP* violation in decay may arise, and there is no straightforward interpretation of $S_{b\to u\bar{u}d}$ and $C_{b\to u\bar{u}d}$. An isospin analysis [419] can be used to disentangle the contributions and extract α.

For the non-*CP* eigenstate $\rho^\pm\pi^\mp$, both BABAR [281] and Belle [283,284] have performed time-dependent Dalitz plot analyses of the $\pi^+\pi^-\pi^0$ final state [279]; such analyses allow direct measurements of the phases. Both experiments have measured the U and I parameters discussed in Sect. 4.2.5 and defined in Table 22. We have performed a full correlated average of these parameters, the results of which are summarised in Fig. 33.

Both experiments have also extracted the Q2B parameters. We have performed a full correlated average of these parameters, which is equivalent to determining the values from the averaged U and I parameters. The results are given in Table 45.[35] Averages of the $B^0 \to \rho^0\pi^0$ Q2B parameters are shown in Figs. 34 and 35.

With the notation described in Sect. 4.2 (Eq. (131)), the time-dependent parameters for the Q2B $B^0 \to \rho^\pm\pi^\mp$ analysis are, neglecting penguin contributions, given by

$$S_{\rho\pi} = \sqrt{1-\left(\frac{\Delta C}{2}\right)^2}\sin(2\alpha)\cos(\delta)$$
$$\Delta S_{\rho\pi} = \sqrt{1-\left(\frac{\Delta C}{2}\right)^2}\cos(2\alpha)\sin(\delta) \qquad (161)$$

and $C_{\rho\pi} = \mathcal{A}^{\rho\pi}_{CP} = 0$, where $\delta = \arg(A_{-+}A^*_{+-})$ is the strong phase difference between the $\rho^-\pi^+$ and $\rho^+\pi^-$ decay amplitudes. In the presence of the penguin contribution, there is no straightforward interpretation of the Q2B observables in the $B^0 \to \rho^\pm\pi^\mp$ system in terms of CKM parameters. However, *CP* violation in decay may arise, resulting in either or both of $C_{\rho\pi} \neq 0$ and $\mathcal{A}^{\rho\pi}_{CP} \neq 0$. Equivalently, *CP* violation in decay may be seen by either of the decay-type-specific observables $\mathcal{A}^{+-}_{\rho\pi}$ and $\mathcal{A}^{-+}_{\rho\pi}$, defined in Eq. (132), deviating from zero. Results and averages for these parameters are also given in Table 45. Averages of *CP* violation parameters in $B^0 \to \rho^\pm\pi^\mp$ decays are shown in Fig. 36, both in $\mathcal{A}^{\rho\pi}_{CP}$ *vs.* $C_{\rho\pi}$ space and in $\mathcal{A}^{-+}_{\rho\pi}$ *vs.* $\mathcal{A}^{+-}_{\rho\pi}$ space.

The averages for $S_{b\to u\bar{u}d}$ and $C_{b\to u\bar{u}d}$ in $B^0 \to \pi^+\pi^-$ decays are both more than 5σ away from zero, suggesting that both mixing-induced and *CP* violation in decay are well-established in this channel. The discrepancy between

[35] The $B^0 \to \rho^\pm\pi^\mp$ Q2B parameters are comparable to the parameters used for $B^0 \to a_1^\pm\pi^\mp$ decays, reported in Table 44. For the

Footnote 35 continued
$B^0 \to a_1^\pm\pi^\mp$ case there has not yet been a full amplitude analysis of $B^0 \to \pi^+\pi^-\pi^+\pi^-$ and therefore only the Q2B parameters are available.

Table 44 Averages for $b \to u\bar{u}d$ modes

Experiment	Sample size	S_{CP}	C_{CP}	Correlation
$\pi^+\pi^-$				
BABAR [416]	$N(B\bar{B}) = 467$M	$-0.68 \pm 0.10 \pm 0.03$	$-0.25 \pm 0.08 \pm 0.02$	-0.06
Belle [417]	$N(B\bar{B}) = 772$M	$-0.64 \pm 0.08 \pm 0.03$	$-0.33 \pm 0.06 \pm 0.03$	-0.10
Average		-0.68 ± 0.04	-0.27 ± 0.04	0.14
Confidence level		0.88 (0.2σ)		
$\rho^+\rho^-$				
BABAR [409]	$N(B\bar{B}) = 387$M	$-0.17 \pm 0.20\,^{+0.05}_{-0.06}$	$0.01 \pm 0.15 \pm 0.06$	-0.04
Belle [410]	$N(B\bar{B}) = 772$M	$-0.13 \pm 0.15 \pm 0.05$	$0.00 \pm 0.10 \pm 0.06$	-0.02
Average		-0.14 ± 0.13	0.00 ± 0.09	-0.02
Confidence level		0.99 (0.02σ)		
$\rho^0\rho^0$				
BABAR [411]	$N(B\bar{B}) = 465$M	$0.3 \pm 0.7 \pm 0.2$	$0.2 \pm 0.8 \pm 0.3$	-0.04

Experiment	$N(B\bar{B})$	$A_{CP}^{a_1\pi}$	$C_{a_1\pi}$	$S_{a_1\pi}$	$\Delta C_{a_1\pi}$	$\Delta S_{a_1\pi}$
$a_1^\pm\pi^\mp$						
BABAR [414]	384M	$-0.07 \pm 0.07 \pm 0.02$	$-0.10 \pm 0.15 \pm 0.09$	$0.37 \pm 0.21 \pm 0.07$	$0.26 \pm 0.15 \pm 0.07$	$-0.14 \pm 0.21 \pm 0.06$
Belle [418]	772M	$-0.06 \pm 0.05 \pm 0.07$	$-0.01 \pm 0.11 \pm 0.09$	$-0.51 \pm 0.14 \pm 0.08$	$0.54 \pm 0.11 \pm 0.07$	$-0.09 \pm 0.14 \pm 0.06$
Average		-0.06 ± 0.06	-0.05 ± 0.11	-0.20 ± 0.13	0.43 ± 0.10	-0.10 ± 0.12
Confidence level				0.03 (2.1σ)		

Experiment	$N(B\bar{B})$	$\mathcal{A}_{a_1\pi}^{-+}$	$\mathcal{A}_{a_1\pi}^{+-}$	Correlation
BABAR [414]	384M	$0.07 \pm 0.21 \pm 0.15$	$0.15 \pm 0.15 \pm 0.07$	0.63
Belle [418]	772M	$-0.04 \pm 0.26 \pm 0.19$	$0.07 \pm 0.08 \pm 0.10$	0.61
Average		0.02 ± 0.20	0.10 ± 0.10	0.38
Confidence level			0.92 (0.1σ)	

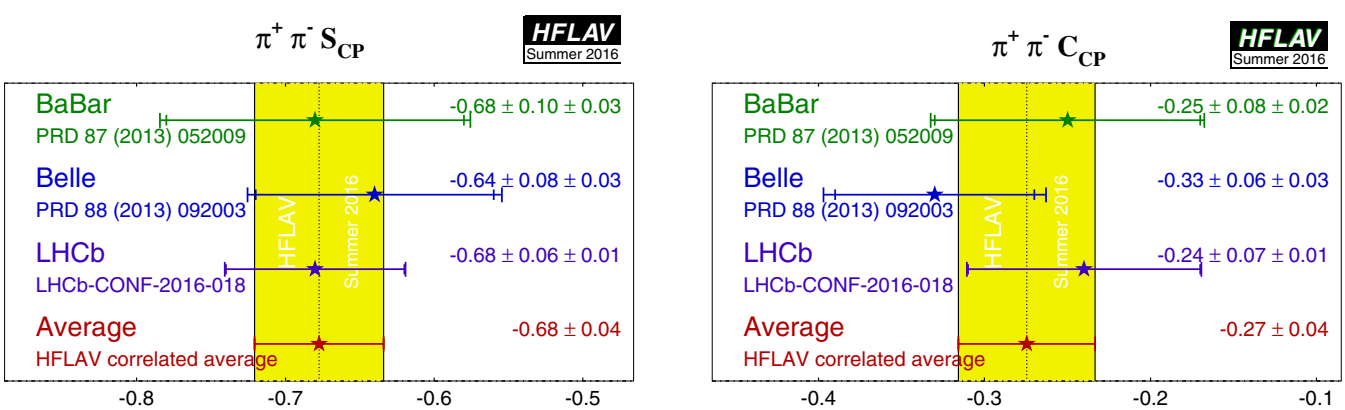

Fig. 29 Averages of (*left*) S_{CP} and (*right*) C_{CP} for the mode $B^0 \to \pi^+\pi^-$

results from BABAR and Belle that used to exist in this channel (see, for example, Ref. [420]) is no longer apparent, and the results from LHCb are also fully consistent with other measurements. Some difference is, however, seen between the BABAR and Belle measurements in the $a_1^\pm\pi^\mp$ system. The confidence level of the five-dimensional average is 0.03, which corresponds to a 2.1σ discrepancy. As seen in Table 44, this discrepancy is primarily in the values of $S_{a_1\pi}$, and is not evident in the $\mathcal{A}_{a_1\pi}^{-+}$ *vs.* $\mathcal{A}_{a_1\pi}^{+-}$ projection shown in Fig. 32. Since there is no evidence of systematic problems in either analysis, we do not rescale the errors of the averages.

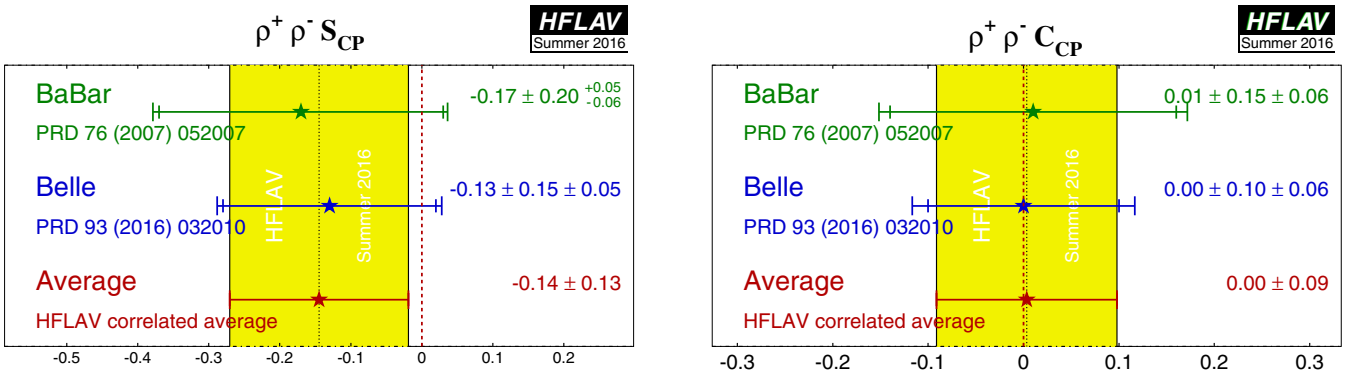

Fig. 30 Averages of (*left*) S_{CP} and (*right*) C_{CP} for the mode $B^0 \to \rho^+\rho^-$

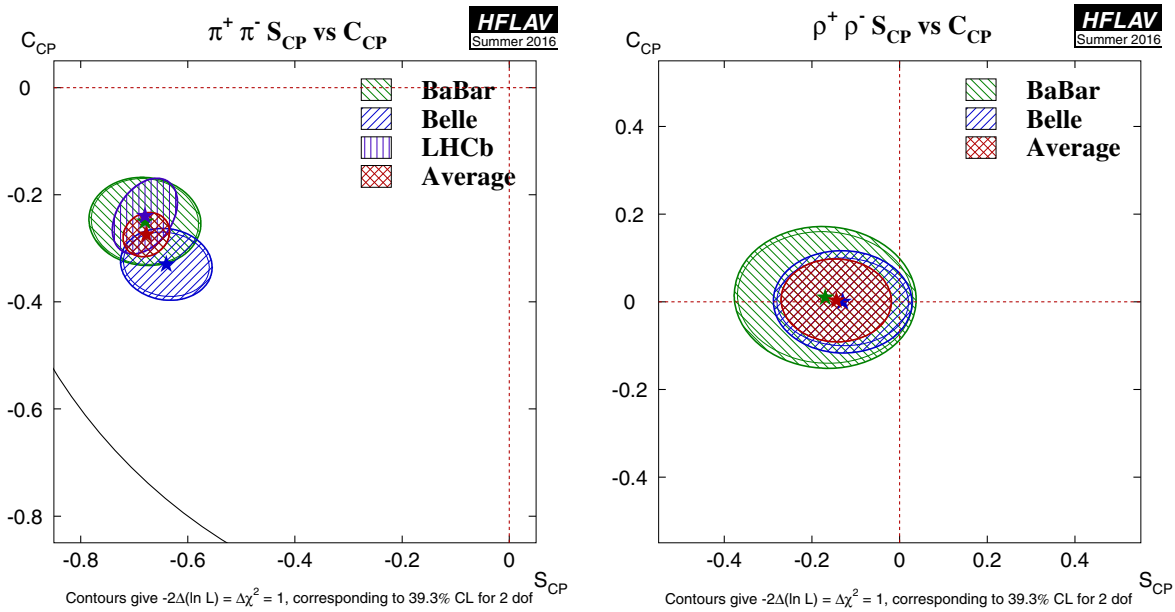

Fig. 31 Averages of $b \to u\bar{u}d$ dominated channels, for which correlated averages are performed, in the S_{CP} *vs*. C_{CP} plane. (*Left*) $B^0 \to \pi^+\pi^-$ and (*right*) $B^0 \to \rho^+\rho^-$

In $B^0 \to \rho^\pm\pi^\mp$ decays, both experiments see an indication of *CP* violation in the $\mathcal{A}_{CP}^{\rho\pi}$ parameter (as seen in Fig. 36). The average is more than 3σ from zero, providing evidence of direct *CP* violation in this channel. In $B^0 \to \rho^+\rho^-$ decays there is no evidence for *CP* violation, either mixing-induced or in decay. The absence of evidence of penguin contributions in this mode leads to strong constraints on $\alpha \equiv \phi_2$.

4.11.1 Constraints on $\alpha \equiv \phi_2$

The precision of the measured *CP* violation parameters in $b \to u\bar{u}d$ transitions allows constraints to be set on the UT angle $\alpha \equiv \phi_2$. Constraints have been obtained with various methods:

- Both BABAR [416] and Belle [417] have performed isospin analyses in the $\pi\pi$ system. Belle exclude $23.8° < \phi_2 < 66.8°$ at 68% CL while BABAR give a confidence level interpretation for α, and constrain $\alpha \in [71°, 109°]$ at 68% CL. Values in the range [23°, 67°] are excluded at 90% CL. In both cases, only solutions in 0°–180° are quoted.
- Both experiments have also performed isospin analyses in the $\rho\rho$ system. The most recent result from BABAR is given in an update of the measurements of the $B^+ \to \rho^+\rho^0$ decay [421], and sets the constraint $\alpha = \left(92.4^{+6.0}_{-6.5}\right)^\circ$. The most recent result from Belle is given in their paper on time-dependent *CP* violation parameters in $B^0 \to \rho^+\rho^-$ decays, and sets the constraint $\phi_2 = (93.7 \pm 10.6)°$ [410].
- The time-dependent Dalitz plot analysis of the $B^0 \to \pi^+\pi^-\pi^0$ decay allows a determination of α without input from any other channels. BABAR [282] present a scan, but not an interval, for α, since their studies indicate that the scan is not statistically robust and cannot be interpreted as 1−CL. Belle [283,284] has obtained a con-

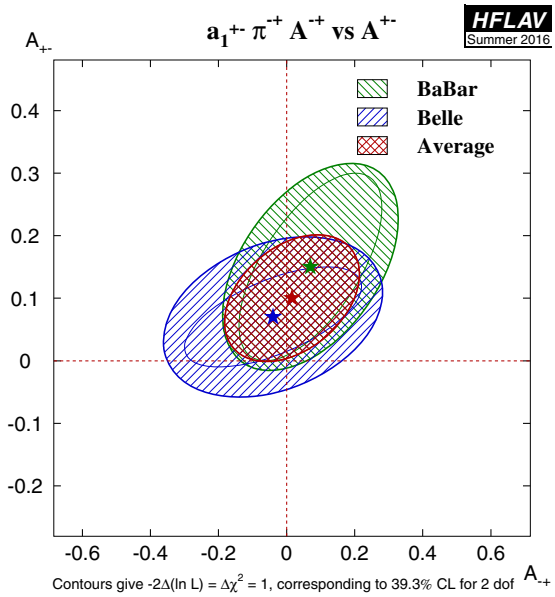

Fig. 32 Averages of *CP* violation parameters in $B^0 \to a_1^{\pm}\pi^{\mp}$ in $\mathcal{A}_{a_1\pi}^{-+}$ *vs.* $\mathcal{A}_{a_1\pi}^{+-}$ space

straint on α using additional information from the SU(2) partners of $B \to \rho\pi$, which can be used to constrain α via an isospin pentagon relation [422]. With this analysis, Belle obtains the constraint $\phi_2 = (83^{+12}_{-23})^\circ$ (where the errors correspond to 1σ, i.e. 68.3% confidence level).

- The results from BABAR on $B^0 \to a_1^{\pm}\pi^{\mp}$ [414] can be combined with results from modes related by flavour symmetries ($a_1 K$ and $K_1\pi$) [423]. This has been done by BABAR [415], resulting in the constraint $\alpha = (79 \pm 7 \pm 11)^\circ$, where the first uncertainty is from the analysis of $B^0 \to a_1^{\pm}\pi^{\mp}$ that obtains $\alpha^{\rm eff}$, and the second is due to the constraint on $|\alpha^{\rm eff} - \alpha|$. This approach gives a result with several ambiguous solutions; that consistent with other determinations of α and with global fits to the CKM matrix parameters is quoted here.
- The CKMfitter [252] and UTFit [339] groups use the measurements from Belle and BABAR given above with other branching fractions and *CP* asymmetries in $B \to \pi\pi$, $\rho\pi$ and $\rho\rho$ modes, to perform isospin analyses for each system, and to obtain combined constraints on α.
- The BABAR and Belle collaborations have combined their results on $B \to \pi\pi$, $\pi\pi\pi^0$ and $\rho\rho$ decays to obtain [424]

$$\alpha \equiv \phi_2 = (88 \pm 5)^\circ . \tag{162}$$

The above solution is that consistent with the Standard Model (an ambiguous solution shifted by 180° exists). The strongest constraint currently comes from the $B \to \rho\rho$ system. The inclusion of results from $B^0 \to a_1^{\pm}\pi^{\mp}$ does not significantly affect the average.

Note that methods based on isospin symmetry make extensive use of measurements of branching fractions and *CP* asymmetries, as averaged by the HFLAV Rare Decays sub-

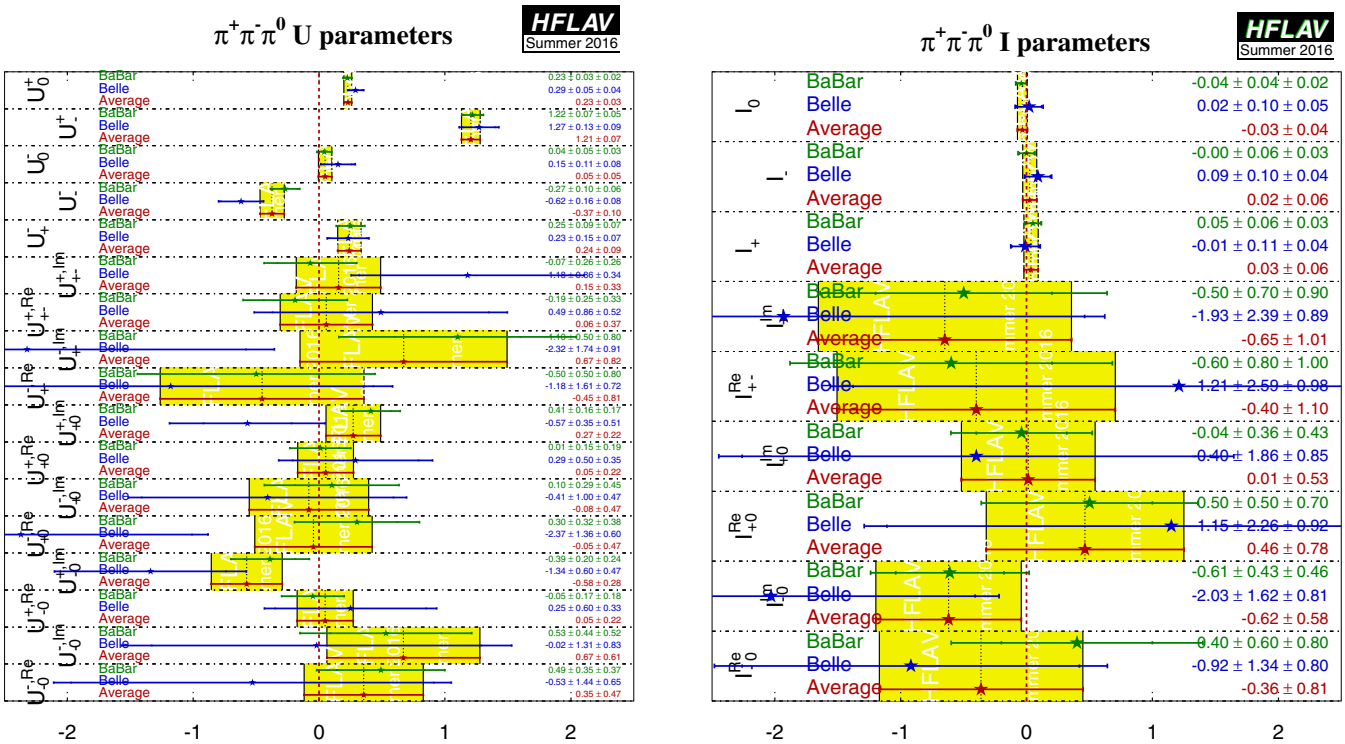

Fig. 33 Summary of the U and I parameters measured in the time-dependent $B^0 \to \pi^+\pi^-\pi^0$ Dalitz plot analysis

Table 45 Averages of quasi-two-body parameters extracted from time-dependent Dalitz plot analysis of $B^0 \to \pi^+\pi^-\pi^0$

Experiment	$N(B\bar{B})$	$\mathcal{A}_{CP}^{\rho\pi}$	$C_{\rho\pi}$	$S_{\rho\pi}$	$\Delta C_{\rho\pi}$	$\Delta S_{\rho\pi}$
BaBar [282]	471M	$-0.10 \pm 0.03 \pm 0.02$	$0.02 \pm 0.06 \pm 0.04$	$0.05 \pm 0.08 \pm 0.03$	$0.23 \pm 0.06 \pm 0.05$	$0.05 \pm 0.08 \pm 0.04$
Belle [283,284]	449M	$-0.12 \pm 0.05 \pm 0.04$	$-0.13 \pm 0.09 \pm 0.05$	$0.06 \pm 0.13 \pm 0.05$	$0.36 \pm 0.10 \pm 0.05$	$-0.08 \pm 0.13 \pm 0.05$
Average		-0.11 ± 0.03	-0.03 ± 0.06	0.06 ± 0.07	0.27 ± 0.06	0.01 ± 0.08
Confidence level				0.63 (0.5σ)		

Experiment	$N(B\bar{B})$	$\mathcal{A}_{\rho\pi}^{-+}$	$\mathcal{A}_{\rho\pi}^{+-}$	Correlation
BaBar [282]	471M	$-0.12 \pm 0.08^{+0.04}_{-0.05}$	$0.09^{+0.05}_{-0.06} \pm 0.04$	0.55
Belle [283,284]	449M	$0.08 \pm 0.16 \pm 0.11$	$0.21 \pm 0.08 \pm 0.04$	0.47
Average		-0.08 ± 0.08	0.13 ± 0.05	0.37
Confidence level		0.47 (0.7σ)		

Experiment	$N(B\bar{B})$	$C_{\rho^0\pi^0}$	$S_{\rho^0\pi^0}$	Correlation
BaBar [282]	471M	$0.19 \pm 0.23 \pm 0.15$	$-0.37 \pm 0.34 \pm 0.20$	0.00
Belle [283,284]	449M	$0.49 \pm 0.36 \pm 0.28$	$0.17 \pm 0.57 \pm 0.35$	0.08
Average		0.27 ± 0.24	-0.23 ± 0.34	0.02
Confidence level		0.68 (0.4σ)		

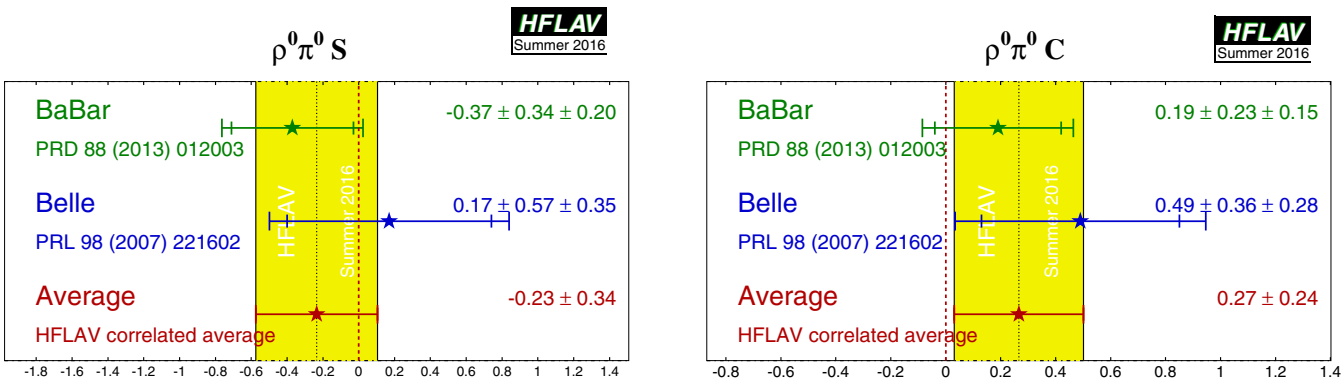

Fig. 34 Averages of (*left*) $S_{b\to u\bar{u}d}$ and (*right*) $C_{b\to u\bar{u}d}$ for the mode $B^0 \to \rho^0\pi^0$

group (Sect. 7). Note also that each method suffers from discrete ambiguities in the solutions. The model assumption in the $B^0 \to \pi^+\pi^-\pi^0$ analysis helps resolve some of the multiple solutions, and results in a single preferred value for α in $[0, \pi]$. All the above measurements correspond to the choice that is in agreement with the global CKM fit.

At present we make no attempt to provide an HFLAV average for $\alpha \equiv \phi_2$. More details on procedures to calculate a best fit value for α can be found in Refs. [252,339].

4.12 Time-dependent CP asymmetries in $b \to c\bar{u}d/u\bar{c}d$ transitions

Non-CP eigenstates such as $D^{\mp}\pi^{\pm}$, $D^{*\mp}\pi^{\pm}$ and $D^{\mp}\rho^{\pm}$ can be produced in decays of B^0 mesons either via Cabibbo favoured ($b \to c$) or doubly Cabibbo suppressed ($b \to u$) tree amplitudes. Since no penguin contribution is possible, these modes are theoretically clean. The ratio of the magnitudes of the suppressed and favoured amplitudes, R, is sufficiently small (predicted to be about 0.02), that $\mathcal{O}(R^2)$ terms can be neglected, and the sine terms give sensitivity to the combination of UT angles $2\beta + \gamma$.

As described in Sect. 4.2.6, the averages are given in terms of the parameters a and c of Eq. (136). CP violation would appear as $a \neq 0$. Results are available from both BaBar and Belle in the modes $D^{\mp}\pi^{\pm}$ and $D^{*\mp}\pi^{\pm}$; for the latter mode both experiments have used both full and partial reconstruction techniques. Results are also available from BaBar using $D^{\mp}\rho^{\pm}$. These results, and their averages, are listed in Table 46, and are shown in Fig. 37. The constraints in c *vs*.

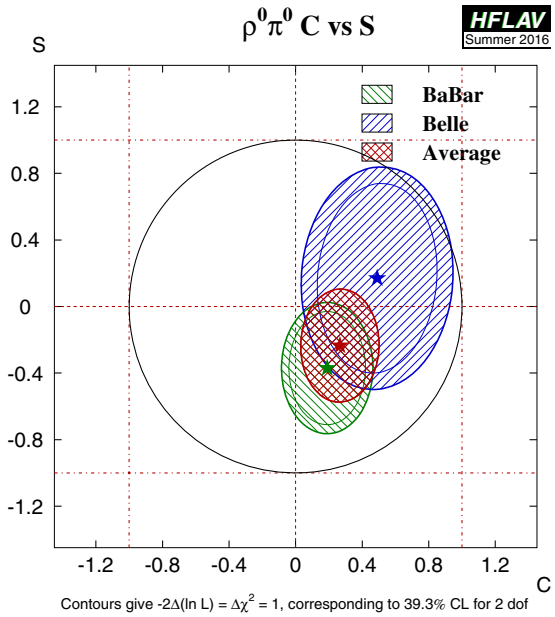

Fig. 35 Averages of $b \to u\bar{u}d$ dominated channels, for the mode $B^0 \to \rho^0\pi^0$ in the S_{CP} *vs.* C_{CP} plane

a space for the $D\pi$ and $D^*\pi$ modes are shown in Fig. 38. It is notable that the average value of a from $D^*\pi$ is more than 3σ from zero, providing evidence of CP violation in this channel.

For each mode, $D\pi$, $D^*\pi$ and $D\rho$, there are two measurements (a and c, or S^+ and S^-) that depend on three unknowns (R, δ and $2\beta+\gamma$), of which two are different for each decay mode. Therefore, there is not enough information to solve directly for $2\beta+\gamma$. However, for each choice of R and $2\beta+\gamma$, one can find the value of δ that allows a and c to be closest to their measured values, and calculate the separation in terms of numbers of standard deviations. (We currently neglect experimental correlations in this analysis.) These values of $N(\sigma)_{\min}$ can then be displayed as a function of R and $2\beta+\gamma$ (and can trivially be converted to confidence levels). These plots are given for the $D\pi$ and $D^*\pi$ modes in Fig. 38; the uncertainties in the $D\rho$ mode are currently too large to give any meaningful constraint.

The constraints can be tightened if one is willing to use theoretical input on the values of R and/or δ. One popular choice is the use of SU(3) symmetry to obtain R by relating the suppressed decay mode to B decays involving D_s mesons. More details can be found in Refs. [295,425–428].

4.13 Time-dependent CP asymmetries in $b \to c\bar{u}s/u\bar{c}s$ transitions

4.13.1 Time-dependent CP asymmetries in $B^0 \to D^{\mp}K^0_S\pi^{\pm}$

Time-dependent analyses of transitions such as $B^0 \to D^{\mp}K^0_S\pi^{\pm}$ can be used to probe $\sin(2\beta+\gamma)$ in a similar way to that discussed above (Sect. 4.12). Since the final state contains three particles, a Dalitz plot analysis is necessary to maximise the sensitivity. BABAR [429] has carried out such an analysis. They obtain $2\beta+\gamma = (83 \pm 53 \pm 20)^\circ$ (with an ambiguity $2\beta+\gamma \leftrightarrow 2\beta+\gamma+\pi$) assuming the ratio of the $b \to u$ and $b \to c$ amplitude to be constant across the Dalitz plot at 0.3.

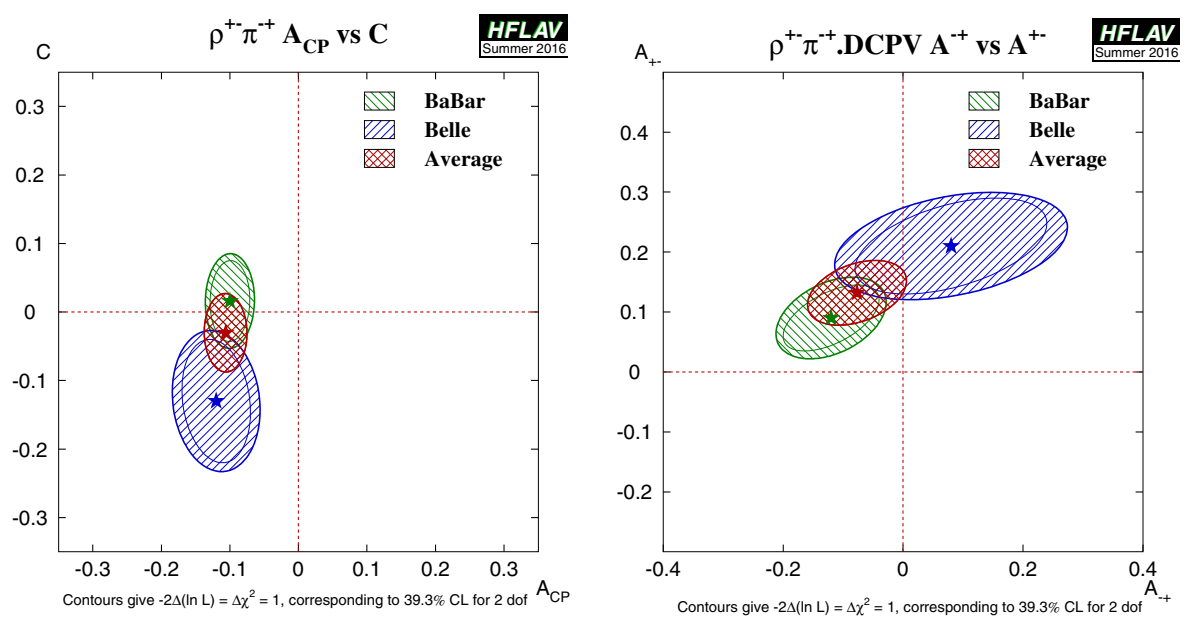

Fig. 36 CP violation in $B^0 \to \rho^{\pm}\pi^{\mp}$ decays. (*Left*) $\mathcal{A}^{\rho\pi}_{CP}$ *vs.* $C_{\rho\pi}$ space, (*right*) $\mathcal{A}^{-+}_{\rho\pi}$ *vs.* $\mathcal{A}^{+-}_{\rho\pi}$ space

Table 46 Averages for $b \to c\bar{u}d/u\bar{c}d$ modes

Experiment	$N(B\bar{B})$	a	c
$D^{\mp}\pi^{\pm}$			
BaBar (full rec.) [290]	232M	$-0.010 \pm 0.023 \pm 0.007$	$-0.033 \pm 0.042 \pm 0.012$
Belle (full rec.) [294]	386M	$-0.050 \pm 0.021 \pm 0.012$	$-0.019 \pm 0.021 \pm 0.012$
Average		-0.030 ± 0.017	-0.022 ± 0.021
Confidence level		0.24 (1.2σ)	0.78 (0.3σ)
$D^{*\mp}\pi^{\pm}$			
BaBar (full rec.) [290]	232M	$-0.040 \pm 0.023 \pm 0.010$	$0.049 \pm 0.042 \pm 0.015$
BaBar (partial rec.) [291]	232M	$-0.034 \pm 0.014 \pm 0.009$	$-0.019 \pm 0.022 \pm 0.013$
Belle (full rec.) [294]	386M	$-0.039 \pm 0.020 \pm 0.013$	$-0.011 \pm 0.020 \pm 0.013$
Belle (partial rec.) [293]	657M	$-0.046 \pm 0.013 \pm 0.015$	$-0.015 \pm 0.013 \pm 0.015$
Average		-0.039 ± 0.010	-0.010 ± 0.013
Confidence level		0.97 (0.03σ)	0.59 (0.6σ)
$D^{\mp}\rho^{\pm}$			
BaBar (full rec.) [290]	232M	$-0.024 \pm 0.031 \pm 0.009$	$-0.098 \pm 0.055 \pm 0.018$

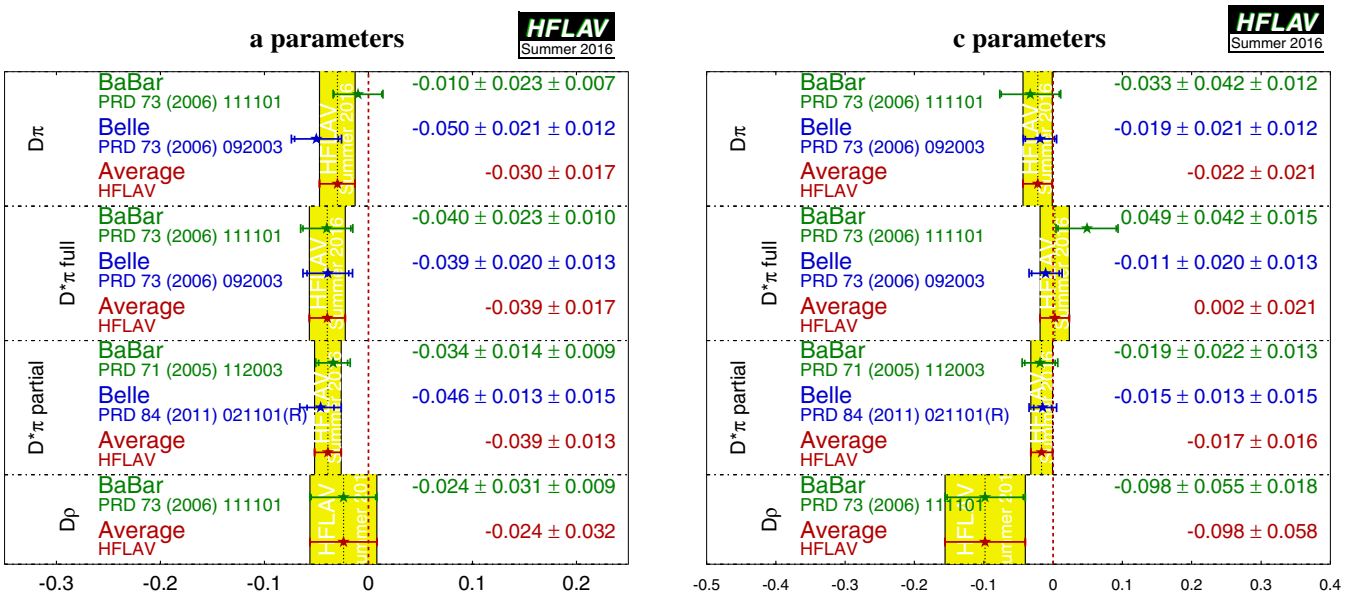

Fig. 37 Averages for $b \to c\bar{u}d/u\bar{c}d$ modes

4.13.2 Time-dependent CP asymmetries in $B_s^0 \to D_s^{\mp}K^{\pm}$

Time-dependent analysis of $B_s^0 \to D_s^{\mp}K^{\pm}$ decays can be used to determine $\gamma - 2\beta_s$ [430,431]. Compared to the situation for $B^0 \to D^{(*)\mp}\pi^{\pm}$ decays discussed in Sect. 4.12, the larger value of the ratio R of the magnitudes of the suppressed and favoured amplitudes allows it to be determined from the data. Moreover, the non-zero value of $\Delta\Gamma_s$ allows the determination of additional terms, labelled $A^{\Delta\Gamma}$ and $\bar{A}^{\Delta\Gamma}$, that break ambiguities in the solutions for $\gamma - 2\beta_s$.

LHCb [296,432] has measured the time-dependent CP violation parameters in $B_s^0 \to D_s^{\mp}K^{\pm}$ decays, using 3.0 fb^{-1} of data. The results are given in Table 47, and correspond to $3.6\,\sigma$ evidence for CP violation in the interference between mixing and $B_s^0 \to D_s^{\mp}K^{\pm}$ decays. From these results, and a constraint on $2\beta_s$ from independent LHCb measurements [202], LHCb determine $\gamma = (127\,^{+17}_{-22})^{\circ}$, $\delta_{D_sK} = (358\,^{+15}_{-16})^{\circ}$ and $R_{D_sK} = 0.37\,^{+0.10}_{-0.09}$.

4.14 Rates and asymmetries in $B \to D^{(*)}K^{(*)}$ decays

As explained in Sect. 4.2.7, rates and asymmetries in $B^+ \to D^{(*)}K^{(*)+}$ decays are sensitive to γ, and have negligible the-

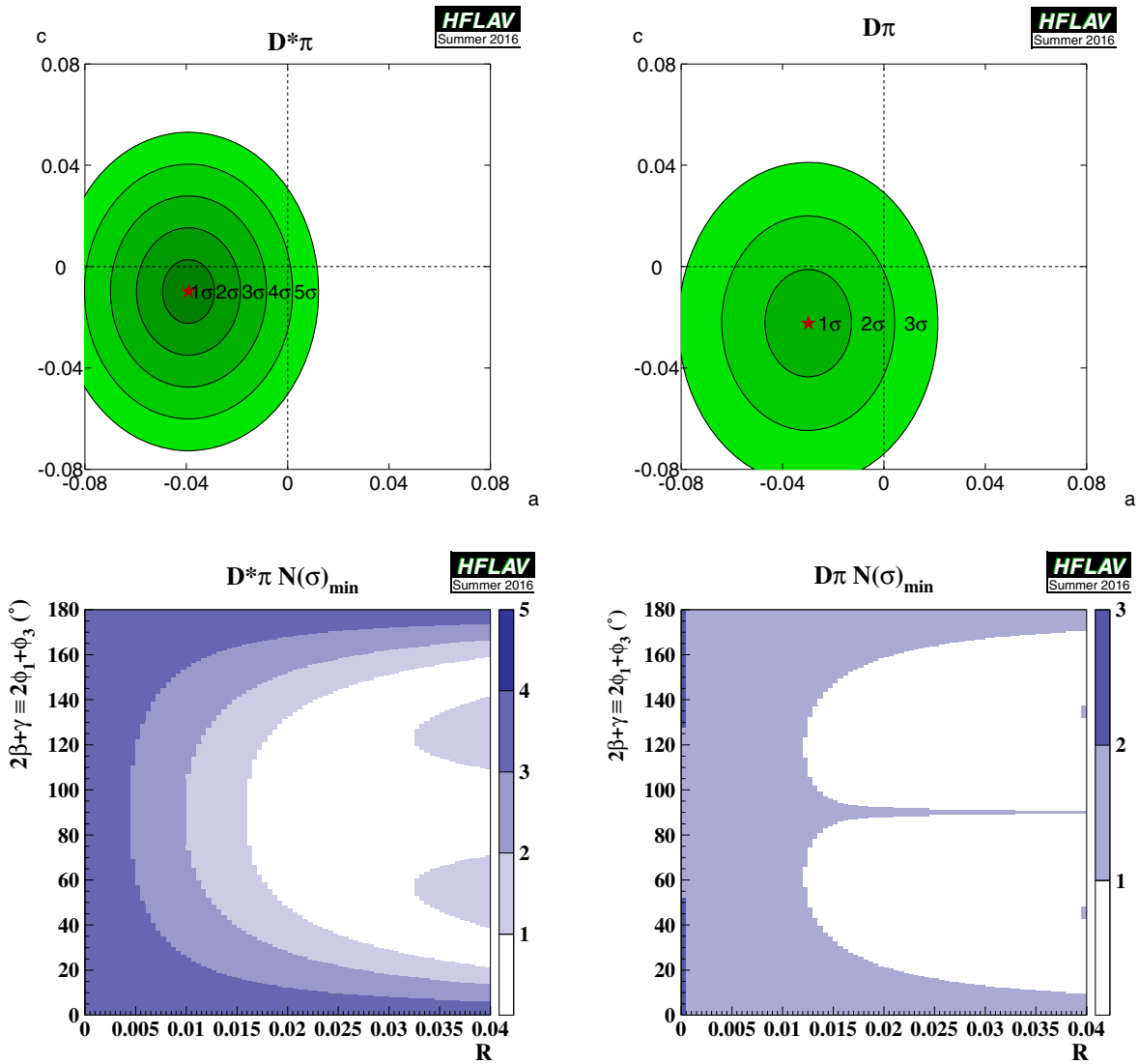

Fig. 38 Results from $b \to c\bar{u}d/u\bar{c}d$ modes. (*Top*) Constraints in c vs. a space. (*Bottom*) Constraints in $2\beta+\gamma$ vs. R space. (*Left*) $D^*\pi$ and (*right*) $D\pi$ modes

Table 47 Results for $B_s^0 \to D_s^{\mp} K^{\pm}$

Experiment	$\int \mathcal{L}\,dt$	C	$A^{\Delta\Gamma}$	$\bar{A}^{\Delta\Gamma}$	S	$\bar{S}$
LHCb [432]	3 fb^{-1}	$0.74 \pm 0.14 \pm 0.05$	$0.40 \pm 0.28 \pm 0.12$	$0.31 \pm 0.27 \pm 0.11$	$-0.52 \pm 0.20 \pm 0.07$	$-0.50 \pm 0.20 \pm 0.07$

oretical uncertainty [311]. Various methods using different $D^{(*)}$ final states have been used.

4.14.1 D decays to CP eigenstates

Results are available from BaBar, Belle, CDF and LHCb on GLW analyses in the decay mode $B^+ \to DK^+$. All experiments use the CP-even D decay final states K^+K^- and $\pi^+\pi^-$; BaBar and Belle in addition use the CP-odd decay modes $K_S^0\pi^0$, $K_S^0\omega$ and $K_S^0\phi$, though care is taken to avoid statistical overlap with the $K_S^0K^+K^-$ sample used for Dalitz plot analyses (see Sect. 4.14.4). BaBar and Belle also have results in the decay mode $B^+ \to D^*K^+$, using both the $D^* \to D\pi^0$ decay, which gives $CP(D^*) = CP(D)$, and the $D^* \to D\gamma$ decays, which gives $CP(D^*) = -CP(D)$. In addition, BaBar and LHCb have results in the decay mode $B^+ \to DK^{*+}$, and LHCb has results in the decay mode $B^+ \to DK^+\pi^+\pi^-$. The results and averages are given in Table 48 and shown in Fig. 39.

LHCb has performed a GLW analysis using the $B^0 \to DK^{*0}$ decay with the CP-even $D \to K^+K^-$ and $D \to \pi^+\pi^-$ channels [441]. The results are presented separately to allow for possible CP violation effects in the charm decays, which are, however, known to be small.

Table 48 Averages from GLW analyses of $b \to c\bar{u}s/u\bar{c}s$ modes. The sample size is given in terms of number of $B\bar{B}$ pairs, $N(B\bar{B})$, for the e^+e^- B factory experiments BABAR and Belle, and in terms of integrated luminosity, $\int \mathcal{L}\,dt$, for the hadron collider experiments CDF and LHCb

Experiment	Sample size	A_{CP+}	A_{CP-}	R_{CP+}	R_{CP-}
$D_{CP}K^+$					
BABAR [433]	467M	$0.25 \pm 0.06 \pm 0.02$	$-0.09 \pm 0.07 \pm 0.02$	$1.18 \pm 0.09 \pm 0.05$	$1.07 \pm 0.08 \pm 0.04$
Belle [434]	275M	$0.06 \pm 0.14 \pm 0.05$	$-0.12 \pm 0.14 \pm 0.05$	$1.13 \pm 0.16 \pm 0.08$	$1.17 \pm 0.14 \pm 0.14$
CDF [435]	$1\,\text{fb}^{-1}$	$0.39 \pm 0.17 \pm 0.04$	–	$1.30 \pm 0.24 \pm 0.12$	–
LHCb KK [436]	$3\,\text{fb}^{-1}$	$0.087 \pm 0.020 \pm 0.008$	–	$0.968 \pm 0.022 \pm 0.021$	–
LHCb $\pi\pi$ [436]	$3\,\text{fb}^{-1}$	$0.128 \pm 0.037 \pm 0.012$	–	$1.002 \pm 0.040 \pm 0.026$	–
LHCb average [436]	$3\,\text{fb}^{-1}$	$0.097 \pm 0.018 \pm 0.009$	–	$0.978 \pm 0.019 \pm 0.018$	–
Average		0.111 ± 0.018	-0.10 ± 0.07	0.995 ± 0.025	1.09 ± 0.08
Confidence level		0.063 (1.9σ)	0.86 (0.2σ)	0.21 (1.3σ)	0.65 (0.5σ)
$D^*_{CP}K^+$					
BABAR [437]	383M	$-0.11 \pm 0.09 \pm 0.01$	$0.06 \pm 0.10 \pm 0.02$	$1.31 \pm 0.13 \pm 0.03$	$1.09 \pm 0.12 \pm 0.04$
Belle [434]	275M	$-0.20 \pm 0.22 \pm 0.04$	$0.13 \pm 0.30 \pm 0.08$	$1.41 \pm 0.25 \pm 0.06$	$1.15 \pm 0.31 \pm 0.12$
Average		-0.12 ± 0.07	0.13 ± 0.07	1.25 ± 0.09	1.06 ± 0.09
Confidence level		0.82 (0.2σ)	0.29 (1.1σ)	0.52 (0.6σ)	0.74 (0.3σ)
$D_{CP}K^{*+}$					
BABAR [438]	379M	$0.09 \pm 0.13 \pm 0.06$	$-0.23 \pm 0.21 \pm 0.07$	$2.17 \pm 0.35 \pm 0.09$	$1.03 \pm 0.27 \pm 0.13$
LHCb KK [439]	$4\,\text{fb}^{-1}$	$0.12 \pm 0.08 \pm 0.01$	–	$1.31 \pm 0.11 \pm 0.05$	–
LHCb $\pi\pi$ [439]	$4\,\text{fb}^{-1}$	$0.08 \pm 0.16 \pm 0.02$	–	$0.98 \pm 0.17 \pm 0.04$	–
LHCb average [439]	$4\,\text{fb}^{-1}$	0.11 ± 0.07	–	1.21 ± 0.10	–
Average		0.11 ± 0.06	-0.23 ± 0.22	1.27 ± 0.10	1.03 ± 0.30
Confidence level		0.97 (0.04σ)		0.01 (2.6σ)	
$D_{CP}K^+\pi^+\pi^-$					
LHCb KK [440]	$3\,\text{fb}^{-1}$	$-0.045 \pm 0.064 \pm 0.011$	–	$1.043 \pm 0.069 \pm 0.034$	–
LHCb $\pi\pi$ [440]	$3\,\text{fb}^{-1}$	$-0.054 \pm 0.101 \pm 0.011$	–	$1.035 \pm 0.108 \pm 0.038$	–
LHCb average [440]	$3\,\text{fb}^{-1}$	-0.048 ± 0.055	–	1.040 ± 0.064	–

The results are given in Table 49 where an average is also reported.

As pointed out in Refs. [313,314], a Dalitz plot analysis of $B^0 \to DK^+\pi^-$ decays provides more sensitivity to $\gamma \equiv \phi_3$ than the quasi-two-body DK^{*0} approach. The analysis provides direct sensitivity to the hadronic parameters r_B and δ_B associated with the $B^0 \to DK^{*0}$ decay amplitudes, rather than effective hadronic parameters averaged over the K^{*0} selection window as in the quasi-two-body case.

Such an analysis has been performed by LHCb. A simultaneous fit is performed to the $B^0 \to DK^+\pi^-$ Dalitz plots with the neutral D meson reconstructed in the $K^+\pi^-$, K^+K^- and $\pi^+\pi^-$ final states. The reported results in Table 50 are for the Cartesian parameters, defined in Eq. (150) associated with the $B^0 \to DK^*(892)^0$ decay. Note that, since the measurements use overlapping data samples, these results cannot be combined with the LHCb results for GLW observables in $B^0 \to DK^*(892)^0$ decays reported in Table 49.

LHCb use these results to obtain confidence levels for γ, $r_B(DK^{*0})$ and $\delta_B(DK^{*0})$. In addition, results are reported for the hadronic parameters needed to relate these results to quasi-two-body measurements of $B^0 \to DK^*(892)^0$ decays, where a selection window of $m(K^+\pi^-)$ within 50 MeV/c^2 of the pole mass and helicity angle satisfying $|\cos(\theta_{K^{*0}})| > 0.4$ is assumed. These parameters are the coherence factor κ, the ratio of quasi-two-body and amplitude level r_B values, $\bar{R}_B = \bar{r}_B/r_B$, and the difference between quasi-two-body and amplitude level δ_B values, $\Delta\bar{\delta}_B = \bar{\delta}_B - \delta_B$. LHCb [442] obtain

$$\begin{aligned} \gamma &= 0.958\,^{+0.005}_{-0.010}\,^{+0.002}_{-0.045}, \\ \bar{R}_B &= 1.02\,^{+0.03}_{-0.01} \pm 0.06, \\ \Delta\bar{\delta}_B &= 0.02\,^{+0.03}_{-0.02} \pm 0.11. \end{aligned} \tag{163}$$

4.14.2 *D decays to quasi-CP eigenstates*

As discussed in Sect. 4.2.7, if a multibody neutral D meson decay can be shown to be dominated by one CP eigenstate,

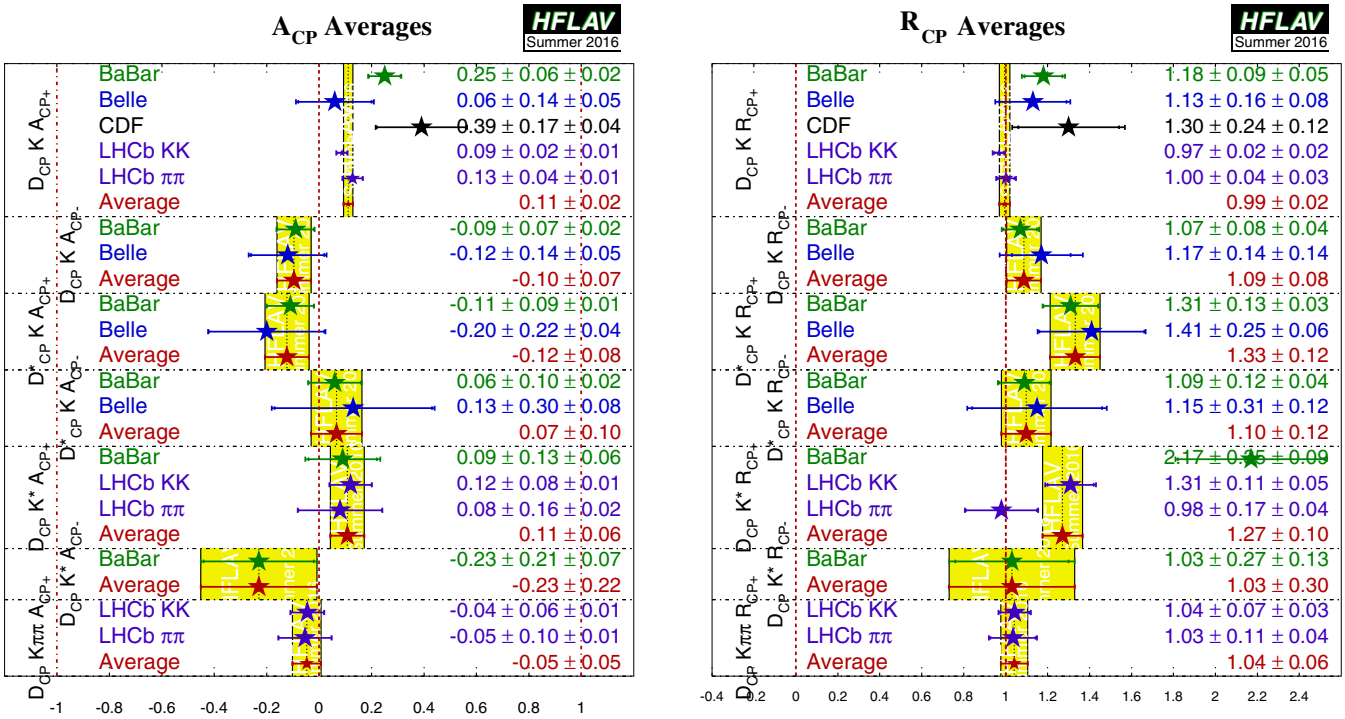

Fig. 39 Averages of A_{CP} and R_{CP} from GLW analyses

Table 49 Results from GLW analysis of $B^0 \to DK^{*0}$

Experiment	Sample size	A_{CP+}	R_{CP+}
LHCb KK [441]	$\int \mathcal{L}\,dt = 3\,\text{fb}^{-1}$	$-0.20 \pm 0.15 \pm 0.02$	$1.05\,^{+0.17}_{-0.15} \pm 0.04$
LHCb $\pi\pi$ [441]	$\int \mathcal{L}\,dt = 3\,\text{fb}^{-1}$	$-0.09 \pm 0.22 \pm 0.02$	$1.21\,^{+0.28}_{-0.25} \pm 0.05$
Average		-0.16 ± 0.12	1.10 ± 0.14

Table 50 Results from Dalitz plot analysis of $B^0 \to DK^+\pi^-$ decays with $D \to K^+K^-$ and $\pi^+\pi^-$

Experiment	$\int \mathcal{L}\,dt$	x_+	y_+	x_-	y_-
LHCb [442]	$3\,\text{fb}^{-1}$	$0.04 \pm 0.16 \pm 0.11$	$-0.47 \pm 0.28 \pm 0.22$	$-0.02 \pm 0.13 \pm 0.14$	$-0.35 \pm 0.26 \pm 0.41$

Table 51 Averages from GLW-like analyses of $b \to c\bar{u}s/u\bar{c}s$ modes

Experiment	Sample size	A_{qGLW}	R_{qGLW}
$D_{\pi^+\pi^-\pi^0}K^+$			
LHCb [444]	$\int \mathcal{L}\,dt = 3\,\text{fb}^{-1}$	$0.05 \pm 0.09 \pm 0.01$	$0.98 \pm 0.11 \pm 0.05$
BABAR [322]	$N(B\bar{B}) = 324\text{M}$	$-0.02 \pm 0.15 \pm 0.03$	–
Average		0.03 ± 0.08	0.98 ± 0.12
Confidence level		$0.68\ (0.4\sigma)$	–
$D_{K^+K^-\pi^0}K^+$			
LHCb [444]	$\int \mathcal{L}\,dt = 3\,\text{fb}^{-1}$	$0.30 \pm 0.20 \pm 0.02$	$0.95 \pm 0.22 \pm 0.04$
$D_{\pi^+\pi^-\pi^+\pi^-}K^+$			
LHCb [436]	$\int \mathcal{L}\,dt = 3\,\text{fb}^{-1}$	$0.10 \pm 0.03 \pm 0.02$	$0.97 \pm 0.04 \pm 0.02$

it can be used in a "GLW-like" (sometimes called "quasi-GLW") analysis [318]. The same observables R_{CP}, A_{CP} as for the GLW case are measured, but an additional factor of $(2F_+ - 1)$, where F_+ is the fractional CP-even content, enters the expressions relating these observables to $\gamma \equiv \phi_3$. The F_+ factors have been measured using CLEO-c data to

Table 52 Averages from ADS analyses of $b \to c\bar{u}s/u\bar{c}s$ modes

Experiment	Sample size	$A_{\rm ADS}$	$R_{\rm ADS}$
DK^+, $D \to K^-\pi^+$			
BaBar [445]	$N(B\bar{B}) = 467$M	$-0.86 \pm 0.47\,^{+0.12}_{-0.16}$	$0.011 \pm 0.006 \pm 0.002$
Belle [446]	$N(B\bar{B}) = 772$M	$-0.39\,^{+0.26}_{-0.28}\,^{+0.04}_{-0.03}$	$0.0163\,^{+0.0044}_{-0.0041}\,^{+0.0007}_{-0.0013}$
CDF [447]	$\int \mathcal{L}\,dt = 7\,\text{fb}^{-1}$	$-0.82 \pm 0.44 \pm 0.09$	$0.0220 \pm 0.0086 \pm 0.0026$
LHCb [436]	$\int \mathcal{L}\,dt = 3\,\text{fb}^{-1}$	$-0.403 \pm 0.056 \pm 0.011$	$0.0188 \pm 0.0011 \pm 0.0010$
Average		-0.415 ± 0.055	0.0183 ± 0.0014
Confidence level		0.64 (0.5σ)	0.61 (0.5σ)
DK^+, $D \to K^-\pi^+\pi^0$			
BaBar [448]	474M	–	$0.0091\,^{+0.0082}_{-0.0076}\,^{+0.0014}_{-0.0037}$
Belle [449]	772M	$0.41 \pm 0.30 \pm 0.05$	$0.0198 \pm 0.0062 \pm 0.0024$
LHCb [444]	$\int \mathcal{L}\,dt = 3\,\text{fb}^{-1}$	$-0.20 \pm 0.27 \pm 0.03$	$0.0140 \pm 0.0047 \pm 0.0019$
Average		0.07 ± 0.20	0.0148 ± 0.0036
Confidence level		0.13 (1.5σ)	0.59 (0.5σ)
DK^+, $D \to K^-\pi^+\pi^+\pi^-$			
LHCb [436]	$\int \mathcal{L}\,dt = 3\,\text{fb}^{-1}$	$-0.313 \pm 0.102 \pm 0.038$	$0.0140 \pm 0.0015 \pm 0.0006$
D^*K^+, $D^* \to D\pi^0$, $D \to K^-\pi^+$			
BaBar [445]	$N(B\bar{B}) = 467$M	$0.77 \pm 0.35 \pm 0.12$	$0.018 \pm 0.009 \pm 0.004$
D^*K^+, $D^* \to D\gamma$, $D \to K^-\pi^+$			
BaBar [445]	$N(B\bar{B}) = 467$M	$0.36 \pm 0.94\,^{+0.25}_{-0.41}$	$0.013 \pm 0.014 \pm 0.008$
DK^{*+}, $D \to K^-\pi^+$, $K^{*+} \to K^0_S\pi^+$			
BaBar [438]	$N(B\bar{B}) = 379$M	$-0.34 \pm 0.43 \pm 0.16$	$0.066 \pm 0.031 \pm 0.010$
LHCb [439]	$\int \mathcal{L}\,dt = 4\,\text{fb}^{-1}$	–	0.003 ± 0.004
Average		-0.34 ± 0.46	0.004 ± 0.004
Confidence level		–	0.06 (1.9σ)
$DK^+\pi^+\pi^-$, $D \to K^-\pi^+$			
LHCb [440]	$\int \mathcal{L}\,dt = 3\,\text{fb}^{-1}$	$-0.32\,^{+0.27}_{-0.34}$	$0.0082\,^{+0.0038}_{-0.0030}$

be $F_+(\pi^+\pi^-\pi^0) = 0.973 \pm 0.017$, $F_+(K^+K^-\pi^0) = 0.732 \pm 0.055$, $F_+(\pi^+\pi^-\pi^+\pi^-) = 0.737 \pm 0.028$ [443].

The GLW-like observables for $D \to \pi^+\pi^-\pi^0$, $K^+K^-\pi^0$ and $D \to \pi^+\pi^-\pi^+\pi^-$ have been measured by LHCb. The $A_{\rm qGLW}$ observable for $D \to \pi^+\pi^-\pi^0$ was measured in an earlier analysis by BaBar, from which additional observables, discussed in Sect. 4.2.7 and reported in Table 55 below, were reported. The results are given in Table 51.

4.14.3 D decays to suppressed final states

For ADS analyses, all of BaBar, Belle, CDF and LHCb have studied the modes $B^+ \to DK^+$ and $B^+ \to D\pi^+$. BaBar has also analysed the $B^+ \to D^*K^+$ mode. There is an effective shift of π in the strong phase difference between the cases that the D^* is reconstructed as $D\pi^0$ and $D\gamma$ [315], therefore these modes are studied separately. In addition, BaBar has studied the $B^+ \to DK^{*+}$ mode, where K^{*+} is reconstructed as $K^0_S\pi^+$, and LHCb has studied the $B^+ \to DK^+\pi^+\pi^-$ mode. In all the above cases the suppressed decay $D \to K^-\pi^+$ has been used. BaBar, Belle and LHCb also have results using $B^+ \to DK^+$ with $D \to K^-\pi^+\pi^0$, while LHCb has results using $B^+ \to DK^+$ with $D \to K^-\pi^+\pi^+\pi^-$. The results and averages are given in Table 52 and shown in Fig. 40.

Similar phenomenology as for $B \to DK$ decays holds for $B \to D\pi$ decays, though in this case the interference is between $b \to c\bar{u}d$ and $b \to u\bar{c}d$ transitions, and the ratio of suppressed to favoured amplitudes is expected to be much smaller, $\mathcal{O}(1\%)$. For most D meson final states this implies that the interference effect is too small to be of interest, but in the case of ADS analysis it is possible that effects due to γ may be observable. Accordingly, the experiments now measure the corresponding observables in the $D\pi$ final states. The results and averages are given in Table 53 and shown in Fig. 41.

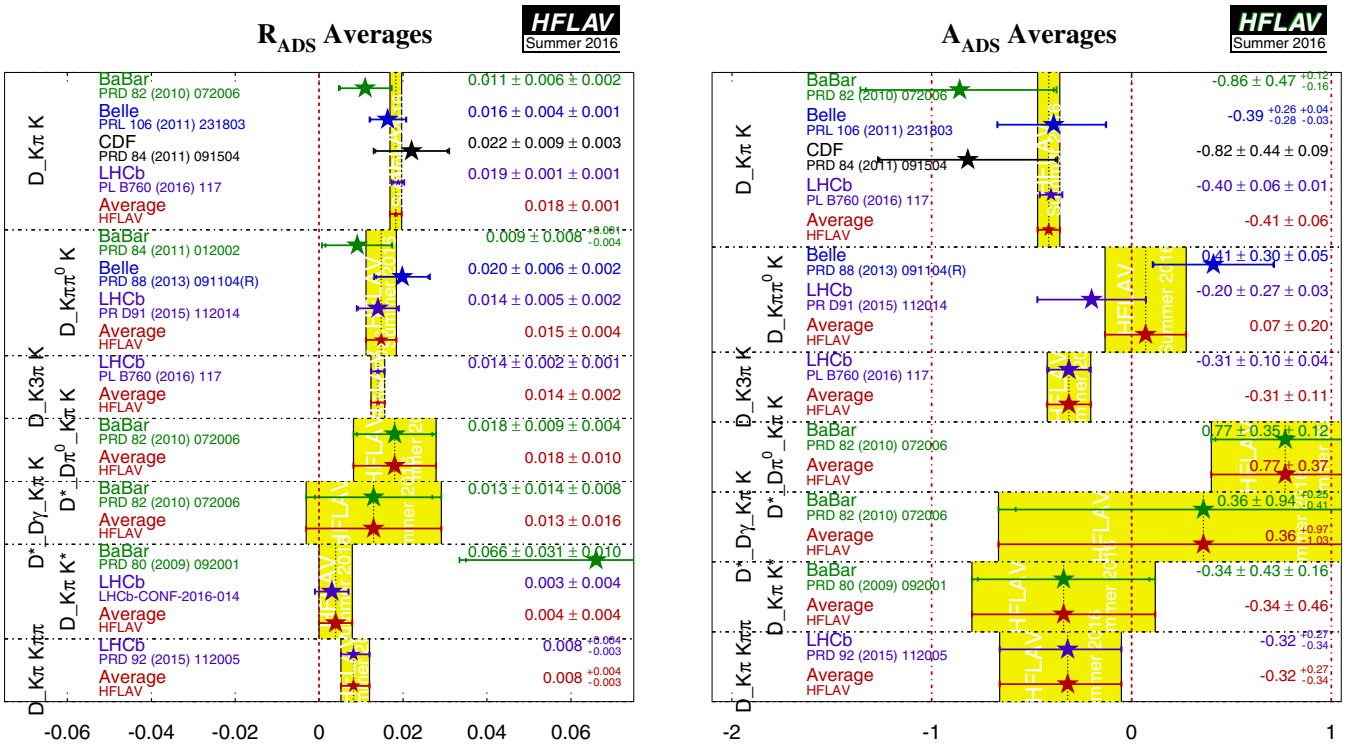

Fig. 40 Averages of R_{ADS} and A_{ADS} for $B \to D^{(*)}K^{(*)}$ decays

Table 53 Averages from ADS analyses of $b \to c\bar{u}d/u\bar{c}d$ modes

Experiment	Sample size	A_{ADS}	R_{ADS}
$D\pi^+, D \to K^-\pi^+$			
BaBar [445]	$N(B\bar{B}) = 467\mathrm{M}$	$0.03 \pm 0.17 \pm 0.04$	$0.0033 \pm 0.0006 \pm 0.0004$
Belle [446]	$N(B\bar{B}) = 772\mathrm{M}$	$-0.04 \pm 0.11\,^{+0.02}_{-0.01}$	$0.00328\,^{+0.00038}_{-0.00036}\,^{+0.00012}_{-0.00018}$
CDF [447]	$\int \mathcal{L}\,dt = 7\,\mathrm{fb}^{-1}$	$0.13 \pm 0.25 \pm 0.02$	$0.0028 \pm 0.0007 \pm 0.0004$
LHCb [436]	$\int \mathcal{L}\,dt = 3\,\mathrm{fb}^{-1}$	$0.100 \pm 0.031 \pm 0.009$	$0.00360 \pm 0.00012 \pm 0.00009$
Average		0.088 ± 0.030	0.00353 ± 0.00014
Confidence level		$0.66\ (0.4\sigma)$	$0.68\ (0.4\sigma)$
$D\pi^+, D \to K^-\pi^+\pi^0$			
Belle [449]	772M	$0.16 \pm 0.27\,^{+0.03}_{-0.04}$	$0.00189 \pm 0.00054\,^{+0.00022}_{-0.00025}$
LHCb [444]	$\int \mathcal{L}\,dt = 3\,\mathrm{fb}^{-1}$	$0.44 \pm 0.19 \pm 0.01$	$0.00235 \pm 0.00049 \pm 0.00004$
Average		0.35 ± 0.16	0.00216 ± 0.00038
Confidence level		$0.40\ (0.8\sigma)$	$0.55\ (0.6\sigma)$
$D\pi^+, D \to K^-\pi^+\pi^+\pi^-$			
LHCb [436]	$\int \mathcal{L}\,dt = 3\,\mathrm{fb}^{-1}$	$0.023 \pm 0.048 \pm 0.005$	$0.00377 \pm 0.00018 \pm 0.00006$
$D^*\pi^+, D^* \to D\pi^0, D \to K^-\pi^+$			
BaBar [445]	467M	$-0.09 \pm 0.27 \pm 0.05$	$0.0032 \pm 0.0009 \pm 0.0008$
$D^*\pi^+, D^* \to D\gamma, D \to K^-\pi^+$			
BaBar [445]	467M	$-0.65 \pm 0.55 \pm 0.22$	$0.0027 \pm 0.0014 \pm 0.0022$
$D\pi^+\pi^+\pi^-, D \to K^-\pi^+$			
LHCb [440]	$\int \mathcal{L}\,dt = 3\,\mathrm{fb}^{-1}$	-0.003 ± 0.090	0.00427 ± 0.00043

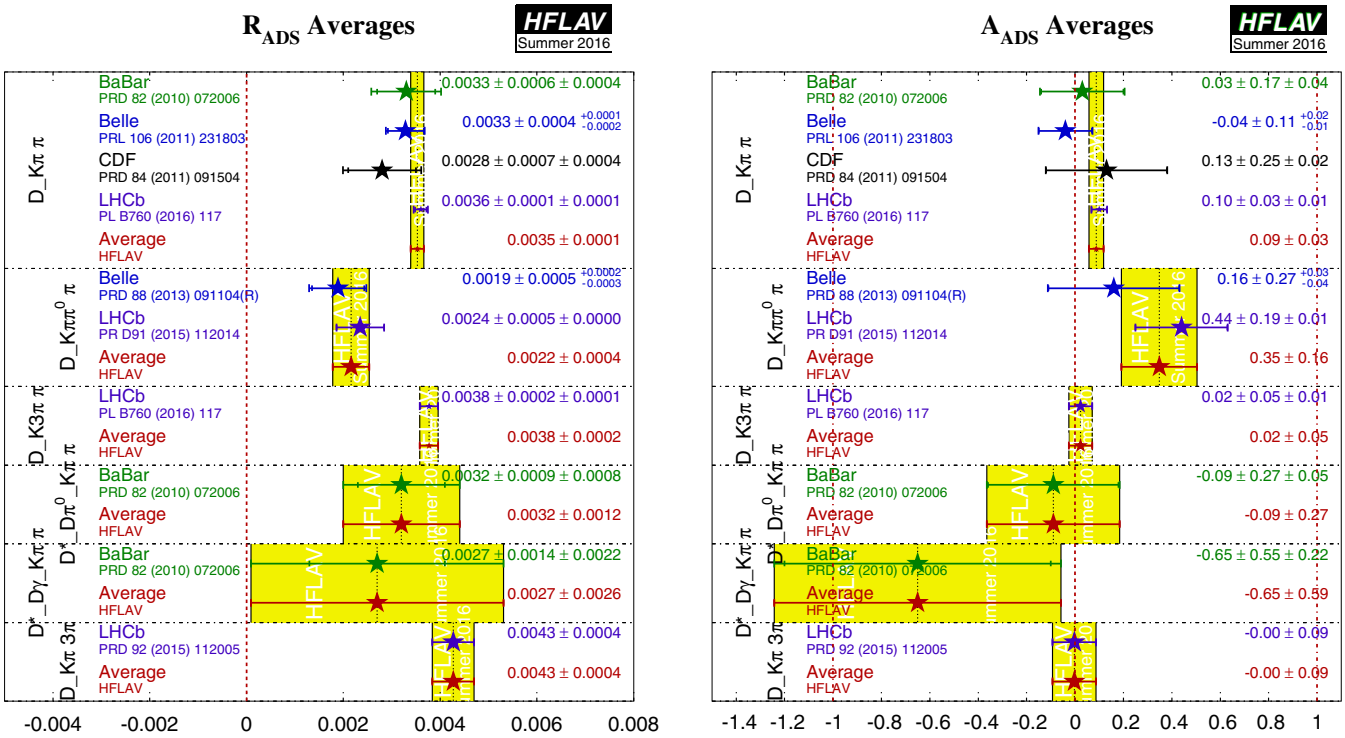

Fig. 41 Averages of R_{ADS} and A_{ADS} for $B \to D^{(*)}\pi$ decays

Table 54 Results from ADS analysis of $B^0 \to DK^{*0}$, $D \to K^-\pi^+$

Experiment	Sample size	R_+	R_-
LHCb [441]	$\int \mathcal{L}\,dt = 3\mathrm{fb}^{-1}$	$0.06 \pm 0.03 \pm 0.01$	$0.06 \pm 0.03 \pm 0.01$

BABAR, Belle and LHCb have also presented results from a similar analysis method with self-tagging neutral B decays: $B^0 \to DK^{*0}$ with $D \to K^-\pi^+$ (all), $D \to K^-\pi^+\pi^0$ and $D \to K^-\pi^+\pi^+\pi^-$ (BABAR only). All these results are obtained with the $K^{*0} \to K^+\pi^-$ decay. Effects due to the natural width of the K^{*0} are handled using the parametrisation suggested by Gronau [312].

The following 95% CL limits are set by BABAR [450]:

$$R_{\mathrm{ADS}}(K\pi) < 0.244 \quad R_{\mathrm{ADS}}(K\pi\pi^0) < 0.181$$
$$R_{\mathrm{ADS}}(K\pi\pi\pi) < 0.391, \tag{164}$$

while Belle [451] obtain

$$R_{\mathrm{ADS}}(K\pi) < 0.16. \tag{165}$$

The results from LHCb, which are presented in terms of the parameters R_+ and R_- instead of R_{ADS} and A_{ADS}, are given in Table 54.

Combining the results and using additional input from CLEO-c [452,453] a limit on the ratio between the $b \to u$ and $b \to c$ amplitudes of $\bar{r}_B(DK^{*0}) \in [0.07, 0.41]$ at 95% CL limit is set by BABAR. Belle set a limit of $\bar{r}_B < 0.4$ at 95% CL. LHCb take input from Sect. 8 and obtain $\bar{r}_B = 0.240^{+0.055}_{-0.048}$ (different from zero with 2.7σ significance).

4.14.4 *D decays to multiparticle self-conjugate final states (model-dependent analysis)*

For the model-dependent Dalitz plot analysis, both BABAR and Belle have studied the modes $B^+ \to DK^+$, $B^+ \to D^*K^+$ and $B^+ \to DK^{*+}$. For $B^+ \to D^*K^+$, both experiments have used both D^* decay modes, $D^* \to D\pi^0$ and $D^* \to D\gamma$, taking the effective shift in the strong phase difference into account.[36] In all cases the decay $D \to K^0_S\pi^+\pi^-$ has been used. BABAR also used the decay $D \to K^0_S K^+K^-$. LHCb has also studied $B^+ \to DK^+$ decays with $D \to K^0_S\pi^+\pi^-$. BABAR has also performed an analysis of $B^+ \to DK^+$ with $D \to \pi^+\pi^-\pi^0$. Results and averages are given in Table 55, and shown in Figs. 42 and 43. The third error on each measurement is due to D decay model uncertainty.

[36] Belle [454] quote separate results for $B^+ \to D^*K^+$ with $D^* \to D\pi^0$ and $D^* \to D\gamma$. The results quoted in Table 55 are from our average, performed using the statistical correlations provided, and neglecting all systematic correlations; model uncertainties are not included. The first uncertainty on the quoted results is combined statistical and systematic, the second is the model error (taken from the Belle results on $B^+ \to D^*K^+$ with $D^* \to D\pi^0$).

Table 55 Averages from model-dependent Dalitz plot analyses of $b \to c\bar{u}s/u\bar{c}s$ modes. Note that the uncertainties assigned to the averages do not include model errors

Experiment	Sample size	x_+	y_+	x_-	y_-
$DK^+, D \to K_S^0\pi^+\pi^-$					
BaBar [455]	$N(B\bar{B}) = 468$M	$-0.103 \pm 0.037 \pm 0.006 \pm 0.007$	$-0.021 \pm 0.048 \pm 0.004 \pm 0.009$	$0.060 \pm 0.039 \pm 0.007 \pm 0.006$	$0.062 \pm 0.045 \pm 0.004 \pm 0.006$
Belle [454]	$N(B\bar{B}) = 657$M	$-0.107 \pm 0.043 \pm 0.011 \pm 0.055$	$-0.067 \pm 0.059 \pm 0.018 \pm 0.063$	$0.105 \pm 0.047 \pm 0.011 \pm 0.064$	$0.177 \pm 0.060 \pm 0.018 \pm 0.054$
LHCb [456]	$\int \mathcal{L}\,dt = 1\,\text{fb}^{-1}$	$-0.084 \pm 0.045 \pm 0.009 \pm 0.005$	$-0.032 \pm 0.048\,^{+0.010}_{-0.009} \pm 0.008$	$0.027 \pm 0.044\,^{+0.010}_{-0.008} \pm 0.001$	$0.013 \pm 0.048\,^{+0.009}_{-0.007} \pm 0.003$
Average		-0.098 ± 0.024	-0.036 ± 0.030	0.070 ± 0.025	0.075 ± 0.029
Confidence level			0.52 (0.7σ)		
$D^*K^+, D^* \to D\pi^0$ or $D\gamma$, $D \to K_S^0\pi^+\pi^-$					
BaBar [455]	$N(B\bar{B}) = 468$M	$0.147 \pm 0.053 \pm 0.017 \pm 0.003$	$-0.032 \pm 0.077 \pm 0.008 \pm 0.006$	$-0.104 \pm 0.051 \pm 0.019 \pm 0.002$	$-0.052 \pm 0.063 \pm 0.009 \pm 0.007$
Belle [454]	$N(B\bar{B}) = 657$M	$0.100 \pm 0.074 \pm 0.081$	$0.155 \pm 0.101 \pm 0.063$	$-0.023 \pm 0.112 \pm 0.090$	$-0.252 \pm 0.112 \pm 0.049$
Average		0.132 ± 0.044	0.037 ± 0.061	-0.081 ± 0.049	-0.107 ± 0.055
Confidence level			0.22 (1.2σ)		
$DK^{*+}, D \to K_S^0\pi^+\pi^-$					
BaBar [455]	$N(B\bar{B}) = 468$M	$-0.151 \pm 0.083 \pm 0.029 \pm 0.006$	$0.045 \pm 0.106 \pm 0.036 \pm 0.008$	$0.075 \pm 0.096 \pm 0.029 \pm 0.007$	$0.127 \pm 0.095 \pm 0.027 \pm 0.006$
Belle [457]	$N(B\bar{B}) = 386$M	$-0.105\,^{+0.177}_{-0.167} \pm 0.006 \pm 0.088$	$-0.004\,^{+0.164}_{-0.156} \pm 0.013 \pm 0.095$	$-0.784\,^{+0.249}_{-0.295} \pm 0.029 \pm 0.097$	$-0.281\,^{+0.440}_{-0.335} \pm 0.046 \pm 0.086$
Average		-0.152 ± 0.077	0.024 ± 0.091	-0.043 ± 0.094	0.091 ± 0.096
Confidence level			0.011 (2.5σ)		
$DK^{*0}, D \to K_S^0\pi^+\pi^-, K^{*0} \to K^+\pi^-$					
LHCb [458]	$\int \mathcal{L}\,dt = 3\,\text{fb}^{-1}$	$0.05 \pm 0.24 \pm 0.04 \pm 0.01$	$-0.65\,^{+0.24}_{-0.23} \pm 0.08 \pm 0.01$	$-0.15 \pm 0.14 \pm 0.03 \pm 0.01$	$0.25 \pm 0.15 \pm 0.06 \pm 0.01$
Experiment	$N(B\bar{B})$	ρ^+	θ^+	ρ^-	θ^-
$DK^+, D \to \pi^+\pi^-\pi^0$					
BaBar [322]	324M	$0.75 \pm 0.11 \pm 0.04$	$147 \pm 23 \pm 1$	$0.72 \pm 0.11 \pm 0.04$	$173 \pm 42 \pm 2$

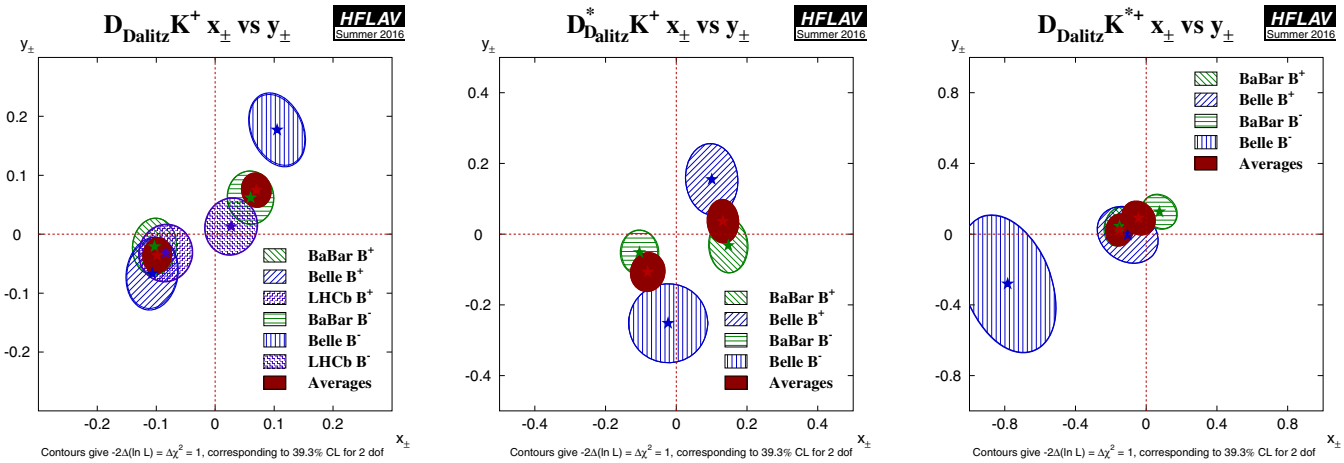

Fig. 42 Contours in the $(x_\pm, y_\pm)$ from model-dependent analysis of $B^+ \to D^{(*)}K^{(*)+}$, $D \to K^0_S h^+ h^-$ $(h = \pi, K)$. (*Left*) $B^+ \to DK^+$, (*middle*) $B^+ \to D^*K^+$, (*right*) $B^+ \to DK^{*+}$. Note that the uncertainties assigned to the averages given in these plots do not include model errors

The parameters measured in the analyses are explained in Sect. 4.2.7. All experiments measure the Cartesian variables, defined in Eq. (150), and perform frequentist statistical procedures, to convert these into measurements of γ, r_B and δ_B. In the $B^+ \to DK^+$ with $D \to \pi^+\pi^-\pi^0$ analysis, the parameters $(\rho^\pm, \theta^\pm)$ are used instead.

Both experiments reconstruct K^{*+} as $K^0_S\pi^+$, but the treatment of possible nonresonant $K^0_S\pi^+$ differs: Belle assign an additional model uncertainty, while BaBar use a parametrisation suggested by Gronau [312]. The parameters r_B and δ_B are replaced with effective parameters $\kappa\bar{r}_B$ and $\bar{\delta}_B$; no attempt is made to extract the true hadronic parameters of the $B^+ \to DK^{*+}$ decay.

We perform averages using the following procedure, which is based on a set of reasonable, though imperfect, assumptions.

- It is assumed that effects due to the different D decay models used by the two experiments are negligible. Therefore, we do not rescale the results to a common model.
- It is further assumed that the model uncertainty is 100% correlated between experiments, and therefore this source of error is not used in the averaging procedure. (This approximation is compromised by the fact that the BaBar results include $D \to K^0_S K^+K^-$ decays in addition to $D \to K^0_S\pi^+\pi^-$.)
- We include in the average the effect of correlations within each experiment's set of measurements.
- At present it is unclear how to assign an average model uncertainty. We have not attempted to do so. Our average includes only statistical and systematic errors. An unknown amount of model uncertainty should be added to the final error.
- We follow the suggestion of Gronau [312] in making the DK^* averages. Explicitly, we assume that the selection of $K^{*+} \to K^0_S\pi^+$ is the same in both experiments (so that κ, $\bar{r}_B$ and $\bar{\delta}_B$ are the same), and drop the additional source of model uncertainty assigned by Belle due to possible nonresonant decays.
- We do not consider common systematic errors, other than the D decay model.

Constraints on $\gamma \equiv \phi_3$

The measurements of $(x_\pm, y_\pm)$ can be used to obtain constraints on $\gamma \equiv \phi_3$, as well as the hadronic parameters r_B and δ_B. BaBar [455], Belle [454,457] and LHCb [456] have all done so using a frequentist procedure (there are some differences in the details of the techniques used).

- BaBar obtain $\gamma = (68^{+15}_{-14} \pm 4 \pm 3)^\circ$ from DK^+, D^*K^+ and DK^{*+}.
- Belle obtain $\phi_3 = (78^{+11}_{-12} \pm 4 \pm 9)^\circ$ from DK^+ and D^*K^+.
- LHCb obtain $\gamma = (84^{+49}_{-42})^\circ$ from DK^+ using 1 fb^{-1} of data (a more precise result using 3 fb^{-1} and the model-independent method is reported below).
- The experiments also obtain values for the hadronic parameters as detailed in Table 56.
- In the BaBar analysis of $B^+ \to DK^+$ with $D \to \pi^+\pi^-\pi^0$ decays [322], a constraint of $-30^\circ < \gamma < 76^\circ$ is obtained at the 68% confidence level.
- The results discussed here are included in the HFLAV combination to obtain a world average value for $\gamma \equiv \phi_3$, as discussed in Sect. 4.14.7.

BaBar and LHCb have performed a similar analysis using the self-tagging neutral B decay $B^0 \to DK^{*0}$ (with $K^{*0} \to K^+\pi^-$). Effects due to the natural width of the

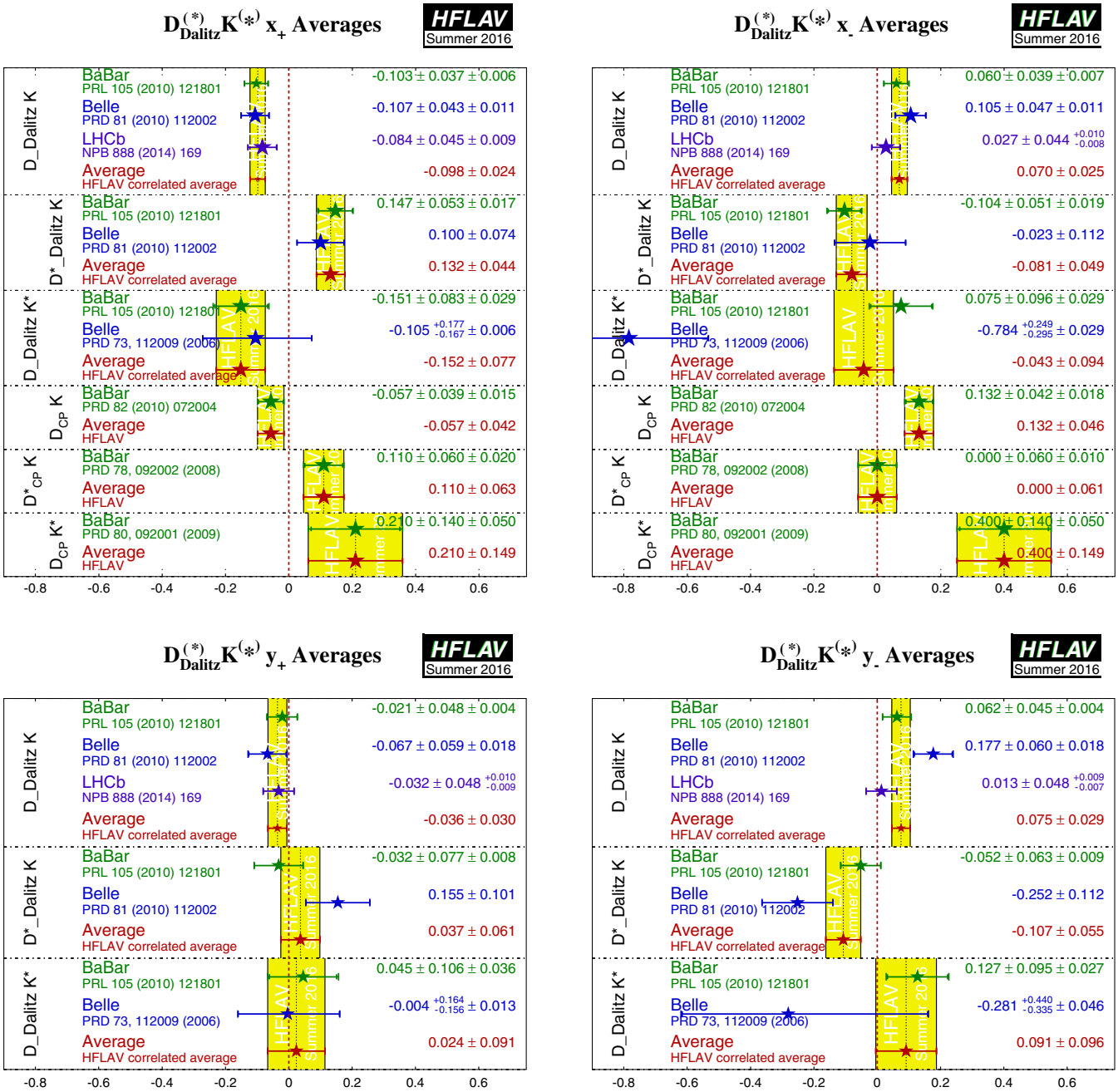

Fig. 43 Averages of $(x_\pm, y_\pm)$ from model-dependent analyses of $B^+ \to D^{(*)}K^{(*)+}$ with $D \to K^0_S h^+h^-$ $(h = \pi, K)$. (*Top left*) x_+, (*top right*) x_-, (*bottom left*) y_+, (*bottom right*) y_-. The *top plots* include constraints on $x_\pm$ obtained from GLW analyses (see Sect. 4.14.1). Note that the uncertainties assigned to the averages given in these plots do not include model errors

K^{*0} are handled using the parametrisation suggested by Gronau [312]. LHCb give results in terms of the Cartesian parameters, as shown in Table 55. BaBar [459] present results only in terms of γ and the hadronic parameters. The obtained constraints on $\gamma \equiv \phi_3$ are

- BaBar obtain $\gamma = (162 \pm 56)^\circ$
- LHCb obtain $\gamma = (80\,^{+21}_{-22})^\circ$
- Values for the hadronic parameters are given in Table 56.

4.14.5 *D decays to multiparticle self-conjugate final states (model-independent analysis)*

A model-independent approach to the analysis of $B^+ \to D^{(*)}K^+$ with multibody D decays was proposed by Giri, Grossman, Soffer and Zupan [309], and further developed by Bondar and Poluektov [319,320]. The method relies on information on the average strong phase difference between D^0 and $\overline{D}^0$ decays in bins of Dalitz plot position that can be obtained from quantum-correlated $\psi(3770) \to D^0\overline{D}^0$

Table 56 Summary of constraints on hadronic parameters from model-dependent analyses of $B^+ \to D^{(*)}K^{(*)+}$ and $B^0 \to DK^{*0}$ decays. Note the alternative parametrisation of the hadronic parameters used by BABAR in the DK^{*+} mode

	r_B	δ_B
In DK^+		
BABAR	$0.096 \pm 0.029 \pm 0.005 \pm 0.004$	$(119\,^{+19}_{-20} \pm 3 \pm 3)^\circ$
Belle	$0.160\,^{+0.040}_{-0.038} \pm 0.011\,^{+0.05}_{-0.010}$	$(138\,^{+13}_{-16} \pm 4 \pm 23)^\circ$
LHCb	0.06 ± 0.04	$(115\,^{+41}_{-51})^\circ$
In D^*K^+		
BABAR	$0.133\,^{+0.042}_{-0.039} \pm 0.014 \pm 0.003$	$(-82 \pm 21 \pm 5 \pm 3)^\circ$
Belle	$0.196\,^{+0.072}_{-0.069} \pm 0.012\,^{+0.062}_{-0.012}$	$(342\,^{+19}_{-21} \pm 3 \pm 23)^\circ$
	$\bar{r}_B$	$\bar{\delta}_B$
In DK^{*+}		
BABAR	$\kappa\bar{r}_B = 0.149\,^{+0.066}_{-0.062} \pm 0.026 \pm 0.006$	$(111 \pm 32 \pm 11 \pm 3)^\circ$
Belle	$0.56\,^{+0.22}_{-0.16} \pm 0.04 \pm 0.08$	$(243\,^{+20}_{-23} \pm 3 \pm 50)^\circ$
In DK^{*0}		
BABAR	<0.55 at 95% probability	$(62 \pm 57)^\circ$
LHCb	0.39 ± 0.13	$(197\,^{+24}_{-20})^\circ$

events. This information is measured in the form of parameters c_i and s_i that are the amplitude weighted averages of the cosine and sine of the strong phase difference in a Dalitz plot bin labelled by i, respectively. These quantities have been obtained for $D \to K^0_S\pi^+\pi^-$ (and $D \to K^0_S K^+K^-$) decays by CLEO-c [263,460].

Belle [461] and LHCb [462] have used the model-independent Dalitz plot analysis approach to study the mode $B^+ \to DK^+$. Both Belle [463] and LHCb [464] have also used this approach to study $B^0 \to DK^*(892)^0$ decays. In both cases, the experiments use $D \to K^0_S\pi^+\pi^-$ decays while LHCb has also included the $D \to K^0_S K^+K^-$ decay. The Cartesian variables $(x_\pm, y_\pm)$, defined in Eq. (150), are determined from the data. Note that due to the strong statistical and systematic correlations with the model-dependent results given in Sect. 4.14.4, these results cannot be combined.

The results and averages are given in Table 57, and shown in Fig. 44. Most results have three sets of errors, which are statistical, systematic, and uncertainty coming from the knowledge of c_i and s_i respectively. To perform the average, we remove the last uncertainty, which should be 100% correlated between the measurements. Since the size of the uncertainty from c_i and s_i is found to depend on the size of the $B \to DK$ data sample, we assign the LHCb uncertainties (which are mostly the smaller of the Belle and LHCb values) to the averaged result. This procedure should be conservative. In the LHCb $B^0 \to DK^*(892)^0$ results [464], the values of c_i and s_i are constrained to their measured values within uncertainties in the fit to data, and hence the effect is absorbed in their statistical uncertainties. The $B^0 \to DK^*(892)^0$ average is performed neglecting the model uncertainties on the Belle results.

Constraints on $\gamma \equiv \phi_3$

The measurements of $(x_\pm, y_\pm)$ can be used to obtain constraints on γ, as well as the hadronic parameters r_B and δ_B. The experiments have done so using frequentist procedures (there are some differences in the details of the techniques used) (Table 58).

- From $B^+ \to DK^+$, Belle [461] obtain $\phi_3 = (77.3\,^{+15.1}_{-14.9} \pm 4.1 \pm 4.3)^\circ$.
- From $B^+ \to DK^+$, LHCb [462] obtain $\gamma = (62\,^{+15}_{-14})^\circ$.
- From $B^0 \to DK^*(892)^0$, LHCb [464] obtain $\gamma = (71 \pm 20)^\circ$.
- The experiments also obtain values for the hadronic parameters as detailed in Table 59.
- The results discussed here are included in the HFLAV combination to obtain a world average value for $\gamma \equiv \phi_3$, as discussed in Sect. 4.14.7.

4.14.6 *D decays to multiparticle non-self-conjugate final states (model-independent analysis)*

Following the original suggestion of Grossman, Ligeti and Soffer [317], decays of D mesons to $K^0_S K^\pm\pi^\mp$ can be used in a similar approach to that discussed above to determine $\gamma \equiv \phi_3$. Since these decays are less abundant, the event samples available to date have not been sufficient for a fine binning of the Dalitz plots, but the analysis can be performed using only an overall coherence factor and related strong phase difference for the decay. These quantities have been

Table 57 Averages from model-independent Dalitz plot analyses of $b \to c\bar{u}s/u\bar{c}s$ modes

Experiment	Sample size	x_+	y_+	x_-	y_-
$DK^+, D \to K^0_S\pi^+\pi^-$					
Belle [461]	$N(B\bar{B}) = 772$M	$-0.110 \pm 0.043 \pm 0.014 \pm 0.007$	$-0.050^{+0.052}_{-0.055} \pm 0.011 \pm 0.007$	$0.095 \pm 0.045 \pm 0.014 \pm 0.010$	$0.137^{+0.053}_{-0.057} \pm 0.015 \pm 0.023$
LHCb [462]	$\int \mathcal{L}\,dt = 3\text{fb}^{-1}$	$-0.077 \pm 0.024 \pm 0.010 \pm 0.004$	$-0.022 \pm 0.025 \pm 0.004 \pm 0.010$	$0.025 \pm 0.025 \pm 0.010 \pm 0.005$	$0.075 \pm 0.029 \pm 0.005 \pm 0.014$
Average		$-0.085 \pm 0.023 \pm 0.04$	$-0.027 \pm 0.023 \pm 0.010$	$0.044 \pm 0.023 \pm 0.005$	$0.090 \pm 0.026 \pm 0.014$
Confidence level			0.39 (0.9σ)		
$DK^{*0}, D \to K^0_S\pi^+\pi^-$					
Belle [463]	$N(B\bar{B}) = 772$M	$0.1^{+0.7}_{-0.4}{}^{+0.0}_{-0.1} \pm 0.1$	$0.3^{+0.5}_{-0.8}{}^{+0.0}_{-0.1} \pm 0.1$	$0.4^{+1.0}_{-0.6}{}^{+0.0}_{-0.1} \pm 0.0$	$-0.6^{+0.8}_{-1.0}{}^{+0.1}_{-0.0} \pm 0.1$
LHCb [464]	$\int \mathcal{L}\,dt = 3\text{fb}^{-1}$	$0.05 \pm 0.35 \pm 0.02$	$-0.81 \pm 0.28 \pm 0.06$	$-0.31 \pm 0.20 \pm 0.04$	$0.31 \pm 0.21 \pm 0.05$
Average		0.10 ± 0.30	-0.63 ± 0.26	-0.27 ± 0.20	0.27 ± 0.21
Confidence level			0.38 (0.9σ)		

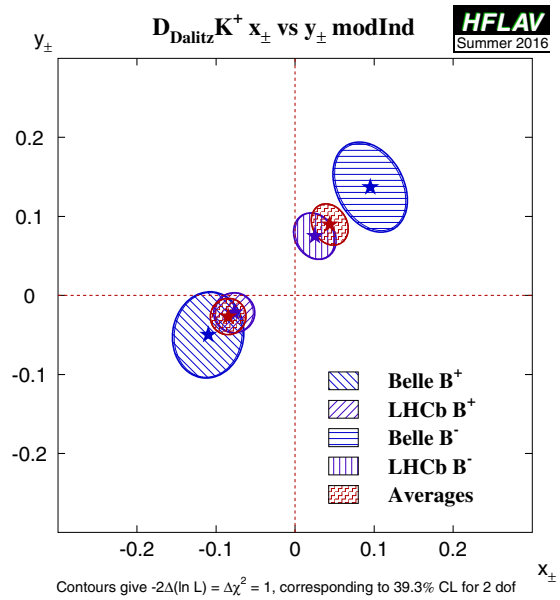

Fig. 44 Contours in the $(x_\pm, y_\pm)$ plane from model-independent analysis of $B^+ \to DK^+$ with $D \to K^0_S h^+h^-$ $(h = \pi, K)$

determined by CLEO-c [466] both for the full Dalitz plots and in a restricted region $\pm 100\,\text{MeV}/c^2$ around the peak of the $K^*(892)^\pm$ resonance.

LHCb [465] has reported results of an analysis of $B^+ \to DK^+$ and $B^+ \to D\pi^+$ decays with $D \to K^0_S K^\pm \pi^\mp$. The decays with different final states of the D meson are distinguished by the charge of the kaon from the decay of the D meson relative to the charge of the B meson, and are labelled "same sign" (SS) and "opposite sign" (OS). Six observables potentially sensitive to $\gamma \equiv \phi_3$ are measured: two ratios of rates for DK and $D\pi$ decays (one each for SS and OS) and four asymmetries (for DK and $D\pi$, SS and OS). This is done both for the full Dalitz plot of the D decay and for the $K^*(892)^\pm$-dominated region (with the same boundaries as used by CLEO-c). Note that there is a significant overlap of events between the two samples. The results, shown in Table 58 do not yet have sufficient precision to set significant constraints on $\gamma \equiv \phi_3$.

4.14.7 Combinations of results on rates and asymmetries in $B \to D^{(*)}K^{(*)}$ decays to obtain constraints on $\gamma \equiv \phi_3$

BABAR and LHCb have both produced constraints on $\gamma \equiv \phi_3$ from combinations of their results on $B^+ \to DK^+$ and related processes. The experiments use a frequentist procedure (there are some differences in the details of the techniques used).

- BABAR [467] use results from DK, D^*K and DK^* modes with GLW, ADS and GGSZ analyses, to obtain $\gamma = (69^{+17}_{-16})^\circ$.

Table 58 Results from model-independent Dalitz plot analysis of $B^+ \to DK^+$, $D \to K_S^0 K^\pm \pi^\mp$

Experiment	$\int \mathcal{L}\,dt$	R_{SS}	R_{OS}	$A_{SS,DK}$	$A_{OS,DK}$	$A_{SS,D\pi}$	$A_{OS,D\pi}$
$D \to K_S^0 K^\pm \pi^\mp$ (whole Dalitz plot)							
LHCb [465]	3 fb^{-1}	$0.092 \pm 0.009 \pm 0.004$	$0.066 \pm 0.009 \pm 0.002$	$0.040 \pm 0.091 \pm 0.018$	$0.233 \pm 0.129 \pm 0.024$	$-0.025 \pm 0.024 \pm 0.010$	$-0.052 \pm 0.029 \pm 0.017$
$D \to K^*(892)^\pm K^\mp$							
LHCb [465]	3 fb^{-1}	$0.084 \pm 0.011 \pm 0.003$	$0.056 \pm 0.013 \pm 0.002$	$0.026 \pm 0.109 \pm 0.029$	$0.336 \pm 0.208 \pm 0.026$	$-0.012 \pm 0.028 \pm 0.010$	$-0.054 \pm 0.043 \pm 0.017$

- LHCb [468] use results from the DK^+ mode with GLW, GLW-like, ADS, GGSZ ($K_S^0 h^+ h^-$) and GLS ($K_S^0 K^\pm \pi^\mp$) analyses, as well as DK^{*0} with GLW, ADS and GGSZ analyses, $DK^+\pi^-$ GLW Dalitz plot analysis, $DK^+\pi^-\pi^+$ with GLW and ADS analyses and $B_s^0 \to D_s^\mp K^\pm$ decays. The LHCb combination takes into account subleading effects due to charm mixing and CP violation [469]. The result is $\gamma = (72.2\,^{+6.8}_{-7.3})^\circ$.
- All the combinations use inputs determined from $\psi(3770) \to D^0\overline{D}^0$ data samples (and/or from the HFLAV Charm Physics subgroup global fits on charm mixing parameters; see Sect. 8.1) to constrain the hadronic parameters in the charm system.
- Constraints are also obtained on the hadronic parameters involved in the decays. A summary of these is given in Table 60.
- The CKMfitter [252] and UTFit [339] groups perform similar combinations of all available results to obtain combined constraints on $\gamma \equiv \phi_3$.

Independently from the constraints on $\gamma \equiv \phi_3$ obtained by the experiments, the results summarised in Sect. 4.14 are statistically combined to produce world average constraints on $\gamma \equiv \phi_3$ and the hadronic parameters involved. The combination is performed with the GammaCombo framework [470] and follows a frequentist procedure, similar to those used by the experiments [467,468,471].

The input measurements used in the combination are listed in Table 61. Individual measurements are used as inputs, rather than the averages presented in Sect. 4.14, in order to facilitate cross-checks and to ensure the most appropriate treatment of correlations. A combination based on our averages for each of the quantities measured by experiments gives consistent results.

All results from GLW and GLW-like analyses of $B^+ \to D^{(*)}K^{(*)+}$ modes, as listed in Tables 48 and 51, are used. All results from ADS analyses of $B^+ \to D^{(*)}K^{(*)+}$ as listed in Table 52 are also used. Regarding $B^0 \to DK^{*0}$ decays, the results of the $B^0 \to DK^+\pi^-$ GLW–Dalitz analysis (Table 50) are included, as are the LHCb results of the ADS analysis of $B^0 \to DK^{*0}$ (Table 54). Concerning results of GGSZ analyses of $B^+ \to D^{(*)}K^{(*)+}$ with $D \to K_S^0 h^+ h^-$, the model-dependent results, as listed in Table 55, are used for the BaBar and Belle experiments, whilst the model-independent results, as listed in Table 57, are used for LHCb. This choice is made in order to maintain consistency of the approach across experiments whilst maximising the size of the samples used to obtain inputs for the combination. For GGSZ analyses of $B^0 \to DK^{*0}$ with $D \to K_S^0 h^+ h^-$ the model-independent result from LHCb (given in Table 57) is used for consistency with the treatment of the LHCb $B^+ \to DK^+$ GGSZ result; the model-

Table 59 Summary of constraints on hadronic parameters from model-independent analyses of $B^+ \to DK^+$ and $B^0 \to DK^{*0}$, $D \to K_S^0 h^+ h^-$ ($h = \pi, K$) decays

	$r_B(DK^+)$	$\delta_B(DK^+)$
Belle	$0.145 \pm 0.030 \pm 0.010 \pm 0.011$	$(129.9 \pm 15.0 \pm 3.8 \pm 4.7)^\circ$
LHCb	$0.080\,^{+0.019}_{-0.021}$	$(134\,^{+14}_{-15})^\circ$
	$\bar{r}_B(DK^{*0})$	$\bar{\delta}_B(DK^{*0})$
Belle	<0.87 at 68% confidence level	
LHCb	0.56 ± 0.17	$(204\,^{+21}_{-20})^\circ$

Table 60 Summary of constraints on hadronic parameters obtained from global combinations of results in $B^+ \to D^{(*)}K^{(*)+}$ and $B^0 \to DK^{*0}$ decays

	$r_B(DK^+)$	$\delta_B(DK^+)$
BaBar	$0.092\,^{+0.013}_{-0.012}$	$(105\,^{+16}_{-17})^\circ$
LHCb	0.1019 ± 0.0056	$(142.6\,^{+5.7}_{-6.6})^\circ$
	$r_B(DK^{*0})$	$\delta_B(DK^{*0})$
LHCb	$0.218\,^{+0.045}_{-0.047}$	$(189\,^{+23}_{-20})^\circ$

independent result by Belle is also included. The result of the GLS analysis of $B^+ \to DK^+$ with $D \to K^{*\pm}K^\mp$ from LHCb (Table 58) are used. Finally, results from the time-dependent analysis of $B_s^0 \to D_s^\mp K^\pm$ from LHCb (Table 47) are used.

Several results with sensitivity to γ are not included in the combination. Results from time-dependent analyses of $B^0 \to D^{(*)\mp}\pi^\pm$ and $D^\mp\rho^\pm$ (Table 46) are not used as there are insufficient constraints on the associated hadronic parameters. Similarly, results from $B^0 \to D^\mp K_S^0\pi^\pm$ (Sect. 4.13.1) are not used. Results from the LHCb $B^0 \to DK^{*0}$ GLW analysis (Table 49) are not used because of the statistical overlap with the GLW–Dalitz analysis which is used instead. Limits on ADS parameters reported in Sect. 4.14.3 are not used. Results on $B^+ \to D\pi^+$ decays, given in Table 53, are not used since the small value of $r_B(D\pi^+)$ means these channels have less sensitivity to γ and are more vulnerable to biases due to subleading effects [468]. Results from the BaBar Dalitz plot analysis of $B^+ \to DK^+$ with $D \to \pi^+\pi^-\pi^0$ (given in Table 55) are not included due to their limited sensitivity. Results from the $B^+ \to DK^+$, $D \to K_S^0\pi^+\pi^-$ GGSZ model-dependent analysis by LHCb (given in Table 55), and of the model-independent analysis of the same decay by Belle (given in Table 57) are not included due to the statistical overlap with results from model-(in)dependent analyses of the same data.

Auxiliary inputs are used in the combination in order to constrain the D system parameters and subsequently improve the determination of $\gamma \equiv \phi_3$. These include the ratio of suppressed to favoured decay amplitudes and the strong phase difference for $D \to K^\pm\pi^\mp$ decays, taken from the HFLAV Charm Physics subgroup global fits (see Sect. 8). The amplitude ratios, strong phase differences and coherence factors of $D \to K^\pm\pi^\mp\pi^0$, $D \to K^\pm\pi^\mp\pi^+\pi^-$ and $D \to K_S^0K^\pm\pi^\pm$ decays are taken from CLEO-c and LHCb measurements [466,472,473]. The fraction of CP-even content for quasi-GLW $D \to \pi^+\pi^-\pi^+\pi^-$, $D \to K^+K^-\pi^0$ and $D \to \pi^+\pi^-\pi^0$ decays are taken from CLEO-c measurements [443]. Constraints required to relate the hadronic parameters of the $B^0 \to DK^{*0}$ GLW–Dalitz analysis to the effective hadronic parameters of the quasi-two-body approaches are taken from LHCb measurements [442]. Finally, the value of $-2\beta_s$ is taken from the HFLAV Lifetimes and Oscillations subgroup (see Sect. 3); this is required to obtain sensitivity to $\gamma \equiv \phi_3$ from the time-dependent analysis of $B_s^0 \to D_s^\mp K^\pm$ decays. A summary of the auxiliary constraints is given in Table 62.

The following reasonable, although imperfect, assumptions are made when performing the averages.

- CP violation in $D \to K^+K^-$ and $D \to \pi^+\pi^-$ decays is assumed to be zero. The results of Sect. 8 anyhow suggest such effects to be negligible.
- The combination is potentially sensitive to subleading effects from D^0–$\overline{D}^0$ mixing which is not accounted for [469,474,475]. The effect is expected to be small given that $r_B \gtrsim 0.1$ (for all included modes) whilst $r_D \approx 0.05$.
- All $B^+ \to DK^{*+}$ modes are treated as two-body decays. In other words any dilution caused by non-K^{*+} contributions in the selected regions of the $DK_S^0\pi^+$ or $DK^+\pi^0$ Dalitz plots is assumed to be negligible. As a check of this assumption, it was found that including a coherence factor for $B^+ \to DK^{*+}$ modes, $\kappa_B(DK^{*+}) = 0.9$, had negligible impact on the results.
- All of the inputs are assumed to be completely uncorrelated. Whilst this is true of the statistical uncertainties, it is not necessarily the case for systematic uncertainties. In particular, the model uncertainties for different model-dependent GGSZ analyses are fully correlated (when the same model is used) and similarly the model-independent GGSZ analyses have correlated systematic uncertainties originating from the knowledge of the strong phase variation across the Dalitz plot. The effect of including these correlations is estimated to be $<1^\circ$.

Table 61 List of measurements used in the γ combination

B decay	D decay	Method	Experiment	Refs.
$B^+ \to DK^+$	$D \to K^+K^-$, $D \to \pi^+\pi^-$, $D \to K_S^0\pi^0$, $D \to K_S^0\omega$, $D \to K_S^0\phi$	GLW	BaBar	[433]
$B^+ \to DK^+$	$D \to K^+K^-$, $D \to \pi^+\pi^-$, $D \to K_S^0\pi^0$, $D \to K_S^0\omega$, $D \to K_S^0\phi$	GLW	Belle	[434]
$B^+ \to DK^+$	$D \to K^+K^-$, $D \to \pi^+\pi^-$	GLW	CDF	[435]
$B^+ \to DK^+$	$D \to K^+K^-$, $D \to \pi^+\pi^-$	GLW	LHCb	[436]
$B^+ \to D^*K^+$ $D^* \to D\gamma\ (\pi^0)$	$D \to K^+K^-$, $D \to \pi^+\pi^-$, $D \to K_S^0\pi^0$, $D \to K_S^0\omega$, $D \to K_S^0\phi$	GLW	BaBar	[437]
$B^+ \to D^*K^+$ $D^* \to D\gamma\ (\pi^0)$	$D \to K^+K^-$, $D \to \pi^+\pi^-$, $D \to K_S^0\pi^0$, $D \to K_S^0\omega$, $D \to K_S^0\phi$	GLW	Belle	[434]
$B^+ \to DK^{*+}$	$D \to K^+K^-$, $D \to \pi^+\pi^-$, $D \to K_S^0\pi^0$, $D \to K_S^0\omega$, $D \to K_S^0\phi$	GLW	BaBar	[438]
$B^+ \to DK^{*+}$	$D \to K^+K^-$, $D \to \pi^+\pi^-$,	GLW	LHCb	[439]
$B^+ \to DK^+\pi^+\pi^-$	$D \to K^+K^-$, $D \to \pi^+\pi^-$	GLW	LHCb	[440]
$B^+ \to DK^+$	$D \to \pi^+\pi^-\pi^0$	GLW-like	BaBar	[322]
$B^+ \to DK^+$	$D \to h^+h^-\pi^0$	GLW-like	LHCb	[444]
$B^+ \to DK^+$	$D \to \pi^+\pi^-\pi^+\pi^-$	GLW-like	LHCb	[436]
$B^+ \to DK^+$	$D \to K^\pm\pi^\mp$	ADS	BaBar	[445]
$B^+ \to DK^+$	$D \to K^\pm\pi^\mp$	ADS	Belle	[446]
$B^+ \to DK^+$	$D \to K^\pm\pi^\mp$	ADS	CDF	[447]
$B^+ \to DK^+$	$D \to K^\pm\pi^\mp$	ADS	LHCb	[436]
$B^+ \to DK^+$	$D \to K^\pm\pi^\mp\pi^0$	ADS	BaBar	[448]
$B^+ \to DK^+$	$D \to K^\pm\pi^\mp\pi^0$	ADS	Belle	[449]
$B^+ \to DK^+$	$D \to K^\pm\pi^\mp\pi^0$	ADS	LHCb	[444]
$B^+ \to DK^+$	$D \to K^\pm\pi^\mp\pi^+\pi^-$	ADS	LHCb	[436]
$B^+ \to D^*K^+$ $D^* \to D\gamma$	$D \to K^\pm\pi^\mp$	ADS	BaBar	[445]
$B^+ \to D^*K^+$ $D^* \to D\pi^0$	$D \to K^\pm\pi^\mp$	ADS	BaBar	[445]
$B^+ \to DK^{*+}$	$D \to K^\pm\pi^\mp$	ADS	BaBar	[438]
$B^+ \to DK^{*+}$	$D \to K^\pm\pi^\mp$	ADS	LHCb	[439]
$B^+ \to DK^+\pi^+\pi^-$	$D \to K^\pm\pi^\mp$	ADS	LHCb	[440]
$B^+ \to DK^+$	$D \to K_S^0\pi^+\pi^-$	GGSZ MD	BaBar	[455]
$B^+ \to DK^+$	$D \to K_S^0\pi^+\pi^-$	GGSZ MD	Belle	[454]
$B^+ \to D^*K^+$ $D^* \to D\gamma\ (\pi^0)$	$D \to K_S^0\pi^+\pi^-$	GGSZ MD	BaBar	[455]
$B^+ \to D^*K^+$ $D^* \to D\gamma\ (\pi^0)$	$D \to K_S^0\pi^+\pi^-$	GGSZ MD	Belle	[454]
$B^+ \to DK^{*+}$	$D \to K_S^0\pi^+\pi^-$	GGSZ MD	BaBar	[455]
$B^+ \to DK^{*+}$	$D \to K_S^0\pi^+\pi^-$	GGSZ MD	Belle	[457]
$B^+ \to DK^+$	$D \to K_S^0\pi^+\pi^-$	GGSZ MI	LHCb	[462]
$B^+ \to DK^+$	$D \to K_S^0K^+\pi^-$	GLS	LHCb	[465]
$B^0 \to DK^{*0}$	$D \to K^\pm\pi^\mp$	ADS	LHCb	[441]
$B^0 \to DK^+\pi^-$	$D \to h^+h^-$	GLW–Dalitz	LHCb	[442]
$B^0 \to DK^{*0}$	$D \to K_S^0h^+h^-$	GGSZ MI	Belle	[463]
$B^0 \to DK^{*0}$	$D \to K_S^0h^+h^-$	GGSZ MI	LHCb	[464]
$B_s^0 \to D_s^\mp K^\pm$	$D_s^+ \to h^+h^-\pi^+$	TD	LHCb	[432]

Table 62 List of the auxiliary inputs used in the combinations

Decay	Parameters	Source	Refs.
$D \to K^{\pm}\pi^{\mp}$	$r_D^{K\pi}$, $\delta_D^{K\pi}$	HFLAV	Sect. 8
$D \to K^{\pm}\pi^{\mp}\pi^{+}\pi^{-}$	$\delta_D^{K3\pi}$, $\kappa_D^{K3\pi}$, $r_D^{K3\pi}$	CLEO+LHCb	[472]
$D \to \pi^{+}\pi^{-}\pi^{+}\pi^{-}$	$F_{+}(\pi^{+}\pi^{-}\pi^{+}\pi^{-})$	CLEO	[443]
$D \to K^{\pm}\pi^{\mp}\pi^{0}$	$\delta_D^{K2\pi}$, $\kappa_D^{K2\pi}$, $r_D^{K2\pi}$	CLEO+LHCb	[472]
$D \to h^{+}h^{-}\pi^{0}$	$F_{+}(\pi^{+}\pi^{-}\pi^{0})$, $F_{+}(K^{+}K^{-}\pi^{0})$	CLEO	[443]
$D \to K_S^0 K^{+}\pi^{-}$	$\delta_D^{K_SK\pi}$, $\kappa_D^{K_SK\pi}$, $r_D^{K_SK\pi}$	CLEO	[466]
	$r_D^{K_SK\pi}$	LHCb	[473]
$B^0 \to DK^{*0}$	$\kappa_B(DK^{*0})$, $\bar{R}_B^{DK^{*0}}$, $\bar{\Delta}_B^{DK^{*0}}$	LHCb	[442]
$B_s^0 \to D_s^{\mp}K^{\pm}$	ϕ_s	HFLAV	Sect. 3

Table 63 Averages values obtained for the hadronic parameters in $B \to D^{(*)}K^{(*)}$ decays

Parameter	Value
$r_B(DK^{+})$	0.104 ± 0.005
$r_B(D^{*}K^{+})$	0.12 ± 0.02
$r_B(DK^{*+})$	0.05 ± 0.03
$r_B(DK^{*0})$	0.55 ± 0.16
$\delta_B(DK^{+})$	$(137.7\,^{+5.1}_{-6.0})^{\circ}$
$\delta_B(D^{*}K^{+})$	$(311\,^{+13}_{-17})^{\circ}$
$\delta_B(DK^{*+})$	$(108\,^{+33}_{-74})^{\circ}$
$\delta_B(DK^{*0})$	$(203\,^{+22}_{-20})^{\circ}$

Table 64 Averages of $\gamma \equiv \phi_3$ split by B meson decay mode

Decay mode	Value
$B_s^0 \to D_s^{\mp}K^{\pm}$	$(128\,^{+18}_{-22})^{\circ}$
$B^{+} \to DK^{*+}$	$(33\,^{+30}_{-20})^{\circ}$
$B^{+} \to D^{*}K^{+}$	$(64\,^{+18}_{-19})^{\circ}$
$B^{0} \to DK^{*0}$	$(92\,^{+23}_{-21})^{\circ}$
$B^{+} \to DK^{+}$	$(72.2\,^{+5.9}_{-7.0})^{\circ}$

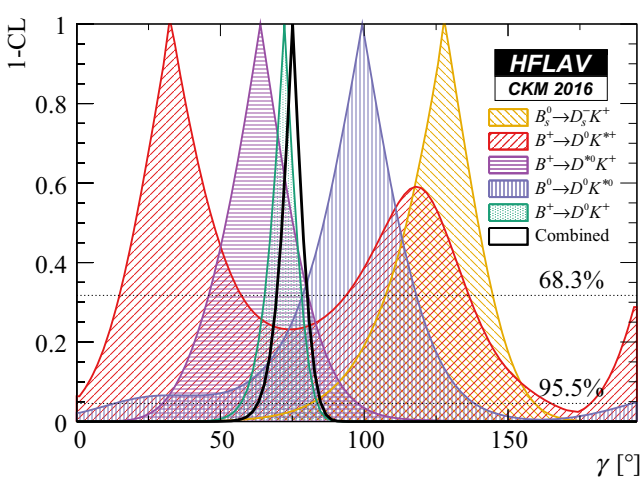

Fig. 45 World average of $\gamma \equiv \phi_3$, in terms of 1−CL, split by decay mode

Table 65 Averages of $\gamma \equiv \phi_3$ split by method. For GLW method only the solution nearest the combined average is shown

Method	Value
GLW	$(82.7\,^{+5.5}_{-6.9})^{\circ}$
ADS	$(72\,^{+12}_{-18})^{\circ}$
GGSZ	$(67.3\,^{+8.1}_{-7.8})^{\circ}$

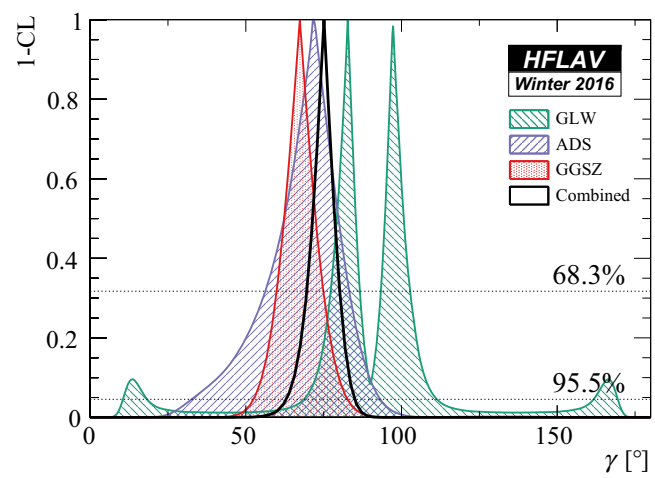

Fig. 46 World average of $\gamma \equiv \phi_3$, in terms of 1−CL, split by analysis method

In total, there are 116 observables and 33 free parameters. The combination has a χ^2 value of 95.5, which corresponds to a global p-value of 0.164. The obtained world average for the Unitarity Triangle angle $\gamma \equiv \phi_3$ is

$$\gamma \equiv \phi_3 = (74.0\,^{+5.8}_{-6.4})^{\circ}. \tag{166}$$

An ambiguous solution at $\gamma \equiv \phi_3 \longrightarrow \gamma \equiv \phi_3 + \pi$ also exists. The results for the hadronic parameters are listed in Table 63. Results for input analyses as split by B meson decay mode are shown in Table 64 and Fig. 45. Results for

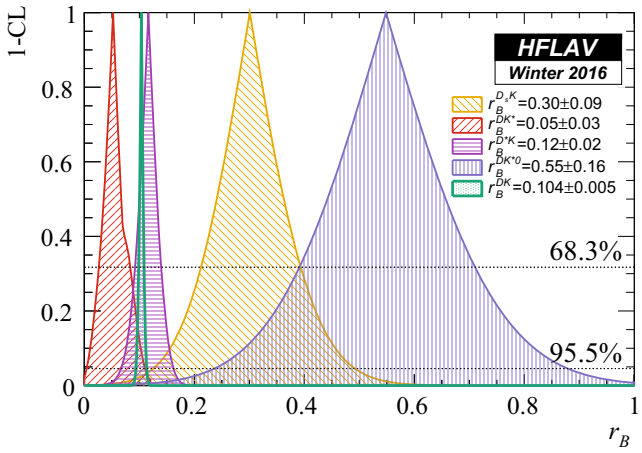

Fig. 47 World averages for the hadronic parameters r_B in the different decay modes, in terms of 1−CL

input analyses as split by the method are shown in Table 65 and Fig. 46. Results for the hadronic ratios, r_B, are shown in Fig. 47. A demonstration of how the various analyses contribute to the combination is shown in Fig. 48.

5 Semileptonic B decays

This section contains our averages for semileptonic B meson decays, i.e. decays of the type $B \to X\ell\nu_\ell$, where X refers to one or more hadrons, ℓ to a charged lepton and ν_ℓ to its associated neutrino. Unless otherwise stated, ℓ stands for an electron *or* a muon, lepton universality is assumed, and both charge conjugate states are combined. Some averages assume isospin symmetry, this will be explicitly mentioned at every instance.

Averages are presented separately for CKM favored $b \to c$ quark transitions and CKM suppressed $b \to u$ transitions. Among these transitions we distinguish *exclusive* decays involving a specific meson ($X = D, D^*, \pi, \rho, \ldots$) from *inclusive* decay modes, i.e. the sum over all possible hadronic states, one or more mesons and baryons. Semileptonic decays proceed via first order weak interactions and are well described in the framework of the standard model (SM). Their decay rates are sensitive to the magnitude squared of the CKM elements V_{cb} and V_{ub}, and their determination is one of the primary goals for the study of these decays. Semileptonic

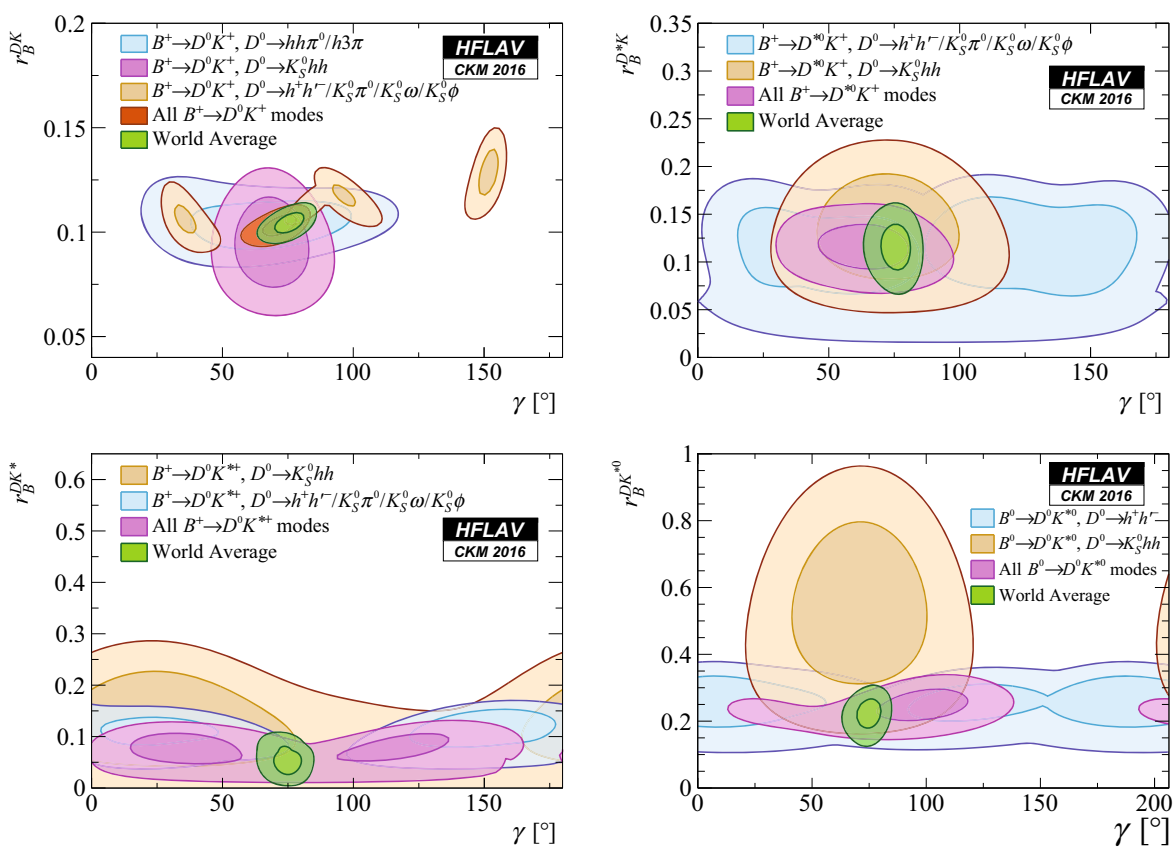

Fig. 48 Contributions to the combination from different input measurements, shown in the plane of the relevant r_B parameter *vs.* $\gamma \equiv \phi_3$. From *left to right*, *top to bottom*: $B^+ \to DK^+$, $B^+ \to D^*K^+$, $B^+ \to DK^{*+}$ and $B^0 \to DK^{*0}$. Contours show the two-dimensional 68 % and 95 % CL regions

decays involving the τ lepton might be sensitive to beyond SM processes because of the high τ mass, which might result in enhanced couplings to a hypothetical charged Higgs boson or leptoquarks.

The technique for obtaining the averages follows the general HFLAV procedure (Sect. 2) unless otherwise stated. More information on the averages, in particular on the common input parameters is available on the HFLAV semileptonic webpage.

5.1 Exclusive CKM-favoured decays

5.1.1 $\bar{B} \to D^* \ell^- \bar{\nu}_\ell$

The recoil variable w used to describe $\bar{B} \to D^* \ell^- \bar{\nu}_\ell$ decays is the product of the four-velocities of the initial and final state mesons, $w = v_B \cdot v_{D^{(*)}}$. The differential decay rate for massless fermions as a function of w is given by (see, e.g., [476])

$$\frac{d\Gamma(\bar{B} \to D^* \ell^- \bar{\nu}_\ell)}{dw} = \frac{G_F^2 m_{D^*}^3}{48\pi^3}(m_B - m_{D^*})^2 \times \chi(w)\eta_{EW}^2 \mathcal{F}^2(w)|V_{cb}|^2, \quad (167)$$

where G_F is Fermi's constant, m_B and m_{D^*} are the B and D^* meson masses, $\chi(w)$ is a known expression of w and η_{EW} is a small electroweak correction [477]. Some authors also include a long-distance EM radiation effect (Coulomb correction) in this factor. The form factor $\mathcal{F}(w)$ for the $\bar{B} \to D^* \ell^- \bar{\nu}_\ell$ decay contains three independent functions, $h_{A_1}(w)$, $R_1(w)$ and $R_2(w)$,

$$\chi(w)\mathcal{F}^2(w) = h_{A_1}^2(w)\sqrt{w^2-1}(w+1)^2 \times \left\{ 2\left[\frac{1-2wr+r^2}{(1-r)^2}\right]\left[1 + R_1^2(w)\frac{w^2-1}{w+1}\right] + \left[1 + (1-R_2(w))\frac{w-1}{1-r}\right]^2 \right\}, \quad (168)$$

where $r = m_{D^*}/m_B$.

To extract $|V_{cb}|$, the experimental analyses we consider in this section use the parametrization of these form factor functions by Caprini, Lellouch and Neubert (CLN) [478],

$$h_{A_1}(w) = h_{A_1}(1)\left[1 - 8\rho^2 z + (53\rho^2 - 15)z^2 - (231\rho^2 - 91)z^3\right], \quad (169)$$

$$R_1(w) = R_1(1) - 0.12(w-1) + 0.05(w-1)^2, \quad (170)$$

$$R_2(w) = R_2(1) + 0.11(w-1) - 0.06(w-1)^2, \quad (171)$$

where $z = (\sqrt{w+1} - \sqrt{2})/(\sqrt{w+1} + \sqrt{2})$. The form factor $\mathcal{F}(w)$ is thus described by the slope ρ^2 and the ratios $R_1(1)$ and $R_2(1)$.

We use the measurements of these form factor parameters shown in Table 66 and rescale them to the latest values of the input parameters (mainly branching fractions of charmed mesons) [479]. Most of the measurements in Table 66 are based on the decay $\bar{B}^0 \to D^{*+}\ell^-\bar{\nu}_\ell$. Some measurements [480,481] are sensitive also to the $B^- \to D^{*0}\ell^-\bar{\nu}_\ell$, and one measurement [482] is based on the decay $B^- \to D^{*0}\ell^-\bar{\nu}_\ell$. Isospin symmetry is assumed in this average. The earlier results for the LEP experiments and CLEO have significantly rescaled results, and significantly larger uncertainties than the recent measurements by the B-factories Belle and BaBar.

In the next step, we perform a four parameter fit of $\eta_{EW}\mathcal{F}(1)|V_{cb}|$, ρ^2, $R_1(1)$ and $R_2(1)$ to the rescaled measurements, taking into account correlated statistical and systematic uncertainties. Only two measurements constrain all four parameters [483,484], the remaining measurements determine only the normalization $\eta_{EW}\mathcal{F}(1)|V_{cb}|$ and the slope ρ^2. The result of the fit is

$$\eta_{EW}\mathcal{F}(1)|V_{cb}| = (35.61 \pm 0.43) \times 10^{-3}, \quad (172)$$

$$\rho^2 = 1.205 \pm 0.026, \quad (173)$$

$$R_1(1) = 1.404 \pm 0.032, \quad (174)$$

$$R_2(1) = 0.854 \pm 0.020, \quad (175)$$

and the correlation coefficients are

$$\rho_{\eta_{EW}\mathcal{F}(1)|V_{cb}|,\rho^2} = 0.338, \quad (176)$$

$$\rho_{\eta_{EW}\mathcal{F}(1)|V_{cb}|,R_1(1)} = -0.104, \quad (177)$$

$$\rho_{\eta_{EW}\mathcal{F}(1)|V_{cb}|,R_2(1)} = -0.071, \quad (178)$$

$$\rho_{\rho^2,R_1(1)} = 0.570, \quad (179)$$

$$\rho_{\rho^2,R_2(1)} = -0.810, \quad (180)$$

$$\rho_{R_1(1),R_2(1)} = -0.758. \quad (181)$$

The uncertainties and correlations quoted here include both statistical and systematic contributions. The χ^2 of the fit is 30.2 for 23 degrees of freedom, which corresponds to a confidence level of 14.4%. An illustration of this fit result is given in Fig. 49.

Using the latest update from the Fermilab Lattice and MILC Collaborations [489], the form factor normalization $\eta_{EW}\mathcal{F}(1)$ is

$$\eta_{EW}\mathcal{F}(1) = 0.912 \pm 0.014, \quad (182)$$

where $\eta_{EW} = 1.0066 \pm 0.0050$ has been used. The central value of this number corresponds to the electroweak correc-

Table 66 Measurements of the Caprini, Lellouch and Neubert (CLN) [478] form factor parameters in $\bar{B} \to D^* \ell^- \bar{\nu}_\ell$ before and after rescaling. Most analyses (except [483,484]) measure only $\eta_{\rm EW}\mathcal{F}(1)|V_{cb}|$, and ρ^2, so only these two parameters are shown here

Experiment	$\eta_{\rm EW}\mathcal{F}(1)\|V_{cb}\|[10^{-3}]$ (rescaled) $\eta_{\rm EW}\mathcal{F}(1)\|V_{cb}\|[10^{-3}]$ (published)	ρ^2 (rescaled) ρ^2 (published)
ALEPH [485]	$30.97 \pm 1.78_{\rm stat} \pm 1.29_{\rm syst}$	$0.491 \pm 0.227_{\rm stat} \pm 0.146_{\rm syst}$
	$31.9 \pm 1.8_{\rm stat} \pm 1.9_{\rm syst}$	$0.37 \pm 0.26_{\rm stat} \pm 0.14_{\rm syst}$
CLEO [480]	$39.67 \pm 1.22_{\rm stat} \pm 1.62_{\rm syst}$	$1.366 \pm 0.085_{\rm stat} \pm 0.087_{\rm syst}$
	$43.1 \pm 1.3_{\rm stat} \pm 1.8_{\rm syst}$	$1.61 \pm 0.09_{\rm stat} \pm 0.21_{\rm syst}$
OPAL excl [486]	$35.81 \pm 1.57_{\rm stat} \pm 1.62_{\rm syst}$	$1.205 \pm 0.207_{\rm stat} \pm 0.153_{\rm syst}$
	$36.8 \pm 1.6_{\rm stat} \pm 2.0_{\rm syst}$	$1.31 \pm 0.21_{\rm stat} \pm 0.16_{\rm syst}$
OPAL partial reco [486]	$36.98 \pm 1.19_{\rm stat} \pm 2.32_{\rm syst}$	$1.149 \pm 0.145_{\rm stat} \pm 0.296_{\rm syst}$
	$37.5 \pm 1.2_{\rm stat} \pm 2.5_{\rm syst}$	$1.12 \pm 0.14_{\rm stat} \pm 0.29_{\rm syst}$
DELPHI partial reco [487]	$35.15 \pm 1.39_{\rm stat} \pm 2.30_{\rm syst}$	$1.168 \pm 0.126_{\rm stat} \pm 0.381_{\rm syst}$
	$35.5 \pm 1.4_{\rm stat}\ ^{+2.3}_{-2.4}{}_{\rm syst}$	$1.34 \pm 0.14_{\rm stat}\ ^{+0.24}_{-0.22}{}_{\rm syst}$
DELPHI excl [488]	$35.85 \pm 1.68_{\rm stat} \pm 1.98_{\rm syst}$	$1.084 \pm 0.143_{\rm stat} \pm 0.151_{\rm syst}$
	$39.2 \pm 1.8_{\rm stat} \pm 2.3_{\rm syst}$	$1.32 \pm 0.15_{\rm stat} \pm 0.33_{\rm syst}$
Belle [483]	$34.39 \pm 0.17_{\rm stat} \pm 1.01_{\rm syst}$	$1.213 \pm 0.034_{\rm stat} \pm 0.008_{\rm syst}$
	$34.6 \pm 0.2_{\rm stat} \pm 1.0_{\rm syst}$	$1.214 \pm 0.034_{\rm stat} \pm 0.009_{\rm syst}$
BaBar excl [484]	$33.59 \pm 0.29_{\rm stat} \pm 1.03_{\rm syst}$	$1.184 \pm 0.048_{\rm stat} \pm 0.029_{\rm syst}$
	$34.7 \pm 0.3_{\rm stat} \pm 1.1_{\rm syst}$	$1.18 \pm 0.05_{\rm stat} \pm 0.03_{\rm syst}$
BaBar D^{*0} [482]	$34.96 \pm 0.58_{\rm stat} \pm 1.32_{\rm syst}$	$1.126 \pm 0.058_{\rm stat} \pm 0.055_{\rm syst}$
	$35.9 \pm 0.6_{\rm stat} \pm 1.4_{\rm syst}$	$1.16 \pm 0.06_{\rm stat} \pm 0.08_{\rm syst}$
BaBar global fit [481]	$35.49 \pm 0.20_{\rm stat} \pm 1.09_{\rm syst}$	$1.185 \pm 0.020_{\rm stat} \pm 0.061_{\rm syst}$
	$35.7 \pm 0.2_{\rm stat} \pm 1.2_{\rm syst}$	$1.21 \pm 0.02_{\rm stat} \pm 0.07_{\rm syst}$
Average	$35.61 \pm 0.11_{\rm stat} \pm 0.41_{\rm syst}$	$1.205 \pm 0.015_{\rm stat} \pm 0.021_{\rm syst}$

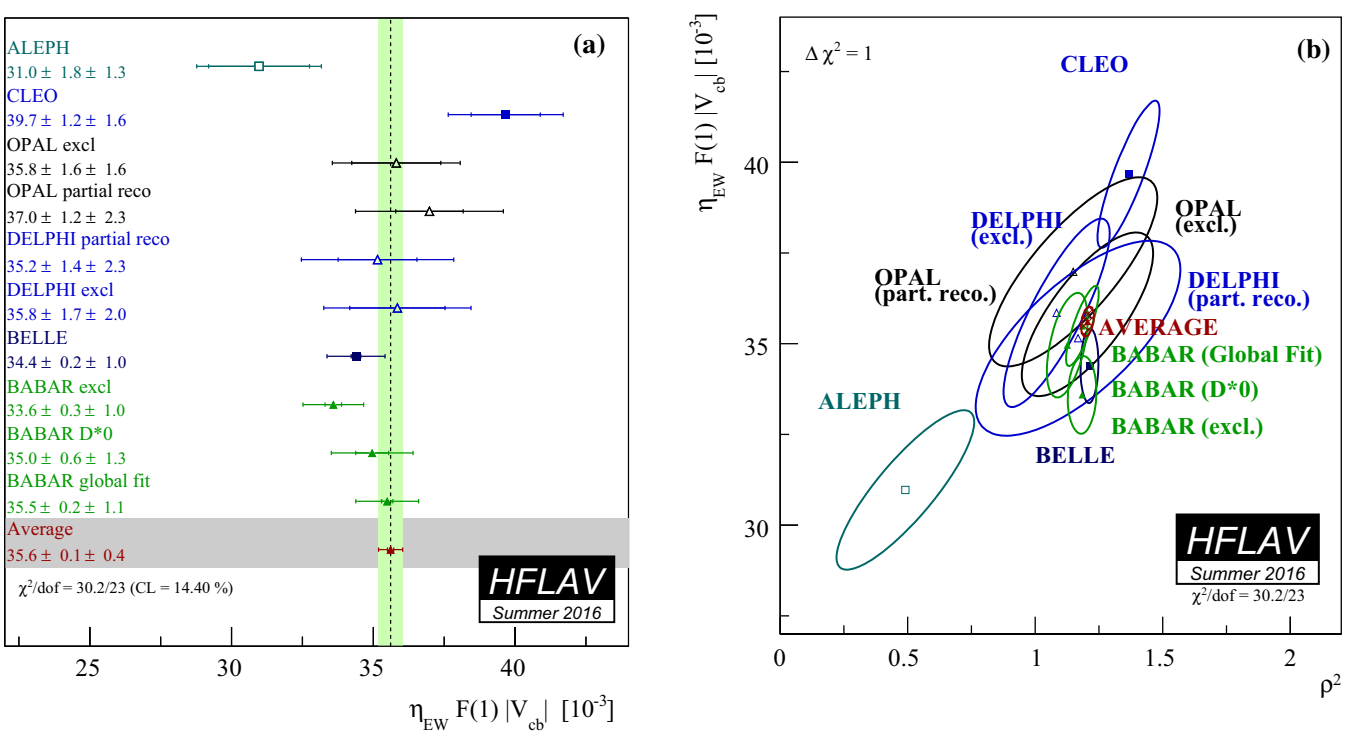

Fig. 49 Illustration of **a** the average and **b** the dependence of $\eta_{\rm EW}\mathcal{F}(1)|V_{cb}|$ on ρ^2. The error ellipses correspond to $\Delta\chi^2 = 1$ (CL = 39%)

Table 67 $\overline{B}^0 \to D^{*+}\ell^-\overline{\nu}_\ell$ branching fractions calculated from the rescaled CLN parameters in Table 66. For Ref. [482] the published value of $\mathcal{B}(B^- \to D^{*0}\ell^-\bar{\nu}_\ell)$ has been rescaled by the factor $\tau(B^0)/\tau(B^+)$ for comparison to the other measurements

Experiment	$\mathcal{B}(\overline{B}^0 \to D^{*+}\ell^-\overline{\nu}_\ell)$ [%] (calculated)	$\mathcal{B}(\overline{B}^0 \to D^{*+}\ell^-\overline{\nu}_\ell)$ [%] (published)
ALEPH [485]	$5.26 \pm 0.25_{\text{stat}} \pm 0.30_{\text{syst}}$	$5.53 \pm 0.26_{\text{stat}} \pm 0.52_{\text{syst}}$
CLEO [480]	$5.55 \pm 0.17_{\text{stat}} \pm 0.24_{\text{syst}}$	$6.09 \pm 0.19_{\text{stat}} \pm 0.40_{\text{syst}}$
OPAL excl [486]	$4.93 \pm 0.18_{\text{stat}} \pm 0.43_{\text{syst}}$	$5.11 \pm 0.19_{\text{stat}} \pm 0.49_{\text{syst}}$
OPAL partial reco [486]	$5.42 \pm 0.25_{\text{stat}} \pm 0.52_{\text{syst}}$	$5.92 \pm 0.27_{\text{stat}} \pm 0.68_{\text{syst}}$
DELPHI partial reco [487]	$4.85 \pm 0.13_{\text{stat}} \pm 0.72_{\text{syst}}$	$4.70 \pm 0.13_{\text{stat}}\ ^{+0.36}_{-0.31}\ _{\text{syst}}$
DELPHI excl [488]	$5.27 \pm 0.20_{\text{stat}} \pm 0.37_{\text{syst}}$	$5.90 \pm 0.22_{\text{stat}} \pm 0.50_{\text{syst}}$
Belle [483]	$4.51 \pm 0.03_{\text{stat}} \pm 0.26_{\text{syst}}$	$4.58 \pm 0.03_{\text{stat}} \pm 0.26_{\text{syst}}$
BaBar excl [484]	$4.45 \pm 0.04_{\text{stat}} \pm 0.26_{\text{syst}}$	$4.69 \pm 0.04_{\text{stat}} \pm 0.34_{\text{syst}}$
BaBar D^{*0} [482]	$4.90 \pm 0.07_{\text{stat}} \pm 0.34_{\text{syst}}$	$5.15 \pm 0.07_{\text{stat}} \pm 0.38_{\text{syst}}$
BaBar global fit [481]	$4.90 \pm 0.02_{\text{stat}} \pm 0.19_{\text{syst}}$	$5.00 \pm 0.02_{\text{stat}} \pm 0.19_{\text{syst}}$
Average	$4.88 \pm 0.01_{\text{stat}} \pm 0.10_{\text{syst}}$	$\chi^2/\text{dof} = 30.2/23$ (CL = 14.4%)

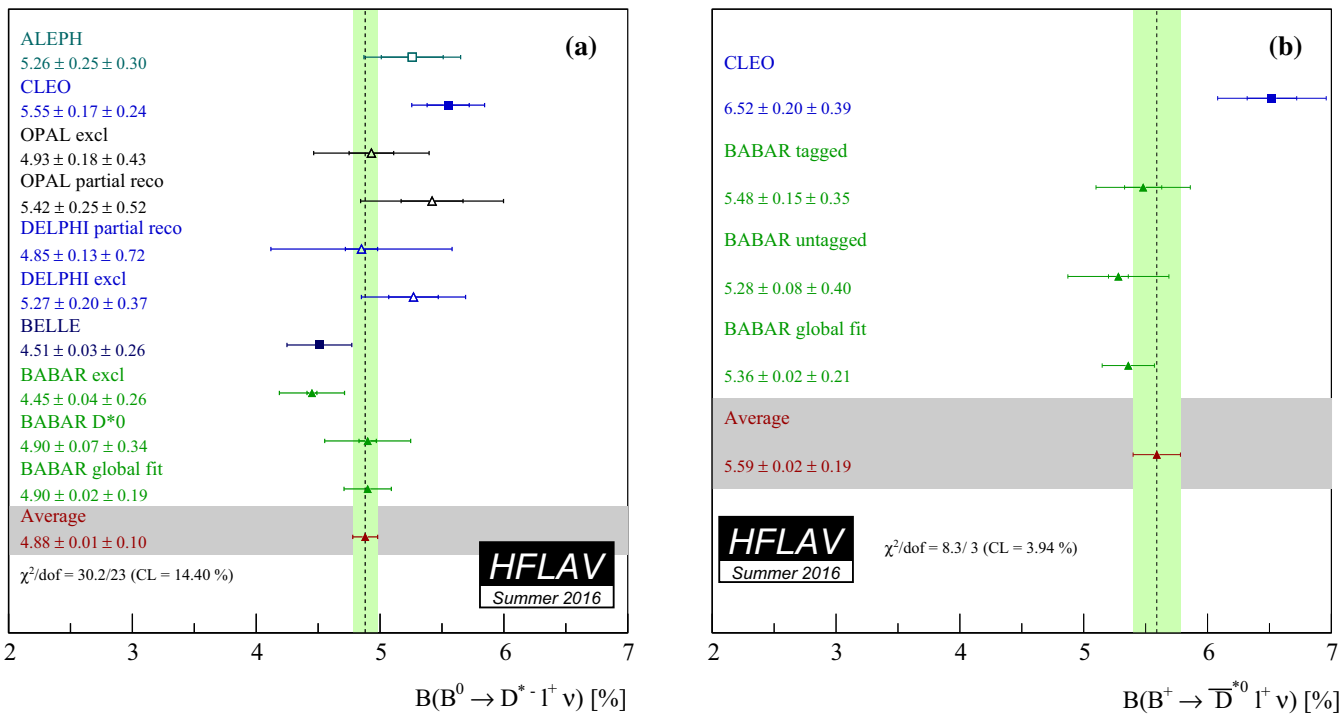

Fig. 50 Branching fractions of exclusive semileptonic B decays: **a** $\overline{B}^0 \to D^{*+}\ell^-\overline{\nu}_\ell$ (Table 67) and **b** $B^- \to D^{*0}\ell^-\bar{\nu}_\ell$ (Table 68)

tion only. The uncertainty has been increased to accommodate the Coulomb effect. Based on Eq. (172), this results in

$$|V_{cb}| = (39.05 \pm 0.47_{\text{exp}} \pm 0.58_{\text{th}}) \times 10^{-3}, \tag{183}$$

where the first uncertainty is experimental and the second error is theoretical (lattice QCD calculation and electro-weak correction).

From each rescaled measurements in Table 66, we calculate the $\bar{B} \to D^*\ell^-\bar{\nu}_\ell$ form factor $\eta_{\text{EW}}\mathcal{F}(w)$ and, by numerical integration, the branching ratio of the decay $\bar{B}^0 \to D^{*+}\ell^-\bar{\nu}_\ell$. For measurements that do not determine the parameters $R_1(1)$ and $R_2(1)$ we assume the average values given in Eqs. (174) and (175). The results are quoted in Table 67 and Fig. 50a. The branching ratio is

$$\mathcal{B}(\overline{B}^0 \to D^{*+}\ell^-\overline{\nu}_\ell) = (4.88 \pm 0.10)\%. \tag{184}$$

We have also performed a one-dimensional average of measurements of the decay $B^- \to D^{*0}\ell^-\bar{\nu}_\ell$, which is shown in Table 68 and Fig. 50b. The result of this average, $(5.59 \pm 0.02 \pm 0.19)\%$, is consistent with the average including both

Table 68 Average of the $B^- \to D^{*0}\ell^-\bar{\nu}_\ell$ branching fraction measurements

Experiment	$\mathcal{B}(B^- \to D^{*0}\ell^-\bar{\nu}_\ell)$ [%] (rescaled)	$\mathcal{B}(B^- \to D^{*0}\ell^-\bar{\nu}_\ell)$ [%] (published)
CLEO [480]	$6.52 \pm 0.20_{\text{stat}} \pm 0.39_{\text{syst}}$	$6.50 \pm 0.20_{\text{stat}} \pm 0.43_{\text{syst}}$
BABARtagged [490]	$5.48 \pm 0.15_{\text{stat}} \pm 0.35_{\text{syst}}$	$5.83 \pm 0.15_{\text{stat}} \pm 0.30_{\text{syst}}$
BABAR [482]	$5.28 \pm 0.08_{\text{stat}} \pm 0.40_{\text{syst}}$	$5.56 \pm 0.08_{\text{stat}} \pm 0.41_{\text{syst}}$
BABAR [481]	$5.36 \pm 0.02_{\text{stat}} \pm 0.21_{\text{syst}}$	$5.40 \pm 0.02_{\text{stat}} \pm 0.21_{\text{syst}}$
Average	$5.59 \pm 0.02_{\text{stat}} \pm 0.19_{\text{syst}}$	$\chi^2/\text{dof} = 8.3/3$ (CL = 3.94%)

charge states given in Eq. (184) rescaled by the lifetime ratio $\tau(B^+)/\tau(B^0)$, $(5.26 \pm 0.11)\%$.

5.1.2 $\bar{B} \to D\ell^-\bar{\nu}_\ell$

The differential decay rate for massless fermions as a function of w (introduced in the previous section) is given by (see, e.g., [476])

$$\frac{\bar{B} \to D\ell^-\bar{\nu}_\ell}{dw} = \frac{G_F^2 m_D^3}{48\pi^3}(m_B + m_D)^2(w^2-1)^{3/2} \times \eta_{EW}^2 \mathcal{G}^2(w)|V_{cb}|^2, \tag{185}$$

where G_F is Fermi's constant, and m_B and m_D are the B and D meson masses. Again, η_{EW} is the electroweak correction introduced in the previous section. In contrast to $\bar{B} \to D^*\ell^-\bar{\nu}_\ell$, $\mathcal{G}(w)$ contains a single form-factor function $f_+(w)$,

$$\mathcal{G}^2(w) = \frac{4r}{(1+r)^2} f_+^2(w), \tag{186}$$

where $r = m_D/m_B$.

As for $\bar{B} \to D^*\ell^-\bar{\nu}_\ell$ decays, we adopt the prescription by Caprini, Lellouch and Neubert [478], which describes the shape and normalization of the measured decay distributions in terms of two parameters: the normalization $\mathcal{G}(1)$ and the slope ρ^2,

$$\mathcal{G}(z) = \mathcal{G}(1)\big[1 - 8\rho^2 z + (51\rho^2 - 10)z^2 - (252\rho^2 - 84)z^3\big], \tag{187}$$

where $z = (\sqrt{w+1} - \sqrt{2})/(\sqrt{w+1} + \sqrt{2})$.

Table 69 shows experimental measurements of the two CLN parameters, which are corrected to match the latest values of the input parameters [479]. Both measurements of $\overline{B}^0 \to D^+\ell^-\overline{\nu}_\ell$ and $B^- \to D^0\ell^-\bar{\nu}_\ell$ are used and isospin symmetry is assumed in the analysis.

The form factor parameters are extracted by a two-parameter fit to the rescaled measurements of $\eta_{EW}\mathcal{G}(1)|V_{cb}|$ and ρ^2 taking into account correlated statistical and systematic uncertainties. The result of the fit is

$$\eta_{EW}\mathcal{G}(1)|V_{cb}| = (41.57 \pm 1.00) \times 10^{-3}, \tag{188}$$

$$\rho^2 = 1.128 \pm 0.033, \tag{189}$$

with a correlation of

$$\rho_{\eta_{EW}\mathcal{G}(1)|V_{cb}|,\rho^2} = 0.751. \tag{190}$$

The uncertainties and the correlation coefficient include both statistical and systematic contributions. The χ^2 of the fit is 4.7

Table 69 Measurements of the Caprini, Lellouch and Neubert (CLN) [478] form factor parameters in $\bar{B} \to D\ell^-\bar{\nu}_\ell$ before and after rescaling

Experiment	$\eta_{EW}\mathcal{G}(1)\lvert V_{cb}\rvert$ [10^{-3}] (rescaled) $\eta_{EW}\mathcal{G}(1)\lvert V_{cb}\rvert$ [10^{-3}] (published)	ρ^2 (rescaled) ρ^2 (published)
ALEPH [485]	$36.67 \pm 10.05_{\text{stat}} \pm 7.33_{\text{syst}}$	$0.845 \pm 0.879_{\text{stat}} \pm 0.448_{\text{syst}}$
	$31.1 \pm 9.9_{\text{stat}} \pm 8.6_{\text{syst}}$	$0.70 \pm 0.98_{\text{stat}} \pm 0.50_{\text{syst}}$
CLEO [491]	$44.18 \pm 5.70_{\text{stat}} \pm 3.47_{\text{syst}}$	$1.270 \pm 0.215_{\text{stat}} \pm 0.121_{\text{syst}}$
	$44.8 \pm 6.1_{\text{stat}} \pm 3.7_{\text{syst}}$	$1.30 \pm 0.27_{\text{stat}} \pm 0.14_{\text{syst}}$
Belle [492]	$41.94 \pm 0.60_{\text{stat}} \pm 1.21_{\text{syst}}$	$1.090 \pm 0.036_{\text{stat}} \pm 0.019_{\text{syst}}$
	42.29 ± 1.37	1.09 ± 0.05
BABAR global fit [481]	$42.23 \pm 0.74_{\text{stat}} \pm 2.14_{\text{syst}}$	$1.186 \pm 0.035_{\text{stat}} \pm 0.062_{\text{syst}}$
	$43.1 \pm 0.8_{\text{stat}} \pm 2.3_{\text{syst}}$	$1.20 \pm 0.04_{\text{stat}} \pm 0.07_{\text{syst}}$
BABAR tagged [493]	$42.60 \pm 1.71_{\text{stat}} \pm 1.26_{\text{syst}}$	$1.200 \pm 0.088_{\text{stat}} \pm 0.043_{\text{syst}}$
	$42.3 \pm 1.9_{\text{stat}} \pm 1.0_{\text{syst}}$	$1.20 \pm 0.09_{\text{stat}} \pm 0.04_{\text{syst}}$
Average	$41.57 \pm 0.45_{\text{stat}} \pm 0.89_{\text{syst}}$	$1.128 \pm 0.024_{\text{stat}} \pm 0.023_{\text{syst}}$

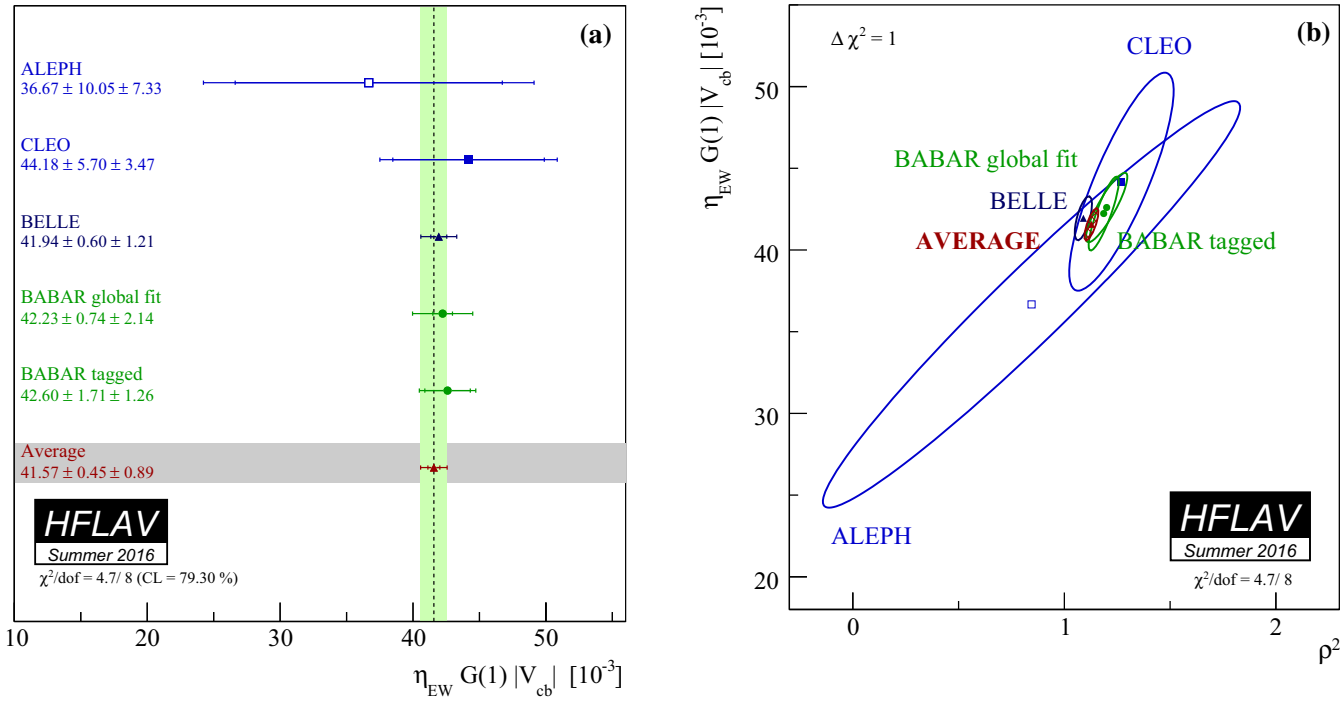

Fig. 51 Illustration of **a** the average and **b** dependence of $\eta_{\rm EW}\mathcal{G}(w)|V_{cb}|$ on ρ^2. The error ellipses correspond to $\Delta\chi^2 = 1$ (CL = 39%)

Table 70 $\bar{B}^0 \to D^+\ell^-\bar{\nu}_\ell$ branching fractions calculated from the rescaled CLN parameters in Table 69, which are based on both charged and neutral B decays, combined under the assumption of isospin symmetry

Experiment	$\mathcal{B}(\bar{B}^0 \to D^+\ell^-\bar{\nu}_\ell)$ [%] (calculated)	$\mathcal{B}(\bar{B}^0 \to D^+\ell^-\bar{\nu}_\ell)$ [%] (published)
ALEPH [485]	$2.09 \pm 0.15_{\rm stat} \pm 0.37_{\rm syst}$	$2.35 \pm 0.20_{\rm stat} \pm 0.44_{\rm syst}$
CLEO [491]	$2.12 \pm 0.23_{\rm stat} \pm 0.29_{\rm syst}$	$2.20 \pm 0.16_{\rm stat} \pm 0.19_{\rm syst}$
Belle [492]	$2.24 \pm 0.03_{\rm stat} \pm 0.11_{\rm syst}$	$2.31 \pm 0.03_{\rm stat} \pm 0.11_{\rm syst}$
BABAR global fit [481]	$2.09 \pm 0.03_{\rm stat} \pm 0.13_{\rm syst}$	$2.34 \pm 0.03_{\rm stat} \pm 0.13_{\rm syst}$
BABAR tagged [493]	$2.10 \pm 0.07_{\rm stat} \pm 0.08_{\rm syst}$	$2.23 \pm 0.11_{\rm stat} \pm 0.11_{\rm syst}$
Average	$2.13 \pm 0.02_{\rm stat} \pm 0.07_{\rm syst}$	$\chi^2/{\rm dof} = 4.7/8$ (CL = 79.3%)

for 8 degrees of freedom, which corresponds to a probability of 79.3%. An illustration of this fit result is given in Fig. 51.

The most recent lattice QCD result obtained for the form factor normalization is [494]

$$\mathcal{G}(1) = 1.0541 \pm 0.0083. \tag{191}$$

Using again $\eta_{\rm EW} = 1.0066 \pm 0.0050$, we determine $|V_{cb}|$ from Eq. (188),

$$|V_{cb}| = (39.18 \pm 0.94_{\rm exp} \pm 0.36_{\rm th}) \times 10^{-3}, \tag{192}$$

where the first error is experimental and the second theoretical. This number is in excellent agreement with $|V_{cb}|$ obtained from $\bar{B} \to D^*\ell^-\bar{\nu}_\ell$ decays given in Eq. (183).

From each rescaled measurement in Table 69, we have calculated the $\bar{B} \to D\ell^-\bar{\nu}_\ell$ form factor $\mathcal{G}(w)$ and, by numerical integration, the branching ratio of the decay $\overline{B}^0 \to D^+\ell^-\overline{\nu}_\ell$. The results are quoted in Table 70 and illustrated in Fig. 52. The branching ratio for the average values of $\eta_{\rm EW}\mathcal{G}(1)|V_{cb}|$ and ρ^2 is

$$\mathcal{B}(\overline{B}^0 \to D^+\ell^-\overline{\nu}_\ell) = (2.13 \pm 0.07)\%. \tag{193}$$

We have also performed one-dimensional averages of measurements of $\overline{B}^0 \to D^+\ell^-\overline{\nu}_\ell$ and $B^- \to D^0\ell^-\bar{\nu}_\ell$ decays. The results are shown in Tables 71 and 72. The $\overline{B}^0 \to D^+\ell^-\overline{\nu}_\ell$ average, $(2.20 \pm 0.04 \pm 0.09)\%$, is consistent with the result in Eq. (193), $(2.13 \pm 0.07)\%$. The $B^- \to D^0\ell^-\bar{\nu}_\ell$ average, $(2.33 \pm 0.04 \pm 0.09)\%$, also compares well to the result in Eq. (193), rescaled by the lifetime ratio $\tau(B^+)/\tau(B^0)$, $(2.30 \pm 0.07)\%$.

5.1.3 $\bar{B} \to D^{(*)}\pi\ell^-\bar{\nu}_\ell$

The average inclusive branching fractions for $\bar{B} \to D^{(*)}\pi\ell^-\bar{\nu}_\ell$ decays, where no constraint is applied to the $D^{(*)}\pi$

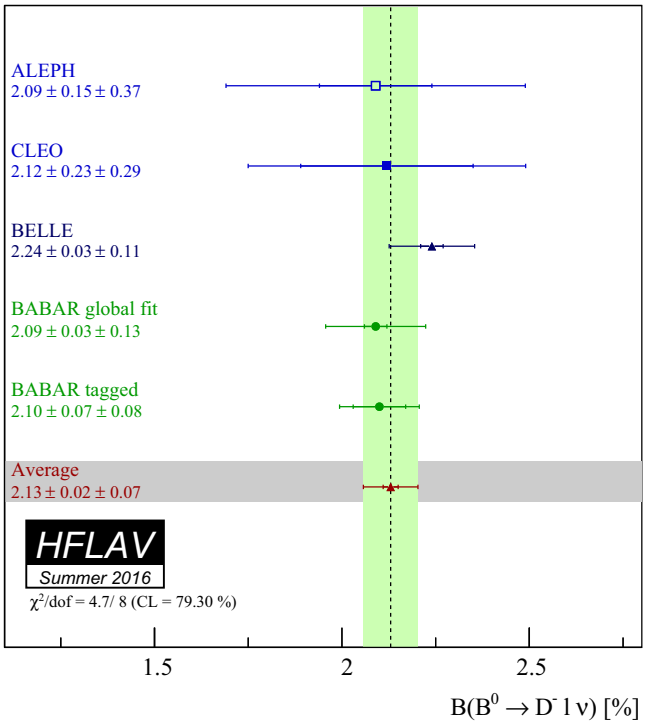

Fig. 52 Illustration of Table 70

system, are determined by the combination of the results provided in Table 73 for $\bar{B}^0 \to D^0\pi^+\ell^-\bar{\nu}_\ell$, $\bar{B}^0 \to D^{*0}\pi^+\ell^-\bar{\nu}_\ell$, $B^- \to D^+\pi^-\ell^-\bar{\nu}_\ell$, and $B^- \to D^{*+}\pi^-\ell^-\bar{\nu}_\ell$ decays. The measurements included in the average are scaled to a consistent set of input parameters and their uncertainties [479]. For both the BaBar and Belle results, the B semileptonic signal yields are extracted from a fit to the missing mass squared distribution for a sample of fully reconstructed $B\overline{B}$ events. Figure 53 shows the measurements and the resulting average for the four decay modes.

5.1.4 $\bar{B} \to D^{**}\ell^-\bar{\nu}_\ell$

D^{**} mesons contain one charm quark and one light antiquark with relative angular momentum $L = 1$. According to Heavy Quark Symmetry (HQS) [496], they form one doublet of states with angular momentum $j \equiv s_q + L = 3/2$ $\left[D_1(2420), D_2^*(2460)\right]$ and another doublet with $j = 1/2$ $\left[D_0^*(2400), D_1'(2430)\right]$, where s_q is the light quark spin. Parity and angular momentum conservation constrain the decays allowed for each state. The D_1 and D_2^* states decay via a D-wave to $D^*\pi$ and $D^{(*)}\pi$, respectively, and have small decay widths, while the D_0^* and D_1' states decay via an S-wave to $D\pi$ and $D^*\pi$ and are very broad. For the narrow states, the averages are determined by the combination of the results provided in Tables 74 and 75 for $\mathcal{B}(B^- \to D_1^0\ell^-\bar{\nu}_\ell) \times \mathcal{B}(D_1^0 \to D^{*+}\pi^-)$ and $\mathcal{B}(B^- \to D_2^0\ell^-\bar{\nu}_\ell) \times \mathcal{B}(D_2^0 \to D^{*+}\pi^-)$. For the broad states, the averages are determined by the combination of the results provided in Tables 76 and 77 for $\mathcal{B}(B^- \to D_1'^0\ell^-\bar{\nu}_\ell) \times \mathcal{B}(D_1'^0 \to D^{*+}\pi^-)$ and $\mathcal{B}(B^- \to D_0^{*0}\ell^-\bar{\nu}_\ell) \times \mathcal{B}(D_0^{*0} \to D^+\pi^-)$. The measurements are scaled to a consistent set of input parameters and their uncertainties [479].

For both the B-factory and the LEP and Tevatron results, the B semileptonic signal yields are extracted from a fit to the invariant mass distribution of the $D^{(*)+}\pi^-$ system. Apart for the CLEO, Belle and BaBar results, the other measurements are for the $\bar{B} \to D^{**}(D^*\pi^-)X\ell^-\bar{\nu}_\ell$ final state and we assume that no particles are left in the X system. The BaBar tagged $\bar{B} \to D_2^*\ell^-\bar{\nu}_\ell$ has been measured selecting $D_s^* \to D\pi$ final state and it has been translated in a result on $D_2^* \to D^*\pi$ decay mode, assuming $\mathcal{B}(D_2^* \to D\pi)/\mathcal{B}(D_2^* \to D^*\pi) = 1.54 \pm 0.15$ [327]. Figures 54 and 55 show the measurements and the resulting averages.

Table 71 Average of $\overline{B}^0 \to D^+\ell^-\overline{\nu}_\ell$ branching fraction measurements

Experiment	$\mathcal{B}(\overline{B}^0 \to D^+\ell^-\overline{\nu}_\ell)$ [%] (rescaled)	$\mathcal{B}(\overline{B}^0 \to D^+\ell^-\overline{\nu}_\ell)$ [%] (published)
ALEPH [485]	$2.14 \pm 0.18_{\text{stat}} \pm 0.36_{\text{syst}}$	$2.35 \pm 0.20_{\text{stat}} \pm 0.44_{\text{syst}}$
CLEO [491]	$2.09 \pm 0.13_{\text{stat}} \pm 0.16_{\text{syst}}$	$2.20 \pm 0.16_{\text{stat}} \pm 0.19_{\text{syst}}$
Belle [492]	$2.30 \pm 0.04_{\text{stat}} \pm 0.12_{\text{syst}}$	$2.39 \pm 0.04_{\text{stat}} \pm 0.11_{\text{syst}}$
BaBar [490]	$2.08 \pm 0.11_{\text{stat}} \pm 0.14_{\text{syst}}$	$2.21 \pm 0.11_{\text{stat}} \pm 0.12_{\text{syst}}$
Average	$2.20 \pm 0.04_{\text{stat}} \pm 0.09_{\text{syst}}$	$\chi^2/\text{dof} = 1.7/3$ (CL = 63.9%)

Table 72 Average of $B^- \to D^0\ell^-\bar{\nu}_\ell$ branching fraction measurements

Experiment	$\mathcal{B}(B^- \to D^0\ell^-\bar{\nu}_\ell)$ [%] (rescaled)	$\mathcal{B}(B^- \to D^0\ell^-\bar{\nu}_\ell)$ [%] (published)
CLEO [491]	$2.16 \pm 0.13_{\text{stat}} \pm 0.17_{\text{syst}}$	$2.32 \pm 0.17_{\text{stat}} \pm 0.20_{\text{syst}}$
BaBar [490]	$2.21 \pm 0.09_{\text{stat}} \pm 0.12_{\text{syst}}$	$2.33 \pm 0.09_{\text{stat}} \pm 0.09_{\text{syst}}$
Belle [492]	$2.48 \pm 0.04_{\text{stat}} \pm 0.12_{\text{syst}}$	$2.54 \pm 0.04_{\text{stat}} \pm 0.13_{\text{syst}}$
Average	$2.33 \pm 0.04_{\text{stat}} \pm 0.09_{\text{syst}}$	$\chi^2/\text{dof} = 2.8/2$ (CL = 25.2%)

Table 73 Averages of the $B \to D^{(*)}\pi^-\ell^-\bar{\nu}_\ell$ branching fractions and individual results

Experiment	$\mathcal{B}(B^- \to D^+\pi^-\ell^-\bar{\nu}_\ell)[\%]$ (rescaled)	$\mathcal{B}(B^- \to D^+\pi^-\ell^-\bar{\nu}_\ell)[\%]$ (published)
Belle [495]	$0.42 \pm 0.04_{\text{stat}} \pm 0.05_{\text{syst}}$	$0.40 \pm 0.04_{\text{stat}} \pm 0.06_{\text{syst}}$
BaBar [490]	$0.40 \pm 0.06_{\text{stat}} \pm 0.03_{\text{syst}}$	$0.42 \pm 0.06_{\text{stat}} \pm 0.03_{\text{syst}}$
Average	0.41 ± 0.04	$\chi^2/\text{dof} = 0.073$ (CL = 78.9%)
Experiment	$\mathcal{B}(B^- \to D^{*+}\pi^-\ell^-\bar{\nu}_\ell)[\%]$ (rescaled)	$\mathcal{B}(B^- \to D^{*+}\pi^-\ell^-\bar{\nu}_\ell)[\%]$ (published)
Belle [495]	$0.68 \pm 0.08_{\text{stat}} \pm 0.07_{\text{syst}}$	$0.64 \pm 0.08_{\text{stat}} \pm 0.09_{\text{syst}}$
BaBar [490]	$0.57 \pm 0.05_{\text{stat}} \pm 0.04_{\text{syst}}$	$0.59 \pm 0.05_{\text{stat}} \pm 0.04_{\text{syst}}$
Average	0.60 ± 0.06	$\chi^2/\text{dof}= 0.778$ (CL = 37.9%)
Experiment	$\mathcal{B}(\bar{B}^0 \to D^0\pi^+\ell^-\bar{\nu}_\ell)[\%]$ (rescaled)	$\mathcal{B}(\bar{B}^0 \to D^0\pi^+\ell^-\bar{\nu}_\ell)[\%]$ (published)
Belle [495]	$0.43 \pm 0.07_{\text{stat}} \pm 0.05_{\text{syst}}$	$0.42 \pm 0.07_{\text{stat}} \pm 0.06_{\text{syst}}$
BaBar [490]	$0.40 \pm 0.08_{\text{stat}} \pm 0.03_{\text{syst}}$	$0.43 \pm 0.08_{\text{stat}} \pm 0.03_{\text{syst}}$
Average	0.42 ± 0.06	$\chi^2/\text{dof}= 0.061$ (CL = 80.5%)
Experiment	$\mathcal{B}(\bar{B}^0 \to D^{*0}\pi^+\ell^-\bar{\nu}_\ell)[\%]$ (rescaled)	$\mathcal{B}(\bar{B}^0 \to D^{*0}\pi^+\ell^-\bar{\nu}_\ell)[\%]$ (published)
Belle [495]	$0.58 \pm 0.21_{\text{stat}} \pm 0.07_{\text{syst}}$	$0.56 \pm 0.21_{\text{stat}} \pm 0.08_{\text{syst}}$
BaBar [490]	$0.46 \pm 0.08_{\text{stat}} \pm 0.04_{\text{syst}}$	$0.48 \pm 0.08_{\text{stat}} \pm 0.04_{\text{syst}}$
Average	0.47 ± 0.08	$\chi^2/\text{dof}= 0.262$ (CL = 60.9%)

5.2 Inclusive CKM-favored decays

5.2.1 Global analysis of $\bar{B} \to X_c\ell^-\bar{\nu}_\ell$

The semileptonic decay width $\Gamma(\bar{B} \to X_c\ell^-\bar{\nu}_\ell)$ has been calculated in the framework of the operator production expansion (OPE) [55–57]. The result is a double-expansion in Λ_{QCD}/m_b and α_s, which depends on a number of non-perturbative parameters. These parameters describe the dynamics of the b-quark inside the B hadron and can be measured using observables in $\bar{B} \to X_c\ell^-\bar{\nu}_\ell$ decays, such as the moments of the lepton energy and the hadronic mass spectrum.

Two renormalization schemes are commonly used to defined the b-quark mass and other theoretical quantities: the kinetic [504–507] and the 1S [508] schemes. An independent set of theoretical expressions is available for each, with several non-perturbative parameters. The non-perturbative parameters in the kinetic scheme are: the quark masses m_b and m_c, μ_π^2 and μ_G^2 at $O(1/m_b^2)$, and ρ_D^3 and ρ_{LS}^3 at $O(1/m_b^3)$. In the 1S scheme, the parameters are: m_b, λ_1 at $O(1/m_b^2)$, and ρ_1, τ_1, τ_2 and τ_3 at $O(1/m_b^3)$. Note that the numerical values of the kinetic and 1S b-quark masses cannot be compared without converting one or the other, or both, to the same renormalization scheme.

We used two kinematic distributions for $\bar{B} \to X_c\ell^-\bar{\nu}_\ell$ decays, the hadron effective mass to derive moments $\langle M_X^n\rangle$ of order $n = 2, 4, 6$, and the charged lepton momentum to derive moments $\langle E_\ell^n\rangle$ of order $n = 0, 1, 2, 3$. Moments are determined for different values of E_{cut}, the lower limit on the minimum lepton momentum. The moments derived from the same distributions with different value of E_{cut} are highly correlated. The list of measurements is given in Table 78. The only input is the average lifetime τ_B of neutral and charged B mesons, taken to be (1.579 ± 0.004) ps (Sect. 3).

In the kinetic and 1S schemes, the moments in $\bar{B} \to X_c\ell^-\bar{\nu}_\ell$ are not sufficient to determine the b-quark mass precisely. In the kinetic scheme analysis we constrain the c-quark mass (defined in the $\overline{\text{MS}}$ scheme) to the value of Ref. [515],

$$m_c^{\overline{\text{MS}}}(3\text{ GeV}) = 0.986 \pm 0.013\text{ GeV}. \tag{194}$$

In the 1S scheme analysis, the b-quark mass is constrained by measurements of the photon energy moments in $B \to X_s\gamma$ [516–519].

5.2.2 Analysis in the kinetic scheme

The fit relies on the calculations of the lepton energy and hadron mass moments in $\bar{B} \to X_c\ell^-\bar{\nu}_\ell$ decays described in Refs. [506,507] and closely follows the procedure of Ref. [520]. The analysis determines $|V_{cb}|$ and the six non-perturbative parameters mentioned above.

The detailed fit result and the matrix of the correlation coefficients is given in Table 79. The fit to the lepton energy and hadronic mass moments is shown in Figs. 56 and 57, respectively. The result in terms of the main parameters is

$$|V_{cb}| = (42.19 \pm 0.78) \times 10^{-3}, \tag{195}$$

$$m_b^{\text{kin}} = 4.554 \pm 0.018\text{ GeV}, \tag{196}$$

$$\mu_\pi^2 = 0.464 \pm 0.076\text{ GeV}^2, \tag{197}$$

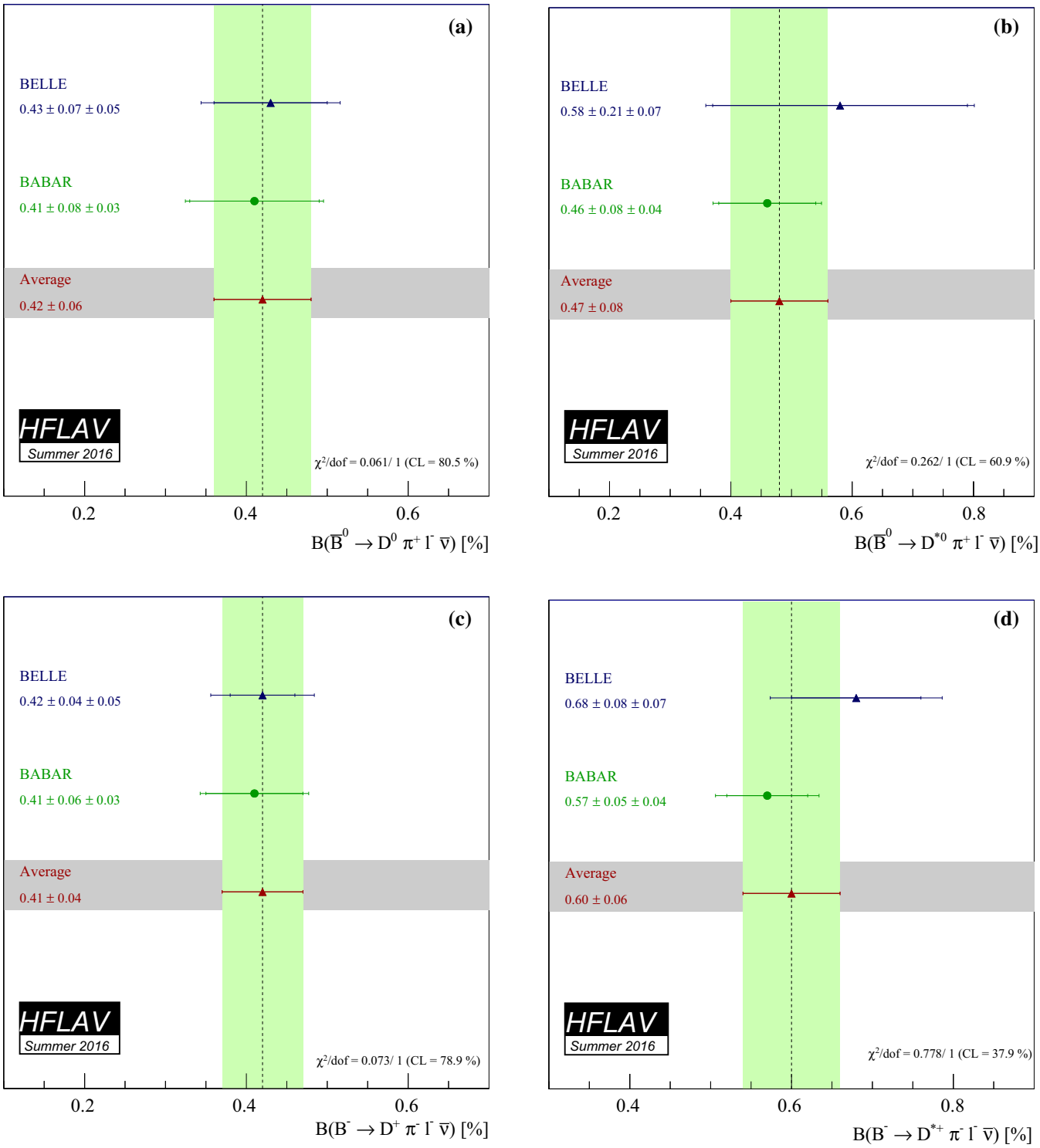

Fig. 53 Average branching fraction of exclusive semileptonic B decays **a** $\bar{B}^0 \to D^0\pi^+\ell^-\bar{\nu}_\ell$, **b** $\bar{B}^0 \to D^{*0}\pi^+\ell^-\bar{\nu}_\ell$, **c** $B^- \to D^+\pi^-\ell^-\bar{\nu}_\ell$, and **d** $B^- \to D^{*+}\pi^-\ell^-\bar{\nu}_\ell$. The corresponding individual results are also shown

with a χ^2 of 15.6 for 43 degrees of freedom. The scale μ of the quantities in the kinematic scheme is 1 GeV.

The inclusive $\bar{B} \to X_c\ell^-\bar{\nu}_\ell$ branching fraction determined by this analysis is

$$\mathcal{B}(\bar{B} \to X_c\ell^-\bar{\nu}_\ell) = (10.65 \pm 0.16)\%. \tag{198}$$

Including the rate of charmless semileptonic decays (Sect. 5.4), $\mathcal{B}(\bar{B} \to X_u\ell^-\bar{\nu}_\ell) = (2.13 \pm 0.31) \times 10^{-3}$, we obtain the semileptonic branching fraction,

$$\mathcal{B}(\bar{B} \to X\ell^-\bar{\nu}_\ell) = (10.86 \pm 0.16)\%. \tag{199}$$

Table 74 Published and rescaled individual measurements and their averages for of the branching fraction $\mathcal{B}(B^- \to D_1^0 \ell^- \bar{\nu}_\ell) \times \mathcal{B}(D_1^0 \to D^{*+}\pi^-)$

Experiment	$\mathcal{B}(B^- \to D_1^0(D^{*+}\pi^-)\ell^-\bar{\nu}_\ell)[\%]$ (rescaled)	$\mathcal{B}(B^- \to D_1^0(D^{*+}\pi^-)\ell^-\bar{\nu}_\ell)[\%]$ (published)
ALEPH [497]	$0.437 \pm 0.085_{\text{stat}} \pm 0.056_{\text{syst}}$	$0.47 \pm 0.10_{\text{stat}} \pm 0.07_{\text{syst}}$
OPAL [498]	$0.570 \pm 0.210_{\text{stat}} \pm 0.101_{\text{syst}}$	$0.70 \pm 0.21_{\text{stat}} \pm 0.10_{\text{syst}}$
CLEO [499]	$0.347 \pm 0.085_{\text{stat}} \pm 0.056_{\text{syst}}$	$0.373 \pm 0.085_{\text{stat}} \pm 0.057_{\text{syst}}$
D0 [500]	$0.214 \pm 0.018_{\text{stat}} \pm 0.035_{\text{syst}}$	$0.219 \pm 0.018_{\text{stat}} \pm 0.035_{\text{syst}}$
Belle Tagged B^- [495]	$0.443 \pm 0.070_{\text{stat}} \pm 0.059_{\text{syst}}$	$0.42 \pm 0.07_{\text{stat}} \pm 0.07_{\text{syst}}$
Belle Tagged B^0 [495]	$0.612 \pm 0.200_{\text{stat}} \pm 0.077_{\text{syst}}$	$0.42 \pm 0.07_{\text{stat}} \pm 0.07_{\text{syst}}$
BaBar Tagged [501]	$0.274 \pm 0.030_{\text{stat}} \pm 0.029_{\text{syst}}$	$0.29 \pm 0.03_{\text{stat}} \pm 0.03_{\text{syst}}$
BaBar Untagged B^- [502]	$0.290 \pm 0.017_{\text{stat}} \pm 0.016_{\text{syst}}$	$0.30 \pm 0.02_{\text{stat}} \pm 0.02_{\text{syst}}$
BaBar Untagged B^0 [502]	$0.294 \pm 0.026_{\text{stat}} \pm 0.027_{\text{syst}}$	$0.30 \pm 0.02_{\text{stat}} \pm 0.02_{\text{syst}}$
Average	$0.281 \pm 0.010 \pm 0.015$	$\chi^2/\text{dof} = 12.7/8$ (CL = 11.7%)

Table 75 Published and rescaled individual measurements and their averages for $\mathcal{B}(B^- \to D_2^0 \ell^- \bar{\nu}_\ell) \times \mathcal{B}(D_2^0 \to D^{*+}\pi^-)$

Experiment	$\mathcal{B}(B^- \to D_2^0(D^{*+}\pi^-)\ell^-\bar{\nu}_\ell)[\%]$ (rescaled)	$\mathcal{B}(B^- \to D_2^0(D^{*+}\pi^-)\ell^-\bar{\nu}_\ell)[\%]$ (published)
CLEO [499]	$0.055 \pm 0.066_{\text{stat}} \pm 0.011_{\text{syst}}$	$0.059 \pm 0.066_{\text{stat}} \pm 0.011_{\text{syst}}$
D0 [500]	$0.086 \pm 0.018_{\text{stat}} \pm 0.020_{\text{syst}}$	$0.088 \pm 0.018_{\text{stat}} \pm 0.020_{\text{syst}}$
Belle [495]	$0.190 \pm 0.060_{\text{stat}} \pm 0.025_{\text{syst}}$	$0.18 \pm 0.06_{\text{stat}} \pm 0.03_{\text{syst}}$
BaBar tagged [501]	$0.075 \pm 0.013_{\text{stat}} \pm 0.009_{\text{syst}}$	$0.078 \pm 0.013_{\text{stat}} \pm 0.010_{\text{syst}}$
BaBar untagged B^- [502]	$0.087 \pm 0.009_{\text{stat}} \pm 0.007_{\text{syst}}$	$0.087 \pm 0.013_{\text{stat}} \pm 0.007_{\text{syst}}$
BaBar untagged B^0 [502]	$0.065 \pm 0.010_{\text{stat}} \pm 0.004_{\text{syst}}$	$0.087 \pm 0.013_{\text{stat}} \pm 0.007_{\text{syst}}$
Average	$0.077 \pm 0.006 \pm 0.004$	$\chi^2/\text{dof} = 5.3/5$ (CL = 37.7%)

Table 76 Published and rescaled individual measurements and their averages for $\mathcal{B}(B^- \to D_1^{'0} \ell^- \bar{\nu}_\ell) \times \mathcal{B}(D_1^{'0} \to D^{*+}\pi^-)$

Experiment	$\mathcal{B}(B^- \to D_1^{'0}(D^{*+}\pi^-)\ell^-\bar{\nu}_\ell)[\%]$ (rescaled)	$\mathcal{B}(B^- \to D_1^{'0}(D^{*+}\pi^-)\ell^-\bar{\nu}_\ell)[\%]$ (published)
DELPHI [503]	$0.71 \pm 0.17_{\text{stat}} \pm 0.18_{\text{syst}}$	$0.83 \pm 0.17_{\text{stat}} \pm 0.18_{\text{syst}}$
Belle [495]	$-0.03 \pm 0.06_{\text{stat}} \pm 0.07_{\text{syst}}$	$-0.03 \pm 0.06_{\text{stat}} \pm 0.07_{\text{syst}}$
BaBar [501]	$0.26 \pm 0.04_{\text{stat}} \pm 0.04_{\text{syst}}$	$0.27 \pm 0.04_{\text{stat}} \pm 0.05_{\text{syst}}$
Average	$0.13 \pm 0.03 \pm 0.02$	$\chi^2/\text{dof} = 18./2$ (CL = 0.0001%)

Table 77 Published and rescaled individual measurements and their averages for $\mathcal{B}(B^- \to D_0^{*0} \ell^- \bar{\nu}_\ell) \times \mathcal{B}(D_0^{*0} \to D^+\pi^-)$

Experiment	$\mathcal{B}(B^- \to D_0^{*0}(D^+\pi^-)\ell^-\bar{\nu}_\ell)[\%]$ (rescaled)	$\mathcal{B}(B^- \to D_0^{*0}(D^+\pi^-)\ell^-\bar{\nu}_\ell)[\%]$ (published)
Belle Tagged B^- [495]	$0.25 \pm 0.04_{\text{stat}} \pm 0.06_{\text{syst}}$	$0.24 \pm 0.04_{\text{stat}} \pm 0.06_{\text{syst}}$
Belle Tagged B^0 [495]	$0.23 \pm 0.08_{\text{stat}} \pm 0.06_{\text{syst}}$	$0.24 \pm 0.04_{\text{stat}} \pm 0.06_{\text{syst}}$
BaBar Tagged [501]	$0.31 \pm 0.04_{\text{stat}} \pm 0.05_{\text{syst}}$	$0.26 \pm 0.05_{\text{stat}} \pm 0.04_{\text{syst}}$
Average	$0.28 \pm 0.03 \pm 0.04$	$\chi^2/\text{dof} = 0.49/2$ (CL = 78.0%)

5.2.3 Analysis in the 1S scheme

The fit relies on the same set of moment measurements and the calculations of the spectral moments described in Ref. [508]. The theoretical uncertainties are estimated as explained in Ref. [521]. Only trivial theory correlations, i.e. between the same moment at the same threshold are included in the analysis. The fit determines $|V_{cb}|$ and the six non-perturbative parameters mentioned above.

The detailed result of the fit using the $B \to X_s\gamma$ constraint is given in Table 80. The result in terms of the main parameters is

$$|V_{cb}| = (41.98 \pm 0.45) \times 10^{-3}, \tag{200}$$

$$m_b^{1S} = 4.691 \pm 0.037 \text{ GeV}, \tag{201}$$

$$\lambda_1 = -0.362 \pm 0.067 \text{ GeV}^2, \tag{202}$$

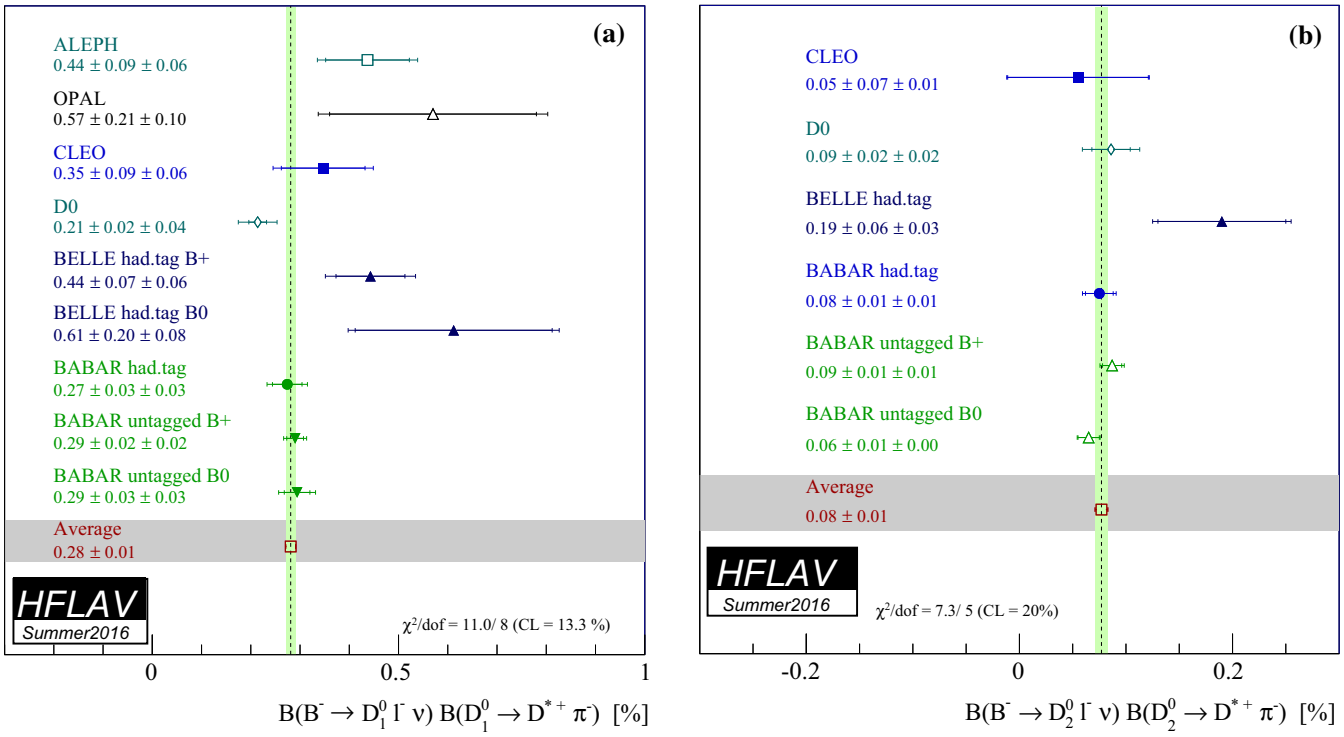

Fig. 54 Rescaled individual measurements and their averages for **a** $\mathcal{B}(B^- \to D_1^0 \ell^- \bar{\nu}_\ell) \times \mathcal{B}(D_1^0 \to D^{*+}\pi^-)$ and **b** $\mathcal{B}(B^- \to D_2^0 \ell^- \bar{\nu}_\ell) \times \mathcal{B}(D_2^0 \to D^{*+}\pi^-)$

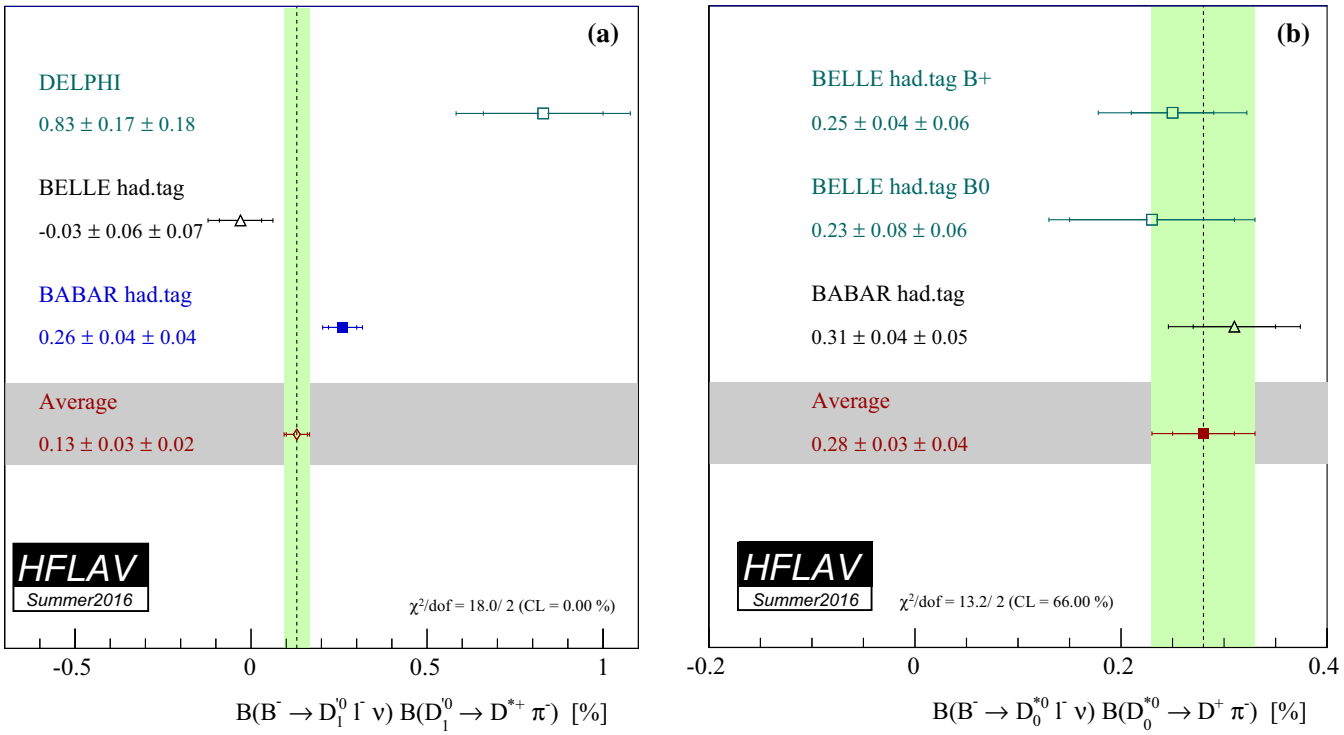

Fig. 55 Rescaled individual measurements and their averages for **a** $\mathcal{B}(B^- \to D_1'^0 \ell^- \bar{\nu}_\ell) \times \mathcal{B}(D_1'^0 \to D^{*+}\pi^-)$ and **b** $\mathcal{B}(B^- \to D_0^{*0} \ell^- \bar{\nu}_\ell) \times \mathcal{B}(D_0^{*0} \to D^+\pi^-)$

with a χ^2 of 23.0 for 59 degrees of freedom. We find a good agreement in the central values of $|V_{cb}|$ between the kinetic and 1S scheme analyses. No conclusion should, however, been drawn regarding the uncertainties in $|V_{cb}|$ as the two approaches are not equivalent in the number of higher-order corrections included.

Table 78 Experimental inputs used in the global analysis of $\bar{B} \to X_c \ell^- \bar{\nu}_\ell$. n is the order of the moment, c is the threshold value of the lepton momentum in GeV. In total, there are 23 measurements from BaBar, 15 measurements from Belle and 12 from other experiments

Experiment	Hadron moments $\langle M_X^n \rangle$	Lepton moments $\langle E_\ell^n \rangle$
BaBar	$n = 2, c = 0.9, 1.1, 1.3, 1.5$	$n = 0, c = 0.6, 1.2, 1.5$
	$n = 4, c = 0.8, 1.0, 1.2, 1.4$	$n = 1, c = 0.6, 0.8, 1.0, 1.2, 1.5$
	$n = 6, c = 0.9, 1.3$ [509]	$n = 2, c = 0.6, 1.0, 1.5$
		$n = 3, c = 0.8, 1.2$ [509,510]
Belle	$n = 2, c = 0.7, 1.1, 1.3, 1.5$	$n = 0, c = 0.6, 1.4$
	$n = 4, c = 0.7, 0.9, 1.3$ [511]	$n = 1, c = 1.0, 1.4$
		$n = 2, c = 0.6, 1.4$
		$n = 3, c = 0.8, 1.2$ [512]
CDF	$n = 2, c = 0.7$	
	$n = 4, c = 0.7$ [513]	
CLEO	$n = 2, c = 1.0, 1.5$	
	$n = 4, c = 1.0, 1.5$ [514]	
DELPHI	$n = 2, c = 0.0$	$n = 1, c = 0.0$
	$n = 4, c = 0.0$	$n = 2, c = 0.0$
	$n = 6, c = 0.0$ [503]	$n = 3, c = 0.0$ [503]

Table 79 Fit result in the kinetic scheme, using a precise c-quark mass constraint. The error matrix of the fit contains experimental and theoretical contributions. In the lower part of the table, the correlation matrix of the parameters is given. The scale μ of the quantities in the kinematic scheme is 1 GeV

	$\lvert V_{cb}\rvert$ (10^{-3})	$m_b^{\rm kin}$ (GeV)	$m_c^{\overline{\rm MS}}$ (GeV)	μ_π^2 (GeV^2)	ρ_D^3 (GeV^3)	μ_G^2 (GeV^2)	ρ_{LS}^3 (GeV^3)
Value	42.19	4.554	0.987	0.464	0.169	0.333	−0.153
Error	0.78	0.018	0.015	0.076	0.043	0.053	0.096
$\lvert V_{cb}\rvert$	1.000	−0.257	−0.078	0.354	0.289	−0.080	−0.051
$m_b^{\rm kin}$		1.000	0.769	−0.054	0.097	0.360	−0.087
$m_c^{\overline{\rm MS}}$			1.000	−0.021	0.027	0.059	−0.013
μ_π^2				1.000	0.732	0.012	0.020
ρ_D^3					1.000	−0.173	−0.123
μ_G^2						1.000	0.066
ρ_{LS}^3							1.000

5.3 Exclusive CKM-suppressed decays

In this section, we give results on exclusive charmless semileptonic branching fractions and the determination of $|V_{ub}|$ based on $B \to \pi l \nu$ decays. The measurements are based on two different event selections: tagged events, in which the second B meson in the event is fully (or partially) reconstructed, and untagged events, for which the momentum of the undetected neutrino is inferred from measurements of the total momentum sum of the detected particles and the knowledge of the initial state. The LHCb experiment recently reported a direct measurement of $|V_{ub}|/|V_{cb}|$ [522] reconstructing the $\Lambda_b^0 \to p\mu\nu$ decays and normalizing the branching fraction to the $\Lambda_b^0 \to \Lambda_c^+(\to pK\pi)\mu\nu$ decays. We show a combination of $|V_{ub}| - |V_{cb}|$ using the LHCb constraint on $|V_{ub}|/|V_{cb}|$, the exclusive determination of $|V_{ub}|$ from $B \to \pi l \nu$ and $|V_{cb}|$ from both $B \to D^* \ell \nu$ and $B \to D \ell \nu$. We also present branching fraction averages for $B^0 \to \rho \ell^+ \nu$, $B^+ \to \omega \ell^+ \nu$, $B^+ \to \eta \ell^+ \nu$ and $B^+ \to \eta' \ell^+ \nu$.

5.3.1 $B \to \pi l \nu$ branching fraction and q^2 spectrum

Currently, the four most precise measurements of the differential $B \to \pi l \nu$ decay rate as a function of the four-momentum transfer squared, q^2, from BaBar and Belle [523–526] are used to obtain an average q^2 spectrum and an average for the total branching fraction. The measurements are presented in Fig. 58. From the two untagged BaBar analyses [525,526], the combined results for $B^0 \to \pi^- \ell^+ \nu$ and $B^+ \to \pi^0 \ell^+ \nu$ decays based on isospin symmetry are used. The hadronic-tag analysis

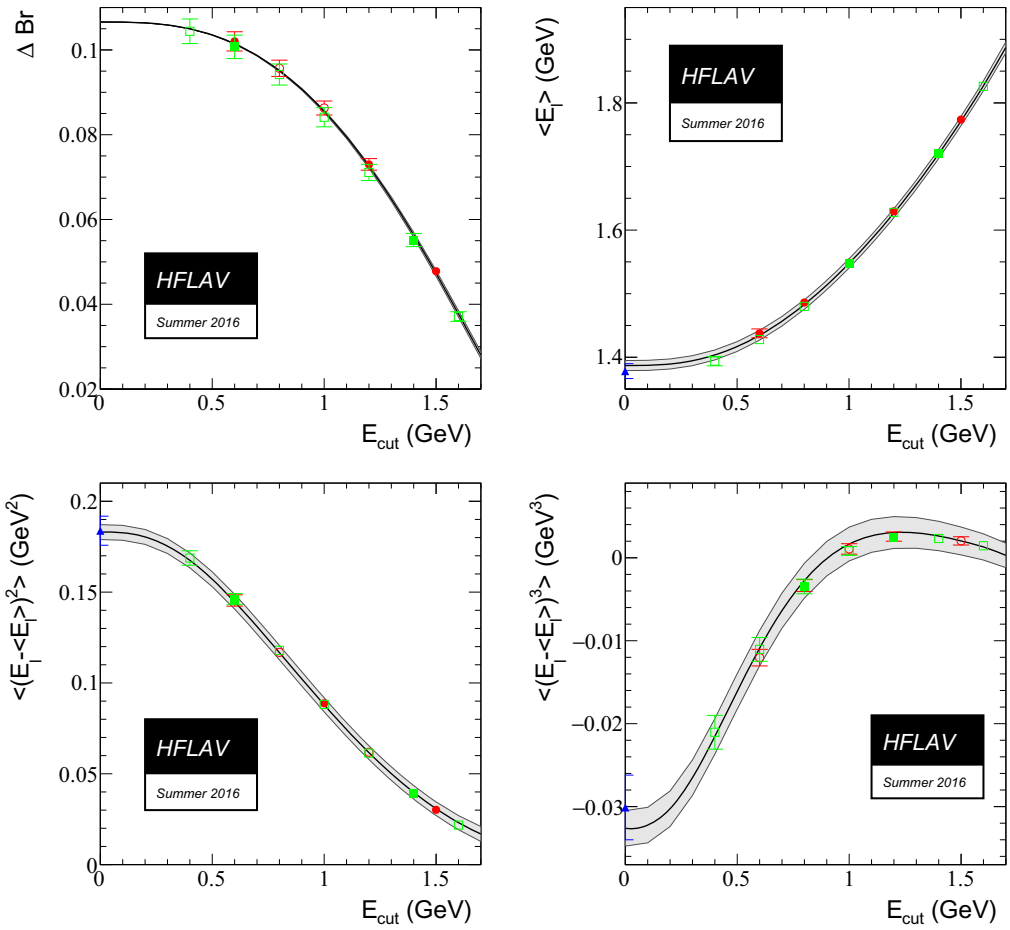

Fig. 56 Fit to the inclusive partial semileptonic branching ratios and to the lepton energy moments in the kinetic mass scheme. In all plots, the *grey band* is the theory prediction with total theory error. BABAR data are shown by *circles*, Belle by *squares* and other experiments (DELPHI, CDF, CLEO) by *triangles*. *Filled symbols* mean that the point was used in the fit. *Open symbols* are measurements that were not used in the fit

by Belle [524] provides results for $B^0 \to \pi^-\ell^+\nu$ and $B^+ \to \pi^0\ell^+\nu$ separately, but not for the combination of both channels. In the untagged analysis by Belle [523], only $B^0 \to \pi^-\ell^+\nu$ decays were measured. The experimental measurements use different binnings in q^2, but have matching bin edges, which allows them to be easily combined.

To arrive at an average q^2 spectrum, a binned maximum-likelihood fit to determine the average partial branching fraction in each q^2 interval is performed differentiating between common and individual uncertainties and correlations for the various measurements. Shared sources of systematic uncertainty of all measurements are included in the likelihood as nuisance parameters constrained using standard normal distributions. The most important shared sources of uncertainty are due to continuum subtraction, branching fractions, the number of B-meson pairs (only correlated among measurement by the same experiment), tracking efficiency (only correlated among measurements by the same experiment), uncertainties from modelling the $b \to u\,\ell\,\bar{\nu}_\ell$ contamination, modelling of final state radiation, and contamination from $b \to c\,\ell\bar{\nu}_\ell$ decays.

The averaged q^2 spectrum is shown in Fig. 58. The probability of the average is computed as the χ^2 probability quantifying the agreement between the input spectra and the averaged spectrum and amounts to 6%. The partial branching fractions and the full covariance matrix obtained from the likelihood fit are given in Tables 81 and 82. The average for the total $B^0 \to \pi^-\ell^+\nu_\ell$ branching fraction is obtained by summing up the partial branching fractions:

$$\mathcal{B}(B^0 \to \pi^-\ell^+\nu_\ell) = (1.50 \pm 0.02_{\text{stat}} \pm 0.06_{\text{syst}}) \times 10^{-4}. \tag{203}$$

5.3.2 $|V_{ub}|$ from $B \to \pi l \nu$

The $|V_{ub}|$ average can be determined from the averaged q^2 spectrum in combination with a prediction for the normalization of the $B \to \pi$ form factor. The differential decay rate for light leptons (e, μ) is given by

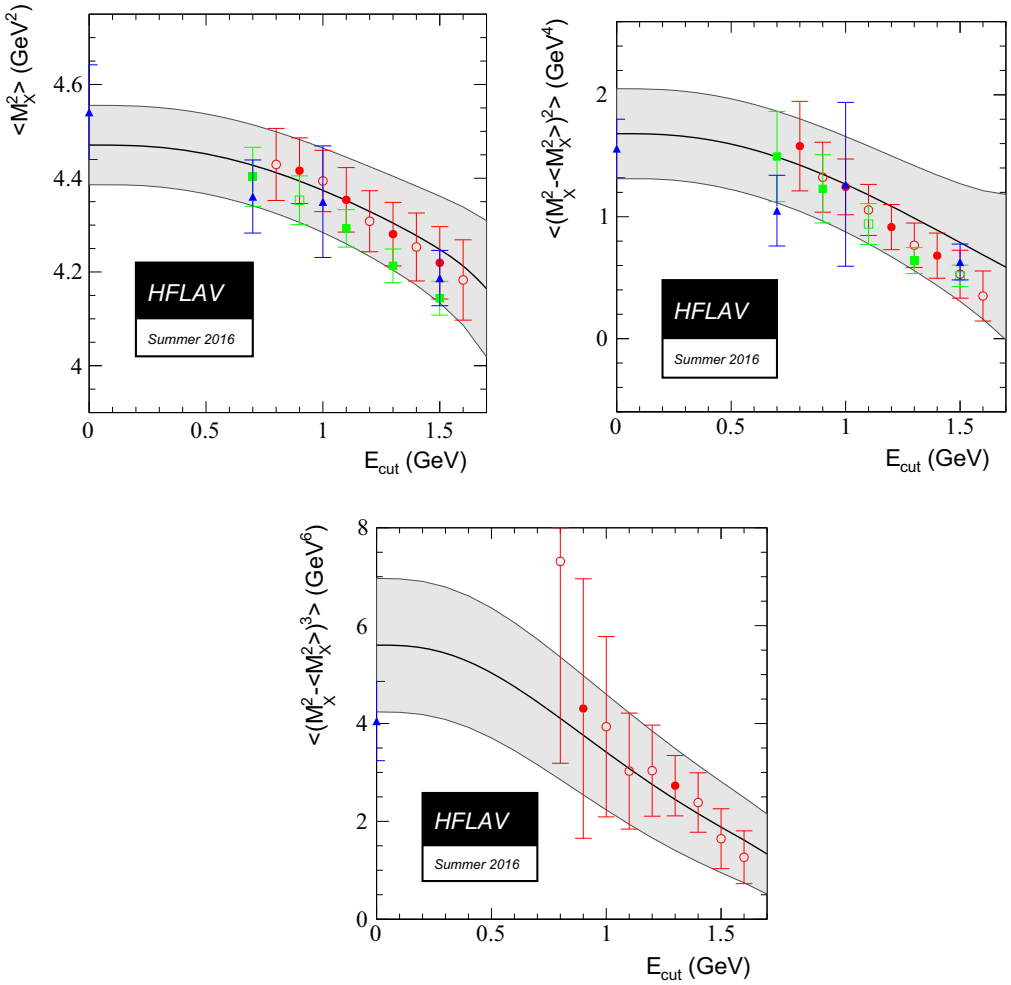

Fig. 57 Same as Fig. 56 for the fit to the hadronic mass moments in the kinetic mass scheme

Table 80 Fit result in the 1S scheme, using $B \to X_s\gamma$ moments as a constraint. In the lower part of the table, the correlation matrix of the parameters is given

	m_b^{1S} (GeV)	λ_1 (GeV^2)	ρ_1 (GeV^3)	τ_1 (GeV^3)	τ_2 (GeV^3)	τ_3 (GeV^3)	$\lvert V_{cb}\rvert$ (10^{-3})
Value	4.691	−0.362	0.043	0.161	−0.017	0.213	41.98
Error	0.037	0.067	0.048	0.122	0.062	0.102	0.45
m_b^{1S}	1.000	0.434	0.213	−0.058	−0.629	−0.019	−0.215
λ_1		1.000	−0.467	−0.602	−0.239	−0.547	−0.403
ρ_1			1.000	0.129	−0.624	0.494	0.286
τ_1				1.000	0.062	−0.148	0.194
τ_2					1.000	−0.009	−0.145
τ_3						1.000	0.376
$\lvert V_{cb}\rvert$							1.000

$$\Delta\Gamma = \Delta\Gamma(q^2_{\rm low}, q^2_{\rm high}) = \int_{q^2_{\rm low}}^{q^2_{\rm high}} {\rm d}q^2 \left[\frac{8|\vec{p}_\pi|}{3} \frac{G_F^2\,|V_{ub}|^2 q^2}{256\,\pi^3\,m_B^2} H_0^2(q^2) \right], \qquad (204)$$

where G_F is Fermi's constant, $|\vec{p}_\pi|$ is the absolute four-momentum of the final state π (a function of q^2), m_B the B^0-meson mass, and $H_0(q^2)$ the only non-zero helicity amplitude. The helicity amplitude is a function of the form factor f_+,

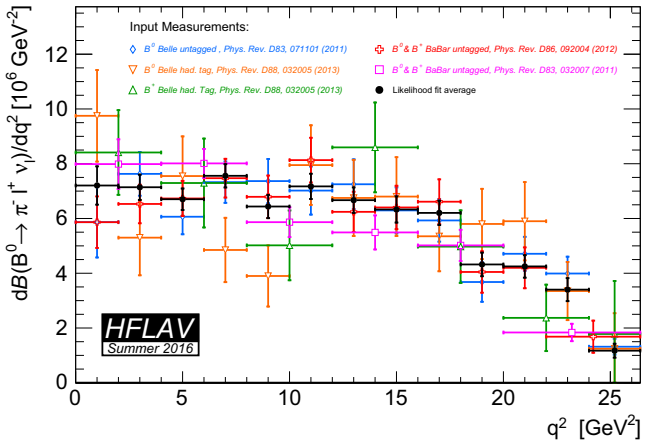

Fig. 58 The $B \to \pi l \nu$ q^2 spectrum measurements and the average spectrum obtained from the likelihood combination (shown in *black*)

$$H_0 = \frac{2m_B\,|\vec{p}_\pi|}{\sqrt{q^2}} f_+(q^2). \tag{205}$$

The form factor f_+ can be calculated with non-perturbative methods, but its general form can be constrained by the differential $B \to \pi l \nu$ spectrum. Here, we parametrize the form factor using the BCL parametrization [527].

The decay rate is proportional to $|V_{ub}|^2 |f_+(q^2)|^2$. Thus to extract $|V_{ub}|$ one needs to determine $f_+(q^2)$ (at least at one value of q^2). In order to enhance the precision, a binned χ^2 fit is performed using a χ^2 function of the form

$$\chi^2 = \left(\vec{\mathcal{B}} - \Delta\vec{\Gamma}\,\tau\right)^T C^{-1} \left(\vec{\mathcal{B}} - \Delta\vec{\Gamma}\,\tau\right) + \chi^2_{\mathrm{LQCD}} + \chi^2_{\mathrm{LCSR}} \tag{206}$$

with C denoting the covariance matrix given in Table 82, $\vec{\mathcal{B}}$ the vector of averaged branching fractions and $\Delta\vec{\Gamma}\,\tau$ the product of the vector of theoretical predictions of the partial decay rates and the B^0-meson lifetime. The form factor normalization is included in the fit by the two extra terms in Eq. (206): χ_{LQCD} uses the latest FLAG lattice average [222] from two state-of-the-art unquenched lattice QCD calculations [528,529]. The resulting constraints are quoted directly in terms of the coefficients b_j of the BCL parameterization and enter Eq. (206) as

$$\chi^2_{\mathrm{LQCD}} = \left(\vec{b} - \vec{b}_{\mathrm{LQCD}}\right)^T C^{-1}_{\mathrm{LQCD}} \left(\vec{b} - \vec{b}_{\mathrm{LQCD}}\right), \tag{207}$$

with $\vec{b}$ the vector containing the free parameters of the χ^2 fit constraining the form factor, $\vec{b}_{\mathrm{LQCD}}$ the averaged values from Ref. [222], and C_{LQCD} their covariance matrix. Additional information about the form factor can be obtained from light-cone sum rule calculations. The state-of-the-art calculation includes up to two-loop contributions [530]. It is included in Eq. (206) via

$$\chi^2_{\mathrm{LQCR}} = \left(f_+^{\mathrm{LCSR}} - f_+(q^2 = 0; \vec{b})\right)^2 / \sigma^2_{f_+^{\mathrm{LCSR}}}. \tag{208}$$

The $|V_{ub}|$ average is obtained for two versions: the first combines the data with the LQCD constraints and the second additionally includes the information from the LCSR calculation. The resulting values for $|V_{ub}|$ are

Table 81 Partial $B^0 \to \pi^- \ell^+ \nu_\ell$ branching fractions per GeV^2 for the input measurements and the average obtained from the likelihood fit. The uncertainties are the combined statistical and systematic uncertainties

Δq^2 (GeV^2)	$\Delta\mathcal{B}(B^0 \to \pi^- \ell^+ \nu_\ell)/\Delta q^2$ $[10^{-7}]$					
	Belle untagged (B^0)	Belle tagged (B^0)	Belle tagged (B^+)	BaBar untagged ($B^{0,+}$, 12 bins)	BaBar untagged ($B^{0,+}$, 6 bins)	Average
0–2	58.7 ± 12.9	97.5 ± 16.7	84.1 ± 15.5	58.7 ± 9.4	79.9 ± 9.1	72.0 ± 7.0
2–4	76.3 ± 8.0	53.0 ± 13.8		65.3 ± 7.1		71.4 ± 4.6
4–6	60.6 ± 6.4	75.5 ± 14.5	73.0 ± 16.2	67.3 ± 6.4	80.1 ± 5.3	67.0 ± 3.9
6–8	73.3 ± 7.6	48.5 ± 11.8		74.7 ± 7.1		75.6 ± 4.3
8–10	73.7 ± 8.1	39.0 ± 11.2	50.2 ± 12.8	67.9 ± 7.8	58.7 ± 5.5	64.4 ± 4.3
10–12	70.2 ± 8.8	79.5 ± 14.6		81.3 ± 8.2		71.7 ± 4.6
12–14	72.5 ± 9.1	67.5 ± 13.9	86.0 ± 16.4	62.4 ± 7.4	54.9 ± 6.2	66.7 ± 4.7
14–16	63.0 ± 8.4	68.0 ± 14.4		64.0 ± 7.9		63.3 ± 4.8
16–18	59.3 ± 7.8	53.5 ± 12.8	49.7 ± 13.3	66.1 ± 8.2	50.2 ± 5.7	62.0 ± 4.4
18–20	36.8 ± 7.2	58.0 ± 12.8		40.5 ± 7.6		43.2 ± 4.3
20–22	47.1 ± 6.2	59.0 ± 14.3	23.7 ± 12.1	42.0 ± 7.5	18.4 ± 3.2	42.5 ± 4.1
22–24	39.9 ± 6.2	33.5 ± 10.6		16.8 ± 5.9		34.0 ± 4.2
24–26.4	13.2 ± 2.9	12.4 ± 13.0	17.8 ± 19.4			11.7 ± 2.6

Table 82 Covariance matrix of the averaged partial branching fractions per GeV^2 in units of 10^{-14}

Δq^2 (GeV^2)	0–2	2–4	4–6	6–8	8–10	10–12	12–14	14–16	16–18	18–20	20–22	22–24	24–26.4
0–2	49.091	1.164	8.461	7.996	7.755	9.484	7.604	9.680	8.868	7.677	7.374	7.717	2.877
2–4		21.487	−0.0971	7.155	4.411	5.413	4.531	4.768	4.410	3.442	3.597	3.388	1.430
4–6			15.489	−0.563	5.818	4.449	4.392	4.157	4.024	3.185	3.169	3.013	1.343
6–8				18.2	2.377	7.889	6.014	5.938	5.429	4.096	3.781	3.863	1.428
8–10					18.124	1.540	7.496	5.224	5.441	4.197	3.848	4.094	1.673
10–12						21.340	4.213	7.696	6.493	5.170	4.686	4.888	1.950
12–14							21.875	0.719	6.144	3.846	3.939	3.922	1.500
14–16								23.040	5.219	6.123	4.045	4.681	1.807
16–18									19.798	1.662	4.362	4.140	1.690
18–20										18.0629	2.621	3.957	1.438
20–22											16.990	1.670	1.127
22–24												17.774	−0.293
24–26.4													6.516

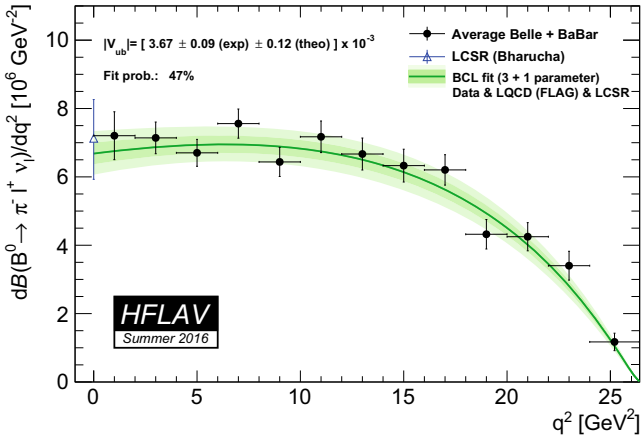

Fig. 59 Fit of the BCL parametrization to the averaged q^2 spectrum from BABAR and Belle and the LQCD and LCSR calculations. The *error bands* represent the 1 σ (*dark green*) and 2 σ (*light green*) uncertainties of the fitted spectrum

Table 83 Best fit values and uncertainties for the combined fit to data, LQCD and LCSR results

Parameter	Value
$\lvert V_{ub}\rvert$	$(3.67 \pm 0.15) \times 10^{-3}$
b_0	0.418 ± 0.012
b_1	-0.399 ± 0.033
b_2	-0.578 ± 0.130

$$|V_{ub}| = \Big(3.70 \pm 0.10\,(\text{exp}) \pm 0.12\,(\text{theo})\Big) \times 10^{-3}\,(\text{data} + \text{LQCD}), \tag{209}$$

$$|V_{ub}| = \Big(3.67 \pm 0.09\,(\text{exp}) \pm 0.12\,(\text{theo})\Big) \times 10^{-3}\,(\text{data} + \text{LQCD} + \text{LCSR}), \tag{210}$$

for the first and second fit version, respectively. The result of the fit including both LQCD and LCSR is shown in Fig. 59. The χ^2 probability of the fit is 47%. We quote the result of the fit including both LQCD and LCSR calculations as our average for $|V_{ub}|$. The best fit values for $|V_{ub}|$ and the BCL parameters and their covariance matrix are given in Tables 83 and 84.

5.3.3 Combined extraction of $|V_{ub}|$ and $|V_{cb}|$

The LHCb experiment reported the first observation of the CKM suppressed decay $\Lambda_b^0 \to p\mu\nu$ [522] and the measurement of the ratio of partial branching fractions at high q^2 for $\Lambda_b^0 \to p\mu\nu$ and $\Lambda_b^0 \to \Lambda_c^+(\to pK\pi)\mu\nu$ decays

Table 84 Covariance matrix for the combined fit to data, LQCD and LCSR results

Parameter	$\|V_{ub}\|$	b_0	b_1	b_2
$\|V_{ub}\|$	2.064×10^{-8}	-1.321×10^{-6}	-1.881×10^{-6}	7.454×10^{-6}
b_0		1.390×10^{-4}	8.074×10^{-5}	-8.953×10^{-4}
b_1			1.053×10^{-3}	-2.879×10^{-3}
b_2				1.673×10^{-2}

$$R = \frac{\mathcal{B}(\Lambda_b^0 \to p\mu\nu)_{q^2>15\ GeV^2}}{\mathcal{B}(\Lambda_b^0 \to \Lambda_c^+\mu\nu)_{q^2>7\ GeV^2}} = (1.00 \pm 0.04 \pm 0.08) \times 10^{-2}. \quad (211)$$

The ratio R is proportional to $(|V_{ub}|/|V_{cb}|)^2$ and sensitive to the form factors of $\Lambda_b^0 \to p$ and $\Lambda_b^0 \to \Lambda_c^+$ transitions that have to be computed with non-perturbative methods, like lattice QCD. The uncertainty on $\mathcal{B}(\Lambda_c^+ \to pK\pi)$ is the largest source of systematic uncertainties on R. Using the recent HFLAV average $\mathcal{B}(\Lambda_c^+ \to pK\pi) = (6.46 \pm 0.24)\%$ reported in Table 296, which includes the recent BESIII measurements [531], the rescaled value for R is

$$R = (0.95 \pm 0.04 \pm 0.07) \times 10^{-2} \quad (212)$$

With the precise lattice QCD prediction [532] of the form factors in the experimentally interesting q^2 region considered, results in

$$\frac{|V_{ub}|}{|V_{cb}|} = 0.080 \pm 0.004_{Exp.} \pm 0.004_{F.F.} \quad (213)$$

where the first uncertainty is the total experimental error and the second one is due to the knowledge of the form factors. A combined fit for $|V_{ub}|$ and $|V_{cb}|$ that includes the constraint from LHCb, and the determination of $|V_{ub}|$ and $|V_{cb}|$ from exclusive B meson decays, results in

$$|V_{ub}| = (3.50 \pm 0.13) \times 10^{-3} \quad (214)$$

$$|V_{cb}| = (39.13 \pm 0.59) \times 10^{-3} \quad (215)$$

$$\rho(|V_{ub}||, |V_{cb}|) = 0.14 \quad (216)$$

where the uncertainties are considered uncorrelated. The χ^2 of the fit is 4.4 for 2 d.o.f corresponding to a $P(\chi^2)$ of 11.0%. The fit result is shown in Fig. 60, where both the $\Delta\chi^2$ and the two-dimensional 68% C.L. contours are indicated. The $|V_{ub}|/|V_{cb}|$ value extracted from R is more compatible with the exclusive determinations of $|V_{ub}|$. Another recent calculation, by Faustov and Galkin [533], based on a relativistic quark model, gives a value of $|V_{ub}|/|V_{cb}|$ closer to the inclusive determinations.

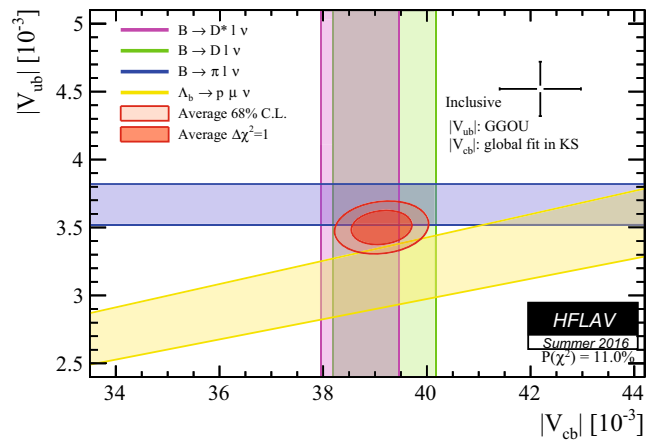

Fig. 60 $|V_{ub}|$-$|V_{cb}|$ combined average including the LHCb measurement of $|V_{ub}|/|V_{cb}|$, the exclusive $|V_{ub}|$ measurement from $B \to \pi l\nu$, and $|V_{cb}|$ measurements from both $B \to D^*\ell\nu$ and $B \to D\ell\nu$. The *point* with the *error bars* corresponds to the inclusive $|V_{cb}|$ from the kinetic scheme Sect. 5.2.2, and the inclusive $|V_{ub}|$ from GGOU calculation Sect. 5.4.3

Table 85 Summary of exclusive determinations of $B^0 \to \rho\ell^+\nu$. The errors quoted correspond to statistical and systematic uncertainties, respectively

	$\mathcal{B}$ [10^{-4}]
CLEO (untagged) ρ^+ [536]	$2.77 \pm 0.41 \pm 0.52$
CLEO (untagged) ρ^+ [537]	$2.93 \pm 0.37 \pm 0.37$
Belle (hadronic tag) ρ^+ [524]	$3.22 \pm 0.27 \pm 0.24$
Belle (hadronic tag) ρ^0 [524]	$3.39 \pm 0.18 \pm 0.18$
Belle (semileptonic tag) ρ^+ [538]	$2.24 \pm 0.54 \pm 0.31$
Belle (semileptonic tag) ρ^0 [538]	$2.50 \pm 0.43 \pm 0.33$
BABAR (untagged) ρ^+ [525]	$1.96 \pm 0.21 \pm 0.38$
BABAR (untagged) ρ^0 [525]	$1.86 \pm 0.19 \pm 0.32$
Average	$2.94 \pm 0.09 \pm 0.17$

5.3.4 *Other exclusive charmless semileptonic B decays*

We report the branching fraction average for $B^0 \to \rho\ell^+\nu$, $B^+ \to \omega\ell^+\nu$, $B^+ \to \eta\ell^+\nu$ and $B^+ \to \eta'\ell^+\nu$ decays. The measurements and their averages are listed in Tables 85, 86, 87, 88, and presented in Figs. 61 and 62.

Table 86 Summary of exclusive determinations of $B^+ \to \omega\ell^+\nu$. The errors quoted correspond to statistical and systematic uncertainties, respectively

	$\mathcal{B}$ [10^{-4}]
Belle (untagged) [539]	$1.30 \pm 0.40 \pm 0.36$
BaBar (loose ν reco.) [526]	$1.19 \pm 0.16 \pm 0.09$
BaBar (untagged) [540]	$1.21 \pm 0.14 \pm 0.08$
Belle (hadronic tag) [524]	$1.07 \pm 0.16 \pm 0.07$
BaBar (semileptonic tag) [541]	$1.35 \pm 0.21 \pm 0.11$
Average	$1.19 \pm 0.08 \pm 0.06$

Table 87 Summary of exclusive determinations of $B^+ \to \eta\ell^+\nu$. The errors quoted correspond to statistical and systematic uncertainties, respectively

	$\mathcal{B}$ [10^{-4}]
CLEO [542]	$0.45 \pm 0.23 \pm 0.11$
BaBar (untagged) [543]	$0.31 \pm 0.06 \pm 0.08$
BaBar (semileptonic tag) [544]	$0.64 \pm 0.20 \pm 0.04$
BaBar (loose ν-reco.) [526]	$0.38 \pm 0.05 \pm 0.05$
Average	$0.38 \pm 0.04 \pm 0.04$

In the $B^0 \to \rho^-\ell^+\nu$ average, both the $B^0 \to \rho^-\ell^+\nu$ and $B^+ \to \rho^0\ell^+\nu$ decays are used, where the $B^+ \to \rho^0\ell^+\nu$ are rescaled by $2\tau_{B^0}/\tau_{B^+}$ assuming the isospin symmetry. For $B^+ \to \omega\ell^+\nu$ and $B^+ \to \eta\ell^+\nu$ decays, the agreement between the different measurements is good. $B^+ \to \eta'\ell^+\nu$ shows a discrepancy between the old CLEO measurement and the BaBar untagged analysis, but the statistical uncertainties of the CLEO measurement are large. The $B^0 \to \rho\ell^+\nu$ results, instead, show significant differences, in particular the BaBar untagged analysis gives a branching fraction significantly lower (by about 2σ) that the Belle measurement based on the hadronic-tag. A possible reason for such discrepancy could be the broad nature of the ρ resonance that makes the control of the background under the ρ mass peak more difficult in the untagged analysis than in the hadronic-tag analysis.

We do not report $|V_{ub}|$ for these exclusive charmless decays, because the form factor calculations have not yet reached the precision achieved for $B \to \pi\ell\nu$ decays. Unquenched lattice QCD calculations of the form factors are not available for these decays, but LCSR calculations exist for all these decay modes. The most recent of these calculations for the $B \to \rho\ell\nu$ and $B \to \omega\ell\nu$ decays are reported in Refs. [534,535].

5.4 Inclusive CKM-suppressed decays

Measurements of $B \to X_u\ell^+\nu$ decays are very challenging because of the fifty times larger rates Cabibbo-favoured $B \to X_c\ell^+\nu$ decays. Cuts designed to suppress this dominant background severely complicate the perturbative QCD calculations required to extract $|V_{ub}|$. For strict phase space limitations, parameterizations of the so-called shape functions are required to describe the unmeasured regions of the phase space. In this update, we use several theoretical calculations to extract $|V_{ub}|$ and do not advocate the use of one method over another. The authors of the different calculations have provided codes to compute the partial rates in limited regions of phase space covered by the measurements. Latest results by Belle [545] and BaBar [546] explore large portions of phase space, with a consequent reduction of the theoretical uncertainties.

Table 88 Summary of exclusive determinations of $B^+ \to \eta'\ell^+\nu$. The errors quoted correspond to statistical and systematic uncertainties, respectively

	$\mathcal{B}$ [10^{-4}]
CLEO [542]	$2.71 \pm 0.80 \pm 0.56$
BaBar (semileptonic tag) [544]	$0.04 \pm 0.22 \pm 0.04$, (<0.47 @ 90%$C.L.$)
BaBar (untagged) [526]	$0.24 \pm 0.08 \pm 0.03$
Average	$0.23 \pm 0.08 \pm 0.03$

In the averages, the systematic errors associated with the modeling of $B \to X_c\ell^+\nu_\ell$ and $B \to X_u\ell^+\nu_\ell$ decays and the theoretical uncertainties are taken as fully correlated among all measurements. Reconstruction-related uncertainties are taken as fully correlated within a given experiment. Measurements of partial branching fractions for $B \to X_u\ell^+\nu_\ell$ transitions from $\Upsilon(4S)$ decays, together with the corresponding selected region, are given in Table 89. The signal yields for all the measurements shown in Table 89 are not rescaled to common input values of the B meson lifetime (see Sect. 3) and the semileptonic width [327]. We use all results published by BaBar in Ref. [546], since the statistical correlations are given. To make use of the theoretical calculations of Ref. [547], we restrict the kinematic range of the invariant mass of the hadronic system, M_X, and the square of the invariant mass of the lepton pair, q^2. This reduces the size of the data sample significantly, but also the theoretical uncertainty, as stated by the authors [547]. The dependence of the quoted error on the measured value for each source of uncertainty is taken into account in the calculation of the averages.

It has been first suggested by Neubert [548] and later detailed by Leibovich, Low, and Rothstein (LLR) [549] and Lange, Neubert and Paz (LNP) [550], that the uncertainty of the leading shape functions can be eliminated by comparing inclusive rates for $B \to X_u\ell^+\nu_\ell$ decays with the inclusive photon spectrum in $B \to X_s\gamma$, based on the assumption that

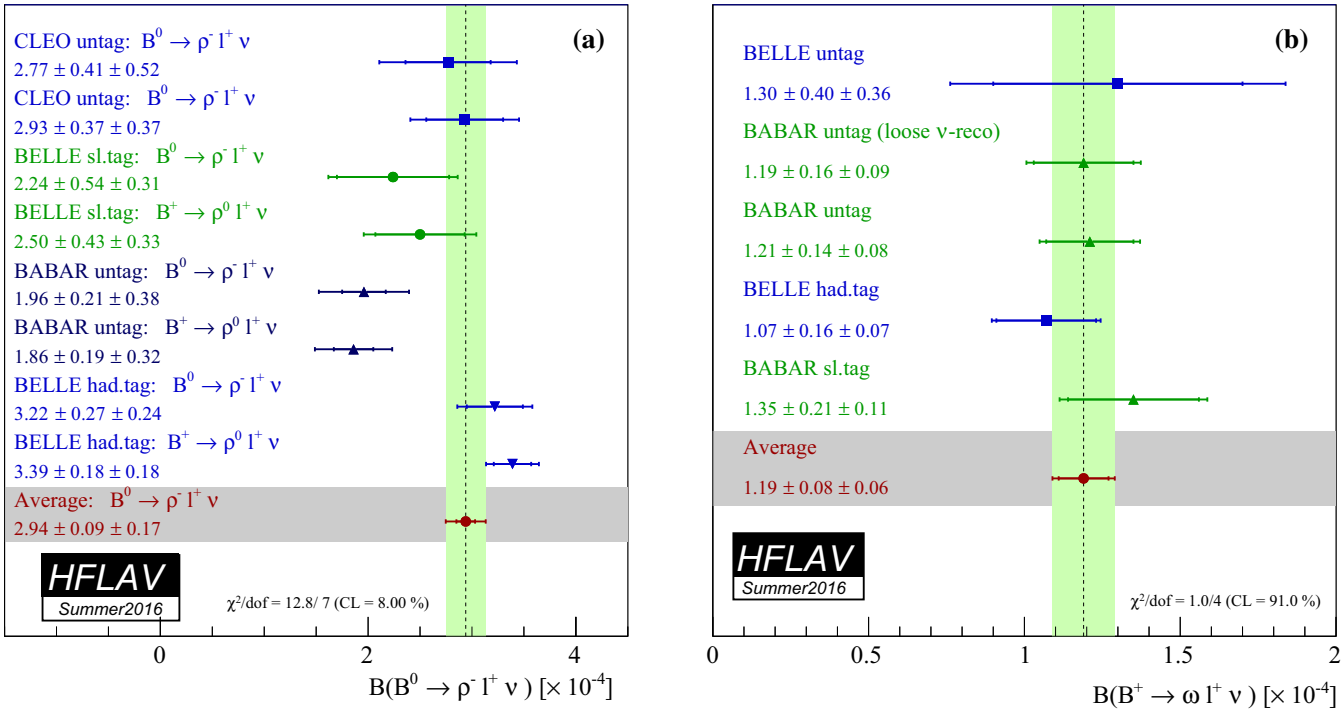

Fig. 61 **a** Summary of exclusive determinations of $\mathcal{B}(B^0 \to \rho\ell^+\nu)$ and their average. Measurements of $B^+ \to \rho^0\ell^+\nu$ branching fractions have been multiplied by $2\tau_{B^0}/\tau_{B^+}$ in accordance with isospin symmetry. **b** Summary of exclusive determinations of $B^+ \to \omega\ell^+\nu$ and their average

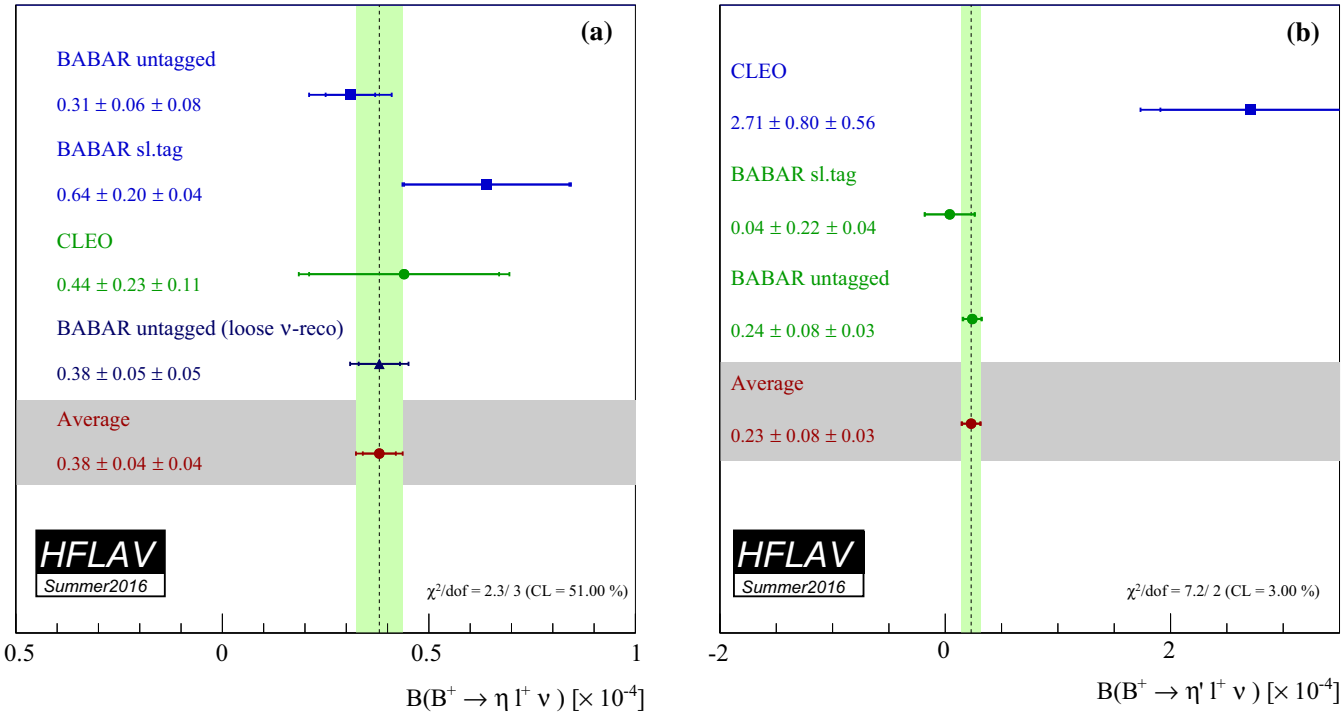

Fig. 62 **a** Summary of exclusive determinations of $\mathcal{B}(B^+ \to \eta\ell^+\nu)$ and their average. **b** Summary of exclusive determinations of $\mathcal{B}(B^+ \to \eta'\ell^+\nu)$ and their average

the shape functions for transitions to light quarks, u or s, are the same at first order. However, shape function uncertainties are only eliminated at the leading order and they still enter via the signal models used for the determination of efficiency.

Table 89 Summary of measurements of partial branching fractions for $B \to X_u \ell^+ \nu_\ell$ decays. The errors quoted on $\Delta\mathcal{B}$ correspond to statistical and systematic uncertainties. E_e is the electron energy in the B rest frame, p^* the lepton momentum in the B frame and m_X is the invariant mass of the hadronic system. The light-cone momentum P_+ is defined in the B rest frame as $P_+ = E_X - |\mathbf{p}_X|$. The $s_\mathrm{h}^\mathrm{max}$ variable is described in Refs. [552,553]

Measurement	Accepted region	$\Delta\mathcal{B}\,[10^{-4}]$	Notes
CLEO [554]	$E_e > 2.1\,\mathrm{GeV}$	$3.3 \pm 0.2 \pm 0.7$	
BaBar [553]	$E_e > 2.0\,\mathrm{GeV}$, $s_\mathrm{h}^\mathrm{max} < 3.5\,\mathrm{GeV}^2$	$4.4 \pm 0.4 \pm 0.4$	
BaBar [555]	$E_e > 2.0\,\mathrm{GeV}$	$5.7 \pm 0.4 \pm 0.5$	
Belle [556]	$E_e > 1.9\,\mathrm{GeV}$	$8.5 \pm 0.4 \pm 1.5$	
BaBar [546]	$M_X < 1.7\,\mathrm{GeV}/c^2$, $q^2 > 8\,\mathrm{GeV}^2/c^4$	$6.9 \pm 0.6 \pm 0.4$	
Belle [557]	$M_X < 1.7\,\mathrm{GeV}/c^2$, $q^2 > 8\,\mathrm{GeV}^2/c^4$	$7.4 \pm 0.9 \pm 1.3$	
Belle [558]	$M_X < 1.7\,\mathrm{GeV}/c^2$, $q^2 > 8\,\mathrm{GeV}^2/c^4$	$8.5 \pm 0.9 \pm 1.0$	Used only in BLL average
BaBar [546]	$P_+ < 0.66\,\mathrm{GeV}$	$9.9 \pm 0.9 \pm 0.8$	
BaBar [546]	$M_X < 1.7\,\mathrm{GeV}/c^2$	$11.6 \pm 1.0 \pm 0.8$	
BaBar [546]	$M_X < 1.55\,\mathrm{GeV}/c^2$	$10.9 \pm 0.8 \pm 0.6$	
Belle [545]	(M_X, q^2) fit, $p_\ell^* > 1\,\mathrm{GeV}/c$	$19.6 \pm 1.7 \pm 1.6$	
BaBar [546]	(M_X, q^2) fit, $p_\ell^* > 1\,\mathrm{GeV}/c$	$18.2 \pm 1.3 \pm 1.5$	
BaBar [546]	$p_\ell^* > 1.3\,\mathrm{GeV}/c$	$15.5 \pm 1.3 \pm 1.4$	

In the following, the different theoretical methods and the resulting averages are described. A recent BaBar measurement of the inclusive electron spectrum [551] was released at the time of this writing and could not be included in the averages.

5.4.1 BLNP

Bosch, Lange, Neubert and Paz (BLNP) [559–562] provide theoretical expressions for the triple differential decay rate for $B \to X_u \ell^+ \nu_\ell$ events, incorporating all known contributions, whilst smoothly interpolating between the "shape-function region" of large hadronic energy and small invariant mass, and the "OPE region" in which all hadronic kinematical variables scale with the b-quark mass. BLNP assign uncertainties to the b-quark mass, which enters through the leading shape function, to sub-leading shape function forms, to possible weak annihilation contribution, and to matching scales. The BLNP calculation uses the shape function renormalization scheme; the heavy quark parameters determined from the global fit in the kinetic scheme, described in Sect. 5.2.2, were therefore translated into the shape function scheme by using a prescription by Neubert [563,564]. The resulting parameters are $m_b(\mathrm{SF}) = (4.582 \pm 0.023 \pm 0.018)$ GeV, $\mu_\pi^2(\mathrm{SF}) = (0.202 \pm 0.089^{+0.020}_{-0.040})\,\mathrm{GeV}/c^2$, where the second uncertainty is due to the scheme translation. The extracted values of $|V_{ub}|$ for each measurement along with their average are given in Table 90 and illustrated in Fig. 63a. The total uncertainty is $^{+5.8}_{-6.0}\%$ and is due to: statistics ($^{+2.1}_{-2.1}\%$), detector effects ($^{+1.7}_{-1.8}\%$), $B \to X_c \ell^+ \nu_\ell$ model ($^{+1.2}_{-1.2}\%$), $B \to X_u \ell^+ \nu_\ell$ model ($^{+1.8}_{-1.7}\%$), heavy quark parameters ($^{+2.6}_{-2.6}\%$), SF functional form ($^{+0.2}_{-0.3}\%$), sub-leading shape functions ($^{+0.6}_{-0.7}\%$), BLNP theory: matching scales μ, μ_i, μ_h ($^{+3.8}_{-3.7}\%$), and weak annihilation ($^{+0.0}_{-1.4}\%$). The error assigned to the matching scales is the source of the largest uncertainty, while the uncertainty due to HQE parameters (b-quark mass and μ_π^2) is second. The uncertainty due to weak annihilation has been assumed to be asymmetric, i.e. it only tends to decrease $|V_{ub}|$.

5.4.2 DGE

Andersen and Gardi (Dressed Gluon Exponentiation, DGE) [565] provide a framework where the on-shell b-quark calculation, converted into hadronic variables, is directly used as an approximation to the meson decay spectrum without the use of a leading-power non-perturbative function (or, in other words, a shape function). The on-shell mass of the b-quark within the B-meson (m_b) is required as input. The DGE calculation uses the $\overline{MS}$ renormalization scheme. The heavy quark parameters determined from the global fit in the kinetic scheme, described in Sect. 5.2.2, were therefore translated into the $\overline{MS}$ scheme by using a calculation by Gardi, giving $m_b(\overline{MS}) = (4.188 \pm 0.043)$ GeV. The extracted values of $|V_{ub}|$ for each measurement along with their average are given in Table 90 and illustrated in Fig. 63b. The total error is $^{+4.8}_{-4.8}\%$, whose breakdown is: statistics ($^{+1.9}_{-1.9}\%$), detector effects ($^{+1.7}_{-1.7}\%$), $B \to X_c \ell^+ \nu_\ell$ model ($^{+1.3}_{-1.3}\%$), $B \to X_u \ell^+ \nu_\ell$ model ($^{+2.1}_{-1.7}\%$), strong coupling α_s ($^{+0.5}_{-0.5}\%$), m_b ($^{+3.2}_{-2.9}\%$), weak annihilation ($^{+0.0}_{-1.8}\%$),

Table 90 Summary of input parameters used by the different theory calculations, corresponding inclusive determinations of $|V_{ub}|$ and their average. The errors quoted on $|V_{ub}|$ correspond to experimental and theoretical uncertainties, respectively

	BLNP	DGE	GGOU	ADFR	BLL
Input parameters					
Scheme	SF	$\overline{MS}$	Kinetic	$\overline{MS}$	$1S$
Refs.	[563,564]	Ref. [565]	See Sect. 5.2.2	Ref. [566]	Ref. [547]
m_b (GeV)	4.582 ± 0.026	4.188 ± 0.043	4.554 ± 0.018	4.188 ± 0.043	4.704 ± 0.029
μ_π^2 (GeV^2)	$0.145\ ^{+0.091}_{-0.097}$	–	0.414 ± 0.078	–	–
Ref.	$\|V_{ub}\|$ values $[10^{-3}]$				
CLEO E_e [554]	$4.22 \pm 0.49^{+0.29}_{-0.34}$	$3.86 \pm 0.45^{+0.25}_{-0.27}$	$4.23 \pm 0.49^{+0.22}_{-0.31}$	$3.42 \pm 0.40^{+0.17}_{-0.17}$	–
Belle M_X, q^2 [557]	$4.51 \pm 0.47^{+0.27}_{-0.29}$	$4.43 \pm 0.47^{+0.19}_{-0.21}$	$4.52 \pm 0.48^{+0.25}_{-0.28}$	$3.93 \pm 0.41^{+0.18}_{-0.17}$	$4.68 \pm 0.49^{+0.30}_{-0.30}$
Belle E_e [556]	$4.93 \pm 0.46^{+0.26}_{-0.29}$	$4.82 \pm 0.45^{+0.23}_{-0.23}$	$4.95 \pm 0.46^{+0.16}_{-0.21}$	$4.48 \pm 0.42^{+0.20}_{-0.20}$	–
BaBarE_e [555]	$4.52 \pm 0.26^{+0.26}_{-0.30}$	$4.30 \pm 0.24^{+0.23}_{-0.25}$	$4.52 \pm 0.26^{+0.17}_{-0.24}$	$3.93 \pm 0.22^{+0.20}_{-0.20}$	–
BaBar $E_e, s_{\rm h}^{\rm max}$ [553]	$4.71 \pm 0.32^{+0.33}_{-0.38}$	$4.35 \pm 0.29^{+0.28}_{-0.30}$	–	$3.81 \pm 0.19^{+0.19}_{-0.18}$	
Belle $p_\ell^*, (M_X, q^2)$ fit [545]	$4.50 \pm 0.27^{+0.20}_{-0.22}$	$4.62 \pm 0.28^{+0.13}_{-0.13}$	$4.62 \pm 0.28^{+0.09}_{-0.10}$	$4.50 \pm 0.30^{+0.20}_{-0.20}$	–
BaBar M_X [546]	$4.24 \pm 0.19^{+0.25}_{-0.25}$	$4.47 \pm 0.20^{+0.19}_{-0.24}$	$4.30 \pm 0.20^{+0.20}_{-0.21}$	$3.83 \pm 0.18^{+0.20}_{-0.19}$	–
BaBar M_X [546]	$4.03 \pm 0.22^{+0.22}_{-0.22}$	$4.22 \pm 0.23^{+0.21}_{-0.27}$	$4.10 \pm 0.23^{+0.16}_{-0.17}$	$3.75 \pm 0.21^{+0.18}_{-0.18}$	–
BaBar M_X, q^2 [546]	$4.32 \pm 0.23^{+0.26}_{-0.28}$	$4.24 \pm 0.22^{+0.18}_{-0.21}$	$4.33 \pm 0.23^{+0.24}_{-0.27}$	$3.75 \pm 0.20^{+0.17}_{-0.17}$	$4.50 \pm 0.24^{+0.29}_{-0.29}$
BaBar P_+ [546]	$4.09 \pm 0.25^{+0.25}_{-0.25}$	$4.17 \pm 0.25^{+0.28}_{-0.37}$	$4.25 \pm 0.26^{+0.26}_{-0.27}$	$3.57 \pm 0.22^{+0.19}_{-0.18}$	–
BaBar $p_\ell^*, (M_X, q^2)$ fit [546]	$4.33 \pm 0.24^{+0.19}_{-0.21}$	$4.45 \pm 0.24^{+0.12}_{-0.13}$	$4.44 \pm 0.24^{+0.09}_{-0.10}$	$4.33 \pm 0.24^{+0.19}_{-0.19}$	–
BaBar p_ℓ^* [546]	$4.34 \pm 0.27^{+0.20}_{-0.21}$	$4.43 \pm 0.27^{+0.13}_{-0.13}$	$4.43 \pm 0.27^{+0.09}_{-0.11}$	$4.28 \pm 0.27^{+0.19}_{-0.19}$	–
Belle M_X, q^2 [558]	–	–	–	–	$5.01 \pm 0.39^{+0.32}_{-0.32}$
Average	$4.44 \pm 0.15^{+0.21}_{-0.22}$	$4.52 \pm 0.16^{+0.15}_{-0.16}$	$4.52 \pm 0.15^{+0.11}_{-0.14}$	$4.08 \pm 0.13^{+0.18}_{-0.12}$	$4.62 \pm 0.20^{+0.29}_{-0.29}$

matching scales in DGE ($^{+0.5}_{-0.4}$%). The largest contribution to the total error is due to the effect of the uncertainty on m_b. The uncertainty due to weak annihilation has been assumed to be asymmetric, i.e. it only tends to decrease $|V_{ub}|$.

5.4.3 GGOU

Gambino, Giordano, Ossola and Uraltsev (GGOU) [567] compute the triple differential decay rates of $B \to X_u \ell^+ \nu_\ell$, including all perturbative and non–perturbative effects through $O(\alpha_s^2 \beta_0)$ and $O(1/m_b^3)$. The Fermi motion is parameterized in terms of a single light–cone function for each structure function and for any value of q^2, accounting for all subleading effects. The calculations are performed in the kinetic scheme, a framework characterized by a Wilsonian treatment with a hard cutoff $\mu \sim 1$ GeV. GGOU have not included calculations for the "(E_e, s_h^{max})" analysis [553]. The heavy quark parameters determined from the global fit in the kinetic scheme, described in Sect. 5.2.2, are used as inputs: $m_b^{kin} = (4.554 \pm 0.018)$ GeV, $\mu_\pi^2 = (0.464 \pm 0.076)$ GeV$/c^2$. The extracted values of $|V_{ub}|$ for each measurement along with their average are given in Table 90 and illustrated in Fig. 64a. The total error is $^{+4.2}_{-4.6}$% whose breakdown is: statistics ($^{+2.0}_{-2.0}$%), detector effects ($^{+1.7}_{-1.7}$%), $B \to X_c \ell^+ \nu_\ell$ model ($^{+1.3}_{-1.3}$%), $B \to X_u \ell^+ \nu_\ell$ model ($^{+1.8}_{-1.8}$%), α_s, m_b and other non-perturbative parameters ($^{+1.4}_{-1.4}$%), higher order perturbative and non-perturbative corrections ($^{+1.5}_{-1.5}$%), modelling of the q^2 tail ($^{+1.2}_{-1.2}$%), weak annihilations matrix element ($^{+0.0}_{-1.9}$%), functional form of the distribution functions ($^{+0.2}_{-0.2}$%). The leading uncertainties on $|V_{ub}|$ are both from theory, and are due to perturbative and non-perturbative parameters and the modelling of the q^2 tail. The uncertainty due to weak annihilation has been assumed to be asymmetric, i.e. it only tends to decrease $|V_{ub}|$.

5.4.4 ADFR

Aglietti, Di Lodovico, Ferrera and Ricciardi (ADFR) [568] use an approach to extract $|V_{ub}|$, that makes use of the ratio of the $B \to X_c \ell^+ \nu_\ell$ and $B \to X_u \ell^+ \nu_\ell$ widths. The normalized triple differential decay rate for $B \to X_u \ell^+ \nu_\ell$ [566,569–571] is calculated with a model based on (i) soft-gluon resummation to next-to-next-leading order and (ii) an effective QCD coupling without Landau pole. This coupling is constructed by means of an extrapola-

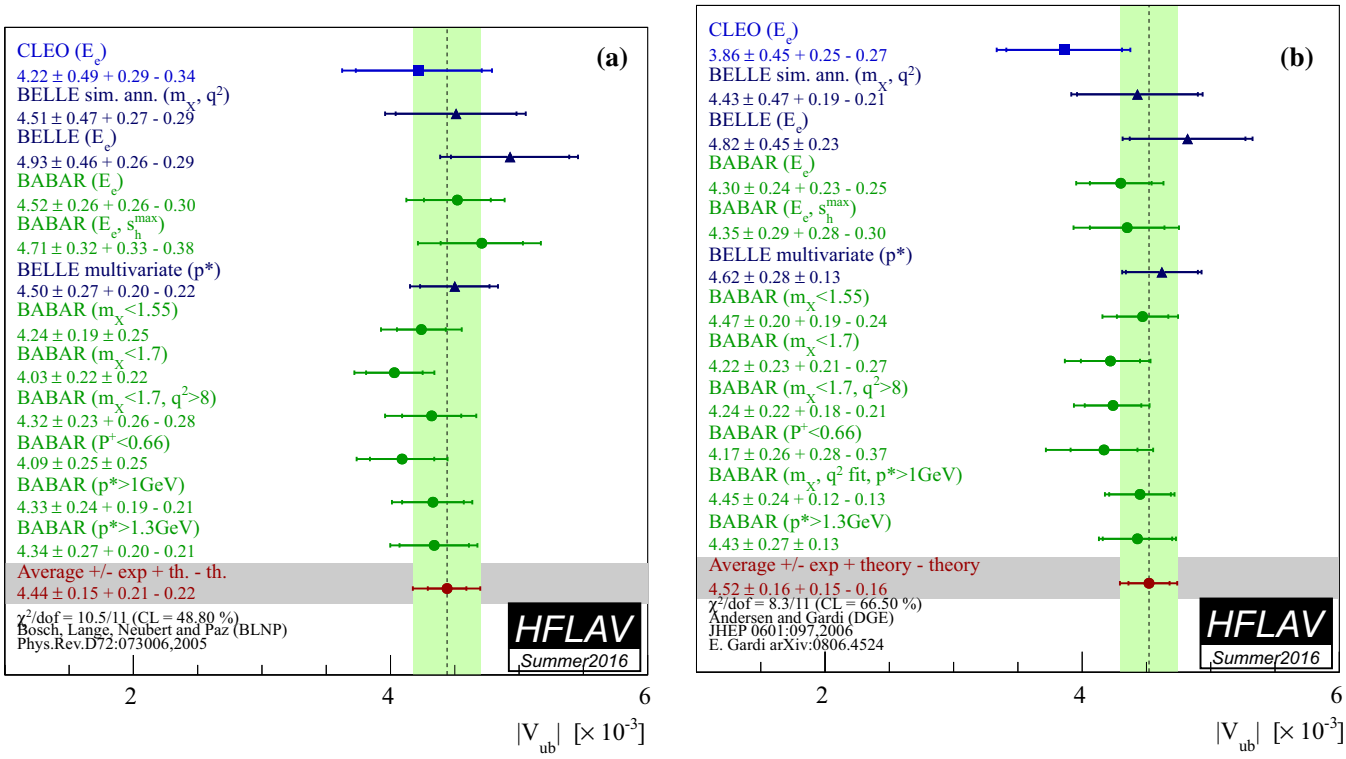

Fig. 63 Measurements of $|V_{ub}|$ from inclusive semileptonic decays and their average based on the BLNP (**a**) and DGE (**b**) prescription. The *labels* indicate the variables and selections used to define the signal regions in the different analyses

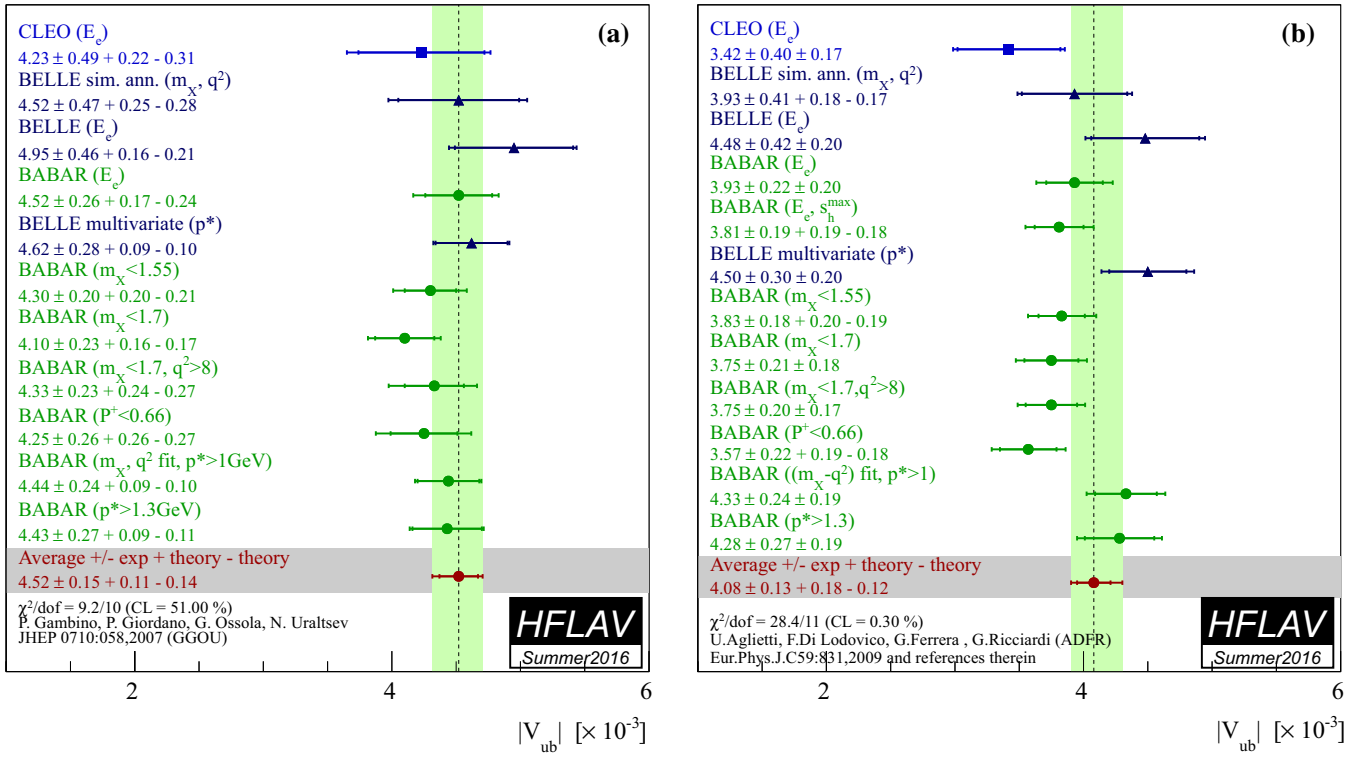

Fig. 64 Measurements of $|V_{ub}|$ from inclusive semileptonic decays and their average based on the GGOU (**a**) and ADFR (**b**) prescription. The *labels* indicate the variables and selections used to define the signal regions in the different analyses

tion to low energy of the high-energy behaviour of the standard coupling. More technically, an analyticity principle is used. The lower cut on the electron energy for the endpoint analyses is 2.3 GeV [566]. The ADFR calculation uses the $\overline{MS}$ renormalization scheme; the heavy quark parameters determined from the global fit in the kinetic scheme, described in Sect. 5.2.2, were therefore translated into the $\overline{MS}$ scheme by using a calculation by Gardi, giving $m_b(\overline{MS}) = (4.188 \pm 0.043)$ GeV. The extracted values of $|V_{ub}|$ for each measurement along with their average are given in Table 90 and illustrated in Fig. 64b. The total error is $^{+5.5}_{-5.5}\%$ whose breakdown is: statistics ($^{+1.9}_{-1.9}\%$), detector effects ($^{+1.7}_{-1.7}\%$), $B \to X_c \ell^+ \nu_\ell$ model ($^{+1.3}_{-1.3}\%$), $B \to X_u \ell^+ \nu_\ell$ model ($^{+1.3}_{-1.3}\%$), α_s ($^{+1.1}_{-1.0}\%$), $|V_{cb}|$ ($^{+1.9}_{-1.9}\%$), m_b ($^{+0.7}_{-0.7}\%$), m_c ($^{+1.3}_{-1.3}\%$), semileptonic branching fraction ($^{+0.8}_{-0.7}\%$), theory model ($^{+3.6}_{-3.6}\%$). The leading uncertainty is due to the theory model.

5.4.5 BLL

Bauer, Ligeti, and Luke (BLL) [547] give a HQET-based prescription that advocates combined cuts on the dilepton invariant mass, q^2, and hadronic mass, m_X, to minimise the overall uncertainty on $|V_{ub}|$. In their reckoning a cut on m_X only, although most efficient at preserving phase space (∼80%), makes the calculation of the partial rate untenable due to uncalculable corrections to the b-quark distribution function or shape function. These corrections are suppressed if events in the low q^2 region are removed. The cut combination used in measurements is $M_x < 1.7$ GeV$/c^2$ and $q^2 > 8$ GeV$^2/c^4$. The extracted values of $|V_{ub}|$ for each measurement along with their average are given in Table 90 and illustrated in Fig. 65. The total error is $^{+7.7}_{-7.7}\%$ whose breakdown is: statistics ($^{+3.3}_{-3.3}\%$), detector effects ($^{+3.0}_{-3.0}\%$), $B \to X_c \ell^+ \nu_\ell$ model ($^{+1.6}_{-1.6}\%$), $B \to X_u \ell^+ \nu_\ell$ model ($^{+1.1}_{-1.1}\%$), spectral fraction (m_b) ($^{+3.0}_{-3.0}\%$), perturbative approach: strong coupling α_s ($^{+3.0}_{-3.0}\%$), residual shape function ($^{+2.5}_{-2.5}\%$), third order terms in the OPE ($^{+4.0}_{-4.0}\%$). The leading uncertainties, both from theory, are due to residual shape function effects and third order terms in the OPE expansion. The leading experimental uncertainty is due to statistics.

5.4.6 Summary

The averages presented in several different frameworks are presented in Table 91. In summary, we recognize that the experimental and theoretical uncertainties play out differently between the schemes and the theoretical assumptions for the theory calculations are different. Therefore, it is difficult to perform an average between the various determinations of $|V_{ub}|$. Since the methodology is similar to that used to determine the inclusive $|V_{cb}|$ average, we choose to quote as reference value the average determined by the GGOU calculation, which gives $|V_{ub}| = (4.52 \pm 0.15^{+0.11}_{-0.14}) \times 10^{-3}$.

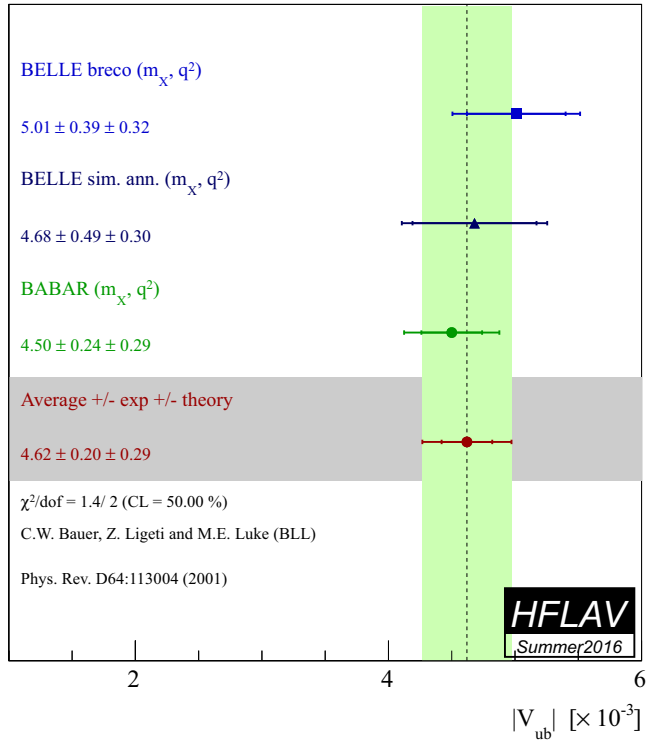

Fig. 65 Measurements of $|V_{ub}|$ from inclusive semileptonic decays and their average in the BLL prescription

Table 91 Summary of inclusive determinations of $|V_{ub}|$. The errors quoted on $|V_{ub}|$ correspond to experimental and theoretical uncertainties

Framework	$\lvert V_{ub}\rvert$ (10^{-3})
BLNP	$4.44 \pm 0.15^{+0.21}_{-0.22}$
DGE	$4.52 \pm 0.16^{+0.15}_{-0.16}$
GGOU	$4.52 \pm 0.15^{+0.11}_{-0.14}$
ADFR	$4.08 \pm 0.13^{+0.18}_{-0.12}$
BLL (m_X/q^2 only)	$4.62 \pm 0.20 \pm 0.29$

5.5 $B \to D^{(*)} \tau \nu_\tau$ decays

In the SM the semileptonic decay are tree level processes which proceed via coupling to the $W^\pm$ boson. These couplings are assumed to be universal for all leptons and are well understood theoretically, (see Sects. 5.1, 5.2). This universality has been tested in purely leptonic and semileptonic B meson decays involving a τ lepton, which might be sensitive to a hypothetical charged Higgs boson or other non-SM processes.

Table 92 Measurements of $\mathcal{R}(D^*)$ and $\mathcal{R}(D)$, their correlations and the combined average

Experiment	$\mathcal{R}(D^*)$	$\mathcal{R}(D)$	ρ
BABAR [574,575]	$0.332 \pm 0.024_{\text{stat}} \pm 0.018_{\text{syst}}$	$0.440 \pm 0.058_{\text{stat}} \pm 0.042_{\text{syst}}$	−0.27
Belle [582]	$0.293 \pm 0.038_{\text{stat}} \pm 0.015_{\text{syst}}$	$0.375 \pm 0.064_{\text{stat}} \pm 0.026_{\text{syst}}$	−0.49
LHCb [583]	$0.336 \pm 0.027_{\text{stat}} \pm 0.030_{\text{syst}}$		
Belle [584]	$0.302 \pm 0.030_{\text{stat}} \pm 0.011_{\text{syst}}$		
Belle [585]	$0.270 \pm 0.035_{\text{stat}}{}^{+0.028}_{-0.025}{}_{\text{syst}}$		
Average	$0.310 \pm 0.015 \pm 0.008$	$0.403 \pm 0.040 \pm 0.024$	−0.23

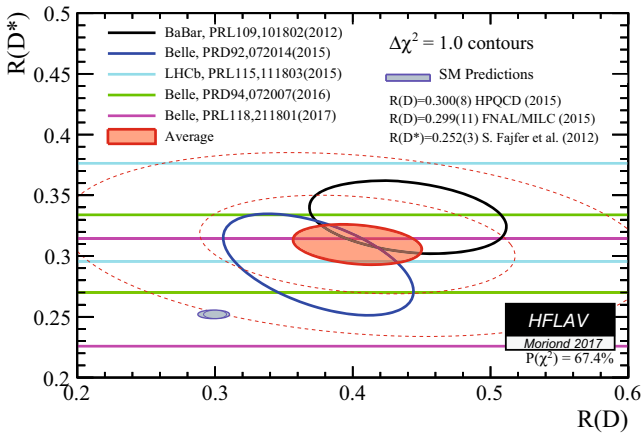

Fig. 66 Measurement of $\mathcal{R}(D)$ and $\mathcal{R}(D^*)$ and their average compared with the prediction for $\mathcal{R}(D^*)$ [577] and $\mathcal{R}(D)$ [494,573]. The *dashed ellipses* corresponds to the 2 and 4 σ contours

Compared to $B^+ \to \tau\nu_\tau$, the $B \to D^{(*)}\tau\nu_\tau$ decay has advantages: the branching fraction is relatively high, because it is not Cabibbo-suppressed, and it is a three-body decay allowing access to many observables besides the branching fraction, such as $D^{(*)}$ momentum, q^2 distributions, and measurements of the D^* and τ polarisations (see Ref. [572] and references therein for recent calculations).

Experiments have measured two ratios of branching fractions defined as

$$\mathcal{R}(D) = \frac{\mathcal{B}(B \to D\tau\nu_\tau)}{\mathcal{B}(B \to D\ell\nu_\ell)}, \tag{217}$$

$$\mathcal{R}(D^*) = \frac{\mathcal{B}(B \to D^*\tau\nu_\tau)}{\mathcal{B}(B \to D^*\ell\nu_\ell)} \tag{218}$$

where ℓ refers either to electron or μ. These ratios are independent of $|V_{cb}|$ and to a large extent, also of the $B \to D^{(*)}$ form factors. As a consequences the SM predictions for these ratios are quite precise:

- $\mathcal{R}(D) = 0.300 \pm 0.008$, which is an average obtained by FLAG [222] by combining the most recent lattice calculations of the $B \to D\ell\nu$ form factors [494,573];
- $\mathcal{R}(D^*) = 0.252 \pm 0.003$, which is a prediction, [574,575] that updates recent QCD calculations [576,577] based on the recent $B \to D^*$ measurements from the B-Factories.

Recently, in Ref. [578] Bigi and Gambino re-analysed the recent experimental results and theoretical calculation of $B \to D\ell\nu$ obtaining $\mathcal{R}(D) = 0.299 \pm 0.003$, compatible with the predictions reported above but with a total error reduced by a factor three.

From the experimental side, in the case of the leptonic τ decay, the ratios $\mathcal{R}(D^{(*)})$ can be directly measured, and many systematic uncertainties cancel in the measurement. The $B^0 \to D^{*+}\tau\nu_\tau$ decay was first observed by Belle [579] performing an "inclusive" reconstruction, which is based on the reconstruction of the B_{tag} from all the particles of the events, other than the $D^{(*)}$ and the lepton candidate, without looking for any specific B_{tag} decay chain. Since then, both BABAR and Belle have published improved measurements and have found evidence for the $B \to D\tau\nu_\tau$ decays [580,581].

The most powerful way to study these decays at the B-Factories exploits the hadronic B_{tag}. Using the full dataset and an improved B_{tag} selection, BABAR measured [574]:

$$\mathcal{R}(D) = 0.440 \pm 0.058 \pm 0.042,$$
$$\mathcal{R}(D^*) = 0.332 \pm 0.024 \pm 0.018 \tag{219}$$

where decays to both $e^\pm$ and $\mu^\pm$ were summed and B^0 and B^- were combined in a isospin-constrained fit. The fact that the BABAR result exceeded SM predictions by 3.4σ, raised considerable interest.

Belle published various measurements using different techniques, and LHCb also joined the effort with a measurement of $R(D^*)$. The most important sources of systematic uncertainties correlated for the different measurement is due to the $B \to D^{**}$ background components that are difficult to disentangle from the signal. In the average the systematic uncertainties due to the $B \to D^{**}$ composition and kinematics are considered fully correlated among the measurements.

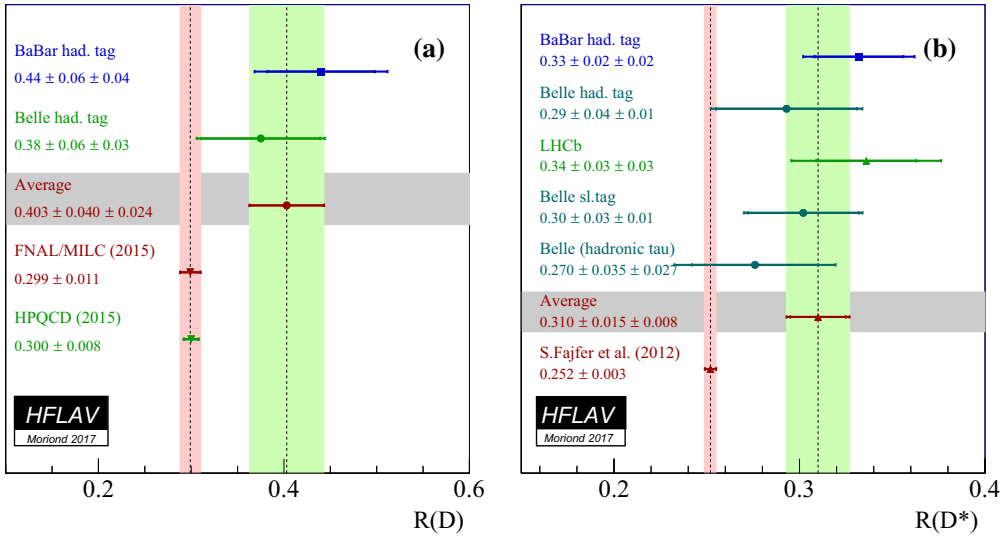

Fig. 67 **a** Measurement of $\mathcal{R}(D)$ and **b** $\mathcal{R}(D^*)$. The average is the projection of the average obtained from the combined fit

The results of the individual measurements, their averages and correlations are presented in Table 92 and Fig. 66. The combined results, projected separately on $\mathcal{R}(D)$ and $\mathcal{R}(D^*)$, are reported in Fig. 67a, b respectively.

The averaged $\mathcal{R}(D)$ and $\mathcal{R}(D^*)$ exceed the SM predictions by 2.2σ and 3.4σ respectively. Considering the $\mathcal{R}(D)$ and $\mathcal{R}(D^*)$ total correlation of -0.23, the difference with respect to the SM is about 3.9 σ, the combined $\chi^2 = 18.83$ for 2 degrees of freedom corresponds to a p-value of 8.3×10^{-5}, assuming Gaussian error distributions.

6 Decays of *b*-hadrons into open or hidden charm hadrons

Ground state B mesons and b baryons dominantly decay to particles containing a charm quark via the $b \to c$ quark transition. In this section, measurements of such decays to hadronic final states are considered; semileptonic decay modes, which are usually used to determine the strength of the $b \to c$ transition as quantified in the magnitude of the CKM matrix element $|V_{cb}|$, are discussed in Sect. 5. Some B meson decays to open or hidden charm hadrons that are fundamental for the measurements of CP-violation phases – like $\phi_s^{c\bar{c}s}$ (Sect. 3), $\beta \equiv \phi_1$ and $\gamma \equiv \phi_3$ (Sect. 4) – are discussed elsewhere in this report. Similarly, the use of $b \to c$ decay modes for the determination of important properties of b-hadrons, like their masses or (absolute, relative or effective) lifetimes, is discussed in Sect. 3. The properties of certain b hadron decays to open or hidden charm hadrons, such as small Q values and similar topologies for different modes, allow the minimization of systematic uncertainties in these measurements.

The fact that decays to final states containing open or hidden charm hadrons dominate the b-hadron widths makes them a very important part of the experimental programme in heavy flavor physics. Understanding the rate of charm production in b-hadron decays is crucial to validate the HQE that underpins much of the theoretical framework for b physics (see, for example, Ref. [586] for a review). Moreover, such decays are often used as normalization modes for measurements of rarer decays. In addition, they are the dominant background in many analyses. To model accurately such backgrounds with simulated data, it is essential to have precise knowledge of the contributing decay modes. In particular, with the expected increase in the data samples at LHCb and Belle II, the enhanced statistical sensitivity has to be matched by low systematic uncertainties due to knowledge of the dominant b-hadron decay modes. For multibody decays, knowledge of the distribution of decays across the phase-space (e.g., the Dalitz plot density for three-body decays or the polarization amplitudes for vector-vector final states) is required in addition to the total branching fraction.

The large yields of $b \to c$ decays to multibody final states make them ideal to study the spectroscopy of both open and hidden charm hadrons. In particular, they have been used to both discover, and measure the properties of, exotic particles such as the $X(3872)$ [587,588], $Z(4430)^+$ [589,590] and $P_c(4450)^+$ [591] states. The large yields available similarly make decays involving $b \to c$ transitions very useful to study baryon-antibaryon pair production.

In addition to the dominant b-hadron decays to final states containing charmed hadrons, there are several decays in this category that are expected to be highly suppressed in the Standard Model. These are of interest to probe particular decay topologies (e.g., the $B^- \to D_s^- \phi$ decay, which is dominated by the annihilation diagram) and thereby constrain effects in other hadronic decays or to search for new physics. There are also other decays involving $b \to c$ transitions, such as $\overline{B}^0 \to D_s^- \pi^+$, that are mediated by the W emission involving the $|V_{ub}|$ CKM matrix element. Finally, some $b \to c$ decays involving lepton flavour or number violation are extremely suppressed in the Standard Model, and therefore provide highly sensitive null tests.

In this section, we give an exhaustive list of measured branching ratios of decay modes to hadrons containing charm quarks. The averaging procedure follows the methodology described in Sect. 2. Where available, correlations between measurements are taken into account. If an insignificant measurement and a limit for the same parameter are provided the former is taken so that it can be included in averages. The confidence level of an average is quoted if it is below 1%. We provide averages of the polarization amplitudes of B meson decays to vector-vector states, but we do not currently provide detailed averages of quantities obtained from Dalitz plot analyses, due to the complications arising from the dependence on the model used.

The results are presented in subsections organized according to the type of decaying bottom hadron: $\overline{B}^0$ (Sect. 6.1), B^- (Sect. 6.2), $\overline{B}^0/B^-$ admixture (Sect. 6.3), $\overline{B}_s^0$ (Sect. 6.4), B_c^- (Sect. 6.5), b baryons (Sect. 6.6). For each subsection the measurements are arranged according to the final state into the following groups: a single charmed meson, two charmed mesons, a charmonium state, a charm baryon, or other states, like for example the $X(3872)$ meson. The individual measurements and averages are shown as numerical values in tables followed by a graphical representation of the averages. The symbol $\mathcal{B}$ is used for branching ratios, f for production fractions (see Sect. 3), and σ for cross sections. The decay amplitudes for longitudinal, parallel, and perpendicular transverse polarization in pseudoscalar to vector-vector decays are denoted $\mathcal{A}_0$, $\mathcal{A}_\parallel$, and $\mathcal{A}_\perp$, respectively, and the definitions $\delta_\parallel = \arg(\mathcal{A}_\parallel/\mathcal{A}_0)$ and $\delta_\perp = \arg(\mathcal{A}_\perp/\mathcal{A}_0)$ are used for their relative phases. The inclusion of charge conjugate modes is always implied.

Following the approach used by the PDG [327], for decays that involve neutral kaons we mainly quote results in terms of final states including either a K^0 or $\overline{K}^0$ meson (instead of a K_S^0 or K_L^0). In some cases where the decay is not flavour-specific and the final state is not self-conjugate, the inclusion of the conjugate final state neutral kaon is implied – in fact, the flavour of the neutral kaon is never determined experimentally, and so the specification as K^0 or $\overline{K}^0$ simply follows the quark model expectation for the dominant decay. An exception occurs for some B_s^0 decays, specifically those to CP eigenstates, where the width difference between the mass eigenstates (see Sect. 3) means that the measured branching fraction, integrated over decay time, is specific to the studied final state [592]. Therefore it is appropriate to quote the branching fraction for, e.g., $\overline{B}_s^0 \to J/\psi K_S^0$ instead of $\overline{B}_s^0 \to J/\psi \overline{K}^0$.

Several measurements assume $\Gamma(\Upsilon(4S) \to B^+B^-) = \Gamma(\Upsilon(4S) \to B^0\bar{B}^0)$. While there is no evidence for isospin violation in $\Upsilon(4S)$ decays, deviations from this assumptions can be of the order of a few percent, see Sect. 3.1.1 and Ref. [593]. As the effect is negligible for many averages, we do not apply a correction or additional systematic uncertainty, but we point out that it can be relevant for averages with a percent level uncertainty.

6.1 Decays of $\bar{B}^0$ mesons

Measurements of $\bar{B}^0$ decays to charmed hadrons are summarized in Sects. 6.1.1–6.1.5.

6.1.1 Decays to a single open charm meson

Averages of $\bar{B}^0$ decays to a single open charm meson are shown in Tables 93, 94, 95, 96, 97, 98, 99, 100, 101, 102, 103, 104, 105 and Figs. 68, 69, 70, 71, 72, 73, 74, 75, 76, 77, 78, 79, 80. In this section D^{**} refers to the sum of all the non-strange charm meson states with masses in the range 2.2–2.8 GeV/c^2.

Table 93 Decays to a $D^{(*)}$ meson and one or more pions I [10^{-3}]

Parameter	Measurements	Average
$\mathcal{B}(\bar{B}^0 \to D^+\pi^-)$	BaBar [594]: 2.55 ± 0.05 ± 0.16	2.65 ± 0.15
	BaBar [595]: 3.03 ± 0.23 ± 0.23	
$\mathcal{B}(\bar{B}^0 \to D^*(2010)^+\pi^-)$	BaBar [594]: 2.79 ± 0.08 ± 0.17	2.84 ± 0.16
	BaBar [595]: 2.99 ± 0.23 ± 0.24	
$\mathcal{B}(\bar{B}^0 \to D^*(2010)^+\pi^-\pi^+\pi^-)$	Belle [596]: 6.81 ± 0.23 ± 0.72	7.19 ± 0.30
	BaBar [597]: 7.26 ± 0.11 ± 0.31	
$\mathcal{B}(\bar{B}^0 \to D^*(2007)^0\pi^-\pi^+\pi^-\pi^+)$	Belle [596]: 2.60 ± 0.47 ± 0.37	2.60 ± 0.60
$\mathcal{B}(\bar{B}^0 \to D^*(2010)^+\pi^-\pi^+\pi^-\pi^+\pi^-)$	Belle [596]: 4.72 ± 0.59 ± 0.71	4.72 ± 0.92
$\mathcal{B}(\bar{B}^0 \to D^*(2010)^+\omega(782)\pi^-)$	Belle [598]: 2.31 ± 0.11 ± 0.14	2.41 ± 0.16
	BaBar [599]: 2.88 ± 0.21 ± 0.31	

Table 94 Decays to a $D^{(*)}$ meson and one or more pions II [10^{-4}]

Parameter	Measurements	Average
$\mathcal{B}(\bar{B}^0 \to D^0\pi^0)$	Belle [600]: 2.25 ± 0.14 ± 0.35	2.62 ± 0.15
	BaBar [601]: 2.69 ± 0.09 ± 0.13	
$\mathcal{B}(\bar{B}^0 \to D^*(2007)^0\pi^0)$	Belle[600]: 1.39 ± 0.18 ± 0.26	2.23 ± 0.22 CL = 0.2‰
	BaBar [601]: 3.05 ± 0.14 ± 0.28	
$\mathcal{B}(\bar{B}^0 \to D^0\pi^+\pi^-)$	LHCb [602]: 8.46 ± 0.14 ± 0.49	8.42 ± 0.49
	Belle [603]: 8.0 ± 0.6 ± 1.5	8.42 ± 0.49
$\mathcal{B}(\bar{B}^0 \to D^*(2007)^0\pi^+\pi^-)$	Belle [603]: 6.2 ± 1.2 ± 1.8	6.2 ± 2.2

Table 95 Decays to a $D^{(*)0}$ meson and a light meson [10^{-4}]

Parameter	Measurements	Average
$\mathcal{B}(\bar{B}^0 \to D^0\rho(770)^0)$	Belle [603]: 2.9 ± 1.0 ± 0.4	2.9 ± 1.1
$\mathcal{B}(\bar{B}^0 \to D^*(2007)^0\rho(770)^0)$	Belle [603]: <5.1	<5.1
$\mathcal{B}(\bar{B}^0 \to D^0\eta)$	Belle [600]: 1.77 ± 0.16 ± 0.21	2.36 ± 0.13
	BaBar [601]: 2.53 ± 0.09 ± 0.11	
$\mathcal{B}(\bar{B}^0 \to D^*(2007)^0\eta)$	Belle [600]: 1.40 ± 0.28 ± 0.26	2.26 ± 0.22 CL = 5.8‰
	BaBar [601]: 2.69 ± 0.14 ± 0.23	
$\mathcal{B}(\bar{B}^0 \to D^0\eta'(958))$	Belle [604]: $1.14 \pm 0.20^{+0.10}_{-0.13}$	1.38 ± 0.12
	BaBar [601]: 1.48 ± 0.13 ± 0.07	
$\mathcal{B}(\bar{B}^0 \to D^*(2007)^0\eta'(958))$	Belle [604]: 1.21 ± 0.34 ± 0.22	1.40 ± 0.22
	BaBar [601]: 1.48 ± 0.22 ± 0.13	
$\mathcal{B}(\bar{B}^0 \to D^0\omega(782))$	LHCb [602]: $2.81 \pm 0.72^{+0.30}_{-0.33}$	
	Belle [600]: 2.37 ± 0.23 ± 0.28	2.54 ± 0.16
	BaBar [601]: 2.57 ± 0.11 ± 0.14	
$\mathcal{B}(\bar{B}^0 \to D^*(2007)^0\omega(782))$	Belle [600]: 2.29 ± 0.39 ± 0.40	3.64 ± 0.35 CL = 1.8‰
	BaBar [601]: 4.55 ± 0.24 ± 0.39	$1.61^{+0.22}_{-0.21}$
$\mathcal{B}(\bar{B}^0 \to D^0 f_2(1270))$	LHCb [602]: $1.61 \pm 0.11^{+0.19}_{-0.18}$	

Table 96 Decays to a $D^{(*)+}$ meson and one or more kaons [10^{-3}]

Parameter	Measurements	Average
$\mathcal{B}(\bar{B}^0 \to D^+ K^-)$	LHCb [47]: 0.220 ± 0.003 ± 0.013	0.219 ± 0.013
	Belle [605]: 0.204 ± 0.045 ± 0.034	
$\mathcal{B}(\bar{B}^0 \to D^*(2010)^+ K^-)$	Belle [605]: 0.204 ± 0.041 ± 0.023	0.204 ± 0.047
$\mathcal{B}(\bar{B}^0 \to D^+ K^*(892)^-)$	BaBar [606]: 0.46 ± 0.06 ± 0.05	0.46 ± 0.08
$\mathcal{B}(\bar{B}^0 \to D^*(2010)^+ K^*(892)^-)$	BaBar [606]: 0.32 ± 0.06 ± 0.03	0.32 ± 0.07
$\mathcal{B}(\bar{B}^0 \to D^+ K^0 \pi^-)$	BaBar [606]: 0.49 ± 0.07 ± 0.05	0.49 ± 0.09
$\mathcal{B}(\bar{B}^0 \to D^*(2010)^+ K^0 \pi^-)$	BaBar [606]: 0.30 ± 0.07 ± 0.03	0.30 ± 0.08
$\mathcal{B}(\bar{B}^0 \to D^+ K^- K^0)$	Belle [607]: <0.31	<0.31
$\mathcal{B}(\bar{B}^0 \to D^*(2010)^+ K^- K^0)$	Belle [607]: <0.47	<0.47
$\mathcal{B}(\bar{B}^0 \to D^+ K^- K^*(892)^0)$	Belle [607]: 0.88 ± 0.11 ± 0.15	0.88 ± 0.19
$\mathcal{B}(\bar{B}^0 \to D^*(2010)^+ K^- K^*(892)^0)$	Belle [607]: 1.29 ± 0.22 ± 0.25	1.29 ± 0.33

Table 97 Decays to a $D^{(*)0}$ meson and a kaon [10^{-4}]

Parameter	Measurements	Average
$\mathcal{B}(\bar{B}^0 \to D^0 \bar{K}^0)$	Belle [608]: $0.50\,^{+0.13}_{-0.12} \pm 0.06$	0.52 ± 0.07
	BaBar [609]: 0.53 ± 0.07 ± 0.03	
$\mathcal{B}(\bar{B}^0 \to D^*(2007)^0 \bar{K}^0)$	Belle [608]: <0.66	0.36 ± 0.12
	BaBar [609]: 0.36 ± 0.12 ± 0.03	
$\mathcal{B}(\bar{B}^0 \to D^0 K^- \pi^+)$	BaBar [610]: 0.88 ± 0.15 ± 0.09	0.88 ± 0.17
$\mathcal{B}(\bar{B}^0 \to D^0 \bar{K}^*(892)^0)$	Belle [608]: $0.48\,^{+0.11}_{-0.10} \pm 0.05$	0.42 ± 0.06
	BaBar [609]: 0.40 ± 0.07 ± 0.03	
$\mathcal{B}(\bar{B}^0 \to D^0 \bar{K}^*(892)^0) \times \mathcal{B}(\bar{K}^*(892)^0 \to K^- \pi^+)$	BaBar [610]: 0.38 ± 0.06 ± 0.04	0.38 ± 0.07
$\mathcal{B}(\bar{B}^0 \to D^*(2007)^0 \bar{K}^*(892)^0)$	Belle [608]: <0.69	<0.69
$\mathcal{B}(\bar{B}^0 \to \bar{D}^*(2007)^0 \bar{K}^*(892)^0)$	Belle [608]: <0.40	<0.40
$\mathcal{B}(\bar{B}^0 \to \bar{D}^0 K^- \pi^+)$	BaBar [610]: <0.19	<0.19
$\mathcal{B}(\bar{B}^0 \to \bar{D}^0 \bar{K}^*(892)^0)$	Belle [608]: <0.18	0.00 ± 0.06
	BaBar [609]: 0.00 ± 0.05 ± 0.03	

Table 98 Decays to a $D_s^{(*)}$ meson [10^{-4}]

Parameter	Measurements	Average
$\mathcal{B}(\bar{B}^0 \to D_s^- \pi^+)$	Belle [611]: 0.199 ± 0.026 ± 0.018	0.216 ± 0.026
	BaBar [612]: 0.25 ± 0.04 ± 0.02	
$\mathcal{B}(\bar{B}^0 \to D_s^{*-} \pi^+)$	Belle [613]: 0.175 ± 0.034 ± 0.020	0.207 ± 0.032
	BaBar [612]: $0.26\,^{+0.05}_{-0.04} \pm 0.02$	
$\mathcal{B}(\bar{B}^0 \to D_s^- \rho(770)^+)$	BaBar [612]: $0.11\,^{+0.09}_{-0.08} \pm 0.03$	$0.11\,^{+0.09}_{-0.09}$
$\mathcal{B}(\bar{B}^0 \to D_s^{*-} \rho(770)^+)$	BaBar [612]: $0.41\,^{+0.13}_{-0.12} \pm 0.04$	$0.41\,^{+0.14}_{-0.13}$
$\mathcal{B}(\bar{B}^0 \to D_s^- a_0(980)^+)$	BaBar [614]: $0.06\,^{+0.14}_{-0.11} \pm 0.01$	$0.06\,^{+0.14}_{-0.11}$
$\mathcal{B}(\bar{B}^0 \to D_s^{*-} a_0(980)^+)$	BaBar [614]: $0.14\,^{+0.21}_{-0.16} \pm 0.03$	$0.14\,^{+0.21}_{-0.16}$
$\mathcal{B}(\bar{B}^0 \to D_s^- a_2(1320)^+)$	BaBar [614]: $0.64\,^{+1.04}_{-0.57} \pm 0.15$	$0.64\,^{+1.05}_{-0.59}$
$\mathcal{B}(\bar{B}^0 \to D_s^{*-} a_2(1320)^+)$	BaBar [614]: <2.0	<2.0
$\mathcal{B}(\bar{B}^0 \to D_s^+ K^-)$	Belle [611]: 0.191 ± 0.024 ± 0.017	0.221 ± 0.025
	BaBar [612]: 0.29 ± 0.04 ± 0.02	
$\mathcal{B}(\bar{B}^0 \to D_s^{*+} K^-)$	Belle [613]: 0.202 ± 0.033 ± 0.022	0.219 ± 0.031
	BaBar [612]: 0.24 ± 0.04 ± 0.02	
$\mathcal{B}(\bar{B}^0 \to D_s^+ K^*(892)^-)$	BaBar [612]: $0.35\,^{+0.10}_{-0.09} \pm 0.04$	$0.35\,^{+0.11}_{-0.10}$
$\mathcal{B}(\bar{B}^0 \to D_s^{*+} K^*(892)^-)$	BaBar [612]: $0.32\,^{+0.14}_{-0.12} \pm 0.04$	$0.32\,^{+0.15}_{-0.13}$
$\mathcal{B}(\bar{B}^0 \to D_s^+ K_S^0 \pi^-)$	BaBar [615]: 0.55 ± 0.13 ± 0.10	0.55 ± 0.17
$\mathcal{B}(\bar{B}^0 \to D_s^{*+} K^0 \pi^-)$	BaBar [615]: <0.55	<0.55

Table 99 Relative decay rates I

Parameter	Measurements	Average
$\mathcal{B}(\bar{B}^0 \to D^0\rho(770)^0)/\mathcal{B}(\bar{B}^0 \to D^0\omega(782))$	Belle [603]: 1.6 ± 0.8	1.6 ± 0.8
$\mathcal{B}(\bar{B}^0 \to D^+\pi^+\pi^-\pi^-)/\mathcal{B}(\bar{B}^0 \to D^+\pi^-)$	LHCb [616]: $2.38 \pm 0.11 \pm 0.21$	2.38 ± 0.24
$\mathcal{B}(\bar{B}^0 \to D^*(2010)^+\pi^-)/\mathcal{B}(\bar{B}^0 \to D^+\pi^-)$	BaBar [595]: $0.99 \pm 0.11 \pm 0.08$	0.99 ± 0.14
$\mathcal{B}(\bar{B}^0 \to D^{**+}\pi^-)/\mathcal{B}(\bar{B}^0 \to D^+\pi^-)$	BaBar [595]: $0.77 \pm 0.22 \pm 0.29$	0.77 ± 0.36
$\mathcal{B}(\bar{B}^0 \to D_s^+K^-\pi^+\pi^-)/\mathcal{B}(\bar{B}_s^0 \to D_s^+K^-\pi^+\pi^-)$	LHCb [617]: $0.54 \pm 0.07 \pm 0.07$	0.54 ± 0.10

Table 100 Relative decay rates II

Parameter	Measurements	Average
$\mathcal{B}(\bar{B}^0 \to D^0K^-\pi^+)/\mathcal{B}(\bar{B}^0 \to D^0\pi^-\pi^+)$	LHCb [618]: $0.106 \pm 0.007 \pm 0.008$	0.106 ± 0.011
$\mathcal{B}(\bar{B}^0 \to \bar{D}^0K^-K^+)/\mathcal{B}(\bar{B}^0 \to \bar{D}^0\pi^-\pi^+)$	LHCb [619]: $0.056 \pm 0.110 \pm 0.007$	0.056 ± 0.110
$\mathcal{B}(\bar{B}^0 \to D^+K^-)/\mathcal{B}(\bar{B}^0 \to D^+\pi^-)$	LHCb [47]: $0.0822 \pm 0.0011 \pm 0.0025$	0.0818 ± 0.0027
	Belle [605]: $0.068 \pm 0.015 \pm 0.007$	
$\mathcal{B}(\bar{B}^0 \to D^+K^-\pi^+\pi^-)/\ \mathcal{B}(\bar{B}^0 \to D^+\pi^+\pi^-\pi^-)$	LHCb [620]: $0.059 \pm 0.011 \pm 0.005$	0.059 ± 0.012
$\mathcal{B}(\bar{B}^0 \to D^*(2010)^+K^-)/\mathcal{B}(\bar{B}^0 \to D^*(2010)^+\pi^-)$	Belle [605]: $0.074 \pm 0.015 \pm 0.006$	0.0773 ± 0.0043
	BaBar [610]: $0.0776 \pm 0.0034 \pm 0.0029$	
$\mathcal{B}(\bar{B}^0 \to D_s^+K^-)/\mathcal{B}(\bar{B}^0 \to D^+\pi^-)$	LHCb [621]: $0.0129 \pm 0.0005 \pm 0.0008$	0.0129 ± 0.0009

Table 101 Absolute product decay rates to excited D mesons I [10^{-4}]

Parameter	Measurements	Average
$\mathcal{B}(\bar{B}^0 \to D_1(2420)^+\pi^-) \times \mathcal{B}(D_1(2420)^+ \to D^+\pi^-\pi^+)$	Belle [622]: $0.89 \pm 0.15\,^{+0.17}_{-0.31}$	$0.89\,^{+0.23}_{-0.34}$
$\mathcal{B}(\bar{B}^0 \to D_1^0(H)\omega(782)) \times \mathcal{B}(D_1^0(H) \to D^*(2010)^+\pi^-)$	BaBar [599]: $4.1 \pm 1.2 \pm 1.1$	4.1 ± 1.6

Table 102 Absolute product decay rates to excited D mesons II [10^{-5}]

Parameter	Measurements	Average
$\mathcal{B}(\bar{B}^0 \to D_1(2420)^+\pi^-) \times \mathcal{B}(D_1(2420)^+ \to D^*(2010)^+\pi^-\pi^+)$	Belle [622]: <3.3	<3.3
$\mathcal{B}(\bar{B}^0 \to D_2^*(2460)^+\pi^-) \times \mathcal{B}(D_2^*(2460)^+ \to D^*(2010)^+\pi^-\pi^+)$	Belle [622]: <2.4	<2.4
$\mathcal{B}(\bar{B}^0 \to D_2^*(2460)^+K^-) \times \mathcal{B}(D_2^*(2460)^+ \to D^0\pi^+)$	BaBar [610]: $1.83 \pm 0.40 \pm 0.31$	1.83 ± 0.51
$\mathcal{B}(\bar{B}^0 \to D_{sJ}(2460)^-\pi^+) \times \mathcal{B}(D_{sJ}(2460)^- \to D_s^-\gamma)$	Belle [623]: <0.40	<0.40
$\mathcal{B}(\bar{B}^0 \to D_{sJ}^+(2460)K^-) \times \mathcal{B}(D_{sJ}^+(2460) \to D_s^+\gamma)$	Belle [623]: <0.94	<0.94
$\mathcal{B}(\bar{B}^0 \to D_{sJ}^*(2317)^-\pi^+) \times \mathcal{B}(D_{sJ}^*(2317)^- \to D_s^-\pi^0)$	Belle [623]: <2.5	<2.5
$\mathcal{B}(\bar{B}^0 \to D_{sJ}^*(2317)^+K^-) \times \mathcal{B}(D_{sJ}^*(2317)^+ \to D_s^+\pi^0)$	Belle [623]: $5.3\,^{+1.5}_{-1.3} \pm 1.6$	$5.3\,^{+2.2}_{-2.0}$

Table 103 Absolute and relative decay rates to excited D mesons [10^{-2}]

Parameter	Measurements	Average
$\mathcal{B}(\bar{B}^0 \to D^{**+}\pi^-)$	BaBar [595]: $0.234 \pm 0.065 \pm 0.088$	0.234 ± 0.109
$[\mathcal{B}(\bar{B}^0 \to D_1^+\pi^-) \times \mathcal{B}(D_1^+ \to D^+\pi^+\pi^-)]/$ $\mathcal{B}(\bar{B}^0 \to D^+\pi^+\pi^-\pi^-)$	LHCb [616]: $2.1 \pm 0.5\,^{+0.3}_{-0.5}$	$2.1\,^{+0.6}_{-0.7}$

Table 104 Baryonic decays I [10^{-4}]

Parameter	Measurements	Average
$\mathcal{B}(\bar{B}^0 \to D^+ p\bar{p}\pi^-)$	BaBar [624]: 3.32 ± 0.10 ± 0.29	3.32 ± 0.31
$\mathcal{B}(\bar{B}^0 \to D^*(2010)^+ p\bar{p}\pi^-)$	BaBar [624]: 4.55 ± 0.16 ± 0.39	4.55 ± 0.42
$\mathcal{B}(\bar{B}^0 \to D^0 p\bar{p}\pi^-\pi^+)$	BaBar [624]: 2.99 ± 0.21 ± 0.45	2.99 ± 0.50
$\mathcal{B}(\bar{B}^0 \to D^*(2007)^0 p\bar{p}\pi^-\pi^+)$	BaBar [624]: 1.91 ± 0.36 ± 0.29	1.91 ± 0.46

Table 105 Baryonic decays II [10^{-5}]

Parameter	Measurements	Average
$\mathcal{B}(\bar{B}^0 \to D^0 p\bar{p})$	Belle [625]: 11.8 ± 1.5 ± 1.6	10.4 ± 0.7
	BaBar [624]: 10.2 ± 0.4 ± 0.6	
$\mathcal{B}(\bar{B}^0 \to D^*(2007)^0 p\bar{p})$	Belle [625]: $12.0\,^{+3.3}_{-2.9}$ ± 2.1	9.9 ± 1.1
	BaBar [624]: 9.7 ± 0.7 ± 0.9	
$\mathcal{B}(\bar{B}^0 \to D_s^+ \Lambda\bar{p})$	Belle [626]: 2.9 ± 0.7 ± 0.6	2.9 ± 0.9
$\mathcal{B}(\bar{B}^0 \to D^0 \Lambda^0 \bar{\Lambda}^0)$	Belle [627]: $1.05\,^{+0.57}_{-0.44}$ ± 0.14	1.00 ± 0.28
	BaBar [628]: $0.98\,^{+0.29}_{-0.26}$ ± 0.19	
$\mathcal{B}(\bar{B}^0 \to D^0 \Sigma^0 \bar{\Lambda} + \bar{B}^0 \to D^0 \Lambda \bar{\Sigma}^0)$	BaBar [628]: $1.5\,^{+0.9}_{-0.8}$ ± 0.3	$1.5\,^{+0.9}_{-0.9}$
$\mathcal{B}(\bar{B}^0 \to D^+ \Lambda\bar{p})$	Belle [629]: 3.36 ± 0.63 ± 0.44	3.36 ± 0.77
$\mathcal{B}(\bar{B}^0 \to D^{*+} \Lambda\bar{p})$	Belle [629]: 2.51 ± 0.26 ± 0.35	2.51 ± 0.44

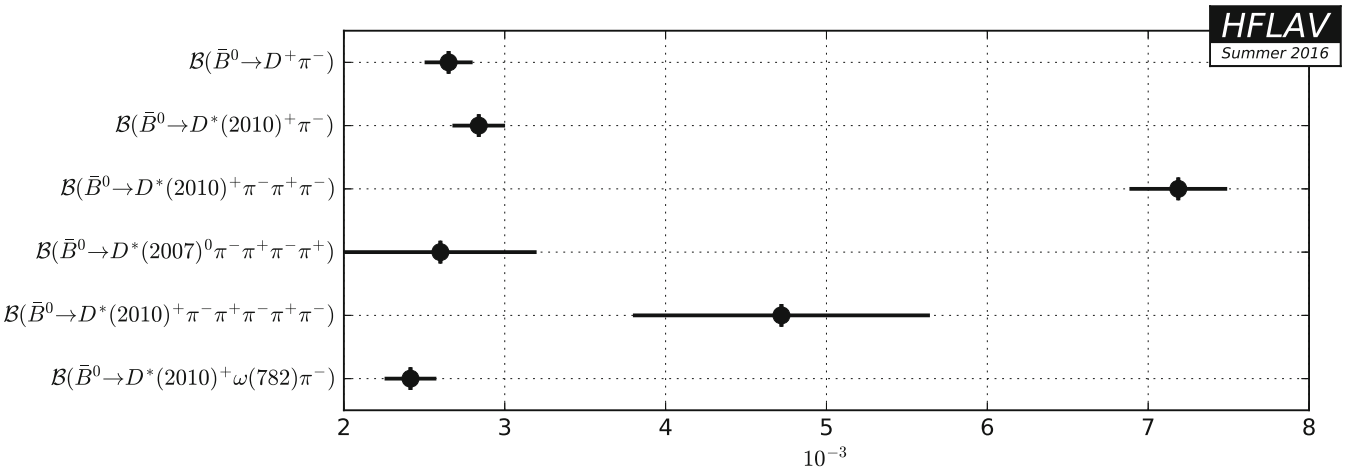

Fig. 68 Summary of the averages from Table 93

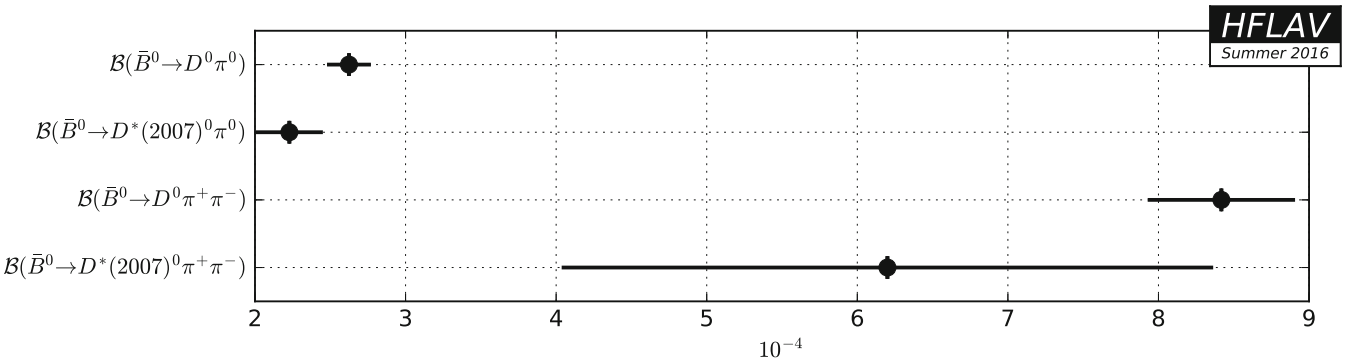

Fig. 69 Summary of the averages from Table 94

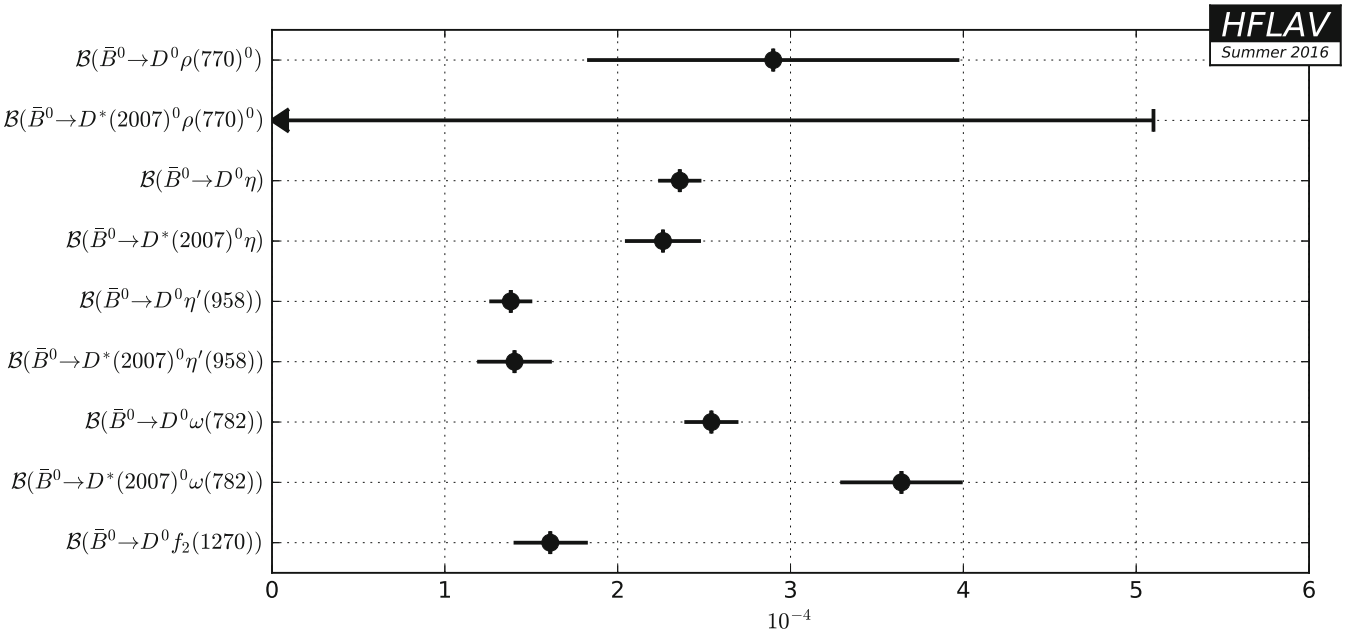

Fig. 70 Summary of the averages from Table 95

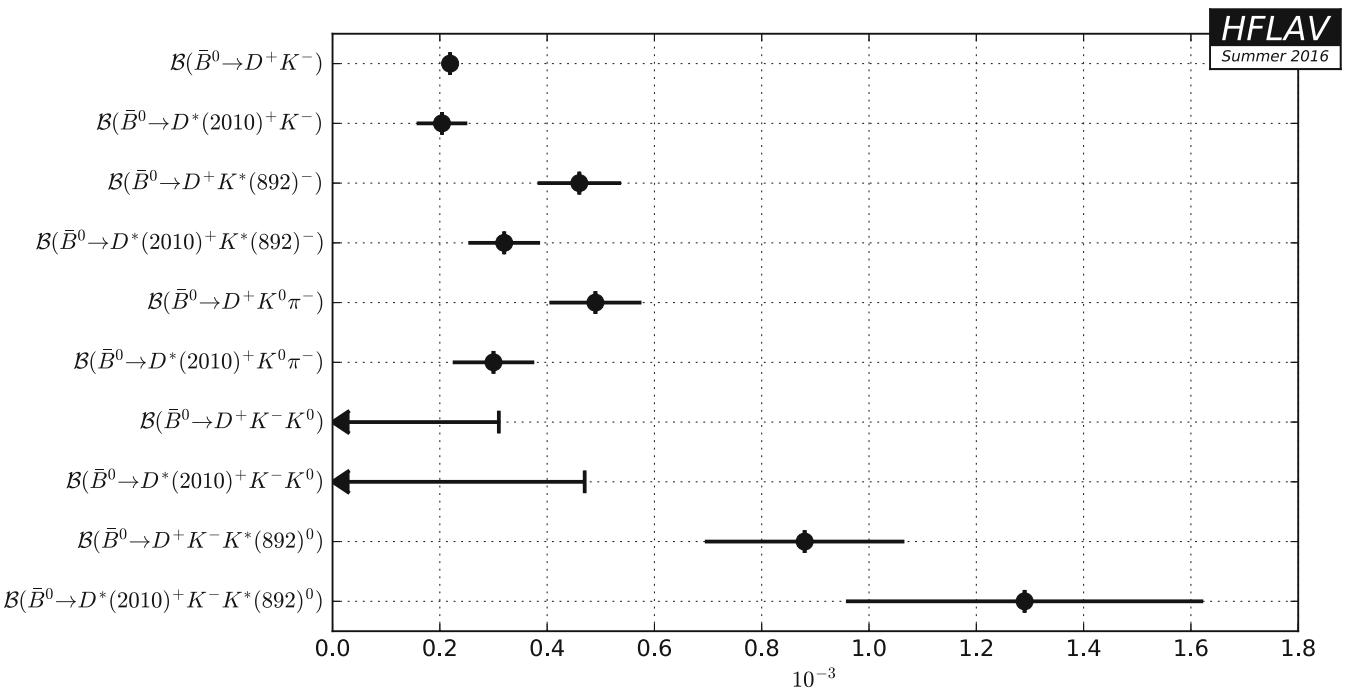

Fig. 71 Summary of the averages from Table 96

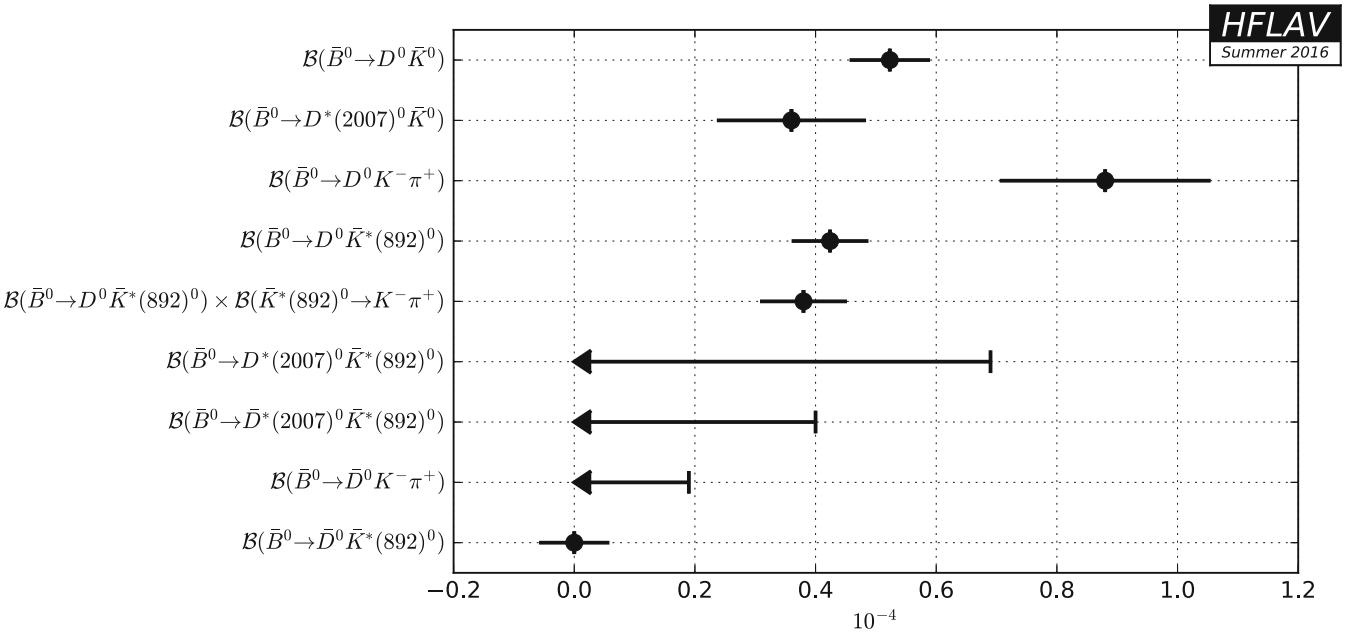

Fig. 72 Summary of the averages from Table 97

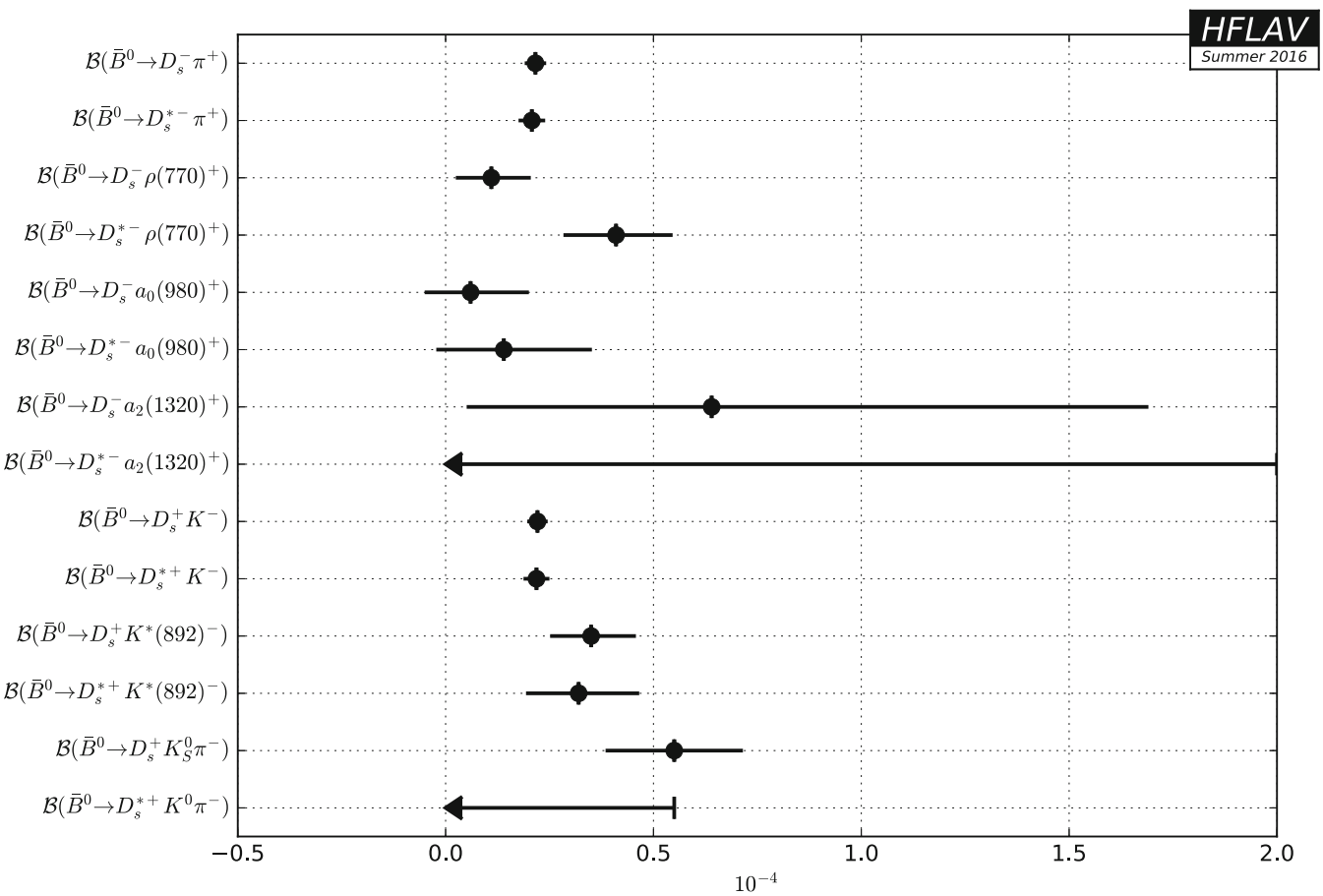

Fig. 73 Summary of the averages from Table 98

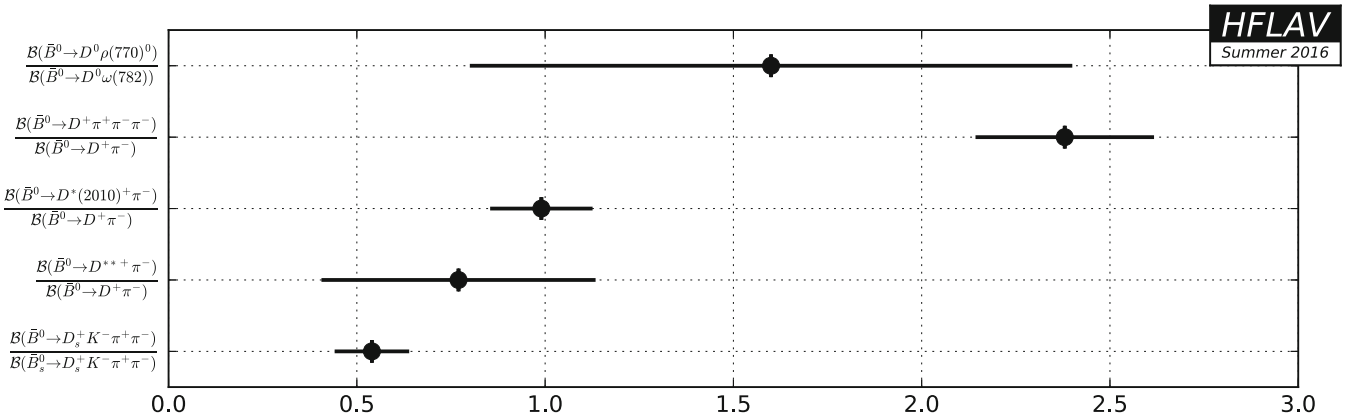

Fig. 74 Summary of the averages from Table 99

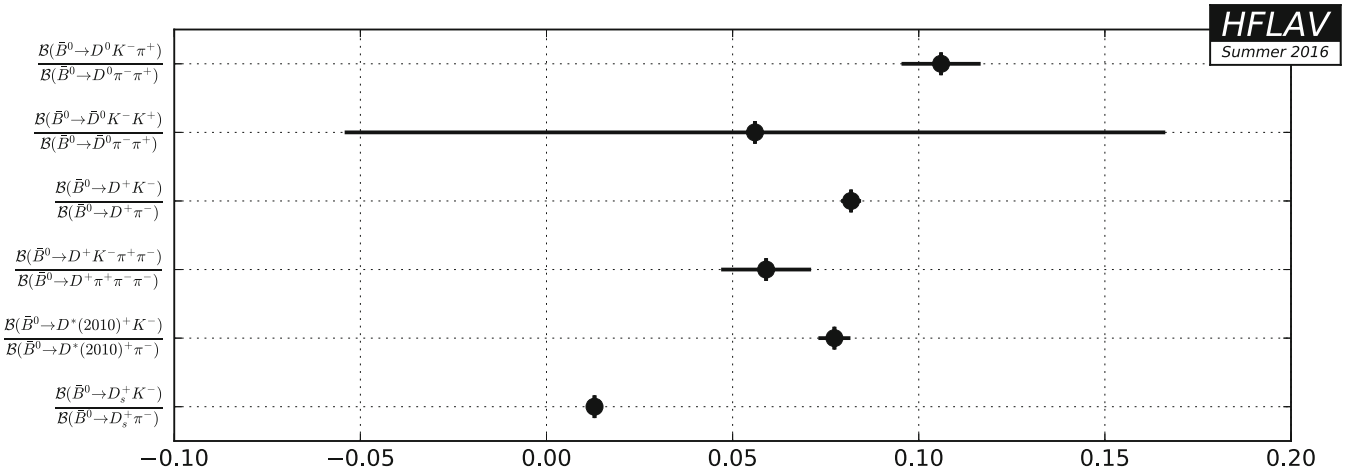

Fig. 75 Summary of the averages from Table 100

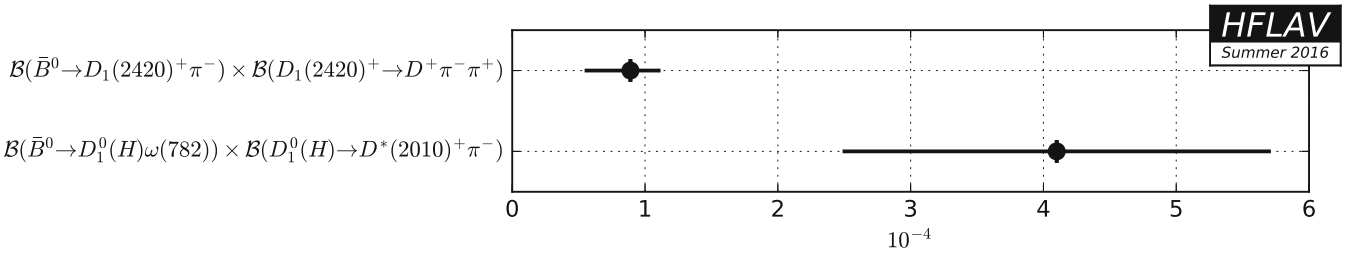

Fig. 76 Summary of the averages from Table 101

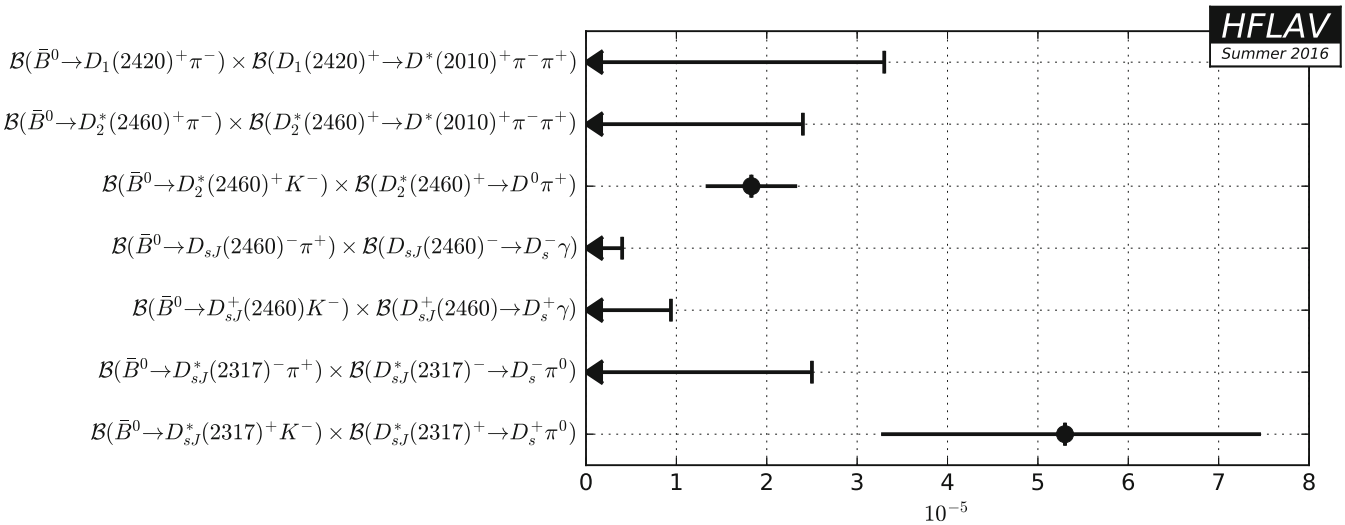

Fig. 77 Summary of the averages from Table 102

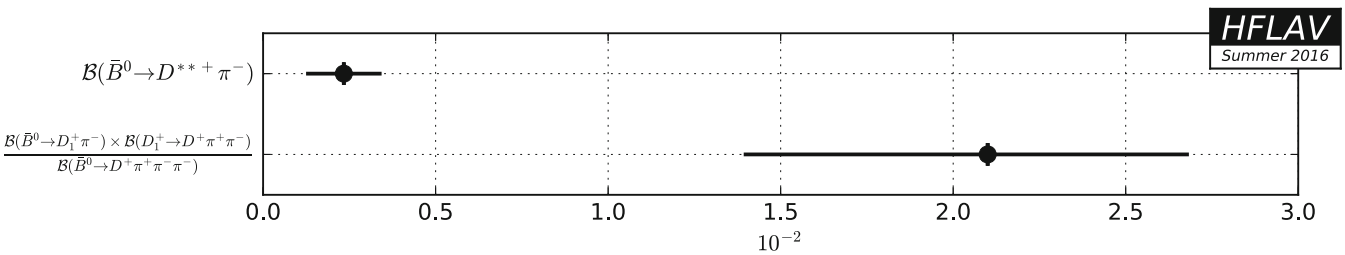

Fig. 78 Summary of the averages from Table103

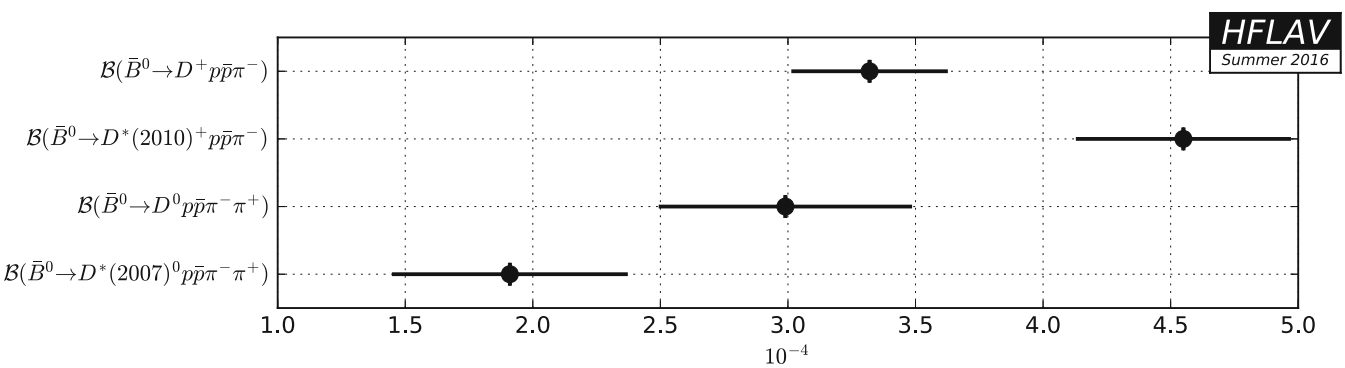

Fig. 79 Summary of the averages from Table 104

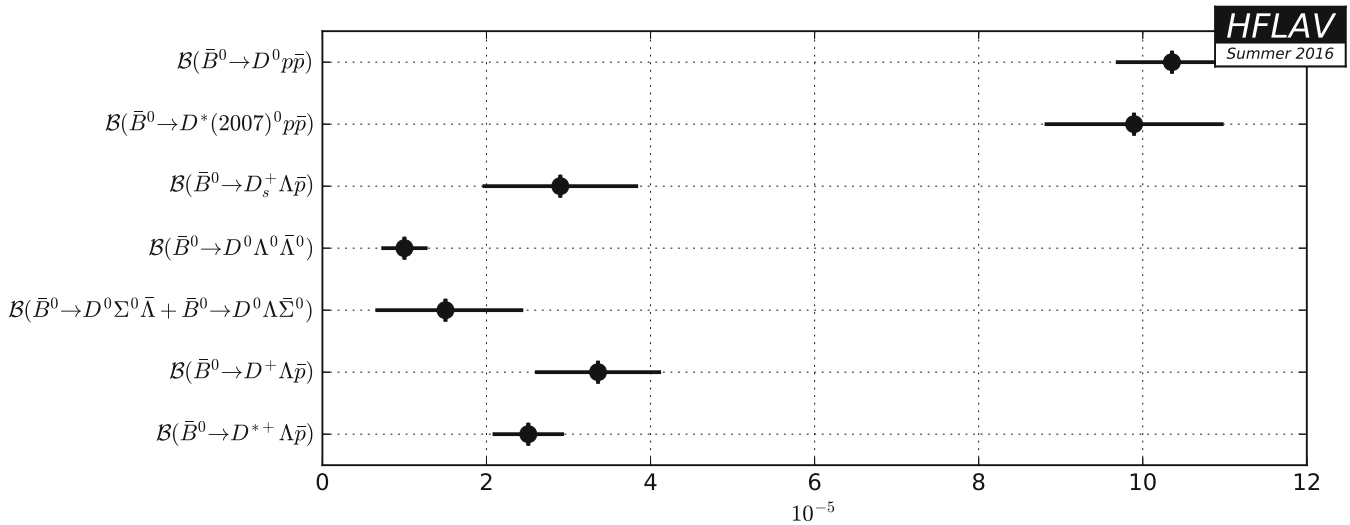

Fig. 80 Summary of the averages from Table 105

6.1.2 Decays to two open charm mesons

Averages of $\bar{B}^0$ decays to two open charm mesons are shown in Tables 106, 107, 108, 109, 110, 111, 112, 113, 114, 115 and Figs. 81, 82, 83, 84, 85, 86, 87, 88, 89.

Table 106 Decays to $D^{(*)+}D^{(*)-}$ [10^{-3}]

Parameter	Measurements	Average
$\mathcal{B}(\bar{B}^0 \to D^+D^-)$	Belle [287]: 0.212 ± 0.016 ± 0.018	0.220 ± 0.023
	BaBar [630]: 0.28 ± 0.04 ± 0.05	
$\mathcal{B}(\bar{B}^0 \to D^*(2010)^-D^+)$	Belle [287]: 0.614 ± 0.029 ± 0.050	0.603 ± 0.050
	BaBar [630]: 0.57 ± 0.07 ± 0.07	
$\mathcal{B}(\bar{B}^0 \to D^*(2010)^-D^*(2010)^+)$	Belle [352]: 0.782 ± 0.038 ± 0.060	0.790 ± 0.061
	BaBar [630]: 0.81 ± 0.06 ± 0.10	
$\mathcal{B}(\bar{B}^0 \to D^0\bar{D}^0)$	Belle [631]: <0.043	<0.043
	BaBar [630]: <0.06	
$\mathcal{B}(\bar{B}^0 \to D^0\bar{D}^*(2007)^0)$	BaBar [630]: <0.29	<0.29
$\mathcal{B}(\bar{B}^0 \to D^*(2007)^0\bar{D}^*(2007)^0)$	BaBar [630]: <0.09	<0.09

Table 107 Decays to two D mesons and a kaon I [10^{-3}]

Parameter	Measurements	Average
$\mathcal{B}(\bar{B}^0 \to D^*(2010)^+D^-\bar{K}^0)$	BaBar [632]: 6.41 ± 0.36 ± 0.39	6.41 ± 0.53
$\mathcal{B}(\bar{B}^0 \to D^*(2010)^-D^*(2010)^+\bar{K}^0)$	BaBar [632]: 8.26 ± 0.43 ± 0.67	8.26 ± 0.80
$\mathcal{B}(\bar{B}^0 \to D^*(2010)^+D^*(2010)^-K_S^0)$	Belle [266]: 3.4 ± 0.4 ± 0.7	3.9 ± 0.6
	BaBar [265]: 4.4 ± 0.4 ± 0.7	
$\mathcal{B}(\bar{B}^0 \to D^*(2010)^+\bar{D}^0K^-)$	BaBar [632]: 2.47 ± 0.10 ± 0.18	2.47 ± 0.21
$\mathcal{B}(\bar{B}^0 \to D^+\bar{D}^*(2007)^0K^-)$	BaBar [632]: 3.46 ± 0.18 ± 0.37	3.46 ± 0.41
$\mathcal{B}(\bar{B}^0 \to D^*(2010)^+\bar{D}^*(2007)^0K^-)$	BaBar [632]: 10.6 ± 0.3 ± 0.9	10.6 ± 0.9
$\mathcal{B}(\bar{B}^0 \to D^0\bar{D}^*(2007)^0\bar{K}^0)$	BaBar [632]: 1.08 ± 0.32 ± 0.36	1.08 ± 0.48
$\mathcal{B}(\bar{B}^0 \to D^*(2007)^0\bar{D}^*(2007)^0\bar{K}^0)$	BaBar [632]: 2.40 ± 0.55 ± 0.67	2.40 ± 0.87

Table 108 Decays to two D mesons and a kaon II [10^{-4}]

Parameter	Measurements	Average
$\mathcal{B}(\bar{B}^0 \to D^+ D^- \bar{K}^0)$	BaBar [632]: $7.5 \pm 1.2 \pm 1.2$	7.5 ± 1.7
$\mathcal{B}(\bar{B}^0 \to D^+ \bar{D}^0 K^-)$	BaBar [632]: $10.7 \pm 0.7 \pm 0.9$	10.7 ± 1.1
$\mathcal{B}(\bar{B}^0 \to D^0 \bar{D}^0 \bar{K}^0)$	BaBar [632]: $2.7 \pm 1.0 \pm 0.5$	2.7 ± 1.1
$\mathcal{B}(\bar{B}^0 \to D^0 \bar{D}^0 \pi^0 \bar{K}^0)$	Belle [633]: $1.73 \pm 0.70^{+0.31}_{-0.53}$	$1.73^{+0.77}_{-0.88}$

Table 109 Decays to $D_s^{(*)-} D^{(*)+}$ I [10^{-3}]

Parameter	Measurements	Average
$\mathcal{B}(\bar{B}^0 \to D_s^- D^+)$	Belle [634]: $7.5 \pm 0.2 \pm 1.1$	7.8 ± 1.0
	BaBar [635]: $9.0 \pm 1.8 \pm 1.4$	
$\mathcal{B}(\bar{B}^0 \to D_s^- D^*(2010)^+)$	BaBar [635]: $5.7 \pm 1.6 \pm 0.9$	6.8 ± 1.6
	BaBar [636]: $10.3 \pm 1.4 \pm 2.9$	
$\mathcal{B}(\bar{B}^0 \to D_s^{*-} D^*(2010)^+)$	BaBar [635]: $16.5 \pm 2.3 \pm 1.9$	
	BaBar [637]: $18.8 \pm 0.9 \pm 1.7$	18.1 ± 1.6
	BaBar [636]: $19.7 \pm 1.5 \pm 5.7$	
$\mathcal{B}(\bar{B}^0 \to D_s^{*-} D^+)$	BaBar [635]: $6.7 \pm 2.0 \pm 1.1$	6.7 ± 2.3

Table 110 Decays to $D_s^{(*)-} D^{(*)+}$ II [10^{-4}]

Parameter	Measurements	Average
$\mathcal{B}(\bar{B}^0 \to D_s^- D^+) \times \mathcal{B}(D_s^- \to \phi(1020)\pi^-)$	BaBar [635]: $2.67 \pm 0.61 \pm 0.47$	2.67 ± 0.77
$\mathcal{B}(\bar{B}^0 \to D_s^- D^*(2010)^+) \times \mathcal{B}(D_s^- \to \phi(1020)\pi^-)$	BaBar [635]: $5.11 \pm 0.94 \pm 0.72$	5.11 ± 1.18
$\mathcal{B}(\bar{B}^0 \to D_s^{*-} D^+) \times \mathcal{B}(D_s^- \to \phi(1020)\pi^-)$	BaBar [635]: $4.14 \pm 1.19 \pm 0.94$	4.14 ± 1.52
$\mathcal{B}(\bar{B}^0 \to D_s^{*-} D^*(2010)^+) \times \mathcal{B}(D_s^- \to \phi(1020)\pi^-)$	BaBar [635]: $12.2 \pm 2.2 \pm 2.2$	12.2 ± 3.1

Table 111 Decays to $D_s^{(*)+} D_s^{(*)-}$ [10^{-3}]

Parameter	Measurements	Average
$\mathcal{B}(\bar{B}^0 \to D_s^- D_s^+)$	Belle [634]: <0.036	<0.036
	BaBar [638]: <0.10	
$\mathcal{B}(\bar{B}^0 \to D_s^- D_s^{*+})$	BaBar [638]: <0.13	<0.13
$\mathcal{B}(\bar{B}^0 \to D_s^{*+} D_s^{*-})$	BaBar [638]: <0.24	<0.24

Table 112 Relative decay rates [10^{-3}]

Parameter	Measurements	Average
$\mathcal{B}(\bar{B}^0 \to D^0 \bar{D}^0)/\mathcal{B}(\bar{B}^- \to D^0 \bar{D}_s^-)$	LHCb [639]: $1.4 \pm 0.6 \pm 0.2$	1.4 ± 0.6

Table 113 Absolute decay rates to excited D_s mesons [10^{-3}]

Parameter	Measurements	Average
$\mathcal{B}(\bar{B}^0 \to D_{sJ}(2460)^- D^+)$	BaBar [635]: $2.6 \pm 1.5 \pm 0.7$	2.6 ± 1.7
$\mathcal{B}(\bar{B}^0 \to D_{sJ}(2460)^- D^*(2010)^+)$	BaBar [635]: $8.8 \pm 2.0 \pm 1.4$	8.8 ± 2.4
$\mathcal{B}(\bar{B}^0 \to D_{s1}(2536)^- D^*(2010)^+)$	BaBar [265]: $92 \pm 24 \pm 1$	92 ± 24

Table 114 Product decay rates to excited D_s mesons I [10^{-3}]

Parameter	Measurements	Average
$\mathcal{B}(\bar{B}^0 \to D^+ D_{sJ}(2460)^-) \times \mathcal{B}(D_{sJ}(2460)^- \to D_s^- \gamma)$	Belle [640]: $0.82^{+0.22}_{-0.19} \pm 0.25$	0.81 ± 0.23
	BaBar [641]: $0.8 \pm 0.2^{+0.3}_{-0.2}$	
$\mathcal{B}(\bar{B}^0 \to D^+ D_{sJ}(2460)^-) \times \mathcal{B}(D_{sJ}(2460)^- \to D_s^{*-} \pi^0)$	Belle [640]: $2.27^{+0.73}_{-0.62} \pm 0.68$	2.47 ± 0.76
	BaBar [641]: $2.8 \pm 0.8^{+1.1}_{-0.8}$	
$\mathcal{B}(\bar{B}^0 \to D_{sJ}(2460)^- D^*(2010)^+) \times \mathcal{B}(D_{sJ}(2460)^- \to D_s^{*-} \pi^0)$	BaBar [641]: $5.5 \pm 1.2^{+2.1}_{-1.6}$	$5.5^{+2.5}_{-2.0}$
$\mathcal{B}(\bar{B}^0 \to D_{sJ}(2460)^- D^*(2010)^+) \times \mathcal{B}(D_{sJ}(2460)^- \to D_s^- \gamma)$	BaBar [641]: $2.3 \pm 0.3^{+0.9}_{-0.6}$	$2.3^{+0.9}_{-0.7}$
$\mathcal{B}(\bar{B}^0 \to D_{sJ}^*(2317)^- D^*(2010)^+) \times \mathcal{B}(D_{sJ}^*(2317)^- \to D_s^- \pi^0)$	BaBar [641]: $1.5 \pm 0.4^{+0.5}_{-0.4}$	$1.5^{+0.7}_{-0.5}$
$\mathcal{B}(\bar{B}^0 \to D^+ D_{sJ}^*(2317)^-) \times \mathcal{B}(D_{sJ}^*(2317)^- \to D_s^- \pi^0)$	Belle [642]: $1.02^{+0.13}_{-0.12} \pm 0.11$	1.03 ± 0.16
	BaBar [641]: $1.8 \pm 0.4^{+0.7}_{-0.5}$	
$\mathcal{B}(\bar{B}^0 \to D^+ D_{sJ}^*(2317)^-) \times \mathcal{B}(D_{sJ}^*(2317)^- \to D_s^{*-} \gamma)$	Belle [640]: <0.95	<0.95

Table 115 Product decay rates to excited D_s mesons II [10^{-4}]

Parameter	Measurements	Average
$\mathcal{B}(\bar{B}^0 \to D_{s1}(2536)^- D^+) \times \mathcal{B}(D_{s1}(2536)^- \to D^*(2010)^- \bar{K}^0)$	BaBar [643]: $2.61 \pm 1.03 \pm 0.31$	2.61 ± 1.08
$\mathcal{B}(\bar{B}^0 \to D_{s1}(2536)^- D^+) \times \mathcal{B}(D_{s1}(2536)^- \to K^- \bar{D}^*(2007)^0)$	BaBar [643]: $1.71 \pm 0.48 \pm 0.32$	1.71 ± 0.58
$\mathcal{B}(\bar{B}^0 \to D_{s1}(2536)^- D^*(2010)^+) \times \mathcal{B}(D_{s1}(2536)^- \to D^*(2010)^- \bar{K}^0)$	BaBar [643]: $5.00 \pm 1.51 \pm 0.67$	5.00 ± 1.65
$\mathcal{B}(\bar{B}^0 \to D_{s1}(2536)^- D^*(2010)^+) \times \mathcal{B}(D_{s1}(2536)^- \to \bar{D}^*(2007)^0 K^+)$	BaBar [643]: $3.32 \pm 0.88 \pm 0.66$	3.32 ± 1.10
$\mathcal{B}(\bar{B}^0 \to D_{s1}(2536)^+ D^-) \times \mathcal{B}(D_{s1}(2536)^+ \to D^*(2007)^0 K^+ + D^*(2010)^+ K^0)$	Belle [644]: $2.75 \pm 0.62 \pm 0.36$	2.75 ± 0.72
$\mathcal{B}(\bar{B}^0 \to D_{s1}(2536)^+ D^*(2010)^-) \times \mathcal{B}(D_{s1}(2536)^+ \to D^*(2007)^0 K^+ + D^*(2010)^+ K^0)$	Belle [644]: $5.01 \pm 1.21 \pm 0.70$	5.01 ± 1.40
$\mathcal{B}(\bar{B}^0 \to D_{s1}(2536)^+ D^*(2010)^-) \times \mathcal{B}(D_{s1}(2536)^+ \to D^*(2010)^+ K_S^0)$	Belle [266]: <6.0	<6.0
$\mathcal{B}(\bar{B}^0 \to D^+ D_{sJ}(2460)^-) \times \mathcal{B}(D_{sJ}(2460)^- \to D_s^- \pi^+ \pi^-)$	Belle [640]: <2.0	<2.0
$\mathcal{B}(\bar{B}^0 \to D^+ D_{sJ}(2460)^-) \times \mathcal{B}(D_{sJ}(2460)^- \to D_s^- \pi^0)$	Belle [640]: <3.6	<3.6
$\mathcal{B}(\bar{B}^0 \to D^+ D_{sJ}(2460)^-) \times \mathcal{B}(D_{sJ}(2460)^- \to D_s^{*-} \gamma)$	Belle [640]: <6.0	<6.0

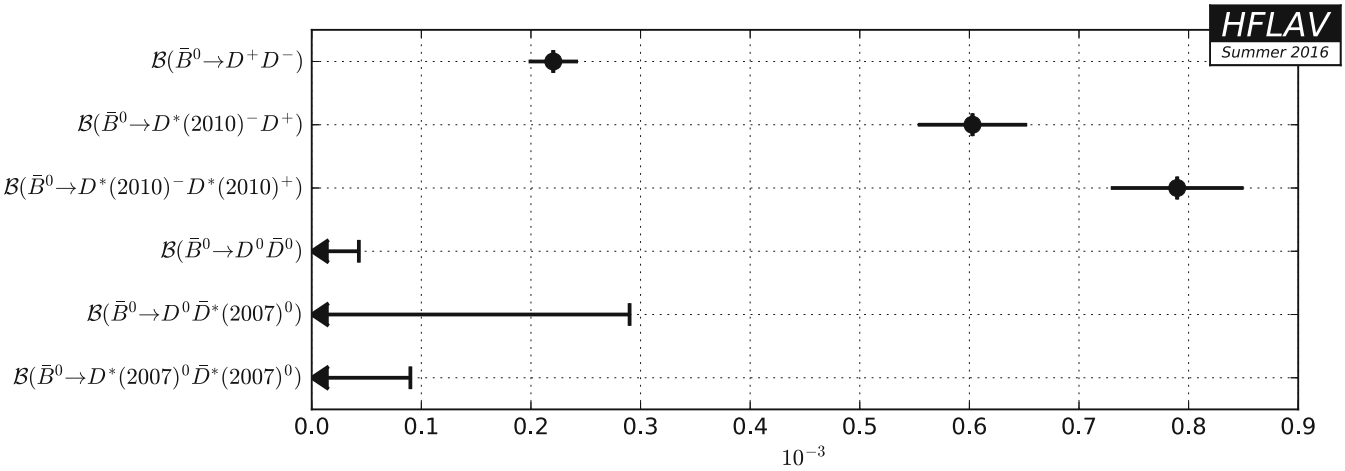

Fig. 81 Summary of the averages from Table 106

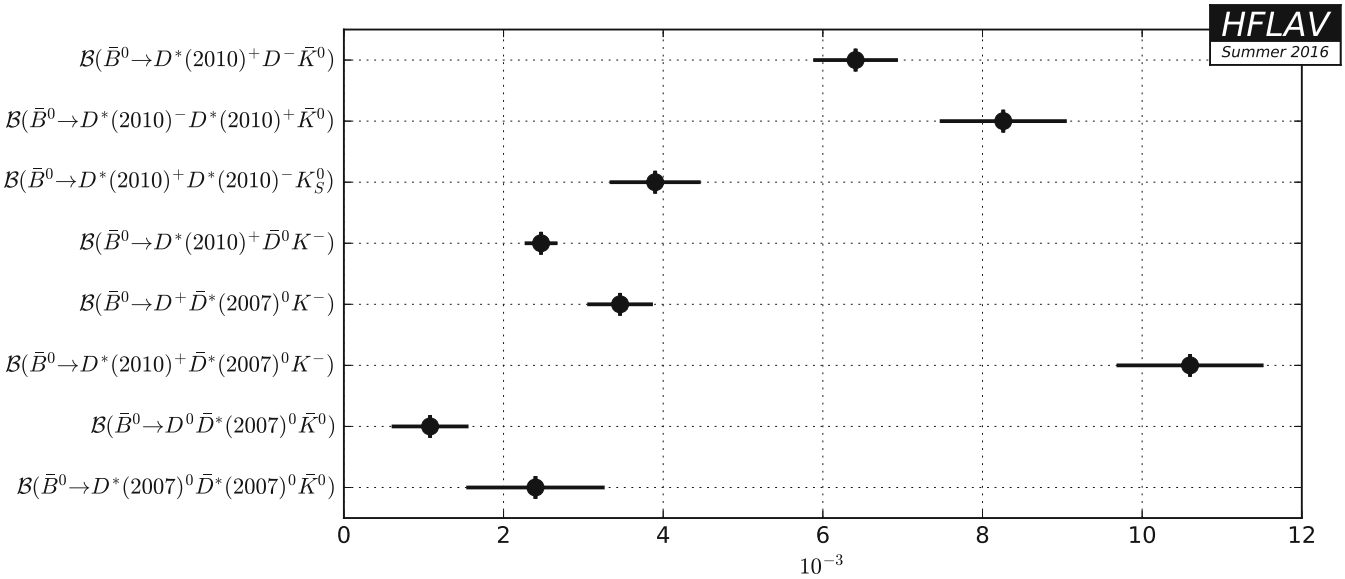

Fig. 82 Summary of the averages from Table 107

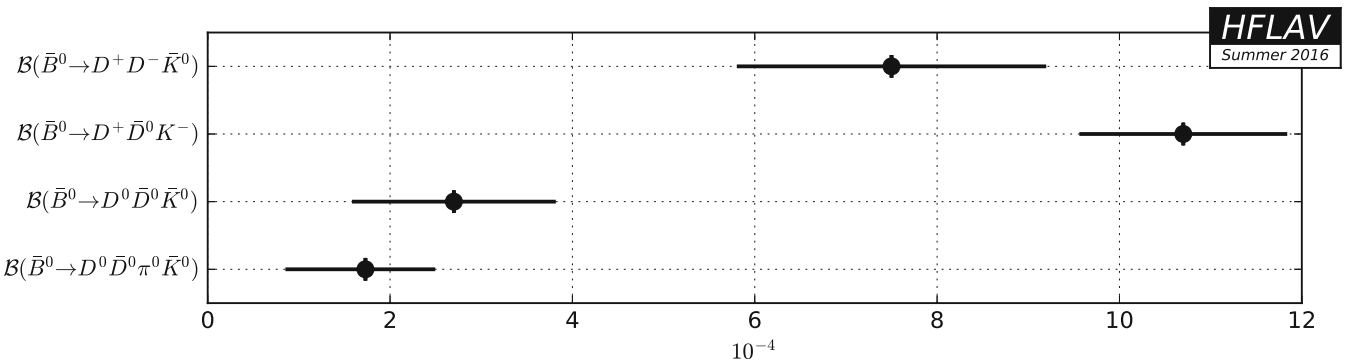

Fig. 83 Summary of the averages from Table 108

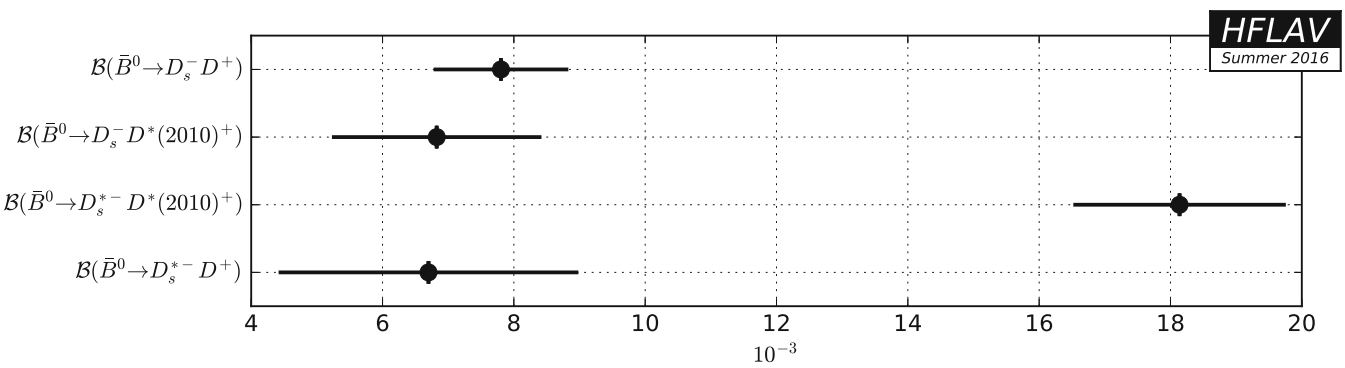

Fig. 84 Summary of the averages from Table 109

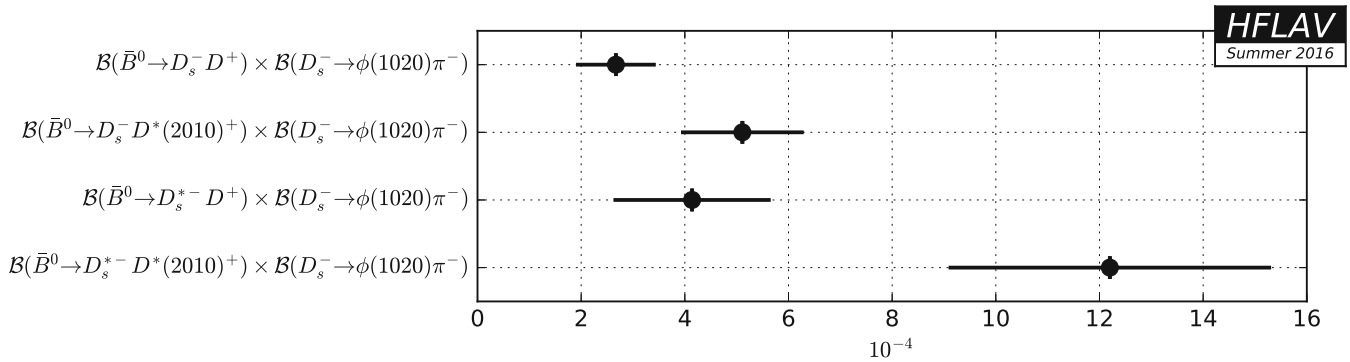

Fig. 85 Summary of the averages from Table 110

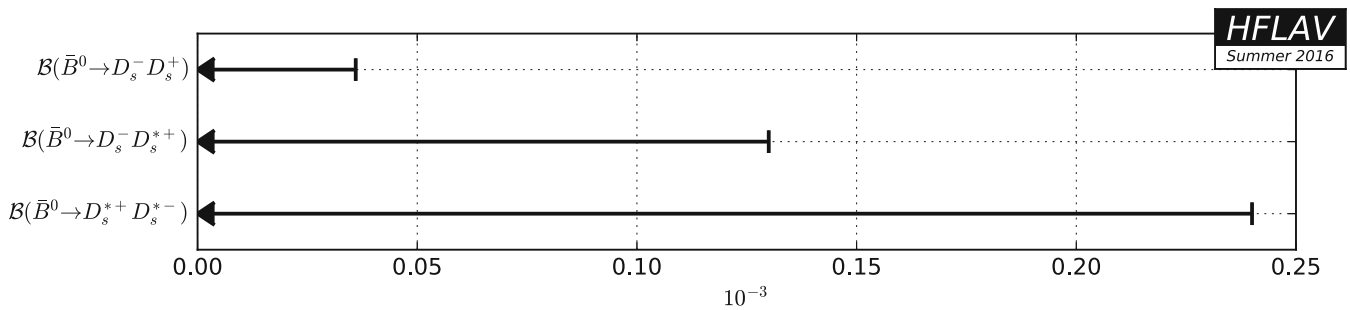

Fig. 86 Summary of the averages from Table 111

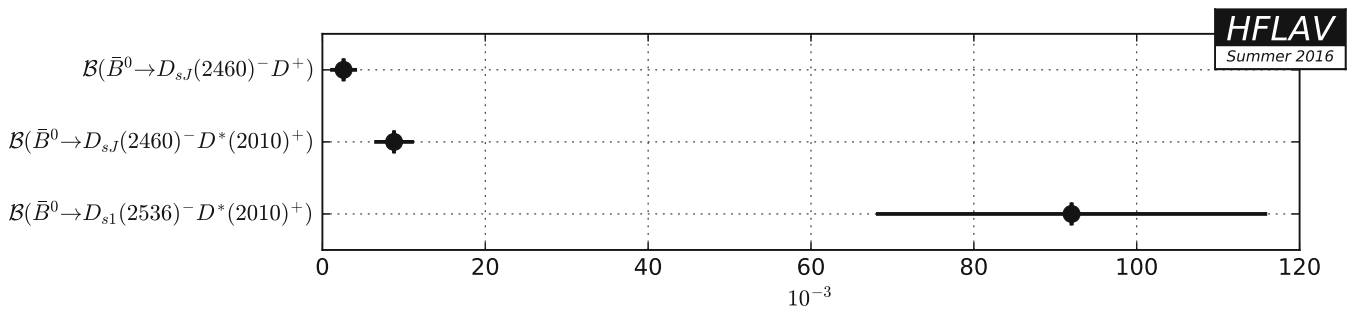

Fig. 87 Summary of the averages from Table 113

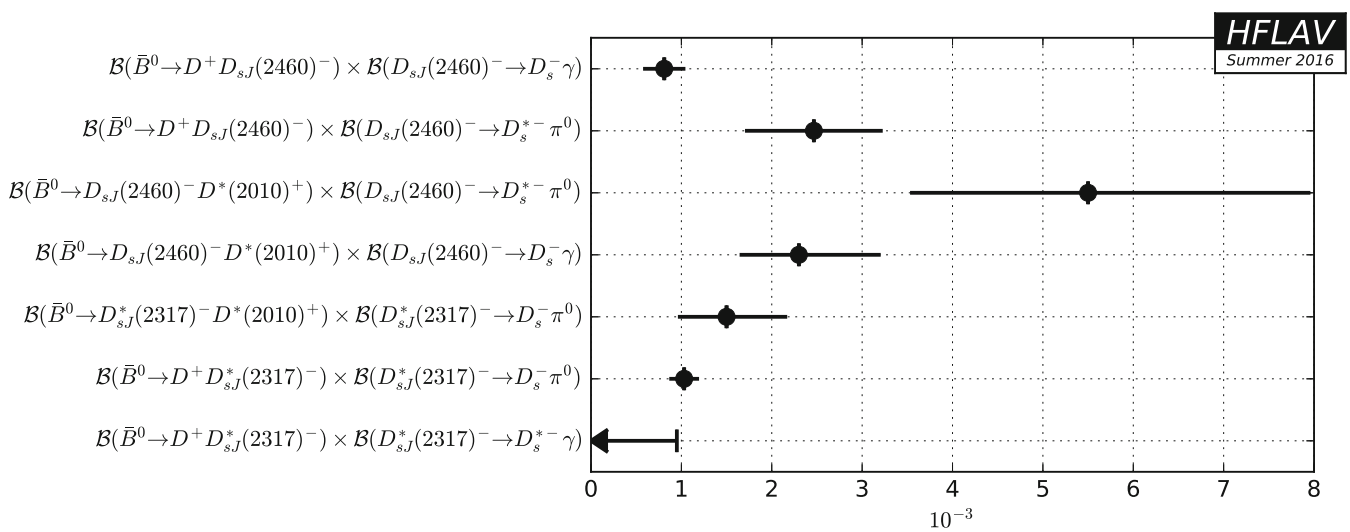

Fig. 88 Summary of the averages from Table 114

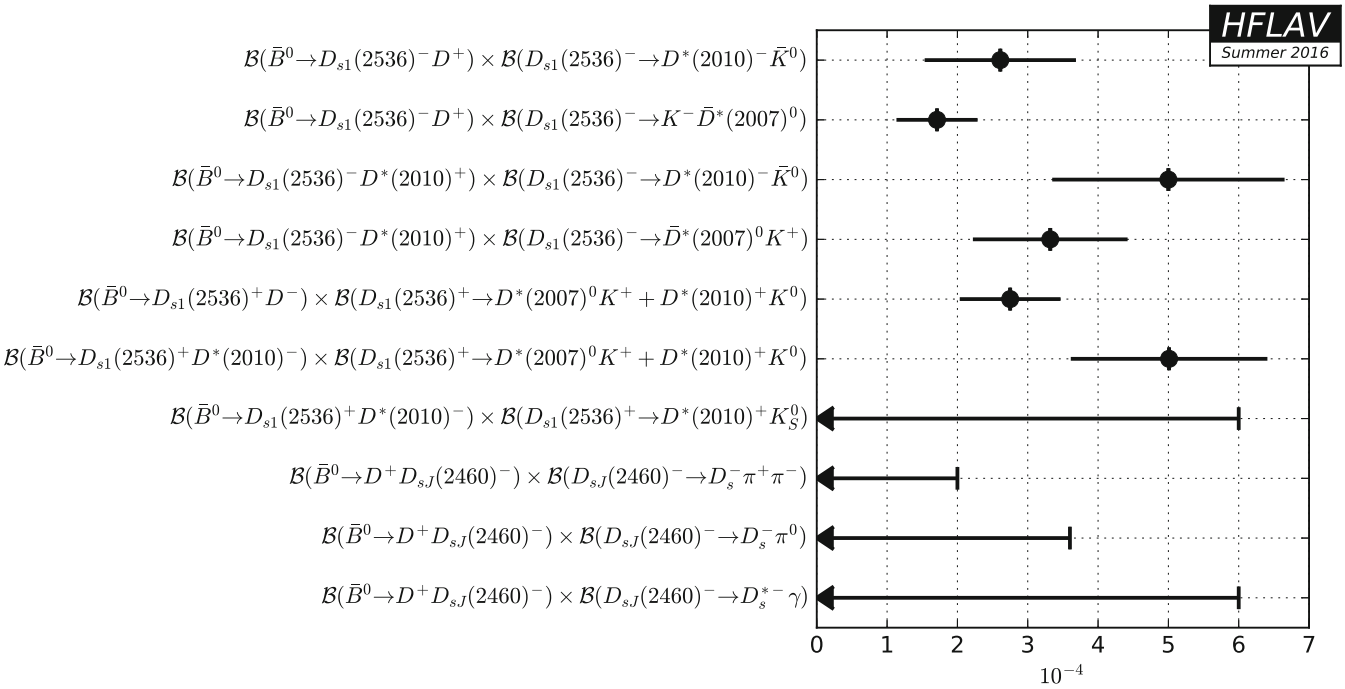

Fig. 89 Summary of the averages from Table 115

6.1.3 Decays to charmonium states

Averages of $\bar{B}^0$ decays to charmonium states are shown in Tables 116, 117, 118, 119, 120, 121, 122, 123, 124 and Figs. 90, 91, 92, 93, 94, 95, 96, 97, 98.

Table 116 Decays to J/ψ and one kaon [10^{-3}]

Parameter	Measurements	Average
$\mathcal{B}(\bar{B}^0 \to J/\psi \bar{K}^0)$	CDF [645]: 1.15 ± 0.23 ± 0.17	
	Belle [646]: 0.79 ± 0.04 ± 0.09	0.863 ± 0.035
	BaBar [10]: 0.869 ± 0.022 ± 0.030	
$\mathcal{B}(\bar{B}^0 \to J/\psi K^- \pi^+)$	Belle [647]: 1.15 ± 0.01 ± 0.05	1.15 ± 0.05
$\mathcal{B}(\bar{B}^0 \to J/\psi \bar{K}^*(892)^0)$	CDF [648]: 1.74 ± 0.20 ± 0.18	
	Belle [647]: 1.19 ± 0.01 ± 0.08	1.270 ± 0.056
	BaBar [10]: 1.309 ± 0.026 ± 0.077	
$\mathcal{B}(\bar{B}^0 \to J/\psi \bar{K}^0 \pi^+ \pi^-)$	LHCb [649]: 0.430 ± 0.030 ± 0.037	
	CDF [650]: 1.03 ± 0.33 ± 0.15	0.440 ± 0.047
$\mathcal{B}(\bar{B}^0 \to J/\psi \bar{K}^0 \rho(770)^0)$	CDF [650]: 0.54 ± 0.29 ± 0.09	0.54 ± 0.30
$\mathcal{B}(\bar{B}^0 \to J/\psi K^*(892)^- \pi^+)$	CDF [650]: 0.77 ± 0.41 ± 0.13	0.77 ± 0.43
$\mathcal{B}(\bar{B}^0 \to J/\psi \omega(782) \bar{K}^0)$	BaBar [651]: 0.23 ± 0.03 ± 0.03	0.23 ± 0.04
$\mathcal{B}(\bar{B}^0 \to J/\psi \phi(1020) \bar{K}^0)$	BaBar [652]: 0.102 ± 0.038 ± 0.010	0.102 ± 0.039
$\mathcal{B}(\bar{B}^0 \to J/\psi \bar{K}_1^0(1270))$	Belle [653]: 1.30 ± 0.34 ± 0.31	1.30 ± 0.46
$\mathcal{B}(\bar{B}^0 \to J/\psi \eta K_S^0)$	Belle [654]: 0.0522 ± 0.0078 ± 0.0049	0.0540 ± 0.0089
	BaBar [655]: 0.084 ± 0.026 ± 0.027	
$\mathcal{B}(\bar{B}^0 \to J/\psi \bar{K}^*(892)^0 \pi^+ \pi^-)$	CDF [650]: 0.66 ± 0.19 ± 0.11	0.66 ± 0.22

Table 117 Decays to charmonium other than J/ψ and one kaon I [10^{-3}]

Parameter	Measurements	Average
$\mathcal{B}(\bar{B}^0 \to \psi(2S)\bar{K}^0)$	Belle [646]: 0.67 ± 0.11	0.655 ± 0.066
	BaBar [10]: $0.646 \pm 0.065 \pm 0.051$	
$\mathcal{B}(\bar{B}^0 \to \psi(2S)\bar{K}^*(892)^0)$	CDF [648]: $0.90 \pm 0.22 \pm 0.09$	0.696 ± 0.103
	BaBar [10]: $0.649 \pm 0.059 \pm 0.097$	
$\mathcal{B}(\bar{B}^0 \to \psi(2S)K^0)$	LHCb [649]: $0.47 \pm 0.07 \pm 0.07$	0.47 ± 0.10
$\mathcal{B}(\bar{B}^0 \to K^*(892)^0\psi(2S))$	Belle [656]: $0.552\,^{+0.035}_{-0.032}\,^{+0.053}_{-0.058}$	$0.552\,^{+0.064}_{-0.066}$
$\mathcal{B}(\bar{B}^0 \to \psi(2S)K^0) \times \mathcal{B}(\psi(2S) \to \chi_{c1}\gamma)$	Belle [657]: $0.68 \pm 0.10 \pm 0.07$	0.68 ± 0.12
$\mathcal{B}(\bar{B}^0 \to \psi(2S)K^0) \times \mathcal{B}(\psi(2S) \to \chi_{c2}\gamma)$	Belle [657]: $0.47 \pm 0.16 \pm 0.08$	0.47 ± 0.18
$\mathcal{B}(\bar{B}^0 \to \chi_{c0}\bar{K}^0)$	BaBar [658]: <1.24	<1.24
$\mathcal{B}(\bar{B}^0 \to \chi_{c0}\bar{K}^*(892)^0)$	BaBar [658]: <0.77	0.17 ± 0.04
	BaBar [659]: $0.17 \pm 0.03 \pm 0.02$	
$\mathcal{B}(\bar{B}^0 \to \chi_{c1}\bar{K}^0)$	Belle [660]: $0.378\,^{+0.017}_{-0.016} \pm 0.033$	0.396 ± 0.028
	BaBar [661]: $0.42 \pm 0.03 \pm 0.03$	
$\mathcal{B}(\bar{B}^0 \to \chi_{c1}K^-\pi^+)$	Belle [662]: $0.497 \pm 0.012 \pm 0.028$	0.500 ± 0.027
	BaBar [663]: $0.511 \pm 0.014 \pm 0.058$	
$\mathcal{B}(\bar{B}^0 \to \chi_{c1}\bar{K}^*(892)^0)$	Belle [664]: $0.31 \pm 0.03 \pm 0.07$	
	BaBar [661]: $0.25 \pm 0.02 \pm 0.02$	0.26 ± 0.03
$\mathcal{B}(\bar{B}^0 \to \chi_{c1}K^-\pi^+\pi^0)$	Belle [662]: $0.352 \pm 0.052 \pm 0.024$	0.352 ± 0.057
$\mathcal{B}(\bar{B}^0 \to \chi_{c1}\bar{K}^0\pi^+\pi^-)$	Belle [662]: $0.316 \pm 0.035 \pm 0.032$	0.316 ± 0.047
$\mathcal{B}(\bar{B}^0 \to \eta_c\bar{K}^0)$	Belle [665]: $1.23 \pm 0.23\,^{+0.40}_{-0.41}$	
	BaBar [666]: $0.64\,^{+0.22}_{-0.20}\,^{+0.28}_{-0.16}$	0.85 ± 0.24
	BaBar [667]: $1.14 \pm 0.15 \pm 0.34$	
$\mathcal{B}(\bar{B}^0 \to \eta_c\bar{K}^*(892)^0)$	Belle [665]: $1.62 \pm 0.32\,^{+0.55}_{-0.60}$	
	BaBar [668]: $0.57 \pm 0.06 \pm 0.09$	0.61 ± 0.10
	BaBar [666]: $0.80\,^{+0.21}_{-0.19}\,^{+0.37}_{-0.23}$	
$\mathcal{B}(\bar{B}^0 \to \eta_c(2S)\bar{K}^*(892)^0)$	BaBar [668]: <0.39	<0.39
$\mathcal{B}(\bar{B}^0 \to h_c(1P)\bar{K}^*(892)^0) \times \mathcal{B}(h_c(1P) \to \eta_c\gamma)$	BaBar [668]: <0.22	<0.22

Table 118 Decays to charmonium other than J/ψ and one kaon II [10^{-4}]

Parameter	Measurements	Average
$\mathcal{B}(\bar{B}^0 \to \psi(3770)\bar{K}^0) \times \mathcal{B}(\psi(3770) \to D^0\bar{D}^0)$	BaBar [643]: <1.23	<1.23
$\mathcal{B}(\bar{B}^0 \to \psi(3770)\bar{K}^0) \times \mathcal{B}(\psi(3770) \to D^+D^-)$	BaBar [643]: <1.88	<1.88
$\mathcal{B}(\bar{B}^0 \to \chi_{c2}\bar{K}^0)$	Belle [660]: <0.15	0.15 ± 0.09
	BaBar [661]: $0.15 \pm 0.09 \pm 0.03$	
$\mathcal{B}(\bar{B}^0 \to \chi_{c2}\bar{K}^*(892)^0)$	BaBar [661]: $0.66 \pm 0.18 \pm 0.05$	0.66 ± 0.19
$\mathcal{B}(\bar{B}^0 \to \chi_{c2}K^-\pi^+)$	Belle [662]: $0.72 \pm 0.09 \pm 0.05$	0.72 ± 0.10

Table 119 Decays to charmonium and light mesons I [10^{-5}]

Parameter	Measurements	Average
$\mathcal{B}(\bar{B}^0 \to J/\psi\pi^0)$	Belle [646]: $2.3 \pm 0.5 \pm 0.2$	1.74 ± 0.15
	BaBar [353]: $1.69 \pm 0.14 \pm 0.07$	
$\mathcal{B}(\bar{B}^0 \to J/\psi\pi^+\pi^-)$	BaBar [669]: <1.2	<1.2
$\mathcal{B}(\bar{B}^0 \to J/\psi\rho(770)^0)$	BaBar [669]: $2.7 \pm 0.3 \pm 0.2$	2.7 ± 0.4
$\mathcal{B}(\bar{B}^0 \to J/\psi\eta)$	Belle [670]: $1.23^{+0.18}_{-0.17} \pm 0.07$	$1.23^{+0.19}_{-0.18}$
	BaBar [652]: <2.7	
$\mathcal{B}(\bar{B}^0 \to J/\psi\eta'(958))$	Belle [670]: <0.74	
	BaBar [652]: <6.3	<0.74
$\mathcal{B}(\bar{B}^0 \to J/\psi f_2(1270))$	BaBar [669]: <0.46	<0.46
$\mathcal{B}(\bar{B}^0 \to J/\psi f_1(1285))$	LHCb [671]: $0.837 \pm 0.195^{+0.079}_{-0.075}$	$0.837^{+0.210}_{-0.209}$
$\mathcal{B}(\bar{B}^0 \to J/\psi K^0 K^\pm \pi^\mp)$	LHCb [649]: <2.1	<2.1
$\mathcal{B}(\bar{B}^0 \to J/\psi K^0 K^+ K^-)$	LHCb [649]: $2.02 \pm 0.43 \pm 0.19$	2.02 ± 0.47
$\mathcal{B}(\bar{B}^0 \to \chi_{c1}\pi^0)$	Belle [672]: $1.12 \pm 0.25 \pm 0.12$	1.12 ± 0.28

Table 120 Decays to charmonium and light mesons II [10^{-5}]

Parameter	Measurements	Average
$\mathcal{B}(\bar{B}^0 \to J/\psi a_0(980)) \times \mathcal{B}(a_0(980) \to K^+K^-)$	LHCb [673]: <0.090	<0.090
$\mathcal{B}(\bar{B}^0 \to J/\psi f_0(980)) \times \mathcal{B}(f_0(980) \to \pi^+\pi^-)$	LHCb [674]: <0.11	<0.11
$\mathcal{B}(\bar{B}^0 \to J/\psi f_1(1285)) \times \mathcal{B}(f_1(1285) \to \pi^+\pi^-\pi^+\pi^-)$	LHCb [671]: $0.0921 \pm 0.0214 \pm 0.0064$	0.0921 ± 0.0223
$\mathcal{B}(\bar{B}^0 \to J/\psi K^+K^-)$	LHCb [673]: $0.253 \pm 0.031 \pm 0.019$	0.253 ± 0.036
$\mathcal{B}(\bar{B}^0 \to J/\psi\phi(1020))$	LHCb [673]: <0.019	
	Belle [675]: <0.094	<0.019
	BaBar [652]: <0.9	

Table 121 Decays to J/ψ and photons, baryons, or heavy mesons [10^{-5}]

Parameter	Measurements	Average
$\mathcal{B}(\bar{B}^0 \to J/\psi\gamma)$	LHCb [676]: <0.15	<0.15
	BaBar [677]: <0.16	
$\mathcal{B}(\bar{B}^0 \to J/\psi\bar{p}p)$	LHCb [678]: <0.052	
	Belle [679]: <0.083	<0.052
	BaBar [680]: <0.19	
$\mathcal{B}(\bar{B}^0 \to J/\psi D^0)$	Belle [681]: <2.0	<1.3
	BaBar [682]: <1.3	

Table 122 Relative decay rates I

Parameter	Measurements	Average
$\mathcal{B}(\bar{B}^0 \to J/\psi \bar{K}_1^0(1270))/\mathcal{B}(B^- \to J/\psi K^-)$	Belle [653]: $1.30 \pm 0.34 \pm 0.28$	1.30 ± 0.44
$\mathcal{B}(\bar{B}^0 \to J/\psi \bar{K}^*(892)^0)/\mathcal{B}(\bar{B}^0 \to J/\psi \bar{K}^0)$	CDF [683]: $1.39 \pm 0.36 \pm 0.10$	
	BaBar [10]: $1.51 \pm 0.05 \pm 0.08$	1.50 ± 0.09
$\mathcal{B}(\bar{B}^0 \to J/\psi \omega(782))/\mathcal{B}(\bar{B}^0 \to J/\psi \rho)$	LHCb [684]: $0.89 \pm 0.19\,^{+0.07}_{-0.13}$	$0.89\,^{+0.20}_{-0.23}$
$\mathcal{B}(\bar{B}^0 \to J/\psi \omega(782)\bar{K}^0)/\mathcal{B}(B^- \to J/\psi \omega(782) K^-)$	BaBar [651]: $0.7 \pm 0.1 \pm 0.1$	0.7 ± 0.1
$\mathcal{B}(\bar{B}^0 \to J/\psi K_S^0 \pi^- \pi^+)/\mathcal{B}(\bar{B}^0 \to J/\psi K_S^0)$	LHCb [649]: $0.493 \pm 0.034 \pm 0.027$	0.493 ± 0.043
$[\mathcal{B}(\bar{B}^0 \to \psi(2S) K_S^0) \times \mathcal{B}(\psi(2S) \to J/\psi \pi^- \pi^+)]/\mathcal{B}(\bar{B}^0 \to J/\psi K_S^0)$	LHCb [649]: $0.183 \pm 0.027 \pm 0.015$	0.183 ± 0.031
$\mathcal{B}(\bar{B}^0 \to \psi(2S) \bar{K}^*(892)^0)/\mathcal{B}(\bar{B}^0 \to \psi(2S) \bar{K}^0)$	BaBar [10]: $1.00 \pm 0.14 \pm 0.09$	1.00 ± 0.17
$\mathcal{B}(\bar{B}^0 \to \psi(2S) K(892)^{*0})/\mathcal{B}(\bar{B}^0 \to J/\psi K(892)^{*0})$	LHCb [685]: $0.476 \pm 0.014 \pm 0.016$	0.476 ± 0.021
$\mathcal{B}\bar{B}^0 \to \psi(2S)\pi^+\pi^-/\mathcal{B}\bar{B}^0 \to J/\psi \pi^+ \pi^-$	LHCb [686]: $0.56 \pm 0.07 \pm 0.05$	0.56 ± 0.09
$\mathcal{B}(\bar{B}^0 \to \eta_c \bar{K}^0)/\mathcal{B}(B^- \to \eta_c K^-)$	BaBar [667]: $0.87 \pm 0.13 \pm 0.07$	0.87 ± 0.15
$\mathcal{B}(\bar{B}^0 \to \eta_c \bar{K}^0)/\mathcal{B}(\bar{B}^0 \to J/\psi \bar{K}^0)$	BaBar [667]: $1.34 \pm 0.19 \pm 0.40$	1.34 ± 0.44
$\mathcal{B}(\bar{B}^0 \to \eta_c \bar{K}^*(892)^0)/\mathcal{B}(B^- \to \eta_c K^-)$	BaBar [668]: $0.62 \pm 0.06 \pm 0.05$	0.62 ± 0.08
$\mathcal{B}(\bar{B}^0 \to \eta_c \bar{K}^*(892)^0)/\mathcal{B}(\bar{B}^0 \to \eta_c \bar{K}^0)$	Belle [665]: $1.33 \pm 0.36\,^{+0.24}_{-0.33}$	$1.33\,^{+0.43}_{-0.49}$
$\mathcal{B}(\bar{B}^0 \to \chi_{c1} K^- \pi^+)/\mathcal{B}(\bar{B}^0 \to J/\psi K^- \pi^+)$	BaBar [663]: $0.474 \pm 0.013 \pm 0.054$	0.474 ± 0.056
$\mathcal{B}(\bar{B}^0 \to \chi_{c1} \bar{K}^*(892)^0)/\mathcal{B}(\bar{B}^0 \to \chi_{c1} \bar{K}^0)$	BaBar [10]: $0.72 \pm 0.11 \pm 0.12$	0.72 ± 0.16
$[\mathcal{B}(\bar{B}^0 \to h_c(1P) \bar{K}^*(892)^0) \times \mathcal{B}(h_c(1P) \to \eta_c \gamma)]/\mathcal{B}(B^- \to \eta_c K^-)$	BaBar [668]: <0.236	<0.236

Table 123 Relative decay rates II

Parameter	Measurements	Average
$\mathcal{B}(\bar{B}^0 \to J/\psi \eta)/\mathcal{B}(\bar{B}_s^0 \to J/\psi \eta)$	LHCb [687]: $0.0185 \pm 0.0061 \pm 0.0014$	0.0185 ± 0.0063
$\mathcal{B}(\bar{B}^0 \to J/\psi \eta')/\mathcal{B}(\bar{B}_s^0 \to J/\psi \eta')$	LHCb [687]: $0.0228 \pm 0.0065 \pm 0.0016$	0.0228 ± 0.0067
$\mathcal{B}(\bar{B}^0 \to J/\psi K_S^0 K^\pm \pi^\mp)/\mathcal{B}(\bar{B}^0 \to J/\psi K_S^0 \pi^+ \pi^-)$	LHCb [649]: <0.048	<0.048
$\mathcal{B}(\bar{B}^0 \to J/\psi K_S^0 K^+ K^-)/\mathcal{B}(\bar{B}^0 \to J/\psi K_S^0 \pi^+ \pi^-)$	LHCb [649]: $0.047 \pm 0.010 \pm 0.004$	0.047 ± 0.011

Table 124 Polarization fractions

Parameter	Measurements	Average
$\lvert\mathcal{A}_0\rvert^2(B^0 \to J/\psi \bar{K}^*(892)^0)/\lvert\mathcal{A}_0\rvert^2(\bar{B}^0 \to J/\psi \bar{K}^*(892)^0)$	BaBar [688]: <0.32	<0.32
$\lvert\mathcal{A}_0\rvert^2(\bar{B}^0 \to J/\psi K^*(892)^0)/\lvert\mathcal{A}_0\rvert^2(B^0 \to J/\psi K^*(892)^0)$	BaBar [688]: <0.26	<0.26

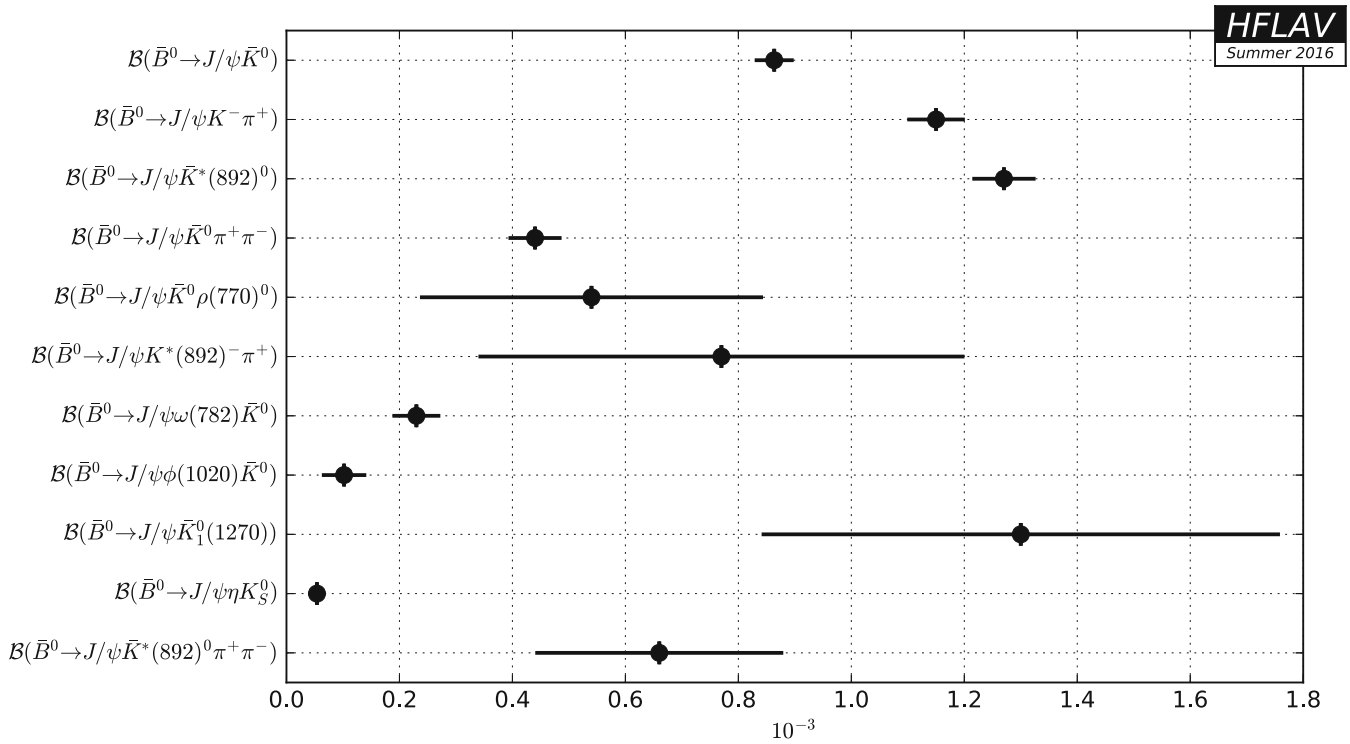

Fig. 90 Summary of the averages from Table 116

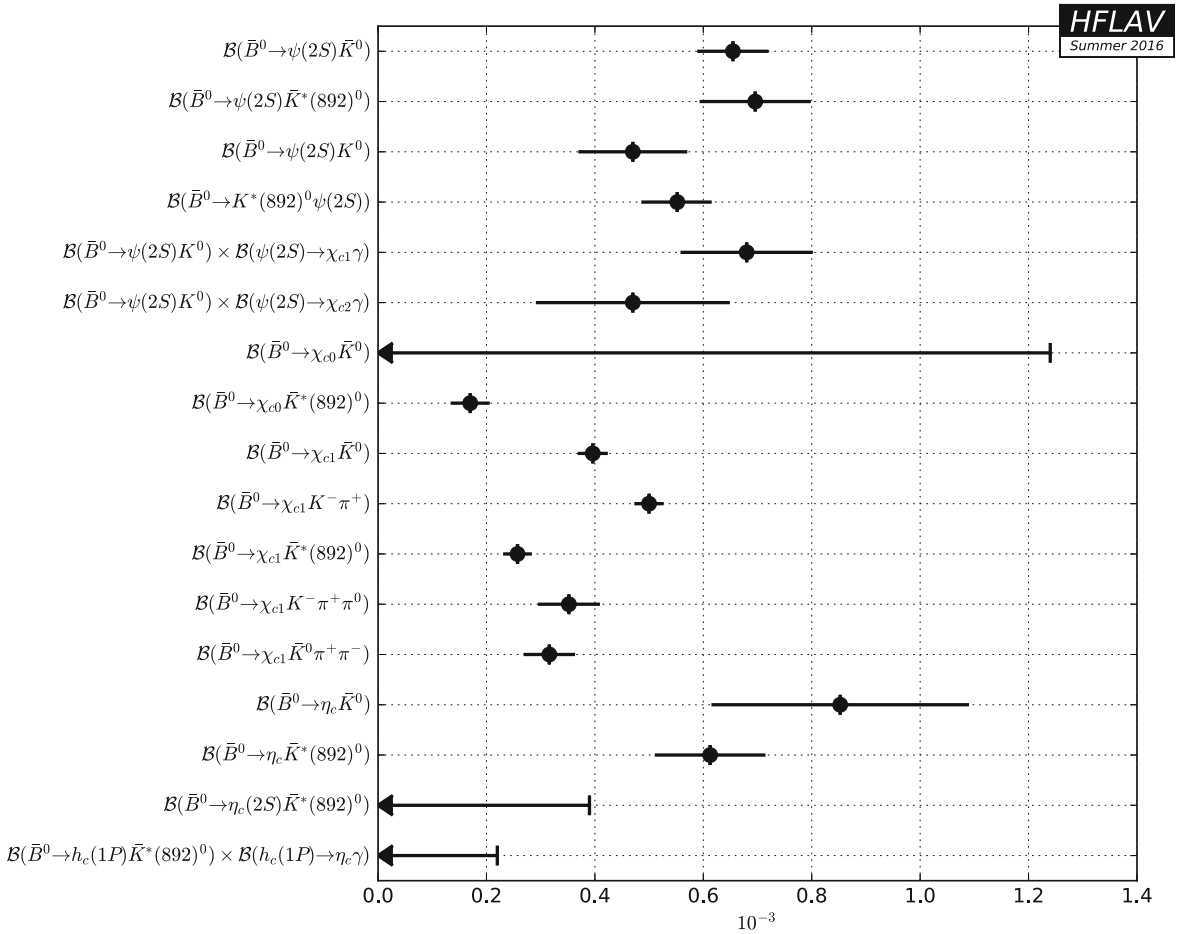

Fig. 91 Summary of the averages from Table 117

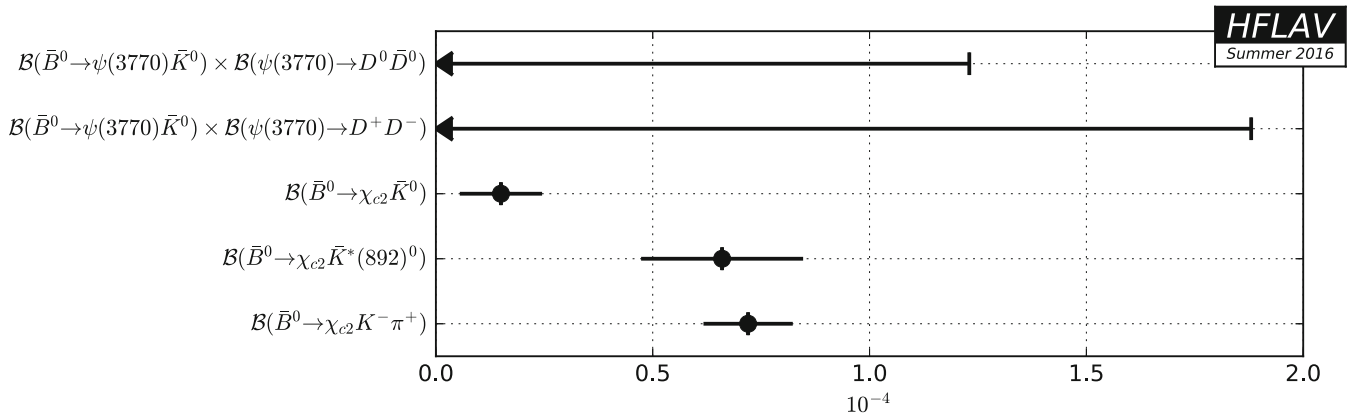

Fig. 92 Summary of the averages from Table 118

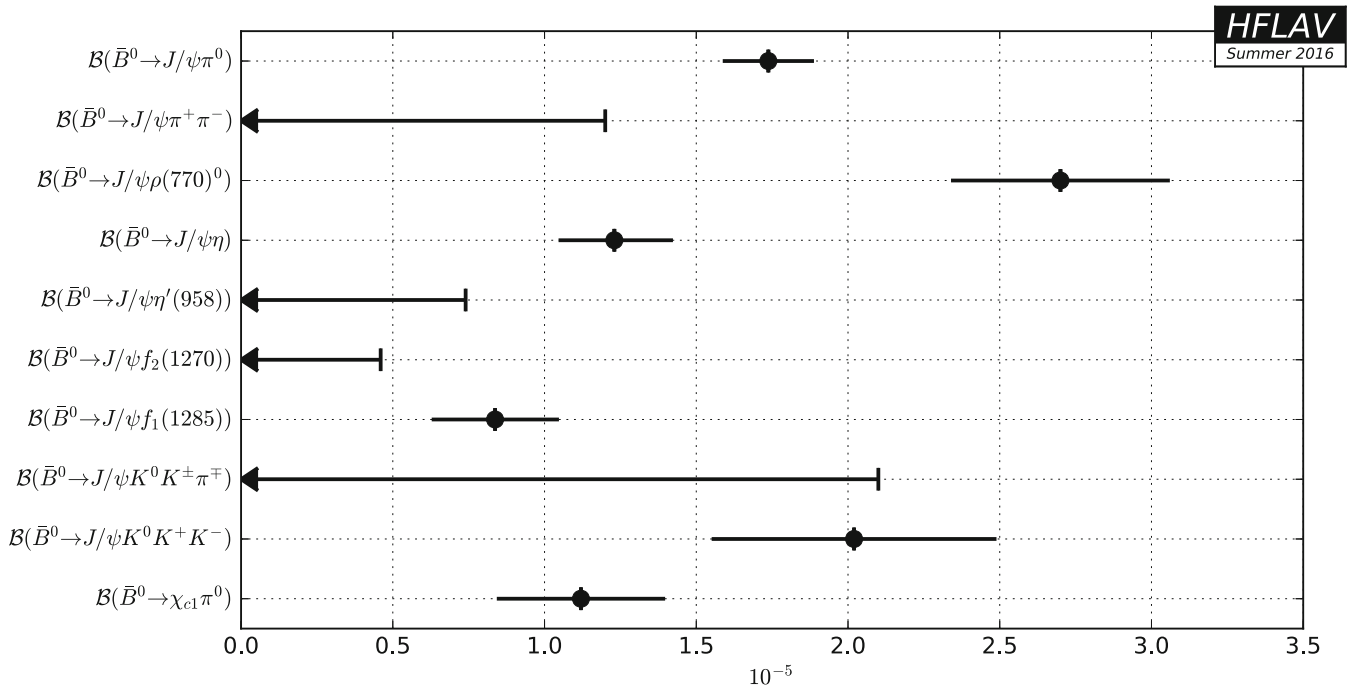

Fig. 93 Summary of the averages from Table 119

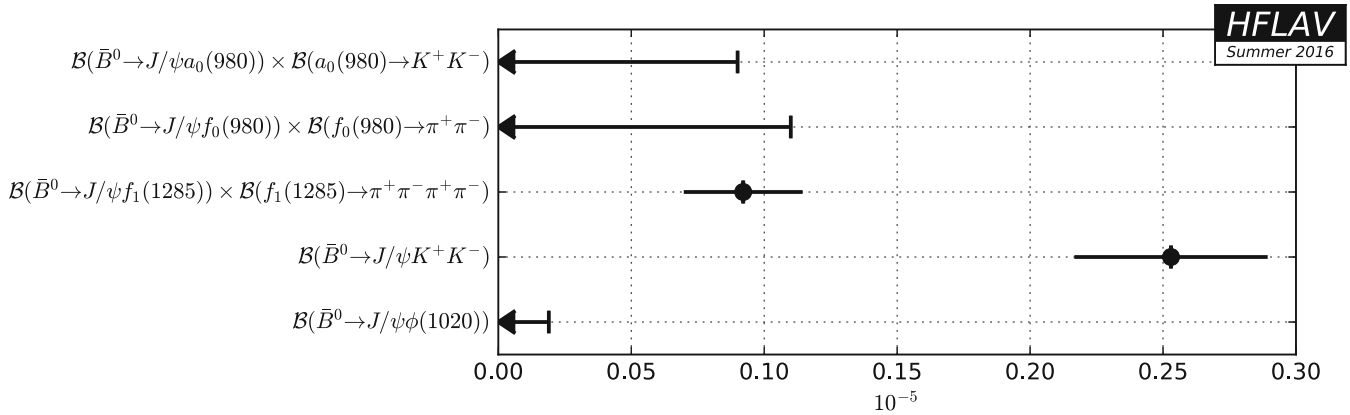

Fig. 94 Summary of the averages from Table 120

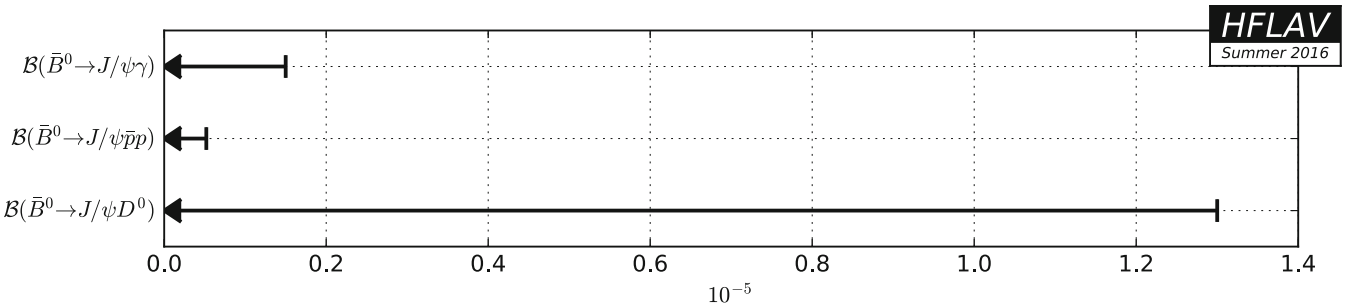

Fig. 95 Summary of the averages from Table 121

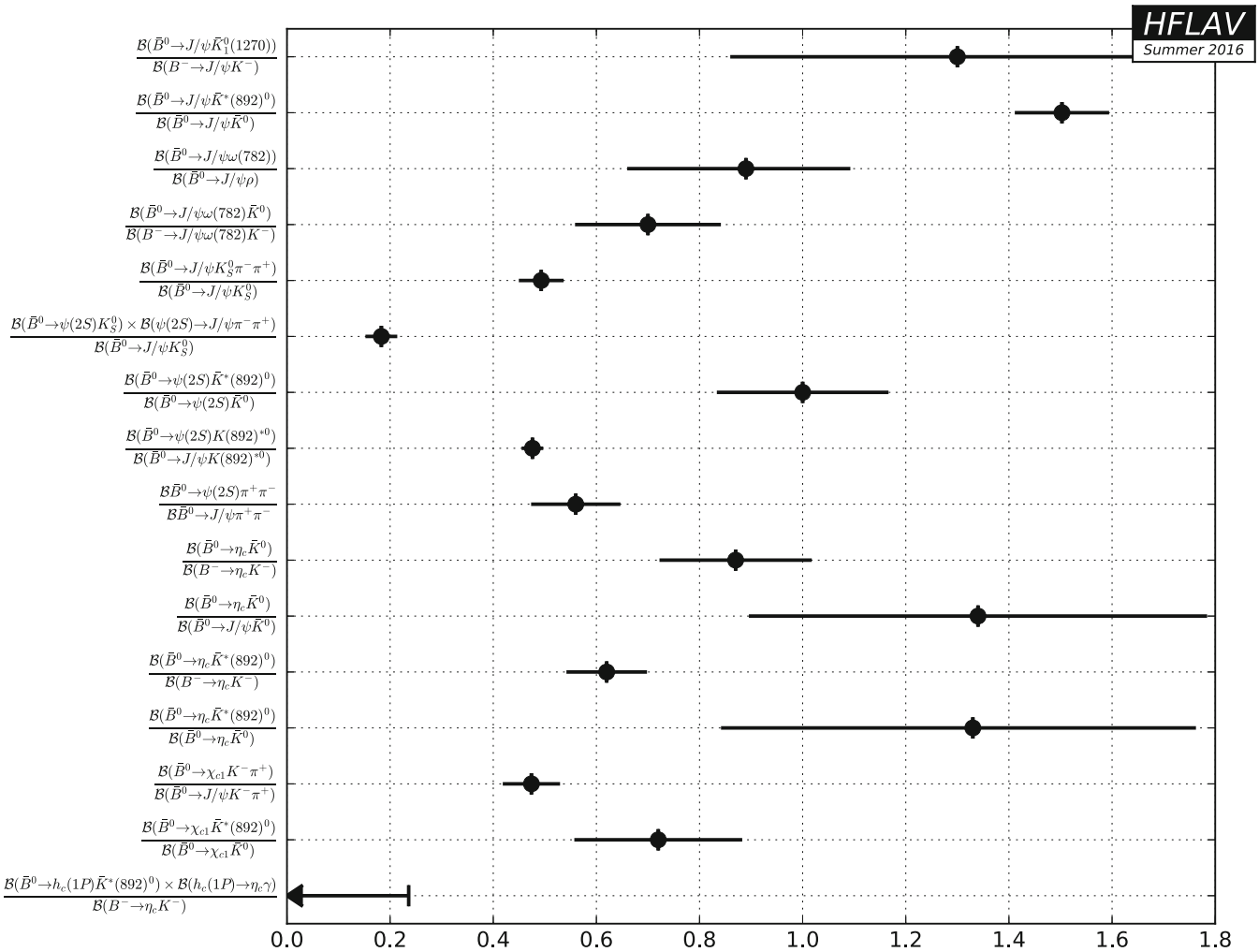

Fig. 96 Summary of the averages from Table 122

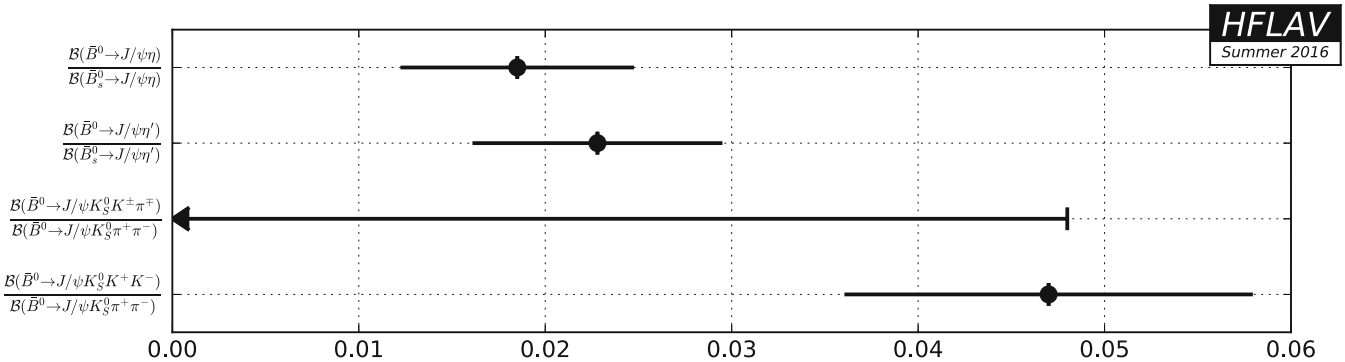

Fig. 97 Summary of the averages from Table 123

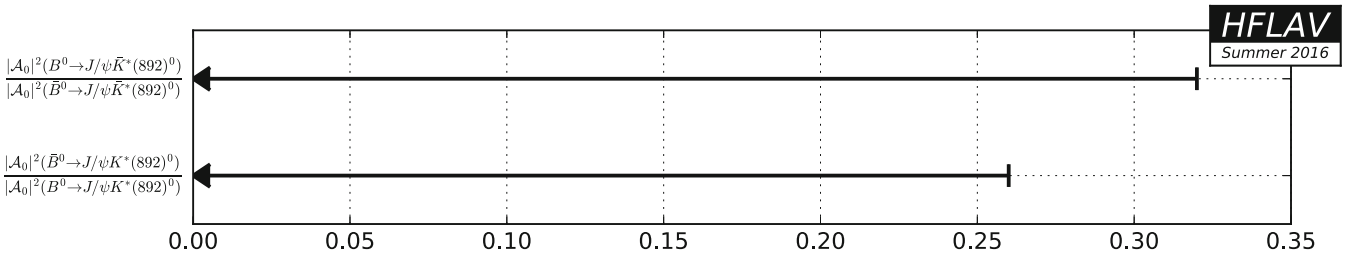

Fig. 98 Summary of the averages from Table 124

6.1.4 Decays to charm baryons

Averages of $\bar{B}^0$ decays to charm baryons are shown in Tables 125, 126, 127, 128 and Figs. 99, 100, 101.

Table 125 Absolute decay rates to charm baryons I [10^{-4}]

Parameter	Measurements	Average
$\mathcal{B}(\bar{B}^0 \to \Lambda_c^+ \bar{p}\pi^0)$	BaBar [689]: $1.94 \pm 0.17 \pm 0.52$	1.94 ± 0.55
$\mathcal{B}(\bar{B}^0 \to \Lambda_c^+ \bar{p}\pi^+\pi^-)$	Belle [690]: $11.0\,^{+1.2}_{-1.2} \pm 3.5$	
	BaBar [691]: $12.3 \pm 0.5 \pm 3.3$	11.9 ± 3.2
$\mathcal{B}(\bar{B}^0 \to \Sigma_c^{++} \bar{p}\pi^-)$	Belle [692]: $2.1 \pm 0.2 \pm 0.6$	
	BaBar [691]: $2.13 \pm 0.10 \pm 0.56$	2.12 ± 0.55
$\mathcal{B}(\bar{B}^0 \to \Sigma_c^{*++} \bar{p}\pi^-)$	Belle [692]: $1.2 \pm 0.1 \pm 0.4$	
	BaBar [691]: $1.15 \pm 0.10 \pm 0.30$	1.16 ± 0.32
$\mathcal{B}(\bar{B}^0 \to \Sigma_c^0 \bar{p}\pi^+)$	Belle [692]: $1.4 \pm 0.2 \pm 0.4$	
	BaBar [691]: $0.91 \pm 0.07 \pm 0.24$	0.77 ± 0.23
$\mathcal{B}(\bar{B}^0 \to \Lambda_c^+ \Lambda_c^- \bar{K}^0)$	Belle [693]: $7.9\,^{+2.9}_{-2.3} \pm 4.3$	
	BaBar [694]: $3.8 \pm 3.1 \pm 2.1$	4.8 ± 3.5
$\mathcal{B}(\bar{B}^0 \to \Lambda_c^+ \bar{p}\pi^+\pi^-_{\mathrm{non}-\Sigma_c})$	BaBar [691]: $7.9 \pm 0.4 \pm 2.0$	7.9 ± 2.1

Table 126 Absolute decay rates to charm baryons II [10^{-5}]

Parameter	Measurements	Average
$\mathcal{B}(\bar{B}^0 \to \Lambda_c^+ \bar{p} K^+ K^-)$	BaBar [695]: $2.5 \pm 0.4 \pm 0.6$	2.5 ± 0.7
$\mathcal{B}(\bar{B}^0 \to \Lambda_c^+ \bar{p} \phi(1020))$	BaBar [695]: <1.2	<1.2
$\mathcal{B}(\bar{B}^0 \to \Sigma_c^{*0} \bar{p} \pi^+)$	Belle [692]: <3.3	
	BaBar [691]: $2.2 \pm 0.7 \pm 0.6$	2.2 ± 0.9
$\mathcal{B}(\bar{B}^0 \to \Lambda_c^+ \bar{p})$	Belle [696]: $2.19\,^{+0.56}_{-0.49} \pm 0.65$	
	BaBar [697]: $1.89 \pm 0.21 \pm 0.49$	1.90 ± 0.54
$\mathcal{B}(\bar{B}^0 \to \Lambda_c^+ \bar{p} \bar{K}^*(892)^0)$	BaBar [698]: $1.60 \pm 0.61 \pm 0.44$	1.60 ± 0.75
$\mathcal{B}(\bar{B}^0 \to \Sigma_c^{++} \bar{p} K^-)$	BaBar [698]: $1.11 \pm 0.30 \pm 0.30$	1.11 ± 0.43
$\mathcal{B}(\bar{B}^0 \to \Xi_c^+ \Lambda_c^-) \times \mathcal{B}(\Xi_c^+ \to \Xi^- \pi^+ \pi^+)$	Belle [699]: $9.3\,^{+3.7}_{-2.8} \pm 3.1$	
	BaBar [694]: $1.5 \pm 1.1 \pm 0.4$	1.7 ± 1.2
$\mathcal{B}(\bar{B}^0 \to \Lambda_c^+ \Lambda_c^-)$	Belle [700]: <5.7	<5.7
$\mathcal{B}(\bar{B}^0 \to \Lambda_c^+ \bar{\Lambda} K^-)$	BaBar [701]: $3.8 \pm 0.8 \pm 1.0$	3.8 ± 1.3
$\mathcal{B}(\bar{B}^0 \to \Lambda_c^+ \bar{p} K^- \pi^+)$	BaBar [698]: $4.33 \pm 0.82 \pm 1.18$	4.33 ± 1.43

Table 127 Absolute decay rates to charm baryons III [10^{-6}]

Parameter	Measurements	Average
$\mathcal{B}(\bar{B}^0 \to \Sigma_c^+ \bar{p}) \times \mathcal{B}(\Lambda_c^+ \to p K^- \pi^+)$	BaBar [689]: <1.5	<1.5
$\mathcal{B}(\bar{B}^0 \to \Lambda_c^+ \bar{p} p \bar{p}) \times \mathcal{B}(\Lambda_c^+ \to p K^- \pi^+)$	BaBar [702]: <0.14	<0.14

Table 128 Relative decay rates to charm baryons [10^{-3}]

Parameter	Measurements	Average
$\mathcal{B}(\bar{B}^0 \to \Lambda_c^- \Lambda_c^+)/\mathcal{B}(\bar{B}^0 \to D^+ D_s^-)$	LHCb [703]: <2	<2

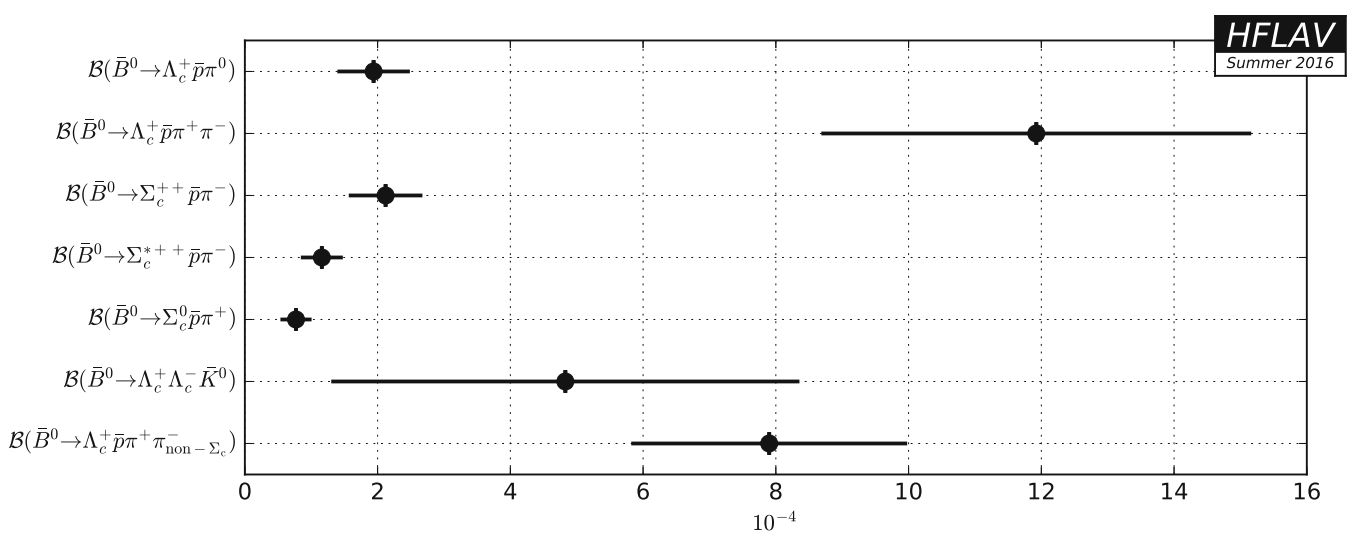

Fig. 99 Summary of the averages from Table 125

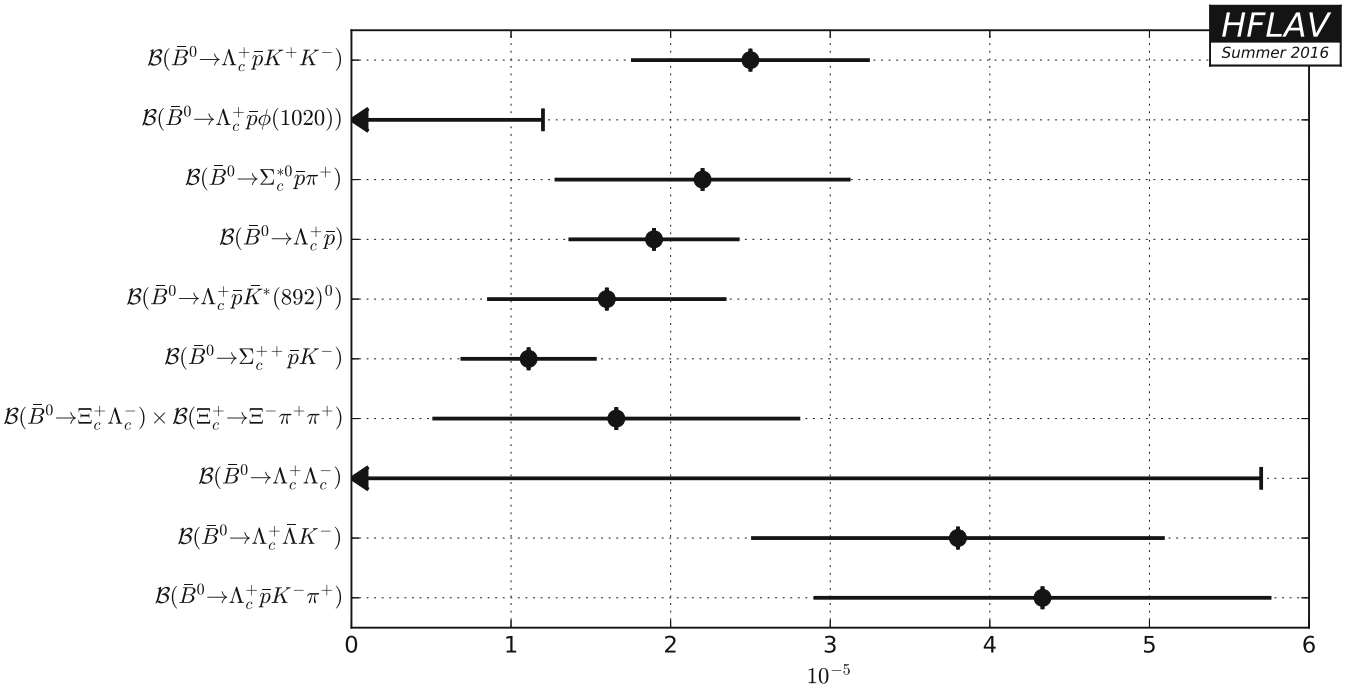

Fig. 100 Summary of the averages from Table 126

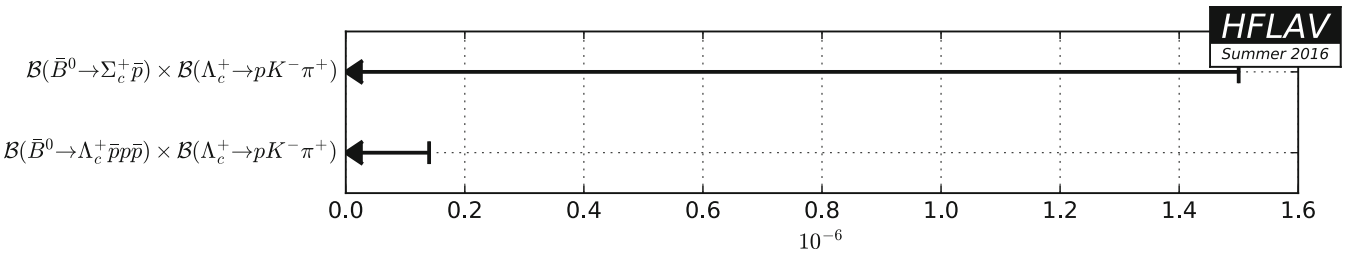

Fig. 101 Summary of the averages from Table 127

6.1.5 Decays to other (XYZ) states

Averages of $\bar{B}^0$ decays to other (XYZ) states are shown in Tables 129, 130, 131, 132, 133, 134 and Figs. 102, 103, 104, 105.

Table 129 Decays to $X(3872)$ $[10^{-5}]$

Parameter	Measurements	Average
$\mathcal{B}(\bar{B}^0 \to X(3872)\bar{K}^0) \times \mathcal{B}(X(3872) \to J/\psi\pi^+\pi^-)$	BaBar [704]: $0.35 \pm 0.19 \pm 0.04$	0.35 ± 0.19
$\mathcal{B}(\bar{B}^0 \to X(3872)\bar{K}^0) \times \mathcal{B}(X(3872) \to J/\psi\omega(782))$	BaBar [651]: $0.6 \pm 0.3 \pm 0.1$	0.6 ± 0.3
$\mathcal{B}(\bar{B}^0 \to X(3872)\bar{K}^0) \times \mathcal{B}(X(3872) \to J/\psi\gamma)$	Belle [660]: $0.24\,^{+0.13}_{-0.14} \pm 0.07$	
	BaBar [661]: $0.26 \pm 0.18 \pm 0.02$	0.25 ± 0.12
$\mathcal{B}(\bar{B}^0 \to X(3872)\bar{K}^*(892)^0) \times \mathcal{B}(X(3872) \to J/\psi\gamma)$	BaBar [661]: $0.07 \pm 0.14 \pm 0.01$	0.07 ± 0.14
$\mathcal{B}(\bar{B}^0 \to X(3872)\bar{K}^0) \times \mathcal{B}(X(3872) \to \psi(2S)\gamma)$	Belle [660]: $0.662\,^{+0.130}_{-0.140} \pm 0.070$	
	BaBar [661]: $1.14 \pm 0.55 \pm 0.10$	0.695 ± 0.147
$\mathcal{B}(\bar{B}^0 \to X(3872)\bar{K}^*(892)^0) \times \mathcal{B}(X(3872) \to \psi(2S)\gamma)$	BaBar [661]: $-0.13 \pm 0.31 \pm 0.03$	-0.13 ± 0.31
$\mathcal{B}(\bar{B}^0 \to X(3872)K^0) \times \mathcal{B}(X(3872) \to \chi_{c1}\gamma)$	Belle [657]: <0.96	<0.96
$\mathcal{B}(\bar{B}^0 \to X(3872)K^0) \times \mathcal{B}(X(3872) \to \chi_{c2}\gamma)$	Belle [657]: <1.22	<1.22

Table 130 Decays to $X(3872)$ with $X(3872) \to D\bar{D}$ [10^{-4}]

Parameter	Measurements	Average
$\mathcal{B}(\bar{B}^0 \to X(3872)\bar{K}^0) \times \mathcal{B}(X(3872) \to \bar{D}^*(2007)^0 D^0)$	BaBar [643]: <4.37	<4.37

Table 131 Decays to neutral states other than $X(3872)$ [10^{-4}]

Parameter	Measurements	Average
$\mathcal{B}(\bar{B}^0 \to X(3823)K^0) \times \mathcal{B}(X(3823) \to \chi_{c1}\gamma)$	Belle [657]: <0.099	<0.099
$\mathcal{B}(\bar{B}^0 \to X(3823)K^0) \times \mathcal{B}(X(3823) \to \chi_{c2}\gamma)$	Belle [657]: <0.228	<0.228
$\mathcal{B}(\bar{B}^0 \to Y(3940)\bar{K}^0) \times \mathcal{B}(Y(3940) \to J/\psi\omega(782))$	BaBar [651]: $0.21 \pm 0.09 \pm 0.03$	0.21 ± 0.09
$\mathcal{B}(\bar{B}^0 \to Z_1(4050)K^-) \times \mathcal{B}(Z_1(4050) \to \chi_{c1}\pi^+)$	Belle [705]: $0.30^{+0.15}_{-0.08}{}^{+0.37}_{-0.16}$	
	BaBar [663]: <0.18	$0.30^{+0.40}_{-0.18}$
$\mathcal{B}(\bar{B}^0 \to Z_2(4250)K^-) \times \mathcal{B}(Z_2(4250) \to \chi_{c1}\pi^+)$	Belle [705]: $0.40^{+0.23}_{-0.09}{}^{+1.97}_{-0.05}$	
	BaBar [663]: <0.47	$0.40^{+1.98}_{-0.10}$

Table 132 Decays to charged states I [10^{-4}]

Parameter	Measurements	Average
$\mathcal{B}(\bar{B}^0 \to X(3872)^+K^-)$	BaBar [706]: <5.0	<5.0

Table 133 Decays to charged states II [10^{-5}]

Parameter	Measurements	Average
$\mathcal{B}(\bar{B}^0 \to X(3872)^+K^-) \times \mathcal{B}(X(3872)^+ \to J/\psi\pi^+\pi^0)$	BaBar [707]: <0.54	<0.54
$\mathcal{B}(\bar{B}^0 \to Z(4430)^+K^-) \times \mathcal{B}(Z(4430)^+ \to J/\psi\pi^+)$	Belle [647]: $0.54^{+0.40}_{-0.10}{}^{+0.11}_{-0.09}$	
	BaBar [708]: $-1.2 \pm 0.4 \pm 0.0$	-0.11 ± 0.24 CL = 0.6‰
$\mathcal{B}(\bar{B}^0 \to Z(4430)^+K^-) \times \mathcal{B}(Z(4430)^+ \to \psi(2S)\pi^+)$	Belle [656]: $3.2^{+1.8}_{-0.9}{}^{+5.3}_{-1.6}$	
	BaBar [708]: $1.9 \pm 0.8 \pm 0.0$	1.9 ± 0.8
$\mathcal{B}(\bar{B}^0 \to Z_c(3900)^+K^-) \times \mathcal{B}(Z_c(3900)^+ \to J/\psi\pi^+)$	Belle [647]: <0.09	<0.09
$\mathcal{B}(\bar{B}^0 \to Z_c(4200)^+K^-) \times \mathcal{B}(Z_c(4200)^+ \to J/\psi\pi^+)$	Belle [647]: $2.2^{+0.7}_{-0.5}{}^{+1.1}_{-0.6}$	$2.2^{+1.3}_{-0.8}$

Table 134 Relative decay rates

Parameter	Measurements	Average
$\mathcal{B}(\bar{B}^0 \to X(3872)\bar{K}^0)/\mathcal{B}(B^- \to X(3872)K^-)$	BaBar [651]: $1.0^{+0.8}_{-0.6}{}^{+0.1}_{-0.2}$	
	BaBar [704]: $0.41 \pm 0.24 \pm 0.05$	0.47 ± 0.23
$\mathcal{B}(\bar{B}^0 \to Y(3940)\bar{K}^0)/\mathcal{B}(B^- \to Y(3940)K^-)$	BaBar [651]: $0.7^{+0.4}_{-0.3} \pm 0.1$	$0.7^{+0.4}_{-0.3}$

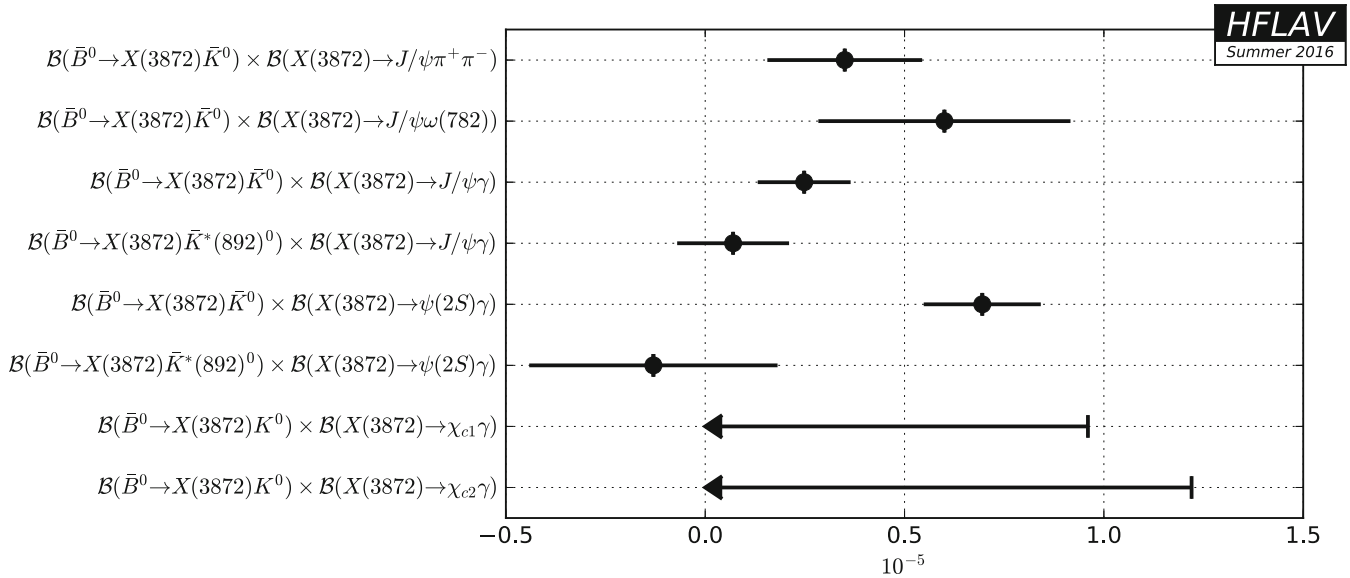

Fig. 102 Summary of the averages from Table 129

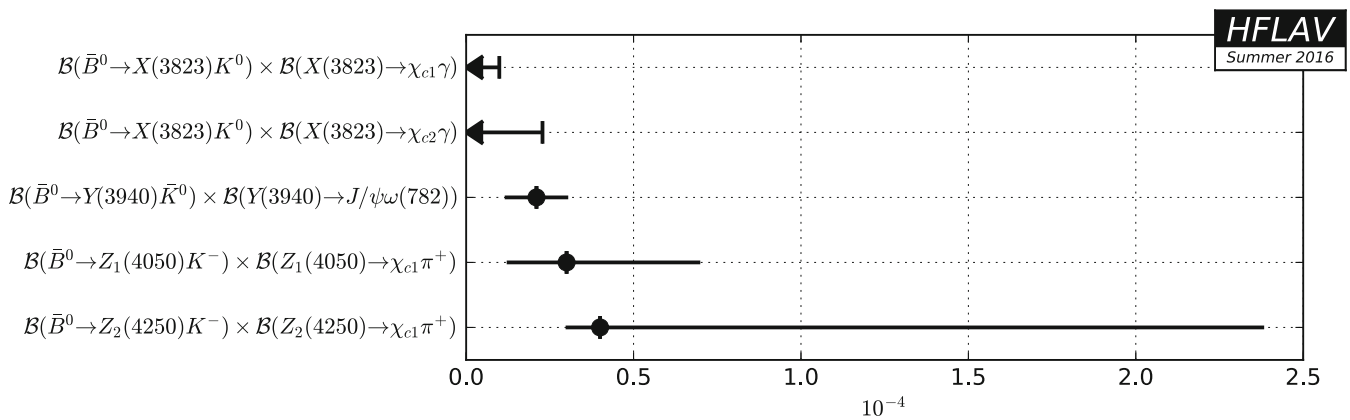

Fig. 103 Summary of the averages from Table 131

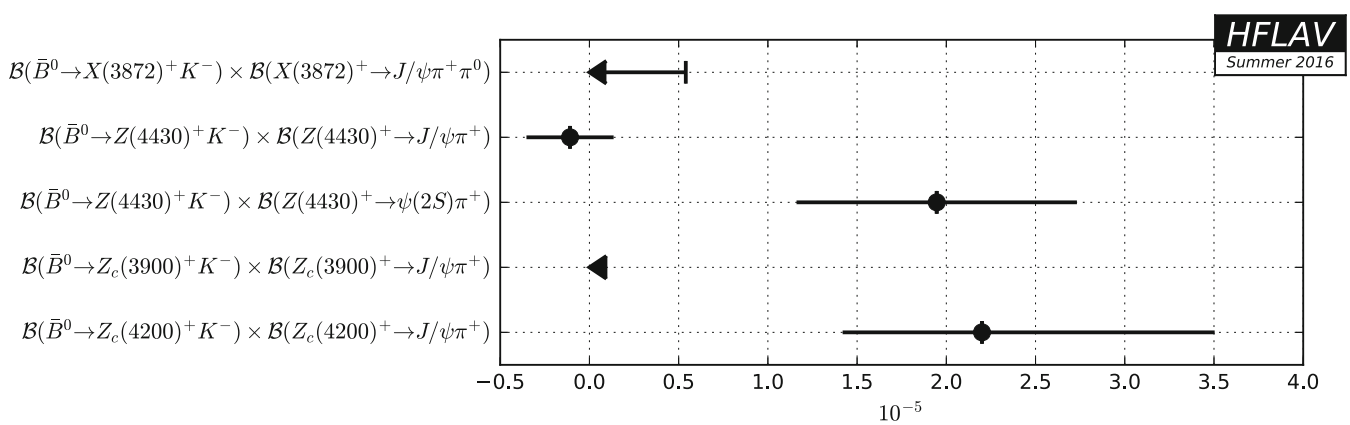

Fig. 104 Summary of the averages from Table 133

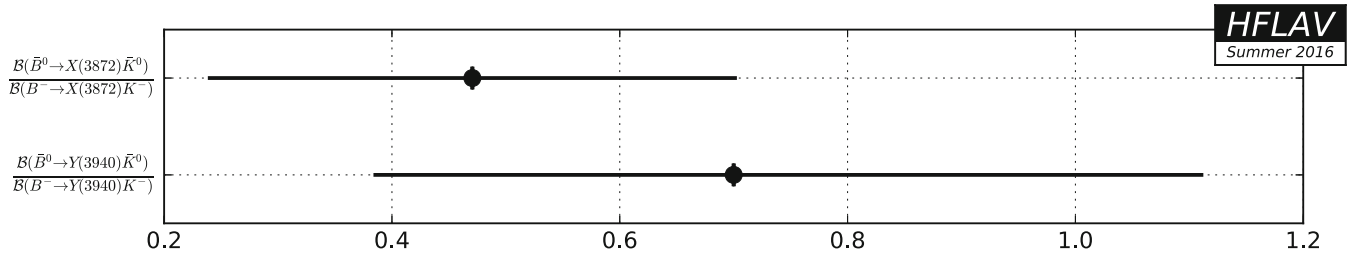

Fig. 105 Summary of the averages from Table 134

6.2 Decays of B^- mesons

Measurements of B^- decays to charmed hadrons are summarized in Sects. 6.2.1–6.2.5.

6.2.1 Decays to a single open charm meson

Averages of B^- decays to a single open charm meson are shown in Tables 135, 136, 137, 138, 139, 140, 141, 142, 143, 144, 145, 146, 147, 148, 149 and Figs. 106, 107, 108, 109, 110, 111, 112, 113, 114, 115, 116, 117, 118, 119. In this section D^{**} refers to the sum of all the non-strange charm meson states with masses in the range 2.2–2.8 GeV/c^2.

Table 135 Decays to a $D^{(*)}$ meson and one or more pions [10^{-2}]

Parameter	Measurements	Average
$\mathcal{B}(B^- \to D^*(2010)^-\pi^0)$	Belle [709]: <0.00036	<0.00036
$\mathcal{B}(B^- \to D^0\pi^-)$	BaBar [594]: 0.490 ± 0.007 ± 0.022	
	BaBar [595]: 0.449 ± 0.021 ± 0.023	0.475 ± 0.019
$\mathcal{B}(B^- \to D^*(2007)^0\pi^-)$	BaBar [594]: 0.552 ± 0.017 ± 0.042	
	BaBar [595]: 0.513 ± 0.022 ± 0.028	0.528 ± 0.028
$\mathcal{B}(B^- \to D^+\pi^-\pi^-)$	Belle [710]: 0.102 ± 0.004 ± 0.015	
	BaBar [711]: 0.108 ± 0.003 ± 0.005	0.107 ± 0.005
$\mathcal{B}(B^- \to D^*(2010)^+\pi^-\pi^-)$	Belle [710]: 0.125 ± 0.008 ± 0.022	
	BaBar [712]: 0.122 ± 0.005 ± 0.018	0.123 ± 0.015
$\mathcal{B}(B^- \to D^*(2007)^0\pi^-\pi^+\pi^-)$	Belle [596]: 1.055 ± 0.047 ± 0.129	1.055 ± 0.137
$\mathcal{B}(B^- \to D^*(2010)^+\pi^-\pi^+\pi^-\pi^-)$	Belle [596]: 0.256 ± 0.026 ± 0.033	0.256 ± 0.042
$\mathcal{B}(B^- \to D^*(2007)^0\pi^-\pi^+\pi^-\pi^+\pi^-)$	Belle [596]: 0.567 ± 0.091 ± 0.085	0.567 ± 0.125

Table 136 Decays to a $D^{(*)0}$ meson and one or more kaons [10^{-3}]

Parameter	Measurements	Average
$\mathcal{B}(B^- \to D^0K^-)$	Belle [713]: 0.383 ± 0.025 ± 0.037	0.383 ± 0.045
$\mathcal{B}(B^- \to D^*(2007)^0K^-)$	Belle [605]: 0.359 ± 0.087 ± 0.051	0.359 ± 0.101
$\mathcal{B}(B^- \to D^0K^-K^0)$	Belle [607]: 0.55 ± 0.14 ± 0.08	0.55 ± 0.16
$\mathcal{B}(B^- \to D^*(2007)^0K^-K^0)$	Belle [607]: <1.06	<1.06
$\mathcal{B}(B^- \to D^0K^-K^*(892)^0)$	Belle [607]: 0.75 ± 0.13 ± 0.11	0.75 ± 0.17
$\mathcal{B}(B^- \to D^*(2007)^0K^-K^*(892)^0)$	Belle [607]: 1.53 ± 0.31 ± 0.29	1.53 ± 0.42
$\mathcal{B}(B^- \to D^0K^*(892)^-)$	BaBar [714]: 0.529 ± 0.030 ± 0.034	0.529 ± 0.045
$\mathcal{B}(B^- \to D^*(2007)^0K^*(892)^-)$	BaBar [715]: 0.83 ± 0.11 ± 0.10	0.83 ± 0.15
$\mathcal{B}(B^- \to D^+K^-\pi^-)$	LHCb [716]: 0.0731 ± 0.0019 ± 0.0045	0.0731 ± 0.0049

Table 137 Decays to a $D^{(*)-}$ meson and a neutral kaon or a kaon and a pion [10^{-6}]

Parameter	Measurements	Average
$\mathcal{B}(B^- \to D^- \bar{K}^0)$	BaBar [717]: $-3.8\,^{+2.2}_{-1.8}\,^{+1.2}_{-1.6}$	$-3.8\,^{+2.5}_{-2.4}$
$\mathcal{B}(B^- \to D^- \bar{K}^*(892)^0)$	BaBar [717]: $-5.3\,^{+2.3}_{-2.0}\,^{+1.4}_{-1.8}$	$-5.3\,^{+2.7}_{-2.7}$
$\mathcal{B}(B^- \to D^- K^- \pi^+)$	LHCb [718]: 5.31 ± 0.90 ± 0.59	5.31 ± 1.08
$\mathcal{B}(B^- \to D^*(2010)^- \bar{K}^0)$	BaBar [719]: <9	<9

Table 138 Relative decay rates to D^0 mesons I

Parameter	Measurements	Average
$\mathcal{B}(B^- \to D^0\pi^-)/\mathcal{B}(\bar{B}^0 \to D^+\pi^-)$	CDF [720]: 1.97 ± 0.10 ± 0.21	1.97 ± 0.23
$\mathcal{B}(B^- \to D^0\pi^+\pi^-\pi^-)/\mathcal{B}(B^- \to D^0\pi^-)$	LHCb [616]: 1.27 ± 0.06 ± 0.11	1.27 ± 0.13

Table 139 Relative decay rates to D^0 mesons II [10^{-2}]

Parameter	Measurements	Average
$\mathcal{B}(B^- \to \bar{D}^0 K^-)/\mathcal{B}(B^- \to D^0 K^-)$	Belle [721]: <19	<19
$\mathcal{B}(B^- \to D^0 K^-)/\mathcal{B}(B^- \to D^0\pi^-)$	LHCb [436]: 7.79 ± 0.06 ± 0.19	
	Belle [721]: 6.77 ± 0.23 ± 0.30	
	Belle [713]: 7.7 ± 0.5 ± 0.6	
	BaBar [722]: 8.31 ± 0.35 ± 0.20	7.69 ± 0.16
$\mathcal{B}(B^- \to D^0 K^-\pi^+\pi^-)/\mathcal{B}(B^- \to D^0\pi^+\pi^-\pi^-)$	LHCb [620]: 9.4 ± 1.3 ± 0.9	9.4 ± 1.6

Table 140 Absolute decay rates to excited D mesons [10^{-3}]

Parameter	Measurements	Average
$\mathcal{B}(B^- \to D^{**0}\pi^-)$	BaBar [595]: 5.50 ± 0.52 ± 1.04	5.50 ± 1.16

Table 141 Absolute product decay rates to excited D mesons I [10^{-3}]

Parameter	Measurements	Average
$\mathcal{B}(B^- \to D_1^0(2420)\pi^-) \times \mathcal{B}(D_1^0(2420) \to D^*(2010)^+\pi^-)$	Belle [710]: 0.68 ± 0.07 ± 0.13	
	BaBar [712]: 0.59 ± 0.03 ± 0.11	0.62 ± 0.09
$\mathcal{B}(B^- \to D_1^0(2420)\pi^-) \times \mathcal{B}(D_1^0(2420) \to D^0\pi^-\pi^+)$	Belle [622]: $0.185 \pm 0.029\,^{+0.035}_{-0.058}$	$0.185\,^{+0.045}_{-0.065}$
$\mathcal{B}(B^- \to D_0^{*0}\pi^-) \times \mathcal{B}(D_0^{*0} \to D^+\pi^-)$	Belle [710]: 0.61 ± 0.06 ± 0.18	
	BaBar [711]: 0.68 ± 0.03 ± 0.20	0.63 ± 0.19
$\mathcal{B}(B^- \to D_1^0(H)\pi^-) \times \mathcal{B}(D_1^0(H) \to D^*(2010)^+\pi^-)$	Belle [710]: 0.50 ± 0.04 ± 0.11	0.50 ± 0.11
$\mathcal{B}(B^- \to D_2^{*0}(2460)\pi^-) \times \mathcal{B}(D_2^{*0}(2460) \to D^*(2010)^+\pi^-)$	Belle [710]: 0.18 ± 0.03 ± 0.04	
	BaBar [712]: 0.18 ± 0.03 ± 0.05	0.18 ± 0.04
$\mathcal{B}(B^- \to D_2^{*0}(2460)\pi^-) \times \mathcal{B}(D_2^{*0}(2460) \to D^+\pi^-)$	Belle [710]: 0.34 ± 0.03 ± 0.07	
	BaBar [711]: 0.35 ± 0.02 ± 0.04	0.35 ± 0.05

Table 142 Absolute product decay rates to excited D mesons II [10^{-5}]

Parameter	Measurements	Average
$\mathcal{B}(B^- \to D_1^0(2420)\pi^-) \times \mathcal{B}(D_1^0(2420) \to D^*(2007)^0\pi^-\pi^+)$	Belle [622]: <0.6	<0.6
$\mathcal{B}(B^- \to D_2^{*0}(2460)\pi^-) \times \mathcal{B}(D_2^{*0}(2460) \to D^*(2007)^0\pi^-\pi^+)$	Belle [622]: <2.2	<2.2

Table 143 Relative decay rates to excited D mesons

Parameter	Measurements	Average
$\mathcal{B}(B^- \to D^*(2007)^0\pi^-)/\mathcal{B}(B^- \to D^0\pi^-)$	BaBar [595]: $1.14 \pm 0.07 \pm 0.04$	1.14 ± 0.08
$\mathcal{B}(B^- \to D^{**0}\pi^-)/\mathcal{B}(B^- \to D^0\pi^-)$	BaBar [595]: $1.22 \pm 0.13 \pm 0.23$	1.22 ± 0.26
$\mathcal{B}(B^- \to D_2^{*0}(2460)\pi^-)/\mathcal{B}(B^- \to D_1^0(2420)\pi^-)$	BaBar [712]: $0.80 \pm 0.07 \pm 0.16$	0.80 ± 0.17
$\mathcal{B}(B^- \to D^*(2007)^0K^-)/\mathcal{B}(B^- \to D^*(2007)^0\pi^-)$	Belle [605]: $0.078 \pm 0.019 \pm 0.009$	
	BaBar [723]: $0.0813 \pm 0.0040\,^{+0.0042}_{-0.0031}$	0.0811 ± 0.0053

Table 144 Relative product decay rates to excited D mesons

Parameter	Measurements	Average
$[\mathcal{B}(B^- \to D_1^0\pi^-) \times \mathcal{B}(D_1^0 \to D^0\pi^+\pi^-)]/\mathcal{B}(B^- \to D^0\pi^+\pi^-\pi^-)$	LHCb [616]: $0.040 \pm 0.007 \pm 0.005$	0.040 ± 0.009
$[\mathcal{B}(B^- \to D_1^{*0}\pi^-) \times \mathcal{B}(D_1^{*0} \to D^{*+}\pi^-)]/\mathcal{B}(B^- \to D^0\pi^+\pi^-\pi^-)$	LHCb [616]: $0.093 \pm 0.016 \pm 0.009$	0.093 ± 0.018
$[\mathcal{B}(B^- \to D_1^{*0}\pi^-) \times \mathcal{B}(D_1^{*0} \to D^0\pi^+\pi^-)]/\mathcal{B}(B^- \to D^0\pi^+\pi^-\pi^-)$	LHCb [616]: $0.103 \pm 0.015 \pm 0.009$	0.103 ± 0.017
$[\mathcal{B}(B^- \to D_2^{*0}\pi^-) \times \mathcal{B}(D_2^{*0} \to D^{*+}\pi^-)]/\mathcal{B}(B^- \to D^0\pi^+\pi^-\pi^-)$	LHCb [616]: $0.039 \pm 0.012 \pm 0.004$	0.039 ± 0.013
$[\mathcal{B}(B^- \to D_2^{*0}\pi^-) \times \mathcal{B}(D_2^{*0} \to D^0\pi^+\pi^-)]/\mathcal{B}(B^- \to D^0\pi^+\pi^-\pi^-)$	LHCb [616]: $0.040 \pm 0.010 \pm 0.004$	0.040 ± 0.011
$[\mathcal{B}(B^- \to D_2^{*+}\pi^-) \times \mathcal{B}(D_2^{*+} \to D^0\pi^-\pi^+)]/\mathcal{B}(B^- \to D^0\pi^+\pi^-\pi^-)$	LHCb [616]: $0.014 \pm 0.006 \pm 0.002$	0.014 ± 0.006

Table 145 Decays to $D_s^{(*)}$ mesons I $[10^{-4}]$

Parameter	Measurements	Average
$\mathcal{B}(B^- \to D_s^+K^-\pi^-)$	Belle [724]: $1.94\,^{+0.09}_{-0.08}\,^{+0.26}_{-0.26}$	1.97 ± 0.23
	BaBar [615]: $2.02 \pm 0.13 \pm 0.38$	
$\mathcal{B}(B^- \to D_s^{*+}K^-\pi^-)$	Belle [724]: $1.47\,^{+0.15}_{-0.14}\,^{+0.23}_{-0.23}$	1.54 ± 0.22
	BaBar [615]: $1.67 \pm 0.16 \pm 0.35$	

Table 146 Decays to $D_s^{(*)}$ mesons I $[10^{-5}]$

Parameter	Measurements	Average
$\mathcal{B}(B^- \to D_s^+K^-K^-)$	BaBar [615]: $1.1 \pm 0.4 \pm 0.2$	1.1 ± 0.4
$\mathcal{B}(B^- \to D_s^{*+}K^-K^-)$	BaBar [615]: <1.5	<1.5
$\mathcal{B}(B^- \to D_s^-\pi^0)$	BaBar [725]: $1.5\,^{+0.5}_{-0.4} \pm 0.2$	$1.5\,^{+0.5}_{-0.5}$
$\mathcal{B}(B^- \to D_s^-\phi(1020))$	LHCb [726]: $0.187\,^{+0.125}_{-0.073} \pm 0.037$	$0.187\,^{+0.130}_{-0.082}$
	BaBar [727]: <0.19	
$\mathcal{B}(B^- \to D_s^{*-}\phi(1020))$	BaBar [727]: <1.2	<1.2

Table 147 Baryonic decays I $[10^{-4}]$

Parameter	Measurements	Average
$\mathcal{B}(B^- \to D^0p\bar{p}\pi^-)$	BaBar [624]: $3.72 \pm 0.11 \pm 0.25$	3.72 ± 0.27
$\mathcal{B}(B^- \to D^*(2007)^0p\bar{p}\pi^-)$	BaBar [624]: $3.73 \pm 0.17 \pm 0.27$	3.73 ± 0.32
$\mathcal{B}(B^- \to D^+p\bar{p}\pi^-\pi^-)$	BaBar [624]: $1.66 \pm 0.13 \pm 0.27$	1.66 ± 0.30
$\mathcal{B}(B^- \to D^*(2010)^+p\bar{p}\pi^-\pi^-)$	BaBar [624]: $1.86 \pm 0.16 \pm 0.19$	1.86 ± 0.25

Table 148 Baryonic decays II $[10^{-5}]$

Parameter	Measurements	Average
$\mathcal{B}(B^- \to D^0\Lambda\bar{p})$	Belle [728]: $1.43\,^{+0.28}_{-0.25} \pm 0.18$	$1.43\,^{+0.33}_{-0.31}$
$\mathcal{B}(B^- \to D^*(2007)^0\Lambda\bar{p})$	Belle [728]: <4.8	<4.8
$\mathcal{B}(B^- \to D^-p\bar{p})$	Belle [625]: <1.5	<1.5
$\mathcal{B}(B^- \to D^*(2010)^-p\bar{p})$	Belle [625]: <1.5	<1.5

Table 149 Lepton number violating decays [10^{-6}]

Parameter	Measurements	Average
$\mathcal{B}(B^- \to D^- e^+ e^+)$	Belle [729]: <2.6	<2.6
$\mathcal{B}(B^- \to D^- e^+ \mu^+)$	Belle [729]: <1.8	<1.8
$\mathcal{B}(B^- \to D^- \mu^+ \mu^+)$	Belle [729]: <1.0	<1.0

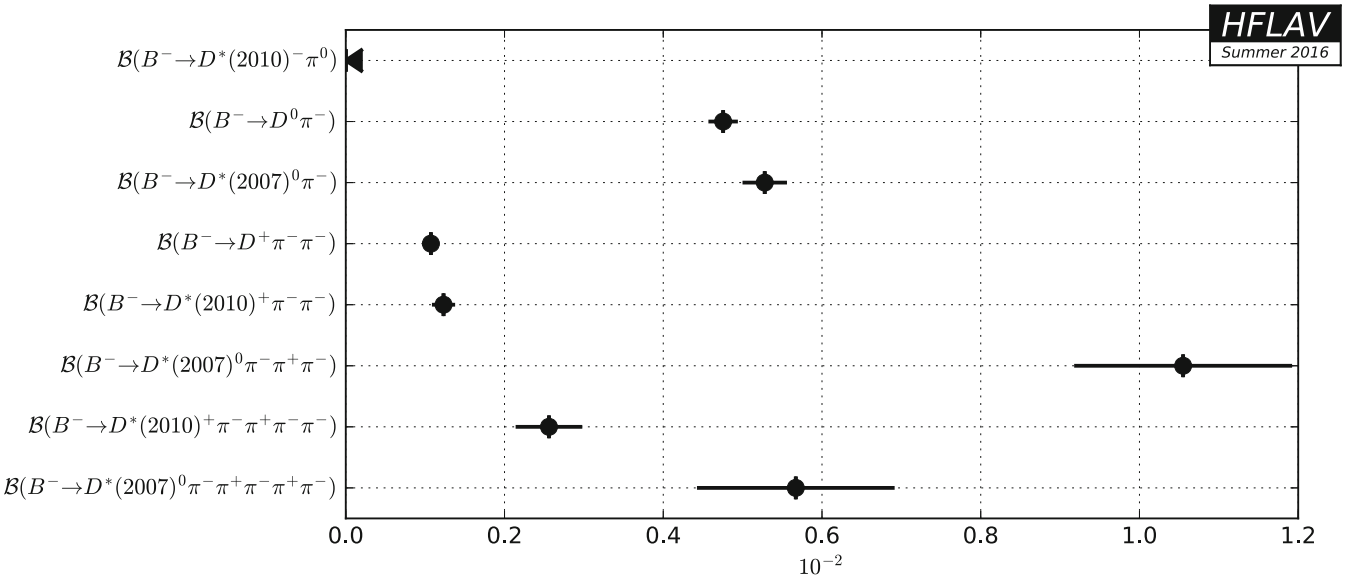

Fig. 106 Summary of the averages from Table 135

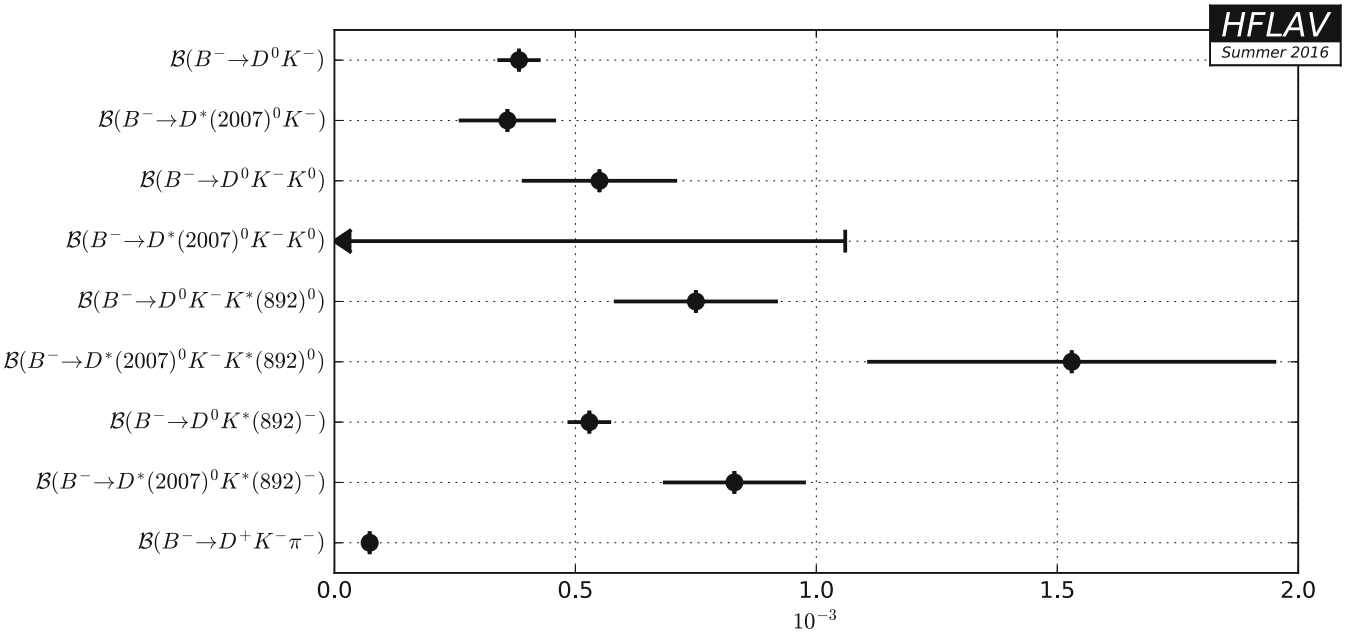

Fig. 107 Summary of the averages from Table 136

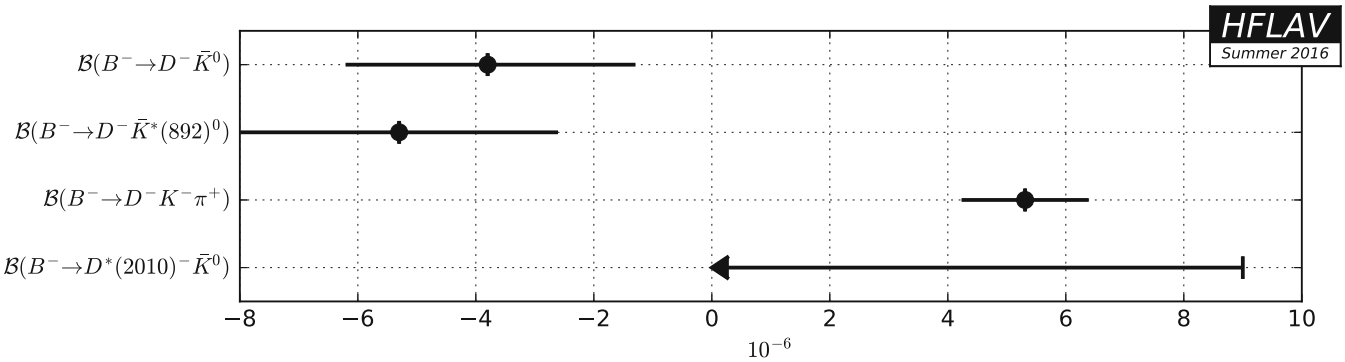

Fig. 108 Summary of the averages from Table 137

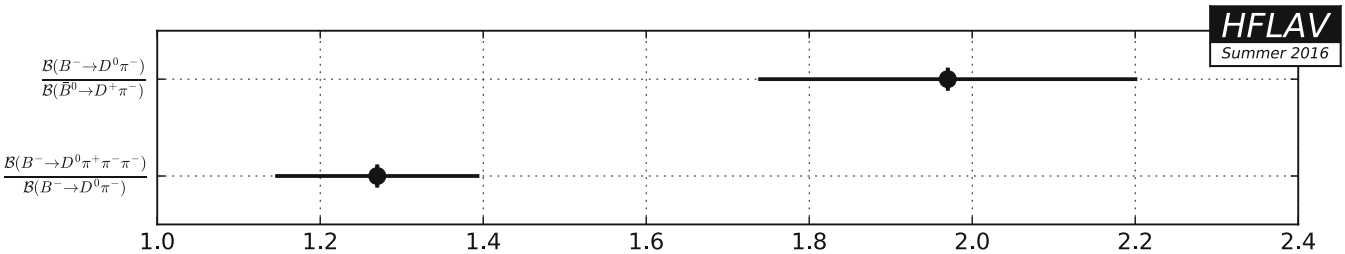

Fig. 109 Summary of the averages from Table 138

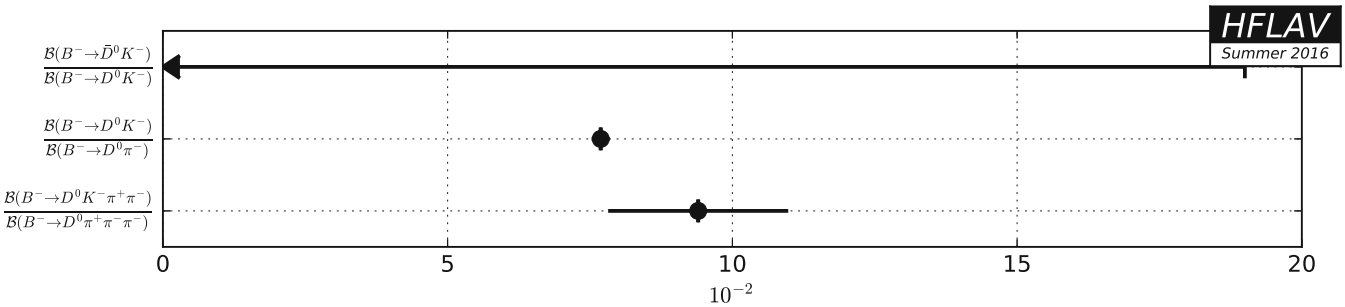

Fig. 110 Summary of the averages from Table 139

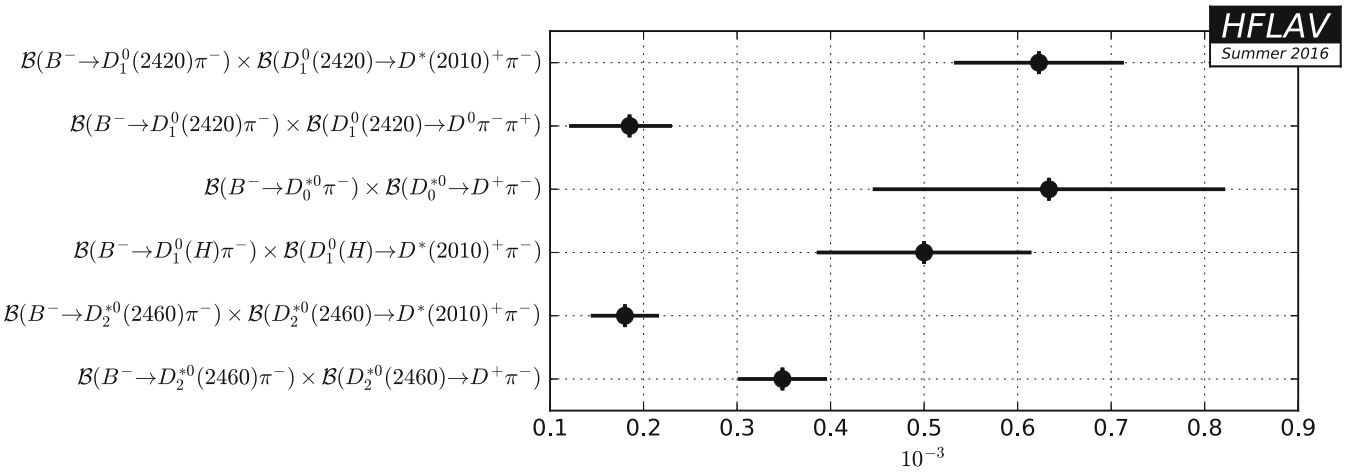

Fig. 111 Summary of the averages from Table 141

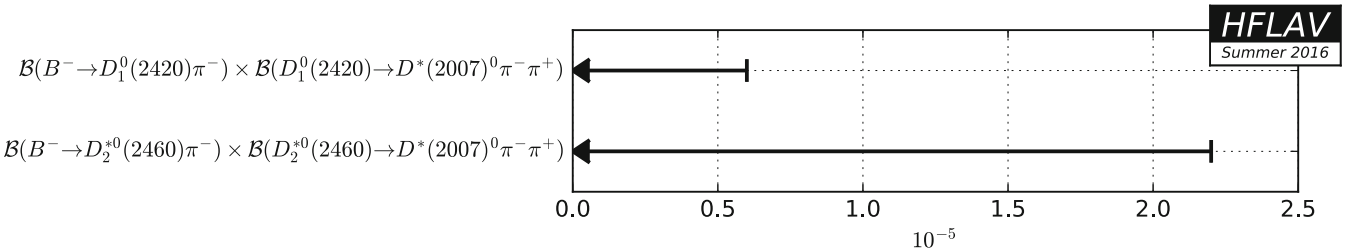

Fig. 112 Summary of the averages from Table 142

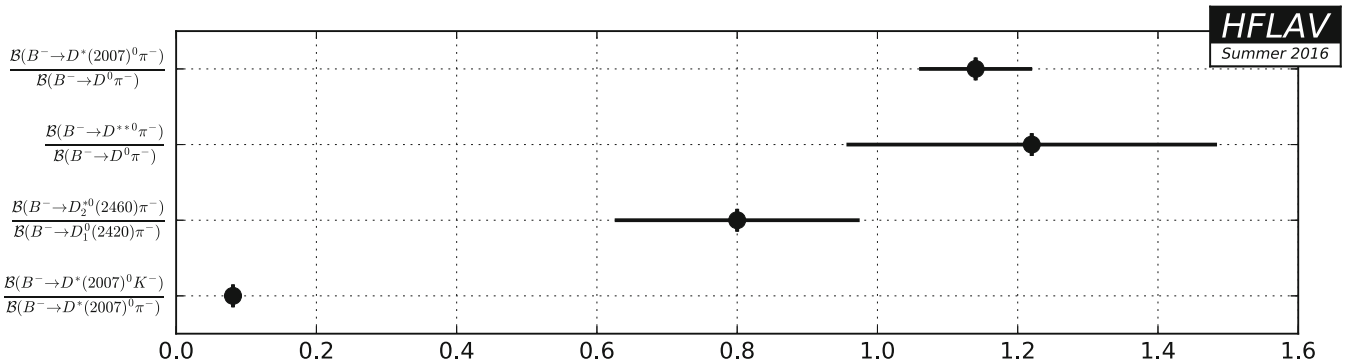

Fig. 113 Summary of the averages from Table 143

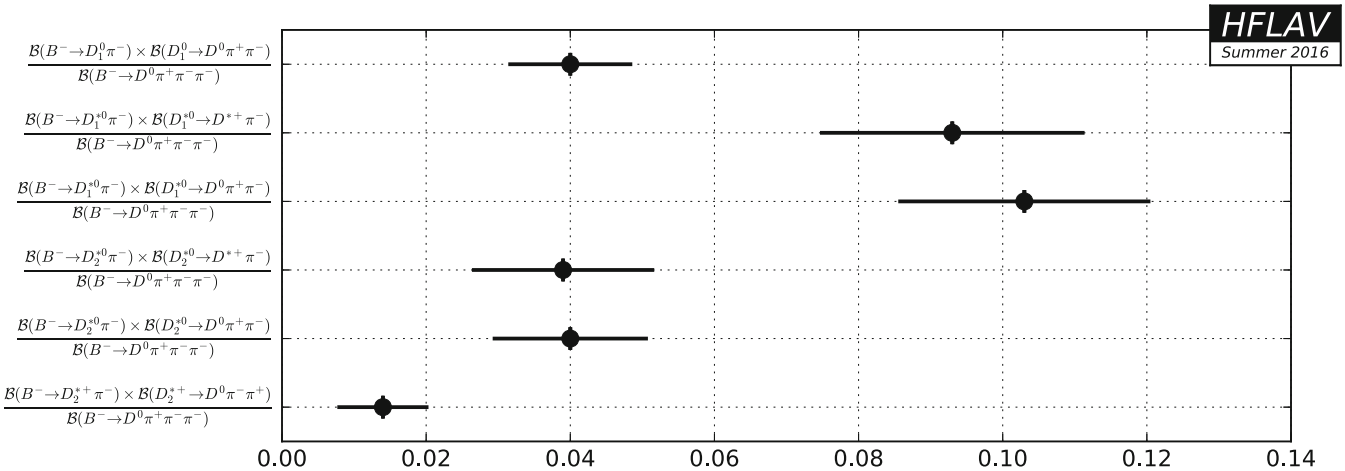

Fig. 114 Summary of the averages from Table 144

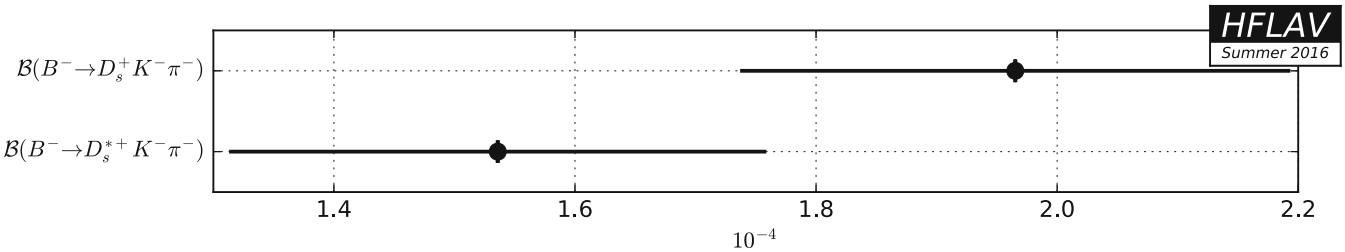

Fig. 115 Summary of the averages from Table 145

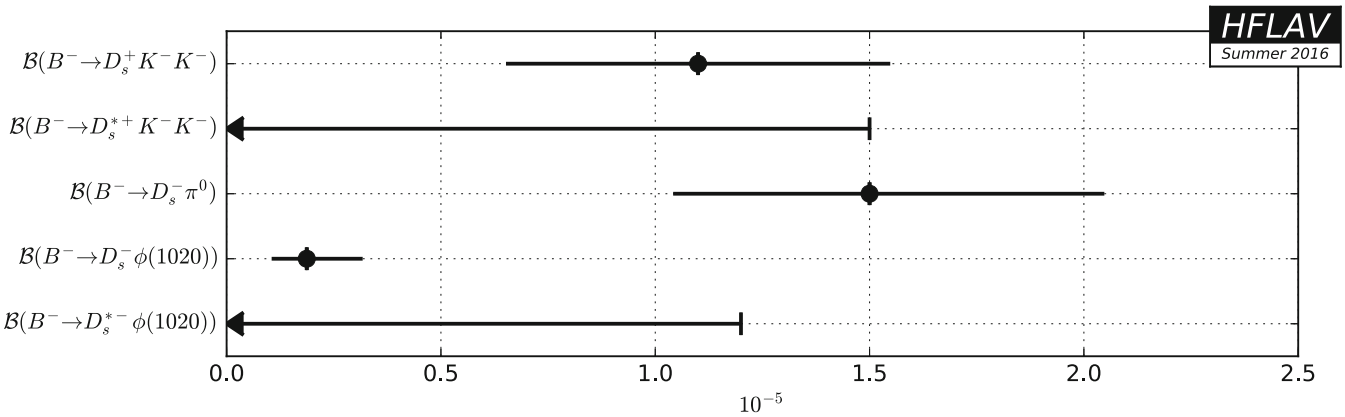

Fig. 116 Summary of the averages from Table 146

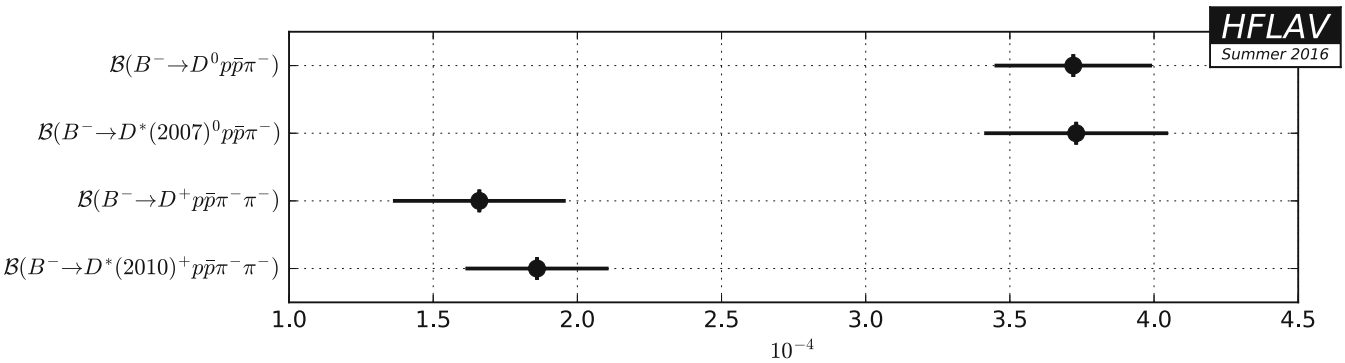

Fig. 117 Summary of the averages from Table 147

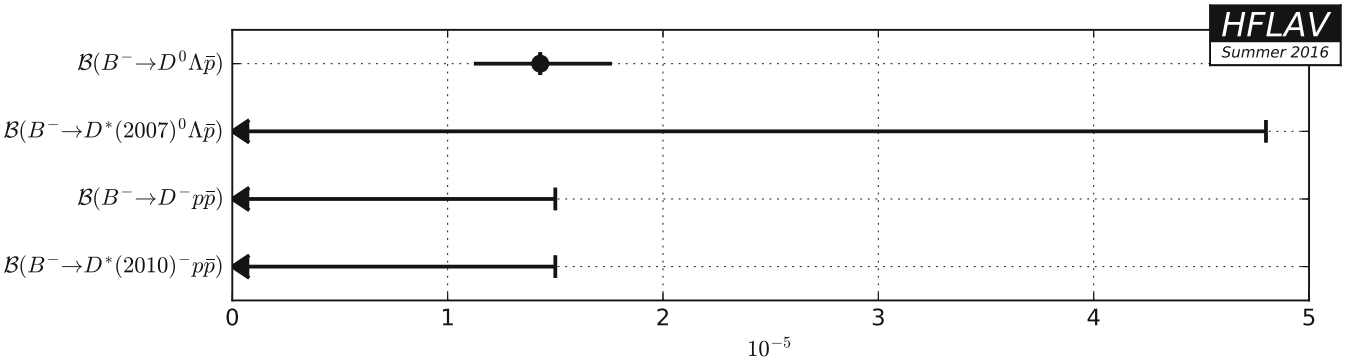

Fig. 118 Summary of the averages from Table 148

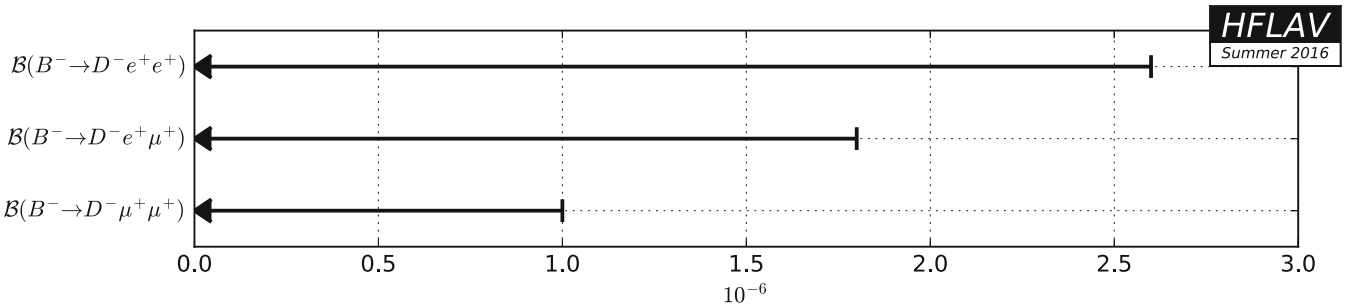

Fig. 119 Summary of the averages from Table 149

6.2.2 Decays to two open charm mesons

Averages of B^- decays to two open charm mesons are shown in Tables 150, 151, 152, 153, 154, 155, 156, 157, 158 and Figs. 120, 121, 122, 123, 124, 125, 126, 127.

Table 150 Decays to $D^{(*)-}D^{(*)0}$ [10^{-3}]

Parameter	Measurements	Average
$\mathcal{B}(B^- \to D^- D^0)$	Belle [631]: 0.385 ± 0.031 ± 0.038	0.384 ± 0.042
	BaBar [630]: 0.38 ± 0.06 ± 0.05	
$\mathcal{B}(B^- \to D^{*0} D^-)$	BaBar [630]: 0.63 ± 0.14 ± 0.10	0.63 ± 0.17
$\mathcal{B}(B^- \to D_s^- D^0)$	Belle [730]: 0.459 ± 0.072 ± 0.056	0.385 ± 0.046
	BaBar [630]: 0.36 ± 0.05 ± 0.04	
$\mathcal{B}(B^- \to D^*(2007)^0 D^*(2010)^-)$	BaBar [630]: 0.81 ± 0.12 ± 0.12	0.81 ± 0.17

Table 151 Decays to two D mesons and a kaon I [10^{-2}]

Parameter	Measurements	Average
$\mathcal{B}(B^- \to D^*(2007)^0 \bar{D}^0 K^-)$	BaBar [632]: 0.226 ± 0.016 ± 0.017	0.226 ± 0.023
$\mathcal{B}(B^- \to D^0 \bar{D}^*(2007)^0 K^-)$	BaBar [632]: 0.632 ± 0.019 ± 0.045	0.632 ± 0.049
$\mathcal{B}(B^- \to \bar{D}^*(2007)^0 D^*(2007)^0 K^-)$	BaBar [632]: 1.123 ± 0.036 ± 0.126	1.123 ± 0.131
$\mathcal{B}(B^- \to D^*(2007)^0 D^- \bar{K}^0)$	BaBar [632]: 0.206 ± 0.038 ± 0.030	0.206 ± 0.048
$\mathcal{B}(B^- \to D^0 D^*(2010)^- \bar{K}^0)$	BaBar [632]: 0.381 ± 0.031 ± 0.023	0.381 ± 0.039
$\mathcal{B}(B^- \to D^*(2007)^0 D^*(2010)^- \bar{K}^0)$	BaBar [632]: 0.917 ± 0.083 ± 0.090	0.917 ± 0.122

Table 152 Decays to two D mesons and a kaon II [10^{-3}]

Parameter	Measurements	Average
$\mathcal{B}(B^- \to D^0 \bar{D}^0 K^-)$	Belle [731]: $2.22 \pm 0.22\,^{+0.26}_{-0.24}$	1.44 ± 0.13
	BaBar [632]: 1.31 ± 0.07 ± 0.12	
$\mathcal{B}(B^- \to D^0 \bar{D}^0 \pi^0 K^-)$	Belle [633]: $0.107 \pm 0.031\,^{+0.019}_{-0.033}$	$0.107\,^{+0.036}_{-0.045}$
$\mathcal{B}(B^- \to D^+ D^- K^-)$	Belle [732]: <0.90	0.22 ± 0.07
	BaBar [632]: 0.22 ± 0.05 ± 0.05	
$\mathcal{B}(B^- \to D^*(2010)^+ D^- K^-)$	BaBar [632]: 0.60 ± 0.10 ± 0.08	0.60 ± 0.13
$\mathcal{B}(B^- \to D^+ D^*(2010)^- K^-)$	BaBar [632]: 0.63 ± 0.09 ± 0.06	0.63 ± 0.11
$\mathcal{B}(B^- \to D^*(2010)^- D^*(2010)^+ K^-)$	BaBar [632]: 1.32 ± 0.13 ± 0.12	1.32 ± 0.18
$\mathcal{B}(B^- \to D^0 D^- \bar{K}^0)$	BaBar [632]: 1.55 ± 0.17 ± 0.13	1.55 ± 0.21

Table 153 Decays to $D_s^{(*)-}D^{(*)+}$ [10^{-2}]

Parameter	Measurements	Average
$\mathcal{B}(B^- \to D_s^- D^0)$	BaBar [635]: 1.33 ± 0.18 ± 0.32	1.33 ± 0.37
$\mathcal{B}(B^- \to D_s^- D^*(2007)^0)$	BaBar [635]: 1.21 ± 0.23 ± 0.20	1.21 ± 0.30
$\mathcal{B}(B^- \to D_s^{*-} D^0)$	BaBar [635]: 0.93 ± 0.18 ± 0.19	0.93 ± 0.26
$\mathcal{B}(B^- \to D_s^{*-} D^*(2007)^0)$	BaBar [635]: 1.70 ± 0.26 ± 0.24	1.70 ± 0.35

Table 154 Product decays rates to $D_s^{(*)-} D^{(*)+}$ [10^{-4}]

Parameter	Measurements	Average
$\mathcal{B}(B^- \to D_s^- D^0) \times \mathcal{B}(D_s^- \to \phi(1020)\pi^-)$	BaBar [635]: 4.00 ± 0.61 ± 0.61	4.00 ± 0.86
$\mathcal{B}(B^- \to D_s^- D^*(2007)^0) \times \mathcal{B}(D_s^- \to \phi(1020)\pi^-)$	BaBar [635]: 2.95 ± 0.65 ± 0.36	2.95 ± 0.74
$\mathcal{B}(B^- \to D_s^{*-} D^0) \times \mathcal{B}(D_s^- \to \phi(1020)\pi^-)$	BaBar [635]: 3.13 ± 1.19 ± 0.58	3.13 ± 1.32
$\mathcal{B}(B^- \to D_s^{*-} D^*(2007)^0) \times \mathcal{B}(D_s^- \to \phi(1020)\pi^-)$	BaBar [635]: 8.57 ± 1.48 ± 1.12	8.57 ± 1.86

Table 155 Relative decay rates

Parameter	Measurements	Average
$\mathcal{B}(B^- \to D_s^- D^0)/\mathcal{B}(\bar{B}^0 \to D_s^+ D^-)$	LHCb [639]: 1.22 ± 0.02 ± 0.07	1.22 ± 0.07

Table 156 Absolute decays rates to excited D_s mesons [10^{-3}]

Parameter	Measurements	Average
$\mathcal{B}(B^- \to D_{sJ}(2460)^- D^0)$	BaBar [635]: 4.3 ± 1.6 ± 1.3	4.3 ± 2.1
$\mathcal{B}(B^- \to D_{sJ}(2460)^- D^*(2007)^0)$	BaBar [635]: 11.2 ± 2.6 ± 2.0	11.2 ± 3.3

Table 157 Product decays rates to excited D_s mesons I [10^{-3}]

Parameter	Measurements	Average
$\mathcal{B}(B^- \to D^0 D_{sJ}(2460)^-) \times \mathcal{B}(D_{sJ}(2460)^- \to D_s^{*-}\pi^0)$	Belle [640]: $1.19^{+0.61}_{-0.49} \pm 0.36$	1.56 ± 0.57
	BaBar [641]: $2.7 \pm 0.7^{+1.0}_{-0.8}$	
$\mathcal{B}(B^- \to D_{sJ}(2460)^- D^*(2007)^0) \times \mathcal{B}(D_{sJ}(2460)^- \to D_s^-\gamma)$	BaBar [641]: $1.4 \pm 0.4^{+0.6}_{-0.4}$	$1.4^{+0.7}_{-0.6}$
$\mathcal{B}(B^- \to D_{sJ}(2460)^- D^*(2007)^0) \times \mathcal{B}(D_{sJ}(2460)^- \to D_s^{*-}\pi^0)$	BaBar [641]: $7.6 \pm 1.7^{+3.2}_{-2.4}$	$7.6^{+3.6}_{-2.9}$

Table 158 Product decays rates to excited D_s mesons II [10^{-3}]

Parameter	Measurements	Average
$\mathcal{B}(B^- \to D^0 D_{sJ}^*(2317)^-) \times \mathcal{B}(D_{sJ}^*(2317)^- \to D_s^-\pi^0)$	Belle [642]: $0.80^{+0.13}_{-0.12} \pm 0.12$	0.82 ± 0.17
	BaBar [641]: $1.0 \pm 0.3^{+0.4}_{-0.2}$	
$\mathcal{B}(B^- \to D^0 D_{sJ}^*(2317)^-) \times \mathcal{B}(D_{sJ}^*(2317)^- \to D_s^{*-}\gamma)$	Belle [640]: <0.76	<0.76
$\mathcal{B}(B^- \to D_{sJ}^*(2317)^- D^*(2007)^0) \times \mathcal{B}(D_{sJ}^*(2317)^- \to D_s^-\pi^0)$	BaBar [641]: $0.9 \pm 0.6^{+0.4}_{-0.3}$	$0.9^{+0.7}_{-0.7}$
$\mathcal{B}(B^- \to D^0 D_{sJ}(2460)^-) \times \mathcal{B}(D_{sJ}(2460)^- \to D_s^-\gamma)$	Belle [640]: $0.56^{+0.16}_{-0.15} \pm 0.17$	0.58 ± 0.18
	BaBar [641]: $0.6 \pm 0.2^{+0.2}_{-0.1}$	
$\mathcal{B}(B^- \to D^0 D_{sJ}(2460)^-) \times \mathcal{B}(D_{sJ}(2460)^- \to D_s^{*-}\gamma)$	Belle [640]: <0.98	<0.98
$\mathcal{B}(B^- \to D^0 D_{sJ}(2460)^-) \times \mathcal{B}(D_{sJ}(2460)^- \to D_s^-\pi^0)$	Belle [640]: <0.27	<0.27
$\mathcal{B}(B^- \to D^0 D_{sJ}(2460)^-) \times \mathcal{B}(D_{sJ}(2460)^- \to D_s^-\pi^+\pi^-)$	Belle [640]: <0.22	<0.22
$\mathcal{B}(B^+ \to D_{s1}(2536)^+ \bar{D}^0) \times \mathcal{B}(D_{s1}(2536)^+ \to D^*(2007)^0 K^+ + D^*(2010)^+ K^0)$	Belle [644]: 0.397 ± 0.085 ± 0.056	0.397 ± 0.102
$\mathcal{B}(B^- \to D_{s1}(2536)^- D^0) \times \mathcal{B}(D_{s1}(2536)^- \to \bar{D}^*(2007)^0 K^-)$	BaBar [643]: 0.216 ± 0.052 ± 0.045	0.216 ± 0.069
$\mathcal{B}(B^- \to D_{s1}(2536)^- D^0) \times \mathcal{B}(D_{s1}(2536)^- \to D^*(2010)^- \bar{K}^0)$	BaBar [643]: 0.230 ± 0.098 ± 0.043	0.230 ± 0.107
$\mathcal{B}(B^- \to D_{s1}(2536)^- \bar{D}^*(2007)^0) \times \mathcal{B}(D_{s1}(2536)^- \to \bar{D}^*(2007)^0 K^-)$	BaBar [643]: 0.546 ± 0.117 ± 0.104	0.546 ± 0.157
$\mathcal{B}(B^- \to D_{s1}(2536)^- D^*(2007)^0) \times \mathcal{B}(D_{s1}(2536)^- \to D^*(2010)^- \bar{K}^0)$	BaBar [643]: <1.069	<1.069

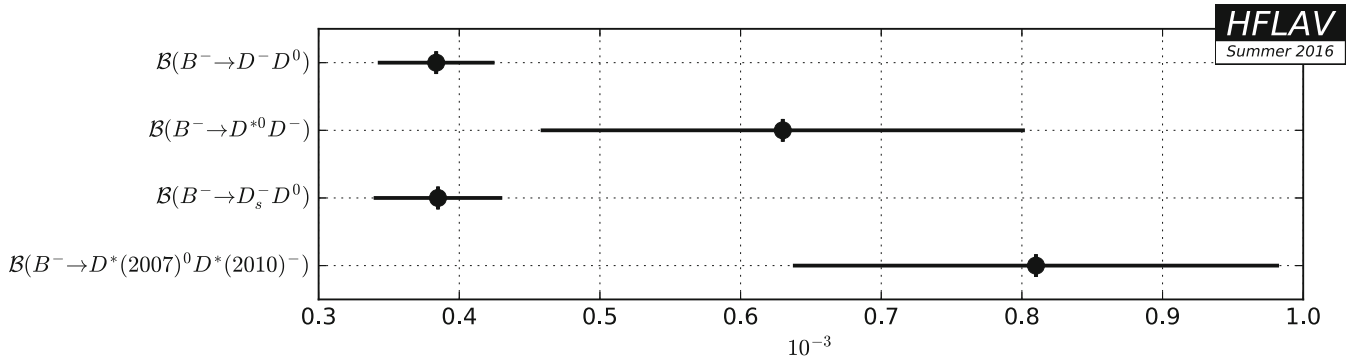

Fig. 120 Summary of the averages from Table 150

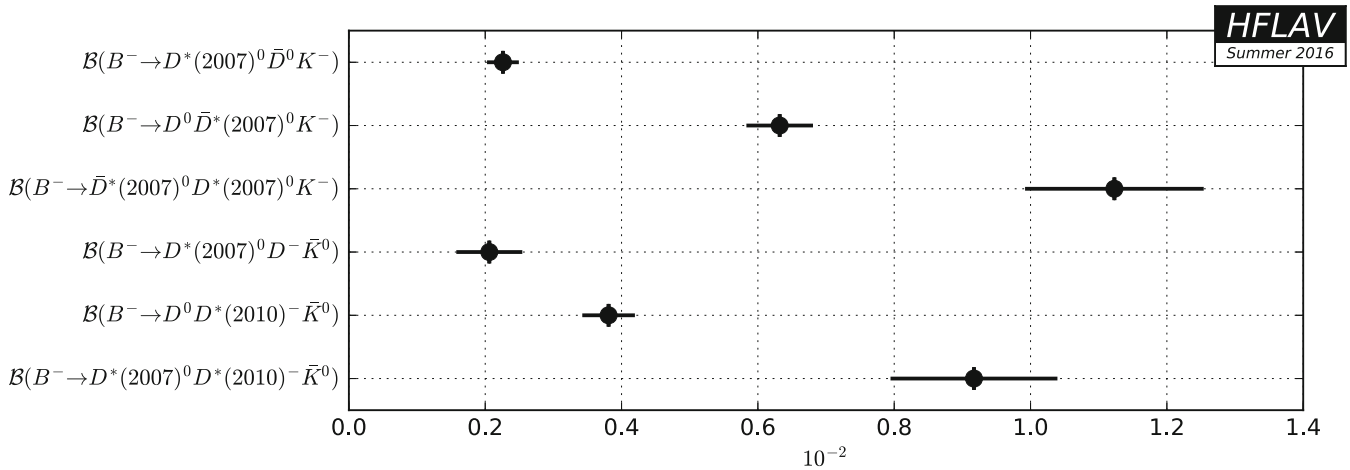

Fig. 121 Summary of the averages from Table 151

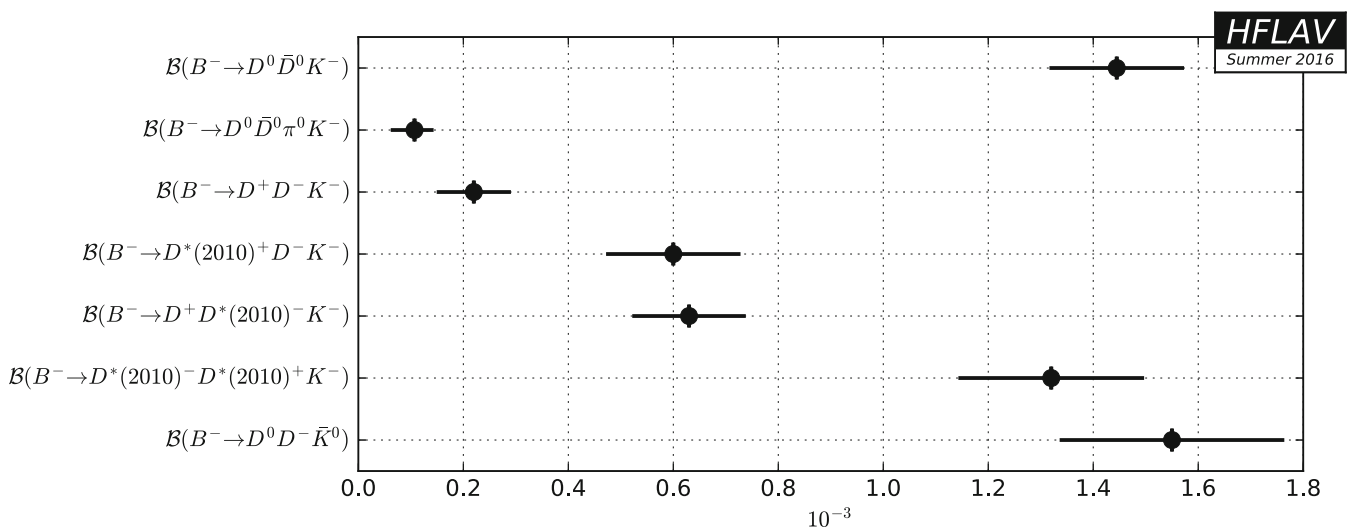

Fig. 122 Summary of the averages from Table 152

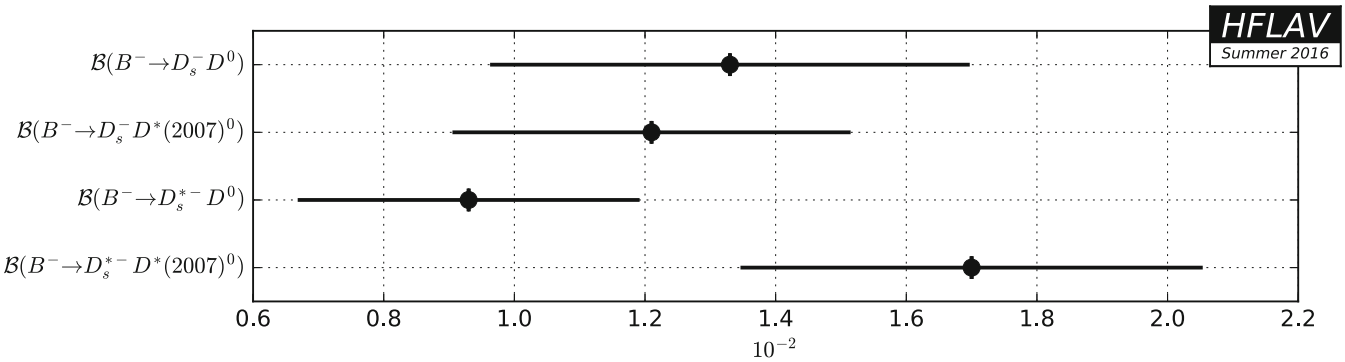

Fig. 123 Summary of the averages from Table 153

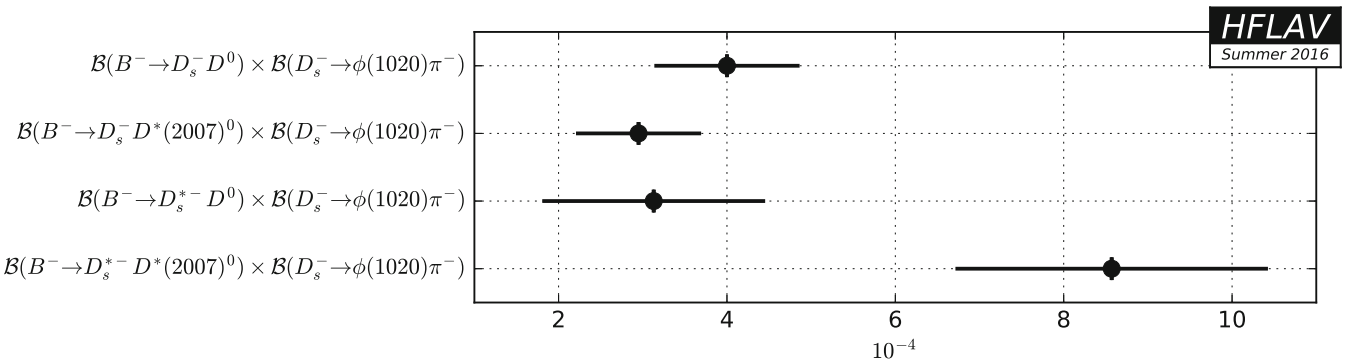

Fig. 124 Summary of the averages from Table 154

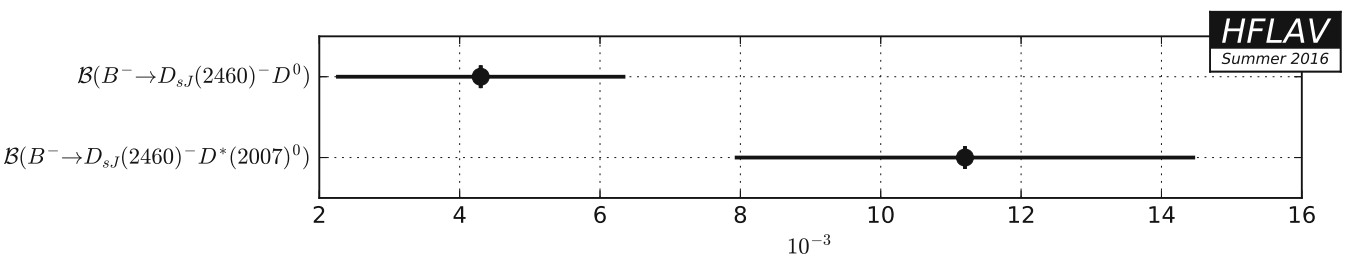

Fig. 125 Summary of the averages from Table 156

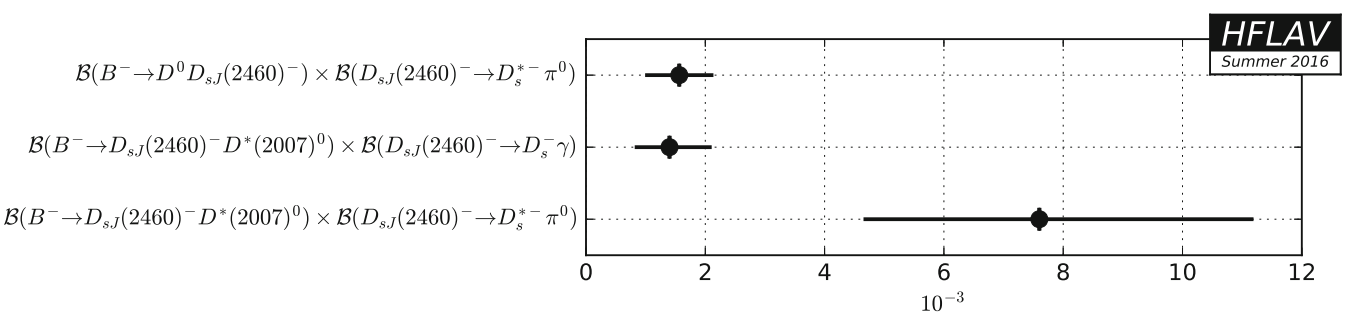

Fig. 126 Summary of the averages from Table 157

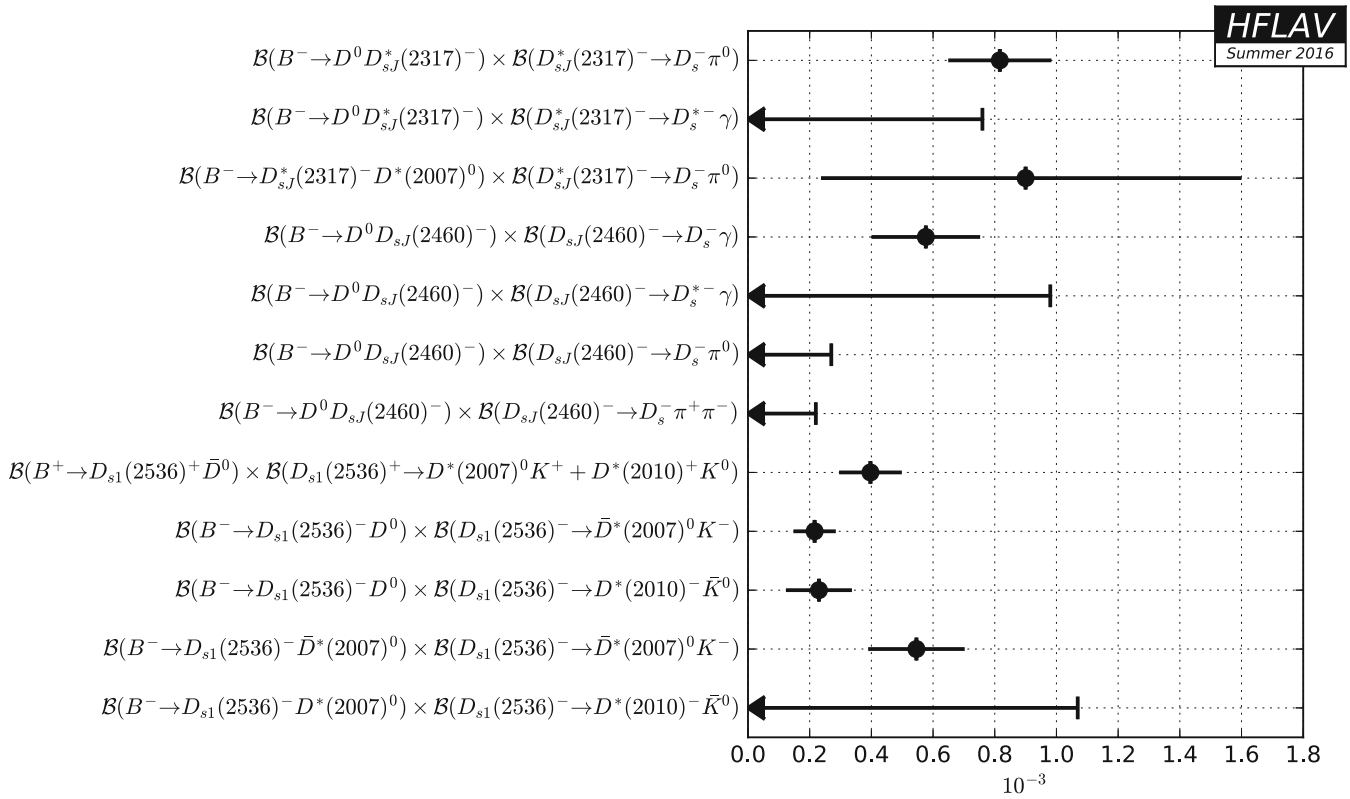

Fig. 127 Summary of the averages from Table 158

6.2.3 Decays to charmonium states

Averages of B^- decays to charmonium states are shown in Tables 159, 160, 161, 162, 163, 164, 165, 166, 167, 168, 169 and Figs. 128, 129, 130, 131, 132, 133, 134, 135, 136, 137, 138.

Table 159 Decays to J/ψ and one kaon I [10^{-3}]

Parameter	Measurements	Average
$\mathcal{B}(B^- \to J/\psi K^-)$	Belle [646]: 1.01 ± 0.02 ± 0.07	
	BaBar [706]: 0.81 ± 0.13 ± 0.07	1.028 ± 0.040
	BaBar [10]: 1.061 ± 0.015 ± 0.048	
$\mathcal{B}(B^- \to J/\psi K^*(892)^-)$	CDF [645]: 1.58 ± 0.47 ± 0.27	
	Belle [733]: 1.28 ± 0.07 ± 0.14	1.404 ± 0.089
	BaBar [10]: 1.454 ± 0.047 ± 0.097	
$\mathcal{B}(B^- \to J/\psi K_1(1270)^-)$	Belle [653]: 1.80 ± 0.34 ± 0.39	1.80 ± 0.52
$\mathcal{B}(B^- \to J/\psi K^- \pi^+ \pi^-)$	CDF [734]: 0.69 ± 0.18 ± 0.12	
	Belle [735]: 0.716 ± 0.010 ± 0.060	0.807 ± 0.052 CL = 2.3‰
	BaBar [736]: 1.16 ± 0.07 ± 0.09	

Table 160 Decays to J/ψ and one kaon II [10^{-4}]

Parameter	Measurements	Average
$\mathcal{B}(B^- \to J/\psi \eta K^-)$	Belle [654]: 1.27 ± 0.11 ± 0.11	1.24 ± 0.14
	BaBar [655]: 1.08 ± 0.23 ± 0.24	
$\mathcal{B}(B^- \to J/\psi \omega(782) K^-)$	BaBar [651]: $3.2 \pm 0.1\,^{+0.6}_{-0.3}$	$3.2\,^{+0.6}_{-0.3}$
$\mathcal{B}(B^- \to J/\psi \phi(1020) K^-)$	BaBar [652]: 0.44 ± 0.14 ± 0.05	0.44 ± 0.15

Table 161 Decays to charmonium other than J/ψ and one kaon I [10^{-3}]

Parameter	Measurements	Average
$\mathcal{B}(B^- \to \psi(2S)K^-)$	CDF [648]: 0.55 ± 0.10 ± 0.06	0.632 ± 0.037
	Belle [646]: 0.69 ± 0.06	
	BaBar [706]: 0.49 ± 0.16 ± 0.04	
	BaBar [10]: 0.617 ± 0.032 ± 0.044	
$\mathcal{B}(B^- \to \psi(2S)K^-) \times \mathcal{B}(\psi(2S) \to \chi_{c1}\gamma)$	Belle [657]: 0.77 ± 0.08 ± 0.09	0.77 ± 0.12
$\mathcal{B}(B^- \to \psi(2S)K^-) \times \mathcal{B}(\psi(2S) \to \chi_{c2}\gamma)$	Belle [657]: 0.63 ± 0.09 ± 0.06	0.63 ± 0.11
$\mathcal{B}(B^- \to \psi(2S)K^*(892)^-)$	BaBar [10]: 0.592 ± 0.085 ± 0.089	0.592 ± 0.123
$\mathcal{B}(B^- \to \psi(2S)K^-\pi^+\pi^-)$	Belle [735]: 0.431 ± 0.020 ± 0.050	0.431 ± 0.054
$\mathcal{B}(B^- \to \psi(3770)K^-)$	Belle [732]: 0.48 ± 0.11 ± 0.07	0.45 ± 0.12
	BaBar [706]: 0.35 ± 0.25 ± 0.03	
$\mathcal{B}(B^- \to \psi(3770)K^-) \times \mathcal{B}(\psi(3770) \to D^+D^-)$	BaBar [643]: 0.084 ± 0.032 ± 0.021	0.084 ± 0.038
$\mathcal{B}(B^- \to \psi(3770)K^-) \times \mathcal{B}(\psi(3770) \to D^0\bar{D}^0)$	BaBar [643]: 0.141 ± 0.030 ± 0.022	0.141 ± 0.037
$\mathcal{B}(B^- \to \chi_{c0}K^-)$	Belle [737]: $0.60^{+0.21}_{-0.18} \pm 0.11$	0.200 ± 0.044
	BaBar [706]: <0.18	
	BaBar [273]: 0.184 ± 0.032 ± 0.031	
$\mathcal{B}(B^- \to \chi_{c0}K^*(892)^-)$	BaBar [658]: <2.86	0.14 ± 0.05
	BaBar [659]: 0.14 ± 0.05 ± 0.02	
$\mathcal{B}(B^- \to \chi_{c1}K^-)$	CDF [734]: 1.55 ± 0.54 ± 0.20	0.479 ± 0.023
	Belle [660]: 0.494 ± 0.011 ± 0.033	
	BaBar [706]: 0.80 ± 0.14 ± 0.07	
	BaBar [661]: 0.45 ± 0.01 ± 0.03	
$\mathcal{B}(B^- \to \chi_{c1}K^*(892)^-)$	Belle [664]: 0.41 ± 0.06 ± 0.09	0.30 ± 0.06
	BaBar [661]: 0.26 ± 0.05 ± 0.04	
$\mathcal{B}(B^- \to \chi_{c1}K^-\pi^0)$	Belle [662]: 0.329 ± 0.029 ± 0.019	0.329 ± 0.035
$\mathcal{B}(B^- \to \chi_{c1}\bar{K}^0\pi^-)$	Belle [662]: 0.575 ± 0.026 ± 0.032	
	BaBar [663]: 0.552 ± 0.026 ± 0.061	0.569 ± 0.035
$\mathcal{B}(B^- \to \chi_{c1}K^-\pi^+\pi^-)$	Belle [662]: 0.374 ± 0.018 ± 0.024	0.374 ± 0.030
$\mathcal{B}(B^- \to \chi_{c2}\bar{K}^0\pi^-)$	Belle [662]: 0.116 ± 0.022 ± 0.012	0.116 ± 0.025
$\mathcal{B}(B^- \to \chi_{c2}K^-\pi^+\pi^-)$	Belle [662]: 0.134 ± 0.017 ± 0.009	0.134 ± 0.019
$\mathcal{B}(B^- \to \eta_c K^-)$	Belle [665]: $1.25 \pm 0.14^{+0.39}_{-0.40}$	
	BaBar [706]: 0.87 ± 0.15	0.92 ± 0.14
	BaBar [667]: 1.29 ± 0.09 ± 0.38	
$\mathcal{B}(B^- \to \eta_c K^*(892)^-)$	BaBar [666]: $1.21^{+0.43}_{-0.35}{}^{+0.64}_{-0.40}$	$1.21^{+0.77}_{-0.53}$
$\mathcal{B}(B^- \to \eta_c(2S)K^-)$	BaBar [706]: 0.34 ± 0.18 ± 0.03	0.34 ± 0.18

Table 162 Decays to charmonium other than J/ψ and one kaon II [10^{-5}]

Parameter	Measurements	Average
$\mathcal{B}(B^- \to \chi_{c2}K^-)$	Belle [660]: $1.11^{+0.36}_{-0.34} \pm 0.09$	1.08 ± 0.31
	BaBar [661]: 1 ± 1 ± 0	
$\mathcal{B}(B^- \to \chi_{c2}K^*(892)^-)$	BaBar [661]: 1.1 ± 4.3 ± 5.5	1.1 ± 7.0
$\mathcal{B}(B^- \to h_c(1P)K^-) \times \mathcal{B}(h_c(1P) \to \eta_c\gamma)$	BaBar [668]: <4.8	<4.8

Table 163 Decays to charmonium other than J/ψ and one kaon III [10^{-6}]

Parameter	Measurements	Average
$\mathcal{B}(B^- \to K^-\eta_c) \times \mathcal{B}(\eta_c \to K^0K^+\pi^+)$	Belle [738]: $0.267 \pm 0.014^{+0.057}_{-0.055}$	$0.267^{+0.059}_{-0.057}$
$\mathcal{B}(B^- \to \eta_c K^-) \times \mathcal{B}(\eta_c \to p\bar{p})$	Belle [739]: $1.42 \pm 0.11^{+0.16}_{-0.20}$	
	BaBar [740]: $1.8^{+0.3}_{-0.2} \pm 0.2$	1.53 ± 0.18
$\mathcal{B}(B^- \to \eta_c K^-) \times \mathcal{B}(\eta_c \to \Lambda\bar{\Lambda})$	Belle [739]: $0.95^{+0.25}_{-0.22}{}^{+0.08}_{-0.11}$	$0.95^{+0.26}_{-0.25}$
$\mathcal{B}(B^- \to K^-\eta_c(2S)) \times \mathcal{B}(\eta_c(2S) \to K^0K^-\pi^+)$	Belle [738]: $0.034^{+0.022}_{-0.015}{}^{+0.005}_{-0.004}$	$0.034^{+0.023}_{-0.016}$
$\mathcal{B}(B^- \to h_c(1P)K^-)$	Belle [741]: <3.8	<3.8
$\mathcal{B}(B^- \to h_c(1P)K^-) \times \mathcal{B}(h_c(1P) \to J/\psi\pi^+\pi^-)$	BaBar [736]: <3.4	<3.4

Table 164 Decays to charmonium and light mesons [10^{-5}]

Parameter	Measurements	Average
$\mathcal{B}(B^- \to J/\psi\pi^-)$	LHCb [742]: $3.88 \pm 0.11 \pm 0.15$	
	Belle [646]: $3.8 \pm 0.6 \pm 0.3$	4.04 ± 0.17
	BaBar [743]: $5.37 \pm 0.45 \pm 0.24$	
$\mathcal{B}(B^- \to J/\psi\pi^-\pi^0)$	BaBar [669]: <0.73	<0.73
$\mathcal{B}(B^- \to J/\psi\rho^-(770))$	BaBar [669]: $5 \pm 1 \pm 0$	5 ± 1
$\mathcal{B}(B^- \to \psi(2S)\pi^-)$	LHCb [742]: $2.52 \pm 0.26 \pm 0.15$	2.52 ± 0.30
$\mathcal{B}(B^- \to \chi_{c0}\pi^-)$	BaBar [744]: <6.1	<6.1
$\mathcal{B}(B^- \to \chi_{c1}\pi^-)$	Belle [745]: $2.2 \pm 0.4 \pm 0.3$	2.2 ± 0.5

Table 165 Decays to J/ψ and a heavy mesons [10^{-4}]

Parameter	Measurements	Average
$\mathcal{B}(B^- \to J/\psi D^-)$	BaBar [682]: <1.2	<1.2
$\mathcal{B}(B^- \to J/\psi D^0\pi^-)$	Belle [681]: <0.25	<0.25
	BaBar [736]: <0.52	

Table 166 Decays with baryons I [10^{-5}]

Parameter	Measurements	Average
$\mathcal{B}(B^- \to J/\psi\Lambda\bar{p})$	Belle [679]: $1.16 \pm 0.28^{+0.18}_{-0.23}$	1.16 ± 0.31
	BaBar [680]: $1.16^{+0.74}_{-0.53}{}^{+0.42}_{-0.18}$	
$\mathcal{B}(B^- \to J/\psi\Sigma^0\bar{p})$	Belle [679]: <1.1	<1.1

Table 167 Decays with baryons II [10^{-6}]

Parameter	Measurements	Average
$\mathcal{B}(B^- \to J/\psi p\bar{p}\pi^-)$	LHCb [678]: <0.50	<0.50
$\mathcal{B}(B^- \to J/\psi K^-) \times \mathcal{B}(J/\psi \to \Lambda\bar{\Lambda})$	Belle [739]: $2.0^{+0.3}_{-0.3} \pm 0.3$	$2.0^{+0.5}_{-0.4}$
$\mathcal{B}(B^- \to J/\psi K^-) \times \mathcal{B}(J/\psi \to p\bar{p})$	Belle [739]: $2.21 \pm 0.13 \pm 0.10$	
	BaBar [740]: $2.2 \pm 0.2 \pm 0.1$	2.21 ± 0.13

Table 168 Relative decay rates I

Parameter	Measurements	Average
$\mathcal{B}(B^- \to J/\psi K^*(892)^-)/\mathcal{B}(B^- \to J/\psi K^-)$	CDF [683]: 1.92 ± 0.60 ± 0.17	1.38 ± 0.09
	BaBar [10]: 1.37 ± 0.05 ± 0.08	
$\mathcal{B}(B^- \to J/\psi K_1(1270)^-)/\mathcal{B}(B^- \to J/\psi K^-)$	Belle [653]: 1.80 ± 0.34 ± 0.34	1.80 ± 0.48
$\mathcal{B}(B^- \to J/\psi K_1^-(1400))/\mathcal{B}(B^- \to J/\psi K_1(1270)^-)$	Belle [653]: <0.30	<0.30
$\mathcal{B}(B^- \to \psi(2S)K^-)/\mathcal{B}(B^- \to J/\psi K^-)$	LHCb [685]: 0.594 ± 0.006 ± 0.022	0.598 ± 0.022
	D0 [746]: 0.65 ± 0.04 ± 0.08	
$\mathcal{B}(B^- \to \psi(2S)K^*(892)^-)/\mathcal{B}(B^- \to \psi(2S)K^-)$	BaBar [10]: 0.96 ± 0.15 ± 0.09	0.96 ± 0.17
$\mathcal{B}(B^- \to \chi_{c0}K^-)/\mathcal{B}(B^- \to J/\psi K^-)$	Belle [737]: $0.60\,^{+0.21}_{-0.18} \pm 0.09$	$0.60\,^{+0.23}_{-0.20}$
$\mathcal{B}(B^- \to \chi_{c1}K^*(892)^-)/\mathcal{B}(B^- \to \chi_{c1}K^-)$	BaBar [10]: 0.51 ± 0.17 ± 0.16	0.51 ± 0.23
$\mathcal{B}(B^- \to \chi_{c1}\bar{K}^0\pi^-)/\mathcal{B}(B^- \to J/\psi \bar{K}^0\pi^-)$	BaBar [663]: 0.501 ± 0.024 ± 0.055	0.501 ± 0.060
$\mathcal{B}(B^- \to \eta_c K^-)/\mathcal{B}(B^- \to J/\psi K^-)$	BaBar [706]: 1.06 ± 0.23 ± 0.04	1.12 ± 0.20
	BaBar [667]: 1.28 ± 0.10 ± 0.38	
$[\mathcal{B}(B^- \to \eta_c K^-) \times \mathcal{B}(\eta_c \to p\bar{p})]/[\mathcal{B}(B^- \to J/\psi K^-) \times \mathcal{B}(J/\psi \to p\bar{p})]$	LHCb [747]: 0.578 ± 0.035 ± 0.027	0.578 ± 0.044

Table 169 Relative decay rates II

Parameter	Measurements	Average
$\mathcal{B}(B^- \to J/\psi\pi^-)/\mathcal{B}(B^- \to J/\psi K^-)$	CDF [748]: $0.050\,^{+0.019}_{-0.017} \pm 0.001$	0.0524 ± 0.0040
	CDF [749]: 0.0486 ± 0.0082 ± 0.0015	
	BaBar [743]: 0.0537 ± 0.0045 ± 0.0011	
$[\mathcal{B}(B^- \to \psi(2S)K^-) \times \mathcal{B}(\psi(2S) \to p\bar{p})]/$ $[\mathcal{B}(B^- \to J/\psi K^-) \times \mathcal{B}(J/\psi \to p\bar{p})]$	LHCb [747]: 0.080 ± 0.012 ± 0.009	0.080 ± 0.015
$\mathcal{B}(B^- \to \chi_{c1}\pi^-)/\mathcal{B}(B^- \to \chi_{c1}K^-)$	Belle [745]: 0.043 ± 0.008 ± 0.003	0.043 ± 0.009
$[\mathcal{B}(B^- \to h_c(1P)K^-) \times \mathcal{B}(h_c(1P) \to \eta_c\gamma)]/\mathcal{B}(B^- \to \eta_c K^-)$	BaBar [668]: <0.052	<0.052

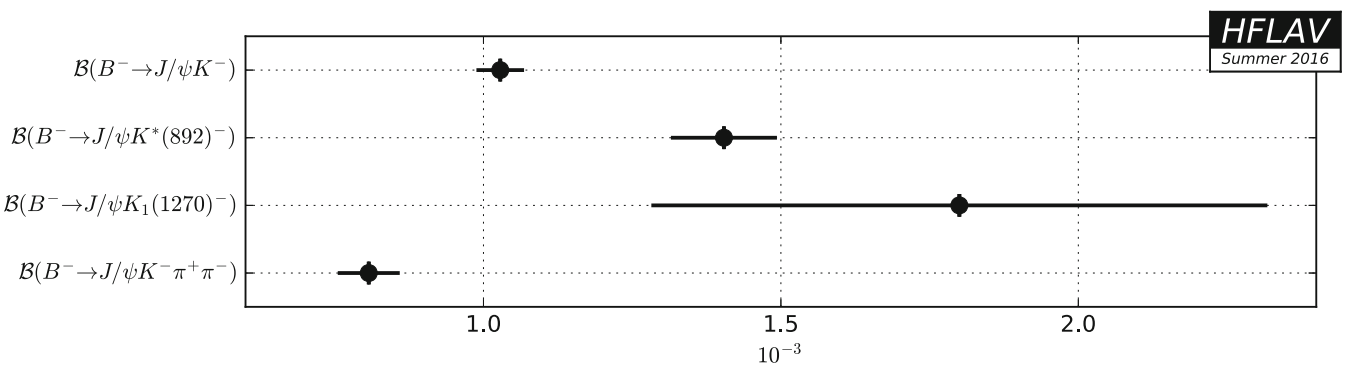

Fig. 128 Summary of the averages from Table 159

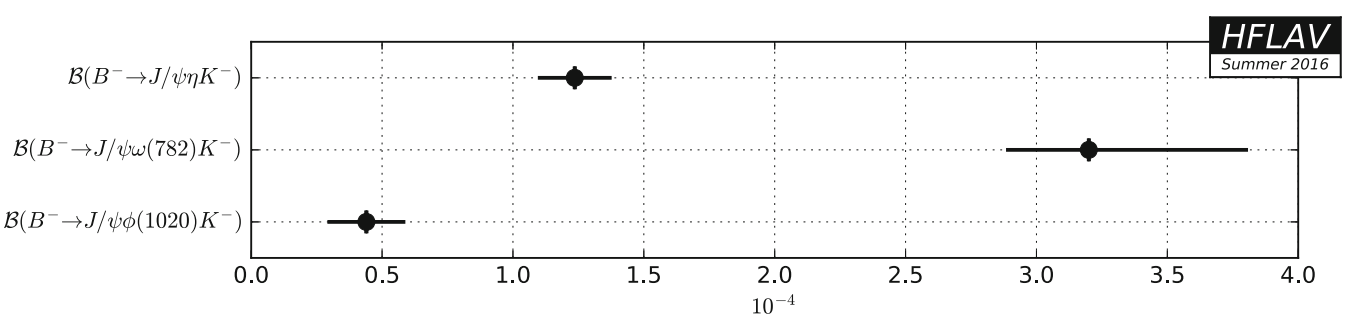

Fig. 129 Summary of the averages from Table 160

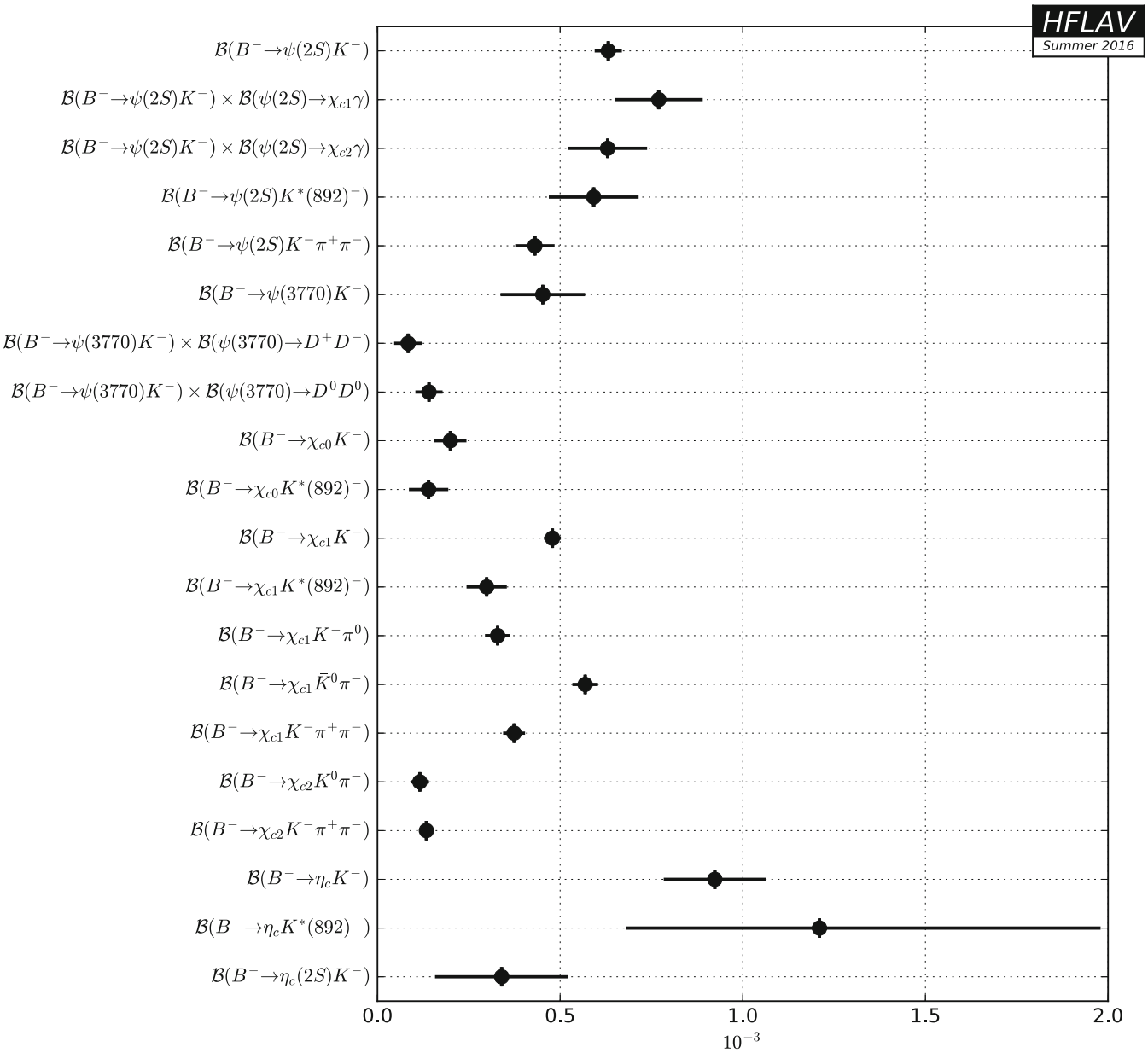

Fig. 130 Summary of the averages from Table 161

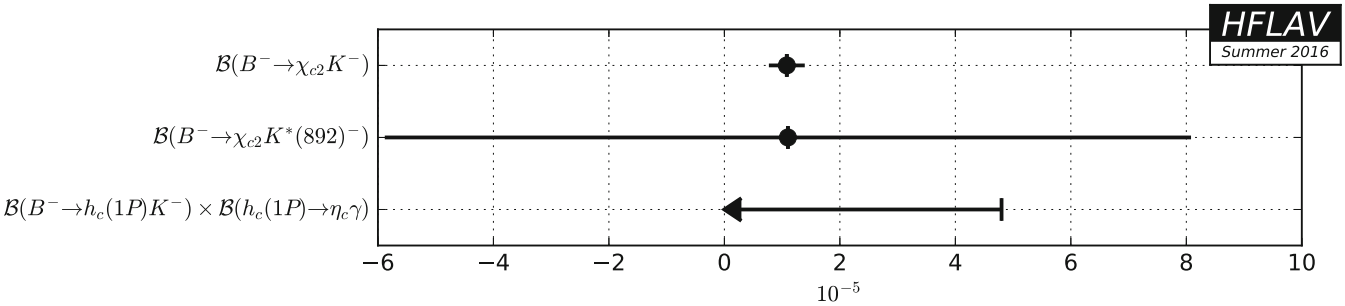

Fig. 131 Summary of the averages from Table 162

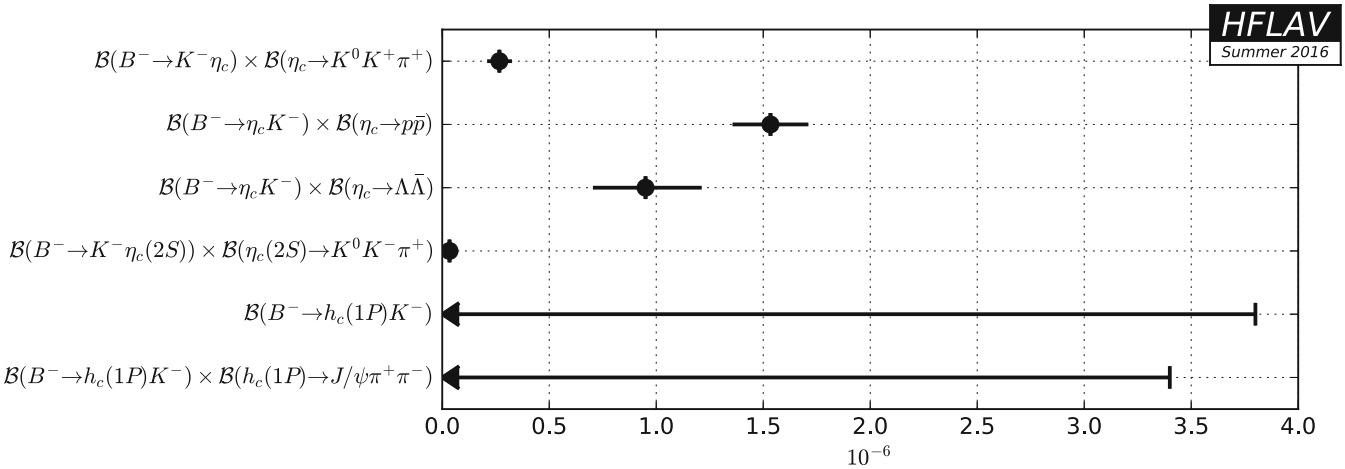

Fig. 132 Summary of the averages from Table 163

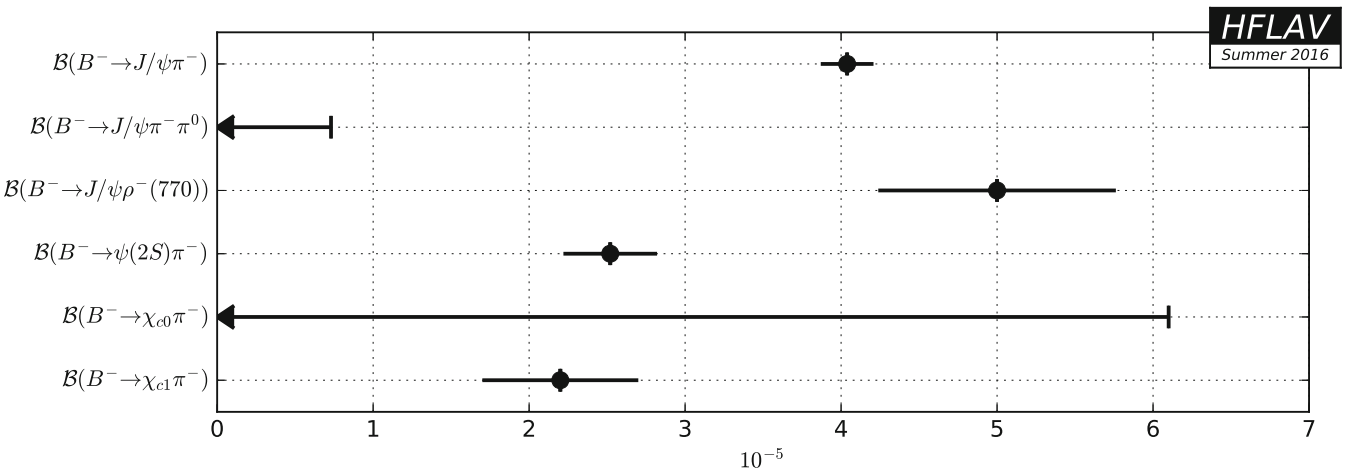

Fig. 133 Summary of the averages from Table 164

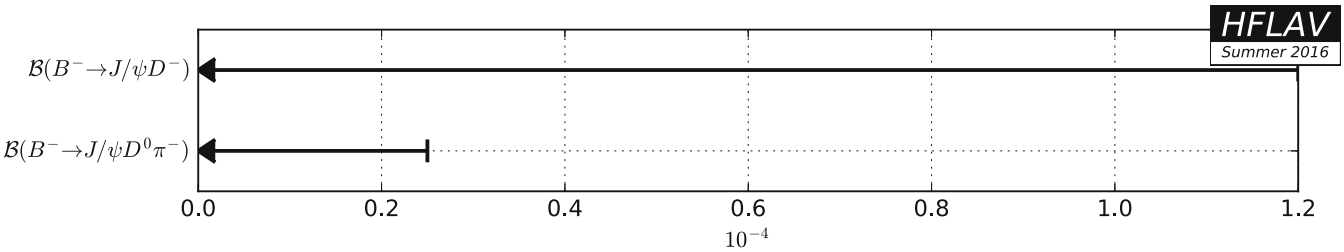

Fig. 134 Summary of the averages from Table 165

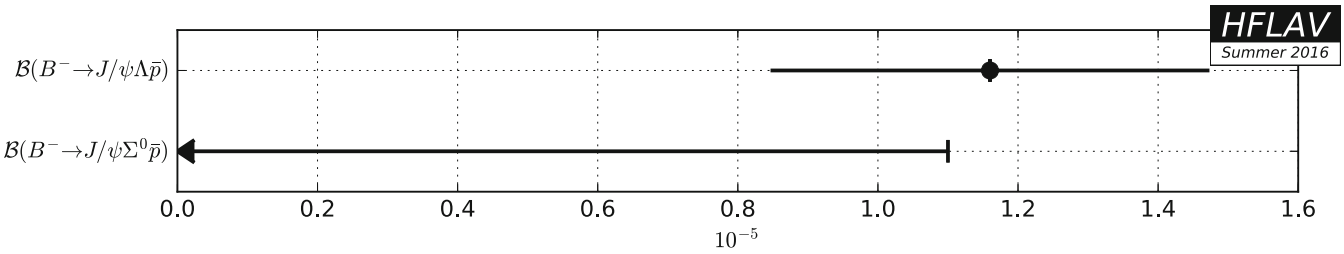

Fig. 135 Summary of the averages from Table 166

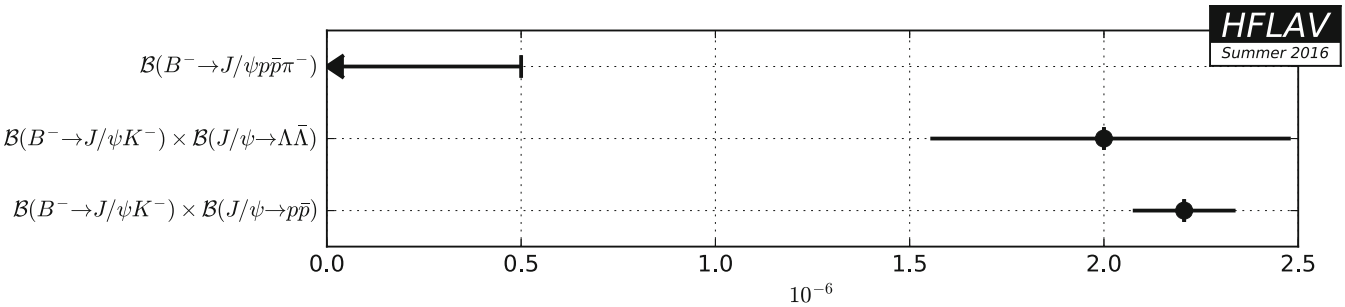

Fig. 136 Summary of the averages from Table 167

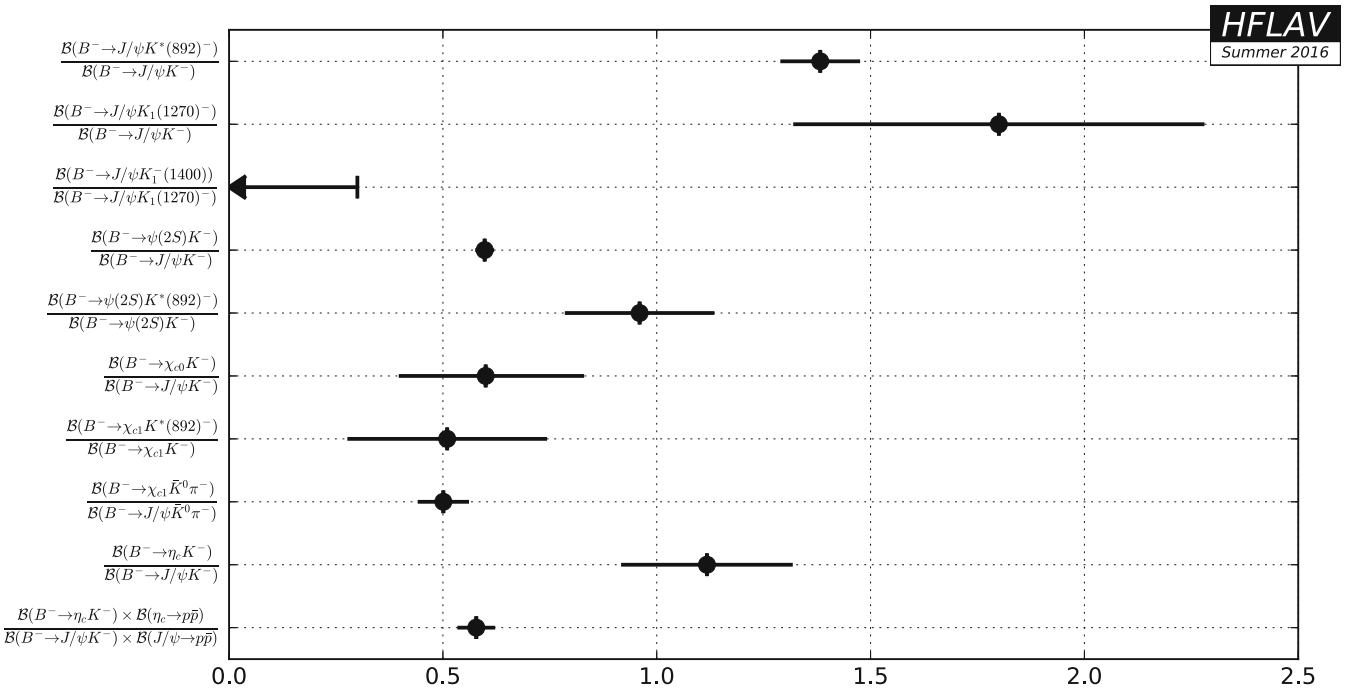

Fig. 137 Summary of the averages from Table 168

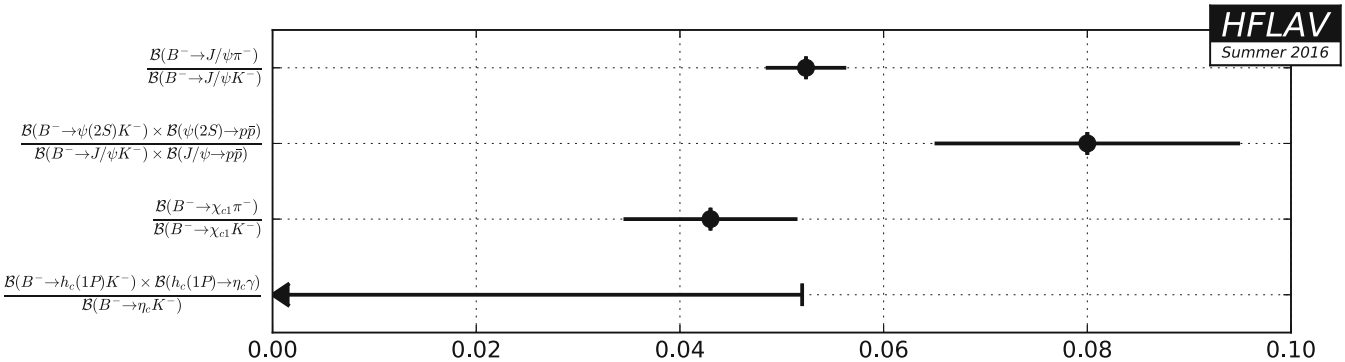

Fig. 138 Summary of the averages from Table 169

6.2.4 Decays to charm baryons

Averages of B^- decays to charm baryons are shown in Tables 170, 171, 172 and Figs. 139, 140.

Table 170 Absolute (product) decay rates [10^{-4}]

Parameter	Measurements	Average
$\mathcal{B}(B^- \to \Lambda_c^+ \Lambda_c^- K^-)$	Belle [693]: $6.5\,^{+1.0}_{-0.9} \pm 3.6$	4.1 ± 3.2
	BaBar [694]: $11.4 \pm 1.5 \pm 6.2$	
$\mathcal{B}(B^- \to \Xi_c^0 \Lambda_c^-) \times \mathcal{B}(\Xi_c^0 \to \Xi^- \pi^+)$	Belle [699]: $0.48\,^{+0.10}_{-0.09} \pm 0.16$	0.221 ± 0.089
	BaBar [694]: $0.208 \pm 0.065 \pm 0.061$	
$\mathcal{B}(B^- \to \Lambda_c^+ \bar{p} \pi^-)$	Belle [690]: $1.87\,^{+0.43}_{-0.40} \pm 0.56$	2.08 ± 0.69
	BaBar [697]: $3.38 \pm 0.12 \pm 0.89$	
$\mathcal{B}(B^- \to \Sigma_c^0 \bar{p})$	Belle [690]: $0.45\,^{+0.26}_{-0.19} \pm 0.14$	$0.45\,^{+0.29}_{-0.24}$
$\mathcal{B}(B^- \to \Sigma_c^{*0} \bar{p})$	Belle [690]: <0.46	<0.46
$\mathcal{B}(B^- \to \Sigma_c^{++} \bar{p} \pi^- \pi^-)$	BaBar [750]: $2.98 \pm 0.16 \pm 0.78$	2.98 ± 0.80

Table 171 Relative decay rates I

Parameter	Measurements	Average
$\mathcal{B}(B^- \to \Lambda_c^+ \bar{p} \pi^-)/\mathcal{B}(\bar{B}^0 \to \Lambda_c^+ \bar{p})$	BaBar [697]: $15.4 \pm 1.8 \pm 0.3$	15.4 ± 1.8

Table 172 Relative decay rates II

Parameter	Measurements	Average
$\mathcal{B}(B^- \to \Sigma_c(2455)^0 \bar{p})/\mathcal{B}(B^- \to \Lambda_c^+ \bar{p} \pi^-)$	BaBar [697]: $0.123 \pm 0.012 \pm 0.008$	0.123 ± 0.014
$\mathcal{B}(B^- \to \Sigma_c(2800)^0 \bar{p})/\mathcal{B}(B^- \to \Lambda_c^+ \bar{p} \pi^-)$	BaBar [697]: $0.117 \pm 0.023 \pm 0.024$	0.117 ± 0.033

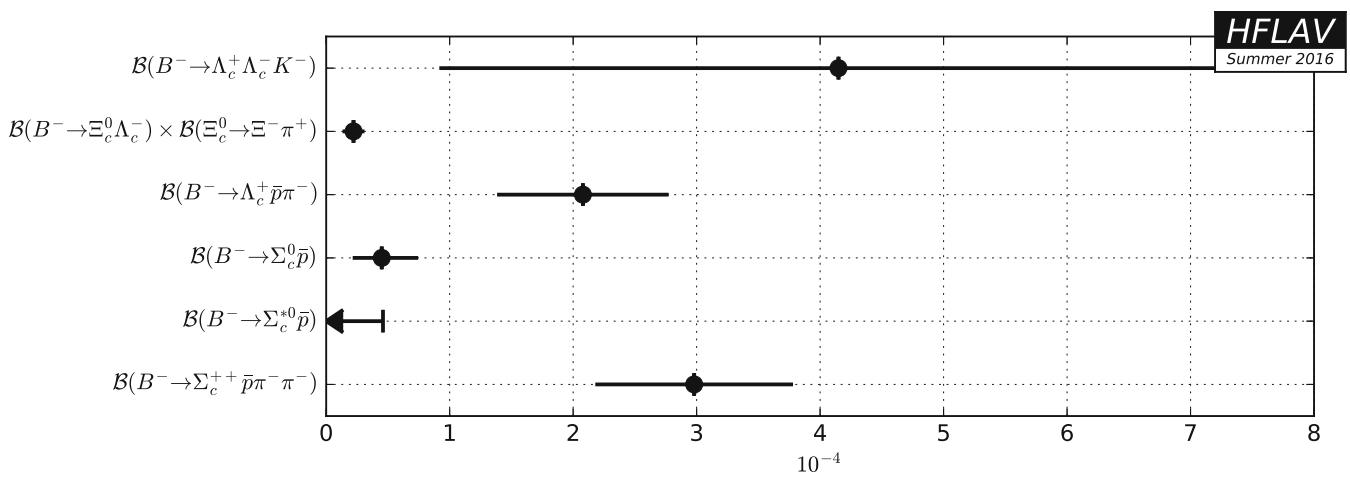

Fig. 139 Summary of the averages from Table 170

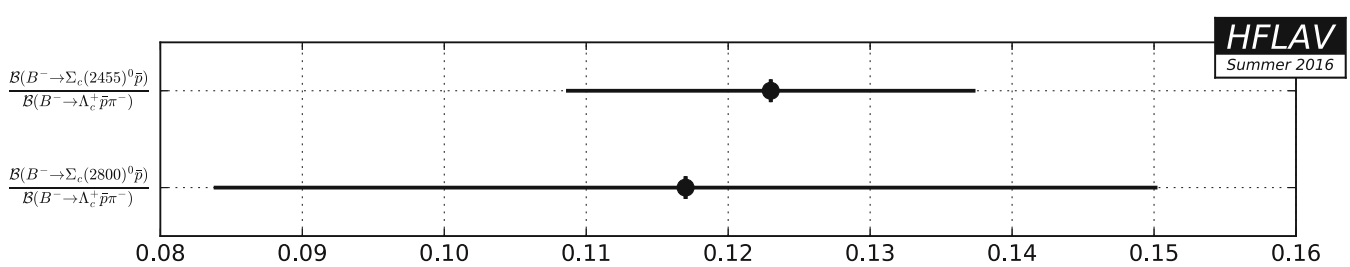

Fig. 140 Summary of the averages from Table 172

6.2.5 Decays to other (XYZ) states

Averages of B^- decays to other (XYZ) states are shown in Tables 173, 174, 175, 176, 177, 178 and Figs. 141, 142, 143, 144, 145.

Table 173 Absolute decay rates $[10^{-4}]$

Parameter	Measurements	Average
$\mathcal{B}(B^- \to X(3872)K^-)$	BaBar [706]: <3.2	<3.2

Table 174 Product decay rates to $X(3872)$ I $[10^{-4}]$

Parameter	Measurements	Average
$\mathcal{B}(B^- \to X(3872)K^-) \times \mathcal{B}(X(3872) \to \bar{D}^*(2007)^0 D^0)$	BaBar [643]: $1.67 \pm 0.36 \pm 0.47$	1.67 ± 0.59
$\mathcal{B}(B^- \to X(3872)K^-) \times \mathcal{B}(X(3872) \to D^0 \bar{D}^0 \pi^0)$	Belle [732]: <0.6	<0.6
$\mathcal{B}(B^- \to X(3872)K^-) \times \mathcal{B}(X(3872) \to D^0 \bar{D}^0)$	Belle [732]: <0.6	<0.6
$\mathcal{B}(B^- \to X(3872)K^-) \times \mathcal{B}(X(3872) \to D^+ D^-)$	Belle [732]: <0.4	<0.4

Table 175 Product decay rates to $X(3872)$ II $[10^{-5}]$

Parameter	Measurements	Average
$\mathcal{B}(B^- \to K^- X(3872)) \times \mathcal{B}(X(3872) \to J/\psi \pi^+ \pi^-)$	Belle [751]: $0.861 \pm 0.062 \pm 0.052$	0.857 ± 0.073
	BaBar [704]: $0.84 \pm 0.15 \pm 0.07$	
$\mathcal{B}(B^- \to X(3872)K^-) \times \mathcal{B}(X(3872) \to J/\psi \omega(782))$	BaBar [651]: $0.6 \pm 0.2 \pm 0.1$	0.6 ± 0.2
$\mathcal{B}(B^- \to X(3872)K^-) \times \mathcal{B}(X(3872) \to J/\psi \eta)$	BaBar [655]: <0.77	<0.77
$\mathcal{B}(B^- \to X(3872)K^-) \times \mathcal{B}(X(3872) \to J/\psi \gamma)$	Belle [660]: $0.178\,^{+0.048}_{-0.044} \pm 0.012$	0.204 ± 0.041
	BaBar [661]: $0.28 \pm 0.08 \pm 0.01$	
$\mathcal{B}(B^- \to X(3872)K^*(892)^-) \times \mathcal{B}(X(3872) \to J/\psi \gamma)$	BaBar [661]: $0.07 \pm 0.26 \pm 0.01$	0.07 ± 0.26
$\mathcal{B}(B^- \to X(3872)K^-) \times \mathcal{B}(X(3872) \to \psi(2S)\gamma)$	Belle [660]: <0.345	0.95 ± 0.28
	BaBar [661]: $0.95 \pm 0.27 \pm 0.06$	
$\mathcal{B}(B^- \to X(3872)K^*(892)^-) \times \mathcal{B}(X(3872) \to \psi(2S)\gamma)$	BaBar [661]: $0.64 \pm 0.98 \pm 0.96$	0.64 ± 1.37
$\mathcal{B}(B^- \to X(3872)K^-) \times \mathcal{B}(X(3872) \to \chi_{c1}\gamma)$	Belle [657]: <0.19	<0.19
$\mathcal{B}(B^- \to X(3872)K^-) \times \mathcal{B}(X(3872) \to \chi_{c2}\gamma)$	Belle [657]: <0.67	<0.67

Table 176 Product decay rates to neutral states other than $X(3872)$ $[10^{-5}]$

Parameter	Measurements	Average
$\mathcal{B}(B^- \to X(3823)K^-) \times \mathcal{B}(X(3823) \to \chi_{c1}\gamma)$	Belle [657]: $0.97 \pm 0.28 \pm 0.11$	0.97 ± 0.30
$\mathcal{B}(B^- \to X(3823)K^-) \times \mathcal{B}(X(3823) \to \chi_{c2}\gamma)$	Belle [657]: <0.36	<0.36
$\mathcal{B}(B^- \to Y(3940)K^-) \times \mathcal{B}(Y(3940) \to J/\psi \gamma)$	BaBar [752]: <1.4	<1.4
$\mathcal{B}(B^- \to Y(3940)K^-) \times \mathcal{B}(Y(3940) \to J/\psi \omega(782))$	BaBar [651]: $3.0\,^{+0.7}_{-0.6}\,^{+0.5}_{-0.3}$	$3.0\,^{+0.9}_{-0.7}$
$\mathcal{B}(B^- \to Y(4260)K^-) \times \mathcal{B}(Y(4260) \to J/\psi \pi^+ \pi^-)$	BaBar [753]: $2.0 \pm 0.7 \pm 0.2$	2.0 ± 0.7

Table 177 Relative product decay rates to states with $s\bar{s}$ component

Parameter	Measurements	Average
$[\mathcal{B}(B^- \to X(4140)K^-) \times \mathcal{B}(X(4140) \to J/\psi \phi(1020))]/\mathcal{B}(B^- \to J/\psi \phi(1020)K^-)$	LHCb [754]: $0.130 \pm 0.032\,^{+0.047}_{-0.020}$	0.148 ± 0.042
	D0 [755]: $0.21 \pm 0.08 \pm 0.04$	
$[\mathcal{B}(B^- \to X(4274)K^-) \times \mathcal{B}(X(4274) \to J/\psi \phi(1020))]/\mathcal{B}(B^- \to J/\psi \phi(1020)K^-)$	LHCb [754]: $0.071 \pm 0.025\,^{+0.035}_{-0.024}$	$0.071\,^{+0.043}_{-0.035}$

Table 178 Product decay rates to charged states [10^{-5}]

Parameter	Measurements	Average
$\mathcal{B}(B^- \to X(3872)^- \bar{K}^0) \times \mathcal{B}(X(3872)^- \to J/\psi\pi^-\pi^0)$	BaBar [707]: <2.2	<2.2
$\mathcal{B}(B^- \to Z(4430)^- \bar{K}^0) \times \mathcal{B}(Z(4430)^- \to J/\psi\pi^-)$	BaBar [708]: $-0.1 \pm 0.8 \pm 0.0$	-0.1 ± 0.8
$\mathcal{B}(B^- \to Z(4430)^- \bar{K}^0) \times \mathcal{B}(Z(4430)^- \to \psi(2S)\pi^-)$	BaBar [708]: $2.0 \pm 1.7 \pm 0.0$	2.0 ± 1.7

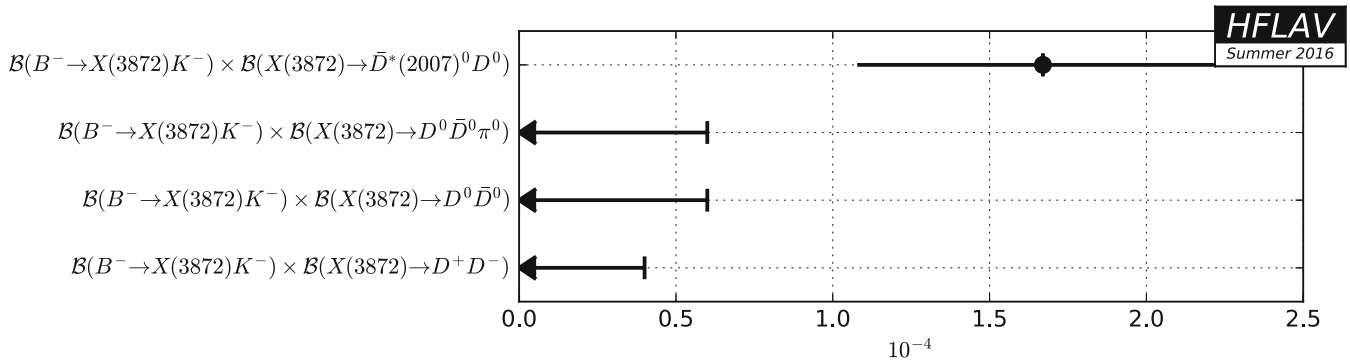

Fig. 141 Summary of the averages from Table 174

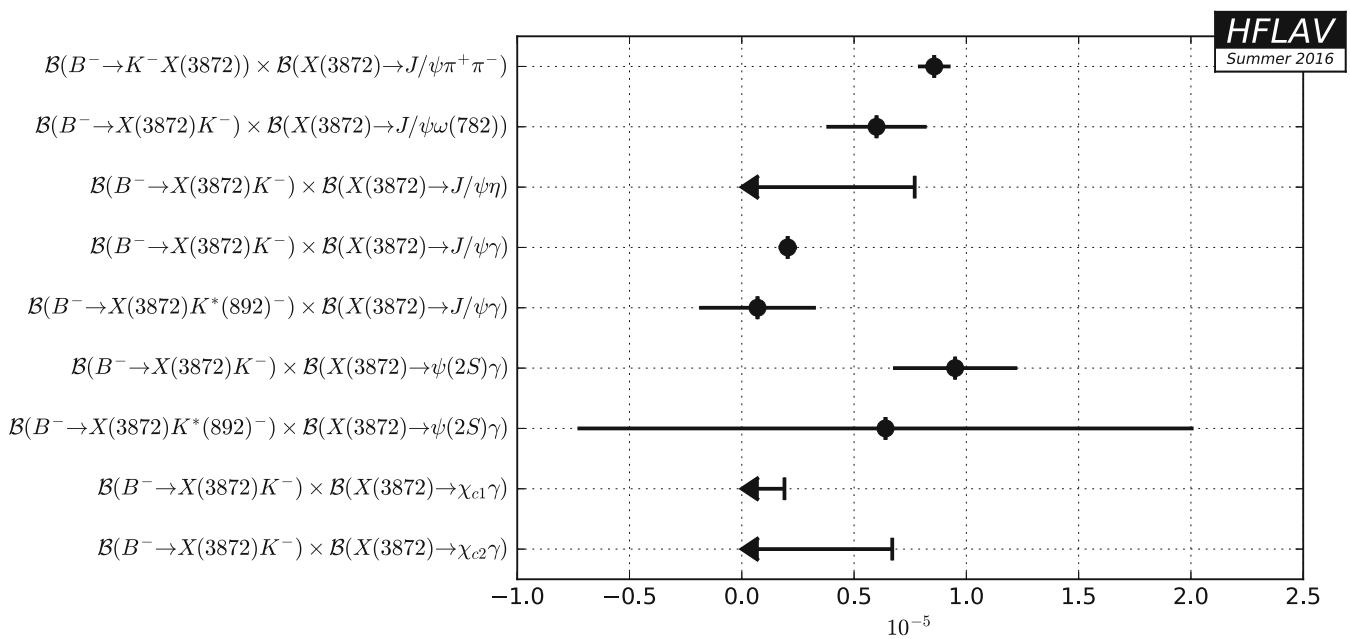

Fig. 142 Summary of the averages from Table 175

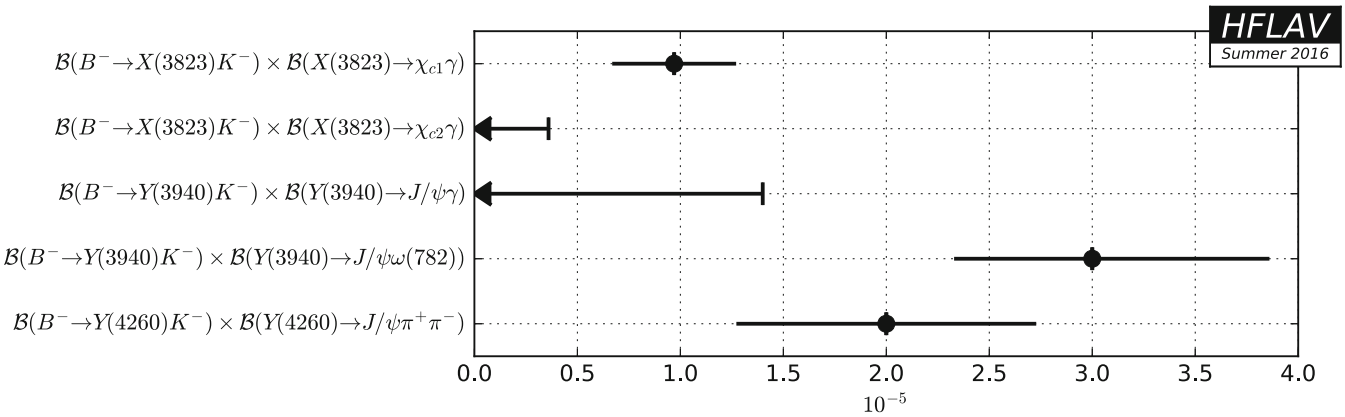

Fig. 143 Summary of the averages from Table 176

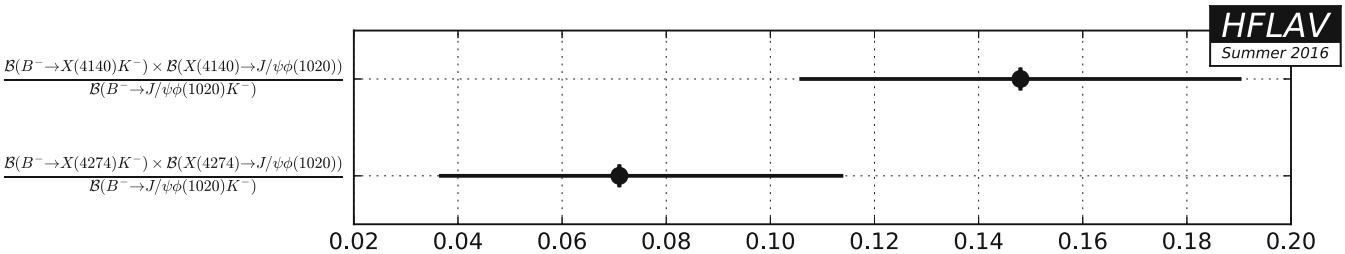

Fig. 144 Summary of the averages from Table 177

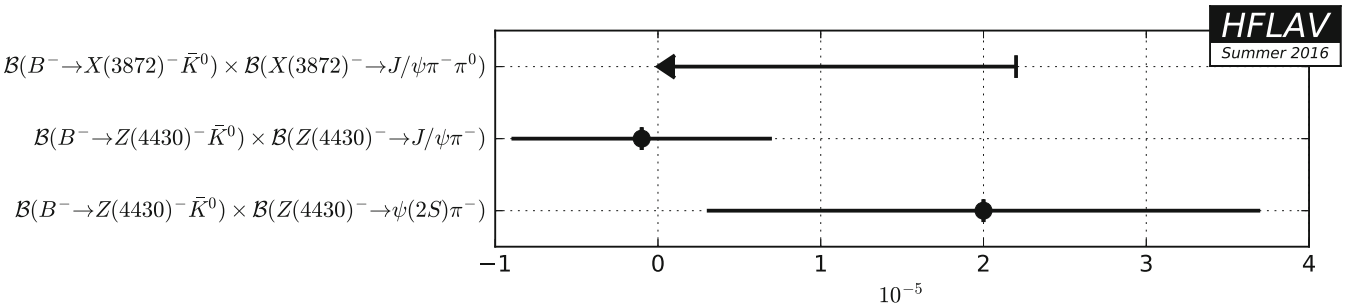

Fig. 145 Summary of the averages from Table 178

6.3 Decays of admixtures of $\bar{B}^0$ / B^- mesons

Measurements of $\bar{B}^0$ / B^- decays to charmed hadrons are summarized in Sects. 6.3.1–6.3.3.

6.3.1 Decays to two open charm mesons

Averages of $\bar{B}^0$ / B^- decays to two open charm mesons are shown in Table 179.

Table 179 B decays to double charm [10^{-4}]

Parameter	Measurements	Average
$\mathcal{B}(B \to D^0\bar{D}^0\pi^0K)$	Belle [633]: $1.27 \pm 0.31\,^{+0.22}_{-0.39}$	$1.27\,^{+0.38}_{-0.50}$

6.3.2 Decays to charmonium states

Averages of $\bar{B}^0$ / B^- decays to charmonium states are shown in Tables 180, 181, 182, 183, 184 and Figs. 146, 147, 148, 149, 150.

Table 180 Decay amplitudes for parallel transverse polarization

Parameter	Measurements	Average
$\lvert\mathcal{A}_\parallel\rvert^2(B \to J/\psi K^*)$	Belle [324]: 0.231 ± 0.012 ± 0.008	0.219 ± 0.009
	BaBar [323]: 0.211 ± 0.010 ± 0.006	
$\lvert\mathcal{A}_\parallel\rvert^2(B \to \chi_{c1} K^*)$	BaBar [323]: 0.20 ± 0.07 ± 0.04	0.20 ± 0.08
$\lvert\mathcal{A}_\parallel\rvert^2(B \to \psi(2S) K^*)$	BaBar [323]: 0.22 ± 0.06 ± 0.02	0.22 ± 0.06

Table 181 Decay amplitudes for perpendicular transverse polarization

Parameter	Measurements	Average
$\lvert\mathcal{A}_\perp\rvert^2(B \to J/\psi K^*)$	Belle [324]: 0.195 ± 0.012 ± 0.008	0.219 ± 0.009
	BaBar [323]: 0.233 ± 0.010 ± 0.005	
$\lvert\mathcal{A}_\perp\rvert^2(B \to \chi_{c1} K^*)$	BaBar [323]: 0.03 ± 0.04 ± 0.02	0.03 ± 0.04
$\lvert\mathcal{A}_\perp\rvert^2(B \to \psi(2S) K^*)$	BaBar [323]: 0.30 ± 0.06 ± 0.02	0.30 ± 0.06

Table 182 Decay amplitudes for longitudinal polarization

Parameter	Measurements	Average
$\lvert\mathcal{A}_0\rvert^2(B \to J/\psi K^*)$	Belle [324]: 0.574 ± 0.012 ± 0.009	0.564 ± 0.010
	BaBar [323]: 0.556 ± 0.009 ± 0.010	
$\lvert\mathcal{A}_0\rvert^2(B \to \chi_{c1} K^*)$	BaBar [323]: 0.77 ± 0.07 ± 0.04	0.77 ± 0.08
$\lvert\mathcal{A}_0\rvert^2(B \to \psi(2S) K^*)$	BaBar [323]: 0.48 ± 0.05 ± 0.02	0.48 ± 0.05

Table 183 Relative phases of parallel transverse polarization decay amplitudes

Parameter	Measurements	Average
$\delta_\parallel(B \to J/\psi K^*)$	Belle [324]: −2.887 ± 0.090 ± 0.008	−2.909 ± 0.064
	BaBar [323]: −2.93 ± 0.08 ± 0.04	
$\delta_\parallel(B \to \chi_{c1} K^*)$	BaBar [323]: 0.0 ± 0.3 ± 0.1	0.0 ± 0.3
$\delta_\parallel(B \to \psi(2S) K^*)$	BaBar [323]: −2.8 ± 0.4 ± 0.1	−2.8 ± 0.4

Table 184 Relative phases of perpendicular transverse polarization decay amplitudes

Parameter	Measurements	Average
$\delta_\perp(B \to J/\psi K^*)$	Belle [324]: 2.938 ± 0.064 ± 0.010	2.923 ± 0.043
	BaBar [323]: 2.91 ± 0.05 ± 0.03	
$\delta_\perp(B \to \psi(2S) K^*)$	BaBar [323]: 2.8 ± 0.3 ± 0.1	2.8 ± 0.3

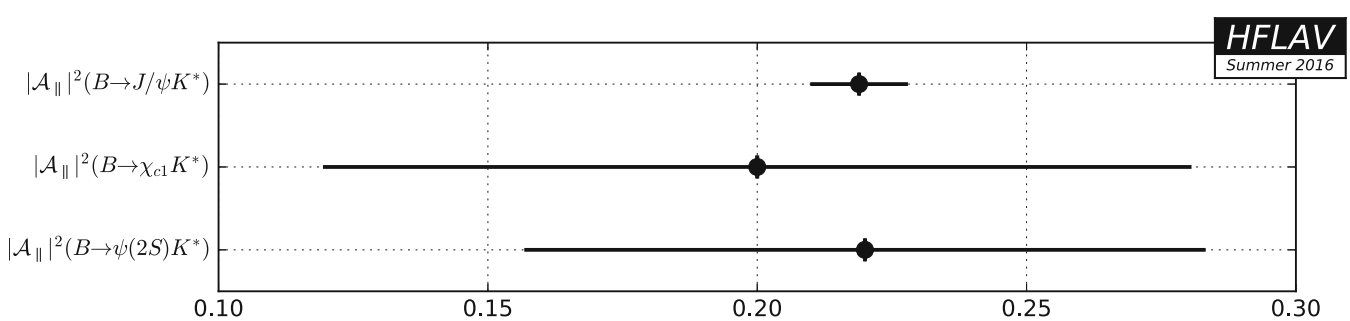

Fig. 146 Summary of the averages from Table 180

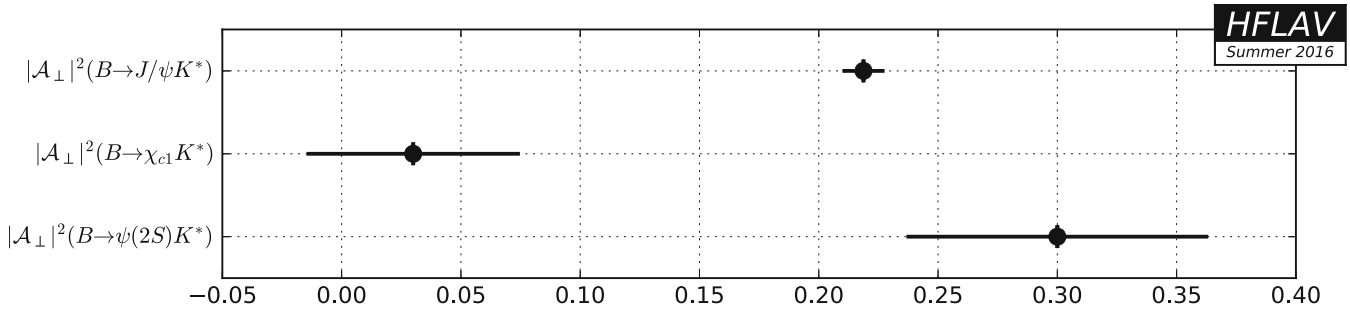

Fig. 147 Summary of the averages from Table 181

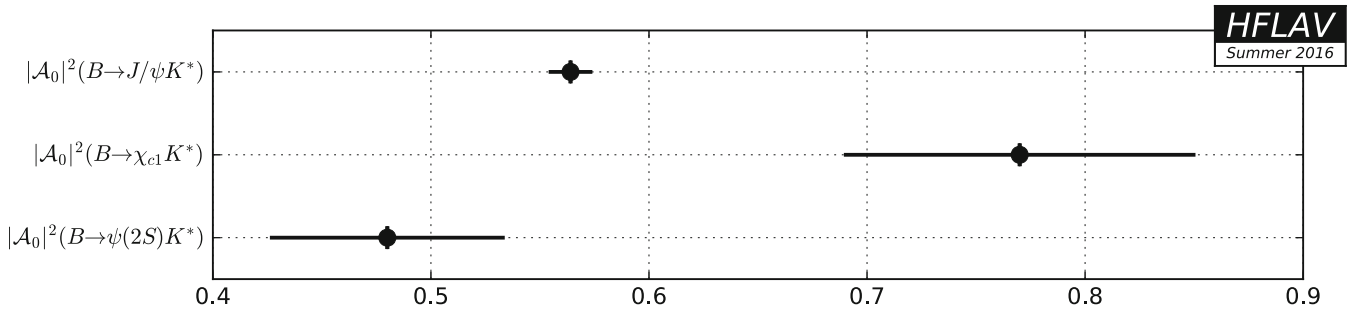

Fig. 148 Summary of the averages from Table 182

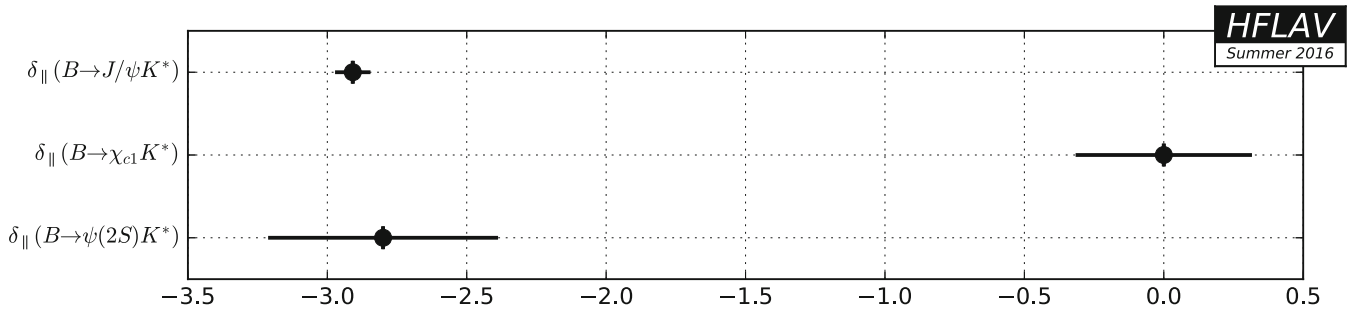

Fig. 149 Summary of the averages from Table 183

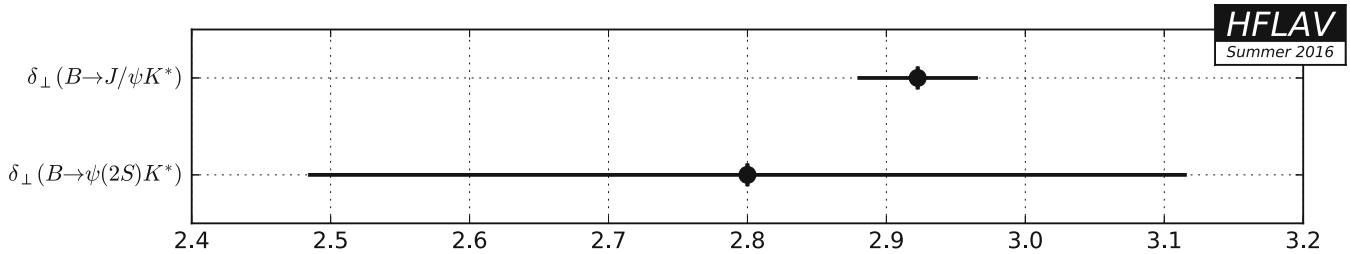

Fig. 150 Summary of the averages from Table 184

6.3.3 *Decays to other (XYZ) states*

Averages of $\bar{B}^0$ / B^- decays to other (XYZ) states are shown in Table 185 and Fig. 151.

6.4 Decays of $\bar{B}_s^0$ mesons

Measurements of $\bar{B}_s^0$ decays to charmed hadrons are summarized in Sects. 6.4.1–6.4.4. These measurements require knowledge of the production rates of $\bar{B}_s^0$ mesons, usually measured relative to those of $\bar{B}^0$ and B^- mesons, in the appropriate experimental environment. Since these production fractions are reasonably well known, see Sect. 3.1, they can be corrected for allowing the results to be presented in terms of the absolute $\bar{B}_s^0$ branching fraction, or the relative branching fraction to a lighter B meson decay mode. This is usually done in the publications; we do not make any attempt to rescale results according to more recent determinations of the relative production fractions. Ratios of branching fractions of two decays of the same hadron do not require any such correction.

6.4.1 *Decays to a single open charm meson*

Averages of $\bar{B}_s^0$ decays to a single open charm meson are shown in Tables 186, 187, 188, 189, 190, 191 and Figs. 152, 153, 154, 155, 156, 157.

Table 185 Absolute decay rates to X/Y states $[10^{-4}]$

Parameter	Measurements	Average
$\mathcal{B}(B \to X(3872)K) \times \mathcal{B}(X(3872) \to D^*(2007)^0\bar{D}^0)$	Belle [756]: $0.80 \pm 0.20 \pm 0.10$	0.80 ± 0.22
$\mathcal{B}(B \to Y(3940)K) \times \mathcal{B}(Y(3940) \to D^*(2007)^0\bar{D}^0)$	Belle [756]: <0.67	<0.67
$\mathcal{B}(B \to KY(3940)) \times \mathcal{B}(Y(3940) \to J/\psi\omega(782))$	Belle [757]: $0.71 \pm 0.13 \pm 0.31$	0.71 ± 0.34

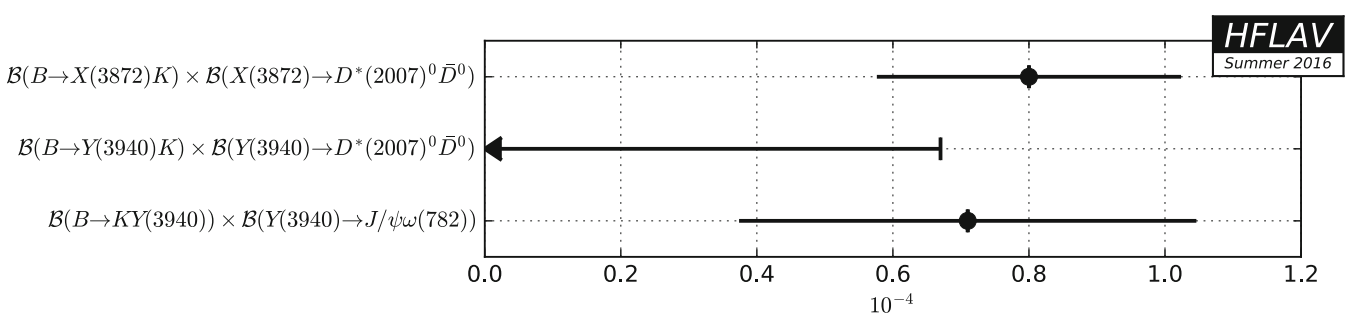

Fig. 151 Summary of the averages from Table 185

Table 186 Decays to a $D_s^{(*)}$ and a light meson I $[10^{-3}]$

Parameter	Measurements	Average
$\mathcal{B}(\bar{B}_s^0 \to D_s^+\pi^-)$	LHCb [758]: $2.95 \pm 0.05\,^{+0.25}_{-0.28}$	3.03 ± 0.25
	Belle [29]: $3.67\,^{+0.35}_{-0.33}\,^{+0.65}_{-0.65}$	
$\mathcal{B}(\bar{B}_s^0 \to D_s^{*+}\pi^-)$	Belle [759]: $2.4\,^{+0.5}_{-0.4} \pm 0.4$	$2.4\,^{+0.7}_{-0.6}$
$\mathcal{B}(\bar{B}_s^0 \to D_s^+\rho^-(770))$	Belle [759]: $8.5\,^{+1.3}_{-1.2} \pm 1.7$	$8.5\,^{+2.1}_{-2.1}$
$\mathcal{B}(\bar{B}_s^0 \to D_s^{*+}\rho^-(770))$	Belle [759]: $11.8\,^{+2.2}_{-2.0} \pm 2.5$	$11.8\,^{+3.3}_{-3.2}$

Table 187 Decays to a $D_s^{(*)}$ and a light meson II $[10^{-4}]$

Parameter	Measurements	Average
$\mathcal{B}(\bar{B}_s^0 \to D_s^+K^-)$	LHCb [758]: $1.90 \pm 0.12\,^{+0.18}_{-0.19}$	1.92 ± 0.22
	Belle [29]: $2.4\,^{+1.2}_{-1.0} \pm 0.4$	
$\mathcal{B}(\bar{B}_s^0 \to D_s^{*+}K^-)$	LHCb [760]: $1.63 \pm 0.12\,^{+0.49}_{-0.48}$	$1.63\,^{+0.50}_{-0.50}$

Table 188 Decays to a $D^{(*)}$ and a light meson I [10^{-4}]

Parameter	Measurements	Average
$\mathcal{B}(\bar{B}_s^0 \to D^0 K^0)$	LHCb [761]: 4.3 ± 0.5 ± 0.8	4.3 ± 0.9
$\mathcal{B}(\bar{B}_s^0 \to D^{*0} K^0)$	LHCb [761]: 2.8 ± 1.0 ± 0.5	2.8 ± 1.1
$\mathcal{B}(\bar{B}_s^0 \to D^0 K^{*0})$	LHCb [762]: 4.72 ± 1.07 ± 0.96	4.72 ± 1.44

Table 189 Decays to a $D^{(*)}$ and a light meson II [10^{-6}]

Parameter	Measurements	Average
$\mathcal{B}(\bar{B}_s^0 \to D^*(2010)^{\pm} \pi^{\mp})$	LHCb [763]: <6.1	<6.1
$\mathcal{B}(\bar{B}_s^0 \to D^0 f_0(980))$	LHCb [764]: <3.1	<3.1

Table 190 Relative decay rates I

Parameter	Measurements	Average
$\mathcal{B}(\bar{B}_s^0 \to D_s^+ \pi^-)/\mathcal{B}(\bar{B}^0 \to D^+ \pi^-)$	CDF [765]: 1.13 ± 0.08 ± 0.23	1.13 ± 0.25
$\mathcal{B}(\bar{B}_s^0 \to D_s^+ \pi^+ \pi^- \pi^-)/\mathcal{B}(\bar{B}_s^0 \to D_s^+ \pi^-)$	LHCb [616]: 2.01 ± 0.37 ± 0.20	2.01 ± 0.42
$\mathcal{B}(\bar{B}_s^0 \to D_s^+ \pi^+ \pi^- \pi^-)/\mathcal{B}(\bar{B}^0 \to D^+ \pi^+ \pi^- \pi^-)$	CDF [765]: 1.05 ± 0.10 ± 0.22	1.05 ± 0.24
$\mathcal{B}(\bar{B}_s^0 \to D^0 K^{*0})/\mathcal{B}(\bar{B}^0 \to D^0 \rho^0)$	LHCb [762]: 1.48 ± 0.34 ± 0.19	1.48 ± 0.39
$\mathcal{B}(\bar{B}_s^0 \to D^0 K^{*0})/\mathcal{B}(\bar{B}^0 \to D^0 \bar{K}^{*0})$	LHCb [766]: 7.8 ± 0.7 ± 0.7	7.8 ± 1.0
$\mathcal{B}(\bar{B}_s^0 \to D^0 K^+ \pi^-)/\mathcal{B}(\bar{B}^0 \to D^0 \pi^- \pi^+)$	LHCb [618]: 1.18 ± 0.05 ± 0.12	1.18 ± 0.13

Table 191 Relative decay rates II [10^{-2}]

Parameter	Measurements	Average
$\mathcal{B}(\bar{B}_s^0 \to D_s^+ K^-)/\mathcal{B}(\bar{B}_s^0 \to D_s^+ \pi^-)$	LHCb [621]: 7.52 ± 0.15 ± 0.19	7.55 ± 0.24
	CDF [767]: 9.7 ± 1.8 ± 0.9	
$\mathcal{B}(\bar{B}_s^0 \to D_s^{*+} K^-)/\mathcal{B}(\bar{B}_s^0 \to D_s^{*+} \pi^-)$	LHCb [760]: $6.8 \pm 0.5\,^{+0.3}_{-0.2}$	$6.8\,^{+0.6}_{-0.5}$
$\mathcal{B}(\bar{B}_s^0 \to D_s^+ K^- \pi^+ \pi^-)/\mathcal{B}(\bar{B}^0 \to D_s^+ \pi^- \pi^+ \pi^-)$	LHCb [617]: 5.2 ± 0.5 ± 0.3	5.2 ± 0.6
$\mathcal{B}(\bar{B}_s^0 \to D^0 \phi(1020))/\mathcal{B}(\bar{B}_s^0 \to D^0 K^{*0})$	LHCb [766]: 6.9 ± 1.3 ± 0.7	6.9 ± 1.5
$[\mathcal{B}(\bar{B}_s^0 \to D_{s1}^+ \pi^-) \times \mathcal{B}(D_{s1}^+ \to D_s^+ \pi^- \pi^+)]/\mathcal{B}(\bar{B}^0 \to D_s^+ \pi^- \pi^+ \pi^-)$	LHCb [617]: 0.40 ± 0.10 ± 0.04	0.40 ± 0.11

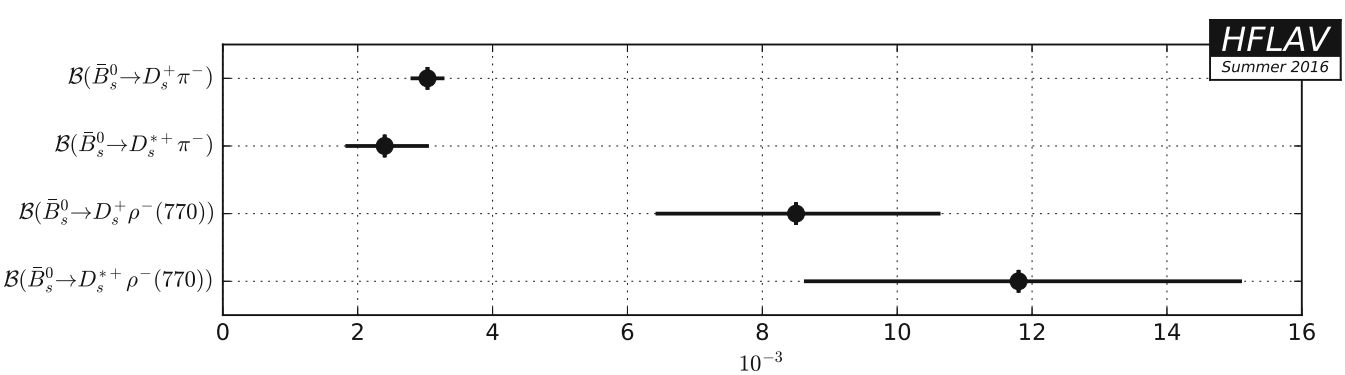

Fig. 152 Summary of the averages from Table 186

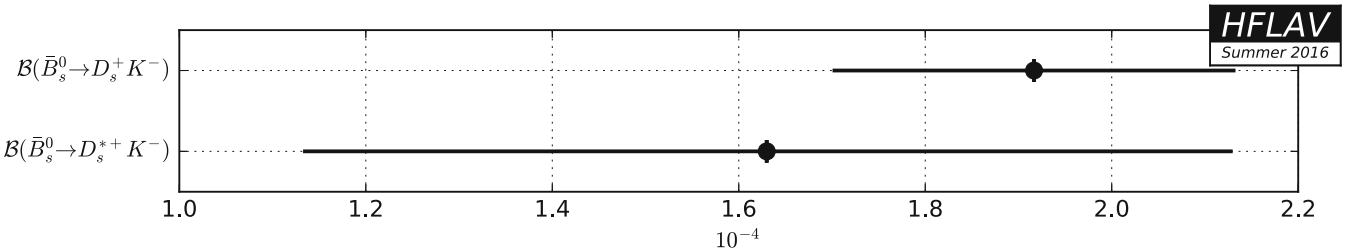

Fig. 153 Summary of the averages from Table 187

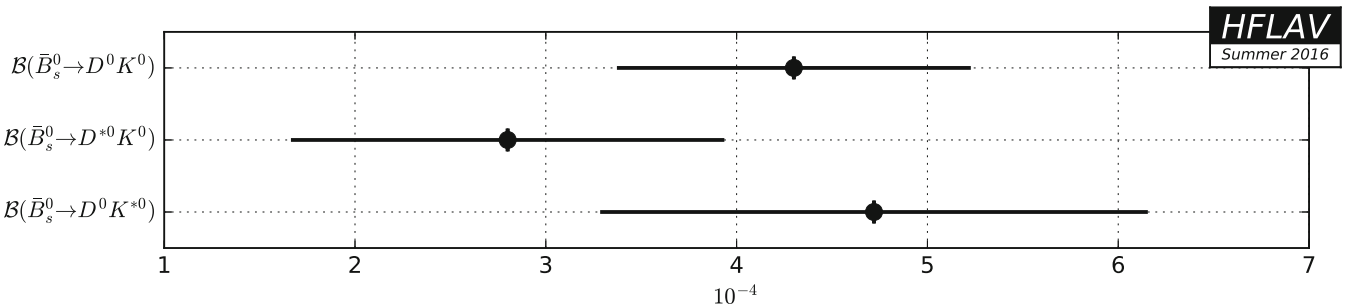

Fig. 154 Summary of the averages from Table 188

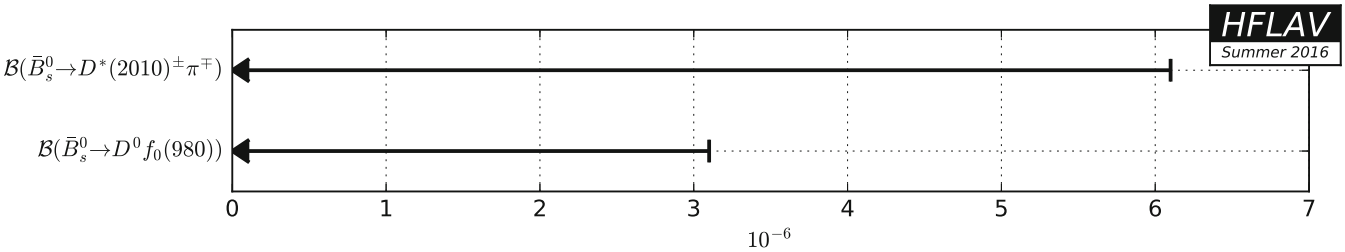

Fig. 155 Summary of the averages from Table 189

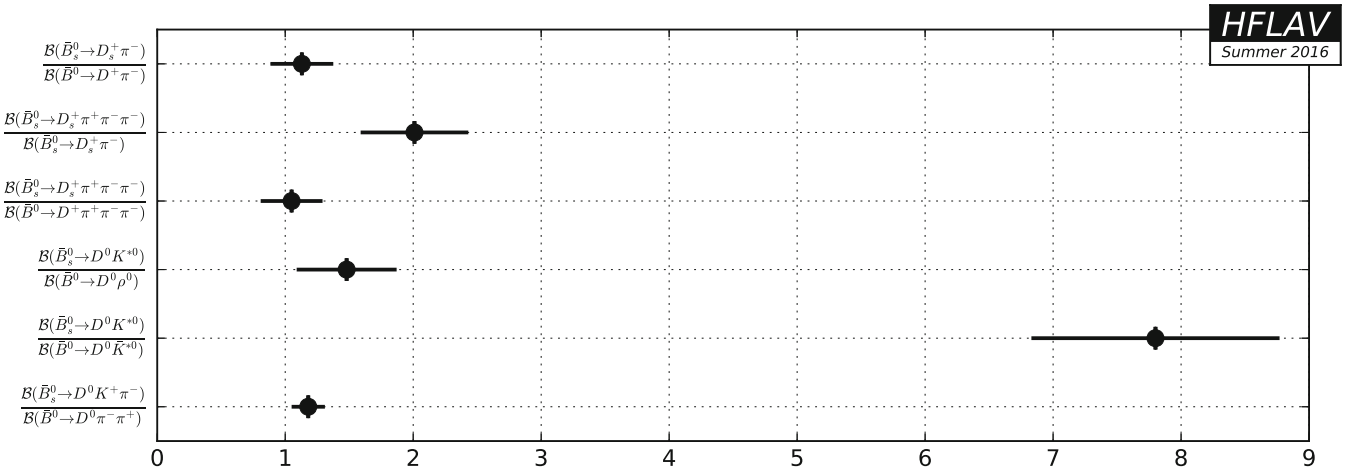

Fig. 156 Summary of the averages from Table 190

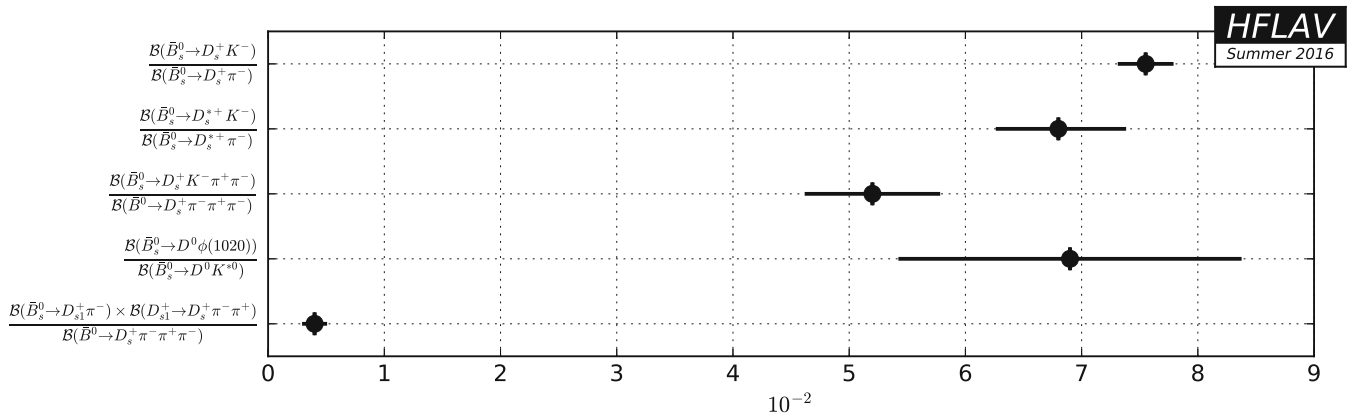

Fig. 157 Summary of the averages from Table 191

6.4.2 *Decays to two open charm mesons*

Averages of $\bar{B}_s^0$ decays to two open charm mesons are shown in Tables 192, 193, 194 and Figs. 158, 159, 160.

Table 192 Absolute decay rates [10^{-2}]

Parameter	Measurements	Average
$\mathcal{B}(\bar{B}_s^0 \to D_s^+ D_s^-)$	CDF [768]: $0.49 \pm 0.06 \pm 0.09$	0.52 ± 0.09
	Belle [20]: $0.58\,^{+0.11}_{-0.09} \pm 0.13$	
$\mathcal{B}(\bar{B}_s^0 \to D_s^+ D_s^{*-})$	LHCb [769]: $1.35 \pm 0.06 \pm 0.17$	
	CDF [768]: $1.13 \pm 0.12 \pm 0.21$	1.38 ± 0.17
	Belle [20]: $1.76\,^{+0.23}_{-0.22} \pm 0.40$	
$\mathcal{B}(\bar{B}_s^0 \to D_s^{*+} D_s^{*-})$	LHCb [769]: $1.27 \pm 0.08 \pm 0.17$	
	CDF [768]: $1.75 \pm 0.19 \pm 0.34$	1.32 ± 0.18
	Belle [20]: $1.98\,^{+0.33}_{-0.31}\,^{+0.51}_{-0.50}$	
$\mathcal{B}(\bar{B}_s^0 \to D_s^{(*)+} D_s^{(*)-})$	LHCb [769]: $3.05 \pm 0.10 \pm 0.39$	3.19 ± 0.37
	D0 [206]: $3.5 \pm 1.0 \pm 1.1$	
	CDF [768]: $3.38 \pm 0.25 \pm 0.64$	
	Belle [20]: $4.32\,^{+0.42}_{-0.39}\,^{+1.04}_{-1.03}$	

Table 193 Relative decay rates I

Parameter	Measurements	Average
$\mathcal{B}(\bar{B}_s^0 \to D^- D^+)/\mathcal{B}(\bar{B}^0 \to D^- D^+)$	LHCb [639]: $1.08 \pm 0.20 \pm 0.10$	1.08 ± 0.22
$\mathcal{B}(\bar{B}_s^0 \to D_s^- D_s^+)/\mathcal{B}(\bar{B}^0 \to D_s^- D^+)$	LHCb [639]: $0.56 \pm 0.03 \pm 0.04$	0.56 ± 0.05

Table 194 Relative decay rates II [10^{-2}]

Parameter	Measurements	Average
$\mathcal{B}(\bar{B}_s^0 \to D_s^+ D^-)/\mathcal{B}(B^0 \to D_s^+ D^-)$	LHCb [639]: $5.0 \pm 0.8 \pm 0.4$	5.0 ± 0.9
$\mathcal{B}(\bar{B}_s^0 \to \bar{D}^0 D^0)/\mathcal{B}(B^- \to D^0 D_s^-)$	LHCb [639]: $1.9 \pm 0.3 \pm 0.3$	1.9 ± 0.4

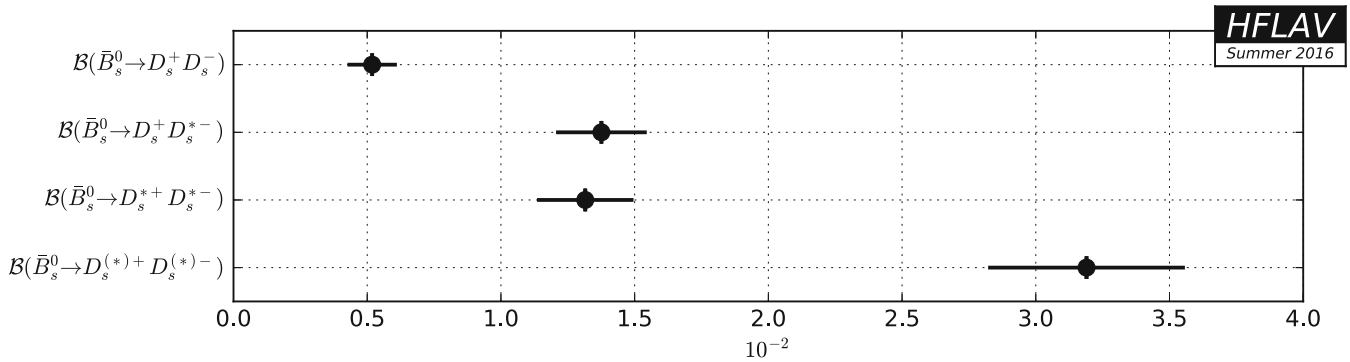

Fig. 158 Summary of the averages from Table 192

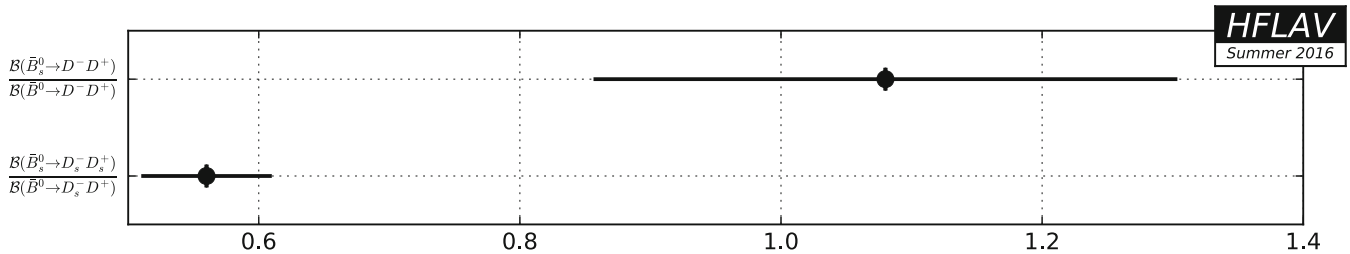

Fig. 159 Summary of the averages from Table 193

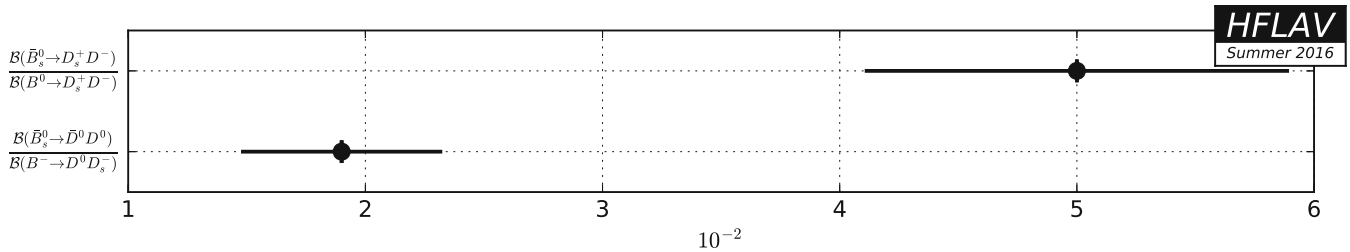

Fig. 160 Summary of the averages from Table 194

6.4.3 Decays to charmonium states

Averages of $\bar{B}_s^0$ decays to charmonium states are shown in Tables 195, 196, 197, 198, 199 and Figs. 161, 162, 163, 164, 165.

Table 195 Absolute decay rates I [10^{-4}]

Parameter	Measurements	Average
$\mathcal{B}(\bar{B}_s^0 \to J/\psi\eta)$	Belle [770]: $5.10 \pm 0.50\,^{+1.17}_{-0.83}$	$5.10\,^{+1.27}_{-0.97}$
$\mathcal{B}(\bar{B}_s^0 \to J/\psi\eta')$	Belle [770]: $3.71 \pm 0.61\,^{+0.85}_{-0.60}$	$3.71\,^{+1.05}_{-0.85}$
$\mathcal{B}(\bar{B}_s^0 \to J/\psi\phi(1020))$	LHCb [771]: $10.5 \pm 0.1 \pm 1.0$	10.0 ± 0.9
	CDF [683]: $9.3 \pm 2.8 \pm 1.7$	
	Belle [772]: $12.5 \pm 0.7 \pm 2.3$	
$\mathcal{B}(\bar{B}_s^0 \to J/\psi K^0 K^\pm \pi^\mp)$	LHCb [649]: $9.1 \pm 0.6 \pm 0.7$	9.1 ± 0.9
$\mathcal{B}(\bar{B}_s^0 \to J/\psi f_0(980)) \times \mathcal{B}(f_0(980) \to \pi^+\pi^-)$	Belle [28]: $1.16\,^{+0.31}_{-0.19}\,^{+0.30}_{-0.25}$	$1.16\,^{+0.43}_{-0.32}$

Table 196 Absolute decay rates II [10^{-5}]

Parameter	Measurements	Average
$\mathcal{B}(\bar{B}_s^0 \to J/\psi \bar{K}^0)$	LHCb [773]: $3.66 \pm 0.42 \pm 0.37$	3.61 ± 0.46
	CDF [774]: $3.5 \pm 0.6 \pm 0.6$	
$\mathcal{B}(\bar{B}_s^0 \to J/\psi K^{*0})$	LHCb [775]: $4.17 \pm 0.18 \pm 0.35$	4.15 ± 0.40
	CDF [774]: $8.3 \pm 1.2 \pm 3.6$	
$\mathcal{B}(\bar{B}_s^0 \to J/\psi p \bar{p})$	LHCb [678]: <0.48	<0.48
$\mathcal{B}(\bar{B}_s^0 \to J/\psi f_1(1285))$	LHCb [671]: $7.14 \pm 0.99 \,^{+0.93}_{-1.00}$	$7.14 \,^{+1.36}_{-1.41}$
$\mathcal{B}(\bar{B}_s^0 \to J/\psi K^0 \pi^+\pi^-)$	LHCb [649]: <4.4	<4.4
$\mathcal{B}(\bar{B}_s^0 \to J/\psi K^0 K^+K^-)$	LHCb [649]: <1.2	<1.2
$\mathcal{B}(\bar{B}_s^0 \to J/\psi f_0(1370)) \times \mathcal{B}(f_0(1370) \to \pi^+\pi^-)$	Belle [28]: $3.4 \,^{+1.1}_{-1.4} \,^{+0.9}_{-0.5}$	$3.4 \,^{+1.4}_{-1.5}$
$\mathcal{B}(\bar{B}_s^0 \to J/\psi f_1(1285)) \times \mathcal{B}(f_1(1285) \to \pi^+\pi^-\pi^+\pi^-)$	LHCb [671]: $0.785 \pm 0.109 \,^{+0.089}_{-0.101}$	$0.785 \,^{+0.141}_{-0.149}$
$\mathcal{B}(\bar{B}_s^0 \to J/\psi \gamma)$	LHCb [676]: <0.73	<0.73

Table 197 Relative decay rates I

Parameter	Measurements	Average
$\mathcal{B}(\bar{B}_s^0 \to J/\psi \eta)/\mathcal{B}(\bar{B}^0 \to J/\psi \rho)$	LHCb [684]: $14.0 \pm 1.2 \,^{+1.6}_{-1.8}$	$14.0 \,^{+2.0}_{-2.2}$
$\mathcal{B}(\bar{B}_s^0 \to J/\psi \eta')/\mathcal{B}(\bar{B}^0 \to J/\psi \rho)$	LHCb [684]: $12.7 \pm 1.1 \,^{+1.1}_{-0.9}$	$12.7 \,^{+1.6}_{-1.4}$
$\mathcal{B}(\bar{B}_s^0 \to J/\psi K_S^0 K^\pm \pi^\mp)/\mathcal{B}(\bar{B}^0 \to J/\psi \pi^+\pi^-)$	LHCb [649]: $2.12 \pm 0.15 \pm 0.18$	2.12 ± 0.23

Table 198 Relative decay rates II

Parameter	Measurements	Average
$\mathcal{B}(\bar{B}_s^0 \to J/\psi \eta)/\mathcal{B}(\bar{B}^0 \to J/\psi \eta')$	Belle [770]: $0.73 \pm 0.14 \pm 0.02$	0.73 ± 0.14
$\mathcal{B}(\bar{B}_s^0 \to J/\psi \eta')/\mathcal{B}(\bar{B}_s^0 \to J/\psi \eta)$	LHCb [684]: $0.90 \pm 0.09 \,^{+0.06}_{-0.02}$	$0.90 \,^{+0.11}_{-0.09}$
$\mathcal{B}(\bar{B}_s^0 \to J/\psi f_2')/\mathcal{B}(\bar{B}_s^0 \to J/\psi \phi(1020))$	LHCb [776]: $0.264 \pm 0.027 \pm 0.024$	0.246 ± 0.031
	D0 [777]: $0.19 \pm 0.05 \pm 0.04$	
$\mathcal{B}(\bar{B}_s^0 \to J/\psi \pi^+\pi^-)/\mathcal{B}(\bar{B}_s^0 \to J/\psi \phi(1020))$	LHCb [778]: $0.162 \pm 0.022 \pm 0.016$	0.162 ± 0.027
$\mathcal{B}\bar{B}_s^0 \to \psi(2S)\pi^+\pi^-/\mathcal{B}\bar{B}_s^0 \to J/\psi \pi^+\pi^-$	LHCb [686]: $0.34 \pm 0.04 \pm 0.03$	0.34 ± 0.05
$\mathcal{B}(\bar{B}_s^0 \to \psi(2S)\phi(1020))/\mathcal{B}(\bar{B}_s^0 \to J/\psi \phi(1020))$	LHCb [685]: $0.489 \pm 0.026 \pm 0.024$	
	D0 [746]: $0.55 \pm 0.11 \pm 0.09$	0.494 ± 0.034
	CDF [779]: $0.52 \pm 0.13 \pm 0.07$	
$\mathcal{B}(\bar{B}_s^0 \to J/\psi K_S^0 \pi^+\pi^-)/\mathcal{B}(\bar{B}^0 \to J/\psi \pi^+\pi^-)$	LHCb [649]: <0.10	<0.10
$[\mathcal{B}(\bar{B}_s^0 \to J/\psi f_0(980)) \times \mathcal{B}(f_0(980) \to \pi^+\pi^-)]/$ $[\mathcal{B}(\bar{B}_s^0 \to J/\psi \phi(1020))) \times \mathcal{B}(\phi \to K^+K^-)]$	LHCb [778]: $0.252 \,^{+0.046}_{-0.032} \,^{+0.027}_{-0.033}$	0.207 ± 0.016 CL = 3.8 ‰
	D0 [780]: $0.275 \pm 0.041 \pm 0.061$	
	CMS [781]: $0.140 \pm 0.008 \pm 0.023$	
	CDF [128]: $0.257 \pm 0.020 \pm 0.014$	

Table 199 Relative decay rates III [10^{-2}]

Parameter	Measurements	Average
$\mathcal{B}(\bar{B}_s^0 \to J/\psi K_S^0)/\mathcal{B}(\bar{B}^0 \to J/\psi K_S^0)$	LHCb [773]: 4.20 ± 0.49 ± 0.40	4.20 ± 0.63
$\mathcal{B}(\bar{B}_s^0 \to J/\psi\phi(1020)\phi(1020))/\mathcal{B}(\bar{B}_s^0 \to J/\psi\phi(1020))$	LHCb [782]: $1.15 \pm 0.12\,^{+0.05}_{-0.09}$	$1.15\,^{+0.13}_{-0.15}$
$\mathcal{B}(\bar{B}_s^0 \to \psi(2S)K^+\pi^-)/\mathcal{B}(\bar{B}^0 \to \psi(2S)K^+\pi^-)$	LHCb [783]: 5.38 ± 0.36 ± 0.38	5.38 ± 0.52
$\mathcal{B}(\bar{B}_s^0 \to \psi(2S)K^{*0})/\mathcal{B}(\bar{B}^0 \to \psi(2S)K^{*0})$	LHCb [783]: 5.38 ± 0.57 ± 0.51	5.38 ± 0.77
$\mathcal{B}(\bar{B}_s^0 \to J/\psi K_S^0 K^+K^-)/\mathcal{B}(\bar{B}^0 \to J/\psi\pi^+\pi^-)$	LHCb [649]: <2.7	<2.7
$[\mathcal{B}(\bar{B}_s^0 \to J/\psi f_0(500)) \times \mathcal{B}(f_0(500) \to \pi^+\pi^-)]/$ $[\mathcal{B}(\bar{B}_s^0 \to J/\psi f_0(980))) \times \mathcal{B}(f_0(500) \to \pi^+\pi^-)]$	LHCb [784]: <3.4	<3.4

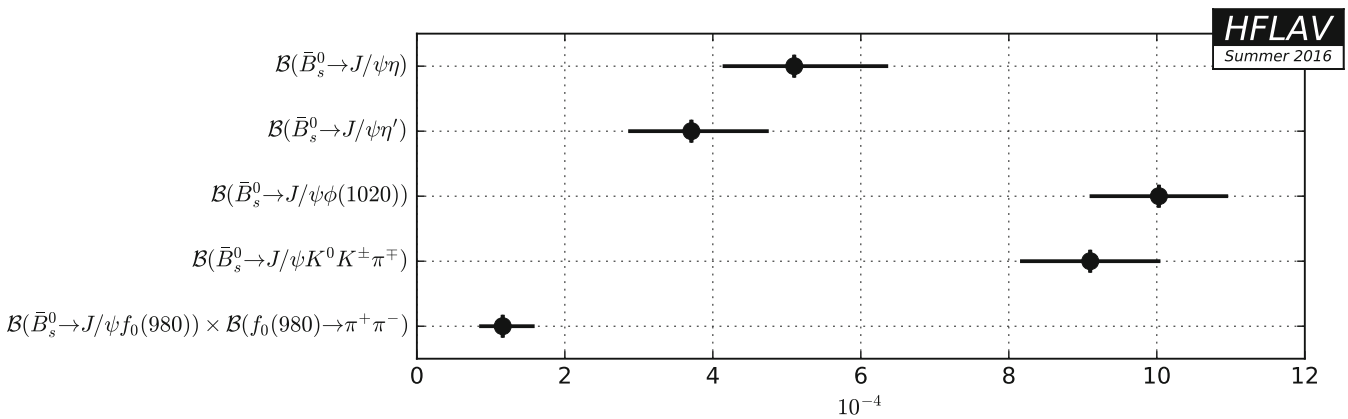

Fig. 161 Summary of the averages from Table 195

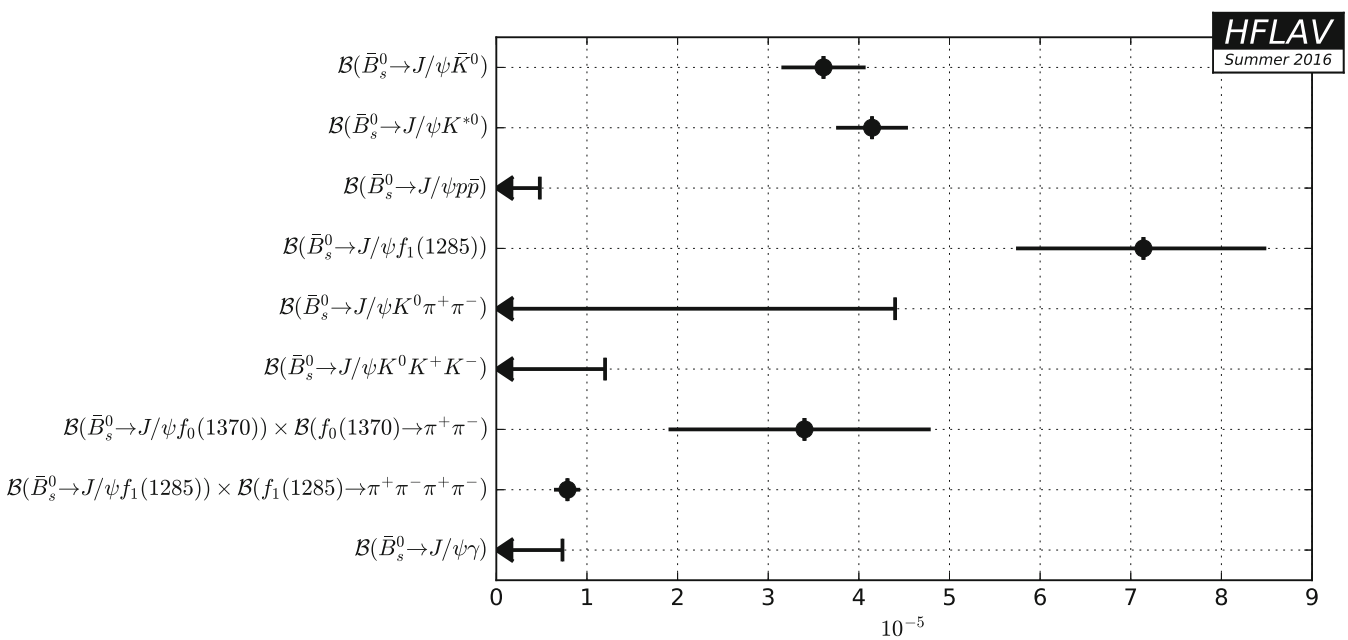

Fig. 162 Summary of the averages from Table 196

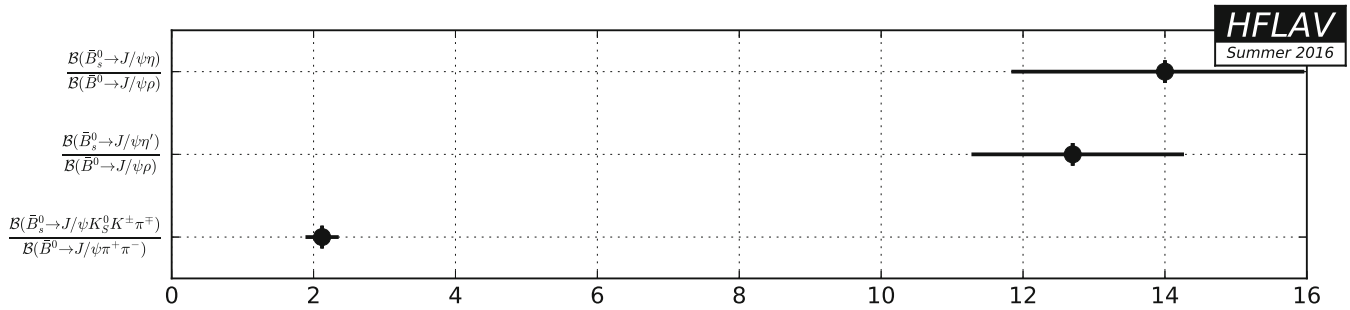

Fig. 163 Summary of the averages from Table 197

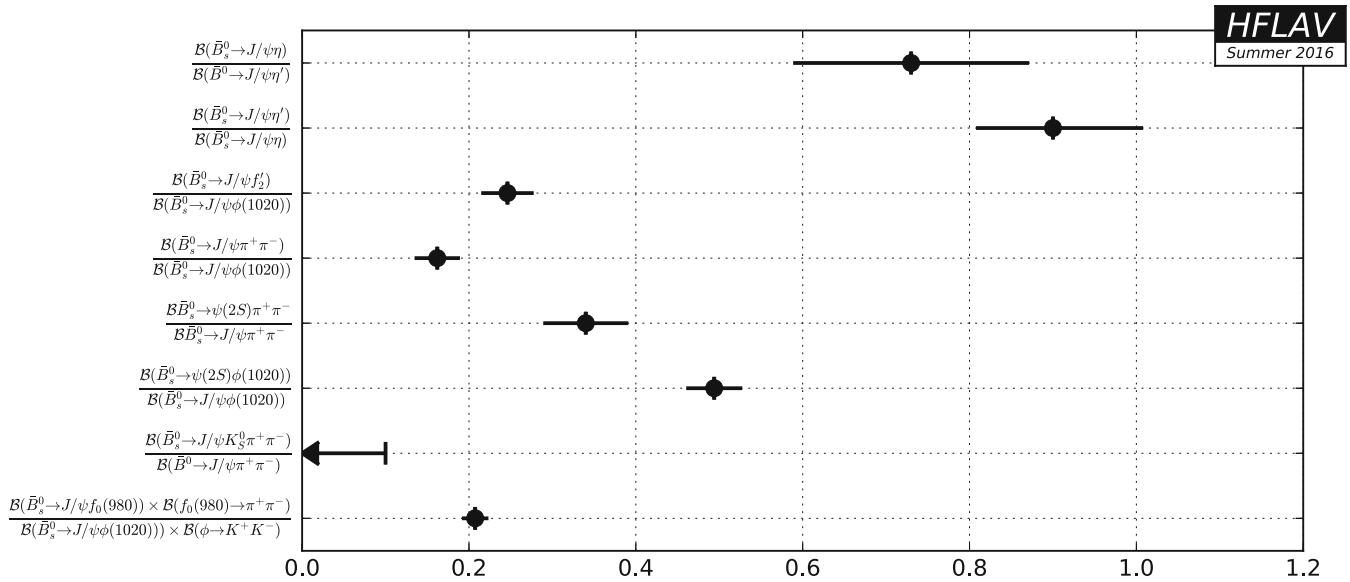

Fig. 164 Summary of the averages from Table 198

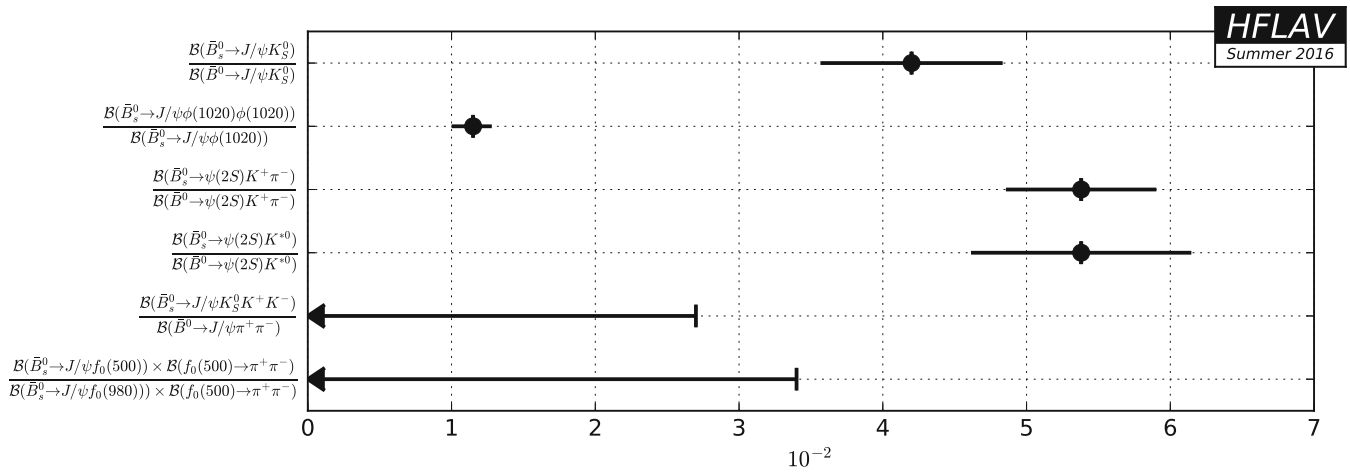

Fig. 165 Summary of the averages from Table 199

Table 200 Decays to one charm baryon [10^{-4}]

Parameter	Measurements	Average
$\mathcal{B}(\bar{B}_s^0 \to \Lambda_c^+ \bar{\Lambda}\pi^-)$	Belle [785]: $3.6 \pm 1.1\,^{+1.2}_{-1.2}$	$3.6\,^{+1.6}_{-1.7}$

Table 201 Decays to two charm baryons

Parameter	Measurements	Average
$\mathcal{B}(\bar{B}_s^0 \to \Lambda_c^- \Lambda_c^+)/\mathcal{B}(\bar{B}_s^0 \to D^- D_s^+)$	LHCb [703]: <0.30	<0.30

6.4.4 *Decays to charm baryons*

Averages of $\bar{B}_s^0$ decays to charm baryons are shown in Tables 200 and 201.

6.5 Decays of B_c^- mesons

Measurements of B_c^- decays to charmed hadrons are summarized in Sects. 6.5.1–6.5.2. Since the absolute cross-section for B_c^- meson production in any production environment is currently not known, it is not possible to determine absolute branching fractions. Instead, results are presented either as ratios of branching fractions of different B_c^- decays, or are normalised to the branching fraction of the decay of a lighter B meson (usually B^-). In the latter case the measured quantity is the absolute or relative B_c^- branching fraction multiplied by the ratio of cross-sections (or, equivalently, production fractions) of the B_c^- and the lighter B meson.

It should be noted that the ratio of cross-sections for different b hadron species can depend on production environment, and on the fiducial region accessed by each experiment. While this has been studied for certain b hadron species (see Sect. 3.1), there is currently little published data that would allow to investigate the effect for B_c^- mesons. Therefore, we do not attempt to apply any correction for this effect.

6.5.1 *Decays to charmonium states*

Averages of B_c^- decays to charmonium states are shown in Tables 202, 203, 204, 205 and Figs. 166, 167.

6.5.2 *Decays to a B meson*

Averages of B_c^- decays to a B meson are shown in Table 206.

6.6 Decays of b baryons

Measurements of b baryons decays to charmed hadrons are summarized in Sects. 6.6.1–6.6.3. Comments regarding the production rates of $\bar{B}_s^0$ and B_c^- mesons relative to lighter B mesons, in Sects. 6.4 and 6.5 respectively, are also appropriate here. Specifically, since the cross-

Table 202 Relative decay rates I

Parameter	Measurements	Average
$\mathcal{B}(B_c^- \to J/\psi D_s^-)/\mathcal{B}(B_c^- \to J/\psi\pi^-)$	LHCb [786]: $2.90 \pm 0.57 \pm 0.24$	3.09 ± 0.55
	ATLAS [787]: $3.8 \pm 1.1 \pm 0.4$	
$\mathcal{B}(B_c^- \to J/\psi D_s^{*-})/\mathcal{B}(B_c^- \to J/\psi D_s^-)$	ATLAS [787]: $2.8\,^{+1.2}_{-0.8} \pm 0.3$	$2.8\,^{+1.2}_{-0.9}$
$\mathcal{B}(B_c^- \to J/\psi D_s^{*-})/\mathcal{B}(B_c^- \to J/\psi\pi^-)$	ATLAS [787]: $10.4 \pm 3.1 \pm 1.6$	10.4 ± 3.5
$\mathcal{B}(B_c^- \to J/\psi\pi^+\pi^-\pi^-)/\mathcal{B}(B_c^- \to J/\psi\pi^-)$	LHCb [788]: $2.41 \pm 0.30 \pm 0.33$	
	CMS [789]: $2.55 \pm 0.80\,^{+0.33}_{-0.33}$	2.44 ± 0.40

Table 203 Relative decay rates II

Parameter	Measurements	Average
$\mathcal{B}(B_c^- \to J/\psi K^-)/\mathcal{B}(B_c^- \to J/\psi\pi^-)$	LHCb [790]: $0.069 \pm 0.019 \pm 0.005$	0.069 ± 0.020
$\mathcal{B}(B_c^- \to J/\psi K^- K^+\pi^-)/\mathcal{B}(B_c^- \to J/\psi\pi^-)$	LHCb [791]: $0.53 \pm 0.10 \pm 0.05$	0.53 ± 0.11
$\mathcal{B}(B_c^- \to \psi(2S)\pi^-)/\mathcal{B}(B_c^- \to J/\psi\pi^-)$	LHCb [792]: $0.268 \pm 0.032 \pm 0.009$	0.268 ± 0.033

Table 204 Relative production times decay rates [10^{-3}]

Parameter	Measurements	Average
$[\sigma(B_c^-) \times \mathcal{B}(B_c^- \to J/\psi\pi^-)]/[\sigma(B^-) \times \mathcal{B}(B^- \to J/\psi K^-)]$	LHCb [793]: $6.83 \pm 0.18 \pm 0.09$	
	LHCb [794]: $6.8 \pm 1.0 \pm 0.6$	6.72 ± 0.19
	CMS [789]: $4.8 \pm 0.5 \pm 0.6$	

Table 205 Decay rates times relative production rates [10^{-6}]

Parameter	Measurements	Average
$[\sigma(B_c^-)/\sigma(B^-)] \times \mathcal{B}(B_c^- \to \chi_{c0}\pi^-)$	LHCb [795]: $9.8\,^{+3.4}_{-3.0} \pm 0.8$	$9.8\,^{+3.5}_{-3.1}$

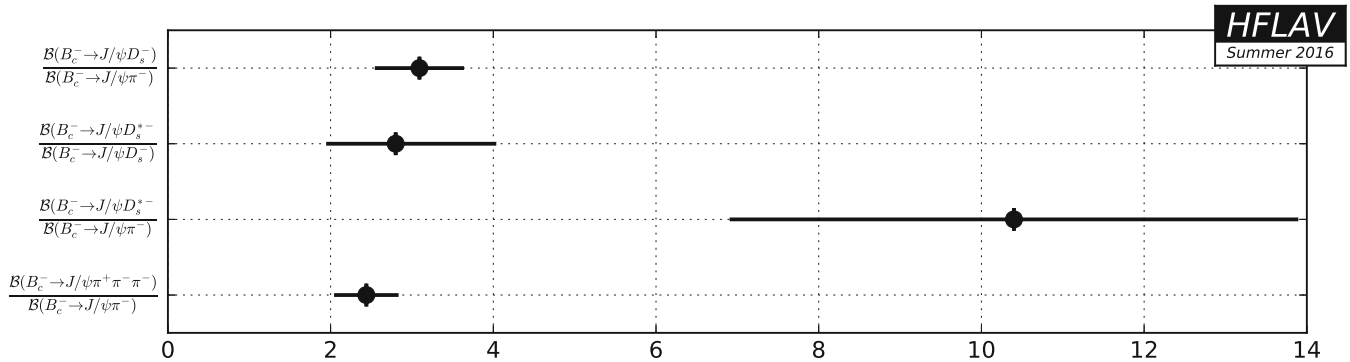

Fig. 166 Summary of the averages from Table 202

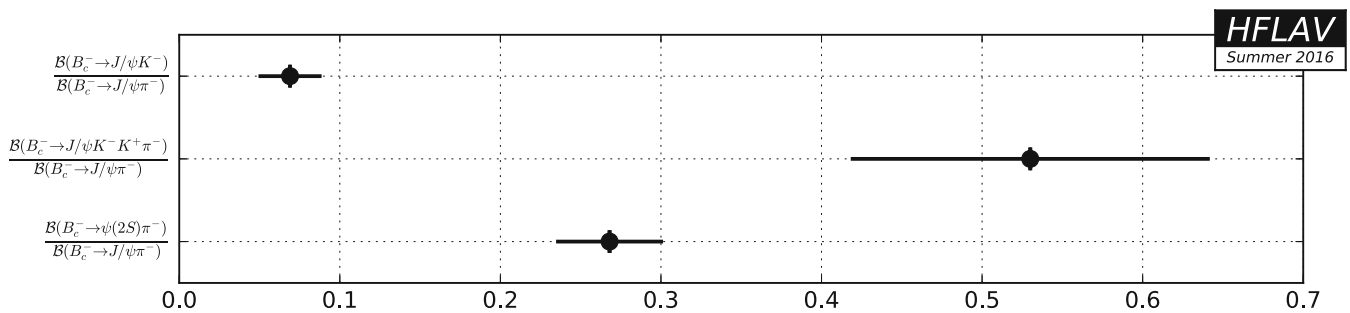

Fig. 167 Summary of the averages from Table 203

Table 206 Decays to B_s^0 meson [10^{-3}]

Parameter	Measurements	Average
$[\sigma(B_c^+)/\sigma(B_s^0)] \times \mathcal{B}(B_c^+ \to B_s^0\pi^+)$	LHCb [796]: $2.37 \pm 0.31\,^{+0.20}_{-0.17}$	$2.37\,^{+0.37}_{-0.35}$

Table 207 Relative decay rates to D^0 mesons

Parameter	Measurements	Average
$\mathcal{B}(\Lambda_b^0 \to D^0 pK^-)/\mathcal{B}(\Lambda_b^0 \to D^0 p\pi^-)$	LHCb [797]: $0.073 \pm 0.008\,^{+0.005}_{-0.006}$	$0.073\,^{+0.009}_{-0.010}$
$[\mathcal{B}(\Lambda_b^0 \to D^0 p\pi^-) \times \mathcal{B}(D^0 \to K^+\pi^-)]/$ $[\mathcal{B}(\Lambda_b^0 \to \Lambda_c^+\pi^-) \times \mathcal{B}(\Lambda_c^+ \to pK^-\pi^+)]$	LHCb [797]: $0.0806 \pm 0.0023 \pm 0.0035$	0.0806 ± 0.0042
$[f_{\Xi_b^0} \times \mathcal{B}(\Xi_b^0 \to D^0 pK^-)]/[f_{\Lambda_b^0} \times \mathcal{B}(\Lambda_b^0 \to D^0 pK^-)]$	LHCb [797]: $0.44 \pm 0.09 \pm 0.06$	0.44 ± 0.11

section for production of Λ_b^0 baryons is reasonably well-known, it is possible to determine absolute or relative branching fractions for its decays (although some older measurements are presented as products involving the cross-section). The cross-sections for production of heavier b baryons are not known, and therefore measured quantities are presented as absolute or relative branching fraction multiplied by a ratio of cross-sections (or, equivalently, production fractions).

6.6.1 Decays to a single open charm meson

Averages of b baryons decays to a single open charm meson are shown in Table 207 and Fig. 168.

6.6.2 Decays to charmonium states

Averages of b baryons decays to charmonium states are shown in Tables 208, 209, 210, 211, 212 and Figs. 169, 170, 171.

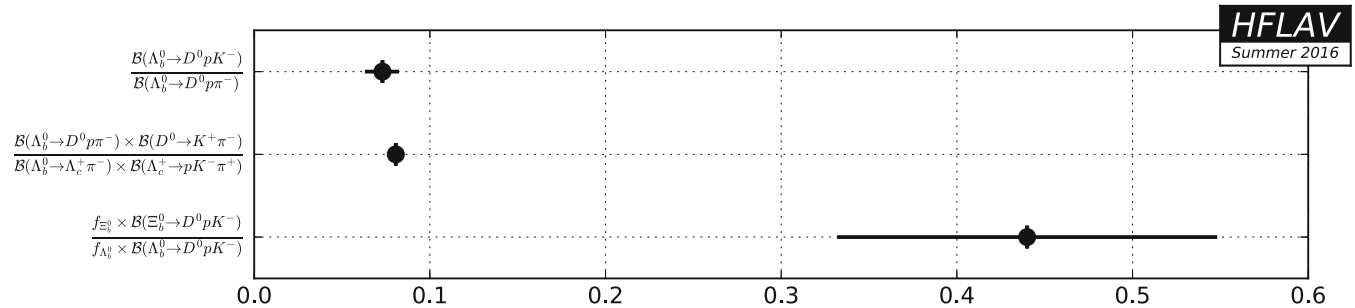

Fig. 168 Summary of the averages from Table 207

Table 208 Λ_b^0 decays to charmonium [10^{-4}]

Parameter	Measurements	Average
$\mathcal{B}(\Lambda_b^0 \to J/\psi pK^-)$	LHCb [798]: $3.17 \pm 0.04\,^{+0.46}_{-0.29}$	$3.17\,^{+0.46}_{-0.29}$
$\mathcal{B}(\Lambda_b^0 \to J/\psi \Lambda)$	CDF [799]: $4.7 \pm 2.1 \pm 1.9$	4.7 ± 2.8

Table 209 f_b times Λ_b^0 decay to charmonium [10^{-5}]

Parameter	Measurements	Average
$f_{\Lambda_b} \times \mathcal{B}(\Lambda_b^0 \to J/\psi \Lambda)$	D0 [800]: $6.01 \pm 0.60 \pm 0.64$	6.01 ± 0.88

Table 210 Relative Λ_b^0 decay rates

Parameter	Measurements	Average
$\mathcal{B}(\Lambda_b^0 \to \psi(2S)\Lambda)/\mathcal{B}(\Lambda_b^0 \to J/\psi \Lambda)$	ATLAS [801]: $0.501 \pm 0.033 \pm 0.019$	0.501 ± 0.038
$\mathcal{B}(\Lambda_b^0 \to J/\psi p\pi^-)/\mathcal{B}(\Lambda_b^0 \to J/\psi pK^-)$	LHCb [802]: $0.0824 \pm 0.0025 \pm 0.0042$	0.0824 ± 0.0049
$\mathcal{B}(\Lambda_b^0 \to J/\psi \pi^+\pi^- pK^-)/\mathcal{B}(\Lambda_b^0 \to J/\psi pK^-)$	LHCb [803]: $0.2086 \pm 0.0096 \pm 0.0134$	0.2086 ± 0.0165
$\mathcal{B}(\Lambda_b^0 \to \psi(2S)pK^-)/\mathcal{B}(\Lambda_b^0 \to J/\psi pK^-)$	LHCb [803]: $0.2070 \pm 0.0076 \pm 0.0059$	0.2070 ± 0.0096

Table 211 Ξ_b^- and Ω_b^- decays to charmonium

Parameter	Measurements	Average
$[\sigma(\Xi_b^-) \times \mathcal{B}(\Xi_b^- \to J/\psi \Xi^-)]/[\sigma(\Lambda_b^0) \times \mathcal{B}(\Lambda_b^0 \to J/\psi \Lambda)]$	CDF [45]: $0.167\,^{+0.037}_{-0.025} \pm 0.012$	$0.167\,^{+0.039}_{-0.028}$
$[\sigma(\Omega_b^-) \times \mathcal{B}(\Omega_b^- \to J/\psi \Omega^-)]/[\sigma(\Lambda_b^0) \times \mathcal{B}(\Lambda_b^0 \to J/\psi \Lambda)]$	CDF [45]: $0.045\,^{+0.017}_{-0.012} \pm 0.004$	$0.045\,^{+0.017}_{-0.013}$

Table 212 Parity violation in Λ_b^0 decays to charmonium

Parameter	Measurements	Average
$\alpha_b(\Lambda_b^0 \to J/\psi \Lambda)$	ATLAS [804]: $0.30 \pm 0.16 \pm 0.06$	0.30 ± 0.17

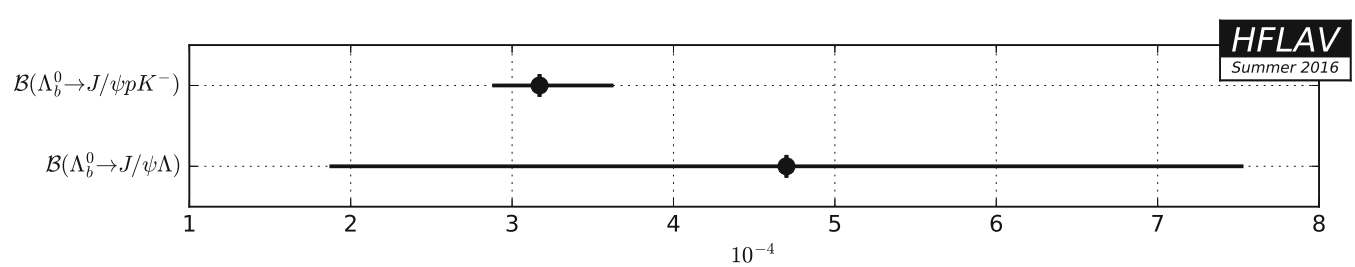

Fig. 169 Summary of the averages from Table 208

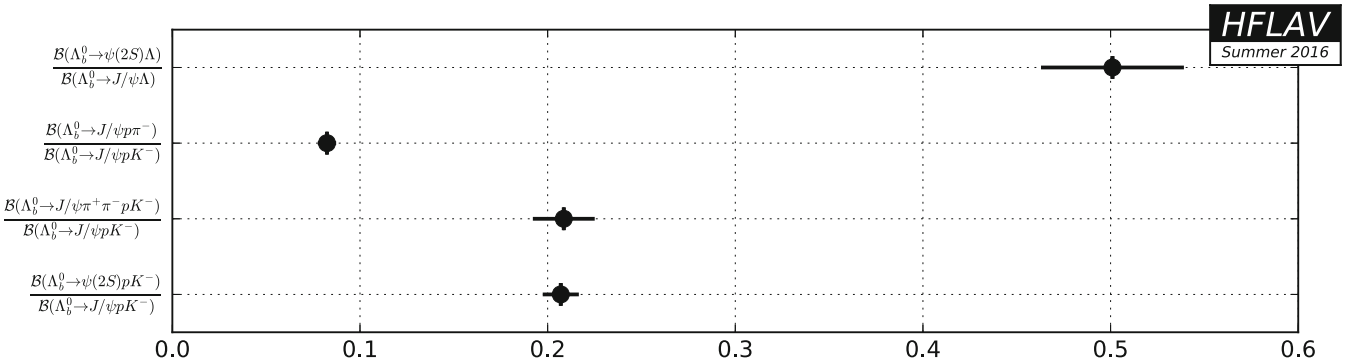

Fig. 170 Summary of the averages from Table 210

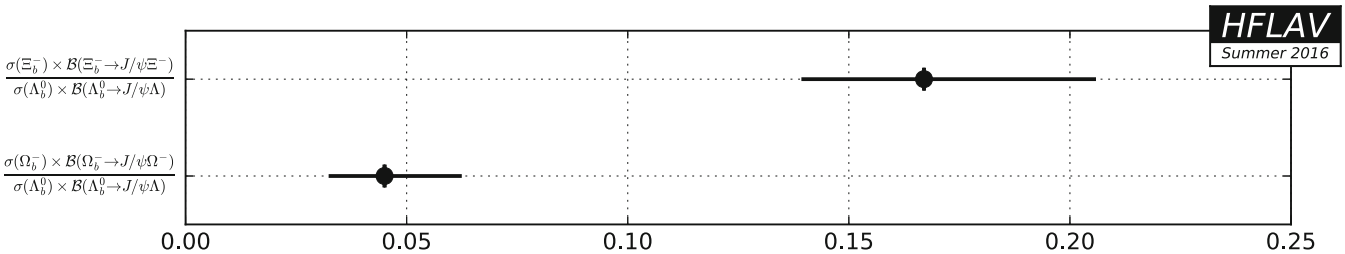

Fig. 171 Summary of the averages from Table 211

6.6.3 Decays to charm baryons

Averages of b baryons decays to charm baryons are shown in Tables 213, 214, 215, 216, 217 and Figs. 172, 173, 174, 175.

Table 213 Absolute decay rates [10^{-2}]

Parameter	Measurements	Average
$\mathcal{B}(\Lambda_b^0 \to \Lambda_c^+\pi^-)$	LHCb [48]: $0.430 \pm 0.003\,^{+0.036}_{-0.035}$	$0.430\,^{+0.036}_{-0.035}$
$\mathcal{B}(\Lambda_b^0 \to \Lambda_c^+\pi^+\pi^-\pi^-)$	CDF [805]: $2.68 \pm 0.29\,^{+1.15}_{-1.09}$	$2.68\,^{+1.19}_{-1.12}$

Table 214 Relative decay rates to Λ_c I

Parameter	Measurements	Average
$\mathcal{B}(\Lambda_b^0 \to \Lambda_c^+\pi^-)/\mathcal{B}(\bar{B}^0 \to D^+\pi^-)$	CDF [806]: $3.3 \pm 0.3 \pm 1.2$	3.3 ± 1.2
$\mathcal{B}(\Lambda_b^0 \to \Lambda_c^+\pi^+\pi^-\pi^-)/\mathcal{B}(\Lambda_b^0 \to \Lambda_c^+\pi^-)$	LHCb [616]: $1.43 \pm 0.16 \pm 0.13$	
	CDF [805]: $3.04 \pm 0.33\,^{+0.70}_{-0.55}$	1.55 ± 0.20
$[\mathcal{B}(\Xi_b^0 \to \Lambda_c^+K^-) \times \mathcal{B}(\Lambda_c^+ \to pK^-\pi^+)]/$ $[\mathcal{B}(\Xi_b^0 \to D^0pK^-) \times \mathcal{B}(D^0 \to K^+\pi^-)]$	LHCb [797]: $0.57 \pm 0.22 \pm 0.21$	0.57 ± 0.30

Table 215 Relative decay rates to Λ_c II [10^{-2}]

Parameter	Measurements	Average
$\mathcal{B}(\Lambda_b^0 \to \Lambda_c^+K^-)/\mathcal{B}(\Lambda_b^0 \to \Lambda_c^+\pi^-)$	LHCb [797]: $7.31 \pm 0.16 \pm 0.16$	7.31 ± 0.23
$\mathcal{B}(\Lambda_b^0 \to \Lambda_c^+D^-)/\mathcal{B}(\Lambda_b^0 \to \Lambda_c^+D_s^-)$	LHCb [703]: $4.2 \pm 0.3 \pm 0.3$	4.2 ± 0.4

Table 216 Relative decay rates to excited or Σ_c states

Parameter	Measurements	Average
$[\mathcal{B}(\Lambda_b^0 \to \Lambda_c(2595)^+\pi^-) \times \mathcal{B}(\Lambda_c(2595)^+ \to \Lambda_c^+\pi^+\pi^-)]/\mathcal{B}(\Lambda_b^0 \to \Lambda_c^+\pi^+\pi^-\pi^-)$	LHCb [616]: $0.044 \pm 0.017\,^{+0.006}_{-0.004}$	$0.044\,^{+0.018}_{-0.017}$
$[\mathcal{B}(\Lambda_b^0 \to \Lambda_c(2625)^+\pi^-) \times \mathcal{B}(\Lambda_c(2625)^+ \to \Lambda_c^+\pi^+\pi^-)]/\mathcal{B}(\Lambda_b^0 \to \Lambda_c^+\pi^+\pi^-\pi^-)$	LHCb [616]: $0.043 \pm 0.015 \pm 0.004$	0.043 ± 0.016
$[\mathcal{B}(\Lambda_b^0 \to \Sigma_c^0\pi^+\pi^-) \times \mathcal{B}(\Sigma_c^0 \to \Lambda_c^+\pi^-)]/\mathcal{B}(\Lambda_b^0 \to \Lambda_c^+\pi^+\pi^-\pi^-)$	LHCb [616]: $0.074 \pm 0.024 \pm 0.012$	0.074 ± 0.027
$[\mathcal{B}(\Lambda_b^0 \to \Sigma_c^{++}\pi^-\pi^-) \times \mathcal{B}(\Sigma_c^{++} \to \Lambda_c^+\pi^+)]/\mathcal{B}(\Lambda_b^0 \to \Lambda_c^+\pi^+\pi^-\pi^-)$	LHCb [616]: $0.042 \pm 0.018 \pm 0.007$	0.042 ± 0.019

Table 217 Ξ_b decay rates [10^{-4}]

Parameter	Measurements	Average
$[f_{\Xi_b^-}/f_{\Lambda_b^0}] \times \mathcal{B}(\Xi_b^- \to \Lambda_b^0\pi^-)$	LHCb [807]: $5.7 \pm 1.8\,^{+0.8}_{-0.9}$	$5.7\,^{+2.0}_{-2.0}$

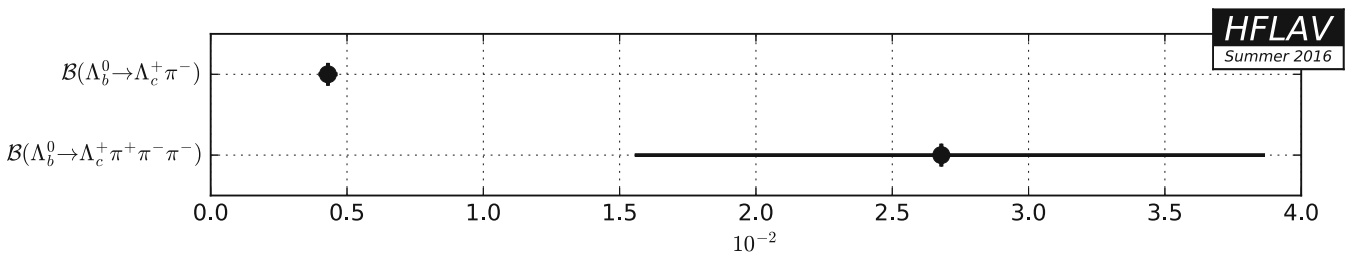

Fig. 172 Summary of the averages from Table 213

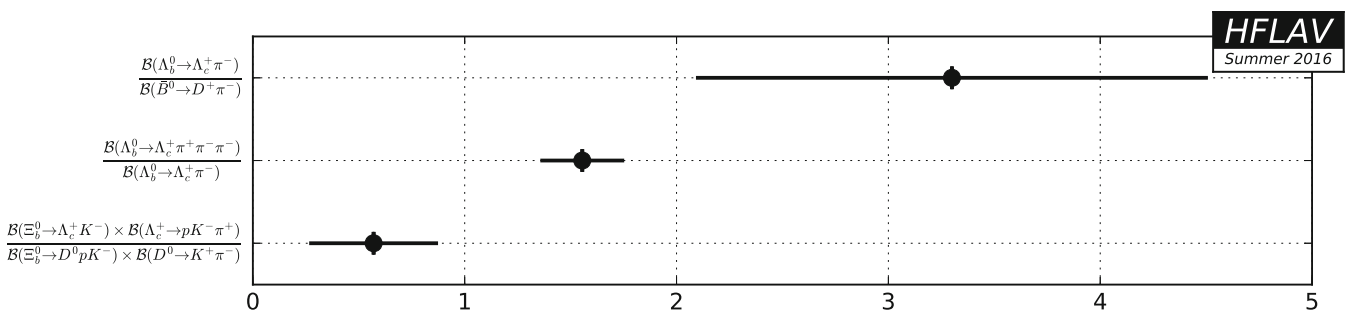

Fig. 173 Summary of the averages from Table 214

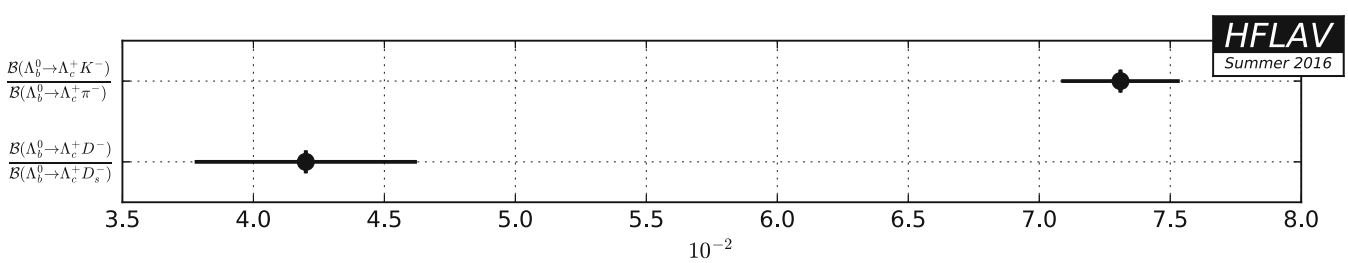

Fig. 174 Summary of the averages from Table 215

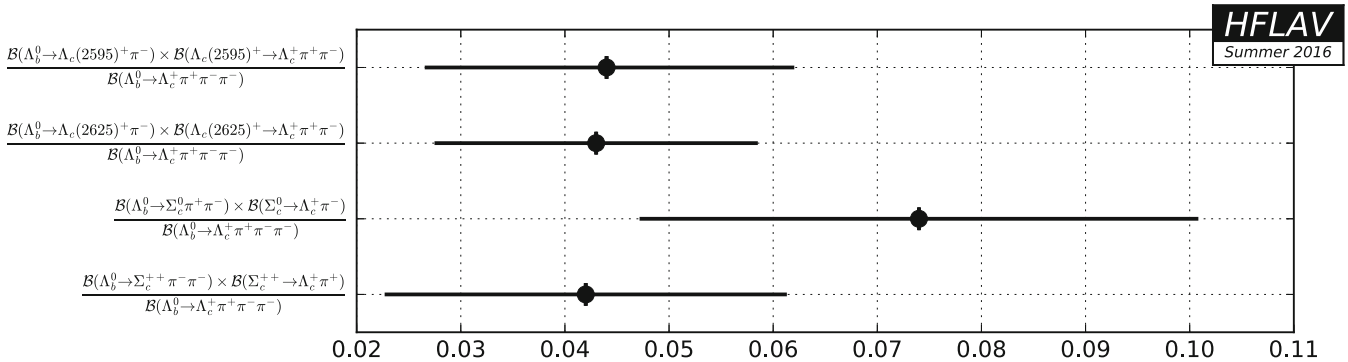

Fig. 175 Summary of the averages from Table 216

7 *B* decays to charmless final states

This section provides branching fractions (BF), polarization fractions, partial rate asymmetries (A_{CP}) and other observables of B decays to final states that do not contain charm hadrons or charmonia mesons. The order of entries in the tables corresponds to that in PDG2014 [327], and the quoted RPP numbers are the PDG numbers of the corresponding branching fractions. The asymmetry is defined as

$$A_{CP} = \frac{N_b - N_{\bar{b}}}{N_b + N_{\bar{b}}}, \tag{220}$$

where N_b ($N_{\bar{b}}$) is the number of hadrons containing a b ($\bar{b}$) quark decaying into a specific final state. This definition is consistent with that of Eq. (104) in Sect. 4.2.1. Four different B^0 and B^+ decay categories are considered: charmless mesonic (i.e., final states containing only mesons), baryonic (only hadrons, but including a baryon-antibaryon pair), radiative (including a photon or a lepton-antilepton pair) and semileptonic/leptonic (including/only leptons). We also include measurements of B_s^0, B_c^+ and b-baryon decays. Measurements supported with written documents are accepted in the averages; written documents include journal papers, conference contributed papers, preprints or conference proceedings. In all the tables of this section, values in red (blue) are new published (preliminary) results since PDG2014. Results from A_{CP} measurements obtained from time-dependent analyses are listed and described in Sect. 4.

Most of the branching fractions from BaBar and Belle assume equal production of charged and neutral B pairs. The best measurements to date show that this is still a reasonable approximation (see Sect. 3). For branching fractions, we provide either averages or the most stringent upper limits. If one or more experiments have measurements with $> 4\sigma$ for a decay channel, all available central values for that channel are used in the averaging. We also give central values and errors for cases where the significance of the average value is at least 3σ, even if no single measurement is above 4σ. For A_{CP} we provide averages in all cases. At the end of some of the tables we give a list of results that were not included. Typical cases are the measurements of distributions, such as differential branching fractions or longitudinal polarizations, which are measured in different binning schemes by the different collaborations, and thus cannot be directly used to obtain averages.

Our averaging is performed by maximizing the likelihood, $\mathcal{L} = \prod_i \mathcal{P}_i(x)$, where $\mathcal{P}_i$ is the probability density function (PDF) of the ith measurement, and x is, e.g., the branching fraction or A_{CP}. The PDF is modelled by an asymmetric Gaussian function with the measured central value as its most probable value and the quadratic sum of the statistical and systematic errors as the standard deviation. The experimental uncertainties are considered to be uncorrelated with each other when the averaging is performed. As mentioned in Sect. 2, no error scaling is applied when the fit χ^2 is greater than 1, except for cases of extreme disagreement (at present we have no such cases).

The largest improvement since the last report has come from the inclusion of a variety of new measurements from the LHC, especially LHCb. The measurements of B_s^0 decays are particularly noteworthy.

Sections 7.1 and 7.2 provide compilations of branching fractions of B^0 and B^+ to mesonic and baryonic charmless final states, respectively, while Sect. 7.3 gives branching fractions of b-baryon decays. In Sects. 7.4 and 7.5 various observables of interest are given in addition to branching fractions: in the former, branching fractions of B_s^0-meson charmless decays, and in the latter observables related to leptonic and radiative B^0 and B^+ meson decays, including processes in which the photon yields a pair of charged or neutral leptons. Section 7.5 also reports limits from searches for lepton-flavor/number-violating decays. Sections 7.6 and 7.7 give CP asymmetries and results of polarization measurements, respectively, in various b-hadron charmless decays. Finally, Sect. 7.8 gives branching fractions of B_c^+ meson decays to charmless final states.

7.1 Mesonic decays of B^0 and B^+ mesons

This section provides branching fractions of charmless mesonic decays: Tables 218, 219 and 220 for B^+ and

Table 218 Branching fractions of charmless mesonic B^+ decays with kaons (part 1) in units of $\times 10^{-6}$. Upper limits are at 90% CL. Where values are shown in red (blue), this indicates that they are new published (preliminary) results since PDG2014

RPP#	Mode	PDG2014 Avg.	BaBar		Belle		CLEO		CDF	LHCb	Our Avg.
262	$K^0\pi^+$	23.7±0.8	23.9±1.1±1.0	[398]	23.97±0.53±0.71	[808]	$18.8^{+3.7+2.1}_{-3.3-1.8}$	[809]			23.79±0.75
263	$K^+\pi^0$	12.9±0.5	13.6±0.6±0.7	[810]	12.62±0.31±0.56	[808]	$12.9^{+2.4+1.2}_{-2.2-1.1}$	[809]			$12.94^{+0.52}_{-0.51}$
264	$\eta' K^+$	70.6±2.5	71.5±1.3±3.2	[811]	69.2±2.2±3.7	[812]					70.6±2.7
265	$\eta' K^{*+}$	$4.8^{+1.8}_{-1.6}$	$4.8^{+1.6}_{-1.4}$±0.8	[813]	< 2.9	[814]					$4.8^{+1.8}_{-1.6}$
266	$\eta' K_0^*(1430)^+$	5.2±2.1	5.2±1.9±1.0	[813]							5.2±2.1
267	$\eta' K_2^*(1430)^+$	28±5	$28.0^{+4.6}_{-4.3}$±2.6	[813]							$28.0^{+5.3}_{-5.0}$
268	ηK^+	2.4±0.4	$2.94^{+0.39}_{-0.34}$±0.21	[811]	2.12±0.23±0.11	[815]	$2.2^{+2.8}_{-2.2}$	[816]			$2.36^{+0.22}_{-0.21}$
269	ηK^{*+}	19.3±1.6	18.9±1.8±1.3	[817]	$19.3^{+2.0}_{-1.9}$±1.5	[818]	$26.4^{+9.6}_{-8.2}$±3.3	[816]			19.3±1.6
270	$\eta K_0^*(1430)^+$	18±4	18.2±2.6±2.6	[817]							18.2±3.7
271	$\eta K_2^*(1430)^+$	9.1±3.0	9.1±2.7±1.4	[817]							9.1±3.0
272	$\eta(1295)K^+$ †	$2.9^{+0.8}_{-0.7}$	$2.9^{+0.8}_{-0.7}$±0.2 ‡	[819]							$2.9^{+0.8}_{-0.7}$
274	$\eta(1405)K^+$ †	< 1.2	< 1.2	[819]							< 1.2
275	$\eta(1475)K^+$ †	$13.8^{+2.1}_{-1.8}$	$13.8^{+1.8+1.0}_{-1.7-0.6}$	[819]							$13.8^{+2.1}_{-1.8}$
276	$f_1(1285)K^+$	< 2.0	< 2.0	[819]							< 2.0
277	$f_1(1420)K^+$ †	< 2.9	< 2.9	[819]							< 2.9
279	$\phi(1680)K^+$ †	< 3.4	< 3.4	[819]							< 3.4
280	$f_0(1500)K^+$	3.7±2.2	3.7±2.2 §	[271,278]							3.7±2.2
281	ωK^+	6.7±0.8	6.3±0.5±0.3	[820]	6.8±0.4±0.4	[389]	$3.2^{+2.4}_{-1.9}$±0.8	[821]			6.5±0.4
282	ωK^{*+}	< 7.4	< 7.4	[822]							< 7.4
283	$\omega(K\pi)_0^{*+}$	28±4	$27.5^{+3.0}_{-2.6}$	[822]							$27.5^{+3.0}_{-2.6}$
284	$\omega K_0^*(1430)^+$	24±5	24.0±2.6±4.4	[822]							24.0±5.1
285	$\omega K_2^*(1430)^+$	21±4	21.5±3.6±2.4	[822]							21.5±4.3
286	$a_0(980)^+K^0$ †	< 3.9	< 3.9	[823]							< 3.9
287	$a_0(980)^0K^+$ †	< 2.5	< 2.5	[823]							< 2.5
288	$K^{*0}\pi^+$	10.1±0.9	10.8±0.6$^{+1.2}_{-1.4}$	[278]	9.7±0.6$^{+0.8}_{-0.9}$	[276]					$10.1^{+0.8}_{-0.9}$
289	$K^{*+}\pi^0$	8.2±1.9	8.2±1.5±1.1	[824]			$7.1^{+11.4}_{-7.1}$±1.0	[821]			8.2±1.8
290	$K^+\pi^+\pi^-$	51±2.9	54.4±1.1±4.6	[278]	48.8±1.1±3.6	[276]					51.0±3.0
291	$K^+\pi^+\pi^-$ (NR)	$16.3^{+2.1}_{-1.5}$	9.3±1.0$^{+6.9}_{-1.7}$	[278]	16.9±1.3$^{+1.7}_{-1.6}$	[276]					16.3±2.0
292	$\omega(782)K^+$ $(K^+\pi^+\pi^-)$	6±9	$5.9^{+8.8+0.5}_{-9.0-0.4}$	[278]							$5.9^{+8.8}_{-9.0}$
293	$f_0(980)K^+$ $(K^+\pi^+\pi^-)$ †	$9.4^{+1.0}_{-1.2}$	10.3±0.5$^{+2.0}_{-1.4}$	[278]	8.8±0.8$^{+0.9}_{-1.8}$	[276]					$9.4^{+0.9}_{-1.0}$

Table 218 continued

RPP#	Mode	PDG2014 Avg.	BABAR		Belle		CLEO		CDF	LHCb		Our Avg.
294	$f_2(1270)^0 K^+ \ (K^+\pi^+\pi^-)$	1.07±0.27	$0.88^{+0.38+0.01}_{-0.33-0.03}$	[278]	$1.33\pm0.30^{+0.23}_{-0.34}$	[276]						1.07±0.29
295	$f_0(1370)^0 K^+ \ (K^+\pi^+\pi^-)$ †	< 10.7	< 10.7	[277]								< 10.7
296	$\rho(1450)^0 K^+ \ (K^+\pi^+\pi^-)$	< 11.7	< 11.7	[277]								< 11.7
297	$f_2'(1525) K^+ \ (K^+\pi^+\pi^-)$	< 3.4	< 3.4	[277]								< 3.4
298	$\rho^0 K^+ \ (K^+\pi^+\pi^-)$	3.7±0.5	$3.56\pm0.45^{+0.57}_{-0.46}$	[278]	$3.89\pm0.47^{+0.43}_{-0.41}$	[276]						$3.74^{+0.49}_{-0.45}$
299	$K_0^*(1430)^0\pi^+ \ (K^+\pi^+\pi^-)$	45^{+9}_{-7}	$32.0\pm1.2^{+10.8}_{-6.0}$	[278]	$51.6\pm1.7^{+7.0}_{-7.5}$	[276]						45.1±6.3
300	$K_2^*(1430)^0\pi^+ \ (K^+\pi^+\pi^-)$	$5.6^{+2.2}_{-1.5}$	$5.6\pm1.2^{+1.8}_{-0.8}$	[278]	< 6.9	[272]						$5.6^{+2.2}_{-1.4}$
301	$K^*(1410)^0\pi^+ \ (K^+\pi^+\pi^-)$	< 45			< 45	[272]						< 45
302	$K^*(1680)^0\pi^+ \ (K^+\pi^+\pi^-)$	< 12	< 15	[277]	< 12	[272]						< 12
303	$K^+\pi^0\pi^0$	16.2±1.9	16.2±1.2±1.5	[824]								16.2±1.9
304	$f_0(980) K^+ \ (K^+\pi^0\pi^0)$	2.8±0.8	2.8±0.6±0.5	[824]								2.8±0.8
305	$K^-\pi^+\pi^+$	< 0.95	< 0.95	[825]	< 4.5	[826]				< 0.046	[827]	< 0.046
306	$K^-\pi^+\pi^+ \ (NR)$	< 56					< 56	[828]				< 56
307	$K_1(1270)^0\pi^+$	< 40	< 40	[415]								< 40
308	$K_1(1400)^0\pi^+$	< 39	< 39	[415]								< 39
309	$K^0\pi^+\pi^0$	< 66					< 66	[829]				< 66
310	$\rho^+K^0(K^0\pi^+\pi^0)$	8.0±1.5	$8.0^{+1.4}_{-1.3}\pm0.6$	[830]								$8.0^{+1.5}_{-1.4}$
311	$K^{*+}\pi^+\pi^-$	75±10	75.3±6.0±8.1	[831]								75.3±10.1
312	$K^{*+}\rho^0$	4.6±1.1	4.6±1.0±0.4	[832]								4.6±1.1
313	$f_0(980) K^{*+}$ †	4.2±0.7	4.2±0.6±0.3	[832]								4.2±0.7

Results for LHCb are relative BFs converted to absolute BFs.
CLEO upper limits that have been greatly superseded are not shown.
† In this product of BFs, all daughter BFs not shown are set to 100%.
‡ The value quoted is $\mathcal{B}(B^+ \to \eta(1295)K^+) \times \mathcal{B}(\eta(1295) \to \eta\pi\pi)$.
§ Average of results in $K_S^0K^+K^-$, $K_S^0K_S^0K^+$ [271] and $K^+\pi^+\pi^-$ [278]. Includes an f_X resonance with parameters that are compatible with $f_0(1500)$.

Table 219 Branching fractions of charmless mesonic B^+ decays with kaons (part 2) in units of $\times 10^{-6}$. Upper limits are at 90% CL. Where values are shown in red (blue), this indicates that they are new published (preliminary) results since PDG2014

RPP#	Mode	PDG2014 Avg.	BABAR		Belle		CLEO		CDF		LHCb		Our Avg.
314	$a_1^+ K^0$	35±7	34.9±5.0±4.4	[833]									34.9±6.7
315	$b_1^+ K^0$ †	9.6±1.9	9.6±1.7±0.9	[834]									9.6±1.9
317	$K_1(1400)^+ \rho^0$	< 780	< 780 ¶	[835]									< 780 ¶
318	$K_2(1430)^+ \rho^0$	< 1500	< 1500 ¶	[835]									< 1500 ¶
319	$b_1^0 K^+$ †	9.1±2.0	9.1±1.7±1.0	[836]									9.1±2.0
320	$b_1^+ K^{*0}$ †	< 5.9	< 5.9	[837]									< 5.9
321	$b_1^0 K^{*+}$ †	< 6.7	< 6.7	[837]									< 6.7
322	$K^+ \overline{K}^0$	1.31±0.17	1.61±0.44±0.09	[398]	1.11±0.19±0.05	[808]					1.52±0.21±0.05	[838]	1.32±0.14
323	$\overline{K}^0 K^+ \pi^0$	< 24					< 24	[829]					< 24
324	$K^+ K_S K_S$	10.8±0.6	10.6±0.5±0.3	[271]	13.4±1.9±1.5	[826]							10.8±0.6
325	$f_0(980) K^+$ $(K^+ K_S K_S)$	14.7±3.3	14.7±2.8±1.8	[271]									14.7±3.3
326	$f_0(1710) K^+$ $(K^+ K_S K_S)$	$0.48^{+0.40}_{-0.26}$	$0.48^{+0.40}_{-0.24}$±0.11	[271]									$0.48^{+0.41}_{-0.26}$
327	$K^+ K_S K_S$ (NR)	20±4	19.8±3.7±2.5	[271]									19.8±4.5
328	$K_S K_S \pi^+$	< 0.51	< 0.51	[839]	< 3.2	[826]							< 0.51
329	$K^+ K^- \pi^+$	5.0±0.7	5.0±0.5±0.5	[840]	< 13	[826]							5.0±0.7
330	$K^+ K^- \pi^+$ (NR)	< 75					< 75	[828]					< 75
331	$\overline{K}^{*0} K^+$ $(K^+ K^- \pi^+)$	< 1.1	< 1.1	[841]									< 1.1
332	$\overline{K}_0^*(1430)^0 K^+$ $(K^+ K^- \pi^+)$	< 2.2	< 2.2	[841]									< 2.2
333	$K^+ K^+ \pi^-$	< 0.16	< 0.16	[825]	< 2.4	[826]					< 0.011	[827]	< 0.011
334	$K^+ K^+ \pi^-$ (NR)	< 87.9											< 87.9
335	$f_2'(1525) K^+$	1.8±0.5	1.8±0.5 ‡	[271]	< 8	[272]							1.8±0.5
336	$f_J(2220) K^+$	< 1.2			< 1.2	[842]							< 1.2
337	$K^{*+} \pi^+ K^-$	< 11.8	< 11.8	[831]									< 11.8
338	$K^{*+} \overline{K}^{*0}$	1.2±0.5	1.2±0.5±0.1	[843]	< 1.31	[844]							1.2±0.5
339	$K^{*+} K^+ \pi^-$	< 6.1	< 6.1	[831]									< 6.1
340	$K^+ K^- K^+$	34.0±1.4	34.6±0.6±0.9	[271]	30.6±1.2±2.3	[272]							34.0±1.0
341	ϕK^+ $(K^+ K^- K^+)$	$8.8^{+0.7}_{-0.6}$	$9.2 \pm 0.4^{+0.7}_{-0.5}$	[271]	$9.6 \pm 0.9^{+1.1}_{-0.8}$	[272]	$5.5^{+2.1}_{-1.8} \pm 0.6$	[845]	7.6±1.3±0.6	[846]			8.8±0.5
342	$f_0(980) K^+$ $(K^+ K^- K^+)$	9.4±3.2	$9.4^{+1.6}_{-2.8}$	[271]									$9.4^{+1.6}_{-2.8}$
343	$a_2(1320) K^+$ $(K^+ K^- K^+)$ †	< 1.1			< 1.1	[272]							< 1.1
344	$X_0(1550) K^+$ $(K^+ K^- K^+)$	4.3±0.7	4.3±0.60±0.30	[847]									4.30±0.67
345	$\phi(1680) K^+$ $(K^+ K^- K^+)$ †	< 0.8			< 0.8	[272]							< 0.8
346	$f_0(1710) K^+$ $(K^+ K^- K^+)$ †	1.1±0.6	1.12±0.25±0.50	[271]									1.12±0.56

Table 219 continued

RPP#	MODE	PDG2014 AVG.	BaBar		BELLE		CLEO		CDF	LHCB	OURAVG.
347	$K^+K^-K^+$ (NR)	$23.8^{+2.8}_{-5.0}$	22.8±2.7±7.6	[271]	$24.0\pm1.5^{+2.6}_{-6.0}$	[272]					$23.8^{+2.9}_{-5.1}$
348	$K^{*+}K^+K^-$	36±5	36.2±3.3±3.6	[831]							36.2±4.9
349	ϕK^{*+}	10.0±2.0	11.2±1.0±0.9	[848]	$6.7^{+2.1+0.7}_{-1.9-1.0}$	[849]	$10.6^{+6.4+1.8}_{-4.9-1.6}$	[845]			10.0±1.1
350	$\phi(K\pi)^{*+}_0$	8.3±1.6	$8.3^{+1.4}_{-0.8}$	[850]							$8.3^{+1.4}_{-0.8}$
351	$\phi K_1(1270)^+$	6.1±1.9	6.1±1.6±1.1	[850]							6.1±1.9
352	$\phi K_1(1400)^+$	< 3.2	< 3.2	[850]							< 3.2
353	$\phi K^*(1410)^+$	< 4.3	< 4.3	[850]							< 4.3
354	$\phi K^*_0(1430)^+$	7.0±1.6	7.0±1.3±0.9	[850]							7.0±1.6
355	$\phi K^*_2(1430)^+$	8.4±2.1	8.4±1.8±1.0	[850]							8.4±2.1
356	$\phi K_2(1770)^+$	< 15	< 15	[850]							< 15
357	$\phi K_2(1820)^+$	< 16.3	< 16.3	[850]							< 16.3
358	$a_1^+K^{*0}$	< 3.6	< 3.6	[851]							< 3.6
359	$\phi\phi K^+$ §	5.0±1.2	5.6±0.5±0.3	[852]	$2.6^{+1.1}_{-0.9}\pm0.3$	[842]					5.0±0.5
360	$\eta'\eta' K^+$	< 25	< 25	[853]							< 25
361	$K^+\omega\phi$	< 1.9			< 1.9	[854]					< 1.9
362	$K^+X(1812)$ †	< 0.32			< 0.32	[854]					< 0.32

Results for CDF and LHCb are relative BFs converted to absolute BFs.
CLEO upper limits that have been greatly superseded are not shown.
† In this product of BFs, all daughter BFs not shown are set to 100%.
‡ Average of results in $K^0_SK^+K^-$, $K^0_SK^0_SK^+$ [271].
§ $M_{\phi\phi} < 2.85$ GeV/c^2.
¶ Result from ARGUS. Cited in the BaBar column to avoid adding a column to the table.

Table 220 Branching fractions of charmless mesonic B^+ decays without kaons in units of $\times 10^{-6}$. Upper limits are at 90% CL. Where values are shown in red (blue), this indicates that they are new published (preliminary) results since PDG2014

RPP#	Mode	PDG2014 Avg.	BABAR		Belle		CLEO		CDF	LHCb		Our Avg.
379	$\pi^+\pi^0$	5.5±0.4	5.02±0.46±0.29	[810]	5.86±0.26±0.38	[808]	$4.6^{+1.8+0.6}_{-1.6-0.7}$	[809]				$5.48^{+0.35}_{-0.34}$
380	$\pi^+\pi^+\pi^-$	15.2±1.4	15.2±0.6±1.3	[855]								15.2±1.4
381	$\rho^0\pi^+$	8.3±1.2	$8.1\pm0.7^{+1.3}_{-1.6}$	[855]	$8.0^{+2.3}_{-2.0}\pm0.7$	[856]	$10.4^{+3.3}_{-3.4}\pm2.1$	[821]				$8.3^{+1.2}_{-1.3}$
382	$f_0(980)\pi^{+\,\dagger}$	< 1.5	< 1.5	[855]								< 1.5
383	$f_2(1270)\pi^+$	$1.6^{+0.7}_{-0.4}$	$1.57\pm0.42^{+0.55}_{-0.25}$	[855]								$1.57^{+0.69}_{-0.49}$
384	$\rho(1450)^0\pi^{+\,\dagger}$	$1.4^{+0.6}_{-0.9}$	$1.4\pm0.4^{+0.5}_{-0.8}$	[855]								$1.4^{+0.6}_{-0.9}$
385	$f_0(1370)\pi^{+\,\dagger}$	< 4.0	< 4.0	[855]								< 4.0
387	$\pi^+\pi^-\pi^+(NR)$	$5.3^{+1.5}_{-1.1}$	$5.3\pm0.7^{+1.3}_{-0.8}$	[855]								$5.3^{+1.5}_{-1.1}$
388	$\pi^+\pi^0\pi^0$	< 890	< 890 ‡	[857]								< 890 ‡
389	$\rho^+\pi^0$	10.9±1.4	10.2±1.4±0.9	[858]	$13.2\pm2.3^{+1.4}_{-1.9}$	[859]					$10.9^{+1.4}_{-1.5}$	
391	$\rho^+\rho^0$	24.0±1.9	23.7±1.4±1.4	[421]	$31.7\pm7.1^{+3.8}_{-6.7}$	[860]						$24.0^{+1.9}_{-2.0}$
392	$f_0(980)\rho^{+\,\dagger}$	< 2.0	< 2.0	[421]								< 2.0
393	$a_1^+\pi^0$	26±7	26.4±5.4±4.1	[861]								26.4±6.8
394	$a_1^0\pi^+$	20±6	20.4±4.7±3.4	[861]								20.4±5.8
395	$\omega\pi^+$	6.9±0.5	6.7±0.5±0.4	[820]	6.9±0.6±0.5	[862]	$11.3^{+3.3}_{-2.9}\pm1.4$	[821]				6.9±0.5
396	$\omega\rho^+$	15.9±2.1	15.9±1.6±1.4	[822]								15.9±2.1
397	$\eta\pi^+$	4.02±0.27	4.00±0.40±0.24	[811]	4.07±0.26±0.21	[815]	$1.2^{+2.8}_{-1.2}$	[816]				4.02±0.27
398	$\eta\rho^+$	7.0±2.9	9.9±1.2±0.8	[863]	$4.1^{+1.4}_{-1.3}\pm0.4$	[818]	$4.8^{+5.2}_{-3.8}$	[816]				6.9±1.0
399	$\eta'\pi^+$	2.7±0.9	3.5±0.6±0.2	[811]	$1.8^{+0.7}_{-0.6}\pm0.1$	[812]	$1.0^{+5.8}_{-1.0}$	[816]				$2.7^{+0.5}_{-0.4}$
400	$\eta'\rho^+$	9.7±2.2	$9.7^{+1.9}_{-1.8}\pm1.1$	[813]	< 5.8	[814]						$9.7^{+2.2}_{-2.1}$
401	$\phi\pi^+$	< 0.15	< 0.24	[864]	< 0.33	[865]				< 0.15	[866]	< 0.15
402	$\phi\rho^+$	< 3.0	< 3.0	[867]								< 3.0
403	$a_0(980)^0\pi^{+\,\dagger}$	< 5.8	< 5.8	[823]								< 5.8
404	$a_0(980)^+\pi^{0\,\dagger}$	< 1.4	< 1.4	[868]								< 1.4
405	$\pi^+\pi^+\pi^+\pi^-\pi^-$	< 860	< 860 ‡	[857]								< 860 ‡
406	$\rho^0 a_1(1260)^+$	< 620					< 620	[869]				< 620
407	$\rho^0 a_2(1320)^+$	< 720					< 720	[869]				< 720
408	$b_1^0\pi^{+\,\dagger}$	6.7±2.0	6.7±1.7±1.0	[836]								6.7±2.0
409	$b_1^+\pi^{0\,\dagger}$	< 3.3	< 3.3	[834]								< 3.3

Table 220 continued

RPP#	Mode	PDG2014 Avg.	BABAR	Belle	CLEO	CDF	LHCb	Our Avg.
410	$\pi^+\pi^+\pi^+\pi^-\pi^-\pi^0$	< 6300	< 6300 ‡	[857]				< 6300 ‡
411	$b_1^+\rho^0$ †	< 5.2	< 5.2	[837]			< 5.2	
413	$b_1^0\rho^+$ †	< 3.3	< 3.3	[837]			< 3.3	

Results for LHCb are relative BFs converted to absolute BFs.
CLEO upper limits that have been greatly superseded are not shown.
† In this product of BFs, all daughter BFs not shown are set to 100%.
‡ Result from ARGUS. Cited in the BABAR column to avoid adding a column to the table.

Tables 221, 222, 223 and 224 for B^0 mesons. The tables are separated according to the presence or absence of kaons in the final state. Finally, Table 225 details several relative branching fractions of B^0 decays.

Figure 176 gives a graphic representation of a selection of high-precision branching fractions given in this section. Footnote symbols indicate that the footnote in the corresponding table should be consulted.

7.2 Baryonic decays of B^+ and B^0 mesons

This section provides branching fractions of charmless baryonic decays of B^+ and B^0 mesons in Tables 226 and 227, respectively. Relative branching fractions are given in Table 228.

Figures 177 and 178 show graphic representations of a selection of results given in this section. Footnote symbols indicate that the footnote in the corresponding table should be consulted.

7.3 Decays of b baryons

A compilation of branching fractions of Λ_b^0 baryon decays is given in Table 229. Table 230 provides the partial branching fractions of $\Lambda_b^0 \to \Lambda\mu^+\mu^-$ decays. A compilation of branching fractions of Ξ_b^0 baryon decays is given in Table 231.

Figure 179 shows a graphic representation of branching fractions of Λ_b^0 decays. Footnote symbols indicate that the footnote in the corresponding table should be consulted.

List of other measurements that are not included in the tables:

- In Ref. [928], LHCb provides a measurement of the differential $\Lambda_b^0 \to \Lambda\mu^+\mu^-$ branching fraction. It is given in bins of $m^2(\mu^+\mu^-)$ that are different from those used in the past by the LHCb and CDF collaborations (see table of differential branching fractions).
- In the paper [929], LHCb measures the ratios

$$\frac{\sigma(pp \to \Xi_b'^- X)\mathcal{B}(\Xi_b'^- \to \Xi_b^0\pi^-)}{\sigma(pp \to \Xi_b^0 X)},$$
$$\frac{\sigma(pp \to \Xi_b'^- X)\mathcal{B}(\Xi_b^{*-} \to \Xi_b^0\pi^-)}{\sigma(pp \to \Xi_b'^- X)\mathcal{B}(\Xi_b'^- \to \Xi_b^0\pi^-)}.$$

- In the paper [930], LHCb measures the ratio

$$\frac{\sigma(pp \to \Xi_b^{*-} X)\mathcal{B}(\Xi_b^{*-} \to \Xi_b^0\pi^-)}{\sigma(pp \to \Xi_b^0 X)}.$$

Table 221 Branching fractions of charmless mesonic B^0 decays with kaons (part 1) in units of $\times 10^{-6}$. Upper limits are at 90% CL. Where values are shown in red (blue), this indicates that they are new published (preliminary) results since PDG2014

RPP#	Mode	PDG2014 Avg.	BABAR		Belle		CLEO		CDF	LHCb	Our Avg.
227	$K^+\pi^-$	19.6 ± 0.5	$19.1 \pm 0.6 \pm 0.6$	[870]	$20.0 \pm 0.34 \pm 0.60$	[808]	$18.0^{+2.3+1.2}_{-2.1-0.9}$	[809]			$19.57^{+0.53}_{-0.52}$
228	$K^0\pi^0$	9.9 ± 0.5	$10.1 \pm 0.6 \pm 0.4$	[416]	$9.68 \pm 0.46 \pm 0.50$	[808]	$12.8^{+4.0+1.7}_{-3.3-1.4}$	[809]			9.93 ± 0.49
229	$\eta' K^0$	66 ± 4	$68.5 \pm 2.2 \pm 3.1$	[811]	$58.9^{+3.6}_{-3.5} \pm 4.3$	[812]	$89^{+18}_{-16} \pm 9$	[816]			66.1 ± 3.1
230	$\eta' K^{*0}$	3.1 ± 0.9	$3.1^{+0.9}_{-0.8} \pm 0.3$	[813]	$2.6 \pm 0.7 \pm 0.2$	[871]	$7.8^{+7.7}_{-5.7}$	[816]			$2.8^{+0.6}_{-0.5}$
231	$\eta' K_0^*(1430)^0$	6.3 ± 1.6	$6.3 \pm 1.3 \pm 0.9$	[813]							6.3 ± 1.6
232	$\eta' K_2^*(1430)^0$	13.7 ± 3.2	$13.7^{+3.0}_{-1.9} \pm 1.2$	[813]							$13.7^{+3.2}_{-2.2}$
233	ηK^0	$1.23^{+0.27}_{-0.24}$	$1.15^{+0.43}_{-0.38} \pm 0.09$	[811]	$1.27^{+0.33}_{-0.29} \pm 0.08$	[815]	$0.0^{+3.0}_{-0.0}$	[816]			$1.23^{+0.27}_{-0.24}$
234	ηK^{*0}	15.9 ± 1.0	$16.5 \pm 1.1 \pm 0.8$	[817]	$15.2 \pm 1.2 \pm 1.0$	[818]	$13.8^{+5.5}_{-4.6} \pm 1.6$	[816]			15.9 ± 1.0
235	$\eta K_0^*(1430)^0$	11.0 ± 2.2	$11.0 \pm 1.6 \pm 1.5$	[817]							11.0 ± 2.2
236	$\eta K_2^*(1430)^0$	9.6 ± 2.1	$9.6 \pm 1.8 \pm 1.1$	[817]							9.6 ± 2.1
237	ωK^0	5.0 ± 0.6	$5.4 \pm 0.8 \pm 0.3$	[820]	$4.5 \pm 0.4 \pm 0.3$	[389]	$10.0^{+5.4}_{-4.2} \pm 1.4$	[821]			4.8 ± 0.4
238	$a_0(980)^0 K^0$ †	< 7.8	< 7.8	[823]							< 7.8
239	$b_1^0 K^0$ †	< 7.8	< 7.8	[834]							< 7.8
240	$a_0(980)^- K^+$ †	< 1.9	< 1.9	[872]							< 1.9
241	$b_1^- K^+$ †	7.4 ± 1.4	$7.4 \pm 1.0 \pm 1.0$	[836]							7.4 ± 1.4
242	$b_1^0 K^{*0}$ †	< 8.0	< 8.0	[837]							< 8.0
243	$b_1^- K^{*+}$ †	< 5.0	< 5.0	[837]							< 5.0
244	$a_0(1450)^- K^+$ †	< 3.1	< 3.1	[872]							< 3.1
245	$K_S X^0$(Familon) †	< 53					< 53	[873]			< 53
246	ωK^{*0}	2.0 ± 0.5	$2.2 \pm 0.6 \pm 0.2$	[822]	$1.8 \pm 0.7^{+0.3}_{-0.2}$	[874]					2.0 ± 0.5
247	ωK^{*0}	18.4 ± 2.5	$18.4^{+1.8}_{-1.7}$	[822]							$18.4^{+1.8}_{-1.7}$
248	$\omega K_0^*(1430)^0$	16.0 ± 3.4	$16.0 \pm 1.6 \pm 3.0$	[822]							16.0 ± 3.4
249	$\omega K_2^*(1430)^0$	10.1 ± 2.3	$10.1 \pm 2.0 \pm 1.1$	[822]							10.1 ± 2.3
250	$\omega K^+\pi^-$ (NR) [1]	5.1 ± 1.0			$5.1 \pm 0.7 \pm 0.7$	[874]					5.1 ± 1.0
251	$K^+\pi^-\pi^0$	37.8 ± 3.2	$38.5 \pm 1.0 \pm 3.9$	[875]	$36.6^{+4.2}_{-4.3} \pm 3.0$	[876]					37.8 ± 3.2
252	$\rho^- K^+$	7.0 ± 0.9	$6.6 \pm 0.5 \pm 0.8$	[875]	$15.1^{+3.4+2.4}_{-3.3-2.6}$	[876]					7.0 ± 0.9
253	$\rho(1450)^- K^+$	2.4 ± 1.2	$2.4 \pm 1.0 \pm 0.6$	[875]							2.4 ± 1.2
254	$\rho(1700)^- K^+$	0.6 ± 0.7	$0.6 \pm 0.6 \pm 0.4$	[875]							0.6 ± 0.7
255	$K^+\pi^-\pi^0$ (NR)	2.8 ± 0.6	$2.8 \pm 0.5 \pm 0.4$	[875]	< 9.4	[876]					2.8 ± 0.6
256	$(K\pi)_0^{*+}\pi^-$	34 ± 5	$34.2 \pm 2.4 \pm 4.1$	[875]							34.2 ± 4.8
257	$(K\pi)_0^{*+}\pi^0$	8.5 ± 1.7	$8.6^{+1.1}_{-1.3}$	[875]							$8.6^{+1.1}_{-1.3}$
258	$K_2^*(1430)^0\pi^0$	< 4.0	< 4.0	[877]							< 4.0

Table 221 continued

RPP#	Mode	PDG2014 Avg.	BaBar		Belle		CLEO		CDF	LHCb		Our Avg.
259	$K^*(1680)^0\pi^0$	< 7.5	< 7.5	[877]							< 7.5	
260	$K_x^{*0}\pi^0$ [2]	6.1 ± 1.6			$6.1^{+1.6+0.5}_{-1.5-0.6}$	[876]					$6.1^{+1.7}_{-1.6}$	
261	$K^0\pi^+\pi^-$	65 ± 8	$50.2 \pm 1.5 \pm 1.8$	[274]	$47.5 \pm 2.4 \pm 3.7$	[878]	$50^{+10}_{-9} \pm 7$	[829]		$65.2^{+6.0}_{-5.1}$ ‡	[879]	51.8 ± 1.9
262	$K^0\pi^+\pi^-$ (NR)	$14.7^{+4.0}_{-2.6}$	$11.1^{+2.5}_{-1.0} \pm 0.9$	[274]	$19.9 \pm 2.5^{+1.7}_{-2.0}$	[878]					14.7 ± 2.0	
263	$\rho^0 K^0$	4.7 ± 0.6	$4.4 \pm 0.7 \pm 0.3$	[274]	$6.1 \pm 1.0^{+1.1}_{-1.2}$	[878]					4.7 ± 0.7	
264	$K^{*+}\pi^-$	8.4 ± 0.8	8.2 ± 0.9 [3]	[274, 875]	$8.4 \pm 1.1^{+1.0}_{-0.9}$	[878]	$16^{+6}_{-5} \pm 2$	[829]			8.4 ± 0.8	
265	$K_0^*(1430)^+\pi^-$	33 ± 7	$29.9^{+2.3}_{-1.7} \pm 3.6$	[274]	$49.7 \pm 3.8^{+6.8}_{-8.2}$	[878]					$33.5^{+3.9}_{-3.8}$	
266	$K_x^{*+}\pi^-$ [2]	5.1 ± 1.6			$5.1^{+1.5+0.6}_{-1.5-0.7}$	[876]					$5.1^{+1.6}_{-1.7}$	
267	$K^*(1410)^+\pi^-$ †	< 3.8			< 3.8	[878]					< 3.8	
268	$f_0(980)K^0$ †	7.0 ± 0.9	$6.9 \pm 0.8 \pm 0.6$	[274]	$7.6 \pm 1.7^{+0.9}_{-1.3}$	[878]					7.0 ± 0.9	
269	$f_2(1270)^0 K^0$	$2.7^{+1.3}_{-1.2}$	$2.7^{+1.0}_{-0.8} \pm 0.9$	[274]	< 2.5 †	[878]					$2.7^{+1.3}_{-1.2}$	
270	$f_x(1300)^0 K^0$	1.8 ± 0.7	$1.81^{+0.55}_{-0.45} \pm 0.48$	[274]							$1.81^{+0.73}_{-0.66}$	

Results for LHCb are relative BFs converted to absolute BFs.
CLEO upper limits that have been greatly superseded are not shown.
† In this product of BFs, all daughter BFs not shown are set to 100%.
‡ Obtained from a fit to the ratios of BFs measured by LHCb (Ref. [879]) and to the averages of the BFs in their numerators, as measured by other experiments (RPP 292 and 298).
[1] $0.755 < M(K\pi) < 1.250$ GeV/c^2. [2] K_x^{*0} stands for the possible candidates for $K^*(1410), K_0^*(1430), K_2^*(1430)$.
[3] Average of BaBar results from $B^0 \to K^+\pi^-\pi^0$ [875] and $B^0 \to K^0\pi^+\pi^-$ [274].

Table 222 Branching fractions of charmless mesonic B^0 decays with kaons (part 2) in units of $\times 10^{-6}$. Upper limits are at 90% CL. Where values are shown in red (blue), this indicates that they are new published (preliminary) results since PDG2014

RPP#	Mode	PDG2014 Avg.	BaBar		Belle		CLEO		CDF		LHCb		Our Avg.
271	$K^{*0}\pi^0$	3.3 ± 0.6	$3.3 \pm 0.5 \pm 0.4$	[875]	< 3.5	[876]							3.3 ± 0.6
272	$K_2^*(1430)^+\pi^-$	< 6	< 16.2	[877]	< 6.3	[878]							< 6.3
273	$K^*(1680)^+\pi^-$	< 10	< 25	[877]	< 10.1	[878]							< 10.1
275	$\rho^0 K^+\pi^-$	2.8 ± 0.7			$2.8 \pm 0.5 \pm 0.5$ [2]	[880]							2.8 ± 0.7
276	$f_0(980)K^+\pi^-$	$1.4^{+0.5}_{-0.6}$			$1.4 \pm 0.4^{+0.3}_{-0.4}$ [2]	[880]							$1.4^{+0.5}_{-0.6}$
277	$K^+\pi^-\pi^+\pi^-$	< 2.1			< 2.1	[880]							< 2.1
278	$K^{*0}\pi^+\pi^-$	55 ± 5	$54.5 \pm 2.9 \pm 4.3$	[881]									54.5 ± 5.2
279	$K^{*0}\rho^0$	3.9 ± 1.3	$5.1 \pm 0.6^{+0.6}_{-0.8}$	[882]	$2.1^{+0.8+0.9}_{-0.7-0.5}$	[880]							3.9 ± 0.8
280	$f_0(980)K^{*0}$ †	$3.9^{+2.1}_{-1.8}$	$5.7 \pm 0.6 \pm 0.4$	[882]	$1.4^{+0.6+0.6}_{-0.5-0.4}$	[880]							3.9 ± 0.5
281	$K_1(1270)^+\pi^-$	< 30	17^{+6}_{-25}	[415]									17^{+6}_{-25}
282	$K_1(1400)^+\pi^-$	< 27	16^{+8}_{-24}	[415]									16^{+8}_{-24}
283	$a_1^- K^+$	16 ± 4	$16.3 \pm 2.9 \pm 2.3$	[833]									16.3 ± 3.7
284	$K^{*+}\rho^-$	10.3 ± 0.26	$10.3 \pm 2.3 \pm 1.3$	[882]									10.3 ± 2.6
285	$K_0(1430)^+\rho^-$	28 ± 12	$28 \pm 10 \pm 6$	[882]									28 ± 11
287	$K_0^*(1430)^0\rho^0$	27 ± 6	$27 \pm 4 \pm 4$	[882]									27 ± 5
288	$K_0^*(1430)^0 f_0(980)$	2.7 ± 0.9	$2.7 \pm 0.7 \pm 0.6$	[882]									2.7 ± 0.9
289	$K_2^*(1430)^0 f_0(980)$	8.6 ± 2.0	$8.6 \pm 1.7 \pm 1.0$	[882]									8.6 ± 2.0
290	K^+K^-	0.13 ± 0.05	< 0.5	[870]	$0.10 \pm 0.08 \pm 0.04$	[808]			$0.23 \pm 0.10 \pm 0.10$	[883]	$0.0780 \pm 0.0127 \pm 0.0084$	[884]	0.0803 ± 0.0147
291	$K^0\overline{K}^0$	1.21 ± 0.16	$1.08 \pm 0.28 \pm 0.11$	[398]	$1.26 \pm 0.19 \pm 0.05$	[808]							1.21 ± 0.16
292	$K^0K^-\pi^+$	7.3 ± 1.1	$6.4 \pm 1.0 \pm 0.6$	[885]	< 18	[826]					6.64 ± 0.99 [1]	[879]	6.54 ± 0.75
293	$K^{*0}\overline{K}^0$ ‡	< 1.9	< 1.9	[886]							< 0.96	[887]	< 0.96
	$K^{*\mp}K^\pm$										< 0.4	[888]	< 0.4
294	$K^+K^-\pi^0$	2.2 ± 0.6			$2.17 \pm 0.60 \pm 0.24$	[889]							2.17 ± 0.65
295	$K_SK_S\pi^0$	< 0.9	< 0.9	[890]									< 0.9
296	$K_SK_S\eta$	< 1.0	< 1.0	[890]									< 1.0
297	$K_SK_S\eta'$	< 2.0	< 2.0	[890]									< 2.0
298	$K^+K^-K^0$	26.3 ± 1.5	$26.5 \pm 0.9 \pm 0.8$	[271]	$28.3 \pm 3.3 \pm 4.0$	[826]					19.1 ± 1.9 [1]	[879]	24.5 ± 1.0
299	ϕK^0	7.3 ± 0.7	$7.1 \pm 0.6^{+0.4}_{-0.3}$	[271]	$9.0^{+2.2}_{-1.8} \pm 0.7$	[849]	$5.4^{+3.7}_{-2.7} \pm 0.7$	[845]					$7.3^{+0.7}_{-0.6}$
300	$f_0(980)K^0$ †	$7.0^{+3.5}_{-3.0}$	$7.0^{+2.6}_{-1.8} \pm 2.4$	[271]									$7.0^{+3.5}_{-3.0}$
301	$f_0(1500)K^0$ †	13^{+7}_{-5}	$13.3^{+5.8}_{-4.4} \pm 3.2$	[271]									$13.3^{+6.6}_{-5.4}$

Table 222 continued

RPP#	Mode	PDG2014 Avg.	BaBar		Belle		CLEO		CDF	LHCb	Our Avg.
302	$f_2'(1525)K^0$	$0.3^{+0.5}_{-0.4}$	$0.29^{+0.27}_{-0.18}\pm0.36$	[271]							$0.29^{+0.45}_{-0.40}$
303	$f_0(1710)K^0$ †	4.4 ± 0.9	$4.4\pm0.7\pm0.5$	[271]							4.4 ± 0.9
304	$K^0K^+K^-$ (NR)	33 ± 10	$33\pm5\pm9$	[271]							33 ± 10
305	$K_SK_SK_S$	$6.2^{+1.2}_{-1.1}$	$6.19\pm0.48\pm0.19$	[387]	$4.2^{+1.6}_{-1.3}\pm0.8$	[826]					6.04 ± 0.50
306	$f_0(980)K_S$ †	2.7 ± 1.8	$2.7^{+1.3}_{-1.2}\pm1.3$ †	[387]							2.7 ± 1.8
307	$f_0(1710)K_S$ †	$0.50^{+0.050}_{-0.026}$	$0.50^{+0.46}_{-0.24}\pm0.11$ †	[387]							$0.50^{+0.47}_{-0.26}$
308	$f_0(2010)K_S$ †	0.5 ± 0.6	$0.54^{+0.21}_{-0.20}\pm0.52$ †	[387]							0.54 ± 0.56
309	$K_SK_SK_S(NR)$	13.3 ± 3.1	$13.3^{+2.2}_{-2.3}\pm2.2$	[387]							$13.3^{+3.1}_{-3.2}$
310	$K_SK_SK_L$	<16	<16 [2]	[891]							<16 [2]
311	$K^{*0}K^+K^-$	27.5 ± 2.6	$27.5\pm1.3\pm2.2$	[881]							27.5 ± 2.6
312	ϕK^{*0}	10.0 ± 0.5	$9.7\pm0.5\pm0.6$	[391]	$10.4\pm0.5\pm0.6$	[892]	$11.5^{+4.5+1.8}_{-3.7-1.7}$	[845]			$10.1^{+0.6}_{-0.5}$
313	$K^+\pi^-\pi^+K^-$	<72			<72 [3]	[893]					<72 [3]
314	$K^{*0}\pi^+K^-$	4.5 ± 1.3	$4.6\pm1.1\pm0.8$	[881]	<13.9 [3]	[893]					4.6 ± 1.4
315	$K^{*0}\overline{K}^{*0}$	0.8 ± 0.5	$1.28^{+0.35}_{-0.30}\pm0.11$	[894]	$0.26^{+0.33+0.10}_{-0.29-0.08}$	[893]					0.81 ± 0.23
316	$K^+\pi^-K^+\pi^-(NR)$	<6.0			<6.0 [3]	[893]					<6.0 [3]
317	$K^{*0}K^+\pi^-$	<2.2	<2.2	[881]	<7.6 [3]	[893]					<2.2
318	$K^{*0}K^{*0}$	<0.2	<0.41	[894]	<0.2	[893]					<0.2
319	$K^{*+}K^{*-}$	<2.0	<2.0	[895]							<2.0
320	$K_1^*(1400)^0\phi$	<5000	<5000 [5]	[835]							<5000 [5]
321	$(K\pi)_0^{*0}\phi$	4.3 ± 0.4	$4.3\pm0.4\pm0.4$	[391]	$4.3\pm0.4\pm0.4$	[892]					4.3 ± 0.4
322	$(K\pi)_0^{*0}\phi$ [4]	<1.7	<1.7	[896]							<1.7
323	$K_0^*(1430)^0\pi^+K^-$	<31.8			<31.8 [3]	[893]					<31.8 [3]
324	$K_0^*(1430)^0\overline{K}^{*0}$	<3.3			<3.3	[893]					<3.3

Results for CDF and LHCb are relative BFs converted to absolute BFs.
CLEO upper limits that have been greatly superseded are not shown.
† In this product of BFs, all daughter BFs not shown are set to 100%. ‡ Includes two distinct decay processes: $\mathcal{B}(B^0\to f)+\mathcal{B}(B^0\to\overline{f})$.
[1] Obtained from a fit to the ratios of BFs measured by LHCb (Ref. [879]) and to the averages of the BFs therein, as measured by other experiments (excluding the present line).
[2] $0.75<M(K\pi)<1.20$ GeV/c^2. [3] $0.70<M(K\pi)<1.70$ GeV/c^2. [4] $1.60<M(K\pi)<2.15$ GeV/c^2.
[5] Result from ARGUS. Cited in the BaBar column to avoid adding a column to the table.

Table 223 Branching fractions of charmless mesonic B^0 decays with kaons (part 3) in units of $\times 10^{-6}$. Upper limits are at 90% CL. Where values are shown in red (blue), this indicates that they are new published (preliminary) results since PDG2014

RPP#	Mode	PDG2014 Avg.	BABAR		Belle		CLEO	CDF	LHCb	Our Avg.
325	$K_0^*(1430)^0\overline{K}_0^*(1430)^0$	< 8.4			< 8.4	[893]				< 8.4
326	$\phi K_0^*(1430)^0$	3.9 ± 0.8	$3.9 \pm 0.5 \pm 0.6$	[391]	$4.3 \pm 0.4 \pm 0.4$	[892]				4.2 ± 0.5
327	$K_0^*(1430)^0 K^{*0}$	< 1.7			< 1.7	[893]				< 1.7
328	$K_0^*(1430)^0 K_0^*(1430)^0$	< 4.7			< 4.7	[893]				< 4.7
329	$\phi K^*(1680)^0$	< 3.5	< 3.5	[896]						< 3.5
330	$\phi K_3^*(1780)^0$	< 2.7	< 2.7	[896]						< 2.7
331	$\phi K_4^*(2045)^0$	< 15.3	< 15.3	[896]						< 15.3
332	$\rho^0 K_2^*(1430)^0$	< 1100	< 1100 ‡	[835]						< 1100 ‡
333	$\phi K_2^*(1430)^0$	6.8 ± 0.9	$7.5 \pm 0.9 \pm 0.5$	[391]	$5.5^{+0.9}_{-0.7} \pm 1.0$	[892]				6.8 ± 0.8
334	$\phi\phi K^0$ †	4.5 ± 0.9	$4.5 \pm 0.8 \pm 0.3$	[852]						4.5 ± 0.9
335	$\eta'\eta' K^0$	< 31	< 31	[853]						< 31

† $M_{\phi\phi} < 2.85$ GeV/c^2.
‡ Result from ARGUS. Cited in the BABAR column to avoid adding a column to the table.

Table 224 Branching fractions of charmless mesonic B^0 decays without kaons in units of $\times 10^{-6}$. Upper limits are at 90% CL. Where values are shown in red (blue), this indicates that they are new published (preliminary) results since PDG2014

RPP#	Mode	PDG2014 Avg.	BABAR		Belle		CLEO		CDF		LHCb		Our Avg.
356	$\pi^+\pi^-$	5.15 ± 0.19	$5.5 \pm 0.4 \pm 0.3$	[870]	$5.04 \pm 0.21 \pm 0.18$	[808]	$4.5^{+1.4+0.5}_{-1.2-0.4}$	[809]	$5.02 \pm 0.33 \pm 0.35$ ‡	[897]	$5.08 \pm 0.17 \pm 0.37$	[898]	5.10 ± 0.19
357	$\pi^0\pi^0$	1.91 ± 0.22	$1.83 \pm 0.21 \pm 0.13$	[416]	$2.3^{+0.4+0.2}_{-0.5-0.3}$	[899]							$1.91^{+0.22}_{-0.23}$
358	$\eta\pi^0$	< 1.5	< 1.5	[863]	$4.1^{+1.7+0.5}_{-1.5-0.7}$	[900]	< 2.9	[816]					$4.1^{+1.8}_{-1.7}$
359	$\eta\eta$	< 1.0	< 1.0	[811]	$0.76^{+0.27+0.14}_{-0.23-0.16}$	[901]							$0.76^{+0.30}_{-0.28}$
360	$\eta'\pi^0$	1.2 ± 0.6	$0.9 \pm 0.4 \pm 0.1$	[863]	$2.8 \pm 1.0 \pm 0.3$	[812]	$0.0^{+1.8}_{-0.0}$	[816]					1.2 ± 0.4
361	$\eta'\eta'$	< 1.7	< 1.7	[811]	< 6.5	[814]							< 1.7
362	$\eta'\eta$	< 1.2	< 1.2	[863]	< 4.5	[814]							< 1.2
363	$\eta'\rho^0$	< 1.3	< 2.8	[813]	< 1.3	[814]							< 1.3
364	$f_0(980)\eta'$ †	< 0.9	< 0.9	[813]									< 0.9
365	$\eta\rho^0$	< 1.5	< 1.5	[872]	< 1.9	[818]							< 1.5
366	$f_0(980)\eta$ †	< 0.4	< 0.4	[872]									< 0.4
367	$\omega\eta$	$0.94^{+0.40}_{-0.31}$	$0.94^{+0.35}_{-0.30} \pm 0.09$	[811]									$0.94^{+0.36}_{-0.31}$
368	$\omega\eta'$	$1.0^{+0.5}_{-0.4}$	$1.01^{+0.46}_{-0.38} \pm 0.09$	[811]	< 2.2	[814]							$1.01^{+0.47}_{-0.39}$
369	$\omega\rho^0$	< 1.6	< 1.6	[822]									< 1.6
370	$f_0(980)\omega$ †	< 1.5	< 1.5	[822]									< 1.5
371	$\omega\omega$	1.2 ± 0.4	$1.2 \pm 0.3^{+0.3}_{-0.2}$	[902]									1.2 ± 0.4
372	$\phi\pi^0$	< 0.15	< 0.28	[864]	< 0.15	[865]							< 0.15
373	$\phi\eta$	< 0.5	< 0.5	[811]									< 0.5
374	$\phi\eta'$	< 0.5	< 1.1	[811]	< 0.5	[814]							< 0.5
375	$\phi\rho^0$	< 0.33	< 0.33	[867]									< 0.33
376	$f_0(980)\phi$ †	< 0.38	< 0.38	[867]									< 0.38
377	$\omega\phi$	< 0.7	< 0.7	[902]									< 0.7
378	$\phi\phi$	< 0.2	< 0.2	[867]							< 0.028	[903]	< 0.028
379	$a_0^{\mp}(980)\pi^{\pm}$ †	< 3.1	< 3.1	[872]									< 3.1
379	$a_0^{\mp}(1450)\pi^{\pm}$	< 2.3	< 2.3	[872]									< 2.3
380	$a_0^{\mp}(1450)\pi^{\pm}$ †	< 2.3	< 2.3	[872]									< 2.3
382	$\rho^0\pi^0$	2.0 ± 0.5	$1.4 \pm 0.6 \pm 0.3$	[904]	$3.0 \pm 0.5 \pm 0.7$	[284]	$1.6^{+2.0}_{-1.4} \pm 0.8$	[821]					2.0 ± 0.5
383	$\rho^{\mp}\pi^{\pm}$	23.0 ± 2.3	$22.6 \pm 1.8 \pm 2.2$	[288]	$22.6 \pm 1.1 \pm 4.4$	[284]	$27.6^{+8.4}_{-7.4} \pm 4.2$	[821]					23.0 ± 2.3
384	$\pi^+\pi^-\pi^+\pi^-$	< 19.3	< 23.1	[411]	< 11.2	[412]							< 11.2
385	$\rho^0\pi^+\pi^-(NR)$	< 8.8	< 8.8	[411]	< 12	[412]							< 8.8
386	$\rho^0\rho^0$	0.73 ± 0.28	$0.92 \pm 0.32 \pm 0.14$	[411]	$1.02 \pm 0.30 \pm 0.15$	[412]					$0.94 \pm 0.17 \pm 0.11$ ‡	[413]	0.95 ± 0.16
387	$f_0(980)\pi^+\pi^-(NR)$ †	< 3.8			< 3.0	[412]							< 3.0

Table 224 continued

RPP#	Mode	PDG2014 Avg.	BABAR		Belle		CLEO	CDF	LHCb		Our Avg.
388	$f_0(980)\rho^0$ †	< 0.3	< 0.40	[411]	$0.78 \pm 0.22 \pm 0.11$	[412]					0.78 ± 0.25
389	$f_0(980)\, f_0(980)$ †	< 0.1	< 0.19	[411]	< 0.2	[412]					< 0.19
391	$a_1^{\mp}\pi^{\pm}$	26 ± 5	$33.2 \pm 3.8 \pm 3.0$	[905]	$22.2 \pm 2.0 \pm 2.8$	[418]					25.9 ± 2.8
392	$a_2^{\mp}\pi^{\pm}$	< 6.3			< 6.3	[418]					< 6.3
393	$\pi^+\pi^-\pi^0\pi^0$	< 3100	< 3100 ¶	[857]							< 3100 ¶
394	$\rho^+\rho^-$	24.2 ± 3.1	$25.5 \pm 2.1^{+3.6}_{-3.9}$	[409]	$22.8 \pm 3.8^{+2.3}_{-2.6}$	[906]					$24.2^{+3.1}_{-3.2}$
395	$a_1(1260)^0\pi^0$	< 1100	< 1100 ¶	[857]							< 1100 ¶
396	$\omega\pi^0$	< 0.5	< 0.5	[863]	< 2.0	[862]					< 0.5
397	$\pi + \pi^+\pi^-\pi^-\pi^0$	< 9000	< 9000 ¶	[857]							< 9000 ¶
398	$a_1^{\pm}\rho^{\mp}$	< 61	< 61	[907]							< 61
399	$a_1^{\pm}\rho^0$	< 600	< 6000 ¶	[857]							< 6000 ¶
400	$b_1^{\mp}\pi^{\pm}$ †	10.9 ± 1.5	$10.9 \pm 1.2 \pm 0.9$	[836]							10.9 ± 1.5
401	$b_1^0\pi^0$ †	< 1.9	< 1.9	[834]							< 1.9
402	$b_1^{\pm}\rho^{\mp}$ †	< 1.4	< 1.4	[837]							< 1.4
403	$b_1^0\rho^0$ †	< 3.4	< 3.4	[837]							< 3.4
404	$\pi^+\pi^+\pi^+\pi^-\pi^-\pi^-$	< 3000	< 3000 ¶	[857]							< 3000 ¶
405	$a_1^{\pm}a_1^{\mp}$	11.8 ± 2.6	11.8 ± 2.6	[908]							11.8 ± 2.6
406	$\pi + \pi^+\pi^+\pi^-\pi^-\pi^-\pi^0$	< 11000	< 11000 ¶	[857]							< 11000 ¶
	$\phi\pi^+\pi^-$								$0.182 \pm 0.048 \pm 0.014$ §	[909]	0.182 ± 0.050

Results for CDF and LHCb are relative BFs converted to absolute BFs.
CLEO upper limits that have been greatly superseded are not shown.
† In this product of BFs, all daughter BFs not shown are set to 100%.
‡ Result given as $0.94 \pm 0.17 \pm 0.09 \pm 0.06$ where last error is from $\mathcal{B}(B^0 \to \phi K^{*0})$.
§ In the mass range $400 < m(\pi^+\pi^-) < 1600$ GeV/c^2.
¶ Result from ARGUS. Cited in the BABAR column to avoid adding a column to the table.

Table 225 Relative branching fractions of charmless mesonic B^0 decays. Upper limits are at 90% CL. Where values are shown in red (blue), this indicates that they are new published (preliminary) results since PDG2014

RPP#	Mode	PDG2014 Avg.	CDF		LHCb		Our Avg.
273	$\mathcal{B}(B^0 \to K^+K^-)/\mathcal{B}(B^0 \to K^+\pi^-)$		$0.012 \pm 0.005 \pm 0.005$	[883]	$0.00398 \pm 0.00065 \pm 0.00042$	[884]	0.00416 ± 0.00099
356	$\mathcal{B}(B^0 \to \pi^+\pi^-)/\mathcal{B}(B^0 \to K^+\pi^-)$	0.261 ± 0.010	$0.259 \pm 0.017 \pm 0.016$	[897]	$0.262 \pm 0.009 \pm 0.017$	[898]	0.261 ± 0.015
	$\mathcal{B}(B^0 \to K^{*\mp}K^{\pm})/\mathcal{B}(B^0 \to K^{*+}\pi^-)$				< 0.05	[888]	< 0.05
	$\mathcal{B}(B^0 \to K_S^0 K^{*0})/\mathcal{B}(B^0 \to K_S^0\pi^+\pi^-)$ †				< 0.020	[887]	< 0.020

† Numerator includes two distinct decay processes: $\mathcal{B}(B^0 \to f) + \mathcal{B}(B^0 \to \overline{f})$.

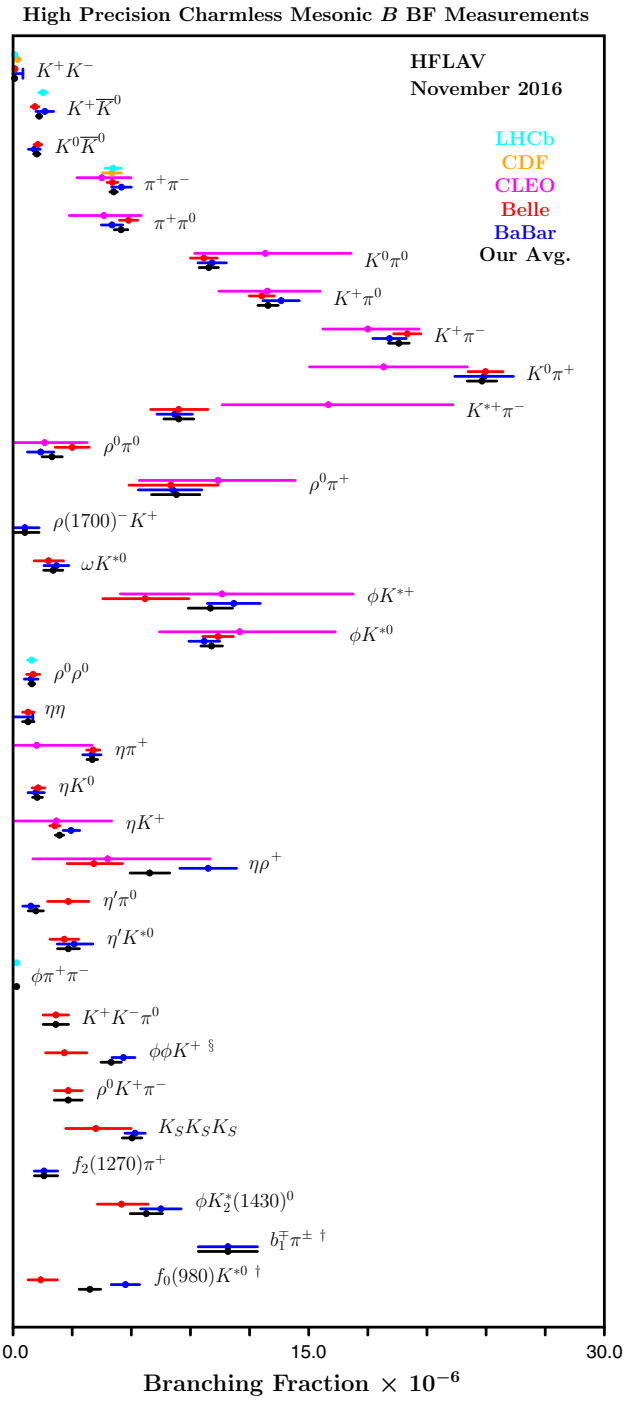

Fig. 176 Selection of high-precision charmless mesonic B meson branching fraction measurements

7.4 Decays of B_s^0 mesons

Tables 232 and 233 detail branching fractions and relative branching fractions of B_s^0 meson decays, respectively.

Figures 180 and 181 show graphic representations of a selection of results given in this section. Footnote symbols

indicate that the footnote in the corresponding table should be consulted.

List of other measurements that are not included in the tables:

- $B_s^0 \to \phi\mu^+\mu^-$: LHCb measures the differential BF in bins of $m^2(\mu^+\mu^-)$. It also performs an angular analysis and measures F_L, S_3, S_4, S_7, A_5, A_6, A_8 and A_9 in bins of $m^2(\mu^+\mu^-)$ [948].
- $B_s^0 \to \phi\gamma$: LHCb has measured the photon polarization [407].

7.5 Radiative and leptonic decays of B^0 and B^+ mesons.

This section reports different observables for leptonic and radiative B^0 and B^+ meson decays, including processes in which the photon yields a pair of charged or neutral leptons. Tables 234 and 235 provide compilations of branching fractions of B^+mesons to radiative, and lepton-flavor/number-violating final states, respectively. Tables 236 and 237 provide compilations of branching fractions of B^0 mesons, and $B^\pm/B^0$ meson admixture, respectively. Table 238 contains branching fractions of leptonic and radiative-leptonic B^+ and B^0 decays. It is followed by Tables 239 and 240, which give relative branching fractions of B^+ decays and a compilations of inclusive decays, respectively. Table 241 contains isospin asymmetry measurements.

Figures 182, 183, 184, 185, 186 and 187 show graphic representations of a selection of results given in this section. Footnote symbols indicate that the footnote in the corresponding table should be consulted.

List of other measurements that are not included in the tables:

- $B^+ \to K^+\pi^-\pi^+\gamma$: LHCb has measured the up-down asymmetries in bins of the $K\pi\pi\gamma$ mass [1022].
- In Ref. [1023], LHCb has also measured the branching fraction of $B^+ \to K^+e^-e^+$ in the $m^2(\ell\ell)$ bin $[1, 6]$ GeV$^2/c^4$.
- In the $B^+ \to \pi^+\mu^+\mu^-$ paper [966], LHCb has also measured the differential branching fraction in bins of $m^2(\ell\ell)$.
- For $B \to K\ell^-\ell^+$, LHCb has measured F_H and $A_{\rm FB}$ in 17 (5) bins of $m^2(\ell\ell)$ for the K^+ (K_S^0) final state [1024]. Belle has measured F_L and $A_{\rm FB}$ in 6 $m^2(\ell\ell)$ bins [1025].
- For the $B \to K^*\ell^-\ell^+$ analyses, partial branching fractions and angular observables in bins of $m^2(\ell\ell)$ are also available:
  - $B^0 \to K^{*0}e^-e^+$: LHCb has measured F_L, $A_T^{(2)}$, $A_T^{\rm Im}$, $A_T^{\rm Re}$ in the $[0.002, 1.120]$GeV$^2/c^4$ bin of $m^2(\ell\ell)$ [1026], and has also determined the branching fraction in the dilepton mass region $[10, 1000]$MeV$/c^2$ [1023].
  - $B \to K^*\ell^-\ell^+$: Belle has measured F_L, $A_{\rm FB}$, isospin asymmetry in 6 $m^2(\ell\ell)$ bins [970] and P_4', P_5', P_6', P_8' in 4 $m^2(\ell\ell)$ bins [1025]. BaBar has measured F_L, $A_{\rm FB}$, P_2 in 5 $m^2(\ell\ell)$ bins [1027].
  - $B^0 \to K^{*0}\mu^-\mu^+$: LHCb has measured F_L, $A_{\rm FB}$, $S_3 - S_9$, $A_3 - A_9$, $P_1 - P_3$, $P_4' - P_8'$ in 8 $m^2(\ell\ell)$ bins [1028]. CMS has measured F_L and $A_{\rm FB}$ in 7 $m^2(\ell\ell)$ bins [1029].
- For $B \to X_s\ell^-\ell^+$ (X_s is a hadronic system with an s quark), Belle has measured $A_{\rm FB}$ in bins of $m^2(\ell\ell)$ with a sum of 10 exclusive final states [1030].
- $B^0 \to K^+\pi^-\mu^+\mu^-$, with $1330 < m(K^+\pi^-) < 1530$ GeV$/c^2$: LHCb has measured the partial branching fraction in bins of $m^2(\mu^-\mu^+)$ in the range $[0.1, 8.0]$ GeV$^2/c^4$, and has also determined angular moments [1031].

7.6 Charge asymmetries in b-hadron decays

This section contains, in Tables 242, 243, 244, 245, 246 247, compilations of CP asymmetries in decays of various b-hadrons: B^+, B^0 mesons, $B^\pm/B^0$ admixtures, B_s^0 mesons and finally Λ_b^0 baryons. Measurements of time-dependent CP asymmetries are not listed here but are discussed in Sect. 4.

Figure 188 shows a graphic representation of a selection of results given in this section. Footnote symbols indicate that the footnote in the corresponding table should be consulted.

List of other measurements that are not included in the tables:

- In the paper [1044], LHCb has measured the triple-product asymmetries for the decays $\Lambda_b^0 \to p\pi^-\pi^+\pi^-$ and $\Lambda_b^0 \to p\pi^-K^+K^-$.

7.7 Polarization measurements in b-hadron decays

In this section, compilations of polarization measurements in b-hadron decays are given. Tables 248 (249) details measurements of the longitudinal fraction, f_L, in B^+ (B^0) decays, and Tables 250 (251) the results of the full angular analyses of B^+ (B^0) $\to \phi K^*$ decays. Table 252 gives results of the full angular analysis of $B^0 \to \phi K_2^{*0}(1430)$ decays. Tables 253, 254 and 255 detail quantities of B_s^0 decays: f_L measurements, and observables from full angular analyses of decays to $\phi\phi$ and $\phi\overline{K}^{*0}$.

Figures 189 and 190 show graphic representations of a selection of results shown in this section. Footnote symbols indicate that the footnote in the corresponding table should be consulted (Table 256).

7.8 Decays of B_c^+ mesons

Table 257 details branching fractions of B_c^+ meson decays to charmless hadronic final states.

Table 226 Branching fractions of charmless baryonic B^+ decays in units of $\times 10^{-6}$. Upper limits are at 90% CL. Where values are shown in red (blue), this indicates that they are new published (preliminary) results since PDG2014

RPP#	Mode	PDG2014 Avg.	BABAR		Belle		LHCb		Our Avg.
417	$p\overline{p}\pi^+$	1.62±0.20	1.69±0.29±0.26 †	[666]	$1.60^{+0.22}_{-0.19}\pm0.12$	[910]			$1.62^{+0.21}_{-0.20}$
417	$p\overline{p}\pi^+$ §						1.07±0.11±0.11	[911]	1.07±0.16
420	$p\overline{p}K^+$	5.9±0.5	6.7±0.5±0.4 †	[740]	$5.54^{+0.27}_{-0.25}\pm0.36$	[910]	4.46±0.21±0.27 ¶	[747]	5.14±0.25
421	$\Theta^{++}\overline{p}$ [1]	< 0.091	< 0.09	[740]	< 0.091	[912]			< 0.09
422	$f_J(2221)K^+$ [2]	< 0.41			< 0.41	[912]			< 0.41
423	$p\overline{\Lambda}(1520)$	< 1.5	< 1.5	[740]			0.315±0.048±0.027	[911]	0.315±0.055
425	$p\overline{p}K^{*+}$	$3.6^{+0.8}_{-0.7}$	5.3±1.5±1.3 †	[666]	$3.38^{+0.73}_{-0.60}\pm0.39$ ‡	[913]			$3.64^{+0.79}_{-0.70}$
426	$f_J(2221)K^{*+}$ [2]	< 0.77	< 0.77	[666]					< 0.77
427	$p\overline{\Lambda}$	< 0.32			< 0.32	[914]			< 0.32
429	$p\overline{\Lambda}\pi^0$	$3.00^{+0.7}_{-0.6}$			$3.00^{+0.61}_{-0.53}\pm0.33$	[915]			$3.00^{+0.69}_{-0.62}$
430	$p\overline{\Sigma}(1385)^0$	< 0.47			< 0.47	[915]			< 0.47
431	$\Delta^+\overline{\Lambda}$	< 0.82			< 0.82	[915]			< 0.82
433	$p\overline{\Lambda}\pi^+\pi^-$ (NR)	5.9±1.1			$5.92^{+0.88}_{-0.84}\pm0.69$	[916]			$5.92^{+1.12}_{-1.09}$
434	$p\overline{\Lambda}\rho^0$	4.8±0.9			$4.78^{+0.67}_{-0.64}\pm0.60$	[916]			$4.78^{+0.90}_{-0.88}$
435	$p\overline{\Lambda}f_2(1270)$	2.0±0.8			$2.03^{+0.77}_{-0.72}\pm0.27$	[916]			$2.03^{+0.82}_{-0.77}$
436	$\Lambda\overline{\Lambda}\pi^+$	< 0.94			< 0.94 §	[627]			< 0.94 §
437	$\Lambda\overline{\Lambda}K^+$	3.4±0.6			$3.38^{+0.41}_{-0.36}\pm0.41$ ‡	[627]			$3.38^{+0.58}_{-0.55}$
438	$\Lambda\overline{\Lambda}K^{*+}$	$2.2^{+1.2}_{-0.9}$			$2.19^{+1.13}_{-0.88}\pm0.33$ §	[627]			$2.19^{+1.18}_{-0.94}$
439	$\overline{\Delta}^0 p$	< 1.38			< 1.38 §	[910]			< 1.38 §
440	$\Delta^{++}\overline{p}$	< 0.14			< 0.14 §	[910]			< 0.14 §

Results for LHCb are relative BFs converted to absolute BFs.
† Charmonium decays to $p\overline{p}$ have been statistically subtracted.
‡ The charmonium mass region has been vetoed.
§ Di-baryon mass is less than 2.85 GeV/c^2.
¶ Includes contribution where $p\overline{p}$ is produced in charmonia decays.
[1] $\Theta(1540)^{++} \to K^+p$ (pentaquark candidate).
[2] In this product of BFs, all daughter BFs not shown are set to 100%.

Table 227 Branching fractions of charmless baryonic B^0 decays in units of $\times 10^{-6}$. Upper limits are at 90% CL. Where values are shown in red (blue), this indicates that they are new published (preliminary) results since PDG2014

RPP#	Mode	PDG2014 Avg.	BaBar		Belle		LHCb		Our Avg.
407	$p\overline{p}$	$0.015^{+0.007}_{-0.005}$	< 0.27	[917]	< 0.11	[914]	$0.0147^{+0.0062+0.0035}_{-0.0051-0.0014}$	[918]	$0.0150^{+0.0070}_{-0.0050}$
409	$p\overline{p}K^0$	2.66 ± 0.32	$3.0\pm0.5\pm0.3$ †	[666]	$2.51^{+0.35}_{-0.29}\pm0.21$ ‡	[913]			$2.66^{+0.34}_{-0.32}$
410	$\Theta^+\overline{p}$ §	< 0.05	< 0.05	[666]	< 0.23	[912]			< 0.05
411	$f_J(2221)K^0$ ¶	< 0.45	< 0.45	[666]					< 0.45
412	$p\overline{p}K^{*0}$	$1.24^{+0.28}_{-0.25}$	$1.47\pm0.45\pm0.40$ †	[666]	$1.18^{+0.29}_{-0.25}\pm0.11$ ‡	[913]			$1.24^{+0.28}_{-0.25}$
413	$f_J(2221)K^{*0}$ ¶	< 0.15	< 0.15	[666]					< 0.15
414	$p\overline{\Lambda}\pi^-$	3.14 ± 0.29	$3.07\pm0.31\pm0.23$	[919]	$3.23^{+0.33}_{-0.29}\pm0.29$	[915]			$3.14^{+0.29}_{-0.28}$
415	$p\overline{\Sigma}(1385)^-$	< 0.26			< 0.26	[915]			< 0.26
416	$\Delta^0\overline{\Lambda}$	< 0.93			< 0.93	[915]			< 0.93
417	$p\overline{\Lambda}K^-$	< 0.82			< 0.82	[920]			< 0.82
418	$p\overline{\Sigma}^0\pi^-$	< 3.8			< 3.8	[920]			< 3.8
419	$\overline{\Lambda}\Lambda$	< 0.32			< 0.32	[914]			< 0.32
420	$\overline{\Lambda}\Lambda K^0$	$4.8^{+1.0}_{-0.9}$			$4.76^{+0.84}_{-0.68}\pm0.61$ ‡	[627]			$4.76^{+1.04}_{-0.91}$
421	$\Lambda\overline{\Lambda}K^{*0}$	$2.5^{+0.9}_{-0.8}$			$2.46^{+0.87}_{-0.72}\pm0.34$ ‡	[627]			$2.46^{+0.93}_{-0.80}$

Results for LHCb are relative BFs converted to absolute BFs.
† Charmonium decays to $p\overline{p}$ have been statistically subtracted.
‡ The charmonium mass region has been vetoed.
§ $\Theta(1540)^+ \to pK^0$ (pentaquark candidate).
¶ In this product of BFs, all daughter BFs not shown are set to 100%.

Table 228 Relative branching fractions of charmless baryonic B decays. Where values are shown in red (blue), this indicates that they are new published (preliminary) results since PDG2014

RPP#	Mode	PDG2014 Avg.	LHCb		Our Avg.
417	$\mathcal{B}(B^+ \to p\bar{p}\pi^+, m_{p\bar{p}} < 2.85\ \mathrm{GeV}/c^2)/\mathcal{B}(B^+ \to J/\psi(\to p\bar{p})\pi^+)$		12.0±1.2±0.3	[911]	12.0±1.2
420	$\mathcal{B}(B^+ \to p\bar{p}K^+)/\mathcal{B}(B^+ \to J/\psi(\to p\bar{p})K^+)$		4.91±0.19±0.14 †	[747]	4.91±0.24
420	$\mathcal{B}(B^+ \to p\bar{p}K^+)/\mathcal{B}(B^+ \to J/\psi K^+)$	0.0104±0.0005±0.0001	0.0104±0.0005±0.0001 †‡	[747]	0.0104±0.0005
423	$\mathcal{B}(B^+ \to \bar{\Lambda}(1520)(\to K^+\bar{p})p)/\mathcal{B}(B^+ \to J/\psi(\to p\bar{p})\pi^+)$		0.033±0.005±0.007	[911]	0.033±0.009

† Includes contribution where $p\bar{p}$ is produced in charmonia decays.
‡ Original experimental relative BF multiplied by the best values (PDG2014) of certain reference BFs. The first error is experimental, and the second is from the reference BFs.

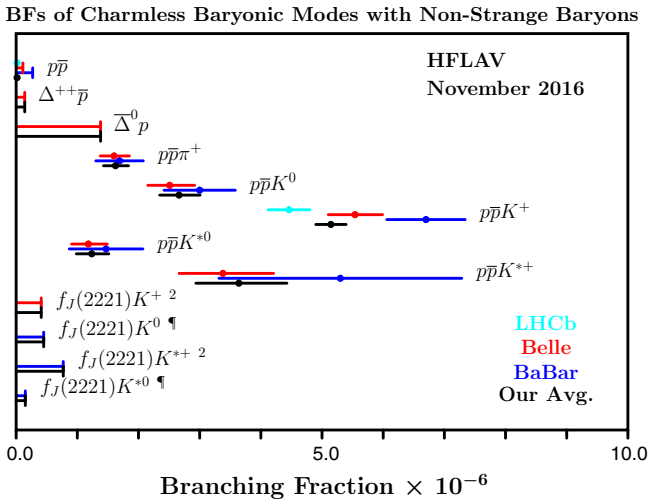

Fig. 177 Branching fractions of charmless baryonic modes with non-strange baryons

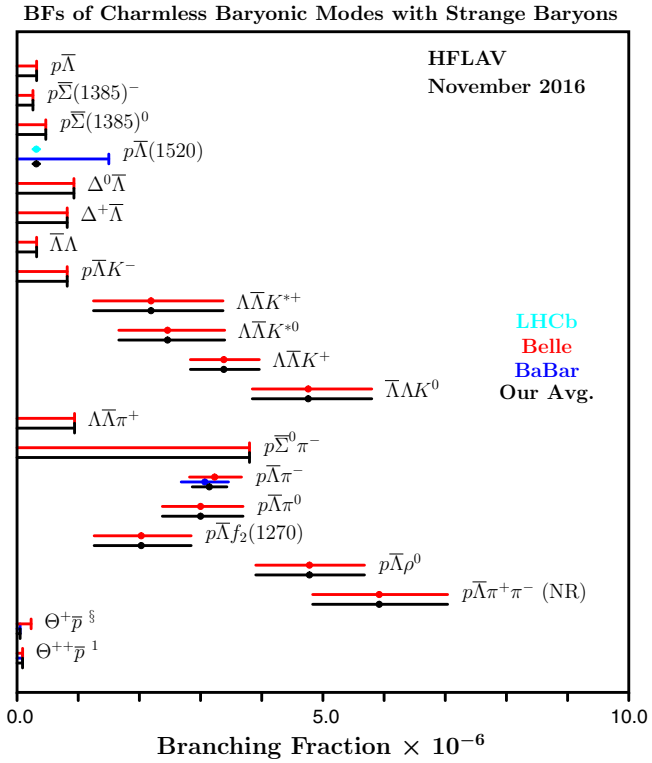

Fig. 178 Branching fractions of charmless baryonic modes with strange baryons

Table 229 Branching fractions of charmless Λ_b^0 decays in units of $\times 10^{-6}$. Upper limits are at 90% CL. Where values are shown in red (blue), this indicates that they are new published (preliminary) results since PDG2014

RPP#	Mode	PDG2014 Avg.	CDF		LHCb		Our Avg.
19	$p\pi^-$	3.5±0.8±0.6	3.5±0.8±0.6	[921]			3.5±1.0
20	pK^-	5.5±1.0±1.0	5.5±1.0±1.0	[921]			5.5±1.4
21	$\Lambda\mu^+\mu^-$	1.73±0.42±0.55	1.73±0.42±0.55	[922]	0.96±0.16±0.25	[923]	1.08±0.27
	$\Lambda\eta$				$9.3^{+7.3}_{-5.3}$ ¶	[924]	$9.3^{+7.3}_{-5.3}$
	$\Lambda\eta'$				< 3.1	[924]	< 3.1
	$\Lambda\phi$				$5.18\pm1.04\pm0.35^{+0.67}_{-0.62}$ ‡	[925]	$5.18^{+1.29}_{-1.26}$
	$\bar{K}^0 p\pi^-$				1.26±0.19±0.09±0.34±0.05 §	[926]	1.26±0.40
	$K^0 pK^-$				< 3.5	[926]	< 3.5
	$\Lambda\pi^+\pi^-$				4.6±1.2±1.4±0.6 †	[927]	4.6±1.9
	$\Lambda K^+\pi^-$				5.6±0.8±0.8±0.7 †	[927]	5.6±1.3
	ΛK^+K^-				15.9±1.2±1.2±2.0 †	[927]	15.9±2.6

Results for CDF and LHCb are relative BFs converted to absolute BFs.
† Last quoted uncertainty is due to the precision with which the normalization channel branching fraction is known.
‡ Third uncertainty is related to external inputs.
§ Third uncertainty is from the ratio of fragmentation fractions $f_{\Lambda_b^0}/f_d$, and the fourth is due to the uncertainty on $\mathcal{B}(B^0 \to K^0\pi^+\pi^-)$.
¶ Result at 68% CL.

Table 230 Partial branching fractions of $\Lambda_b^0 \to \mu^+\mu^-$ decays in intervals of $q^2 = m^2(\mu^+\mu^-)$ in units of $\times 10^{-6}$. Where values are shown in red (blue), this indicates that they are new published (preliminary) results since PDG2014

RPP#	Mode	q^2 [GeV$^2/c^4$] †	PDG2014 Avg.	CDF		LHCb		Our Avg.
21	$\Lambda\mu^+\mu^-$ ‡	< 2.0	0.15±2.01±0.05	0.15±2.01±0.05	[922]	0.56±0.76±0.80	[923]	0.41±0.87
	$\Lambda\mu^+\mu^-$	[2.0, 4.3]	1.8±1.7±0.6	1.8±1.7±0.6		0.71±0.60±0.10		0.91±0.55
	$\Lambda\mu^+\mu^-$	[4.3, 8.68]	−0.2±1.6±0.1	−0.2±1.6±0.1		0.66±0.72±0.16		0.40±0.62
	$\Lambda\mu^+\mu^-$	[10.09, 12.86]	3.0±1.5±1.0	3.0±1.5±1.0		1.55±0.58±0.55		1.96±0.68
	$\Lambda\mu^+\mu^-$	[14.18, 16.00]	1.0±0.7±0.3	1.0±0.7±0.3		1.44±0.44±0.42		1.19±0.40
	$\Lambda\mu^+\mu^-$	> 16.00	7.0±1.9±2.2	7.0±1.9±2.2		4.7±0.8±1.2		5.5±1.2

Results for CDF and LHCb are relative BFs converted to absolute BFs.
† See the original paper for the exact $m^2(\mu^+\mu^-)$ selection.
‡ The LHCb measurement was superseded with a more accurate result in different $m^2(\mu^+\mu^-)$ bins (see list of not-included results).

Table 231 Branching fractions of charmless Ξ_b^0 decays in units of $\times 10^{-6}$. Upper limits are at 90% CL. Where values are shown in red (blue), this indicates that they are new published (preliminary) results since PDG2014

RPP#	Mode	PDG2014 Avg.	LHCb		Our Avg.
	$\Lambda\pi^+\pi^-$		< 1.7	[927]	< 1.7
	$\Lambda K^+\pi^-$		< 0.8	[927]	< 0.8
	ΛK^+K^-		< 0.3	[927]	< 0.3
	$\bar{K}^0 p\pi^-$		< 1.6	[926]	< 1.6
	$\bar{K}^0 pK^-$		< 1.1	[926]	< 1.1

Results for LHCb are relative BFs converted to absolute BFs

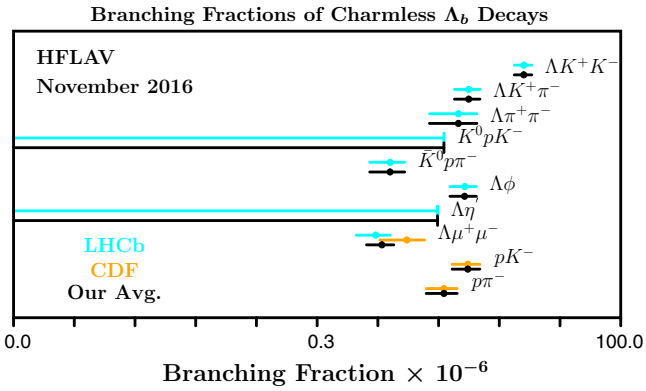

Fig. 179 Branching fractions of charmless Λ_b^0 decays

Table 232 Branching fractions of charmless B_s^0 decays in units of $\times 10^{-6}$. Upper limits are at 90% CL. Where values are shown in red (blue), this indicates that they are new published (preliminary) results since PDG2014

RPP#	Mode	PDG2014 Avg.	Belle		CDF		D0		LHCb		CMS		ATLAS		Our Avg.
45	$\pi^+\pi^-$	0.76±0.19	< 12	[931]	0.60±0.17±0.04 ‡	[883]			0.691±0.083±0.044 ‡	[884]					0.671±0.083
51	$\phi\phi$	19.1±3.1			19.1±2.6±1.6 †	[932]			18.4±0.5±1.8 §	[933]					18.6±1.6
52	π^+K^-	5.5±0.6	< 26	[931]	5.3±0.9±0.3 †	[921]			5.6±0.6±0.3 †	[898]					5.5±0.5
53	K^+K^-	24.9±1.7	$38^{+10}_{-9}\pm7$	[931]	25.9±2.2±1.7 †	[897]			23.7±1.6±1.5 †	[898]					24.8±1.7
54	$K^0\overline{K}^0$	< 66	$19.6^{+5.8}_{-5.1}\pm1.0\pm2.0$	‡[934]											$19.6^{+6.2}_{-5.6}$
55	$K^0\pi^+\pi^-$	19±5							19±5±2 †	[879]					19±5
56	$K^0K^-\pi^+$ ¶	97±17							97±12±12 †	[879]					97±16
57	$K^0K^+K^-$	< 4							< 4 †	[879]					< 4 †
	$K^{*\pm}K^{\mp}$								12.7±1.9±1.9	[888]					12.7±2.7
	$K^{*-}\pi^+$								3.3±1.1±0.5	[888]					3.3±1.2
59	$K^{*0}\overline{K}^{*0}$	28.1±4.6±5.6							10.8±1.4±1.5 §	[935]					10.8±2.1
60	$\phi\overline{K}^{*0}$	1.13±0.3							1.13±0.29±0.06 †	[936]					1.13±0.30
61	$p\overline{p}$	$0.028^{+0.022}_{-0.017}$							$0.0284^{+0.0203+0.0085}_{-0.0168-0.0018}$	[918]					$0.0280^{+0.0220}_{-0.0170}$
63	$\gamma\gamma$	< 8.7	< 3.1	[937]											< 3.1
64	$\phi\gamma$	36±4	36±5±7	[937]					35.1±3.5±1.2 †	[938]					35.2±3.4
65	$\mu^+\mu^-$	0.0031±0.0007			$0.013^{+0.009}_{-0.007}$	[939]	< 0.012	[940]	$0.0029^{+0.0011+0.0003}_{-0.0010-0.0001}$	[941]	$0.0030^{+0.0010}_{-0.0009}$	[942]	< 0.003 [1]	[943]	$0.0029^{+0.0007}_{-0.0006}$ [3]
66	e^+e^-	< 0.28			< 0.28	[944]									< 0.28
67	$e^\pm\mu^\mp$	< 0.011			< 0.20	[944]			< 0.011	[945]					< 0.011
68	$\mu^+\mu^-\mu^+\mu^-$	< 0.012							< 0.012	[946]					< 0.012
70	$\phi\mu^+\mu^-$	0.76±0.15					< 3.2	[947]	$0.797^{+0.045}_{-0.043}\pm0.068$	[948]					$0.797^{+0.082}_{-0.080}$
	$\eta'\eta'$								33.1±7.0±1.2 †	[949]					33.1±7.1
	$\pi^+\pi^-\mu^+\mu^-$								0.086±0.015±0.010 [2]	[933]					0.086±0.018
	$K^0\overline{K}^{*0}$ ¶								16.4±3.4±2.3	[887]					16.4±4.1
	$\phi\pi^+\pi^-$								3.48±0.29±0.35 [4]	[909]					3.48±0.46
	$\phi f_0(980)$, $f_0(980) \to \pi^+\pi^-$								1.12±0.18±0.11	[909]					1.12±0.21
	$\phi f_2(1270)$, $f_2(1270) \to \pi^+\pi^-$								$0.61^{+0.18}_{-0.14}\pm0.06$	[909]					$0.61^{+0.19}_{-0.15}$
	$\phi\rho^0(770)$								0.27±0.07±0.02	[909]					0.27±0.07

Results for CDF, D0, LHCb, CMS and ATLAS are relative BFs converted to absolute BFs.

† The first error is experimental, and the second is from the reference BF.

‡ Last error represents the uncertainty due to the total number of $B_s^0\overline{B}_s^0$ pairs.

§ Last error takes into account $\mathcal{B}(B^0 \to \phi K^{*0})$ and f_d/f_s.

¶ Includes two distinct decay processes: $\mathcal{B}(B_s^0 \to f) + \mathcal{B}(B_s^0 \to \overline{f})$.

[1] UL at 95% CL.

[2] Muon pairs do not originate from resonances and $0.5 < m(\pi^+\pi^-) < 1.3$ GeV/c^2.

[3] The average is done between the combined LHCb and CMS result, $0.0028^{+0.0007}_{-0.0006}$ (Ref. [950]) and CDF.

[4] In the mass range $400 < m(\pi^+\pi^-) < 1600$ GeV/c^2.

Table 233 Relative branching fractions of charmless B_s^0 decays. Upper limits are at 90% CL. Where values are shown in red (blue), this indicates that they are new published (preliminary) results since PDG2014

RPP#	Mode	PDG2014 Avg.	CDF		LHCb		Our Avg.
45	$f_s\mathcal{B}(B_s^0 \to \pi^+\pi^-)/f_d\mathcal{B}(B^0 \to K^+\pi^-)$		0.008±0.002±0.001	[883]	0.00915±0.00071±0.00083	[884]	0.00880±0.00090
45	$f_s\mathcal{B}(B_s^0 \to \pi^+\pi^-)/f_d\mathcal{B}(B^0 \to \pi^+\pi^-)$				$0.050^{+0.011}_{-0.009}\pm0.004$	[898]	$0.050^{+0.012}_{-0.010}$
51	$\mathcal{B}(B_s^0 \to \phi\phi)/\mathcal{B}(B_s^0 \to J/\psi\phi)$		0.0178±0.0014±0.0020	[932]			0.0180±0.0020
	$\mathcal{B}(B_s^0 \to \phi\phi)/\mathcal{B}(B^0 \to \phi K^*)$				1.84±0.05±0.13	[933]	1.84±0.14
52	$f_s\mathcal{B}(B_s^0 \to K^+\pi^-)/f_d\mathcal{B}(B_d^0 \to K^+\pi^-)$		0.071±0.010±0.007	[921]	0.074±0.006±0.006	[898]	0.073±0.007
53	$f_s\mathcal{B}(B_s^0 \to K^+K^-)/f_d\mathcal{B}(B_d^0 \to K^+\pi^-)$		0.347±0.020±0.021	[897]	0.316±0.009±0.019	[898]	0.327±0.017
55	$\mathcal{B}(B_s^0 \to K^0\pi^+\pi^-)/\mathcal{B}(B^0 \to K^0\pi^+\pi^-)$				0.29±0.06±0.04	[879]	0.29±0.07
56	$\mathcal{B}(B_s^0 \to K^0K^-\pi^+)/\mathcal{B}(B^0 \to K^0K^-\pi^+)$ †				1.48±0.12±0.14	[879]	1.48±0.18
57	$\mathcal{B}(B_s^0 \to K^0K^+K^-)/\mathcal{B}(B^0 \to K^0K^+K^-)$				< 0.068	[879]	< 0.068
	$\mathcal{B}(B_s^0 \to K^{*-}K^+)/\mathcal{B}(B^0 \to K^{*+}\pi^-)$				1.49±0.22±0.18	[888]	1.49±0.28
	$\mathcal{B}(B_s^0 \to K^{*-}\pi^+)/\mathcal{B}(B^0 \to K^{*+}\pi^-)$				0.39±0.13±0.05	[888]	0.39±0.14
59	$\mathcal{B}(B_s^0 \to K^{*0}\overline{K}^{*0})/\mathcal{B}(B^0 \to K^{*+}\pi^-)$				1.11±0.22±0.13	[935]	1.11±0.26
60	$\mathcal{B}(B_s^0 \to \phi\overline{K}^{*0})/\mathcal{B}(B^0 \to \phi K^{*0})$				0.113±0.024±0.016	[946]	0.113±0.029
64	$\mathcal{B}(B_s^0 \to \phi\gamma)/\mathcal{B}(B^0 \to K^{*0}\gamma)$				0.81±0.04±0.07	[938]	0.81±0.08
70	$\mathcal{B}(B_s^0 \to \phi\mu^+\mu^-)/\mathcal{B}(B_s^0 \to J/\psi\phi) \times 10^4$	7.1±1.3			$7.41^{+0.42}_{-0.40}\pm0.29$	[948]	$7.41^{+0.51}_{-0.49}$
	$\mathcal{B}(B_s^0 \to K_S^0K^{*0})/\mathcal{B}(B^0 \to K_S^0\pi^+\pi^-)$ †				0.33±0.07±0.04	[887]	0.33±0.08

† Numerator includes two distinct decay processes: $\mathcal{B}(B_s^0 \to f) + \mathcal{B}(B_s^0 \to \overline{f})$.

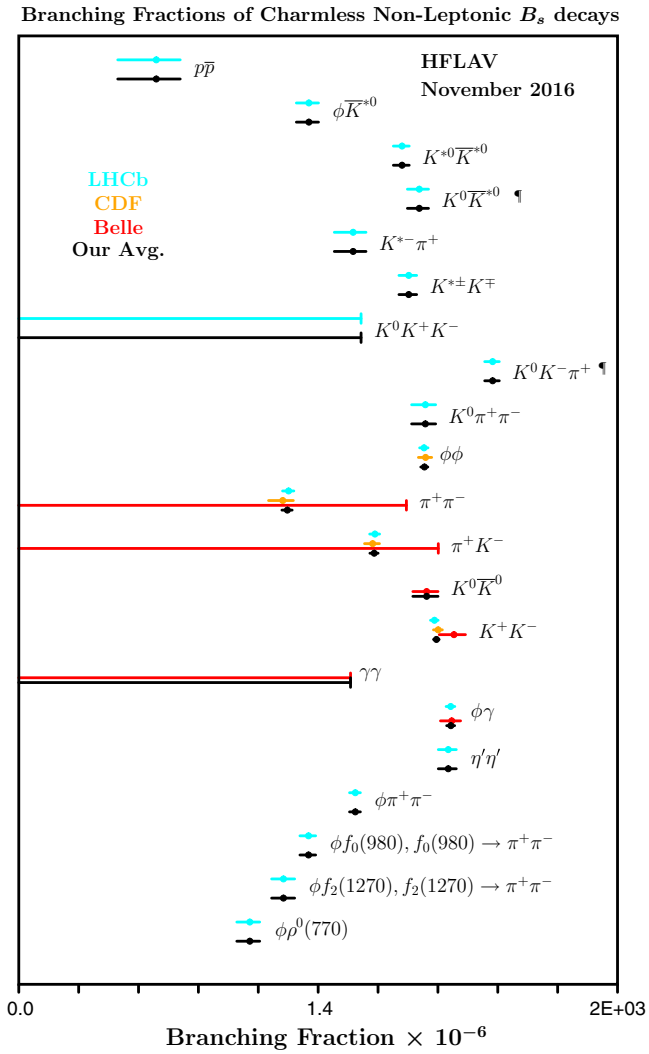

Fig. 180 Branching fractions of charmless non-leptonic B_s^0 decays

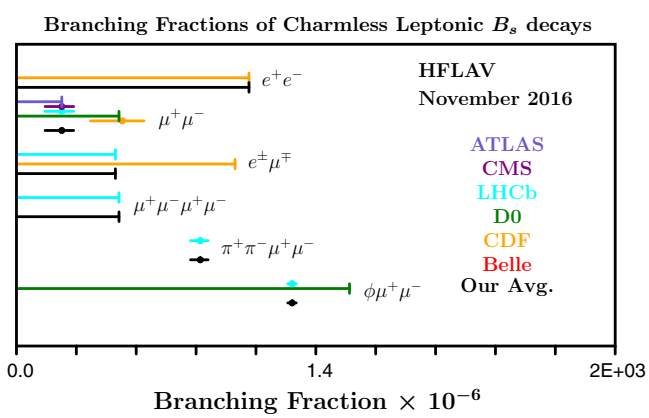

Fig. 181 Branching fractions of charmless leptonic B_s^0 decays

Table 234 Branching fractions of charmless semileptonic and radiative B^+ decays in units of $\times 10^{-6}$. Upper limits are at 90% CL. Where values are shown in red (blue), this indicates that they are new published (preliminary) results since PDG2014

RPP#	Mode	PDG2014 Avg.	BABAR		Belle		CLEO		LHCb		Our Avg.
363	$K^{*+}\gamma$	42.1±1.8	42.2±1.4±1.6	[951]	42.5±3.1±2.4	[952]	$37.6^{+8.9}_{-8.3}$±2.8	[953]			42.1±1.8
364	$K_1^+(1270)\gamma$	43±13	$44.1^{+6.3}_{-4.4}$±5.8 †	[401]	43±9±9	[954]					$43.8^{+7.1}_{-6.3}$
365	$K^+\eta\gamma$	7.9±0.9	7.7±1.0±0.4	[405]	$8.4^{+1.5}_{-1.2}$±0.9	[955]					7.9±0.9
366	$K^+\eta'\gamma$	$2.9^{+1.0}_{-0.9}$	$1.9^{+1.5}_{-1.2}$±0.1	[956]	3.6±1.2±0.4	[957]					$2.9^{+1.0}_{-0.9}$
367	$K^+\phi\gamma$	2.7±0.4	3.5±0.6±0.4	[958]	2.48±0.30±0.24	[406]					2.71±0.34
368	$K^+\pi^-\pi^+\gamma$	27.6±2.2	24.5±0.9±1.2 †	[401]	25.0±1.8±2.2 ‡	[954]					24.6±1.3
369	$K^{*0}\pi^+\gamma$ §	20^{+7}_{-6}	$23.4\pm0.9^{+0.8}_{-0.7}$ †	[401]	20^{+7}_{-6}±2	[959]					$23.3^{+1.2}_{-1.1}$
370	$K^+\rho^0\gamma$ §	< 20	8.2±0.4±0.8 †	[401]	< 20	[959]					8.2±0.9
	$(K\pi)_0^{*0}\pi^+\gamma$		$10.3^{+0.7+1.5}_{-0.8-2.0}$ †	[401]							$10.3^{+1.7}_{-2.2}$
371	$K^+\pi^-\pi^+\gamma$ (N.R.) §	< 9.2	$9.9\pm0.7^{+1.5}_{-1.9}$ †	[401]	< 9.2	[959]					$9.9^{+1.7}_{-2.0}$
	$K_0^*(1430)\pi^+\gamma$		$1.32^{+0.09+0.24}_{-0.10-0.30}$ †	[401]							$1.32^{+0.26}_{-0.32}$
372	$K^0\pi^+\pi^0\gamma$	46±5	45.6±4.2±3.1 †	[960]							45.6±5.2
373	$K_1^+(1400)\gamma$	< 15	$9.7^{+4.6+2.9}_{-2.9-2.4}$ †	[401]	< 15	[954]					$9.7^{+5.4}_{-3.8}$
	$K^{*+}(1410)\gamma$		$27.1^{+5.4+5.9}_{-4.8-3.7}$ †	[401]							$27.1^{+8.0}_{-6.1}$
374	$K_2^*(1430)^+\gamma$	14±4	$8.7^{+7.0+8.7}_{-5.3-10.4}$ †	[401]							$8.7^{+11.2}_{-11.7}$
375	$K^{*+}(1680)\gamma$	< 1900	$66.7^{+9.3+14.4}_{-7.8-11.4}$ †	[401]							$66.7^{+17.1}_{-13.8}$
376	$K_3^*(1780)^+\gamma$	< 39			< 39	[955]					< 39
378	$\rho^+\gamma$	0.98±0.25	$1.20^{+0.42}_{-0.37}$±0.20	[961]	$0.87^{+0.29+0.09}_{-0.27-0.11}$	[962]					$0.98^{+0.25}_{-0.24}$
428	$p\overline{\Lambda}\gamma$	$2.4^{+0.5}_{-0.4}$			$2.45^{+0.44}_{-0.38}$±0.22	[915]					$2.45^{+0.49}_{-0.44}$
432	$p\overline{\Sigma^0}\gamma$	< 4.6			< 4.6	[963]					< 4.6
467	$\pi^+\ell^+\ell^-$	< 0.049	< 0.066	[964]	< 0.049	[965]					< 0.049
468	$\pi^+e^+e^-$	< 0.080	< 0.125	[964]	< 0.080	[965]					< 0.080
469	$\pi^+\mu^+\mu^-$	< 0.055	< 0.055	[964]	< 0.069	[965]			0.0183±0.0024±0.0005 [1]	[966]	0.0180±0.0020
470	$\pi^+\nu\overline{\nu}$	< 98	< 100	[967]	< 98	[968]					< 98
471	$K^+\ell^+\ell^-$	0.451±0.023	0.48±0.09±0.02	[969]	$0.53^{+0.06}_{-0.05}$±0.03	[970]					0.51±0.05
472	$K^+e^+e^-$	0.55±0.07	$0.51^{+0.12}_{-0.11}$±0.02	[969]	$0.57^{+0.09}_{-0.08}$±0.03	[970]					0.55±0.07
473	$K^+\mu^+\mu^-$	0.449±0.023	$0.41^{+0.16}_{-0.15}$±0.02	[969]	$0.53\pm0.08^{+0.07}_{-0.03}$	[970]			0.429±0.007±0.021	[971]	0.435±0.021
	$K^+\tau^+\tau^-$		< 2250	[972]							< 2250

Table 234 continued

RPP#	Mode	PDG2014 Avg.	BABAR		Belle		CLEO	LHCb		Our Avg.
476	$K^+\nu\overline{\nu}$	< 16	< 16	[973]	< 55	[968]				< 16
477	$\rho^+\nu\overline{\nu}$	< 213			< 213	[968]				< 213
478	$K^{*+}\ell^+\ell^-$	1.29 ± 0.21	$1.40^{+0.40}_{-0.37}\pm0.09$	[969]	$1.24^{+0.23}_{-0.21}\pm0.13$	[970]				$1.29^{+0.22}_{-0.21}$
479	$K^{*+}e^+e^-$	$1.55^{+0.40}_{-0.31}$	$1.38^{+0.47}_{-0.42}\pm0.08$	[969]	$1.73^{+0.50}_{-0.42}\pm0.20$	[970]				$1.55^{+0.35}_{-0.32}$
480	$K^{*+}\mu^+\mu^-$	1.12 ± 0.15	$1.46^{+0.79}_{-0.75}\pm0.12$	[969]	$1.11^{+0.32}_{-0.27}\pm0.10$	[970]		$0.924\pm0.093\pm0.067$	[974]	$0.958^{+0.107}_{-0.104}$
481	$K^{*+}\nu\overline{\nu}$	< 40	< 64	[973]	< 40	[968]				< 40
	$K^+\pi^+\pi^-\mu^+\mu^-$							$0.436^{+0.029}_{-0.027}\pm0.028$ [2]	[975]	$0.436^{+0.040}_{-0.039}$
	$K^+\phi\mu^+\mu^-$							$0.082^{+0.019+0.029}_{-0.017-0.027}$	[975]	$0.082^{+0.035}_{-0.032}$

Results for LHCb are relative BFs converted to absolute BFs.
CLEO upper limits that have been greatly superseded are not shown.
† $M_{K\pi\pi} < 1.8$ GeV/c^2.
‡ $1.0 < M_{K\pi\pi} < 2.0$ GeV/c^2.
§ $M_{K\pi\pi} < 2.4$ GeV/c^2.
[1] PDG2014 cites only the measurement: $\mathcal{B}(\pi^+\mu^+\mu^-)/\mathcal{B}(K^+\mu^+\mu^-) = 0.053 \pm 0.014 \pm 0.01$.
[2] Differential BF in bins of $m(\mu^+\mu^-)$ is also available.

Table 235 Branching fractions of charmless semileptonic B^+ decays to LFV and LNV final states in units of $\times 10^{-6}$. Upper limits are at 90% CL. Where values are shown in red (blue), this indicates that they are new published (preliminary) results since PDG2014

RPP#	Mode	PDG2014 Avg.	BABAR		LHCb		Our Avg.
484	$\pi^+ e^\pm \mu^\mp$	< 0.17	< 0.17	[976]			< 0.17
485	$\pi^+ e^+ \tau^-$	< 74	< 74	[977]			< 74
486	$\pi^+ e^- \tau^+$	< 20	< 20	[977]			< 20
487	$\pi^+ e^\pm \tau^\mp$	< 75	< 75	[977]			< 75
488	$\pi^+ \mu^+ \tau^-$	< 62	< 62	[977]			< 62
489	$\pi^+ \mu^- \tau^+$	< 45	< 45	[977]			< 45
490	$\pi^+ \mu^\pm \tau^\mp$	< 72	< 72	[977]			< 72
491	$K^+ e^+ \mu^-$	< 0.091	< 0.091	[978]			< 0.091
492	$K^+ e^- \mu^+$	< 0.13	< 0.13	[978]			< 0.13
493	$K^+ e^\pm \mu^\mp$	< 0.091	< 0.091	[978]			< 0.091
494	$K^+ e^+ \tau^-$	< 43	< 43	[977]			< 43
495	$K^+ e^- \tau^+$	< 15	< 15	[977]			< 15
496	$K^+ e^\pm \tau^\mp$	< 30	< 30	[977]			< 30
497	$K^+ \mu^+ \tau^-$	< 45	< 45	[977]			< 45
498	$K^+ \mu^- \tau^+$	< 28	< 28	[977]			< 28
499	$K^+ \mu^\pm \tau^\mp$	< 48	< 48	[977]			< 48
500	$K^{*+} e^+ \mu^-$	< 1.3	< 1.3	[978]			< 1.3
501	$K^{*+} e^- \mu^+$	< 0.99	< 0.99	[978]			< 0.99
502	$K^{*+} e^\pm \mu^\mp$	< 1.4	< 1.4	[978]			< 1.4
503	$\pi^- e^+ e^+$	< 0.023	< 0.023	[979]			< 0.023
504	$\pi^- \mu^+ \mu^+$	< 0.013	< 0.107	[979]	< 0.004 †	[980]	< 0.004
505	$\pi^- e^+ \mu^+$	< 0.15	< 0.15	[981]			< 0.15
506	$\rho^- e^+ e^+$	< 0.17	< 0.17	[981]			< 0.17
507	$\rho^- \mu^+ \mu^+$	< 0.42	< 0.42	[981]			< 0.42
508	$\rho^- e^+ \mu^+$	< 0.47	< 0.47	[981]			< 0.47
509	$K^- e^+ e^+$	< 0.03	< 0.03	[979]			< 0.03
510	$K^- \mu^+ \mu^+$	< 0.041	< 0.067	[979]	< 0.041	[982]	< 0.041
511	$K^- e^+ \mu^+$	< 0.16	< 0.16	[981]			< 0.16
512	$K^{*-} e^+ e^+$	< 0.40	< 0.40	[981]			< 0.40
513	$K^{*-} \mu^+ \mu^+$	< 0.59	< 0.59	[981]			< 0.59
514	$K^{*-} e^+ \mu^+$	< 0.30	< 0.30	[981]			< 0.30

Results for LHCb are relative BFs converted to absolute BFs.
CLEO upper limits that have been greatly superseded are not shown.
† UL at 95% CL.

Table 236 Branching fractions of charmless semileptonic and radiative B^0 decays in units of $\times 10^{-6}$. Upper limits are at 90% CL. Where values are shown in red (blue), this indicates that they are new published (preliminary) results since PDG2014

RPP#	Mode	PDG2014 Avg.	BABAR		Belle		CLEO		LHCb		Our Avg.
336	$K^0\eta\gamma$	7.6±1.8	$7.1^{+2.1}_{-2.0}\pm0.4$	[405]	$8.7^{+3.1+1.9}_{-2.7-1.6}$	[955]					$7.6^{+1.8}_{-1.7}$
337	$K^0\eta'\gamma$	< 6.4	< 6.6	[956]	< 6.4	[957]					< 6.4
338	$K^0\phi\gamma$	2.7±0.7	< 2.7	[958]	2.74±0.60±0.32	[406]					2.74±0.68
339	$K^+\pi^-\gamma$ §	4.6±1.4			$4.6^{+1.3+0.5}_{-1.2-0.7}$	[959]					4.6±1.4
340	$K^{*0}\gamma$	43.3±1.5	44.7±1.0±1.6	[951]	40.1±2.1±1.7	[952]	$45.5^{+7.2}_{-6.8}\pm3.4$	[953]			43.3±1.5
341	$K^*(1410)^0\gamma$	< 130			< 130	[959]					< 130
342	$K^+\pi^-\gamma$ (N.R.) §	< 2.6			< 2.6	[959]					< 2.6
344	$K^0\pi^+\pi^-\gamma$	19.5±2.2	18.5±2.1±1.2 †	[960]	24±4±3 ‡	[954]					19.5±2.2
345	$K^+\pi^-\pi^0\gamma$	41±4	40.7±2.2±3.1 †	[960]							40.7±3.8
346	$K_1^0(1270)\gamma$	< 58			< 58	[954]					< 58
347	$K_1^0(1400)\gamma$	< 12			< 12	[954]					< 12
348	$K_2^*(1430)^0\gamma$	12.4±2.4	12.2±2.5±1.0	[983]	13±5±1	[959]					12.4±2.4
350	$K_3^*(1780)^0\gamma$	< 83			< 83	[955]					< 83
352	$\rho^0\gamma$	0.86±0.15	$0.97^{+0.24}_{-0.22}\pm0.06$	[961]	$0.78^{+0.17+0.09}_{-0.16-0.10}$	[962]					$0.86^{+0.15}_{-0.14}$
354	$\omega\gamma$	$0.44^{+0.18}_{-0.16}$	$0.50^{+0.27}_{-0.23}\pm0.09$	[961]	$0.40^{+0.19}_{-0.17}\pm0.13$	[962]					$0.44^{+0.18}_{-0.16}$
355	$\phi\gamma$	< 0.85	< 0.85	[984]	< 0.1	[985]					< 0.1
	$p\overline{\Lambda}\pi^-\gamma$				< 0.65	[986]					< 0.65
465	$\pi^0\ell^+\ell^-$	< 0.053	< 0.053	[964]	< 0.154	[965]					< 0.053
466	$\pi^0e^+e^-$	< 0.084	< 0.084	[964]	< 0.227	[965]					< 0.084
467	$\pi^0\mu^+\mu^-$	< 0.069	< 0.069	[964]	< 0.184	[965]					< 0.069
468	$\eta\ell^+\ell^-$	< 0.064	< 0.064	[964]							< 0.064
469	ηe^+e^-	< 0.108	< 0.108	[964]							< 0.108
470	$\eta\mu^+\mu^-$	< 0.112	< 0.112	[964]							< 0.112
471	$\pi^0\nu\overline{\nu}$	< 69			< 69	[968]					< 69
472	$K^0\ell^+\ell^-$	$0.31^{+0.08}_{-0.07}$	$0.21^{+0.15}_{-0.13}\pm0.02$	[969]	$0.34^{+0.09}_{-0.08}\pm0.02$	[970]					$0.31^{+0.08}_{-0.07}$
473	$K^0e^+e^-$	$0.16^{+0.10}_{-0.08}$	$0.08^{+0.15}_{-0.12}\pm0.01$	[969]	$0.20^{+0.14}_{-0.10}\pm0.01$	[970]					$0.16^{+0.10}_{-0.08}$
474	$K^0\mu^+\mu^-$	0.34±0.05	$0.49^{+0.29}_{-0.25}\pm0.03$	[969]	$0.44^{+0.13}_{-0.10}\pm0.03$	[970]			0.327±0.034±0.017	[974]	$0.343^{+0.036}_{-0.035}$
475	$K^0\nu\overline{\nu}$	< 49	< 49	[973]	< 194	[968]					< 49
476	$\rho^0\nu\overline{\nu}$	< 208			< 208	[968]					< 208
477	$K^{*0}\ell^+\ell^-$	$0.99^{+0.12}_{-0.11}$	$1.03^{+0.22}_{-0.21}\pm0.07$	[969]	$0.97^{+0.13}_{-0.11}\pm0.07$	[970]					$0.99^{+0.13}_{-0.11}$
478	$K^{*0}e^+e^-$	$1.03^{+0.19}_{-0.17}$	$0.86^{+0.26}_{-0.24}\pm0.05$	[969]	$1.18^{+0.27}_{-0.22}\pm0.09$	[970]					$1.03^{+0.19}_{-0.17}$
479	$K^{*0}\mu^+\mu^-$	1.05±0.10	$1.35^{+0.40}_{-0.37}\pm0.10$	[969]	$1.06^{+0.19}_{-0.14}\pm0.07$	[970]			$1.036^{+0.018}_{-0.017}\pm0.071$ ¶	[987]	$1.049^{+0.067}_{-0.065}$
480	$K^{*0}\nu\overline{\nu}$	< 55	< 120	[973]	< 55	[968]					< 55

Table 236 continued

RPP#	Mode	PDG2014 Avg.	BABAR		Belle		CLEO	LHCb		Our Avg.
481	$\phi\nu\nu$	< 127			< 127	[968]				< 127
	$\pi^+\pi^-\mu^+\mu^-$							$0.0211\pm0.0051\pm0.0022$ [1]	[933]	0.0210 ± 0.0060
483	$\pi^0 e^\pm\mu^\mp$	< 0.14	< 0.14	[976]						< 0.14
484	$K^0 e^\pm\mu^\mp$	< 0.27	< 0.27	[978]						< 0.27
485	$K^{*0} e^\pm\mu^\mp$	< 0.53	< 0.53	[978]						< 0.53

Results for LHCb are relative BFs converted to absolute BFs.
CLEO upper limits that have been greatly superseded are not shown.
† $M_{K\pi\pi} < 1.8$ GeV/c^2.
‡ $1.0 < M_{K\pi\pi} < 2.0$ GeV/c^2.
§ $1.25 < M_{K\pi} < 1.60$ GeV/c^2.
¶ This result takes into account the S-wave fraction in the $K\pi$ system.
[1] Muon pairs do not originate from resonances and $0.5 < m(\pi^+\pi^-) < 1.3$ GeV/c^2.

Table 237 Branching fractions of charmless semileptonic and radiative decays of $B^{\pm}/B^{0}$ admixture in units of $\times 10^{-6}$. Upper limits are at 90% CL. Where values are shown in red (blue), this indicates that they are new published (preliminary) results since PDG2014

RPP#	Mode	PDG2014 Avg.	BABAR		Belle		CLEO		CDF		Our Avg.
66	$K\eta\gamma$	$8.5^{+1.8}_{-1.6}$			$8.5^{+1.3}_{-1.2}\pm0.9$	[955]					$8.5^{+1.6}_{-1.5}$
68	$K_2^*(1430)\gamma$	17^{+6}_{-5}					$17\pm6\pm1$	[953]			17 ± 6
70	$K_3^*(1780)\gamma$	< 37			< 2.8 [§]	[955]					< 2.8
77	$s\gamma$ [†]	340 ± 21	341 ± 28 [1]	[988–990]	328 ± 20 [1]	[518,991,992]	$329\pm44\pm29$	[519]			332 ± 15
77	$s\gamma$ [2]		308 ± 22 [1]	[988–990]	305 ± 16 [1]	[991,992]					306 ± 13
78	$d\gamma$	9.2 ± 3.0	$9.2\pm2.0\pm2.3$	[993]							9.2 ± 3.0
84	$\rho\gamma$	1.39 ± 0.25	$1.73^{+0.34}_{-0.32}\pm0.17$	[961]	$1.21^{+0.24}_{-0.22}\pm0.12$	[962]					$1.39^{+0.22}_{-0.21}$
85	$\rho/\omega\gamma$	1.30 ± 0.23	$1.63^{+0.30}_{-0.28}\pm0.16$	[961]	$1.14\pm0.20^{+0.10}_{-0.12}$	[962]					$1.30^{+0.18}_{-0.19}$
119	se^+e^- [‡]	4.7 ± 1.3	$7.69^{+0.82+0.71}_{-0.77-0.60}$	[994]							$7.69^{+1.08}_{-0.98}$
120	$s\mu^+\mu^-$ [‡]	4.3 ± 1.2	$4.41^{+1.31+0.63}_{-1.17-0.50}$	[994]							$4.41^{+1.45}_{-1.27}$
121	$s\ell^+\ell^-$ [‡]	4.5 ± 1.0	$6.73^{+0.70+0.60}_{-0.64-0.56}$	[994]							$6.73^{+0.92}_{-0.85}$
122	$\pi\ell^+\ell^-$	< 0.059	< 0.059	[964]	< 0.062	[965]					< 0.059
123	πe^+e^-	< 0.110	< 0.110	[964]							< 0.110
124	$\pi\mu^+\mu^-$	< 0.050	< 0.050	[964]							< 0.050
125	Ke^+e^-	0.44 ± 0.06	$0.39^{+0.09}_{-0.08}\pm0.02$	[969]	$0.48^{+0.08}_{-0.07}\pm0.03$	[970]					0.44 ± 0.06
126	$K^*e^+e^-$	1.19 ± 0.20	$0.99^{+0.23}_{-0.21}\pm0.06$	[969]	$1.39^{+0.23}_{-0.20}\pm0.12$	[970]					$1.19^{+0.17}_{-0.16}$
127	$K\mu^+\mu^-$	0.44 ± 0.04	$0.41^{+0.13}_{-0.12}\pm0.02$	[969]	$0.50\pm0.06\pm0.03$	[970]			$0.42\pm0.04\pm0.02$	[922]	0.44 ± 0.04
128	$K^*\mu^+\mu^-$	1.06 ± 0.09	$1.35^{+0.35}_{-0.33}\pm0.10$	[969]	$1.10^{+0.16}_{-0.14}\pm0.08$	[970]			$1.01\pm0.10\pm0.05$	[922]	1.06 ± 0.09
129	$K\ell^+\ell^-$	0.48 ± 0.04	$0.47\pm0.06\pm0.02$	[995]	$0.48^{+0.05}_{-0.04}\pm0.03$	[970]					0.48 ± 0.04
130	$K^*\ell^+\ell^-$	1.05 ± 0.10	$1.02^{+0.14}_{-0.13}\pm0.05$	[995]	$1.07^{+0.11}_{-0.10}\pm0.09$	[970]					1.05 ± 0.10
131	$K\nu\overline{\nu}$	< 17	< 17	[973]							< 17
132	$K^*\nu\overline{\nu}$	< 76	< 76	[973]							< 76
134	$\pi e^{\pm}\mu^{\mp}$	< 0.092	< 0.092	[976]							< 0.092
135	$\rho e^{\pm}\mu^{\mp}$	< 3.2					< 3.2	[996]			< 3.2
136	$Ke^{\pm}\mu^{\mp}$	< 0.038	< 0.038	[978]							< 0.038
137	$K^*e^{\pm}\mu^{\mp}$	< 0.51	< 0.51	[978]							< 0.51

Results for CDF are relative BFs converted to absolute BFs.
CLEO upper limits that have been greatly superseded are not shown.
[†] Results extrapolated to $E_\gamma > 1.6$ GeV, using the method of Ref. [997].
[‡] Belle: $m(\ell^+\ell^-) > 0.2$ GeV/c^2, BABAR: $m^2(\ell^+\ell^-) > 0.1$ GeV$^2/c^4$.
[§] The value quoted is $\mathcal{B}(B \to K_3^*\gamma) \times \mathcal{B}(K_3^* \to K\eta)$. PDG gives the BF assuming $\mathcal{B}(K_3^* \to K\eta) = 11^{+5}_{-4}\%$.
[1] Average of several results, obtained with different methods.
[2] Only results originally measured in the interval $E_\gamma > 1.9$ GeV (also taken into account in the previous line).

Table 238 Branching fractions of leptonic and radiative-leptonic B^+ and B^0 decays in units of $\times 10^{-6}$. Upper limits are at 90% CL. Where values are shown in red (blue), this indicates that they are new published (preliminary) results since PDG2014

RPP#	Mode	PDG2014 Avg.	BaBar		Belle		CDF		LHCb		CMS		ATLAS		Our Avg.
29	$e^+\nu$	< 0.98	< 1.9	[998]	< 0.98 †	[999]									< 0.98 †
30	$\mu^+\nu$	< 1.0	< 1.0	[998]	< 1.7 †	[999]									< 1.0
31	$\tau^+\nu$	114 ± 27	179 ± 48 ‡	[1000]	$91\pm19\pm11$ ‡	[1001]									106 ± 19
32	$\ell^+\nu_\ell\gamma$	< 15.6	< 15.6	[1002]	< 3.5	[1003]									< 3.5
33	$e^+\nu_e\gamma$	< 17	< 17	[1002]	< 6.1	[1003]									< 6.1
34	$\mu^+\nu_\mu\gamma$	< 24	< 24	[1002]	< 3.4	[1003]									< 3.4
457	$\gamma\gamma$	< 0.32	< 0.32	[1004]	< 0.62	[1005]									< 0.32
458	e^+e^-	< 0.083	< 0.113	[1006]	< 0.19	[1007]	< 0.083	[944]							< 0.083
459	$e^+e^-\gamma$	< 0.12	< 0.12	[1008]											< 0.12
460	$\mu^+\mu^-$	< 0.00063	< 0.052	[1006]	< 0.16	[1007]	< 0.0038	[939]	< 00074 ¶	[941]	< 00110 ¶	[942]	< 0.00042 ¶	[943]	$0.00039^{+0.00016}_{-0.00014}$ §
461	$\mu^+\mu^-\gamma$	< 0.16	< 0.16	[1008]											< 0.16
462	$\mu^+\mu^-\mu^+\mu^-$	< 0.0053							< 0.0053	[946]					< 0.0053
464	$\tau^+\tau^-$	< 4100	< 4100	[1009]											< 4100
482	$e^\pm\mu^\mp$	< 0.0028	< 0.092	[1006]	< 0.17	[1007]	< 0.064	[944]	< 0.0028	[945]					< 0.0028
488	$e^\pm\tau^\mp$	< 28	< 28	[1010]											< 28
489	$\mu^\pm\tau^\mp$	< 22	< 22	[1010]											< 22
490	$\nu\bar{\nu}$	< 24	< 24	[1011]	< 130	[1012]									< 24
491	$\nu\bar{\nu}\gamma$	< 17	< 17	[1011]											< 17

Results for CDF, LHCb, CMS and ATLAS are relative BFs converted to absolute BFs.
† More recent results exist, with hadronic tagging [1013], which do not improve the limits (< 3.5 and < 2.7) for $e^+\nu$ and $\mu^+\nu$, respectively).
‡ The authors make the average with their previous results, derived from statistically independent samples [1014, 1015].
§ This is the combined result obtained by the LHCb and CMS collaborations [950].
¶ UL at 95% CL.

Table 239 Relative branching fractions of semileptonic and radiative B^+ decays. Where values are shown in red (blue), this indicates that they are new published (preliminary) results since PDG2014

RPP#	Mode	PDG2014 AVG.	Belle		BABAR		LHCb		Our Avg.
	$10^4 \times \mathcal{B}(K^+\pi^+\pi^-\mu^+\mu^-)/\mathcal{B}(\psi(2S)K^+)$						$6.95^{+0.46}_{-0.43}\pm0.34$	[975]	$6.95^{+0.57}_{-0.55}$
	$10^4 \times \mathcal{B}(K^+\phi\mu^+\mu^-)/\mathcal{B}(\psi(2S)K^+)$						$1.58^{+0.36+0.19}_{-0.32-0.07}$	[975]	$1.58^{+0.41}_{-0.33}$
469	$\mathcal{B}(\pi^+\mu^+\mu^-)/\mathcal{B}(K^+\mu^+\mu^-)$ †	$0.053\pm0.014\pm0.01$					$0.038\pm0.009\pm0.001$	[966]	0.038 ± 0.009
473	$\mathcal{B}(K^+\mu^+\mu^-)/\mathcal{B}(K^+e^+e^-)$ ‡						$0.745^{+0.090}_{-0.074}\pm0.036$	[1016]	$0.745^{+0.097}_{-0.082}$
473	$\mathcal{B}(K^+\mu^+\mu^-)/\mathcal{B}(K^+e^+e^-)$ §		$1.03\pm0.19\pm0.06$	[970]					1.03 ± 0.20
473	$\mathcal{B}(K^+\mu^+\mu^-)/\mathcal{B}(K^+e^+e^-)$ ¶				$1.00^{+0.31}_{-0.25}\pm0.07$	[995]			$1.00^{+0.32}_{-0.26}$
	$\mathcal{B}(K^*\mu^+\mu^-)/\mathcal{B}(K^*e^+e^-)$ §		$0.83\pm0.17\pm0.08$	[970]					0.83 ± 0.19
	$\mathcal{B}(K^*\mu^+\mu^-)/\mathcal{B}(K^*e^+e^-)$ ¶				$1.013^{+0.34}_{-0.26}\pm0.010$	[995]			$1.013^{+0.340}_{-0.260}$

† For $0.1 < m^2(\ell^+\ell^-) < 6.0$ GeV$^2/c^4$.
‡ For $1.0 < m^2(\ell^+\ell^-) < 6.0$ GeV$^2/c^4$.
§ For the full $m^2(\ell^+\ell^-)$ range.
¶ For $0.10 < m^2(\ell^+\ell^-) < 8.12$ GeV$^2/c^4$ and $m^2(\ell^+\ell^-) > 10.11$ GeV$^2/c^4$.

Table 240 Branching fractions of $B^+/B^0 \to \bar{q}$ gluon decays in units of $\times 10^{-6}$. Upper limits are at 90% CL. Where values are shown in red (blue), this indicates that they are new published (preliminary) results since PDG2014

RPP#	Mode	PDG2014 Avg.	BABAR		Belle		CLEO		Our Avg.
80	ηX	260^{+50}_{-80}			$261\pm30^{+44}_{-74}$ §	[1017]	< 440	[1018]	261^{+53}_{-79}
81	$\eta' X$	420 ± 90	$390\pm80\pm90$ †	[1019]			$460\pm110\pm60$ †	[1020]	423 ± 86
82	K^+X	< 187	< 187 ‡	[1021]					< 187
83	K^0X	195^{+71}_{-67}	$195^{+51}_{-45}\pm50$ ‡	[1021]					195^{+71}_{-67}
94	π^+X	370 ± 80	$372^{+50}_{-47}\pm59$ ¶	[1021]					372^{+77}_{-75}

† $2.0 < p^*(\eta') < 2.7$ GeV/c.
‡ $m_X < 1.69$ GeV/c^2.
§ $0.4 < m_X < 2.6$ GeV/c^2.
¶ $m_X < 1.71$ GeV/c^2

Table 241 Isospin asymmetry in radiative and semileptonic B meson decays. The notations are those adopted by the PDG. Where values are shown in red (blue), this indicates that they are new published (preliminary) results since PDG2014

Parameter	PDG2014 Avg.	BABAR		Belle		LHCb		Our Avg.
$\Delta_{0^-}(X_s\gamma)$	-0.01 ± 0.06	-0.01 ± 0.06 ‡	[516,988]					-0.01 ± 0.06
$\Delta_{0^+}(K^*\gamma)$	0.052 ± 0.026	$0.066\pm0.021\pm0.022$	[951]	$0.012\pm0.044\pm0.026$	[952]			0.052 ± 0.026
$\Delta_{\rho\gamma}$	-0.46 ± 0.17	$-0.43^{+0.25}_{-0.22}\pm0.10$	[961]	$-0.48^{+0.21+0.08}_{-0.19-0.09}$	[962]			$-0.46^{+0.17}_{-0.16}$
$\Delta_{0-}(K\ell\ell)$ †	-0.37 ± 0.13	$-0.41\pm0.25\pm0.01$	[995]	$-0.41^{+0.25}_{-0.20}\pm0.07$	[970]	$-0.10^{+0.08}_{-0.09}\pm0.02$ §	[974]	-0.16 ± 0.08
$\Delta_{0-}(K^*\ell\ell)$ †	-0.22 ± 0.10	$-0.20^{+0.30}_{-0.23}\pm0.03$	[995]	$0.33^{+0.37}_{-0.43}\pm0.08$	[970]	$0.00^{+0.12}_{-0.10}\pm0.02$ §	[974]	$-0.01^{+0.11}_{-0.09}$

In some of the B-factory results it is assumed that $\mathcal{B}(\Upsilon(4S) \to B^+B^-) = \mathcal{B}(\Upsilon(4S) \to B^0\overline{B}^0)$, and in others a measured value of the ratio of branching fractions is used. See original papers for details. The averages quoted above are computed naively and should be treated with caution.
† Results given for the bin $1 < m^2(\ell^+\ell^-) < 6$ GeV$^2/c^4$, see references for the other bins.
‡ Average of two independent measurements from BABAR.
§ Only muons are used

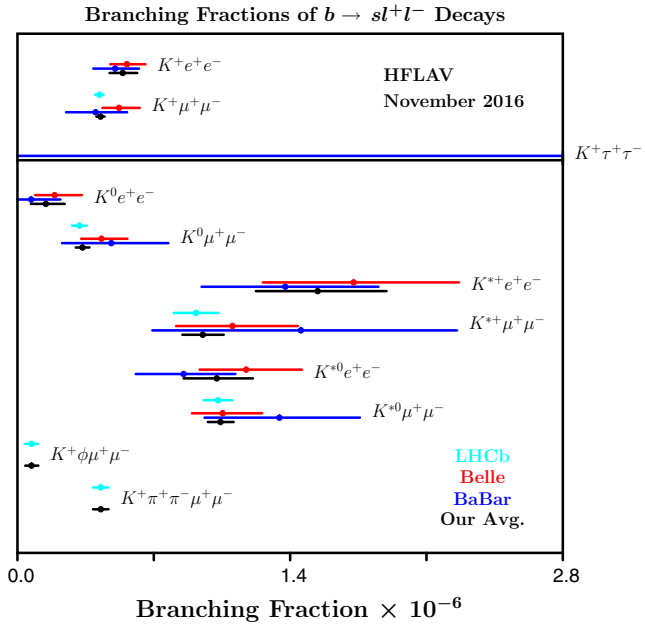

Fig. 182 Branching fractions of $b \to s\ell^+\ell^-$ decays

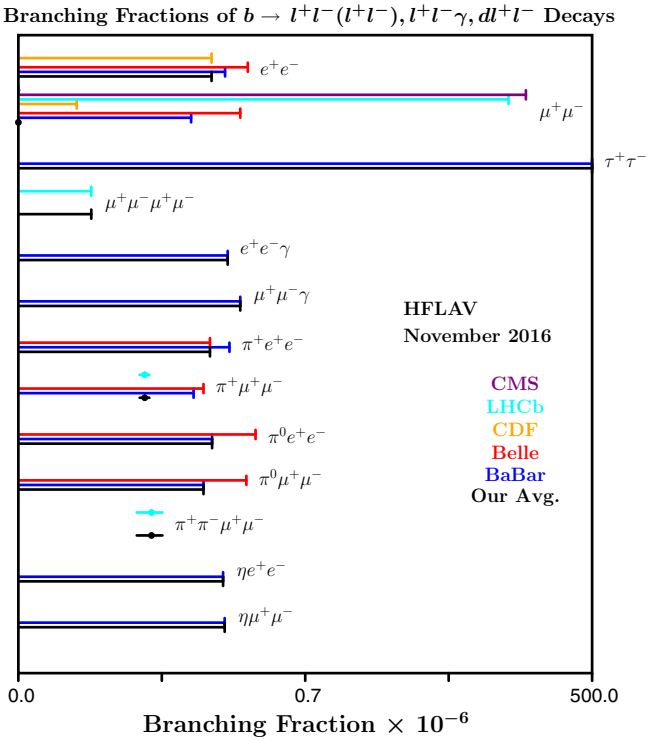

Fig. 183 Branching fractions of $b \to \ell^+\ell^-(\ell^+\ell^-)$, $\ell^+\ell^-\gamma$ and $b \to d\ell^+\ell^-$ decays

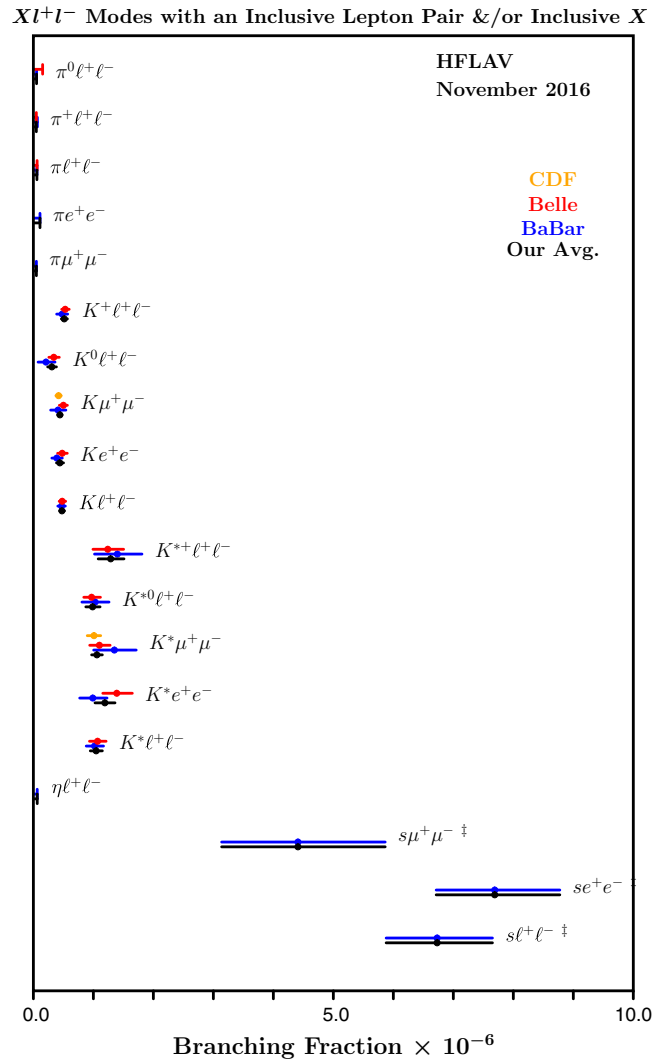

Fig. 184 $X\ell^+\ell^-$ modes with an inclusive lepton pair and/or inclusive X

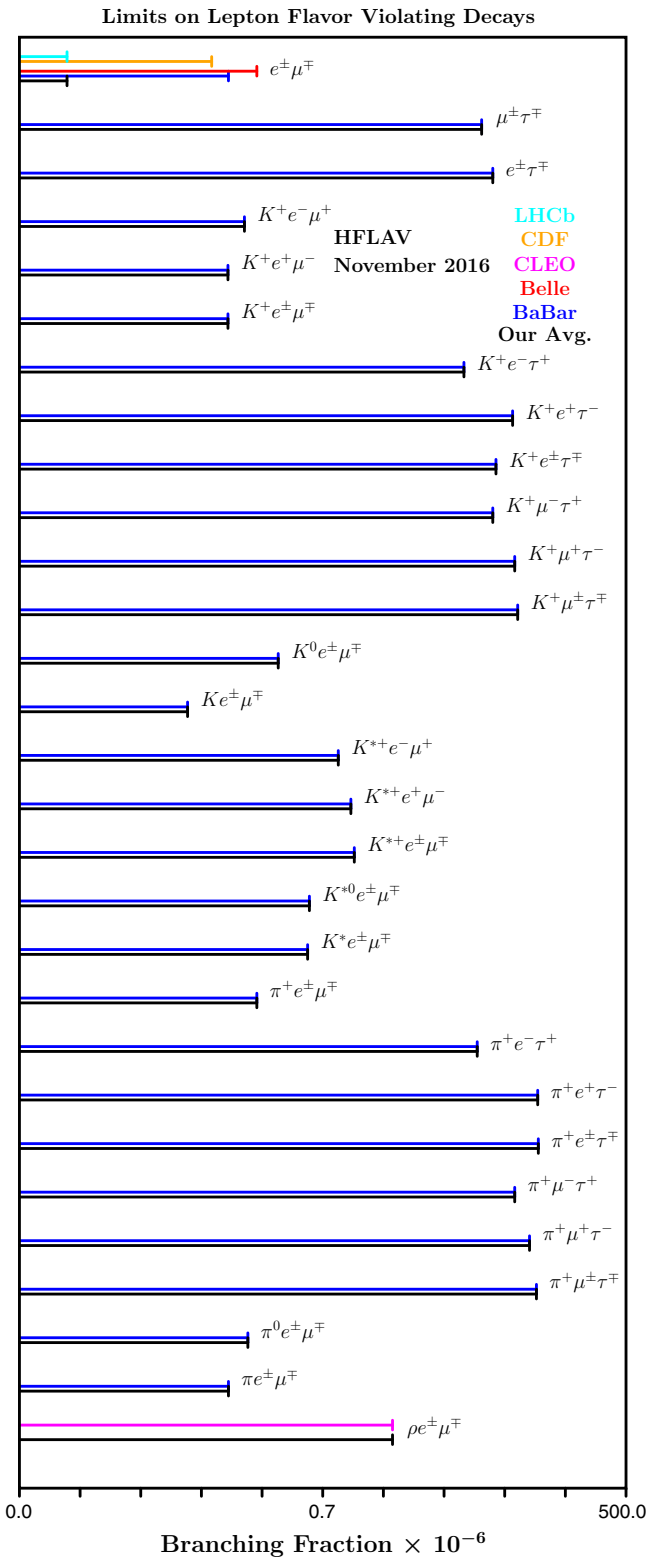

Fig. 185 Limits on lepton-flavor-violating decays

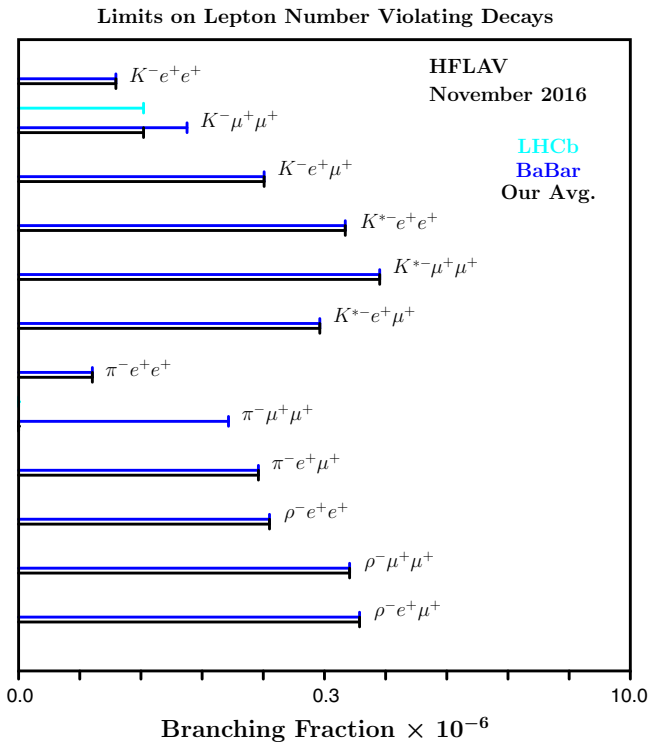

Fig. 186 Limits on lepton-number-violating decays

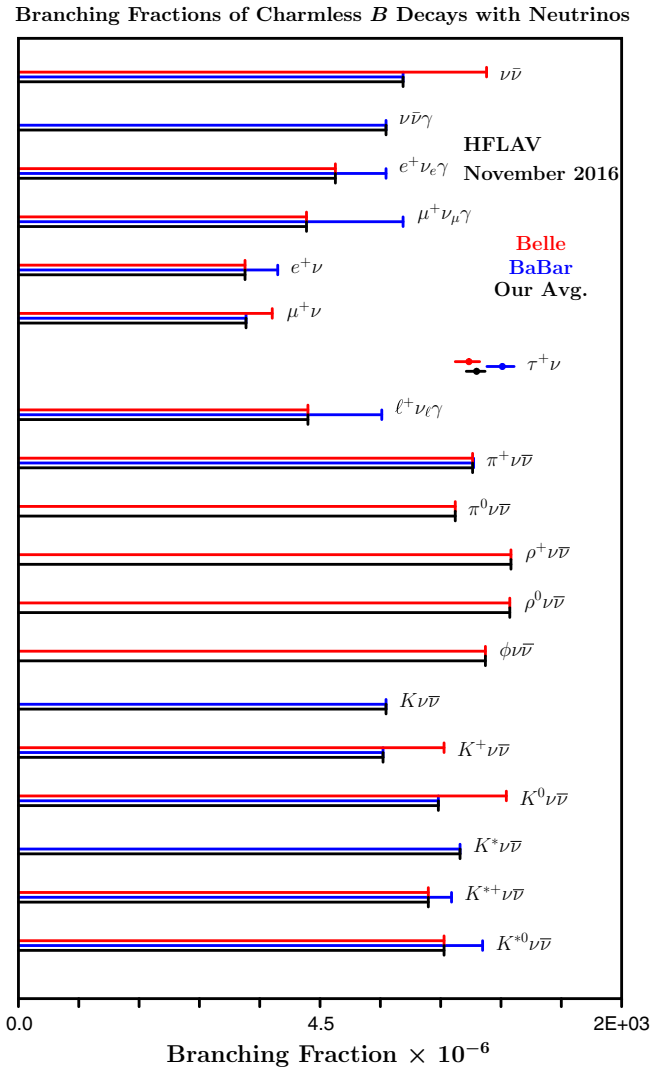

Fig. 187 Branching fractions of charmless B decays with neutrinos

Table 242 *CP* asymmetries of charmless hadronic B^+ decays (part 1). Where values are shown in red (blue), this indicates that they are new published (preliminary) results since PDG2014

RPP#	Mode	PDG2014 Avg.	BABAR		Belle		CDF	LHCb		Our Avg.
262	$K^0\pi^+$	-0.017 ± 0.016	$-0.029\pm0.039\pm0.010$	[398]	$-0.011\pm0.021\pm0.006$	[808]		$-0.022\pm0.025\pm0.010$	[838]	-0.017 ± 0.016
263	$K^+\pi^0$	0.037 ± 0.021 ‡	$0.030\pm0.039\pm0.010$	[810]	$0.043\pm0.024\pm0.002$	[808]				0.040 ± 0.021
264	$\eta' K^+$	0.013 ± 0.017	$0.008^{+0.017}_{-0.018}\pm0.009$	[811]	$0.028\pm0.028\pm0.021$	[812]				0.013 ± 0.017
265	$\eta' K^{*+}$	-0.26 ± 0.27	$-0.26\pm0.27\pm0.02$	[813]						-0.26 ± 0.27
266	$\eta' K_0^*(1430)^+$	0.06 ± 0.20	$0.06\pm0.20\pm0.02$	[813]						0.06 ± 0.20
267	$\eta' K_2^*(1430)^+$	0.15 ± 0.13	$0.15\pm0.13\pm0.02$	[813]						0.15 ± 0.13
268	ηK^+	-0.37 ± 0.08	$-0.36\pm0.11\pm0.03$	[811]	$-0.38\pm0.11\pm0.01$	[815]				-0.37 ± 0.08
269	ηK^{*+}	0.02 ± 0.06	$0.01\pm0.08\pm0.02$	[817]	$0.03\pm0.10\pm0.01$	[818]				0.02 ± 0.06
270	$\eta K_0^*(1430)^+$	$0.05\pm0.13\pm0.02$	$0.05\pm0.13\pm0.02$	[817]						0.05 ± 0.13
271	$\eta K_2^*(1430)^+$	$-0.45\pm0.30\pm0.02$	$-0.45\pm0.30\pm0.02$	[817]						-0.45 ± 0.30
281	ωK^+	0.02 ± 0.05	$-0.01\pm0.07\pm0.01$	[820]	$-0.03\pm0.04\pm0.01$	[1032]				-0.02 ± 0.04
282	ωK^{*+}	0.29 ± 0.35	$0.29\pm0.35\pm0.02$	[822]						0.29 ± 0.35
284	$\omega K_0^*(1430)^+$	-0.10 ± 0.09	$-0.10\pm0.09\pm0.02$	[822]						-0.10 ± 0.09
285	$\omega K_2^*(1430)^+$	0.14 ± 0.15	$0.14\pm0.15\pm0.02$	[822]						0.14 ± 0.15
288	$K^{*0}\pi^+$	-0.04 ± 0.09	$0.032\pm0.052^{+0.016}_{-0.013}$	[278]	$-0.149\pm0.064\pm0.022$	[276]				-0.038 ± 0.042
289	$K^{*+}\pi^0$	-0.06 ± 0.24	$-0.06\pm0.24\pm0.04$	[824]						-0.06 ± 0.24
290	$K^+\pi^+\pi^-$	0.033 ± 0.010	$0.028\pm0.020\pm0.023$	[278]	$0.049\pm0.026\pm0.020$	[276]		$0.025\pm0.004\pm0.008$	[1033]	0.027 ± 0.008
293	$f_0(980)K^+$	-0.08 ± 0.09 †	$-0.106\pm0.050^{+0.036}_{-0.015}$	[278]	$-0.077\pm0.065^{+0.046}_{-0.026}$	[276]				$-0.095^{+0.049}_{-0.042}$
294	$f_2(1270)K^+$	$-0.68^{+0.19}_{-0.017}$	$-0.85\pm0.22^{+0.26}_{-0.13}$	[278]	$-0.59\pm0.22\pm0.04$	[276]				$-0.68^{+0.20}_{-0.18}$
295	$f_0(1370)K^+$	$0.28^{+0.30}_{-0.29}$	$0.28\pm0.26^{+0.15}_{-0.14}$	[278]						$0.28^{+0.30}_{-0.29}$
298	$\rho^0 K^+$	0.37 ± 0.10	$0.44\pm0.10^{+0.06}_{-0.14}$	[278]	$0.30\pm0.11^{+0.11}_{-0.05}$	[276]				0.37 ± 0.11
299	$K_0^*(1430)^0\pi^+$	0.055 ± 0.033	$0.032\pm0.035^{+0.034}_{-0.028}$	[278]	$0.076\pm0.038^{+0.028}_{-0.022}$	[276]				$0.055^{+0.034}_{-0.032}$
300	$K_2^*(1430)^0\pi^+$	$0.05^{+0.29}_{-0.24}$	$0.05\pm0.23^{+0.18}_{-0.08}$	[278]						$0.05^{+0.29}_{-0.24}$
303	$K^+\pi^0\pi^0$	-0.06 ± 0.07	$-0.06\pm0.06\pm0.04$	[824]						-0.06 ± 0.07
310	$\rho^+ K^0$	-0.12 ± 0.17	$-0.12\pm0.17\pm0.02$	[830]						-0.12 ± 0.17
311	$K^{*+}\pi^+\pi^-$	0.07 ± 0.08	$0.07\pm0.07\pm0.04$	[831]						0.07 ± 0.08
312	$K^{*+}\rho^0$	0.31 ± 0.13	$0.31\pm0.13\pm0.03$	[832]						0.31 ± 0.13
313	$f_0(980)K^{*+}$	-0.15 ± 0.12	$-0.15\pm0.12\pm0.03$	[832]						-0.15 ± 0.12
314	$a_1^+ K^0$	0.12 ± 0.11	$0.12\pm0.11\pm0.02$	[833]						0.12 ± 0.11
315	$b_1^+ K^0$	-0.03 ± 0.15	$-0.03\pm0.15\pm0.02$	[834]						-0.03 ± 0.15
312	$K^{*0}\rho^+$	-0.01 ± 0.16	$-0.01\pm0.16\pm0.02$	[1034]						-0.01 ± 0.16
319	$b_1^0 K^+$	-0.46 ± 0.20	$-0.46\pm0.20\pm0.02$	[836]						-0.46 ± 0.20

Table 242 continued

RPP#	Mode	PDG2014 Avg.	BABAR		Belle		CDF		LHCb		Our Avg.
322	$K^+\overline{K}^0$	0.04±0.14	0.10±0.26±0.03	[398]	0.014±0.168±0.002	[808]			−0.21±0.14±0.01	[838]	−0.087±0.100
324	$K^+K_SK_S$	$0.04^{+0.04}_{-0.05}$	$0.04^{+0.04}_{-0.05}\pm0.02$	[271]							$0.04^{+0.04}_{-0.05}$
329	$K^+K^-\pi^+$	−0.12±0.05	0.00±0.10±0.03	[840]					−0.123±0.017±0.014	[1033]	−0.118±0.022
340	$K^+K^-K^+$	−0.036±0.012	$-0.017^{+0.019}_{-0.014}\pm0.014$	[271]					−0.036±0.004±0.007	[1033]	−0.033±0.007
341	ϕK^+	0.04±0.04	0.128±0.044±0.013	[271]	0.01±0.12±0.05	[849]	$-0.07\pm0.17^{+0.03}_{-0.02}$	[846]	0.022±0.021±0.009	[866]	0.041±0.020

† PDG takes the value from the BABAR amplitude analysis of $B^+ \to K^+K^-K^+$, while our numbers are from amplitude analyses of $B^+ \to K^+\pi^-\pi^+$
‡ PDG uses also a result from CLEO

Table 243 *CP* asymmetries of charmless hadronic B^+ decays (part 2). Where values are shown in red (blue), this indicates that they are new published (preliminary) results since PDG2014

RPP#	Mode	PDG2014 Avg.	BABAR		Belle		CDF	LHCb		Our Avg.
348	$K^{*+}K^+K^-$	0.11±0.09	0.11±0.08±0.03	[831]						0.11±0.09
349	ϕK^{*+}	−0.01±0.08	0.00±0.09±0.04	[848]	−0.02±0.14±0.03	[1035]				−0.01±0.08
351	$\phi K_1(1270)^+$	0.15±0.20	0.15±0.19±0.05	[850]						0.15±0.20
354	$\phi K_0^*(1430)^+$	0.04±0.15	0.04±0.15±0.04	[850]						0.04±0.15
355	$\phi K_2^*(1430)^+$	−0.23±0.20	−0.23±0.19±0.06	[850]						−0.23±0.20
359	$\phi\phi K^+$	−0.10±0.08	−0.10±0.08	[852]						−0.10±0.08
363	$K^{*+}\gamma$	0.18±0.29	0.18±0.28±0.07	[951]	0.007±0.074±0.017	[952]				0.018±0.073
365	$K^+\eta\gamma$	−0.12±0.07	−0.09±0.10±0.01	[405]	−0.16±0.09±0.06	[955]				−0.12±0.07
367	$K^+\phi\gamma$	−0.13±0.11	−0.26±0.14±0.05	[958]	−0.03±0.11±0.08	[406]				−0.13±0.10
378	$\rho^+\gamma$	−0.11±0.33			−0.11±0.32±0.09	[962]				−0.11±0.33
379	$\pi^+\pi^0$	0.03±0.04	0.03±0.08±0.01	[810]	0.025±0.043±0.007	[808]				0.026±0.039
380	$\pi^+\pi^-\pi^+$	0.105±0.029	$0.032\pm0.044^{+0.040}_{-0.037}$	[855]				0.058±0.008±0.011	[1033]	0.057±0.014
381	$\rho^0\pi^+$	$0.18^{+0.09}_{-0.17}$	$0.18\pm0.07^{+0.05}_{-0.15}$	[855]						$0.18^{+0.09}_{-0.17}$
383	$f_2(1270)\pi^+$	$0.41^{+0.31}_{-0.29}$	$0.41\pm0.25^{+0.18}_{-0.15}$	[855]						$0.41^{+0.31}_{-0.29}$
384	$\rho(1450)^0\pi^+$	$-0.06^{+0.36}_{-0.42}$	$-0.06\pm0.28^{+0.23}_{-0.32}$	[855]						$-0.06^{+0.36}_{-0.42}$
385	$f_0(1370)\pi^+$	0.72±0.22	0.72±0.15±0.16	[855]						0.72±0.22
387	$\pi^+\pi^-\pi^+(NR)$	$-0.14^{+0.23}_{-0.16}$	$-0.14\pm0.14^{+0.18}_{-0.08}$	[855]						$-0.14^{+0.23}_{-0.16}$
389	$\rho^+\pi^0$	0.02±0.11	−0.01±0.13±0.02	[858]	$0.06\pm0.17^{+0.04}_{-0.05}$	[859]				0.02±0.11
391	$\rho^+\rho^0$	−0.05±0.05	−0.054±0.055±0.010	[421]	0.00±0.22±0.03	[860]				−0.051±0.054
397	$\eta\pi^+$	−0.14±0.07	−0.03±0.09±0.03	[811]	−0.19±0.06±0.01	[815]				−0.14±0.05
398	$\eta\rho^+$	0.11±0.11	0.13±0.11±0.02	[863]	$-0.04^{+0.34}_{-0.32}\pm0.01$	[818]				0.11±0.11
399	$\eta'\pi^+$	0.06±0.16	0.03±0.17±0.02	[811]	$0.20^{+0.37}_{-0.36}\pm0.04$	[812]				0.06±0.15
400	$\eta'\rho^+$	0.26±0.17	0.26±0.17±0.02	[813]						0.26±0.17
401	$\omega\pi^+$	−0.04±0.06 †	−0.02±0.08±0.01	[820]	−0.02±0.09±0.01	[862]				−0.02±0.06
402	$\omega\rho^+$	−0.20±0.09	−0.20±0.09±0.02	[822]						−0.20±0.09
408	$b_1^0\pi^+$	0.05±0.16	0.05±0.16±0.02	[836]						0.05±0.16
417	$p\overline{p}\pi^+$	0.00±0.04	0.04±0.07±0.04	[666]	−0.17±0.10±0.02 ‡	[910]				−0.04±0.06
420	$p\overline{p}K^+$	−0.08±0.04	−0.16±0.08±0.04	[740]	−0.02±0.05±0.02 ‡	[910]		−0.047±0.036±0.007	[1036]	−0.051±0.029
425	$p\overline{p}K^{*+}$	0.21±0.16	0.32±0.13±0.05	[666]	−0.01±0.19±0.02	[913]				0.21±0.11
428	$p\overline{\Lambda}\gamma$	0.17±0.17			0.17±0.16±0.05	[915]				0.17±0.17
429	$p\overline{\Lambda}\pi^0$	0.01±0.17			0.01±0.17±0.04	[915]				0.01±0.17

Table 243 continued

RPP#	Mode	PDG2014 Avg.	BABAR		Belle		CDF	LHCb		Our Avg.
471	$K^+\ell\ell$	-0.02 ± 0.08	$-0.03\pm0.14\pm0.01$ §	[995]	$0.04\pm0.10\pm0.02$	[970]				0.02 ± 0.08
472	$K^+e^+e^-$	0.14 ± 0.14			$0.14\pm0.14\pm0.03$	[970]				0.14 ± 0.14
473	$K^+\mu^+\mu^-$	-0.003 ± 0.033			$-0.05\pm0.13\pm0.03$	[970]		$0.012\pm0.017\pm0.001$ ¶	[1037]	0.011 ± 0.017
478	$K^{*+}\ell\ell$	-0.09 ± 0.14	$0.01^{+0.26}_{-0.24}\pm0.02$	[969]	$-0.13^{+0.17}_{-0.16}\pm0.01$	[970]				$-0.09^{+0.14}_{-0.13}$
479	$K^{*+}e^+e^-$	$-0.14^{+0.23}_{-0.22}$			$-0.14^{+0.23}_{-0.22}\pm0.02$	[970]				$-0.14^{+0.23}_{-0.22}$
480	$K^{*+}\mu^+\mu^-$	-0.12 ± 0.24			$-0.12\pm0.24\pm0.02$	[970]		$-0.035\pm0.024\pm0.003$ ¶	[1037]	-0.036 ± 0.024
480	$\pi^+\mu^+\mu^-$							$-0.11\pm0.12\pm0.01$	[966]	-0.11 ± 0.12

† PDG uses also a result from CLEO.
‡ PDG swaps the Belle results corresponding to $A_{CP}(p\overline{p}\pi^+)$ and $A_{CP}(p\overline{p}K^+)$.
§ PDG uses also a previous result from *BABAR* ([969]).
¶ LHCb also quotes results in bins of $m(\ell^+\ell^-)^2$.

Table 244 *CP* asymmetries of charmless hadronic B^0 decays. Where values are shown in red (blue), this indicates that they are new published (preliminary) results since PDG2014

RPP#	Mode	PDG2014 Avg.	BABAR		Belle		CDF		LHCb		Our Avg.
227	$K^+\pi^-$	-0.082 ± 0.006 †	$-0.107\pm0.016^{+0.006}_{-0.004}$	[416]	$-0.069\pm0.014\pm0.007$	[808]	$-0.083\pm0.013\pm0.004$	[1038]	$-0.080\pm0.007\pm0.003$	[1039]	-0.082 ± 0.006
230	$\eta' K^{*0}$	0.02 ± 0.23	$0.02\pm0.23\pm0.02$	[813]	$-0.22\pm0.29\pm0.07$	[871]					-0.07 ± 0.18
231	$\eta' K_0^*(1430)^0$	-0.19 ± 0.17	$-0.19\pm0.17\pm0.02$	[813]							-0.19 ± 0.17
232	$\eta' K_2^*(1430)^0$	0.14 ± 0.18	$0.14\pm0.18\pm0.02$	[813]							0.14 ± 0.18
234	ηK^{*0}	0.19 ± 0.05	$0.21\pm0.06\pm0.02$	[817]	$0.17\pm0.08\pm0.01$	[818]					0.19 ± 0.05
235	$\eta K_0^*(1430)^0$	0.06 ± 0.13	$0.06\pm0.13\pm0.02$	[817]							0.06 ± 0.13
236	$\eta K_2^*(1430)^0$	-0.07 ± 0.19	$-0.07\pm0.19\pm0.02$	[817]							-0.07 ± 0.19
241	$b_1^- K^+$	-0.07 ± 0.12	$-0.07\pm0.12\pm0.02$	[836]							-0.07 ± 0.12
246	ωK^{*0}	0.45 ± 0.25	$0.45\pm0.25\pm0.02$	[822]							0.45 ± 0.25
248	$\omega K_0^*(1430)^0$	-0.07 ± 0.09	$-0.07\pm0.09\pm0.02$	[822]							-0.07 ± 0.09
249	$\omega K_2^*(1430)^0$	-0.37 ± 0.17	$-0.37\pm0.17\pm0.02$	[822]							-0.37 ± 0.17
251	$K^+\pi^-\pi^0$	0.00 ± 0.06	$-0.030^{+0.045}_{-0.051}\pm0.055$	[877]	$0.07\pm0.11\pm0.01$	[876]					$0.000^{+0.059}_{-0.061}$
252	$\rho^- K^+$	0.20 ± 0.11	$0.20\pm0.09\pm0.08$	[875]	$0.22^{+0.22+0.06}_{-0.23-0.02}$	[876]					0.20 ± 0.11
253	$\rho(1450)^- K^+$	-0.10 ± 0.33	$-0.10\pm0.32\pm0.09$	[875]							-0.10 ± 0.33
254	$\rho(1700)^- K^+$	-0.36 ± 0.61	$-0.36\pm0.57\pm0.23$	[875]							-0.36 ± 0.61
255	$K^+\pi^-\pi^0(NR)$	0.10 ± 0.18	$0.10\pm0.16\pm0.08$	[875]							0.10 ± 0.18
257	$K_0^*(1430)^0\pi^0$	-0.15 ± 0.11	$-0.15\pm0.10\pm0.04$	[875]							-0.15 ± 0.11
261	$K^0\pi^+\pi^-$	-0.01 ± 0.05	$-0.01\pm0.05\pm0.01$	[274]							-0.01 ± 0.05
264	$K^{*+}\pi^-$	-0.22 ± 0.06 †	$-0.24\pm0.07\pm0.02$ ‡	[875]	$-0.21\pm0.11\pm0.07$	[275]					-0.23 ± 0.06
265	$K_0^*(1430)^+\pi^-$	0.09 ± 0.07	$0.09\pm0.07\pm0.03$	[274]							0.09 ± 0.08
271	$K^{*0}\pi^0$	-0.15 ± 0.13	$-0.15\pm0.12\pm0.04$	[875]							-0.15 ± 0.13
278	$K^{*0}\pi^+\pi^-$	0.07 ± 0.05	$0.07\pm0.04\pm0.03$	[881]							0.07 ± 0.05
279	$K^{*0}\rho^0$	-0.06 ± 0.09	$-0.06\pm0.09\pm0.02$	[882]							-0.06 ± 0.09
280	$f_0(980)K^{*0}$	0.07 ± 0.10	$0.07\pm0.10\pm0.02$	[882]							0.07 ± 0.10
283	$a_1^- K^+$	-0.16 ± 0.12	$-0.16\pm0.12\pm0.01$	[833]							-0.16 ± 0.12
284	$K^{*+}\rho^-$	0.21 ± 0.15	$0.21\pm0.15\pm0.02$	[882]							0.21 ± 0.15
311	$K^{*0}K^+K^-$	0.01 ± 0.05	$0.01\pm0.05\pm0.02$	[881]							0.01 ± 0.05
312	ϕK^{*0}	0.00 ± 0.04	$0.01\pm0.06\pm0.03$	[391]	$-0.007\pm0.048\pm0.021$	[892]			$-0.015\pm0.032\pm0.10$ ¶	[1040]	-0.003 ± 0.038
314	$K^{*0}\pi^+K^-$	0.22 ± 0.39	$0.22\pm0.33\pm0.20$	[881]							0.22 ± 0.39
326	$\phi K_0^*(1430)^0$	0.12 ± 0.08	$0.20\pm0.14\pm0.06$	[391]	$0.093\pm0.094\pm0.017$	[892]					0.124 ± 0.081
333	$\phi K_2^*(1430)^0$	-0.11 ± 0.10	$-0.08\pm0.12\pm0.05$	[391]	$-0.155^{+0.152}_{-0.133}\pm0.033$	[892]					$-0.113^{+0.102}_{-0.096}$
340	$K^{*0}\gamma$	-0.002 ± 0.015	$-0.016\pm0.022\pm0.007$	[951]	$-0.030\pm0.055\pm0.014$	[952]			$0.008\pm0.017\pm0.009$	[938]	-0.003 ± 0.014
357	$\pi^0\pi^0$	0.43 ± 0.14	$0.43\pm0.26\pm0.05$	[416]	$0.44^{+0.52}_{-0.53}\pm0.17$	[899]					0.43 ± 0.24
391	$a_1^\mp\pi^\pm$	-0.07 ± 0.06	$-0.07\pm0.07\pm0.02$	[836]	$-0.06\pm0.05\pm0.07$	[418]					-0.07 ± 0.06

Table 244 continued

RPP#	Mode	PDG2014 Avg.	BABAR		Belle		CDF	LHCb		Our Avg.
400	$b_1^{\mp}\pi^{\pm}$	-0.05 ± 0.10	$-0.05\pm0.10\pm0.02$	[836]						-0.05 ± 0.10
412	$p\overline{p}K^{*0}$	0.05 ± 0.12	$0.11\pm0.13\pm0.06$	[666]	$-0.08\pm0.20\pm0.02$	[913]				0.05 ± 0.12
414	$p\overline{\Lambda}\pi^{-}$	0.04 ± 0.07	$-0.10\pm0.10\pm0.02$ §	[919]	$-0.02\pm0.10\pm0.03$	[915]				-0.06 ± 0.07
477	$K^{*0}\ell\ell$	-0.05 ± 0.10	$0.02\pm0.20\pm0.02$	[969]	$-0.08\pm0.12\pm0.02$	[970]				-0.05 ± 0.10
478	$K^{*0}e^{+}e^{-}$	-0.21 ± 0.19			$-0.21\pm0.19\pm0.02$	[970]				-0.21 ± 0.19
479	$K^{*0}\mu^{+}\mu^{-}$	-0.07 ± 0.04			$0.00\pm0.15\pm0.03$	[970]		$-0.035\pm0.024\pm0.003$ ◇	[1037]	-0.034 ± 0.024

Measurements of time-dependent CP asymmetries are listed in Sec. 4.

† PDG uses also a result from CLEO.

‡ Average of BABAR results from $B^0 \to K^+\pi^-\pi^0$ and $B^0 \to K^0\pi^+\pi^-$.

§ PDG quotes the opposite asymmetry.

¶ Extracted from measured $\Delta A_{CP} = A_{CP}(\phi K^{*0}) - A_{CP}(J/\psi K^{*0}) = 0.015 \pm 0.032 \pm 0.005$.

◇ LHCb also quotes results in bins of $m(\ell^+\ell^-)^2$.

Table 245 *CP* asymmetries of charmless hadronic decays of $B^{\pm}/B^0$ admixture. Where values are shown in red (blue), this indicates that they are new published (preliminary) results since PDG2014

RPP#	Mode	PDG2014 Avg.	BABAR		Belle		Our Avg.
65	$K^*\gamma$	-0.003 ± 0.017 †	$-0.003\pm0.017\pm0.007$	[951]	$-0.015\pm0.044\pm0.012$	[952]	-0.005 ± 0.017
77	$s\gamma$	-0.008 ± 0.029	$0.017\pm0.019\pm0.010$ ‡	[1041]	$0.002\pm0.050\pm0.030$	[1042]	0.015 ± 0.020
	$(s+d)\gamma$	-0.01 ± 0.05	$0.057\pm0.060\pm0.018$ §	[989]	$0.022\pm0.039\pm0.009$ ◇	[1032]	0.032 ± 0.034
80	$s\eta$	$-0.13^{+0.04}_{-0.05}$			$-0.13\pm0.04^{+0.02}_{-0.03}$	[1017]	$-0.13^{+0.04}_{-0.05}$
86	π^+X	0.10 ± 0.17	$0.10\pm0.16\pm0.05$	[1021]			0.10 ± 0.17
121	$s\ell\ell$	-0.22 ± 0.26	$0.04\pm0.11\pm0.01$	[994]			0.04 ± 0.11
126	$K^*e^+e^-$	-0.18 ± 0.15			$-0.18\pm0.15\pm0.01$	[970]	-0.18 ± 0.15
128	$K^*\mu^+\mu^-$	-0.03 ± 0.13			$-0.03\pm0.13\pm0.02$	[970]	-0.03 ± 0.13
129	$K\ell\ell$		$-0.03\pm0.14\pm0.01$	[995]			-0.03 ± 0.14
130	$K^*\ell\ell$	-0.04 ± 0.07	$0.03\pm0.13\pm0.01$ ¶	[995]	$-0.10\pm0.10\pm0.01$	[970]	-0.05 ± 0.08

† PDG includes also a result from CLEO.
‡ BABAR also measures the difference in direct *CP* asymmetry for charged and neutral B mesons: $\Delta A_{CP} = +(5.0 \pm 3.9 \pm 1.5)\%$.
§ There is another BABAR result using the recoil method [988], and a CLEO result [1043] that are used in the PDG average.
¶ Previous BABAR result is also included in the PDG Average.
◇ Requires $E_\gamma > 2.1$ GeV.

Table 246 *CP* asymmetries of charmless hadronic B_s^0 decays. Where values are shown in red (blue), this indicates that they are new published (preliminary) results since PDG2014

RPP#	Mode	PDG2014 Avg.	CDF		LHCb		Our Avg.
52	π^+K^-	0.28 ± 0.04	$0.22\pm0.07\pm0.02$	[1038]	$0.27\pm0.04\pm0.01$	[1039]	0.26 ± 0.04

Table 247 *CP* asymmetries of charmless hadronic Λ_b^0 decays. Where values are shown in red (blue), this indicates that they are new published (preliminary) results since PDG2014

RPP#	Mode	PDG2014 Avg.	CDF		LHCb		Our Avg.
21	$p\pi^-$	0.03 ± 0.18	$0.06\pm0.07\pm0.03$	[1038]			0.06 ± 0.08
22	pK^-	0.37 ± 0.17	$-0.10\pm0.08\pm0.04$	[1038]			-0.10 ± 0.09
	$\overline{K}^0p\pi^-$				$0.22\pm0.13\pm0.03$	[926]	0.22 ± 0.13
	$\Lambda K^+\pi^-$				$-0.53\pm0.23\pm0.11$	[927]	-0.53 ± 0.26
	ΛK^+K^-				$-0.28\pm0.10\pm0.07$	[927]	-0.28 ± 0.12

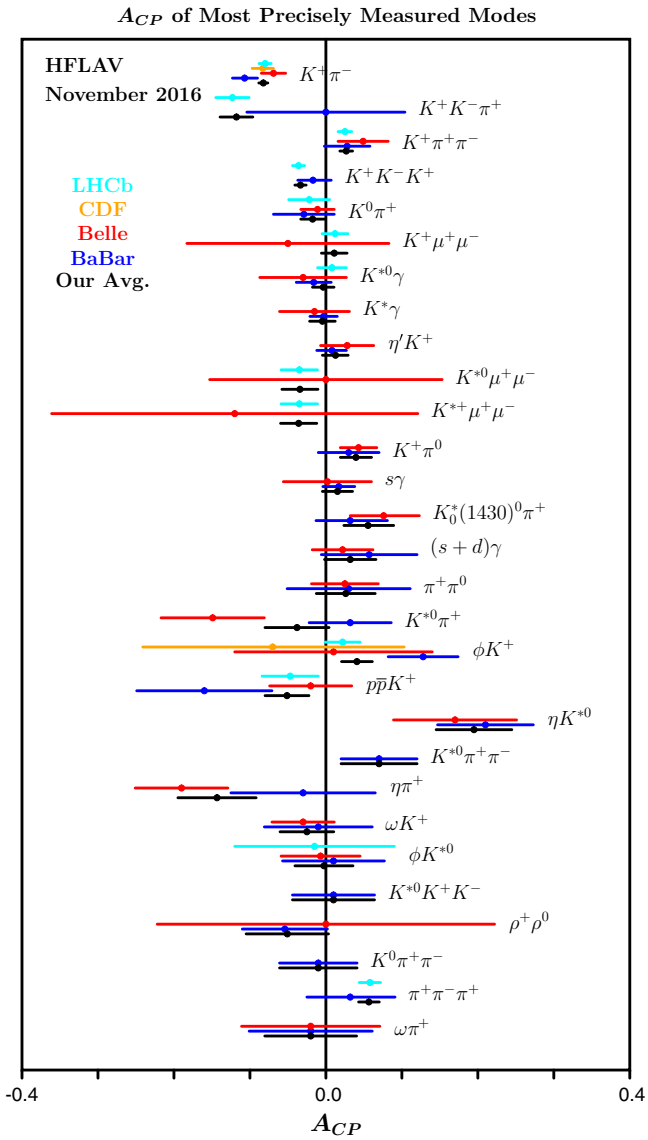

Fig. 188 A_{CP} of most precisely measured modes

Table 248 Longitudinal polarizat ion fraction f_L for B^+ decays. Where values are shown in red (blue), this indicates that they are new published (preliminary) results since PDG2014

RPP#	Mode	PDG2014 Avg.	BABAR		Belle		Our Avg.
282	ωK^{*+}	0.41±0.18±0.05	0.41±0.18±0.05	[822]			0.41±0.19
285	$\omega K_2^*(1430)^+$	0.56±0.10±0.04	0.56±0.10±0.04	[822]			0.56±0.11
312	$K^{*+}\rho^0$	0.78±0.12±0.03	0.78±0.12±0.03	[832]			0.78±0.12
316	$K^{*0}\rho^+$	0.48±0.08	0.52±0.10±0.04	[1034]	$0.43\pm0.11^{+0.05}_{-0.02}$	[1045]	0.48±0.08
338	$K^{*+}\overline{K}^{*0}$	$0.75^{+0.16}_{-0.26}\pm0.03$	$0.75^{+0.16}_{-0.26}\pm0.03$	[843]			$0.75^{+0.16}_{-0.26}$
349	ϕK^{*+}	0.50±0.05	0.49±0.05±0.03	[848]	0.52±0.08±0.03	[1035]	0.50±0.05
351	$\phi K_1(1270)^+$	$0.46^{+0.12+0.06}_{-0.13-0.07}$	$0.46^{+0.12+0.06}_{-0.13-0.07}$	[850]			$0.46^{+0.13}_{-0.15}$
355	$\phi K_2^*(1430)^+$	$0.80^{+0.09}_{-0.10}\pm0.03$	$0.80^{+0.09}_{-0.10}\pm0.03$	[850]			0.80±0.10
391	$\rho^+\rho^0$	0.950±0.016	0.950±0.015±0.006	[421]	0.95±0.11±0.02	[860]	0.950±0.016
396	$\omega\rho^+$	0.90±0.05±0.03	0.90±0.05±0.03	[822]			0.90±0.06

Table 249 Longitudinal polarization fraction f_L for B^0 decays. Where values are shown in red (blue), this indicates that they are new published (preliminary) results since PDG2014

RPP#	Mode	PDG2014 Avg.	BaBar		Belle		LHCb		Our Avg.
246	ωK^{*0}	0.69±0.13	0.72±0.14±0.02	[822]	$0.56\pm0.29^{+0.18}_{-0.08}$	[874]			0.70±0.13
249	$\omega K_2^*(1430)^0$	0.45±0.12±0.02	0.45±0.12±0.02	[822]					0.45±0.12
279	$K^{*0}\rho^0$	0.40±0.08±0.11	0.40±0.08±0.11	[882]					0.40±0.14
284	$K^{*+}\rho^-$	0.38±0.13±0.03	0.38±0.13±0.03	[882]					0.38±0.13
312	ϕK^{*0}	0.497±0.025	0.494±0.034±0.013	[391]	0.499±0.030±0.018	[892]	0.497±0.019±0.015	[1040]	0.497±0.017
315	$K^{*0}\overline{K}^{*0}$	$0.80^{+0.10}_{-0.12}\pm0.06$	$0.80^{+0.10}_{-0.12}\pm0.06$	[894]					$0.80^{+0.12}_{-0.13}$
333	$\phi K_2^*(1430)^0$	$0.901^{+0.046}_{-0.058}\pm0.037$	$0.901^{+0.046}_{-0.058}\pm0.037$	[391]					$0.901^{+0.059}_{-0.069}$
386	$\rho^0\rho^0$	$0.75^{+0.11}_{-0.14}\pm0.05$	$0.75^{+0.11}_{-0.14}\pm0.05$	[411]	$0.21^{+0.18}_{-0.22}\pm0.15$	[412]	$0.745^{+0.048}_{-0.058}\pm0.034$	[413]	$0.714^{+0.055}_{-0.062}$
394	$\rho^+\rho^-$	$0.977^{+0.028}_{-0.024}$	$0.992\pm0.024^{+0.026}_{-0.013}$	[409]	$0.941^{+0.034}_{-0.040}\pm0.030$	[906]			$0.978^{+0.025}_{-0.022}$
405	$a_1^\pm a_1^\mp$	0.31±0.22±0.10	0.31±0.22±0.10	[908]					0.31±0.24

Table 250 Results of the full angular analyses of $B^+ \to \phi K^{*+}$ decays. Where values are shown in red (blue), this indicates that they are new published (preliminary) results since PDG2014

Parameter	PDG2014 Avg.	BaBar		Belle		Our Avg.
$f_\perp = A_{\perp\perp}$	0.20±0.05	0.21±0.05±0.02	[848]	0.19±0.08±0.02	[1035]	0.20±0.05
$\phi_\parallel$	2.34±0.18	2.47±0.20±0.07		2.10±0.28±0.04		2.34±0.17
$\phi_\perp$	2.58±0.17	2.69±0.20±0.03		2.31±0.30±0.07		2.58±0.17
δ_0	3.07±0.18±0.06	3.07±0.18±0.06				3.07±0.19
A_{CP}^0	0.17±0.11±0.02	0.17±0.11±0.02				0.17±0.11
$A_{CP}^\perp$	0.22±0.24±0.08	0.22±0.24±0.08				0.22±0.25
$\Delta\phi_\parallel$	0.07±0.20±0.05	0.07±0.20±0.05				0.07±0.21
$\Delta\phi_\perp$	0.19±0.20±0.07	0.19±0.20±0.07				0.19±0.21
$\Delta\delta_0$	0.20±0.18±0.03	0.20±0.18±0.03				0.20±0.18

Angles (ϕ, δ) are in radians. BF, f_L and A_{CP} are tabulated separately

Table 251 Results of the full angular analyses of $B^0 \to \phi K^{*0}$ decays. Where values are shown in red (blue), this indicates that they are new published (preliminary) results since PDG2014

Parameter	PDG2014 Avg.	BABAR		Belle		LHCb		Our Avg.
$f_\perp = A_{\perp\perp}$	0.228±0.021	0.212±0.032±0.013	[391]	0.238±0.026±0.008	[892]	0.221±0.016±0.013	[1040]	0.225±0.015
$f_S(K\pi)$						0.143±0.013±0.012		0.143±0.018
$f_S(KK)$						0.122±0.013±0.008		0.122±0.015
$\phi_\parallel$	2.28±0.08	2.40±0.13±0.08		2.23±0.10±0.02		2.562±0.069±0.040		2.430±0.058
$\phi_\perp$	2.36±0.09	2.35±0.13±0.09		2.37±0.10±0.04		2.633±0.062±0.037		2.527±0.056
δ_0	2.88±0.10	2.82±0.15±0.09		2.91±0.10±0.08				2.88±0.10
$\phi_S(K\pi)$ †						2.222±0.063±0.081		2.222±0.103
$\phi_S(KK)$ †						2.481±0.072±0.048		2.481±0.087
A_{CP}^0	−0.01±0.05	0.01±0.07±0.02		−0.03±0.06±0.01		−0.003±0.038±0.005		−0.007±0.030
$A_{CP}^\perp$	−0.11±0.09	−0.04±0.15±0.06		−0.14±0.11±0.01		0.047±0.072±0.009		−0.014±0.057
$\mathcal{A}_{CP}^S(K\pi)$						0.073±0.091±0.035		0.073±0.097
$\mathcal{A}_{CP}^S(KK)$						−0.209±0.105±0.012		−0.209±0.106
$\Delta\phi_\parallel$	0.06±0.11	0.22±0.12±0.08		−0.02±0.10±0.01		0.045±0.068±0.015		0.051±0.053
$\Delta\phi_\perp$	0.10±0.08	0.21±0.13±0.08		0.05±0.10±0.02		0.062±0.062±0.006		0.075±0.050
$\Delta\delta_0$	0.13±0.09	0.27±0.14±0.08		0.08±0.10±0.01				0.13±0.08
$\Delta\phi_S(K\pi)$ †						0.062±0.062±0.022		0.062±0.066
$\Delta\phi_S(KK)$ †						0.022±0.072±0.004		0.022±0.072

Angles (ϕ, δ) are in radians. BF, f_L and A_{CP} are tabulated separately
† Original LHCb notation adapted to match similar existing quantities

Table 252 Results of the full angular analyses of $B^0 \to \phi K_2^{*0}(1430)$ decays. Where values are shown in red (blue), this indicates that they are new published (preliminary) results since PDG2014

Parameter	PDG2014 Avg.	BABAR		Belle		Our Avg.
$f_\perp = A_{\perp\perp}$	$0.027^{+0.031}_{-0.025}$	$0.002^{+0.018}_{-0.002}\pm0.031$	[391]	$0.056^{+0.050}_{-0.035}\pm0.009$	[892]	$0.027^{+0.027}_{-0.024}$
$\phi_\parallel$	4.0 ± 0.4	$3.96\pm0.38\pm0.06$		$3.76\pm2.88\pm1.32$		3.96 ± 0.38
$\phi_\perp$	4.5 ± 0.4			$4.45^{+0.43}_{-0.38}\pm0.13$		$4.45^{+0.45}_{-0.40}$
δ_0	3.46 ± 0.14	$3.41\pm0.13\pm0.13$		$3.53\pm0.11\pm0.19$		3.46 ± 0.14
A^0_{CP}	-0.03 ± 0.04	$-0.05\pm0.06\pm0.01$		$-0.016^{+0.066}_{-0.051}\pm0.008$		$-0.032^{+0.043}_{-0.038}$
$A^\perp_{CP}$	$0.0^{+0.9}_{-0.7}$			$-0.01^{+0.85}_{-0.67}\pm0.09$		$-0.01^{+0.85}_{-0.68}$
$\Delta\phi_\parallel$	-0.9 ± 0.4	$-1.00\pm0.38\pm0.09$		$-0.02\pm1.08\pm1.01$		-0.94 ± 0.38
$\Delta\phi_\perp$	-0.2 ± 0.4			$-0.19\pm0.42\pm0.11$		-0.19 ± 0.43
$\Delta\delta_0$	0.08 ± 0.09	$0.11\pm0.13\pm0.06$		$0.06\pm0.11\pm0.02$		0.08 ± 0.09

Angles (ϕ, δ) are in radians. BF, f_L and A_{CP} are tabulated separately

Table 253 Longitudinal polarization fraction f_L for B^0_s decays. Where values are shown in red (blue), this indicates that they are new published (preliminary) results since PDG2014

RPP#	Mode	PDG2014 Avg.	CDF		LHCb		Our Avg.
51	$\phi\phi$	0.361 ± 0.022	$0.348\pm0.041\pm0.021$	[932]	$0.365\pm0.022\pm0.012$	[1046]	0.361 ± 0.022
59	$K^{*0}\overline{K}^{*0}$	0.31 ± 0.13			$0.201\pm0.057\pm0.040$	[935]	0.201 ± 0.070
60	$\phi\overline{K}^{*0}$	0.51 ± 0.17			$0.51\pm0.15\pm0.07$	[936]	0.51 ± 0.17

Table 254 Results of the full angular analyses of $B^0_s \to \phi\phi$ decays. Where values are shown in red (blue), this indicates that they are new published (preliminary) results since PDG2014

Parameter	PDG2014 Avg.	CDF		LHCb		Our Avg.
$f_\perp = A_{\perp\perp}$	0.306 ± 0.030	$0.365\pm0.044\pm0.027$	[932]	$0.291\pm0.024\pm0.010$	[1046]	0.306 ± 0.023
$\phi_\parallel$	2.59 ± 0.15	$2.71^{+0.31}_{-0.36}\pm0.22$		$2.57\pm0.15\pm0.06$		2.59 ± 0.15

The parameter ϕ is in radians. BF, f_L and A_{CP} are tabulated separately

Table 255 Results of the full angular analyses of $B^0_s \to \phi\overline{K}^{*0}$ decays. Where values are shown in red (blue), this indicates that they are new published (preliminary) results since PDG2014

Parameter	PDG2014 Avg.	LHCb		Our Avg.
$f_\perp = A_{\perp\perp}$		$0.28\pm0.12\pm0.03$	[936]	0.28 ± 0.12
f_0		$0.51\pm0.15\pm0.07$		0.51 ± 0.17
$f_\parallel$	0.21 ± 0.11	$0.21\pm0.11\pm0.02$		0.21 ± 0.11
$\phi_\parallel$ †	$1.75\pm0.53\pm0.29$	$1.75^{+0.59+0.38}_{-0.53-0.30}$		$1.75^{+0.70}_{-0.61}$

The parameter ϕ is in radians. BF, f_L and A_{CP} are tabulated separately.
† Converted from the measurement of $\cos(\phi_\parallel)$. PDG takes the smallest resulting asymmetric error as parabolic

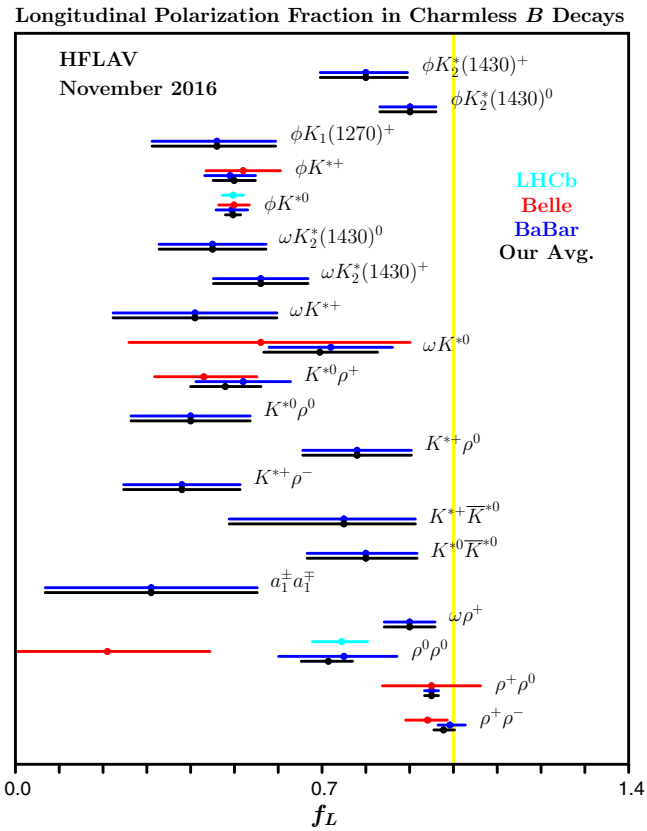

Fig. 189 Longitudinal polarization fraction in charmless B decays

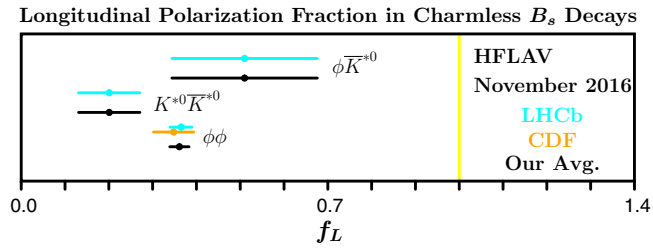

Fig. 190 Longitudinal polarization fraction in charmless B_s^0 decays

Table 256 Results of the full angular analyses of $B_s^0 \to K^{*0}\overline{K}^{*0}$ decays. Where values are shown in red (blue), this indicates that they are new published (preliminary) results since PDG2014

Parameter	PDG2014 Avg.	LHCb		Our Avg.
f_L	0.31±0.12±0.04	0.201±0.057±0.040	[935]	0.201±0.070
$f_\parallel$		0.215±0.046±0.015		0.215±0.048
$\lvert A_s^+\rvert^2$		0.114±0.037±0.023		0.114±0.044
$\lvert A_s^-\rvert^2$		0.485±0.051±0.019		0.485±0.054
$\lvert A_{ss}\rvert^2$		0.066±0.022±0.007		0.066±0.023
$\delta_\parallel$		5.31±0.24±0.14		5.31±0.28
$\delta_\perp - \delta_s^+$		1.95±0.21±0.04		1.95±0.21
δ_s^-		1.79±0.19±0.19		1.79±0.27
δ_{ss}		1.06±0.27±0.23		1.06±0.35

Table 257 Relative branching fractions of B_c^+ decays. Where values are shown in red (blue), this indicates that they are new published (preliminary) results since PDG2014

RPP#	Mode	PDG2014 AVG.	LHCb		Our Avg.
	$f_c\mathcal{B}(B_c^+ \to K^+K^0)/f_u\mathcal{B}(B^+ \to K_S^0\pi^+)$	‡	$< 5.8 \times 10^{-2}$	[838]	$< 5.8 \times 10^{-2}$
	$f_c\mathcal{B}(B_c^+ \to p\bar{p}\pi^+)/f_u$		$< 2.8 \times 10^{-8}$	[1047]	$< 2.8 \times 10^{-8}$
	$\sigma(B_c^+)\mathcal{B}(B_c^+ \to K^+K^-\pi^+)/\sigma(B^+)$ †		$< 15 \times 10^{-8}$	[795]	$< 15 \times 10^{-8}$

† Measured in the annihilation region $m(K^-\pi^+) < 1.834\text{GeV}/c^2$.
‡ PDG converts the LHCb result to $f_c\mathcal{B}(B_c^+ \to K^+K^0) < 4.6 \times 10^{-7}$

8 Charm physics

8.1 D^0-$\bar{D}^0$ mixing and CP violation

8.1.1 Introduction

In 2007 Belle [1048] and BaBar [1049] obtained the first evidence of D^0-$\bar{D}^0$ mixing, for which experiments had searched for more than two decades. These results were later confirmed by CDF [1050] and more recently by LHCb [1051]. There are now numerous measurements of D^0-$\bar{D}^0$ mixing with various levels of sensitivity. All measurements are input into a global fit to determine world average values of mixing parameters, CP-violation (CPV) parameters, and strong phase differences.

Our notation is as follows. The mass eigenstates are denoted

$$D_1 = p|D^0\rangle - q|\bar{D}^0\rangle \tag{221}$$

$$D_2 = p|D^0\rangle + q|\bar{D}^0\rangle, \tag{222}$$

where we use the convention [1052] $CP|D^0\rangle = -|\bar{D}^0\rangle$ and $CP|\bar{D}^0\rangle = -|D^0\rangle$. Thus in the absence of CP violation, D_1 is CP-even and D_2 is CP-odd. The weak phase ϕ is defined as $\mathrm{Arg}(q/p)$. The mixing parameters are defined as $x \equiv (m_1 - m_2)/\Gamma$ and $y \equiv (\Gamma_1 - \Gamma_2)/(2\Gamma)$, where m_1, m_2 and Γ_1, Γ_2 are the masses and decay widths for the mass eigenstates, and $\Gamma \equiv (\Gamma_1 + \Gamma_2)/2$.

The global fit determines central values and errors for ten underlying parameters. These consist of the mixing parameters x and y; indirect CPV parameters $|q/p|$ and ϕ; the ratio of decay rates $R_D \equiv [\Gamma(D^0 \to K^+\pi^-) + \Gamma(\bar{D}^0 \to K^-\pi^+)]/[\Gamma(D^0 \to K^-\pi^+) + \Gamma(\bar{D}^0 \to K^+\pi^-)]$; direct CPV asymmetries A_D, A_K, and A_π in $D^0 \to K^+\pi^-$, K^+K^-, and $\pi^+\pi^-$ decays, respectively; the strong phase difference δ between $\bar{D}^0 \to K^-\pi^+$ and $D^0 \to K^-\pi^+$ amplitudes; and the strong phase difference $\delta_{K\pi\pi}$ between $\bar{D}^0 \to K^-\rho^+$ and $D^0 \to K^-\rho^+$ amplitudes.

The fit uses 50 observables from measurements of $D^0 \to K^+\ell^-\bar{\nu}$, $D^0 \to K^+K^-$, $D^0 \to \pi^+\pi^-$, $D^0 \to K^+\pi^-$, $D^0 \to K^+\pi^-\pi^0$, $D^0 \to K^0_S\pi^+\pi^-$, $D^0 \to \pi^0\pi^+\pi^-$, $D^0 \to K^0_S K^+K^-$, and $D^0 \to K^+\pi^-\pi^+\pi^-$ decays,[37] and from double-tagged branching fractions measured at the $\psi(3770)$ resonance. The relationships between the measured observables and the fitted parameters are given in Table 258. Correlations among observables are accounted for by using covariance matrices provided by the experimental collaborations. Errors are assumed to be Gaussian, and systematic errors among different experiments are assumed to be uncorrelated unless specific correlations have been identified. We have checked this method with a second method that adds together three-dimensional log-likelihood functions for x, y, and δ obtained from several analyses; this combination accounts for non-Gaussian errors. When both methods are applied to the same set of measurements, equivalent results are obtained.

Mixing in the D^0, B^0, and B^0_s heavy flavor systems is governed by a short-distance box diagram. In the D^0 system, this diagram is doubly-Cabibbo-suppressed *relative to amplitudes dominating the decay width*. In addition, because the d and s quark masses are sufficiently close, this diagram is also GIM-suppressed. Thus the short-distance mixing rate is extremely small, and D^0-$\bar{D}^0$ mixing is expected to be dominated by long-distance processes. These are difficult to calculate, and theoretical estimates for x and y range over three orders of magnitude (up to the percent level) [1053–1056].

Almost all methods besides that of the $\psi(3770) \to \overline{D}D$ measurements [1057] identify the flavor of the D^0 or $\bar{D}^0$ when produced by reconstructing the decay $D^{*+} \to D^0\pi^+$ or $D^{*-} \to \bar{D}^0\pi^-$. The charge of the pion, which has low momentum relative to that of the D^0 and is often referred to as the "soft" pion, identifies the D flavor. For this decay $M_{D^*} - M_{D^0} - M_{\pi^+} \equiv Q \approx 6$ MeV, which is close to the kinematic threshold; thus analyses typically require that the reconstructed Q be small to suppress backgrounds. An LHCb measurement [1058] of the difference between time-integrated CP asymmetries $A_{CP}(K^+K^-) - A_{CP}(\pi^+\pi^-)$ identifies the flavor of the D^0 by partially reconstructing $\overline{B} \to D^0\mu^-X$ decays (and charge-conjugates); in this case the charge of the muon originating from the B decay identifies the flavor of the D^0.

For time-dependent measurements, the D^0 decay time is calculated as $M_{D^0} \times (\vec{\mathbf{d}} \cdot \vec{\mathbf{p}})/(cp^2)$, where $\vec{\mathbf{d}}$ is the displacement vector between the D^* and D^0 decay vertices, $\vec{\mathbf{p}}$ is the reconstructed D^0 momentum, and p and M_{D^0} are in GeV. The D^* vertex position is taken to be the intersection of the D^0 momentum vector with the beamspot profile for e^+e^- experiments, and at the primary interaction vertex for $\bar{p}p$ and pp experiments [1050,1051].

8.1.2 Input observables

The global fit determines central values and errors for ten underlying parameters using a χ^2 statistic. The fitted parameters are x, y, R_D, A_D, $|q/p|$, ϕ, δ, $\delta_{K\pi\pi}$, A_K, and A_π. In the $D \to K^+\pi^-\pi^0$ Dalitz plot analysis [1059], the phases of intermediate resonances in the $\bar{D}^0 \to K^+\pi^-\pi^0$ decay amplitude are determined relative to the phase for $\mathcal{A}(\bar{D}^0 \to K^+\rho^-)$, and the phases of intermediate resonances for $D^0 \to K^+\pi^-\pi^0$ are determined relative to the phase for $\mathcal{A}(D^0 \to K^+\rho^-)$. As the $\bar{D}^0$ and D^0 Dalitz plots are fitted independently, the phase difference $\delta_{K\pi\pi}$ between the

[37] Charge-conjugate modes are implicitly included.

Table 258 Left: decay modes used to determine fitted parameters x, y, δ, $\delta_{K\pi\pi}$, R_D, A_D, A_K, A_π, $|q/p|$, and ϕ. Middle: the observables measured for each decay mode. Right: the relationships between the observables measured and the fitted parameters. $\langle t\rangle$ is the mean reconstructed decay time for $D^0 \to K^+K^-$ or $D^0 \to \pi^+\pi^-$ decays

Decay Mode	Observables	Relationship
$D^0 \to K^+K^-/\pi^+\pi^-$	y_{CP} A_Γ	$2y_{CP} = \Big(\lvert q/p\rvert + \lvert p/q\rvert\Big) y\cos\phi - \Big(\lvert q/p\rvert - \lvert p/q\rvert\Big) x\sin\phi$ $2A_\Gamma = \Big(\lvert q/p\rvert - \lvert p/q\rvert\Big) y\cos\phi - \Big(\lvert q/p\rvert + \lvert p/q\rvert\Big) x\sin\phi$
$D^0 \to K^0_S\pi^+\pi^-$	x y $\lvert q/p\rvert$ ϕ	
$D^0 \to K^+\ell^-\nu$	R_M	$R_M = (x^2+y^2)/2$
$D^0 \to K^+\pi^-\pi^0$ (Dalitz plot analysis)	x'' y''	$x'' = x\cos\delta_{K\pi\pi} + y\sin\delta_{K\pi\pi}$ $y'' = y\cos\delta_{K\pi\pi} - x\sin\delta_{K\pi\pi}$
"Double-tagged" branching fractions measured in $\psi(3770) \to DD$ decays	R_M y R_D $\sqrt{R_D}\cos\delta$	$R_M = (x^2+y^2)/2$
$D^0 \to K^+\pi^-$	x'^2, y' x'^{2+}, x'^{2-} y'^+, y'^-	$x' = x\cos\delta + y\sin\delta$ $y' = y\cos\delta - x\sin\delta$ $A_M \equiv (\lvert q/p\rvert^4 - 1)/(\lvert q/p\rvert^4 + 1)$ $x'^\pm = [(1 \pm A_M)/(1\mp A_M)]^{1/4} \times (x'\cos\phi \pm y'\sin\phi)$ $y'^\pm = [(1 \pm A_M)/(1\mp A_M)]^{1/4} \times (y'\cos\phi \mp x'\sin\phi)$
$D^0 \to K^+\pi^-/K^-\pi^+$ (time-integrated)	$\frac{\Gamma(D^0\to K^+\pi^-)+\Gamma(\bar D^0\to K^-\pi^+)}{\Gamma(D^0\to K^-\pi^+)+\Gamma(\bar D^0\to K^+\pi^-)}$ $\frac{\Gamma(D^0\to K^+\pi^-)-\Gamma(\bar D^0\to K^-\pi^+)}{\Gamma(D^0\to K^+\pi^-)+\Gamma(\bar D^0\to K^-\pi^+)}$	R_D A_D
$D^0 \to K^+K^-/\pi^+\pi^-$ (time-integrated)	$\frac{\Gamma(D^0\to K^+K^-)-\Gamma(\bar D^0\to K^+K^-)}{\Gamma(D^0\to K^+K^-)+\Gamma(\bar D^0\to K^+K^-)}$ $\frac{\Gamma(D^0\to \pi^+\pi^-)-\Gamma(\bar D^0\to \pi^+\pi^-)}{\Gamma(D^0\to \pi^+\pi^-)+\Gamma(\bar D^0\to \pi^+\pi^-)}$	$A_K + \frac{\langle t\rangle}{\tau_D}\mathcal{A}_{CP}^{\text{indirect}}$ $(\mathcal{A}_{CP}^{\text{indirect}} \approx -A_\Gamma)$ $A_\pi + \frac{\langle t\rangle}{\tau_D}\mathcal{A}_{CP}^{\text{indirect}}$ $(\mathcal{A}_{CP}^{\text{indirect}} \approx -A_\Gamma)$

two reference amplitudes cannot be determined from these fits. However, the phase difference can be constrained in the global fit and thus is included as a fitted parameter.

All input measurements are listed in Tables 259, 260 and 261. The observable $R_M = (x^2+y^2)/2$ is measured in both $D^0 \to K^+\pi^-\pi^+\pi^-$ [1061] and $D^0 \to K^+\ell^-\nu$ decays. In the case of the latter, the HFLAV world average [1060] is used in the global fit. The inputs used for this average [1062–1065] are plotted in Fig. 191. The observables

$$y_{CP} = \frac{1}{2}\left(\left|\frac{q}{p}\right| + \left|\frac{p}{q}\right|\right) y\cos\phi - \frac{1}{2}\left(\left|\frac{q}{p}\right| - \left|\frac{p}{q}\right|\right) x\sin\phi \tag{223}$$

$$A_\Gamma = \frac{1}{2}\left(\left|\frac{q}{p}\right| - \left|\frac{p}{q}\right|\right) y\cos\phi - \frac{1}{2}\left(\left|\frac{q}{p}\right| + \left|\frac{p}{q}\right|\right) x\sin\phi \tag{224}$$

are also HFLAV world average values [1060]; the inputs used for these averages are plotted in Figs. 192 and 193, respectively. The $D^0 \to K^+\pi^-$ measurements used are from Belle [1066,1067], BaBar [1049], CDF [1068], and more recently LHCb [1051,1069]; earlier measurements have much less precision and are not used. The observables from $D^0 \to K^0_S\pi^+\pi^-$ decays are measured in two ways: assuming CP conservation (D^0 and $\bar D^0$ decays combined), and allowing for CP violation (D^0 and $\bar D^0$ decays fitted separately). The no-CPV measurements are from Belle [1070], BaBar [1071], and LHCb [1072], but for the CPV-allowed case only Belle measurements [1070] are available. The $D^0 \to K^+\pi^-\pi^0$, $D^0 \to K^0_S K^+K^-$, and $D^0 \to \pi^0\pi^+\pi^-$ results are from BaBar [1059,1073], the $D^0 \to K^+\pi^-\pi^+\pi^-$ results are from LHCb [1061], and the $\psi(3770) \to \overline{D}D$ results are from CLEOc [1057].

The relationships between the observables and the fitted parameters are listed in Table 258. For each set of correlated observables we construct a difference vector $\vec{V}$ between measured values and those calculated from fitted parame-

Table 259 Observables used in the global fit except those from time-dependent $D^0 \to K^+\pi^-$ measurements, and those from direct *CPV* measurements. The $D^0 \to K^+\pi^-\pi^0$ observables are $x'' \equiv x\cos\delta_{K\pi\pi} + y\sin\delta_{K\pi\pi}$ and $y'' \equiv -x\sin\delta_{K\pi\pi} + y\cos\delta_{K\pi\pi}$

Mode	Observable	Values	Correlation coefficients
$D^0 \to K^+K^-/\pi^+\pi^-$, ϕK_S^0 [1060]	y_{CP}	$(0.835 \pm 0.155)\%$	
	A_Γ	$(-0.032 \pm 0.026)\%$	
$D^0 \to K_S^0\pi^+\pi^-$ [1070] (Belle: no *CPV*)	x	$(0.56 \pm 0.19\,^{+0.067}_{-0.127})\%$	
	y	$(0.30 \pm 0.15\,^{+0.050}_{-0.078})\%$	$+0.012$
$D^0 \to K_S^0\pi^+\pi^-$ [1070] (Belle: no direct *CPV*)	$\lvert q/p\rvert$	$0.90\,^{+0.16+0.078}_{-0.15-0.064}$	
	ϕ	$(-6 \pm 11\,^{+4.2}_{-5.0})$ degrees	
$D^0 \to K_S^0\pi^+\pi^-$ [1070] (Belle: direct *CPV* allowed)	x	$(0.58 \pm 0.19^{+0.0734}_{-0.1177})\%$	$\begin{Bmatrix} 1 & 0.054 & -0.074 & -0.031 \\ 0.054 & 1 & 0.034 & -0.019 \\ -0.074 & 0.034 & 1 & 0.044 \\ -0.031 & -0.019 & 0.044 & 1 \end{Bmatrix}$
	y	$(0.27 \pm 0.16^{+0.0546}_{-0.0854})\%$	
	$\lvert q/p\rvert$	$0.82\,^{+0.20+0.0807}_{-0.18-0.0645}$	
	ϕ	$(-13\,^{+12}_{-13}\,^{+4.15}_{-4.77})$ degrees	
$D^0 \to K_S^0\pi^+\pi^-$ [1072]	x	$(-0.86 \pm 0.53 \pm 0.17)\%$	$+0.37$
(LHCb: no *CPV*)	y	$(0.03 \pm 0.46 \pm 0.13)\%$	
$D^0 \to K_S^0\pi^+\pi^-$ [1071] $K_S^0K^+K^-$	x	$(0.16 \pm 0.23 \pm 0.12 \pm 0.08)\%$	$+0.0615$
(BaBar: no *CPV*)	y	$(0.57 \pm 0.20 \pm 0.13 \pm 0.07)\%$	
$D^0 \to \pi^0\pi^+\pi^-$ [1073]	x	$(1.5 \pm 1.2 \pm 0.6)\%$	-0.006
(BaBar: no *CPV*)	y	$(0.2 \pm 0.9 \pm 0.5)\%$	
$D^0 \to K^+\ell^-\nu$ [1060]	$R_M = (x^2+y^2)/2$	$(0.0130 \pm 0.0269)\%$	
$D^0 \to K^+\pi^-\pi^0$ [1059]	x''	$(2.61\,^{+0.57}_{-0.68} \pm 0.39)\%$	-0.75
	y''	$(-0.06\,^{+0.55}_{-0.64} \pm 0.34)\%$	
$D^0 \to K^+\pi^-\pi^+\pi^-$ [1061]	$R_M/2$	$(4.8 \pm 1.8) \times 10^{-5}$	$\begin{Bmatrix} 1 & 0 & 0 & -0.42 & 0.01 \\ & 1 & -0.73 & 0.39 & 0.02 \\ & & 1 & -0.53 & -0.03 \\ & & & 1 & 0.04 \\ & & & & 1 \end{Bmatrix}$
	R_D	$(0.533 \pm 0.107 \pm 0.045)\%$	
$\psi(3770) \to \overline{D}D$ [1057]	x^2	$(0.06 \pm 0.23 \pm 0.11)\%$	
(CLEOc)	y	$(4.2 \pm 2.0 \pm 1.0)\%$	
	$\cos\delta$	$0.81\,^{+0.22}_{-0.18}\,^{+0.07}_{-0.05}$	
	$\sin\delta$	$-0.01 \pm 0.41 \pm 0.04$	

ters using these relations; e.g., for $D^0 \to K_S^0\pi^+\pi^-$ decays, $\vec{V} = (\Delta x, \Delta y, \Delta|q/p|, \Delta\phi)$. The contribution of a set of observables to the fit χ^2 is calculated as $\vec{V}\cdot(M^{-1})\cdot\vec{V}^T$, where M^{-1} is the inverse of the covariance matrix for the measurement. Covariance matrices are constructed from the correlation coefficients among the measured observables. These correlation coefficients are also listed in Tables 259, 260 and 261.

8.1.3 Fit results

The global fit uses MINUIT with the MIGRAD minimizer, and all errors are obtained from MINOS [1090]. Four separate fits are performed:

1. assuming *CP* conservation, i.e., fixing $A_D = 0$, $A_K = 0$, $A_\pi = 0$, $\phi = 0$, and $|q/p| = 1$;
2. assuming no direct *CPV* in doubly Cabibbo-suppressed (DCS) decays ($A_D = 0$) and fitting for parameters $(x, y, |q/p|)$ or (x, y, ϕ);
3. assuming no direct *CPV* in DCS decays and fitting for alternative parameters [1091,1092] $x_{12} = 2|M_{12}|/\Gamma$, $y_{12} = |\Gamma_{12}|/\Gamma$, and $\phi_{12} = \mathrm{Arg}(M_{12}/\Gamma_{12})$, where M_{12} and Γ_{12} are the off-diagonal elements of the D^0-$\bar{D}^0$ mass and decay matrices, respectively. The parameter ϕ_{12} is a weak phase that is responsible for *CP* violation in mixing.
4. allowing full *CPV* (floating all parameters).

For fits (2) and (3) assuming no direct *CPV* in DCS decays, in addition to $A_D = 0$ we impose other constraints that reduce four independent parameters to three.[38] For fit (2) we impose

[38] One can also use Eq. (15) of Ref. [1091] to reduce four parameters to three.

Table 260 Time-dependent $D^0 \to K^+\pi^-$ observables used for the global fit. The observables R_D^+ and R_D^- are related to parameters R_D and A_D via $R_D^\pm = R_D(1 \pm A_D)$

Mode	Observable	Values	Correlation coefficients
$D^0 \to K^+\pi^-$ [1049] (BaBar 384 fb^{-1})	R_D	$(0.303 \pm 0.0189)\%$	$\begin{Bmatrix} 1 & 0.77 & -0.87 \\ 0.77 & 1 & -0.94 \\ -0.87 & -0.94 & 1 \end{Bmatrix}$
	x'^{2+}	$(-0.024 \pm 0.052)\%$	
	y'^{+}	$(0.98 \pm 0.78)\%$	
$\bar{D}^0 \to K^-\pi^+$ [1049] (BaBar 384 fb^{-1})	A_D	$(-2.1 \pm 5.4)\%$	
	x'^{2-}	$(-0.020 \pm 0.050)\%$	Same as above
	y'^{-}	$(0.96 \pm 0.75)\%$	
$D^0 \to K^+\pi^-$ [1067] (Belle 976 fb^{-1} No *CPV*)	R_D	$(0.353 \pm 0.013)\%$	$\begin{Bmatrix} 1 & 0.737 & -0.865 \\ 0.737 & 1 & -0.948 \\ -0.865 & -0.948 & 1 \end{Bmatrix}$
	x'^{2}	$(0.009 \pm 0.022)\%$	
	y'	$(0.46 \pm 0.34)\%$	
$D^0 \to K^+\pi^-$ [1066] (Belle 400 fb^{-1} *CPV*-allowed)	R_D	$(0.364 \pm 0.018)\%$	$\begin{Bmatrix} 1 & 0.655 & -0.834 \\ 0.655 & 1 & -0.909 \\ -0.834 & -0.909 & 1 \end{Bmatrix}$
	x'^{2+}	$(0.032 \pm 0.037)\%$	
	y'^{+}	$(-0.12 \pm 0.58)\%$	
$\bar{D}^0 \to K^-\pi^+$ [1066] (Belle 400 fb^{-1} *CPV*-allowed)	A_D	$(+2.3 \pm 4.7)\%$	
	x'^{2-}	$(0.006 \pm 0.034)\%$	Same as above
	y'^{-}	$(0.20 \pm 0.54)\%$	
$D^0 \to K^+\pi^-$ [1068] (CDF 9.6 fb^{-1} No *CPV*)	R_D	$(0.351 \pm 0.035)\%$	$\begin{Bmatrix} 1 & 0.90 & -0.97 \\ 0.90 & 1 & -0.98 \\ -0.97 & -0.98 & 1 \end{Bmatrix}$
	x'^{2}	$(0.008 \pm 0.018)\%$	
	y'	$(0.43 \pm 0.43)\%$	
$D^0 \to K^+\pi^-$ [1069] (LHCb 3.0 fb^{-1} *CPV*-allowed)	R_D^+	$(0.3474 \pm 0.0081)\%$	$\begin{Bmatrix} 1 & 0.823 & -0.920 \\ 0.823 & 1 & -0.962 \\ -0.920 & -0.962 & 1 \end{Bmatrix}$
	x'^{2+}	$(0.0011 \pm 0.0065)\%$	
	y'^{+}	$(0.597 \pm 0.125)\%$	
$\bar{D}^0 \to K^-\pi^+$ [1069] (LHCb 3.0 fb^{-1} *CPV*-allowed)	R_D^-	$(0.3591 \pm 0.0081)\%$	$\begin{Bmatrix} 1 & 0.812 & -0.918 \\ 0.812 & 1 & -0.956 \\ -0.918 & -0.956 & 1 \end{Bmatrix}$
	x'^{2-}	$(0.0061 \pm 0.0061)\%$	
	y'^{-}	$(0.450 \pm 0.121)\%$	

the relation [1092,1093] $\tan\phi = (1-|q/p|^2)/(1+|q/p|^2)\times(x/y)$ in two ways: first we float parameters x, y, and ϕ and from these derive $|q/p|$; we then repeat the fit floating x, y, and $|q/p|$ and from these derive ϕ. The central values returned by the two fits are identical, but the first fit yields MINOS errors for ϕ, while the second fit yields MINOS errors for $|q/p|$. For no-direct-*CPV* fit (3), we fit for underlying parameters x_{12}, y_{12}, and ϕ_{12}, and from these calculate x, y, $|q/p|$, and ϕ to which measured observables are compared. All fit results are listed in Table 262. For the *CPV*-allowed fit, individual contributions to the χ^2 are listed in Table 263. The total χ^2 is 76.8 for $50 - 10 = 40$ degrees of freedom.

Confidence contours in the two dimensions (x, y) or $(|q/p|, \phi)$ are obtained by allowing, for any point in the two-dimensional plane, all other fitted parameters to take their preferred values. The resulting $1\sigma - 5\sigma$ contours are shown in Fig. 194 for the *CP*-conserving case, in Fig. 195 for the no-direct-*CPV* case, and in Fig. 196 for the *CPV*-allowed case. The contours are determined from the increase of the χ^2 above the minimum value. One observes that the (x, y) contours for the no-*CPV* fit are very similar to those for the

Table 261 Measurements of time-integrated CP asymmetries. The observable $A_{CP}(f) \equiv [\Gamma(D^0 \to f) - \Gamma(\bar{D}^0 \to f)]/[\Gamma(D^0 \to f) + \Gamma(\bar{D}^0 \to f)]$, and $\Delta\langle t\rangle$ is the difference between the mean reconstructed decay times for $D^0 \to K^+K^-$ and $D^0 \to \pi^+\pi^-$ decays (due to different trigger and reconstruction efficiencies)

Mode	Observable	Values	$\Delta\langle t\rangle/\tau_D$
$D^0 \to h^+h^-$ [1074] (BaBar 386 fb^{-1})	$A_{CP}(K^+K^-)$	$(+0.00 \pm 0.34 \pm 0.13)\%$	
	$A_{CP}(\pi^+\pi^-)$	$(-0.24 \pm 0.52 \pm 0.22)\%$	0
$D^0 \to h^+h^-$ [1075] (Belle 976 fb^{-1})	$A_{CP}(K^+K^-)$	$(-0.32 \pm 0.21 \pm 0.09)\%$	
	$A_{CP}(\pi^+\pi^-)$	$(+0.55 \pm 0.36 \pm 0.09)\%$	0
$D^0 \to h^+h^-$ [1076,1077] (CDF 9.7 fb^{-1})	$A_{CP}(K^+K^-) - A_{CP}(\pi^+\pi^-)$	$(-0.62 \pm 0.21 \pm 0.10)\%$	
	$A_{CP}(K^+K^-)$	$(-0.32 \pm 0.21)\%$	
	$A_{CP}(\pi^+\pi^-)$	$(+0.31 \pm 0.22)\%$	0.27 ± 0.01
$D^0 \to h^+h^-$ [1078](LHCb 3.0 fb^{-1}, $D^{*+} \to D^0\pi^+$ tag)	$A_{CP}(K^+K^-) - A_{CP}(\pi^+\pi^-)$	$(-0.10 \pm 0.08 \pm 0.03)\%$	$0.1153 \pm 0.0007 \pm 0.0018$
$D^0 \to h^+h^-$ [1058] (LHCb 3 fb^{-1}, $\overline{B} \to D^0\mu^-X$ tag)	$A_{CP}(K^+K^-) - A_{CP}(\pi^+\pi^-)$	$(+0.14 \pm 0.16 \pm 0.08)\%$	0.014 ± 0.004

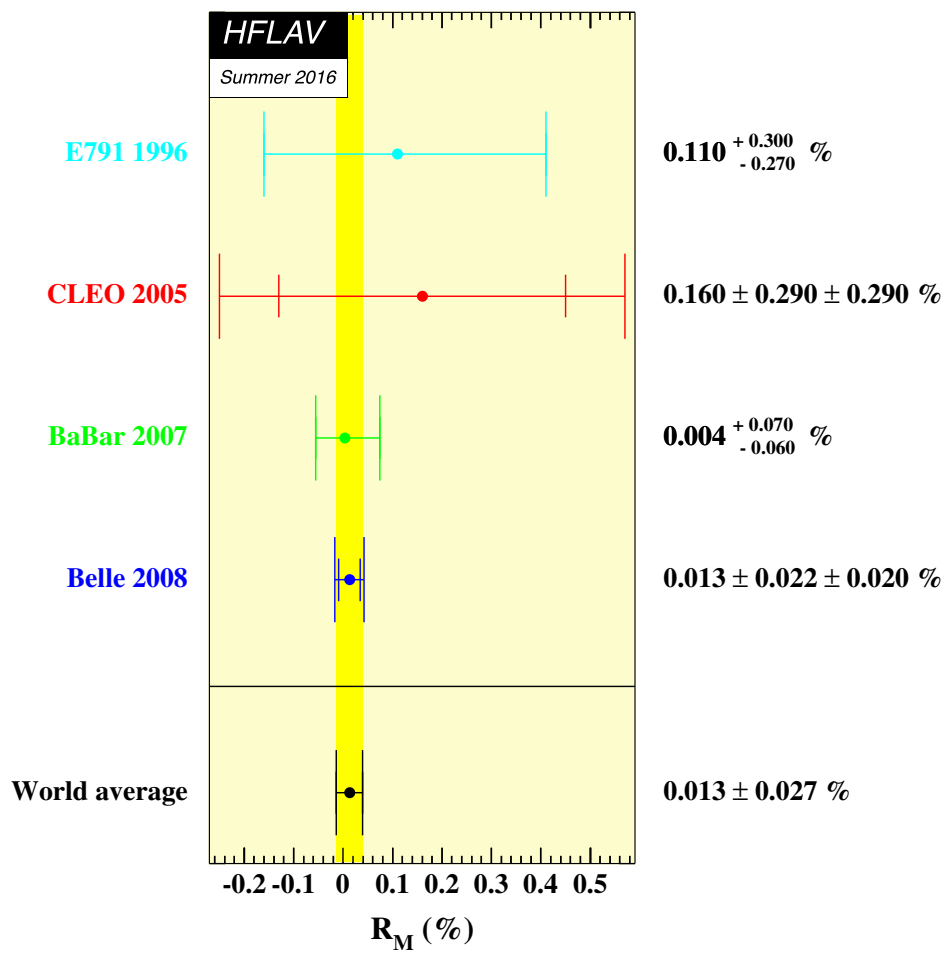

Fig. 191 World average value of $R_M = (x^2 + y^2)/2$ from Ref. [1060], as calculated from $D^0 \to K^+\ell^-\bar{\nu}$ measurements [1062–1065]

CPV-allowed fit. In the latter fit, the χ^2 at the no-mixing point $(x, y) = (0, 0)$ is 450 units above the minimum value, which, for two degrees of freedom, corresponds to a confidence level[39] (C.L.) $> 11.5\sigma$. Thus, no mixing is excluded at this high level. In the $(|q/p|, \phi)$ plot, the no-CPV point (1, 0)

[39] This is the limit of the CERNLIB PROB routine [1094] used for this calculation.

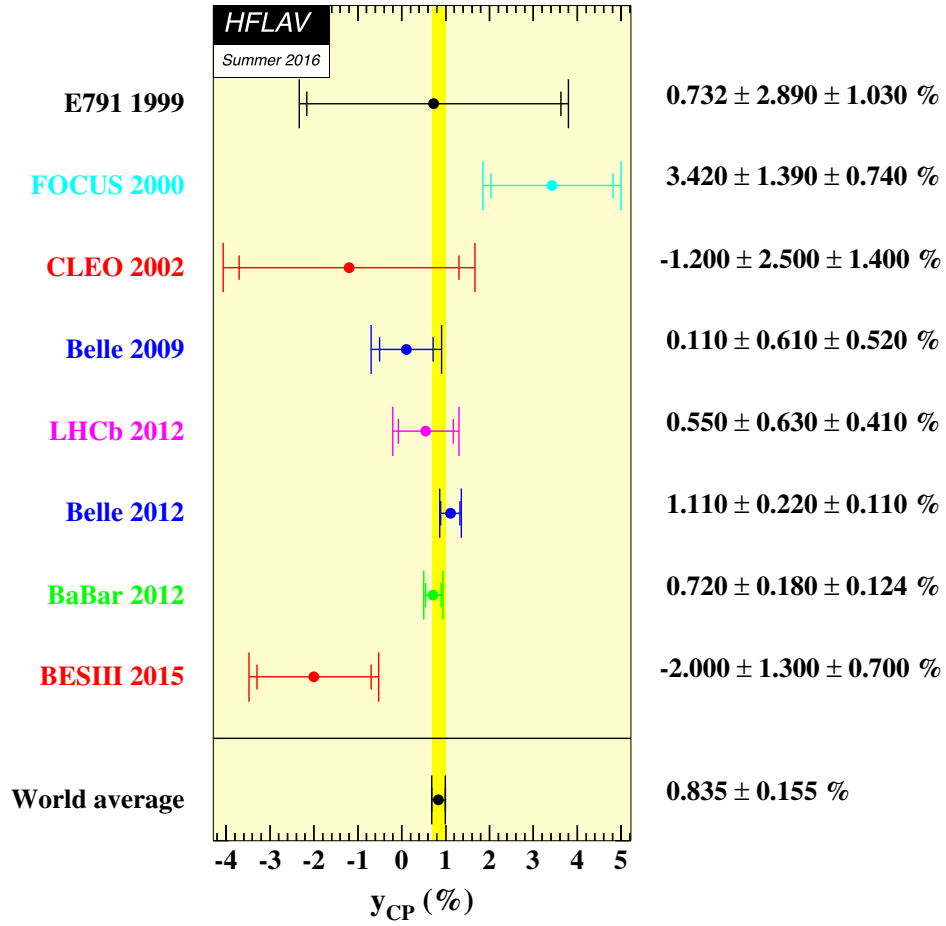

Fig. 192 World average value of y_{CP} from Ref. [1060], as calculated from $D^0 \to K^+K^-, \pi^+\pi^-$ measurements [1079–1086]

is within the 1σ contour; thus the data is consistent with *CP* conservation.

One-dimensional likelihood curves for individual parameters are obtained by allowing, for a fixed value of a selected parameter, all other fitted parameters to take their preferred values. The resulting functions $\Delta\chi^2 = \chi^2 - \chi^2_{\rm min}$ ($\chi^2_{\rm min}$ is the minimum value) are shown in Fig. 197. The points where $\Delta\chi^2 = 3.84$ determine 95% C.L. intervals for the parameters. These intervals are listed in Table 262.

8.1.4 Conclusions

From the fit results listed in Table 262 and shown in Figs. 196 and 197, we conclude that:

- the experimental data consistently indicate that D^0 mesons mix. The no-mixing point $x = y = 0$ is excluded at $> 11.5\sigma$. The parameter x differs from zero by 1.9σ, and y differs from zero by 9.4σ. This mixing is presumably dominated by long-distance processes, which are difficult to calculate. Thus unless it turns out that $|x| \gg |y|$ [1053], which is not indicated, it will be difficult to identify new physics from (x, y) alone.
- Since y_{CP} is positive, the *CP*-even state is shorter-lived as in the K^0-$\bar{K}^0$ system. However, since x also appears to be positive, the *CP*-even state is heavier, unlike in the K^0-$\bar{K}^0$ system.
- There is no evidence for *CPV* arising from D^0-$\bar{D}^0$ mixing ($|q/p| \neq 1$) or from a phase difference between the mixing amplitude and a direct decay amplitude ($\phi \neq 0$). The CDF experiment (and initially LHCb) measured a time-integrated asymmetry in $D^0 \to K^+K^-, \pi^+\pi^-$ decays that hints at direct *CPV* (see Table 261); however, recent measurements from LHCb with higher statistics disfavor this hypothesis and are consistent with zero.

8.2 *CP* asymmetries

One way *CP* violation manifests itself is if the decay rate for a particle differs from that of its *CP*-conjugate[1095]. Such phenomena can be classified into two broad categories, termed *direct CP* violation and *indirect CP* violation [1096]. Direct *CP* violation refers to charm changing, $\Delta C = 1$, processes and can occur in both charged and neutral charm hadron decays. It results from interference between two different decay amplitudes (e.g., a penguin and tree amplitude)

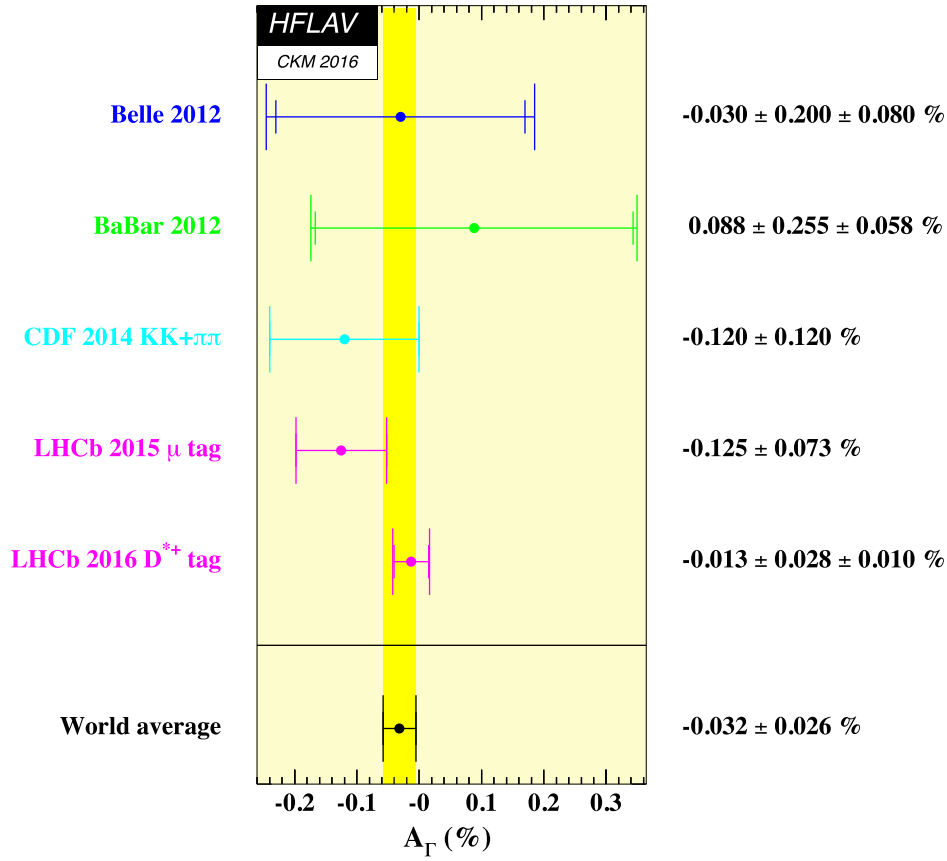

Fig. 193 World average value of A_Γ from Ref. [1060], as calculated from $D^0 \to K^+K^-$, $\pi^+\pi^-$ measurements [1084,1085, 1087–1089]

Table 262 Results of the global fit for different assumptions concerning *CPV*

Parameter	No *CPV*	No direct *CPV* in DCS decays	*CPV*-allowed	*CPV*-allowed 95% C.L. interval
x (%)	$0.46^{+0.14}_{-0.15}$	$0.41^{+0.14}_{-0.15}$	0.32 ± 0.14	[0.04, 0.62]
y (%)	0.62 ± 0.08	0.61 ± 0.07	$0.69^{+0.06}_{-0.07}$	[0.50, 0.80]
$\delta_{K\pi}$ (°)	$8.0^{+9.7}_{-11.2}$	$4.8^{+10.4}_{-12.3}$	$15.2^{+7.6}_{-10.0}$	[−16.8, 30.1]
R_D (%)	$0.348^{+0.004}_{-0.003}$	$0.347^{+0.004}_{-0.003}$	$0.349^{+0.004}_{-0.003}$	[0.342, 0.356]
A_D (%)	–	–	-0.88 ± 0.99	[−2.8, 1.0]
$\lvert q/p \rvert$	–	0.999 ± 0.014	$0.89^{+0.08}_{-0.07}$	[0.77, 1.12]
ϕ (°)	–	$0.05^{+0.54}_{-0.53}$	$-12.9^{+9.9}_{-8.7}$	[−30.2, 10.6]
$\delta_{K\pi\pi}$ (°)	$20.4^{+23.3}_{-23.8}$	$22.6^{+24.1}_{-24.4}$	$31.7^{+23.5}_{-24.2}$	[−16.4, 77.7]
A_π(%)	–	$+0.02 \pm 0.13$	$+0.01 \pm 0.14$	[−0.25, 0.28]
A_K(%)	–	-0.11 ± 0.13	-0.11 ± 0.13	[−0.37, 0.14]
x_{12} (%)	–	$0.41^{+0.14}_{-0.15}$		[0.10, 0.67]
y_{12}(%)	–	0.61 ± 0.07		[0.47, 0.75]
ϕ_{12}(°)	–	-0.17 ± 1.8		[−5.3, 4.4]

that have different weak (CKM) and strong phases.[40] In the Standard Model a difference in strong phases may arise for example due to final-state interactions (FSI)[1097], different isospin amplitudes, intermediate resonance contributions, or different partial waves. A difference in weak phases arises from different CKM vertex couplings, as is often the case for tree and penguin diagrams. Within the SM direct *CP* violation is expected only in Singly Cabibbo Suppressed (SCS) charm decays, as only these decays receive a contribution from the penguin amplitude. This type of *CP* violation depends on the decay mode, the SM asymmetries may reach

[40] The weak phase difference will have opposite signs for $D \to f$ and $\overline{D} \to \bar{f}$ decays, while the strong phase difference will have the same sign. As a result, squaring the total amplitudes to obtain the decay rates gives interference terms having opposite sign, i.e., non-identical decay rates.

Table 263 Individual contributions to the χ^2 for the *CPV*-allowed fit

Observable	χ^2	$\sum\chi^2$
y_{CP}	1.19	1.19
A_Γ	0.83	2.01
$x_{K^0_S\pi^+\pi^-}$ Belle	1.33	3.35
$y_{K^0_S\pi^+\pi^-}$ Belle	5.30	8.64
$\lvert q/p\rvert_{K^0_S\pi^+\pi^-}$ Belle	0.10	8.74
$\phi_{K^0_S\pi^+\pi^-}$ Belle	0.23	8.97
$x_{K^0_S\pi^+\pi^-}$ LHCb	4.51	13.48
$y_{K^0_S\pi^+\pi^-}$ LHCb	0.40	13.88
$x_{K^0_S h^+h^-}$ BaBar	0.36	14.24
$y_{K^0_S h^+h^-}$ BaBar	0.19	14.43
$x_{\pi^0\pi^+\pi^-}$ BaBar	0.77	15.20
$y_{\pi^0\pi^+\pi^-}$ BaBar	0.22	15.42
$(x^2+y^2)_{K^+\ell^-\nu}$	0.14	15.56
$x_{K^+\pi^-\pi^0}$ BaBar	7.10	22.67
$y_{K^+\pi^-\pi^0}$ BaBar	3.92	26.58
CLEOc $(x/y/R_D/\cos\delta/\sin\delta)$	10.53	37.12
$R_D^+/x'^{2+}/y'^+$ BaBar	11.13	48.25
$R_D^-/x'^{2-}/y'^-$ BaBar	6.04	54.29
$R_D^+/x'^{2+}/y'^+$ Belle	2.08	56.36
$R_D^-/x'^{2-}/y'^-$ Belle	3.22	59.58
$R_D/x'^2/y'$ CDF	1.29	60.87
$R_D^+/x'^{2+}/y'^+$ LHCb	0.58	61.46
$R_D^-/x'^{2-}/y'^-$ LHCb	1.65	63.11
$A_{KK}/A_{\pi\pi}$ BaBar	0.30	63.41
$A_{KK}/A_{\pi\pi}$ Belle	2.89	66.30
$A_{KK}/A_{\pi\pi}$ CDF	4.63	70.94
$A_{KK}-A_{\pi\pi}$ LHCb ($D^{*+}\to D^0\pi^+$ tag)	0.12	71.05
$A_{KK}-A_{\pi\pi}$ LHCb ($\overline{B}\to D^0\mu^-X$ tag)	2.24	73.30
$(x^2+y^2)_{K^+\pi^-\pi^+\pi^-}$ LHCb	3.48	76.78

a percent level. Indirect *CP* violation refers to $\Delta C=2$ processes and arises in D^0 decays due to $D^0-\bar{D}^0$ mixing. It can occur as an asymmetry in the mixing itself, or it can result from interference between a decay amplitude following mixing and a non-mixed amplitude. Within the SM charm indirect *CP* asymmetry is expected to be universal.

The *CP* asymmetry is defined as the difference between D and $\overline{D}$ partial widths divided by their sum:

$$A_{CP}=\frac{\Gamma(D)-\Gamma(\overline{D})}{\Gamma(D)+\Gamma(\overline{D})}. \tag{225}$$

In the case of D^+ and D_s^+ decays, A_{CP} measures direct *CP* violation; in the case of D^0 decays, A_{CP} measures direct and indirect *CP* violation combined (see also Sect. 8.4).

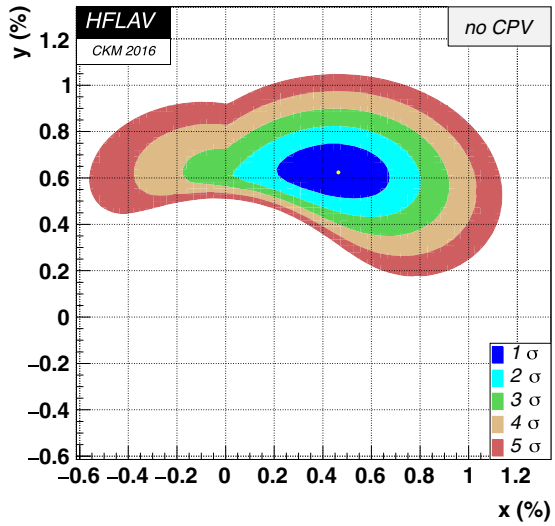

Fig. 194 Two-dimensional contours for mixing parameters (x, y), for no *CPV*

In each experiment, care must be taken to correct for production and detection asymmetries. To take into account differences in production rates between D and $\overline{D}$ (which would affect the number of respective decays observed), some experiments (like FOCUS and E791) normalize to a Cabibbo-favored mode. In this case there is the additional benefit that most corrections due to reconstruction inefficiencies cancel out, reducing systematic uncertainties. An implicit assumption is that there is no measurable *CP* violation in the Cabibbo-favored normalizing mode. The *CP* asymmetry is calculated as

$$A_{CP}=\frac{\eta(D)-\eta(\overline{D})}{\eta(D)+\eta(\overline{D})}, \tag{226}$$

where (considering, for example, $D^0\to K^-K^+$)

$$\eta(D)=\frac{N(D^0\to K^-K^+)}{N(D^0\to K^-\pi^+)}, \tag{227}$$

$$\eta(\overline{D})=\frac{N(\bar{D}^0\to K^-K^+)}{N(\bar{D}^0\to K^+\pi^-)}. \tag{228}$$

Other experiments (like LHCb) determine A_{CP} through the relation:

$$A_{\text{meas}}=A_{CP}+A_{\text{prod}}+A_{\text{det}}, \tag{229}$$

where A_{meas} is the measured asymmetry, A_{prod} is the asymmetry in the charm meson production, and A_{det} is due to difference in detection efficiencies between positively and negatively charged hadrons.

Values of A_{CP} for D^+, D^0 and D_s^+ decays are listed in Tables 264, 265, 266, 267 and 268 respectively. In these tables we report asymmetries for the actual final state, i.e., resonant substructure is implicitly included but not considered separately. The high accuracy of these measurements

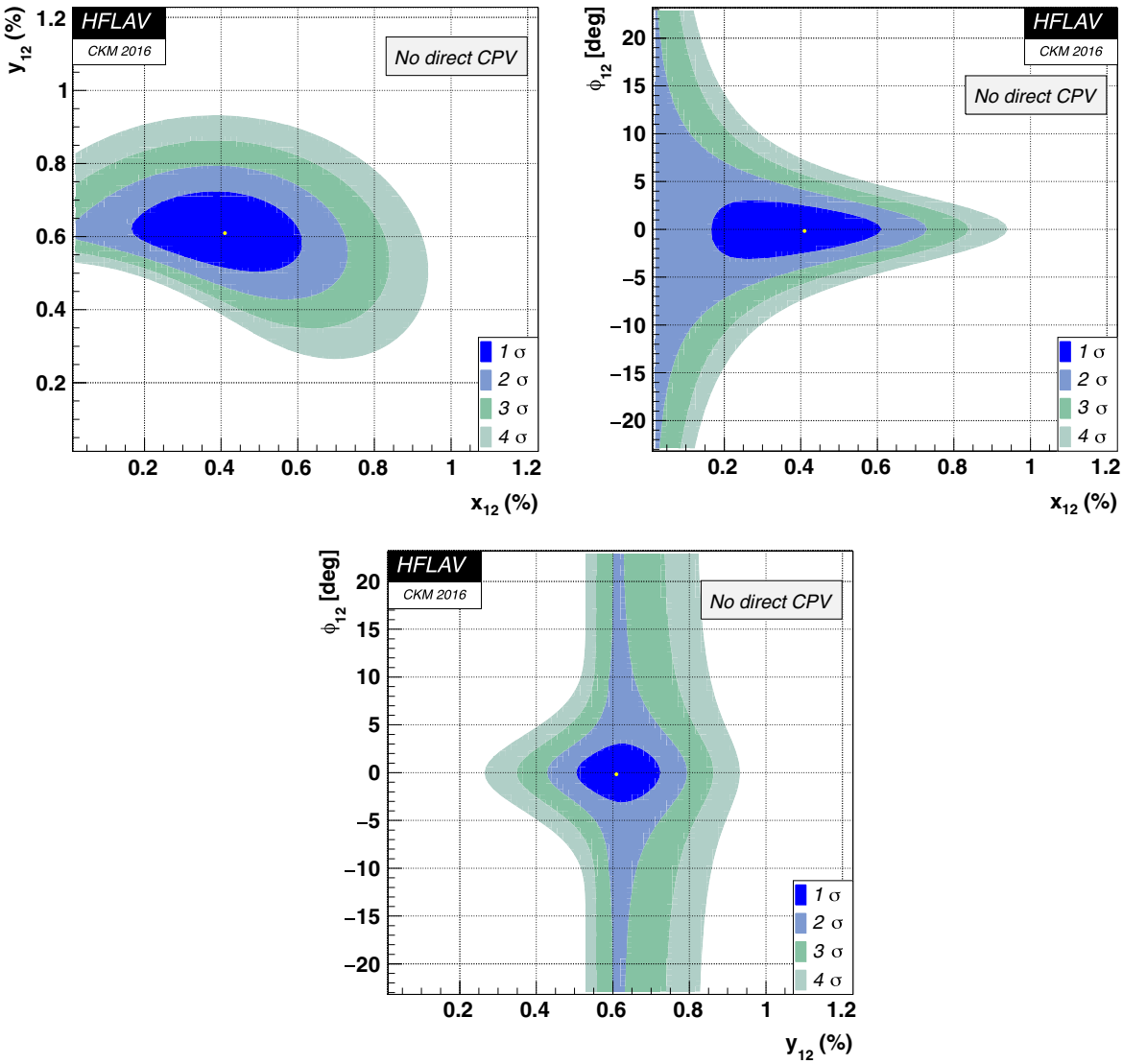

Fig. 195 Two-dimensional contours for theoretical parameters (x_{12}, y_{12}) (*top left*), (x_{12}, ϕ_{12}) (*top right*), and (y_{12}, ϕ_{12}) (*bottom*), for no direct *CPV* in DCS decays

allows one to see and correct for *CP* violation due to the CPV in K^0-$\bar{K}^0$ mixing [1098]. For example, the decay modes $D^+ \to (\bar{K}^0/K^0)K^+$ and $D_s^+ \to (\bar{K}^0/K^0)\pi^+$ (shown in Tables 264 and 268, respectively) are the modes $D^+ \to K_s^0 K^+$ and $D_s^+ \to K_s^0 \pi^+$ after subtracting for this effect. For multi-body decays some experiments use model independent techniques to reveal local *CP* asymmetry. The first technique (Miranda method) [1099] uses a binned χ^2 approach to compare the relative density in a bin of phase space of a decay with that of its *CP* conjugate. In the Energy Test technique [1100] two event samples are compared and a test statistic variable (T) is used to determine the average distances of events in phase space. If the distributions of events in both samples are identical, T will randomly fluctuate around a value close to zero.

Overall, *CP* asymmetry measurements have been carried out for 49 charm decay modes, and in several modes the sensitivity is well below 5×10^{-3}. There is currently no evidence for *CP* violation in the charm meson sector. The *CP* asymmetry observed in the mode $D^+ \to K_s^0 \pi^+$ is consistent with what expected from the $K^0 - \bar{K}^0$ system [1098], and thus it is not attributed to charm.

Neither in the charm baryon sector there is evidence of *CP* asymmetry. These are just two measurements on Λ_C^+, with limited sensitivity, done by FOCUS [1101] and by CLEO [1102].

Taken together, the limits obtained for *CP* asymmetries in the charm sector pose tight constraints on new physics models.

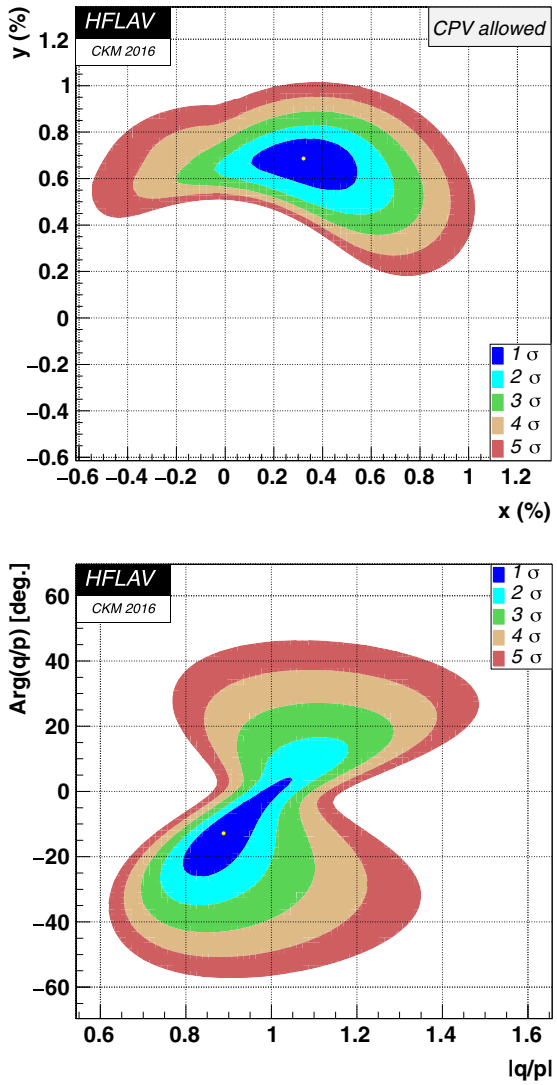

Fig. 196 Two-dimensional contours for parameters (x, y) (*top*) and $(|q/p|, \phi)$ (*bottom*), allowing for *CPV*

8.3 T-odd asymmetries

Measuring T-odd asymmetries provides an alternative way to search for *CP* violation in the charm sector, due to *CPT* invariance. T-odd asymmetries are measured using triple-product correlations of the form $\vec{a} \cdot (\vec{b} \times \vec{c})$, where a, b, and c are spins or momenta; this combination is odd under time reversal (T). If the triple-product is formed using *both* spin and momenta, i.e.,

$$\vec{s}_1 \cdot (\vec{p}_2 \times \vec{p}_3), \tag{230}$$

then it is even for P-conjugation. However, if only momenta are used, then it is odd for P-conjugation. In this case the asymmetry allows one to probe *CP* violation occurring via P-violation. This may arise in P-odd amplitudes, which are allowed in decays to final states with 4 spinless particles.

Taking as an example the decay mode $D^0 \to K^+K^-\pi^+\pi^-$, one forms the triple-product correlation using the momenta of the final state particles. We note that when using only momenta, at least four daughter particles are required to give a nonzero correlation (as three daughters decay in a plane). Defining for D^0 the T-odd correlation

$$C_T \equiv \vec{p}_{K^+} \cdot (\vec{p}_{\pi^+} \times \vec{p}_{\pi^-}), \tag{231}$$

and the corresponding quantity for $\bar{D}^0$

$$\overline{C}_T \equiv \vec{p}_{K^-} \cdot (\vec{p}_{\pi^-} \times \vec{p}_{\pi^+}), \tag{232}$$

one constructs the asymmetry

$$A_T = \frac{\Gamma(C_T > 0) - \Gamma(C_T < 0)}{\Gamma(C_T > 0) + \Gamma(C_T < 0)} \tag{233}$$

for D^0 decays and

$$\overline{A}_T = \frac{\Gamma(-\overline{C}_T > 0) - \Gamma(-\overline{C}_T < 0)}{\Gamma(-\overline{C}_T > 0) + \Gamma(-\overline{C}_T < 0)} \tag{234}$$

for $\bar{D}^0$ decays. In these expressions, Γ represents a partial width. The asymmetries A_T and $\overline{A}_T$ depend on the angular distribution of the daughter particles and may be nonzero due to final state interactions or P-violation in weak decays.

Since $P(C_T) = -C_T$ and $C(C_T) = \overline{C_T}$, $CP(A_T) = \overline{A}_T$. One can thus construct the *CP*-odd (and P-odd, T-odd) quantity

$$\mathcal{A}_T \equiv \frac{A_T - \overline{A}_T}{2}; \tag{235}$$

a nonzero value indicates *CP* violation (see Refs. [1140–1145]).

Recently, this topic has been revisited (see Refs. [1146, 1147]) with the suggestion to use other asymmetries constructed from triple products in multi-body decays to probe C, P, and *CP* symmetries. Up until now, experiments have measured only the asymmetry $\mathcal{A}_T$ defined in Eq. (235). (Note that this asymmetry is referred to in the literature by several names: $A_{T\,\mathrm{viol}}$, a_{CP}^{P}, and $a_{CP}^{T-\mathrm{odd}}$.)

Values of $\mathcal{A}_T$ for D^+, D_s^+, and D^0 decay modes are listed in Table 269. The first measurements were made by FOCUS, and subsequent BABAR measurements reached a sensitivity of $\sim 1\%$. Currently the best sensitivity is from LHCb.

However, despite relatively high precision ($<1\%$), there is no evidence for *CP* violation.

8.4 Interplay of direct and indirect *CP* violation

In decays of D^0 mesons, *CP* asymmetry measurements have contributions from both direct and indirect *CP* violation as discussed in Sect. 8.1. The contribution from indirect *CP* violation depends on the decay-time distribution of the data

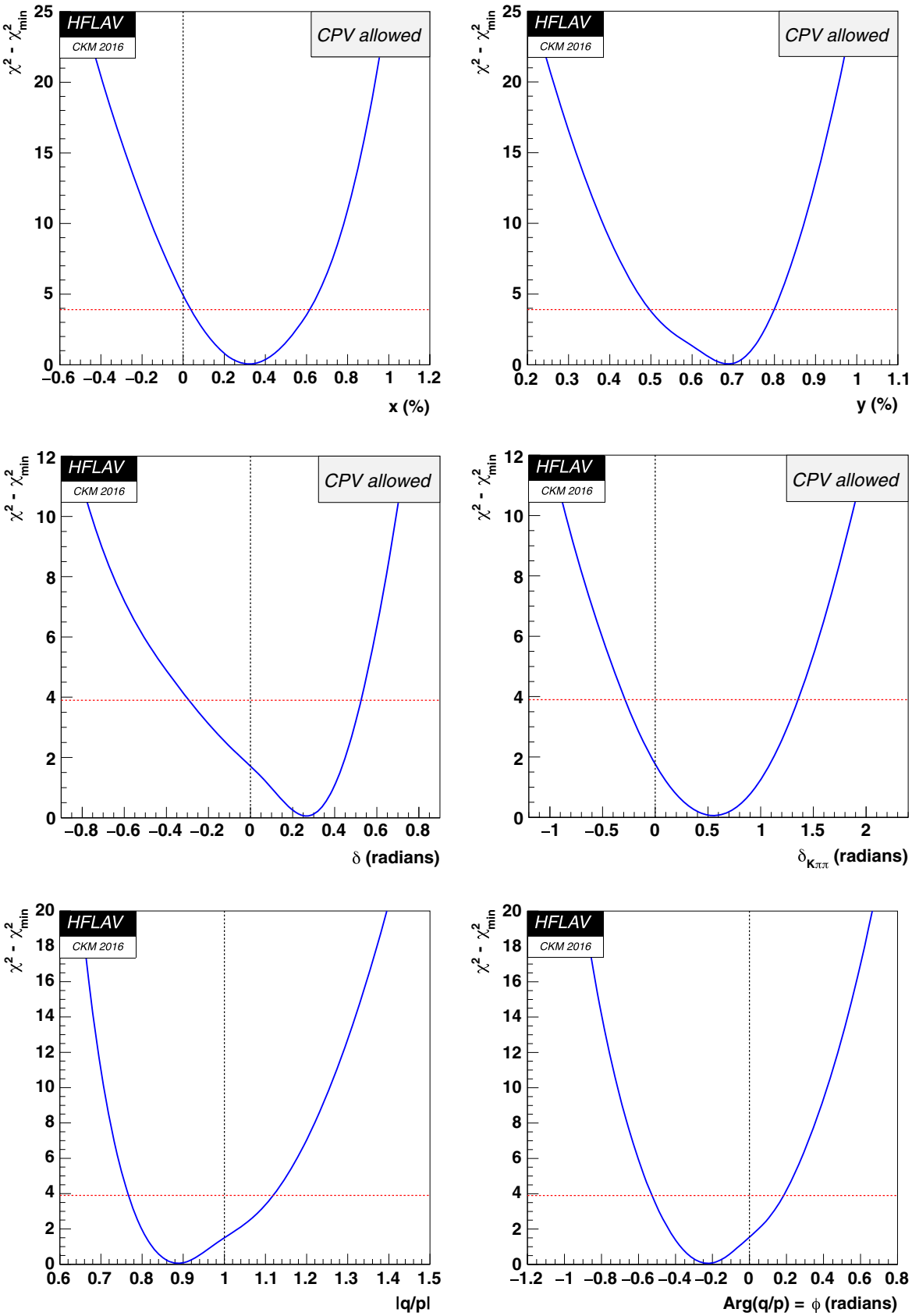

Fig. 197 The function $\Delta\chi^2 = \chi^2 - \chi^2_{\text{min}}$ for fitted parameters x, y, δ, $\delta_{K\pi\pi}$, $|q/p|$, and ϕ. The points where $\Delta\chi^2 = 3.84$ (denoted by dashed horizontal lines) determine 95% C.L. intervals

Table 264 *CP* asymmetries $A_{CP} = [\Gamma(D^+) - \Gamma(D^-)]/[\Gamma(D^+) + \Gamma(D^-)]$ for two-body $D^\pm$ decays

Mode	Year	Collaboration	A_{CP}
$D^+ \to \mu^+\nu$	2008	CLEO [1103]	$+0.08 \pm 0.08$
$D^+ \to \pi^+\pi^0$	2010	CLEO [1104]	$+0.029 \pm 0.029 \pm 0.003$
$D^+ \to \pi^+\eta$	2011	Belle [1105]	$+0.0174 \pm 0.0113 \pm 0.0019$
	2010	CLEO [1104]	$-0.020 \pm 0.023 \pm 0.003$
		HFLAV average	$+0.010 \pm 0.010$
$D^+ \to \pi^+\eta'$	2011	Belle [1105]	$-0.0012 \pm 0.0112 \pm 0.0017$
	2010	CLEO [1104]	$-0.040 \pm 0.034 \pm 0.003$
		HFLAV average	-0.005 ± 0.011
$D^+ \to K^+\pi^0$	2010	CLEO [1104]	$-0.035 \pm 0.107 \pm 0.009$
$D^+ \to K_s^0\pi^+$	2014	CLEO [1106]	$-0.011 \pm 0.006 \pm 0.002$
	2012	Belle [1107]	$-0.00363 \pm 0.00094 \pm 0.00067$
	2011	BaBar [1108]	$-0.0044 \pm 0.0013 \pm 0.0010$
	2002	FOCUS [1109]	$-0.016 \pm 0.015 \pm 0.009$
		HFLAV average	-0.0041 ± 0.0009
$D^+ \to K_s^0K^+$	2013	BaBar [1110]	$+0.0013 \pm 0.0036 \pm 0.0025$
	2013	Belle [1111]	$-0.0025 \pm 0.0028 \pm 0.0014$
	2010	CLEO [1104]	$-0.002 \pm 0.015 \pm 0.009$
	2002	FOCUS [1109]	$+0.071 \pm 0.061 \pm 0.012$
		HFLAV average	-0.0011 ± 0.0025
$D^+ \to (\overline{K}^0/K^0)K^+$	2014	LHCb [1112]	$+0.0003 \pm 0.0017 \pm 0.0014$
	2013	BaBar [1110]	$+0.0046 \pm 0.0036 \pm 0.0025$
	2013	Belle [1111]	$-0.0008 \pm 0.0028 \pm 0.0014$
		HFLAV average	$+0.0011 \pm 0.0017$

Table 265 *CP* asymmetries $A_{CP} = [\Gamma(D^+) - \Gamma(D^-)]/[\Gamma(D^+) + \Gamma(D^-)]$ for three- and four-body $D^\pm$ decays

Mode	Year	Collaboration	A_{CP}
$D^+ \to \pi^+\pi^-\pi^+$	2014	LHCb [1113]	Model independent technique, no evidence for *CP* violation
	1997	E791 [1114]	-0.017 ± 0.042 (stat.)
$D^+ \to K^-\pi^+\pi^+$	2014	D0 [1115]	$-0.0016 \pm 0.0015 \pm 0.0009$
	2014	CLEO [1106]	$-0.003 \pm 0.002 \pm 0.004$
		HFLAV average	-0.0018 ± 0.0016
$D^+ \to K_s^0\pi^+\pi^0$	2014	CLEO [1106]	$-0.001 \pm 0.007 \pm 0.002$
$D^+ \to K^+K^-\pi^+$	2014	CLEO [1106]	$-0.001 \pm 0.009 \pm 0.004$
	2013	BaBar [1116]	$+0.0037 \pm 0.0030 \pm 0.0015$
	2008	CLEO [1117]	Dalitz plot analysis, no evidence for *CP* violation
	2000	FOCUS [1118]	$+0.006 \pm 0.011 \pm 0.005$
	1997	E791 [1114]	-0.014 ± 0.029 (stat.)
		HFLAV average	$+0.0032 \pm 0.0031$
$D^+ \to K^-\pi^+\pi^+\pi^0$	2014	CLEO [1106]	$-0.003 \pm 0.006 \pm 0.004$
$D^+ \to K_s^0\pi^+\pi^+\pi^-$	2014	CLEO [1106]	$+0.000 \pm 0.012 \pm 0.003$
$D^+ \to K_s^0K^+\pi^+\pi^-$	2005	FOCUS [1119]	$-0.042 \pm 0.064 \pm 0.022$

Table 266 *CP* asymmetries $A_{CP} = [\Gamma(D^0) - \Gamma(\bar{D}^0)]/[\Gamma(D^0) + \Gamma(\bar{D}^0)]$ for two-body D^0, $\bar{D}^0$ decays

Mode	Year	Collaboration	A_{CP}
$D^0 \to \pi^+\pi^-$	2014	LHCb [1058]	$-0.0020 \pm 0.0019 \pm 0.0010$
	2012	CDF [1120]	$+0.0022 \pm 0.0024 \pm 0.0011$
	2008	BaBar [1074]	$-0.0024 \pm 0.0052 \pm 0.0022$
	2012	Belle [1121]	$+0.0043 \pm 0.0052 \pm 0.0012$
	2002	CLEO [1081]	$+0.019 \pm 0.032 \pm 0.008$
	2000	FOCUS [1118]	$+0.048 \pm 0.039 \pm 0.025$
	1998	E791 [1122]	$-0.049 \pm 0.078 \pm 0.030$
		HFLAV average	$+0.0000 \pm 0.0015$
$D^0 \to \pi^0\pi^0$	2014	Belle [1123]	$-0.0003 \pm 0.0064 \pm 0.0010$
	2001	CLEO [1124]	$+0.001 \pm 0.048$ (stat. and syst. combined)
		HFLAV average	-0.0003 ± 0.0064
$D^0 \to K_s^0\pi^0$	2014	Belle [1123]	$-0.0021 \pm 0.0016 \pm 0.0007$
	2001	CLEO [1124]	$+0.001 \pm 0.013$ (stat. and syst. combined)
		HFLAV average	-0.0020 ± 0.0017
$D^0 \to K_s^0\eta$	2011	Belle [1125]	$+0.0054 \pm 0.0051 \pm 0.0016$
$D^0 \to K_s^0\eta'$	2011	Belle [1125]	$+0.0098 \pm 0.0067 \pm 0.0014$
$D^0 \to K_s^0K_s^0$	2015	LHCb [1126]	$-0.029 \pm 0.052 \pm 0.022$
	2001	CLEO [1124]	-0.23 ± 0.19 (stat. and syst. combined)
		HFLAV average	-0.046 ± 0.054
$D^0 \to K^-\pi^+$	2014	CLEO [1106]	$+0.003 \pm 0.003 \pm 0.006$
$D^0 \to K^+K^-$	2014	LHCb [1058]	$-0.0006 \pm 0.0015 \pm 0.0010$
	2012	CDF [1120]	$-0.0024 \pm 0.0022 \pm 0.0009$
	2008	BaBar [1074]	$+0.0000 \pm 0.0034 \pm 0.0013$
	2012	Belle [1121]	$-0.0043 \pm 0.0030 \pm 0.0011$
	2002	CLEO [1081]	$+0.000 \pm 0.022 \pm 0.008$
	2000	FOCUS [1118]	$-0.001 \pm 0.022 \pm 0.015$
	1998	E791 [1122]	$-0.010 \pm 0.049 \pm 0.012$
		HFLAV average	-0.0016 ± 0.0012

Table 267 *CP* asymmetries $A_{CP} = [\Gamma(D^0) - \Gamma(\bar{D}^0)]/[\Gamma(D^0) + \Gamma(\bar{D}^0)]$ for three- and four-body D^0, $\bar{D}^0$ decays

Mode	Year	Collaboration	A_{CP}
$D^0 \to \pi^+\pi^-\pi^0$	2015	LHCb [1127]	Model independent technique, no evidence for *CP* violation
	2008	BaBar [1128]	$+0.0031 \pm 0.0041 \pm 0.0017$
	2008	Belle [1129]	$+0.0043 \pm 0.0130$ (stat. and syst. combined)
	2005	CLEO [1130]	$+0.01^{+0.09}_{-0.07} \pm 0.05$
		HFLAV average	$+0.0032 \pm 0.0042$
$D^0 \to K^-\pi^+\pi^0$	2014	CLEO [1106]	$+0.001 \pm 0.003 \pm 0.004$
$D^0 \to K^+\pi^-\pi^0$	2005	Belle [1131]	-0.006 ± 0.053 (stat.)
	2001	CLEO [1132]	$+0.09^{+0.25}_{-0.22}$ (stat.)
		HFLAV average	-0.0014 ± 0.0517
$D^0 \to K_s^0\pi^+\pi^-$	2012	CDF [1133]	$-0.0005 \pm 0.0057 \pm 0.0054$
	2004	CLEO [1134]	$-0.009 \pm 0.021^{+0.016}_{-0.057}$
		HFLAV average	-0.0008 ± 0.0077
$D^0 \to K_s^0 + K^-\pi^+$	2016	LHCb [473]	Amplitude analysis, no evidence for *CP* violation
$D^0 \to K_s^0 + K^+\pi^-$	2016	LHCb [473]	Amplitude analysis, no evidence for *CP* violation

Table 267 continued

Mode	Year	Collaboration	A_{CP}
$D^0 \to K^+K^-\pi^0$	2008	BaBar [1128]	$-0.0100 \pm 0.0167 \pm 0.0025$
$D^0 \to \pi^-\pi^-\pi^+\pi^+$	2013	LHCb [1135]	Model independent technique, no evidence for CP violation
$D^0 \to K^-\pi^+\pi^+\pi^-$	2014	CLEO [1106]	$+0.002 \pm 0.003 \pm 0.004$
$D^0 \to K^+\pi^-\pi^+\pi^-$	2005	Belle [1131]	-0.018 ± 0.044 (stat.)
$D^0 \to K^+K^-\pi^+\pi^-$	2013	LHCb [1135]	Model independent technique, no evidence for CP violation
	2012	CLEO [1136]	Amplitude analysis, no evidence for CP violation
	2005	FOCUS [1119]	$-0.082 \pm 0.056 \pm 0.047$

Table 268 CP asymmetries $A_{CP} = [\Gamma(D_s^+) - \Gamma(D_s^-)]/[\Gamma(D_s^+) + \Gamma(D_s^-)]$ for $D_s^\pm$ decays

Mode	Year	Collaboration	A_{CP}
$D_s^+ \to \mu^+\nu$	2009	CLEO [1137]	$+0.048 \pm 0.061$
$D_s^+ \to \pi^+\eta$	2013	CLEO [1138]	$+0.011 \pm 0.030 \pm 0.008$
$D_s^+ \to \pi^+\eta'$	2013	CLEO [1138]	$-0.022 \pm 0.022 \pm 0.006$
$D_s^+ \to K_s^0\pi^+$	2013	BaBar [1110]	$+0.006 \pm 0.020 \pm 0.003$
	2010	Belle [1139]	$+0.0545 \pm 0.0250 \pm 0.0033$
	2010	CLEO [1104]	$+0.163 \pm 0.073 \pm 0.003$
		HFLAV average	$+0.0311 \pm 0.0154$
$D_s^+ \to (\bar{K}^0/K^0)\pi^+$	2014	LHCb [1112]	$+0.0038 \pm 0.0046 \pm 0.0017$
	2013	BaBar [1110]	$+0.003 \pm 0.020 \pm 0.003$
		HFLAV average	$+0.0038 \pm 0.0048$
$D_s^+ \to K_s^0K^+$	2013	CLEO [1138]	$+0.026 \pm 0.015 \pm 0.006$
	2013	BaBar [1110]	$-0.0005 \pm 0.0023 \pm 0.0024$
	2010	Belle [1139]	$+0.0012 \pm 0.0036 \pm 0.0022$
		HFLAV average	$+0.0008 \pm 0.0026$
$D_s^+ \to K^+\pi^0$	2010	CLEO [1104]	$+0.266 \pm 0.228 \pm 0.009$
$D_s^+ \to K^+\eta$	2010	CLEO [1104]	$+0.093 \pm 0.152 \pm 0.009$
$D_s^+ \to K^+\eta'$	2010	CLEO [1104]	$+0.060 \pm 0.189 \pm 0.009$
$D_s^+ \to \pi^+\pi^+\pi^-$	2013	CLEO [1138]	$-0.007 \pm 0.030 \pm 0.006$
$D_s^+ \to \pi^+\pi^0\eta$	2013	CLEO [1138]	$-0.005 \pm 0.039 \pm 0.020$
$D_s^+ \to \pi^+\pi^0\eta'$	2013	CLEO [1138]	$-0.004 \pm 0.074 \pm 0.019$
$D_s^+ \to K_s^0K^+\pi^0$	2013	CLEO [1138]	$-0.016 \pm 0.060 \pm 0.011$
$D_s^+ \to K_s^0K_s^0\pi^+$	2013	CLEO [1138]	$+0.031 \pm 0.052 \pm 0.006$
$D_s^+ \to K^+\pi^+\pi^-$	2013	CLEO [1138]	$+0.045 \pm 0.048 \pm 0.006$
$D_s^+ \to K^+K^-\pi^+$	2013	CLEO [1138]	$-0.005 \pm 0.008 \pm 0.004$
$D_s^+ \to K_s^0K^-\pi^+\pi^+$	2013	CLEO [1138]	$+0.041 \pm 0.027 \pm 0.009$
$D_s^+ \to K_s^0K^+\pi^+\pi^-$	2013	CLEO [1138]	$-0.057 \pm 0.053 \pm 0.009$
$D_s^+ \to K^+K^-\pi^+\pi^0$	2013	CLEO [1138]	$+0.000 \pm 0.027 \pm 0.012$

sample [1092]. This section describes a combination of measurements that allows the extraction of the individual contributions of the two types of CP violation. At the same time, the level of agreement for a no-CP-violation hypothesis is tested. The observables are:

$$A_\Gamma \equiv \frac{\tau(\bar{D}^0 \to h^+h^-) - \tau(D^0 \to h^+h^-)}{\tau(\bar{D}^0 \to h^+h^-) + \tau(D^0 \to h^+h^-)}, \tag{236}$$

where h^+h^- can be K^+K^- or $\pi^+\pi^-$, and

$$\Delta A_{CP} \equiv A_{CP}(K^+K^-) - A_{CP}(\pi^+\pi^-), \tag{237}$$

where A_{CP} are time-integrated CP asymmetries. The underlying theoretical parameters are:

$$a_{CP}^{\rm dir} \equiv \frac{|\mathcal{A}_{D^0\to f}|^2 - |\mathcal{A}_{\bar{D}^0\to f}|^2}{|\mathcal{A}_{D^0\to f}|^2 + |\mathcal{A}_{\bar{D}^0\to f}|^2},$$

Table 269 Measurements of the T-odd asymmetry $\mathcal{A}_T = (A_T - \overline{A}_T)/2$

Mode	Year	Collaboration	$\mathcal{A}_T$
$D^0 \to K^+K^-\pi^+\pi^-$	2014	LHCb [1148]	$+0.0018 \pm 0.0029 \pm 0.0004$
	2010	BaBar [1149]	$+0.0010 \pm 0.0051 \pm 0.0044$
	2005	FOCUS [1119]	$+0.010 \pm 0.057 \pm 0.037$
		HFLAV average	$+0.0017 \pm 0.0027$
$D^+ \to K_s^0K^+\pi^+\pi^-$	2011	BaBar [1150]	$-0.0120 \pm 0.0100 \pm 0.0046$
	2005	FOCUS [1119]	$+0.023 \pm 0.062 \pm 0.022$
		HFLAV average	-0.0110 ± 0.0109
$D_s^+ \to K_s^0K^+\pi^+\pi^-$	2011	BaBar [1150]	$-0.0136 \pm 0.0077 \pm 0.0034$
	2005	FOCUS [1119]	$-0.036 \pm 0.067 \pm 0.023$
		HFLAV average	-0.0139 ± 0.0084

Table 270 Inputs to the fit for direct and indirect CP violation. The first uncertainty listed is statistical, and the second is systematic

Year	Experiment	Results	$\Delta\langle t\rangle/\tau$	$\langle t\rangle/\tau$	References
2012	BaBar	$A_\Gamma = (+0.09 \pm 0.26 \pm 0.06)\%$	–	–	[1085]
2016	LHCb prompt	$A_\Gamma(KK) = (-0.030 \pm 0.032 \pm 0.010)\%$	–	–	[1089]
		$A_\Gamma(\pi\pi) = (+0.046 \pm 0.058 \pm 0.012)\%$	–	–	
2014	CDF	$A_\Gamma = (-0.12 \pm 0.12)\%$	–	–	[1087]
2015	LHCb SL	$A_\Gamma = (-0.125 \pm 0.073)\%$	–	–	[1088]
2015	Belle	$A_\Gamma = (-0.03 \pm 0.20 \pm 0.07)\%$	–	–	[1084]
2008	BaBar	$A_{CP}(KK) = (+0.00 \pm 0.34 \pm 0.13)\%$			
		$A_{CP}(\pi\pi) = (-0.24 \pm 0.52 \pm 0.22)\%$	0.00	1.00	[1074]
2012	Belle prel.	$\Delta A_{CP} = (-0.87 \pm 0.41 \pm 0.06)\%$	0.00	1.00	[1153]
2012	CDF	$\Delta A_{CP} = (-0.62 \pm 0.21 \pm 0.10)\%$	0.25	2.58	[1077]
2014	LHCb SL	$\Delta A_{CP} = (+0.14 \pm 0.16 \pm 0.08)\%$	0.01	1.07	[1058]
2016	LHCb prompt	$\Delta A_{CP} = (-0.10 \pm 0.08 \pm 0.03)\%$	0.12	2.10	[1078]

$$a_{CP}^{\rm ind} \equiv \frac{1}{2}\left[\left(\left|\frac{q}{p}\right| + \left|\frac{p}{q}\right|\right)x\sin\phi - \left(\left|\frac{q}{p}\right| - \left|\frac{p}{q}\right|\right)y\cos\phi\right], \tag{238}$$

where $\mathcal{A}_{D\to f}$ is the amplitude for $D \to f$ [1151]. We use the following relations between the observables and the underlying parameters [1152]:

$$A_\Gamma = -a_{CP}^{\rm ind} - a_{CP}^{\rm dir} y_{CP}, \tag{239}$$

$$\Delta A_{CP} = \Delta a_{CP}^{\rm dir}\left(1 + y_{CP}\frac{\overline{\langle t\rangle}}{\tau}\right) + a_{CP}^{\rm ind}\frac{\Delta\langle t\rangle}{\tau} + \overline{a_{CP}^{\rm dir}}\, y_{CP}\frac{\Delta\langle t\rangle}{\tau},$$
$$\approx \Delta a_{CP}^{\rm dir}\left(1 + y_{CP}\frac{\overline{\langle t\rangle}}{\tau}\right) + a_{CP}^{\rm ind}\frac{\Delta\langle t\rangle}{\tau}. \tag{240}$$

Equation (239) constrains mostly indirect CP violation, and the direct CP violation contribution can differ for different final states. In Eq. (240), $\langle t\rangle/\tau$ denotes the mean decay time in units of the D^0 lifetime; ΔX denotes the difference in quantity X between K^+K^- and $\pi^+\pi^-$ final states; and $\overline{X}$ denotes the average for quantity X. We neglect the last term in this relation as all three factors are $\mathcal{O}(10^{-2})$ or smaller, and thus this term is negligible with respect to the other two terms. Note that $\Delta\langle t\rangle/\tau \ll \langle t\rangle/\tau$, and it is expected that $|a_{CP}^{\rm dir}| < |\Delta a_{CP}^{\rm dir}|$ because $a_{CP}^{\rm dir}(K^+K^-)$ and $a_{CP}^{\rm dir}(\pi^+\pi^-)$ are expected to have opposite signs in the Standard Model [1151].

A χ^2 fit is performed in the plane $\Delta a_{CP}^{\rm dir}$ vs. $a_{CP}^{\rm ind}$. For the BaBar result the difference of the quoted values for $A_{CP}(K^+K^-)$ and $A_{CP}(\pi^+\pi^-)$ is calculated, adding all uncertainties in quadrature. This may overestimate the systematic uncertainty for the difference as it neglects correlated errors; however, the result is conservative and the effect is small as all measurements are statistically limited. For all measurements, statistical and systematic uncertainties are added in quadrature when calculating the χ^2. We use the current world average value $y_{CP} = (0.835 \pm 0.155)\%$ (see Sect. 8.1) and the measurements listed in Table 270.

In this fit, $A_\Gamma(KK)$ and $A_\Gamma(\pi\pi)$ are assumed to be identical. This assumption (expected to hold in the Standard Model) is supported by all measurements to date. A sig-

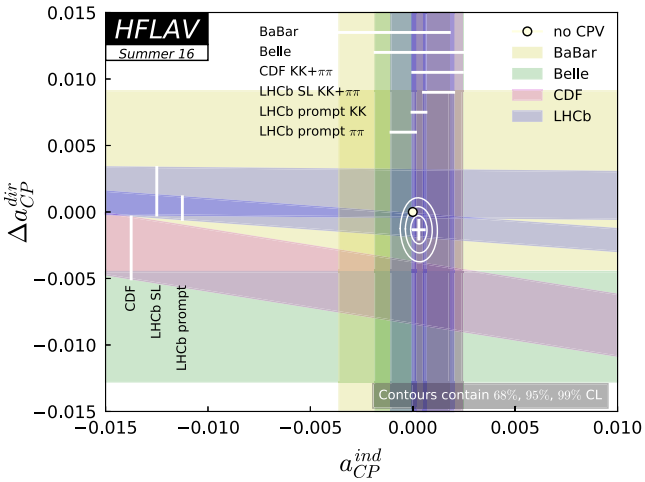

Fig. 198 Plot of all data and the fit result. Individual measurements are plotted as bands showing their $\pm 1\sigma$ range. The no-*CPV* point (0,0) is shown as a filled circle, and the best fit value is indicated by a cross showing the one-dimensional uncertainties. Two-dimensional 68% C.L., 95% C.L., and 99.7% C.L. regions are plotted as ellipses

nificant relative shift due to final-state dependent A_Γ values between ΔA_{CP} measurements with different mean decay times is excluded by these measurements.

The combination plot (see Fig. 198) shows the measurements listed in Table 270 for ΔA_{CP} and A_Γ.

From the fit, the change in χ^2 from the minimum value for the no-*CPV* point (0,0) is 4.7, which corresponds to a C.L. of 9.3×10^{-2} for two degrees of freedom. Thus the data are consistent with the no-*CP*-violation hypothesis at 9.3% C.L. This p-value corresponds to 1.7σ. The central values and $\pm 1\sigma$ uncertainties for the individual parameters are

$$\begin{aligned} a_{CP}^{\text{ind}} &= (+0.030 \pm 0.026)\% \\ \Delta a_{CP}^{\text{dir}} &= (-0.134 \pm 0.070)\%. \end{aligned} \tag{241}$$

Compared to the previous average, the tension in the difference between direct *CP* violation in the two final states is reduced, while the common indirect *CP* violation moved away from the no-*CP*-violation point by about one standard deviation.

8.5 Semileptonic decays

8.5.1 Introduction

Semileptonic decays of D mesons involve the interaction of a leptonic current with a hadronic current. The latter is non-perturbative and cannot be calculated from first principles; thus it is usually parameterized in terms of form factors. The transition matrix element is written

$$\mathcal{M} = -i\,\frac{G_F}{\sqrt{2}}\,V_{cq}\,L^\mu H_\mu, \tag{242}$$

where G_F is the Fermi constant and V_{cq} is a CKM matrix element. The leptonic current L^μ is evaluated directly from the lepton spinors and has a simple structure; this allows one to extract information about the form factors (in H_μ) from data on semileptonic decays [1154]. Conversely, because there are no strong final-state interactions between the leptonic and hadronic systems, semileptonic decays for which the form factors can be calculated allow one to determine V_{cq} [2].

8.5.2 $D \to P\bar{\ell}\nu_\ell$ decays

When the final state hadron is a pseudoscalar, the hadronic current is given by

$$\begin{aligned} H_\mu &= \langle P(p)|\bar{q}\gamma_\mu c|D(p')\rangle \\ &= f_+(q^2) \times \left[(p'+p)_\mu - \frac{m_D^2 - m_P^2}{q^2} q_\mu\right] \\ &\quad + f_0(q^2)\frac{m_D^2 - m_P^2}{q^2} q_\mu, \end{aligned} \tag{243}$$

where m_D and p' are the mass and four momentum of the parent D meson, m_P and p are those of the daughter meson, $f_+(q^2)$ and $f_0(q^2)$ are form factors, and $q = p' - p$. Kinematics require that $f_+(0) = f_0(0)$. The contraction $q_\mu L^\mu$ results in terms proportional to m_ℓ[1155], and thus for $\ell = e$ the terms proportionals to q_μ in Eq. (243) are negligible. For light leptons only the $f_+(q^2)$ vector form factor is relevant and the differential partial width is

$$\frac{d\Gamma(D \to P\bar{\ell}\nu_\ell)}{dq^2\, d\cos\theta_\ell} = \frac{G_F^2 |V_{cq}|^2}{32\pi^3} p^{*3} |f_+(q^2)|^2 \sin\theta_\ell^2, \tag{244}$$

where p^* is the magnitude of the momentum of the final state hadron in the D rest frame, and θ_ℓ is the angle of the lepton in the $\ell\nu$ rest frame with respect to the direction of the pseudoscalar meson in the D rest frame.

8.5.3 Form factor parameterizations

The form factor is traditionally parameterized with an explicit pole and a sum of effective poles:

$$\begin{aligned} f_+(q^2) = \frac{f_+(0)}{(1-\alpha)}\Bigg[&\left(\frac{1}{1 - q^2/m_{\text{pole}}^2}\right) \\ &+ \sum_{k=1}^{N} \frac{\rho_k}{1 - q^2/(\gamma_k\, m_{\text{pole}}^2)}\Bigg], \end{aligned} \tag{245}$$

where ρ_k and γ_k are expansion parameters and α is a parameter that normalizes the form factor at $q^2 = 0$, $f_+(0)$. The parameter m_{pole} is the mass of the lowest-lying $c\bar{q}$ resonance with the vector quantum numbers; this is expected to provide the largest contribution to the form factor for the $c \to q$ transition. The sum over N gives the contribution

Table 271 Results for $m_{\rm pole}$ and $\alpha_{\rm BK}$ from various experiments for $D^0 \to K^-\ell^+\nu$ and $D^+ \to \bar{K}^0\ell^+\nu$ decays

$D \to K\ell\nu_\ell$ Expt.	Mode	Refs.	$m_{\rm pole}$ (GeV/c^2)	$\alpha_{\rm BK}$
CLEO III	$(D^0; \ell = e, \mu)$	[1175]	$1.89 \pm 0.05^{+0.04}_{-0.03}$	$0.36 \pm 0.10^{+0.03}_{-0.07}$
FOCUS	$(D^0; \ell = \mu)$	[1176]	$1.93 \pm 0.05 \pm 0.03$	$0.28 \pm 0.08 \pm 0.07$
Belle	$(D^0; \ell = e, \mu)$	[1171]	$1.82 \pm 0.04 \pm 0.03$	$0.52 \pm 0.08 \pm 0.06$
BaBar	$(D^0; \ell = e)$	[1172]	$1.889 \pm 0.012 \pm 0.015$	$0.366 \pm 0.023 \pm 0.029$
CLEO-c (tagged)	$(D^0, D^+; \ell = e)$	[1173]	$1.93 \pm 0.02 \pm 0.01$	$0.30 \pm 0.03 \pm 0.01$
CLEO-c (untagged)	$(D^0; \ell = e)$	[1174]	$1.97 \pm 0.03 \pm 0.01$	$0.21 \pm 0.05 \pm 0.03$
CLEO-c (untagged)	$(D^+; \ell = e)$	[1174]	$1.96 \pm 0.04 \pm 0.02$	$0.22 \pm 0.08 \pm 0.03$
BESIII	$(D^0; \ell = e)$	[1169]	$1.921 \pm 0.010 \pm 0.007$	$0.309 \pm 0.020 \pm 0.013$
BESIII	$(D^+; \ell = e)$	[1170]	$1.953 \pm 0.044 \pm 0.036$	$0.239 \pm 0.077 \pm 0.065$

Table 272 Results for $m_{\rm pole}$ and $\alpha_{\rm BK}$ from various experiments for $D^0 \to \pi^-\ell^+\nu$ and $D^+ \to \pi^0\ell^+\nu$ decays

$D \to \pi\ell\nu_\ell$ Expt.	Mode	Refs.	$m_{\rm pole}$ (GeV/c^2)	$\alpha_{\rm BK}$
CLEO III	$(D^0; \ell = e, \mu)$	[1175]	$1.86^{+0.10+0.07}_{-0.06-0.03}$	$0.37^{+0.20}_{-0.31} \pm 0.15$
FOCUS	$(D^0; \ell = \mu)$	[1176]	$1.91^{+0.30}_{-0.15} \pm 0.07$	–
Belle	$(D^0; \ell = e, \mu)$	[1171]	$1.97 \pm 0.08 \pm 0.04$	$0.10 \pm 0.21 \pm 0.10$
CLEO-c (tagged)	$(D^0, D^+; \ell = e)$	[1173]	$1.91 \pm 0.02 \pm 0.01$	$0.21 \pm 0.07 \pm 0.02$
CLEO-c (untagged)	$(D^0; \ell = e)$	[1174]	$1.87 \pm 0.03 \pm 0.01$	$0.37 \pm 0.08 \pm 0.03$
CLEO-c (untagged)	$(D^+; \ell = e)$	[1174]	$1.97 \pm 0.07 \pm 0.02$	$0.14 \pm 0.16 \pm 0.04$
BES III	$(D^0; \ell = e)$	[1169]	$1.911 \pm 0.012 \pm 0.004$	$0.279 \pm 0.035 \pm 0.011$
BaBar	$(D^0; \ell = e)$	[1168]	$1.906 \pm 0.029 \pm 0.023$	$0.268 \pm 0.074 \pm 0.059$

of higher mass states. For example, for $D \to \pi$ transitions the dominant resonance is expected to be $D^*(2010)$, and thus $m_{\rm pole} = m_{D^*(2010)}$. For $D \to K$ transitions, the dominant contribution is expected from $D_s^*(2112)$, with $m_{\rm pole} = m_{D_s^*(2112)}$.

8.5.4 Simple pole

Equation (245) can be simplified by neglecting the sum over effective poles, leaving only the explicit vector meson pole. This approximation is referred to as "nearest pole dominance" or "vector-meson dominance." The resulting parameterization is

$$f_+(q^2) = \frac{f_+(0)}{(1 - q^2/m_{\rm pole}^2)}. \tag{246}$$

However, values of $m_{\rm pole}$ that give a good fit to the data do not agree with the expected vector meson masses [1156]. To address this problem, the "modified pole" or Becirevic–Kaidalov (BK) parameterization [1157] was introduced. $m_{\rm pole}/\sqrt{\alpha_{\rm BK}}$ is interpreted as the mass of an effective pole, higher than $m_{\rm pole}$, thus it is expected that $\alpha_{\rm BK} < 1$.

The parameterization takes the form

$$f_+(q^2) = \frac{f_+(0)}{(1 - q^2/m_{\rm pole}^2)} \frac{1}{\left(1 - \alpha_{\rm BK} \frac{q^2}{m_{\rm pole}^2}\right)}. \tag{247}$$

These parameterizations are used by several experiments to determine form factor parameters. Measured values of $m_{\rm pole}$ and $\alpha_{\rm BK}$ are listed in Tables 271 and 272 for $D \to K\ell\nu_\ell$ and $D \to \pi\ell\nu_\ell$ decays, respectively.

8.5.5 z expansion

An alternative series expansion around some value $q^2 = t_0$ to parameterize $f_+(q^2)$ can be used [1154,1158–1160]. This parameterization is model independent and satisfies general QCD constraints, being suitable for fitting experimental data. The expansion is given in terms of a complex parameter z, which is the analytic continuation of q^2 into the complex plane:

$$z(q^2, t_0) = \frac{\sqrt{t_+ - q^2} - \sqrt{t_+ - t_0}}{\sqrt{t_+ - q^2} + \sqrt{t_+ - t_0}}, \tag{248}$$

where $t_\pm \equiv (m_D \pm m_P)^2$ and t_0 is the (arbitrary) q^2 value corresponding to $z = 0$. The physical region corresponds

to $\pm|z|_{max} = \pm 0.051$ for $D \to K\ell\nu_\ell$ and $= \pm 0.17$ for $D \to \pi\ell\nu_\ell$, using $t_0 = t_+(1-\sqrt{1-t_-/t_+})$.

The form factor is expressed as

$$f_+(q^2) = \frac{1}{P(q^2)\,\phi(q^2,t_0)} \sum_{k=0}^{\infty} a_k(t_0)[z(q^2,t_0)]^k, \tag{249}$$

where the $P(q^2)$ factor accommodates sub-threshold resonances via

$$P(q^2) \equiv \begin{cases} 1 & (D \to \pi) \\ z(q^2, M^2_{D^*_s}) & (D \to K). \end{cases} \tag{250}$$

The "outer" function $\phi(t,t_0)$ can be any analytic function, but a preferred choice (see, e.g. Refs. [1158,1159,1161]) obtained from the Operator Product Expansion (OPE) is

$$\phi(q^2,t_0) = \alpha\left(\sqrt{t_+-q^2}+\sqrt{t_+-t_0}\right) \times \frac{t_+-q^2}{(t_+-t_0)^{1/4}} \frac{\left(\sqrt{t_+-q^2}+\sqrt{t_+-t_-}\right)^{3/2}}{\left(\sqrt{t_+-q^2}+\sqrt{t_+}\right)^5}, \tag{251}$$

with $\alpha = \sqrt{\pi m_c^2/3}$. The OPE analysis provides a constraint upon the expansion coefficients, $\sum_{k=0}^{N} a_k^2 \le 1$. These coefficients receive $1/M_D$ corrections, and thus the constraint is only approximate. However, the expansion is expected to converge rapidly since $|z| < 0.051$ (0.17) for $D \to K$ ($D \to \pi$) over the entire physical q^2 range, and Eq. (249) remains a useful parameterization. The main disadvantage as compared to phenomenological approaches is that there is no physical interpretation of the fitted coefficients a_K.

8.5.6 Three-pole formalism

An update of the vector pole dominance model has been developed for the $D \to \pi\ell\nu_\ell$ channel [1162]. It uses information of the residues of the semileptonic form factor at its first two poles, the $D^*(2010)$ and $D^{*'}(2600)$ resonances. The form factor is expressed as an infinite sum of residues from $J^P = 1^-$ states with masses $m_{D^*_n}$:

$$f_+(q^2) = \sum_{n=0}^{\infty} \frac{\operatorname*{Res}_{q^2=m^2_{D^*_n}} f_+(q^2)}{m^2_{D^*_n}-q^2}, \tag{252}$$

with the residues given by

$$\operatorname*{Res}_{q^2=m^2_{D^*_n}} f_+(q^2) = \frac{1}{2} m_{D^*_n} f_{D^*_n} g_{D^*_n D\pi}. \tag{253}$$

Values of the f_{D^*} and $f_{D^{*\prime}}$ decay constants have been obtained by lattice QCD calculations, relative to f_D, with 2% and 28% precision, respectively [1162]. The couplings to the $D\pi$ state, $g_{D^*D\pi}$ and $g_{D^{*\prime}D\pi}$, are extracted from measurements of the $D^*(2010)$ and $D^{*'}(2600)$ widths by BABAR and LHCb experiments [1163–1165]. Thus the contribution from the first pole is known with a 3% accuracy. The contribution from the $D^{*'}(2600)$ is determined with poorer accuracy, ~30%, mainly due to lattice uncertainties. A *superconvergence* condition [1166] is applied:

$$\sum_{n=0}^{\infty} \operatorname*{Res}_{q^2=m^2_{D^*_n}} f_+(q^2) = 0, \tag{254}$$

protecting the form factor behavior at large q^2. Within this model the first two poles are not sufficient to describe the data, and a third effective pole needs to be included.

One of the advantages of this phenomenological model is that it can be extrapolated outside the charm physical region, providing a method to extract the CKM matrix element V_{ub} using the ratio of the form factors of the $D \to \pi\ell\nu$ and $B \to \pi\ell\nu$ decay channels. It will be used once lattice calculations provide the form factor ratio $f^+_{B\pi}(q^2)/f^+_{D\pi}(q^2)$ at the same pion energy.

This form factor description can be extended to the $D \to K\ell\nu$ decay channel, considering the contribution of several $c\bar{s}$ resonances with $J^P = 1^-$. The first two pole masses contributing to the form factor correspond to the $D^*_s(2112)$ and $D^*_{s1}(2700)$ resonant states [327]. A constraint on the first residue can be obtained using information of the f_K decay constant [327] and the g coupling extracted from the D^{*+} width [1163]. The contribution from the second pole can be evaluated using the decay constants from [1167], the measured total width and the ratio of D^*K and DK decay branching fractions [327].

8.5.7 Experimental techniques and results

Different techniques by several experiments are used to measure D meson semileptonic decays having a pseudoscalar particle in the final state. The most recent results are provided by the BABAR [1168] and BES III [1169,1170] collaborations. Belle [1171], BABAR [1172], and CLEO-c [1173,1174] have all previously reported results. Belle fully reconstructs $e^+e^- \to D\bar{D}X$ events from the continuum under the $\Upsilon(4S)$ resonance, achieving very good q^2 resolution (15 MeV^2) and a low background level but with a low efficiency. Using 282 fb^{-1} of data, about 1300 and 115 signal semileptonic decays are isolated for both lepton channels together ($e+\mu$), for the Cabibbo-favored and Cabibbo-suppressed modes, respectively. The BABAR experiment uses a partial reconstruction technique in which the semileptonic decays are tagged via $D^{*+} \to D^0\pi^+$ decays. The D direction and neutrino energy are obtained using information from the rest of the event. With 75 fb^{-1} of data, 74,000 signal events in the $D^0 \to K^-e^+\nu$ mode are obtained. This

Table 273 Results for r_1 and r_2 from various experiments for the $D \to K\ell\nu_\ell$ decay channel. The correlation coefficient between these parameters is larger than 0.9

Expt. $D \to K\ell\nu_\ell$	Mode	Refs.	r_1	r_2
BaBar	$(D^0; \ell = e)$	[1172]	$-2.5 \pm 0.2 \pm 0.2$	$0.6 \pm 6.0 \pm 5.0$
CLEO-c (tagged)	$(D^0; \ell = e)$	[1173]	$-2.65 \pm 0.34 \pm 0.08$	$13 \pm 9 \pm 1$
CLEO-c (tagged)	$(D^+; \ell = e)$	[1173]	$-1.66 \pm 0.44 \pm 0.10$	$-14 \pm 11 \pm 1$
CLEO-c (untagged)	$(D^0; \ell = e)$	[1174]	$-2.4 \pm 0.4 \pm 0.1$	$21 \pm 11 \pm 2$
CLEO-c (untagged)	$(D^+; \ell = e)$	[1174]	$-2.8 \pm 6 \pm 2$	$32 \pm 18 \pm 4$
BES III	$(D^0; \ell = e)$	[1169]	$-2.334 \pm 0.159 \pm 0.080$	$3.42 \pm 3.91 \pm 2.41$
BES III	$(D^+; \ell = e)$	[1170]	$-2.23 \pm 0.42 \pm 0.53$	$11.3 \pm 8.5 \pm 8.7$

Table 274 Results for r_1 and r_2 from various experiments, for $D \to \pi\ell\nu_\ell$. The correlation coefficient between these parameters is larger than 0.9

Expt. $D \to \pi\ell\nu_\ell$	Mode	Refs.	r_1	r_2
CLEO-c (tagged)	$(D^0; \ell = e)$	[1173]	$-2.80 \pm 0.49 \pm 0.04$	$6 \pm 3 \pm 0$
CLEO-c (tagged)	$(D^+; \ell = e)$	[1173]	$-1.37 \pm 0.88 \pm 0.24$	$-4 \pm 5 \pm 1$
CLEO-c (untagged)	$(D^0; \ell = e)$	[1174]	$-2.1 \pm 0.7 \pm 0.3$	$-1.2 \pm 4.8 \pm 1.7$
CLEO-c (untagged)	$(D^+; \ell = e)$	[1174]	$-0.2 \pm 1.5 \pm 0.4$	$-9.8 \pm 9.1 \pm 2.1$
BES III	$(D^0; \ell = e)$	[1169]	$-1.85 \pm 0.22 \pm 0.07$	$-1.4 \pm 1.5 \pm 0.5$
BaBar	$(D^0; \ell = e)$	[1168]	$-1.31 \pm 0.70 \pm 0.43$	$-4.2 \pm 4.0 \pm 1.9$

technique provides a large signal yield but also a high background level and a poor q^2 resolution (ranging from 66 to 219 MeV^2). In this case the measurement of the branching fraction is obtained by normalizing to the $D^0 \to K^-\pi^+$ decay channel; thus the measurement would benefit from future improvements in the determination of this reference channel. The Cabibbo-suppressed mode has been recently measured using the same technique and 350 fb^{-1} data. For this measurement, 5000 $D^0 \to \pi^-e^+\nu$ signal events were reconstructed [1168].

The CLEO-c experiment uses two different methods to measure charm semileptonic decays. Tagged analyses [1173] rely on the full reconstruction of $\Psi(3770) \to D\overline{D}$ events. One of the D mesons is reconstructed in a hadronic decay mode, the other in the semileptonic channel. The only missing particle is the neutrino so the q^2 resolution is very good and the background level very low. With the entire CLEO-c data sample, 818 pb^{-1}, 14,123 and 1374 signal events are reconstructed for the $D^0 \to K^-e^+\nu$ and $D^0 \to \pi^-e^+\nu$ channels, and 8467 and 838 for the $D^+ \to \overline{K}^0e^+\nu$ and $D^+ \to \pi^0e^+\nu$ decays, respectively. Another technique without tagging the D meson in a hadronic mode ("untagged" in the following) has been also used by CLEO-c [1174]. In this method, the entire missing energy and momentum in an event are associated with the neutrino four momentum, with the penalty of larger background as compared to the tagged method. Using the "tagged" method the BES III experiment measures the $D^0 \to K^-e^+\nu$ and $D^0 \to \pi^-e^+\nu$ decay channels. With 2.9 fb^{-1} they fully reconstruct 70,700 and 6300 signal events for each channel, respectively[1169]. In a separated analysis the BES III experiment measures also the D^+ decay mode into $D^+ \to K_L^0e^+\nu$ [1170]. Using several tagged hadronic events they reconstruct 20,100 semileptonic candidates.

Previous measurements were also performed by several experiments. Events registered at the $\Upsilon(4S)$ energy corresponding to an integrated luminosity of 7 fb^{-1} were analyzed by CLEO III [1175]. Fixed target photo-production experiments performed also measurements of the normalized form factor distribution (FOCUS [1176]) and total decay rates (Mark-III [1177], E653 [1178,1179], E687 [1180,1181], E691 [1182], BES II [1183,1184], CLEO II [1185]). In the FOCUS fixed target photo-production experiment, D^0 semimuonic events were obtained from the decay of a D^{*+}, with a kaon or a pion detected.

Results of the hadronic form factor parameters, m_{pole} and α_{BK}, obtained from the measurements discussed above, are given in Tables 271 and 272.

The z-expansion formalism has been used by BaBar [1168, 1172], BES III[1186] and CLEO-c [1173], [1174]. Their fits use the first three terms of the expansion, and the results for the ratios $r_1 \equiv a_1/a_0$ and $r_2 \equiv a_2/a_0$ are listed in Tables 273 and 274.

8.5.8 Combined results for the $D \to K\ell\nu_\ell$ channel

The q^2 distribution provided by each individual measurement is used to determine a combined result by performing a fit to the z-expansion formalism at second order. Results for the form factor normalization $f_+^K(0)|V_{cs}|$ and the shape param-

Table 275 Results of the fits to $D \to K\ell\nu_\ell$ measurements from several experiments, using the z-expansion. External inputs have been updated to PDG [327]. The correlation coefficients listed in the last column refer to $\rho_{12} \equiv \rho_{|V_{cs}|f_+^K(0),r_1}$, $\rho_{13} \equiv \rho_{|V_{cs}|f_+^K(0),r_2}$, and $\rho_{23} \equiv \rho_{r_1,r_2}$ and are for the total uncertainties (statistical $\oplus$ systematic). The result for the $D^+ \to K_L^0 e^+\nu_e$ decay channel from BES III [1170] is included in the combined results as a constraint on the normalization, $|V_{cs}|f_+^K(0)$. The entry *others* refers to total decay rates measured by Mark-III [1177], E653 [1178,1179], E687[1180,1181], E691 [1182], BES II [1183,1184] and CLEO II [1185]

Expt. $D \to K\ell\nu_\ell$	Mode	$\lvert V_{cs}\rvert f_+^K(0)$	r_1	r_2	$\rho_{12}/\rho_{13}/\rho_{23}$
BES III (tagged) [1169]	(D^0)	0.7195(35)(43)	−2.33(16)(8)	3.4(4.0)(2.5)	−0.21/0.58/−0.81
CLEO-c (tagged) [1173]	(D^0, D^+)	0.7189(64)(48)	−2.29(28)(27)	3.0(7.0)(1.0)	−0.19/0.58/−0.81
CLEO-c (untagged) [1174]	(D^0, D^+)	0.7436(76)(79)	−2.57(33)(18)	23.9(8.9)(4.3)	−0.34/0.66/−0.84
BaBar [1172]	(D^0)	0.7241(64)(60)	−2.45(20)(18)	−0.6(6.0)(3.8)	−0.36/0.59/−0.82
Belle [1171]	(D^0)	0.700(19)	−3.06(71)	−3.3(17.9)	−0.20/0.66/−0.81
FOCUS [1176] and others		0.724(29)	−2.54(75)	7.0(12.8)	−0.02/0.02/−0.97
Combined	(D^0, D^+)	0.7226(22)(26)	−2.38(11)(6)	4.7(2.6)(1.4)	−0.19/0.51/− 0.84

Table 276 Results for the $D^0 \to K^-\ell^+\nu_\ell$ and $D^+ \to \bar{K}^0\ell^+\nu_\ell$ decays channels using the z-expansion formalism at second order

Fit value	$D^0 \to K^-\ell^+\nu_\ell$	$D^+ \to \bar{K}^0\ell^+\nu_\ell$
$\lvert V_{cs}\rvert f_+^K(0)$	0.7219 ± 0.0024 ± 0.0027	0.726 ± 0.005 ± 0.007
r_1	−2.41 ± 0.11 ± 0.07	−2.07 ± 0.38 ± 0.10
r_2	4.7 ± 2.7 ± 1.4	5.4 ± 8.2 ± 4.6
$\rho_{12}/\rho_{13}/\rho_{23}$	−0.19/0.51/−0.84	−0.10/0.39/−0.84

eters r_1 and r_2 for each individual measurement and for the combination are presented in Table 275. Measurements have been corrected with respect to the original ones using recent values from PDG [327]. This includes updated branching fractions of normalization channels, corrected CKM matrix elements and the D meson lifetime. The BaBar measurement has been corrected accounting for final-state radiation. The result for the $D^+ \to K_L^0 e^+\nu_e$ decay channel from BES III [1170] is included as a constraint in the combined result since correlation matrices are not provided. Correlation coefficients of the parameters are quoted in the last column of Table 275. The χ^2 per degree of freedom is 114.7/101. Results are shown in Fig. 201.

In the combination of the electron and muon channels, the measurements with muons are corrected for the reduction of phase space and for the $f_0(q^2)$ contribution [1187]. Channels with a D^0 or a D^+ are combined assuming isospin invariance and using physical meson and lepton masses. These combined results are noted as $D \to K\ell\nu_\ell$ in the following. Hadronic form factors are assumed to be the same for charged and neutral D mesons. Separate results for the $D^0 \to K^-\ell^+\nu_\ell$ and $D^+ \to \bar{K}^0\ell^+\nu_\ell$ decay channels are shown in Table 276 and Fig. 200. Using the fitted parameters and integrating over the full q^2 range, the combined semileptonic branching fraction, expressed in terms of the D^0 decay channel gives:

$$\mathcal{B}(D^0 \to K^-\ell^+\nu_\ell) = (3.490 \pm 0.011 \pm 0.020)\% \quad (255)$$

Table 277 Results of the three-pole model form factors obtained from a fit to all measurements. Fitted parameters are the first two residues γ_0^K and γ_1^K, which are constrained using present measurements of masses and widths of the D_s^* and D_{s1}^* mesons, and lattice computations of decay constants, and the effective mass, $m_{D_{s\,\mathrm{eff}}^{*\prime\prime}}$, accounting for higher mass hadronic contributions

Parameter	Combined result ($D \to K\ell\nu_\ell$)
γ_0^K	4.85 ± 0.08 GeV^2
γ_1^K	−1.2 ± 0.30 GeV^2
$m_{D_{s\,\mathrm{eff}}^{*\prime\prime}}$	4.46 ± 0.26 GeV

Data from the different experiments are also fitted within the three-pole form factor formalism. Constraints on the first and second poles are imposed using information of the $D_s^*(2112)$ and $D_{s1}^*(2700)$ resonances. Results are presented in Table 277. Fitted parameters are the first two residues $\gamma_0^K = \operatorname*{Res}_{q^2=m^2_{D_s^*(2112)}} f_+^K(q^2)$ and $\gamma_1^\pi = \operatorname*{Res}_{q^2=m^2_{D_{s1}^*(2700)}} f_+^K(q^2)$ and an effective mass, $m_{D_{s\,\mathrm{eff}}^{*\prime\prime}}$, accounting for higher mass hadronic contributions. It is found that the fitted effective third pole mass is larger than the mass of the second radial excitation, around 3.2 GeV/c^2, as expected. The contribution to the form factor by only the D_s^* resonance is disfavoured by the data. Figure 199 (left) shows the result of the fitted form factors for the z-expansion and three-pole parametrizations (Figs. 200, 201).

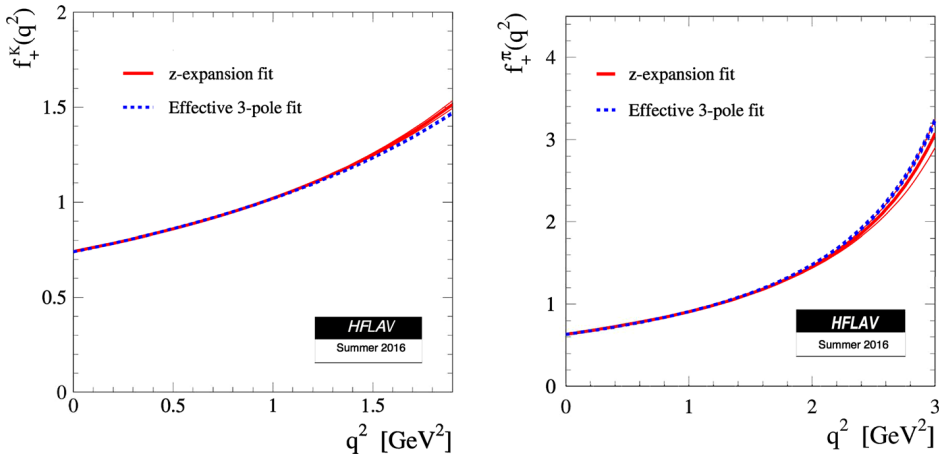

Fig. 199 Form factors as function of q^2 for the $D \to K\ell\nu_\ell$ (*left*) and $D \to \pi\ell\nu_\ell$ (*right*) channels, obtained from a fit to all experimental data. Central values (*central lines*) and uncertainties (one σ deviation) are shown for the z-expansion and the 3-pole parameterization

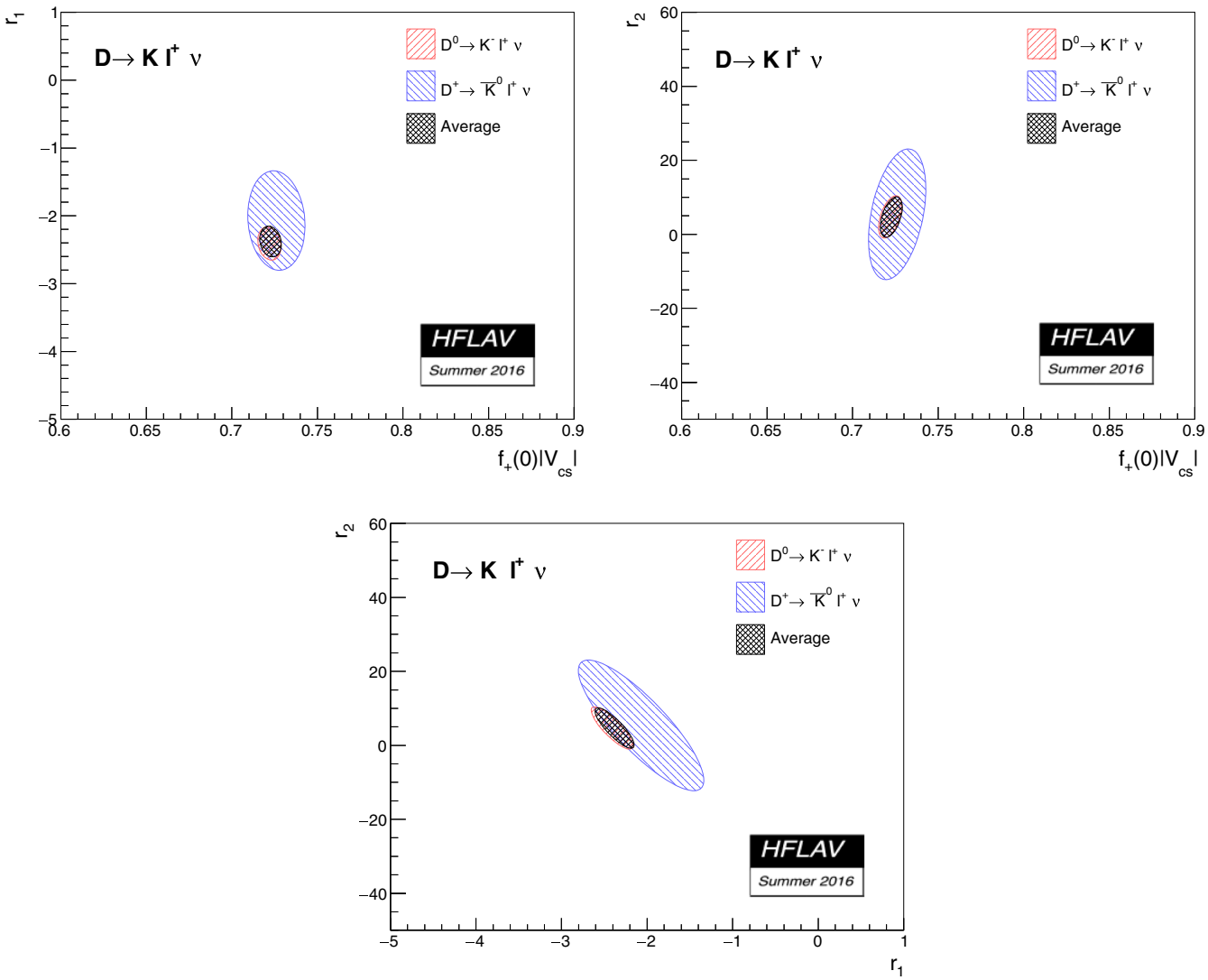

Fig. 200 Results of the combined fit shown separately for the $D^0 \to K^-\ell^+\nu$ and $D^+ \to \bar{K}^0\ell^+\nu$ decay channels. Ellipses are shown for 68% C.L

8.5.9 Combined results for the $D \to \pi\ell\nu_\ell$ channel

The combined result for the $D \to \pi\ell\nu_\ell$ decay channel is obtained from a fit to BABAR, Belle, BES III, and CLEO-c data, with updated input values from [327]. The available measurements are fitted in bins of q^2 to the z-expansion model at second order. Results of the individual fits for each experiment and the combined result are shown in

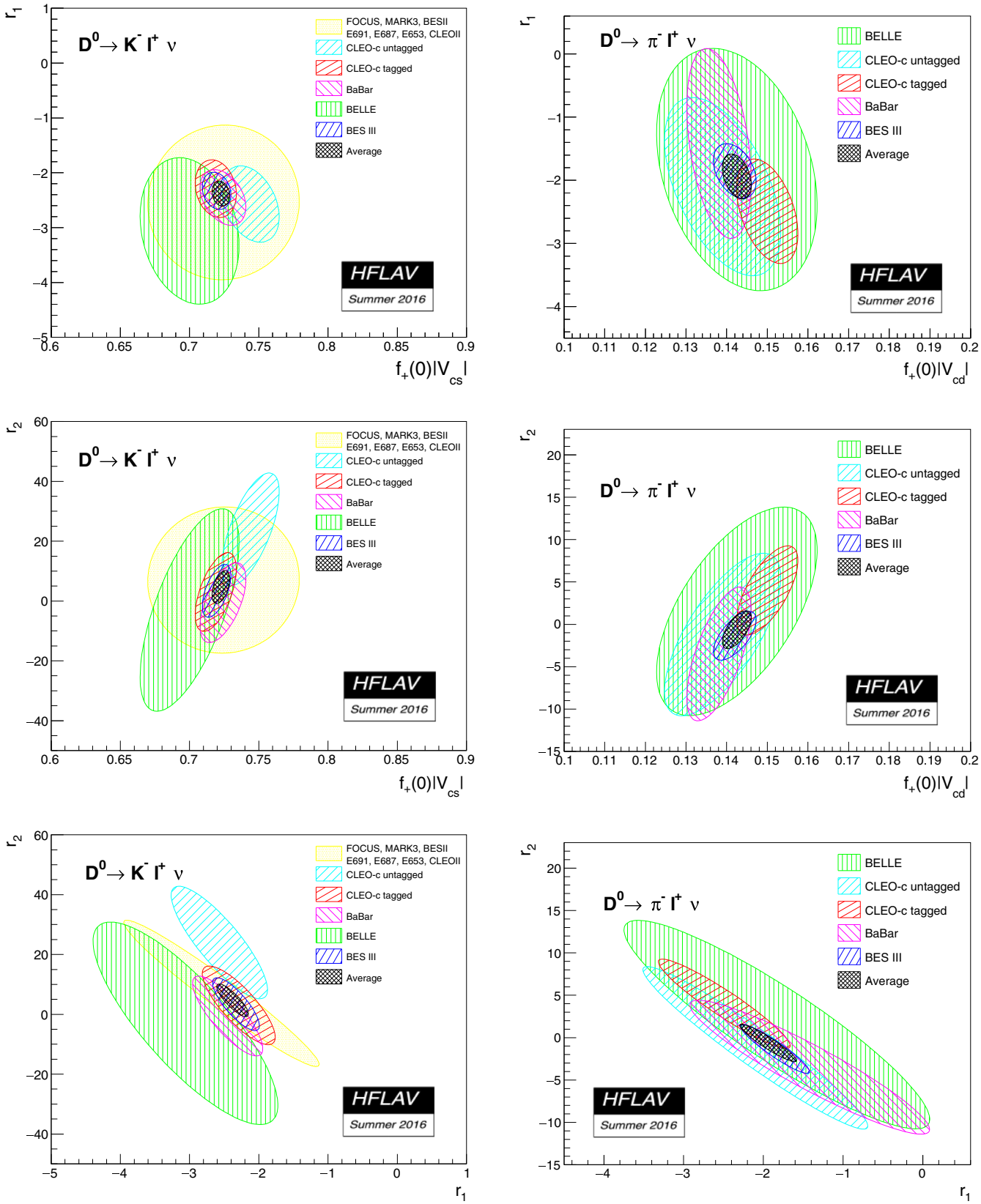

Fig. 201 The $D^0 \to K^-\ell^+\nu$ (*left*) and $D^0 \to \pi^-\ell^+\nu$ (*right*) 68% C.L. error ellipses from the average fit of the 3-parameter z-expansion results

Table 278 Results of the fits to $D \to \pi \ell \nu_\ell$ measurements from several experiments, using the z-expansion. External inputs are updated to PDG [327]. The correlation coefficients listed in the last column refer to $\rho_{12} \equiv \rho_{|V_{cd}|f_+^\pi(0),r_1}$, $\rho_{13} \equiv \rho_{|V_{cd}|f_+^\pi(0),r_2}$, and $\rho_{23} \equiv \rho_{r_1,r_2}$ and are for the total uncertainties (statistical $\oplus$ systematic)

Expt. $D \to \pi \ell \nu_\ell$	mode	$\lvert V_{cd}\rvert f_+^\pi(0)$	r_1	r_2	$\rho_{12}/\rho_{13}/\rho_{23}$
BES III (tagged) [1169]	(D^0)	0.1422(25)(10)	−1.86(23)(7)	−1.24(1.51)(47)	−0.37/0.64/−0.93
CLEO-c (tagged) [1173]	(D^0, D^+)	0.1507(42)(11)	−2.45(43)(9)	3.8(2.8)(6)	−0.43/0.67/−0.94
CLEO-c (untagged) [1174]	(D^0, D^+)	0.1394(58)(25)	−1.71(62)(25)	−2.8(4.0)(1.6)	−0.50/0.69/−0.96
BABAR [1172]	(D^0)	0.1381(36)(22)	−1.42(66)(45)	−3.5(3.7)(2.0)	−0.40/0.57/−0.97
Belle [1171]	(D^0)	0.142(11)	−1.83(1.00)	1.5(6.5)	−0.30/0.59/−0.91
Combined	(D^0, D^+)	0.1426(17)(8)	−1.95(18)(1)	−0.52(1.17)(32)	−0.37/0.63/−0.94

Table 279 Results of the three-pole model to BABAR, Belle, BES III and CLEO-c (tagged and untagged) data. Fitted parameters are the first two residues γ_0^π and γ_1^π, which are constrained using present measurements of masses and widths of the D^* and $D^{*'}$ mesons, and lattice computations of decay constants, and the effective mass, $m_{D^{*''}_{\rm eff}}$, accounting for higher mass hadronic contributions

Parameter	Combined result ($D \to \pi \ell \nu_\ell$)
γ_0^π	3.881 ± 0.093 GeV^2
γ_1^π	-1.18 ± 0.30 GeV^2
$m_{D^{*''}_{\rm eff}}$	4.17 ± 0.42 GeV

Table 278. The χ^2 per degree of freedom of the combined fit is 51/55.

Using the fitted parameters and integrating over the full q^2 range, the combined semileptonic branching fraction, expressed in terms of the D^0 decay channel gives:

$$\mathcal{B}(D^0 \to \pi^- \ell^+ \nu_\ell) = (2.891 \pm 0.030 \pm 0.022) \times 10^{-3} \tag{256}$$

Results of the three-pole model to the $D \to \pi \ell \nu_\ell$ data are shown in Table 279. Fitted parameters are the first two residues $\gamma_0^\pi = \operatorname*{Res}_{q^2=m^2_{D^*}} f_+^\pi(q^2)$ and $\gamma_1^\pi = \operatorname*{Res}_{q^2=m^2_{D^{*'}}} f_+^\pi(q^2)$ (which are constrained using present measurements of masses and widths of the $D^*(2010)$ and $D^{*'}(2600)$ mesons, and lattice computations of decay constants, following [1162]), and an effective mass, $m_{D^{*''}_{\rm eff}}$, accounting for higher mass hadronic contributions. The V_{cd} value entering in the fit is given in Eq. (257). The χ^2 per degree of freedom of the combined fit is 57.5/57.

The effective mass $m_{D^{*''}_{\rm eff}}$ is larger than the predicted mass of the second radially excited state with $J^P = 1^-$ ($\sim$ 3.11 GeV), indicating that more contributions are needed to explain the form factor. Figure 199 (right) shows the result of the combined form factor for the z-expansion and three-pole parameterizations.

8.5.10 V_{cs} and V_{cd} determination

Assuming unitarity of the CKM matrix, the values of the CKM matrix elements entering in charm semileptonic decays are evaluated from the V_{ud}, V_{td} and V_{cb} elements [327]:

$$\begin{aligned} |V_{cs}| &= 0.97343 \pm 0.00015, \\ |V_{cd}| &= 0.22521 \pm 0.00061. \end{aligned} \tag{257}$$

Using the combined values of $f_+^K(0)|V_{cs}|$ and $f_+^\pi(0)|V_{cd}|$ in Tables 275 and 278, leads to the form factor values:

$$\begin{aligned} f_+^K(0) &= 0.7423 \pm 0.0035, \\ f_+^\pi(0) &= 0.6327 \pm 0.0086, \end{aligned}$$

which are in agreement with present lattice QCD computations [222]: $f_+^K(0) = 0.747 \pm 0.019$ and $f_+^\pi(0) = 0.666 \pm 0.029$. The experimental accuracy is at present higher than the one from lattice calculations. If instead one assumes the lattice QCD form factor values, one obtains for the CKM matrix elements using the combined results in Tables 275 and 278:

$$\begin{aligned} |V_{cs}| &= 0.967 \pm 0.025, \\ |V_{cd}| &= 0.2140 \pm 0.0097, \end{aligned}$$

still compatible with unitarity of the CKM matrix.

8.5.11 $D \to V \bar{\ell} \nu_\ell$ decays

When the final state hadron is a vector meson, the decay can proceed through both vector and axial vector currents, and four form factors are needed. The hadronic current is $H_\mu = V_\mu + A_\mu$, where [1155]

$$\begin{aligned} V_\mu &= \langle V(p,\varepsilon)|\bar{q}\gamma_\mu c|D(p')\rangle \\ &= \frac{2V(q^2)}{m_D + m_V}\varepsilon_{\mu\nu\rho\sigma}\varepsilon^{*\nu}p'^\rho p^\sigma \\ A_\mu &= \langle V(p,\varepsilon)| - \bar{q}\gamma_\mu\gamma_5 c|D(p')\rangle \\ &= -i\,(m_D + m_V)A_1(q^2)\varepsilon^*_\mu \end{aligned} \tag{258}$$

$$+ i \frac{A_2(q^2)}{m_D + m_V}(\varepsilon^* \cdot q)(p' + p)_\mu$$
$$+ i \frac{2m_V}{q^2}\Big(A_3(q^2) - A_0(q^2)\Big)[\varepsilon^* \cdot (p' + p)]q_\mu. \tag{259}$$

In this expression, m_V is the daughter meson mass and

$$A_3(q^2) = \frac{m_D + m_V}{2m_V}A_1(q^2) - \frac{m_D - m_V}{2m_V}A_2(q^2). \tag{260}$$

Kinematics require that $A_3(0) = A_0(0)$. Terms proportional to q_μ are only important for the case of τ leptons. Thus, only three form factors are relevant in the decays involving μ or e: $A_1(q^2)$, $A_2(q^2)$ and $V(q^2)$. The differential partial width is

$$\frac{d\Gamma(D \to V\bar{\ell}\nu_\ell)}{dq^2\, d\cos\theta_\ell} = \frac{G_F^2\,|V_{cq}|^2}{128\pi^3 m_D^2}\, p^*\, q^2 \times \Bigg[\frac{(1-\cos\theta_\ell)^2}{2}|H_-|^2 + \frac{(1+\cos\theta_\ell)^2}{2}|H_+|^2 + \sin^2\theta_\ell |H_0|^2\Bigg], \tag{261}$$

where $H_\pm$ and H_0 are helicity amplitudes, corresponding to helicities of the V meson or virtual W, given by

$$H_\pm = \frac{1}{m_D + m_V}\Big[(m_D + m_V)^2 A_1(q^2) \mp 2m_D\, p^* V(q^2)\Big] \tag{262}$$

$$H_0 = \frac{1}{|q|}\frac{m_D^2}{2m_V(m_D + m_V)} \times \Bigg[\Bigg(1 - \frac{m_V^2 - q^2}{m_D^2}\Bigg) \times (m_D + m_V)^2 A_1(q^2) - 4p^{*2} A_2(q^2)\Bigg]. \tag{263}$$

p^* is the magnitude of the three-momentum of the V system, measured in the D rest frame, and θ_ℓ is the angle of the lepton momentum, in the W rest frame, with respect to the opposite direction of the D meson [see Fig. 202 for the electron case (θ_e)]. The left-handed nature of the quark current manifests itself as $|H_-| > |H_+|$. The differential decay rate for $D \to V\ell\nu$ followed by the vector meson decaying into two pseudoscalars is

$$\frac{d\Gamma(D \to V\bar{\ell}\nu,\, V \to P_1P_2)}{dq^2 d\cos\theta_V d\cos\theta_\ell d\chi} = \frac{3G_F^2}{2048\pi^4}|V_{cq}|^2 \frac{p^*(q^2)q^2}{m_D^2}\mathcal{B}(V \to P_1P_2) \times \Big\{(1 + \cos\theta_\ell)^2 \sin^2\theta_V |H_+(q^2)|^2 + (1 - \cos\theta_\ell)^2 \sin^2\theta_V |H_-(q^2)|^2 + 4\sin^2\theta_\ell \cos^2\theta_V |H_0(q^2)|^2 - 4\sin\theta_\ell(1 + \cos\theta_\ell) \times \sin\theta_V \cos\theta_V \cos\chi\, H_+(q^2)H_0(q^2) + 4\sin\theta_\ell(1 - \cos\theta_\ell) \times \sin\theta_V \cos\theta_V \cos\chi\, H_-(q^2)H_0(q^2) - 2\sin^2\theta_\ell \sin^2\theta_V \cos 2\chi\, H_+(q^2)H_-(q^2)\Big\}, \tag{264}$$

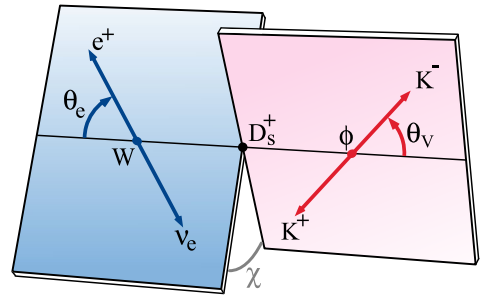

Fig. 202 Decay angles θ_V, θ_ℓ and χ. Note that the angle χ between the decay planes is defined in the D-meson reference frame, whereas the angles θ_V and θ_ℓ are defined in the V meson and W reference frames, respectively

where the helicity angles θ_ℓ, θ_V, and acoplanarity angle χ are defined in Fig. 202.

Ratios between the values of the hadronic form factors expressed at $q^2 = 0$ are usually introduced:

$$r_V \equiv V(0)/A_1(0), \quad r_2 \equiv A_2(0)/A_1(0). \tag{265}$$

8.5.12 *Form factor measurements*

In 2002 FOCUS reported [1188] an asymmetry in the observed $\cos(\theta_V)$ distribution in $D^+ \to K^-\pi^+\mu^+\nu$ decays. This is interpreted as evidence for an S-wave $K^-\pi^+$ component in the decay amplitude. Since H_0 typically dominates over $H_\pm$, the distribution given by Eq. (264) is, after integration over χ, roughly proportional to $\cos^2\theta_V$. Inclusion of a constant S-wave amplitude of the form $A\,e^{i\delta}$ leads to an interference term proportional to $|AH_0 \sin\theta_\ell \cos\theta_V|$; this term causes an asymmetry in $\cos(\theta_V)$. When FOCUS fit their data including this S-wave amplitude, they obtained $A = 0.330 \pm 0.022 \pm 0.015\,\text{GeV}^{-1}$ and $\delta = 0.68 \pm 0.07 \pm 0.05$ [1189]. Both BaBar [1190] and CLEO-c [1191] have also found evidence for an $f_0 \to K^+K^-$ component in semileptonic D_s decays.

The CLEO-c collaboration extracted the form factors $H_+(q^2)$, $H_-(q^2)$, and $H_0(q^2)$ from 11000 $D^+ \to K^-\pi^+\ell^+\nu_\ell$ events in a model-independent fashion directly as functions of q^2 [1192]. They also determined the S-wave form factor $h_0(q^2)$ via the interference term, despite the fact that the $K\pi$ mass distribution appears dominated by the vector $K^*(892)$ state. It is observed that $H_0(q^2)$ dominates over a wide range of q^2, especially at low q^2. The transverse form factor $H_t(q^2)$, which can be related to $A_3(q^2)$, is small compared to lattice gauge theory calculations and suggests that the form factor ratio $r_3 \equiv A_3(0)/A_1(0)$ is large and negative.

BaBar [1193] selected a large sample of 244×10^3 $D^+ \to K^-\pi^+e^+\nu_e$ candidates with a ratio $S/B \sim 2.3$ from an analyzed integrated luminosity of 347 fb^{-1}. With four particles emitted in the final state, the differential decay rate depends on five variables. In addition to the four variables defined in previous sections there is also m^2, the mass squared of the $K\pi$ system. To analyze the $D^+ \to K^-\pi^+e^+\nu_e$ decay channel it is assumed that all form factors have a q^2 variation given by the simple pole model and the effective pole mass value, $m_A = (2.63 \pm 0.10 \pm 0.13)$ GeV/c^2, is fitted for the axial vector form factors. This value is compatible with expectations when comparing with the mass of $J^P = 1^+$ charm mesons. For the mass dependence of the form factors, a Breit–Wigner with a mass dependent width and a Blatt–Weisskopf damping factor is used. For the S-wave amplitude, considering what was measured in $D^+ \to K^-\pi^+\pi^+$ decays, a polynomial variation below the $\overline{K}_0^*(1430)$ and a Breit–Wigner distribution, above are assumed. For the polynomial part, a linear term is sufficient to fit data. It is verified that the variation of the S-wave phase is compatible with expectations from elastic $K\pi$ [343,1194] (after correcting for $\delta^{3/2}$) according to the Watson theorem. At variance with elastic scattering, a negative relative sign between the S- and P-waves is measured; this is compatible with the previous theorem. Contributions from other spin-1 and spin-2 resonances decaying into $K^-\pi^+$ are considered.

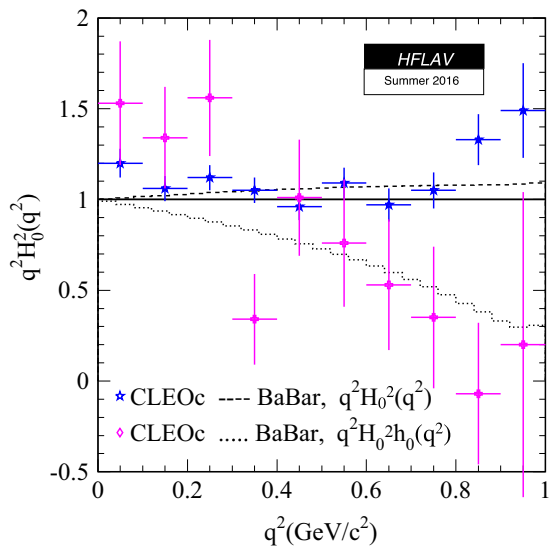

Fig. 203 Comparison between CLEO-c and BaBar results for the quantities $q^2H_0^2(q^2)$ and $q^2h_0(q^2)H_0(q^2)$

In Fig. 203, measured values from CLEO-c of the products $q^2H_0^2(q^2)$ and $q^2h_0(q^2)H_0(q^2)$ are compared with corresponding results from BaBar illustrating the difference in behavior of the scalar h_0 component and the H_0 form factor. For this comparison, the plotted values from BaBar for the two distributions are fixed to 1 at $q^2 = 0$. The different behavior of $h_0(q^2)$ and $H_0(q^2)$ can be explained by their different dependence in the p^* variable.

Table 280 lists measurements of r_V and r_2 from several experiments. Most of the measurements assume that the q^2 dependence of hadronic form factors is given by the simple pole ansatz. Some of these measurements do not consider a S-wave contribution and it is included in the measured values. The measurements are plotted in Fig. 204, which shows that they are all consistent.

Table 280 Results for r_V and r_2 from various experiments

Experiment	Refs.	r_V	r_2
$D^+ \to \overline{K}^{*0}l^+\nu$			
E691	[1195]	$2.0 \pm 0.6 \pm 0.3$	$0.0 \pm 0.5 \pm 0.2$
E653	[1196]	$2.00 \pm 0.33 \pm 0.16$	$0.82 \pm 0.22 \pm 0.11$
E687	[1197]	$1.74 \pm 0.27 \pm 0.28$	$0.78 \pm 0.18 \pm 0.11$
E791 (e)	[1198]	$1.90 \pm 0.11 \pm 0.09$	$0.71 \pm 0.08 \pm 0.09$
E791 (μ)	[1199]	$1.84 \pm 0.11 \pm 0.09$	$0.75 \pm 0.08 \pm 0.09$
Beatrice	[1200]	$1.45 \pm 0.23 \pm 0.07$	$1.00 \pm 0.15 \pm 0.03$
FOCUS	[1189]	$1.504 \pm 0.057 \pm 0.039$	$0.875 \pm 0.049 \pm 0.064$
$D^0 \to \overline{K}^0\pi^-\mu^+\nu$			
FOCUS	[1201]	$1.706 \pm 0.677 \pm 0.342$	$0.912 \pm 0.370 \pm 0.104$
BaBar	[1193]	$1.493 \pm 0.014 \pm 0.021$	$0.775 \pm 0.011 \pm 0.011$
$D_s^+ \to \phi\, e^+\nu$			
BaBar	[1190]	$1.849 \pm 0.060 \pm 0.095$	$0.763 \pm 0.071 \pm 0.065$
$D^0, D^+ \to \rho\, e\nu$			
CLEO	[1202]	$1.40 \pm 0.25 \pm 0.03$	$0.57 \pm 0.18 \pm 0.06$

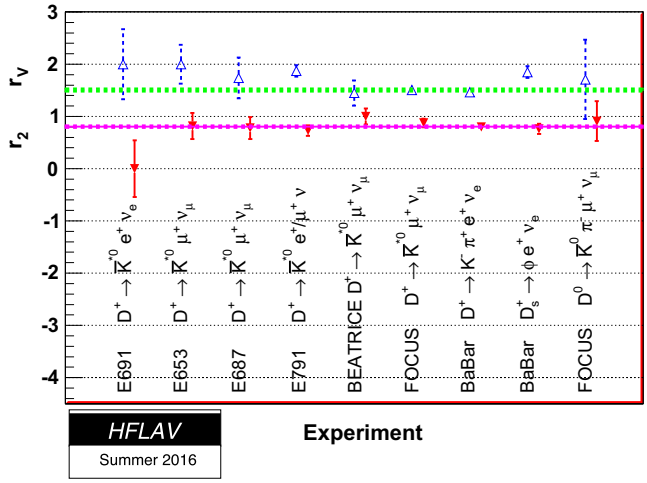

Fig. 204 A comparison of r_2 (*filled inverted triangles*) and r_V (*open triangles*) values from various experiments. The first seven measurements are for $D^+ \to K^-\pi^+l^+\nu_l$ decays. Also shown as a *line* with 1-σ limits is the average of these. The last two points are D_s^+ and D^0 decays

8.6 Leptonic decays

Purely leptonic decays of D^+ and D_s^+ mesons are among the simplest and theoretically cleanest probes of $c \to d$ and $c \to s$ quark flavor-changing transitions. The branching fraction of leptonic decays that proceed via the annihilation of the initial quark-antiquark pair ($c\bar{d}$ or $c\bar{s}$) into a virtual W^+ that finally materializes as an antilepton-neutrino pair ($\ell^+\nu_\ell$). Their Standard Model branching fraction is given by

$$\mathcal{B}(D_q^+ \to \ell^+\nu_\ell) = \frac{G_F^2}{8\pi}\tau_{D_q} f_{D_q}^2 |V_{cq}|^2 m_{D_q} m_\ell^2 \left(1 - \frac{m_\ell^2}{m_{D_q}^2}\right)^2. \quad (266)$$

Here, m_{D_q} is the D_q meson mass, τ_{D_q} is its lifetime, m_ℓ is the charged lepton mass, $|V_{cq}|$ is the magnitude of the relevant CKM matrix element, and G_F is the Fermi coupling constant. The parameter f_{D_q} is the D_q meson decay constant and is related to the wave-function overlap of the meson's constituent quark and anti-quark. The decay constants have been predicted using several methods, the most accurate and robust being the lattice gauge theory (LQCD) calculations. The Flavor Lattice Averaging Group [222] combines all LQCD calculations and provides averaged values for f_D and f_{D_s} (see Table 281) that are used within this section to extract the magnitudes of the V_{cd} and V_{cs} CKM matrix elements from experimentally measured branching fractions of $D^+ \to \ell^+\nu_\ell$ and $D_s^+ \to \ell^+\nu_\ell$ decays, respectively.

The leptonic decays of pseudoscalar mesons are helicity-suppressed and their decay rates are thus proportional to the square of the charged lepton mass. Leptonic decays into electrons, with expected $\mathcal{B} \lesssim 10^{-7}$, are not experimentally observable yet, whereas decays to taus are favored over decays to muons. In particular, the ratio of the latter decays is equal to $R_{\tau/\mu}^{D_q} \equiv \mathcal{B}(D_q^+ \to \tau^+\nu_\tau)/\mathcal{B}(D_q^+ \to \mu^+\nu_\mu) = m_\tau^2/m_\mu^2 \cdot (1 - m_\tau^2/m_{D_q}^2)^2/(1 - m_\mu^2/m_{D_q}^2)^2$, and amounts to 9.76 ± 0.03 in the case of D_s^+ decays and to 2.67 ± 0.01 in the case of D^+ decays based on the world average values of masses of the muon, tau and D_q meson given in Ref. [6]. Any deviation from this expectation could only be interpreted as violation of lepton universality in charged currents and would hence point to NP effects [1203].

Table 281 The LQCD average for D and D_s meson decay constants and their ratio from the Flavor Lattice Averaging Group [222]

Quantity	Value
f_D	212.15 ± 1.45 MeV
f_{D_s}	248.83 ± 1.27 MeV
f_{D_s}/f_D	1.1716 ± 0.0032

Averages presented within this subsection are weighted averages, in which correlations between measurements and dependencies on input parameters are taken into account. There is only one new experimental result on leptonic charm decays since our last report from 2014 – the measurements of $\mathcal{B}(D_s^+ \to \mu^+\nu_\mu)$ and $\mathcal{B}(D_s^+ \to \tau^+\nu_\tau)$ by BESIII collaboration [1204]. The Lattice QCD calculations of the D and D_s meson decay constants have improved significantly since our last report and we use the latest averages of $N_f = 2+1+1$ calculations provided by the Flavour Lattice Averaging Group [222] in our determinations of the CKM matrix elements $|V_{cd}|$ and $|V_{cs}|$.

8.6.1 $D^+ \to \ell^+\nu_\ell$ decays and $|V_{cd}|$

We use measurements of the branching fraction $\mathcal{B}(D^+ \to \mu^+\nu_\mu)$ from CLEO-c [1103] and BESIII [1205] to calculate the world average (WA) value. We obtain

$$\mathcal{B}^{\mathrm{WA}}(D^+ \to \mu^+\nu_\mu) = (3.74 \pm 0.17) \times 10^{-4}, \quad (267)$$

from which we determine the product of the decay constant and the CKM matrix element to be

$$f_D|V_{cd}| = (45.9 \pm 1.1)\ \mathrm{MeV}, \quad (268)$$

where the uncertainty includes the uncertainty on $\mathcal{B}^{\mathrm{WA}}(D^+ \to \mu^+\nu_\mu)$ and external inputs[41] needed to extract $f_D|V_{cd}|$ from the measured branching fraction using Eq. (266). Using the LQCD value for f_D from Table 281 we finally obtain the CKM matrix element V_{cd} to be

$$|V_{cd}| = 0.2164 \pm 0.0050(\mathrm{exp.}) \pm 0.0015(\mathrm{LQCD}), \quad (269)$$

[41] These values (taken from the PDG 2014 edition [327]) are $m_\mu = (0.1056583715 \pm 0.0000000035)$ GeV/c^2, $m_D = (1.86961 \pm 0.00009)$ GeV/c^2 and $\tau_D = (1040 \pm 7) \times 10^{-15}$ s.

Table 282 Experimental results and world averages for $\mathcal{B}(D^+ \to \ell^+\nu_\ell)$ and $f_D|V_{cd}|$. The first uncertainty is statistical and the second is experimental systematic. The third uncertainty in the case of $f_{D^+}|V_{cd}|$ is due to external inputs (dominated by the uncertainty of τ_D)

Mode	$\mathcal{B}$ (10^{-4})	$f_D\|V_{cd}\|$ (MeV)	References
$\mu^+\nu_\mu$	$3.82 \pm 0.32 \pm 0.09$	$46.4 \pm 1.9 \pm 0.5 \pm 0.2$	CLEO-c [1103]
	$3.71 \pm 0.19 \pm 0.06$	$45.7 \pm 1.2 \pm 0.4 \pm 0.2$	BESIII [1205]
	$3.74 \pm 0.16 \pm 0.05$	$45.9 \pm 1.0 \pm 0.3 \pm 0.2$	Average
$e^+\nu_e$	<0.088 at 90% C.L.		CLEO-c [1103]
$\tau^+\nu_\tau$	<12 at 90% C.L.		CLEO-c [1103]

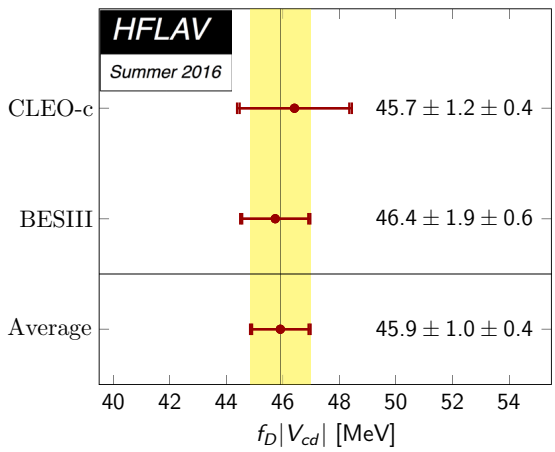

Fig. 205 WA value for $f_D|V_{cd}|$. For each point, the first error listed is the statistical and the second error is the systematic error

where the uncertainties are from the experiments and lattice calculations, respectively. All input values and the resulting world averages are summarized in Table 282 and plotted in Fig. 205.

The upper limit on the ratio of branching fractions is found to be $R^D_{\tau/\mu} < 3.2$ at 90% C.L., which is just slightly above the SM expected value.

8.6.2 $D_s^+ \to \ell^+\nu_\ell$ decays and $|V_{cs}|$

We use measurements of the absolute branching fraction $\mathcal{B}(D_s^+ \to \mu^+\nu_\mu)$ from CLEO-c [1137], BaBar [1206], Belle [1207], and BESIII [1204], and obtain a WA value of

$$\mathcal{B}^{\rm WA}(D_s^+ \to \mu^+\nu_\mu) = (5.54 \pm 0.23) \times 10^{-3}. \quad (270)$$

The WA value for $\mathcal{B}(D_s^+ \to \tau^+\nu_\tau)$ is also calculated from CLEO-c, BaBar, Belle, and BESIII measurements. CLEO-c made separate measurements for $\tau^+ \to e^+\nu_e\overline{\nu}_\tau$ [1208], $\tau^+ \to \pi^+\overline{\nu}_\tau$ [1137], and $\tau^+ \to \rho^+\overline{\nu}_\tau$ [1209], BaBarmade separate measurements for $\tau^+ \to e^+\nu_e\overline{\nu}_\tau$ [1206] and $\tau^+ \to \mu^+\nu_\mu\overline{\nu}_\tau$, Belle made separate measurements for $\tau^+ \to e^+\nu_e\overline{\nu}_\tau$, $\tau^+ \to \mu^+\nu_\mu\overline{\nu}_\tau$, and $\tau^+ \to \pi^+\overline{\nu}_\tau$ [1207], and BESIII made measurements using $\tau^+ \to \pi^+\overline{\nu}_\tau$ [1204] decays. Combining all of them we obtain the WA value of

$$\mathcal{B}^{\rm WA}(D_s^+ \to \tau^+\nu_\tau) = (5.51 \pm 0.24) \times 10^{-2}. \quad (271)$$

The ratio of branching fractions is found to be

$$R^{D_s}_{\tau/\mu} = 9.95 \pm 0.57, \quad (272)$$

and is consistent with the value expected in the SM.

From the average values of branching fractions of muonic and tauonic decays we determine[42] the product of D_s meson decay constant and the $|V_{cs}|$ CKM matrix element to be

$$f_{D_s}|V_{cs}| = (250.3 \pm 4.5)\ \text{MeV}, \quad (273)$$

where the uncertainty is due to the uncertainties on $\mathcal{B}^{\rm WA}(D_s^+ \to \mu^+\nu_\mu)$ and $\mathcal{B}^{\rm WA}(D_s^+ \to \tau^+\nu_\tau)$ and the external inputs. All input values and the resulting world averages are summarized in Table 283 and plotted in Fig. 206. To obtain the averages given within this subsection and in Table 283 we have taken into account the correlations within each experiment[43] for the uncertainties related to: normalization, tracking, particle identification, signal and background parameterizations, and peaking background contributions.

Using the LQCD value for f_{D_s} from Table 281, we finally obtain the magnitude of the CKM matrix element V_{cs} to be

$$|V_{cs}| = 1.006 \pm 0.018(\text{exp.}) \pm 0.005(\text{LQCD}), \quad (274)$$

where the uncertainties are from the experiments and lattice calculations, respectively.

8.6.3 Comparison with other determinations of $|V_{cd}|$ and $|V_{cs}|$

Table 284 summarizes and Fig. 207 shows all determinations of the CKM matrix elements $|V_{cd}|$ and $|V_{cs}|$. As can be seen, the most precise direct determinations of these CKM

[42] We use the following values (taken from PDG 2014 edition [327]) for external parameters entering Eq. (266): $m_\tau = (1.77686 \pm 0.00012)$ GeV/c^2, $m_{D_s} = (1.96830 \pm 0.00010)$ GeV/c^2 and $\tau_{D_s} = (500 \pm 7) \times 10^{-15}$ s.

[43] In the case of BaBar we use the covariance matrix from the errata of Ref. [1206].

Table 283 Experimental results and world averages for $\mathcal{B}(D_s^+ \to \ell^+\nu_\ell)$ and $f_{D_s}|V_{cs}|$. The first uncertainty is statistical and the second is experimental systematic. The third uncertainty in the case of $f_{D_s}|V_{cs}|$ is due to external inputs (dominated by the uncertainty of τ_{D_s}). We have recalculated $\mathcal{B}(D_s^+ \to \tau^+\nu_\tau)$ quoted by CLEO-c and BaBar using the latest values for branching fractions of τ decays to electron, muon, or pion and neutrinos [6]. CLEO-c and BaBar include statistical uncertainty of number of D_s tags (denominator in the calculation of branching fraction) in the statistical uncertainty of measured $\mathcal{B}$. We subtract this uncertainty from the statistical one and add it to the systematic uncertainty

Mode	$\mathcal{B}$ (10^{-2})	$f_{D_s}\|V_{cs}\|$ (MeV)	References
$\mu^+\nu_\mu$	$0.565 \pm 0.044 \pm 0.020$	$250.8 \pm 9.8 \pm 4.4 \pm 1.8$	CLEO-c [1137]
	$0.602 \pm 0.037 \pm 0.032$	$258.9 \pm 8.0 \pm 6.9 \pm 1.8$	BaBar [1206]
	$0.531 \pm 0.028 \pm 0.020$	$243.1 \pm 6.4 \pm 4.6 \pm 1.7$	Belle [1207]
	$0.517 \pm 0.075 \pm 0.021$	$239.9 \pm 17.4 \pm 4.9 \pm 1.7$	BESIII [1204]
	$0.554 \pm 0.020 \pm 0.013$	$248.2 \pm 4.4 \pm 2.8 \pm 1.7$	Average
$\tau^+(e^+)\nu_\tau$	$5.31 \pm 0.47 \pm 0.22$	$246.1 \pm 10.9 \pm 5.1 \pm 1.7$	CLEO-c [1209]
$\tau^+(\pi^+)\nu_\tau$	$6.46 \pm 0.80 \pm 0.23$	$271.4 \pm 16.8 \pm 4.8 \pm 1.9$	CLEO-c [1137]
$\tau^+(\rho^+)\nu_\tau$	$5.50 \pm 0.54 \pm 0.24$	$250.4 \pm 12.3 \pm 5.5 \pm 1.8$	CLEO-c [1208]
$\tau^+\nu_\tau$	$5.57 \pm 0.32 \pm 0.15$	$252.0 \pm 7.2 \pm 3.4 \pm 1.8$	CLEO-c average
$\tau^+(e^+)\nu_\tau$	$5.08 \pm 0.52 \pm 0.68$	$240.7 \pm 12.3 \pm 16.1 \pm 1.7$	BaBar [1206]
$\tau^+(\mu^+)\nu_\tau$	$4.90 \pm 0.46 \pm 0.54$	$236.4 \pm 11.1 \pm 13.0 \pm 1.7$	BaBar [1206]
$\tau^+\nu_\tau$	$4.95 \pm 0.36 \pm 0.58$	$237.6 \pm 8.6 \pm 13.8 \pm 1.7$	BaBar average
$\tau^+(e^+)\nu_\tau$	$5.37 \pm 0.33^{+0.35}_{-0.31}$	$247.4 \pm 7.6^{+8.1}_{-7.1} \pm 1.7$	Belle [1207]
$\tau^+(\mu^+)\nu_\tau$	$5.86 \pm 0.37^{+0.34}_{-0.59}$	$258.5 \pm 8.2^{+7.5}_{-13.0} \pm 1.8$	Belle [1207]
$\tau^+(\pi^+)\nu_\tau$	$6.04 \pm 0.43^{+0.46}_{-0.40}$	$262.4 \pm 9.3^{+10.0}_{-8.7} \pm 1.8$	Belle [1207]
$\tau^+\nu_\tau$	$5.70 \pm 0.21 \pm 0.31$	$254.9 \pm 4.7 \pm 6.9 \pm 1.8$	Belle average
$\tau^+(\pi^+)\nu_\tau$	$3.28 \pm 1.83 \pm 0.37$	$194 \pm 54 \pm 11 \pm 1$	BESIII [1204]
$\tau^+\nu_\tau$	$5.51 \pm 0.18 \pm 0.16$	$250.9 \pm 4.0 \pm 3.7 \pm 1.8$	All average
$\mu^+\nu_\mu + \tau^+\nu_\tau$		$250.3 \pm 3.1 \pm 2.7 \pm 1.8$	All average
$e^+\nu_e$	<0.0083 at 90% C.L.		Belle [1207]

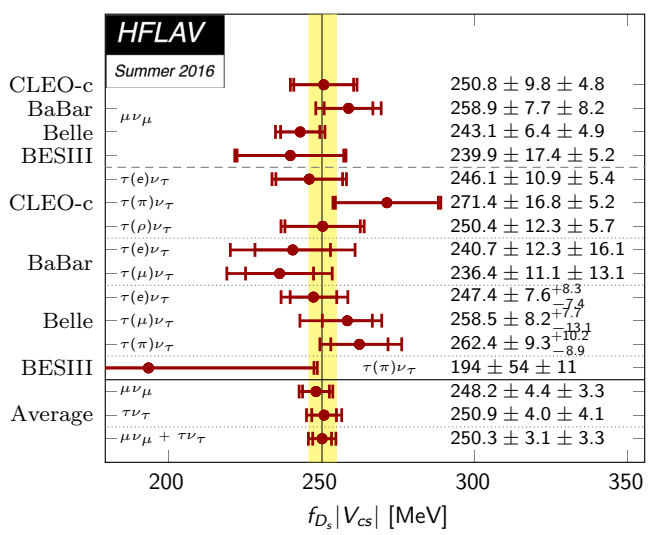

Fig. 206 WA value for $f_{D_s}|V_{cs}|$. For each point, the first error listed is the statistical and the second error is the systematic error

matrix elements are those from leptonic and semileptonic $D_{(s)}$ decays. The values are in agreement within uncertainties with the values obtained from the global fit assuming CKM matrix unitarity.

8.6.4 *Extraction of $D_{(s)}$ meson decay constants*

Assuming unitarity of the CKM matrix, the values of the elements relevant in the case of (semi-)leptonic charm decays are known from the global fit of the CKM matrix and are given in Table 284. These values can be used to extract the D and D_s meson decay constants from the experimentally measured products $f_D|V_{cd}|$ and $f_{D_s}|V_{cs}|$ using Eq. (268) and Eq. (273), respectively. This leads to the experimentally measured $D_{(s)}$ meson decay constants to be:

$$f_D^{\text{exp}} = (203.7 \pm 4.9)\ \text{MeV}, \tag{275}$$

$$f_{D_s}^{\text{exp}} = (257.1 \pm 4.6)\ \text{MeV}, \tag{276}$$

and the ratio of the constants is determined to be

$$f_{D_s}^{\text{exp}}/f_D^{\text{exp}} = 1.262 \pm 0.037. \tag{277}$$

The values are in agreement with the LQCD determinations given in Table 281 within the uncertainties. The largest discrepancy is in the determinations of the ratio of the decay constants where the agreement is only at the level of 2.4σ.

Table 284 Average of the magnitudes of the CKM matrix elements $|V_{cd}|$ and $|V_{cs}|$ determined from the leptonic and semileptonic D and D_s decays. In the calculation of average values we assume 100% correlations in uncertainties due to LQCD. The values determined from neutrino scattering or W decays and determination from the global fit to the CKM matrix are given for comparison as well

Method	References	Value
		$\|V_{cd}\|$
$D \to \ell\nu_\ell$	This section	$0.2164 \pm 0.0050(\text{exp.}) \pm 0.0015(\text{LQCD})$
$D \to \pi\ell\nu_\ell$	Section 8.5	$0.2141 \pm 0.0029(\text{exp.}) \pm 0.0093(\text{LQCD})$
	Average	0.216 ± 0.005
νN	PDG [6]	0.230 ± 0.011
Global CKM Fit	CKMFitter [252]	$0.22529^{+0.00041}_{-0.00032}$
		$\|V_{cs}\|$
$D_s \to \ell\nu_\ell$	This section	$1.006 \pm 0.018(\text{exp.}) \pm 0.005(\text{LQCD})$
$D \to K\ell\nu_\ell$	Section 8.5	$0.967 \pm 0.005(\text{exp.}) \pm 0.025(\text{LQCD})$
	Average	0.997 ± 0.017
$W \to c\bar{s}$	PDG [6]	$0.94^{+0.32}_{-0.26} \pm 0.13$
Global CKM Fit	CKMFitter [252]	$0.973394^{+0.000074}_{-0.000096}$

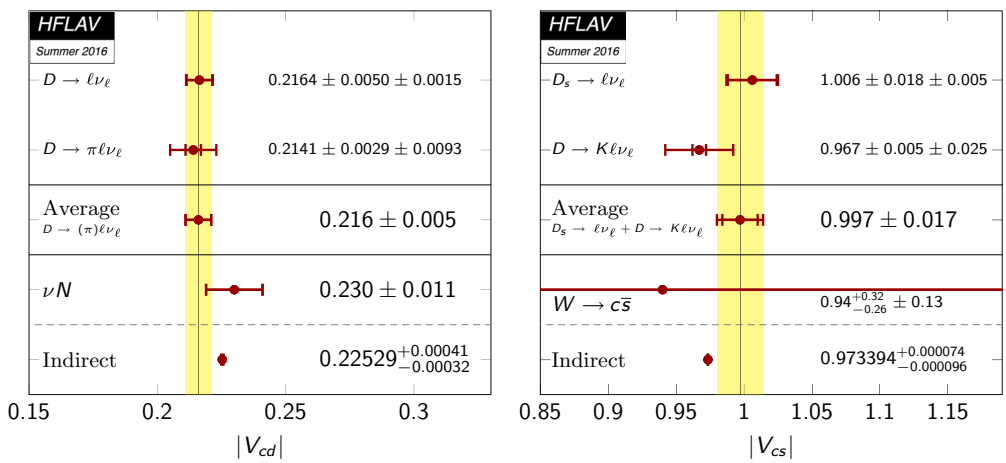

Fig. 207 Comparison of magnitudes of the CKM matrix elements $|V_{cd}|$ (*left*) and $|V_{cs}|$ (*right*) determined from the (semi-)leptonic charm decays and from neutrino scattering data or W decays and determination from the global fit assuming CKM unitarity [252]

8.7 Hadronic decays of D_s mesons

BABAR, CLEO-c and Belle collaborations have measured the absolute branching fractions of hadronic decays, $D_s^+ \to K^-K^+\pi^+$, $D_s^+ \to \overline{K}^0\pi^+$, and $D_s^+ \to \eta\pi^+$. The first two decay modes are the reference modes for the measurements of branching fractions of the D_s^+ decays to any other final state. Table 285 and Fig. 208 summarise the individual measurements and averaged values, which are found to be

$$\mathcal{B}^{\text{WA}}(D_s^+ \to K^-K^+\pi^+) = (5.44 \pm 0.14)\%, \quad (278)$$

$$\mathcal{B}^{\text{WA}}(D_s^+ \to \overline{K}^0\pi^+) = (3.00 \pm 0.09)\%, \quad (279)$$

$$\mathcal{B}^{\text{WA}}(D_s^+ \to \eta\pi^+) = (1.71 \pm 0.08)\%, \quad (280)$$

where the uncertainties are total uncertainties. These averages are the same as in our previous report from 2014. The $\mathcal{B}(D_s^+ \to K^-K^+\pi^+)$ is for a phase space integrated decay and therefore includes all intermediate resonances.

8.8 Two-body hadronic D^0 decays and final state radiation

Measurements of the branching fractions for the decays $D^0 \to K^-\pi^+$, $D^0 \to \pi^+\pi^-$, and $D^0 \to K^+K^-$ have reached sufficient precision to allow averages with $\mathcal{O}(1\%)$ relative uncertainties. At these precisions, Final State Radiation (FSR) must be treated correctly and consistently across the input measurements for the accuracy of the averages to match the precision. The sensitivity of measurements to FSR arises because of a tail in the distribution of radiated energy that extends to the kinematic limit. The tail beyond $\sum E_\gamma \approx 30$ MeV causes typical selection variables like the hadronic invariant mass to shift outside the selection range dictated by experimental resolution, as shown in Fig. 209. While the differential rate for the tail is small, the integrated rate amounts to several percent of the total $h^+h^-(n\gamma)$ rate because of the tail's extent. The tail therefore trans-

Table 285 Experimental results and world averages for branching fractions of $D_s^+ \to K^-K^+\pi^+$, $D_s^+ \to \overline{K}^0K^+$, and $D_s^+ \to \eta\pi^+$ decays. The first uncertainty is statistical and the second is experimental systematic. CLEO-c reports in Ref. [1138] $\mathcal{B}(D_s^+ \to K_S^0K^+)$. We include it in the average of $\mathcal{B}(D_s^+ \to \overline{K}^0K^+)$ by using the relation $\mathcal{B}(D_s^+ \to \overline{K}^0K^+) \equiv 2\mathcal{B}(D_s^+ \to K_S^0K^+)$

Mode	$\mathcal{B}$ (10^{-2})	References
$K^-K^+\pi^+$	5.78 ± 0.20 ± 0.30	BABAR [1206]
	5.55 ± 0.14 ± 0.13	CLEO-c [1138]
	5.06 ± 0.15 ± 0.21	Belle [1207]
	5.44 ± 0.09 ± 0.11	Average
$\overline{K}^0K^+$	3.04 ± 0.10 ± 0.06	CLEO-c [1138]
	2.95 ± 0.11 ± 0.09	Belle [1207]
	3.00 ± 0.07 ± 0.05	Average
$\eta\pi^+$	1.67 ± 0.08 ± 0.06	CLEO-c [1138]
	1.82 ± 0.14 ± 0.07	Belle [1207]
	1.71 ± 0.07 ± 0.08	Average

lates directly into a several percent loss in experimental efficiency.

All measurements that include an FSR correction have a correction based on the use of PHOTOS [1210–1213] within the experiment's Monte Carlo simulation. PHOTOS itself, however, has evolved, over the period spanning the set of measurements. In particular, the incorporation of interference between radiation off the two separate mesons has proceeded in stages: it was first available for particle–antiparticle pairs in version 2.00 (1993), extended to any two-body, all-charged, final states in version 2.02 (1999), and further extended to multi-body final states in version 2.15 (2005). The effects of interference are clearly visible, as shown in Fig. 209, and cause a roughly 30% increase in the integrated rate into the high energy photon tail. To evaluate the FSR correction incorporated into a given measurement, we must therefore note whether any correction was made, the version of PHOTOS used in correction, and whether the interference terms in PHOTOS were turned on.

8.8.1 Branching fraction corrections

Before averaging the measured branching fractions, the published results are updated, as necessary, to the FSR prediction of PHOTOS 2.15 with interference included. The correction will always shift a branching fraction to a higher value: with no FSR correction or with no interference term in the correction, the experimental efficiency determination will be biased high, and therefore the branching fraction will be biased low.

Most of the branching fraction analyses used the kinematic quantity sensitive to FSR in the candidate selection criteria. For the analyses at the $\psi(3770)$, this variable was

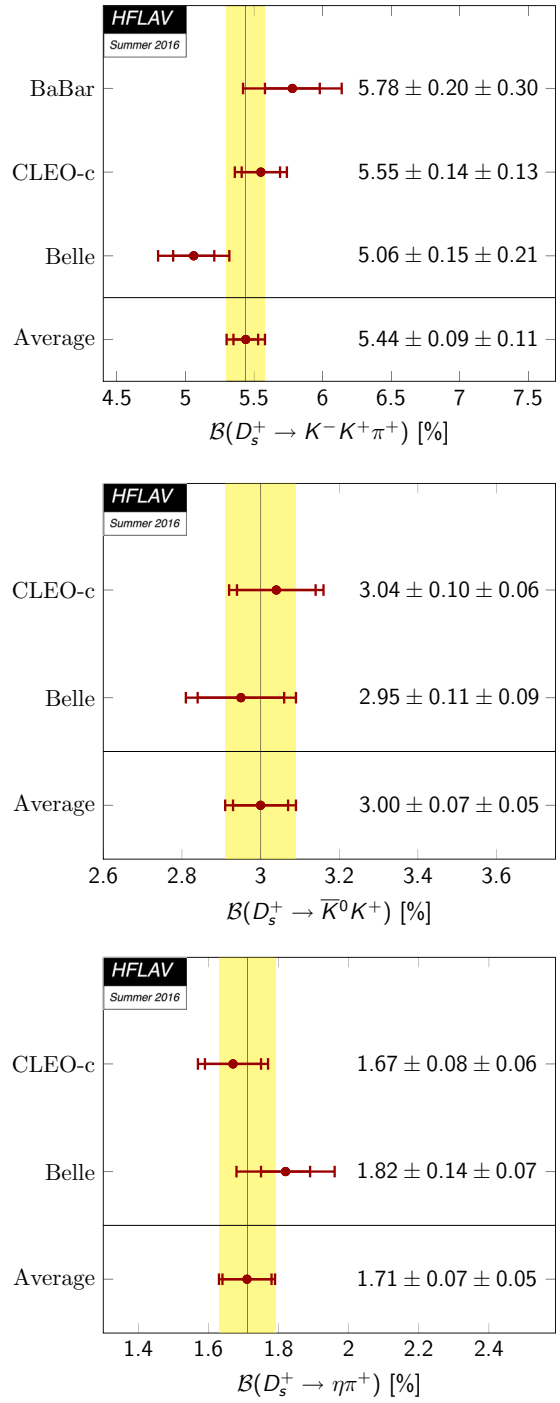

Fig. 208 WA values for $\mathcal{B}(D_s^+ \to K^-K^+\pi^+)$ (*top*), $\mathcal{B}(D_s^+ \to \overline{K}^0\pi^+)$ (*middle*), $\mathcal{B}(D_s^+ \to \eta\pi^+)$ (*bottom*). For each point, the first error listed is the statistical and the second error is the systematic error

ΔE, the difference between the candidate D^0 energy and the beam energy (e.g., $E_K + E_\pi - E_{\text{beam}}$ for $D^0 \to K^-\pi^+$). In the remainder of the analyses, the relevant quantity was the reconstructed hadronic two-body mass $m_{h^+h^-}$. To make the correction, we only need to evaluate the fraction of decays that FSR moves outside of the range accepted for the analysis.

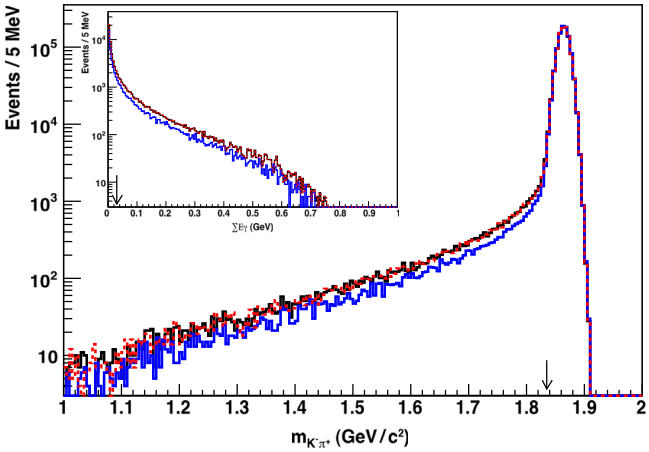

Fig. 209 The $K\pi$ invariant mass distribution for $D^0 \to K^-\pi^+(n\gamma)$ decays. The three curves correspond to three different configurations of PHOTOS for modeling FSR: version 2.02 without interference (*blue*/*grey*), version 2.02 with interference (*red dashed*) and version 2.15 with interference (*black*). The true invariant mass has been smeared with a typical experimental resolution of 10 MeV/c^2. *Inset* The corresponding spectrum of total energy radiated per event. The *arrow* indicates the $\sum E_\gamma$ value that begins to shift kinematic quantities outside of the range typically accepted in a measurement

The corrections were evaluated using an event generator (EvtGen [1214]) that incorporates PHOTOS to simulate the portions of the decay process most relevant to the correction. We compared corrections determined both with and without smearing to account for experimental resolution. The differences were negligible, typically of $\mathcal{O}(1\%)$ of the correction itself. The immunity of the correction to resolution effects comes about because most of the long FSR-induced tail in, for example, the $m_{h^+h^-}$ distribution resides well away from the selection boundaries. The smearing from resolution, on the other hand, mainly affects the distribution of events right at the boundary.

For measurements incorporating an FSR correction that did not include interference, we update by assessing the FSR-induced efficiency loss for both the PHOTOS version and configuration used in the analysis and our nominal version 2.15 with interference. For measurements that published their sensitivity to FSR, our generator-level predictions for the original efficiency loss agreed to within a few percent of the correction. This agreement lends additional credence to the procedure.

Once the event loss from FSR in the most sensitive kinematic quantity is accounted for, the event loss in other quantities is very small. For example, analyses using D^{*+} tags show little sensitivity to FSR in the reconstructed $D^{*+} - D^0$ mass difference, i.e., in $m_{K^-\pi^+\pi^+} - m_{K^-\pi^+}$. In this case the effect of FSR tends to cancel in the difference of reconstructed masses. In the $\psi(3770)$ analyses, the beam-constrained mass distributions ($\sqrt{E^2_{\text{beam}} - |\vec{p}_K + \vec{p}_\pi|^2}$) also show much smaller sensitivity than does the two-body mass.

The FOCUS [1215] analysis of the branching fraction ratios $\mathcal{B}(D^0 \to \pi^+\pi^-)/\mathcal{B}(D^0 \to K^-\pi^+)$ and $\mathcal{B}(D^0 \to K^+K^-)/\mathcal{B}(D^0 \to K^-\pi^+)$ obtained yields using fits to the two-body mass distributions. FSR will both distort the low end of the signal mass peak, and will contribute a signal component to the low side tail used to estimate the background. The fitting procedure is not sensitive to signal events out in the FSR tail, which would be counted as part of the background.

A more complex toy Monte Carlo procedure was required to analyze the effect of FSR on the fitted yields, which were published with no FSR corrections applied. A detailed description of the procedure and results is available on the HFLAV web site, and a brief summary is provided here. Determining the correction involved an iterative procedure in which samples of similar size to the FOCUS sample were generated and then fit using the FOCUS signal and background parameterizations. The MC parameterizations were tuned based on differences between the fits to the toy MC data and the FOCUS fits, and the procedure was repeated. These steps were iterated until the fit parameters matched the original FOCUS parameters.

The toy MC samples for the first iteration were based on the generator-level distribution of $m_{K^-\pi^+}$, $m_{\pi^+\pi^-}$, and $m_{K^+K^-}$, including the effects of FSR, smeared according to the original FOCUS resolution function, and on backgrounds generated using the parameterization from the final FOCUS fits. For each iteration, 400–1600 individual data-sized samples were generated and fit. The means of the parameters from these fits determined the corrections to the generator parameters for the following iteration. The ratio between the number of signal events generated and the final signal yield provides the required FSR correction in the final iteration. Only a few iterations were required in each mode. Figure 210 shows the FOCUS data, the published FOCUS fits, and the final toy MC parameterizations. The toy MC provides an excellent description of the data.

The corrections obtained to the individual FOCUS yields were 1.0298 ± 0.0001 for $K^-\pi^+$, 1.062 ± 0.001 for $\pi^+\pi^-$, and 1.0183 ± 0.0003 for K^+K^-. These corrections tend to cancel in the branching ratios, leading to corrections of 1.031 ± 0.001 for $\mathcal{B}(D^0 \to \pi^+\pi^-)/\mathcal{B}(D^0 \to K^-\pi^+)$, and 0.9888 ± 0.0003 for $\mathcal{B}(D^0 \to K^+K^-)/\mathcal{B}(D^0 \to K^-\pi^+)$.

Table 286 summarizes the corrected branching fractions. The published FSR-related modeling uncertainties have been replaced by with a new, common, estimate based on the assumption that the dominant uncertainty in the FSR corrections comes from the fact that the mesons are treated like structureless particles. No contributions from structure-dependent terms in the decay process (e.g., radiation off individual quarks) are included in PHOTOS. Internal studies done by various experiments have indicated that in $K\pi$ decays, the PHOTOS corrections agree with data at the 20–

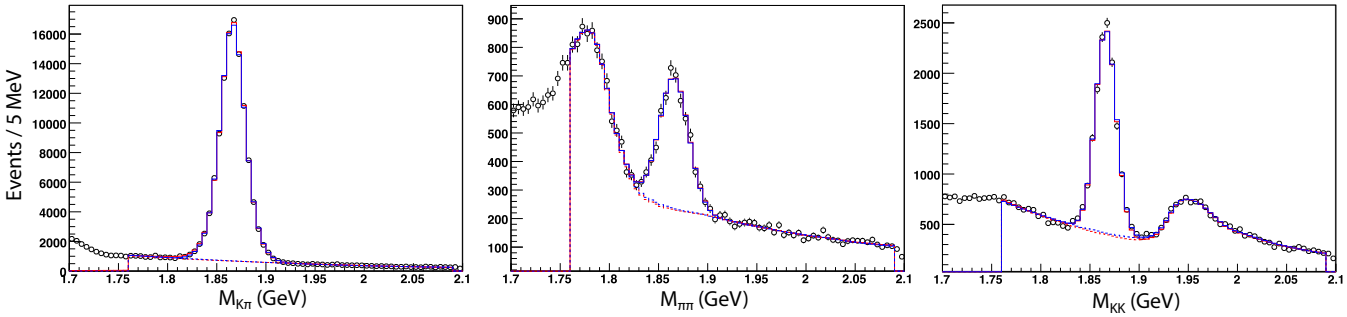

Fig. 210 FOCUS data (*dots*), original fits (*blue*) and toy MC parameterization (*red*) for $D^0 \to K^-\pi^+$ (*left*), $D^0 \to \pi^+\pi^-$ (*center*), and $D^0 \to \pi^+\pi^-$ (*right*)

Table 286 The experimental measurements relating to $\mathcal{B}(D^0 \to K^-\pi^+)$, $\mathcal{B}(D^0 \to \pi^+\pi^-)$, and $\mathcal{B}(D^0 \to K^+K^-)$ after correcting to the common version and configuration of PHOTOS. The uncertainties are statistical and total systematic, with the FSR-related systematic estimated in this procedure shown in parentheses. Also listed are the percent shifts in the results from the correction, if any, applied here, as well as the original PHOTOS and interference configuration for each publication

Experiment (acronym)	Result (rescaled)	Correction (%)	PHOTOS
$D^0 \to K^-\pi^+$			
CLEO-c 14 (CC14) [1106]	$3.934 \pm 0.021 \pm 0.061(31)\%$	–	2.15/yes
BABAR 07 (BB07) [1216]	$4.035 \pm 0.037 \pm 0.074(24)\%$	0.69	2.02/no
CLEO II 98 (CL98) [1217]	$3.920 \pm 0.154 \pm 0.168(32)\%$	2.80	None
ALEPH 97 (AL97) [1218]	$3.930 \pm 0.091 \pm 0.125(32)\%$	0.79	2.0/no
ARGUS 94 (AR94) [1219]	$3.490 \pm 0.123 \pm 0.288(24)\%$	2.33	None
CLEO II 93 (CL93) [1220]	$3.960 \pm 0.080 \pm 0.171(15)\%$	0.38	2.0/no
ALEPH 91 (AL91) [1221]	$3.730 \pm 0.351 \pm 0.455(34)\%$	3.12	None
$D^0 \to \pi^+\pi^-/D^0 \to K^-\pi^+$			
CLEO-c 10 (CC10) [1104]	$0.0370 \pm 0.0006 \pm 0.0009(02)$	–	2.15/yes
CDF 05 (CD05) [1222]	$0.03594 \pm 0.00054 \pm 0.00043(15)$	–	2.15/yes
FOCUS 02 (FO02) [1215]	$0.0364 \pm 0.0012 \pm 0.0006(02)$	3.10	None
$D^0 \to K^+K^-/D^0 \to K^-\pi^+$			
CLEO-c 10 [1104]	$0.1041 \pm 0.0011 \pm 0.0012(03)$	–	2.15/yes
CDF 05 [1222]	$0.0992 \pm 0.0011 \pm 0.0012(01)$	–	2.15/yes
FOCUS 02 [1215]	$0.0982 \pm 0.0014 \pm 0.0014(01)$	-1.12	None

30% level. We therefore attribute a 25% uncertainty to the FSR prediction from potential structure-dependent contributions. For the other two modes, the only difference in structure is the final state valence quark content. While radiative corrections typically come in with a $1/M$ dependence, one would expect the additional contribution from the structure terms to come in on time scales shorter than the hadronization time scale. In this case, you might expect $\Lambda_{\rm QCD}$ to be the relevant scale, rather than the quark masses, and therefore that the amplitude is the same for the three modes. In treating the correlations among the measurements this is what we assume. We also assume that the PHOTOS amplitudes and any missing structure amplitudes are relatively real with constructive interference. The uncertainties largely cancel in the branching fraction ratios. For the final average branching fractions, the FSR uncertainty on $K\pi$ dominates. Note that because of the relative sizes of FSR in the different modes, the $\pi\pi/K\pi$ branching ratio uncertainty from FSR is positively correlated with that for the $K\pi$ branching fraction, while the $KK/K\pi$ branching ratio FSR uncertainty is negatively correlated.

The $\mathcal{B}(D^0 \to K^-\pi^+)$ measurement of reference [1223], the $\mathcal{B}(D^0 \to \pi^+\pi^-)/\mathcal{B}(D^0 \to K^-\pi^+)$ measurements of references [1122] and [1081], and the $\mathcal{B}(D^0 \to K^+K^-)/\mathcal{B}(D^0 \to K^-\pi^+)$ measurement of reference [1081] are excluded from the branching fraction averages presented here. These measurements appear not to have incorporated any FSR corrections, and insufficient information is available to determine the 2–3% corrections that would be required.

Table 287 The correlation matrix corresponding to the full covariance matrix. Subscripts h denote which of the $D^0 \to h^+h^-$ decay results from a single experiment is represented in that row or column

	CC14	BB07	CL98	AL97	AR94	CL93	AL91	$FO02_\pi$	$CD05_\pi$	$CC10_\pi$	$FO02_K$	$CD05_K$	$CC10_K$
CC14	1.000	0.139	0.057	0.084	0.031	0.033	0.023	0.070	0.103	0.068	−0.019	−0.032	−0.085
BB07	0.139	1.000	0.035	0.051	0.019	0.020	0.014	0.042	0.062	0.041	−0.012	−0.019	−0.051
CL98	0.057	0.035	1.000	0.021	0.008	0.298	0.006	0.017	0.026	0.017	−0.005	−0.008	−0.021
AL97	0.084	0.051	0.021	1.000	0.011	0.012	0.116	0.025	0.038	0.025	−0.007	−0.012	−0.031
AR94	0.031	0.019	0.008	0.011	1.000	0.004	0.003	0.009	0.014	0.009	−0.003	−0.004	−0.011
CL93	0.033	0.020	0.298	0.012	0.004	1.000	0.003	0.010	0.015	0.010	−0.003	−0.005	−0.012
AL91	0.023	0.014	0.006	0.116	0.003	0.003	1.000	0.007	0.010	0.007	−0.002	−0.003	−0.009
$FO02_\pi$	0.070	0.042	0.017	0.025	0.009	0.010	0.007	1.000	0.031	0.021	−0.006	−0.010	−0.026
$CD05_\pi$	0.103	0.062	0.026	0.038	0.014	0.015	0.010	0.031	1.000	0.031	−0.009	−0.014	−0.038
$CC10_\pi$	0.068	0.041	0.017	0.025	0.009	0.010	0.007	0.021	0.031	1.000	−0.006	−0.010	−0.025
$FO02_K$	−0.019	−0.012	−0.005	−0.007	−0.003	−0.003	−0.002	−0.006	−0.009	−0.006	1.000	0.003	0.007
$CD05_K$	−0.032	−0.019	−0.008	−0.012	−0.004	−0.005	−0.003	−0.010	−0.014	−0.010	0.003	1.000	0.012
$CC10_K$	−0.085	−0.051	−0.021	−0.031	−0.011	−0.012	−0.009	−0.026	−0.038	−0.025	0.007	0.012	1.000

8.8.2 Average branching fractions

The average branching fractions for $D^0 \to K^-\pi^+$, $D^0 \to \pi^+\pi^-$ and $D^0 \to K^+K^-$ decays are obtained from a single χ^2 minimization procedure, in which the three branching fractions are floating parameters. The central values are obtained from a fit in which the full covariance matrix – accounting for all statistical, systematic (excluding FSR), and FSR measurement uncertainties – is used. Table 287 presents the correlation matrix for this nominal fit. We then obtain the three reported uncertainties on those central values as follows: The statistical uncertainties are obtained from a fit using only the statistical covariance matrix. The systematic uncertainties are obtained by subtracting (in quadrature) the statistical uncertainties from the uncertainties determined via a fit using a covariance matrix that accounts for both statistical and systematic measurement uncertainties. The FSR uncertainties are obtained by subtracting (in quadrature) the uncertainties determined via a fit using a covariance matrix that accounts for both statistical and systematic measurement uncertainties from the uncertainties determined via the fit using the full covariance matrix.

In forming the full covariance matrix, the FSR uncertainties are treated as fully correlated (or anti-correlated) as described above. For the covariance matrices involving systematic measurement uncertainties, ALEPH's systematic uncertainties in the θ_{D^*} parameter are treated as fully correlated between the ALEPH 97 and ALEPH 91 measurements. Similarly, the tracking efficiency uncertainties in the CLEO II 98 and the CLEO II 93 measurements are treated as fully correlated.

The averaging procedure results in a final χ^2 of 11.0 for 10 (13 − 3) degrees of freedom. The branching fractions obtained are

$$\mathcal{B}(D^0 \to K^-\pi^+) = (3.962 \pm 0.017 \pm 0.038 \pm 0.027)\,\%, \tag{281}$$

$$\mathcal{B}(D^0 \to \pi^+\pi^-) = (0.144 \pm 0.002 \pm 0.002 \pm 0.002)\,\%, \tag{282}$$

$$\mathcal{B}(D^0 \to K^+K^-) = (0.399 \pm 0.003 \pm 0.005 \pm 0.002)\,\%. \tag{283}$$

The uncertainties, estimated as described above, are statistical, systematic (excluding FSR), and FSR modeling. The correlation coefficients from the fit using the total uncertainties are

	$K^-\pi^+$	$\pi^+\pi^-$	K^+K^-
$K^-\pi^+$	1.00	0.71	0.76
$\pi^+\pi^-$	0.71	1.00	0.53
K^+K^-	0.76	0.53	1.00

As the χ^2 would suggest and Fig. 211 shows, the average value for $\mathcal{B}(D^0 \to K^-\pi^+)$ and the input branching fractions agree very well. With the estimated uncertainty in the FSR modeling used here, the FSR uncertainty dominates the statistical uncertainty in the average, suggesting that experimental work in the near future should focus on verification of FSR with $\sum E_\gamma \gtrsim 100$ MeV. Note that the systematic uncertainty excluding FSR is still larger than the FSR uncertainty; in the most precise measurements of these branching fractions, the largest systematic uncertainty is the uncertainty on the tracking efficiency. The $\mathcal{B}(D^0 \to K^+K^-)$ and $\mathcal{B}(D^0 \to \pi^+\pi^-)$ measurements inferred from the branching ratio measurements also agree well (Fig. 212).

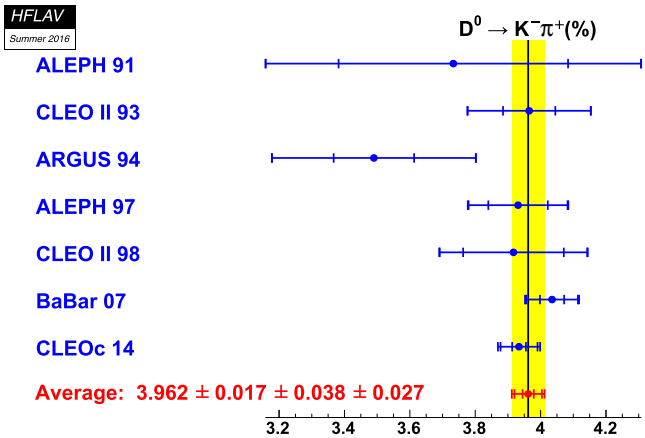

Fig. 211 Comparison of measurements of $\mathcal{B}(D^0 \to K^-\pi^+)$ (*blue*) with the average branching fraction obtained here (*red*, and *yellow band*)

The $\mathcal{B}(D^0 \to K^-\pi^+)$ average obtained here is approximately two statistical standard deviations higher than the 2016 PDG update average [6]. Table 288 shows the evolution from a fit similar to the PDG's (no FSR corrections or correlations, reference [1223] included) to the average presented here. There are two main contributions to the difference. The branching fraction in reference [1223] is low, and its exclusion shifts the result upwards. The dominant shift (+0.017%) is due to the FSR corrections, which as expected shift the result upwards.

There is no reason to presume that the effects of FSR should be different in $D^0 \to K^+\pi^-$ and $D^0 \to K^-\pi^+$ decays, as both decay to one charged kaon and one charged pion. Measurements of the relative branching fraction ratio between the doubly Cabibbo-suppressed decay $D^0 \to K^+\pi^-$ and the Cabibbo-favored decay $D^0 \to K^-\pi^+$ (R_D, determined in Sect. 8.1) are now approaching $\mathcal{O}(1\%)$ relative uncertainties. This makes it worthwhile to combine our R_D average with the $\mathcal{B}(D^0 \to K^-\pi^+)$ average obtained in Eq. (281), to provide measurements of the branching fraction:

$$\mathcal{B}(D^0 \to K^+\pi^-) = (1.379 \pm 0.023) \times 10^{-4} \text{ (assuming no } CPV), \quad (284)$$

$$\mathcal{B}(D^0 \to K^+\pi^-) = (1.383 \pm 0.023) \times 10^{-4} \text{ (} CPV \text{ allowed)}. \quad (285)$$

Note that, by definition of R_D, these branching fractions do not include any contribution from Cabibbo-favored $\overline{D}^0 \to K^+\pi^-$ decays.

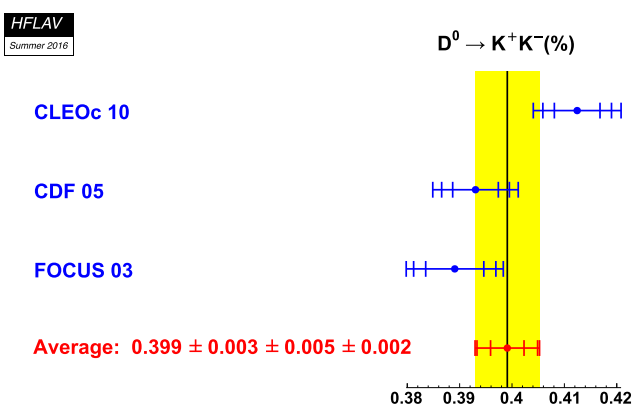

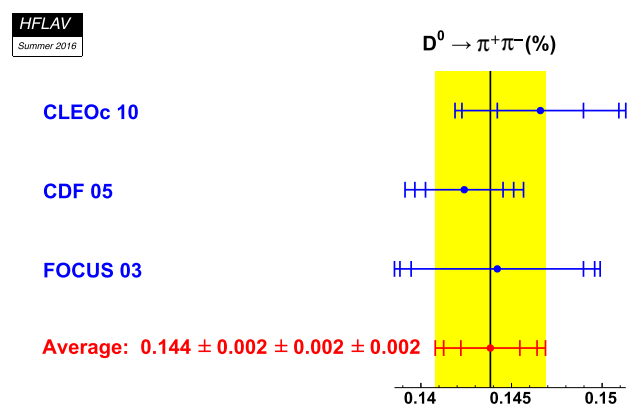

Fig. 212 The $\mathcal{B}(D^0 \to K^+K^-)$ (*left*) and $\mathcal{B}(D^0 \to \pi^+\pi^-)$ (right) values obtained by scaling the measured branching ratios with the $\mathcal{B}(D^0 \to K^-\pi^+)$ branching fraction average obtained here. For the measurements (*blue points*), the error bars correspond to the statistical, systematic and $K\pi$ normalization uncertainties. The average obtained here (*red point*, *yellow band*) lists the statistical, systematics excluding FSR, and the FSR systematic

Table 288 Evolution of the $D^0 \to K^-\pi^+$ branching fraction from a fit with no FSR corrections or correlations (similar to the average in the PDG 2016 update [6]) to the nominal fit presented here

Modes fit	Description	$\mathcal{B}(D^0 \to K^-\pi^+)$ (%)	χ^2/(deg. of freedom)
$K^-\pi^+$	PDG 2016 [6] equivalent	$3.930 \pm 0.017 \pm 0.042$	$4.5/(8-1) = 0.64$
$K^-\pi^+$	Drop Ref. [1223]	$3.938 \pm 0.017 \pm 0.042$	$4.5/(7-1) = 0.75$
$K^-\pi^+$	Add FSR corrections	$3.955 \pm 0.017 \pm 0.038 \pm 0.018$	$3.5/(7-1) = 0.58$
$K^-\pi^+$	Add FSR correlations	$3.956 \pm 0.017 \pm 0.038 \pm 0.027$	$3.6/(7-1) = 0.60$
All	–	$3.962 \pm 0.017 \pm 0.038 \pm 0.027$	$11.0/(13-3) = 1.10$

Table 289 Recent measurements of mass and width for different excited D_s mesons. The column J^P list the most significant assignment of spin and parity. If possible an average mass or width is calculated

Resonance	J^P	Decay mode	Mass (MeV/c^2)	Width (MeV)	Measured by	References
$D_{s0}^*(2317)^\pm$	0^+	$D_s^+\pi^0$	$2319.6 \pm 0.2 \pm 1.4$		BaBar	[1244]
		$D_s^+\pi^0$	$2317.3 \pm 0.4 \pm 0.8$		BaBar	[1227]
			2318.0 ± 0.8		Our average	
$D_{s1}(2460)^\pm$	1^+	$D_s^{*+}\pi^0$, $D_s^+\pi^0\gamma$, $D_s^+\gamma$, $D_s^+\pi^+\pi^-$	$2460.1 \pm 0.2 \pm 0.8$		BaBar	[1244]
		$D_s^+\pi^0\gamma$	$2458 \pm 1.0 \pm 1.0$		BaBar	[1227]
			2459.6 ± 0.7		Our average	
$D_{s1}(2536)^\pm$	1^+	$D^{*+}K_S^0$	$2535.7 \pm 0.6 \pm 0.5$		DØ	[1245]
		$D^{*+}K_S^0$, $D^{*0}K^+$	$2534.78 \pm 0.31 \pm 0.40$		BaBar	[643]
		$D_s^+\pi^+\pi^-$	$2534.6 \pm 0.3 \pm 0.7$		BaBar	[1244]
		$D^{*+}K_S^0$, $D^{*0}K^+$	$2535.0 \pm 0.6 \pm 1.0$		E687	[1246]
		$D^{*0}K^+$	$2535.3 \pm 0.2 \pm 0.5$		CLEO	[1247]
		$D^{*+}K_S^0$	$2534.8 \pm 0.6 \pm 0.6$		CLEO	[1247]
		$D^{*0}K^+$	$2535.2 \pm 0.5 \pm 1.5$		ARGUS	[1248]
		$D^{*+}K_S^0$	$2535.6 \pm 0.7 \pm 0.4$		CLEO	[1249]
		$D^{*+}K_S^0$	$2535.9 \pm 0.6 \pm 2.0$		ARGUS	[1250]
		$D^{*+}K_S^0$		$0.92 \pm 0.03 \pm 0.04$	BaBar	[1251]
			2535.10 ± 0.26	0.92 ± 0.05	Our average	
$D_{s2}^*(2573)^\pm$	2^+	D^0K^+, $D^{*+}K_S^0$	$2568.39 \pm 0.29 \pm 0.26$	$16.9 \pm 0.5 \pm 0.6$	LHCb	[1252]
		$D^+K_S^0$, D^0K^+	$2569.4 \pm 1.6 \pm 0.5$	$12.1 \pm 4.5 \pm 1.6$	LHCb	[1253]
		$D^+K_S^0$, D^0K^+	$2572.2 \pm 0.3 \pm 1.0$	$27.1 \pm 0.6 \pm 5.6$	BaBar	[1254]
		D^0K^+	$2574.25 \pm 3.3 \pm 1.6$	$10.4 \pm 8.3 \pm 3.0$	ARGUS	[1255]
		D^0K^+	$2573.2^{+1.7}_{-1.6} \pm 0.9$	$16^{+5}_{-4} \pm 3$	CLEO	[1256]
			2569.08 ± 0.35	16.9 ± 0.8	Our average	
$D_{s1}^*(2700)^\pm$	1^-	$D^{*+}K_S^0$, $D^{*0}K^+$	$2732.3 \pm 4.3 \pm 5.8$	$136 \pm 19 \pm 24$	LHCb	[1241]
		D^0K^+	2699^{+14}_{-7}	127^{+24}_{-19}	BaBar	[1257]
		$D^{*+}K_S^0$, $D^{*0}K^+$	$2709.2 \pm 1.9 \pm 4.5$	$115.8 \pm 7.3 \pm 12.1$	LHCb	[1239]
		DK, D^*K	$2710 \pm 2^{+12}_{-7}$	$149 \pm 7^{+39}_{-52}$	BaBar	[1238]
		D^0K^+	$2708 \pm 9^{+11}_{-10}$	$108 \pm 2^{+36}_{-31}$	Belle	[731]
			2712.0 ± 1.5	121.5 ± 10.2	Our average	
$D_{s1}^*(2860)^\pm$	1	D^0K^+	$2859 \pm 12 \pm 24$	$159 \pm 23 \pm 77$	LHCb	[1240]
$D_{s3}^*(2860)^\pm$	3^-	$D^{*+}K_S^0$, $D^{*0}K^+$	$2867.1 \pm 4.3 \pm 1.9$	$50 \pm 11 \pm 13$	LHCb	[1241]
		D^0K^+	$2860.5 \pm 2.6 \pm 6.5$	$53 \pm 7 \pm 7$	LHCb	[1240]
			2865.0 ± 3.9	52.2 ± 8.6	Our average	
$D_{sJ}(3040)^\pm$	Unnatural	D^*K	$3044 \pm 8^{+30}_{-5}$	$239 \pm 35^{+46}_{-42}$	BaBar (m and Γ) + LHCb(J^P)	[1238]+[1241]

8.9 Excited $D_{(s)}$ mesons

Excited charm meson states have received increased attention since the first observation of states that could not be accommodated by QCD predictions [1224–1227]. Tables 289, 290 and 291 summarize recent measurements of the masses and widths of excited D and D_s mesons, respectively. If a preferred assignment of spin and parity was measured it is listed in the column J^P, where the label natural denotes $J^P = 0^-, 1^+, 2^- \ldots$ and unnatural $J^P = 0^+, 1^-, 2^+ \ldots$. If possible, an average mass and width are calculated. The calculation of the averages assumes no correlation between individual measurements. A summary of the averaged masses and widths is shown in Fig. 213.

The masses and widths of narrow ($\Gamma < 50$ MeV) orbitally excited D mesons (1P states, denoted D^{**}), both neutral

Table 290 Recent measurements of mass and width for different excited D mesons. The column J^P list the most significant assignment of spin and parity. If possible an average mass or width is calculated

Resonance	J^P	Decay mode	Mass (MeV/c^2)	Width (MeV)	Measured by	References
$D_0^*(2400)^0$	0^+	$D^+\pi^-$	$2297 \pm 8 \pm 20$	$273 \pm 12 \pm 48$	BaBar	[711]
		$D^+\pi^-$	$2308 \pm 17 \pm 32$	$276 \pm 21 \pm 63$	Belle	[710]
		$D^+\pi^-$	$2407 \pm 21 \pm 35$	$240 \pm 55 \pm 59$	FOCUS	[1228]
			2318.2 ± 16.9	267.4 ± 35.6	Our average	
$D_0^*(2400)^\pm$	0^+	$D^0\pi^+$	$2349 \pm 6 \pm 1 \pm 4$	$217 \pm 13 \pm 5 \pm 12$	LHCb	[602]
		$D^0\pi^+$	$2360 \pm 15 \pm 12 \pm 28$	$255 \pm 26 \pm 20 \pm 47$	LHCb	[1258]
		$D^0\pi^+$	$2403 \pm 14 \pm 35$	$283 \pm 24 \pm 34$	FOCUS (m and Γ) + Belle(J^P)	[1228] + [1259]
			2350.6 ± 5.9	233.7 ± 15.5	Our average	
$D_1(2420)^0$	1^+	$D^{*+}\pi^-$	$2419.6 \pm 0.1 \pm 0.7$	$35.2 \pm 0.4 \pm 0.9$	LHCb	[1165]
		$D^{*+}\pi^-$	$2423.1 \pm 1.5^{+0.4}_{-1.0}$	$38.8 \pm 5^{+1.9}_{-5.4}$	Zeus	[1260]
		$D^{*+}\pi^-$	$2420.1 \pm 0.1 \pm 0.8$	$31.4 \pm 0.5 \pm 1.3$	BaBar	[1164]
		$D^{*+}\pi^-$	$20.0 \pm 1.7 \pm 1.3$		CDF	[1261]
		$D^0\pi^+\pi^-$	$2426 \pm 3 \pm 1$	$24 \pm 7 \pm 8$	Belle	[622]
		$D^{*+}\pi^-$	$2421.4 \pm 1.5 \pm 0.9$	$23.7 \pm 2.7 \pm 4.0$	Belle	[710]
		$D^{*+}\pi^-$	$2421^{+1}_{-2} \pm 2$	20^{+6+3}_{-5-3}	CLEO	[1262]
		$D^{*+}\pi^-$	$2422 \pm 2 \pm 2$	$15 \pm 8 \pm 4$	E687	[1246]
		$D^{*+}\pi^-$	$2428 \pm 3 \pm 2$	23^{+8+10}_{-6-4}	CLEO	[1249]
		$D^{*+}\pi^-$	$2414 \pm 2 \pm 5$	$13 \pm 6^{+10}_{-5}$	ARGUS	[1263]
		$D^{*+}\pi^-$	$2428 \pm 8 \pm 5$	$58 \pm 14 \pm 10$	TPS	[1264]
			2420.5 ± 0.5	31.7 ± 0.7	Our average	
$D_1(2420)^\pm$	1^+	$D^{*0}\pi^+$	$2421.9 \pm 4.7^{+3.4}_{-1.2}$		Zeus	[1260]
		$D^+\pi^-\pi^+$	$2421 \pm 2 \pm 1$	$21 \pm 5 \pm 8$	Belle	[622]
		$D^{*0}\pi^+$	$2425 \pm 2 \pm 2$	$26^{+8}_{-7} \pm 4$	CLEO	[1265]
		$D^{*0}\pi^+$	$2443 \pm 7 \pm 5$	$41 \pm 19 \pm 8$	TPS	[1264]
			2423.2 ± 1.6	25.2 ± 6.0	Our average	
$D_1(2430)^0$	1^+	$D^{*+}\pi^-$	$2427 \pm 26 \pm 25$	$384^{+107}_{-75} \pm 74$	Belle	[710]
$D_2^*(2460)^0$	2^+	$D^{*+}\pi^-$	$2464.0 \pm 1.4 \pm 0.5 \pm 0.2$	$43.8 \pm 2.9 \pm 1.7 \pm 0.6$	LHCb	[716]
		$D^{*+}\pi^-$	$2460.4 \pm 0.4 \pm 1.2$	$43.2 \pm 1.2 \pm 3.0$	LHCb	[1165]
		$D^+\pi^-$	$2460.4 \pm 0.1 \pm 0.1$	$45.6 \pm 0.4 \pm 1.1$	LHCb	[1165]
		$D^{*+}\pi^-$, $D^+\pi^-$	$2462.5 \pm 2.4^{+1.3}_{-1.1}$	$46.6 \pm 8.1^{+5.9}_{-3.8}$	Zeus	[1260]
		$D^+\pi^-$	$2462.2 \pm 0.1 \pm 0.8$	$50.5 \pm 0.6 \pm 0.7$	BaBar	[1164]
		$D^+\pi^-$	$2460.4 \pm 1.2 \pm 2.2$	$41.8 \pm 2.5 \pm 2.9$	BaBar	[711]
		$D^+\pi^-$		$49.2 \pm 2.3 \pm 1.3$	CDF	[1261]
		$D^+\pi^-$	$2461.6 \pm 2.1 \pm 3.3$	$45.6 \pm 4.4 \pm 6.7$	Belle	[710]
		$D^+\pi^-$	$2464.5 \pm 1.1 \pm 1.9$	$38.7 \pm 5.3 \pm 2.9$	FOCUS	[1228]
		$D^+\pi^-$	$2465 \pm 3 \pm 3$	$28^{+8}_{-7} \pm 6$	CLEO	[1262]
		$D^+\pi^-$	$2453 \pm 3 \pm 2$	$25 \pm 10 \pm 5$	E687	[1246]
		$D^{*+}\pi^-$	$2461 \pm 3 \pm 1$	$20^{+9}_{-12}{}^{+9}_{-10}$	CLEO	[1249]
		$D^+\pi^-$	$2455 \pm 3 \pm 5$	15^{+13+5}_{-10-10}	ARGUS	[1266]
		$D^+\pi^-$	$2459 \pm 3 \pm 2$	$20 \pm 10 \pm 5$	TPS	[1264]
			2460.49 ± 0.17	47.52 ± 0.65	Our average	

Table 291 Recent measurements of mass and width for different excited D mesons. The column J^P list the most significant assignment of spin and parity. If possible an average mass or width is calculated

Resonance	J^P	Decay mode	Mass (MeV/c^2)	Width (MeV)	Measured by	References
$D_2^*(2460)^\pm$	2^+	$D^0\pi^+$	$2468.6 \pm 0.6 \pm 0.0 \pm 0.3$	$47.3 \pm 1.5 \pm 0.3 \pm 0.6$	LHCb	[602]
		$D^0\pi^+$	$2465.6 \pm 1.8 \pm 0.5 \pm 1.2$	$46.0 \pm 3.4 \pm 1.4 \pm 2.9$	LHCb	[1258]
		$D^0\pi^+$	$2463.1 \pm 0.2 \pm 0.6$	$48.6 \pm 1.3 \pm 1.9$	LHCb	[1165]
		$D^{*0}\pi^+$, $D^0\pi^+$	$2460.6 \pm 4.4^{+3.6}_{-0.8}$		Zeus	[1260]
		$D^0\pi^+$	$2465.4 \pm 0.2 \pm 1.1$		BABAR	[1164]
		$D^0\pi^+$	$2465.7 \pm 1.8^{+1.4}_{-4.8}$	$49.7 \pm 3.8 \pm 6.4$	Belle	[1259]
		$D^0\pi^+$	$2467.6 \pm 1.5 \pm 0.8$	$34.1 \pm 6.5 \pm 4.2$	FOCUS	[1228]
		$D^0\pi^+$	$2463 \pm 3 \pm 3$	$27^{+11}_{-8} \pm 5$	CLEO	[1265]
		$D^0\pi^+$	$2453 \pm 3 \pm 2$	$23 \pm 9 \pm 5$	E687	[1246]
		$D^0\pi^+$	$2469 \pm 4 \pm 6$		ARGUS	[1267]
			2465.55 ± 0.40	46.7 ± 1.2	Our average	
$D(2550)^0$	0^-	$D^{*+}\pi^-$	$2539.4 \pm 4.5 \pm 6.8$	$130 \pm 12 \pm 13$	BABAR	[1164]
$D(2580)^0$	Unnatural	$D^{*+}\pi^-$	$2579.5 \pm 3.4 \pm 5.5$	$117.5 \pm 17.8 \pm 46.0$	LHCb	[1165]
$D(2600)^0$	Natural	$D^+\pi^-$	$2608.7 \pm 2.4 \pm 2.5$	$93 \pm 6 \pm 13$	BABAR	[1164]
$D(2600)^\pm$	Natural	$D^0\pi^+$	$2621.3 \pm 3.7 \pm 4.2$		BABAR	[1164]
$D^*(2640)^\pm$	1^-	$D^{*+}\pi^+\pi^-$	$2637 \pm 2 \pm 6$		Delphi	[1268]
$D^*(2650)^0$	Natural	$D^{*+}\pi^-$	$2649.2 \pm 3.5 \pm 3.5$	$140.2 \pm 17.1 \pm 18.6$	LHCb	[1165]
$D(2740)^0$	Unnatural	$D^{*+}\pi^-$	$2737.0 \pm 3.5 \pm 11.2$	$73.2 \pm 13.4 \pm 25.0$	LHCb	[1165]
$D(2750)^0$		$D^{*+}\pi^-$	$2752.4 \pm 1.7 \pm 2.7$	$71 \pm 6 \pm 11$	BABAR	[1164]
$D_1^*(2760)^0$	1^+	$D^+\pi^-$	$2781 \pm 18 \pm 11 \pm 6$	$177 \pm 32 \pm 20 \pm 7$	LHCb	[716]
		$D^{*+}\pi^-$	$2761.1 \pm 5.1 \pm 6.5$	$74.4 \pm 3.4 \pm 37.0$	LHCb	[1165]
		$D^+\pi^-$	$2760.1 \pm 1.1 \pm 3.7$	$74.4 \pm 3.4 \pm 19.1$	LHCb	[1165]
		$D^+\pi^-$	$2763.3 \pm 2.3 \pm 2.3$	$60.9 \pm 5.1 \pm 3.6$	BABAR	[1164]
			2762.1 ± 2.4	65.1 ± 5.8	Our average	
$D_3^*(2760)^\pm$	3^-	$D^0\pi^+$	$2798 \pm 7 \pm 1 \pm 7$	$105 \pm 18 \pm 6 \pm 23$	LHCb	[602]
		$D^0\pi^+$	$2771.7 \pm 1.7 \pm 3.8$	$66.7 \pm 6.6 \pm 10.5$	LHCb	[1165]
		$D^0\pi^+$	$2769.7 \pm 3.8 \pm 1.5$		BABAR	[1164]
			2773.9 ± 3.3	72.3 ± 11.5	Our average	

Table 292 Product of B meson branching fraction and (daughter) excited D meson branching fraction

Resonance	Decay	$\mathcal{B}$ [10^{-4}]	Measured by	References
$D_0^*(2400)^0$	$B^- \to D_0^*(2400)^0(\to D^+\pi^-)\pi^-$	$6.1 \pm 0.6 \pm 1.8$	Belle	[710]
		$6.8 \pm 0.3 \pm 2.0$	BaBar	[711]
		6.4 ± 1.4	Our average	
	$B^- \to D_0^*(2400)^0(\to D^+\pi^-)K^-$	$0.061 \pm 0.019 \pm 0.005 \pm 0.014 \pm 0.004$	LHCb	[716]
$D_0^*(2400)^\pm$	$\overline{B}^0 \to D_0^*(2400)^+(\to D^0\pi^+)\pi^-$	$0.77 \pm 0.05 \pm 0.03 \pm 0.03 \pm 0.04$	LHCb	[602]
		$0.60 \pm 0.13 \pm 0.27$	Belle	[1259]
		0.76 ± 0.07	Our average	
	$\overline{B}^0 \to D_0^*(2400)^+(\to D^0\pi^+)K^-$	$0.177 \pm 0.026 \pm 0.019 \pm 0.067 \pm 0.20$	LHCb	[1258]
$D_1(2420)^0$	$B^- \to D_1(2420)^0(\to D^{*+}\pi^-)\pi^-$	$6.8 \pm 0.7 \pm 1.3$	Belle	[710]
	$B^- \to D_1(2420)^0(\to D^0\pi^+\pi^-)\pi^-$	$1.85 \pm 0.29 \pm 0.27 \pm 0.41$	Belle	[622]
	$\overline{B}^0 \to D_1(2420)^0(\to D^{*+}\pi^-)\omega$	$0.7 \pm 0.2^{+0.1}_{-0.0} \pm 0.1$	Belle	[598]
$D_1(2420)^\pm$	$\overline{B}^0 \to D_1(2420)^+(\to D^+\pi^-\pi^+)\pi^-$	$0.89 \pm 0.15 \pm 0.22$	Belle	[622]
$D_1(2430)^0$	$B^- \to D_1(2430)^0(\to D^{*+}\pi^-)\pi^-$	$5.0 \pm 0.4 \pm 1.08$	Belle	[710]
	$\overline{B}^0 \to D_1(2430)^0(\to D^{*+}\pi^-)\omega$	$2.5 \pm 0.4^{+0.7+0.4}_{-0.2-0.1}$	Belle	[598]
$D_2^*(2460)^0$	$B^- \to D_2^*(2460)^0(\to D^+\pi^-)\pi^-$	$3.4 \pm 0.3 \pm 0.7$	Belle	[710]
		$3.5 \pm 0.2 \pm 0.5$	BaBar	[711]
		3.4 ± 0.3	Our average	
	$B^- \to D_2^*(2460)^0(\to D^{*+}\pi^-)\pi^-$	$1.8 \pm 0.3 \pm 0.4$	Belle	[710]
	$B^- \to D_2^*(2460)^0(\to D^{*+}\pi^-)\omega$	$0.4 \pm 0.1^{+0.0}_{-0.1} \pm 0.1$	Belle	[598]
	$B^- \to D_2^*(2460)^0(\to D^+\pi^-)K^-$	$0.232 \pm 0.011 \pm 0.006 \pm 0.010 \pm 0.016$	LHCb	[716]
$D_2^*(2460)^\pm$	$\overline{B}^0 \to D_2^*(2460)^+(\to D^0\pi^+)\pi^-$	$2.44 \pm 0.07 \pm 0.10 \pm 0.04 \pm 0.12$	LHCb	[602]
		$2.15 \pm 0.17 \pm 0.31$	Belle	[1259]
		2.38 ± 0.16	Our average	
	$\overline{B}^0 \to D_2^*(2460)^+(\to D^0\pi^+)K^-$	$0.212 \pm 0.010 \pm 0.011 \pm 0.011 \pm 0.25$	LHCb	[1258]
$D_1^*(2760)^0$	$B^- \to D_1^*(2760)^0(\to D^+\pi^-)K^-$	$0.036 \pm 0.009 \pm 0.003 \pm 0.007 \pm 0.002$	LHCb	[716]
$D_3^*(2760)^\pm$	$\overline{B}^0 \to D_3^*(2760)^0(\to D^0\pi^+)\pi^-$	$0.103 \pm 0.016 \pm 0.007 \pm 0.008 \pm 0.005$	LHCb	[602]

and charged, are well-established. Measurements of broad states ($\Gamma \sim 200$–400 MeV) are less abundant, as identifying the signal is more challenging. There is a slight discrepancy between the $D_0^*(2400)^0$ masses measured by the Belle [710] and FOCUS [1228] experiments. No data exist yet for the $D_1(2430)^\pm$ state. Dalitz plot analyses of $B \to \overline{D}^{(*)}\pi\pi$ decays strongly favor the assignments 0^+ and 1^+ for the spin-parity quantum numbers of the $D_0^*(2400)^0/D_0^*(2400)^\pm$ and $D_1(2430)^0$ states, respectively. The measured masses and widths, as well as the J^P values, are in agreement with theoretical predictions based on potential models [496,1229–1231].

Tables 292 and 293 summarize the branching fractions of B meson decays to excited D and D_s states, respectively. It is notable that the branching fractions for B mesons decaying to a narrow D^{**} state and a pion are similar for charged and neutral B initial states, while the branching fractions to a broad D^{**} state and π^+ are much larger for B^+ than for B^0. This may be due to the fact that color-suppressed amplitudes contribute only to the B^+ decay and not to the B^0 decay (for a theoretical discussion, see Refs. [1232,1233]). Measurements of individual branching fractions of D mesons are difficult due to the unknown fragmentation of a c quark to D^{**} or due to the unknown $B \to D^{**}X$ branching fractions.

The discoveries of the $D_{s0}^*(2317)^\pm$ and $D_{s1}(2460)^\pm$ have triggered increased interest in properties of, and searches for, excited D_s mesons (here generically denoted D_s^{**}). While the masses and widths of $D_{s1}(2536)^\pm$ and $D_{s2}^*(2573)^\pm$ states are in relatively good agreement with potential model predictions, the masses of $D_{s0}^*(2317)^\pm$ and $D_{s1}(2460)^\pm$ states are significantly lower than expected (see Ref. [1234] for a discussion of $c\bar{s}$ models). Moreover, the mass splitting between these two states greatly exceeds that between the $D_{s1}(2536)^\pm$ and $D_{s2}(2573)^\pm$. These unexpected properties have led to interpretations of the $D_{s0}^*(2317)^\pm$ and $D_{s1}(2460)^\pm$ as exotic four-quark states [1235,1236].

While there are few measurements of the J^P values of $D_{s0}^*(2317)^\pm$ and $D_{s1}(2460)^\pm$, the available data favor 0^+ and 1^+, respectively. A molecule-like (DK) interpre-

Table 293 Product of B meson branching fraction and (daughter) excited D_s meson branching fraction

Resonance	Decay	$\mathcal{B}$ [10^{-4}]	Measured by	References
$D_{s0}^*(2317)^\pm$	$B^0 \to D_{s0}^*(2317)^+(\to D_s^+\pi^0)D^-$	$8.6^{+3.3}_{-2.6} \pm 2.6$	Belle	[640]
		$18.0 \pm 4.0^{+6.7}_{-5.0}$	BaBar	[641]
		$10.1^{+1.3}_{-1.2} \pm 1.0 \pm 0.4$	Belle	[642]
		10.2 ± 1.5	Our average	
	$B^+ \to D_{s0}^*(2317)^+(\to D_s^+\pi^0)\overline{D}^0$	$8.0^{+1.3}_{-1.2} \pm 1.0 \pm 0.4$	Belle	[642]
	$B^0 \to D_{s0}^*(2317)^+(\to D_s^+\pi^0)K^-$	$0.53^{+0.15}_{-0.13} \pm 0.16$	Belle	[623]
$D_{s1}(2460)^\pm$	$B^0 \to D_{s1}(2460)^+(\to D_s^{*+}\pi^0)D^-$	$22.7^{+7.3}_{-6.2} \pm 6.8$	Belle	[640]
		$28.0 \pm 8.0^{+11.2}_{-7.8}$	BaBar	[641]
		24.7 ± 7.6	Our average	
	$B^0 \to D_{s1}(2460)^+(\to D_s^{*+}\gamma)D^-$	$8.2^{+2.2}_{-1.9} \pm 2.5$	Belle	[640]
		$8.0 \pm 2.0^{+3.2}_{-2.3}$	BaBar	[641]
		8.1 ± 2.3	Our average	
	$D_{s1}(2460)^+ \to D_s^{*+}\pi^0$	$(56 \pm 13 \pm 9)\%$	BaBar	[635]
	$D_{s1}(2460)^+ \to D_s^{*+}\gamma$	$(16 \pm 4 \pm 3)\%$	BaBar	[635]
	$B^0 \to D_{s1}(2536)^+(\to D^{*0}K^+)D^-$	$1.71 \pm 0.48 \pm 0.32$	BaBar	[643]
	$B^0 \to D_{s1}(2536)^+(\to D^{*+}K^0)D^-$	$2.61 \pm 1.03 \pm 0.31$	BaBar	[643]
	$B^0 \to D_{s1}(2536)^+(\to D^{*0}K^+)D^{*-}$	$3.32 \pm 0.88 \pm 0.66$	BaBar	[643]
$D_{s1}(2536)^\pm$	$B^0 \to D_{s1}(2536)^+(\to D^{*+}K^0)D^{*-}$	$5.00 \pm 1.51 \pm 0.67$	BaBar	[643]
	$B^+ \to D_{s1}(2536)^+(\to D^{*0}K^+)\overline{D}^0$	$2.16 \pm 0.52 \pm 0.45$	BaBar	[643]
	$B^+ \to D_{s1}(2536)^+(\to D^{*+}K^0)\overline{D}^0$	$2.30 \pm 0.98 \pm 0.43$	BaBar	[643]
	$B^+ \to D_{s1}(2536)^+(\to D^{*0}K^+)\overline{D}^{*0}$	$5.46 \pm 1.17 \pm 1.04$	BaBar	[643]
	$B^+ \to D_{s1}(2536)^+(\to D^{*+}K^0)\overline{D}^{*0}$	$3.92 \pm 2.46 \pm 0.83$	BaBar	[643]
$D_{s2}^*(2573)^\pm$	$B^0 \to D_{s2}^*(2573)(\to D^0K^+)D^-$	$0.34 \pm 0.17 \pm 0.05$	BaBar	[1257]
	$B^+ \to D_{s2}^*(2573)(\to D^0K^+)\overline{D}^0$	$0.08 \pm 14 \pm 0.05$	BaBar	[1257]
$D_{s1}{}^*(2700)^\pm$	$B^+ \to D_{s1}{}^*(2700)^+(\to D^0K^+)\overline{D}^0$	$11.3 \pm 2.2^{+1.4}_{-2.8}$	Belle	[731]
		$5.02 \pm 0.71 \pm 0.93$	BaBar	[1257]
		5.83 ± 1.09	Our average	
	$B^0 \to D_{s1}{}^*(2700)^+(\to D^0K^+)D^-$	$7.14 \pm 0.96 \pm 0.69$	BaBar	[1257]

tation of the $D_{s0}^*(2317)^\pm$ and $D_{s1}(2460)^\pm$ [1235,1236] that can account for their low masses and isospin-breaking decay modes is tested by searching for charged and neutral isospin partners of these states; thus far such searches have yielded negative results. Therefore the subset of models that predict equal production rates for different charged states is excluded. The molecular picture can also be tested by measuring the rates for the radiative processes $D_{s0}^*(2317)^\pm/D_{s1}(2460)^\pm \to D_s^{(*)}\gamma$ and comparing to theoretical predictions. The predicted rates, however, are below the sensitivity of current experiments.

Another model successful in explaining the total widths and the $D_{s0}^*(2317)^\pm - D_{s1}(2460)^\pm$ mass splitting is based on the assumption that these states are chiral partners of the ground states D_s^+ and D_s^* [1237]. While some measured branching fraction ratios agree with predicted values, further experimental tests with better sensitivity are needed to confirm or refute this scenario. A summary of the mass difference measurements is given in Table 294.

Measurements by BaBar [1238] and LHCb [1239] first indicated the existence of a strange-charm $D_{sJ}^*(2860)^\pm$ meson. An LHCb study of $B_s^0 \to \overline{D}^0K^-\pi^+$ decays, in which they searched for excited D_s mesons [1240], showed with 10σ significance that this state is comprised of two different particles, one of spin 1 and one of spin 3. This represents the first measurement of a heavy flavored spin-3 particle, and the first observation of B meson decays to spin 3 particles. A subsequent study of D_{sJ} mesons by the LHCb collaboration [1241] supports the natural parity assignment for this state ($J^P = 3^-$). This study also shows weak evidence for a further structure at a mass around 3040 MeV/c^2 with unnatural parity, which was first hinted at by a BaBar analysis [1238].

Table 294 Mass difference measurements for excited D mesons

Resonance	Relative to	Δm (MeV/c^2)	Measured by	References
$D_1^*(2420)^0$	D^{*+}	$410.2 \pm 2.1 \pm 0.9$	Zeus	[1269]
		$411.7 \pm 0.7 \pm 0.4$	CDF	[1261]
		411.5 ± 0.8	Our average	
$D_1(2420)^\pm$	$D_1^*(2420)^0$	$4^{+2}_{-3} \pm 3$	CLEO	[1265]
$D_2^*(2460)^0$	D^+	$593.9 \pm 0.6 \pm 0.5$	CDF	[1261]
	D^{*+}	$458.8 \pm 3.7^{+1.2}_{-1.3}$	Zeus	[1269]
$D_2^*(2460)^\pm$	$D_2^*(2460)^0$	$3.1 \pm 1.9 \pm 0.9$	FOCUS	[1228]
		$-2 \pm 4 \pm 4$	CLEO	[1265]
		$14 \pm 5 \pm 8$	ARGUS	[1267]
		3.0 ± 1.9	Our average	
$D_{s0}^*(2317)^\pm$	$D_s^\pm$	$348.7 \pm 0.5 \pm 0.7$	Belle	[1226]
		$350.0 \pm 1.2 \pm 1.0$	CLEO	[1225]
		$351.3 \pm 2.1 \pm 1.9$	Belle	[640]
		349.2 ± 0.7	Our average	
$D_{s1}(2460)^\pm$	$D_s^{*\pm}$	$344.1 \pm 1.3 \pm 1.1$	Belle	[1226]
		$351.2 \pm 1.7 \pm 1.0$	CLEO	[1225]
		$346.8 \pm 1.6 \pm 1.9$	Belle	[640]
		347.1 ± 1.1	Our average	
	$D_s^\pm$	$491.0 \pm 1.3 \pm 1.9$	Belle	[1226]
		$491.4 \pm 0.9 \pm 1.5$	Belle	[1226]
		491.3 ± 1.4	Our average	
$D_{s1}(2536)^\pm$	$D^*(2010)^\pm$	$524.83 \pm 0.01 \pm 0.04$	BaBar	[1251]
		$525.30^{+0.44}_{-0.41} \pm 0.10$	Zeus	[1269]
		$525.3 \pm 0.6 \pm 0.1$	ALEPH	[1270]
		524.84 ± 0.04	Our average	
	$D^*(2007)^0$	$528.7 \pm 1.9 \pm 0.5$	ALEPH	[1270]
$D_{s2}^*(2573)^\pm$	D^0	$704 \pm 3 \pm 1$	ALEPH	[1270]

Recent evidence shows that the 1D family of charm resonances can be explored in the Dalitz plot analyses of B-meson decays in the same way as seen for the charm-strange resonances. The LHCb collaboration performed an analysis of $B^0 \to \overline{D}^0\pi^+\pi^-$ decays, in which they measured the spin-parity assignment of the state $D_3^*(2760)^\pm$, which was observed previously by BaBar [1164] and LHCb [1165], to be $J^P = 3^-$. The measurement suggests a spectroscopic assignment of $^3D_3$. This is the second observation of a spin-3 charm meson.

Other observed excited D_s states include $D_{s1}^*(2700)^\pm$ and $D_{s2}^*(2573)^\pm$. The properties of both (mass, width, J^P) have been measured and determined in several analyses. A theoretical discussion [1242] investigates the possibility that the $D_{s1}(2700)^\pm$ could represent radial excitations of the $D_s^{*\pm}$. Similarly, the $D_{s1}^*(2860)^\pm$ and $D_{sJ}(3040)^\pm$ could be excitations of $D_{s0}^*(2317)^\pm$ and $D_{s1}(2460)^\pm$ or $D_{s1}(2536)^\pm$, respectively.

Table 295 Measurements of polarization amplitudes for excited D mesons

Resonance	A_D	Measured by	References
$D_1(2420)^0$	$7.8^{+6.7+4.6}_{-2.7-1.8}$	ZEUS	[1260]
	5.72 ± 0.25	BaBar	[1164]
	$5.9^{+3.0+2.4}_{-1.7-1.0}$	ZEUS	[1269]
	$3.8 \pm 0.6 \pm 0.8$	BaBar	[502]
	5.61 ± 0.24	Our average	
$D_1(2420)^\pm$	$3.8 \pm 0.6 \pm 0.8$	BaBar	[502]
$D_2^*(2460)^0$	-1.16 ± 0.35	ZEUS	[1260]
$D(2750)^0$	-0.33 ± 0.28	BaBar	[1164]

Table 295 summarizes measurements of the helicity parameter A_D (also referred to as polarization amplitude). In D^{**} meson decays to $D^{**} \to D^*\pi$, $D^* \to D\pi$, the helicity distribution varies like $1 + A_D \cos^2\theta_H$, where θ_H is

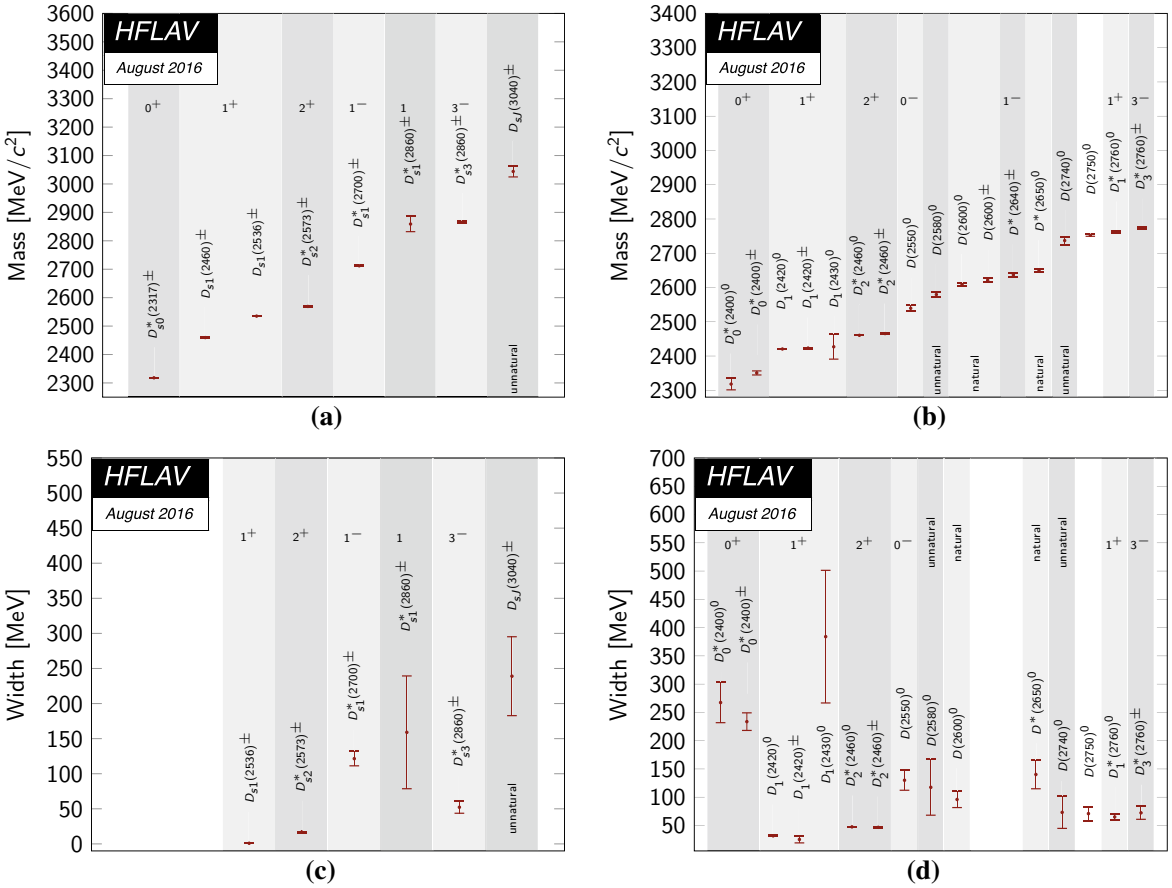

Fig. 213 Averaged masses for excited D_s mesons are shown in (**a**) and for D mesons in (**b**). The average widths for excited D_s mesons are shown in (**c**) and for excited D mesons in (**d**). The *vertical shaded regions* distinguish between different spin parity states

the angle in the D^* rest frame between the two pions emitted by decay $D^{**} \to D^*\pi$ and the $D^* \to D\pi$. The parameter is sensitive to possible S-wave contributions in the decay. In the case of a D meson decay decaying purely via D-wave, the helicity parameter is predicted to give $A_D = 3$. Studies of the $D_1(2420)^0$ meson by the ZEUS and BABAR collaborations suggest that there is an S-wave admixture in the decay, which is contrary to Heavy Quark Effective Theory calculations [476,1243].

8.10 Λ_c^+ branching fractions

Charmed baryon decays play an important role in studies of weak and strong interactions. For example, they provide crucial input for measurements of exclusive and inclusive decay rates of b-flavored mesons and baryons, and also for measurements of fragmentation fractions of charm and bottom quarks. In spite of this importance, experimental data on Λ_c^+ baryon decays was scarce until 2014, when Belle published the first model-independent measurement of the branching fraction for $\Lambda_c^+ \to pK^-\pi^+$ [1271]. This measurement improved upon the precision of previous (model-dependent) measurements by a factor of five. Since then the precision of other Λ_c^+ branching fractions has improved due to measurements based on threshold data performed by BESIII [531]. BESIII also reported the first measurement of the branching fraction for the semileptonic decay $\Lambda_c^+ \to \Lambda e^+\nu_e$ [1272]. Here we present a global fit for branching fractions of Cabbibo-favored Λ_c^+ decays, taking into account all relevant experimental measurements and their correlations. All measurements used assume unpolarised production of the Λ_c^+.

The measurements listed in Table 296 are input to a least-squares fit minimizing a χ^2 statistic. The fitted quantities are the Λ_c^+ branching fractions for twelve hadronic modes and one semileptonic mode. The measurements are labelled using the Γ_n notation employed by the Particle Data Group [6], where n is an integer that specifies the decay mode. The fitted output consists of 13 quantities – twelve hadronic and one semileptonic branching fraction. The advantage of our fit is that it takes into account correlations among measurements from the same experiment, i.e., systematic uncertainties related to normalization, track-finding efficiency, particle identification efficiency, and π^0, K_S^0, and Λ reconstruction efficiencies. For the twelve hadronic branching fractions

Table 296 Experimental results and world averages for branching fractions of twelve hadronic and one semileptonic Λ_c^+ decay. The first uncertainty is statistical and the second is systematic

Λ_c^+ branching fraction	Value	References
$\Gamma_1 = pK_S^0$	$(1.59 \pm 0.07)\%$	HFLAV Fit
BESIII	$(1.52 \pm 0.08 \pm 0.03)\%$	[531]
$\frac{\Gamma_1}{\Gamma_2} = \frac{pK_S^0}{pK^-\pi^+}$	0.246 ± 0.009	HFLAV Fit
CLEO	$0.22 \pm 0.04 \pm 0.03$	[1273]
CLEO	$0.23 \pm 0.01 \pm 0.02$	[1274]
$\Gamma_2 = pK^-\pi^+$	$(6.46 \pm 0.24)\%$	HFLAV Fit
Belle	$(6.84 \pm 0.24^{+0.21}_{-0.27})\%$	[1271]
BESIII	$(5.84 \pm 0.27 \pm 0.23)\%$	[531]
$\Gamma_7 = pK_S^0\pi^0$	$(2.03 \pm 0.12)\%$	HFLAV Fit
BESIII	$(1.87 \pm 0.13 \pm 0.05)\%$	[531]
$\frac{\Gamma_7}{\Gamma_2} = \frac{pK_S^0\pi^0}{pK^-\pi^+}$	0.314 ± 0.017	HFLAV Fit
CLEO	$0.33 \pm 0.03 \pm 0.04$	[1274]
$\Gamma_9 = pK_S^0\pi^+\pi^-$	$(1.69 \pm 0.11)\%$	HFLAV Fit
BESIII	$(1.53 \pm 0.11 \pm 0.09)\%$	[531]
$\frac{\Gamma_9}{\Gamma_2} = \frac{pK_S^0\pi^+\pi^-}{pK^-\pi^+}$	0.261 ± 0.013	HFLAV Fit
CLEO	$0.22 \pm 0.06 \pm 0.02$	[1273]
CLEO	$0.26 \pm 0.02 \pm 0.03$	[1274]
$\Gamma_{10} = pK^-\pi^+\pi^0$	$(5.05 \pm 0.29)\%$	HFLAV Fit
BESIII	$(4.53 \pm 0.23 \pm 0.30)\%$	[531]
$\frac{\Gamma_{10}}{\Gamma_2} = \frac{pK^-\pi^+\pi^0}{pK^-\pi^+}$	0.781 ± 0.031	HFLAV Fit
CLEO	$0.67 \pm 0.04 \pm 0.11$	[1274]
$\Gamma_{23} = \Lambda\pi^+$	$(1.28 \pm 0.06)\%$	HFLAV Fit
BESIII	$(1.24 \pm 0.07 \pm 0.03)\%$	[531]
$\frac{\Gamma_{23}}{\Gamma_2} = \frac{\Lambda\pi^+}{pK^-\pi^+}$	0.198 ± 0.008	HFLAV Fit
CLEO	$0.18 \pm 0.03 \pm 0.03$	[1273]
ARGUS	$0.18 \pm 0.03 \pm 0.04$	[1275]
FOCUS	$0.217 \pm 0.013 \pm 0.020$	[1276]
$\Gamma_{24} = \Lambda\pi^+\pi^0$	$(7.09 \pm 0.36)\%$	HFLAV Fit
BESIII	$(7.01 \pm 0.37 \pm 0.19)\%$	[531]
$\frac{\Gamma_{24}}{\Gamma_2} = \frac{\Lambda\pi^+\pi^0}{pK^-\pi^+}$	1.10 ± 0.05	HFLAV Fit
CLEO	$0.73 \pm 0.09 \pm 0.16$	[1277]
$\Gamma_{26} = \Lambda\pi^+\pi^-\pi^+$	$(3.73 \pm 0.21)\%$	HFLAV Fit
BESIII	$(3.81 \pm 0.24 \pm 0.18)\%$	[531]
$\frac{\Gamma_{26}}{\Gamma_2} = \frac{\Lambda\pi^+\pi^-\pi^+}{pK^-\pi^+}$	0.577 ± 0.022	HFLAV Fit
CLEO	$0.65 \pm 0.11 \pm 0.12$	[1273]
FOCUS	$0.508 \pm 0.024 \pm 0.024$	[1276]
ARGUS	$0.61 \pm 0.16 \pm 0.04$	[1278]

Table 296 continued

Λ_c^+ branching fraction	Value	References
$\Gamma_{39} = \Sigma^0\pi^+$	$(1.31 \pm 0.07)\%$	HFLAV Fit
BESIII	$(1.27 \pm 0.08 \pm 0.03)\%$	[531]
$\frac{\Gamma_{39}}{\Gamma_2} = \frac{\Sigma^0\pi^+}{pK^-\pi^+}$	0.202 ± 0.009	HFLAV Fit
CLEO	$0.21 \pm 0.02 \pm 0.04$	[1277]
ARGUS	$0.17 \pm 0.06 \pm 0.04$	[1275]
$\frac{\Gamma_{39}}{\Gamma_{23}} = \frac{\Sigma^0\pi^+}{\Lambda\pi^+}$	1.02 ± 0.03	HFLAV Fit
FOCUS	$1.09 \pm 0.11 \pm 0.19$	[1276]
BaBar	$0.997 \pm 0.015 \pm 0.051$	[1279]
$\Gamma_{40} = \Sigma^+\pi^0$	$(1.25 \pm 0.09)\%$	HFLAV Fit
BESIII	$(1.18 \pm 0.10 \pm 0.03)\%$	[531]
$\frac{\Gamma_{40}}{\Gamma_2} = \frac{\Sigma^+\pi^0}{pK^-\pi^+}$	0.193 ± 0.014	HFLAV Fit
CLEO	$0.20 \pm 0.03 \pm 0.03$	[1280]
$\Gamma_{42} = \Sigma^+\pi^+\pi^-$	$(4.64 \pm 0.24)\%$	HFLAV Fit
BESIII	$(4.25 \pm 0.24 \pm 0.20)\%$	[531]
$\frac{\Gamma_{42}}{\Gamma_2} = \frac{\Sigma^+\pi^+\pi^-}{pK^-\pi^+}$	0.719 ± 0.028	HFLAV Fit
CLEO	$0.74 \pm 0.07 \pm 0.09$	[1280]
$\Gamma_{48} = \Sigma^+\omega$	$(1.77 \pm 0.21)\%$	HFLAV Fit
BESIII	$(1.56 \pm 0.20 \pm 0.07)\%$	[531]
$\frac{\Gamma_{48}}{\Gamma_2} = \frac{\Sigma^+\omega}{pK^-\pi^+}$	0.274 ± 0.031	HFLAV Fit
CLEO	$0.54 \pm 0.13 \pm 0.06$	[1280]
$\Gamma_{64} = \Lambda e^+\nu_e$	$(3.18 \pm 0.32)\%$	HFLAV Fit
BESIII	$(3.63 \pm 0.38 \pm 0.20)\%$	[1272]
$\frac{\Gamma_{64}}{\Gamma_2} = \frac{\Lambda e^+\nu_e}{pK^-\pi^+}$	0.492 ± 0.049	HFLAV Fit
CLEO	0.43 ± 0.08	[1281]
ARGUS	0.36 ± 0.14	[1282]

measured by BESIII, we use BESIII's published correlation matrix [531].

The resulting fitted values for the branching fractions are given in Table 296. The overall χ^2 of the fit is 30.0 for 23 degrees of freedom, which corresponds to a p value of 0.149. The correlation matrix for the fitted branching fractions is shown in Fig. 214, and constraints from individual measurements for pairs of fitted branching fractions are shown in Fig. 215. The branching fraction of the normalisation decay $\Lambda_c^+ \to pK^-\pi^+$ is found to be

$$\mathcal{B}(\Lambda_c^+ \to pK^-\pi^+) = (6.46 \pm 0.24)\%.$$

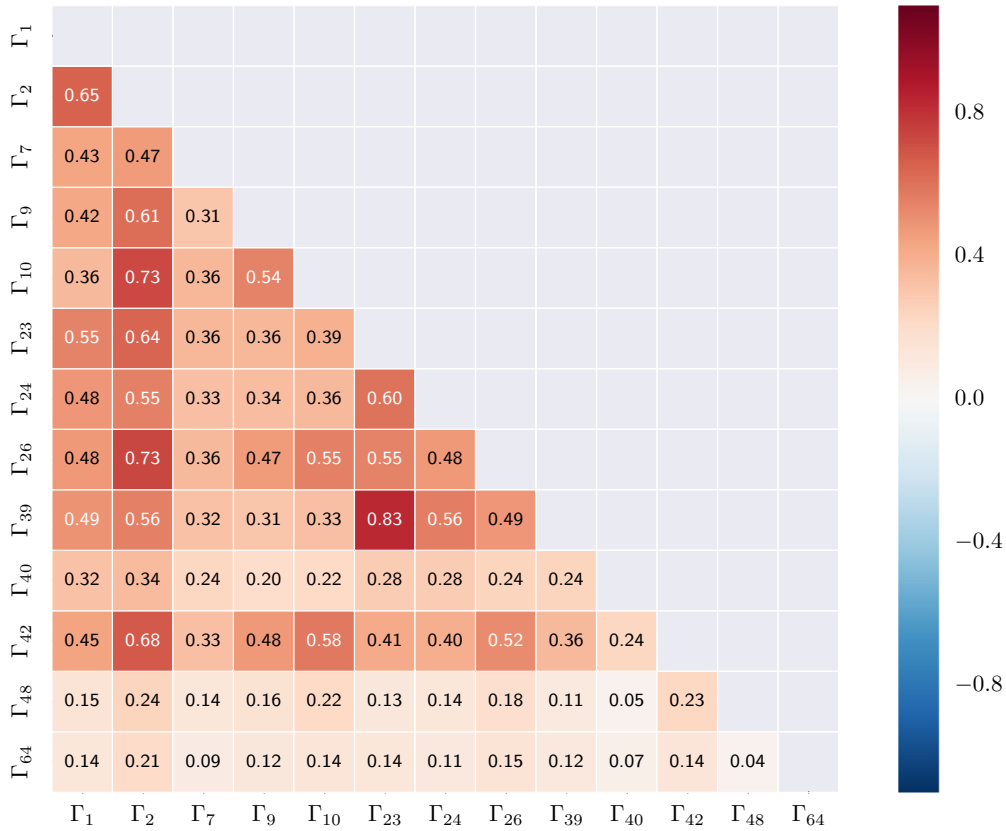

Fig. 214 Correlation coefficients between averaged Λ_c^+ branching fractions

8.11 Excited charm baryons

In this section we summarize the present status of excited charmed baryons, decaying strongly or electromagnetically. We list their masses (or the mass difference between the excited baryon and the corresponding ground state), natural widths, decay modes, and assigned quantum numbers. The present ground-state measurements are: $M(\Lambda_c^+) = 2286.46 \pm 0.14$ MeV/c^2 measured by BaBar [1283], $M(\Xi_c^0) = (2470.85^{+0.28}_{-0.04})$ MeV/c^2 and $M(\Xi_c^+) = (2467.93^{+0.28}_{-0.40})$ MeV/c^2, both dominated by CDF [145], and $M(\Omega_c^0) = (2695.2 \pm 1.7)$ MeV/c^2, dominated by Belle [1284]. Should these values change, so will some of the values for the masses of the excited states.

Table 297 summarizes the excited Λ_c^+ baryons. The first two states listed, namely the $\Lambda_c(2595)^+$ and $\Lambda_c(2625)^+$, are well-established. The measured masses and decay patterns suggest that they are orbitally excited Λ_c^+ baryons with total angular momentum of the light quarks $L = 1$. Thus their quantum numbers are assigned to be $J^P = (\frac{1}{2})^-$ and $J^P = (\frac{3}{2})^-$, respectively. Their mass measurements are dominated by CDF [1285]: $M(\Lambda_c(2595)^+) = (2592.25 \pm 0.24 \pm 0.14)$ MeV/c^2 and $M(\Lambda_c(2625)^+) = (2628.11 \pm 0.13 \pm 0.14)$ MeV/c^2. Earlier measurements did not fully take into account the restricted phase-space of the $\Lambda_c(2595)^+$ decays.

The next two states, $\Lambda_c(2765)^+$ and $\Lambda_c(2880)^+$, were discovered by CLEO [1286] in the $\Lambda_c^+\pi^+\pi^-$ final state. CLEO found that a significant fraction of the $\Lambda_c(2880)^+$ decays proceeds via an intermediate $\Sigma_c(2445)^{++/0}\pi^{-/+}$. Later, BaBar [1287] observed that this state has also a D^0p decay mode. This was the first example of an excited charmed baryon decaying into a charm meson plus a baryon; previously all excited charmed baryon were found in their hadronic transitions into lower lying charmed baryons. In the same analysis, BaBarobserved for the first time an additional state, $\Lambda_c(2940)^+$, decaying into D^0p. Studying the D^+p final state, BaBar found no signal; this implies that the $\Lambda_c(2880)^+$ and $\Lambda_c(2940)^+$ are Λ_c^+ excited states rather than Σ_c excitations. Belle reported the result of an angular analysis that favors 5/2 for the $\Lambda_c(2880)^+$ spin hypothesis. Moreover, the measured ratio of branching fractions $\mathcal{B}(\Lambda_c(2880)^+ \to \Sigma_c(2520)\pi^\pm)/\mathcal{B}(\Lambda_c(2880)^+ \to \Sigma_c(2455)\pi^\pm) = (0.225 \pm 0.062 \pm 0.025)$, combined with theoretical predictions based on HQS [496,1288], favor even parity. However this prediction is only valid if the P-wave portion of $\Sigma_c(2520)\pi$ is suppressed. The current open questions in the excited Λ_c^+ family include the determination of quantum numbers for the other states, and the nature of the $\Lambda_c(2765)^+$ state, in particular whether it is an excited Σ_c^+ or Λ_c^+. However, there is no doubt that the state exists, as it is clearly visible in Belle data.

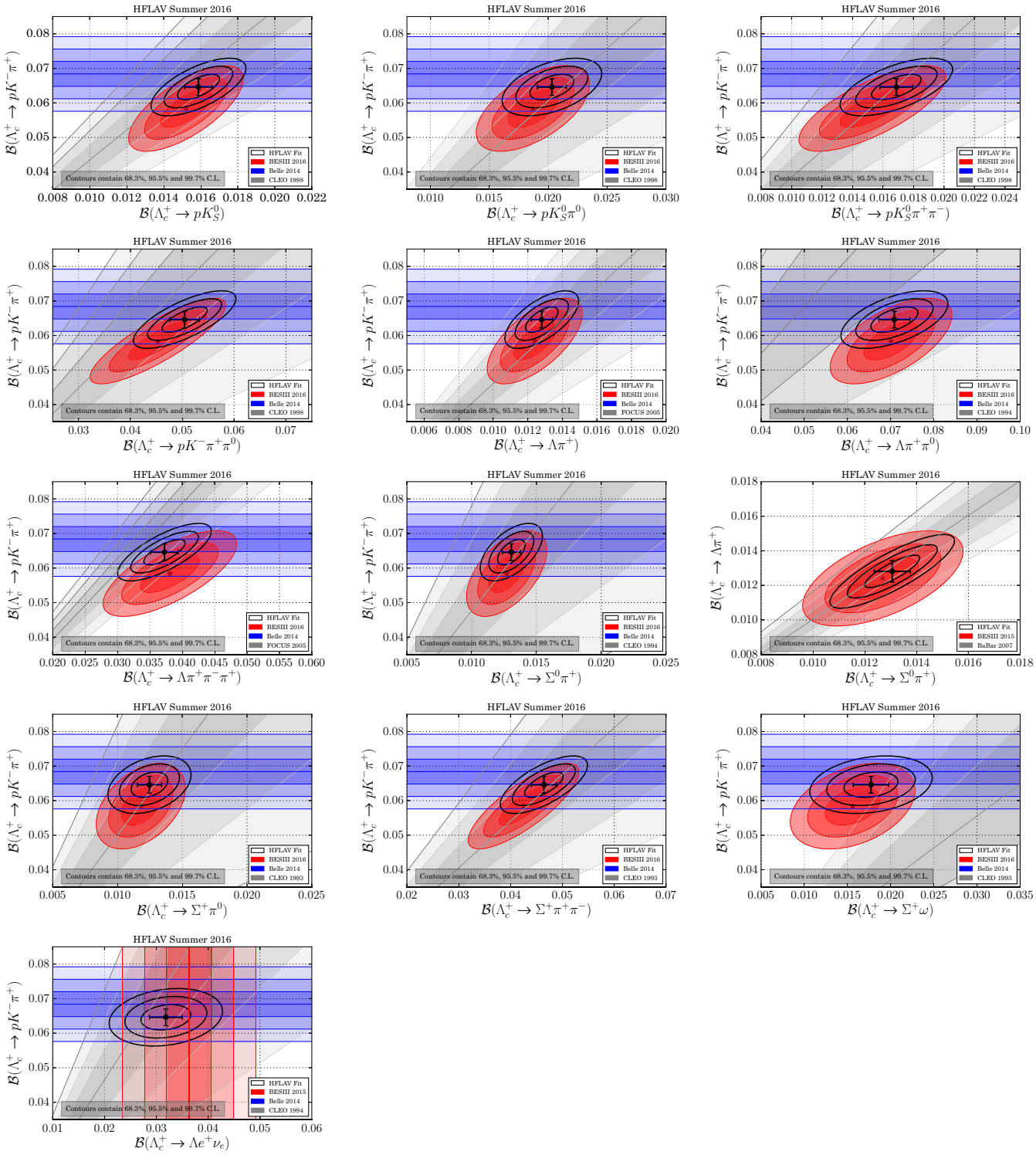

Fig. 215 Plots of all individual measurements and the fitted averages. Individual measurements are plotted as bands (*ellipses*) showing their $\pm 1\sigma$, $\pm 2\sigma$, and $\pm 3\sigma$ ranges. The best fit value is indicated by a *cross* showing the one-dimensional errors. In cases where multiple ratio measurements exists (Γ_i / Γ_j), only the most precise one is plotted

Table 297 Summary of excited Λ_c^+ baryons

Charmed baryon excited state	Mode	Mass (MeV/c^2)	Natural width (MeV)	J^P
$\Lambda_c(2595)^+$	$\Lambda_c^+\pi^+\pi^-$, $\Sigma_c(2455)\pi$	2592.25 ± 0.28	2.59 ± 0.30 ± 0.47	$1/2^-$
$\Lambda_c(2625)^+$	$\Lambda_c^+\pi^+\pi^-$	2628.11 ± 0.19	<0.97	$3/2^-$
$\Lambda_c(2765)^+$	$\Lambda_c^+\pi^+\pi^-$, $\Sigma_c(2455)\pi$	2766.6 ± 2.4	50	?
$\Lambda_c(2880)^+$	$\Lambda_c^+\pi^+\pi^-$, $\Sigma_c(2455)\pi$, $\Sigma_c(2520)\pi$, D^0p	2881.53 ± 0.35	5.8 ± 1.1	$5/2^+$
$\Lambda_c(2940)^+$	D^0p, $\Sigma_c(2455)\pi$	$2939.3^{+1.4}_{-1.5}$	17^{+8}_{-6}	?

Table 298 Summary of the excited $\Sigma_c^{++,+,0}$ baryon family

Charmed baryon excited state	Mode	ΔM (MeV/c^2)	Natural width (MeV)	J^P
$\Sigma_c(2455)^{++}$	$\Lambda_c^+\pi^+$	167.510 ± 0.17	$1.89^{+0.09}_{-0.18}$	$1/2^+$
$\Sigma_c(2455)^+$	$\Lambda_c^+\pi^0$	166.4 ± 0.4	<4.6 @ 90% C.L.	$1/2^+$
$\Sigma_c(2455)^0$	$\Lambda_c^+\pi^-$	167.29 ± 0.17	$1.83^{+0.11}_{-0.19}$	$1/2^+$
$\Sigma_c(2520)^{++}$	$\Lambda_c^+\pi^+$	$231.95^{+0.17}_{-0.12}$	$14.78^{+0.30}_{-0.40}$	$3/2^+$
$\Sigma_c(2520)^+$	$\Lambda_c^+\pi^0$	231.0 ± 2.3	<17 @ 90% C.L.	$3/2^+$
$\Sigma_c(2520)^0$	$\Lambda_c^+\pi^-$	$232.02^{+0.15}_{-0.14}$	$15.3^{+0.4}_{-0.5}$	$3/2^+$
$\Sigma_c(2800)^{++}$	$\Lambda_c^+\pi^+$	514^{+4}_{-6}	75^{+18+12}_{-13-11}	$3/2^-$?
$\Sigma_c(2800)^+$	$\Lambda_c^+\pi^0$	505^{+15}_{-5}	62^{+37+52}_{-23-38}	
$\Sigma_c(2800)^0$	$\Lambda_c^+\pi^-$	519^{+5}_{-7}	72^{+22}_{-15}	
	$\Lambda_c^+\pi^-$	560 ± 8 ± 10	86^{+33}_{-22}	

Table 299 Summary of excited $\Xi_c^{+,0}$ and Ω_c^0 baryon families. For the first four iso-doublets, the mass difference with respect to the ground state is given, as the uncertainties are dominated by the uncertainty in the ground state mass. In the remaining cases, the uncertainty on the measurement of the excited state itself dominates

Charmed baryon excited state	Mode	Mass or mass difference (MeV/c^2)	Natural width (MeV)	J^P
$\Xi_c'^+$	$\Xi_c^+\gamma$	110.5 ± 0.4		$1/2^+$
$\Xi_c'^0$	$\Xi_c^0\gamma$	108.3 ± 0.4		$1/2^+$
$\Xi_c(2645)^+$	$\Xi_c^0\pi^+$	178.5 ± 0.1	2.1 ± 0.2	$3/2^+$
$\Xi_c(2645)^0$	$\Xi_c^+\pi^-$	174.7 ± 0.1	2.4 ± 0.2	$3/2^+$
$\Xi_c(2790)^+$	$\Xi_c'^0\pi^+$	320.7 ± 0.5	9 ± 1	$1/2^-$
$\Xi_c(2790)^0$	$\Xi_c'^+\pi^-$	323.8 ± 0.5	10 ± 1	$1/2^-$
$\Xi_c(2815)^+$	$\Xi_c(2645)^0\pi^+$	348.8 ± 0.1	2.43 ± 0.23	$3/2^-$
$\Xi_c(2815)^0$	$\Xi_c(2645)^+\pi^-$	349.4 ± 0.1	2.54 ± 0.23	$3/2^-$
$\Xi_c(2930)^0$	$\Lambda_c^+K^-$	2931.6 ± 6	36 ± 13	?
$\Xi_c(2970)^+$	$\Lambda_c^+K^-\pi^+$, $\Sigma_c^{++}K^-$, $\Xi_c(2645)^0\pi^+$	2967.2 ± 0.8	21 ± 3	?
$\Xi_c(2970)^0$	$\Xi_c(2645)^+\pi^-$	2970.4 ± 0.8	28 ± 3	?
$\Xi_c(3055)^+$	$\Sigma_c^{++}K^-$, ΛD	3055.7 ± 0.4	8.0 ± 1.9	?
$\Xi_c(3055)^0$	ΛD	3059.0 ± 0.8	6.2 ± 2.4	?
$\Xi_c(3080)^+$	$\Lambda_c^+K^-\pi^+$, $\Sigma_c^{++}K^-$, $\Sigma_c(2520)^{++}K^-$, ΛD	3077.8 ± 0.3	3.6 ± 0.7	?
$\Xi_c(3080)^0$	$\Lambda_c^+K_S^0\pi^-$, $\Sigma_c^0K_S^0$, $\Sigma_c(2520)^0K_S^0$	3079.9 ± 1.0	5.6 ± 2.2	?
$\Omega_c(2770)^0$	$\Omega_c^0\gamma$	2765.9 ± 2.0	$70.7^{+0.8}_{-0.9}$	$3/2^+$

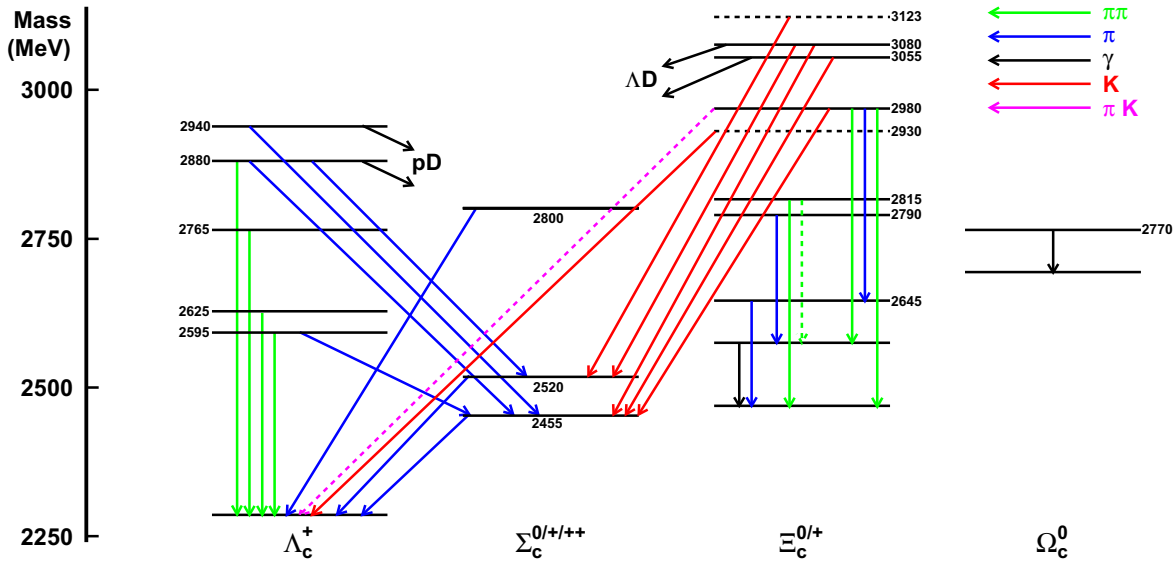

Fig. 216 Level diagram for multiplets and transitions for excited charm baryons

Table 298 summarizes the excited $\Sigma_c^{++,+,0}$ baryons. The ground iso-triplets of $\Sigma_c(2455)^{++,+,0}$ and $\Sigma_c(2520)^{++,+,0}$ baryons are well-established. Belle [1289]precisely measured the mass differences and widths of the doubly charged and neutral members of this triplet. The short list of excited Σ_c baryons is completed by the triplet of $\Sigma_c(2800)$ states observed by Belle [1290]. Based on the measured masses and theoretical predictions [1291,1292], these states are assumed to be members of the predicted Σ_{c2} $3/2^-$ triplet. From a study of resonant substructure in $B^- \to \Lambda_c^+ \bar{p}\pi^-$ decays, BaBar found a significant signal in the $\Lambda_c^+\pi^-$ final state with a mean value higher than measured for the $\Sigma_c(2800)$ by Belle by about 3σ (Table 298). The decay widths measured by Belle and BaBar are consistent, but it is an open question if the observed state is the same as the Belle state.

Table 299 summarizes the excited $\Xi_c^{+,0}$ and Ω_c^0 baryons. The list of excited Ξ_c baryons has several states, of unknown quantum numbers, having masses above 2900 MeV/c^2 and decaying into three different types of decay modes: $\Lambda_c/\Sigma_c n\pi$, $\Xi_c n\pi$ and the most recently observed ΛD. Some of these states ($\Xi_c(2970)^+$, $\Xi_c(3055)$ and $\Xi_c(3080)^{+,0}$) have been observed by both Belle [1293–1295] and BaBar [694] and are considered well-established. The $\Xi_c(2930)^0$ state decaying into $\Lambda_c^+ K^-$ is seen only by BaBar [1296] and needs confirmation. The $\Xi_c(3123)^+$ observed by BaBar [694] in the $\Sigma_c(2520)^{++}\pi^-$ final state has not been confirmed by Belle [1294] with twice the statistics; thus its existence in doubt and it is omitted from Table 299.

Several of the width and mass measurements for the $\Xi_c(3055)$ and $\Xi_c(3080)$ iso-doublets are only in marginal agreement between experiments and decay modes. However, there seems little doubt that the differing measurements are of the same particle.

Belle [1297] has recently analyzed large samples of Ξ_c', $\Xi_c(2645)$, $\Xi_c(2790)$, $\Xi_c(2815)$ and $\Xi_c(2970)$ decays. From this analysis they obtain the most precise mass measurements of all five iso-doublets, and the first significant width measurements of the $\Xi_c(2645)$, $\Xi_c(2790)$ and $\Xi_c(2815)$. The level of agreement in the different measurements of the mass and width of the $\Xi_c(2970)$, formerly named by the PDG as the $\Xi_c(2980)$, is not satisfactory. This leaves open the possibility of there being other resonances nearby or that threshold effects have not been fully understood. The present situation in the excited Ξ_c sector is summarized in Table 299.

The excited Ω_c^0 doubly strange charmed baryon has been seen by both BaBar [1298] and Belle [1284]. The mass differences $\delta M = M(\Omega_c^{*0}) - M(\Omega_c^0)$ measured by the experiments are in good agreement and are also consistent with most theoretical predictions [1299–1302]. No higher mass Ω_c states have yet been observed.

Figure 216 shows the levels of excited charm baryons along with corresponding transitions between them, and also transitions to the ground states.

We note that Belle and BaBar recently discovered that transitions between families are possible, i.e., between the Ξ_c and Λ_c^+ families of excited charmed baryons [694,1293] and that highly excited states are found to decay into a non-charmed baryons and a D meson[1287,1295].

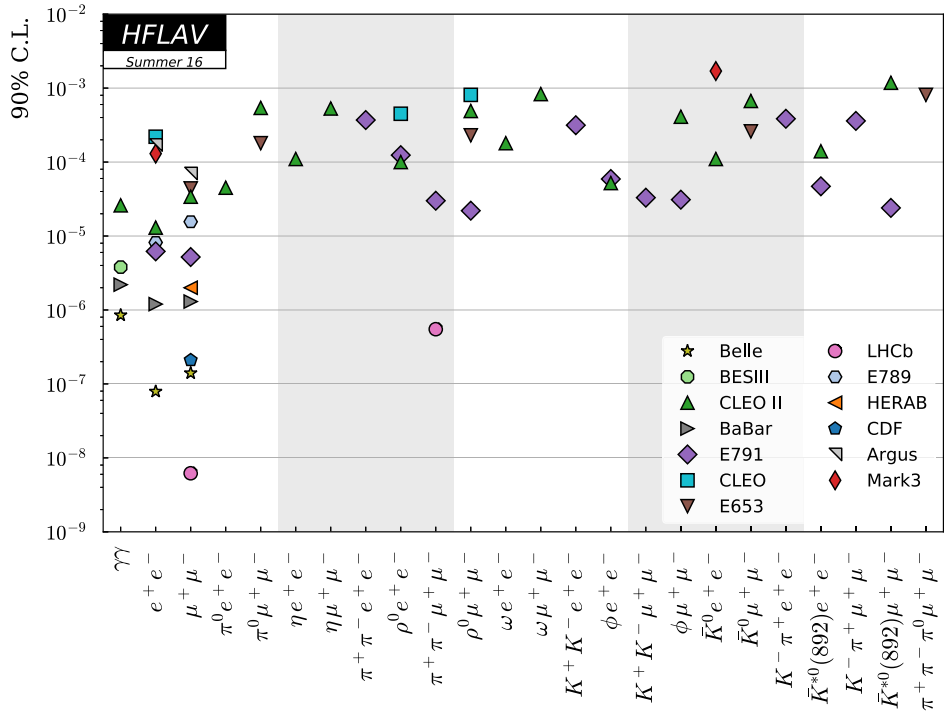

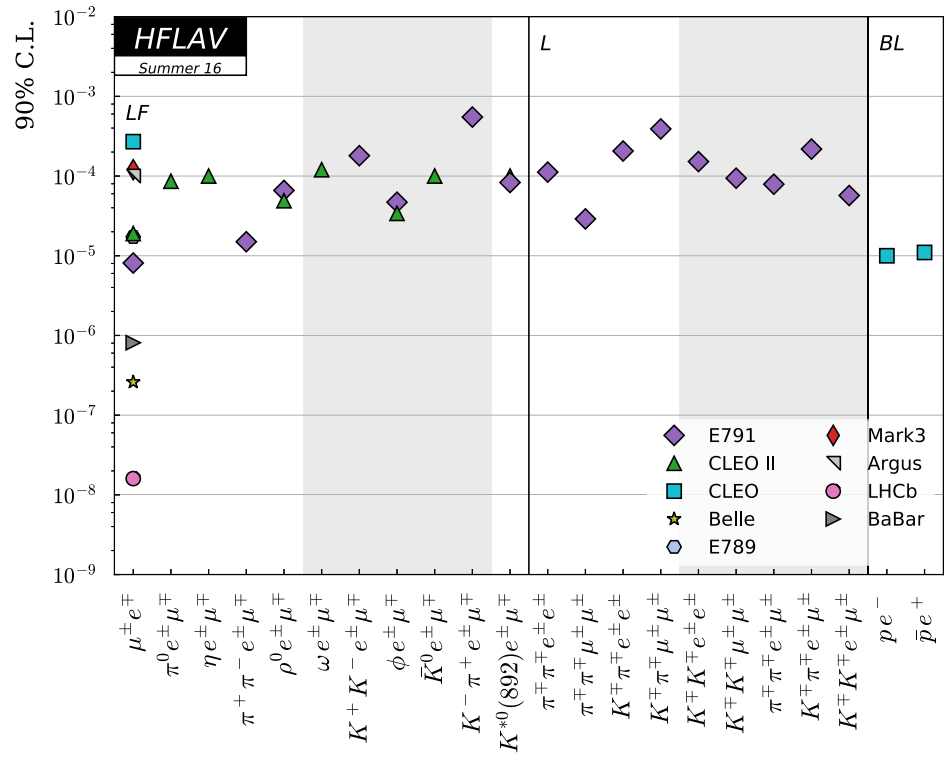

Fig. 217 Upper limits at 90% C.L. for D^0 decays. The *top plot* shows flavor-changing neutral current decays, and the *bottom plot* shows lepton-flavor-changing (LF), lepton-number-changing (L), and both baryon- and lepton-number-changing (BL) decays

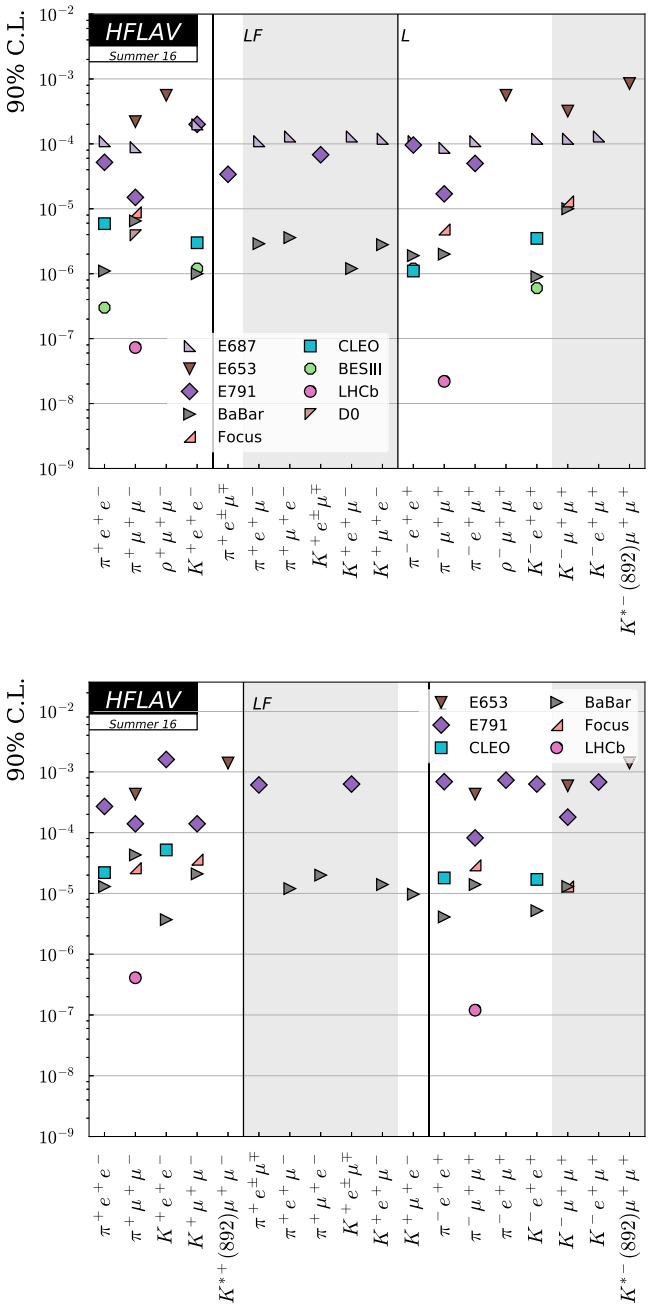

Fig. 218 Upper limits at 90% C.L. for D^+ (*top*) and D_s^+ (*bottom*) decays. *Each plot* shows flavor-changing neutral current decays, lepton-flavor-changing decays (LF), and lepton-number-changing (L) decays

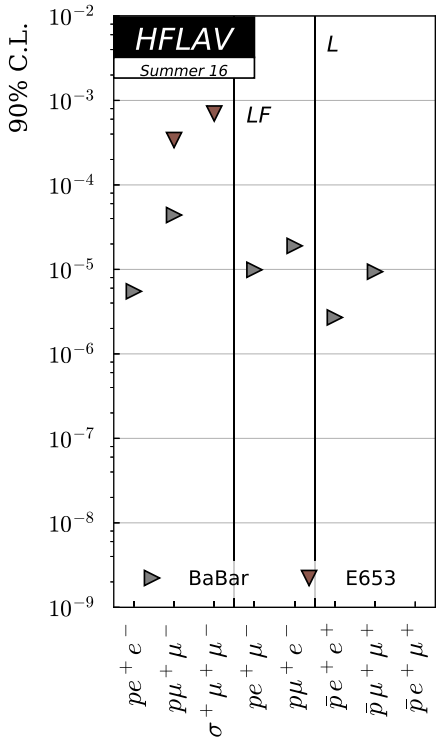

Fig. 219 Upper limits at 90% C.L. for Λ_c^+ decays. Shown are flavor-changing neutral current decays, lepton-flavor-changing (LF) decays, and lepton-number-changing (L) decays

8.12 Rare and forbidden decays

This section provides a summary of searches for rare and forbidden charm decays in tabular form. The decay modes can be categorized as flavor-changing neutral currents, lepton-flavor-violating, lepton-number-violating, and both baryon- and lepton-number-violating decays. Figures 217, 218 and 219 plot the upper limits for D^0, D^+, D_s^+, and Λ_c^+ decays. Tables 300, 301, 302 and 303 give the corresponding numerical results. Some theoretical predictions are given in Refs. [1303–1310].

In several cases the rare-decay final states have been observed with the di-lepton pair being the decay product of a vector meson. For these measurements the quoted limits are those expected for the non-resonant di-lepton spectrum. For the extrapolation to the full spectrum a phase-space distribution of the non-resonant component has been assumed. This applies to the CLEO measurement of the decays $D_{(s)}^+ \to (K^+, \pi^+)e^+e^-$ [1311], to the D0 measurements of the decays $D_{(s)}^+ \to \pi^+\mu^+\mu^-$ [1312], and to the BaBar measurements of the decays $D_{(s)}^+ \to (K^+, \pi^+)e^+e^-$ and $D_{(s)}^+ \to (K^+, \pi^+)\mu^+\mu^-$, where the contribution from $\phi \to l^+l^-$ ($l = e, \mu$) has been excluded. In the case of the LHCb measurements of the decays $D^0 \to \pi^+\pi^-\mu^+\mu^-$ [1313] as well as the decays $D_{(s)}^+ \to \pi^+\mu^+\mu^-$ [1314] the contributions from $\phi \to l^+l^-$ as well as from $\rho, \omega \to l^+l^-$ ($l = e, \mu$) have been excluded.

Table 300 Upper limits at 90% C.L. for D^0 decays

Decay	Limit $\times 10^6$	Experiment	References
$\gamma\gamma$	26.0	CLEO II	[1315]
	3.8	BESIII	[1316]
	2.2	BaBar	[1317]
	0.85	Belle	[1318]
e^+e^-	220.0	CLEO	[1319]
	170.0	Argus	[1320]
	130.0	Mark3	[1321]
	13.0	CLEO II	[1322]
	8.19	E789	[1323]
	6.2	E791	[1324]
	1.2	BaBar	[1325]
	0.079	Belle	[1326]
$\mu^+\mu^-$	70.0	Argus	[1320]
	44.0	E653	[1327]
	34.0	CLEO II	[1322]
	15.6	E789	[1323]
	5.2	E791	[1324]
	2.0	HERAb	[1328]
	1.3	BaBar	[1325]
	0.21	CDF	[1329]
	0.14	Belle	[1326]
	0.0062	LHCb	[1330]
$\pi^0 e^+e^-$	45.0	CLEO II	[1322]
$\pi^0\mu^+\mu^-$	540.0	CLEO II	[1322]
	180.0	E653	[1327]
$\eta\, e^+e^-$	110.0	CLEO II	[1322]
$\eta\,\mu^+\mu^-$	530.0	CLEO II	[1322]
$\pi^+\pi^-e^+e^-$	370.0	E791	[1331]
$\rho^0 e^+e^-$	450.0	CLEO	[1319]
	124.0	E791	[1331]
	100.0	CLEO II	[1322]
$\pi^+\pi^-\mu^+\mu^-$	30.0	E791	[1331]
	0.55	LHCb	[1313]
$\rho^0\mu^+\mu^-$	810.0	CLEO	[1319]
	490.0	CLEO II	[1322]
	230.0	E653	[1327]
	22.0	E791	[1331]
$\omega\, e^+e^-$	180.0	CLEO II	[1322]
$\omega\,\mu^+\mu^-$	830.0	CLEO II	[1322]
$K^+K^-e^+e^-$	315.0	E791	[1331]
$\phi\, e^+e^-$	59.0	E791	[1331]
	52.0	CLEO II	[1322]
$K^+K^-\mu^+\mu^-$	33.0	E791	[1331]
$\phi\,\mu^+\mu^-$	410.0	CLEO II	[1322]
	31.0	E791	[1331]
$\overline{K}^0 e^+e^-$	1700.0	Mark3	[1332]
	110.0	CLEO II	[1322]
$\overline{K}^0\mu^+\mu^-$	670.0	CLEO II	[1322]
	260.0	E653	[1327]
$K^-\pi^+e^+e^-$	385.0	E791	[1331]
$\overline{K}^{*0}(892)e^+e^-$	140.0	CLEO II	[1322]
	47.0	E791	[1331]
$K^-\pi^+\mu^+\mu^-$	360.0	E791	[1331]
$\overline{K}^{*0}(892)\mu^+\mu^-$	1180.0	CLEO II	[1322]
	24.0	E791	[1331]
$\pi^+\pi^-\pi^0\mu^+\mu^-$	810.0	E653	[1327]
$\mu^\pm e^\mp$	270.0	CLEO	[1319]
	120.0	Mark3	[1333]
	100.0	Argus	[1320]
	19.0	CLEO II	[1322]
	17.2	E789	[1323]
	8.1	E791	[1324]
	0.81	BaBar	[1325]
	0.26	Belle	[1326]
	0.016	LHCb	[1334]
$\pi^0 e^\pm\mu^\mp$	86.0	CLEO II	[1322]
$\eta\, e^\pm\mu^\mp$	100.0	CLEO II	[1322]
$\pi^+\pi^-e^\pm\mu^\mp$	15.0	E791	[1331]
$\rho^0 e^\pm\mu^\mp$	66.0	E791	[1331]
	49.0	CLEO II	[1322]
$\omega\, e^\pm\mu^\mp$	120.0	CLEO II	[1322]
$K^+K^-e^\pm\mu^\mp$	180.0	E791	[1331]
$\phi\, e^\pm\mu^\mp$	47.0	E791	[1331]
	34.0	CLEO II	[1322]
$\overline{K}^0 e^\pm\mu^\mp$	100.0	CLEO II	[1322]
$K^-\pi^+e^\pm\mu^\mp$	550.0	E791	[1331]
$K^{*0}(892)e^\pm\mu^\mp$	100.0	CLEO II	[1322]
	83.0	E791	[1331]
$\pi^\mp\pi^\mp e^\pm e^\pm$	112.0	E791	[1331]
$\pi^\mp\pi^\mp\mu^\pm\mu^\pm$	29.0	E791	[1331]
$K^\mp\pi^\mp e^\pm e^\pm$	206.0	E791	[1331]
$K^\mp\pi^\mp\mu^\pm\mu^\pm$	390.0	E791	[1331]
$K^\mp K^\mp e^\pm e^\pm$	152.0	E791	[1331]
$K^\mp K^\mp\mu^\pm\mu^\pm$	94.0	E791	[1331]
$\pi^\mp\pi^\mp e^\pm\mu^\pm$	79.0	E791	[1331]
$K^\mp\pi^\mp e^\pm\mu^\pm$	218.0	E791	[1331]
$K^\mp K^\mp e^\pm\mu^\pm$	57.0	E791	[1331]
$p\, e^-$	10.0	CLEO	[1335]
$\overline{p}\, e^+$	11.0	CLEO	[1335]

Table 301 Upper limits at 90% C.L. for D^+ decays

Decay	Limit $\times 10^6$	Experiment	References
$\pi^+e^+e^-$	110.0	E687	[1336]
	52.0	E791	[1324]
	5.9	CLEO	[1311]
	1.1	BaBar	[1337]
	0.3	BESIII	[1338]
$\pi^+\mu^+\mu^-$	220.0	E653	[1327]
	89.0	E687	[1336]
	15.0	E791	[1324]
	8.8	Focus	[1339]
	6.5	BaBar	[1337]
	3.9	D0	[1312]
	0.073	LHCb	[1314]
$\rho^+\mu^+\mu^-$	560.0	E653	[1327]
$K^+e^+e^-$	200.0	E687	[1336]
	3.0	CLEO	[1311]
	1.2	BESIII	[1338]
	1.0	BaBar	[1337]
$\pi^+e^\pm\mu^\mp$	34.0	E791	[1324]
$\pi^+e^+\mu^-$	110.0	E687	[1336]
	2.9	BaBar	[1337]
$\pi^+\mu^+e^-$	130.0	E687	[1336]
	3.6	BaBar	[1337]
$K^+e^\pm\mu^\mp$	68.0	E791	[1324]
$K^+e^+\mu^-$	130.0	E687	[1336]
	1.2	BaBar	[1337]
$K^+\mu^+e^-$	120.0	E687	[1336]
	2.8	BaBar	[1337]
$\pi^-e^+e^+$	110.0	E687	[1336]
	96.0	E791	[1324]
	1.9	BaBar	[1337]
	1.2	BESIII	[1338]
	1.1	CLEO	[1311]
$\pi^-\mu^+\mu^+$	87.0	E687	[1336]
	17.0	E791	[1324]
	4.8	Focus	[1339]
	2.0	BaBar	[1337]
	0.022	LHCb	[1314]
$\pi^-e^+\mu^+$	110.0	E687	[1336]
	50.0	E791	[1324]
$\rho^-\mu^+\mu^+$	560.0	E653	[1327]
$K^-e^+e^+$	120.0	E687	[1336]
	3.5	CLEO	[1311]
	0.9	BaBar	[1337]
	0.6	BESIII	[1338]
$K^-\mu^+\mu^+$	320.0	E653	[1327]
	120.0	E687	[1336]
	13.0	Focus	[1339]
	10.0	BaBar	[1337]
$K^-e^+\mu^+$	130.0	E687	[1336]
$K^{*-}(892)\mu^+\mu^+$	850.0	E653	[1327]

Table 302 Upper limits at 90% C.L. for D_s^+ decays

Decay	Limit $\times 10^6$	Experiment	References
$\pi^+e^+e^-$	270.0	E791	[1324]
	22.0	CLEO	[1311]
	13.0	BaBar	[1337]
$\pi^+\mu^+\mu^-$	430.0	E653	[1327]
	140.0	E791	[1324]
	43.0	BaBar	[1337]
	26.0	Focus	[1339]
	0.41	LHCb	[1314]
$K^+e^+e^-$	1600.0	E791	[1324]
	52.0	CLEO	[1311]
	3.7	BaBar	[1337]
$K^+\mu^+\mu^-$	140.0	E791	[1324]
	36.0	Focus	[1339]
	21.0	BaBar	[1337]
$K^{*+}(892)\mu^+\mu^-$	1400.0	E653	[1327]
$\pi^+e^\pm\mu^\mp$	610.0	E791	[1324]
$\pi^+e^+\mu^-$	12.0	BaBar	[1337]
$\pi^+\mu^+e^-$	20.0	BaBar	[1337]
$K^+e^\pm\mu^\mp$	630.0	E791	[1324]
$K^+e^+\mu^-$	14.0	BaBar	[1337]
$K^+\mu^+e^-$	9.7	BaBar	[1337]
$\pi^-e^+e^+$	690.0	E791	[1324]
	18.0	CLEO	[1311]
	4.1	BaBar	[1337]
$\pi^-\mu^+\mu^+$	430.0	E653	[1327]
	82.0	E791	[1324]
	29.0	Focus	[1339]
	14.0	BaBar	[1337]
	0.12	LHCb	[1314]
$\pi^-e^+\mu^+$	730.0	E791	[1324]
$K^-e^+e^+$	630.0	E791	[1324]
	17.0	CLEO	[1311]
	5.2	BaBar	[1337]
$K^-\mu^+\mu^+$	590.0	E653	[1327]
	180.0	E791	[1324]
	13.0	BaBar	[1337]
$K^-e^+\mu^+$	680.0	E791	[1324]
$K^{*-}(892)\mu^+\mu^+$	1400.0	E653	[1327]

Table 303 Upper limits at 90% C.L. for Λ_c^+ decays

Decay	Limit $\times 10^6$	Experiment	References
pe^+e^-	5.5	BaBar	[1337]
$p\mu^+\mu^-$	340.0	E653	[1327]
	44.0	BaBar	[1337]
$\sigma^+\mu^+\mu^-$	700.0	E653	[1327]
$pe^+\mu^-$	9.9	BaBar	[1337]
$p\mu^+e^-$	19.0	BaBar	[1337]
$\overline{p}\,e^+e^+$	2.7	BaBar	[1337]
$\overline{p}\,\mu^+\mu^+$	9.4	BaBar	[1337]

9 Tau lepton properties

We present averages of a selection of τ lepton quantities with the goal to provide the best tests of the universality of the charged-current weak interaction (Sect. 9.2) and of the Cabibbo–Kobayashi–Maskawa (CKM) matrix coefficient $|V_{us}|$ from τ decays (Sect. 9.4). We focus on the averages that benefit most from the adoption of the HFLAV methodology [420], namely a global fit of the τ branching fractions that best exploits the available experimental information. Since the 2016 edition, the HFLAV-Tau group has collaborated to the determination of the τ-lepton branching fractions based on a global fit and to the related mini-review that are included in the "Review of particle physics" [6]. The differences between the PDG 2016 fit and the fit presented here are detailed in Sect. 9.1.4.

All relevant published statistical correlations are used, and a selection of measurements, particularly the most precise and the most recent ones, was studied to take into account the significant systematic dependencies from external parameters and common sources of systematic uncertainty.

Finally, we report in Sect. 9.5 the latest limits on the lepton-flavour-violating τ branching fractions and in Sect. 9.6 we determine the combined upper limits for the branching fractions that have multiple experimental results.

The τ lepton results are obtained from inputs available through summer 2016 and have been published on the web in 2016 with the label "Summer 2016". However, there have been minor revisions since then, and we have updated tables and plots in this report with the label "Spring 2017".

9.1 Branching fraction fit

A global fit of the available experimental measurements is used to determine the τ branching fractions, together with their uncertainties and statistical correlations. The τ branching fractions provide a test for theory predictions based on the Standard Model (SM) EW and QCD interactions and can be further elaborated to test the EW charged-current universality for leptons, to determine the CKM matrix coefficient $|V_{us}|$ (and the QCD coupling constant α_s at the τ mass).

The measurements used in the fit are listed in Table 304 and consist of either τ decay branching fractions, labelled as Γ_i, or ratios of two τ decay branching fractions, labelled as Γ_i/Γ_j. A minimum χ^2 fit is performed for all the measured quantities and for some additional branching fractions and ratios of branching fractions, and all fit results are listed in Table 304. Some fitted quantities are equal to the ratio of two other fitted quantities, as documented with the notation Γ_i/Γ_j in Table 304. Some fitted quantities are sums of other fitted quantities, for instance $\Gamma_8 = B(\tau \to h^-\nu_\tau)$ is the sum of $\Gamma_9 = B(\tau \to \pi^-\nu_\tau)$ and $\Gamma_{10} = B(\tau \to K^-\nu_\tau)$. The symbol h is used to mean either a π or K. Section 9.1.7 lists all equations relating one quantity to the sum of other quantities. In the following, we refer to both types of relations between fitted quantities collectively as constraint equations or constraints. The fit χ^2 is minimized subject to all the above mentioned constraints, listed in Table 304 and Sect. 9.1.7. The fit procedure is equivalent to that employed in the previous HFLAV reports [5,234,420].

9.1.1 Technical implementation of the fit procedure

The fit computes the quantities q_i by minimizing a χ^2 while respecting a series of equality constraints on the q_i. The χ^2 is computed using the measurements x_i and their covariance matrix V_{ij} as

$$\chi^2 = (x_i - A_{ik}q_k)^t V_{ij}^{-1}(x_j - A_{jl}q_l), \tag{286}$$

where the model matrix A_{ij} is used to get the vector of the predicted measurements x_i' from the vector of the fit parameters q_j as $x_i' = A_{ij}q_j$. In this particular implementation, the measurements are grouped according to the measured quantity, and all quantities with at least one measurement correspond to a fit parameter. Therefore, the matrix A_{ij} has one row per measurement x_i and one column per fitted quantity q_j, with unity coefficients for the rows and column that identify a measurement x_i of the quantity q_j. In summary, the χ^2 given in Eq. (286) is minimized subject to the constraints

$$f_r(q_s) - c_r = 0, \tag{287}$$

where Eq. (287) corresponds to the constraint equations, written as a set of "constraint expressions" that are equated to zero. Using the method of Lagrange multipliers, a set of equations is obtained by taking the derivatives with respect to the fitted quantities q_k and the Lagrange multipliers λ_r of the sum of the χ^2 and the constraint expres-

Table 304 HFLAV Spring 2017 branching fractions fit results

τ lepton branching fraction	Fit value/Exp.	HFLAV fit/Refs.
$\Gamma_1 = (\text{particles})- \geq 0\,\text{neutrals} \geq 0 K^0 \nu_\tau$	0.8519 ± 0.0011	HFLAV Spring 2017 fit
$\Gamma_2 = (\text{particles})^- \geq 0\,\text{neutrals} \geq 0 K^0_L \nu_\tau$	0.8453 ± 0.0010	HFLAV Spring 2017 fit
$\Gamma_3 = \mu^- \bar{\nu}_\mu \bar{\nu}_\tau$	0.17392 ± 0.00040	HFLAV Spring 2017 fit
$0.17319 \pm 0.00077 \pm 0.00000$	ALEPH	[1344]
$0.17325 \pm 0.00095 \pm 0.00077$	DELPHI	[1345]
$0.17342 \pm 0.00110 \pm 0.00067$	L3	[1346]
$0.17340 \pm 0.00090 \pm 0.00060$	OPAL	[1347]
$\frac{\Gamma_3}{\Gamma_5} = \frac{\mu^- \bar{\nu}_\mu \bar{\nu}_\tau}{e^- \bar{\nu}_e \bar{\nu}_\tau}$	0.9762 ± 0.0028	HFLAV Spring 2017 fit
$0.9970 \pm 0.0350 \pm 0.0400$	ARGUS	[1348]
$0.9796 \pm 0.0016 \pm 0.0036$	BaBar	[1349]
$0.9777 \pm 0.0063 \pm 0.0087$	CLEO	[1350]
$\Gamma_5 = e^- \bar{\nu}_e \bar{\nu}_\tau$	0.17816 ± 0.00041	HFLAV Spring 2017 fit
$0.17837 \pm 0.00080 \pm 0.00000$	ALEPH	[1344]
$0.17760 \pm 0.00060 \pm 0.00170$	CLEO	[1350]
$0.17877 \pm 0.00109 \pm 0.00110$	DELPHI	[1345]
$0.17806 \pm 0.00104 \pm 0.00076$	L3	[1346]
$0.17810 \pm 0.00090 \pm 0.00060$	OPAL	[1351]
$\Gamma_7 = h^- \geq 0 K^0_L \nu_\tau$	0.12023 ± 0.00054	HFLAV Spring 2017 fit
$0.12400 \pm 0.00700 \pm 0.00700$	DELPHI	[1352]
$0.12470 \pm 0.00260 \pm 0.00430$	L3	[1353]
$0.12100 \pm 0.00700 \pm 0.00500$	OPAL	[1354]
$\Gamma_8 = h^- \nu_\tau$	0.11506 ± 0.00054	HFLAV Spring 2017 fit
$0.11524 \pm 0.00105 \pm 0.00000$	ALEPH	[1344]
$0.11520 \pm 0.00050 \pm 0.00120$	CLEO	[1350]
$0.11571 \pm 0.00120 \pm 0.00114$	DELPHI	[1355]
$0.11980 \pm 0.00130 \pm 0.00160$	OPAL	[1356]
$\frac{\Gamma_8}{\Gamma_5} = \frac{h^- \nu_\tau}{e^- \bar{\nu}_e \nu_\tau}$	0.6458 ± 0.0033	HFLAV Spring 2017 fit
$\Gamma_9 = \pi^- \nu_\tau$	0.10810 ± 0.00053	HFLAV Spring 2017 fit
$\frac{\Gamma_9}{\Gamma_5} = \frac{\pi^- \nu_\tau}{e^- \bar{\nu}_e \nu_\tau}$	0.6068 ± 0.0032	HFLAV Spring 2017 fit
$0.5945 \pm 0.0014 \pm 0.0061$	BABAR	[1349]
$\Gamma_{10} = K^- \nu_\tau$	$(0.6960 \pm 0.0096) \cdot 10^{-2}$	HFLAV Spring 2017 fit
$(0.6960 \pm 0.0287 \pm 0.0000) \cdot 10^{-2}$	ALEPH	[1357]
$(0.6600 \pm 0.0700 \pm 0.0900) \cdot 10^{-2}$	CLEO	[1358]
$(0.8500 \pm 0.1800 \pm 0.0000) \cdot 10^{-2}$	DELPHI	[1359]
$(0.6580 \pm 0.0270 \pm 0.0290) \cdot 10^{-2}$	OPAL	[1360]
$\frac{\Gamma_{10}}{\Gamma_5} = \frac{K^- \nu_\tau}{e^- \bar{\nu}_e \nu_\tau}$	$(3.906 \pm 0.054) \cdot 10^{-2}$	HFLAV Spring 2017 fit
$(3.882 \pm 0.032 \pm 0.057) \cdot 10^{-2}$	BaBar	[1349]
$\frac{\Gamma_{10}}{\Gamma_9} = \frac{K^- \nu_\tau}{\pi^- \nu_\tau}$	$(6.438 \pm 0.094) \cdot 10^{-2}$	HFLAV Spring 2017 fit
$\Gamma_{11} = \text{h}^- \geq 1\,\text{neutrals} \geq \nu_\tau$	0.36973 ± 0.00097	HFLAV Spring 2017 fit
$\Gamma_{12} = h^- \pi^0 \nu_\tau\ (\text{ex.} K^0)$	0.36475 ± 0.00097	HFLAV Spring 2017 fit
$\Gamma_{13} = h^- \pi^0 \nu_\tau$	0.25935 ± 0.00091	HFLAV Spring 2017 fit
$0.25924 \pm 0.00129 \pm 0.00000$	ALEPH	[1344]
$0.25670 \pm 0.00010 \pm 0.00390$	Belle	[1361]
$0.25870 \pm 0.00120 \pm 0.00420$	CLEO	[1362]
$0.25740 \pm 0.00201 \pm 0.00138$	DELPHI	[1355]

Table 304 continued

τ lepton branching fraction	Fit value/Exp.	HFLAV fit/Refs.
$0.25050 \pm 0.00350 \pm 0.00500$	L3	[1353]
$0.25890 \pm 0.00170 \pm 0.00290$	OPAL	[1356]
$\Gamma_{14} = \pi^- \pi^0 \nu_\tau$	0.25502 ± 0.00092	HFLAV Spring 2017 fit
$\Gamma_{16} = K^- \pi^0 \nu_\tau$	$(0.4327 \pm 0.0149) \cdot 10^{-2}$	HFLAV Spring 2017 fit
$(0.4440 \pm 0.0354 \pm 0.0000) \cdot 10^{-2}$	ALEPH	[1357]
$(0.4160 \pm 0.0030 \pm 0.0180) \cdot 10^{-2}$	BaBar	[1363]
$(0.5100 \pm 0.1000 \pm 0.0700) \cdot 10^{-2}$	CLEO	[1358]
$(0.4710 \pm 0.0590 \pm 0.0230) \cdot 10^{-2}$	OPAL	[1364]
$\Gamma_{17} = h^- \geq 2\pi^0 \nu_\tau$	0.10775 ± 0.00095	HFLAV Spring 2017 fit
$0.09910 \pm 0.00310 \pm 0.00270$	OPAL	[1356]
$\Gamma_{18} = h^- 2\pi^0 \nu_\tau$	$(9.458 \pm 0.097) \cdot 10^{-2}$	HFLAV Spring 2017 fit
$\Gamma_{19} = h^- 2\pi^0 \nu_\tau$ (ex.K^0)	$(9.306 \pm 0.097) \cdot 10^{-2}$	HFLAV Spring 2017 fit
$(9.295 \pm 0.122 \pm 0.000) \cdot 10^{-2}$	ALEPH	[1344]
$(9.498 \pm 0.320 \pm 0.275) \cdot 10^{-2}$	DELPHI	[1355]
$(8.880 \pm 0.370 \pm 0.420) \cdot 10^{-2}$	L3	[1353]
$\frac{\Gamma_{19}}{\Gamma_{13}} = \frac{h^- 2\pi^0 \nu_\tau \text{ (ex.} K^0)}{h^- \pi^0 \nu_\tau}$	0.3588 ± 0.0044	HFLAV Spring 2017 fit
$0.3420 \pm 0.0060 \pm 0.0160$	CLEO	[1365]
$\Gamma_{20} = \pi^- 2\pi^0 \nu_\tau$ (ex.K^0)	$(9.242 \pm 0.100) \cdot 10^{-2}$	HFLAV Spring 2017 fit
$\Gamma_{23} = K^- 2\pi^0 \nu_\tau$ (ex.K^0)	$(0.0640 \pm 0.0220) \cdot 10^{-2}$	HFLAV Spring 2017 fit
$(0.0560 \pm 0.0250 \pm 0.0000) \cdot 10^{-2}$	ALEPH	[1357]
$(0.0900 \pm 0.1000 \pm 0.0300) \cdot 10^{-2}$	CLEO	[1358]
$\Gamma_{24} = h^- \geq 3\pi^0 \nu_\tau$	$(1.318 \pm 0.065) \cdot 10^{-2}$	HFLAV Spring 2017 fit
$\Gamma_{25} = h^- \geq 3\pi^0 \nu_\tau$ (ex.K^0)	$(1.233 \pm 0.065) \cdot 10^{-2}$	HFLAV Spring 2017 fit
$(1.403 \pm 0.214 \pm 0.224) \cdot 10^{-2}$	DELPHI	[1355]
$\Gamma_{26} = h^- 3\pi^0 \nu_\tau$	$(1.158 \pm 0.072) \cdot 10^{-2}$	HFLAV Spring 2017 fit
$(1.082 \pm 0.093 \pm 0.000) \cdot 10^{-2}$	ALEPH	[1344]
$(1.700 \pm 0.240 \pm 0.380) \cdot 10^{-2}$	L3	[1353]
$\frac{\Gamma_{26}}{\Gamma_{13}} = \frac{h^- 3\pi^0 \nu_\tau}{h^- \pi^0 \nu_\tau}$	$(4.465 \pm 0.277) \cdot 10^{-2}$	HFLAV Spring 2017 fit
$(4.400 \pm 0.300 \pm 0.500) \cdot 10^{-2}$	CLEO	[1365]
$\Gamma_{27} = \pi^- \geq 3\pi^0 \nu_\tau$ (ex.K^0)	$(1.029 \pm 0.075) \cdot 10^{-2}$	HFLAV Spring 2017 fit
$\Gamma_{28} = K^- \geq 3\pi^0 \nu_\tau$ (ex.K^0, η)	$(4.283 \pm 2.161) \cdot 10^{-2}$	HFLAV Spring 2017 fit
$(3.700 \pm 2.371 \pm 0.000) \cdot 10^{-4}$	ALEPH	[1357]
$\Gamma_{29} = h^- \geq 4\pi^0 \nu_\tau$ (ex.K^0)	$(0.1568 \pm 0.0391) \cdot 10^{-2}$	HFLAV Spring 2017 fit
$(0.1600 \pm 0.0500 \pm 0.0500) \cdot 10^{-2}$	CLEO	[1365]
$\Gamma_{30} = h^- \geq 4\pi^0 \nu_\tau$ (ex.K^0, η)	$(0.1099 \pm 0.0391) \cdot 10^{-2}$	HFLAV Spring 2017 fit
$(0.1120 \pm 0.0509 \pm 0.0000) \cdot 10^{-2}$	ALEPH	[1344]
$\Gamma_{31} = K^- \geq 0\pi^0 \geq 0K^0 \geq 0\gamma \nu_\tau$	$(1.545 \pm 0.030) \cdot 10^{-2}$	HFLAV Spring 2017 fit
$(1.700 \pm 0.120 \pm 0.190) \cdot 10^{-2}$	CLEO	[1358]
$(1.540 \pm 0.240 \pm 0.000) \cdot 10^{-2}$	DELPHI	[1359]
$(1.528 \pm 0.039 \pm 0.040) \cdot 10^{-2}$	OPAL	[1360]
$\Gamma_{32} = K^- \geq 1(\pi^0 \text{ or } K^0 \text{ or } \gamma)\nu_\tau$	$(0.8528 \pm 0.0286) \cdot 10^{-2}$	HFLAV Spring 2017 fit
$\Gamma_{33} = K^0_S(\text{particles})\nu_\tau$	$(0.9372 \pm 0.0292) \cdot 10^{-2}$	HFLAV Spring 2017 fit
$(0.9700 \pm 0.0849 \pm 0.0000) \cdot 10^{-2}$	ALEPH	[1343]
$(0.9700 \pm 0.0900 \pm 0.0600) \cdot 10^{-2}$	OPAL	[1366]
$\Gamma_{34} = h^- \bar{K}^0 \nu_\tau$	$(0.9865 \pm 0.0139) \cdot 10^{-2}$	HFLAV Spring 2017 fit
$(0.8550 \pm 0.0360 \pm 0.0730) \cdot 10^{-2}$	CLEO	[1367]

Table 304 continued

τ lepton branching fraction	Fit value/Exp.	HFLAV fit/Refs.
$\Gamma_{35} = \pi^- \bar{K}^0 \nu_\tau$	$(0.8386 \pm 0.0141) \cdot 10^{-2}$	HFLAV Spring 2017 fit
$(0.9280 \pm 0.0564 \pm 0.0000) \cdot 10^{-2}$	ALEPH	[1357]
$(0.8320 \pm 0.0025 \pm 0.0150) \cdot 10^{-2}$	Belle	[1342]
$(0.9500 \pm 0.1500 \pm 0.0600) \cdot 10^{-2}$	L3	[1368]
$(0.9330 \pm 0.0680 \pm 0.0490) \cdot 10^{-2}$	OPAL	[1369]
$\Gamma_{37} = K^- K^0 \nu_\tau$	$(0.1479 \pm 0.0053) \cdot 10^{-2}$	HFLAV Spring 2017 fit
$(0.1580 \pm 0.0453 \pm 0.0000) \cdot 10^{-2}$	ALEPH	[1343]
$(0.1620 \pm 0.0237 \pm 0.0000) \cdot 10^{-2}$	ALEPH	[1357]
$(0.1480 \pm 0.0013 \pm 0.0055) \cdot 10^{-2}$	Belle	[1342]
$(0.1510 \pm 0.0210 \pm 0.0220) \cdot 10^{-2}$	CLEO	[1367]
$\Gamma_{38} = K^- K^0 \nu_\tau \geq 0\pi^0 \nu_\tau$	$(0.2982 \pm 0.0079) \cdot 10^{-2}$	HFLAV Spring 2017 fit
$(0.3300 \pm 0.0550 \pm 0.0390) \cdot 10^{-2}$	OPAL	[1369]
$\Gamma_{39} = h^- \overline{K}^0 \pi^0 \nu_\tau$	$(0.5314 \pm 0.0134) \cdot 10^{-2}$	HFLAV Spring 2017 fit
$(0.5620 \pm 0.0500 \pm 0.0480) \cdot 10^{-2}$	CLEO	[1367]
$\Gamma_{40} = \pi^- \overline{K}^0 \pi^0 \nu_\tau$	$(0.3812 \pm 0.0129) \cdot 10^{-2}$	HFLAV Spring 2017 fit
$(0.2940 \pm 0.0818 \pm 0.0000) \cdot 10^{-2}$	ALEPH	[1343]
$(0.3470 \pm 0.0646 \pm 0.0000) \cdot 10^{-2}$	ALEPH	[1357]
$(0.3860 \pm 0.0031 \pm 0.0135) \cdot 10^{-2}$	Belle	[1342]
$(0.4100 \pm 0.1200 \pm 0.0300) \cdot 10^{-2}$	L3	[1368]
$\Gamma_{42} = K^- \pi^0 K^0 \nu_\tau$	$(0.1502 \pm 0.0071) \cdot 10^{-2}$	HFLAV Spring 2017 fit
$(0.1520 \pm 0.0789 \pm 0.0000) \cdot 10^{-2}$	ALEPH	[1343]
$(0.1430 \pm 0.0291 \pm 0.0000) \cdot 10^{-2}$	ALEPH	[1357]
$(0.1496 \pm 0.0019 \pm 0.0073) \cdot 10^{-2}$	Belle	[1342]
$(0.1450 \pm 0.0360 \pm 0.0200) \cdot 10^{-2}$	CLEO	[1367]
$\Gamma_{43} = \pi^- \overline{K}^0 \geq 1\pi^0 \nu_\tau$	$(0.4046 \pm 0.0260) \cdot 10^{-2}$	HFLAV Spring 2017 fit
$(0.3240 \pm 0.0740 \pm 0.0660) \cdot 10^{-2}$	OPAL	[1369]
$\Gamma_{44} = \pi^- \overline{K}^0 \pi^0 \pi^0 \nu_\tau$ (ex.K^0)	$(2.340 \pm 2.306) \cdot 10^{-4}$	HFLAV Spring 2017 fit
$(2.600 \pm 2.400 \pm 0.000) \cdot 10^{-4}$	ALEPH	[1370]
$\Gamma_{46} = \pi^- K^0 \overline{K}^0 \nu_\tau$	$(0.1513 \pm 0.0247) \cdot 10^{-2}$	HFLAV Spring 2017 fit
$\Gamma_{47} = \pi^- K^0_S K^0_S \nu_\tau$	$(2.332 \pm 0.065) \cdot 10^{-4}$	HFLAV Spring 2017 fit
$(2.600 \pm 1.118 \pm 0.000) \cdot 10^{-4}$	ALEPH	[1343]
$(2.310 \pm 0.040 \pm 0.080) \cdot 10^{-4}$	BaBar	[1371]
$(2.330 \pm 0.033 \pm 0.093) \cdot 10^{-4}$	Belle	[1342]
$(2.300 \pm 0.500 \pm 0.300) \cdot 10^{-4}$	CLEO	[1367]
$\Gamma_{48} = \pi^- K^0_S K^0_L \nu_\tau$	$(0.1047 \pm 0.0247) \cdot 10^{-2}$	HFLAV Spring 2017 fit
$(0.1010 \pm 0.0264 \pm 0.0000) \cdot 10^{-2}$	ALEPH	[1343]
$\Gamma_{49} = \pi^- K^0 \overline{K}^0 \pi^0 \nu_\tau$	$(3.540 \pm 1.193) \cdot 10^{-4}$	HFLAV Spring 2017 fit
$\Gamma_{50} = \pi^- \pi^0 K^0_S K^0_S \nu_\tau$	$(1.815 \pm 0.207) \cdot 10^{-5}$	HFLAV Spring 2017 fit
$(1.600 \pm 0.200 \pm 0.220) \cdot 10^{-5}$	BaBar	[1371]
$(2.000 \pm 0.216 \pm 0.202) \cdot 10^{-5}$	Belle	[1342]
$\Gamma_{51} = \pi^- \pi^0 K^0_S K^0_L \nu_\tau$	$(3.177 \pm 1.192) \cdot 10^{-4}$	HFLAV Spring 2017 fit
$(3.100 \pm 1.100 \pm 0.500) \cdot 10^{-4}$	ALEPH	[1343]
$\Gamma_{53} = \overline{K}^0 h^- h^- h^+ \nu_\tau$	$(2.218 \pm 2.024) \cdot 10^{-4}$	HFLAV Spring 2017 fit
$(2.300 \pm 2.025 \pm 0.000) \cdot 10^{-4}$	ALEPH	[1343]

Table 304 continued

τ lepton branching fraction	Fit value/Exp.	HFLAV fit/Refs.
$\Gamma_{54} = h^- h^- h^+ \geq 0\,\text{neutrals} \geq 0 K_L^0 \nu_\tau$	0.15215 ± 0.00061	HFLAV Spring 2017 fit
$0.15000 \pm 0.00400 \pm 0.00300$	CELLO	[1372]
$0.14400 \pm 0.00600 \pm 0.00300$	L3	[1373]
$0.15100 \pm 0.00800 \pm 0.00600$	TPC	[1374]
$\Gamma_{55} = h^- h^- h^+ \geq 0\,\text{neutrals}\, \nu_\tau\ (\text{ex.}K^0)$	0.14567 ± 0.00057	HFLAV Spring 2017 fit
$0.14556 \pm 0.00105 \pm 0.00076$	L3	[1375]
$0.14960 \pm 0.00090 \pm 0.00220$	OPAL	[1376]
$\Gamma_{56} = h^- h^- h^+ \nu_\tau$	$(9.780 \pm 0.054) \cdot 10^{-2}$	HFLAV Spring 2017 fit
$\Gamma_{57} = h^- h^- h^+ \nu_\tau\ (\text{ex.}K^0)$	$(9.439 \pm 0.053) \cdot 10^{-2}$	HFLAV Spring 2017 fit
$(9.510 \pm 0.070 \pm 0.200) \cdot 10^{-2}$	CLEO	[1377]
$(9.317 \pm 0.090 \pm 0.082) \cdot 10^{-2}$	DELPHI	[1355]
$\frac{\Gamma_{57}}{\Gamma_{55}} = \frac{h^- h^- h^+ \nu_\tau\ (\text{ex.}K^0)}{h^- h^- h^+ \geq 0\,\text{neutrals}\, \nu_\tau\ (\text{ex.}K^0)}$	0.6480 ± 0.0030	HFLAV Spring 2017 fit
$0.6600 \pm 0.0040 \pm 0.0140$	OPAL	[1376]
$\Gamma_{58} = h^- h^- h^+ \nu_\tau\ (\text{ex.}K^0, \omega)$	$(9.408 \pm 0.053) \cdot 10^{-2}$	HFLAV Spring 2017 fit
$(9.469 \pm 0.096 \pm 0.000) \cdot 10^{-2}$	ALEPH	[1344]
$\Gamma_{59} = \pi^- \pi^+ \pi^- \nu_\tau$	$(9.290 \pm 0.052) \cdot 10^{-2}$	HFLAV Spring 2017 fit
$\Gamma_{60} = \pi^- \pi^+ \pi^- \nu_\tau\ (\text{ex.}K^0)$	$(9.000 \pm 0.051) \cdot 10^{-2}$	HFLAV Spring 2017 fit
$(8.830 \pm 0.010 \pm 0.130) \cdot 10^{-2}$	BaBar	[1378]
$\left(8.420 \pm 0.000^{+0.260}_{-0.250}\right) \cdot 10^{-2}$	Belle	[1379]
$(9.130 \pm 0.050 \pm 0.460) \cdot 10^{-2}$	CLEO3	[1380]
$\Gamma_{62} = \pi^- \pi^- \pi^+ \nu_\tau\ (\text{ex.}K^0, \omega)$	$(8.970 \pm 0.052) \cdot 10^{-2}$	HFLAV Spring 2017 fit
$\Gamma_{63} = h^- h^- h^+ \geq 1\,\text{neutrals}\, \nu_\tau$	$(5.325 \pm 0.050) \cdot 10^{-2}$	HFLAV Spring 2017 fit
$\Gamma_{64} = h^- h^- h^+ \geq 1\pi^0\, \nu_\tau\ (\text{ex.}K^0)$	$(5.120 \pm 0.049) \cdot 10^{-2}$	HFLAV Spring 2017 fit
$\Gamma_{65} = h^- h^- h^+ \geq \pi^0$	$(4.790 \pm 0.052) \cdot 10^{-2}$	HFLAV Spring 2017 fit
$\Gamma_{66} = h^- h^- h^+ \geq \pi^0\, \nu_\tau\ (\text{ex.}K^0)$	$(4.606 \pm 0.051) \cdot 10^{-2}$	HFLAV Spring 2017 fit
$(4.734 \pm 0.077 \pm 0.000) \cdot 10^{-2}$	ALEPH	[1344]
$(4.230 \pm 0.060 \pm 0.220) \cdot 10^{-2}$	CLEO	[1377]
$(4.545 \pm 0.106 \pm 0.103) \cdot 10^{-2}$	DELPHI	[1355]
$\Gamma_{67} = h^- h^- h^+ \pi^0 \nu_\tau\ (\text{ex.}K^0, \omega)$	$(2.820 \pm 0.070) \cdot 10^{-2}$	HFLAV Spring 2017 fit
$\Gamma_{68} = \pi^- \pi^+ \pi^- \pi^0\, \nu_\tau$	$(4.651 \pm 0.053) \cdot 10^{-2}$	HFLAV Spring 2017 fit
$\Gamma_{69} = \pi^- \pi^+ \pi^- \pi^0\, \nu_\tau\ (\text{ex.}K^0)$	$(4.519 \pm 0.052) \cdot 10^{-2}$	HFLAV Spring 2017 fit
$(4.190 \pm 0.100 \pm 0.210) \cdot 10^{-2}$	CLEO	[1381]
$\Gamma_{70} = \pi^- \pi^- \pi^+ \pi^0\, \nu_\tau\ (\text{ex.}K^0, \omega)$	$(2.769 \pm 0.071) \cdot 10^{-2}$	HFLAV Spring 2017 fit
$\Gamma_{74} = h^- h^- h^+ \geq 2\pi^0\, \nu_\tau\ (\text{ex.}K^0)$	$(0.5135 \pm 0.0312) \cdot 10^{-2}$	HFLAV Spring 2017 fit
$(0.5610 \pm 0.0680 \pm 0.0950) \cdot 10^{-2}$	DELPHI	[1355]
$\Gamma_{75} = h^- h^- h^+ 2\pi^0\, \nu_\tau$	$(0.5024 \pm 0.0310) \cdot 10^{-2}$	HFLAV Spring 2017 fit
$\Gamma_{76} = h^- h^- h^+ \geq 2\pi^0\, \nu_\tau\ (\text{ex.}K^0)$	$(0.4925 \pm 0.0310) \cdot 10^{-2}$	HFLAV Spring 2017 fit
$(0.4350 \pm 0.0461 \pm 0.0000) \cdot 10^{-2}$	ALEPH	[1344]
$\frac{\Gamma_{76}}{\Gamma_{54}} = \frac{h^- h^- h^+ 2\pi^0\, \nu_\tau\ (\text{ex.}K^0)}{h^- h^- h^+ \geq 0\,\text{neutrals} \geq 0 K_L^0\, \nu_\tau}$	$(3.237 \pm 0.202) \cdot 10^{-2}$	HFLAV Spring 2017 fit
$(3.400 \pm 0.200 \pm 0.300) \cdot 10^{-2}$	CLEO	[1382]
$\Gamma_{77} = h^- h^- h^+ 2\pi^0\, \nu_\tau\ (\text{ex.}K^0, \omega, \eta)$	$(9.759 \pm 3.550) \cdot 10^{-4}$	HFLAV Spring 2017 fit
$\Gamma_{78} = h^- h^- h^+ 3\pi^0\, \nu_\tau$	$(2.107 \pm 0.299) \cdot 10^{-4}$	HFLAV Spring 2017 fit
$(2.200 \pm 0.300 \pm 0.400) \cdot 10^{-4}$	CLEO	[1383]
$\Gamma_{79} = K^- h^- h^+ \geq 0\,\text{neutrals}\, \nu_\tau$	$(0.6297 \pm 0.0141) \cdot 10^{-2}$	HFLAV Spring 2017 fit

Table 304 continued

τ lepton branching fraction	Fit value/Exp.	HFLAV fit/Refs.
$\Gamma_{80} = K^-\pi^-h^+\nu_\tau$ (ex.K^0)	$(0.4363 \pm 0.0073) \cdot 10^{-2}$	HFLAV Spring 2017 fit
$\frac{\Gamma_{80}}{\Gamma_{60}} = \frac{K^-\pi^-h^+\nu_\tau\,(\mathrm{ex}.K^0)}{\pi^-\pi^+\pi^-\nu_\tau\,(\mathrm{ex}.K^0)}$	$(4.847 \pm 0.080) \cdot 10^{-2}$	HFLAV Spring 2017 fit
$(5.440 \pm 0.210 \pm 0.530) \cdot 10^{-2}$	CLEO	[1384]
$\Gamma_{81} = K^-\pi^-h^+\pi^0\,\nu_\tau$ (ex.K^0)	$(8.726 \pm 1.177) \cdot 10^{-4}$	HFLAV Spring 2017 fit
$\frac{\Gamma_{81}}{\Gamma_{69}} = \frac{K^-\pi^-h^+\pi^0\,\nu_\tau\,(\mathrm{ex}.K^0)}{\pi^-\pi^+\pi^-\pi^0\,\nu_\tau\,(\mathrm{ex}.K^0)}$	$(1.931 \pm 0.266) \cdot 10^{-2}$	HFLAV Spring 2017 fit
$(2.610 \pm 0.450 \pm 0.420) \cdot 10^{-2}$	CLEO	[1384]
$\Gamma_{82} = K^-\pi^-\pi^+ \geq 0$ neutrals ν_τ	$(0.4780 \pm 0.0137) \cdot 10^{-2}$	HFLAV Spring 2017 fit
$\left(0.5800^{+0.1500}_{-0.1300} \pm 0.1200\right) \cdot 10^{-2}$	TPC	[1385]
$\Gamma_{83} = K^-\pi^-\pi^+ \geq 0\pi^0\,\nu_\tau$ (ex.K^0)	$(0.3741 \pm 0.0135) \cdot 10^{-2}$	HFLAV Spring2017 fit
$\Gamma_{84} = K^-\pi^-\pi^+\nu_\tau$	$(0.3441 \pm 0.0070) \cdot 10^{-2}$	HFLAV Spring 2017 fit
$\Gamma_{85} = K^-\pi^+\pi^-\nu_\tau$ (ex.K^0)	$(0.2929 \pm 0.0067) \cdot 10^{-2}$	HFLAV Spring2017 fit
$(0.2140 \pm 0.0470 \pm 0.0000) \cdot 10^{-2}$	ALEPH	[1386]
$(0.2730 \pm 0.0020 \pm 0.0090) \cdot 10^{-2}$	BaBar	[1378]
$\left(0.3300 \pm 0.0010^{+0.0160}_{-0.0170}\right) \cdot 10^{-2}$	Belle	[1379]
$(0.3840 \pm 0.0140 \pm 0.0380) \cdot 10^{-2}$	CLE03	[1380]
$(0.4150 \pm 0.0530 \pm 0.0400) \cdot 10^{-2}$	OPAL	[1364]
$\frac{\Gamma_{85}}{\Gamma_{60}} = \frac{K^-\pi^+\pi^-\nu_\tau\,(\mathrm{ex}.K^0)}{\pi^-\pi^+\pi^-\nu_\tau\,(\mathrm{ex}.K^0)}$	$(3.254 \pm 0.074) \cdot 10^{-2}$	HFLAV Spring 2017 fit
$\Gamma_{87} = K^-\pi^-\pi^+\pi^0\,\nu_\tau$	$(0.1331 \pm 0.0119) \cdot 10^{-2}$	HFLAV Spring 2017 fit
$\Gamma_{88} = K^-\pi^-\pi^+\pi^0\,\nu_\tau$ (ex.K^0)	$(8.115 \pm 1.168) \cdot 10^{-4}$	HFLAV Spring 2017 fit
$(6.100 \pm 4.295 \pm 0.000) \cdot 10^{-4}$	ALEPH	[1386]
$(7.400 \pm 0.800 \pm 1.100) \cdot 10^{-4}$	CLE03	[1387]
$\Gamma_{89} = K^-\pi^-\pi^+\pi^0\,\nu_\tau$ (ex.K^0, η)	$(7.761 \pm 1.168) \cdot 10^{-4}$	HFLAV Spring 2017 fit
$\Gamma_{92} = \pi^-K^-K^+ \geq 0$ neutrals ν_τ	$(0.1495 \pm 0.0033) \cdot 10^{-2}$	HFLAV Spring 2017 fit
$(0.1590 \pm 0.0530 \pm 0.0200) \cdot 10^{-2}$	OPAL	[1388]
$\left(0.1500^{+0.0900}_{-0.0700} \pm 0.0300\right).10^{-2}$	TPC	[1385]
$\Gamma_{93} = \pi^-K^-K^+\nu_\tau$	$(0.1434 \pm 0.0027) \cdot 10^{-2}$	HFLAV Spring 2017 fit
$(0.1630 \pm 0.0270 \pm 0.0000) \cdot 10^{-2}$	ALEPH	[1386]
$(0.1346 \pm 0.0010 \pm 0.0036) \cdot 10^{-2}$	BaBar	[1378]
$\left(0.1550 \pm 0.0010^{+0.0060}_{-0.0050}\right).10^{-2}$	Belle	[1379]
$(0.1550 \pm 0.0060 \pm 0.0090) \cdot 10^{-2}$	CLE03	[1380]
$\frac{\Gamma_{93}}{\Gamma_{60}} = \frac{\pi^-K^-K^+\nu_\tau}{\pi^-\pi^+\pi^-\nu_\tau\,(\mathrm{ex}.K^0)}$	$(1.593 \pm 0.030) \cdot 10^{-2}$	HFLAV Spring2017 fit
$(1.600 \pm 0.150 \pm 0.300) \cdot 10^{-2}$	CLEO	[1384]
$\Gamma_{94} = \pi^-K^-K^+\pi^0\,\nu_\tau$	$(0.611 \pm 0.183) \cdot 10^{-4}$	HFLAV Spring 2017 fit
$(7.500 \pm 3.265 \pm 0.000) \cdot 10^{-4}$	ALEPH	[1386]
$(0.550 \pm 0.140 \pm 0.120) \cdot 10^{-4}$	CLE03	[1387]
$\frac{\Gamma_{94}}{\Gamma_{69}} = \frac{\pi^-K^-K^+\pi^0\,\nu_\tau}{\pi^-\pi^+\pi^-\pi^0\,\nu_\tau\,(\mathrm{ex}.K^0)}$	$(0.1353 \pm 0.0405) \cdot 10^{-2}$	HFLAV Spring 2017 fit
$(0.7900 \pm 0.4400 \pm 0.1600) \cdot 10^{-2}$	CLEO	[1384]
$\Gamma_{96} = K^-K^-K^+\nu_\tau$	$(2.174 \pm 0.800) \cdot 10^{-5}$	HFLAV Spring 2017 fit
$(1.578 \pm 0.130 \pm 0.123) \cdot 10^{-5}$	BaBar	[1378]
$\left(3.290 \pm 0.170^{+0.190}_{-0.200}\right).10^{-5}$	Belle	[1379]

Table 304 continued

τ lepton branching fraction	Fit value/Exp.	HFLAV fit/Refs.
$\Gamma_{102} = 3h^- 2h^+ \geq 0\,\text{neutrals}\,\nu_\tau\ \left(\text{ex. } K^0\right)$	$(0.0985 \pm 0.0037) \cdot 10^{-2}$	HFLAV Spring 2017 fit
$(0.0970 \pm 0.0050 \pm 0.0110) \cdot 10^{-2}$	CLEO	[1389]
$(0.1020 \pm 0.0290 \pm 0.0000) \cdot 10^{-2}$	HRS	[1390]
$(0.1700 \pm 0.0220 \pm 0.0260) \cdot 10^{-2}$	L3	[1375]
$\Gamma_{103} = 3h^- 2h^+ \nu_\tau\ \left(\text{ex.} K^0\right)$	$(8.216 \pm 0.316) \cdot 10^{-4}$	HFLAV Spring 2017 fit
$(7.200 \pm 1.500 \pm 0.000) \cdot 10^{-4}$	ALEPH	[1344]
$(6.400 \pm 2.300 \pm 1.000) \cdot 10^{-4}$	ARGUS	[1391]
$(7.700 \pm 0.500 \pm 0.900) \cdot 10^{-4}$	CLEO	[1389]
$(9.700 \pm 1.500 \pm 0.500) \cdot 10^{-4}$	DELPHI	[1355]
$(5.100 \pm 2.000 \pm 0.000) \cdot 10^{-4}$	HRS	[1390]
$(9.100 \pm 1.400 \pm 0.600) \cdot 10^{-4}$	OPAL	[1392]
$\Gamma_{104} = 3h^- 2h^+ \pi^0\,\nu_\tau\ \left(\text{ex. } K^0\right)$	$(1.634 \pm 0.114) \cdot 10^{-4}$	HFLAV Spring 2017 fit
$(2.100 \pm 0.700 \pm 0.900) \cdot 10^{-4}$	ALEPH	[1344]
$(1.700 \pm 0.200 \pm 0.200) \cdot 10^{-4}$	CLEO	[1383]
$(1.600 \pm 1.200 \pm 0.600) \cdot 10^{-4}$	DELPHI	[1355]
$(2.700 \pm 1.800 \pm 0.900) \cdot 10^{-4}$	OPAL	[1392]
$\Gamma_{106} = (5\pi)^-\,\nu_\tau$	$(0.7748 \pm 0.0534) \cdot 10^{-2}$	HFLAV Spring 2017 fit
$\Gamma_{110} = X_s^- \nu_\tau$	$(2.909 \pm 0.048) \cdot 10^{-2}$	HFLAV Spring 2017 fit
$\Gamma_{126} = \pi^- \pi^0\,\eta\nu_\tau$	$(0.1386 \pm 0.0072) \cdot 10^{-2}$	HFLAV Spring 2017 fit
$(0.1800 \pm 0.0447 \pm 0.0000) \cdot 10^{-2}$	ALEPH	[1393]
$(0.1350 \pm 0.0030 \pm 0.0070) \cdot 10^{-2}$	Belle	[1394]
$(0.1700 \pm 0.0200 \pm 0.0200) \cdot 10^{-2}$	CLEO	[1395]
$\Gamma_{128} = K^- \eta\nu_\tau$	$(1.547 \pm 0.080) \cdot 10^{-4}$	HFLAV Spring 2017 fit
$\left(2.900^{+1.300}_{-1.200} \pm 0.700\right) .10^{-4}$	ALEPH	[1393]
$(1.420 \pm 0.110 \pm 0.070) \cdot 10^{-4}$	BaBar	[1396]
$(1.580 \pm 0.050 \pm 0.090) \cdot 10^{-4}$	Belle	[1394]
$(2.600 \pm 0.500 \pm 0.500) \cdot 10^{-4}$	CLEO	[1397]
$\Gamma_{130} = K^- \pi^0\,\eta\nu_\tau$	$(0.483 \pm 0.116) \cdot 10^{-4}$	HFLAV Spring 2017 fit
$(0.460 \pm 0.110 \pm 0.040) \cdot 10^{-4}$	Belle	[1394]
$(1.770 \pm 0.560 \pm 0.710) \cdot 10^{-4}$	CLEO	[1398]
$\Gamma_{132} = \pi^- \bar{K}^0 \eta\nu_\tau$	$(0.937 \pm 0.149) \cdot 10^{-4}$	HFLAV Spring 2017 fit
$(0.880 \pm 0.140 \pm 0.060) \cdot 10^{-4}$	Belle	[1394]
$(2.200 \pm 0.700 \pm 0.220) \cdot 10^{-4}$	CLEO	[1398]
$\Gamma_{136} = \pi^- \pi^+ \pi^- \eta\nu_\tau\ \left(\text{ex. } K^0\right)$	$(2.184 \pm 0.130) \cdot 10^{-4}$	HFLAV Spring 2017 fit
$\Gamma_{149} = h^- \omega \geq 0\,\text{neutrals}\,\nu_\tau$	$(2.401 \pm 0.075) \cdot 10^{-2}$	HFLAV Spring 2017 fit
$\Gamma_{150} = h^- \omega\nu_\tau$	$(1.995 \pm 0.064) \cdot 10^{-2}$	HFLAV Spring 2017 fit
$(1.910 \pm 0.092 \pm 0.000) \cdot 10^{-2}$	ALEPH	[1393]
$(1.600 \pm 0.270 \pm 0.410) \cdot 10^{-2}$	CLEO	[1399]
$\frac{\Gamma_{150}}{\Gamma_{66}} = \frac{h^- \omega\nu_\tau}{h^- h^- h^+ \pi^0\,\nu_\tau\,(\text{ex. } K^0)}$	0.4332 ± 0.0139	HFLAV Spring 2017 fit
$0.4310 \pm 0.0330 \pm 0.0000$	ALEPH	[1400]
$0.4640 \pm 0.0160 \pm 0.0170$	CLEO	[1377]
$\Gamma_{151} = K^- \omega\nu_\tau$	$(4.100 \pm 0.922) \cdot 10^{-4}$	HFLAV Spring 2017 fit
$(4.100 \pm 0.600 \pm 0.700) \cdot 10^{-4}$	CLE03	[1387]
$\Gamma_{152} = h^- \pi^0\,\omega\nu_\tau$	$(0.4058 \pm 0.0419) \cdot 10^{-2}$	HFLAV Spring 2017 fit

Table 304 continued

τ lepton branching fraction	Fit value/Exp.	HFLAV fit/Refs.
$(0.4300 \pm 0.0781 \pm 0.0000) \cdot 10^{-2}$	ALEPH	[1393]
$\frac{\Gamma_{152}}{\Gamma_{54}} = \frac{h^-\omega\pi^0\nu_\tau}{h^-h^-h^+\geq 0\,\text{neutrals}\geq 0 K_L^0\nu_\tau}$	$(2.667 \pm 0.275) \cdot 10^{-2}$	HFLAV Spring 2017 fit
$\frac{\Gamma_{152}}{\Gamma_{76}} = \frac{h^-\omega\pi^0\nu_\tau}{h^-h^-h^+2\pi^0\nu_\tau\,(\text{ex. } K^0)}$	0.8241 ± 0.0757	HFLAV Spring 2017 fit
$0.8100 \pm 0.0600 \pm 0.0600$	CLEO	[1382]
$\Gamma_{167} = K^-\phi\nu_\tau$	$(4.445 \pm 1.636) \cdot 10^{-5}$	HFLAV Spring 2017 fit
$\Gamma_{168} = K^-\phi\nu_\tau(\phi \to K^+K^-)$	$(2.174 \pm 0.800) \cdot 10^{-5}$	HFLAV Spring 2017 fit
$\Gamma_{169} = K^-\phi\nu_\tau(\phi \to K_S^0K_L^0)$	$(1.520 \pm 0.560) \cdot 10^{-5}$	HFLAV Spring 2017 fit
$\Gamma_{800} = \pi^-\omega\nu_\tau$	$(1.954 \pm 0.065) \cdot 10^{-2}$	HFLAV Spring 2017 fit
$\Gamma_{802} = K^-\pi^-\pi^+\nu_\tau\,(\text{ex. } K^0, \omega)$	$(0.2923 \pm 0.0067) \cdot 10^{-2}$	HFLAV Spring 2017 fit
$\Gamma_{803} = K^-\pi^-\pi^+\pi^0\,\nu_\tau\,(\text{ex. } K^0, \omega, \eta)$	$(4.103 \pm 1.429) \cdot 10^{-4}$	HFLAV Spring 2017 fit
$\Gamma_{804} = \pi^-K_L^0K_L^0\nu_\tau$	$(2.332 \pm 0.065) \cdot 10^{-4}$	HFLAV Spring 2017 fit
$\Gamma_{805} = a_1^-(\to \pi^-\gamma)\nu_\tau$	$(4.000 \pm 2.000) \cdot 10^{-4}$	HFLAV Spring 2017 fit
$(4.000 \pm 2.000 \pm 0.000) \cdot 10^{-4}$	ALEPH	[1344]
$\Gamma_{806} = \pi^-\pi^0\,K_L^0K_L^0\nu_\tau$	$(1.815 \pm 0.207) \cdot 10^{-5}$	HFLAV Spring 2017 fit
$\Gamma_{810} = 2\pi^-\pi^+3\pi^0\,\nu_\tau\,(\text{ex. } K^0)$	$(1.924 \pm 0.298) \cdot 10^{-4}$	HFLAV Spring 2017 fit
$\Gamma_{811} = \pi^-2\pi^0\,\omega\nu_\tau\,(\text{ex. } K^0)$	$(7.105 \pm 1.586) \cdot 10^{-5}$	HFLAV Spring 2017 fit
$(7.300 \pm 1.200 \pm 1.200) \cdot 10^{-5}$	BaBar	[1401]
$\Gamma_{812} = 2\pi^-\pi^+3\pi^0\,\nu_\tau\,(\text{ex. } K^0, \eta, \omega, f_1)$	$(1.344 \pm 2.683) \cdot 10^{-5}$	HFLAV Spring 2017 fit
$(1.000 \pm 0.800 \pm 3.000) \cdot 10^{-5}$	BaBar	[1401]
$\Gamma_{820} = 3\pi^-2\pi^+\nu_\tau\,(\text{ex. } K^0, \omega)$	$(8.197 \pm 0.315) \cdot 10^{-4}$	HFLAV Spring 2017 fit
$\Gamma_{821} = 3\pi^-2\pi^+\nu_\tau\,(\text{ex. } K^0, \omega, f_1)$	$(7.677 \pm 0.297) \cdot 10^{-4}$	HFLAV Spring 2017 fit
$(7.680 \pm 0.040 \pm 0.400) \cdot 10^{-4}$	BaBar	[1401]
$\Gamma_{822} = K^-2\pi^-2\pi^+\nu_\tau\,(\text{ex. } K^0)$	$(0.596 \pm 1.208) \cdot 10^{-6}$	HFLAV Spring 2017 fit
$(0.600 \pm 0.500 \pm 1.100) \cdot 10^{-6}$	BaBar	[1401]
$\Gamma_{830} = 3\pi^-2\pi^+\pi^0\,\nu_\tau\,(\text{ex. } K^0)$	$(1.623 \pm 0.114) \cdot 10^{-4}$	HFLAV Spring 2017 fit
$\Gamma_{831} = 2\pi^-\pi^+\omega\nu_\tau\,(\text{ex. } K^0)$	$(8.359 \pm 0.626) \cdot 10^{-5}$	HFLAV Spring2017 fit
$(8.400 \pm 0.400 \pm 0.600) \cdot 10^{-5}$	BaBar	[1401]
$\Gamma_{832} = 3\pi^-2\pi^+\pi^0\,\nu_\tau\,(\text{ex. } K^0, \eta, \omega, f_1)$	$(3.771 \pm 0.875) \cdot 10^{-5}$	HFLAV Spring 2017 fit
$(3.600 \pm 0.300 \pm 0.900) \cdot 10^{-5}$	BaBar	[1401]
$\Gamma_{833} = K^-2\pi^-2\pi^+\pi^0\,\nu_\tau\,(\text{ex. } K^0)$	$(1.108 \pm 0.566) \cdot 10^{-6}$	HFLAV Spring 2017 fit
$(1.100 \pm 0.400 \pm 0.400) \cdot 10^{-6}$	BaBar	[1401]
$\Gamma_{910} = 2\pi^-\pi^+\eta\nu_\tau\,\left(\eta \to 3\pi^0\right)\,(\text{ex. } K^0)$	$(7.136 \pm 0.424) \cdot 10^{-5}$	HFLAV Spring 2017 fit
$(8.270 \pm 0.880 \pm 0.810) \cdot 10^{-5}$	BaBar	[1401]
$\Gamma_{911} = \pi^-2\pi^0\,\eta\nu_\tau\,\left(\eta \to \pi^+\pi^-\pi^0\right)\,\left(\text{ex. } K^0\right)$	$(4.420 \pm 0.867) \cdot 10^{-5}$	HFLAV Spring 2017 fit
$(4.570 \pm 0.770 \pm 0.500) \cdot 10^{-5}$	BaBar	[1401]
$\Gamma_{920} = \pi^-f_1\nu_\tau(f_1 \to 2\pi^-2\pi^+)$	$(5.197 \pm 0.444) \cdot 10^{-5}$	HFLAV Spring 2017 fit
$(5.200 \pm 0.310 \pm 0.370) \cdot 10^{-5}$	BaBar	[1401]
$\Gamma_{930} = 2\pi^-\pi^+\eta\nu_\tau(\eta \to \pi^+\pi^-\pi^0)\,(\text{ex. } K^0)$	$(5.005 \pm 0.297) \cdot 10^{-5}$	HFLAV Spring 2017 fit
$(5.390 \pm 0.270 \pm 0.410) \cdot 10^{-5}$	BaBar	[1401]
$\Gamma_{944} = 2\pi^-\pi^+\eta\nu_\tau(\eta \to \gamma\gamma)\,(\text{ex. } K^0)$	$(8.606 \pm 0.511) \cdot 10^{-5}$	HFLAV Spring 2017 fit
$(8.260 \pm 0.350 \pm 0.510) \cdot 10^{-5}$	BaBar	[1401]
$\Gamma_{945} = \pi^-2\pi^0\,\eta\nu_\tau$	$(1.929 \pm 0.378) \cdot 10^{-4}$	HFLAV Spring 2017 fit
$\Gamma_{998} = 1 - \Gamma_{\text{ALL}}$	$(0.0355 \pm 0.1031) \cdot 10^{-2}$	HFLAV Spring 2017 fit

sions multiplied by the Lagrange multipliers λ_r, one for each constraint:

$$\min\left[(A_{ik}q_k - x_i)^t V_{ij}^{-1}(A_{jl}q_l - x_j) + 2\lambda_r(f_r(q_s) - c_r)\right] \tag{288}$$

$$(\partial/\partial q_k, \partial/\partial\lambda_r)\,[\text{expression above}] = 0. \tag{289}$$

Equation (289) defines a set of equations for the vector of the unknowns (q_k, λ_r), some of which may be non-linear, in case of non-linear constraints. An iterative minimization procedure approximates at each step the non-linear constraint expressions by their first order Taylor expansion around the current values of the fitted quantities, $\bar{q}_s$:

$$f_r(q_s) - c_r \simeq f_r(\bar{q}_s) + \left.\frac{\partial f_r(q_s)}{\partial q_s}\right|_{\bar{q}_s}(q_s - \bar{q}_s) - c_r, \tag{290}$$

which can be written as

$$B_{rs}q_s - c'_r, \tag{291}$$

where c'_r are the resulting constant known terms, independent of q_s at first order. After linearization, the differentiation by q_k and λ_r is trivial and leads to a set of linear equations

$$A^t_{ki}V^{-1}_{ij}A_{jl}q_l + B^t_{kr}\lambda_r = A^t_{ki}V^{-1}_{ij}x_j \tag{292}$$

$$B_{rs}q_s = c'_r, \tag{293}$$

which can be expressed as:

$$F_{ij}u_j = v_i, \tag{294}$$

where $u_j = (q_k, \lambda_r)$ and v_i is the vector of the known constant terms running over the index k and then r in the right terms of Eqs. (292) and (293). Solving the equation set in Eq. (294) gives the fitted quantities and their covariance matrix, using the measurements and their covariance matrix.

The fit procedure starts by computing the linear approximation of the non-linear constraint expressions around the quantities seed values. With an iterative procedure, the unknowns are updated at each step by solving the equations and the equations are then linearized around the updated values, until the RMS average of relative variation of the fitted unknowns is reduced below 10^{-12}.

9.1.2 Fit results

The fit output consists of 135 fitted quantities that correspond to either branching fractions or ratios of branching fractions. The fitted quantities values and uncertainties are listed in Table 304. The off-diagonal statistical correlation terms between a subset of 47 "basis quantities" are listed in Sect. 9.1.6. All the remaining statistical correlation terms can be obtained using the constraint equations listed in Table 304 and Sect. 9.1.7.

The fit has $\chi^2/\text{d.o.f.} = 137/123$, corresponding to a confidence level CL = 17.84%. We use a total of 170 measurements to fit the above mentioned 135 quantities subjected to 88 constraints. Although the unitarity constraint is not applied, the fit is statistically consistent with unitarity, where the residual is $\Gamma_{998} = 1 - \Gamma_{\text{All}} = (0.0355 \pm 0.1031) \cdot 10^{-2}$.

A scale factor of 5.44 (as in the three previous reports [5, 234,420]) has been applied to the published uncertainties of the two severely inconsistent measurements of $\Gamma_{96} = \tau \to KKK\nu$ by BABAR and Belle. The scale factor has been determined using the PDG procedure, i.e., to the proper size in order to obtain a reduced χ^2 equal to 1 when fitting just the two Γ_{96} measurements.

For several old results, for historical reasons, the table reports the total error (statistical plus systematic) in the position of the statistical error and zero in the position of the systematic error. Since the fit depends only on the total errors, the results are unaffected.

9.1.3 Changes with respect to the previous report

The following changes have been introduced with respect to the previous HFLAV report [5].

Two old preliminary results have been removed:

- $\Gamma_{35} = B(\tau \to \pi K_S \nu)$, BABAR [1340],
- $\Gamma_{40} = B(\tau \to \pi K_S \pi^0 \nu)$, BABAR [1341].

They were announced in 2008 and 2009 but have not been published.

In the 2014 report, for several BABAR and Belle experimental results we used more precise numerical values than the published ones, using internal information from the Collaborations. We revert to the published figures in this report, as the improvements in the fit results were negligible. In so doing, we use in this report the same values that are used in the PDG 2016 fit.

The Belle result on $\tau^- \to K^0_S(\text{particles})^-\nu_\tau$ [1342] has been discarded, because it was determined that the published information does not permit a reliable determination of the correlations with the other results in the same paper. The correlations estimated for the HFLAV 2014 report were inconsistent. As a result, both the covariance matrix of the Belle results and the overall correlation matrix for the branching ratio fit results were non-positive-definite. It has been found that the inconsistency had negligible impact on lepton universality tests and on the $|V_{us}|$ measurements.

The ALEPH result on $\Gamma_{46}(\tau^- \to \pi^- K^0 \bar{K}^0 \nu_\tau)$ [1329] has been removed from the fit inputs, since it is simply the sum of twice $\Gamma_{47} = \pi^- K^0_S K^0_S \nu_\tau$ and $\Gamma_{48} = \pi^- K^0_S K^0_L \nu_\tau$ from the same paper, hence 100% correlated with them.

Several minor corrections have been applied to the constraints. The list of constraints included in the following fully documents the changes when compared with the same list in the 2014 edition. In some cases the relation equating one decay mode to a sum of modes included some minor terms that did not match the mode definitions. In other cases, the sum included modes with overlapping components. The effects on the 2014 fit results have been found to be modest with respect to the quoted uncertainties. For instance, the definition of the total branching fraction has been updated as follows:

$$\begin{aligned}\Gamma_{\text{All}} = {} & \Gamma_3 + \Gamma_5 + \Gamma_9 + \Gamma_{10} + \Gamma_{14} + \Gamma_{16} + \Gamma_{20} + \Gamma_{23} \\ & + \Gamma_{27} + \Gamma_{28} + \Gamma_{30} + \Gamma_{35} + \Gamma_{37} + \Gamma_{40} + \Gamma_{42} \\ & + \Gamma_{47} \cdot (1 + ((\Gamma_{<K^0|K_L>} \cdot \Gamma_{<\bar{K}^0|K_L>})/(\Gamma_{<K^0|K_S>} \\ & \cdot \Gamma_{<\bar{K}^0|K_S>}))) + \Gamma_{48} + \Gamma_{62} \\ & + \Gamma_{70} + \Gamma_{77} + \Gamma_{811} + \Gamma_{812} + \Gamma_{93} \\ & + \Gamma_{94} + \Gamma_{832} + \Gamma_{833} + \Gamma_{126} + \Gamma_{128} + \Gamma_{802} + \Gamma_{803} \\ & + \Gamma_{800} + \Gamma_{151} + \Gamma_{130} + \Gamma_{132} + \Gamma_{44} + \Gamma_{53} \\ & + \Gamma_{50} \cdot (1 + ((\Gamma_{<K^0|K_L>} \cdot \Gamma_{<\bar{K}^0|K_L>})/(\Gamma_{<K^0|K_S>} \\ & \cdot \Gamma_{<\bar{K}^0|K_S>}))) + \Gamma_{51} \\ & + \Gamma_{167} \cdot (\Gamma_{\phi \to K^+K^-} + \Gamma_{\phi \to K_S K_L}) + \Gamma_{152} + \Gamma_{920} \\ & + \Gamma_{821} + \Gamma_{822} + \Gamma_{831} + \Gamma_{136} + \Gamma_{945} + \Gamma_{805}\end{aligned}$$

In the 2014 definition, the term $\Gamma_{78} = h^- h^- h^+ 3\pi^0 \nu_\tau$ included the contributions of $\Gamma_{50} = \pi^- \pi^0 K^0_S K^0_S \nu_\tau$ and $\Gamma_{132} = \pi^- \bar{K}^0 \eta \nu_\tau$, which were already included explicitly in Γ_{All}. In the present definition, Γ_{78} has been replaced with modes whose sum corresponds to

$$\Gamma_{810} = 2\pi^- \pi^+ 3\pi^0 \nu_\tau \text{ (ex. } K^0)$$

As in 2014, the total τ branching fraction Γ_{All} definition includes two modes that have overlapping final states, to a minor extent, which we consider negligible:

$$\begin{aligned}\Gamma_{50} &= \pi^- \pi^0 K^0_S K^0_S \nu_\tau \\ \Gamma_{132} &= \pi^- \bar{K}^0 \eta \nu_\tau.\end{aligned}$$

Finally, we updated to the PDG 2015 results [327] all the parameters corresponding to the measurements' systematic biases and uncertainties and all the parameters appearing in the constraint equations in Sect. 9.1.7 and Table 304.

9.1.4 Differences between the HFLAV Spring 2017 fit and the PDG 2016 fit

As is standard for the PDG branching fraction fits, the PDG 2016 τ branching fraction fit is unitarity constrained, while the HFLAV 2016 fit is unconstrained.

The HFLAV-Tau fit uses the ALEPH measurements of branching fractions defined according to the final state content of "hadrons" and kaons, where a "hadron" corresponds to either a pion or a kaon, since this set of results is closer to the actual experimental measurements and facilitates a more comprehensive treatment of the experimental results correlations [420]. The PDG 2016 fit on the other hand continues to use – as in the past editions – the ALEPH measurements of modes with pions and kaons, which correspond to the final set of published measurements of the collaboration. It is planned eventually to update the PDG fit to use the same ALEPH measurement set that is used by HFLAV.

The HFLAV Spring 2017 fit, as in 2014, uses the ALEPH estimate for $\Gamma_{805} = B(\tau \to a_1^-(\to \pi^- \gamma)\nu_\tau)$, which is not a direct measurement. The PDG 2016 fit uses the PDG average of $B(a_1 \to \pi\gamma)$ as a parameter and defines $\Gamma_{805} = B(a_1 \to \pi\gamma) \times B(\tau \to 3\pi\nu)$. As a consequence, the PDG fit procedure does not take into account the large uncertainty on $B(a_1 \to \pi\gamma)$, resulting in an underestimated fit uncertainty on Γ_{805}. Therefore, in this case an appropriate correction has to be applied after the fit.

9.1.5 Branching ratio fit results and experimental inputs

Table 304 reports the τ branching ratio fit results and experimental inputs.

9.1.6 Correlation terms between basis branching fractions uncertainties

The following tables report the correlation coefficients between basis quantities, in percent (Tables 305, 306, 307, 308, 309, 310, 311, 312, 313, 314).

9.1.7 Equality constraints

We list in the following the equality constraints that relate a branching fraction to a sum of branching fractions. The constraint equations include as coefficients the values of some non-tau branching fractions, denoted e.g., with the self-describing notation $\Gamma_{K_S \to \pi^0 \pi^0}$. Some coefficients are probabilities corresponding to modulus square amplitudes describing quantum mixtures of states such as K^0, $\bar{K}^0$, K_S, K_L, denoted with e.g., $\Gamma_{<K^0|K_S>} = |<K^0|K_S>|^2$. All non-tau quantities are taken from the PDG 2015 [327] fits (when available) or averages, and are used without accounting for

Table 305 Basis quantities correlation coefficients in percent, subtable 1

Γ_5	23													
Γ_9	7	5												
Γ_{10}	3	5	1											
Γ_{14}	−13	−14	−12	−3										
Γ_{16}	0	−1	2	−1	−16									
Γ_{20}	−5	−5	−7	−1	−40	2								
Γ_{23}	0	0	0	−2	2	−13	−22							
Γ_{27}	−4	−3	−8	−1	0	3	−36	6						
Γ_{28}	0	0	0	−2	2	−13	5	−21	−29					
Γ_{30}	−5	−4	−11	−2	−9	0	6	0	−42	0				
Γ_{35}	0	0	0	0	0	0	0	1	0	1	0			
Γ_{37}	0	0	0	0	0	−2	1	−3	1	−3	0	−22		
Γ_{40}	0	0	0	0	0	1	0	1	−2	1	0	−12	4	
	Γ_3	Γ_5	Γ_9	Γ_{10}	Γ_{14}	Γ_{16}	Γ_{20}	Γ_{23}	Γ_{27}	Γ_{28}	Γ_{30}	Γ_{35}	Γ_{37}	Γ_{40}

Table 306 Basis quantities correlation coefficients in percent, subtable 2

Γ_{42}	0	0	0	0	1	−3	1	−5	1	−5	0	2	−21	−20
Γ_{44}	0	0	0	0	0	0	0	0	0	0	0	−1	0	−4
Γ_{47}	0	0	0	0	0	0	0	0	0	0	0	−1	1	−4
Γ_{48}	0	0	0	0	0	0	0	0	0	0	0	−3	0	−2
Γ_{50}	0	0	0	0	0	0	0	−1	0	−1	0	0	7	0
Γ_{51}	0	0	0	0	0	0	0	0	0	0	0	−1	0	−1
Γ_{53}	0	0	0	0	0	0	0	0	0	0	0	0	0	0
Γ_{62}	−3	−5	8	0	−4	5	−7	−1	−5	−1	−5	0	0	0
Γ_{70}	−6	−6	−7	−1	−8	−1	−1	0	−1	0	3	0	0	0
Γ_{77}	−1	0	−3	−1	−2	0	0	0	2	0	2	0	0	0
Γ_{93}	−1	−1	3	0	−1	2	−1	0	−1	0	−1	0	0	0
Γ_{94}	0	0	0	0	0	0	0	0	0	0	0	0	0	0
Γ_{126}	0	0	0	0	0	0	−1	0	0	0	−2	0	0	0
Γ_{128}	0	0	1	0	0	1	0	−1	0	−1	0	0	0	0
	Γ_3	Γ_5	Γ_9	Γ_{10}	Γ_{14}	Γ_{16}	Γ_{20}	Γ_{23}	Γ_{27}	Γ_{28}	Γ_{30}	Γ_{35}	Γ_{37}	Γ_{40}

Table 307 Basis quantities correlation coefficients in percent, subtable 3

Γ_{130}	0	0	0	0	0	0	0	0	0	0	0	0	0	0
Γ_{132}	0	0	0	0	0	0	0	0	0	0	0	0	0	0
Γ_{136}	0	0	0	0	0	0	0	0	0	0	0	0	0	0
Γ_{151}	0	0	0	0	0	0	0	0	0	0	0	0	0	0
Γ_{152}	−1	0	−3	−1	−2	0	−1	0	2	0	2	0	0	0
Γ_{167}	0	0	0	0	0	0	0	0	0	0	0	0	0	0
Γ_{800}	−2	−2	−2	0	−3	0	0	0	0	0	1	0	0	0
Γ_{802}	−1	−1	0	0	−1	0	−2	0	−2	0	−1	0	0	0
Γ_{803}	0	0	0	0	0	0	0	0	0	0	0	0	0	0
Γ_{805}	0	0	0	0	0	0	0	0	0	0	0	0	0	0
Γ_{811}	0	0	0	0	0	0	0	0	0	0	0	0	0	0
Γ_{812}	0	1	0	0	0	0	0	0	0	0	0	0	0	0
Γ_{821}	0	0	1	0	0	0	−1	0	0	0	−1	0	0	0
Γ_{822}	0	0	0	0	0	0	0	0	0	0	0	0	0	0
	Γ_3	Γ_5	Γ_9	Γ_{10}	Γ_{14}	Γ_{16}	Γ_{20}	Γ_{23}	Γ_{27}	Γ_{28}	Γ_{30}	Γ_{35}	Γ_{37}	Γ_{40}

Table 308 Basis quantities correlation coefficients in percent, subtable 4

Γ_{831}	0	0	0	0	0	0	0	0	0	0	0	0	0	0
Γ_{832}	0	0	0	0	0	0	0	0	0	0	0	0	0	0
Γ_{833}	0	0	0	0	0	0	0	0	0	0	0	0	0	0
Γ_{920}	0	0	0	0	0	0	0	0	0	0	0	0	0	0
Γ_{945}	0	0	0	0	0	0	0	0	0	0	0	0	0	0
	Γ_{3}	Γ_{5}	Γ_{9}	Γ_{10}	Γ_{14}	Γ_{16}	Γ_{20}	Γ_{23}	Γ_{27}	Γ_{28}	Γ_{30}	Γ_{35}	Γ_{37}	Γ_{40}

Table 309 Basis quantities correlation coefficients in percent, subtable 5

Γ_{44}	0													
Γ_{47}	1	0												
Γ_{48}	−1	−6	0											
Γ_{50}	5	0	−7	0										
Γ_{51}	0	−3	0	−6	0									
Γ_{53}	0	0	0	0	0	0								
Γ_{62}	0	0	1	0	0	0	0							
Γ_{70}	0	0	0	0	0	0	0	−20						
Γ_{77}	0	0	0	0	0	0	0	−1	−7					
Γ_{93}	0	0	0	0	0	0	0	14	−4	0				
Γ_{94}	0	0	0	0	0	0	0	0	−2	0	0			
Γ_{126}	0	0	1	0	0	0	0	1	0	−5	0	0		
Γ_{128}	0	0	1	0	0	0	0	2	0	0	1	0	4	
	Γ_{42}	Γ_{44}	Γ_{47}	Γ_{48}	Γ_{50}	Γ_{51}	Γ_{53}	Γ_{62}	Γ_{70}	Γ_{77}	Γ_{93}	Γ_{94}	Γ_{126}	Γ_{128}

Table 310 Basis quantities correlation coefficients in percent, subtable 6

Γ_{130}	0	0	0	0	0	0	0	0	0	−1	0	0	1	1
Γ_{132}	0	0	0	0	0	0	0	0	0	0	0	0	2	1
Γ_{136}	0	0	0	0	0	0	0	0	−1	0	0	0	0	0
Γ_{151}	0	0	0	0	0	0	0	0	12	0	0	0	0	0
Γ_{152}	0	0	0	0	0	0	0	−1	−11	−64	0	0	0	0
Γ_{167}	0	0	0	0	0	0	0	−1	0	0	1	0	0	0
Γ_{800}	0	0	0	0	0	0	0	−8	−69	−2	−1	0	0	0
Γ_{802}	0	0	0	0	0	0	0	16	−6	0	0	0	0	0
Γ_{803}	0	0	0	0	0	0	0	−1	−19	0	0	−2	0	−1
Γ_{805}	0	0	0	0	0	0	0	0	0	0	0	0	0	0
Γ_{811}	0	0	0	0	0	0	0	0	0	0	0	0	0	0
Γ_{812}	0	0	0	0	−1	0	0	0	−1	0	0	0	0	0
Γ_{821}	0	0	0	0	0	0	0	0	−1	0	0	0	0	0
Γ_{822}	0	0	0	0	0	0	0	0	0	0	0	0	0	0
	Γ_{42}	Γ_{44}	Γ_{47}	Γ_{48}	Γ_{50}	Γ_{51}	Γ_{53}	Γ_{62}	Γ_{70}	Γ_{77}	Γ_{93}	Γ_{94}	Γ_{126}	Γ_{128}

Table 311 Basis quantities correlation coefficients in percent, subtable 7

Γ_{831}	0	0	0	0	0	0	0	0	0	0	0	0	0	0
Γ_{832}	0	0	0	0	0	0	0	0	0	0	0	0	0	0
Γ_{833}	0	0	0	0	0	0	0	0	0	0	0	0	0	0
Γ_{920}	0	0	0	0	0	0	0	0	0	0	0	0	0	0
Γ_{945}	0	0	0	0	0	0	0	0	0	0	0	0	0	0
	Γ_{42}	Γ_{44}	Γ_{47}	Γ_{48}	Γ_{50}	Γ_{51}	Γ_{53}	Γ_{62}	Γ_{70}	Γ_{77}	Γ_{93}	Γ_{94}	Γ_{126}	Γ_{128}

Table 312 Basis quantities correlation coefficients in percent, subtable 8

Γ_{132}	0													
Γ_{136}	0	0												
Γ_{151}	0	0	0											
Γ_{152}	0	0	0	0										
Γ_{167}	0	0	0	0	0									
Γ_{800}	0	0	0	−14	−3	0								
Γ_{802}	0	0	0	−2	0	1	−1							
Γ_{803}	0	0	0	−58	0	0	9	1						
Γ_{805}	0	0	0	0	0	0	0	0	0					
Γ_{811}	0	−1	20	0	0	0	0	0	0	0				
Γ_{812}	0	−2	−8	0	0	0	0	0	0	0	−16			
Γ_{821}	0	0	47	0	0	0	0	0	0	0	8	−4		
Γ_{822}	0	0	−1	0	0	0	0	0	0	0	0	0	−1	
	Γ_{130}	Γ_{132}	Γ_{136}	Γ_{151}	Γ_{152}	Γ_{167}	Γ_{800}	Γ_{802}	Γ_{803}	Γ_{805}	Γ_{811}	Γ_{812}	Γ_{821}	Γ_{822}

Table 313 Basis quantities correlation coefficients in percent, subtable 9

Γ_{831}	0	0	39	0	0	0	0	0	0	0	14	−4	39	−1
Γ_{832}	0	0	3	0	0	0	0	0	0	0	2	0	3	0
Γ_{833}	0	0	−1	0	0	0	0	0	0	0	0	0	−1	0
Γ_{920}	0	0	21	0	0	0	0	0	0	0	3	−2	35	−1
Γ_{945}	0	−1	25	0	0	0	0	0	0	0	10	−11	10	0
	Γ_{130}	Γ_{132}	Γ_{136}	Γ_{151}	Γ_{152}	Γ_{167}	Γ_{800}	Γ_{802}	Γ_{803}	Γ_{805}	Γ_{811}	Γ_{812}	Γ_{821}	Γ_{822}

Table 314 Basis quantities correlation coefficients in percent, subtable 10

Γ_{832}	−2				
Γ_{833}	−1	−1			
Γ_{920}	17	1	0		
Γ_{945}	17	2	0	4	
	Γ_{831}	Γ_{832}	Γ_{833}	Γ_{920}	Γ_{945}

their uncertainties, which are however in general small with respect to the uncertainties on the τ branching fractions.

The following list does not include the constraints listed in Table 304, where some measured ratios of branching fractions are expressed as ratios of two branching fractions.

$$
\begin{aligned}
\Gamma_1 = {} & \Gamma_3 + \Gamma_5 + \Gamma_9 + \Gamma_{10} + \Gamma_{14} + \Gamma_{16} \\
& + \Gamma_{20} + \Gamma_{23} + \Gamma_{27} + \Gamma_{28} + \Gamma_{30} + \Gamma_{35} \\
& + \Gamma_{40} + \Gamma_{44} + \Gamma_{37} + \Gamma_{42} + \Gamma_{47} + \Gamma_{48} \\
& + \Gamma_{804} + \Gamma_{50} + \Gamma_{51} + \Gamma_{806} + \Gamma_{126} \cdot \Gamma_{\eta\to\text{neutral}} \\
& + \Gamma_{128} \cdot \Gamma_{\eta\to\text{neutral}} + \Gamma_{130} \cdot \Gamma_{\eta\to\text{neutral}} \\
& + \Gamma_{132} \cdot \Gamma_{\eta\to\text{neutral}} + \Gamma_{800} \cdot \Gamma_{\omega\to\pi^0\gamma} \\
& + \Gamma_{151} \cdot \Gamma_{\omega\to\pi^0\gamma} + \Gamma_{152} \cdot \Gamma_{\omega\to\pi^0\gamma} \\
& + \Gamma_{167} \cdot \Gamma_{\phi\to K_S K_L}
\end{aligned}
$$

$$
\begin{aligned}
\Gamma_2 = {} & \Gamma_3 + \Gamma_5 \\
& + \Gamma_9 + \Gamma_{10} + \Gamma_{14} + \Gamma_{16} \\
& + \Gamma_{20} + \Gamma_{23} + \Gamma_{27} + \Gamma_{28} + \Gamma_{30} \\
& + \Gamma_{35} \cdot (\Gamma_{<\bar{K}^0|K_S>} \cdot \Gamma_{K_S\to\pi^0\pi^0} \\
& + \Gamma_{<\bar{K}^0|K_L>}) + \Gamma_{40} \cdot (\Gamma_{<\bar{K}^0|K_S>} \cdot \Gamma_{K_S\to\pi^0\pi^0} \\
& + \Gamma_{<\bar{K}^0|K_L>}) + \Gamma_{44} \cdot (\Gamma_{<\bar{K}^0|K_S>} \cdot \Gamma_{K_S\to\pi^0\pi^0} \\
& + \Gamma_{<\bar{K}^0|K_L>}) + \Gamma_{37} \cdot (\Gamma_{<\bar{K}^0|K_S>} \cdot \Gamma_{K_S\to\pi^0\pi^0} \\
& + \Gamma_{<\bar{K}^0|K_L>}) + \Gamma_{42} \cdot (\Gamma_{<\bar{K}^0|K_S>} \cdot \Gamma_{K_S\to\pi^0\pi^0} \\
& + \Gamma_{<\bar{K}^0|K_L>}) + \Gamma_{47} \cdot (\Gamma_{K_S\to\pi^0\pi^0} \cdot \Gamma_{K_S\to\pi^0\pi^0}) \\
& + \Gamma_{48} \cdot \Gamma_{K_S\to\pi^0\pi^0} + \Gamma_{804} \\
& + \Gamma_{50} \cdot (\Gamma_{K_S\to\pi^0\pi^0} \cdot \Gamma_{K_S\to\pi^0\pi^0}) + \Gamma_{51} \cdot \Gamma_{K_S\to\pi^0\pi^0} \\
& + \Gamma_{806} + \Gamma_{126} \cdot \Gamma_{\eta\to\text{neutral}} + \Gamma_{128} \cdot \Gamma_{\eta\to\text{neutral}} \\
& + \Gamma_{130} \cdot \Gamma_{\eta\to\text{neutral}} \\
& + \Gamma_{132} \cdot (\Gamma_{\eta\to\text{neutral}} \cdot (\Gamma_{<\bar{K}^0|K_S>} \cdot \Gamma_{K_S\to\pi^0\pi^0} \\
& + \Gamma_{<\bar{K}^0|K_L>})) + \Gamma_{800} \cdot \Gamma_{\omega\to\pi^0\gamma} \\
& + \Gamma_{151} \cdot \Gamma_{\omega\to\pi^0\gamma} + \Gamma_{152} \cdot \Gamma_{\omega\to\pi^0\gamma} \\
& + \Gamma_{167} \cdot (\Gamma_{\phi\to K_S K_L} \cdot \Gamma_{K_S\to\pi^0\pi^0})
\end{aligned}
$$

$$
\begin{aligned}
\Gamma_7 = {} & \Gamma_{35} \cdot \Gamma_{<\bar{K}^0|K_L>} + \Gamma_9 + \Gamma_{804} + \Gamma_{37} \cdot \Gamma_{<K^0|K_L>} \\
& + \Gamma_{10}
\end{aligned}
$$

$$\Gamma_8 = \Gamma_9 + \Gamma_{10}$$

$$\begin{aligned}\Gamma_{11} =& \Gamma_{14} + \Gamma_{16} + \Gamma_{20} + \Gamma_{23} + \Gamma_{27} + \Gamma_{28} \\ &+ \Gamma_{30} + \Gamma_{35} \cdot (\Gamma_{<K^0|K_S>} \cdot \Gamma_{K_S\to\pi^0\pi^0}) \\ &+ \Gamma_{37} \cdot (\Gamma_{<K^0|K_S>} \cdot \Gamma_{K_S\to\pi^0\pi^0}) \\ &+ \Gamma_{40} \cdot (\Gamma_{<K^0|K_S>} \cdot \Gamma_{K_S\to\pi^0\pi^0}) \\ &+ \Gamma_{42} \cdot (\Gamma_{<K^0|K_S>} \cdot \Gamma_{K_S\to\pi^0\pi^0}) \\ &+ \Gamma_{47} \cdot (\Gamma_{K_S\to\pi^0\pi^0} \cdot \Gamma_{K_S\to\pi^0\pi^0}) \\ &+ \Gamma_{50} \cdot (\Gamma_{K_S\to\pi^0\pi^0} \cdot \Gamma_{K_S\to\pi^0\pi^0}) \\ &+ \Gamma_{126} \cdot \Gamma_{\eta\to\text{neutral}} + \Gamma_{128} \cdot \Gamma_{\eta\to\text{neutral}} \\ &+ \Gamma_{130} \cdot \Gamma_{\eta\to\text{neutral}} \\ &+ \Gamma_{132} \cdot (\Gamma_{<K^0|K_S>} \cdot \Gamma_{K_S\to\pi^0\pi^0} \cdot \Gamma_{\eta\to\text{neutral}}) \\ &+ \Gamma_{151} \cdot \Gamma_{\omega\to\pi^0\gamma} \\ &+ \Gamma_{152} \cdot \Gamma_{\omega\to\pi^0\gamma} + \Gamma_{800} \cdot \Gamma_{\omega\to\pi^0\gamma}\end{aligned}$$

$$\begin{aligned}\Gamma_{12} =& \Gamma_{128} \cdot \Gamma_{\eta\to3\pi^0} + \Gamma_{30} + \Gamma_{23} + \Gamma_{28} + \Gamma_{14} \\ &+ \Gamma_{16} + \Gamma_{20} + \Gamma_{27} \\ &+ \Gamma_{126} \cdot \Gamma_{\eta\to3\pi^0} + \Gamma_{130} \cdot \Gamma_{\eta\to3\pi^0}\end{aligned}$$

$$\Gamma_{13} = \Gamma_{14} + \Gamma_{16}$$

$$\begin{aligned}\Gamma_{17} =& \Gamma_{128} \cdot \Gamma_{\eta\to3\pi^0} + \Gamma_{30} + \Gamma_{23} + \Gamma_{28} \\ &+\Gamma_{35} \cdot (\Gamma_{<K^0|K_S>} \cdot \Gamma_{K_S\to\pi^0\pi^0}) \\ &+\Gamma_{40} \cdot (\Gamma_{<K^0|K_S>} \cdot \Gamma_{K_S\to\pi^0\pi^0}) \\ &+\Gamma_{42} \cdot (\Gamma_{<K^0|K_S>} \cdot \Gamma_{K_S\to\pi^0\pi^0}) \\ &+\Gamma_{20} + \Gamma_{27} + \Gamma_{47} \cdot (\Gamma_{K_S\to\pi^0\pi^0} \cdot \Gamma_{K_S\to\pi^0\pi^0}) \\ &+\Gamma_{50} \cdot (\Gamma_{K_S\to\pi^0\pi^0} \cdot \Gamma_{K_S\to\pi^0\pi^0}) \\ &+\Gamma_{126} \cdot \Gamma_{\eta\to3\pi^0} + \Gamma_{37} \cdot (\Gamma_{<K^0|K_S>} \cdot \Gamma_{K_S\to\pi^0\pi^0}) \\ &+\Gamma_{130} \cdot \Gamma_{\eta\to3\pi^0}\end{aligned}$$

$$\begin{aligned}\Gamma_{18} =& \Gamma_{23} + \Gamma_{35} \cdot (\Gamma_{<K^0|K_S>} \cdot \Gamma_{K_S\to\pi^0\pi^0}) \\ &+\Gamma_{20} + \Gamma_{37} \cdot (\Gamma_{<K^0|K_S>} \cdot \Gamma_{K_S\to\pi^0\pi^0})\end{aligned}$$

$$\Gamma_{19} = \Gamma_{23} + \Gamma_{20}$$

$$\begin{aligned}\Gamma_{24} =& \Gamma_{27} + \Gamma_{28} + \Gamma_{30} \\ &+\Gamma_{40} \cdot (\Gamma_{<K^0|K_S>} \cdot \Gamma_{K_S\to\pi^0\pi^0}) \\ &+\Gamma_{42} \cdot (\Gamma_{<K^0|K_S>} \cdot \Gamma_{K_S\to\pi^0\pi^0}) \\ &+\Gamma_{47} \cdot (\Gamma_{K_S\to\pi^0\pi^0} \cdot \Gamma_{K_S\to\pi^0\pi^0}) \\ &+\Gamma_{50} \cdot (\Gamma_{K_S\to\pi^0\pi^0} \cdot \Gamma_{K_S\to\pi^0\pi^0}) \\ &+\Gamma_{126} \cdot \Gamma_{\eta\to3\pi^0} + \Gamma_{128} \cdot \Gamma_{\eta\to3\pi^0} \\ &+\Gamma_{130} \cdot \Gamma_{\eta\to3\pi^0} \\ &+\Gamma_{132} \cdot (\Gamma_{<K^0|K_S>} \cdot \Gamma_{K_S\to\pi^0\pi^0} \cdot \Gamma_{\eta\to3\pi^0})\end{aligned}$$

$$\begin{aligned}\Gamma_{25} =& \Gamma_{128} \cdot \Gamma_{\eta\to3\pi^0} + \Gamma_{30} + \Gamma_{28} \\ &+\Gamma_{27} + \Gamma_{126} \cdot \Gamma_{\eta\to3\pi^0} \\ &+\Gamma_{130} \cdot \Gamma_{\eta\to3\pi^0} \\ &+\Gamma_{30} + \Gamma_{28} + \Gamma_{27} + \Gamma_{126} \cdot \Gamma_{\eta\to3\pi^0} \\ &+\Gamma_{130} \cdot \Gamma_{\eta\to3\pi^0}\end{aligned}$$

$$\begin{aligned}\Gamma_{26} =& \Gamma_{128} \cdot \Gamma_{\eta\to3\pi^0} + \Gamma_{27} \\ &+\Gamma_{28} + \Gamma_{40} \cdot (\Gamma_{<K^0|K_S>} \cdot \Gamma_{K_S\to\pi^0\pi^0}) \\ &+\Gamma_{42} \cdot (\Gamma_{<K^0|K_S>} \cdot \Gamma_{K_S\to\pi^0\pi^0})\end{aligned}$$

$$\Gamma_{29} = \Gamma_{30} + \Gamma_{126} \cdot \Gamma_{\eta\to3\pi^0} + \Gamma_{130} \cdot \Gamma_{\eta\to3\pi^0}$$

$$\begin{aligned}\Gamma_{31} =& \Gamma_{128} \cdot \Gamma_{\eta\to\text{neutral}} + \Gamma_{23} \\ &+\Gamma_{28} + \Gamma_{42} + \Gamma_{16} \\ &+\Gamma_{37} + \Gamma_{10} + \Gamma_{167} \cdot (\Gamma_{\phi\to K_S K_L} \cdot \Gamma_{K_S\to\pi^0\pi^0})\end{aligned}$$

$$\begin{aligned}\Gamma_{32} =& \Gamma_{16} + \Gamma_{23} + \Gamma_{28} + \Gamma_{37} \\ &+\Gamma_{42} + \Gamma_{128} \cdot \Gamma_{\eta\to\text{neutral}} \\ &+\Gamma_{130} \cdot \Gamma_{\eta\to\text{neutral}} \\ &+\Gamma_{167} \cdot (\Gamma_{\phi\to K_S K_L} \cdot \Gamma_{K_S\to\pi^0\pi^0})\end{aligned}$$

$$\begin{aligned}\Gamma_{33} =& \Gamma_{35} \cdot \Gamma_{<\bar{K}^0|K_S>} + \Gamma_{40} \cdot \Gamma_{<\bar{K}^0|K_S>} \\ &+\Gamma_{42} \cdot \Gamma_{<K^0|K_S>} \\ &+\Gamma_{47} + \Gamma_{48} + \Gamma_{50} + \Gamma_{51} \\ &+\Gamma_{37} \cdot \Gamma_{<K^0|K_S>} \\ &+\Gamma_{132} \cdot (\Gamma_{<\bar{K}^0|K_S>} \cdot \Gamma_{\eta\to\text{neutral}}) \\ &+\Gamma_{44} \cdot \Gamma_{<\bar{K}^0|K_S>} + \Gamma_{167} \cdot \Gamma_{\phi\to K_S K_L}\end{aligned}$$

$$\Gamma_{34} = \Gamma_{35} + \Gamma_{37}$$

$$\Gamma_{38} = \Gamma_{42} + \Gamma_{37}$$

$$\Gamma_{39} = \Gamma_{40} + \Gamma_{42}$$

$$\Gamma_{43} = \Gamma_{40} + \Gamma_{44}$$

$$\Gamma_{46} = \Gamma_{48} + \Gamma_{47} + \Gamma_{804}$$

$$\Gamma_{49} = \Gamma_{50} + \Gamma_{51} + \Gamma_{806}$$

$$\begin{aligned}\Gamma_{54} =& \Gamma_{35} \cdot (\Gamma_{<K^0|K_S>} \cdot \Gamma_{K_S\to\pi^+\pi^-}) \\ &+\Gamma_{37} \cdot (\Gamma_{<K^0|K_S>} \cdot \Gamma_{K_S\to\pi^+\pi^-}) \\ &+\Gamma_{40} \cdot (\Gamma_{<K^0|K_S>} \cdot \Gamma_{K_S\to\pi^+\pi^-}) \\ &+\Gamma_{42} \cdot (\Gamma_{<K^0|K_S>} \cdot \Gamma_{K_S\to\pi^+\pi^-}) \\ &+\Gamma_{47} \cdot (2 \cdot \Gamma_{K_S\to\pi^+\pi^-} \cdot \Gamma_{K_S\to\pi^0\pi^0}) \\ &+\Gamma_{48} \cdot \Gamma_{K_S\to\pi^+\pi^-} \\ &+\Gamma_{50} \cdot (2 \cdot \Gamma_{K_S\to\pi^+\pi^-} \cdot \Gamma_{K_S\to\pi^0\pi^0}) \\ &+\Gamma_{51} \cdot \Gamma_{K_S\to\pi^+\pi^-} \\ &+\Gamma_{53} \cdot (\Gamma_{<\bar{K}^0|K_S>} \cdot \Gamma_{K_S\to\pi^0\pi^0} + \Gamma_{<\bar{K}^0|K_L>}) \\ &+\Gamma_{62} + \Gamma_{70} \\ &+\Gamma_{77} + \Gamma_{78} + \Gamma_{93} \\ &+\Gamma_{94} + \Gamma_{126} \cdot \Gamma_{\eta\to\text{charged}} \\ &+\Gamma_{128} \cdot \Gamma_{\eta\to\text{charged}} + \Gamma_{130} \cdot \Gamma_{\eta\to\text{charged}} \\ &+\Gamma_{132} \cdot (\Gamma_{<\bar{K}^0|K_L>} \cdot \Gamma_{\eta\to\pi^+\pi^-\pi^0} \\ &+\Gamma_{<\bar{K}^0|K_S>} \cdot \Gamma_{K_S\to\pi^0\pi^0} \cdot \Gamma_{\eta\to\pi^+\pi^-\pi^0} \\ &+\Gamma_{<\bar{K}^0|K_S>} \cdot \Gamma_{K_S\to\pi^+\pi^-} \cdot \Gamma_{\eta\to3\pi^0}) \\ &+\Gamma_{151} \cdot (\Gamma_{\omega\to\pi^+\pi^-\pi^0} + \Gamma_{\omega\to\pi^+\pi^-}) \\ &+\Gamma_{152} \cdot (\Gamma_{\omega\to\pi^+\pi^-\pi^0} + \Gamma_{\omega\to\pi^+\pi^-}) \\ &+\Gamma_{167} \cdot (\Gamma_{\phi\to K^+K^-} + \Gamma_{\phi\to K_S K_L} \cdot \Gamma_{K_S\to\pi^+\pi^-}) \\ &+\Gamma_{802} + \Gamma_{803}\end{aligned}$$

$$+\Gamma_{800}\cdot(\Gamma_{\omega\to\pi^+\pi^-\pi^0}+\Gamma_{\omega\to\pi^+\pi^-})$$

$$\Gamma_{55}=\Gamma_{128}\cdot\Gamma_{\eta\to\text{charged}}$$
$$+\Gamma_{152}\cdot(\Gamma_{\omega\to\pi^+\pi^-\pi^0}+\Gamma_{\omega\to\pi^+\pi^-})+\Gamma_{78}$$
$$+\Gamma_{77}+\Gamma_{94}+\Gamma_{62}+\Gamma_{70}+\Gamma_{93}$$
$$+\Gamma_{126}\cdot\Gamma_{\eta\to\text{charged}}$$
$$+\Gamma_{802}+\Gamma_{803}+\Gamma_{800}\cdot(\Gamma_{\omega\to\pi^+\pi^-\pi^0}+\Gamma_{\omega\to\pi^+\pi^-})$$
$$+\Gamma_{151}\cdot(\Gamma_{\omega\to\pi^+\pi^-\pi^0}$$
$$+\Gamma_{\omega\to\pi^+\pi^-})$$
$$+\Gamma_{130}\cdot\Gamma_{\eta\to\text{charged}}+\Gamma_{168}$$

$$\Gamma_{56}=\Gamma_{35}\cdot(\Gamma_{<K^0|K_S>}\cdot\Gamma_{K_S\to\pi^+\pi^-})$$
$$+\Gamma_{62}+\Gamma_{93}+\Gamma_{37}\cdot(\Gamma_{<K^0|K_S>}\cdot\Gamma_{K_S\to\pi^+\pi^-})$$
$$+\Gamma_{802}+\Gamma_{800}\cdot\Gamma_{\omega\to\pi^+\pi^-}$$
$$+\Gamma_{151}\cdot\Gamma_{\omega\to\pi^+\pi^-}+\Gamma_{168}$$

$$\Gamma_{57}=\Gamma_{62}+\Gamma_{93}+\Gamma_{802}$$
$$+\Gamma_{800}\cdot\Gamma_{\omega\to\pi^+\pi^-}$$
$$+\Gamma_{151}\cdot\Gamma_{\omega\to\pi^+\pi^-}$$
$$+\Gamma_{167}\cdot\Gamma_{\phi\to K^+K^-}$$

$$\Gamma_{58}=\Gamma_{62}+\Gamma_{93}+\Gamma_{802}+\Gamma_{167}\cdot\Gamma_{\phi\to K^+K^-}$$
$$\Gamma_{59}=\Gamma_{35}\cdot(\Gamma_{<K^0|K_S>}\cdot\Gamma_{K_S\to\pi^+\pi^-})$$
$$+\Gamma_{62}+\Gamma_{800}\cdot\Gamma_{\omega\to\pi^+\pi^-}$$
$$\Gamma_{60}=\Gamma_{62}+\Gamma_{800}\cdot\Gamma_{\omega\to\pi^+\pi^-}$$
$$\Gamma_{63}=\Gamma_{40}\cdot(\Gamma_{<K^0|K_S>}\cdot\Gamma_{K_S\to\pi^+\pi^-})$$
$$+\Gamma_{42}\cdot(\Gamma_{<K^0|K_S>}\cdot\Gamma_{K_S\to\pi^+\pi^-})$$
$$+\Gamma_{47}\cdot(2\cdot\Gamma_{K_S\to\pi^+\pi^-}\cdot\Gamma_{K_S\to\pi^0\pi^0})$$
$$+\Gamma_{50}\cdot(2\cdot\Gamma_{K_S\to\pi^+\pi^-}\cdot\Gamma_{K_S\to\pi^0\pi^0})$$
$$+\Gamma_{70}+\Gamma_{77}+\Gamma_{78}$$
$$+\Gamma_{94}+\Gamma_{126}\cdot\Gamma_{\eta\to\text{charged}}$$
$$+\Gamma_{128}\cdot\Gamma_{\eta\to\text{charged}}+\Gamma_{130}\cdot\Gamma_{\eta\to\text{charged}}$$
$$+\Gamma_{132}\cdot(\Gamma_{<\bar{K}^0|K_S>}\cdot\Gamma_{K_S\to\pi^+\pi^-}\cdot\Gamma_{\eta\to\text{neutral}}$$
$$+\Gamma_{<\bar{K}^0|K_S>}\cdot\Gamma_{K_S\to\pi^0\pi^0}\cdot\Gamma_{\eta\to\text{charged}})$$
$$+\Gamma_{151}\cdot\Gamma_{\omega\to\pi^+\pi^-\pi^0}+\Gamma_{152}\cdot(\Gamma_{\omega\to\pi^+\pi^-\pi^0}$$
$$+\Gamma_{\omega\to\pi^+\pi^-})+\Gamma_{800}\cdot\Gamma_{\omega\to\pi^+\pi^-\pi^0}+\Gamma_{803}$$
$$\Gamma_{64}=\Gamma_{78}+\Gamma_{77}+\Gamma_{94}+\Gamma_{70}$$
$$+\Gamma_{126}\cdot\Gamma_{\eta\to\pi^+\pi^-\pi^0}$$
$$+\Gamma_{128}\cdot\Gamma_{\eta\to\pi^+\pi^-\pi^0}$$
$$+\Gamma_{130}\cdot\Gamma_{\eta\to\pi^+\pi^-\pi^0}$$
$$+\Gamma_{800}\cdot\Gamma_{\omega\to\pi^+\pi^-\pi^0}$$
$$+\Gamma_{151}\cdot\Gamma_{\omega\to\pi^+\pi^-\pi^0}$$
$$+\Gamma_{152}\cdot(\Gamma_{\omega\to\pi^+\pi^-\pi^0}+\Gamma_{\omega\to\pi^+\pi^-})$$
$$+\Gamma_{803}$$
$$\Gamma_{65}=\Gamma_{40}\cdot(\Gamma_{<K^0|K_S>}\cdot\Gamma_{K_S\to\pi^+\pi^-})$$
$$+\Gamma_{42}\cdot(\Gamma_{<K^0|K_S>}\cdot\Gamma_{K_S\to\pi^+\pi^-})+\Gamma_{70}+\Gamma_{94}$$
$$+\Gamma_{128}\cdot\Gamma_{\eta\to\pi^+\pi^-\pi^0}$$
$$+\Gamma_{151}\cdot\Gamma_{\omega\to\pi^+\pi^-\pi^0}$$
$$+\Gamma_{152}\cdot\Gamma_{\omega\to\pi^+\pi^-}$$
$$+\Gamma_{800}\cdot\Gamma_{\omega\to\pi^+\pi^-\pi^0}+\Gamma_{803}$$
$$\Gamma_{66}=\Gamma_{70}+\Gamma_{94}+\Gamma_{128}\cdot\Gamma_{\eta\to\pi^+\pi^-\pi^0}$$
$$+\Gamma_{151}\cdot\Gamma_{\omega\to\pi^+\pi^-\pi^0}$$
$$+\Gamma_{152}\cdot\Gamma_{\omega\to\pi^+\pi^-}$$
$$+\Gamma_{800}\cdot\Gamma_{\omega\to\pi^+\pi^-\pi^0}+\Gamma_{803}$$

$$\Gamma_{67}=\Gamma_{70}+\Gamma_{94}$$
$$+\Gamma_{128}\cdot\Gamma_{\eta\to\pi^+\pi^-\pi^0}+\Gamma_{803}$$
$$\Gamma_{68}=\Gamma_{40}\cdot(\Gamma_{<K^0|K_S>}\cdot\Gamma_{K_S\to\pi^+\pi^-})$$
$$+\Gamma_{70}+\Gamma_{152}\cdot\Gamma_{\omega\to\pi^+\pi^-}$$
$$+\Gamma_{800}\cdot\Gamma_{\omega\to\pi^+\pi^-\pi^0}$$
$$\Gamma_{69}=\Gamma_{152}\cdot\Gamma_{\omega\to\pi^+\pi^-}+\Gamma_{70}$$
$$+\Gamma_{800}\cdot\Gamma_{\omega\to\pi^+\pi^-\pi^0}$$
$$\Gamma_{74}=\Gamma_{152}\cdot\Gamma_{\omega\to\pi^+\pi^-\pi^0}+\Gamma_{78}$$
$$+\Gamma_{77}+\Gamma_{126}\cdot\Gamma_{\eta\to\pi^+\pi^-\pi^0}$$
$$+\Gamma_{130}\cdot\Gamma_{\eta\to\pi^+\pi^-\pi^0}$$
$$\Gamma_{75}=\Gamma_{152}\cdot\Gamma_{\omega\to\pi^+\pi^-\pi^0}$$
$$+\Gamma_{47}\cdot(2\cdot\Gamma_{K_S\to\pi^+\pi^-}\cdot\Gamma_{K_S\to\pi^0\pi^0})$$
$$+\Gamma_{77}+\Gamma_{126}\cdot\Gamma_{\eta\to\pi^+\pi^-\pi^0}$$
$$+\Gamma_{130}\cdot\Gamma_{\eta\to\pi^+\pi^-\pi^0}$$
$$\Gamma_{76}=\Gamma_{152}\cdot\Gamma_{\omega\to\pi^+\pi^-\pi^0}+\Gamma_{77}$$
$$+\Gamma_{126}\cdot\Gamma_{\eta\to\pi^+\pi^-\pi^0}$$
$$+\Gamma_{130}\cdot\Gamma_{\eta\to\pi^+\pi^-\pi^0}$$
$$\Gamma_{78}=\Gamma_{810}+\Gamma_{50}\cdot(2\cdot\Gamma_{K_S\to\pi^+\pi^-}\cdot\Gamma_{K_S\to\pi^0\pi^0})$$
$$+\Gamma_{132}\cdot(\Gamma_{<\bar{K}^0|K_S>}\cdot\Gamma_{K_S\to\pi^+\pi^-}\cdot\Gamma_{\eta\to3\pi^0})$$
$$\Gamma_{79}=\Gamma_{37}\cdot(\Gamma_{<K^0|K_S>}\cdot\Gamma_{K_S\to\pi^+\pi^-})$$
$$+\Gamma_{42}\cdot(\Gamma_{<K^0|K_S>}\cdot\Gamma_{K_S\to\pi^+\pi^-})$$
$$+\Gamma_{93}+\Gamma_{94}+\Gamma_{128}\cdot\Gamma_{\eta\to\text{charged}}$$
$$+\Gamma_{151}\cdot(\Gamma_{\omega\to\pi^+\pi^-\pi^0}$$
$$+\Gamma_{\omega\to\pi^+\pi^-})+\Gamma_{168}+\Gamma_{802}+\Gamma_{803}$$
$$\Gamma_{80}=\Gamma_{93}+\Gamma_{802}+\Gamma_{151}\cdot\Gamma_{\omega\to\pi^+\pi^-}$$
$$\Gamma_{81}=\Gamma_{128}\cdot\Gamma_{\eta\to\pi^+\pi^-\pi^0}+\Gamma_{94}$$
$$+\Gamma_{803}+\Gamma_{151}\cdot\Gamma_{\omega\to\pi^+\pi^-\pi^0}$$
$$\Gamma_{82}=\Gamma_{128}\cdot\Gamma_{\eta\to\text{charged}}$$
$$+\Gamma_{42}\cdot(\Gamma_{<K^0|K_S>}\cdot\Gamma_{K_S\to\pi^+\pi^-})+\Gamma_{802}$$
$$+\Gamma_{803}+\Gamma_{151}\cdot(\Gamma_{\omega\to\pi^+\pi^-\pi^0}+\Gamma_{\omega\to\pi^+\pi^-})$$
$$+\Gamma_{37}\cdot(\Gamma_{<K^0|K_S>}\cdot\Gamma_{K_S\to\pi^+\pi^-})$$
$$\Gamma_{83}=\Gamma_{128}\cdot\Gamma_{\eta\to\pi^+\pi^-\pi^0}+\Gamma_{802}$$
$$+\Gamma_{803}+\Gamma_{151}\cdot(\Gamma_{\omega\to\pi^+\pi^-\pi^0}$$
$$+\Gamma_{\omega\to\pi^+\pi^-})$$
$$\Gamma_{84}=\Gamma_{802}+\Gamma_{151}\cdot\Gamma_{\omega\to\pi^+\pi^-}$$
$$+\Gamma_{37}\cdot(\Gamma_{<K^0|K_S>}\cdot\Gamma_{K_S\to\pi^+\pi^-})$$

$$
\begin{aligned}
\Gamma_{85} &= \Gamma_{802} + \Gamma_{151} \cdot \Gamma_{\omega\to\pi^+\pi^-} \\
\Gamma_{87} &= \Gamma_{42} \cdot (\Gamma_{<K^0|K_S>} \cdot \Gamma_{K_S\to\pi^+\pi^-}) \\
&\quad + \Gamma_{128} \cdot \Gamma_{\eta\to\pi^+\pi^-\pi^0} \\
&\quad + \Gamma_{151} \cdot \Gamma_{\omega\to\pi^+\pi^-\pi^0} + \Gamma_{803} \\
\Gamma_{88} &= \Gamma_{128} \cdot \Gamma_{\eta\to\pi^+\pi^-\pi^0} + \Gamma_{803} + \Gamma_{151} \cdot \Gamma_{\omega\to\pi^+\pi^-\pi^0} \\
\Gamma_{89} &= \Gamma_{803} + \Gamma_{151} \cdot \Gamma_{\omega\to\pi^+\pi^-\pi^0} \\
\Gamma_{92} &= \Gamma_{94} + \Gamma_{93} \\
\Gamma_{96} &= \Gamma_{167} \cdot \Gamma_{\phi\to K^+K^-} \\
\Gamma_{102} &= \Gamma_{103} + \Gamma_{104} \\
\Gamma_{103} &= \Gamma_{820} + \Gamma_{822} + \Gamma_{831} \cdot \Gamma_{\omega\to\pi^+\pi^-} \\
\Gamma_{104} &= \Gamma_{830} + \Gamma_{833} \\
\Gamma_{106} &= \Gamma_{30} + \Gamma_{44} \cdot \Gamma_{<\bar{K}^0|K_S>} \\
&\quad + \Gamma_{47} + \Gamma_{53} \cdot \Gamma_{<K^0|K_S>} \\
&\quad + \Gamma_{77} + \Gamma_{103} + \Gamma_{126} \cdot (\Gamma_{\eta\to 3\pi^0} + \Gamma_{\eta\to\pi^+\pi^-\pi^0}) \\
&\quad + \Gamma_{152} \cdot \Gamma_{\omega\to\pi^+\pi^-\pi^0} \\
\Gamma_{110} &= \Gamma_{10} + \Gamma_{16} + \Gamma_{23} + \Gamma_{28} + \Gamma_{35} + \Gamma_{40} \\
&\quad + \Gamma_{128} + \Gamma_{802} + \Gamma_{803} + \Gamma_{151} + \Gamma_{130} + \Gamma_{132} \\
&\quad + \Gamma_{44} + \Gamma_{53} + \Gamma_{168} + \Gamma_{169} \\
&\quad + \Gamma_{822} + \Gamma_{833} \\
\Gamma_{149} &= \Gamma_{152} + \Gamma_{800} + \Gamma_{151} \\
\Gamma_{150} &= \Gamma_{800} + \Gamma_{151}
\end{aligned}
$$

$$
\begin{aligned}
\Gamma_{168} &= \Gamma_{167} \cdot \Gamma_{\phi\to K^+K^-} \\
\Gamma_{169} &= \Gamma_{167} \cdot \Gamma_{\phi\to K_SK_L} \\
\Gamma_{804} &= \Gamma_{47} \cdot ((\Gamma_{<K^0|K_L>} \cdot \Gamma_{<\bar{K}^0|K_L>})/ \\
&\quad (\Gamma_{<K^0|K_S>} \cdot \Gamma_{<\bar{K}^0|K_S>})) \\
\Gamma_{806} &= \Gamma_{50} \cdot ((\Gamma_{<K^0|K_L>} \cdot \Gamma_{<\bar{K}^0|K_L>})/ \\
&\quad (\Gamma_{<K^0|K_S>} \cdot \Gamma_{<\bar{K}^0|K_S>})) \\
\Gamma_{810} &= \Gamma_{910} + \Gamma_{911} + \Gamma_{811} \cdot \Gamma_{\omega\to\pi^+\pi^-\pi^0} + \Gamma_{812} \\
\Gamma_{820} &= \Gamma_{920} + \Gamma_{821} \\
\Gamma_{830} &= \Gamma_{930} + \Gamma_{831} \cdot \Gamma_{\omega\to\pi^+\pi^-\pi^0} + \Gamma_{832} \\
\Gamma_{910} &= \Gamma_{136} \cdot \Gamma_{\eta\to 3\pi^0} \\
\Gamma_{911} &= \Gamma_{945} \cdot \Gamma_{\eta\to\pi^+\pi^-\pi^0} \\
\Gamma_{930} &= \Gamma_{136} \cdot \Gamma_{\eta\to\pi^+\pi^-\pi^0} \\
\Gamma_{944} &= \Gamma_{136} \cdot \Gamma_{\eta\to\gamma\gamma} \\
\Gamma_{\mathrm{All}} &= \Gamma_3 + \Gamma_5 + \Gamma_9 + \Gamma_{10} + \Gamma_{14} + \Gamma_{16} \\
&\quad + \Gamma_{20} + \Gamma_{23} + \Gamma_{27} + \Gamma_{28} + \Gamma_{30} + \Gamma_{35} \\
&\quad + \Gamma_{37} + \Gamma_{40} + \Gamma_{42} \\
&\quad + \Gamma_{47} \cdot (1 + ((\Gamma_{<K^0|K_L>} \\
&\quad \cdot \Gamma_{<\bar{K}^0|K_L>})/(\Gamma_{<K^0|K_S>} \cdot \Gamma_{<\bar{K}^0|K_S>}))) \\
&\quad + \Gamma_{48} + \Gamma_{62} + \Gamma_{70} + \Gamma_{77} + \Gamma_{811} + \Gamma_{812} \\
&\quad + \Gamma_{93} + \Gamma_{94} + \Gamma_{832} + \Gamma_{833} + \Gamma_{126} + \Gamma_{128} \\
&\quad + \Gamma_{802} + \Gamma_{803} + \Gamma_{800} + \Gamma_{151} + \Gamma_{130} + \Gamma_{132} \\
&\quad + \Gamma_{44} + \Gamma_{53} + \Gamma_{50} \cdot (1 + ((\Gamma_{<K^0|K_L>} \cdot \Gamma_{<\bar{K}^0|K_L>})/ \\
&\quad (\Gamma_{<K^0|K_S>} \cdot \Gamma_{<\bar{K}^0|K_S>}))) + \Gamma_{51} + \Gamma_{167} \\
&\quad \cdot (\Gamma_{\phi\to K^+K^-} + \Gamma_{\phi\to K_SK_L}) + \Gamma_{152} + \Gamma_{920} \\
&\quad + \Gamma_{821} + \Gamma_{822} + \Gamma_{831} + \Gamma_{136} + \Gamma_{945} + \Gamma_{805}
\end{aligned}
$$

9.2 Tests of lepton universality

Lepton universality tests probe the Standard Model prediction that the charged weak current interaction has the same coupling for all lepton generations. The precision of such tests has been significantly improved since the 2014 edition by the addition of the Belle τ lifetime measurement [1402], while improvements from the τ branching fraction fit are negligible. We compute the universality tests as in the previous report by using ratios of the partial widths of a heavier lepton λ decaying to a lighter lepton ρ [1403],

$$
\begin{aligned}
\Gamma(\lambda \to \nu_\lambda \rho \overline{\nu}_\rho(\gamma)) &= \frac{\mathcal{B}(\lambda \to \nu_\lambda \rho \overline{\nu}_\rho)}{\tau_\lambda} \\
&= \frac{G_\lambda G_\rho m_\lambda^5}{192\pi^3} f\left(\frac{m_\rho^2}{m_\lambda^2}\right) R_W^\lambda R_\gamma^\lambda,
\end{aligned}
$$

where

$$
G_\rho = \frac{g_\rho^2}{4\sqrt{2}M_W^2},
$$

$$
f(x) = 1 - 8x + 8x^3 - x^4 - 12x^2 \ln x,
$$

$$
R_W^\lambda = 1 + \frac{3}{5}\frac{m_\lambda^2}{M_W^2} + \frac{9}{5}\frac{m_\rho^2}{M_W^2} \; [1390 - 1392],
$$

$$
R_\gamma^\lambda = 1 + \frac{\alpha(m_\lambda)}{2\pi}\left(\frac{25}{4} - \pi^2\right).
$$

We use $R_\gamma^\tau = 1 - 43.2 \cdot 10^{-4}$ and $R_\gamma^\mu = 1 - 42.4 \cdot 10^{-4}$ [1403] and M_W from PDG 2015 [327]. We use HFLAV Spring 2017 averages and PDG 2015 for the other quantities. Using pure leptonic processes we obtain

$$
\left(\frac{g_\tau}{g_\mu}\right) = 1.0010 \pm 0.0015,
$$

$$
\left(\frac{g_\tau}{g_e}\right) = 1.0029 \pm 0.0015,
$$

$$
\left(\frac{g_\mu}{g_e}\right) = 1.0019 \pm 0.0014.
$$

Using the expressions for the τ semi-hadronic partial widths, we obtain

$$
\left(\frac{g_\tau}{g_\mu}\right)^2 = \frac{B(\tau \to h\nu_\tau)}{B(h \to \mu\bar{\nu}_\mu)} \frac{2m_h m_\mu^2 \tau_h}{(1+\delta R_{\tau/h}) m_\tau^3 \tau_\tau} \left(\frac{1 - m_\mu^2/m_h^2}{1 - m_h^2/m_\tau^2}\right)^2,
$$

where $h = \pi$ or K and the radiative corrections are $\delta R_{\tau/\pi} = (0.16 \pm 0.14)\%$ and $\delta R_{\tau/K} = (0.90 \pm 0.22)\%$ [1407–1410]. We measure:

$$
\left(\frac{g_\tau}{g_\mu}\right)_\pi = 0.9961 \pm 0.0027,
$$

Table 315 Universality coupling ratios correlation coefficients (%)

$\left(\frac{g_\tau}{g_e}\right)$	53			
$\left(\frac{g_\mu}{g_e}\right)$	−49	48		
$\left(\frac{g_\tau}{g_\mu}\right)_\pi$	24	26	2	
$\left(\frac{g_\tau}{g_\mu}\right)_K$	11	10	−1	6
	$\left(\frac{g_\tau}{g_\mu}\right)$	$\left(\frac{g_\tau}{g_e}\right)$	$\left(\frac{g_\mu}{g_e}\right)$	$\left(\frac{g_\tau}{g_\mu}\right)_\pi$

$$\left(\frac{g_\tau}{g_\mu}\right)_K = 0.9860 \pm 0.0070.$$

Similar tests could be performed with decays to electrons, however they are less precise because the hadron two body decays to electrons are helicity-suppressed. Averaging the three g_τ/g_μ ratios we obtain

$$\left(\frac{g_\tau}{g_\mu}\right)_{\tau+\pi+K} = 1.0000 \pm 0.0014,$$

accounting for statistical correlations. Table 315 reports the statistical correlation coefficients for the fitted coupling ratios.

Since there is 100% correlation between g_τ/g_μ, g_τ/g_e and g_μ/g_e, the correlation matrix is expected to be positive semi-definite, with one eigenvalue equal to zero. Due to numerical inaccuracies, one eigenvalue is expected to be close to zero rather than exactly zero.

9.3 Universality improved $B(\tau \to e\nu\bar{\nu})$ and R_{had}

We compute two quantities that are used in this report and that have been traditionally used for further elaborations and tests involving the τ branching fractions:

- the "universality improved" experimental determination of $B_e = B(\tau \to e\nu\bar{\nu})$, which relies on the assumption that the Standard Model and lepton universality hold;
- the ratio R_{had} between the total branching fraction of the τ to hadrons and the universality improved $\mathcal{B}_e$, which is the same as the ratio of the two respective partial widths.

Following Ref. [1411], we obtain a more precise experimental determination of B_e using the τ branching fraction to $\mu\nu\bar{\nu}$, B_μ, and the τ lifetime. We average:

- the B_e fit value Γ_5,
- the B_e determination from the $B_\mu = B(\tau \to \mu\nu\bar{\nu})$ fit value Γ_3 assuming that $g_\mu/g_e = 1$, hence (see also Sect. 9.2) $B_e = B_\mu \cdot f(m_e^2/m_\tau^2)/f(m_\mu^2/m_\tau^2)$,
- the B_e determination from the τ lifetime assuming that $g_\tau/g_\mu = 1$, hence $B_e = B(\mu \to e\bar{\nu}_e\nu_\mu) \cdot (\tau_\tau/\tau_\mu) \cdot (m_\tau/m_\mu)^5 \cdot f(m_e^2/m_\tau^2)/f(m_e^2/m_\mu^2) \cdot (\delta_\gamma^\tau\delta_W^\tau)/(\delta_\gamma^\mu\delta_W^\mu)$ where $B(\mu \to e\bar{\nu}_e\nu_\mu) = 1$.

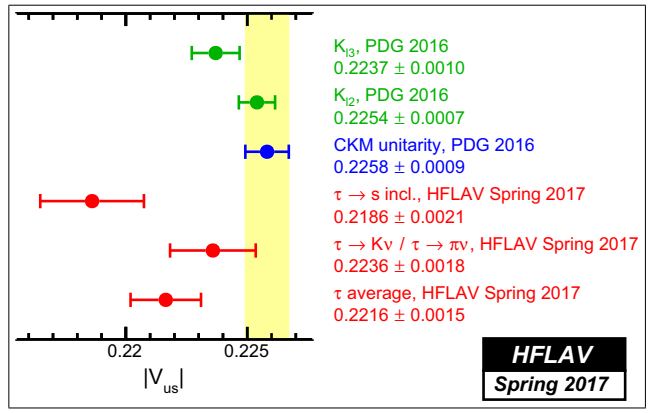

Fig. 220 $|V_{us}|$ averages

Accounting for statistical correlations, we obtain

$$B_e^{\text{uni}} = (17.815 \pm 0.023)\%.$$

We use B_e^{uni} to obtain the ratio

$$R_{\text{had}} = \frac{\Gamma(\tau \to \text{hadrons})}{\Gamma(\tau \to e\nu\bar{\nu})} = \frac{\Gamma_{\text{hadrons}}}{B_e^{\text{uni}}} = 3.6349 \pm 0.0082,$$

where $\Gamma(\tau \to \text{hadrons})$ and $\Gamma(\tau \to e\nu\bar{\nu})$ indicate the partial widths and Γ_{hadrons} is the total branching fraction of the τ to hadrons, or the total branching fraction in any measured final state minus the leptonic branching fractions, i.e., with our notation $\Gamma_{\text{hadrons}} = \Gamma_{\text{All}} - \Gamma_3 - \Gamma_5 = (64.76 \pm 0.10)\%$ (see Sect. 9.1 and Table 304 for the definitions of $\Gamma_{\text{All}}, \Gamma_3, \Gamma_5$). We underline that this report's definition of Γ_{hadrons} corresponds to summing all τ hadronic decay modes, like in the previous report, rather than – as done elsewhere – subtracting the leptonic branching fractions from unity, i.e., $\Gamma_{\text{hadrons}} = 1 - \Gamma_3 - \Gamma_5$.

9.4 $|V_{us}|$ measurement

The CKM matrix element magnitude $|V_{us}|$ is most precisely determined from kaon decays [1412] (see Fig. 220), and its precision is limited by the uncertainties of the lattice QCD estimates of the meson decay constants $f_+^{K\pi}(0)$ and f_K/f_π. Using the τ branching fractions, it is possible to determine $|V_{us}|$ in an alternative way [1413,1414] that does not depend on lattice QCD and has small theory uncertainties (as discussed in Sect. 9.4.1). Moreover, $|V_{us}|$ can be determined using the τ branching fractions similarly to the kaon case, using the same meson decay constants from Lattice QCD.

9.4.1 $|V_{us}|$ from $B(\tau \to X_s \nu)$

The τ hadronic partial width is the sum of the τ partial widths to strange and to non-strange hadronic final states, $\Gamma_{\text{had}} = \Gamma_s + \Gamma_{\text{VA}}$. The suffix "VA" traditionally denotes the sum of the τ partial widths to non-strange final states, which proceed through either vector or axial-vector currents.

Dividing any partial width Γ_x by the electronic partial width, Γ_e, we obtain partial width ratios R_x (which are equal to the respective branching fraction ratios B_x/B_e) for which $R_{\text{had}} = R_s + R_{\text{VA}}$. In terms of such ratios, $|V_{us}|$ can be measured as [1413,1414]

$$|V_{us}|_{\tau s} = \sqrt{R_s / \left[\frac{R_{\text{VA}}}{|V_{ud}|^2} - \delta R_{\text{theory}} \right]},$$

where δR_{theory} can be determined in the context of low energy QCD theory, partly relying on experimental low energy scattering data. The literature reports several calculations [1415–1417]. In this report we use Ref. [1415], whose estimated uncertainty size is intermediate between the two other ones. We use the information in that paper and the PDG 2015 value for the s-quark mass $m_s = 95.00 \pm 5.00$ MeV [327] to calculate $\delta R_{\text{theory}} = 0.242 \pm 0.032$..

We proceed following the same procedure of the 2012 HFLAV report [234]. We sum the relevant τ branching fractions to compute B_{VA} and B_s and we use the universality improved B_e^{uni} (see Sect. 9.3) to compute the R_{VA} and R_s ratios. In past determinations of $|V_{us}|$, for example in the 2009 HFLAV report [420], the total hadronic branching fraction has been computed using unitarity as $B_{\text{had}}^{\text{uni}} = 1 - B_e - B_\mu$, obtaining then B_s from the sum of the strange branching fractions and B_{VA} from $B_{\text{had}}^{\text{uni}} - B_s$. We prefer to use the more direct experimental determination of B_{VA} for two reasons. First, both methods result in comparable uncertainties on $|V_{us}|$, since the better precision on $B_{\text{had}}^{\text{uni}} = 1 - B_e - B_\mu$ is vanified by increased statistical correlations in the expressions $(1 - B_e - B_\mu)/B_e^{\text{univ}}$ and $B_s/(B_{\text{had}} - B_s)$ in the $|V_{us}|$ calculation. Second, if there are unobserved τ hadronic decay modes, they would affect B_{VA} and B_s in a more asymmetric way when using unitarity.

Using the τ branching fraction fit results with their uncertainties and correlations (Sect. 9.1), we compute $B_s = (2.909 \pm 0.048)\%$ (see also Table 316) and $B_{\text{VA}} = B_{\text{hadrons}} - B_s = (61.85 \pm 0.10))\%$, where B_{hadrons} is equal to Γ_{hadrons} defined in Sect. 9.3. PDG 2015 averages are used for non-τ quantities, and $|V_{ud}| = 0.97417 \pm 0.00021$ [1418].

We obtain $|V_{us}|_{\tau s} = 0.2186 \pm 0.0021$, which is 3.1σ lower than the unitarity CKM prediction $|V_{us}|_{\text{uni}} = 0.22582 \pm 0.00089$, from $(|V_{us}|_{\text{uni}})^2 = 1 - |V_{ud}|^2$. The $|V_{us}|_{\tau s}$ uncertainty includes a systematic error contribution of 0.47% from the theory uncertainty on δR_{theory}. There is no significant change with respect to the previous HFLAV report.

Table 316 HFLAV Spring 2017 τ branching fractions to strange final states

Branching fraction	HFLAV Spring 2017 fit (%)
$K^-\nu_\tau$	0.6960 ± 0.0096
$K^-\pi^0\nu_\tau$	0.4327 ± 0.0149
$K^-2\pi^0\nu_\tau$ (ex. K^0)	0.0640 ± 0.0220
$K^-3\pi^0\nu_\tau$ (ex. K^0, η)	0.0428 ± 0.0216
$\pi^-\bar{K}^0\nu_\tau$	0.8386 ± 0.0141
$\pi^-\bar{K}^0\pi^0\nu_\tau$	0.3812 ± 0.0129
$\pi^-\bar{K}^0\pi^0\pi^0\nu_\tau$(ex.$K^0$)	0.0234 ± 0.0231
$\bar{K}^0h^-h^-h+\nu_\tau$	0.0222 ± 0.0202
$K^-\eta\nu_\tau$	0.0155 ± 0.0008
$K^-\pi^0\eta\nu_\tau$	0.0048 ± 0.0012
$\pi^-\bar{K}^0\eta\nu_\tau$	0.0094 ± 0.0015
$K^-\omega\nu_\tau$	0.0410 ± 0.0092
$K^-\phi\nu_\tau(\phi \to K^+K-)$	0.0022 ± 0.0008
$K^-\phi\nu_\tau(\phi \to K_S^0K_L^0)$	0.0015 ± 0.0006
$K^-\pi^-\pi^+\nu_\tau$(ex.K^0, ω)	0.2923 ± 0.0067
$K^-\pi^-\pi^+\pi^0\nu_\tau$(ex.$K^0, \omega\eta$)	0.0410 ± 0.0143
$K^-2\pi^-2\pi^+\nu_\tau$(ex.K^0)	0.0001 ± 0.0001
$K^-2\pi^-2\pi^+\pi^0\nu_\tau$(ex.$K^0$)	0.0001 ± 0.0001
$X_s^-\nu_\tau$	2.9087 ± 0.0482

9.4.2 $|V_{us}|$ from $B(\tau \to K\nu)/B(\tau \to \pi\nu)$

We compute $|V_{us}|$ from the ratio of branching fractions $B(\tau \to K^-\nu_\tau)/B(\tau \to \pi^-\nu_\tau) = (6.438 \pm 0.094)$ from the equation [1404]:

$$\frac{B(\tau \to K^-\nu_\tau)}{B(\tau \to \pi^-\nu_\tau)} = \frac{f_K^2|V_{us}|^2}{f_\pi^2|V_{ud}|^2} \times \frac{(m_\tau^2 - m_K^2)^2}{(m_\tau^2 - m_\pi^2)^2} \frac{1 + \delta R_{\tau/K}}{1 + \delta R_{\tau/\pi}} (1 + \delta R_{K/\pi})$$

We use $f_K/f_\pi = 1.1930 \pm 0.0030$ from the FLAG 2016 Lattice averages with $N_f = 2 + 1 + 1$ [222],

$$\frac{1 + \delta R_{\tau/K}}{1 + \delta R_{\tau/\pi}} = \frac{1 + (1.1930 \pm 0.0030)\%}{1 + (0.16 \pm 0.14)\%} \; [1393 - 1396],$$

$$1 + \delta R_{K/\pi} = 1 + (-1.13 \pm 0.23)\% \; [1390, 1405, 1406].$$

We compute $|V_{us}|_{\tau K/\pi} = 0.2236 \pm 0.0018$, 1.1σ below the CKM unitarity prediction.

9.4.3 $|V_{us}|$ from τ summary

We summarize the $|V_{us}|$ results reporting the values, the discrepancy with respect to the $|V_{us}|$ determination from CKM unitarity, and an illustration of the measurement method:

$$\begin{aligned}
|V_{us}|_{\text{uni}} &= 0.22582 \pm 0.00089 \\
&\quad [\text{from } \sqrt{1-|V_{ud}|^2} \quad \text{(CKM unitarity)}], \\
|V_{us}|_{\tau s} &= 0.2186 \pm 0.0021 \quad -3.1\sigma \\
&\quad [\text{from } \Gamma(\tau^- \to X_s^- \nu_\tau)], \\
|V_{us}|_{\tau K/\pi} &= 0.2236 \pm 0.0018 \quad -1.1\sigma \\
&\quad [\text{from } \Gamma(\tau^- \to K^- \nu_\tau)/\Gamma(\tau^- \to \pi^- \nu_\tau)].
\end{aligned}$$

Averaging the two above $|V_{us}|$ determinations that rely on the τ branching fractions (taking into account all correlations due to the τ HFLAV and other mentioned inputs) we obtain, for $|V_{us}|$ and its discrepancy:

$$\begin{aligned}
|V_{us}|_{\tau} &= 0.2216 \pm 0.0015 \quad -2.4\sigma \\
&\quad [\text{average of } 2|V_{us}|\ \tau \text{ measurements}].
\end{aligned}$$

All $|V_{us}|$ determinations based on measured τ branching fractions are lower than both the kaon and the CKM-unitarity determinations. This is correlated with the fact that the direct measurements of the three major τ branching fractions to kaons [$B(\tau \to K^-\nu_\tau)$, $B(\tau \to K^-\pi^0\nu_\tau)$ and $B(\tau \to \pi^-\bar{K}^0\nu_\tau)$] are lower than their determinations from the kaon branching fractions into final states with leptons within the SM [1404,1421,1422].

A recent determination of $|V_{us}|$ [1423,1424] that relies on the τ spectral functions in addition to the inclusive $\tau \to X_s\nu$ branching fraction reports a $|V_{us}|$ value about 1σ lower than the CKM-unitarity determination. This determination uses inputs that are partially different from the ones used in this report. Specifically, the HFLAV average of $B(\tau \to K^-\nu_\tau)$ has been replaced with the SM prediction based on the measured $B(K^- \to \mu^-\bar{\nu}_\mu)$ and the HFLAV average of $B(\tau \to K^-\pi^0\nu_\tau)$ has been replaced with an in-progress BaBar measurement that is published in a PhD thesis. Both changes increase the resulting $\tau \to X_s\nu$ inclusive branching fraction. This study claims that the newly proposed $|V_{us}|$ calculation has a more stable and reliable theory uncertainty, which could possibly have been underestimated in former studies, which are used for the HFLAV $|V_{us}|$ average.

In previous editions of the HFLAV report, we also computed $|V_{us}|$ using the branching fraction $B(\tau \to K\nu)$ and without taking the ratio with $B(\tau \to \pi\nu)$. We do not report this additional determination because it did not include the long-distance radiative corrections in addition to the short-distance contribution, and because it had a negligible effect on the overall precision of the $|V_{us}|$ calculation with τ data.

Figure 220 reports the HFLAV $|V_{us}|$ determinations that use the τ branching fractions, compared to two $|V_{us}|$ determinations based on kaon data [6] and to $|V_{us}|$ obtained from $|V_{ud}|$ and the CKM matrix unitarity [6].

9.5 Upper limits on τ lepton-flavour-violating branching fractions

The Standard Model predicts that the τ lepton-flavour-violating (LFV) branching fractions are too small to be measured with the available experimental precision. We report in Table 317 and Fig. 221 the experimental upper limits on these branching fractions that have been published by the B-factories BaBar and Belle and later experiments. We omit previous weaker upper limits (mainly from CLEO) and all preliminary results presented several years ago. The previous HFLAV report [5] still included a few preliminary results, which have all been removed now.

9.6 Combination of upper limits on τ lepton-flavour-violating branching fractions

Combining upper limits is a delicate issue, since there is no standard and generally agreed procedure. Furthermore, the τ LFV searches published limits are extracted from the data with a variety of methods, and cannot be directly combined with a uniform procedure. It is however possible to use a single and effective upper limit combination procedure for all modes by re-computing the published upper limits with just one extraction method, using the published information that documents the upper limit determination: number of observed candidates, expected background, signal efficiency and number of analyzed τ decays.

We chose to use the CL_s method [1443] to re-compute the τ LFV upper limits, since it is well known and widely used (see the Statistics review of PDG 2013 [6]), and since the limits computed with the CL_s method can be combined in a straightforward way (see below). The CL_s method is based on two hypotheses: signal plus background and background only. We calculate the observed confidence levels for the two hypotheses:

$$\text{CL}_{s+b} = P_{s+b}(Q \le Q_{obs}) = \int_{-\infty}^{Q_{obs}} \frac{dP_{s+b}}{dQ} dQ, \tag{295}$$

$$\text{CL}_b = P_b(Q \le Q_{obs}) = \int_{-\infty}^{Q_{obs}} \frac{dP_b}{dQ} dQ, \tag{296}$$

where CL_{s+b} is the confidence level observed for the signal plus background hypotheses, CL_b is the confidence level observed for the background only hypothesis, $\frac{dP_{s+b}}{dQ}$ and $\frac{dP_b}{dQ}$ are the probability distribution functions (PDFs) for the two corresponding hypothesis and Q is called the test statistic.

Table 317 Experimental upper limits on lepton flavour violating τ decays. The modes are grouped according to the properties of their final states. Modes with baryon number violation are labelled with "BNV"

Decay mode	Category	90% CL Limit	Exp.	Refs.
$\Gamma_{156} = e^-\gamma$	ℓ_γ	$3.3 \cdot 10^{-8}$	BaBaR	[1425]
$\Gamma_{156} = e^-\gamma$		$1.2 \cdot 10^{-7}$	Belle	[1426]
$\Gamma_{157} = \mu^-\gamma$		$4.4 \cdot 10^{-8}$	BaBaR	[1425]
$\Gamma_{157} = \mu^-\gamma$		$4.5 \cdot 10^{-8}$	Belle	[1426]
$\Gamma_{158} = e^-\pi^0$	ℓP^0	$1.3 \cdot 10^{-7}$	BaBaR	[1427]
$\Gamma_{158} = e^-\pi^0$		$8.0 \cdot 10^{-8}$	Belle	[1428]
$\Gamma_{159} = \nu^-\pi^0$		$1.1 \cdot 10^{-7}$	BaBaR	[1427]
$\Gamma_{159} = \nu^-\pi^0$		$1.2 \cdot 10^{-7}$	Belle	[1428]
$\Gamma_{160} = e^-{K_S}^0$		$3.3 \cdot 10^{-8}$	BaBaR	[1429]
$\Gamma_{160} = e^-{K_S}^0$		$2.6 \cdot 10^{-8}$	Belle	[1430]
$\Gamma_{161} = \mu^-{K_S}^0$		$4.0 \cdot 10^{-8}$	BaBaR	[1429]
$\Gamma_{161} = \mu^-{K_S}^0$		$2.3 \cdot 10^{-8}$	Belle	[1430]
$\Gamma_{162} = e^-\eta$		$1.6 \cdot 10^{-7}$	BaBaR	[1427]
$\Gamma_{162} = e^-\eta$		$9.2 \cdot 10^{-8}$	Belle	[1428]
$\Gamma_{163} = \nu^-\eta$		$1.5 \cdot 10^{-7}$	BaBaR	[1427]
$\Gamma_{163} = \nu^-\eta$		$6.5 \cdot 10^{-8}$	Belle	[1428]
$\Gamma_{172} = e^-\eta'(958)$		$2.4 \cdot 10^{-7}$	BaBaR	[1427]
$\Gamma_{172} = e^-\eta'(958)$		$1.6 \cdot 10^{-7}$	Belle	[1428]
$\Gamma_{173} = \nu^-\eta'(958)$		$1.4 \cdot 10^{-7}$	BaBaR	[1427]
$\Gamma_{173} = \nu^-\eta'(958)$		$1.3 \cdot 10^{-7}$	Belle	[1428]
$\Gamma_{164} = e^-\rho^0$	ℓV^0	$4.6 \cdot 10^{-8}$	BaBaR	[1431]
$\Gamma_{164} = e^-\rho^0$		$1.8 \cdot 10^{-8}$	Belle	[1432]
$\Gamma_{165} = \mu^-\rho^0$		$2.6 \cdot 10^{-8}$	BaBaR	[1431]
$\Gamma_{165} = \mu^-\rho^0$		$1.2 \cdot 10^{-8}$	Belle	[1432]
$\Gamma_{166} = e^-\omega$		$1.1 \cdot 10^{-7}$	BaBaR	[1433]
$\Gamma_{166} = e^-\omega$		$4.8 \cdot 10^{-8}$	Belle	[1432]
$\Gamma_{167} = \mu^-\omega$		$1.0 \cdot 10^{-7}$	BaBaR	[1433]
$\Gamma_{167} = \mu^-\omega$		$4.7 \cdot 10^{-8}$	Belle	[1432]
$\Gamma_{168} = e^-K^*(892)^0$		$5.9 \cdot 10^{-8}$	BaBaR	[1431]
$\Gamma_{168} = e^-K^*(892)^0$		$3.2 \cdot 10^{-8}$	Belle	[1432]
$\Gamma_{169} = \mu^-K^*(892)^0$		$1.7 \cdot 10^{-7}$	BaBaR	[1431]
$\Gamma_{169} = \mu^-K^*(892)^0$		$7.2 \cdot 10^{-8}$	Belle	[1432]
$\Gamma_{170} = e^-\bar{K}^*(892)^0$		$4.6 \cdot 10^{-8}$	BaBaR	[1431]
$\Gamma_{170} = e^-\bar{K}^*(892)^0$		$3.4 \cdot 10^{-8}$	Belle	[1432]
$\Gamma_{171} = \mu^-\bar{K}^*(892)^0$		$7.3 \cdot 10^{-8}$	BaBaR	[1431]
$\Gamma_{171} = \mu^-\bar{K}^*(892)^0$		$7.0 \cdot 10^{-8}$	Belle	[1432]
$\Gamma_{176} = e^-\phi$		$3.1 \cdot 10^{-8}$	BaBaR	[1431]
$\Gamma_{176} = e^-\phi$		$3.1 \cdot 10^{-8}$	Belle	[1432]
$\Gamma_{177} = \mu^-\phi$		$1.9 \cdot 10^{7}$	BaBaR	[1431]
$\Gamma_{177} = \mu^-\phi$		$8.4 \cdot 10^{8}$	Belle	[1432]
$\Gamma_{174} = e^-f_0(980)$	ℓS^0	$3.2 \cdot 10^{8}$	Belle	[1434]
$\Gamma_{175} = \mu^-f_0(980)$		$3.4 \cdot 10^{8}$	Belle	[1434]
$\Gamma_{178} = e^-e^+e^-$	$\ell\ell\ell$	$2.9 \cdot 10^{8}$	BaBaR	[1435]
$\Gamma_{178} = e^-e^+e^-$		$2.7 \cdot 10^{8}$	Belle	[1436]
$\Gamma_{179} = e^-\mu^+\mu^-$		$3.2 \cdot 10^{8}$	BaBaR	[1435]
$\Gamma_{179} = e^-\mu^+\mu^-$		$2.7 \cdot 10^{8}$	Belle	[1436]

Table 317 continued

Decay mode	Category	90% CL Limit	Exp.	Refs.
$\Gamma_{180} = \mu^- e^+ \mu^-$		$2.6 \cdot 10^8$	BABAR	[1435]
$\Gamma_{180} = \mu^- e^+ \mu^-$		$1.7 \cdot 10^8$	Belle	[1436]
$\Gamma_{181} = \mu^- e^+ e^-$		$2.2 \cdot 10^8$	BABAR	[1435]
$\Gamma_{181} = \mu^- e^+ e^-$		$1.8 \cdot 10^8$	Belle	[1436]
$\Gamma_{182} = e^- \mu^+ e^-$		$1.8 \cdot 10^8$	BABAR	[1435]
$\Gamma_{182} = e^- \mu^+ e^-$		$1.5 \cdot 10^8$	Belle	[1436]
$\Gamma_{183} = \mu^- \mu^+ \mu^-$		$3.8 \cdot 10^7$	ATLAS	[1437]
$\Gamma_{183} = \mu^- \mu^+ \mu^-$		$3.3 \cdot 10^8$	BABAR	[1435]
$\Gamma_{183} = \mu^- \mu^+ \mu^-$		$2.1 \cdot 10^8$	Belle	[1436]
$\Gamma_{183} = \mu^- \mu^+ \mu^-$		$4.6 \cdot 10^8$	LHCb	[1438]
$\Gamma_{184} = e^- \pi^+ \pi^-$	ℓhh	$1.2 \cdot 10^7$	BABAR	[1439]
$\Gamma_{184} = e^- \pi^+ \pi^-$		$2.3 \cdot 10^8$	Belle	[1440]
$\Gamma_{185} = e^- \pi^+ \pi^-$		$2.7 \cdot 10^7$	BABAR	[1439]
$\Gamma_{185} = e^- \pi^+ \pi^-$		$2.0 \cdot 10^8$	Belle	[1440]
$\Gamma_{186} = \mu^- \pi^+ \pi^-$		$2.9 \cdot 10^7$	BABAR	[1439]
$\Gamma_{186} = \mu^- \pi^+ \pi^-$		$2.1 \cdot 10^8$	Belle	[1440]
$\Gamma_{187} = \mu^- \pi^+ \pi^-$		$7.0 \cdot 10^8$	BABAR	[1439]
$\Gamma_{187} = \mu^- \pi^+ \pi^-$		$3.9 \cdot 10^8$	Belle	[1440]
$\Gamma_{188} = e^- \pi^+ K^-$		$3.2 \cdot 10^7$	BABAR	[1439]
$\Gamma_{188} = e^- K^+ \pi^-$		$3.7 \cdot 10^8$	Belle	[1440]
$\Gamma_{189} = e^- K^+ \pi^-$		$1.7 \cdot 10^7$	BABAR	[1439]
$\Gamma_{189} = e^- K^+ \pi^-$		$3.1 \cdot 10^8$	Belle	[1440]
$\Gamma_{190} = e^+ \pi^- K^-$		$1.8 \cdot 10^7$	BABAR	[1439]
$\Gamma_{190} = e^+ K^- \pi^-$		$3.2 \cdot 10^8$	Belle	[1440]
$\Gamma_{191} = e^+ K^- \pi^-$		$7.1 \cdot 10^8$	Belle	[1430]
$\Gamma_{192} = e^- K_S^0 K_S^0$		$1.4 \cdot 10^7$	BABAR	[1439]
$\Gamma_{192} = e^- K^+ K^-$		$3.4 \cdot 10^8$	Belle	[1440]
$\Gamma_{193} = e^- K^+ K^-$		$1.5 \cdot 10^7$	BABAR	[1439]
$\Gamma_{193} = e^- K^- K^-$		$3.3 \cdot 10^8$	Belle	[1440]
$\Gamma_{194} = \mu^- \pi^+ K^-$		$2.6 \cdot 10^7$	BABAR	[1439]
$\Gamma_{194} = \mu^- \pi^+ K^-$		$8.6 \cdot 10^8$	Belle	[1440]
$\Gamma_{195} = \mu^- K^+ \pi^-$		$3.2 \cdot 10^7$	BABAR	[1439]
$\Gamma_{195} = \mu^- K^+ \pi^-$		$4.5 \cdot 10^8$	Belle	[1440]
$\Gamma_{196} = \mu^+ \pi^- K^-$		$2.2 \cdot 10^{-7}$	BABAR	[1439]
$\Gamma_{196} = \mu^+ \pi^- K^-$		$4.8 \cdot 10^{-8}$	Belle	[1440]
$\Gamma_{197} = \mu^- K_S^0 K_S^0$		$8.0 \cdot 10^{-8}$	Belle	[1430]
$\Gamma_{198} = \mu^- K^+ K^-$		$2.5 \cdot 10^{-7}$	BABAR	[1439]
$\Gamma_{198} = \mu^- K^+ K^-$		$4.4 \cdot 10^8$	Belle	[1440]
$\Gamma_{199} = \mu^- K^+ K^-$		$4.8 \cdot 10^{-7}$	BABAR	[1439]
$\Gamma_{199} = \mu^- K^+ K^-$		$4.7 \cdot 10^8$	Belle	[1440]
$\Gamma_{211} = \pi^- \Lambda$	BNV	$7.2 \cdot 10^{-8}$	Belle	[1441]
$\Gamma_{212} = \pi^- \bar{\Lambda}$		$1.4 \cdot 10^{-7}$	Belle	[1441]
$\Gamma_{215} = p \mu^- \mu^-$		$4.4 \cdot 10^{-7}$	LHCb	[1442]
$\Gamma_{216} = \bar{p} \mu^+ \mu^-$		$3.3 \cdot 10^{-7}$	LHCb	[1442]

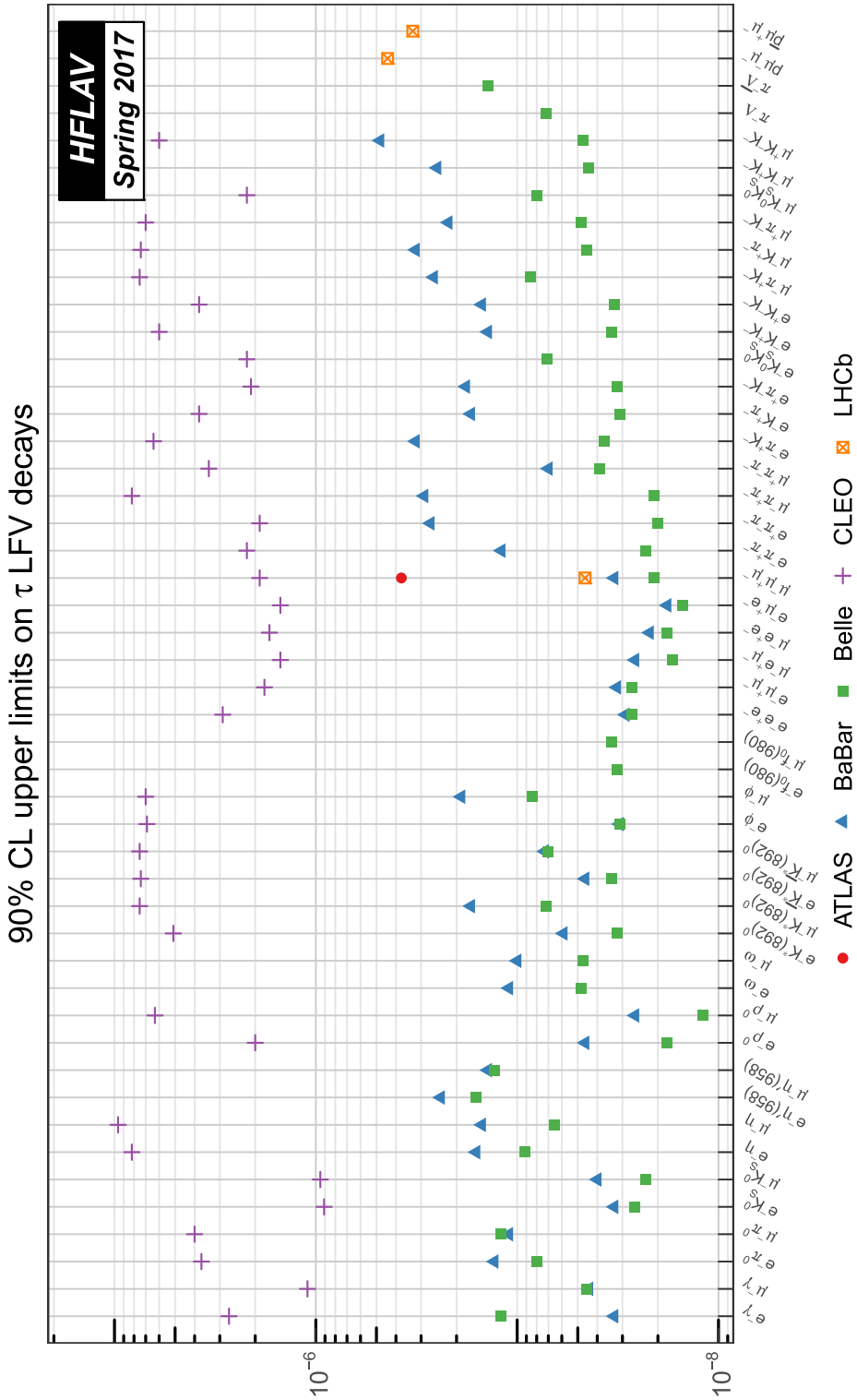

Fig. 221 Tau lepton-flavor-violating branching fraction upper limits summary plot. In order to appreciate the physics reach improvement over time, the plot includes also the CLEO upper limits reported by PDG 2016 [6]

The CL_s value is defined as the ratio between the confidence level for the signal plus background hypothesis and the confidence level for the background hypothesis:

$$\mathrm{CL}_s = \frac{\mathrm{CL}_{s+b}}{\mathrm{CL}_b}. \tag{297}$$

When multiple results are combined, the PDFs in Eqs. (295) and (296) are the product of the individual PDFs,

$$\mathrm{CL}_s = \frac{\prod_{i=1}^{N} \sum_{n=0}^{n_i} \frac{e^{-(s_i+b_i)}(s_i+b_i)^n}{n!}}{\prod_{i=1}^{N} \sum_{n=0}^{n_i} \frac{e^{-b_i} b_i^n}{n!}}$$

Table 318 Combinations of upper limits on lepton flavour violating τ decay modes. The modes are grouped according to the properties of their final states. Modes with baryon number violation are labelled with "BNV"

Decay mode	Category	90% CL limit	Refs.
$\Gamma_{156} = e^-\gamma$	$\ell\gamma$	$5.4 \cdot 10^{-8}$	[1425,1426]
$\Gamma_{157} = \mu^-\gamma$		$5.0 \cdot 10^{-8}$	[1425,1426]
$\Gamma_{158} = e^-\pi^0$	ℓP^0	$4.9 \cdot 10^{-8}$	[1427,1428]
$\Gamma_{159} = \mu^-\pi^0$		$3.6 \cdot 10^{-8}$	[1427,1428]
$\Gamma_{160} = e^- K_S^0$		$1.4 \cdot 10^{-8}$	[1429,1430]
$\Gamma_{161} = \mu^- K_S^0$		$1.5 \cdot 10^{-8}$	[1429,1430]
$\Gamma_{162} = e^-\eta$		$5.5 \cdot 10^{-8}$	[1427,1428]
$\Gamma_{163} = \mu^-\eta$		$3.8 \cdot 10^{-8}$	[1427,1428]
$\Gamma_{172} = e^-\eta'(958)$		$9.9 \cdot 10^{-8}$	[1427,1428]
$\Gamma_{173} = \mu^-\eta'(958)$		$6.3 \cdot 10^{-8}$	[1427,1428]
$\Gamma_{164} = e^-\rho^0$	ℓV^0	$1.5 \cdot 10^{-8}$	[1431,1432]
$\Gamma_{165} = \mu^-\rho^0$		$1.5 \cdot 10^{-8}$	[1431,1432]
$\Gamma_{166} = e^-\omega$		$3.3 \cdot 10^{-8}$	[1432,1433]
$\Gamma_{167} = \mu^-\omega$		$4.0 \cdot 10^{-8}$	[1432,1433]
$\Gamma_{168} = e^- K^*(892)^0$		$2.3 \cdot 10^{-8}$	[1431,1432]
$\Gamma_{169} = \mu^- K^*(892)^0$		$6.0 \cdot 10^{-8}$	[1431,1432]
$\Gamma_{170} = e^- \bar{K}^*(892)^0$		$2.2 \cdot 10^{-8}$	[1431,1432]
$\Gamma_{171} = \mu^- \bar{K}^*(892)^0$		$4.2 \cdot 10^{-8}$	[1431,1432]
$\Gamma_{176} = e^-\phi$		$2.0 \cdot 10^{-8}$	[1431,1432]
$\Gamma_{177} = \mu^-\phi$		$6.8 \cdot 10^{-8}$	[1431,1432]
$\Gamma_{178} = e^-e^+e^-$	$\ell\ell\ell$	$1.4 \cdot 10^{-8}$	[1435,1436]
$\Gamma_{179} = e^-\mu^+\mu^-$		$1.6 \cdot 10^{-8}$	[1435,1436]
$\Gamma_{180} = \mu^-e^+\mu^-$		$9.8 \cdot 10^{-9}$	[1435,1436]
$\Gamma_{181} = \mu^-e^+e^-$		$1.1 \cdot 10^{-8}$	[1435,1436]
$\Gamma_{182} = e^-\mu^+e^-$		$8.4 \cdot 10^{-9}$	[1435,1436]
$\Gamma_{183} = \mu^-\mu^+\mu^-$		$1.2 \cdot 10^{-8}$	[1435,1436,1438]

$$\times \frac{\prod_{j=1}^{N}\left[s_i S_i(x_{ij}) + b_i B_i(x_{ij})\right]}{\prod_{j=1}^{N} B_i(x_{ij})}, \tag{298}$$

where N is the number of results (or channels), and, for each channel i, n_i is the number of observed candidates, x_{ij} are the values of the discriminating variables (with index j), s_i and b_i are the number of signal and background events and S_i, B_i are the probability distribution functions of the discriminating variables. The discriminating variables x_{ij} are assumed to be uncorrelated. The expected signal s_i is related to the τ lepton branching fraction $B(\tau \to f_i)$ into the searched final state f_i by $s_i = N_i \epsilon_i B(\tau \to f_i)$, where N_i is the number of produced τ leptons and ϵ_i is the detection efficiency for observing the decay $\tau \to f_i$. For e^+e^- experiments, $N_i = 2\mathcal{L}_i \sigma_{\tau\tau}$, where $\mathcal{L}_i$ is the integrated luminosity and $\sigma_{\tau\tau}$ is the τ pair production cross section $\sigma(e^+e^- \to \tau^+\tau^-)$ [1444]. In experiments where τ leptons are produced in more complex multiple reactions, the effective N_i is typically estimated with Monte Carlo simulations calibrated with related data yields.

The extraction of the upper limits is performed using the code provided by Tom Junk [1445]. The systematic uncertainties are modeled in the Monte Carlo toy experiments by convolving the S_i and B_i PDFs with Gaussian distributions corresponding to the nuisance parameters.

Table 318 reports the HFLAV combinations of the τ LFV limits. Since there is negligible gain in combining limits of very different strength, the combinations do not include the CLEO searches and do not include results where the single event sensitivity is more than a factor of 5 lower than the value for the search with the best limit.

Figure 222 reports a graphical representation of the limits in Table 318. The published information that has been used to obtain these limits is reported in Table 319.

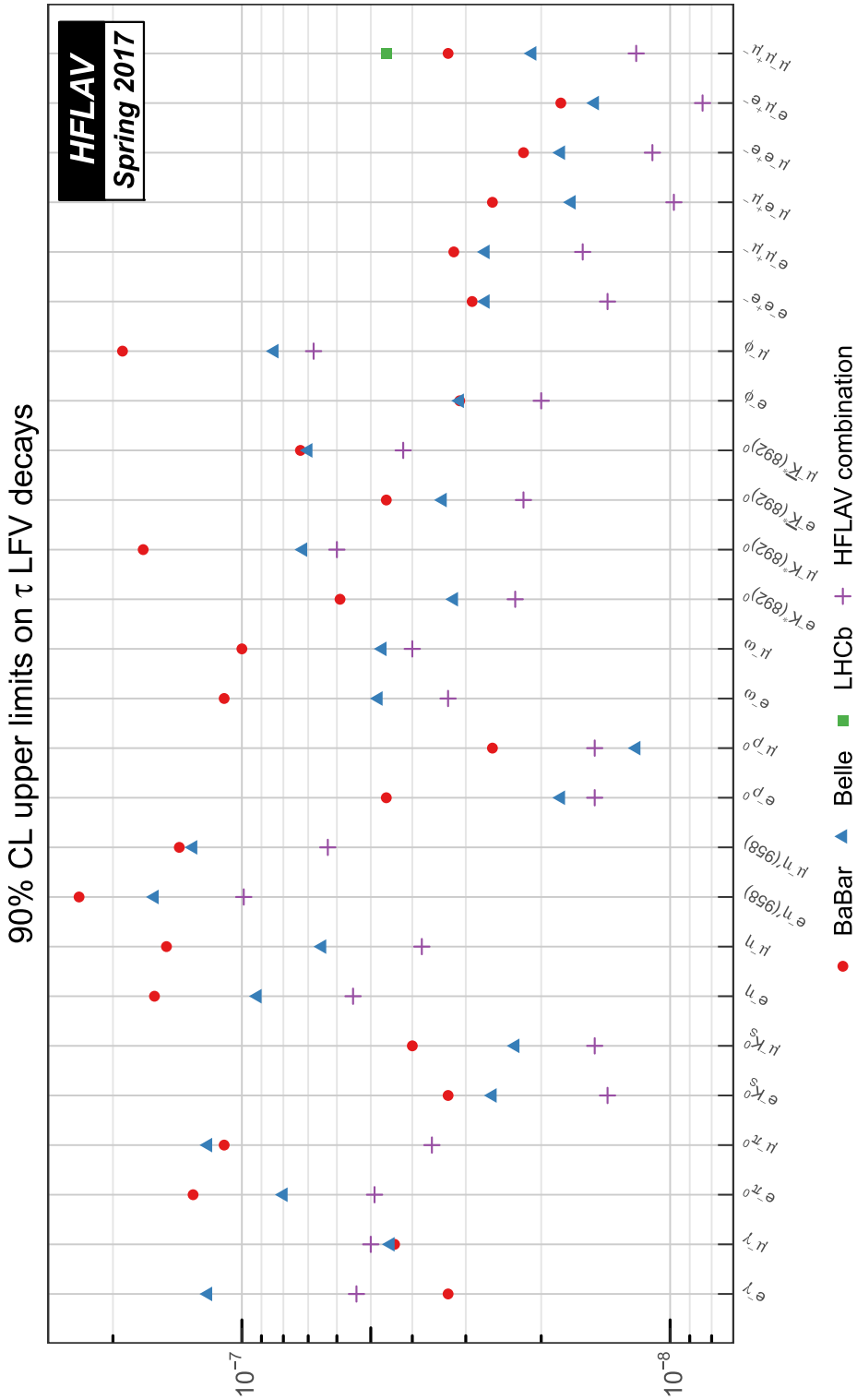

Fig. 222 Tau lepton-flavour-violating branching fraction upper limits combinations summary plot. For each channel we report the HFLAV combined limit, and the experimental published limits. In some cases, the combined limit is weaker than the limit published by a single experiment. This arises since the CL_s method used in the combination can be more conservative compared to other legitimate methods, especially when the number of observed events fluctuates below the expected background

Table 319 Published information that has been used to re-compute upper limits with the CL_s method, i.e. the number of τ leptons produced, the signal detection efficiency and its uncertainty, the number of expected background events and its uncertainty, and the number of observed events. The uncertainty on the efficiency includes the minor uncertainty contribution on the number of τ leptons (typically originating on the uncertainties on the integrated luminosity and on the production cross-section). The additional limit used in the combinations (from LHCb) has been originally determined with the CL_s method

Decay mode	Exp.	Refs.	N_τ(millions)	Efficiency (%)	N_{bkg}	N_{obs}
$\Gamma_{156} = e^-\gamma$	BaBar	[1425]	963	3.90 ± 0.30	1.60 ± 0.40	0
$\Gamma_{156} = e^-\gamma$	Belle	[1426]	983	3.00 ± 0.10	5.14 ± 3.30	5
$\Gamma_{157} = \mu^-\gamma$	BaBar	[1425]	963	6.10 ± 0.50	3.60 ± 0.70	2
$\Gamma_{157} = \mu^-\gamma$	Belle	[1426]	983	5.07 ± 0.20	13.90 ± 5.00	10
$\Gamma_{158} = e^-\pi^0$	BaBar	[1427]	339	2.83 ± 0.25	0.17 ± 0.04	0
$\Gamma_{158} = e^-\pi^0$	Belle	[1428]	401	3.93 ± 0.18	0.20 ± 0.20	0
$\Gamma_{159} = \mu^-\pi^0$	BaBar	[1427]	339	4.75 ± 0.37	1.33 ± 0.15	1
$\Gamma_{159} = \mu^-\pi^0$	Belle	[1428]	401	4.53 ± 0.20	0.58 ± 0.34	1
$\Gamma_{160} = e^-K^0_S$	BaBar	[1429]	862	9.10 ± 1.73	0.59 ± 0.25	1
$\Gamma_{160} = e^-K^0_S$	Belle	[1430]	1274	10.20 ± 0.67	0.18 ± 0.18	0
$\Gamma_{161} = \mu^-K^0_S$	BaBar	[1429]	862	6.14 ± 0.20	0.30 ± 0.18	1
$\Gamma_{161} = \mu^-K^0_S$	Belle	[1430]	1274	10.70 ± 0.73	0.35 ± 0.21	0
$\Gamma_{162} = e^-\eta$	BaBar	[1427]	339	2.12 ± 0.20	0.22 ± 0.05	0
$\Gamma_{162} = e^-\eta$	Belle	[1428]	401	2.87 ± 0.20	0.78 ± 0.78	0
$\Gamma_{163} = \mu^-\eta$	BaBar	[1427]	339	3.59 ± 0.41	0.75 ± 0.08	1
$\Gamma_{163} = \mu^-\eta$	Belle	[1428]	401	4.08 ± 0.28	0.64 ± 0.04	0
$\Gamma_{172} = e^-\eta'(958)$	BaBar	[1427]	339	1.53 ± 0.16	0.12 ± 0.03	0
$\Gamma_{172} = e^-\eta'(958)$	Belle	[1428]	401	1.59 ± 0.13	0.01 ± 0.41	0
$\Gamma_{173} = \mu^-\eta'(958)$	BaBar	[1427]	339	2.18 ± 0.26	0.49 ± 0.26	0
$\Gamma_{173} = \mu^-\eta'(958)$	Belle	[1428]	401	2.47 ± 0.20	0.23 ± 0.46	0
$\Gamma_{164} = e^-\rho^0$	BaBar	[1431]	829	7.31 ± 0.20	1.32 ± 0.17	1
$\Gamma_{164} = e^-\rho^0$	Belle	[1432]	1554	7.58 ± 0.41	0.29 ± 0.15	0
$\Gamma_{165} = \mu^-\rho^0$	BaBar	[1431]	829	4.52 ± 0.40	2.04 ± 0.19	0
$\Gamma_{165} = \mu^-\rho^0$	Belle	[1432]	1554	7.09 ± 0.37	1.48 ± 0.35	0
$\Gamma_{166} = e^-\omega$	BaBar	[1433]	829	2.96 ± 0.13	0.35 ± 0.06	0
$\Gamma_{166} = e^-\omega$	Belle	[1432]	1554	2.92 ± 0.18	0.30 ± 0.14	0
$\Gamma_{167} = \mu^-\omega$	BaBar	[1433]	829	2.56 ± 0.16	0.73 ± 0.03	0
$\Gamma_{167} = \mu^-\omega$	Belle	[1432]	1554	2.38 ± 0.14	0.72 ± 0.18	0
$\Gamma_{168} = e^-K^*(892)^0$	BaBar	[1431]	829	8.00 ± 0.20	1.65 ± 0.23	2
$\Gamma_{168} = e^-K^*(892)^0$	Belle	[1432]	1554	4.37 ± 0.24	0.29 ± 0.14	0
$\Gamma_{169} = \mu^-K^*(892)^0$	BaBar	[1431]	829	4.60 ± 0.40	1.79 ± 0.21	4
$\Gamma_{169} = \mu^-K^*(892)^0$	Belle	[1432]	1554	3.39 ± 0.19	0.53 ± 0.20	1
$\Gamma_{170} = e^-\bar{K}^*(892)^0$	BaBar	[1431]	829	7.80 ± 0.20	2.76 ± 0.28	2
$\Gamma_{170} = e^-\bar{K}^*(892)^0$	Belle	[1432]	1554	4.41 ± 0.25	0.08 ± 0.08	0
$\Gamma_{171} = \mu^-\bar{K}^*(892)^0$	BaBar	[1431]	829	4.10 ± 0.30	1.72 ± 0.17	1
$\Gamma_{171} = \mu^-\bar{K}^*(892)^0$	Belle	[1432]	1554	3.60 ± 0.20	0.45 ± 0.17	1
$\Gamma_{176} = e^-\phi$	BaBar	[1431]	829	6.40 ± 0.20	0.68 ± 0.12	0
$\Gamma_{176} = e^-\phi$	Belle	[1432]	1554	4.18 ± 0.25	0.47 ± 0.19	0
$\Gamma_{177} = \mu^-\phi$	BaBar	[1431]	829	5.20 ± 0.30	2.76 ± 0.16	6
$\Gamma_{177} = \mu^-\phi$	Belle	[1432]	1554	3.21 ± 0.19	0.06 ± 0.06	1
$\Gamma_{178} = e^-e^+e^-$	BaBar	[1435]	868	8.60 ± 0.20	0.12 ± 0.02	0
$\Gamma_{178} = e^-e^+e^-$	Belle	[1436]	1437	6.00 ± 0.59	0.21 ± 0.15	0

Table 319 continued

Decay mode	Exp.	Refs.	N_τ (millions)	Efficiency (%)	$N_{\rm bkg}$	$N_{\rm obs}$
$\Gamma_{179} = e^-\mu^+\mu^-$	BaBar	[1435]	868	6.40 ± 0.40	0.54 ± 0.14	0
$\Gamma_{179} = e^-\mu^+\mu^-$	Belle	[1436]	1437	6.10 ± 0.58	0.10 ± 0.04	0
$\Gamma_{180} = \mu^-e^+\mu^-$	BaBar	[1435]	868	10.20 ± 0.60	0.03 ± 0.02	0
$\Gamma_{180} = \mu^-e^+\mu^-$	Belle	[1436]	1437	10.10 ± 0.77	0.02 ± 0.02	0
$\Gamma_{181} = \mu^-e^+e^-$	BaBar	[1435]	868	8.80 ± 0.50	0.64 ± 0.19	0
$\Gamma_{181} = \mu^-e^+e^-$	Belle	[1436]	1437	9.30 ± 0.73	0.04 ± 0.04	0
$\Gamma_{182} = e^-\mu^+e^-$	BaBar	[1435]	868	12.70 ± 0.70	0.34 ± 0.12	0
$\Gamma_{182} = e^-\mu^+e^-$	Belle	[1436]	1437	11.50 ± 0.89	0.01 ± 0.01	0
$\Gamma_{183} = \mu^-\mu^+\mu^-$	BaBar	[1435]	868	6.60 ± 0.60	0.44 ± 0.17	0
$\Gamma_{183} = \mu^-\mu^+\mu^-$	Belle	[1436]	1437	7.60 ± 0.56	0.13 ± 0.20	0

10 Summary

This article provides updated world averages of measurements of b-hadron, c-hadron, and τ-lepton properties using results available through Summer 2016. A small selection of highlights of the results described in Sects. 3–9 is given in Table 320.

Since the previous version of this document [5], the b-hadron lifetime and mixing averages have mostly made gradual progress in precision. Notable exceptions with significant improvement are the averages for the mass difference in the $B^0 - \bar{B}^0$ system (Δm_d) and the CP violation parameter in $B_s^0 - \bar{B}_s^0$ system ($|q_s/p_s|$). In total eleven new results (of which ten from the LHC Run 1 data and one from the Tevatron data) have been incorporated in these averages. On the other hand, all results that remained unpublished and for which there is no publication plan, have been removed from the averages.

The lifetime hierarchy for the most abundant weakly decaying b-hadron species is well established, with impressive precisions of 5 fs or less for the most common B^0, B^+ and B_s^0 mesons, and compatible with the expectations from the Heavy Quark Expansion. However, statistics are still lacking for b baryons heavier than Λ_b^0 (Ξ_b^-, Ξ_b^0, Ω_b, and all other yet-to-be-discovered b baryons), but this will surely come from the LHC with sufficient time. A sizable value of the decay width difference in the $B_s^0 - \bar{B}_s^0$ system is measured with a relative precision of 7% and is well predicted by the Standard Model (SM). In contrast, the experimental results for the decay width difference in the $B^0 - \bar{B}^0$ system are not yet precise enough to distinguish the small (expected) value from zero. The mass differences in both systems are known very accurately, to the (few) per mil level. On the other hand, CP violation in the mixing of either system has not been observed yet, with asymmetries known within a couple per mil but still consistent both with zero and their SM predictions. A similar conclusion holds for the CP violation induced by B_s^0 mixing in the $b \to c\bar{c}s$ transition, although in this case the experimental precision on the corresponding weak phase is an order of magnitude larger, but now becoming just smaller than the SM central value. Many measurements are still dominated by statistical uncertainties and will improve once new results from the LHC Run 2 become available.

The measurement of $\sin 2\beta \equiv \sin 2\phi_1$ from $b \to c\bar{c}s$ transitions such as $B^0 \to J/\psi K_S^0$ has reached $< 2.5\,\%$ precision: $\sin 2\beta \equiv \sin 2\phi_1 = 0.691 \pm 0.017$. Measurements of the same parameter using different quark-level processes provide a consistency test of the Standard Model and allow insight into possible new physics. All results among hadronic $b \to s$ penguin dominated decays of B^0 mesons are currently consistent with the Standard Model expectations. Measurements of CP violation parameters in $B_s^0 \to \phi\phi$ allow a similar comparison to the value of $\phi_s^{c\bar{c}s}$; again, results are consistent with the SM expectation (which in this case is very close to zero). Among measurements related to the Unitarity Triangle angle $\alpha \equiv \phi_2$, results from the $\rho\rho$ system allow constraints at the level of $\approx 6°$. These remain the strongest constraints, although results from all of BaBar, Belle and LHCb lead to good precision on the CP violation parameters in $B^0 \to \pi^+\pi^-$ decays. Knowledge of the third angle $\gamma \equiv \phi_3$ also continues to improve, with the current world average being $(74.0\,^{+5.8}_{-6.4})°$. The precision is expected to improve further as more data becomes available at LHCb and Belle II.

In semileptonic B meson decays, the anomalies reported in the last version of the document have remained: The discrepancy between $|V_{cb}|$ measured with inclusive and exclusive decays is of the order of 3σ (3.2σ for $|V_{cb}|$ from $\bar{B} \to D^*\ell^-\bar{\nu}_\ell$, 2.4σ for $|V_{cb}|$ from $\bar{B} \to D\ell^-\bar{\nu}_\ell$). The difference between $|V_{ub}|$ measured with inclusive decays $\bar{B} \to X_u\ell^-\bar{\nu}_\ell$ and $|V_{ub}|$ from $\bar{B} \to \pi\ell^-\bar{\nu}_\ell$ has risen to 3.6σ. An important new contribution to the determination

Table 320 Selected world averages. Where two uncertainties are given the first is statistical and the second is systematic, except where indicated otherwise

b-hadron lifetimes	
$\tau(B^0)$	1.520 ± 0.004 ps
$\tau(B^+)$	1.638 ± 0.004 ps
$\bar{\tau}(B_s^0) = 1/\Gamma_s$	1.505 ± 0.005 ps
$\tau(B_{s\mathrm{L}}^0)$	1.413 ± 0.006 ps
$\tau(B_{s\mathrm{H}}^0)$	1.609 ± 0.010 ps
$\tau(B_c^+)$	0.507 ± 0.009 ps
$\tau(\Lambda_b^0)$	1.470 ± 0.010 ps
$\tau(\Xi_b^-)$	1.571 ± 0.040 ps
$\tau(\Xi_b^0)$	1.479 ± 0.031 ps
$\tau(\Omega_b^-)$	$1.64^{+0.18}_{-0.17}$ ps
B^0 and B_s^0 mixing/CP violation parameters	
Δm_d	0.5064 ± 0.0019 ps^{-1}
$\Delta\Gamma_d/\Gamma_d$	-0.002 ± 0.010
$\lvert q_d/p_d \rvert$	1.0009 ± 0.0013
Δm_s	17.757 ± 0.021 ps^{-1}
$\Delta\Gamma_s$	$+0.086 \pm 0.006$ ps^{-1}
$\lvert q_s/p_s \rvert$	1.0003 ± 0.0014
$\phi_s^{c\bar{c}s}$	-0.030 ± 0.033
Parameters related to Unitarity Triangle angles	
$\sin 2\beta \equiv \sin 2\phi_1$	0.691 ± 0.017
$\beta \equiv \phi_1$	$(21.9 \pm 0.7)^\circ$
$-\eta S_{\phi K_S^0}$	$0.74^{+0.11}_{-0.13}$
$-\eta S_{\eta' K^0}$	0.63 ± 0.06
$-\eta S_{K_S^0 K_S^0 K_S^0}$	0.72 ± 0.19
$\phi_s(\phi\phi)$	$-0.17 \pm 0.15 \pm 0.03$ rad
$-\eta S_{J/\psi\pi^0}$	0.93 ± 0.15
$-\eta S_{D^+D^-}$	0.84 ± 0.12
$-\eta S_{J/\psi\rho^0}$	$0.66^{+0.13}_{-0.12}{}^{+0.09}_{-0.03}$
$S_{K^*\gamma}$	-0.16 ± 0.22
$(S_{\pi^+\pi^-}, C_{\pi^+\pi^-})$	$(-0.68 \pm 0.04, -0.27 \pm 0.04)$
$(S_{\rho^+\rho^-}, C_{\rho^+\rho^-})$	$(-0.14 \pm 0.13, 0.00 \pm 0.09)$
$a(D^{*\pm}\pi^\mp)$	-0.039 ± 0.010
$A_{CP}(B \to D_{CP+}K)$	0.111 ± 0.018
$A_{\mathrm{ADS}}(B \to D_{K\pi}K)$	-0.415 ± 0.055
$\gamma \equiv \phi_3$	$(74.0^{+5.8}_{-6.4})^\circ$
Semileptonic B decay parameters	
$\mathcal{B}(\bar{B}^0 \to D^{*+}\ell^-\bar{\nu}_\ell)$	$(4.88 \pm 0.10)\%$
$\mathcal{B}(B^- \to D^{*0}\ell^-\bar{\nu}_\ell)$	$(5.59 \pm 0.19)\%$
$\eta_{\mathrm{EW}}\mathcal{F}(1)\lvert V_{cb}\rvert$	$(35.61 \pm 0.43) \times 10^{-3}$
$\lvert V_{cb}\rvert$ from $\bar{B} \to D^*\ell^-\bar{\nu}_\ell$	$(39.05 \pm 0.47_{\mathrm{exp}} \pm 0.58_{\mathrm{th}}) \times 10^{-3}$
$\mathcal{B}(\bar{B}^0 \to D^+\ell^-\bar{\nu}_\ell)$	$(2.20 \pm 0.10)\%$
$\mathcal{B}(B^- \to D^0\ell^-\bar{\nu}_\ell)$	$(2.33 \pm 0.10)\%$
$\eta_{\mathrm{EW}}\mathcal{G}(1)\lvert V_{cb}\rvert$	$(41.57 \pm 1.00) \times 10^{-3}$
$\lvert V_{cb}\rvert$ from $\bar{B} \to D\ell^-\bar{\nu}_\ell$	$(39.18 \pm 0.94_{\mathrm{exp}} \pm 0.36_{\mathrm{th}}) \times 10^{-3}$

Table 320 continued

$\mathcal{B}(\bar{B} \to X_c \ell^- \bar{\nu}_\ell)$	$(10.65 \pm 0.16)\%$
$\mathcal{B}(\bar{B} \to X \ell^- \bar{\nu}_\ell)$	$(10.86 \pm 0.16)\%$
$\lvert V_{cb}\rvert$ from $\bar{B} \to X \ell^- \bar{\nu}_\ell$	$(42.19 \pm 0.78) \times 10^{-3}$
$\mathcal{B}(\bar{B} \to \pi \ell^- \bar{\nu}_\ell)$	$(1.50 \pm 0.06) \times 10^{-4}$
$\lvert V_{ub}\rvert$ from $\bar{B} \to \pi \ell^- \bar{\nu}_\ell$	$(3.67 \pm 0.15) \times 10^{-3}$
$\lvert V_{ub}\rvert$ from $\bar{B} \to X_u \ell^- \bar{\nu}_\ell$	$(4.52 \pm 0.15_{\text{exp}} \pm 0.13_{\text{th}}) \times 10^{-3}$
$\lvert V_{ub}\rvert/\lvert V_{cb}\rvert$ from $\Lambda_b^0 \to p\mu^- \bar{\nu}_\mu / \Lambda_b^0 \to \Lambda_c^+ \mu^- \bar{\nu}_\mu$	$0.080 \pm 0.004_{\text{exp}} \pm 0.004_{\text{th}}$
$\mathcal{R}(D) = \mathcal{B}(B \to D\tau\nu_\tau)/\mathcal{B}(B \to D\ell\nu_\ell)$	0.403 ± 0.047
$\mathcal{R}(D^*) = \mathcal{B}(B \to D^*\tau\nu_\tau)/\mathcal{B}(B \to D^*\ell\nu_\ell)$	0.310 ± 0.017
b-hadron to charmed hadron decays	
$\mathcal{B}(\bar{B}^0 \to D^+\pi^-)$	$(2.65 \pm 0.15) \times 10^{-3}$
$\mathcal{B}(B^- \to D^0\pi^-)$	$(4.75 \pm 0.19) \times 10^{-3}$
$\mathcal{B}(\bar{B}_s^0 \to D_s^+\pi^-)$	$(3.03 \pm 0.25) \times 10^{-3}$
$\mathcal{B}(\Lambda_b^0 \to \Lambda_c^+\pi^-)$	$(4.30^{+0.36}_{-0.35}) \times 10^{-3}$
$\mathcal{B}(\bar{B}^0 \to J/\psi \bar{K}^0)$	$(0.863 \pm 0.035) \times 10^{-3}$
$\mathcal{B}(B^- \to J/\psi K^-)$	$(1.028 \pm 0.040) \times 10^{-3}$
$\mathcal{B}(\bar{B}_s^0 \to J/\psi \phi)$	$(1.00 \pm 0.09) \times 10^{-3}$
Rare B decays	
$\mathcal{B}(B_s^0 \to \mu^+\mu^-)$	$\left(2.8\,^{+0.07}_{-0.06}\right) \times 10^{-9}$
$\mathcal{B}(B^0 \to \mu^+\mu^-)$	$\left(0.39\,^{+0.16}_{-0.14}\right) \times 10^{-9}$
$\mathcal{B}(B \to X_s\gamma)$ $(E_\gamma > 1.6\ \text{GeV})$	$(3.32 \pm 0.16) \times 10^{-4}$
$\mathcal{B}(B^+ \to \tau^+\nu)$	$(1.06 \pm 0.19) \times 10^{-4}$
$R_K = \mathcal{B}(B^+ \to K^+\mu^+\mu^-)/\mathcal{B}(B^+ \to K^+e^+e^-)$ in $1.0 < m^2_{\ell^+\ell^-} < 6.0\ \text{GeV}^2/c^4$	$0.745^{+0.090}_{-0.074} \pm 0.036$
$A_{CP}(B^0 \to K^+\pi^-)$, $A_{CP}(B^+ \to K^+\pi^0)$	$-0.082 \pm 0.006, 0.040 \pm 0.021$
$A_{CP}(B_s^0 \to K^-\pi^+)$	0.26 ± 0.04
Longitudinal polarisation of $B^0 \to \phi K^{*0}$	0.497 ± 0.017
Longitudinal polarisation of $B_s^0 \to \phi\phi$	0.361 ± 0.022
Observables in $B^0 \to K^{*0}\mu^+\mu^-$ decays in bins of $q^2 = m^2(\mu^+\mu^-)$	See Sect. 7.5
D^0 mixing and CP violation parameters	
x	$(0.32 \pm 0.14)\%$
y	$(0.69\,^{+0.06}_{-0.07})\%$
$\delta_{K\pi}$	$(15.2\,^{+7.6}_{-10.0})^\circ$
A_D	$(-0.88 \pm 0.99)\%$
$\lvert q/p\rvert$	$0.89\,^{+0.08}_{-0.07}$
ϕ	$(-12.9\,^{+9.9}_{-8.7})^\circ$
x_{12} (no direct CP violation)	$(0.41\,^{+0.14}_{-0.15})\%$
y_{12} (no direct CP violation)	$(0.61 \pm 0.07)\%$
ϕ_{12} (no direct CP violation)	$(-0.17 \pm 1.8)^\circ$
a_{CP}^{ind}	$(0.030 \pm 0.026)\%$
$\Delta a_{CP}^{\text{dir}}$	$(-0.134 \pm 0.070)\%$
Leptonic D decays	
f_D	(203.7 ± 4.9) MeV
f_{D_s}	(257.1 ± 4.6) MeV

Table 320 continued

$\|V_{cd}\|$	$0.2164 \pm 0.0050_{\text{exp}} \pm 0.0015_{\text{LQCD}}$
$\|V_{cs}\|$	$1.006 \pm 0.018_{\text{exp}} \pm 0.005_{\text{LQCD}}$
Benchmark charm branching fractions	
$\mathcal{B}(\Lambda_c^+ \to pK^-\pi^+)$	$(6.46 \pm 0.24)\%$
$\mathcal{B}(D^0 \to K^-\pi^+)$	$(3.962 \pm 0.017 \pm 0.038 \pm 0.027_{\text{FSR}})\%$
$\mathcal{B}(D^0 \to K^+\pi^-)/\mathcal{B}(D^0 \to K^-\pi^+)$	$(0.349^{+0.004}_{-0.003})\%$
$\mathcal{B}(D_s^+ \to K^+K^-\pi^+)$	$(5.44 \pm 0.09 \pm 0.11)\%$
τ parameters, lepton universality, and $\|V_{us}\|$	
g_τ/g_μ	1.0010 ± 0.0015
g_τ/g_e	1.0029 ± 0.0015
g_μ/g_e	1.0019 ± 0.0014
$\mathcal{B}_e^{\text{uni}}$	$17.815 \pm 0.023\%$
R_{had}	3.6349 ± 0.0082
$\|V_{us}\|$ from sum of strange branching fractions	0.2186 ± 0.0021
$\|V_{us}\|$ from $\mathcal{B}(\tau^- \to K^-\nu_\tau)/\mathcal{B}(\tau^- \to \pi^-\nu_\tau)$	0.2236 ± 0.0018
$\|V_{us}\|$ τ average	0.2216 ± 0.0015

of the values of $|V_{ub}|$ and $|V_{cb}|$ comes from exclusive b-baryon decays. The largest anomaly however is observed in $B \to D^{(*)}\tau\nu_\tau$ decays: The combined discrepancy of the measured values of $\mathcal{R}(D^*)$ and $\mathcal{R}(D)$ to their standard model expectations is found to be 3.9σ.

The most important new measurements of rare b-hadron decays are coming from the LHC. Precision measurements of B_s^0 decays are particularly noteworthy, including several measurements of the longitudinal polarisation fraction from LHCb. ATLAS, CMS and LHCb have significantly improved the sensitivity to the $B_{(s)}^0 \to \mu^+\mu^-$ decays. Recently, CMS and LHCb published a combined analysis that allowed the first observation of the $B_s^0 \to \mu^+\mu^-$ decay to be obtained, and provided three standard deviations evidence of the $B^0 \to \mu^+\mu^-$ decay. The results are compatible with the SM predictions, and yield constrains on the parameter space of new physics models. CMS and LHCb have also performed angular analyses of the $B^0 \to K^{*0}\mu^+\mu^-$ decay, complementing, extending and improving on the precision of results from BaBar and Belle. One of the observables measured by LHCb, P_5', differs from the SM prediction by 3.7σ in one of the $m^2_{\mu^+\mu^-}$ intervals; results from Belle on this observable are consistent but less precise. Improved measurements from LHCb and other experiments are keenly anticipated. A measurement of the ratio of branching fractions of $B^+ \to K^+\mu^+\mu^-$ and $B^+ \to K^+e^+e^-$ decays (R_K) has been made by LHCb. In the low $m^2_{\ell^+\ell^-}$ region, it differs from the standard model prediction by 2.6σ. Among the CP violating observables in rare decays, the "$K\pi$ puzzle" persists, and important new results have appeared in three-body decays. LHCb has produced many other results on a wide variety of decays, including b-baryon and B_c^+-meson decays. Belle and BaBar continue to produce new results though their output rates are dwindling. It will still be some years before we see new results from the upgraded SuperKEKB B factory and the Belle II experiment.

About 800 b to charm results from BaBar, Belle, CDF, D0, LHCb, CMS, and ATLAS reported in more than 200 papers are compiled in a list of over 600 averages. The huge samples of b hadrons that are available in contemporary experiments allows measurements of decays to states with open or hidden charm content with unprecedented precision. In addition to improvements in precision for branching fractions of $\bar{B}^0$ and B^- mesons, many new decay modes have been discovered. In addition, there is a rapidly increasing set of measurements available for $\bar{B}_s^0$ and B_c^- mesons as well as for b baryon decays.

In the charm sector, $D^0 - \bar{D}^0$ mixing is now well-established and the emphasis has shifted to searching for CP violation. Measurements of 49 observables from the E791, FOCUS, Belle, BaBar, CLEO, BESIII, CDF, and LHCb experiments are input into a global fit for 10 underlying parameters, and the no-mixing hypothesis is excluded at a confidence level $> 11.5\sigma$. The mixing parameters x and y individually differ from zero by 1.9σ and 9.4σ, respectively. The world average value for the observable y_{CP} is positive, indicating that the CP-even state is shorter-lived as in the $K^0 - \bar{K}^0$ system. The CP violation parameters $|q/p|$ and ϕ are consistent with the no-CP violation hypothesis within 1σ. Thus there is no evidence for CP violation arising from mixing ($|q/p| \neq 1$) or from a phase difference between the mixing amplitude and a direct decay amplitude ($\phi \neq 0$). In addition, the most recent data indicates no direct CP violation

in $D^0 \to K^+K^-/\pi^+\pi^-$ decays; performing a global fit to all relevant measurements gives $\Delta a_{CP}^{\rm dir} = (-0.134 \pm 0.070)\%$. The world's most precise measurements of $|V_{cd}|$ and $|V_{cs}|$ are obtained from leptonic $D^+ \to \mu^+\nu$ and $D_s^+ \to \mu^+\nu/\tau^+\nu$ decays, respectively. These measurements have theoretical uncertainties arising from decay constants. However, calculations of decay constants within lattice QCD have improved such that the theory error is $<1/3$ the experimental errors of the measurements.

Since 2016, HFLAV provides the τ branching fraction fit averages for the PDG Review of Particle Physics. For the PDG, a unitarity constrained variant of the fit is performed, using only inputs that are published and included in the PDG. Two preliminary results used in the HFLAV 2014 report have been removed both in the HFLAV and in the PDG variants of the fit. A few minor imperfections of the 2014 fit have been corrected. There are no non-negligible changes to the lepton universality tests and to the $|V_{us}|$ determinations from the τ branching fractions. There is still a large discrepancy between $|V_{us}|$ from τ, $|V_{us}|$ from kaons and $|V_{us}|$ from $|V_{ud}|$ and CKM matrix unitarity. On this topic, recent studies [1423,1424] claim to get a more reliable theory uncertainty on $|V_{us}|$ with a revised calculation method that uses also the τ spectral functions. Just one more τ lepton-flavour-violating branching fraction upper limit has been published, which does not change the computed combined related limit. The list of limits and their combinations has been revised to remove old preliminary results.

Acknowledgements We are grateful for the strong support of the ATLAS, BaBar, Belle, BESIII, CLEO(c), CDF, CMS, D0 and LHCb collaborations, without whom this compilation of results and world averages would not have been possible. The success of these experiments in turn would not have been possible without the excellent operations of the BEPC, CESR, KEKB, LHC, PEP-II, and Tevatron accelerators. We also recognise the interplay between theoretical and experimental communities that has provided a stimulus for many of the measurements in this document. Our averages and this compilation have benefitted greatly from contributions to the Heavy Flavor Averaging Group from numerous individuals. We thank David Kirkby, Yoshihide Sakai, Simon Eidelman, Soeren Prell, and Gianluca Cavoto for their past leadership of HFLAV. We are grateful to Paolo Gambino and Bob Kowalewski for assistance with averages that appear in Sect. 5; to Ruslan Chistov, Lawrence Gibbons, Bostjan Golob, Milind Purohit, and Patrick Roudeau for significant contributions to Sect. 8; and to Michel Davier for providing valuable input to Sect. 9. We especially thank the following for their careful review of the text in preparing this paper for publication: Vanya Belyaev, Guennadi Borissov, Jolanta Brodzicka, Paoti Chang, Paolo Gambino, Martin Jung, Andreas Kronfeld, George Lafferty, Alexander Lenz, Zoltan Ligeti, David London, Vera Lüth, Alexey Petrov, Antonio Pich, and Fernando Martinez Vidal. Finally, we thank the SLAC National Accelerator Laboratory for providing crucial computing resources and support to HFLAV.

References

1. N. Cabibbo, Phys. Rev. Lett. **10**, 531 (1963). https://doi.org/10.1103/PhysRevLett.10.531
2. M. Kobayashi, T. Maskawa, Progr. Theor. Phys. **49**, 652 (1973). https://doi.org/10.1143/PTP.49.652
3. D. Abbaneo et al. (ALEPH, CDF, DELPHI, L3, OPAL, and SLD collaborations), CERN-EP-2000-096 (2000). arXiv:hep-ex/0009052
4. D. Abbaneo et al. (ALEPH, CDF, DELPHI, L3, OPAL, and SLD collaborations), CERN-EP-2001-050 (2001). arXiv:hep-ex/0112028
5. Y. Amhis et al. (Heavy Flavor Averaging Group) (2014). arXiv:1412.7515 [hep-ex]
6. C. Patrignani et al., Particle data group. Chin. Phys. C **40**, 100001 (2016). https://doi.org/10.10z88/1674-1137/40/10/100001
7. J.P. Alexander et al., CLEO collaboration. Phys. Rev. Lett. **86**, 2737 (2001). https://doi.org/10.1103/PhysRevLett.86.2737. arXiv:hep-ex/0006002
8. S.B. Athar et al., CLEO collaboration. Phys. Rev. D **66**, 052003 (2002). https://doi.org/10.1103/PhysRevD.66.052003. arXiv:hep-ex/0202033
9. N.C. Hastings et al., Belle collaboration. Phys. Rev. D **67**, 052004 (2003). https://doi.org/10.1103/PhysRevD.67.052004. arXiv:hep-ex/0212033
10. B. Aubert et al., BaBar collaboration. Phys. Rev. Lett. **94**, 141801 (2005). https://doi.org/10.1103/PhysRevLett.94.141801. arXiv:hep-ex/0412062
11. B. Barish et al., CLEO collaboration. Phys. Rev. D **51**, 1014 (1995). https://doi.org/10.1103/PhysRevD.51.1014. arXiv:hep-ex/9406005
12. B. Aubert et al., BaBar collaboration. Phys. Rev. Lett. **95**, 042001 (2005). https://doi.org/10.1103/PhysRevLett.95.042001. arXiv:hep-ex/0504001
13. B. Aubert et al., BaBar collaboration. Phys. Rev. Lett. **96**, 232001 (2006). https://doi.org/10.1103/PhysRevLett.96.232001. arXiv:hep-ex/0604031
14. A. Sokolov et al., Belle collaboration. Phys. Rev. D **75**, 071103 (2007). https://doi.org/10.1103/PhysRevD.75.071103. arXiv:hep-ex/0611026
15. B. Aubert et al., BaBar collaboration. Phys. Rev. D **78**, 112002 (2008). https://doi.org/10.1103/PhysRevD.78.112002. arXiv:0807.2014 [hep-ex]
16. B. Barish et al., CLEO collaboration. Phys. Rev. Lett. **76**, 1570 (1996). https://doi.org/10.1103/PhysRevLett.76.1570
17. A. Drutskoy et al., Belle collaboration. Phys. Rev. D **81**, 112003 (2010). https://doi.org/10.1103/PhysRevD.81.112003. arXiv:1003.5885 [hep-ex]
18. G.S. Huang et al., CLEO collaboration. Phys. Rev. D **75**, 012002 (2007). https://doi.org/10.1103/PhysRevD.75.012002. arXiv:hep-ex/0610035
19. A. Drutskoy et al., Belle collaboration. Phys. Rev. Lett. **98**, 052001 (2007). https://doi.org/10.1103/PhysRevLett.98.052001. arXiv:hep-ex/0608015
20. S. Esen et al., Belle collaboration. Phys. Rev. D **87**, 031101 (2013). https://doi.org/10.1103/PhysRevD.87.031101. arXiv:1208.0323
21. M. Artuso et al., CLEO collaboration. Phys. Rev. Lett. **95**, 261801 (2005). https://doi.org/10.1103/PhysRevLett.95.261801. arXiv:hep-ex/0508047

22. K.F. Chen et al., Belle collaboration. Phys. Rev. Lett. **100**, 112001 (2008). https://doi.org/10.1103/PhysRevLett.100.112001. arXiv:0710.2577 [hep-ex]
23. A. Garmash et al., Belle collaboration. Phys. Rev. D **91**, 072003 (2015). https://doi.org/10.1103/PhysRevD.91.072003. arXiv:1403.0992 [hep-ex]
24. I. Adachi et al., Belle collaboration. Phys. Rev. Lett. **108**, 032001 (2012). https://doi.org/10.1103/PhysRevLett.108.032001. arXiv:1103.3419 [hep-ex]
25. P. Krokovny et al., Belle collaboration. Phys. Rev. D **88**, 052016 (2013). https://doi.org/10.1103/PhysRevD.88.052016. arXiv:1308.2646 [hep-ex]
26. R. Louvot, PhD thesis #5213, EPFL, Lausanne (2012). https://doi.org/10.5075/epfl-thesis-5213
27. J.P. Lees et al., BaBar collaboration. Phys. Rev. D **85**, 011101 (2012). https://doi.org/10.1103/PhysRevD.85.011101. arXiv:1110.5600 [hep-ex]
28. J. Li et al., Belle collaboration. Phys. Rev. Lett. **106**, 121802 (2011). https://doi.org/10.1103/PhysRevLett.106.121802. arXiv:1102.2759 [hep-ex]
29. R. Louvot et al., Belle collaboration. Phys. Rev. Lett. **102**, 021801 (2009). https://doi.org/10.1103/PhysRevLett.102.021801. arXiv:0809.2526 [hep-ex]
30. P. Abreu et al., DELPHI collaboration. Phys. Lett. B **289**, 199 (1992). https://doi.org/10.1016/0370-2693(92)91385-M
31. P.D. Acton et al., OPAL collaboration. Phys. Lett. B **295**, 357 (1992). https://doi.org/10.1016/0370-2693(92)91578-W
32. D. Buskulic et al., ALEPH collaboration. Phys. Lett. B **361**, 221 (1995). https://doi.org/10.1016/0370-2693(95)01173-N
33. P. Abreu et al., DELPHI collaboration. Z. Phys. C **68**, 375 (1995). https://doi.org/10.1007/BF01620713
34. R. Barate et al., ALEPH collaboration. Eur. Phys. J. C **2**, 197 (1998). https://doi.org/10.1007/s100520050133
35. D. Buskulic et al., ALEPH collaboration. Phys. Lett. B **384**, 449 (1996). https://doi.org/10.1016/0370-2693(96)00925-2
36. J. Abdallah et al., DELPHI collaboration. Eur. Phys. J. C **44**, 299 (2005). https://doi.org/10.1140/epjc/s2005-02388-4. arXiv:hep-ex/0510023
37. R. Barate et al., ALEPH collaboration. Eur. Phys. J. C **5**, 205 (1998). https://doi.org/10.1007/s100520050263
38. J. Abdallah et al., DELPHI collaboration. Phys. Lett. B **576**, 29 (2003). https://doi.org/10.1016/j.physletb.2003.09.070. arXiv:hep-ex/0311005
39. T. Affolder et al., CDF collaboration. Phys. Rev. Lett. **84**, 1663 (2000). https://doi.org/10.1103/PhysRevLett.84.1663. arXiv:hep-ex/9909011
40. T. Aaltonen et al., CDF collaboration. Phys. Rev. D **77**, 072003 (2008). https://doi.org/10.1103/PhysRevD.77.072003. arXiv:0801.4375 [hep-ex]
41. T. Aaltonen et al., CDF collaboration. Phys. Rev. D **79**, 032001 (2009). https://doi.org/10.1103/PhysRevD.79.032001. arXiv:0810.3213 [hep-ex]
42. F. Abe et al., CDF collaboration. Phys. Rev. D **60**, 092005 (1999). https://doi.org/10.1103/PhysRevD.60.092005
43. V.M. Abazov et al., D0 collaboration. Phys. Rev. Lett. **99**, 052001 (2007). https://doi.org/10.1103/PhysRevLett.99.052001. arXiv:0706.1690 [hep-ex]
44. V.M. Abazov et al., D0 collaboration. Phys. Rev. Lett. **101**, 232002 (2008). https://doi.org/10.1103/PhysRevLett.101.232002. arXiv:0808.4142 [hep-ex]
45. T. Aaltonen et al., CDF collaboration. Phys. Rev. D **80**, 072003 (2009). https://doi.org/10.1103/PhysRevD.80.072003. arXiv:0905.3123 [hep-ex]
46. R. Aaij et al. (LHCb collaboration), Phys. Rev. D **85**, 032008 (2012). https://doi.org/10.1103/PhysRevD.85.032008. arXiv:1111.2357 [hep-ex], with numerical results and full covariance matrix available at https://cdsweb.cern.ch/record/1390838
47. R. Aaij et al. (LHCb collaboration), JHEP **04**, 001 (2013). https://doi.org/10.1007/JHEP04(2013)001. arXiv:1301.5286 [hep-ex], with numerical results and full covariance matrix available at http://cdsweb.cern.ch/record/1507868
48. R. Aaij et al., LHCb collaboration. JHEP **08**, 143 (2014). https://doi.org/10.1007/JHEP08(2014)143. arXiv:1405.6842 [hep-ex]
49. G. Aad et al., ATLAS collaboration. Phys. Rev. Lett. **115**, 262001 (2015). https://doi.org/10.1103/PhysRevLett.115.262001. arXiv:1507.08925 [hep-ex]
50. X. Liu, W. Wang, Y. Xie, Phys. Rev. D **89**, 094010 (2014). https://doi.org/10.1103/PhysRevD.89.094010. arXiv:1309.0313 [hep-ph]
51. S. Schael et al., ALEPH, CDF, DELPHI, L3, OPAL, and SLD collaborations, LEP electroweak working group, SLD electroweak and heavy flavour working groups. Phys. Rep. **427**, 257 (2006). https://doi.org/10.1016/j.physrep.2005.12.006. arXiv:hep-ex/0509008
52. V.M. Abazov et al., D0 collaboration. Phys. Rev. D **74**, 092001 (2006). https://doi.org/10.1103/PhysRevD.74.092001. arXiv:hep-ex/0609014
53. D. Acosta et al., CDF collaboration. Phys. Rev. D **69**, 012002 (2004). https://doi.org/10.1103/PhysRevD.69.012002. arXiv:hep-ex/0309030
54. LHCb collaboration, LHCb-CONF-2013-011 (2013). https://cdsweb.cern.ch/record/1559262
55. M.A. Shifman, M.B. Voloshin, Sov. Phys. JETP **64**, 698 (1986)
56. J. Chay, H. Georgi, B. Grinstein, Phys. Lett. B **247**, 399 (1990). https://doi.org/10.1016/0370-2693(90)90916-T
57. I.I. Bigi, N.G. Uraltsev, A.I. Vainshtein, Phys. Lett. B **293**, 430 (1992). https://doi.org/10.1016/0370-2693(92)90908-M. arXiv:hep-ph/9207214. [Erratum ibid. **297**, 477 (1992). doi:10.1016/0370-2693(92)91287-JPhys.Lett.B]
58. M.A. Shifman (2000). arXiv:hep-ph/0009131
59. I.I.Y. Bigi, N. Uraltsev, Int. J. Mod. Phys. A **16**, 5201 (2001). https://doi.org/10.1142/S0217751X01005535. arXiv:hep-ph/0106346
60. T. Jubb, M. Kirk, A. Lenz, G. Tetlalmatzi-Xolocotzi, Nucl. Phys. B **915**, 431 (2017). https://doi.org/10.1016/j.nuclphysb.2016.12.020. arXiv:1603.07770 [hep-ph]
61. K.G. Wilson, Phys. Rev. **179**, 1499 (1969). https://doi.org/10.1103/PhysRev.179.1499
62. M. Ciuchini, E. Franco, V. Lubicz, F. Mescia, Nucl. Phys. B **625**, 211 (2002). https://doi.org/10.1016/S0550-3213(02)00006-8. arXiv:hep-ph/0110375
63. M. Beneke, G. Buchalla, C. Greub, A. Lenz, U. Nierste, Nucl. Phys. B **639**, 389 (2002). https://doi.org/10.1016/S0550-3213(02)00561-8. arXiv:hep-ph/0202106
64. E. Franco, V. Lubicz, F. Mescia, C. Tarantino, Nucl. Phys. B **633**, 212 (2002). https://doi.org/10.1016/S0550-3213(02)00262-6. arXiv:hep-ph/0203089
65. C. Tarantino, Eur. Phys. J. C **33**, S895 (2004). https://doi.org/10.1140/epjcd/s2003-03-1006-y. arXiv:hep-ph/0310241
66. F. Gabbiani, A.I. Onishchenko, A.A. Petrov, Phys. Rev. D **68**, 114006 (2003). https://doi.org/10.1103/PhysRevD.68.114006. arXiv:hep-ph/0303235
67. F. Gabbiani, A.I. Onishchenko, A.A. Petrov, Phys. Rev. D **70**, 094031 (2004). https://doi.org/10.1103/PhysRevD.70.094031. arXiv:hep-ph/0407004
68. A. Lenz, Int. J. Mod. Phys. A **30**, 1543005 (2015). https://doi.org/10.1142/S0217751X15430058
69. A. Lenz (2014). arXiv:1405.3601 [hep-ph]
70. D. Buskulic et al., ALEPH collaboration. Phys. Lett. B **314**, 459 (1993). https://doi.org/10.1016/0370-2693(93)91265-O

71. P. Abreu et al., DELPHI collaboration. Z. Phys. C **63**, 3 (1994). https://doi.org/10.1007/BF01577539
72. P. Abreu et al., DELPHI collaboration. Phys. Lett. B **377**, 195 (1996). https://doi.org/10.1016/0370-2693(96)00452-2
73. J. Abdallah et al., DELPHI collaboration. Eur. Phys. J. C **33**, 307 (2004). https://doi.org/10.1140/epjc/s2004-01599-5. arXiv:hep-ex/0401025
74. M. Acciarri et al., L3 collaboration. Phys. Lett. B **416**, 220 (1998). https://doi.org/10.1016/S0370-2693(97)01379-8
75. K. Ackerstaff et al., OPAL collaboration. Z. Phys. C **73**, 397 (1997). https://doi.org/10.1007/s002880050329
76. K. Abe et al., SLD collaboration. Phys. Rev. Lett. **75**, 3624 (1995). https://doi.org/10.1103/PhysRevLett.75.3624. arXiv:hep-ex/9511005
77. D. Buskulic et al., ALEPH collaboration. Phys. Lett. B **369**, 151 (1996). https://doi.org/10.1016/0370-2693(95)01586-8
78. P.D. Acton et al., OPAL collaboration. Z. Phys. C **60**, 217 (1993). https://doi.org/10.1007/BF01474617
79. F. Abe et al., CDF collaboration. Phys. Rev. D **57**, 5382 (1998). https://doi.org/10.1103/PhysRevD.57.5382
80. R. Barate et al., ALEPH collaboration. Phys. Lett. B **492**, 275 (2000). https://doi.org/10.1016/S0370-2693(00)01093-5. arXiv:hep-ex/0008016
81. D. Buskulic et al., ALEPH collaboration. Z. Phys. C **71**, 31 (1996). https://doi.org/10.1007/s002880050145
82. P. Abreu et al., DELPHI collaboration. Z. Phys. C **68**, 13 (1995). https://doi.org/10.1007/BF01579800
83. W. Adam et al., DELPHI collaboration. Z. Phys. C **68**, 363 (1995). https://doi.org/10.1007/BF01620712
84. P. Abreu et al., DELPHI collaboration. Z. Phys. C **74**, 19 (1997). https://doi.org/10.1007/s002880050367
85. M. Acciarri et al., L3 collaboration. Phys. Lett. B **438**, 417 (1998). https://doi.org/10.1016/S0370-2693(98)01114-9
86. R. Akers et al., OPAL collaboration. Z. Phys. C **67**, 379 (1995). https://doi.org/10.1007/BF01624581
87. G. Abbiendi et al., OPAL collaboration. Eur. Phys. J. C **12**, 609 (2000). https://doi.org/10.1007/s100520000322. arXiv:hep-ex/9901017
88. G. Abbiendi et al., OPAL collaboration. Phys. Lett. B **493**, 266 (2000). https://doi.org/10.1016/S0370-2693(00)01145-X. arXiv:hep-ex/0010013
89. K. Abe et al., SLD collaboration. Phys. Rev. Lett. **79**, 590 (1997). https://doi.org/10.1103/PhysRevLett.79.590
90. F. Abe et al., CDF collaboration. Phys. Rev. D **58**, 092002 (1998). https://doi.org/10.1103/PhysRevD.58.092002. arXiv:hep-ex/9806018
91. D. Acosta et al., CDF collaboration. Phys. Rev. D **65**, 092009 (2002). https://doi.org/10.1103/PhysRevD.65.092009
92. T. Aaltonen et al., CDF collaboration. Phys. Rev. Lett. **106**, 121804 (2011). https://doi.org/10.1103/PhysRevLett.106.121804. arXiv:1012.3138 [hep-ex]
93. V.M. Abazov et al., D0 collaboration. Phys. Rev. Lett. **102**, 032001 (2009). https://doi.org/10.1103/PhysRevLett.102.032001. arXiv:0810.0037 [hep-ex]
94. V.M. Abazov et al., D0 collaboration. Phys. Rev. D **85**, 112003 (2012). https://doi.org/10.1103/PhysRevD.85.112003. arXiv:1204.2340 [hep-ex]
95. V.M. Abazov et al., D0 collaboration. Phys. Rev. Lett. **114**, 062001 (2015). https://doi.org/10.1103/PhysRevLett.114.062001. arXiv:1410.1568 [hep-ex]
96. B. Aubert et al., BaBar collaboration. Phys. Rev. Lett. **87**, 201803 (2001). https://doi.org/10.1103/PhysRevLett.87.201803. arXiv:hep-ex/0107019
97. B. Aubert et al. (BaBar collaboration), Phys. Rev. Lett. **89**, 011802 (2002). https://doi.org/10.1103/PhysRevLett.89.011802. arXiv:hep-ex/0202005. [Erratum ibid. **89**, 169903 (2002). doi:10.1103/PhysRevLett.89.169903]
98. B. Aubert et al., BaBar collaboration. Phys. Rev. D **67**, 072002 (2003). https://doi.org/10.1103/PhysRevD.67.072002. arXiv:hep-ex/0212017
99. B. Aubert et al., BaBar collaboration. Phys. Rev. D **67**, 091101 (2003). https://doi.org/10.1103/PhysRevD.67.091101. arXiv:hep-ex/0212012
100. B. Aubert et al., BaBar collaboration. Phys. Rev. D **73**, 012004 (2006). https://doi.org/10.1103/PhysRevD.73.012004. arXiv:hep-ex/0507054
101. K. Abe et al. (Belle collaboration), Phys. Rev. D **71**, 072003 (2005). https://doi.org/10.1103/PhysRevD.71.072003. arXiv:hep-ex/0408111. [Erratum ibid. **71**, 079903 (2005). doi:10.1103/PhysRevD.71.079903]
102. G. Aad et al., ATLAS collaboration. Phys. Rev. D **87**, 032002 (2013). https://doi.org/10.1103/PhysRevD.87.032002. arXiv:1207.2284 [hep-ex]
103. R. Aaij et al., LHCb collaboration. JHEP **04**, 114 (2014). https://doi.org/10.1007/JHEP04(2014)114. arXiv:1402.2554 [hep-ex]
104. R. Aaij et al., LHCb collaboration. Phys. Lett. B **736**, 446 (2014). https://doi.org/10.1016/j.physletb.2014.07.051. arXiv:1406.7204 [hep-ex]
105. T. Aaltonen et al., CDF collaboration. Phys. Rev. D **83**, 032008 (2011). https://doi.org/10.1103/PhysRevD.83.032008. arXiv:1004.4855 [hep-ex]
106. V.M. Abazov et al., D0 collaboration. Phys. Rev. Lett. **94**, 182001 (2005). https://doi.org/10.1103/PhysRevLett.94.182001. arXiv:hep-ex/0410052
107. M. Artuso, G. Borissov, A. Lenz, Rev. Mod. Phys. **88**, 045002 (2016). https://doi.org/10.1103/RevModPhys.88.045002. arXiv:1511.09466 [hep-ph]
108. S. Laplace, Z. Ligeti, Y. Nir, G. Perez, Phys. Rev. D **65**, 094040 (2002). https://doi.org/10.1103/PhysRevD.65.094040. arXiv:hep-ph/0202010
109. M. Ciuchini, E. Franco, V. Lubicz, F. Mescia, C. Tarantino, JHEP **08**, 031 (2003). https://doi.org/10.1088/1126-6708/2003/08/031. arXiv:hep-ph/0308029
110. M. Beneke, G. Buchalla, A. Lenz, U. Nierste, Phys. Lett. B **576**, 173 (2003). https://doi.org/10.1016/j.physletb.2003.09.089. arXiv:hep-ph/0307344
111. R. Aaij et al., LHCb collaboration. Phys. Rev. Lett. **108**, 241801 (2012). https://doi.org/10.1103/PhysRevLett.108.241801. arXiv:1202.4717 [hep-ex]
112. R. Fleischer, R. Knegjens, Eur. Phys. J. C **71**, 1789 (2011). https://doi.org/10.1140/epjc/s10052-011-1789-9. arXiv:1109.5115 [hep-ph]
113. R. Barate et al., ALEPH collaboration. Eur. Phys. J. C **4**, 367 (1998). https://doi.org/10.1007/s100520050215
114. P. Abreu et al., DELPHI collaboration. Eur. Phys. J. C **18**, 229 (2000). https://doi.org/10.1007/s100520000531. arXiv:hep-ex/0105077
115. K. Ackerstaff et al., OPAL collaboration. Eur. Phys. J. C **2**, 407 (1998). https://doi.org/10.1007/s100520050150. arXiv:hep-ex/9708023
116. D. Buskulic et al., ALEPH collaboration. Phys. Lett. B **377**, 205 (1996). https://doi.org/10.1016/0370-2693(96)00451-0
117. F. Abe et al., CDF collaboration. Phys. Rev. D **59**, 032004 (1999). https://doi.org/10.1103/PhysRevD.59.032004. arXiv:hep-ex/9808003
118. P. Abreu et al., DELPHI collaboration. Eur. Phys. J. C **16**, 555 (2000). https://doi.org/10.1007/s100520000415. arXiv:hep-ex/0107077
119. K. Ackerstaff et al., OPAL collaboration. Phys. Lett. B **426**, 161 (1998). https://doi.org/10.1016/S0370-2693(98)00289-5. arXiv:hep-ex/9802002

120. T. Aaltonen et al., CDF collaboration. Phys. Rev. Lett. **107**, 272001 (2011). https://doi.org/10.1103/PhysRevLett.107.272001. arXiv:1103.1864 [hep-ex]
121. R. Aaij et al., LHCb collaboration. Phys. Rev. Lett. **112**, 111802 (2014). https://doi.org/10.1103/PhysRevLett.112.111802. arXiv:1312.1217 [hep-ex]
122. R. Aaij et al., LHCb collaboration. Phys. Rev. Lett. **113**, 172001 (2014). https://doi.org/10.1103/PhysRevLett.113.172001. arXiv:1407.5873 [hep-ex]
123. V.M. Abazov et al., D0 collaboration. Phys. Rev. Lett. **94**, 042001 (2005). https://doi.org/10.1103/PhysRevLett.94.042001. arXiv:hep-ex/0409043
124. R. Barate et al., ALEPH collaboration. Phys. Lett. B **486**, 286 (2000). https://doi.org/10.1016/S0370-2693(00)00750-4
125. R. Aaij et al., LHCb collaboration. Phys. Lett. B **707**, 349 (2012). https://doi.org/10.1016/j.physletb.2011.12.058. arXiv:1111.0521 [hep-ex]
126. R. Aaij et al., LHCb collaboration. Phys. Lett. B **762**, 484 (2016). https://doi.org/10.1016/j.physletb.2016.10.006. arXiv:1607.06314 [hep-ex]
127. R. Aaij et al., LHCb collaboration. Nucl. Phys. B **873**, 275 (2013). https://doi.org/10.1016/j.nuclphysb.2013.04.021. arXiv:1304.4500 [hep-ex]
128. T. Aaltonen et al., CDF collaboration. Phys. Rev. D **84**, 052012 (2011). https://doi.org/10.1103/PhysRevD.84.052012. arXiv:1106.3682 [hep-ex]
129. V.M. Abazov et al., D0 collaboration. Phys. Rev. D **94**, 012001 (2016). https://doi.org/10.1103/PhysRevD.94.012001. arXiv:1603.01302 [hep-ex]
130. R. Aaij et al., LHCb collaboration. Phys. Rev. D **87**, 112010 (2013). https://doi.org/10.1103/PhysRevD.87.112010. arXiv:1304.2600 [hep-ex]
131. K. Hartkorn, H.G. Moser, Eur. Phys. J. C **8**, 381 (1999). https://doi.org/10.1007/s100520050472
132. R. Aaij et al., LHCb collaboration. Phys. Lett. B **739**, 218 (2014). https://doi.org/10.1016/j.physletb.2014.10.005. arXiv:1408.0275 [hep-ex]
133. F. Abe et al., CDF collaboration. Phys. Rev. Lett. **81**, 2432 (1998). https://doi.org/10.1103/PhysRevLett.81.2432. arXiv:hep-ex/9805034
134. A. Abulencia et al., CDF collaboration. Phys. Rev. Lett. **97**, 012002 (2006). https://doi.org/10.1103/PhysRevLett.97.012002. arXiv:hep-ex/0603027
135. V.M. Abazov et al., D0 collaboration. Phys. Rev. Lett. **102**, 092001 (2009). https://doi.org/10.1103/PhysRevLett.102.092001. arXiv:0805.2614 [hep-ex]
136. T. Aaltonen et al., CDF collaboration. Phys. Rev. D **87**, 011101 (2013). https://doi.org/10.1103/PhysRevD.87.011101. arXiv:1210.2366 [hep-ex]
137. R. Aaij et al., LHCb collaboration. Eur. Phys. J. C **74**, 2839 (2014). https://doi.org/10.1140/epjc/s10052-014-2839-x. arXiv:1401.6932 [hep-ex]
138. R. Aaij et al., LHCb collaboration. Phys. Lett. B **742**, 29 (2015). https://doi.org/10.1016/j.physletb.2015.01.010. arXiv:1411.6899 [hep-ex]
139. P. Abreu et al., DELPHI collaboration. Eur. Phys. J. C **10**, 185 (1999). https://doi.org/10.1007/s100520050582
140. P. Abreu et al., DELPHI collaboration. Z. Phys. C **71**, 199 (1996). https://doi.org/10.1007/s002880050164
141. R. Akers et al., OPAL collaboration. Z. Phys. C **69**, 195 (1996). https://doi.org/10.1007/s002880050020
142. F. Abe et al., CDF collaboration. Phys. Rev. Lett. **77**, 1439 (1996). https://doi.org/10.1103/PhysRevLett.77.1439
143. V.M. Abazov et al., D0 collaboration. Phys. Rev. Lett. **99**, 182001 (2007). https://doi.org/10.1103/PhysRevLett.99.182001. arXiv:0706.2358 [hep-ex]
144. T. Aaltonen et al., CDF collaboration. Phys. Rev. Lett. **104**, 102002 (2010). https://doi.org/10.1103/PhysRevLett.104.102002. arXiv:0912.3566 [hep-ex]
145. T.A. Aaltonen et al., CDF collaboration. Phys. Rev. D **89**, 072014 (2014). https://doi.org/10.1103/PhysRevD.89.072014. arXiv:1403.8126 [hep-ex]
146. S. Chatrchyan et al., CMS collaboration. JHEP **07**, 163 (2013). https://doi.org/10.1007/JHEP07(2013)163. arXiv:1304.7495 [hep-ex]
147. R. Aaij et al., LHCb collaboration. Phys. Lett. B **734**, 122 (2014). https://doi.org/10.1016/j.physletb.2014.05.021. arXiv:1402.6242 [hep-ex]
148. P. Abreu et al., DELPHI collaboration. Z. Phys. C **68**, 541 (1995). https://doi.org/10.1007/BF01565255
149. R. Aaij et al., LHCb collaboration. Phys. Lett. B **736**, 154 (2014). https://doi.org/10.1016/j.physletb.2014.06.064. arXiv:1405.1543 [hep-ex]
150. R. Aaij et al., LHCb collaboration. Phys. Rev. Lett. **113**, 242002 (2014). https://doi.org/10.1103/PhysRevLett.113.242002. arXiv:1409.8568 [hep-ex]
151. R. Aaij et al., LHCb collaboration. Phys. Rev. Lett. **113**, 032001 (2014). https://doi.org/10.1103/PhysRevLett.113.032001. arXiv:1405.7223 [hep-ex]
152. R. Aaij et al., LHCb collaboration. Phys. Rev. D **93**, 092007 (2016). https://doi.org/10.1103/PhysRevD.93.092007. arXiv:1604.01412 [hep-ex]
153. M. Beneke, G. Buchalla, I. Dunietz, Phys. Rev. D **54**, 4419 (1996). https://doi.org/10.1103/PhysRevD.54.4419. arXiv:hep-ph/9605259. [Erratum ibid. **83**, 119902 (2011). doi:10.1103/PhysRevD.83.119902]
154. Y.-Y. Keum, U. Nierste, Phys. Rev. D **57**, 4282 (1998). https://doi.org/10.1103/PhysRevD.57.4282. arXiv:hep-ph/9710512
155. M.B. Voloshin, Phys. Rep. **320**, 275 (1999). https://doi.org/10.1016/S0370-1573(99)00054-X. arXiv:hep-ph/9901445
156. B. Guberina, B. Melic, H. Stefancic, Phys. Lett. B **469**, 253 (1999). https://doi.org/10.1016/S0370-2693(99)01198-3. arXiv:hep-ph/9907468
157. M. Neubert, C.T. Sachrajda, Nucl. Phys. B **483**, 339 (1997). https://doi.org/10.1016/S0550-3213(96)00559-7. arXiv:hep-ph/9603202
158. I.I.Y. Bigi, M.A. Shifman, N. Uraltsev, Ann. Rev. Nucl. Part. Sci. **47**, 591 (1997). https://doi.org/10.1146/annurev.nucl.47.1.591. arXiv:hep-ph/9703290
159. N.G. Uraltsev, Phys. Lett. B **376**, 303 (1996). https://doi.org/10.1016/0370-2693(96)00305-X. arXiv:hep-ph/9602324
160. D. Pirjol, N. Uraltsev, Phys. Rev. D **59**, 034012 (1999). https://doi.org/10.1103/PhysRevD.59.034012. arXiv:hep-ph/9805488
161. P. Colangelo, F. De Fazio, Phys. Lett. B **387**, 371 (1996). https://doi.org/10.1016/0370-2693(96)01049-0. arXiv:hep-ph/9604425
162. M. Di Pierro, C.T. Sachrajda, C. Michael, (UKQCD collaboration), Phys. Lett. B **468**, 143 (1999). https://doi.org/10.1016/S0370-2693(99)01166-1. arXiv:hep-lat/9906031. [Erratum ibid. **525**, 360 (2002). doi:10.1016/S0370-2693(01)01458-7]
163. D. Buskulic et al., ALEPH collaboration. Z. Phys. C **75**, 397 (1997). https://doi.org/10.1007/s002880050483
164. P. Abreu et al., DELPHI collaboration. Z. Phys. C **76**, 579 (1997). https://doi.org/10.1007/s002880050582
165. J. Abdallah et al., DELPHI collaboration. Eur. Phys. J. C **28**, 155 (2003). https://doi.org/10.1140/epjc/s2003-01183-7. arXiv:hep-ex/0303032
166. M. Acciarri et al., L3 collaboration. Eur. Phys. J. C **5**, 195 (1998). https://doi.org/10.1007/s100520050262
167. K. Ackerstaff et al., OPAL collaboration. Z. Phys. C **76**, 417 (1997). https://doi.org/10.1007/s002880050565. arXiv:hep-ex/9707010

168. K. Ackerstaff et al., OPAL collaboration. Z. Phys. C **76**, 401 (1997). https://doi.org/10.1007/s002880050564. arXiv:hep-ex/9707009
169. G. Alexander et al., OPAL collaboration. Z. Phys. C **72**, 377 (1996). https://doi.org/10.1007/s002880050258
170. F. Abe et al., CDF collaboration. Phys. Rev. Lett. **80**, 2057 (1998). https://doi.org/10.1103/PhysRevLett.80.2057. arXiv:hep-ex/9712004
171. F. Abe et al., CDF collaboration. Phys. Rev. D **59**, 032001 (1999). https://doi.org/10.1103/PhysRevD.59.032001. arXiv:hep-ex/9806026
172. F. Abe et al., CDF collaboration. Phys. Rev. D **60**, 051101 (1999). https://doi.org/10.1103/PhysRevD.60.051101
173. F. Abe et al., CDF collaboration. Phys. Rev. D **60**, 072003 (1999). https://doi.org/10.1103/PhysRevD.60.072003. arXiv:hep-ex/9903011
174. T. Affolder et al., CDF collaboration. Phys. Rev. D **60**, 112004 (1999). https://doi.org/10.1103/PhysRevD.60.112004. arXiv:hep-ex/9907053
175. V.M. Abazov et al., D0 collaboration. Phys. Rev. D **74**, 112002 (2006). https://doi.org/10.1103/PhysRevD.74.112002. arXiv:hep-ex/0609034
176. B. Aubert et al., BaBar collaboration. Phys. Rev. Lett. **88**, 221802 (2002). https://doi.org/10.1103/PhysRevLett.88.221802. arXiv:hep-ex/0112044
177. B. Aubert et al., BaBar collaboration. Phys. Rev. D **66**, 032003 (2002). https://doi.org/10.1103/PhysRevD.66.032003. arXiv:hep-ex/0201020
178. B. Aubert et al., BaBar collaboration. Phys. Rev. Lett. **88**, 221803 (2002). https://doi.org/10.1103/PhysRevLett.88.221803. arXiv:hep-ex/0112045
179. Y. Zheng et al., Belle collaboration. Phys. Rev. D **67**, 092004 (2003). arXiv:hep-ex/0211065
180. LHCb collaboration, LHCb-CONF-2011-010 (2011). https://cdsweb.cern.ch/record/1331124, this result has been published in Ref. [206]
181. R. Aaij et al., LHCb collaboration. Phys. Lett. B **719**, 318 (2013). https://doi.org/10.1016/j.physletb.2013.01.019. arXiv:1210.6750 [hep-ex]
182. R. Aaij et al., LHCb collaboration. Eur. Phys. J. C **73**, 2655 (2013). https://doi.org/10.1140/epjc/s10052-013-2655-8. arXiv:1308.1302 [hep-ex]
183. R. Aaij et al., LHCb collaboration. Eur. Phys. J. C **76**, 412 (2016). https://doi.org/10.1140/epjc/s10052-016-4250-2. arXiv:1604.03475 [hep-ex]
184. H. Albrecht et al., ARGUS collaboration. Z. Phys. C **55**, 357 (1992). https://doi.org/10.1007/BF01565092
185. H. Albrecht et al., ARGUS collaboration. Phys. Lett. B **324**, 249 (1994). https://doi.org/10.1016/0370-2693(94)90415-4
186. J.E. Bartelt et al., CLEO collaboration. Phys. Rev. Lett. **71**, 1680 (1993). https://doi.org/10.1103/PhysRevLett.71.1680
187. B.H. Behrens et al., CLEO collaboration. Phys. Lett. B **490**, 36 (2000). https://doi.org/10.1016/S0370-2693(00)00990-4. arXiv:hep-ex/0005013
188. B. Aubert et al., BaBar collaboration. Phys. Rev. Lett. **92**, 181801 (2004). https://doi.org/10.1103/PhysRevLett.92.181801. arXiv:hep-ex/0311037
189. B. Aubert et al., BaBar collaboration. Phys. Rev. D **70**, 012007 (2004). https://doi.org/10.1103/PhysRevD.70.012007. arXiv:hep-ex/0403002
190. T. Higuchi et al., Belle collaboration. Phys. Rev. D **85**, 071105 (2012). https://doi.org/10.1103/PhysRevD.85.071105. arXiv:1203.0930 [hep-ex]
191. T. Gershon, J. Phys. G **38**, 015007 (2011). https://doi.org/10.1088/0954-3899/38/1/015007J. arXiv:1007.5135 [hep-ph]. [Erratum ibid. **42**, 119501 (2015). doi:10.1088/0954-3899/42/11/119501]
192. M. Aaboud et al., ATLAS collaboration. JHEP **06**, 081 (2016). https://doi.org/10.1007/JHEP06(2016)081. arXiv:1605.07485 [hep-ex]
193. J. Charles et al. (CKMfitter group), Phys. Rev. D **84**, 033005 (2011). https://doi.org/10.1103/PhysRevD.84.033005. arXiv:1106.4041 [hep-ph], with updated results and plots available at http://ckmfitter.in2p3.fr
194. M. Bona et al. (UTfit collaboration), JHEP **10**, 081 (2006). https://doi.org/10.1088/1126-6708/2006/10/081. arXiv:hep-ph/0606167, with similar updated results and plots available at http://www.utfit.org
195. V.M. Abazov et al., D0 collaboration. Phys. Rev. D **89**, 012002 (2014). https://doi.org/10.1103/PhysRevD.89.012002. arXiv:1310.0447 [hep-ex]
196. U. Nierste, talk presented at the 8th International Workshop on the CKM unitarity Triangle (CKM 2014) (2014). http://indico.cern.ch/event/253826/contributions/567426/
197. T. Aaltonen et al., CDF collaboration. Phys. Rev. Lett. **109**, 171802 (2012). https://doi.org/10.1103/PhysRevLett.109.171802. arXiv:1208.2967 [hep-ex]
198. V.M. Abazov et al., D0 collaboration. Phys. Rev. D **85**, 032006 (2012). https://doi.org/10.1103/PhysRevD.85.032006. arXiv:1109.3166 [hep-ex]
199. G. Aad et al., ATLAS collaboration. Phys. Rev. D **90**, 052007 (2014). https://doi.org/10.1103/PhysRevD.90.052007. arXiv:1407.1796 [hep-ex]
200. G. Aad et al., ATLAS collaboration. JHEP **08**, 147 (2016). https://doi.org/10.1007/JHEP08(2016)147. arXiv:1601.03297 [hep-ex]
201. V. Khachatryan et al., CMS collaboration. Phys. Lett. B **757**, 97 (2016). https://doi.org/10.1016/j.physletb.2016.03.046. arXiv:1507.07527 [hep-ex]
202. R. Aaij et al., LHCb collaboration. Phys. Rev. Lett. **114**, 041801 (2015). https://doi.org/10.1103/PhysRevLett.114.041801. arXiv:1411.3104 [hep-ex]
203. R. Aaij et al., LHCb collaboration. Phys. Lett. B. **762**, 253 (2016). https://doi.org/10.1016/j.physletb.2016.09.028. arXiv:1608.04855 [hep-ex]
204. A. Lenz, arXiv:1205.1444 [hep-ph] (2012)
205. S. Esen et al., Belle collaboration. Phys. Rev. Lett. **105**, 201802 (2010). https://doi.org/10.1103/PhysRevLett.105.201802. arXiv:1005.5177 [hep-ex]
206. V. Abazov et al., D0 collaboration. Phys. Rev. Lett. **102**, 091801 (2009). https://doi.org/10.1103/PhysRevLett.102.091801. arXiv:0811.2173 [hep-ex]
207. T. Aaltonen et al., CDF collaboration. Phys. Rev. Lett. **100**, 021803 (2008). https://doi.org/10.1103/PhysRevLett.100.021803
208. A. Lenz, U. Nierste, arXiv:1102.4274 [hep-ph] (2011)
209. A. Lenz, U. Nierste, JHEP **06**, 072 (2007). https://doi.org/10.1088/1126-6708/2007/06/072. arXiv:hep-ph/0612167
210. A. Heister et al., ALEPH collaboration. Eur. Phys. J. C **29**, 143 (2003). https://doi.org/10.1140/epjc/s2003-01230-5
211. J. Abdallah et al., DELPHI collaboration. Eur. Phys. J. C **35**, 35 (2004). https://doi.org/10.1140/epjc/s2004-01827-0. arXiv:hep-ex/0404013
212. G. Abbiendi et al., OPAL collaboration. Eur. Phys. J. C **11**, 587 (1999). https://doi.org/10.1007/s100520050658. arXiv:hep-ex/9907061
213. G. Abbiendi et al., OPAL collaboration. Eur. Phys. J. C **19**, 241 (2001). https://doi.org/10.1007/s100520100591. arXiv:hep-ex/0011052
214. K. Abe et al., SLD collaboration. Phys. Rev. D **67**, 012006 (2003). https://doi.org/10.1103/PhysRevD.67.012006. arXiv:hep-ex/0209002

215. K. Abe et al., SLD collaboration. Phys. Rev. D **66**, 032009 (2002). https://doi.org/10.1103/PhysRevD.66.032009. arXiv:hep-ex/0207048
216. F. Abe et al., CDF collaboration. Phys. Rev. Lett. **82**, 3576 (1999). https://doi.org/10.1103/PhysRevLett.82.3576
217. V.M. Abazov et al., D0 collaboration. Phys. Rev. Lett. **97**, 021802 (2006). https://doi.org/10.1103/PhysRevLett.97.021802. arXiv:hep-ex/0603029
218. A. Abulencia et al., CDF collaboration. Phys. Rev. Lett. **97**, 242003 (2006). https://doi.org/10.1103/PhysRevLett.97.242003. arXiv:hep-ex/0609040
219. R. Aaij et al., LHCb collaboration. Phys. Lett. B **709**, 177 (2012). https://doi.org/10.1016/j.physletb.2012.02.031. arXiv:1112.4311 [hep-ex]
220. R. Aaij et al., LHCb collaboration. New J. Phys. **15**, 053021 (2013). https://doi.org/10.1088/1367-2630/15/5/053021. arXiv:1304.4741 [hep-ex]
221. A. Bazavov et al., Fermilab Lattice and MILC collaborations. Phys. Rev. D **93**, 113016 (2016). https://doi.org/10.1103/PhysRevD.93.113016. arXiv:1602.03560 [hep-lat]
222. S. Aoki et al. (FLAG working group), Eur. Phys. J. C **77**, 112 (2017). arXiv:1607.00299 [hep-lat], see also http://itpwiki.unibe.ch/flag/
223. D.E. Jaffe et al., CLEO collaboration. Phys. Rev. Lett. **86**, 5000 (2001). https://doi.org/10.1103/PhysRevLett.86.5000. arXiv:hep-ex/0101006
224. J.P. Lees et al., BaBar collaboration. Phys. Rev. Lett. **114**, 081801 (2015). https://doi.org/10.1103/PhysRevLett.114.081801. arXiv:1411.1842 [hep-ex]
225. F. Abe et al., CDF collaboration. Phys. Rev. D **55**, 2546 (1997). https://doi.org/10.1103/PhysRevD.55.2546
226. R. Barate et al., ALEPH collaboration. Eur. Phys. J. C **20**, 431 (2001)
227. J.P. Lees et al. (BaBar collaboration), Phys. Rev. Lett. **111**, 101802 (2013). https://doi.org/10.1103/PhysRevLett.111.101802. arXiv:1305.1575 [hep-ex]. [Erratum ibid. **111**, 159901 (2013). doi:10.1103/PhysRevLett.111.159901]
228. B. Aubert et al., BaBar collaboration. Phys. Rev. Lett. **96**, 251802 (2006). https://doi.org/10.1103/PhysRevLett.96.251802. arXiv:hep-ex/0603053
229. E. Nakano et al., Belle collaboration. Phys. Rev. D **73**, 112002 (2006). https://doi.org/10.1103/PhysRevD.73.112002. arXiv:hep-ex/0505017
230. M. Beneke, G. Buchalla, I. Dunietz, Phys. Lett. B **393**, 132 (1997). https://doi.org/10.1016/S0370-2693(96)01648-6. arXiv:hep-ph/9609357
231. I. Dunietz, Eur. Phys. J. C **7**, 197 (1999). https://doi.org/10.1007/s100529801005. arXiv:hep-ph/9806521
232. V.M. Abazov et al., D0 collaboration. Phys. Rev. D **86**, 072009 (2012). https://doi.org/10.1103/PhysRevD.86.072009. arXiv:1208.5813 [hep-ex]
233. R. Aaij et al., LHCb collaboration. Phys. Rev. Lett. **114**, 041601 (2015). https://doi.org/10.1103/PhysRevLett.114.041601. arXiv:1409.8586 [hep-ex]
234. Y. Amhis et al. (Heavy Flavor Averaging Group), arXiv:1207.1158 [hep-ex] (2012)
235. V.M. Abazov et al., D0 collaboration. Phys. Rev. Lett. **110**, 011801 (2013). https://doi.org/10.1103/PhysRevLett.110.011801. arXiv:1207.1769 [hep-ex]
236. R. Aaij et al., LHCb collaboration. Phys. Rev. Lett. **117**, 061803 (2016). https://doi.org/10.1103/PhysRevLett.117.061803. arXiv:1605.09768 [hep-ex]
237. A. Lenz, private communication (2017)
238. S. Descotes-Genon, J.F. Kamenik, Phys. Rev. D **87**, 074036 (2013). https://doi.org/10.1103/PhysRevD.87.074036. arXiv:1207.4483 [hep-ph]. [Erratum ibid. **92**, 079903 (2015). doi:10.1103/PhysRevD.92.079903]
239. M. Aaboud et al., ATLAS collaboration. JHEP **02**, 071 (2017). https://doi.org/10.1007/JHEP02(2017)071. arXiv:1610.07869 [hep-ex]
240. R. Aaij et al., LHCb collaboration. Phys. Lett. B. **736**, 186 (2014). https://doi.org/10.1016/j.physletb.2014.06.079. arXiv:1405.4140 [hep-ex]
241. R. Aaij et al., LHCb collaboration. Phys. Rev. D. **86**, 052006 (2012). https://doi.org/10.1103/PhysRevD.86.052006. arXiv:1204.5643 [hep-ex]
242. R. Aaij et al., LHCb collaboration. Phys. Rev. Lett. **113**, 211801 (2014). https://doi.org/10.1103/PhysRevLett.113.211801. arXiv:1409.4619 [hep-ex]
243. R. Aaij et al., LHCb collaboration. Phys. Lett. B **741**, 1 (2015). https://doi.org/10.1016/j.physletb.2014.12.015. arXiv:1408.4368 [hep-ex]
244. L.-L. Chau, W.-Y. Keung, Phys. Rev. Lett. **53**, 1802 (1984). https://doi.org/10.1103/PhysRevLett.53.1802
245. L. Wolfenstein, Phys. Rev. Lett. **51**, 1945 (1983). https://doi.org/10.1103/PhysRevLett.51.1945
246. A.J. Buras, M.E. Lautenbacher, G. Ostermaier, Phys. Rev. D **50**, 3433 (1994). https://doi.org/10.1103/PhysRevD.50.3433. arXiv:hep-ph/9403384
247. C. Jarlskog, Phys. Rev. Lett. **55**, 1039 (1985). https://doi.org/10.1103/PhysRevLett.55.1039
248. C. Jarlskog, Phys. Lett. B. **615**, 207 (2005). https://doi.org/10.1016/j.physletb.2005.04.033. arXiv:hep-ph/0503199
249. P.F. Harrison, S. Dallison, W.G. Scott, Phys. Lett. B **680**, 328 (2009). https://doi.org/10.1016/j.physletb.2009.09.004. arXiv:0904.3077 [hep-ph]
250. P.H. Frampton, X.-G. He, Phys. Lett. B **688**, 67 (2010). https://doi.org/10.1016/j.physletb.2010.03.077. arXiv:1003.0310 [hep-ph]
251. P.H. Frampton, X.-G. He, Phys. Rev. D **82**, 017301 (2010). https://doi.org/10.1103/PhysRevD.82.017301. arXiv:1004.3679 [hep-ph]
252. J. Charles et al. (CKMfitter group), Eur. Phys. J. C **41**, 1 (2005). https://doi.org/10.1140/epjc/s2005-02169-1. arXiv:hep-ph/0406184, see also online updates, http://ckmfitter.in2p3.fr/
253. B. Aubert et al., BaBar collaboration. Phys. Rev. Lett. **86**, 2515 (2001). https://doi.org/10.1103/PhysRevLett.86.2515. arXiv:hep-ex/0102030
254. K. Abe et al., Belle collaboration. Phys. Rev. Lett. **87**, 091802 (2001). https://doi.org/10.1103/PhysRevLett.87.091802. arXiv:hep-ex/0107061
255. A.B. Carter, A.I. Sanda, Phys. Rev. D **23**, 1567 (1981). https://doi.org/10.1103/PhysRevD.23.1567
256. I.I.Y. Bigi, A.I. Sanda, Nucl. Phys. B **193**, 85 (1981). https://doi.org/10.1016/0550-3213(81)90519-8
257. I. Dunietz, R. Fleischer, U. Nierste, Phys. Rev. D **63**, 114015 (2001). https://doi.org/10.1103/PhysRevD.63.114015. arXiv:hep-ph/0012219
258. R. Aaij et al., LHCb collaboration. Phys. Lett. B. **742**, 38 (2015). https://doi.org/10.1016/j.physletb.2015.01.008. arXiv:1411.1634 [hep-ex]
259. B. Aubert et al., BaBar collaboration. Phys. Rev. D **79**, 032002 (2009). https://doi.org/10.1103/PhysRevD.79.032002. arXiv:0808.1866 [hep-ex]
260. P. Krokovny et al., Belle collaboration. Phys. Rev. Lett. **97**, 081801 (2006). https://doi.org/10.1103/PhysRevLett.97.081801. arXiv:hep-ex/0605023
261. B. Aubert et al., BaBar collaboration. Phys. Rev. Lett. **99**, 231802 (2007). https://doi.org/10.1103/PhysRevLett.99.231802. arXiv:0708.1544 [hep-ex]

262. V. Vorobyev et al., Belle collaboration. Phys. Rev. D **94**, 052004 (2016). https://doi.org/10.1103/PhysRevD.94.052004. arXiv:1607.05813 [hep-ex]
263. J. Libby et al., CLEO collaboration. Phys. Rev. D **82**, 112006 (2010). https://doi.org/10.1103/PhysRevD.82.112006. arXiv:1010.2817 [hep-ex]
264. T.E. Browder, A. Datta, P.J. O'Donnell, S. Pakvasa, Phys. Rev. D **61**, 054009 (2000). https://doi.org/10.1103/PhysRevD.61.054009. arXiv:hep-ph/9905425
265. B. Aubert et al., BaBar collaboration. Phys. Rev. D **74**, 091101 (2006). https://doi.org/10.1103/PhysRevD.74.091101. arXiv:hep-ex/0608016
266. J. Dalseno et al., Belle collaboration. Phys. Rev. D **76**, 072004 (2007). https://doi.org/10.1103/PhysRevD.76.072004. arXiv:0706.2045 [hep-ex]
267. R. Aaij et al., LHCb collaboration. Phys. Rev. D **90**, 012003 (2014). https://doi.org/10.1103/PhysRevD.90.012003. arXiv:1404.5673 [hep-ex]
268. J.R. Pelaez, Phys. Rep. **658**, 1 (2016). https://doi.org/10.1016/j.physrep.2016.09.001. arXiv:1510.00653 [hep-ph]
269. B. Aubert et al., BaBar collaboration. Phys. Rev. Lett. **99**, 161802 (2007). https://doi.org/10.1103/PhysRevLett.99.161802. arXiv:0706.3885 [hep-ex]
270. Y. Nakahama et al., Belle collaboration. Phys. Rev. D **82**, 073011 (2010). https://doi.org/10.1103/PhysRevD.82.073011. arXiv:1007.3848 [hep-ex]
271. J.P. Lees et al., BaBar collaboration. Phys. Rev. D. **85**, 112010 (2012). https://doi.org/10.1103/PhysRevD.85.112010. arXiv:1201.5897 [hep-ex]
272. A. Garmash et al., Belle collaboration. Phys. Rev. D **71**, 092003 (2005). https://doi.org/10.1103/PhysRevD.71.092003. arXiv:hep-ex/0412066
273. B. Aubert et al., BaBar collaboration. Phys. Rev. D **74**, 032003 (2006). https://doi.org/10.1103/PhysRevD.74.032003. arXiv:hep-ex/0605003
274. B. Aubert et al., BaBar collaboration. Phys. Rev. D **80**, 112001 (2009). https://doi.org/10.1103/PhysRevD.80.112001. arXiv:0905.3615 [hep-ex]
275. J. Dalseno et al., Belle collaboration. Phys. Rev. D **79**, 072004 (2009). https://doi.org/10.1103/PhysRevD.79.072004. arXiv:0811.3665 [hep-ex]
276. A. Garmash et al., Belle collaboration. Phys. Rev. Lett. **96**, 251803 (2006). https://doi.org/10.1103/PhysRevLett.96.251803. arXiv:hep-ex/0512066
277. B. Aubert, (BaBar collaboration), Phys. Rev. D **72**, 072003 (2005). https://doi.org/10.1103/PhysRevD.72.072003. arXiv:hep-ex/0507004. [Erratum ibid. **74**, 099903 (2006). doi:10.1103/PhysRevD.74.099903]
278. B. Aubert et al., BaBar collaboration. Phys. Rev. D **78**, 012004 (2008). https://doi.org/10.1103/PhysRevD.78.012004. arXiv:0803.4451 [hep-ex]
279. A.E. Snyder, H.R. Quinn, Phys. Rev. D **48**, 2139 (1993). https://doi.org/10.1103/PhysRevD.48.2139
280. H.R. Quinn, J.P. Silva, Phys. Rev. D **62**, 054002 (2000). https://doi.org/10.1103/PhysRevD.62.054002. arXiv:hep-ph/0001290
281. B. Aubert et al., BaBar collaboration. Phys. Rev. D **76**, 012004 (2007). https://doi.org/10.1103/PhysRevD.76.012004. arXiv:hep-ex/0703008
282. J.P. Lees et al., BaBar collaboration. Phys. Rev. D **88**, 012003 (2013). https://doi.org/10.1103/PhysRevD.88.012003. arXiv:1304.3503 [hep-ex]
283. A. Kusaka et al., Belle collaboration. Phys. Rev. Lett. **98**, 221602 (2007). https://doi.org/10.1103/PhysRevLett.98.221602. arXiv:hep-ex/0701015
284. A. Kusaka et al., Belle collaboration. Phys. Rev. D **77**, 072001 (2008). https://doi.org/10.1103/PhysRevD.77.072001. arXiv:0710.4974 [hep-ex]
285. B. Aubert et al., BaBar collaboration. Phys. Rev. Lett. **99**, 071801 (2007). https://doi.org/10.1103/PhysRevLett.99.071801. arXiv:0705.1190 [hep-ex]
286. T. Aushev et al., Belle collaboration. Phys. Rev. Lett. **93**, 201802 (2004). https://doi.org/10.1103/PhysRevLett.93.201802. arXiv:hep-ex/0408051
287. M. Rohrken et al., Belle collaboration. Phys. Rev. D **85**, 091106 (2012). https://doi.org/10.1103/PhysRevD.85.091106. arXiv:1203.6647 [hep-ex]
288. B. Aubert et al., BaBar collaboration. Phys. Rev. Lett. **91**, 201802 (2003). https://doi.org/10.1103/PhysRevLett.91.201802. arXiv:hep-ex/0306030
289. C.C. Wang et al., Belle collaboration. Phys. Rev. Lett. **94**, 121801 (2005). https://doi.org/10.1103/PhysRevLett.94.121801. arXiv:hep-ex/0408003
290. B. Aubert et al., BaBar collaboration. Phys. Rev. D **73**, 111101 (2006). https://doi.org/10.1103/PhysRevD.73.111101. arXiv:hep-ex/0602049
291. B. Aubert et al., BaBar collaboration. Phys. Rev. D **71**, 112003 (2005). https://doi.org/10.1103/PhysRevD.71.112003. arXiv:hep-ex/0504035
292. O. Long, M. Baak, R.N. Cahn, D. Kirkby, Phys. Rev. D **68**, 034010 (2003). https://doi.org/10.1103/PhysRevD.68.034010. arXiv:hep-ex/0303030
293. S. Bahinipati et al., Belle collaboration. Phys. Rev. D **84**, 021101 (2011). https://doi.org/10.1103/PhysRevD.84.021101. arXiv:1102.0888 [hep-ex]
294. F.J. Ronga et al., Belle collaboration. Phys. Rev. D **73**, 092003 (2006). https://doi.org/10.1103/PhysRevD.73.092003. arXiv:hep-ex/0604013
295. R. Fleischer, Nucl. Phys. B **671**, 459 (2003). https://doi.org/10.1016/j.nuclphysb.2003.08.010. arXiv:hep-ph/0304027
296. R. Aaij et al., LHCb collaboration. JHEP **11**, 060 (2014). https://doi.org/10.1007/JHEP11(2014)060. arXiv:1407.6127 [hep-ex]
297. D. Atwood, M. Gronau, A. Soni, Phys. Rev. Lett. **79**, 185 (1997). https://doi.org/10.1103/PhysRevLett.79.185. arXiv:hep-ph/9704272
298. D. Atwood, T. Gershon, M. Hazumi, A. Soni, Phys. Rev. D **71**, 076003 (2005). https://doi.org/10.1103/PhysRevD.71.076003. arXiv:hep-ph/0410036
299. B. Grinstein, Y. Grossman, Z. Ligeti, D. Pirjol, Phys. Rev. D **71**, 011504 (2005). https://doi.org/10.1103/PhysRevD.71.011504. arXiv:hep-ph/0412019
300. B. Grinstein, D. Pirjol, Phys. Rev. D **73**, 014013 (2006). https://doi.org/10.1103/PhysRevD.73.014013. arXiv:hep-ph/0510104
301. M. Matsumori, A.I. Sanda, Phys. Rev. D **73**, 114022 (2006). https://doi.org/10.1103/PhysRevD.73.114022. arXiv:hep-ph/0512175
302. P. Ball, R. Zwicky, Phys. Lett. B **642**, 478 (2006). https://doi.org/10.1016/j.physletb.2006.10.013. arXiv:hep-ph/0609037
303. F. Muheim, Y. Xie, R. Zwicky, Phys. Lett. B **664**, 174 (2008). https://doi.org/10.1016/j.physletb.2008.05.032. arXiv:0802.0876 [hep-ph]
304. I.I.Y. Bigi, A.I. Sanda, Phys. Lett. B **211**, 213 (1988). https://doi.org/10.1016/0370-2693(88)90836-2
305. M. Gronau, D. London, Phys. Lett. B **253**, 483 (1991). https://doi.org/10.1016/0370-2693(91)91756-L
306. M. Gronau, D. Wyler, Phys. Lett. B **265**, 172 (1991). https://doi.org/10.1016/0370-2693(91)90034-N
307. D. Atwood, I. Dunietz, A. Soni, Phys. Rev. Lett. **78**, 3257 (1997). https://doi.org/10.1103/PhysRevLett.78.3257. arXiv:hep-ph/9612433

308. D. Atwood, I. Dunietz, A. Soni, Phys. Rev. D **63**, 036005 (2001). https://doi.org/10.1103/PhysRevD.63.036005. arXiv:hep-ph/0008090
309. A. Giri, Y. Grossman, A. Soffer, J. Zupan, Phys. Rev. D **68**, 054018 (2003). https://doi.org/10.1103/PhysRevD.68.054018. arXiv:hep-ph/0303187
310. A. Poluektov et al., Belle collaboration. Phys. Rev. D **70**, 072003 (2004). https://doi.org/10.1103/PhysRevD.70.072003. arXiv:hep-ex/0406067
311. J. Brod, J. Zupan, JHEP **01**, 051 (2014). https://doi.org/10.1007/JHEP01(2014)051. arXiv:1308.5663 [hep-ph]
312. M. Gronau, Phys. Lett. B **557**, 198 (2003). https://doi.org/10.1016/S0370-2693(03)00192-8. arXiv:hep-ph/0211282
313. T. Gershon, Phys. Rev. D **79**, 051301 (2009). https://doi.org/10.1103/PhysRevD.79.051301. arXiv:0810.2706 [hep-ph]
314. T. Gershon, M. Williams, Phys. Rev. D **80**, 092002 (2009). https://doi.org/10.1103/PhysRevD.80.092002. arXiv:0909.1495 [hep-ph]
315. A. Bondar, T. Gershon, Phys. Rev. D **70**, 091503 (2004). https://doi.org/10.1103/PhysRevD.70.091503. arXiv:hep-ph/0409281
316. D. Atwood, A. Soni, Phys. Rev. D **68**, 033003 (2003). https://doi.org/10.1103/PhysRevD.68.033003. arXiv:hep-ph/0304085
317. Y. Grossman, Z. Ligeti, A. Soffer, Phys. Rev. D **67**, 071301 (2003). https://doi.org/10.1103/PhysRevD.67.071301. arXiv:hep-ph/0210433
318. M. Nayak et al., Phys. Lett. B **740**, 1 (2014). https://doi.org/10.1016/j.physletb.2014.11.022. arXiv:1410.3964 [hep-ex]
319. A. Bondar, A. Poluektov, Eur. Phys. J. C **47**, 347 (2006). https://doi.org/10.1140/epjc/s2006-02590-x. arXiv:hep-ph/0510246
320. A. Bondar, A. Poluektov, Eur. Phys. J. C **55**, 51 (2008). https://doi.org/10.1140/epjc/s10052-008-0600-z. arXiv:0801.0840 [hep-ex]
321. T. Gershon, J. Libby, G. Wilkinson, Phys. Lett. B **750**, 338 (2015). https://doi.org/10.1016/j.physletb.2015.08.063. arXiv:1506.08594 [hep-ph]
322. B. Aubert et al., BaBar collaboration. Phys. Rev. Lett. **99**, 251801 (2007). https://doi.org/10.1103/PhysRevLett.99.251801. arXiv:hep-ex/0703037
323. B. Aubert et al., BaBar collaboration. Phys. Rev. D **76**, 031102 (2007). https://doi.org/10.1103/PhysRevD.76.031102. arXiv:0704.0522 [hep-ex]
324. R. Itoh et al., Belle collaboration. Phys. Rev. Lett. **95**, 091601 (2005). https://doi.org/10.1103/PhysRevLett.95.091601. arXiv:hep-ex/0504030
325. D. Acosta et al., CDF collaboration. Phys. Rev. Lett. **94**, 101803 (2005). https://doi.org/10.1103/PhysRevLett.94.101803. arXiv:hep-ex/0412057
326. R. Aaij et al., LHCb collaboration. Phys. Rev. D **88**, 052002 (2013). https://doi.org/10.1103/PhysRevD.88.052002. arXiv:1307.2782 [hep-ex]
327. K. Olive et al., Particle Data Group. Chin. Phys. C **38**, 090001 (2014). https://doi.org/10.1088/1674-1137/38/9/090001
328. M. Jung, Phys. Rev. D **86**, 053008 (2012). https://doi.org/10.1103/PhysRevD.86.053008. arXiv:1206.2050 [hep-ph]
329. K. De Bruyn, R. Fleischer, JHEP **03**, 145 (2015). https://doi.org/10.1007/JHEP03(2015)145. arXiv:1412.6834 [hep-ph]
330. P. Frings, U. Nierste, M. Wiebusch, Phys. Rev. Lett. **115**, 061802 (2015). https://doi.org/10.1103/PhysRevLett.115.061802. arXiv:1503.00859 [hep-ph]
331. B. Aubert et al., BaBar collaboration. Phys. Rev. D **79**, 072009 (2009). https://doi.org/10.1103/PhysRevD.79.072009. arXiv:0902.1708 [hep-ex]
332. B. Aubert et al., BaBar collaboration. Phys. Rev. D **69**, 052001 (2004). https://doi.org/10.1103/PhysRevD.69.052001. arXiv:hep-ex/0309039
333. I. Adachi et al., Belle collaboration. Phys. Rev. Lett. **108**, 171802 (2012). https://doi.org/10.1103/PhysRevLett.108.171802. arXiv:1201.4643 [hep-ex]
334. R. Barate et al., ALEPH collaboration. Phys. Lett. B **492**, 259 (2000). https://doi.org/10.1016/S0370-2693(00)01091-1. arXiv:hep-ex/0009058
335. K. Ackerstaff et al., OPAL collaboration. Eur. Phys. J. C **5**, 379 (1998). https://doi.org/10.1007/s100520050284. arXiv:hep-ex/9801022
336. A.A. Affolder et al., CDF collaboration. Phys. Rev. D **61**, 072005 (2000). https://doi.org/10.1103/PhysRevD.61.072005. arXiv:hep-ex/9909003
337. R. Aaij et al., LHCb collaboration. Phys. Rev. Lett. **115**, 031601 (2015). https://doi.org/10.1103/PhysRevLett.115.031601. arXiv:1503.07089 [hep-ex]
338. Y. Sato et al., Belle collaboration. Phys. Rev. Lett. **108**, 171801 (2012). https://doi.org/10.1103/PhysRevLett.108.171801. arXiv:1201.3502 [hep-ex]
339. M. Bona et al. (UTfit collaboration), JHEP **07**, 028 (2005). https://doi.org/10.1088/1126-6708/2005/07/028. arXiv:hep-ph/0501199. see also online updates, http://www.utfit.org/
340. E. Lunghi, A. Soni, Phys. Lett. B **666**, 162 (2008). https://doi.org/10.1016/j.physletb.2008.07.015. arXiv:0803.4340 [hep-ph]
341. G. Eigen, G. Dubois-Felsmann, D. Hitlin, F. Porter, Phys. Rev. D **89**, 033004 (2014). https://doi.org/10.1103/PhysRevD.89.033004. arXiv:1301.5867 [hep-ex]
342. I. Dunietz, H.R. Quinn, A. Snyder, W. Toki, H.J. Lipkin, Phys. Rev. D **43**, 2193 (1991). https://doi.org/10.1103/PhysRevD.43.2193
343. D. Aston et al., Nucl. Phys. B **296**, 493 (1988). https://doi.org/10.1016/0550-3213(88)90028-4
344. M. Suzuki, Phys. Rev. D **64**, 117503 (2001). https://doi.org/10.1103/PhysRevD.64.117503. arXiv:hep-ph/0106354
345. B. Aubert et al., BaBar collaboration. Phys. Rev. D **71**, 032005 (2005). https://doi.org/10.1103/PhysRevD.71.032005. arXiv:hep-ex/0411016
346. Y. Grossman, M.P. Worah, Phys. Lett. B **395**, 241 (1997). https://doi.org/10.1016/S0370-2693(97)00068-3. arXiv:hep-ph/9612269
347. R. Fleischer, Phys. Lett. B **562**, 234 (2003). https://doi.org/10.1016/S0370-2693(03)00582-3. arXiv:hep-ph/0301255
348. R. Fleischer, Nucl. Phys. B **659**, 321 (2003). https://doi.org/10.1016/S0550-3213(03)00225-6. arXiv:hep-ph/0301256
349. A. Abdesselam et al., BaBar and Belle collaborations. Phys. Rev. Lett. **115**, 121604 (2015). https://doi.org/10.1103/PhysRevLett.115.121604. arXiv:1505.04147 [hep-ex]
350. A. Bondar, T. Gershon, P. Krokovny, Phys. Lett. B **624**, 1 (2005). https://doi.org/10.1016/j.physletb.2005.07.053. arXiv:hep-ph/0503174
351. F. Botella, J. Silva, Phys. Rev. D **71**, 094008 (2005). https://doi.org/10.1103/PhysRevD.71.094008. arXiv:hep-ph/0503136
352. B. Kronenbitter et al., Belle collaboration. Phys. Rev. D **86**, 071103 (2012). https://doi.org/10.1103/PhysRevD.86.071103. arXiv:1207.5611 [hep-ex]
353. B. Aubert et al., BaBar collaboration. Phys. Rev. Lett. **101**, 021801 (2008). https://doi.org/10.1103/PhysRevLett.101.021801. arXiv:0804.0896 [hep-ex]
354. S.E. Lee et al., Belle collaboration. Phys. Rev. D **77**, 071101 (2008). https://doi.org/10.1103/PhysRevD.77.071101. arXiv:0708.0304 [hep-ex]
355. R. Aaij et al., LHCb collaboration. Phys. Rev. Lett. **117**, 261801 (2016). https://doi.org/10.1103/PhysRevLett.117.261801. arXiv:1608.06620 [hep-ex]

356. J.P. Lees et al., BaBar collaboration. Phys. Rev. D **86**, 112006 (2012). https://doi.org/10.1103/PhysRevD.86.112006. arXiv:1208.1282 [hep-ex]
357. S. Fratina et al., Belle collaboration. Phys. Rev. Lett. **98**, 221802 (2007). https://doi.org/10.1103/PhysRevLett.98.221802. arXiv:hep-ex/0702031
358. R. Fleischer, Eur. Phys. J. C **10**, 299 (1999). https://doi.org/10.1007/s100529900099. arXiv:hep-ph/9903455
359. K. De Bruyn, R. Fleischer, P. Koppenburg, Eur. Phys. J. C **70**, 1025 (2010). https://doi.org/10.1140/epjc/s10052-010-1495-z. arXiv:1010.0089 [hep-ph]
360. R. Aaij et al., LHCb collaboration. JHEP **06**, 131 (2015). https://doi.org/10.1007/JHEP06(2015)131. arXiv:1503.07055 [hep-ex]
361. R. Fleischer, Int. J. Mod. Phys. A **12**, 2459 (1997). https://doi.org/10.1142/S0217751X97001432. arXiv:hep-ph/9612446
362. D. London, A. Soni, Phys. Lett. B **407**, 61 (1997). https://doi.org/10.1016/S0370-2693(97)00695-3. arXiv:hep-ph/9704277
363. M. Ciuchini, E. Franco, G. Martinelli, A. Masiero, L. Silvestrini, Phys. Rev. Lett. **79**, 978 (1997). https://doi.org/10.1103/PhysRevLett.79.978. arXiv:hep-ph/9704274
364. S. Okubo, Phys. Lett. **5**, 165–168 (1963). https://doi.org/10.1016/S0375-9601(63)92548-9
365. G. Zweig, CERN-TH-412 (1964)
366. J. Iizuka, Prog. Theor. Phys. Suppl. **37**, 21–34 (1966). https://doi.org/10.1143/PTPS.37.21
367. T. Gershon, M. Hazumi, Phys. Lett. B **596**, 163 (2004). https://doi.org/10.1016/j.physletb.2004.06.095. arXiv:hep-ph/0402097
368. Y. Grossman, Z. Ligeti, Y. Nir, H. Quinn, Phys. Rev. D **68**, 015004 (2003). https://doi.org/10.1103/PhysRevD.68.015004. arXiv:hep-ph/0303171
369. M. Gronau, J.L. Rosner, Phys. Lett. B **564**, 90 (2003). https://doi.org/10.1016/S0370-2693(03)00702-0. arXiv:hep-ph/0304178
370. M. Gronau, Y. Grossman, J.L. Rosner, Phys. Lett. B **579**, 331 (2004). https://doi.org/10.1016/j.physletb.2003.11.015. arXiv:hep-ph/0310020
371. M. Gronau, J.L. Rosner, J. Zupan, Phys. Lett. B **596**, 107 (2004). https://doi.org/10.1016/j.physletb.2004.06.086. arXiv:hep-ph/0403287
372. H.-Y. Cheng, C.-K. Chua, A. Soni, Phys. Rev. D **72**, 014006 (2005). https://doi.org/10.1103/PhysRevD.72.014006. arXiv:hep-ph/0502235
373. M. Gronau, J.L. Rosner, Phys. Rev. D **71**, 074019 (2005). https://doi.org/10.1103/PhysRevD.71.074019. arXiv:hep-ph/0503131
374. G. Buchalla, G. Hiller, Y. Nir, G. Raz, JHEP **09**, 074 (2005). https://doi.org/10.1088/1126-6708/2005/09/074. arXiv:hep-ph/0503151
375. M. Beneke, Phys. Lett. B **620**, 143 (2005). https://doi.org/10.1016/j.physletb.2005.06.045. arXiv:hep-ph/0505075
376. G. Engelhard, Y. Nir, G. Raz, Phys. Rev. D **72**, 075013 (2005). https://doi.org/10.1103/PhysRevD.72.075013. arXiv:hep-ph/0505194
377. H.-Y. Cheng, C.-K. Chua, A. Soni, Phys. Rev. D **72**, 094003 (2005). https://doi.org/10.1103/PhysRevD.72.094003. arXiv:hep-ph/0506268
378. G. Engelhard, G. Raz, Phys. Rev. D **72**, 114017 (2005). https://doi.org/10.1103/PhysRevD.72.114017. arXiv:hep-ph/0508046
379. M. Gronau, J.L. Rosner, J. Zupan, Phys. Rev. D **74**, 093003 (2006). https://doi.org/10.1103/PhysRevD.74.093003. arXiv:hep-ph/0608085
380. L. Silvestrini, Ann. Rev. Nucl. Part. Sci. **57**, 405 (2007). https://doi.org/10.1146/annurev.nucl.57.090506.123007. arXiv:0705.1624 [hep-ph]
381. R. Dutta, S. Gardner, Phys. Rev. D **78**, 034021 (2008). https://doi.org/10.1103/PhysRevD.78.034021. arXiv:0805.1963 [hep-ph]
382. M. Fujikawa et al., Belle collaboration. Phys. Rev. D **81**, 011101 (2010). https://doi.org/10.1103/PhysRevD.81.011101. arXiv:0809.4366 [hep-ex]
383. K. Abe et al., Belle collaboration. Phys. Rev. D **76**, 091103 (2007). https://doi.org/10.1103/PhysRevD.76.091103. arXiv:hep-ex/0609006
384. B. Aubert et al., BaBar collaboration. Phys. Rev. D **71**, 091102 (2005). https://doi.org/10.1103/PhysRevD.71.091102. arXiv:hep-ex/0502019
385. B. Aubert et al., BaBar collaboration. Phys. Rev. D **79**, 052003 (2009). https://doi.org/10.1103/PhysRevD.79.052003. arXiv:0809.1174 [hep-ex]
386. L. Šantelj et al., Belle collaboration. JHEP **10**, 165 (2014). https://doi.org/10.1007/JHEP10(2014)165. arXiv:1408.5991 [hep-ex]
387. J.P. Lees et al., BaBar collaboration. Phys. Rev. D **85**, 054023 (2012). https://doi.org/10.1103/PhysRevD.85.054023. arXiv:1111.3636 [hep-ex]
388. K.F. Chen et al., Belle collaboration. Phys. Rev. Lett. **98**, 031802 (2007). https://doi.org/10.1103/PhysRevLett.98.031802. arXiv:hep-ex/0608039
389. V. Chobanova et al., Belle collaboration. Phys. Rev. D **90**, 012002 (2014). https://doi.org/10.1103/PhysRevD.90.012002. arXiv:1311.6666 [hep-ex]
390. B. Aubert et al., BaBar collaboration. Phys. Rev. D **76**, 071101 (2007). https://doi.org/10.1103/PhysRevD.76.071101. arXiv:hep-ex/0702010
391. B. Aubert et al., BaBar collaboration. Phys. Rev. D **78**, 092008 (2008). https://doi.org/10.1103/PhysRevD.78.092008. arXiv:0808.3586 [hep-ex]
392. I. Dunietz, FERMILAB-CONF-93-090-T (1993)
393. R. Fleischer, Phys. Lett. B **459**, 306 (1999). https://doi.org/10.1016/S0370-2693(99)00640-1. arXiv:hep-ph/9903456
394. LHCb collaboration, LHCb-CONF-2016-018 (2016)
395. R. Aaij et al., LHCb collaboration. JHEP **10**, 183 (2013). https://doi.org/10.1007/JHEP10(2013)183. arXiv:1308.1428 [hep-ex]
396. M. Raidal, Phys. Rev. Lett. **89**, 231803 (2002). https://doi.org/10.1103/PhysRevLett.89.231803. arXiv:hep-ph/0208091
397. R. Aaij et al., LHCb collaboration. Phys. Rev. D **90**, 052011 (2014). https://doi.org/10.1103/PhysRevD.90.052011. arXiv:1407.2222 [hep-ex]
398. B. Aubert et al. (BaBar collaboration), Phys. Rev. Lett. **97**, 171805 (2006). https://doi.org/10.1103/PhysRevLett.97.171805. arXiv:hep-ex/0608036 [hep-ex]
399. Y. Nakahama et al., Belle collaboration. Phys. Rev. Lett. **100**, 121601 (2008). https://doi.org/10.1103/PhysRevLett.100.121601. arXiv:0712.4234 [hep-ex]
400. S. Akar, Ph.D. thesis, LPNHE, Université Pierre et Marie Curie-Paris VI (2013). https://tel.archives-ouvertes.fr/tel-00998252
401. P. del Amo Sanchez et al., BaBar collaboration. Phys. Rev. D **93**, 052013 (2016). https://doi.org/10.1103/PhysRevD.93.052013. arXiv:1512.03579 [hep-ex]
402. J. Li et al., Belle collaboration. Phys. Rev. Lett. **101**, 251601 (2008). https://doi.org/10.1103/PhysRevLett.101.251601. arXiv:0806.1980 [hep-ex]
403. B. Aubert et al., BaBar collaboration. Phys. Rev. D **78**, 071102 (2008). https://doi.org/10.1103/PhysRevD.78.071102. arXiv:0807.3103 [hep-ex]
404. Y. Ushiroda et al., Belle collaboration. Phys. Rev. D **74**, 111104 (2006). https://doi.org/10.1103/PhysRevD.74.111104. arXiv:hep-ex/0608017
405. B. Aubert et al., BaBar collaboration. Phys. Rev. D **79**, 011102 (2009). https://doi.org/10.1103/PhysRevD.79.011102. arXiv:0805.1317 [hep-ex]
406. H. Sahoo et al., Belle collaboration. Phys. Rev. D **84**, 071101 (2011). https://doi.org/10.1103/PhysRevD.84.071101. arXiv:1104.5590 [hep-ex]

407. R. Aaij et al., LHCb collaboration. Phys. Rev. Lett. **118**, 021801 (2017). https://doi.org/10.1103/PhysRevLett.118.021801. arXiv:1609.02032 [hep-ex]
408. Y. Ushiroda et al., Belle collaboration. Phys. Rev. Lett. **100**, 021602 (2008). https://doi.org/10.1103/PhysRevLett.100.021602. arXiv:0709.2769 [hep-ex]
409. B. Aubert et al., BaBar collaboration. Phys. Rev. D **76**, 052007 (2007). https://doi.org/10.1103/PhysRevD.76.052007. arXiv:0705.2157 [hep-ex]
410. P. Vanhoefer et al., Belle collaboration. Phys. Rev. D **93**, 032010 (2016). https://doi.org/10.1103/PhysRevD.93.032010. arXiv:1510.01245 [hep-ex]
411. B. Aubert et al., BaBar collaboration. Phys. Rev. D **78**, 071104 (2008). https://doi.org/10.1103/PhysRevD.78.071104. arXiv:0807.4977 [hep-ex]
412. I. Adachi et al. (Belle collaboration), Phys. Rev. D **89**, 072008 (2014). https://doi.org/10.1103/PhysRevD.89.072008. arXiv:1212.4015 [hep-ex]. Addendum ibid. **89**, 119903 (2014). doi:10.1103/PhysRevD.89.119903
413. R. Aaij et al., LHCb collaboration. Phys. Lett. B **747**, 468 (2015). https://doi.org/10.1016/j.physletb.2015.06.027. arXiv:1503.07770 [hep-ex]
414. B. Aubert et al., BaBar collaboration. Phys. Rev. Lett. **98**, 181803 (2007). https://doi.org/10.1103/PhysRevLett.98.181803. arXiv:hep-ex/0612050
415. B. Aubert et al., BaBar collaboration. Phys. Rev. D **81**, 052009 (2010). https://doi.org/10.1103/PhysRevD.81.052009. arXiv:0909.2171 [hep-ex]
416. J.P. Lees et al., BaBar collaboration. Phys. Rev. D **87**, 052009 (2013). https://doi.org/10.1103/PhysRevD.87.052009. arXiv:1206.3525 [hep-ex]
417. I. Adachi et al., Belle collaboration. Phys. Rev. D **88**, 092003 (2013). https://doi.org/10.1103/PhysRevD.88.092003. arXiv:1302.0551 [hep-ex]
418. J. Dalseno et al., Belle collaboration. Phys. Rev. D **86**, 092012 (2012). https://doi.org/10.1103/PhysRevD.86.092012. arXiv:1205.5957 [hep-ex]
419. M. Gronau, D. London, Phys. Rev. Lett. **65**, 3381 (1990). https://doi.org/10.1103/PhysRevLett.65.3381
420. D. Asner et al. (Heavy Flavor Averaging Group), (2010). arXiv:1010.1589 [hep-ex]
421. B. Aubert et al., BaBar collaboration. Phys. Rev. Lett. **102**, 141802 (2009). https://doi.org/10.1103/PhysRevLett.102.141802. arXiv:0901.3522 [hep-ex]
422. H.J. Lipkin, Y. Nir, H.R. Quinn, A. Snyder, Phys. Rev. D **44**, 1454 (1991). https://doi.org/10.1103/PhysRevD.44.1454
423. M. Gronau, J. Zupan, Phys. Rev. D **73**, 057502 (2006). https://doi.org/10.1103/PhysRevD.73.057502. arXiv:hep-ph/0512148
424. A. Bevan et al., BaBar and Belle collaborations. Eur. Phys. J. C **74**, 3026 (2014). https://doi.org/10.1140/epjc/s10052-014-3026-9. arXiv:1406.6311 [hep-ex]
425. I. Dunietz, Phys. Lett. B **427**, 179 (1998). https://doi.org/10.1016/S0370-2693(98)00304-9. arXiv:hep-ph/9712401
426. M.A. Baak, Ph.D. thesis, Vrije U., Amsterdam (2007). http://www-public.slac.stanford.edu/sciDoc/docMeta.aspx?slacPubNumber=slac-r-858
427. K. De Bruyn, R. Fleischer, R. Knegjens, M. Merk, M. Schiller, N. Tuning, Nucl. Phys. B **868**, 351 (2013). https://doi.org/10.1016/j.nuclphysb.2012.11.012. arXiv:1208.6463 [hep-ph]
428. M. Kenzie, M. Martinelli, N. Tuning, Phys. Rev. D **94**, 054021 (2016). https://doi.org/10.1103/PhysRevD.94.054021. arXiv:1606.09129 [hep-ph]
429. B. Aubert et al., BaBar collaboration. Phys. Rev. D **77**, 071102 (2008). https://doi.org/10.1103/PhysRevD.77.071102. arXiv:0712.3469 [hep-ex]
430. I. Dunietz, R.G. Sachs, Phys. Rev. D **37**, 3186 (1988). https://doi.org/10.1103/PhysRevD.37.3186. [Erratum ibid. **39** (1989). https://doi.org/10.1103/PhysRevD.39.3515]
431. R. Aleksan, I. Dunietz, B. Kayser, Z. Phys. C **54**, 653 (1992). https://doi.org/10.1007/BF01559494
432. LHCb collaboration, LHCb-CONF-2016-015 (2016)
433. P. del Amo Sanchez et al., BaBar collaboration. Phys. Rev. D **82**, 072004 (2010). https://doi.org/10.1103/PhysRevD.82.072004. arXiv:1007.0504 [hep-ex]
434. K. Abe et al., Belle collaboration. Phys. Rev. D **73**, 051106 (2006). https://doi.org/10.1103/PhysRevD.73.051106. arXiv:hep-ex/0601032
435. T. Aaltonen et al., CDF collaboration. Phys. Rev. D **81**, 031105 (2010). https://doi.org/10.1103/PhysRevD.81.031105. arXiv:0911.0425 [hep-ex]
436. R. Aaij et al., LHCb collaboration. Phys. Lett. B **760**, 117 (2016). https://doi.org/10.1016/j.physletb.2016.06.022. arXiv:1603.08993 [hep-ex]
437. B. Aubert et al., BaBar collaboration. Phys. Rev. D **78**, 092002 (2008). https://doi.org/10.1103/PhysRevD.78.092002. arXiv:0807.2408 [hep-ex]
438. B. Aubert et al., BaBar collaboration. Phys. Rev. D **80**, 092001 (2009). https://doi.org/10.1103/PhysRevD.80.092001. arXiv:0909.3981 [hep-ex]
439. LHCb collaboration, LHCb-CONF-2016-014 (2016)
440. R. Aaij et al., LHCb collaboration. Phys. Rev. D **92**, 112005 (2015). https://doi.org/10.1103/PhysRevD.92.112005. arXiv:1505.07044 [hep-ex]
441. R. Aaij et al., LHCb collaboration. Phys. Rev. D **90**, 112002 (2014). https://doi.org/10.1103/PhysRevD.90.112002. arXiv:1407.8136 [hep-ex]
442. R. Aaij et al., LHCb collaboration. Phys. Rev. D **93**, 112018 (2016). https://doi.org/10.1103/PhysRevD.93.112018. arXiv:1602.03455 [hep-ex]
443. S. Malde et al., Phys. Lett. B **747**, 9 (2015). https://doi.org/10.1016/j.physletb.2015.05.043. arXiv:1504.05878 [hep-ex]
444. R. Aaij et al., LHCb collaboration. Phys. Rev. D **91**, 112014 (2015). https://doi.org/10.1103/PhysRevD.91.112014. arXiv:1504.05442 [hep-ex]
445. P. del Amo Sanchez et al., BaBar collaboration. Phys. Rev. D **82**, 072006 (2010). https://doi.org/10.1103/PhysRevD.82.072006. arXiv:1006.4241 [hep-ex]
446. Y. Horii et al., Belle collaboration. Phys. Rev. Lett. **106**, 231803 (2011). https://doi.org/10.1103/PhysRevLett.106.231803. arXiv:1103.5951 [hep-ex]
447. T. Aaltonen et al., CDF collaboration. Phys. Rev. D **84**, 091504 (2011). https://doi.org/10.1103/PhysRevD.84.091504. arXiv:1108.5765 [hep-ex]
448. J.P. Lees et al., BaBar collaboration. Phys. Rev. D **84**, 012002 (2011). https://doi.org/10.1103/PhysRevD.84.012002. arXiv:1104.4472 [hep-ex]
449. M. Nayak et al., Belle collaboration. Phys. Rev. D **88**, 091104 (2013). https://doi.org/10.1103/PhysRevD.88.091104. arXiv:1310.1741 [hep-ex]
450. B. Aubert et al., BaBar collaboration. Phys. Rev. D **80**, 031102 (2009). https://doi.org/10.1103/PhysRevD.80.031102. arXiv:0904.2112 [hep-ex]
451. K. Negishi et al., Belle collaboration. Phys. Rev. D **86**, 011101 (2012). https://doi.org/10.1103/PhysRevD.86.011101. arXiv:1205.0422 [hep-ex]
452. D.M. Asner et al., CLEO collaboration. Phys. Rev. D **78**, 012001 (2008). https://doi.org/10.1103/PhysRevD.78.012001. arXiv:0802.2268 [hep-ex]
453. N. Lowrey et al., CLEO collaboration. Phys. Rev. D **80**, 031105 (2009). https://doi.org/10.1103/PhysRevD.80.031105. arXiv:0903.4853 [hep-ex]

454. A. Poluektov et al., Belle collaboration. Phys. Rev. D **81**, 112002 (2010). https://doi.org/10.1103/PhysRevD.81.112002. arXiv:1003.3360 [hep-ex]
455. P. del Amo Sanchez et al., BaBar collaboration. Phys. Rev. Lett. **105**, 121801 (2010). https://doi.org/10.1103/PhysRevLett.105.121801. arXiv:1005.1096 [hep-ex]
456. R. Aaij et al., LHCb collaboration. Nucl. Phys. B **888**, 169 (2014). https://doi.org/10.1016/j.nuclphysb.2014.09.015. arXiv:1407.6211 [hep-ex]
457. A. Poluektov et al., Belle collaboration. Phys. Rev. D **73**, 112009 (2006). https://doi.org/10.1103/PhysRevD.73.112009. arXiv:hep-ex/0604054
458. R. Aaij et al., LHCb collaboration. JHEP **08**, 137 (2016). https://doi.org/10.1007/JHEP08(2016)137. arXiv:1605.01082 [hep-ex]
459. B. Aubert et al., BaBar collaboration. Phys. Rev. D **79**, 072003 (2009). https://doi.org/10.1103/PhysRevD.79.072003. arXiv:0805.2001 [hep-ex]
460. R.A. Briere et al., CLEO collaboration. Phys. Rev. D **80**, 032002 (2009). https://doi.org/10.1103/PhysRevD.80.032002. arXiv:0903.1681 [hep-ex]
461. H. Aihara et al., Belle collaboration. Phys. Rev. D **85**, 112014 (2012). https://doi.org/10.1103/PhysRevD.85.112014. arXiv:1204.6561 [hep-ex]
462. R. Aaij et al., LHCb collaboration. JHEP **10**, 97 (2014). https://doi.org/10.1007/JHEP10(2014)097. arXiv:1408.2748 [hep-ex]
463. K. Negishi et al. (Belle collaboration), PTEP **2016**, 043C01 (2016). https://doi.org/10.1093/ptep/ptw030. arXiv:1509.01098 [hep-ex]
464. R. Aaij et al., LHCb collaboration. JHEP **06**, 131 (2016). https://doi.org/10.1007/JHEP06(2016)131. arXiv:1604.01525 [hep-ex]
465. R. Aaij et al., LHCb collaboration. Phys. Lett. B **733**, 36 (2014). https://doi.org/10.1016/j.physletb.2014.03.051. arXiv:1402.2982 [hep-ex]
466. J. Insler et al., CLEO collaboration. Phys. Rev. D **85**, 092016 (2012). https://doi.org/10.1103/PhysRevD.85.092016. arXiv:1203.3804 [hep-ex]
467. J.P. Lees et al., BaBar collaboration. Phys. Rev. D **87**, 052015 (2013). https://doi.org/10.1103/PhysRevD.87.052015. arXiv:1301.1029 [hep-ex]
468. R. Aaij et al., LHCb collaboration. JHEP **12**, 087 (2016). https://doi.org/10.1007/JHEP12(2016)087. arXiv:1611.03076 [hep-ex]
469. M. Rama, Phys. Rev. D **89**, 014021 (2014). https://doi.org/10.1103/PhysRevD.89.014021. arXiv:1307.4384 [hep-ex]
470. GammaCombo framework for combinations of measurements and computation of confidence intervals, CERN. http://gammacombo.hepforge.org/
471. R. Aaij et al., LHCb collaboration. Phys. Lett. B **726**, 151 (2013). https://doi.org/10.1016/j.physletb.2013.08.020. arXiv:1305.2050 [hep-ex]
472. T. Evans, S. Harnew, J. Libby, S. Malde, J. Rademacker, G. Wilkinson, Phys. Lett. B **757**, 520 (2016). https://doi.org/10.1016/j.physletb.2016.04.037. arXiv:1602.07430 [hep-ex]
473. R. Aaij et al., LHCb collaboration. Phys. Rev. D **93**, 052018 (2016). https://doi.org/10.1103/PhysRevD.93.052018. arXiv:1509.06628 [hep-ex]
474. J.P. Silva, A. Soffer, Phys. Rev. D **61**, 112001 (2000). https://doi.org/10.1103/PhysRevD.61.112001. arXiv:hep-ph/9912242
475. Y. Grossman, A. Soffer, J. Zupan, Phys. Rev. D **72**, 031501 (2005). https://doi.org/10.1103/PhysRevD.72.031501. arXiv:hep-ph/0505270
476. M. Neubert, Phys. Rep. **245**, 259 (1994). https://doi.org/10.1016/0370-1573(94)90091-4. arXiv:hep-ph/9306320
477. A. Sirlin, Nucl. Phys. B **196**, 83 (1982). https://doi.org/10.1016/0550-3213(82)90303-0
478. I. Caprini, L. Lellouch, M. Neubert, Nucl. Phys. B **530**, 153 (1998). https://doi.org/10.1016/S0550-3213(98)00350-2. arXiv:hep-ph/9712417
479. *B* semileptonic decays common input parameters. http://www.slac.stanford.edu/xorg/hflav/semi/summer16/common/common.param.summer16
480. N.E. Adam et al., CLEO collaboration. Phys. Rev. D **67**, 032001 (2003). https://doi.org/10.1103/PhysRevD.67.032001. arXiv:hep-ex/0210040
481. B. Aubert et al., BaBar collaboration. Phys. Rev. D **79**, 012002 (2009). https://doi.org/10.1103/PhysRevD.79.012002. arXiv:0809.0828 [hep-ex]
482. B. Aubert et al., BaBar collaboration. Phys. Rev. Lett. **100**, 231803 (2008). https://doi.org/10.1103/PhysRevLett.100.231803. arXiv:0712.3493 [hep-ex]
483. W. Dungel et al., Belle collaboration. Phys. Rev. D **82**, 112007 (2010). https://doi.org/10.1103/PhysRevD.82.112007. arXiv:1010.5620 [hep-ex]
484. B. Aubert et al., BaBar collaboration. Phys. Rev. D **77**, 032002 (2008). https://doi.org/10.1103/PhysRevD.77.032002. arXiv:0705.4008 [hep-ex]
485. D. Buskulic et al., ALEPH collaboration. Phys. Lett. B **395**, 373 (1997). https://doi.org/10.1016/S0370-2693(97)00071-3
486. G. Abbiendi et al., OPAL collaboration. Phys. Lett. B **482**, 15 (2000). https://doi.org/10.1016/S0370-2693(00)00457-3. arXiv:hep-ex/0003013
487. P. Abreu et al., DELPHI collaboration. Phys. Lett. B **510**, 55 (2001). https://doi.org/10.1016/S0370-2693(01)00569-X. arXiv:hep-ex/0104026
488. J. Abdallah et al., DELPHI collaboration. Eur. Phys. J. C **33**, 213 (2004). https://doi.org/10.1140/epjc/s2004-01598-6. arXiv:hep-ex/0401023
489. J.A. Bailey et al., Fermilab Lattice and MILC collaborations. Phys. Rev. D **89**, 114504 (2014). https://doi.org/10.1103/PhysRevD.89.114504. arXiv:1403.0635 [hep-lat]
490. B. Aubert et al., BaBar collaboration. Phys. Rev. Lett. **100**, 151802 (2008). https://doi.org/10.1103/PhysRevLett.100.151802. arXiv:0712.3503 [hep-ex]
491. J.E. Bartelt et al., CLEO collaboration. Phys. Rev. Lett. **82**, 3746 (1999). https://doi.org/10.1103/PhysRevLett.82.3746. arXiv:hep-ex/9811042
492. R. Glattauer et al., Belle collaboration. Phys. Rev. D **93**, 032006 (2016). https://doi.org/10.1103/PhysRevD.93.032006. arXiv:1510.03657 [hep-ex]
493. B. Aubert et al., BaBar collaboration. Phys. Rev. Lett. **104**, 011802 (2010). https://doi.org/10.1103/PhysRevLett.104.011802. arXiv:0904.4063 [hep-ex]
494. J.A. Bailey et al., MILC collaboration. Phys. Rev. D **92**, 034506 (2015). https://doi.org/10.1103/PhysRevD.92.034506. arXiv:1503.07237 [hep-lat]
495. D. Liventsev et al., Belle collaboration. Phys. Rev. D **77**, 091503 (2008). https://doi.org/10.1103/PhysRevD.77.091503. arXiv:0711.3252 [hep-ex]
496. N. Isgur, M.B. Wise, Phys. Rev. Lett. **66**, 1130 (1991). https://doi.org/10.1103/PhysRevLett.66.1130
497. D. Buskulic et al., ALEPH collaboration. Z. Phys. C **73**, 601 (1997). https://doi.org/10.1007/s002880050351
498. G. Abbiendi et al., OPAL collaboration. Eur. Phys. J. C **30**, 467 (2003). https://doi.org/10.1140/epjc/s2003-01322-2. arXiv:hep-ex/0301018
499. A. Anastassov et al., CLEO collaboration. Phys. Rev. Lett. **80**, 4127 (1998). https://doi.org/10.1103/PhysRevLett.80.4127. arXiv:hep-ex/9708035
500. V.M. Abazov et al., D0 collaboration. Phys. Rev. Lett. **95**, 171803 (2005). https://doi.org/10.1103/PhysRevLett.95.171803. arXiv:hep-ex/0507046

501. B. Aubert et al., BaBar collaboration. Phys. Rev. Lett. **101**, 261802 (2008). https://doi.org/10.1103/PhysRevLett.101.261802. arXiv:0808.0528 [hep-ex]
502. B. Aubert et al., BaBar collaboration. Phys. Rev. Lett. **103**, 051803 (2009). https://doi.org/10.1103/PhysRevLett.103.051803. arXiv:0808.0333 [hep-ex]
503. J. Abdallah et al., DELPHI collaboration. Eur. Phys. J. C **45**, 35 (2006). https://doi.org/10.1140/epjc/s2005-02406-7. arXiv:hep-ex/0510024
504. D. Benson, I.I. Bigi, T. Mannel, N. Uraltsev, Nucl. Phys. B **665**, 367 (2003). https://doi.org/10.1016/S0550-3213(03)00452-8. arXiv:hep-ph/0302262
505. P. Gambino, N. Uraltsev, Eur. Phys. J. C **34**, 181 (2004). https://doi.org/10.1140/epjc/s2004-01671-2. arXiv:hep-ph/0401063
506. P. Gambino, JHEP **09**, 055 (2011). https://doi.org/10.1007/JHEP09(2011)055. arXiv:1107.3100 [hep-ph]
507. A. Alberti, P. Gambino, K.J. Healey, S. Nandi, Phys. Rev. Lett. **114**, 061802 (2015). https://doi.org/10.1103/PhysRevLett.114.061802. arXiv:1411.6560 [hep-ph]
508. C.W. Bauer, Z. Ligeti, M. Luke, A.V. Manohar, M. Trott, Phys. Rev. D **70**, 094017 (2004). https://doi.org/10.1103/PhysRevD.70.094017. arXiv:hep-ph/0408002
509. B. Aubert et al., BaBar collaboration. Phys. Rev. D **81**, 032003 (2010). https://doi.org/10.1103/PhysRevD.81.032003. arXiv:0908.0415 [hep-ex]
510. B. Aubert et al., BaBar collaboration. Phys. Rev. D **69**, 111104 (2004). https://doi.org/10.1103/PhysRevD.69.111104. arXiv:hep-ex/0403030
511. C. Schwanda et al., Belle collaboration. Phys. Rev. D **75**, 032005 (2007). https://doi.org/10.1103/PhysRevD.75.032005. arXiv:hep-ex/0611044
512. P. Urquijo et al., Belle collaboration. Phys. Rev. D **75**, 032001 (2007). https://doi.org/10.1103/PhysRevD.75.032001. arXiv:hep-ex/0610012
513. D.E. Acosta et al., CDF collaboration. Phys. Rev. D **71**, 051103 (2005). https://doi.org/10.1103/PhysRevD.71.051103. arXiv:hep-ex/0502003
514. S.E. Csorna et al., CLEO collaboration. Phys. Rev. D **70**, 032002 (2004). https://doi.org/10.1103/PhysRevD.70.032002. arXiv:hep-ex/0403052
515. K. Chetyrkin et al., Phys. Rev. D **80**, 074010 (2009). https://doi.org/10.1103/PhysRevD.80.074010. arXiv:0907.2110 [hep-ph]
516. B. Aubert et al., BaBar collaboration. Phys. Rev. D **72**, 052004 (2005). https://doi.org/10.1103/PhysRevD.72.052004. arXiv:hep-ex/0508004
517. B. Aubert et al., BaBar collaboration. Phys. Rev. Lett. **97**, 171803 (2006). https://doi.org/10.1103/PhysRevLett.97.171803. arXiv:hep-ex/0607071
518. A. Limosani et al., Belle collaboration. Phys. Rev. Lett. **103**, 241801 (2009). https://doi.org/10.1103/PhysRevLett.103.241801. arXiv:0907.1384 [hep-ex]
519. S. Chen et al., CLEO collaboration. Phys. Rev. Lett. **87**, 251807 (2001). https://doi.org/10.1103/PhysRevLett.87.251807. arXiv:hep-ex/0108032
520. P. Gambino, C. Schwanda, Phys. Rev. D **89**, 014022 (2014). https://doi.org/10.1103/PhysRevD.89.014022. arXiv:1307.4551 [hep-ph]
521. C. Schwanda et al., Belle collaboration. Phys. Rev. D **78**, 032016 (2008). https://doi.org/10.1103/PhysRevD.78.032016. arXiv:0803.2158 [hep-ex]
522. R. Aaij et al., LHCb collaboration. Nat. Phys. **11**, 743 (2015). https://doi.org/10.1038/nphys3415. arXiv:1504.01568 [hep-ex]
523. H. Ha et al., Belle collaboration. Phys. Rev. D **83**, 071101 (2011). https://doi.org/10.1103/PhysRevD.83.071101. arXiv:1012.0090 [hep-ex]
524. A. Sibidanov et al., Belle collaboration. Phys. Rev. D **88**, 032005 (2013). https://doi.org/10.1103/PhysRevD.88.032005. arXiv:1306.2781 [hep-ex]
525. P. del Amo Sanchez et al., BaBar collaboration. Phys. Rev. D **83**, 032007 (2011). https://doi.org/10.1103/PhysRevD.83.032007. arXiv:1005.3288 [hep-ex]
526. J.P. Lees et al., BaBar collaboration. Phys. Rev. D **86**, 092004 (2012). https://doi.org/10.1103/PhysRevD.86.092004. arXiv:1208.1253 [hep-ex]
527. C. Bourrely, I. Caprini, L. Lellouch, Phys. Rev. D **79**, 013008 (2009). https://doi.org/10.1103/PhysRevD.79.013008. arXiv:0807.2722 [hep-ph]. [Erratum ibid. **82**, 099902 (2010). doi:10.1103/PhysRevD.82.099902]
528. J.A. Bailey et al., Fermilab Lattice and MILC collaborations. Phys. Rev. D **92**, 014024 (2015). https://doi.org/10.1103/PhysRevD.92.014024. arXiv:1503.07839 [hep-lat]
529. J.M. Flynn, T. Izubuchi, T. Kawanai, C. Lehner, A. Soni, R.S. Van de Water, O. Witzel, RBC and UKQCD collaborations. Phys. Rev. D **91**, 074510 (2015). https://doi.org/10.1103/PhysRevD.91.074510. arXiv:1501.05373 [hep-lat]
530. A. Bharucha, JHEP **05**, 092 (2012). https://doi.org/10.1007/JHEP05(2012)092. arXiv:1203.1359 [hep-ph]
531. M. Ablikim et al., BESIII collaboration. Phys. Rev. Lett. **116**, 052001 (2016). https://doi.org/10.1103/PhysRevLett.116.052001. arXiv:1511.08380 [hep-ex]
532. W. Detmold, C. Lehner, S. Meinel, Phys. Rev. D **92**, 034503 (2015). https://doi.org/10.1103/PhysRevD.92.034503. arXiv:1503.01421 [hep-lat]
533. R.N. Faustov, V.O. Galkin, Phys. Rev. D **94**, 073008 (2016). https://doi.org/10.1103/PhysRevD.94.073008. arXiv:1609.00199 [hep-ph]
534. P. Ball, R. Zwicky, Phys. Rev. D **71**, 014015 (2005). https://doi.org/10.1103/PhysRevD.71.014015. arXiv:hep-ph/0406232
535. A. Bharucha, D.M. Straub, R. Zwicky, JHEP **08**, 098 (2016). https://doi.org/10.1007/JHEP08(2016)098. arXiv:1503.05534 [hep-ph]
536. B.H. Behrens et al., CLEO collaboration. Phys. Rev. D **61**, 052001 (2000). https://doi.org/10.1103/PhysRevD.61.052001. arXiv:hep-ex/9905056
537. N.E. Adam et al., CLEO collaboration. Phys. Rev. Lett. **99**, 041802 (2007). https://doi.org/10.1103/PhysRevLett.99.041802. arXiv:hep-ex/0703041
538. T. Hokuue et al., Belle collaboration. Phys. Lett. B **648**, 139 (2007). https://doi.org/10.1016/j.physletb.2007.02.067. arXiv:hep-ex/0604024
539. C. Schwanda et al., Belle collaboration. Phys. Rev. Lett. **93**, 131803 (2004). https://doi.org/10.1103/PhysRevLett.93.131803. arXiv:hep-ex/0402023
540. J.P. Lees et al., BaBar collaboration. Phys. Rev. D **87**, 032004 (2013). https://doi.org/10.1103/PhysRevD.87.032004. arXiv:1205.6245 [hep-ex]
541. J.P. Lees et al., BaBar collaboration. Phys. Rev. D **88**, 072006 (2013). https://doi.org/10.1103/PhysRevD.88.072006. arXiv:1308.2589 [hep-ex]
542. R. Gray et al., CLEO collaboration. Phys. Rev. D **76**, 012007 (2007). https://doi.org/10.1103/PhysRevD.76.012007. arXiv:hep-ex/0703042
543. B. Aubert et al., BaBar collaboration. Phys. Rev. D **79**, 052011 (2009). https://doi.org/10.1103/PhysRevD.79.052011. arXiv:0808.3524 [hep-ex]
544. B. Aubert et al., BaBar collaboration. Phys. Rev. Lett. **101**, 081801 (2008). https://doi.org/10.1103/PhysRevLett.101.081801. arXiv:0805.2408 [hep-ex]
545. P. Urquijo et al., Belle collaboration. Phys. Rev. Lett. **104**, 021801 (2010). https://doi.org/10.1103/PhysRevLett.104.021801. arXiv:0907.0379 [hep-ex]

546. J.P. Lees et al., BaBar collaboration. Phys. Rev. D **86**, 032004 (2012). https://doi.org/10.1103/PhysRevD.86.032004. arXiv:1112.0702 [hep-ex]
547. C.W. Bauer, Z. Ligeti, M.E. Luke, Phys. Rev. D **64**, 113004 (2001). https://doi.org/10.1103/PhysRevD.64.113004. arXiv:hep-ph/0107074
548. M. Neubert, Phys. Rev. D **49**, 4623 (1994). https://doi.org/10.1103/PhysRevD.49.4623. arXiv:hep-ph/9312311
549. A.K. Leibovich, I. Low, I.Z. Rothstein, Phys. Rev. D **61**, 053006 (2000). https://doi.org/10.1103/PhysRevD.61.053006. arXiv:hep-ph/9909404
550. B.O. Lange, M. Neubert, G. Paz, JHEP **10**, 084 (2005). https://doi.org/10.1088/1126-6708/2005/10/084. arXiv:hep-ph/0508178
551. J.P. Lees et al., BaBar collaboration. Phys. Rev. D **95**, 072001 (2017). https://doi.org/10.1103/PhysRevD.95.072001. arXiv:1611.05624 [hep-ex]
552. R.V. Kowalewski, S. Menke, Phys. Lett. B **541**, 29 (2002). https://doi.org/10.1016/S0370-2693(02)02181-0. arXiv:hep-ex/0205038
553. B. Aubert et al., BaBar collaboration. Phys. Rev. Lett. **95**, 111801 (2005). https://doi.org/10.1103/PhysRevLett.95.111801. arXiv:hep-ex/0506036
554. A. Bornheim et al., CLEO collaboration. Phys. Rev. Lett. **88**, 231803 (2002). https://doi.org/10.1103/PhysRevLett.88.231803. arXiv:hep-ex/0202019
555. B. Aubert et al., BaBar collaboration. Phys. Rev. D **73**, 012006 (2006). https://doi.org/10.1103/PhysRevD.73.012006. arXiv:hep-ex/0509040
556. A. Limosani et al., Belle collaboration. Phys. Lett. B **621**, 28 (2005). https://doi.org/10.1016/j.physletb.2005.06.011. arXiv:hep-ex/0504046
557. H. Kakuno et al., Belle collaboration. Phys. Rev. Lett. **92**, 101801 (2004). https://doi.org/10.1103/PhysRevLett.92.101801. arXiv:hep-ex/0311048
558. I. Bizjak et al., Belle collaboration. Phys. Rev. Lett. **95**, 241801 (2005). https://doi.org/10.1103/PhysRevLett.95.241801. arXiv:hep-ex/0505088
559. B.O. Lange, M. Neubert, G. Paz, Phys. Rev. D **72**, 073006 (2005). https://doi.org/10.1103/PhysRevD.72.073006. arXiv:hep-ph/0504071
560. S.W. Bosch, B.O. Lange, M. Neubert, G. Paz, Nucl. Phys. B **699**, 335 (2004). https://doi.org/10.1016/j.nuclphysb.2004.07.041. arXiv:hep-ph/0402094
561. S.W. Bosch, M. Neubert, G. Paz, JHEP **11**, 073 (2004). https://doi.org/10.1088/1126-6708/2004/11/073. arXiv:hep-ph/0409115
562. M. Neubert, Eur. Phys. J. C **44**, 205 (2005). https://doi.org/10.1140/epjc/s2005-02360-4. arXiv:hep-ph/0411027
563. M. Neubert, Phys. Lett. B **612**, 13 (2005). https://doi.org/10.1016/j.physletb.2005.02.055. arXiv:hep-ph/0412241
564. M. Neubert, Phys. Rev. D **72**, 074025 (2005). https://doi.org/10.1103/PhysRevD.72.074025. arXiv:hep-ph/0506245
565. J.R. Andersen, E. Gardi, JHEP **01**, 097 (2006). https://doi.org/10.1088/1126-6708/2006/01/097. arXiv:hep-ph/0509360
566. U. Aglietti, G. Ferrera, G. Ricciardi, Nucl. Phys. B **768**, 85 (2007). https://doi.org/10.1016/j.nuclphysb.2007.01.014. arXiv:hep-ph/0608047
567. P. Gambino, P. Giordano, G. Ossola, N. Uraltsev, JHEP **10**, 058 (2007). https://doi.org/10.1088/1126-6708/2007/10/058. arXiv:0707.2493 [hep-ph]
568. U. Aglietti, F. Di Lodovico, G. Ferrera, G. Ricciardi, Eur. Phys. J. C **59**, 831 (2009). https://doi.org/10.1140/epjc/s10052-008-0817-x. arXiv:0711.0860 [hep-ph]
569. U. Aglietti, G. Ricciardi, G. Ferrera, Phys. Rev. D **74**, 034004 (2006). https://doi.org/10.1103/PhysRevD.74.034004. arXiv:hep-ph/0507285
570. U. Aglietti, G. Ricciardi, G. Ferrera, Phys. Rev. D **74**, 034005 (2006). https://doi.org/10.1103/PhysRevD.74.034005. arXiv:hep-ph/0509095
571. U. Aglietti, G. Ricciardi, G. Ferrera, Phys. Rev. D **74**, 034006 (2006). https://doi.org/10.1103/PhysRevD.74.034006. arXiv:hep-ph/0509271
572. M. Duraisamy, P. Sharma, A. Datta, Phys. Rev. D **90**, 074013 (2014). https://doi.org/10.1103/PhysRevD.90.074013. arXiv:1405.3719 [hep-ph]
573. H. Na, C.M. Bouchard, G.P. Lepage, C. Monahan, J. Shigemitsu, (HPQCD collaboration), Phys. Rev. D **92**, 054510 (2015). https://doi.org/10.1103/PhysRevD.92.054510. arXiv:1505.03925 [hep-lat]. [Erratum ibid. **93**, 119906 (2016). doi:10.1103/PhysRevD.93.119906]
574. J.P. Lees et al., BaBar collaboration. Phys. Rev. Lett. **109**, 101802 (2012). https://doi.org/10.1103/PhysRevLett.109.101802. arXiv:1205.5442 [hep-ex]
575. J.P. Lees et al., BaBar collaboration. Phys. Rev. D **88**, 072012 (2013). https://doi.org/10.1103/PhysRevD.88.072012. arXiv:1303.0571 [hep-ex]
576. J.F. Kamenik, F. Mescia, Phys. Rev. D **78**, 014003 (2008). https://doi.org/10.1103/PhysRevD.78.014003Phys. arXiv:0802.3790 [hep-ph]
577. S. Fajfer, J.F. Kamenik, I. Nisandzic, Phys. Rev. D **85**, 094025 (2012). https://doi.org/10.1103/PhysRevD.85.094025. arXiv:1203.2654 [hep-ph]
578. D. Bigi, P. Gambino, Phys. Rev. D **94**, 094008 (2016). https://doi.org/10.1103/PhysRevD.94.094008. arXiv:1606.08030 [hep-ph]
579. A. Matyja et al., Belle collaboration. Phys. Rev. Lett. **99**, 191807 (2007). https://doi.org/10.1103/PhysRevLett.99.191807. arXiv:0706.4429 [hep-ex]
580. B. Aubert et al., BaBar collaboration. Phys. Rev. Lett. **100**, 021801 (2008). https://doi.org/10.1103/PhysRevLett.100.021801. arXiv:0709.1698 [hep-ex]
581. A. Bozek et al., Belle collaboration. Phys. Rev. D **82**, 072005 (2010). https://doi.org/10.1103/PhysRevD.82.072005. arXiv:1005.2302 [hep-ex]
582. M. Huschle et al., Belle collaboration. Phys. Rev. D **92**, 072014 (2015). https://doi.org/10.1103/PhysRevD.92.072014. arXiv:1507.03233 [hep-ex]
583. R. Aaij et al. (LHCb collaboration), Phys. Rev. Lett. **115**, 111803 (2015). https://doi.org/10.1103/PhysRevLett.115.111803. arXiv:1506.08614 [hep-ex]. Addendum ibid. **115**, 159901 (2015). doi:10.1103/PhysRevLett.115.159901
584. Y. Sato et al., Belle collaboration. Phys. Rev. D **94**, 072007 (2016). https://doi.org/10.1103/PhysRevD.94.072007. arXiv:1607.07923 [hep-ex]
585. S. Hirose et al., Belle collaboration. Phys. Rev. Lett. **118**(21), 211801 (2017). https://doi.org/10.1103/PhysRevLett.118.211801. arXiv:1612.00529 [hep-ex]
586. A.J. Lenz, J. Phys. G **41**, 103001 (2014). https://doi.org/10.1088/0954-3899/41/10/103001. arXiv:1404.6197 [hep-ph]
587. S. Choi et al. (Belle collaboration), Phys. Rev. Lett. **91**, 262001 (2003). https://doi.org/10.1103/PhysRevLett.91.262001. arXiv:hep-ex/0309032 [hep-ex]
588. R. Aaij et al., LHCb collaboration. Phys. Rev. Lett. **110**, 222001 (2013). https://doi.org/10.1103/PhysRevLett.110.222001. arXiv:1302.6269 [hep-ex]
589. S. Choi et al., Belle collaboration. Phys. Rev. Lett. **100**, 142001 (2008). https://doi.org/10.1103/PhysRevLett.100.142001. arXiv:0708.1790 [hep-ex]
590. R. Aaij et al., LHCb collaboration. Phys. Rev. Lett. **112**, 222002 (2014). https://doi.org/10.1103/PhysRevLett.112.222002. arXiv:1404.1903 [hep-ex]

591. R. Aaij et al., LHCb collaboration. Phys. Rev. Lett. **115**, 072001 (2015). https://doi.org/10.1103/PhysRevLett.115.072001. arXiv:1507.03414 [hep-ex]
592. K. De Bruyn et al., Phys. Rev. D **86**, 014027 (2012). https://doi.org/10.1103/PhysRevD.86.014027. arXiv:1204.1735 [hep-ph]
593. M. Jung, Phys. Lett. B **753**, 187 (2016). https://doi.org/10.1016/j.physletb.2015.12.024. arXiv:1510.03423 [hep-ph]
594. B. Aubert et al. (BaBar collaboration), Phys. Rev. D **75**, 031101 (2007). https://doi.org/10.1103/PhysRevD.75.031101, arXiv:hep-ex/0610027 [hep-ex]
595. B. Aubert et al., BaBar collaboration. Phys. Rev. D **74**, 111102 (2006). https://doi.org/10.1103/PhysRevD.74.111102. arXiv:hep-ex/0609033
596. G. Majumder et al. (Belle collaboration), Phys. Rev. D **70**, 111103 (2004). https://doi.org/10.1103/PhysRevD.70.111103. arXiv:hep-ex/0409008 [hep-ex]
597. J.P. Lees et al., BaBar collaboration. Phys. Rev. D **94**, 091101 (2016). https://doi.org/10.1103/PhysRevD.94.091101. arXiv:1609.06802 [hep-ex]
598. D. Matvienko et al., Belle collaboration. Phys. Rev. D **92**, 012013 (2015). https://doi.org/10.1103/PhysRevD.92.012013. arXiv:1505.03362 [hep-ex]
599. B. Aubert et al., BaBar collaboration. Phys. Rev. D **74**, 012001 (2006). https://doi.org/10.1103/PhysRevD.74.012001. arXiv:hep-ex/0604009
600. S. Blyth et al., Belle collaboration. Phys. Rev. D **74**, 092002 (2006). https://doi.org/10.1103/PhysRevD.74.092002. arXiv:hep-ex/0607029
601. J.P. Lees et al. (BaBar collaboration), Phys. Rev. D **84**, 112007 (2011). https://doi.org/10.1103/PhysRevD.84.112007. arXiv:1107.5751 [hep-ex]. [Erratum ibid. **87**, 039901 (2013). doi:10.1103/PhysRevD.87.039901]
602. R. Aaij et al., LHCb collaboration. Phys. Rev. D **92**, 032002 (2015). https://doi.org/10.1103/PhysRevD.92.032002. arXiv:1505.01710 [hep-ex]
603. A. Satpathy et al., Belle collaboration. Phys. Lett. B **553**, 159 (2003). https://doi.org/10.1016/S0370-2693(02)03198-2. arXiv:hep-ex/0211022
604. J. Schumann et al., Belle collaboration. Phys. Rev. D **72**, 011103 (2005). https://doi.org/10.1103/PhysRevD.72.011103. arXiv:hep-ex/0501013
605. K. Abe et al., Belle collaboration. Phys. Rev. Lett. **87**, 111801 (2001). https://doi.org/10.1103/PhysRevLett.87.111801. arXiv:hep-ex/0104051
606. B. Aubert et al., BaBar collaboration. Phys. Rev. Lett. **95**, 171802 (2005). https://doi.org/10.1103/PhysRevLett.95.171802. arXiv:hep-ex/0412040
607. A. Drutskoy et al., Belle collaboration. Phys. Lett. B **542**, 171 (2002). https://doi.org/10.1016/S0370-2693(02)02373-0. arXiv:hep-ex/0207041
608. P. Krokovny et al., Belle collaboration. Phys. Rev. Lett. **90**, 141802 (2003). https://doi.org/10.1103/PhysRevLett.90.141802. arXiv:hep-ex/0212066
609. B. Aubert et al., BaBar collaboration. Phys. Rev. D **74**, 031101 (2006). https://doi.org/10.1103/PhysRevD.74.031101. arXiv:hep-ex/0604016
610. B. Aubert et al., BaBar collaboration. Phys. Rev. Lett. **96**, 011803 (2006). https://doi.org/10.1103/PhysRevLett.96.011803. arXiv:hep-ex/0509036
611. A. Das et al., Belle collaboration. Phys. Rev. D **82**, 051103 (2010). https://doi.org/10.1103/PhysRevD.82.051103. arXiv:1007.4619 [hep-ex]
612. B. Aubert et al., BaBar collaboration. Phys. Rev. D **78**, 032005 (2008). https://doi.org/10.1103/PhysRevD.78.032005. arXiv:0803.4296 [hep-ex]
613. N. Joshi et al., Belle collaboration. Phys. Rev. D **81**, 031101 (2010). https://doi.org/10.1103/PhysRevD.81.031101. arXiv:0912.2594 [hep-ex]
614. B. Aubert et al., BaBar collaboration. Phys. Rev. D **73**, 071103 (2006). https://doi.org/10.1103/PhysRevD.73.071103. arXiv:hep-ex/0512031
615. B. Aubert et al., BaBar collaboration. Phys. Rev. Lett. **100**, 171803 (2008). https://doi.org/10.1103/PhysRevLett.100.171803. arXiv:0707.1043 [hep-ex]
616. R. Aaij et al. (LHCb collaboration), Phys. Rev. D **84**, 092001 (2011). https://doi.org/10.1103/PhysRevD.84.092001. arXiv:1109.6831 [hep-ex]. [Erratum ibid. **85**, 039904 (2011). doi:10.1103/PhysRevD.85.039904]
617. R. Aaij et al., LHCb collaboration. Phys. Rev. D **86**, 112005 (2012). https://doi.org/10.1103/PhysRevD.86.112005. arXiv:1211.1541 [hep-ex]
618. R. Aaij et al., LHCb collaboration. Phys. Rev. D **87**, 112009 (2013). https://doi.org/10.1103/PhysRevD.87.112009. arXiv:1304.6317 [hep-ex]
619. R. Aaij et al., LHCb collaboration. Phys. Rev. Lett. **109**, 131801 (2012). https://doi.org/10.1103/PhysRevLett.109.131801. arXiv:1207.5991 [hep-ex]
620. R. Aaij et al., LHCb collaboration. Phys. Rev. Lett. **108**, 161801 (2012). https://doi.org/10.1103/PhysRevLett.108.161801. arXiv:1201.4402 [hep-ex]
621. R. Aaij et al., LHCb collaboration. JHEP **05**, 019 (2015). https://doi.org/10.1007/JHEP05(2015)019. arXiv:1412.7654 [hep-ex]
622. K. Abe et al., Belle collaboration. Phys. Rev. Lett. **94**, 221805 (2005). https://doi.org/10.1103/PhysRevLett.94.221805. arXiv:hep-ex/0410091
623. A. Drutskoy et al., Belle collaboration. Phys. Rev. Lett. **94**, 061802 (2005). https://doi.org/10.1103/PhysRevLett.94.061802. arXiv:hep-ex/0409026
624. P. del Amo Sanchez et al., BaBar collaboration. Phys. Rev. D **85**, 092017 (2012). https://doi.org/10.1103/PhysRevD.85.092017. arXiv:1111.4387 [hep-ex]
625. K. Abe et al., Belle collaboration. Phys. Rev. Lett. **89**, 151802 (2002). https://doi.org/10.1103/PhysRevLett.89.151802. arXiv:hep-ex/0205083
626. T. Medvedeva et al., Belle collaboration. Phys. Rev. D **76**, 051102 (2007). https://doi.org/10.1103/PhysRevD.76.051102. arXiv:0704.2652 [hep-ex]
627. Y.W. Chang et al., Belle collaboration. Phys. Rev. D **79**, 052006 (2009). https://doi.org/10.1103/PhysRevD.79.052006. arXiv:0811.3826 [hep-ex]
628. J.P. Lees et al., BaBar collaboration. Phys. Rev. D **89**, 112002 (2014). https://doi.org/10.1103/PhysRevD.89.112002. arXiv:1401.5990 [hep-ex]
629. Y.Y. Chang et al., Belle collaboration. Phys. Rev. Lett. **115**, 221803 (2015). https://doi.org/10.1103/PhysRevLett.115.221803. arXiv:1509.03034 [hep-ex]
630. B. Aubert et al., BaBar collaboration. Phys. Rev. D **73**, 112004 (2006). https://doi.org/10.1103/PhysRevD.73.112004. arXiv:hep-ex/0604037
631. I. Adachi et al., Belle collaboration. Phys. Rev. D **77**, 091101 (2008). https://doi.org/10.1103/PhysRevD.77.091101. arXiv:0802.2988 [hep-ex]
632. P. del Amo Sanchez et al., BaBar collaboration. Phys. Rev. D **83**, 032004 (2011). https://doi.org/10.1103/PhysRevD.83.032004. arXiv:1011.3929 [hep-ex]
633. G. Gokhroo et al., Belle collaboration. Phys. Rev. Lett. **97**, 162002 (2006). https://doi.org/10.1103/PhysRevLett.97.162002. arXiv:hep-ex/0606055
634. A. Zupanc et al., Belle collaboration. Phys. Rev. D **75**, 091102 (2007). https://doi.org/10.1103/PhysRevD.75.091102. arXiv:hep-ex/0703040

635. B. Aubert et al., BaBar collaboration. Phys. Rev. D **74**, 031103 (2006). https://doi.org/10.1103/PhysRevD.74.031103. arXiv:hep-ex/0605036
636. B. Aubert et al., BaBar collaboration. Phys. Rev. D **67**, 092003 (2003). https://doi.org/10.1103/PhysRevD.67.092003. arXiv:hep-ex/0302015
637. B. Aubert et al., BaBar collaboration. Phys. Rev. D **71**, 091104 (2005). https://doi.org/10.1103/PhysRevD.71.091104. arXiv:hep-ex/0502041
638. B. Aubert et al., BaBar collaboration. Phys. Rev. D **72**, 111101 (2005). https://doi.org/10.1103/PhysRevD.72.111101. arXiv:hep-ex/0510051
639. R. Aaij et al., LHCb collaboration. Phys. Rev. D **87**, 092007 (2013). https://doi.org/10.1103/PhysRevD.87.092007. arXiv:1302.5854 [hep-ex]
640. P. Krokovny et al., Belle collaboration. Phys. Rev. Lett. **91**, 262002 (2003). https://doi.org/10.1103/PhysRevLett.91.262002. arXiv:hep-ex/0308019
641. B. Aubert et al., BaBar collaboration. Phys. Rev. Lett. **93**, 181801 (2004). https://doi.org/10.1103/PhysRevLett.93.181801. arXiv:hep-ex/0408041
642. S.K. Choi et al. (Belle collaboration), Phys. Rev. D **91**, 092011 (2015). https://doi.org/10.1103/PhysRevD.91.092011. arXiv:1504.02637 [hep-ex]. Addendum ibid. **92**, 039905 (2015). doi:10.1103/PhysRevD.92.039905
643. B. Aubert et al., BaBar collaboration. Phys. Rev. D **77**, 011102 (2008). https://doi.org/10.1103/PhysRevD.77.011102. arXiv:0708.1565 [hep-ex]
644. T. Aushev et al. (Belle collaboration), Phys. Rev. D **83**, 051102 (2011). https://doi.org/10.1103/PhysRevD.83.059902. arXiv:1102.0935 [hep-ex]. [Erratum ibid. **83**, 051102 (2011). doi:10.1103/PhysRevD.83.051102]
645. F. Abe et al., CDF collaboration. Phys. Rev. Lett. **76**, 2015 (1996). https://doi.org/10.1103/PhysRevLett.76.2015
646. K. Abe et al., Belle collaboration. Phys. Rev. D **67**, 032003 (2003). https://doi.org/10.1103/PhysRevD.67.032003. arXiv:hep-ex/0211047
647. K. Chilikin et al., Belle collaboration. Phys. Rev. D **90**, 112009 (2014). https://doi.org/10.1103/PhysRevD.90.112009. arXiv:1408.6457 [hep-ex]
648. F. Abe et al., CDF collaboration. Phys. Rev. D **58**, 072001 (1998). https://doi.org/10.1103/PhysRevD.58.072001. arXiv:hep-ex/9803013
649. R. Aaij et al., LHCb collaboration. JHEP **07**, 140 (2014). https://doi.org/10.1007/JHEP07(2014)140. arXiv:1405.3219 [hep-ex]
650. T. Affolder et al., CDF collaboration. Phys. Rev. Lett. **88**, 071801 (2002). https://doi.org/10.1103/PhysRevLett.88.071801. arXiv:hep-ex/0108022
651. P. del Amo Sanchez et al., BaBar collaboration. Phys. Rev. D **82**, 011101 (2010). https://doi.org/10.1103/PhysRevD.82.011101. arXiv:1005.5190 [hep-ex]
652. B. Aubert et al., BaBar collaboration. Phys. Rev. Lett. **91**, 071801 (2003). https://doi.org/10.1103/PhysRevLett.91.071801. arXiv:hep-ex/0304014
653. K. Abe et al., Belle collaboration. Phys. Rev. Lett. **87**, 161601 (2001). https://doi.org/10.1103/PhysRevLett.87.161601. arXiv:hep-ex/0105014
654. T. Iwashita et al. (Belle collaboration), PTEP **2014**, 043C01 (2014). https://doi.org/10.1093/ptep/ptu043. arXiv:1310.2704 [hep-ex]
655. B. Aubert et al., BaBar collaboration. Phys. Rev. Lett. **93**, 041801 (2004). https://doi.org/10.1103/PhysRevLett.93.041801. arXiv:hep-ex/0402025
656. R. Mizuk et al., Belle collaboration. Phys. Rev. D **80**, 031104 (2009). https://doi.org/10.1103/PhysRevD.80.031104. arXiv:0905.2869 [hep-ex]
657. V. Bhardwaj et al., Belle collaboration. Phys. Rev. Lett. **111**, 032001 (2013). https://doi.org/10.1103/PhysRevLett.111.032001. arXiv:1304.3975 [hep-ex]
658. B. Aubert et al., BaBar collaboration. Phys. Rev. Lett. **94**, 171801 (2005). https://doi.org/10.1103/PhysRevLett.94.171801. arXiv:hep-ex/0501061
659. B. Aubert et al., BaBar collaboration. Phys. Rev. D **78**, 091101 (2008). https://doi.org/10.1103/PhysRevD.78.091101. arXiv:0808.1487 [hep-ex]
660. V. Bhardwaj et al., Belle collaboration. Phys. Rev. Lett. **107**, 091803 (2011). https://doi.org/10.1103/PhysRevLett.107.091803. arXiv:1105.0177 [hep-ex]
661. B. Aubert et al., BaBar collaboration. Phys. Rev. Lett. **102**, 132001 (2009). https://doi.org/10.1103/PhysRevLett.102.132001. arXiv:0809.0042 [hep-ex]
662. V. Bhardwaj et al., Belle collaboration. Phys. Rev. D **93**, 052016 (2016). https://doi.org/10.1103/PhysRevD.93.052016. arXiv:1512.02672 [hep-ex]
663. J.P. Lees et al., BaBar collaboration. Phys. Rev. D **85**, 052003 (2012). https://doi.org/10.1103/PhysRevD.85.052003. arXiv:1111.5919 [hep-ex]
664. N. Soni et al., Belle collaboration. Phys. Lett. B **634**, 155 (2006). https://doi.org/10.1016/j.physletb.2006.01.013. arXiv:hep-ex/0508032
665. F. Fang et al., Belle collaboration. Phys. Rev. Lett. **90**, 071801 (2003). https://doi.org/10.1103/PhysRevLett.90.071801. arXiv:hep-ex/0208047
666. B. Aubert et al., BaBar collaboration. Phys. Rev. D **76**, 092004 (2007). https://doi.org/10.1103/PhysRevD.76.092004. arXiv:0707.1648 [hep-ex]
667. B. Aubert et al., BaBar collaboration. Phys. Rev. D **70**, 011101 (2004). https://doi.org/10.1103/PhysRevD.70.011101. arXiv:hep-ex/0403007
668. B. Aubert et al., BaBar collaboration. Phys. Rev. D **78**, 012006 (2008). https://doi.org/10.1103/PhysRevD.78.012006. arXiv:0804.1208 [hep-ex]
669. B. Aubert et al., BaBar collaboration. Phys. Rev. D **76**, 031101 (2007). https://doi.org/10.1103/PhysRevD.76.031101. arXiv:0704.1266 [hep-ex]
670. M. Chang et al., Belle collaboration. Phys. Rev. D **85**, 091102 (2012). https://doi.org/10.1103/PhysRevD.85.091102. arXiv:1203.3399 [hep-ex]
671. R. Aaij et al., LHCb collaboration. Phys. Rev. Lett. **112**, 091802 (2014). https://doi.org/10.1103/PhysRevLett.112.091802. arXiv:1310.2145 [hep-ex]
672. R. Kumar et al., Belle collaboration. Phys. Rev. D **78**, 091104 (2008). https://doi.org/10.1103/PhysRevD.78.091104. arXiv:0809.1778 [hep-ex]
673. R. Aaij et al., LHCb collaboration. Phys. Rev. D **88**, 072005 (2013). https://doi.org/10.1103/PhysRevD.88.072005. arXiv:1308.5916 [hep-ex]
674. R. Aaij et al., LHCb collaboration. Phys. Rev. D **87**, 052001 (2013). https://doi.org/10.1103/PhysRevD.87.052001. arXiv:1301.5347 [hep-ex]
675. Y. Liu et al., Belle collaboration. Phys. Rev. D **78**, 011106 (2008). https://doi.org/10.1103/PhysRevD.78.011106. arXiv:0805.3225 [hep-ex]
676. R. Aaij et al., LHCb collaboration. Phys. Rev. D **92**, 112002 (2015). https://doi.org/10.1103/PhysRevD.92.112002. arXiv:1510.04866 [hep-ex]
677. B. Aubert et al., BaBar collaboration. Phys. Rev. D **70**, 091104 (2004). https://doi.org/10.1103/PhysRevD.70.091104. arXiv:hep-ex/0408018
678. R. Aaij et al., LHCb collaboration. JHEP **09**, 006 (2013). https://doi.org/10.1007/JHEP09(2013)006. arXiv:1306.4489 [hep-ex]

679. Q. Xie et al., Belle collaboration. Phys. Rev. D **72**, 051105 (2005). https://doi.org/10.1103/PhysRevD.72.051105. arXiv:hep-ex/0508011
680. B. Aubert et al., BaBar collaboration. Phys. Rev. Lett. **90**, 231801 (2003). https://doi.org/10.1103/PhysRevLett.90.231801. arXiv:hep-ex/0303036
681. L. Zhang et al., Belle collaboration. Phys. Rev. D **71**, 091107 (2005). https://doi.org/10.1103/PhysRevD.71.091107. arXiv:hep-ex/0503037
682. B. Aubert et al., BaBar collaboration. Phys. Rev. D **71**, 091103 (2005). https://doi.org/10.1103/PhysRevD.71.091103. arXiv:hep-ex/0503021
683. F. Abe et al., CDF collaboration. Phys. Rev. D **54**, 6596 (1996). https://doi.org/10.1103/PhysRevD.54.6596. arXiv:hep-ex/9607003
684. R. Aaij et al., LHCb collaboration. Nucl. Phys. B **867**, 547 (2013). https://doi.org/10.1016/j.nuclphysb.2012.10.021. arXiv:1210.2631 [hep-ex]
685. R. Aaij et al., LHCb collaboration. Eur. Phys. J. C **72**, 2118 (2012). https://doi.org/10.1140/epjc/s10052-012-2118-7. arXiv:1205.0918 [hep-ex]
686. R. Aaij et al., LHCb collaboration. Nucl. Phys. B **871**, 403 (2013). https://doi.org/10.1016/j.nuclphysb.2013.03.004. arXiv:1302.6354 [hep-ex]
687. R. Aaij et al., LHCb collaboration. JHEP **01**, 024 (2015). https://doi.org/10.1007/JHEP01(2015)024. arXiv:1411.0943 [hep-ex]
688. B. Aubert et al., BaBar collaboration. Phys. Rev. Lett. **93**, 081801 (2004). https://doi.org/10.1103/PhysRevLett.93.081801. arXiv:hep-ex/0404005
689. B. Aubert et al., BaBar collaboration. Phys. Rev. D **82**, 031102 (2010). https://doi.org/10.1103/PhysRevD.82.031102. arXiv:1007.1370 [hep-ex]
690. N. Gabyshev et al., Belle collaboration. Phys. Rev. D **66**, 091102 (2002). https://doi.org/10.1103/PhysRevD.66.091102. arXiv:hep-ex/0208041
691. J.P. Lees et al., BaBar collaboration. Phys. Rev. D **87**, 092004 (2013). https://doi.org/10.1103/PhysRevD.87.092004. arXiv:1302.0191 [hep-ex]
692. K. Park et al., Belle collaboration. Phys. Rev. D **75**, 011101 (2007). https://doi.org/10.1103/PhysRevD.75.011101. arXiv:hep-ex/0608025
693. K. Abe et al., Belle collaboration. Phys. Rev. Lett. **97**, 202003 (2006). https://doi.org/10.1103/PhysRevLett.97.202003. arXiv:hep-ex/0508015
694. B. Aubert et al., BaBar collaboration. Phys. Rev. D **77**, 012002 (2008). https://doi.org/10.1103/PhysRevD.77.012002. arXiv:0710.5763 [hep-ex]
695. J.P. Lees et al., BaBar collaboration. Phys. Rev. D **91**, 031102 (2015). https://doi.org/10.1103/PhysRevD.91.031102. arXiv:1410.3644 [hep-ex]
696. N. Gabyshev et al., Belle collaboration. Phys. Rev. Lett. **90**, 121802 (2003). https://doi.org/10.1103/PhysRevLett.90.121802. arXiv:hep-ex/0212052
697. B. Aubert et al., BaBar collaboration. Phys. Rev. D **78**, 112003 (2008). https://doi.org/10.1103/PhysRevD.78.112003. arXiv:0807.4974 [hep-ex]
698. B. Aubert et al., BaBar collaboration. Phys. Rev. D **80**, 051105 (2009). https://doi.org/10.1103/PhysRevD.80.051105. arXiv:0907.4566 [hep-ex]
699. R. Chistov et al., Belle collaboration. Phys. Rev. D **74**, 111105 (2006). https://doi.org/10.1103/PhysRevD.74.111105. arXiv:hep-ex/0510074
700. Y. Uchida et al., Belle collaboration. Phys. Rev. D **77**, 051101 (2008). https://doi.org/10.1103/PhysRevD.77.051101. arXiv:0708.1105 [hep-ex]
701. J.P. Lees et al. (BaBar collaboration), Phys. Rev. D **84**, 071102 (2011). https://doi.org/10.1103/PhysRevD.84.071102. arXiv:1108.3211 [hep-ex]. [Erratum ibid. **85**, 039903 (2012). doi:10.1103/PhysRevD.85.039903]
702. J.P. Lees et al., BaBar collaboration. Phys. Rev. D **89**, 071102 (2014). https://doi.org/10.1103/PhysRevD.89.071102. arXiv:1312.6800 [hep-ex]
703. R. Aaij et al., LHCb collaboration. Phys. Rev. Lett. **112**, 202001 (2014). https://doi.org/10.1103/PhysRevLett.112.202001. arXiv:1403.3606 [hep-ex]
704. B. Aubert et al., BaBar collaboration. Phys. Rev. D **77**, 111101 (2008). https://doi.org/10.1103/PhysRevD.77.111101. arXiv:0803.2838 [hep-ex]
705. R. Mizuk et al., Belle collaboration. Phys. Rev. D **78**, 072004 (2008). https://doi.org/10.1103/PhysRevD.78.072004. arXiv:0806.4098 [hep-ex]
706. B. Aubert et al., BaBar collaboration. Phys. Rev. Lett. **96**, 052002 (2006). https://doi.org/10.1103/PhysRevLett.96.052002. arXiv:hep-ex/0510070
707. B. Aubert et al., BaBar collaboration. Phys. Rev. D **71**, 031501 (2005). https://doi.org/10.1103/PhysRevD.71.031501. arXiv:hep-ex/0412051
708. B. Aubert et al., BaBar collaboration. Phys. Rev. D **79**, 112001 (2009). https://doi.org/10.1103/PhysRevD.79.112001. arXiv:0811.0564 [hep-ex]
709. M. Iwabuchi et al., Belle collaboration. Phys. Rev. Lett. **101**, 041601 (2008). https://doi.org/10.1103/PhysRevLett.101.041601. arXiv:0804.0831 [hep-ex]
710. K. Abe et al., Belle collaboration. Phys. Rev. D **69**, 112002 (2004). https://doi.org/10.1103/PhysRevD.69.112002. arXiv:hep-ex/0307021
711. B. Aubert et al., BaBar collaboration. Phys. Rev. D **79**, 112004 (2009). https://doi.org/10.1103/PhysRevD.79.112004. arXiv:0901.1291 [hep-ex]
712. B. Aubert et al. (BaBar collaboration) (2003). arXiv:hep-ex/0308026
713. S. Swain et al., Belle collaboration. Phys. Rev. D **68**, 051101 (2003). https://doi.org/10.1103/PhysRevD.68.051101. arXiv:hep-ex/0304032
714. B. Aubert et al., BaBar collaboration. Phys. Rev. D **73**, 111104 (2006). https://doi.org/10.1103/PhysRevD.73.111104. arXiv:hep-ex/0604017
715. B. Aubert et al., BaBar collaboration. Phys. Rev. Lett. **92**, 141801 (2004). https://doi.org/10.1103/PhysRevLett.92.141801. arXiv:hep-ex/0308057
716. R. Aaij et al. (LHCb collaboration), Phys. Rev. D **91**, 092002 (2015). https://doi.org/10.1103/PhysRevD.91.092002. arXiv:1503.02995 [hep-ex]. [Erratum ibid. **93**, 119901 (2016). doi:10.1103/PhysRevD.93.119901]
717. P. del Amo Sanchez et al., BaBar collaboration. Phys. Rev. D **82**, 092006 (2010). https://doi.org/10.1103/PhysRevD.82.092006. arXiv:1005.0068 [hep-ex]
718. R. Aaij et al. (LHCb collaboration), Phys. Rev. D **93**, 051101 (2016). https://doi.org/10.1103/PhysRevD.93.051101. arXiv:1512.02494 [hep-ex]. [Erratum ibid. **93**, 119902 (2016). doi:10.1103/PhysRevD.93.119902]
719. B. Aubert et al., BaBar collaboration. Phys. Rev. D **72**, 011102 (2005). https://doi.org/10.1103/PhysRevD.72.011102. arXiv:hep-ex/0505099
720. A. Abulencia et al., CDF collaboration. Phys. Rev. Lett. **96**, 191801 (2006). https://doi.org/10.1103/PhysRevLett.96.191801. arXiv:hep-ex/0508014
721. Y. Horii et al., Belle collaboration. Phys. Rev. D **78**, 071901 (2008). https://doi.org/10.1103/PhysRevD.78.071901. arXiv:0804.2063 [hep-ex]

722. B. Aubert et al., BaBar collaboration. Phys. Rev. Lett. **92**, 202002 (2004). https://doi.org/10.1103/PhysRevLett.92.202002. arXiv:hep-ex/0311032
723. B. Aubert et al., BaBar collaboration. Phys. Rev. D **71**, 031102 (2005). https://doi.org/10.1103/PhysRevD.71.031102. arXiv:hep-ex/0411091
724. J. Wiechczynski et al., Belle collaboration. Phys. Rev. D **80**, 052005 (2009). https://doi.org/10.1103/PhysRevD.80.052005. arXiv:0903.4956 [hep-ex]
725. B. Aubert et al., BaBar collaboration. Phys. Rev. Lett. **98**, 171801 (2007). https://doi.org/10.1103/PhysRevLett.98.171801. arXiv:hep-ex/0611030
726. R. Aaij et al., LHCb collaboration. JHEP **02**, 043 (2013). https://doi.org/10.1007/JHEP02(2013)043. arXiv:1210.1089 [hep-ex]
727. B. Aubert et al., BaBar collaboration. Phys. Rev. D **73**, 011103 (2006). https://doi.org/10.1103/PhysRevD.73.011103. arXiv:hep-ex/0512028
728. P. Chen et al., Belle collaboration. Phys. Rev. D **84**, 071501 (2011). https://doi.org/10.1103/PhysRevD.84.071501. arXiv:1108.4271 [hep-ex]
729. O. Seon et al., Belle collaboration. Phys. Rev. D **84**, 071106 (2011). https://doi.org/10.1103/PhysRevD.84.071106. arXiv:1107.0642 [hep-ex]
730. G. Majumder et al., Belle collaboration. Phys. Rev. Lett. **95**, 041803 (2005). https://doi.org/10.1103/PhysRevLett.95.041803. arXiv:hep-ex/0502038
731. J. Brodzicka et al., Belle collaboration. Phys. Rev. Lett. **100**, 092001 (2008). https://doi.org/10.1103/PhysRevLett.100.092001. arXiv:0707.3491 [hep-ex]
732. K. Abe et al., Belle collaboration. Phys. Rev. Lett. **93**, 051803 (2004). https://doi.org/10.1103/PhysRevLett.93.051803. arXiv:hep-ex/0307061
733. K. Abe et al., Belle collaboration. Phys. Lett. B **538**, 11 (2002). https://doi.org/10.1016/S0370-2693(02)01969-X. arXiv:hep-ex/0205021
734. D. Acosta et al., CDF collaboration. Phys. Rev. D **66**, 052005 (2002). https://doi.org/10.1103/PhysRevD.66.052005
735. H. Guler et al., Belle collaboration. Phys. Rev. D **83**, 032005 (2011). https://doi.org/10.1103/PhysRevD.83.032005. arXiv:1009.5256 [hep-ex]
736. B. Aubert et al., BaBar collaboration. Phys. Rev. D **71**, 071103 (2005). https://doi.org/10.1103/PhysRevD.71.071103. arXiv:hep-ex/0406022
737. K. Abe et al., Belle collaboration. Phys. Rev. Lett. **88**, 031802 (2002). https://doi.org/10.1103/PhysRevLett.88.031802. arXiv:hep-ex/0111069
738. A. Vinokurova et al., Belle collaboration. Phys. Lett. B **706**, 139 (2011). https://doi.org/10.1016/j.physletb.2011.11.014. arXiv:1105.0978 [hep-ex]
739. C.-H. Wu et al., Belle collaboration. Phys. Rev. Lett. **97**, 162003 (2006). https://doi.org/10.1103/PhysRevLett.97.162003. arXiv:hep-ex/0606022
740. B. Aubert et al., BaBar collaboration. Phys. Rev. D **72**, 051101 (2005). https://doi.org/10.1103/PhysRevD.72.051101. arXiv:hep-ex/0507012
741. F. Fang et al., Belle collaboration. Phys. Rev. D **74**, 012007 (2006). https://doi.org/10.1103/PhysRevD.74.012007. arXiv:hep-ex/0605007
742. R. Aaij et al., LHCb collaboration. Phys. Rev. D **85**, 091105 (2012). https://doi.org/10.1103/PhysRevD.85.091105. arXiv:1203.3592 [hep-ex]
743. B. Aubert et al., BaBar collaboration. Phys. Rev. Lett. **92**, 241802 (2004). https://doi.org/10.1103/PhysRevLett.92.241802. arXiv:hep-ex/0401035
744. B. Aubert et al., BaBar collaboration. Phys. Rev. D **72**, 052002 (2005). https://doi.org/10.1103/PhysRevD.72.052002. arXiv:hep-ex/0507025
745. R. Kumar et al., Belle collaboration. Phys. Rev. D **74**, 051103 (2006). https://doi.org/10.1103/PhysRevD.74.051103. arXiv:hep-ex/0607008
746. V. Abazov et al., D0 collaboration. Phys. Rev. D **79**, 111102 (2009). https://doi.org/10.1103/PhysRevD.79.111102. arXiv:0805.2576 [hep-ex]
747. R. Aaij et al., LHCb collaboration. Eur. Phys. J. C **73**, 2462 (2013). https://doi.org/10.1140/epjc/s10052-013-2462-2. arXiv:1303.7133 [hep-ex]
748. F. Abe et al., CDF collaboration. Phys. Rev. Lett. **77**, 5176 (1996). https://doi.org/10.1103/PhysRevLett.77.5176
749. A. Abulencia, CDF collaboration. Phys. Rev. D **79**, 112003 (2009). https://doi.org/10.1103/PhysRevD.79.112003. arXiv:0905.2146 [hep-ex]
750. J.P. Lees et al., BaBar collaboration. Phys. Rev. D **86**, 091102 (2012). https://doi.org/10.1103/PhysRevD.86.091102. arXiv:1208.3086 [hep-ex]
751. S.K. Choi et al., Belle collaboration. Phys. Rev. D **84**, 052004 (2011). https://doi.org/10.1103/PhysRevD.84.052004. arXiv:1107.0163 [hep-ex]
752. B. Aubert et al., BaBar collaboration. Phys. Rev. D **74**, 071101 (2006). https://doi.org/10.1103/PhysRevD.74.071101. arXiv:hep-ex/0607050
753. B. Aubert et al., BaBar collaboration. Phys. Rev. D **73**, 011101 (2006). https://doi.org/10.1103/PhysRevD.73.011101. arXiv:hep-ex/0507090
754. R. Aaij et al., LHCb collaboration. Phys. Rev. Lett. **118**, 022003 (2017). https://doi.org/10.1103/PhysRevLett.118.022003. arXiv:1606.07895 [hep-ex]
755. V.M. Abazov et al., D0 collaboration. Phys. Rev. D **89**, 012004 (2014). https://doi.org/10.1103/PhysRevD.89.012004. arXiv:1309.6580 [hep-ex]
756. T. Aushev et al., Belle collaboration. Phys. Rev. D **81**, 031103 (2010). https://doi.org/10.1103/PhysRevD.81.031103. arXiv:0810.0358 [hep-ex]
757. K. Abe et al., Belle collaboration. Phys. Rev. Lett. **94**, 182002 (2005). https://doi.org/10.1103/PhysRevLett.94.182002. arXiv:hep-ex/0408126
758. R. Aaij et al., LHCb collaboration. JHEP **06**, 115 (2012). https://doi.org/10.1007/JHEP06(2012)115. arXiv:1204.1237 [hep-ex]
759. R. Louvot et al., Belle collaboration. Phys. Rev. Lett. **104**, 231801 (2010). https://doi.org/10.1103/PhysRevLett.104.231801. arXiv:1003.5312 [hep-ex]
760. R. Aaij et al., LHCb collaboration. JHEP **06**, 130 (2015). https://doi.org/10.1007/JHEP06(2015)130. arXiv:1503.09086 [hep-ex]
761. R. Aaij et al., LHCb collaboration. Phys. Rev. Lett. **116**, 161802 (2016). https://doi.org/10.1103/PhysRevLett.116.161802. arXiv:1603.02408 [hep-ex]
762. R. Aaij et al., LHCb collaboration. Phys. Lett. B **706**, 32 (2011). https://doi.org/10.1016/j.physletb.2011.10.073. arXiv:1110.3676 [hep-ex]
763. R. Aaij et al., LHCb collaboration. Phys. Rev. D **87**, 071101 (2013). https://doi.org/10.1103/PhysRevD.87.071101. arXiv:1302.6446 [hep-ex]
764. R. Aaij et al., LHCb collaboration. JHEP **08**, 005 (2015). https://doi.org/10.1007/JHEP08(2015)005. arXiv:1505.01654 [hep-ex]
765. A. Abulencia et al., CDF collaboration. Phys. Rev. Lett. **98**, 061802 (2007). https://doi.org/10.1103/PhysRevLett.98.061802. arXiv:hep-ex/0610045
766. R. Aaij et al., LHCb collaboration. Phys. Lett. B **727**, 403 (2013). https://doi.org/10.1016/j.physletb.2013.10.057. arXiv:1308.4583 [hep-ex]

767. T. Aaltonen et al., CDF collaboration. Phys. Rev. Lett. **103**, 191802 (2009). https://doi.org/10.1103/PhysRevLett.103.191802. arXiv:0809.0080 [hep-ex]
768. T. Aaltonen et al., CDF collaboration. Phys. Rev. Lett. **108**, 201801 (2012). https://doi.org/10.1103/PhysRevLett.108.201801. arXiv:1204.0536 [hep-ex]
769. R. Aaij et al., LHCb collaboration. Phys. Rev. D **93**, 092008 (2016). https://doi.org/10.1103/PhysRevD.93.092008. arXiv:1602.07543 [hep-ex]
770. J. Li et al., Belle collaboration. Phys. Rev. Lett. **108**, 181808 (2012). https://doi.org/10.1103/PhysRevLett.108.181808. arXiv:1202.0103 [hep-ex]
771. R. Aaij et al., LHCb collaboration. Phys. Rev. D **87**, 072004 (2013). https://doi.org/10.1103/PhysRevD.87.072004. arXiv:1302.1213 [hep-ex]
772. F. Thorne et al., Belle collaboration. Phys. Rev. D **88**, 114006 (2013). https://doi.org/10.1103/PhysRevD.88.114006. arXiv:1309.0704 [hep-ex]
773. R. Aaij et al., LHCb collaboration. Phys. Lett. B **713**, 172 (2012). https://doi.org/10.1016/j.physletb.2012.05.062. arXiv:1205.0934 [hep-ex]
774. T. Aaltonen et al., CDF collaboration. Phys. Rev. D **83**, 052012 (2011). https://doi.org/10.1103/PhysRevD.83.052012. arXiv:1102.1961 [hep-ex]
775. R. Aaij et al., LHCb collaboration. JHEP **11**, 082 (2015). https://doi.org/10.1007/JHEP11(2015)082. arXiv:1509.00400 [hep-ex]
776. R. Aaij et al., LHCb collaboration. Phys. Rev. Lett. **108**, 151801 (2012). https://doi.org/10.1103/PhysRevLett.108.151801. arXiv:1112.4695 [hep-ex]
777. V.M. Abazov et al., D0 collaboration. Phys. Rev. D **86**, 092011 (2012). https://doi.org/10.1103/PhysRevD.86.092011. arXiv:1204.5723 [hep-ex]
778. R. Aaij et al., LHCb collaboration. Phys. Lett. B **698**, 115 (2011). https://doi.org/10.1016/j.physletb.2011.03.006. arXiv:1102.0206 [hep-ex]
779. A. Abulencia et al., CDF collaboration. Phys. Rev. Lett. **96**, 231801 (2006). https://doi.org/10.1103/PhysRevLett.96.231801. arXiv:hep-ex/0602005
780. V.M. Abazov et al., D0 collaboration. Phys. Rev. D **85**, 011103 (2012). https://doi.org/10.1103/PhysRevD.85.011103. arXiv:1110.4272 [hep-ex]
781. V. Khachatryan et al., CMS collaboration. Phys. Lett. B **756**, 84 (2016). https://doi.org/10.1016/j.physletb.2016.02.047. arXiv:1501.06089 [hep-ex]
782. R. Aaij et al., LHCb collaboration. JHEP **03**, 040 (2016). https://doi.org/10.1007/JHEP03(2016)040. arXiv:1601.05284 [hep-ex]
783. R. Aaij et al., LHCb collaboration. Phys. Lett. B **747**, 484 (2015). https://doi.org/10.1016/j.physletb.2015.06.038. arXiv:1503.07112 [hep-ex]
784. R. Aaij et al., LHCb collaboration. Phys. Rev. D **89**, 092006 (2014). https://doi.org/10.1103/PhysRevD.89.092006. arXiv:1402.6248 [hep-ex]
785. E. Solovieva et al., Belle collaboration. Phys. Lett. B **726**, 206 (2013). https://doi.org/10.1016/j.physletb.2013.08.057. arXiv:1304.6931 [hep-ex]
786. R. Aaij et al., LHCb collaboration. Phys. Rev. D **87**, 112012 (2013). https://doi.org/10.1103/PhysRevD.87.112012. arXiv:1304.4530 [hep-ex]
787. G. Aad et al., ATLAS collaboration. Eur. Phys. J. C **76**, 4 (2016). https://doi.org/10.1140/epjc/s10052-015-3743-8. arXiv:1507.07099 [hep-ex]
788. R. Aaij et al., LHCb collaboration. Phys. Rev. Lett. **108**, 251802 (2012). https://doi.org/10.1103/PhysRevLett.108.251802. arXiv:1204.0079 [hep-ex]
789. V. Khachatryan et al., CMS collaboration. JHEP **01**, 063 (2015). https://doi.org/10.1007/JHEP01(2015)063. arXiv:1410.5729 [hep-ex]
790. R. Aaij et al., LHCb collaboration. JHEP **09**, 075 (2013). https://doi.org/10.1007/JHEP09(2013)075. arXiv:1306.6723 [hep-ex]
791. R. Aaij et al., LHCb collaboration. JHEP **11**, 094 (2013). https://doi.org/10.1007/JHEP11(2013)094. arXiv:1309.0587 [hep-ex]
792. R. Aaij et al., LHCb collaboration. Phys. Rev. D **92**, 072007 (2015). https://doi.org/10.1103/PhysRevD.92.072007. arXiv:1507.03516 [hep-ex]
793. R. Aaij et al., LHCb collaboration. Phys. Rev. Lett. **114**, 132001 (2015). https://doi.org/10.1103/PhysRevLett.114.132001. arXiv:1411.2943 [hep-ex]
794. R. Aaij et al., LHCb collaboration. Phys. Rev. Lett. **109**, 232001 (2012). https://doi.org/10.1103/PhysRevLett.109.232001. arXiv:1209.5634 [hep-ex]
795. R. Aaij et al., LHCb collaboration. Phys. Rev. D **94**, 091102 (2016). https://doi.org/10.1103/PhysRevD.94.091102. arXiv:1607.06134 [hep-ex]
796. R. Aaij et al., LHCb collaboration. Phys. Rev. Lett. **111**, 181801 (2013). https://doi.org/10.1103/PhysRevLett.111.181801. arXiv:1308.4544 [hep-ex]
797. R. Aaij et al., LHCb collaboration. Phys. Rev. D **89**, 032001 (2014). https://doi.org/10.1103/PhysRevD.89.032001. arXiv:1311.4823 [hep-ex]
798. R. Aaij et al., LHCb collaboration. Chin. Phys. C **40**, 011001 (2016). https://doi.org/10.1088/1674-1137/40/1/011001. arXiv:1509.00292 [hep-ex]
799. F. Abe et al., CDF collaboration. Phys. Rev. D **55**, 1142 (1997). https://doi.org/10.1103/PhysRevD.55.1142
800. V.M. Abazov et al., D0 collaboration. Phys. Rev. D **84**, 031102 (2011). https://doi.org/10.1103/PhysRevD.84.031102. arXiv:1105.0690 [hep-ex]
801. G. Aad et al., ATLAS collaboration. Phys. Lett. B **751**, 63 (2015). https://doi.org/10.1016/j.physletb.2015.10.009. arXiv:1507.08202 [hep-ex]
802. R. Aaij et al., LHCb collaboration. JHEP **07**, 103 (2014). https://doi.org/10.1007/JHEP07(2014)103. arXiv:1406.0755 [hep-ex]
803. R. Aaij et al., LHCb collaboration. JHEP **05**, 132 (2016). https://doi.org/10.1007/JHEP05(2016)132. arXiv:1603.06961 [hep-ex]
804. G. Aad et al., ATLAS collaboration. Phys. Rev. D **89**, 092009 (2014). https://doi.org/10.1103/PhysRevD.89.092009. arXiv:1404.1071 [hep-ex]
805. T. Aaltonen et al., CDF collaboration. Phys. Rev. D **85**, 032003 (2012). https://doi.org/10.1103/PhysRevD.85.032003. arXiv:1112.3334 [hep-ex]
806. A. Abulencia et al., CDF collaboration. Phys. Rev. Lett. **98**, 122002 (2007). https://doi.org/10.1103/PhysRevLett.98.122002. arXiv:hep-ex/0601003
807. R. Aaij et al., LHCb collaboration. Phys. Rev. Lett. **115**, 241801 (2015). https://doi.org/10.1103/PhysRevLett.115.241801. arXiv:1510.03829 [hep-ex]
808. Y.T. Duh et al., Belle collaboration. Phys. Rev. D **87**, 031103 (2013). https://doi.org/10.1103/PhysRevD.87.031103. arXiv:1210.1348 [hep-ex]
809. A. Bornheim et al. (CLEO collaboration), Phys. Rev. D **68**, 052002 (2003). https://doi.org/10.1103/PhysRevD.68.052002. arXiv:hep-ex/0302026. [Erratum ibid. **75**, 119907 (2007). doi:10.1103/PhysRevD.75.119907]
810. B. Aubert et al., BaBar collaboration. Phys. Rev. D **76**, 091102 (2007). https://doi.org/10.1103/PhysRevD.76.091102. arXiv:0707.2798 [hep-ex]
811. B. Aubert et al., BaBar collaboration. Phys. Rev. D **80**, 112002 (2009). https://doi.org/10.1103/PhysRevD.80.112002. arXiv:0907.1743 [hep-ex]

812. J. Schumann et al., Belle collaboration. Phys. Rev. Lett. **97**, 061802 (2006). https://doi.org/10.1103/PhysRevLett.97.061802. arXiv:hep-ex/0603001
813. P. del Amo Sanchez et al., BaBar collaboration. Phys. Rev. D **82**, 011502 (2010). https://doi.org/10.1103/PhysRevD.82.011502. arXiv:1004.0240 [hep-ex]
814. J. Schumann et al., Belle collaboration. Phys. Rev. D **75**, 092002 (2007). https://doi.org/10.1103/PhysRevD.75.092002. arXiv:hep-ex/0701046
815. C.T. Hoi et al., Belle collaboration. Phys. Rev. Lett. **108**, 031801 (2012). https://doi.org/10.1103/PhysRevLett.108.031801. arXiv:1110.2000 [hep-ex]
816. S.J. Richichi et al., CLEO collaboration. Phys. Rev. Lett. **85**, 520 (2000). https://doi.org/10.1103/PhysRevLett.85.520. arXiv:hep-ex/9912059
817. B. Aubert et al., BaBar collaboration. Phys. Rev. Lett. **97**, 201802 (2006). https://doi.org/10.1103/PhysRevLett.97.201802. arXiv:hep-ex/0608005
818. C.H. Wang et al., Belle collaboration. Phys. Rev. D **75**, 092005 (2007). https://doi.org/10.1103/PhysRevD.75.092005. arXiv:hep-ex/0701057
819. B. Aubert et al., BaBar collaboration. Phys. Rev. Lett. **101**, 091801 (2008). https://doi.org/10.1103/PhysRevLett.101.091801. arXiv:0804.0411 [hep-ex]
820. B. Aubert et al., BaBar collaboration. Phys. Rev. D **76**, 031103 (2007). https://doi.org/10.1103/PhysRevD.76.031103. arXiv:0706.3893 [hep-ex]
821. C.P. Jessop et al., CLEO collaboration. Phys. Rev. Lett. **85**, 2881 (2000). https://doi.org/10.1103/PhysRevLett.85.2881. arXiv:hep-ex/0006008
822. B. Aubert et al., BaBar collaboration. Phys. Rev. D **79**, 052005 (2009). https://doi.org/10.1103/PhysRevD.79.052005. arXiv:0901.3703 [hep-ex]
823. B. Aubert et al., BaBar collaboration. Phys. Rev. D **70**, 111102 (2004). https://doi.org/10.1103/PhysRevD.70.111102. arXiv:hep-ex/0407013
824. J.P. Lees et al., BaBar collaboration. Phys. Rev. D **84**, 092007 (2011). https://doi.org/10.1103/PhysRevD.84.092007. arXiv:1109.0143 [hep-ex]
825. B. Aubert et al., BaBar collaboration. Phys. Rev. D **78**, 091102 (2008). https://doi.org/10.1103/PhysRevD.78.091102. arXiv:0808.0900 [hep-ex]
826. A. Garmash et al., Belle collaboration. Phys. Rev. D **69**, 012001 (2004). https://doi.org/10.1103/PhysRevD.69.012001. arXiv:hep-ex/0307082
827. R. Aaij et al., LHCb collaboration. Phys. Lett. B **765**, 307 (2017). https://doi.org/10.1016/j.physletb.2016.11.053. arXiv:1608.01478 [hep-ex]
828. T. Bergfeld et al., CLEO collaboration. Phys. Rev. Lett. **77**, 4503 (1996). https://doi.org/10.1103/PhysRevLett.77.4503
829. E. Eckhart et al., CLEO collaboration. Phys. Rev. Lett. **89**, 251801 (2002). https://doi.org/10.1103/PhysRevLett.89.251801. arXiv:hep-ex/0206024
830. B. Aubert et al., BaBar collaboration. Phys. Rev. D **76**, 011103 (2007). https://doi.org/10.1103/PhysRevD.76.011103. arXiv:hep-ex/0702043
831. B. Aubert et al. (BaBar collaboration), Phys. Rev. D **74**, 051104, (2006). https://doi.org/10.1103/PhysRevD.74.051104. arXiv:hep-ex/0607113 [hep-ex]
832. P. del Amo Sanchez et al., BaBar collaboration. Phys. Rev. D **83**, 051101 (2011). https://doi.org/10.1103/PhysRevD.83.051101. arXiv:1012.4044 [hep-ex]
833. B. Aubert et al., BaBar collaboration. Phys. Rev. Lett. **100**, 051803 (2008). https://doi.org/10.1103/PhysRevLett.100.051803. arXiv:0709.4165 [hep-ex]
834. B. Aubert et al., BaBar collaboration. Phys. Rev. D **78**, 011104 (2008). https://doi.org/10.1103/PhysRevD.78.011104. arXiv:0805.1217 [hep-ex]
835. H. Albrecht et al., ARGUS collaboration. Phys. Lett. B **254**, 288 (1991). https://doi.org/10.1016/0370-2693(91)90436-T
836. B. Aubert et al., BaBar collaboration. Phys. Rev. Lett. **99**, 241803 (2007). https://doi.org/10.1103/PhysRevLett.99.241803. arXiv:0707.4561 [hep-ex]
837. B. Aubert et al., BaBar collaboration. Phys. Rev. D **80**, 051101 (2009). https://doi.org/10.1103/PhysRevD.80.051101. arXiv:0907.3485 [hep-ex]
838. R. Aaij et al., LHCb collaboration. Phys. Lett. B **726**, 646 (2013). https://doi.org/10.1016/j.physletb.2013.09.046. arXiv:1308.1277 [hep-ex]
839. B. Aubert et al., BaBar collaboration. Phys. Rev. D **79**, 051101 (2009). https://doi.org/10.1103/PhysRevD.79.051101. arXiv:0811.1979 [hep-ex]
840. B. Aubert et al., BaBar collaboration. Phys. Rev. Lett. **99**, 221801 (2007). https://doi.org/10.1103/PhysRevLett.99.221801. arXiv:0708.0376 [hep-ex]
841. B. Aubert et al., BaBar collaboration. Phys. Rev. D **76**, 071103 (2007). https://doi.org/10.1103/PhysRevD.76.071103. arXiv:0706.1059 [hep-ex]
842. H.C. Huang et al., Belle collaboration. Phys. Rev. Lett. **91**, 241802 (2003). https://doi.org/10.1103/PhysRevLett.91.241802. arXiv:hep-ex/0305068
843. B. Aubert et al., BaBar collaboration. Phys. Rev. D **79**, 051102 (2009). https://doi.org/10.1103/PhysRevD.79.051102. arXiv:0901.1223 [hep-ex]
844. Y.M. Goh et al., Belle collaboration. Phys. Rev. D **91**, 071101 (2015). https://doi.org/10.1103/PhysRevD.91.071101. arXiv:1502.00381 [hep-ex]
845. R.A. Briere et al., CLEO collaboration. Phys. Rev. Lett. **86**, 3718 (2001). https://doi.org/10.1103/PhysRevLett.86.3718. arXiv:hep-ex/0101032
846. D. Acosta et al., CDF collaboration. Phys. Rev. Lett. **95**, 031801 (2005). https://doi.org/10.1103/PhysRevLett.95.031801. arXiv:hep-ex/0502044
847. A. Abulencia et al., CDF collaboration. Phys. Rev. D **73**, 032003 (2006). https://doi.org/10.1103/PhysRevD.73.032003. arXiv:hep-ex/0510048
848. B. Aubert et al., BaBar collaboration. Phys. Rev. Lett. **99**, 201802 (2007). https://doi.org/10.1103/PhysRevLett.99.201802. arXiv:0705.1798 [hep-ex]
849. K.F. Chen et al., Belle collaboration. Phys. Rev. Lett. **91**, 201801 (2003). https://doi.org/10.1103/PhysRevLett.91.201801. arXiv:hep-ex/0307014
850. B. Aubert et al., BaBar collaboration. Phys. Rev. Lett. **101**, 161801 (2008). https://doi.org/10.1103/PhysRevLett.101.161801. arXiv:0806.4419 [hep-ex]
851. P. del Amo Sanchez et al., BaBar collaboration. Phys. Rev. D **82**, 091101 (2010). https://doi.org/10.1103/PhysRevD.82.091101. arXiv:1007.2732 [hep-ex]
852. J.P. Lees et al., BaBar collaboration. Phys. Rev. D **84**, 012001 (2011). https://doi.org/10.1103/PhysRevD.84.012001. arXiv:1105.5159 [hep-ex]
853. B. Aubert et al., BaBar collaboration. Phys. Rev. D **74**, 031105 (2006). https://doi.org/10.1103/PhysRevD.74.031105. arXiv:hep-ex/0605008
854. C. Liu et al., Belle collaboration. Phys. Rev. D **79**, 071102 (2009). https://doi.org/10.1103/PhysRevD.79.071102. arXiv:0902.4757 [hep-ex]
855. B. Aubert et al., BaBar collaboration. Phys. Rev. D **79**, 072006 (2009). https://doi.org/10.1103/PhysRevD.79.072006. arXiv:0902.2051 [hep-ex]

856. A. Gordon et al., Belle collaboration. Phys. Lett. B **542**, 183 (2002). https://doi.org/10.1016/S0370-2693(02)02374-2. arXiv:hep-ex/0207007
857. H. Albrecht et al., ARGUS collaboration. Phys. Lett. B **241**, 278 (1990). https://doi.org/10.1016/0370-2693(90)91293-K
858. B. Aubert et al., BaBar collaboration. Phys. Rev. D **75**, 091103 (2007). https://doi.org/10.1103/PhysRevD.75.091103. arXiv:hep-ex/0701035
859. J. Zhang et al., Belle collaboration. Phys. Rev. Lett. **94**, 031801 (2005). https://doi.org/10.1103/PhysRevLett.94.031801. arXiv:hep-ex/0406006
860. J. Zhang et al., Belle collaboration. Phys. Rev. Lett. **91**, 221801 (2003). https://doi.org/10.1103/PhysRevLett.91.221801. arXiv:hep-ex/0306007
861. B. Aubert et al., BaBar collaboration. Phys. Rev. Lett. **99**, 261801 (2007). https://doi.org/10.1103/PhysRevLett.99.261801/. arXiv:0708.0050 [hep-ex]
862. C.M. Jen et al., Belle collaboration. Phys. Rev. D **74**, 111101 (2006). https://doi.org/10.1103/PhysRevD.74.111101. arXiv:hep-ex/0609022
863. B. Aubert et al., BaBar collaboration. Phys. Rev. D **78**, 011107 (2008). https://doi.org/10.1103/PhysRevD.78.011107. arXiv:0804.2422 [hep-ex]
864. B. Aubert et al., BaBar collaboration. Phys. Rev. D **74**, 011102 (2006). https://doi.org/10.1103/PhysRevD.74.011102. arXiv:hep-ex/0605037
865. J.H. Kim et al., Belle collaboration. Phys. Rev. D **86**, 031101 (2012). https://doi.org/10.1103/PhysRevD.86.031101. arXiv:1206.4760 [hep-ex]
866. R. Aaij et al., LHCb collaboration. Phys. Lett. B **728**, 85 (2014). https://doi.org/10.1016/j.physletb.2013.11.036. arXiv:1309.3742 [hep-ex]
867. B. Aubert et al., BaBar collaboration. Phys. Rev. Lett. **101**, 201801 (2008). https://doi.org/10.1103/PhysRevLett.101.201801. arXiv:0807.3935 [hep-ex]
868. B. Aubert et al., BaBar collaboration. Phys. Rev. D **77**, 011101 (2008). https://doi.org/10.1103/PhysRevD.77.011101. arXiv:0708.0963 [hep-ex]
869. D. Bortoletto et al., CLEO collaboration. Phys. Rev. Lett. **62**, 2436 (1989). https://doi.org/10.1103/PhysRevLett.62.2436
870. B. Aubert et al., BaBar collaboration. Phys. Rev. D **75**, 012008 (2007). https://doi.org/10.1103/PhysRevD.75.012008. arXiv:hep-ex/0608003
871. S. Sato et al., Belle collaboration. Phys. Rev. D **90**, 072009 (2014). https://doi.org/10.1103/PhysRevD.90.072009. arXiv:1408.6343 [hep-ex]
872. B. Aubert et al., BaBar collaboration. Phys. Rev. D **75**, 111102 (2007). https://doi.org/10.1103/PhysRevD.75.111102. arXiv:hep-ex/0703038
873. R. Ammar et al., CLEO collaboration. Phys. Rev. Lett. **87**, 271801 (2001). https://doi.org/10.1103/PhysRevLett.87.271801. arXiv:hep-ex/0106038
874. P. Goldenzweig et al., Belle collaboration. Phys. Rev. Lett. **101**, 231801 (2008). https://doi.org/10.1103/PhysRevLett.101.231801. arXiv:0807.4271 [hep-ex]
875. J.P. Lees et al., BaBar collaboration. Phys. Rev. D **83**, 112010 (2011). https://doi.org/10.1103/PhysRevD.83.112010. arXiv:1105.0125 [hep-ex]
876. P. Chang et al., Belle collaboration. Phys. Lett. B **599**, 148 (2004). https://doi.org/10.1016/j.physletb.2004.07.063. arXiv:hep-ex/0406075
877. B. Aubert et al., BaBar collaboration. Phys. Rev. D **78**, 052005 (2008). https://doi.org/10.1103/PhysRevD.78.052005. arXiv:0711.4417 [hep-ex]
878. A. Garmash et al., Belle collaboration. Phys. Rev. D **75**, 012006 (2007). https://doi.org/10.1103/PhysRevD.75.012006. arXiv:hep-ex/0610081
879. R. Aaij et al., LHCb collaboration. JHEP **10**, 143 (2013). https://doi.org/10.1007/JHEP10(2013)143. arXiv:1307.7648 [hep-ex]
880. S.H. Kyeong et al., Belle collaboration. Phys. Rev. D **80**, 051103 (2009). https://doi.org/10.1103/PhysRevD.80.051103. arXiv:0905.0763 [hep-ex]
881. B. Aubert et al., BaBar collaboration. Phys. Rev. D **76**, 071104 (2007). https://doi.org/10.1103/PhysRevD.76.071104. arXiv:0708.2543 [hep-ex]
882. J.P. Lees et al., BaBar collaboration. Phys. Rev. D **85**, 072005 (2012). https://doi.org/10.1103/PhysRevD.85.072005. arXiv:1112.3896 [hep-ex]
883. T. Aaltonen et al., CDF collaboration. Phys. Rev. Lett. **108**, 211803 (2012). https://doi.org/10.1103/PhysRevLett.108.211803. arXiv:1111.0485 [hep-ex]
884. R. Aaij et al., LHCb collaboration. Phys. Rev. Lett. **118**, 081801 (2017). https://doi.org/10.1103/PhysRevLett.118.081801. arXiv:1610.08288 [hep-ex]
885. P. del Amo Sanchez et al., BaBar collaboration. Phys. Rev. D **82**, 031101 (2010). https://doi.org/10.1103/PhysRevD.82.031101. arXiv:1003.0640 [hep-ex]
886. B. Aubert et al. (BaBar collaboration), Phys. Rev. D **74**, 072008 (2006). https://doi.org/10.1103/PhysRevD.74.072008. arXiv:hep-ex/0606050 [hep-ex]
887. R. Aaij et al., LHCb collaboration. JHEP **01**, 012 (2016). https://doi.org/10.1007/JHEP01(2016)012. arXiv:1506.08634 [hep-ex]
888. R. Aaij et al., LHCb collaboration. New J. Phys. **16**, 123001 (2014). https://doi.org/10.1088/1367-2630/16/12/123001. arXiv:1407.7704 [hep-ex]
889. V. Gaur et al., Belle collaboration. Phys. Rev. D **87**, 091101 (2013). https://doi.org/10.1103/PhysRevD.87.091101. arXiv:1304.5312 [hep-ex]
890. B. Aubert et al., BaBar collaboration. Phys. Rev. D **80**, 011101 (2009). https://doi.org/10.1103/PhysRevD.80.011101. arXiv:0905.0868 [hep-ex]
891. B. Aubert et al., BaBar collaboration. Phys. Rev. D **74**, 032005 (2006). https://doi.org/10.1103/PhysRevD.74.032005. arXiv:hep-ex/0606031
892. M. Prim et al., Belle collaboration. Phys. Rev. D **88**, 072004 (2013). https://doi.org/10.1103/PhysRevD.88.072004. arXiv:1308.1830 [hep-ex]
893. C.C. Chiang et al., Belle collaboration. Phys. Rev. D **81**, 071101 (2010). https://doi.org/10.1103/PhysRevD.81.071101. arXiv:1001.4595 [hep-ex]
894. B. Aubert et al., BaBar collaboration. Phys. Rev. Lett. **100**, 081801 (2008). https://doi.org/10.1103/PhysRevLett.100.081801. arXiv:0708.2248 [hep-ex]
895. B. Aubert et al., BaBar collaboration. Phys. Rev. D **78**, 051103 (2008). https://doi.org/10.1103/PhysRevD.78.051103. arXiv:0806.4467 [hep-ex]
896. B. Aubert et al., BaBar collaboration. Phys. Rev. D **76**, 051103 (2007). https://doi.org/10.1103/PhysRevD.76.051103. arXiv:0705.0398 [hep-ex]
897. T. Aaltonen et al., CDF collaboration. Phys. Rev. Lett. **106**, 181802 (2011). https://doi.org/10.1103/PhysRevLett.106.181802. arXiv:1103.5762 [hep-ex]
898. R. Aaij et al., LHCb collaboration. JHEP **10**, 037 (2012). https://doi.org/10.1007/JHEP10(2012)037. arXiv:1206.2794 [hep-ex]
899. K. Abe et al., Belle collaboration. Phys. Rev. Lett. **94**, 181803 (2005). https://doi.org/10.1103/PhysRevLett.94.181803. arXiv:hep-ex/0408101
900. B. Pal et al., Belle collaboration. Phys. Rev. D **92**, 011101 (2015). https://doi.org/10.1103/PhysRevD.92.011101. arXiv:1504.00957 [hep-ex]

901. A. Abdesselam et al. (Belle collaboration) (2016). arXiv:1609.03267 [hep-ex]
902. J.P. Lees et al., BaBar collaboration. Phys. Rev. D **89**, 051101 (2014). https://doi.org/10.1103/PhysRevD.89.051101. arXiv:1312.0056 [hep-ex]
903. R. Aaij et al., LHCb collaboration. JHEP **10**, 053 (2015). https://doi.org/10.1007/JHEP10(2015)053. arXiv:1508.00788 [hep-ex]
904. B. Aubert et al., BaBar collaboration. Phys. Rev. Lett. **93**, 051802 (2004). https://doi.org/10.1103/PhysRevLett.93.051802. arXiv:hep-ex/0311049
905. B. Aubert et al., BaBar collaboration. Phys. Rev. Lett. **97**, 051802 (2006). https://doi.org/10.1103/PhysRevLett.97.051802. arXiv:hep-ex/0603050
906. A. Somov et al., Belle collaboration. Phys. Rev. Lett. **96**, 171801 (2006). https://doi.org/10.1103/PhysRevLett.96.171801. arXiv:hep-ex/0601024
907. B. Aubert et al., BaBar collaboration. Phys. Rev. D **74**, 031104 (2006). https://doi.org/10.1103/PhysRevD.74.031104. arXiv:hep-ex/0605024
908. B. Aubert et al., BaBar collaboration. Phys. Rev. D **80**, 092007 (2009). https://doi.org/10.1103/PhysRevD.80.092007. arXiv:0907.1776 [hep-ex]
909. R. Aaij et al., LHCb collaboration. Phys. Rev. D **95**, 012006 (2017). https://doi.org/10.1103/PhysRevD.95.012006. arXiv:1610.05187 [hep-ex]
910. J.T. Wei et al., Belle collaboration. Phys. Lett. B **659**, 80 (2008). https://doi.org/10.1016/j.physletb.2007.11.063. arXiv:0706.4167 [hep-ex]
911. R. Aaij et al., LHCb collaboration. Phys. Rev. Lett. **113**, 141801 (2014). https://doi.org/10.1103/PhysRevLett.113.141801. arXiv:1407.5907 [hep-ex]
912. M.Z. Wang et al., Belle collaboration. Phys. Lett. B **617**, 141 (2005). https://doi.org/10.1016/j.physletb.2005.05.008. arXiv:hep-ex/0503047
913. J.H. Chen et al., Belle collaboration. Phys. Rev. Lett. **100**, 251801 (2008). https://doi.org/10.1103/PhysRevLett.100.251801. arXiv:0802.0336 [hep-ex]
914. Y.T. Tsai et al., Belle collaboration. Phys. Rev. D **75**, 111101 (2007). https://doi.org/10.1103/PhysRevD.75.111101. arXiv:hep-ex/0703048
915. M.Z. Wang et al., Belle collaboration. Phys. Rev. D **76**, 052004 (2007). https://doi.org/10.1103/PhysRevD.76.052004. arXiv:0704.2672 [hep-ex]
916. P. Chen et al., Belle collaboration. Phys. Rev. D **80**, 111103 (2009). https://doi.org/10.1103/PhysRevD.80.111103. arXiv:0910.5817 [hep-ex]
917. B. Aubert et al., BaBar collaboration. Phys. Rev. D **69**, 091503 (2004). https://doi.org/10.1103/PhysRevD.69.091503. arXiv:hep-ex/0403003
918. R. Aaij et al., LHCb collaboration. JHEP **10**, 005 (2013). https://doi.org/10.1007/JHEP10(2013)005. arXiv:1308.0961 [hep-ex]
919. B. Aubert et al., BaBar collaboration. Phys. Rev. D **79**, 112009 (2009). https://doi.org/10.1103/PhysRevD.79.112009. arXiv:0904.4724 [hep-ex]
920. M.Z. Wang et al., Belle collaboration. Phys. Rev. Lett. **90**, 201802 (2003). https://doi.org/10.1103/PhysRevLett.90.201802. arXiv:hep-ex/0302024
921. T. Aaltonen et al., CDF collaboration. Phys. Rev. Lett. **103**, 031801 (2009). https://doi.org/10.1103/PhysRevLett.103.031801. arXiv:0812.4271 [hep-ex]
922. T. Aaltonen et al., CDF collaboration. Phys. Rev. Lett. **107**, 201802 (2011). https://doi.org/10.1103/PhysRevLett.107.201802. arXiv:1107.3753 [hep-ex]
923. R. Aaij et al., LHCb collaboration. Phys. Lett. B **725**, 25 (2013). https://doi.org/10.1016/j.physletb.2013.06.060. arXiv:1306.2577 [hep-ex]
924. R. Aaij et al., LHCb collaboration. JHEP **09**, 006 (2015). https://doi.org/10.1007/JHEP09(2015)006. arXiv:1505.03295 [hep-ex]
925. R. Aaij et al., LHCb collaboration. Phys. Lett. B **759**, 282 (2016). https://doi.org/10.1016/j.physletb.2016.05.077. arXiv:1603.02870 [hep-ex]
926. R. Aaij et al., LHCb collaboration. JHEP **04**, 087 (2014). https://doi.org/10.1007/JHEP04(2014)087. arXiv:1402.0770 [hep-ex]
927. R. Aaij et al., LHCb collaboration. JHEP **05**, 081 (2016). https://doi.org/10.1007/JHEP05(2016)081. arXiv:1603.00413 [hep-ex]
928. R. Aaij et al., LHCb collaboration. JHEP **06**, 115 (2015). https://doi.org/10.1007/JHEP06(2015)115. arXiv:1503.07138 [hep-ex]
929. R. Aaij et al., LHCb collaboration. Phys. Rev. Lett. **114**, 062004 (2015). https://doi.org/10.1103/PhysRevLett.114.062004. arXiv:1411.4849 [hep-ex]
930. R. Aaij et al., LHCb collaboration. JHEP **05**, 161 (2016). https://doi.org/10.1007/JHEP05(2016)161. arXiv:1604.03896 [hep-ex]
931. C.C. Peng et al., Belle collaboration. Phys. Rev. D **82**, 072007 (2010). https://doi.org/10.1103/PhysRevD.82.072007. arXiv:1006.5115 [hep-ex]
932. T. Aaltonen et al., CDF collaboration. Phys. Rev. Lett. **107**, 261802 (2011). https://doi.org/10.1103/PhysRevLett.107.261802. arXiv:1107.4999 [hep-ex]
933. R. Aaij et al., LHCb collaboration. Phys. Lett. B **743**, 46 (2015). https://doi.org/10.1016/j.physletb.2015.02.010. arXiv:1412.6433 [hep-ex]
934. B. Pal et al., Belle collaboration. Phys. Rev. Lett. **116**, 161801 (2016). https://doi.org/10.1103/PhysRevLett.116.161801. arXiv:1512.02145 [hep-ex]
935. R. Aaij et al., LHCb collaboration. JHEP **07**, 166 (2015). https://doi.org/10.1007/JHEP07(2015)166. arXiv:1503.05362 [hep-ex]
936. R. Aaij et al., LHCb collaboration. JHEP **11**, 092 (2013). https://doi.org/10.1007/JHEP11(2013)092. arXiv:1306.2239 [hep-ex]
937. D. Dutta et al., Belle collaboration. Phys. Rev. D **91**, 011101 (2015). https://doi.org/10.1103/PhysRevD.91.011101. arXiv:1411.7771 [hep-ex]
938. R. Aaij et al., LHCb collaboration. Nucl. Phys. B **867**, 1 (2013). https://doi.org/10.1016/j.nuclphysb.2012.09.013. arXiv:1209.0313 [hep-ex]
939. T. Aaltonen et al., CDF collaboration. Phys. Rev. D **87**, 072003 (2013). https://doi.org/10.1103/PhysRevD.87.072003. arXiv:1301.7048 [hep-ex]
940. V.M. Abazov et al., D0 collaboration. Phys. Rev. D **87**, 072006 (2013). https://doi.org/10.1103/PhysRevD.87.072006. arXiv:1301.4507 [hep-ex]
941. R. Aaij et al., LHCb collaboration. Phys. Rev. Lett. **111**, 101805 (2013). https://doi.org/10.1103/PhysRevLett.111.101805. arXiv:1307.5024 [hep-ex]
942. S. Chatrchyan et al., CMS collaboration. Phys. Rev. Lett. **111**, 101804 (2013). https://doi.org/10.1103/PhysRevLett.111.101804. arXiv:1307.5025 [hep-ex]
943. M. Aaboud et al., ATLAS collaboration. Eur. Phys. J. C **76**, 513 (2016). https://doi.org/10.1140/epjc/s10052-016-4338-8. arXiv:1604.04263 [hep-ex]
944. T. Aaltonen et al., CDF collaboration. Phys. Rev. Lett. **102**, 201801 (2009). https://doi.org/10.1103/PhysRevLett.102.201801. arXiv:0901.3803 [hep-ex]
945. R. Aaij et al., LHCb collaboration. Phys. Rev. Lett. **111**, 141801 (2013). https://doi.org/10.1103/PhysRevLett.111.141801. arXiv:1307.4889 [hep-ex]
946. R. Aaij et al., LHCb collaboration. Phys. Rev. Lett. **110**, 211801 (2013). https://doi.org/10.1103/PhysRevLett.110.211801. arXiv:1303.1092 [hep-ex]
947. V.M. Abazov et al., D0 collaboration. Phys. Rev. D **74**, 031107 (2006). https://doi.org/10.1103/PhysRevD.74.031107. arXiv:hep-ex/0604015

948. R. Aaij et al., LHCb collaboration. JHEP **09**, 179 (2015). https://doi.org/10.1007/JHEP09(2015)179. arXiv:1506.08777 [hep-ex]
949. R. Aaij et al., LHCb collaboration. Phys. Rev. Lett. **115**, 051801 (2015). https://doi.org/10.1103/PhysRevLett.115.051801. arXiv:1503.07483 [hep-ex]
950. V. Khachatryan et al., CMS and LHCb collaborations. Nature **522**, 68 (2015). https://doi.org/10.1038/nature14474. arXiv:1411.4413 [hep-ex]
951. B. Aubert et al., BaBar collaboration. Phys. Rev. Lett. **103**, 211802 (2009). https://doi.org/10.1103/PhysRevLett.103.211802. arXiv:0906.2177 [hep-ex]
952. M. Nakao et al., Belle collaboration. Phys. Rev. D **69**, 112001 (2004). https://doi.org/10.1103/PhysRevD.69.112001. arXiv:hep-ex/0402042
953. T.E. Coan et al., CLEO collaboration. Phys. Rev. Lett. **84**, 5283 (2000). https://doi.org/10.1103/PhysRevLett.84.5283. arXiv:hep-ex/9912057
954. H. Yang et al., Belle collaboration. Phys. Rev. Lett. **94**, 111802 (2005). https://doi.org/10.1103/PhysRevLett.94.111802. arXiv:hep-ex/0412039
955. S. Nishida et al., Belle collaboration. Phys. Lett. B **610**, 23 (2005). https://doi.org/10.1016/j.physletb.2005.01.097. arXiv:hep-ex/0411065
956. B. Aubert et al., BaBar collaboration. Phys. Rev. D **74**, 031102 (2006). https://doi.org/10.1103/PhysRevD.74.031102. arXiv:hep-ex/0603054
957. R. Wedd et al., Belle collaboration. Phys. Rev. D **81**, 111104 (2010). https://doi.org/10.1103/PhysRevD.81.111104. arXiv:0810.0804 [hep-ex]
958. B. Aubert et al., BaBar collaboration. Phys. Rev. D **75**, 051102 (2007). https://doi.org/10.1103/PhysRevD.75.051102. arXiv:hep-ex/0611037
959. S. Nishida et al., Belle collaboration. Phys. Rev. Lett. **89**, 231801 (2002). https://doi.org/10.1103/PhysRevLett.89.231801. arXiv:hep-ex/0205025
960. B. Aubert et al. (BaBar collaboration), Phys. Rev. Lett. **98**, 211804 (2007). https://doi.org/10.1103/PhysRevLett.100.189903. arXiv:hep-ex/0507031. [Erratum ibid. **100**, 199905 (2008). doi:10.1103/PhysRevLett.100.199905]
961. B. Aubert et al., BaBar collaboration. Phys. Rev. D **78**, 112001 (2008). https://doi.org/10.1103/PhysRevD.78.112001. arXiv:0808.1379 [hep-ex]
962. N. Taniguchi et al. (Belle collaboration), Phys. Rev. Lett. **101**, 111801 (2008). https://doi.org/10.1103/PhysRevLett.101.111801. arXiv:0804.4770 [hep-ex]. [Erratum ibid. **101**, 129904 (2008). doi:10.1103/PhysRevLett.101.129904]
963. Y.J. Lee et al., Belle collaboration. Phys. Rev. Lett. **95**, 061802 (2005). https://doi.org/10.1103/PhysRevLett.95.061802. arXiv:hep-ex/0503046
964. J.P. Lees et al., BaBar collaboration. Phys. Rev. D **88**, 032012 (2013). https://doi.org/10.1103/PhysRevD.88.032012. arXiv:1303.6010 [hep-ex]
965. J.T. Wei et al., Belle collaboration. Phys. Rev. D **78**, 011101 (2008). https://doi.org/10.1103/PhysRevD.78.011101. arXiv:0804.3656 [hep-ex]
966. R. Aaij et al., LHCb collaboration. JHEP **10**, 034 (2015). https://doi.org/10.1007/JHEP10(2015)034. arXiv:1509.00414 [hep-ex]
967. B. Aubert et al., BaBar collaboration. Phys. Rev. Lett. **94**, 101801 (2005). https://doi.org/10.1103/PhysRevLett.94.101801. arXiv:hep-ex/0411061
968. O. Lutz et al., Belle collaboration. Phys. Rev. D **87**, 111103 (2013). https://doi.org/10.1103/PhysRevD.87.111103. arXiv:1303.3719 [hep-ex]
969. B. Aubert et al., BaBar collaboration. Phys. Rev. Lett. **102**, 091803 (2009). https://doi.org/10.1103/PhysRevLett.102.091803. arXiv:0807.4119 [hep-ex]
970. J.T. Wei et al., Belle collaboration. Phys. Rev. Lett. **103**, 171801 (2009). https://doi.org/10.1103/PhysRevLett.103.171801. arXiv:0904.0770 [hep-ex]
971. R. Aaij et al., LHCb collaboration. JHEP **02**, 105 (2013). https://doi.org/10.1007/JHEP02(2013)105. arXiv:1209.4284 [hep-ex]
972. J.P. Lees et al., BaBar collaboration. Phys. Rev. Lett. **118**, 031802 (2017). https://doi.org/10.1103/PhysRevLett.118.031802. arXiv:1605.09637 [hep-ex]
973. J.P. Lees et al., BaBar collaboration. Phys. Rev. D **87**, 112005 (2013). https://doi.org/10.1103/PhysRevD.87.112005. arXiv:1303.7465 [hep-ex]
974. R. Aaij et al., LHCb collaboration. JHEP **06**, 133 (2014). https://doi.org/10.1007/JHEP06(2014)133. arXiv:1403.8044 [hep-ex]
975. R. Aaij et al., LHCb collaboration. JHEP **10**, 064 (2014). https://doi.org/10.1007/JHEP10(2014)064. arXiv:1408.1137 [hep-ex]
976. B. Aubert et al., BaBar collaboration. Phys. Rev. Lett. **99**, 051801 (2007). https://doi.org/10.1103/PhysRevLett.99.051801. arXiv:hep-ex/0703018
977. J.P. Lees et al., BaBar collaboration. Phys. Rev. D **86**, 012004 (2012). https://doi.org/10.1103/PhysRevD.86.012004. arXiv:1204.2852 [hep-ex]
978. B. Aubert et al., BaBar collaboration. Phys. Rev. D **73**, 092001 (2006). https://doi.org/10.1103/PhysRevD.73.092001. arXiv:hep-ex/0604007
979. J.P. Lees et al., BaBar collaboration. Phys. Rev. D **85**, 071103 (2012). https://doi.org/10.1103/PhysRevD.85.071103. arXiv:1202.3650 [hep-ex]
980. R. Aaij et al., LHCb collaboration. Phys. Rev. Lett. **112**, 131802 (2014). https://doi.org/10.1103/PhysRevLett.112.131802. arXiv:1401.5361 [hep-ex]
981. J.P. Lees et al., BaBar collaboration. Phys. Rev. D **89**, 011102 (2014). https://doi.org/10.1103/PhysRevD.89.011102. arXiv:1310.8238 [hep-ex]
982. R. Aaij et al., LHCb collaboration. Phys. Rev. Lett. **108**, 101601 (2012). https://doi.org/10.1103/PhysRevLett.108.101601. arXiv:1110.0730 [hep-ex]
983. B. Aubert et al., BaBar collaboration. Phys. Rev. D **70**, 091105 (2004). https://doi.org/10.1103/PhysRevD.70.091105. arXiv:hep-ex/0409035
984. B. Aubert et al., BaBar collaboration. Phys. Rev. D **72**, 091103 (2005). https://doi.org/10.1103/PhysRevD.72.091103. arXiv:hep-ex/0501038
985. Z. King et al., Belle collaboration. Phys. Rev. D **93**, 111101 (2016). https://doi.org/10.1103/PhysRevD.93.111101. arXiv:1603.06546 [hep-ex]
986. Y.T. Lai et al., Belle collaboration. Phys. Rev. D **89**, 051103 (2014). https://doi.org/10.1103/PhysRevD.89.051103. arXiv:1312.4228 [hep-ex]
987. R. Aaij et al., LHCb collaboration. JHEP **11**, 047 (2016). https://doi.org/10.1007/JHEP11(2016)047. arXiv:1606.04731 [hep-ex]
988. B. Aubert et al., BaBar collaboration. Phys. Rev. D **77**, 051103 (2008). https://doi.org/10.1103/PhysRevD.77.051103. arXiv:0711.4889 [hep-ex]
989. J.P. Lees et al., BaBar collaboration. Phys. Rev. Lett. **109**, 191801 (2012). https://doi.org/10.1103/PhysRevLett.109.191801. arXiv:1207.2690 [hep-ex]
990. J.P. Lees et al., BaBar collaboration. Phys. Rev. D **86**, 052012 (2012). https://doi.org/10.1103/PhysRevD.86.052012. arXiv:1207.2520 [hep-ex]
991. T. Saito et al., Belle collaboration. Phys. Rev. D **91**, 052004 (2015). https://doi.org/10.1103/PhysRevD.91.052004. arXiv:1411.7198 [hep-ex]
992. A. Abdesselam et al. (Belle collaboration) (2016). arXiv:1608.02344 [hep-ex]

993. P. del Amo Sanchez et al., BaBar collaboration. Phys. Rev. D **82**, 051101 (2010). https://doi.org/10.1103/PhysRevD.82.051101. arXiv:1005.4087 [hep-ex]
994. J.P. Lees et al., BaBar collaboration. Phys. Rev. Lett. **112**, 211802 (2014). https://doi.org/10.1103/PhysRevLett.112.211802. arXiv:1312.5364 [hep-ex]
995. J.P. Lees et al., BaBar collaboration. Phys. Rev. D **86**, 032012 (2012). https://doi.org/10.1103/PhysRevD.86.032012. arXiv:1204.3933 [hep-ex]
996. K.W. Edwards et al., CLEO collaboration. Phys. Rev. D **65**, 111102 (2002). https://doi.org/10.1103/PhysRevD.65.111102. arXiv:hep-ex/0204017
997. O. Buchmuller, H. Flacher, Phys. Rev. D **73**, 073008 (2006). https://doi.org/10.1103/PhysRevD.73.073008. arXiv:hep-ph/0507253
998. B. Aubert et al., BaBar collaboration. Phys. Rev. D **79**, 091101 (2009). https://doi.org/10.1103/PhysRevD.79.091101. arXiv:0903.1220 [hep-ex]
999. N. Satoyama et al. (Belle collaboration), Phys. Lett. B **647**, 67 (2007). https://doi.org/10.1016/j.physletb.2007.01.068. arXiv:hep-ex/0611045 [hep-ex]
1000. J.P. Lees et al., BaBar collaboration. Phys. Rev. D **88**, 031102 (2013). https://doi.org/10.1103/PhysRevD.88.031102. arXiv:1207.0698 [hep-ex]
1001. B. Kronenbitter et al., Belle collaboration. Phys. Rev. D **92**, 051102 (2015). https://doi.org/10.1103/PhysRevD.92.051102. arXiv:1503.05613 [hep-ex]
1002. B. Aubert et al., BaBar collaboration. Phys. Rev. D **80**, 111105 (2009). https://doi.org/10.1103/PhysRevD.80.111105. arXiv:0907.1681 [hep-ex]
1003. A. Heller et al., Belle collaboration. Phys. Rev. D **91**, 112009 (2015). https://doi.org/10.1103/PhysRevD.91.112009. arXiv:1504.05831 [hep-ex]
1004. P. del Amo Sanchez et al., BaBar collaboration. Phys. Rev. D **83**, 032006 (2011). https://doi.org/10.1103/PhysRevD.83.032006. arXiv:1010.2229 [hep-ex]
1005. S. Villa et al., Belle collaboration. Phys. Rev. D **73**, 051107 (2006). https://doi.org/10.1103/PhysRevD.73.051107. arXiv:hep-ex/0507036
1006. B. Aubert et al., BaBar collaboration. Phys. Rev. D **77**, 032007 (2008). https://doi.org/10.1103/PhysRevD.77.032007. arXiv:0712.1516 [hep-ex]
1007. M.C. Chang et al., Belle collaboration. Phys. Rev. D **68**, 111101 (2003). https://doi.org/10.1103/PhysRevD.68.111101. arXiv:hep-ex/0309069
1008. B. Aubert et al., BaBar collaboration. Phys. Rev. D **77**, 011104 (2008). https://doi.org/10.1103/PhysRevD.77.011104. arXiv:0706.2870 [hep-ex]
1009. B. Aubert et al., BaBar collaboration. Phys. Rev. Lett. **96**, 241802 (2006). https://doi.org/10.1103/PhysRevLett.96.241802. arXiv:hep-ex/0511015
1010. B. Aubert et al., BaBar collaboration. Phys. Rev. D **77**, 091104 (2008). https://doi.org/10.1103/PhysRevD.77.091104. arXiv:0801.0697 [hep-ex]
1011. J.P. Lees et al., BaBar collaboration. Phys. Rev. D **86**, 051105 (2012). https://doi.org/10.1103/PhysRevD.86.051105. arXiv:1206.2543 [hep-ex]
1012. C.L. Hsu et al., Belle collaboration. Phys. Rev. D **86**, 032002 (2012). https://doi.org/10.1103/PhysRevD.86.032002. arXiv:1206.5948 [hep-ex]
1013. Y. Yook et al., Belle collaboration. Phys. Rev. D **91**, 052016 (2015). https://doi.org/10.1103/PhysRevD.91.052016. arXiv:1406.6356 [hep-ex]
1014. B. Aubert et al., BaBar collaboration. Phys. Rev. D **81**, 051101 (2010). https://doi.org/10.1103/PhysRevD.81.051101. arXiv:0912.2453 [hep-ex]
1015. I. Adachi et al., Belle collaboration. Phys. Rev. Lett. **110**, 131801 (2013). https://doi.org/10.1103/PhysRevLett.110.131801. arXiv:1208.4678 [hep-ex]
1016. R. Aaij et al., LHCb collaboration. Phys. Rev. Lett. **113**, 151601 (2014). https://doi.org/10.1103/PhysRevLett.113.151601. arXiv:1406.6482 [hep-ex]
1017. K. Nishimura et al., Belle collaboration. Phys. Rev. Lett. **105**, 191803 (2010). https://doi.org/10.1103/PhysRevLett.105.191803. arXiv:0910.4751 [hep-ex]
1018. T.E. Browder et al., CLEO collaboration. Phys. Rev. Lett. **81**, 1786 (1998). https://doi.org/10.1103/PhysRevLett.81.1786. arXiv:hep-ex/9804018
1019. B. Aubert et al., BaBar collaboration. Phys. Rev. Lett. **93**, 061801 (2004). https://doi.org/10.1103/PhysRevLett.93.061801. arXiv:hep-ex/0401006
1020. G. Bonvicini et al., CLEO collaboration. Phys. Rev. D **68**, 011101 (2003). https://doi.org/10.1103/PhysRevD.68.011101. arXiv:hep-ex/0303009
1021. P. del Amo Sanchez et al., BaBar collaboration. Phys. Rev. D **83**, 031103 (2011). https://doi.org/10.1103/PhysRevD.83.031103. arXiv:1012.5031 [hep-ex]
1022. R. Aaij et al., LHCb collaboration. Phys. Rev. Lett. **112**, 161801 (2014). https://doi.org/10.1103/PhysRevLett.112.161801. arXiv:1402.6852 [hep-ex]
1023. R. Aaij et al., LHCb collaboration. JHEP **05**, 159 (2013). https://doi.org/10.1007/JHEP05(2013)159. arXiv:1304.3035 [hep-ex]
1024. R. Aaij et al., LHCb collaboration. JHEP **05**, 082 (2014). https://doi.org/10.1007/JHEP05(2014)082. arXiv:1403.8045 [hep-ex]
1025. A. Abdesselam et al. (Belle collaboration) (2016). arXiv:1604.04042 [hep-ex]
1026. R. Aaij et al., LHCb collaboration. JHEP **04**, 064 (2015). https://doi.org/10.1007/JHEP04(2015)064. arXiv:1501.03038 [hep-ex]
1027. J.P. Lees et al., BaBar collaboration. Phys. Rev. D **93**, 052015 (2016). https://doi.org/10.1103/PhysRevD.93.052015. arXiv:1508.07960 [hep-ex]
1028. R. Aaij et al., LHCb collaboration. JHEP **02**, 104 (2016). https://doi.org/10.1007/JHEP02(2016)104. arXiv:1512.04442 [hep-ex]
1029. V. Khachatryan et al., CMS collaboration. Phys. Lett. B **753**, 424 (2016). https://doi.org/10.1016/j.physletb.2015.12.020. arXiv:1507.08126 [hep-ex]
1030. Y. Sato et al. (Belle collaboration), Phys. Rev. D **93**, 032008 (2016). https://doi.org/10.1103/PhysRevD.93.032008. arXiv:1402.7134 [hep-ex]. Addendum ibid. **93**, 059901 (2016). doi:10.1103/PhysRevD.93.059901
1031. R. Aaij et al., LHCb collaboration. JHEP **12**, 065 (2016). https://doi.org/10.1007/JHEP12(2016)065. arXiv:1609.04736 [hep-ex]
1032. L. Pesántez et al., Belle collaboration. Phys. Rev. Lett. **114**, 151601 (2015). https://doi.org/10.1103/PhysRevLett.114.151601. arXiv:1501.01702 [hep-ex]
1033. R. Aaij et al., LHCb collaboration. Phys. Rev. D **90**, 112004 (2014). https://doi.org/10.1103/PhysRevD.90.112004. arXiv:1408.5373 [hep-ex]
1034. B. Aubert et al., BaBar collaboration. Phys. Rev. Lett. **97**, 201801 (2006). https://doi.org/10.1103/PhysRevLett.97.201801. arXiv:hep-ex/0607057
1035. K.F. Chen et al., Belle collaboration. Phys. Rev. Lett. **94**, 221804 (2005). https://doi.org/10.1103/PhysRevLett.94.221804. arXiv:hep-ex/0503013
1036. R. Aaij et al., LHCb collaboration. Phys. Rev. D **88**, 052015 (2013). https://doi.org/10.1103/PhysRevD.88.052015. arXiv:1307.6165 [hep-ex]
1037. R. Aaij et al., LHCb collaboration. JHEP **09**, 177 (2014). https://doi.org/10.1007/JHEP09(2014)177. arXiv:1408.0978 [hep-ex]
1038. T.A. Aaltonen et al., CDF collaboration. Phys. Rev. Lett. **113**, 242001 (2014). https://doi.org/10.1103/PhysRevLett.113.242001. arXiv:1403.5586 [hep-ex]

1039. R. Aaij et al., LHCb collaboration. Phys. Rev. Lett. **110**, 221601 (2013). https://doi.org/10.1103/PhysRevLett.110.221601. arXiv:1304.6173 [hep-ex]
1040. R. Aaij et al., LHCb collaboration. JHEP **05**, 069 (2014). https://doi.org/10.1007/JHEP05(2014)069. arXiv:1403.2888 [hep-ex]
1041. J.P. Lees et al., BaBar collaboration. Phys. Rev. D **90**, 092001 (2014). https://doi.org/10.1103/PhysRevD.90.092001. arXiv:1406.0534 [hep-ex]
1042. S. Nishida et al., Belle collaboration. Phys. Rev. Lett. **93**, 031803 (2004). https://doi.org/10.1103/PhysRevLett.93.031803. arXiv:hep-ex/0308038
1043. T.E. Coan et al., CLEO collaboration. Phys. Rev. Lett. **86**, 5661 (2001). https://doi.org/10.1103/PhysRevLett.86.5661. arXiv:hep-ex/0010075
1044. R. Aaij et al., LHCb collaboration. Nat. Phys. **13**, 391 (2017). https://doi.org/10.1038/nphys4021. arXiv:1609.05216 [hep-ex]
1045. J. Zhang et al., Belle collaboration. Phys. Rev. Lett. **95**, 141801 (2005). https://doi.org/10.1103/PhysRevLett.95.141801. arXiv:hep-ex/0408102
1046. R. Aaij et al., LHCb collaboration. Phys. Lett. B **713**, 369 (2012). https://doi.org/10.1016/j.physletb.2012.06.012. arXiv:1204.2813 [hep-ex]
1047. R. Aaij et al., LHCb collaboration. Phys. Lett. B **759**, 313 (2016). https://doi.org/10.1016/j.physletb.2016.05.074. arXiv:1603.07037 [hep-ex]
1048. M. Staric et al., Belle collaboration. Phys. Rev. Lett. **98**, 211803 (2007). https://doi.org/10.1103/PhysRevLett.98.211803. arXiv:hep-ex/0703036
1049. B. Aubert et al., BaBar collaboration. Phys. Rev. Lett. **98**, 211802 (2007). https://doi.org/10.1103/PhysRevLett.98.211802. arXiv:hep-ex/0703020
1050. T. Aaltonen et al., CDF collaboration. Phys. Rev. Lett. **100**, 121802 (2008). https://doi.org/10.1103/PhysRevLett.100.121802. arXiv:0712.1567 [hep-ex]
1051. R. Aaij et al., LHCb collaboration. Phys. Rev. Lett. **111**, 251801 (2013). https://doi.org/10.1103/PhysRevLett.111.251801. arXiv:1309.6534 [hep-ex]
1052. S. Bergmann, Y. Grossman, Z. Ligeti, Y. Nir, A.A. Petrov, Phys. Lett. B **486**, 418 (2000). https://doi.org/10.1016/S0370-2693(00)00772-3. arXiv:hep-ph/0005181
1053. I.I.Y. Bigi, N.G. Uraltsev, Nucl. Phys. B **592**, 92 (2001). https://doi.org/10.1016/S0550-3213(00)00604-0. arXiv:hep-ph/0005089
1054. A.A. Petrov (2003). arXiv:hep-ph/0311371
1055. A.A. Petrov, Nucl. Phys. Proc. Suppl. **142**, 333 (2005). https://doi.org/10.1016/j.nuclphysbps.2005.01.057. arXiv:hep-ph/0409130
1056. A.F. Falk, Y. Grossman, Z. Ligeti, Y. Nir, A.A. Petrov, Phys. Rev. D **69**, 114021 (2004). https://doi.org/10.1103/PhysRevD.69.114021. arXiv:hep-ph/0402204
1057. D. Asner et al., CLEO collaboration. Phys. Rev. D **86**, 112001 (2012). https://doi.org/10.1103/PhysRevD.86.112001. arXiv:1210.0939 [hep-ex]
1058. R. Aaij et al., LHCb collaboration. JHEP **07**, 041 (2014). https://doi.org/10.1007/JHEP07(2014)041. arXiv:1405.2797 [hep-ex]
1059. B. Aubert et al., BaBar collaboration. Phys. Rev. Lett. **103**, 211801 (2009). https://doi.org/10.1103/PhysRevLett.103.211801. arXiv:0807.4544 [hep-ex]
1060. Heavy Flavor Averaging Group: charm physics parameters. http://www.slac.stanford.edu/xorg/hflav/charm/index.html
1061. R. Aaij et al., LHCb collaboration. Phys. Rev. Lett. **116**, 241801 (2016). https://doi.org/10.1103/PhysRevLett.116.241801. arXiv:1602.07224 [hep-ex]
1062. E.M. Aitala et al., Fermilab E791 collaboration. Phys. Rev. Lett. **77**, 2384 (1996). https://doi.org/10.1103/PhysRevLett.77.2384. arXiv:hep-ex/9606016
1063. C. Cawlfield et al. (CLEO collaboration), Phys. Rev. D **71**, 077101 (2005). https://doi.org/10.1103/PhysRevD.71.077101. arXiv:hep-ex/0502012
1064. B. Aubert et al., BaBar collaboration. Phys. Rev. D **76**, 014018 (2007). https://doi.org/10.1103/PhysRevD.76.014018. arXiv:0705.0704 [hep-ex]
1065. U. Bitenc et al., Belle collaboration. Phys. Rev. D **77**, 112003 (2008). https://doi.org/10.1103/PhysRevD.77.112003. arXiv:0802.2952 [hep-ex]
1066. L.M. Zhang et al., Belle collaboration. Phys. Rev. Lett. **96**, 151801 (2006). https://doi.org/10.1103/PhysRevLett.96.151801. arXiv:hep-ex/0601029
1067. B.R. Ko et al., Belle collaboration. Phys. Rev. Lett. **112**, 111801 (2014). https://doi.org/10.1103/PhysRevLett.112.111801. arXiv:1401.3402 [hep-ex]
1068. T.A. Aaltonen et al., CDF collaboration. Phys. Rev. Lett. **111**, 231802 (2013). https://doi.org/10.1103/PhysRevLett.111.231802. arXiv:1309.4078 [hep-ex]
1069. R. Aaij et al., LHCb collaboration. Phys. Rev. D **95**, 052004 (2017). https://doi.org/10.1103/PhysRevD.95.052004. arXiv:1611.06143 [hep-ex]
1070. T. Peng et al., Belle collaboration. Phys. Rev. D **89**, 091103 (2014). https://doi.org/10.1103/PhysRevD.89.091103. arXiv:1404.2412 [hep-ex]
1071. P. del Amo Sanchez et al., BaBar collaboration. Phys. Rev. Lett. **105**, 081803 (2010). https://doi.org/10.1103/PhysRevLett.105.081803. arXiv:1004.5053 [hep-ex]
1072. R. Aaij et al., LHCb collaboration. JHEP **04**, 033 (2016). https://doi.org/10.1007/JHEP04(2016)033. arXiv:1510.01664 [hep-ex]
1073. J.P. Lees et al., BaBar collaboration. Phys. Rev. D **93**, 112014 (2016). https://doi.org/10.1103/PhysRevD.93.112014. arXiv:1604.00857 [hep-ex]
1074. B. Aubert et al., BaBar collaboration. Phys. Rev. Lett. **100**, 061803 (2008). https://doi.org/10.1103/PhysRevLett.100.061803. arXiv:0709.2715 [hep-ex]
1075. B.R. Ko, (Belle collaboration) (2012). arXiv:1212.5320 [hep-ex]
1076. CDF collaboration, CDF note 10784 (2012). http://www-cdf.fnal.gov/physics/new/bottom/120216.blessed-CPVcharm10fb/
1077. T. Aaltonen et al., CDF collaboration. Phys. Rev. Lett. **109**, 111801 (2012). https://doi.org/10.1103/PhysRevLett.109.111801. arXiv:1207.2158 [hep-ex]
1078. R. Aaij et al., LHCb collaboration. Phys. Rev. Lett. **116**, 191601 (2016). https://doi.org/10.1103/PhysRevLett.116.191601. arXiv:1602.03160 [hep-ex]
1079. E.M. Aitala et al., Fermilab E791 collaboration. Phys. Rev. Lett. **83**, 32 (1999). https://doi.org/10.1103/PhysRevLett.83.32. arXiv:hep-ex/9903012
1080. J.M. Link et al., FOCUS collaboration. Phys. Lett. B **485**, 62 (2000). https://doi.org/10.1016/S0370-2693(00)00694-8. arXiv:hep-ex/0004034
1081. S.E. Csorna et al., CLEO collaboration. Phys. Rev. D **65**, 092001 (2002). https://doi.org/10.1103/PhysRevD.65.092001. arXiv:hep-ex/0111024
1082. A. Zupanc et al., Belle collaboration. Phys. Rev. D **80**, 052006 (2009). https://doi.org/10.1103/PhysRevD.80.052006. arXiv:0905.4185 [hep-ex]
1083. R. Aaij et al., LHCb collaboration. JHEP **04**, 129 (2012). https://doi.org/10.1007/JHEP04(2012)129. arXiv:1112.4698 [hep-ex]
1084. M. Staric et al., Belle collaboration. Phys. Lett. B **753**, 412–418 (2016). https://doi.org/10.1016/j.physletb.2015.12.025. arXiv:1509.08266 [hep-ex]
1085. J.P. Lees et al., BaBar collaboration. Phys. Rev. D **87**, 012004 (2013). https://doi.org/10.1103/PhysRevD.87.012004. arXiv:1209.3896 [hep-ex]

1086. M. Ablikim et al., BESIII collaboration. Phys. Lett. B **744**, 339 (2015). https://doi.org/10.1016/j.physletb.2015.04.008. arXiv:1501.01378 [hep-ex]
1087. T.A. Aaltonen et al., CDF collaboration. Phys. Rev. D **90**, 111103 (2014). https://doi.org/10.1103/PhysRevD.90.111103. arXiv:1410.5435 [hep-ex]
1088. R. Aaij et al., LHCb collaboration. JHEP **04**, 043 (2015). https://doi.org/10.1007/JHEP04(2015)043. arXiv:1501.06777 [hep-ex]
1089. R. Aaij et al., LHCb collaboration. Phys. Rev. Lett. **118**, 261803 (2017). arXiv:1702.06490 [hep-ex]
1090. F. James, MINUIT–Function Minimization and Error Analysis, Reference Manual Version 94.1, CERN Program Library Long Writeup D506. http://wwwasdoc.web.cern.ch/wwwasdoc/minuit/minmain.html
1091. Y. Grossman, Y. Nir, G. Perez, Phys. Rev. Lett. **103**, 071602 (2009). https://doi.org/10.1103/PhysRevLett.103.071602. arXiv:0904.0305 [hep-ph]
1092. A.L. Kagan, M.D. Sokoloff, Phys. Rev. D **80**, 076008 (2009). https://doi.org/10.1103/PhysRevD.80.076008. arXiv:0907.3917 [hep-ph]
1093. M. Ciuchini et al., Phys. Lett. B **655**, 162 (2007). https://doi.org/10.1016/j.physletb.2007.08.055. arXiv:hep-ph/0703204
1094. Computing and Networks Division, CERNLIB Short Writeups. https://root.cern.ch/sites/d35c7d8c.web.cern.ch/files/cernlib.pdf
1095. I.I.Y. Bigi, A.I. Sanda, Camb. Monogr. Part. Phys. Nucl. Phys. Cosmol. **9**, 1 (2000)
1096. Y. Nir (1999). arXiv:hep-ph/9911321
1097. F. Buccella, M. Lusignoli, G. Miele, A. Pugliese, P. Santorelli, Phys. Rev. D **51**, 3478 (1995). https://doi.org/10.1103/PhysRevD.51.3478. arXiv:hep-ph/9411286
1098. Y. Grossman, Y. Nir, JHEP **04**, 002 (2012). https://doi.org/10.1007/JHEP04(2012)002. arXiv:1110.3790 [hep-ph]
1099. I. Bediaga, I.I. Bigi, A. Gomes, G. Guerrer, J. Miranda, A.C.D. Reis, Phys. Rev. D **80**, 096006 (2009). https://doi.org/10.1103/PhysRevD.80.096006. arXiv:0905.4233 [hep-ph]
1100. B. Aslan, G. Zech, J. Stat. Comput. Simul. **75**, 109 (2005). https://doi.org/10.1080/00949650410001661440
1101. J.M. Link et al., FOCUS collaboration. Phys. Lett. B **634**, 165 (2006). https://doi.org/10.1016/j.physletb.2006.01.017. arXiv:hep-ex/0509042
1102. J.W. Hinson et al., CLEO collaboration. Phys. Rev. Lett. **94**, 191801 (2005). https://doi.org/10.1103/PhysRevLett.94.191801. arXiv:hep-ex/0501002
1103. B.I. Eisenstein et al., CLEO collaboration. Phys. Rev. D **78**, 052003 (2008). https://doi.org/10.1103/PhysRevD.78.052003. arXiv:0806.2112 [hep-ex]
1104. H. Mendez et al., CLEO collaboration. Phys. Rev. D **81**, 052013 (2010). https://doi.org/10.1103/PhysRevD.81.052013. arXiv:0906.3198 [hep-ex]
1105. E. Won et al., Belle collaboration. Phys. Rev. Lett. **107**, 221801 (2011). https://doi.org/10.1103/PhysRevLett.107221801. arXiv:1107.0553 [hep-ex]
1106. G. Bonvicini et al., CLEO collaboration. Phys. Rev. D **89**, 072002 (2014). https://doi.org/10.1103/PhysRevD.89.072002. arXiv:1312.6775 [hep-ex]
1107. B.R. Ko et al., Belle collaboration. Phys. Rev. Lett. **109**, 021601 (2012). https://doi.org/10.1103/PhysRevLett.109.021601. arXiv:1203.6409 [hep-ex]
1108. P. del Amo Sanchez et al., BaBar collaboration. Phys. Rev. D **83**, 071103 (2011). https://doi.org/10.1103/PhysRevD.83.071103. arXiv:1011.5477 [hep-ex]
1109. J.M. Link et al. (FOCUS collaboration), Phys. Rev. Lett. **88**, 041602, 159903(E) (2002). https://doi.org/10.1103/PhysRevLett.88.041602. arXiv:hep-ex/0109022
1110. J.P. Lees et al., BaBar collaboration. Phys. Rev. D **87**, 052012 (2013). https://doi.org/10.1103/PhysRevD.87.052012. arXiv:1212.3003 [hep-ex]
1111. B.R. Ko et al., Belle collaboration. JHEP **02**, 098 (2013). https://doi.org/10.1007/JHEP02(2013)098. arXiv:1212.6112 [hep-ex]
1112. R. Aaij et al., LHCb collaboration. JHEP **10**, 25 (2014). https://doi.org/10.1007/JHEP10(2014)025. arXiv:1406.2624 [hep-ex]
1113. R. Aaij et al., LHCb collaboration. Phys. Lett. B **728**, 585 (2014). https://doi.org/10.1016/j.physletb.2013.12.035. arXiv:1310.7953 [hep-ex]
1114. E.M. Aitala et al., Fermilab E791 collaboration. Phys. Lett. B **403**, 377 (1997). https://doi.org/10.1016/S0370-2693(97)00565-0. arXiv:hep-ex/9612005
1115. V.M. Abazov et al., D0 collaboration. Phys. Rev. D **90**, 111102 (2014). https://doi.org/10.1103/PhysRevD.90.111102. arXiv:1408.6848 [hep-ex]
1116. J.P. Lees et al., BaBar collaboration. Phys. Rev. D **87**, 052010 (2013). https://doi.org/10.1103/PhysRevD.87.052010. arXiv:1212.1856 [hep-ex]
1117. P. Rubin et al., CLEO collaboration. Phys. Rev. D **78**, 072003 (2008). https://doi.org/10.1103/PhysRevD.78.072003. arXiv:0807.4545 [hep-ex]
1118. J.M. Link et al., FOCUS collaboration. Phys. Lett. B **491**, 232 (2000). https://doi.org/10.1016/S0370-2693(00)01039-X. arXiv:hep-ex/0005037
1119. J.M. Link et al., FOCUS collaboration. Phys. Lett. B **622**, 239 (2005). https://doi.org/10.1016/j.physletb.2005.07.024. arXiv:hep-ex/0506012
1120. T. Aaltonen et al., CDF collaboration. Phys. Rev. D **85**, 012009 (2012). https://doi.org/10.1103/PhysRevD.85.012009. arXiv:1111.5023 [hep-ex]
1121. M. Staric et al., Belle collaboration. Phys. Lett. B **670**, 190 (2008). https://doi.org/10.1016/j.physletb.2008.10.052. arXiv:0807.0148 [hep-ex]
1122. E.M. Aitala et al., Fermilab E791 collaboration. Phys. Lett. B **421**, 405 (1998). https://doi.org/10.1016/S0370-2693(97)01570-0. arXiv:hep-ex/9711003
1123. N.K. Nisar et al., Belle collaboration. Phys. Rev. Lett. **112**, 211601 (2014). https://doi.org/10.1103/PhysRevLett.112.211601. arXiv:1404.1266 [hep-ex]
1124. G. Bonvicini et al., CLEO collaboration. Phys. Rev. D **63**, 071101 (2001). https://doi.org/10.1103/PhysRevD.63.071101. arXiv:hep-ex/0012054
1125. B.R. Ko et al., Belle collaboration. Phys. Rev. Lett. **106**, 211801 (2011). https://doi.org/10.1103/PhysRevLett.106.211801. arXiv:1101.3365 [hep-ex]
1126. R. Aaij et al., LHCb collaboration. JHEP **10**, 055 (2015). https://doi.org/10.1007/JHEP10(2015)055. arXiv:1508.06087 [hep-ex]
1127. R. Aaij et al., LHCb collaboration. Phys. Lett. B **740**, 158 (2015). https://doi.org/10.1016/j.physletb.2014.11.043. arXiv:1410.4170 [hep-ex]
1128. B. Aubert et al., BaBar collaboration. Phys. Rev. D **78**, 051102 (2008). https://doi.org/10.1103/PhysRevD.78.051102. arXiv:0802.4035 [hep-ex]
1129. K. Arinstein, Belle collaboration. Phys. Lett. B **662**, 102 (2008). https://doi.org/10.1016/j.physletb.2008.02.054. arXiv:0801.2439 [hep-ex]
1130. D. Cronin-Hennessy et al., CLEO collaboration. Phys. Rev. D **72**, 031102 (2005). https://doi.org/10.1103/PhysRevD.72.031102. arXiv:hep-ex/0503052
1131. X.C. Tian et al., Belle collaboration. Phys. Rev. Lett. **95**, 231801 (2005). https://doi.org/10.1103/PhysRevLett.95.231801. arXiv:hep-ex/0507071
1132. G. Brandenburg et al., CLEO collaboration. Phys. Rev. Lett. **87**, 071802 (2001). https://doi.org/10.1103/PhysRevLett.87.071802. arXiv:hep-ex/0105002

1133. T. Aaltonen et al., CDF collaboration. Phys. Rev. D **86**, 032007 (2012). https://doi.org/10.1103/PhysRevD.86.032007. arXiv:1207.0825 [hep-ex]
1134. D.M. Asner et al., CLEO collaboration. Phys. Rev. D **70**, 091101 (2004). https://doi.org/10.1103/PhysRevD.70.091101. arXiv:hep-ex/0311033
1135. R. Aaij et al., LHCb collaboration. Phys. Lett. B **726**, 623 (2013). https://doi.org/10.1016/j.physletb.2013.09.011. arXiv:1308.3189 [hep-ex]
1136. M. Artuso et al., CLEO collaboration. Phys. Rev. D **85**, 122002 (2012). https://doi.org/10.1103/PhysRevD.85.122002. arXiv:1201.5716 [hep-ex]
1137. J. Alexander et al., CLEO collaboration. Phys. Rev. D **79**, 052001 (2009). https://doi.org/10.1103/PhysRevD.79.052001. arXiv:0901.1216 [hep-ex]
1138. P. Onyisi et al., CLEO collaboration. Phys. Rev. D **88**, 032009 (2013). https://doi.org/10.1103/PhysRevD.88.032009. arXiv:1306.5363 [hep-ex]
1139. B.R. Ko et al., Belle collaboration. Phys. Rev. Lett. **104**, 181602 (2010). https://doi.org/10.1103/PhysRevLett.104.181602. arXiv:1001.3202 [hep-ex]
1140. E. Golowich, G. Valencia, Phys. Rev. D **40**, 112 (1989). https://doi.org/10.1103/PhysRevD.40.112
1141. I.I.Y. Bigi (2001). arXiv:hep-ph/0107102
1142. W. Bensalem, A. Datta, D. London, Phys. Rev. D **66**, 094004 (2002). https://doi.org/10.1103/PhysRevD.66.094004. arXiv:hep-ph/0208054
1143. W. Bensalem, D. London, Phys. Rev. D **64**, 116003 (2001). https://doi.org/10.1103/PhysRevD.64.116003. arXiv:hep-ph/0005018
1144. W. Bensalem, A. Datta, D. London, Phys. Lett. B **538**, 309 (2002). https://doi.org/10.1016/S0370-2693(02)02028-2. arXiv:hep-ph/0205009
1145. M. Gronau, J.L. Rosner, Phys. Rev. D **84**, 096013 (2011). https://doi.org/10.1103/PhysRevD.84.096013. arXiv:1107.1232 [hep-ph]
1146. A.J. Bevan (2015). arXiv:1506.04246 [hep-ex]
1147. G. Durieux, Y. Grossman, Phys. Rev. D **92**, 076013 (2015). https://doi.org/10.1103/PhysRevD.92.076013. arXiv:1508.03054 [hep-ph]
1148. R. Aaij et al., LHCb collaboration. JHEP **10**, 005 (2014). https://doi.org/10.1007/JHEP10(2014)005. arXiv:1408.1299 [hep-ex]
1149. P. del Amo Sanchez et al., BaBar collaboration. Phys. Rev. D **81**, 111103 (2010). https://doi.org/10.1103/PhysRevD.81.111103. arXiv:1003.3397 [hep-ex]
1150. J.P. Lees et al., BaBar collaboration. Phys. Rev. D **84**, 031103 (2011). https://doi.org/10.1103/PhysRevD.84.031103. arXiv:1105.4410 [hep-ex]
1151. Y. Grossman, A.L. Kagan, Y. Nir, Phys. Rev. D **75**, 036008 (2007). https://doi.org/10.1103/PhysRevD.75.036008. arXiv:hep-ph/0609178 [hep-ph]
1152. M. Gersabeck, M. Alexander, S. Borghi, V. Gligorov, C. Parkes, J. Phys. G **39**, 045005 (2012). https://doi.org/10.1088/0954-3899/39/4/045005. arXiv:1111.6515 [hep-ex]
1153. B.R. Ko, (Belle collaboration), PoS **ICHEP2012**, 353 (2013). arXiv:1212.1975
1154. T. Becher, R.J. Hill, Phys. Lett. B **633**, 61 (2006). https://doi.org/10.1016/j.physletb.2005.11.063. arXiv:hep-ph/0509090
1155. F.J. Gilman, R.L. Singleton, Phys. Rev. D **41**, 142 (1990). https://doi.org/10.1103/PhysRevD.41.142
1156. R.J. Hill, eConf **C060409**, 027 (2006). arXiv:hep-ph/0606023
1157. D. Becirevic, A.B. Kaidalov, Phys. Lett. B **478**, 417 (2000). https://doi.org/10.1016/S0370-2693(00)00290-2. arXiv:hep-ph/9904490
1158. C.G. Boyd, B. Grinstein, R.F. Lebed, Phys. Rev. Lett. **74**, 4603 (1995). https://doi.org/10.1103/PhysRevLett.74.4603. arXiv:hep-ph/9412324
1159. C.G. Boyd, M.J. Savage, Phys. Rev. D **56**, 303 (1997). https://doi.org/10.1103/PhysRevD.56.303. arXiv:hep-ph/9702300
1160. M.C. Arnesen, B. Grinstein, I.Z. Rothstein, I.W. Stewart, Phys. Rev. Lett. **95**, 071802 (2005). https://doi.org/10.1103/PhysRevLett.95.071802
1161. C. Bourrely, B. Machet, E. de Rafael, Nucl. Phys. B **189**, 157 (1981). https://doi.org/10.1016/0550-3213(81)90086-9
1162. D. Becirevic, A.L. Yaouanc, A. Oyanguren, P. Roudeau, F. Sanfilippo (2014). arXiv:1407.1019 [hep-ph]
1163. J.P. Lees et al. (BaBar collaboration), Phys. Rev. D **88**, 052003 (2013). https://doi.org/10.1103/PhysRevD.88.052003. arXiv:1304.5009 [hep-ex]. [Erratum ibid. **88**, 079902 (2013). doi:10.1103/PhysRevD.88.079902]
1164. P. del Amo Sanchez et al., BaBar collaboration. Phys. Rev. D **82**, 111101 (2010). https://doi.org/10.1103/PhysRevD.82.111101. arXiv:1009.2076 [hep-ex]
1165. R. Aaij et al., LHCb collaboration. JHEP **09**, 145 (2013). https://doi.org/10.1007/JHEP09(2013)45. arXiv:1307.4556
1166. G. Burdman, J. Kambor, Phys. Rev. D **55**, 2817 (1997). https://doi.org/10.1103/PhysRevD.55.2817. arXiv:hep-ph/9602353
1167. D. Becirevic, A. Le Yaouanc, L. Oliver, J.-C. Raynal, P. Roudeau, J. Serrano, Phys. Rev. D **87**, 054007 (2013). https://doi.org/10.1103/PhysRevD.87.054007. arXiv:1206.5869 [hep-ph]
1168. J.P. Lees et al., BaBar collaboration. Phys. Rev. D **91**, 052022 (2015). https://doi.org/10.1103/PhysRevD.91.052022. arXiv:1412.5502 [hep-ex]
1169. M. Ablikim et al., BESIII collaboration. Phys. Rev. D **92**, 072012 (2015). https://doi.org/10.1103/PhysRevD.92.072012. arXiv:1508.07560 [hep-ex]
1170. M. Ablikim et al., BESIII collaboration. Phys. Rev. D **92**, 112008 (2015). https://doi.org/10.1103/PhysRevD.92.112008. arXiv:1510.00308 [hep-ex]
1171. L. Widhalm et al., Belle collaboration. Phys. Rev. Lett. **97**, 061804 (2006). https://doi.org/10.1103/PhysRevLett.97.061804. arXiv:hep-ex/0604049
1172. B. Aubert et al., BaBar collaboration. Phys. Rev. D **76**, 052005 (2007). https://doi.org/10.1103/PhysRevD.76.052005. arXiv:0704.0020 [hep-ex]
1173. D. Besson et al., CLEO collaboration. Phys. Rev. D **80**, 032005 (2009). https://doi.org/10.1103/PhysRevD.80.032005. arXiv:0906.2983 [hep-ex]
1174. S. Dobbs et al., CLEO collaboration. Phys. Rev. D **77**, 112005 (2008). https://doi.org/10.1103/PhysRevD.77.112005. arXiv:0712.1020 [hep-ex]
1175. G. Huang et al., CLEO collaboration. Phys. Rev. Lett. **94**, 011802 (2005). https://doi.org/10.1103/PhysRevLett.94.011802. arXiv:hep-ex/0407035
1176. J. Link et al., FOCUS collaboration. Phys. Lett. B **607**, 233 (2005). https://doi.org/10.1016/j.physletb.2004.12.036. arXiv:hep-ex/0410037
1177. J. Adler et al., MARK-III collaboration. Phys. Rev. Lett. **62**, 1821 (1989). https://doi.org/10.1103/PhysRevLett.62.1821
1178. K. Kodama et al., Fermilab E653 collaboration. Phys. Rev. Lett. **66**, 1819 (1991). https://doi.org/10.1103/PhysRevLett.66.1819
1179. K. Kodama et al., Fermilab E653 collaboration. Phys. Lett. B **336**, 605 (1994). https://doi.org/10.1016/0370-2693(94)90579-7
1180. P.L. Frabetti et al., Fermilab E687 collaboration. Phys. Lett. B **364**, 127 (1995). https://doi.org/10.1016/0370-2693(95)01368-2
1181. P.L. Frabetti et al., Fermilab E687 collaboration. Phys. Lett. B **315**, 203 (1993). https://doi.org/10.1016/0370-2693(93)90181-G
1182. J.C. Anjos et al., Tagged Photon Spectrometer collaboration. Phys. Rev. Lett. **62**, 1587 (1989). https://doi.org/10.1103/PhysRevLett.62.1587

1183. M. Ablikim et al., BES collaboration. Phys. Lett. B **597**, 39 (2004). https://doi.org/10.1016/j.physletb.2004.07.004. arXiv:hep-ex/0406028
1184. M. Ablikim et al. (BES collaboration) (2006). arXiv:hep-ex/0610019
1185. A. Bean et al., CLEO collaboration. Phys. Lett. B **317**, 647 (1993). https://doi.org/10.1016/0370-2693(93)91385-Z
1186. Y. Zheng, (BESIII collaboration), Presented at the 37th International Conference on High Energy Physics (ICHEP 2014) (2014)
1187. J.G. Korner, G.A. Schuler, Z. Phys. C **46**, 93 (1990). https://doi.org/10.1007/BF02440838
1188. J. Link et al., FOCUS collaboration. Phys. Lett. B **535**, 43 (2002). https://doi.org/10.1016/S0370-2693(02)01715-X. arXiv:hep-ex/0203031
1189. J. Link et al., FOCUS collaboration. Phys. Lett. B **544**, 89 (2002). https://doi.org/10.1016/S0370-2693(02)02386-9. arXiv:hep-ex/0207049
1190. B. Aubert et al., BaBar collaboration. Phys. Rev. D **78**, 051101 (2008). https://doi.org/10.1103/PhysRevD.78.051101. arXiv:0807.1599 [hep-ex]
1191. K.M. Ecklund et al., CLEO collaboration. Phys. Rev. D **80**, 052009 (2009). https://doi.org/10.1103/PhysRevD.80.052009. arXiv:0907.3201 [hep-ex]
1192. R.A. Briere et al., CLEO collaboration. Phys. Rev. D **81**, 112001 (2010). https://doi.org/10.1103/PhysRevD.81.112001. arXiv:1004.1954 [hep-ex]
1193. P. del Amo Sanchez et al., BaBar collaboration. Phys. Rev. D **83**, 072001 (2011). https://doi.org/10.1103/PhysRevD.83.072001. arXiv:1012.1810 [hep-ex]
1194. P. Estabrooks et al., Nucl. Phys. B **133**, 490 (1978). https://doi.org/10.1016/0550-3213(78)90238-9
1195. J. Anjos et al., Fermilab E691 collaboration. Phys. Rev. Lett. **65**, 2630 (1990). https://doi.org/10.1103/PhysRevLett.65.2630
1196. K. Kodama et al., Fermilab E653 collaboration. Phys. Lett. B **274**, 246 (1992). https://doi.org/10.1016/0370-2693(92)90530-H
1197. P. Frabetti et al., Fermilab E687 collaboration. Phys. Lett. B **307**, 262 (1993). https://doi.org/10.1016/0370-2693(93)90216-5
1198. E. Aitala et al., Fermilab E791 collaboration. Phys. Rev. Lett. **80**, 1393 (1998). https://doi.org/10.1103/PhysRevLett.80.1393. arXiv:hep-ph/9710216
1199. E. Aitala et al., Fermilab E791 collaboration. Phys. Lett. B **440**, 435 (1998). https://doi.org/10.1016/S0370-2693(98)01243-X. arXiv:hep-ex/9809026
1200. M. Adamovich et al., BEATRICE collaboration. Eur. Phys. J. C **6**, 35 (1999). https://doi.org/10.1007/s100529801012
1201. J. Link et al. (FOCUS collaboration), Phys. Lett. B **607**, 67 (2005). https://doi.org/10.1016/j.physletb.2004.12.037. arXiv:hep-ex/0410067 [hep-ex]
1202. H. Mahlke, eConf **C0610161**, 014 (2006). arXiv:hep-ex/0702014
1203. A. Filipuzzi, J. Portoles, M. Gonzalez-Alonso, Phys. Rev. D **85**, 116010 (2012). https://doi.org/10.1103/PhysRevD.85.116010. arXiv:1203.2092 [hep-ph]
1204. M. Ablikim et al., BESIII collaboration. Phys. Rev. D **94**, 072004 (2016). https://doi.org/10.1103/PhysRevD.94.072004. arXiv:1608.06732 [hep-ex]
1205. M. Ablikim et al., BESIII collaboration. Phys. Rev. D **89**, 051104 (2014). https://doi.org/10.1103/PhysRevD.89.051104. arXiv:1312.0374 [hep-ex]
1206. P. del Amo Sanchez et al., BaBar collaboration. Phys. Rev. D **82**, 091103 (2010). https://doi.org/10.1103/PhysRevD.82.091103. arXiv:1008.4080 [hep-ex]
1207. A. Zupanc et al., Belle collaboration. JHEP **09**, 139 (2013). https://doi.org/10.1007/JHEP09(2013)139. arXiv:1307.6240 [hep-ex]
1208. P. Naik et al., CLEO collaboration. Phys. Rev. D **80**, 112004 (2009). https://doi.org/10.1103/PhysRevD.80.112004. arXiv:0910.3602 [hep-ex]
1209. P. Onyisi et al., CLEO collaboration. Phys. Rev. D **79**, 052002 (2009). https://doi.org/10.1103/PhysRevD.79.052002. arXiv:0901.1147 [hep-ex]
1210. E. Barberio, B. van Eijk, Z. Was, Comput. Phys. Commun. **66**, 115 (1991). https://doi.org/10.1016/0010-4655(91)90012-A
1211. E. Barberio, Z. Was, Comput. Phys. Commun. **79**, 291 (1994). https://doi.org/10.1016/0010-4655(94)90074-4
1212. P. Golonka, Z. Was, Eur. Phys. J. C **45**, 97 (2006). https://doi.org/10.1140/epjc/s2005-02396-4. arXiv:hep-ph/0506026
1213. P. Golonka, Z. Was, Eur. Phys. J. C **50**, 53 (2007). https://doi.org/10.1140/epjc/s10052-006-0205-3. arXiv:hep-ph/0604232
1214. EVTGEN-V00-11-07 (2005). http://inspirehep.net/record/707695
1215. J.M. Link et al., FOCUS collaboration. Phys. Lett. B **555**, 167 (2003). https://doi.org/10.1016/S0370-2693(03)00053-4. arXiv:hep-ex/0212058
1216. B. Aubert et al., BaBar collaboration. Phys. Rev. Lett. **100**, 051802 (2008). https://doi.org/10.1103/PhysRevLett.100.051802. arXiv:0704.2080 [hep-ex]
1217. M. Artuso et al., CLEO collaboration. Phys. Rev. Lett. **80**, 3193 (1998). https://doi.org/10.1103/PhysRevLett.80.3193. arXiv:hep-ex/9712023
1218. R. Barate et al., ALEPH collaboration. Phys. Lett. B **403**, 367 (1997). https://doi.org/10.1016/S0370-2693(97)00585-6
1219. H. Albrecht et al., ARGUS collaboration. Phys. Lett. B **340**, 125 (1994). https://doi.org/10.1016/0370-2693(94)91308-0
1220. D.S. Akerib et al., CLEO collaboration. Phys. Rev. Lett. **71**, 3070 (1993). https://doi.org/10.1103/PhysRevLett.71.3070
1221. D. Decamp et al., ALEPH collaboration. Phys. Lett. B **266**, 218 (1991). https://doi.org/10.1016/0370-2693(91)90769-M
1222. D.E. Acosta et al., CDF collaboration. Phys. Rev. Lett. **94**, 122001 (2005). https://doi.org/10.1103/PhysRevLett.94.122001. arXiv:hep-ex/0504006
1223. T.E. Coan et al., CLEO collaboration. Phys. Rev. Lett. **80**, 1150 (1998). https://doi.org/10.1103/PhysRevLett.80.1150. arXiv:hep-ex/9710028
1224. B. Aubert et al., BaBar collaboration. Phys. Rev. Lett. **90**, 242001 (2003). https://doi.org/10.1103/PhysRevLett.90.242001. arXiv:hep-ex/0304021
1225. D. Besson et al. (CLEO collaboration), Phys. Rev. D **68**, 032002 (2003). https://doi.org/10.1103/PhysRevD.68.032002. arXiv:hep-ex/0305100. [Erratum ibid. **75**, 119908 (2007). doi:10.1103/PhysRevD.75.119908]
1226. K. Abe et al., Belle collaboration. Phys. Rev. Lett. **92**, 012002 (2004). https://doi.org/10.1103/PhysRevLett.92.012002. arXiv:hep-ex/0307052
1227. B. Aubert et al., BaBar collaboration. Phys. Rev. D **69**, 031101 (2004). https://doi.org/10.1103/PhysRevD.69.031101. arXiv:hep-ex/0310050
1228. J.M. Link et al., FOCUS collaboration. Phys. Lett. B **586**, 11 (2004). https://doi.org/10.1016/j.physletb.2004.02.017. arXiv:hep-ex/0312060
1229. S. Godfrey, N. Isgur, Phys. Rev. D **32**, 189 (1985). https://doi.org/10.1103/PhysRevD.32.189
1230. S. Godfrey, R. Kokoski, Phys. Rev. D **43**, 1679 (1991). https://doi.org/10.1103/PhysRevD.43.1679
1231. P. Schweitzer, S. Boffi, M. Radici, Phys. Rev. D **66**, 114004 (2002). https://doi.org/10.1103/PhysRevD.66.114004. arXiv:hep-ph/0207230
1232. F. Jugeau, A. Le Yaouanc, L. Oliver, J.-C. Raynal, Phys. Rev. D **72**, 094010 (2005). https://doi.org/10.1103/PhysRevD.72.094010. arXiv:hep-ph/0504206

1233. P. Colangelo, F. De Fazio, R. Ferrandes, Mod. Phys. Lett. A **19**, 2083 (2004). https://doi.org/10.1142/S0217732304015269. arXiv:hep-ph/0407137
1234. R.N. Cahn, J.D. Jackson, Phys. Rev. D **68**, 037502 (2003). https://doi.org/10.1103/PhysRevD.68.037502. arXiv:hep-ph/0305012
1235. T. Barnes, F.E. Close, H.J. Lipkin, Phys. Rev. D **68**, 054006 (2003). https://doi.org/10.1103/PhysRevD.68.054006. arXiv:hep-ph/0305025
1236. H. Lipkin, Phys. Lett. B **580**, 50 (2004). https://doi.org/10.1016/j.physletb.2003.10.117. arXiv:hep-ph/0306204
1237. W.A. Bardeen, E.J. Eichten, C.T. Hill, Phys. Rev. D **68**, 054024 (2003). https://doi.org/10.1103/PhysRevD.68.054024. arXiv:hep-ph/0305049
1238. B. Aubert et al., BaBar collaboration. Phys. Rev. D **80**, 092003 (2009). https://doi.org/10.1103/PhysRevD.80.092003. arXiv:0908.0806 [hep-ex]
1239. R. Aaij et al., LHCb collaboration. JHEP **10**, 151 (2012). https://doi.org/10.1007/JHEP10(2012)151. arXiv:1207.6016 [hep-ex]
1240. R. Aaij et al., LHCb collaboration. Phys. Rev. Lett. **113**, 162001 (2014). https://doi.org/10.1103/PhysRevLett.113.162001. arXiv:1407.7574 [hep-ex]
1241. R. Aaij et al., LHCb collaboration. JHEP **02**, 133 (2016). https://doi.org/10.1007/JHEP02(2016)133. arXiv:1601.01495 [hep-ex]
1242. T. Matsuki, T. Morii, K. Sudoh, Eur. Phys. J. A **31**, 701 (2007). https://doi.org/10.1140/epja/i2006-10287-1. arXiv:hep-ph/0610186
1243. N. Isgur, M.B. Wise, Phys. Lett. B **232**, 113 (1989). https://doi.org/10.1016/0370-2693(89)90566-2
1244. B. Aubert et al., BaBar collaboration. Phys. Rev. D **74**, 032007 (2006). https://doi.org/10.1103/PhysRevD.74.032007. arXiv:hep-ex/0604030
1245. V.M. Abazov et al., D0 collaboration. Phys. Rev. Lett. **102**, 051801 (2009). https://doi.org/10.1103/PhysRevLett.102.051801. arXiv:0712.3789 [hep-ex]
1246. P.L. Frabetti et al., Fermilab E687 collaboration. Phys. Rev. Lett. **72**, 324 (1994). https://doi.org/10.1103/PhysRevLett.72.324
1247. J.P. Alexander et al., CLEO collaboration. Phys. Lett. B **303**, 377 (1993). https://doi.org/10.1016/0370-2693(93)91448-V
1248. H. Albrecht et al., ARGUS collaboration. Phys. Lett. B **297**, 425 (1992). https://doi.org/10.1016/0370-2693(92)91282-E
1249. P. Avery et al., CLEO collaboration. Phys. Rev. D **41**, 774 (1990). https://doi.org/10.1103/PhysRevD.41.774
1250. H. Albrecht et al., ARGUS collaboration. Phys. Lett. B **230**, 162 (1989). https://doi.org/10.1016/0370-2693(89)91672-9
1251. J.P. Lees et al., BaBar collaboration. Phys. Rev. D **83**, 072003 (2011). https://doi.org/10.1103/PhysRevD.83.072003. arXiv:1103.2675 [hep-ex]
1252. R. Aaij et al., LHCb collaboration. Phys. Rev. D **90**, 072003 (2014). https://doi.org/10.1103/PhysRevD.90.072003. arXiv:1407.7712 [hep-ex]
1253. R. Aaij et al., LHCb collaboration. Phys. Lett. B **698**, 14 (2011). https://doi.org/10.1016/j.physletb.2011.02.039. arXiv:1102.0348 [hep-ex]
1254. B. Aubert et al., BaBar collaboration. Phys. Rev. Lett. **97**, 222001 (2006). https://doi.org/10.1103/PhysRevLett.97.222001. arXiv:hep-ex/0607082
1255. H. Albrecht et al., ARGUS collaboration. Z. Phys. C **69**, 405 (1996). https://doi.org/10.1007/s002880050040
1256. Y. Kubota et al., CLEO collaboration. Phys. Rev. Lett. **72**, 1972 (1994). https://doi.org/10.1103/PhysRevLett.72.1972. arXiv:hep-ph/9403325
1257. J.P. Lees et al., BaBar collaboration. Phys. Rev. D **91**, 052002 (2015). https://doi.org/10.1103/PhysRevD.91.052002. arXiv:1412.6751 [hep-ex]
1258. R. Aaij et al., LHCb collaboration. Phys. Rev. D **92**, 012012 (2015). https://doi.org/10.1103/PhysRevD.92.012012. arXiv:1505.01505 [hep-ex]
1259. A. Kuzmin et al., Belle collaboration. Phys. Rev. D **76**, 012006 (2007). https://doi.org/10.1103/PhysRevD.76.012006. arXiv:hep-ex/0611054
1260. H. Abramowicz et al., ZEUS collaboration. Nucl. Phys. B **866**, 229 (2013). https://doi.org/10.1016/j.nuclphysb.2012.09.007. arXiv:1208.4468 [hep-ex]
1261. A. Abulencia et al., CDF collaboration. Phys. Rev. D **73**, 051104 (2006). https://doi.org/10.1103/PhysRevD.73.051104. arXiv:hep-ex/0512069
1262. P. Avery et al., CLEO collaboration. Phys. Lett. B **331**, 236 (1994). https://doi.org/10.1016/0370-2693(94)90968-7. arXiv:hep-ph/9403359
1263. H. Albrecht et al., ARGUS collaboration. Phys. Lett. B **232**, 398 (1989). https://doi.org/10.1016/0370-2693(89)90764-8
1264. J.C. Anjos et al., Tagged Photon Spectrometer collaboration. Phys. Rev. Lett. **62**, 1717 (1989). https://doi.org/10.1103/PhysRevLett.62.1717
1265. T. Bergfeld et al., CLEO collaboration. Phys. Lett. B **340**, 194 (1994). https://doi.org/10.1016/0370-2693(94)01348-9
1266. H. Albrecht et al., ARGUS collaboration. Phys. Lett. B **221**, 422 (1989). https://doi.org/10.1016/0370-2693(89)91737-1
1267. H. Albrecht et al., ARGUS collaboration. Phys. Lett. B **231**, 208 (1989). https://doi.org/10.1016/0370-2693(89)90141-X
1268. P. Abreu et al., DELPHI collaboration. Phys. Lett. B **426**, 231 (1998). https://doi.org/10.1016/S0370-2693(98)00346-3
1269. S. Chekanov et al., ZEUS collaboration. Eur. Phys. J. C **60**, 25 (2009). https://doi.org/10.1140/epjc/s10052-009-0881-x. arXiv:0807.1290 [hep-ex]
1270. A. Heister et al., ALEPH collaboration. Phys. Lett. B **526**, 34 (2002). https://doi.org/10.1016/S0370-2693(01)01465-4. arXiv:hep-ex/0112010
1271. A. Zupanc et al., Belle collaboration. Phys. Rev. Lett. **113**, 042002 (2014). https://doi.org/10.1103/PhysRevLett.113.042002. arXiv:1312.7826 [hep-ex]
1272. M. Ablikim et al., BESIII collaboration. Phys. Rev. Lett. **115**, 221805 (2015). https://doi.org/10.1103/PhysRevLett.115.221805. arXiv:1510.02610 [hep-ex]
1273. P. Avery et al., CLEO collaboration. Phys. Rev. D **43**, 3599 (1991). https://doi.org/10.1103/PhysRevD.43.3599
1274. M.S. Alam et al., CLEO collaboration. Phys. Rev. D **57**, 4467 (1998). https://doi.org/10.1103/PhysRevD.57.4467. arXiv:hep-ex/9709012
1275. H. Albrecht et al., ARGUS collaboration. Phys. Lett. B **274**, 239 (1992). https://doi.org/10.1016/0370-2693(92)90529-D
1276. J.M. Link et al., FOCUS collaboration. Phys. Lett. B **624**, 22 (2005). https://doi.org/10.1016/j.physletb.2005.08.014. arXiv:hep-ex/0505077
1277. P. Avery et al., CLEO collaboration. Phys. Lett. B **325**, 257 (1994). https://doi.org/10.1016/0370-2693(94)90100-7
1278. H. Albrecht et al., ARGUS collaboration. Phys. Lett. B **207**, 109 (1988). https://doi.org/10.1016/0370-2693(88)90896-9
1279. B. Aubert et al., BaBar collaboration. Phys. Rev. D **75**, 052002 (2007). https://doi.org/10.1103/PhysRevD.75.052002. arXiv:hep-ex/0601017
1280. Y. Kubota et al., CLEO collaboration. Phys. Rev. Lett. **71**, 3255 (1993). https://doi.org/10.1103/PhysRevLett.71.3255
1281. T. Bergfeld et al., CLEO collaboration. Phys. Lett. B **323**, 219 (1994). https://doi.org/10.1016/0370-2693(94)90295-X. arXiv:hep-ph/9403326
1282. H. Albrecht et al., ARGUS collaboration. Phys. Lett. B **269**, 234 (1991). https://doi.org/10.1016/0370-2693(91)91480-J

1283. B. Aubert et al., BaBar collaboration. Phys. Rev. D **72**, 052006 (2005). https://doi.org/10.1103/PhysRevD.72.052006. arXiv:hep-ex/0507009
1284. E. Solovieva et al., Belle collaboration. Phys. Lett. B **672**, 1 (2009). https://doi.org/10.1016/j.physletb.2008.12.062. arXiv:0808.3677 [hep-ex]
1285. T. Aaltonen et al., CDF collaboration. Phys. Rev. D **84**, 012003 (2011). https://doi.org/10.1103/PhysRevD.84.012003. arXiv:1105.5995 [hep-ex]
1286. M. Artuso et al., CLEO collaboration. Phys. Rev. Lett. **86**, 4479 (2001). https://doi.org/10.1103/PhysRevLett.86.4479. arXiv:hep-ex/0010080
1287. B. Aubert et al., BaBar collaboration. Phys. Rev. Lett. **98**, 012001 (2007). https://doi.org/10.1103/PhysRevLett.98.012001. arXiv:hep-ex/0603052
1288. H.-Y. Cheng, C.-K. Chua, Phys. Rev. D **75**, 014006 (2007). https://doi.org/10.1103/PhysRevD.75.014006. arXiv:hep-ph/0610283
1289. S.H. Lee et al., Belle collaboration. Phys. Rev. D **89**, 091102 (2014). https://doi.org/10.1103/PhysRevD.89.091102. arXiv:1404.5389 [hep-ex]
1290. R. Mizuk et al., Belle collaboration. Phys. Rev. Lett. **94**, 122002 (2005). https://doi.org/10.1103/PhysRevLett.94.122002. arXiv:hep-ex/0412069
1291. L. Copley, N. Isgur, G. Karl, Phys. Rev. D **20**, 768 (1979). https://doi.org/10.1103/PhysRevD.20.768. [Erratum ibid. **23**, 817 (1981). doi:10.1103/PhysRevD.23.817]
1292. D. Pirjol, T.-M. Yan, Phys. Rev. D **56**, 5483 (1997). https://doi.org/10.1103/PhysRevD.56.5483. arXiv:hep-ph/9701291
1293. R. Chistov et al., Belle collaboration. Phys. Rev. Lett. **97**, 162001 (2006). https://doi.org/10.1103/PhysRevLett.97.162001. arXiv:hep-ex/0606051
1294. Y. Kato et al., Belle collaboration. Phys. Rev. D **89**, 052003 (2014). https://doi.org/10.1103/PhysRevD.89.052003. arXiv:1312.1026 [hep-ex]
1295. Y. Kato et al., Belle collaboration. Phys. Rev. D **94**, 032002 (2016). https://doi.org/10.1103/PhysRevD.94.032002. arXiv:1605.09103 [hep-ex]
1296. B. Aubert et al., BaBar collaboration. Phys. Rev. D **77**, 031101 (2008). https://doi.org/10.1103/PhysRevD.77.031101. arXiv:0710.5775 [hep-ex]
1297. J. Yelton et al., Belle collaboration. Phys. Rev. D **94**, 052011 (2016). https://doi.org/10.1103/PhysRevD.94.052011. arXiv:1607.07123 [hep-ex]
1298. B. Aubert et al., BaBar collaboration. Phys. Rev. Lett. **97**, 232001 (2006). https://doi.org/10.1103/PhysRevLett.97.232001. arXiv:hep-ex/0608055
1299. J.L. Rosner, Phys. Rev. D **52**, 6461 (1995). https://doi.org/10.1103/PhysRevD.52.6461. arXiv:hep-ph/9508252
1300. L.Y. Glozman, D. Riska, Nucl. Phys. A **603**, 326 (1996). https://doi.org/10.1016/0375-9474(96)80005-C. arXiv:hep-ph/9509269. [Erratum ibid. 620, 510 (1997). doi:10.1016/S0375-9474(97)00200-5]
1301. E.E. Jenkins, Phys. Rev. D **54**, 4515 (1996). https://doi.org/10.1103/PhysRevD.54.4515. arXiv:hep-ph/9603449
1302. L. Burakovsky, J.T. Goldman, L. Horwitz, Phys. Rev. D **56**, 7124 (1997). https://doi.org/10.1103/PhysRevD.56.7124. arXiv:hep-ph/9706464
1303. G. Burdman, E. Golowich, J.L. Hewett, S. Pakvasa, Phys. Rev. D **66**, 014009 (2002). https://doi.org/10.1103/PhysRevD.66.014009. arXiv:hep-ph/0112235
1304. S. Fajfer, A. Prapotnik, S. Prelovsek, P. Singer, J. Zupan, Nucl. Phys. Proc. Suppl. **115**, 93 (2003). https://doi.org/10.1016/S0920-5632(02)01961-8. arXiv:hep-ph/0208201
1305. S. Fajfer, N. Kosnik, S. Prelovsek, Phys. Rev. D **76**, 074010 (2007). https://doi.org/10.1103/PhysRevD.76.074010. arXiv:0706.1133 [hep-ph]
1306. E. Golowich, J. Hewett, S. Pakvasa, A.A. Petrov, Phys. Rev. D **79**, 114030 (2009). https://doi.org/10.1103/PhysRevD.79.114030. arXiv:0903.2830 [hep-ph]
1307. A. Paul, I.I. Bigi, S. Recksiegel, Phys. Rev. D **82**, 094006 (2010). https://doi.org/10.1103/PhysRevD.82.094006. arXiv:1008.3141 [hep-ph]. [Erratum ibid. **83**, 019901 (2011). doi:10.1103/PhysRevD.83.019901]
1308. A. Borisov (2011). arXiv:1112.3269 [hep-ph]
1309. R.-M. Wang, J.-H. Sheng, J. Zhu, Y.-Y. Fan, Y. Gao, Int. J. Mod. Phys. A **29**, 1450169 (2014). https://doi.org/10.1142/S0217751X14501693
1310. S. de Boer, G. Hiller, Phys. Rev. D **93**, 074001 (2016). https://doi.org/10.1103/PhysRevD.93.074001. arXiv:1510.00311 [hep-ph]
1311. P. Rubin et al., CLEO collaboration. Phys. Rev. D **82**, 092007 (2010). https://doi.org/10.1103/PhysRevD.82.092007. arXiv:1009.1606 [hep-ex]
1312. V. Abazov et al., D0 collaboration. Phys. Rev. Lett. **100**, 101801 (2008). https://doi.org/10.1103/PhysRevLett.100.101801. arXiv:0708.2094 [hep-ex]
1313. R. Aaij et al., LHCb collaboration. Phys. Lett. B **728**, 234 (2014). https://doi.org/10.1016/j.physletb.2013.11.053. arXiv:1310.2535 [hep-ex]
1314. R. Aaij et al., LHCb collaboration. Phys. Lett. B **724**, 203 (2013). https://doi.org/10.1016/j.physletb.2013.06.010. arXiv:1304.6365 [hep-ex]
1315. T. Coan et al., CLEO collaboration. Phys. Rev. Lett. **90**, 101801 (2003). https://doi.org/10.1103/PhysRevLett.90.101801. arXiv:hep-ex/0212045
1316. M. Ablikim et al., BESIII collaboration. Phys. Rev. D **91**, 112015 (2015). https://doi.org/10.1103/PhysRevD.91.112015. arXiv:1505.03087 [hep-ex]
1317. J.P. Lees et al., BaBar collaboration. Phys. Rev. D **85**, 091107 (2012). https://doi.org/10.1103/PhysRevD.85.091107. arXiv:1110.6480 [hep-ex]
1318. N.K. Nisar et al., Belle collaboration. Phys. Rev. D **93**, 051102 (2016). https://doi.org/10.1103/PhysRevD.93.051102. arXiv:1512.02992 [hep-ex]
1319. P. Haas et al., CLEO collaboration. Phys. Rev. Lett. **60**, 1614 (1988). https://doi.org/10.1103/PhysRevLett.60.1614
1320. H. Albrecht et al., ARGUS collaboration. Phys. Lett. B **209**, 380 (1988). https://doi.org/10.1016/0370-2693(88)90967-7
1321. J. Adler et al., MARK-III collaboration. Phys. Rev. D **37**, 2023 (1988). https://doi.org/10.1103/PhysRevD.37.2023. [Erratum ibid. **40**, 3788 (1989). doi:10.1103/PhysRevD.40.3788]
1322. A. Freyberger et al., CLEO collaboration. Phys. Rev. Lett. **76**, 3065 (1996). https://doi.org/10.1103/PhysRevLett.76.3065
1323. D. Pripstein et al., Fermilab E789 collaboration. Phys. Rev. D **61**, 032005 (2000). https://doi.org/10.1103/PhysRevD.61.032005. arXiv:hep-ex/9906022
1324. E. Aitala et al., Fermilab E791 collaboration. Phys. Lett. B **462**, 401 (1999). https://doi.org/10.1016/S0370-2693(99)00902-8. arXiv:hep-ex/9906045
1325. B. Aubert et al., BaBar collaboration. Phys. Rev. Lett. **93**, 191801 (2004). https://doi.org/10.1103/PhysRevLett.93.191801. arXiv:hep-ex/0408023
1326. M. Petric et al., Belle collaboration. Phys. Rev. D **81**, 091102 (2010). https://doi.org/10.1103/PhysRevD.81.091102. arXiv:1003.2345 [hep-ex]
1327. K. Kodama et al., Fermilab E653 collaboration. Phys. Lett. B **345**, 85 (1995). https://doi.org/10.1016/0370-2693(94)01610-O
1328. I. Abt et al., HERA-B collaboration. Phys. Lett. B **596**, 173 (2004). https://doi.org/10.1016/j.physletb.2004.06.097. arXiv:hep-ex/0405059

1329. T. Aaltonen et al., CDF collaboration. Phys. Rev. D **82**, 091105 (2010). https://doi.org/10.1103/PhysRevD.82.091105. arXiv:1008.5077 [hep-ex]
1330. R. Aaij et al., LHCb collaboration. Phys. Lett. B **725**, 15 (2013). https://doi.org/10.1016/j.physletb.2013.06.037. arXiv:1305.5059 [hep-ex]
1331. E. Aitala et al., Fermilab E791 collaboration. Phys. Rev. Lett. **86**, 3969 (2001). https://doi.org/10.1103/PhysRevLett.86.3969. arXiv:hep-ex/0011077
1332. J. Adler et al., MARK-III collaboration. Phys. Rev. D **40**, 906 (1989). https://doi.org/10.1103/PhysRevD.40.906
1333. J. Becker et al., MARK-III collaboration. Phys. Lett. B **193**, 147 (1987). https://doi.org/10.1016/0370-2693(87)90473-4
1334. R. Aaij et al., LHCb collaboration. Phys. Lett. B **754**, 167 (2016). https://doi.org/10.1016/j.physletb.2016.01.029. arXiv:1512.00322 [hep-ex]
1335. P. Rubin et al., CLEO collaboration. Phys. Rev. D **79**, 097101 (2009). https://doi.org/10.1103/PhysRevD.79.097101. arXiv:0904.1619 [hep-ex]
1336. P. Frabetti et al., Fermilab E687 collaboration. Phys. Lett. B **398**, 239 (1997). https://doi.org/10.1016/S0370-2693(97)00229-3
1337. J.P. Lees et al., BaBar collaboration. Phys. Rev. D **84**, 072006 (2011). https://doi.org/10.1103/PhysRevD.84.072006. arXiv:1107.4465 [hep-ex]
1338. M.-G. Zhao, (BESIII collaboration) (2016). arXiv:1605.08952 [hep-ex]
1339. J. Link et al., FOCUS collaboration. Phys. Lett. B **572**, 21 (2003). https://doi.org/10.1016/j.physletb.2003.07.079. arXiv:hep-ex/0306049
1340. B. Aubert et al., BaBar collaboration. Nucl. Phys. Proc. Suppl. **189**, 193 (2009). https://doi.org/10.1016/j.nuclphysbps.2009.03.034. arXiv:0808.1121 [hep-ex]
1341. S. Paramesvaran, (BaBar collaboration) (2009). arXiv:0910.2884 [hep-ex]
1342. S. Ryu et al., Belle collaboration. Phys. Rev. D **89**, 072009 (2014). https://doi.org/10.1103/PhysRevD.89.072009. arXiv:1402.5213 [hep-ex]
1343. R. Barate et al., ALEPH collaboration. Eur. Phys. J. C **4**, 29 (1998). https://doi.org/10.1007/s100529800879
1344. S. Schael et al., (ALEPH collaboration), HFLAV-tau uses measurements of $\tau \to hX$ and $\tau \to KX$ and obtains $\tau \to \pi X$ by difference; the measurement of $\mathcal{B}\left(\tau^- \to 3h^- 2h^+ \pi^0 \nu_\tau (\text{ex.} K^0)\right)$ has been read as $(2.1 \pm 0.7 \pm 0.6) \times 10^{-4}$ whereas PDG11 uses $(2.1 \pm 0.7 \pm 0.9) \times 10^{-4}$. Phys. Rep. **421**, 191 (2005). https://doi.org/10.1016/j.physrep.2005.06.007. arXiv:hep-ex/0506072
1345. P. Abreu et al., DELPHI collaboration. Eur. Phys. J. C **10**, 201 (1999). https://doi.org/10.1007/s100520050583
1346. M. Acciarri et al., L3 collaboration. Phys. Lett. B **507**, 47 (2001). https://doi.org/10.1016/S0370-2693(01)00294-5. arXiv:hep-ex/0102023
1347. G. Abbiendi et al., OPAL collaboration. Phys. Lett. B **551**, 35 (2003). https://doi.org/10.1016/S0370-2693(02)03020-4. arXiv:hep-ex/0211066
1348. H. Albrecht et al., ARGUS collaboration. Z. Phys. C **53**, 367 (1992). https://doi.org/10.1007/BF01625895
1349. B. Aubert et al., BaBar collaboration. Phys. Rev. Lett. **105**, 051602 (2010). https://doi.org/10.1103/PhysRevLett.105.051602. arXiv:0912.0242 [hep-ex]
1350. A. Anastassov et al., CLEO collaboration. Phys. Rev. D **55**, 2559 (1997). https://doi.org/10.1103/PhysRevD.55.2559. [Erratum ibid. **58**, 119903 (1998). doi:10.1103/PhysRevD.58.119903]
1351. G. Abbiendi et al., OPAL collaboration. Phys. Lett. B **447**, 134 (1999). https://doi.org/10.1016/S0370-2693(98)01553-6. arXiv:hep-ex/9812017
1352. P. Abreu et al., DELPHI collaboration. Z. Phys. C **55**, 555 (1992). https://doi.org/10.1007/BF01561293
1353. M. Acciarri et al., L3 collaboration. Phys. Lett. B **345**, 93 (1995). https://doi.org/10.1016/0370-2693(94)01587-3
1354. G. Alexander et al., OPAL collaboration. Phys. Lett. B **266**, 201 (1991). https://doi.org/10.1016/0370-2693(91)90768-L
1355. J. Abdallah et al., DELPHI collaboration. Eur. Phys. J. C **46**, 1 (2006). https://doi.org/10.1140/epjc/s2006-02494-9. arXiv:hep-ex/0603044
1356. K. Ackerstaff et al., OPAL collaboration. Eur. Phys. J. C **4**, 193 (1998). https://doi.org/10.1007/s100520050197. arXiv:hep-ex/9801029
1357. R. Barate et al., ALEPH collaboration. Eur. Phys. J. C **10**, 1 (1999). https://doi.org/10.1007/s100529900146. arXiv:hep-ex/9903014
1358. M. Battle et al., CLEO collaboration. Phys. Rev. Lett. **73**, 1079 (1994). https://doi.org/10.1103/PhysRevLett.73.1079. arXiv:hep-ph/9403329
1359. P. Abreu et al., DELPHI collaboration. Phys. Lett. B **334**, 435 (1994). https://doi.org/10.1016/0370-2693(94)90711-0
1360. G. Abbiendi et al., OPAL collaboration. Eur. Phys. J. C **19**, 653 (2001). https://doi.org/10.1007/s100520100632. arXiv:hep-ex/0009017
1361. M. Fujikawa et al., Belle collaboration. Phys. Rev. D **78**, 072006 (2008). https://doi.org/10.1103/PhysRevD.78.072006. arXiv:0805.3773 [hep-ex]
1362. M. Artuso et al., CLEO collaboration. Phys. Rev. Lett. **72**, 3762 (1994). https://doi.org/10.1103/PhysRevLett.72.3762. arXiv:hep-ph/9404310
1363. B. Aubert et al., BaBar collaboration. Phys. Rev. D **76**, 051104 (2007). https://doi.org/10.1103/PhysRevD.76.051104. arXiv:0707.2922 [hep-ex]
1364. G. Abbiendi et al., OPAL collaboration. Eur. Phys. J. C **35**, 437 (2004). https://doi.org/10.1140/epjc/s2004-01877-2. arXiv:hep-ex/0406007
1365. M. Procario et al., CLEO collaboration. Phys. Rev. Lett. **70**, 1207 (1993). https://doi.org/10.1103/PhysRevLett.70.1207
1366. R. Akers et al., OPAL collaboration. Phys. Lett. B **339**, 278 (1994). https://doi.org/10.1016/0370-2693(94)90645-9
1367. T. Coan et al., CLEO collaboration. Phys. Rev. D **53**, 6037 (1996). https://doi.org/10.1103/PhysRevD.53.6037
1368. M. Acciarri et al., L3 collaboration. Phys. Lett. B **352**, 487 (1995). https://doi.org/10.1016/0370-2693(95)00509-J
1369. G. Abbiendi et al., OPAL collaboration. Eur. Phys. J. C **13**, 213 (2000). https://doi.org/10.1007/s100520000317. arXiv:hep-ex/9911029
1370. R. Barate et al., ALEPH collaboration. Eur. Phys. J. C **11**, 599 (1999). https://doi.org/10.1007/s100520050659. arXiv:hep-ex/9903015
1371. J.P. Lees et al., BaBar collaboration. Phys. Rev. D **86**, 092013 (2012). https://doi.org/10.1103/PhysRevD.86.092013. arXiv:1208.0376 [hep-ex]
1372. H. Behrend et al., CELLO collaboration. Phys. Lett. B **222**, 163 (1989). https://doi.org/10.1016/0370-2693(89)90741-7
1373. B. Adeva et al., L3 collaboration. Phys. Lett. B **265**, 451 (1991). https://doi.org/10.1016/0370-2693(91)90081-Z
1374. H. Aihara et al., TPC/Two Gamma collaboration. Phys. Rev. D **35**, 1553 (1987). https://doi.org/10.1103/PhysRevD.35.1553
1375. P. Achard et al., L3 collaboration. Phys. Lett. B **519**, 189 (2001). https://doi.org/10.1016/S0370-2693(01)01099-1. arXiv:hep-ex/0107055
1376. R. Akers et al., OPAL collaboration. Z. Phys. C **68**, 555 (1995). https://doi.org/10.1007/BF01565256
1377. R. Balest et al., CLEO collaboration. Phys. Rev. Lett. **75**, 3809 (1995). https://doi.org/10.1103/PhysRevLett.75.3809

1378. B. Aubert et al., BaBar collaboration. Phys. Rev. Lett. **100**, 011801 (2008). https://doi.org/10.1103/PhysRevLett.100.011801. arXiv:0707.2981 [hep-ex]
1379. M. Lee et al., Belle collaboration. Phys. Rev. D **81**, 113007 (2010). https://doi.org/10.1103/PhysRevD.81.113007. arXiv:1001.0083 [hep-ex]
1380. R.A. Briere et al., CLEO collaboration. Phys. Rev. Lett. **90**, 181802 (2003). https://doi.org/10.1103/PhysRevLett.90.181802. arXiv:hep-ex/0302028
1381. K. Edwards et al., CLEO collaboration. Phys. Rev. D **61**, 072003 (2000). https://doi.org/10.1103/PhysRevD.61.072003. arXiv:hep-ex/9908024
1382. D. Bortoletto et al., CLEO collaboration. Phys. Rev. Lett. **71**, 1791 (1993). https://doi.org/10.1103/PhysRevLett.71.1791
1383. A. Anastassov et al., CLEO collaboration. Phys. Rev. Lett. **86**, 4467 (2001). https://doi.org/10.1103/PhysRevLett.86.4467. arXiv:hep-ex/0010025
1384. S. Richichi et al., CLEO collaboration. Phys. Rev. D **60**, 112002 (1999). arXiv:hep-ex/9810026
1385. D.A. Bauer et al., TPC/Two Gamma collaboration. Phys. Rev. D **50**, 13 (1994). https://doi.org/10.1103/PhysRevD.50.13
1386. R. Barate et al., ALEPH collaboration. Eur. Phys. J. C **1**, 65 (1998). https://doi.org/10.1007/s100520050062
1387. K.E. Arms et al., CLEO collaboration. Phys. Rev. Lett. **94**, 241802 (2005). https://doi.org/10.1103/PhysRevLett.94.241802. arXiv:hep-ex/0501042
1388. G. Abbiendi et al., OPAL collaboration. Eur. Phys. J. C **13**, 197 (2000). https://doi.org/10.1007/s100520000272. arXiv:hep-ex/9908013
1389. D. Gibaut et al., CLEO collaboration. Phys. Rev. Lett. **73**, 934 (1994). https://doi.org/10.1103/PhysRevLett.73.934
1390. B. Bylsma et al., Phys. Rev. D **35**, 2269 (1987). https://doi.org/10.1103/PhysRevD.35.2269
1391. H. Albrecht et al., ARGUS collaboration. Phys. Lett. B **202**, 149 (1988). https://doi.org/10.1016/0370-2693(88)90870-2
1392. K. Ackerstaff et al., OPAL collaboration. Eur. Phys. J. C **8**, 183 (1999). https://doi.org/10.1007/s100529901057. arXiv:hep-ex/9808011
1393. D. Buskulic et al., ALEPH collaboration. Z. Phys. C **74**, 263 (1997). https://doi.org/10.1007/s002880050387
1394. K. Inami et al., Belle collaboration. Phys. Lett. B **672**, 209 (2009). https://doi.org/10.1016/j.physletb.2009.01.047. arXiv:0811.0088 [hep-ex]
1395. M. Artuso et al., CLEO collaboration. Phys. Rev. Lett. **69**, 3278 (1992). https://doi.org/10.1103/PhysRevLett.69.3278
1396. P. del Amo Sanchez et al., BaBar collaboration. Phys. Rev. D **83**, 032002 (2011). https://doi.org/10.1103/PhysRevD.83.032002. arXiv:1011.3917 [hep-ex]
1397. J.E. Bartelt et al., CLEO collaboration. Phys. Rev. Lett. **76**, 4119 (1996). https://doi.org/10.1103/PhysRevLett.76.4119
1398. M. Bishai et al., CLEO collaboration. Phys. Rev. Lett. **82**, 281 (1999). https://doi.org/10.1103/PhysRevLett.82.281. arXiv:hep-ex/9809012
1399. P. Baringer et al., CLEO collaboration. Phys. Rev. Lett. **59**, 1993 (1987). https://doi.org/10.1103/PhysRevLett.59.1993
1400. D. Buskulic et al., ALEPH collaboration. Z. Phys. C **70**, 579 (1996). https://doi.org/10.1007/s002880050134
1401. J.P. Lees et al., BaBar collaboration. Phys. Rev. D **86**, 092010 (2012). https://doi.org/10.1103/PhysRevD.86.092010. arXiv:1209.2734 [hep-ex]
1402. K. Belous et al., Belle collaboration. Phys. Rev. Lett. **112**, 031801 (2014). https://doi.org/10.1103/PhysRevLett.112.031801. arXiv:1310.8503 [hep-ex]
1403. W. Marciano, A. Sirlin, Phys. Rev. Lett. **61**, 1815 (1988). https://doi.org/10.1103/PhysRevLett.61.1815
1404. A. Pich, Prog. Part. Nucl. Phys. **75**, 41 (2014). https://doi.org/10.1016/j.ppnp.2013.11.002. arXiv:1310.7922 [hep-ph]
1405. A. Ferroglia, C. Greub, A. Sirlin, Z. Zhang, Phys. Rev. D **88**, 033012 (2013). https://doi.org/10.1103/PhysRevD.88.033012. arXiv:1307.6900 [hep-ph]
1406. M. Fael, L. Mercolli, M. Passera, Phys. Rev. D **88**, 093011 (2013). https://doi.org/10.1103/PhysRevD.88.093011. arXiv:1310.1081 [hep-ph]
1407. W.J. Marciano, A. Sirlin, Phys. Rev. Lett. **71**, 3629 (1993). https://doi.org/10.1103/PhysRevLett.71.3629
1408. R. Decker, M. Finkemeier, Phys. Lett. B **334**, 199 (1994). https://doi.org/10.1016/0370-2693(94)90611-4
1409. R. Decker, M. Finkemeier, Nucl. Phys. B **438**, 17 (1995). https://doi.org/10.1016/0550-3213(95)00597-L. arXiv:hep-ph/9403385
1410. R. Decker, M. Finkemeier, Nucl. Phys. Proc. Suppl. **40**, 453 (1995). https://doi.org/10.1016/0920-5632(95)00170-E. arXiv:hep-ph/9411316
1411. M. Davier, A. Hocker, Z. Zhang, Rev. Mod. Phys. **78**, 1043 (2006). https://doi.org/10.1103/RevModPhys.78.1043. arXiv:hep-ph/0507078
1412. M. Antonelli et al., FlaviaNet working group on kaon decays. Eur. Phys. J. C **69**, 399 (2010). https://doi.org/10.1140/epjc/s10052-010-1406-3. arXiv:1005.2323 [hep-ph]
1413. E. Gamiz, M. Jamin, A. Pich, J. Prades, F. Schwab, JHEP **01**, 060 (2003). https://doi.org/10.1088/1126-6708/2003/01/060. arXiv:hep-ph/0212230
1414. E. Gamiz, M. Jamin, A. Pich, J. Prades, F. Schwab, Phys. Rev. Lett. **94**, 011803 (2005). https://doi.org/10.1103/PhysRevLett.94.011803. arXiv:hep-ph/0408044
1415. E. Gamiz, M. Jamin, A. Pich, J. Prades, F. Schwab, Nucl. Phys. Proc. Suppl. **169**, 85 (2007). https://doi.org/10.1016/j.nuclphysbps.2007.02.053. arXiv:hep-ph/0612154
1416. E. Gamiz, M. Jamin, A. Pich, J. Prades, F. Schwab, PoS **KAON**, 008 (2008). arXiv:0709.0282 [hep-ph]
1417. K. Maltman, Nucl. Phys. Proc. Suppl. **218**, 146 (2011). https://doi.org/10.1016/j.nuclphysbps.2011.06.025. arXiv:1011.6391 [hep-ph]
1418. J.C. Hardy, I.S. Towner, Phys. Rev. C **91**, 025501 (2015). https://doi.org/10.1103/PhysRevC.91.025501. arXiv:1411.5987 [nucl-ex]
1419. V. Cirigliano, H. Neufeld, Phys. Lett. B **700**, 7 (2011). https://doi.org/10.1016/j.physletb.2011.04.038. arXiv:1102.0563 [hep-ph]
1420. W.J. Marciano, Phys. Rev. Lett. **93**, 231803 (2004). https://doi.org/10.1103/PhysRevLett.93.231803. arXiv:hep-ph/0402299
1421. M. Jamin, A. Pich, J. Portoles, Phys. Lett. B **664**, 78 (2008). https://doi.org/10.1016/j.physletb.2008.04.049. arXiv:0803.1786 [hep-ph]
1422. M. Antonelli, V. Cirigliano, A. Lusiani, E. Passemar, JHEP **10**, 070 (2013). https://doi.org/10.1007/JHEP10(2013)070. arXiv:1304.8134 [hep-ph]
1423. K. Maltman, R.J. Hudspith, R. Lewis, C.E. Wolfe, J. Zanotti (2015), arXiv:1510.06954 [hep-ph]
1424. R.J. Hudspith, R. Lewis, K. Maltman, J. Zanotti (2017), arXiv:1702.01767 [hep-ph]
1425. B. Aubert et al., BaBar collaboration. Phys. Rev. Lett. **104**, 021802 (2010). https://doi.org/10.1103/PhysRevLett.104.021802. arXiv:0908.2381 [hep-ex]
1426. K. Hayasaka et al., Belle collaboration. Phys. Lett. B **666**, 16 (2008). https://doi.org/10.1016/j.physletb.2008.06.056. arXiv:0705.0650 [hep-ex]
1427. B. Aubert et al., BaBar collaboration. Phys. Rev. Lett. **98**, 061803 (2007). https://doi.org/10.1103/PhysRevLett.98.061803. arXiv:hep-ex/0610067
1428. Y. Miyazaki et al., Belle collaboration. Phys. Lett. B **648**, 341 (2007). https://doi.org/10.1016/j.physletb.2007.03.027. arXiv:hep-ex/0703009

1429. B. Aubert et al., BaBar collaboration. Phys. Rev. D **79**, 012004 (2009). https://doi.org/10.1103/PhysRevD.79.012004. arXiv:0812.3804 [hep-ex]
1430. Y. Miyazaki et al., Belle collaboration. Phys. Lett. B **692**, 4 (2010). https://doi.org/10.1016/j.physletb.2010.07.012. arXiv:1003.1183 [hep-ex]
1431. B. Aubert et al., BaBar collaboration. Phys. Rev. Lett. **103**, 021801 (2009). https://doi.org/10.1103/PhysRevLett.103.021801. arXiv:0904.0339 [hep-ex]
1432. Y. Miyazaki, Belle collaboration. Phys. Lett. B **699**, 251 (2011). https://doi.org/10.1016/j.physletb.2011.04.011. arXiv:1101.0755 [hep-ex]
1433. B. Aubert et al., BaBar collaboration. Phys. Rev. Lett. **100**, 071802 (2008). https://doi.org/10.1103/PhysRevLett.100.071802. arXiv:0711.0980 [hep-ex]
1434. Y. Miyazaki et al., Belle collaboration. Phys. Lett. B **672**, 317 (2009). https://doi.org/10.1016/j.physletb.2009.01.058. arXiv:0810.3519 [hep-ex]
1435. J.P. Lees et al., BaBar collaboration. Phys. Rev. D **81**, 111101 (2010). https://doi.org/10.1103/PhysRevD.81.111101. arXiv:1002.4550 [hep-ex]
1436. K. Hayasaka et al., Belle collaboration. Phys. Lett. B **687**, 139 (2010). https://doi.org/10.1016/j.physletb.2010.03.037. arXiv:1001.3221 [hep-ex]
1437. G. Aad et al., ATLAS collaboration. Eur. Phys. J. C **76**, 232 (2016). https://doi.org/10.1140/epjc/s10052-016-4041-9. arXiv:1601.03567 [hep-ex]
1438. R. Aaij et al., LHCb collaboration. JHEP **02**, 121 (2015). https://doi.org/10.1007/JHEP02(2015)121. arXiv:1409.8548 [hep-ex]
1439. B. Aubert et al., BaBar collaboration. Phys. Rev. Lett. **95**, 191801 (2005). https://doi.org/10.1103/PhysRevLett.95.191801. arXiv:hep-ex/0506066
1440. Y. Miyazaki et al. (Belle collaboration), Phys. Lett. B **719**, 346 (2013). https://doi.org/10.1016/j.physletb.2013.01.032. arXiv:1206.5595 [hep-ex]
1441. Y. Miyazaki et al., Belle collaboration. Phys. Lett. B **632**, 51 (2006). https://doi.org/10.1016/j.physletb.2005.10.024. arXiv:hep-ex/0508044
1442. R. Aaij et al., LHCb collaboration. Phys. Lett. B **724**, 36 (2013). https://doi.org/10.1016/j.physletb.2013.05.063. arXiv:1304.4518 [hep-ex]
1443. A.L. Read, J. Phys. G **28**, 2693 (2002). https://doi.org/10.1088/0954-3899/28/10/313
1444. S. Banerjee, B. Pietrzyk, J.M. Roney, Z. Was, Phys. Rev. D **77**, 054012 (2008). https://doi.org/10.1103/PhysRevD.77.054012. arXiv:0706.3235 [hep-ph]
1445. CDF collaboration, CDF note 8128 (2007). http://www-cdf.fnal.gov/physics/statistics/notes/cdf8128_mclimit_csm_v2.pdf